A Structural Study of the Nature of Molecular Zirconium Species in Aqueous Solution

by

Joe Rawlinson

A thesis submitted in partial fulfilment for the requirements for the degree of Doctor of Philosophy at the University of Central Lancashire

December 2022

RESEARCH STUDENT DECLARATION FORM

Type of Award **Doctor of Philosophy**

School **School of Natural Sciences**

*Sections marked * delete as appropriate*

1. Concurrent registration for two or more academic awards

*I declare that while registered as a candidate for the research degree, I have not been a registered candidate or enrolled student for another award of the University or other academic or professional institution

2. Material submitted for another award

***I** declare that no material contained in the thesis has been used in any other submission for an
academic award and is solely my own work

3. Collaboration

Where a candidate's research programme is part of a collaborative project, the thesis must indicate in addition clearly the candidate's individual contribution and the extent of the collaboration. Please state below:

_____

4. Use of a Proof-reader

*No proof-reading service was used in the compilation of this thesis.

Signature of Candidate

Print name: Joe Rawlinson

Abstract

The structural study of complex molecular ions in solution has often proved difficult but is vital to fully understand how these solutions behave in the reaction pathways of material synthesis. Attempts have been made previously to quantitatively determine the structure of Zr(IV) solutions using a number of techniques. The work presented here aims to determine the optimal method for the study of these solutions and critically compares extended X-ray absorption fine structure (EXAFS), a technique long seen as the logical choice for the study of metal containing complex ions in solution, and X-ray pair distribution function (XPDF).

To initially test the validity of the use of XPDF to study these solutions, structural studies were undertaken on solutions of zirconium-oxychloride, ($ZrOCl_2 \cdot 8H_2O$). This work determined that the tetrameric phase $[Zr_4(OH)_8(OH_2)_{16}]^{8+}$ previously proposed by Clearfield *et al.* [1] is present in solutions and that there is a strong coordination between the complex tetrameric ion and the chloride counter ions. Through the iterative method development that was used to study this zirconium-oxychloride solution, an optimal method was derived to be carried forward for subsequent XPDF studies.

The work then attempts to compare the results of studies performed by other groups using EXAFS to study laboratory synthesised solutions prepared from the addition of acetic acid to $ZrOCl_2 \cdot 8H_2O$ solutions, with commercially available solutions of zirconium-acetate, $[Zr(CH_3COO)_4]$. It was found that the results seen in literature for laboratory synthesised solutions do not match that seen in commercially available materials. The commercial materials showed a tendency towards a tetrameric phase, $[Zr_4(OH)_8(OH_2)_{16}]^{8+}$, up to acetic acid : zirconium ratios well in excess of 5.0 contrary to that seen in laboratory synthesised

material which seem to shower a higher prevalence of the hexameric phase, $Zr_6(O)_4(OH)_4(CH_3COO)_{12}$, at acetic acid : zirconium ratios higher than 0.8.

Alongside this work an ageing study was conducted to determine if the structure or relative composition of tetrameric $[Zr_4(OH)_8(OH_2)_{16}]^{8+}$ and hexameric, $Zr_6(O)_4(OH)_4(CH_3COO)_{12}$, phases could be altered through ageing or varying the solution concentrations. It was found that while all solutions adopt a two phase system of the hexameric and tetrameric phases, and that the main influence on this ratio was concentration, there are potentially two conformations that the hexameric $Zr_6(O)_4(OH)_4(CH_3COO)_{12}$ can adopt, and the validity of both these models is discussed within with a "fixed-core" model being preferred but not being without chemical inconsistencies in the extended length of some of the chelating Zr-O bonds between the core and the carboxylate ligands. Some of these achieving lengths of over the common literature value of 2.2 ± 0.2 Å.

Finally, a model compound synthesis study was undertaken to determine if any of the variations observed in the ageing study described above manifested as variation in final products when these solutions were used as zirconium precursors as they so often are in industrial applications. It was determined that the consistency of the model compound, the microporous zirconosilicate umbite $K_2ZrSi_3O_9{\cdot}H_2O$, is extremely high with a single crystalline phase with consistent orthorhombic lattice parameters (a = 10.2916-10.3131 Å, b = 13.3071-13.3623 Å, c = 7.1845-7.2107 Å) and bond lengths and angles consistent with those reported in literature. The principal variation observed in the zirconosilicate was the quantity of amorphous phase obtained varying from 9.80-88.12% crystallinity. Whilst little seemed to impact the maximum crystallinity that could be achieved for a sample it was noted that higher ratios of acetic acid : zirconium gave a broader range of crystallinity.

It is hoped that the methods developed here can subsequently be applied to alternative solutions and that this is not only limited to zirconium complexes but all metal complex solution species. The information derived on the specific zirconium materials studied here, namely zirconium-oxychloride and zirconium-acetate, can inform their employment in synthesis pathways.

Acknowledgements

My first and greatest thanks must go to my supervisor, Dr. Jennifer Readman, without who I don't think I would have started this journey, let alone finished it. For all the help I have needed for the last 9 (It really has been that long!) years. I know I have grown a few grey hairs in that time and I'm sure I've caused you a good few! For being on call to help me out throughout the whole pandemic when office hours became an abstract concept. Thank you for the endless supply of coffee. I'm sure that your office will be significantly quieter (and possibly a little bit more productive) in future.

I would also like to thank Luxfer MEL Technologies for supporting my research and to Dr. Emiliana Dvininov for your help, supervision, and window (and now door) into the big wide world of industry. Also, to Dr. Hazel Stephenson for believing that I was worth it in the first place. I hope over the last 4 years, even with you being more removed from the project, I have proven you right.

To all of those at UCLan who have made this work possible, I thank you all so much. To all the technical staff, especially Tamar and Pete who had a shrewd ability to spot the confusion on my face from the other side of the room and come and bail me out. To all the good people I get to call friend who I met on this journey, without you I would be far less sane than I am, and although you probably doubt its possible, a lot grumpier. We had some good times when we were allowed to work in the same room, and I will always remember our "productive days".

I must also thank the beamline scientists who have run many of the experiments presented here. All of the staff of 28-ID-1 at NSLS, and I15-1 at DLS, but in particular Dr. Phillip Chater at DLS for your insight.

I cannot understate the thanks I have to give to my parents and the rest of my family. To have put up with me for so long and always to try and complain about me when I am out of earshot (not always successfully). I promise I will get from under your feet and move out soon!

Finally, to the woman who has been my strength for the whole of this PhD project. The only person who truly understood what I was going through and what I needed. Rachel, I know for certain that I couldn't have done this without you there.

After 9 years at UCLan it's the end of an era, and what an era.

Contents

Abstract iii

Acknowledgements vii

Table of Figures xiii

Table of Tables xxviii

Table of Equations xxxv

1.0 Introduction 1

1.1 Background 1

1.2 Aims of Project 2

1.3 Layout of Thesis 2

1.4 Applications of Zirconium Materials 4

1.5 Previous Structural Studies 6

1.6 The Model Compound – Umbite ($K_2ZrSi_3O_9 \cdot H_2O$) 16

2.0 Scattering Techniques 18

2.1 Generation of X-rays 18

2.1.1 Laboratory X-ray Sources 18

2.1.2 Synchrotron Sources 20

2.2 Powder X-ray Diffraction (PXRD) 24

2.2.1 The Rietveld Refinement 27

2.2.2 The Pawley Fit 30

2.2.3 Experimental Setup Used 31

2.3 Total Scattering Pair Distribution Functions (PDF) 33

2.3.1 Refinement Techniques 40

3.0 Non-Scattering Experimental Techniques 43

3.1 X-ray Absorption Spectroscopy (XAS) 43

3.2 Synthesis of the Model Compound – Umbite $K_2ZrSi_3O_9 \cdot H_2O$ 50

3.3 Scanning Electron Microscopy (SEM) 51

3.4 Nitrogen Gas Adsorption 54

4.0 Zirconium-oxychloride Refinements 57

4.1 Preparation of the Refinement Model 58

4.2 Refinement Method Iteration 1 62

4.3 Refinement Method Iteration 2 72

4.4 Refinement Method Iteration 3 80

5.0 Preliminary Investigation of Commercial Samples 90

5.1 Zirconium-acetate Zr K-edge EXAFS 92

5.2 Zirconium-acetate PDF 99

6.0 Zirconium-acetate Refinements 103

6.1 Synthesis of Zirconium-acetate Solutions 104

6.1.1 Physical Observations 106

6.2 9-Month Data Collection (March 2020) 108

6.2.1 Single-phase Refinements 110

6.2.2 Dual-phase Refinements 129

6.2.3 Summary 150

6.3 15-Month Data Collection (September 2020) 152

6.3.1 Summary 172

6.4 18-Month Data Collection (December 2020) 174

6.4.1 Summary 192

6.5 Other Data Collections 194

6.6 Phase Ratio Analysis 201

6.7 Summary of Ageing Study 205

7.0 Model Compound Analysis 206

7.1 Synthesis of Umbite 207

7.2 Yields 208

7.3 Rietveld Refinements 215

7.4 Degree of Crystallinity 221

7.5 Scanning Electron Microscopy 227

7.6 Nitrogen Gas Adsorption 233

7.7 Conclusions of Model Compound Analysis 239

8.0 Conclusions 241

8.1 Future Work 246

References 249

Table of Figures

Figure 1: a)The structure of solid zirconium-oxychloride ($ZrOCl_2 \cdot 8H_2O$) viewed off centre from the c-axis, as proposed by Clearfield and Vaughn [1]. B) The isolated tetrameric unit and 8 nearest neighbouring Cl positions. Hydrogen positions have been omitted for clarity. Key: Zr – Black, O – Red, Cl – Lime Green. 7

Figure 2: Atomic distances between the tetrameric cluster ($[Zr_4(OH)_8(OH_2)_{16}]^{8+}$) and the neighbouring chlorine positions. Key: Zr – Black, O – Red, Cl – Lime Green. 8

Figure 3: The a) single and b) linked tetranuclear structure of zirconium-acetate as proposed by Tosan et al.[42] showing the core structure of $ZrOCl_2 \cdot 8H_2O$ as proposed by Clearfield and Vaughn [1] but with carboxylate groups in the terminal positions. The corner positions represent Zr atoms bridged by pairs of oxygen positions. The carboxylate groups are shown bonded with dashed lines (b). Chlorine is shown in black. 12

Figure 4: Fourier transformed XAS data of $[Zr_4(OH)_8(OH_2)_{16}]^{8+}$ (left) and $Zr_6(O)_4(OH)_4(CH_3COO)_{12}$ (right). (Bottom) the hexanuclear cluster $Zr_6(O)_4(OH)_4(CH_3COO)_{12}$. Zr-Blue, O-Red, C-Grey, H-Grey [2]. 14

Figure 5: Crystal structure of Umbite ($K_2ZrSi_3O_9 \cdot H_2O$) viewed down the c-axis showing the octahedral Zr (Black Polyhedra) and tetrahedral Si (Yellow Polyhedra) of the framework. Within the framework are the counter cations K (Blue Spheres) and the oxygens of the waters of crystallisation (Black Spheres). The unit-cell boundaries are shown in blue dashed lines [46]. 17

Figure 6: An X-ray emission profile showing the Bremsstrahlung continuum and two monochromatic characteristic X-ray peaks [48]. 19

Figure 7: Schematic of a synchrotron facility with key elements highlighted [50]. 21

Figure 8: Diagram showing a system that satisfies Bragg's Law, constructive interference is observed in the out-bound X-rays. 25

Figure 9: X-ray and neutron scattering length of a selection of elements [71]. 34

Figure 10: The exponential characteristics of the RDF. a) the RDF (black) is shown with the asymptotic behaviour in red. b) the associated PDF (black) with the asymptotic behaviour in red and a negative sloping baseline in blue [70]. 35

Figure 11: The raw diffraction data, S(q), and D(r) for a sample of zirconium-acetate solution obtained in the 3-month data collection at DLS. 39

Figure 12: Graphical representations of a series of common thermal parameters used in PDF refinements a) a standard single value B=0.5 b) a spherical function with a gradual rise to low correlated motion c) a spherical system where an immediate range of high correlation which dissipates d) another system of low r bonding which dissipates to a maximum. 41

Figure 13: A typical XAS spectra with the XANES and EXAFS regions highlighted [81]. 45

Figure 14: The schematic of a standard XAS experiment in transmission-mode. 47

Figure 15: Instances of the relationship between atomic spacing and wavelength (Top) causing constructive interference and (Bottom) causing destructive interference. 48

Figure 16: Schematic of a Scanning Electron Microscope. The incident electron beam is denoted in yellow and the secondary electrons which are to be detected are shown in orange. 52

Figure 17: All isotherm types as classified by IUPAC [88] 56

Figure 18: Unit-cell of the Clearfield model of $ZrOCl_2 \cdot 8H_2O$, as viewed down the c axis showing the tetrameric species $[Zr_4(OH)_8(OH_2)_{16}]^{8+}$. Key: Zr–Grey O–Red, Cl–Light Green [1]. 58

Figure 19: The single isolated tetramer unit ($[Zr_4(OH)_8(OH_2)_{16}]^{8+}$) as seen in the Clearfield model [1]. Key: Zr – Black, O – Red. 60

Figure 20: Fourier transformed PDF of zirconium-oxychloride processed using a water filled capillary as a background.....61

Figure 21: The function of effective b value with respect to the distance r between an atomic pair. “rlo” the r value at which correlated motion stops being linear, and “2*radius + rlo” the r value at which the correlation again becomes linear are shown. 63

Figure 22: Resultant refinement of PDF data of zirconium-oxychloride using refinement method 1.....64

Figure 23: Structure of the resultant model ($[Zr_4(OH)_8(OH_2)_{16}]^{8+}$) of the refinement of zirconium-oxychloride using refinement method 1 Key: Zr – Black, O – Red. 64

Figure 24: Fourier transformed PDF of zirconium-oxychloride processed using an empty capillary as a background.....73

Figure 25: The first 8 lines of a Z-matrix used to define the zirconium-oxychloride tetramer showing the definition of the core 4 zirconium positions. This Z-matrix also contains a parameter “=rXZr;” which is used to group common terms. 74

Figure 26: Model resulting from the Z-matrix shown in Figure 25. The core 3 atomic positions (X1, X2 and X3) are shown in yellow and the 4 Zr positions are shown in Grey. The bonds between are representative of the distance =rXZr; from Figure 25.....74

Figure 27: Resultant refinement of PDF data of zirconium-oxychloride using refinement method 2. This refinement iteration modelled the water contribution rather than removing it from the data set as a background measurement. 76

Figure 28: Structure of the resultant model ($[Zr_4(OH)_8(OH_2)_{16}]^{8+}$) of the refinement of zirconium-oxychloride using refinement method 2 Key: Zr – Black, O – Red. 76

Figure 29: Starting model of refinement iteration 3 showing the location of the chlorine positions. Key: Zr – Black, O – Red, Cl – Lime Green. 81

Figure 30: Resultant refinement of PDF data of zirconium-oxychloride using refinement method 3. 82

Figure 31: Structure of the resultant model of the refinement of zirconium-oxychloride using refinement method 3 Key: Zr – Black, O – Red, Cl – Lime Green. 82

Figure 32: The structures of two alternative models which were assessed in this work. Key: Zr – Black, O – Red. 87

Figure 33: Refinement of PDF data of zirconium-oxychloride using the model shown in Figure 32a 88

Figure 34: Refinement of PDF data of zirconium-oxychloride using the model shown in Figure 32b. 88

Figure 35: Absorption spectra of three samples of commercially available zirconium-acetate solutions from Luxfer MEL Technologies. All three samples have had their absorption energy normalised to Zr foil which was used as a reference sample. 92

Figure 36: Zr K-edge k^3 weighted EXAFS after Fourier transform. 93

Figure 37: Fourier transformed XAS data of $[Zr_4(OH)_8(OH_2)_{16}]^{8+}$(left) and $Zr_6(O)_4(OH)_4(CH_3COO)_{12}$ (right) as reported by Hennig et al. Key: Zr-Blue, O, Red, C-Grey, H-Grey [2]. 94

Figure 38: The observed and calculated radial distribution function resulting from the fit of a 30% zirconium-acetate sample to the model proposed by Hennig et al. [2]. 96

Figure 39: The observed and calculated radial distribution function resulting from the fit of 22% zirconium-acetate sample 1 to the model proposed by Hennig et al. [2]. 96

Figure 40: The observed and calculated radial distribution function resulting from the fit of 22% zirconium-acetate sample 2 to the model proposed by Hennig et al. [2]. 97

Figure 41: (Top) Overlay of 3 PDFs of zirconium-acetate solutions of 2 different zirconium concentrations collected on I15-1 as part of the preliminary work with some key features labelled. (Bottom) the Hexameric structure, $Zr_6(O)_4(OH)_4(CH_3COO)_{12}$, with the key contact distances labelled.....100

Figure 42: Overlay of 3 PDFs collected on I15-1 focused on the range of 7 – 15 Å. 101

Figure 43: Overlay of the PDFs collected in the 9-month data collection period over an r-range of 0Å < r < 15Å with a zoom in on the largest peak (Inset) 109

Figure 44: Starting hexameric model showing a symmetrical core used in the first single-phase refinement iteration. Key: Zr – Grey, O – Red, C – Black. 111

Figure 45: a) Observed (black) and calculated (blue) PDF of the first iteration of the single-phase refinement of sample ZAA1 (14% ZrO_2). b) Resultant model of this refinement. Key: Zr – Grey, O – Red, C – Black. R_{wp} = 34.75%. 112

Figure 46: a) Observed (black) and calculated (blue) PDF of the first iteration of the single-phase refinement of sample ZAA4 (22% ZrO_2). b) Resultant model of this refinement. Key: Zr – Grey, O – Red, C – Black. R_{wp} = 34.38%. 112

Figure 47: a) Observed (black) and calculated (blue) PDF of the first iteration of the single-phase refinement of sample ZAA7 (30% ZrO_2). b) Resultant model of this refinement. Key: Zr – Grey, O – Red, C – Black. R_{wp} = 29.15%. 113

Figure 48: A diagram of the movements seen in the carboxylate groups for the refinements presented herein. The model transfers from that seen on the left to the right with the net effect being a change in the carbon position (Δ). Key: Zr – Grey, O – Red, C – Black. 117

Figure 49: An example of a hexameric cluster displaying the chandelier bonding conformation highlighting the axial zirconium positions. Key: Zr Equatorial – Grey, Zr Axial – Blue, O – Red, C – Black. 120

Figure 50: Observed (black) and calculated (blue) PDF of the second iteration of the single-phase refinement of sample ZAA1. R_{wp} = 30.29%. 121
Figure 51: Observed (black) and calculated (blue) PDF of the second iteration of the single-phase refinement of sample ZAA4. R_{wp} = 29.27%. 121
Figure 52: Observed (black) and calculated (blue) PDF of the second iteration of the single-phase refinement of sample ZAA7. R_{wp} = 28.24%. 122
Figure 53: Resultant model of the refinement of data collected on sample ZAA1 using the second iteration single-phase refinement viewed from the axial positions (left) and the equatorial plane (right). Key: Zr – Grey, O – Red, C – Black. 124
Figure 54: Resultant model of the refinement of data collected on sample ZAA4 using the second iteration single-phase refinement viewed from the axial positions (left) and the equatorial plane (right). Key: Zr – Grey, O – Red, C – Black. 124
Figure 55: Resultant model of the refinement of data collected on sample ZAA7 using the second iteration single-phase refinement viewed from the axial positions (left) and the equatorial plane (right). Key: Zr – Grey, O – Red, C – Black. 125
Figure 56: a) Observed (black) and calculated (blue) PDF of the first iteration of the dual-phase refinement of sample ZAA1. Each respective phase has been resolved with the hexameric contribution shown in green, the tetrameric contribution in orange, and the background and water in purple. b) Resultant model of this refinement. Key: Zr – Grey, O – Red, C – Black. R_{wp} = 25.63%.....130
Figure 57: a) Observed (black) and calculated (blue) PDF of the first iteration of the dual-phase refinement of sample ZAA4. Each respective phase has been resolved with the hexameric contribution shown in green, the tetrameric contribution in orange, and the background and

water in purple. b) Resultant model of this refinement. Key: Zr – Grey, O – Red, C – Black. R_{wp} = 26.75%.....130
Figure 58: a) Observed (black) and calculated (blue) PDF of the first iteration of the dual-phase refinement of sample ZAA7. Each respective phase has been resolved with the hexameric contribution shown in green, the tetrameric contribution in orange, and the background and water in purple. b) Resultant model of this refinement. Key: Zr – Grey, O – Red, C – Black. R_{wp} = 26.67%.....131
Figure 59: A comparison of a zirconium position and its surrounding oxygen positions for a) the model refined from zirconium-oxychloride and b) the tetrameric phase of the refinement of sample ZAA1 showing the bond angles between both the in plane and perpendicular terminal oxygen positions.....137
Figure 60: Observed (black) and calculated (blue) PDF of the second iteration of the dual-phase refinement of sample ZAA1. Each respective phase has been resolved with the hexameric contribution shown in green, the tetrameric contribution in orange and the background and water in purple. R_{wp} = 26.07%.....139
Figure 61: Observed (black) and calculated (blue) PDF of the second iteration of the dual-phase refinement of sample ZAA4. Each respective phase has been resolved with the hexameric contribution shown in green, the tetrameric contribution in orange and the background and water in purple. R_{wp} = 25.25%.....139
Figure 62: Observed (black) and calculated (blue) PDF of the second iteration of the dual-phase refinement of sample ZAA7. Each respective phase has been resolved with the hexameric contribution shown in green, the tetrameric contribution in orange and the background and water in purple. R_{wp} = 24.84%.....140

Figure 63: Resultant model of the refinement of data collected on sample ZAA1 using the second iteration dual-phase refinement viewed from the axial positions and the equatorial plane. Key: Zr – Grey, O – Red, C – Black. 143
Figure 64: Resultant model of the refinement of data collected on sample ZAA4 using the second iteration dual-phase refinement viewed from the axial positions and the equatorial plane. Key: Zr – Grey, O – Red, C – Black. 143
Figure 65: Resultant model of the refinement of data collected on sample ZAA7 using the second iteration dual-phase refinement viewed from the axial positions and the equatorial plane. Key: Zr – Grey, O – Red, C – Black. 144
Figure 66: The centre of the hexamer viewed diagonally (110) arising from the a) chandelier model and b) fixed-core model refinements of ZAA1. Key: Zr – Grey, O – Red, C – Black....147
Figure 67: Overlay of the PDFs collected in the 15-month data collection period over an r-range of 0 Å < r < 15 Å. 153
Figure 68: a) Observed (black) and calculated (blue) PDF of the first iteration of the dual-phase refinement of sample ZAA1. Each respective phase has been resolved with the hexameric contribution shown in green, the tetrameric contribution in orange, and the background and water in purple. R_{wp} = 24.77%. b) Resultant model of this refinement. Key: Zr – Grey, O – Red, C – Black. 155
Figure 69: a) Observed (black) and calculated (blue) PDF of the first iteration of the dual-phase refinement of sample ZAA4. Each respective phase has been resolved with the hexameric contribution shown in green, the tetrameric contribution in orange, and the background and water in purple. R_{wp} = 24.38%. b) Resultant model of this refinement. Key: Zr – Grey, O – Red, C – Black. 155

Figure 70: a) Observed (black) and calculated (blue) PDF of the first iteration of the dual-phase refinement of sample ZAA7. Each respective phase has been resolved with the hexameric contribution shown in green, the tetrameric contribution in orange, and the background and water in purple. R_{wp} = 24.17%. b) Resultant model of this refinement. Key: Zr – Grey, O – Red, C – Black. 156

Figure 71: a) Observed (black) and calculated (blue) PDF of the first iteration of the dual-phase refinement of sample ZAA24. Each respective phase has been resolved with the hexameric contribution shown in green, the tetrameric contribution in orange, and the background and water in purple. R_{wp} = 25.53%. b) Resultant model of this refinement. Key: Zr – Grey, O – Red, C – Black. 156

Figure 72: a) Observed (black) and calculated (blue) PDF of the first iteration of the dual-phase refinement of sample ZAA25. Each respective phase has been resolved with the hexameric contribution shown in green, the tetrameric contribution in orange, and the background and water in purple. R_{wp} = 23.06%. b) Resultant model of this refinement. Key: Zr – Grey, O – Red, C – Black. 156

Figure 73: a) Observed (black) and calculated (blue) PDF of the second iteration of the dual-phase refinement of sample ZAA1. Each respective phase has been resolved with the hexameric contribution shown in green, the tetrameric contribution in orange, and the background and water in purple. R_{wp} = 29.36%. b) Resultant model of this refinement. Key: Zr – Grey, O – Red, C – Black. 164

Figure 74: a) Observed (black) and calculated (blue) PDF of the second iteration of the dual-phase refinement of sample ZAA4. Each respective phase has been resolved with the hexameric contribution shown in green, the tetrameric contribution in orange, and the

background and water in purple. R_{wp} = 28.34%. b) Resultant model of this refinement. Key: Zr – Grey, O – Red, C – Black. 164

Figure 75: a) Observed (black) and calculated (blue) PDF of the second iteration of the dual-phase refinement of sample ZAA7. Each respective phase has been resolved with the hexameric contribution shown in green, the tetrameric contribution in orange, and the background and water in purple. R_{wp} = 26.59%. b) Resultant model of this refinement. Key: Zr – Grey, O – Red, C – Black. 164

Figure 76: a) Observed (black) and calculated (blue) PDF of the second iteration of the dual-phase refinement of sample ZAA24. Each respective phase has been resolved with the hexameric contribution shown in green, the tetrameric contribution in orange, and the background and water in purple. R_{wp} = 28.51%. b) Resultant model of this refinement. Key: Zr – Grey, O – Red, C – Black. 165

Figure 77: a) Observed (black) and calculated (blue) PDF of the second iteration of the dual-phase refinement of sample ZAA25. Each respective phase has been resolved with the hexameric contribution shown in green, the tetrameric contribution in orange, and the background and water in purple. R_{wp} = 26.72%. b) Resultant model of this refinement. Key: Zr – Grey, O – Red, C – Black. 165

Figure 78: Overlay of the PDFs of samples ZAA24C, ZAA24A, and ZAA24I, collected as part of the 18 month data collection. 176

Figure 79: Overlay of the PDFs of samples ZAA4C, ZAA4A, and ZAA4I, collected as part of the 18 month data collection. 176

Figure 80: Overlay of the PDFs of samples ZAA25C, ZAA25A, and ZAA25I, collected as part of the 18 month data collection. 177

Figure 81: Observed (black) and calculated (blue) PDF of the fixed-core iteration of the dual-phase refinement of sample ZAA24C. Each respective phase has been resolved with the tetrameric contribution shown in green, the hexameric contribution in orange, and the background and water in purple. R_{wp} = 37.13%. 179
Figure 82: Observed (black) and calculated (blue) PDF of the fixed-core iteration of the dual-phase refinement of sample ZAA24A. Each respective phase has been resolved with the tetrameric contribution shown in green, the hexameric contribution in orange, and the background and water in purple. R_{wp} = 40.55%. 179
Figure 83: Observed (black) and calculated (blue) PDF of the fixed-core iteration of the dual-phase refinement of sample ZAA24I. Each respective phase has been resolved with the tetrameric contribution shown in green, the hexameric contribution in orange, and the background and water in purple. R_{wp} = 37.37%. 180
Figure 84: Observed (black) and calculated (blue) PDF of the fixed-core iteration of the dual-phase refinement of sample ZAA4C. Each respective phase has been resolved with the tetrameric contribution shown in green, the hexameric contribution in orange, and the background and water in purple. R_{wp} = 36.90%. 183
Figure 85: Observed (black) and calculated (blue) PDF of the fixed-core iteration of the dual-phase refinement of sample ZAA4A. Each respective phase has been resolved with the tetrameric contribution shown in green, the hexameric contribution in orange, and the background and water in purple. R_{wp} = 46.09%. 183
Figure 86: Observed (black) and calculated (blue) PDF of the fixed-core iteration of the dual-phase refinement of sample ZAA4I. Each respective phase has been resolved with the tetrameric contribution shown in green, the hexameric contribution in orange, and the background and water in purple. R_{wp} = 39.89%. 184

Figure 87: Observed (black) and calculated (blue) PDF of the fixed-core iteration of the dual-phase refinement of sample ZAA25C. Each respective phase has been resolved with the tetrameric contribution shown in green, the hexameric contribution in orange, and the background and water in purple. R_{wp} = 30.14%. 187
Figure 88: Observed (black) and calculated (blue) PDF of the fixed-core iteration of the dual-phase refinement of sample ZAA25A. Each respective phase has been resolved with the tetrameric contribution shown in green, the hexameric contribution in orange, and the background and water in purple. R_{wp} = 29.31%. 187
Figure 89: Observed (black) and calculated (blue) PDF of the fixed-core iteration of the dual-phase refinement of sample ZAA25I. Each respective phase has been resolved with the tetrameric contribution shown in green, the hexameric contribution in orange, and the background and water in purple. R_{wp} = 30.79%. 188
Figure 90: a) Observed (black) and calculated (blue) PDF of the fixed-core iteration of the dual-phase refinement of sample ZAA29. Each respective phase has been resolved with the tetrameric contribution shown in green, the hexameric contribution in orange, and the background and water in purple. R_{wp} = 24.30% b) The model resulting from this refinement. Key: Zr – Grey, O – Red, C – Black. 195
Figure 91: Observed (black) and calculated (blue) PDF of the fixed-core iteration of the dual-phase refinement of sample ZAA30. Each respective phase has been resolved with the tetrameric contribution shown in green, the hexameric contribution in orange, and the background and water in purple. R_{wp} = 22.45% b) The model resulting from this refinement. Key: Zr – Grey, O – Red, C – Black. 195
Figure 92: Observed (black) and calculated (blue) PDF of the fixed-core iteration of the dual-phase refinement of sample ZAA24. Each respective phase has been resolved with the

tetrameric contribution shown in green, the hexameric contribution in orange, and the background and water in purple. R_{wp} = 26.72% b) The model resulting from this refinement. Key: Zr – Grey, O – Red, C – Black. 196

Figure 93: Observed (black) and calculated (blue) PDF of the fixed-core iteration of the dual-phase refinement of sample ZAA25. Each respective phase has been resolved with the tetrameric contribution shown in green, the hexameric contribution in orange, and the background and water in purple. R_{wp} = 22.91% b) The model resulting from this refinement. Key: Zr – Grey, O – Red, C – Black. 196

Figure 94: Percentage concentration of hexamer found in samples studied at Diamond Light Source (DLS) distributed by acetic acid : zirconium ratio when refined using the fixed-core model. 203

Figure 95: Percentage concentration of hexamer found in samples studied at National Synchrotron Light Source II (NSLS-II) distributed by acetic acid : zirconium ratio when refined using the fixed-core model. 203

Figure 96: Effect of ZrO_2 concentration on the percentage yield of umbite ($K_2ZrSi_3O_9 \cdot H_2O$) obtained. Samples of feedstock 3 are shown in figure A and both feedstocks 1 and 2 in figure B. 209

Figure 97: Effect of feedstock concentration on the percentage yield of umbite ($K_2ZrSi_3O_9 \cdot H_2O$) obtained. Plot includes values from all umbite samples synthesised. 210

Figure 98: Effect of storage temperature on the percentage yield of umbite ($K_2ZrSi_3O_9 \cdot H_2O$) obtained. Samples of feedstock 3 are shown in figure A and both feedstocks 1 and 2 in figure B. 211

Figure 99: Effect of acetic acid : zirconium ratio on the percentage yield of umbite ($K_2ZrSi_3O_9 \cdot H_2O$) obtained. Samples of feedstock 3 are shown in figure A and both feedstocks 1 and 2 in figure B. 211

Figure 100: Effect of sample age on the percentage yield of umbite ($K_2ZrSi_3O_9 \cdot H_2O$) obtained. Plot includes values from all umbite samples synthesised. 213

Figure 101: Observed (black), calculated (blue), and difference (grey) diffraction pattern of a sample of umbite synthesised from ZAA15 after 3 months of ageing.The resultant structure of the refined model is displayed (inset). viewed down the c-axis showing the octahedral Zr (Black Polyhedra) and tetrahedral Si (Yellow Polyhedra) of the framework. Within the framework are the counter cations K (Blue Spheres) and the oxygens of the waters of crystallisation (Black Spheres). The unit-cell boundaries are shown in blue dashed lines ...217

Figure 102: Observed (black) and calculated (blue) diffraction patterns from the crystallinity studies of the sample (sample ZAA21C after 22 months of ageing). The two phases of umbite (amophous in green and crystalline in purple) are displayed above. 223

Figure 103: Observed (black) and calculated (blue) diffraction patterns from the crystallinity studies of the sample (sample ZAA27I after 15 months of ageing). The two phases of umbite (amophous in green and crystalline in purple) are displayed above. 223

Figure 104: Effect of a) storage temperature, b) ZrO_2 concentration, and c) feedstock type on the percentage degree of crystallinity obtained. 224

Figure 105: Effect of sample age on the percentage degree of crystallinity obtained. 225

Figure 106: Effect of acetic acid : zirconium ratio on the percentage degree of crystallinity obtained. 226

Figure 107: SEM image of an umbite sample synthesised from ZAA6C after 15 months of ageing showing the characteristic particle morphology. 228

Figure 108: SEM image of an umbite sample synthesised from ZAA25I after 15 months of ageing showing a characteristic morphology which is covered in an amorphous rough surface that is poorly defined. 229

Figure 109: SEM image of an umbite sample synthesised from a) ZAA27I after 15 months of ageing b) ZAA1C after 22 months of ageing c) ZAA10C after 22 months of ageing and d) ZAA1A after 3 months of ageing. Figures a & b show poor surface morphology and c & d show characteristic morphology. 230

Figure 110: SEM image of umbite synthesised at a) 3 months, b) 7 months, c) 15 months, and d) 22 months from sample ZAA25. 231

Figure 111: SEM images of umbite synthesised from a) ZAA3C and b) ZAA3A synthesised after 15 months of ageing. 232

Figure 112: Isotherm resulting from the nitrogen gas adsorption of sample ZAA3A. The adsorption pathway is shown in black and the desorption pathway in blue. 234

Figure 113: Isotherm resulting from the nitrogen gas adsorption of sample ZAA21A. The adsorption pathway is shown in black and the desorption pathway in blue. 234

Figure 114: Isotherm resulting from the nitrogen gas adsorption of sample ZAA27I. The adsorption pathway is shown in black and the desorption pathway in blue. 235

Figure 115: Results of nitrogen gas adsorption studies of a range of samples showing surface area (red) and total pore volume (green) with the degree of crystallintity results. 235

Figure 116: SEM image of sample ZAA3C with the glass-like phase highlighted in red. 237

Table of Tables

Table 1: The crystal systems, their essential symmetries, and allowed centring options forming the 14 Bravais lattice types. note the primitive form of the rhombohedral unit-cell is traditionally denoted with the letter R [47, 57, 58]. 27

Table 2: X-ray energies, wavelengths, an appropriate Q_{max} values for common laboratory X-ray sources and the dedicated XPDF beamlines I15-1 and 28-ID-1 at Diamond Light Source (DLS) and National Synchrotron Light Source (NSLS-II) respectively [52, 69, 76]. 38

Table 3: Mass of reagents required for the synthesis of samples of umbite ($K_2ZrSi_3O_9 \cdot H_2O$) showing the difference in the amount of zirconium-acetate solution required based on the solution concentration.....50

Table 4: Space group and lattice parameters of the Clearfield model shown above [1]. 58

Table 5: Bond lengths of Zr-O bonds and the resultant oxidation state as derived through bond-valence calculations described by Brown and Altermatt for refinement method 1 [92]..66

Table 6: Bond lengths and angles of the Clearfield model and the model resulting of refinement 1 [1]. 67

Table 7: The resultant oxidation state as derived through bond-valence calculations described by Brown and Altermatt for refinement method 2 [92]. 77

Table 8: Bond lengths and angles of the Clearfield model and the model resulting from refinement 2 [1]. 78

Table 9: Bond lengths and angles of the Clearfield model and the model resulting of refinement 3 [1]. 84

Table 10: The resultant oxidation state as derived through bond-valence calculations described by Brown and Altermatt for refinement method 3 [92].....86

Table 11: Contact distances from EXAFS refinements of zirconium-acetate solutions compared to those obtained in literature by Hennig et al.[2]. 97

Table 12: Comparisons of the literature contact distances of the hexameric cluster and the peak maxima determined from preliminary XPDF. 101

Table 13: All zirconium-acetate samples synthesised for the ageing study and their variables. 105

Table 14: A list of all the zirconium-acetate samples and their phases after 12 months of storage at 45°C. Samples which increased in viscosity are highlighted in orange. 107

Table 15: Details of the zirconium-acetate samples studied in the first data collection in after 9 months ageing.....108

Table 16: Bond lengths and angles of the Hennig model and the models resulting from the first iteration of the single-phase refinement of samples ZAA1, ZAA4, and ZAA7 [2]. 115

Table 17: The resultant oxidation state as derived from the Zr-O bond lengths, through bond-valence calculations described by Brown and Altermatt for the first iteration of the single-phase refinement of samples ZAA1, ZAA4, and ZAA7 [92].....118

Table 18: R_{wp} values of the two single-phase refinements for samples ZAA1, ZAA4, and ZAA7. 122

Table 19: Bond lengths and angles of the Hennig model and the models resulting from the second iteration of the single-phase refinement of samples ZAA1, ZAA4, and ZAA7 [2]. 126

Table 20: The resultant oxidation state as derived through bond-valence calculations described by Brown and Altermatt for the second iteration of the single-phase refinement of samples ZAA1, ZAA4, and ZAA7 [92]. 127

Table 21: R_{wp} values resulting from the two single-phase refinements and the dual-phase refinement. 131

Table 22: Bond lengths and angles of the Hennig model and the hexameric models resulting from the first iteration of the dual-phase refinement of samples ZAA1, ZAA4, and ZAA7 [2].133

Table 23: The resultant oxidation state as derived through bond-valence calculations described by Brown and Altermatt for the first iteration of the dual-phase refinement of samples ZAA1, ZAA4, and ZAA7 [92]. 135

Table 24: Bond lengths and angles of the Clearfield model and the tetrameric models resulting from the first iteration of the dual-phase refinement of samples ZAA1, ZAA4, and ZAA7 [1].136

Table 25: The resultant oxidation state as derived through bond-valence calculations described by Brown and Altermatt for the tetrameric phase of the first iteration of the dual-phase refinement of samples ZAA1, ZAA4, and ZAA7 [92]. 138

Table 26: R_{wp} values arising from all the refinements of data from this period data collection. 141

Table 27: Bond lengths and angles of the Hennig model and the hexameric models resulting from the second iteration of the dual-phase refinement of samples ZAA1, ZAA4, and ZAA7 [2]. 145

Table 28: The resultant oxidation state as derived through bond-valence calculations described by Brown and Altermatt for the hexameric phase of the second iteration of the dual-phase refinement of samples ZAA1, ZAA4, and ZAA7 [92]. 147

Table 29: Bond lengths and angles of the Clearfield model and the tetrameric models resulting from the second iteration of the dual-phase refinement of samples ZAA1, ZAA4, and ZAA7 [1]. 149

Table 30: The resultant oxidation state as derived through bond-valence calculations described by Brown and Altermatt for the tetrameric phase of the second iteration of the dual-phase refinement of samples ZAA1, ZAA4, and ZAA7 [92]. 150

Table 31: Details of the samples studied in the second data collection commencing after 15 months of ageing. 152

Table 32: Bond lengths for the hexamer and angles of the Hennig model and the models resulting from the first iteration of the dual-phase refinements of samples ZAA1, ZAA4, ZAA7, ZAA24, and ZAA25 [2]. 158

Table 33: The resultant oxidation state as derived through bond-valence calculations described by Brown and Altermatt for the hexameric phase of the first iteration of the dual-phase refinement of samples ZAA1, ZAA4, ZAA7, ZAA24, and ZAA25 [92]. 160

Table 34: Bond lengths and angles of the Clearfield model and the tetrameric models resulting from the first iteration of the dual-phase refinement of samples ZAA1, ZAA4, ZAA7, ZAA24 and ZAA25 [1].....161

Table 35: The resultant oxidation state as derived through bond-valence calculations described by Brown and Altermatt for the tetrameric phase of the first iteration of the dual-phase refinement of samples ZAA1, ZAA4, ZAA7, ZAA24, and ZAA25 [92]. 162

Table 36: R_{wp} values arising from all the refinements of data from this period data collection. 166

Table 37: Bond lengths and angles of the Hennig model and the hexamer models resulting from the second iteration of the dual-phase refinements of samples ZAA1, ZAA4, ZAA7, ZAA24, and ZAA25 [2]. 167

Table 38: The resultant oxidation state as derived through bond-valence calculations described by Brown and Altermatt for the hexameric phase of the second iteration of the dual-phase refinement of samples ZAA1, ZAA4, ZAA7, ZAA24, and ZAA25 [92].....168

Table 39: Bond lengths and angles of the Clearfield model and the tetrameric models resulting from the second iteration of the dual-phase refinement of samples ZAA1, ZAA4, ZAA7, ZAA24 and ZAA25 [1].....170

Table 40: The resultant oxidation state as derived through bond-valence calculations described by Brown and Altermatt for the tetrameric phase of the second iteration of the dual-phase refinement of samples ZAA1, ZAA4, ZAA7, ZAA24, and ZAA25 [92]. 171

Table 41: A list of samples studied at NSLS-II as part of the 18 month data collection and the variables that describe them. 174

Table 42: Bond lengths and angles of the Hennig model and the hexamer models resulting from the fixed-core iteration of the dual-phase refinements of samples ZAA24C, ZAA24A,and ZAA24I [2].....182

Table 43: Bond lengths and angles of the Hennig model and the hexamer models resulting from the fixed-core iteration of the dual-phase refinements of samples ZAA4C, ZAA4A,and ZAA4I [2].....185

Table 44: Bond lengths and angles of the Hennig model and the hexamer models resulting from the fixed-core iteration of the dual-phase refinements of samples ZAA25C, ZAA25A,and ZAA25I [2].....190

Table 45: The resultant oxidation state, as derived through bond-valence calculations described by Brown and Altermatt, for the hexameric phase of the fixed-core iteration of the dual-phase refinement of samples ZAA24C-I, ZAA4C-I, and ZAA25C-I [92]. 191

Table 46: The resultant oxidation state, as derived through bond-valence calculations described by Brown and Altermatt, for the tetrameric phase of the fixed-core iteration of the dual-phase refinement of samples ZAA24C-I, ZAA4C-I, and ZAA25C-I [92]. 191

Table 47: Details of the samples studied in the final data collection. *Sample ZAA30 was made of a feedstock similar to 1 but not wholly identical. 194

Table 48: Bond lengths and angles of the Hennig model and the hexamer models resulting from the fixed-core iteration of the dual-phase refinements of samples ZAA29, ZAA30, ZAA24, and ZAA25 [2].....198

Table 49: The resultant oxidation state, as derived through bond-valence calculations described by Brown and Altermatt, for the hexameric phase of the fixed-core iteration of the dual-phase refinement of samples ZAA29, ZAA30, ZAA24, and ZAA25 [92].....199

Table 50: The resultant oxidation state, as derived through bond-valence calculations described by Brown and Altermatt, for the tetrameric phase of the fixed-core iteration of the dual-phase refinement of samples ZAA29, ZAA30, ZAA24, and ZAA25 [92].....200

Table 51: Description of the ageing intervals at which samples were synthesised. 207

Table 52: Table of atomic coordinates, thermal parameters, multiplicity and fractional occupancy arising from the Rietveld refinement of the umbite synthesised from the zirconium-acetate sample ZAA15 after 3 months of ageing. 216

Table 53: Selected crystallographic data and structure refinement parameters of the umbite synthesised from the zirconium-acetate sample ZAA15 after 3 months of ageing. 216

Table 54: Bond lengths from the refined model of umbite synthesised from zirconium-acetate sample ZAA15. 218

Table 55: Minimum and maximum lattice parameters and the range between them as determined from the Rietveld refinement of 190 umbite samples. The reference value is obtained from a Rietveld refinement of a sample of umbite synthesised from $ZrCl_4$. The literature values are according to Poojary et al. [46]. 219

Table 56: Degree of crystallinity, surface area,and total pore volume for a selection of samples from the 15 month synthesis round. Sample names end with the temperature they were stored at (A=ambient, C=chilled, I=incubated). 233

Table of Equations

Equation 1: A single Laue equation. 24

Equation 2: The full set of Laue equations for a 3-Dimensional structure. 25

Equation 3: Bragg's Law [55]. 25

Equation 4: The process of a least-squares refinement. The difference between the calculated and observed intensity is minimised [59] 28

Equation 5:The equation used for the determination of calculated intensity, y, at any point, i. 28

Equation 6: Equation for R_{wp}, where w_m is the weighting given to data point m, $Y_{(OBS, M)}$ and $Y_{(CALC, M)}$ are the observed and calculated data respectively at data point m [60] 30

Equation 7: Equation for calculating R_{exp} where the weighting of each data point, m is given by w_m. $Y_{OBS, M}$ is the observed data at point m, M is the number of data points, P the total number of parameters [60]. 30

Equation 8: Equation of the relationship of goodness of fit to R_{wp} and R_{exp} [60]. 30

Equation 9: The series of equations which are used to represent the calculated intensity of a step wise diffraction pattern at any given step. 31

Equation 10: Scattering vector value (Q). 36

Equation 11: S(Q) defined with respect to I(Q). 37

Equation 12: D(r) defined in terms of ρ(r). 37

Equation 13: Attenuation of X-ray flux. 46

Equation 14: Requirement for constructive interference in XAS experiment. 48

Equation 15: The EXAFS equation [79]. 49

Equation 16: Equation of the minimum lattice parameters of a model used for PDF refinement to avoid intercluster interactions. 60
Equation 17: Equation for determining oxidation state of the Zr atom for Zr-O bonds as determined by Brown and Altermatt [92] where r is the bond length and s is the calculated oxidation state of the Zr atom. 65
Equation 18: Equation of the formula used to determine the relative molar concentration of the two phases.....201
Equation 19: The equilibrium between the hexameric and tetrameric phase. 245

1.0 Introduction

1.1 Background

The shifting climate and a drive for a more sustainable approach to chemistry are ever prevalent in the modern age. One of the key aims of modern chemical science is the reduction of waste, not only for economic reasons, but for ever more pressing environmental concerns. Knowledge of the "shelf stability" of a material is crucial. Underestimation results in high volumes of material being discarded at great cost to users but also with significant impact on the environment. Overestimations, however, may lead to the production of inferior or completely unsuitable end materials once again creating an increase in waste. For these reasons it is critical that the modern chemical industry is aware of the intermediate materials they use and produce and are fully informed of the effects of age on these precursors. It is also critical for solutions manufacturers to understand the effect of storage conditions on the end user of their products. These effects may manifest themselves in a variety of ways, and it is critical that the molecular structure of these materials is known throughout their lifetime of use.

For this reason, this work endeavours to qualitatively and quantitatively assess the structures present in these intermediate materials, namely zirconium-acetate solution. This information ultimately impacts the end user of the material and so it is crucial that this is known and well-studied. This work attempts to use X-ray pair distribution function (XPDF) analysis to achieve this task determining the structure of these aqueous materials through a prolonged and comprehensive ageing study.

1.2 Aims of Project

The work presented here has four principal aims:

- Through the use of EXAFS, determine if the hexameric solution species, $Zr_6(O)_4(OH)_4(CH_3COO)_{12}$, proposed by Hennig *et al.* [2] to be present in laboratory synthesised zirconium-acetate solutions, is present in commercially available zirconium-acetate solutions.
- Develop a method for the study of zirconium-acetate solutions with XPDF using aqueous zirconium-oxychloride ($ZrOCl_2 \cdot 8H_2O$) and the proposed tetrameric species $[Zr_4(OH)_8(OH_2)_{16}]^{8+}$ as a test case.
- Employ the method developed above to a long-term ageing study of commercially available zirconium-acetate solutions covering the effect of storage temperature, relative ZrO_2 concentration, and acetic acid : zirconium ratio, to determine if any structural changes are undergone with time.
- Synthesise the model compound, umbite, periodically through the ageing study using the solutions from the ageing study to determine the impact of the ageing process on the end users of these materials.

1.3 Layout of Thesis

This work is presented as 8 principal chapters. Chapter 1 will outline the background to zirconium materials including their current uses and previously performed structural studies. Chapter 2 introduces the concept of scattering as a structural analysis technique. This chapter outlines the currently held knowledge of X-ray diffraction (XRD) and X-ray pair distribution

function analysis (XPDF) including the generation and sources of X-rays. Chapter 3 looks at the methods of analysis of liquid samples employed by this research project and assesses the methods for analysing solid samples. Chapters 4-7 are chapters which contain results and subsequent analysis and discussion. Chapter 4 covers the method development phase of the XPDF analysis applied to zirconium-oxychloride solutions. Chapter 5 discusses the work performed by Hennig *et al*. on laboratory synthesised zirconium-acetate solutions and aims to reproduce these results with commercially available samples [2]. Chapter 6 contains the XPDF results of the 2+ year ageing study performed on commercially available samples of zirconium-acetate solution. This chapter looks at attempts to model these compounds throughout their ageing process. In an effort to determine the effect of any identified changes in the zirconium-acetate solutions on end users who employ these solutions as precursor materials in their synthetic pathways, Chapter 7 discusses the solid-phase analysis of a model compound, the zircon-silicate, umbite, synthesised at periodic intervals throughout the ageing study. Finally, Chapter 8 brings together the summaries of all the results of this work and aims to draw conclusions from the data and briefly discusses potential future work.

1.4 Applications of Zirconium Materials

Numerous commercially available zirconium sources exist, and are available as both solids and solutions, and these are often used in a wide range of industries to produce a diverse range of products and materials [3-6].

From aerospace to automotive catalysis, the use of zirconium-oxide ceramics is unsurpassed. Its electrical, wear, and heat resistant qualities make it an ideal material for these applications [7-9]. In automotive catalysis it is employed as a catalytic support and, when doped, an oxygen sensor and an oxygen buffer, allowing for optimal conditions for pollutant control and ensuring peak catalytic efficiency [10]. More recently, attempts have been made to apply zirconium oxide materials to the sequestration of CO_2 and H_2 [11]. Their strong resistance, coupled with the ability to modify properties such as surface area stability, porosity, surface acidity/basicity, and crystallinity mean that solid zirconium oxides and hydroxides are vital in industrial catalysis [12-14]. Zirconium-containing Metal Organic Frameworks (MOFs) have shown great potential in gas adsorption with a focus on storage, separation, and purification [15].

It is not just solid zirconium-based materials that have their industrial applications. Zirconium-containing solutions are vital in many commercial processes. An example of this is the use of zirconium lactate as a cross linker in the oil and gas industry during the extraction of unconventional hydrocarbons [16]. Zirconium-oxychloride is often used to produce zirconium-containing materials, to precipitate acid dyes, and to encourage the binding of inks and dyes. It also has an application in the preparation of body deodorants and antiperspirants.

Zirconium-acetate solution has numerous industrial applications. It is often used as a crosslinker in the application of surface coatings, including water repellent and flame-retardant coatings, to paper and textile products [17-19]. It has uses as a binding agent in

ink and dye production, and catalytic applications where it catalyses the curing of silicone resins in water repellent treatments. Recent work has shown its potential as an additive to oil wells as a gelling agent to decrease excessive water production encountered during drilling [20]. Zirconium-acetate is also used during the corrosion inhibiting pre-treatment of some metals. One of the reasons zirconium-acetate is used in industrial applications is that it offers a concentrated source of aqueous zirconium ions without containing any trace of chlorine. This makes it ideal for industrial-scale syntheses where the evolution of toxic chlorine containing pollutants or salt formation is to be avoided. In addition, it is widely used as a precursor to produce many zirconium-containing solids, including, but not limited to, ZrO_2 nanoparticles and ceramics which are extremely important as catalysts and sorbents in industry [21-24].

It is commonly agreed that the structure of the species observed in a precursor material will have driving effects on the nature, structure, and chemical properties of the resultant product of any sol/gel synthesis subsequently employed. It has been theorised, that changes to temperature, pH, and concentrations of the solutions will play a substantial role in the structure of the species found in these solutions and thus the product of any synthetic methods that employ them. Berry *et al.* [25] found in 1999 that the pH of the zirconium-acetate precursor used in the production of zirconia (ZrO_2) influenced the crystallinity of the product formed with lower pH values offering a more crystalline monoclinic zirconia.

1.5 Previous Structural Studies

1.5.1 Zirconium-oxychloride

The study of elements in their aqueous states is not new and has been the interest of chemists for years [26]. Evidence for the hydrolysis of zirconium into a complex ion in aqueous solution has been postulated since 1956. Clearfield and Vaughn [1] grew single-crystal samples from dried zirconium-oxychloride ($ZrOCl_2 \cdot 8H_2O$) solutions and subsequently resolved their structure. They proposed a tetranuclear species, $[Zr_4(OH)_8(OH_2)_{16}]^{8+}$ as a result of single-crystal X-ray diffraction studies. This species is a tetranuclear system with a square Zr(IV) core held together by 8 hydroxyl bridges. Each zirconium atom also bonds to 4 terminal water groups leading to 8-coordinate zirconium positions. The position of the oxygen atoms around the zirconium atoms forms a square antiprism, with the opposite side of each face being offset by 45°. The structure proposed by Clearfield and Vaughn [1] is shown below in Figure 1:

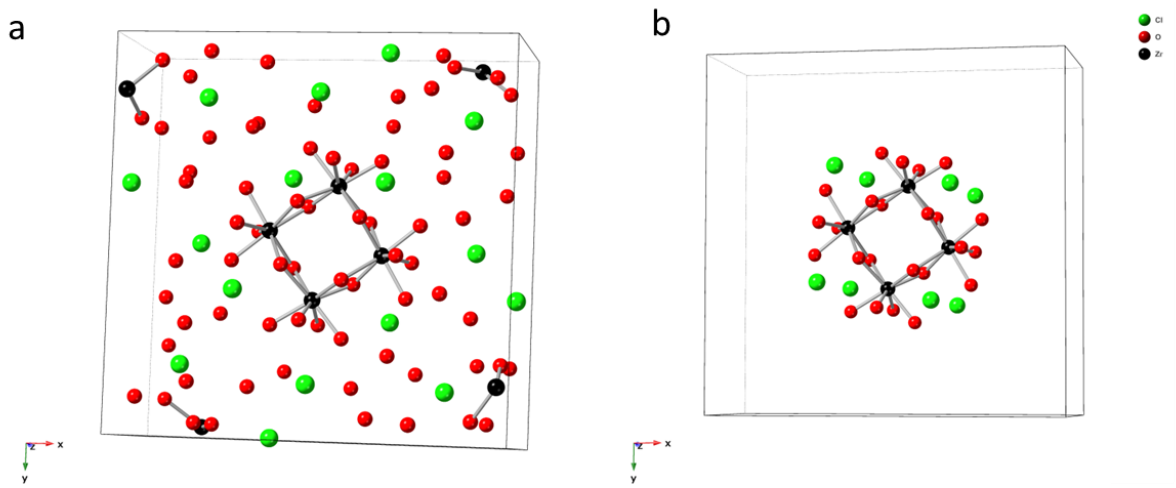

Figure 1: a)The structure of solid zirconium-oxychloride ($ZrOCl_2 \cdot 8H_2O$) viewed off centre from the c-axis, as proposed by Clearfield and Vaughn [1]. b) The isolated tetrameric unit and 8 nearest neighbouring Cl positions. Hydrogen positions have been omitted for clarity. Key: Zr – Black, O – Red, Cl – Lime Green.

Clearfield and Vaughn [1] acknowledge the presence of the chlorine atoms in close proximity to the tetrameric species but explicitly state "There are no zirconium-halogen bonds in this structure". The distances between the chloride positions and the tetrameric structure are shown below in Figure 2. It can be seen that for all the values shown below the distances between atomic pairs is larger than common covalent bonding length.

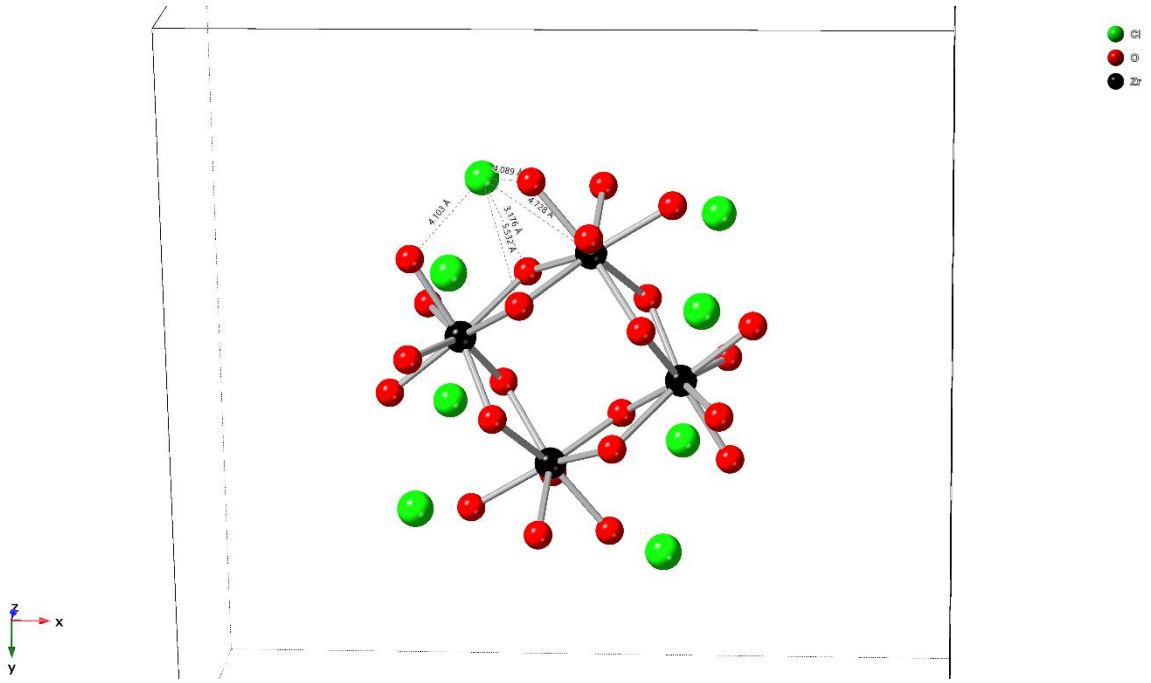

Figure 2: Atomic distances between the tetrameric cluster ($[Zr_4(OH)_8(OH_2)_{16}]^{8+}$) and the neighbouring chlorine positions. Key: Zr – Black, O – Red, Cl – Lime Green.

It was commonly agreed that the species present when these samples are in the aqueous phase is the core tetranuclear cluster and that the water of hydration molecules and the charge balancing chlorine atoms are not bonded to this cluster. The traditional Bragg scattering, which was available when the structure of $ZrOCl_2{\cdot}8H_2O$ was resolved, relied on the presence of long-range order in a solid crystalline material and so the resolution of the aqueous structure was not possible.

Through the use of X-ray scattering, Muha and Vaughan [27] confirmed the existence of a tetrameric species $[Zr_4(OH)_8(OH_2)_{16}]^{8+}$ present in zirconium-oxychloride in the solution phase. In 1968, Mak [28], through single-crystal X-ray diffraction data, suggested that the zirconium positions in the tetrameric cluster $[Zr_4(OH)_8(OH_2)_{16}]^{8+}$ did not adopt the D_{4d} square antiprismatic geometry suggested by Clearfield and supported by Muha and Vaughan, but instead a D_{2d} dodecahedron. This was later supported by Åberg [29] in 1977 through the use of X-ray scattering in the aqueous phase. A polymeric structure was proposed by Singhal *et al.*[30]

at high pH values ($[H^+]$ < 0.05 M) through measuring the radii of gyration with small angle scattering. The structure proposed consisted of several tetrameric units oligomerised to form a longer chain species.

Computational studies performed by Rao *et al.* [31] in 2007 concur with the tetrameric species $[Zr_4(OH)_8(OH_2)_{16}]^{8+}$ which they determined to be a stable phase for these solution species. Due to relaxation in the structure however, they could not conclude whether the zirconium positions formed a D_{2d} dodecahedron or D_{4d} square antiprism. They did however confirm that the structure they had calculated agreed with the principal peaks of EXAFS data collected.

Further Computational studies performed by Messner *et al.* [32] confirm the stability of the tetrameric $[Zr_4(OH)_8(OH_2)_{16}]^{8+}$ unit but did not aim resolve its physical geometry. Instead, their simulations looked at the impact of temperature on the system and proposed that the tetrameric system is stable up to 600 K at which point it undergoes further hydrolysis. Their work confirmed the D_{4d} square antiprismatic geometry.

In 2013, Hu *et al.* [33] using high-energy X-ray scattering (HEXS) and the subsequently obtained PDFs, confirmed the presence of the tetrameric species, $[Zr_4(OH)_8(OH_2)_{16}]^{8+}$, when $ZrOCl_2$ was added to perchloric acid through peak assignment to the model proposed by Clearfield and Vaughan [1].

The work of Sommer *et al.* in 2019 [34] showed how in differing solvent systems the tetrameric species $[Zr_4(OH)_8(OH_2)_{16}]^{8+}$, can be structurally altered. Their work found evidence to suggest oligomer chains of tetrameric units in water, DMF and to a lesser, extent in methanol. Their work also showed how the addition of peroxide to solutions of zirconium oxyperchlorate can yield a variety of different structures including $[Zr_{25}O_{10}(OH)_{50}(O_2)_5(H_2O)_{40}]^{20+}$ and

$[Zr_4(OH)_4(\mu\text{-}O_2)_2(\mu_4\text{-}O)(H_2O)_{12}]^{6+}$ with the former being the largest zirconium cluster species reported that remains soluble in organic solvent systems.

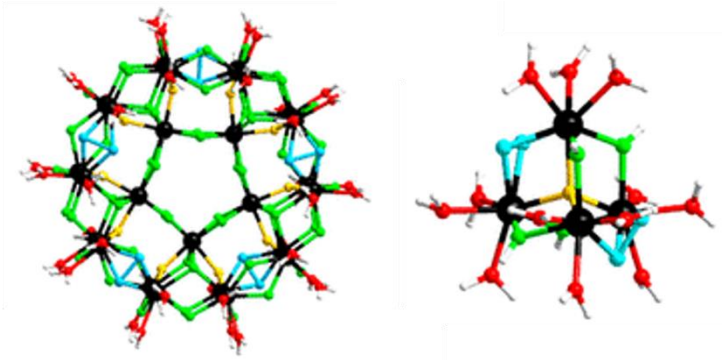

Figure 3: Structure of the $[Zr_{25}O_{10}(OH)_{50}(O_2)_5(H_2O)_{40}]^{20+}$ and $[Zr_4(OH)_4(\mu\text{-}O_2)_2(\mu_4\text{-}O)(H_2O)_{12}]^{6+}$ systems discovered by Sommer et al. [34] Key: Zr – Black, O – Red, Lime Green, Light Blue, and Yellow.

Recently, in 2019 and after the start of this research project, Xu *et al.* [35] reported the presence of the tetrameric species proposed by Clearfield and Vaughan in the aqueous phase through the use of X-ray pair distribution function (XPDF) analysis, but this was done purely through qualitative peak assignment and refining a scale factor. At the time of producing this thesis no attempts to quantitatively refine the structure present in the solution phase have been presented.

In 2021, Stern *et al.* [36] using density functional theory, concluded that the tetrameric species would be the most stable and even though a hexameric species was theoretically possible, it is unlikely.

Most recently, and published during the post experimentation phase of this thesis, Klove *et al.* [37] studied samples of zirconium-oxychloride solutions using XPDF methods. Their work suggests a relaxed tetrameric structure with the same overall formula $[Zr_4(OH)_8(OH_2)_{16}]^{8+}$. They also suggest the strong coordination to the complex molecular ion of the chloride counter ions. These findings corroborate the results presented herein (Chapter 4.0).

1.5.2 Zirconium-acetate

The structures of other zirconium-containing complex ions have been studied in the solution phase [38]. Zirconium-acetate [$Zr(CH_3COO)_4$] is the acetic acid salt of zirconium (IV) and is most commonly available as an aqueous solution. It is noted here that all the work described in the literature sources discussed below, employed the use of zirconium-oxychloride as a zirconium source to which acetic acid was added. This differs from commercially available zirconium-acetate materials which do not start with zirconium-oxychloride as a starting species and so any species present in the work discussed below cannot be assumed to be present in commercial solutions.

Early attempts to resolve the structure produced conflicting results with initial theories suggesting a monomeric solution species[39, 40] . Paul *et al.* [41] postulated a polymeric species with a stoichiometric ratio of 4 : 1 acetic acid to zirconium. Using infrared spectroscopy, Paul *et al.* proved the presence of bridging or bidentate groups, and expected zirconium to occupy a coordination number ≤ 8. Once again, however, this work was performed on solid samples, extracted, and dried under vacuum. The zirconium-acetate samples studied were also synthesised through the addition of acetic acid to zirconium-oxychloride.

An in depth aqueous study was performed using a combination of infrared and Raman spectroscopy by Tosan *et al.* in 1994 [42]. This study analysed the materials in their aqueous environment for up to 1 month of ageing from the first point of synthesis. Acetic acid was added to samples of zirconium-oxychloride and the resultant solution analysed periodically. Tosan *et al.* [42] concluded that they believed that upon this addition the final product, after 1 month of ageing, was an adapted version of Clearfield's Tetramer, with the 4 terminal oxygen positions replaced by a single chelating bidentate carboxylate group, shown in Figure 4. This

would ultimately alter the charge on the cluster species through the replacement of 16 O^{-} groups with 4 CH_3COO^{-} groups.

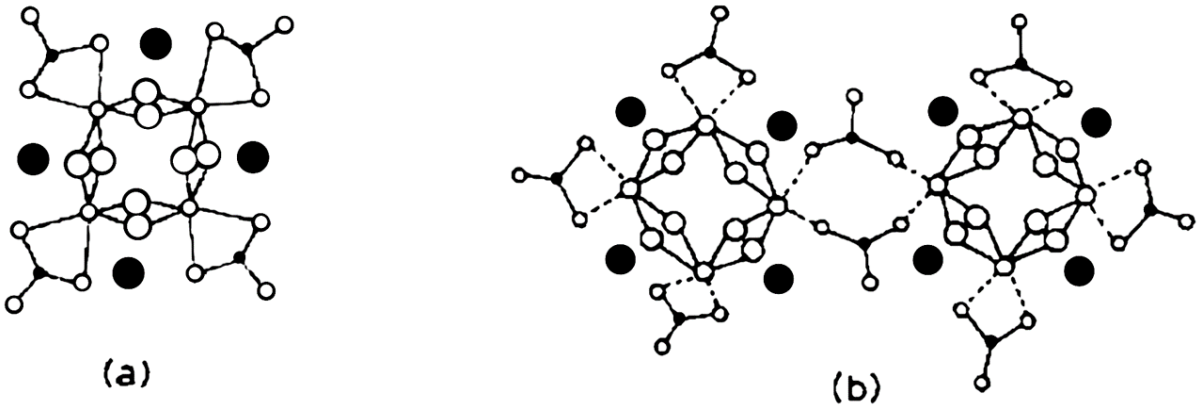

Figure 4: The a) single and b) linked tetranuclear structure of zirconium-acetate as proposed by Tosan et al.[42] showing the core structure of $ZrOCl_2 \cdot 8H_2O$ as proposed by Clearfield and Vaughn [1] but with carboxylate groups in the terminal positions. The corner positions represent Zr atoms bridged by pairs of oxygen positions. The carboxylate groups are shown bonded with dashed lines (b). Chlorine is shown in black.

This substitution of 4 terminal oxygen positions with a single chelating carboxylate group resulted in a zirconium coordination number of 6 and a Zr : acetic acid : Cl ratio of 1:1:1. They argued that the acetate groups adopted only chelating bidentate coordination in the tetrameric species but did not exclusively rule out the presence of bridging ligands connecting the tetrameric species stating "the presence of bridging bidentate carboxylates linked to zirconium ions of different tetrameric entities remains possible" [42]. Interestingly, Tosan's [42] work also postulated that the structural rearrangement that led to this structure was not instantaneous, instead believing that an optimal time of over a month was required to achieve this structural evolution.

Bremholm *et al*. [43] recently applied Small Angle X-ray Scattering (SAXS) to the study of these aqueous zirconium-acetate solutions. They deduced the presence of a polymeric species that formed rod-like structures over 100 Å long with a radius of 4.9 ± 0.9 Å within 24 hours of sample synthesis. This level of extended polymerisation of the structure, they found, was

encouraged by higher concentration solutions with heated samples resulting in oligomer chains of over 400 Å in 20 minutes. It was noted, however, that polymerisation still occurred even at ambient temperatures but at a slower rate. Bremholm [43] did not specify any details on the local structure of these extended chains, instead recommending further investigation.

The most recent work studying the structure of aqueous zirconium-acetate solutions, was performed by Hennig *et al.* in 2017 [2]. This work was done using Zr K-edge X-ray Absorption Spectroscopy (XAS) on samples in the solution phase. The samples used were, once again, synthesised from the addition of varying quantities of acetic acid to 1M solutions of zirconium-oxychloride. The XAS results determined that prior to the addition of acetic acid, the sample was dominated by the presence of the tetranucleic structure, proposed by Clearfield and Vaughn [1]. This manifested as a large Zr-O coordination peak at 2.169(2) Å and two Zr-Zr contact distances, Zr-Zr_S and Zr-Zr_L at 3.620(3) Å and 5.14(1) Å respectively, as shown in Figure 5. The shorter of these two distances was believed to be the two zirconium atoms that make up the neighbouring points in the tetrameric square, and the longer to be the opposite zirconium atom, across the square. As the concentration of acetic acid was increased, the primary Zr-O peak decreased in intensity and splitting was observed, as the Zr-Zr_S increased in intensity. The Zr-Zr_L peak shifted slightly to a lower *r* region. These changes were ascribed to the creation of a new, hexameric structure with a formula of $Zr_6(O)_4(OH)_4(CH_3COO)_{12}$. This structure and the XAS results obtained by Hennig *et al.* [2] are shown in Figure 5.

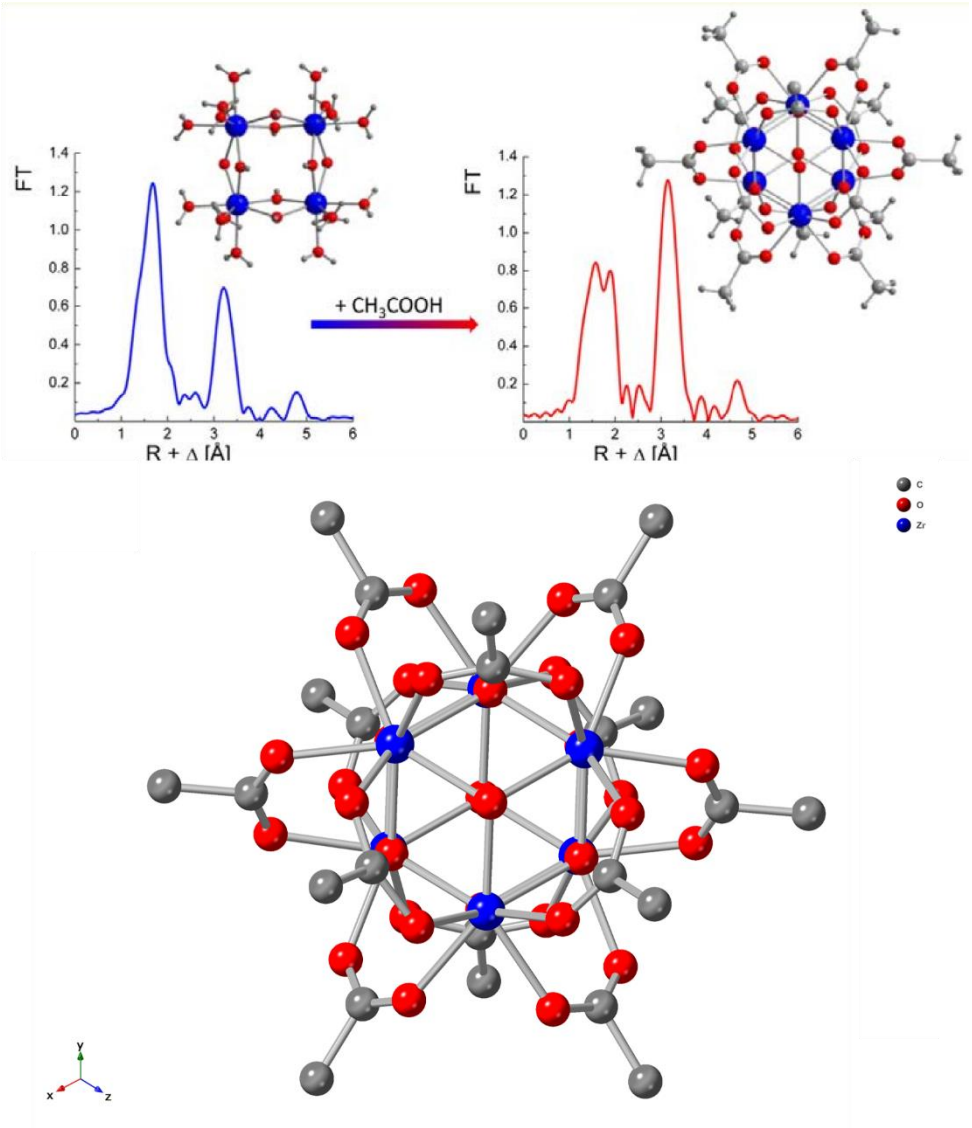

Figure 5: Fourier transformed XAS data of $[Zr_4(OH)_8(OH_2)_{16}]^{8+}$ (left) and $Zr_6(O)_4(OH)_4(CH_3COO)_{12}$ (right). (Bottom) the hexanuclear cluster $Zr_6(O)_4(OH)_4(CH_3COO)_{12}$. Zr-Blue, O-Red, C-Grey, H-Grey [2].

The hexamer proposed has each zirconium atom with a coordination number of 8, with 4 bridging oxo or hydroxo species and 4 bidentate bridging acetate groups. Overall, the structure displays a Zr : Acetate ratio of 1:2 (6:12). The chlorine atoms, present in the samples studied, due to the starting material being zirconium-oxychloride, were not incorporated into the models proposed by Hennig *et al.* [2]

1.5.3 Other Zirconium Solutions

This hexameric model has since been seen in other structural studies of zirconium-containing compounds that are not zirconium-acetate. The MOF UiO-66 displays the core of the hexameric structure as one of its building units [3] and in 2008 Pan *et al.* [44] determined zirconium glycine adopts a similar hexameric structure, through the use of single-crystal X-ray diffraction and infrared spectroscopy. Recently, in 2021, Stern *et al.* [36] proposed that, through density functional theory, that whilst the tetrameric phase seen for zirconium-oxychloride is more stable, an adapted version of the hexameric core with terminal oxygen positions $Zr_6(O)_4(OH)_4(OH_2)_{24}$ is theoretically possible.

After the completion of the work presented in this thesis Pascual-Colino *et al.* [45] studied the initial formation of metal carboxylate clusters in ethanol/water solution, through the use of Fourier transform infrared spectroscopy (FTIR), solid state nuclear magnetic resonance (SS-NMR) and both single crystal and powder X-ray diffraction. Their findings concluded that after the addition of benzoic acid to solutions of zirconium tetrachloride ($ZrCl_4$) that the initial cluster species was actually a pentameric species $[Zr_5O_2(OH)_6(OOCR)_4(solv)_x]^{6+}$ and that ligand-solvent replacement was common. This was seen to evolve into the hexameric species $[Zr_6(O)_4(OH)_4(OOCR)_8(solv)_y]^{4+}$.

1.6 The Model Compound – Umbite ($K_2ZrSi_3O_9 \cdot H_2O$)

To study the impact of any structural changes within the zirconium-acetate solutions on their use as a synthesis precursor, a model compound is needed. This material was synthesised periodically throughout the ageing study and was subsequently analysed through powder X-ray diffraction (PXRD), scanning electron microscopy (SEM) and nitrogen gas adsorption. The material used in this study as a model compound is umbite. Umbite is a naturally occurring zirconosilicate found in northern Russia. It is named after Lake Umbozero, a large lake in the Kola peninsula where umbite was first discovered. It has the chemical formula $K_2ZrSi_3O_9 \cdot H_2O$. Exhibiting the space group $P2_12_12_1$ and an orthorhombic unit-cell, it has lattice parameters of a = 10.2977(2) Å, b = 13.3207(3) Å and c = 7.1956(1) Å [46]. Like many traditional zeolites and zeotypes, umbite has a synthetic analogue that is produced using hydrothermal methods [46]. Each asymmetric unit consists of two cationic positions (K^+), a single Zr atom, a water molecule, and a linear chain trisilicate group. The silicate groups are linked together by octahedrally coordinated Zr atoms. The channels are created by the connection of the trisilicate groups to these Zr atoms to create a 3-dimensional pore system that can be seen in Figure 6.

Umbite was selected for this study due to its robust nature and consistent synthesis. The synthesis of umbite persistently yields high yields ca. 80% with a single-phase and no major impurities. This therefore will mean any variations within the quality of the sample produced can be directly linked to the zirconium-acetate solution as the synthetic pathway rarely shows any variations.

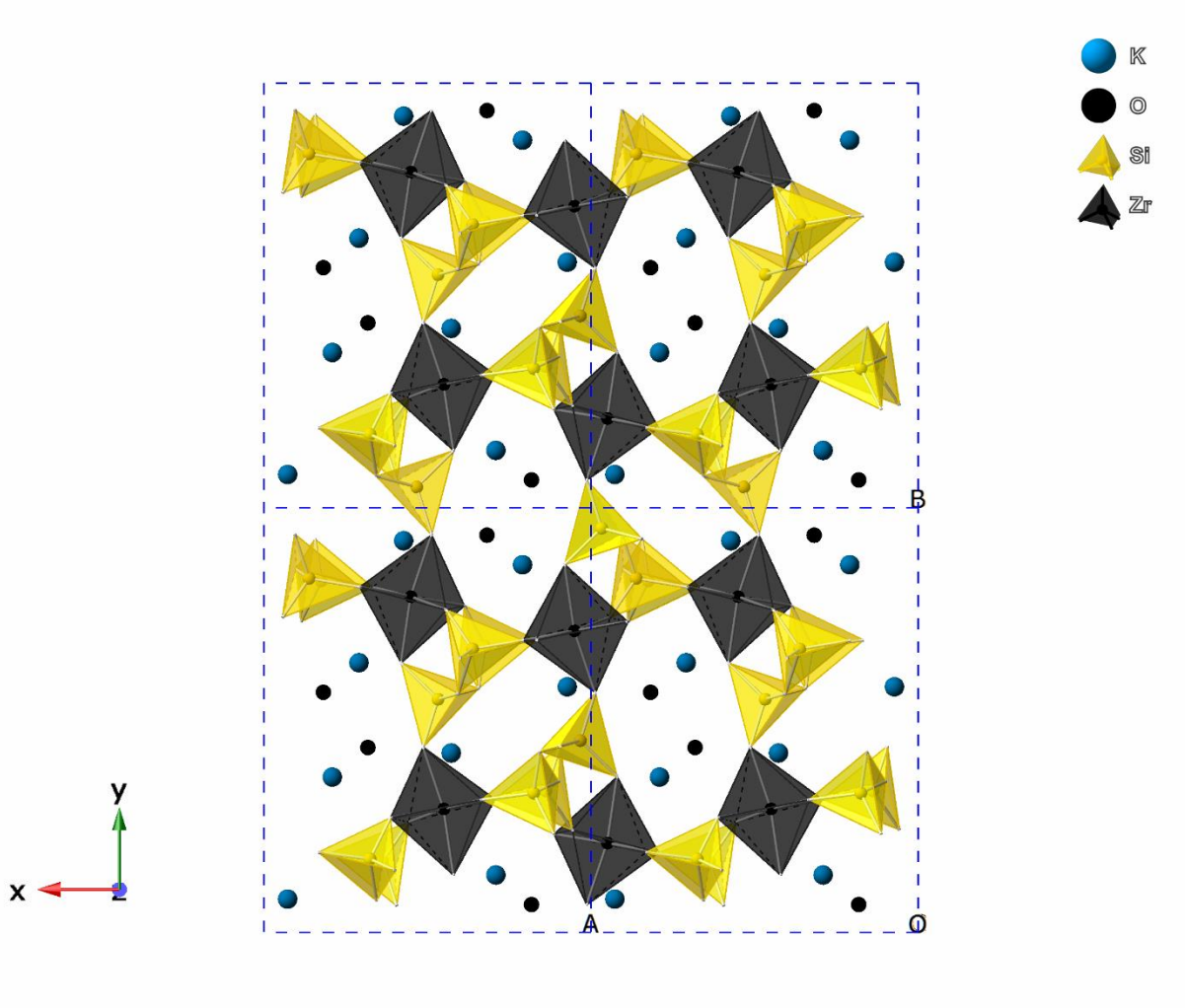

Figure 6: Crystal structure of Umbite ($K_2ZrSi_3O_9 \cdot H_2O$) viewed down the c-axis showing the octahedral Zr (Black Polyhedra) and tetrahedral Si (Yellow Polyhedra) of the framework. Within the framework are the counter cations K (Blue Spheres) and the oxygens of the waters of crystallisation (Black Spheres). The unit-cell boundaries are shown in blue dashed lines [46].

2.0 Scattering Techniques

There are two principal ways in which X-rays can be used to analyse matter: absorption and subsequent spectroscopic methods, or, more widely used, scattering and diffraction. Scattering techniques are primarily composed of diffraction: the study of the Bragg peaks caused by constructive interference, and total scattering: a technique which assesses both the Bragg peaks and the diffuse scatter which occurs. Both scattering techniques were applied to this research project and as such will both be discussed in this chapter.

2.1 Generation of X-rays

With wavelengths ranging from ≈ 25 Å to 0.25 Å and the corresponding energy ranges of 0.5 keV to 500 keV, X-rays form a part of the electromagnetic spectrum and are essential in modern-day structural analysis and crystallography in particular [47].

To enable the process of the analysis of matter with X-rays it is obviously necessary to have the ability to produce characteristic X-rays of a known wavelength: an X-ray source. The two principal methods for the production of X-rays: laboratory sources and synchrotron sources, will be discussed herein.

2.1.1 Laboratory X-ray Sources

Traditionally, in the laboratory, X-rays are generated through the bombardment of a metal source, usually copper but other metals such as molybdenum and silver are often used, with a beam of high-energy electrons accelerated through 30 kV. The conversion rate of electrons from the electron beam to X-rays is extremely small; approximately 1% of the electron beam is converted into characteristic X-rays with the rest being lost as heat or Bremsstrahlung radiation.

During the bombardment, two forms of radiation are formed; a broad spectrum of "white radiation" or Bremsstrahlung radiation, and several fixed monochromatic wavelengths characteristic of the metal source used, as shown in Figure 7. Diffraction experiments concern themselves largely with the latter monochromatic wavelengths and often aim to limit or remove the broader Bremsstrahlung contribution.

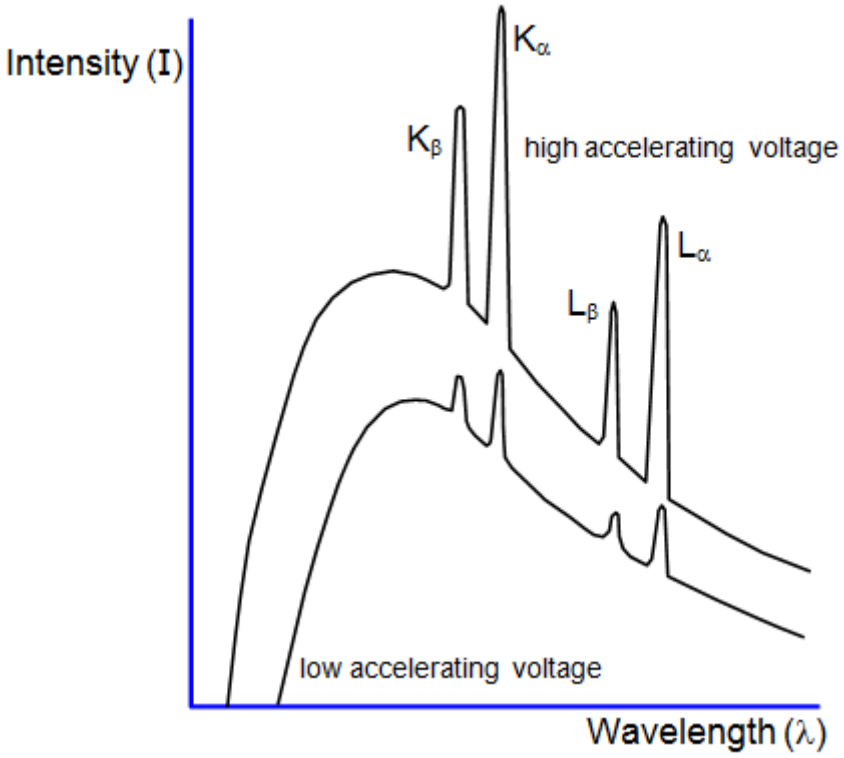

Figure 7: An X-ray emission profile showing the Bremsstrahlung continuum and two monochromatic characteristic X-ray peaks [48].

The monochromatic wavelengths are formed by the interaction of the electron beam with the inner atomic orbitals of the metal target. The incident electrons ionise core 1s K shell electrons on the metal target creating a vacancy. The subsequent dropping of an electron from a higher energy level to fill this vacancy results in an energy emission in the form of X-rays with characteristic wavelengths. The most common orbital transition for copper targets is from a 2p L shell to the 1s K shell. This process produces X-rays of with a

characteristic wavelength of 1.5418 Å and is known as a Kα transition. This is the most common of the transitions that can occur, with the second most common being the Kβ transition of wavelength 1.3922 Å [49]. The Kβ transition occurs when the electron that relaxes to fill the vacancy created in the core originates from the 3p orbital of the M shell. In diffraction experiments this is usually filtered out before the diffracted X-rays reach the detector. The Kα transition, whilst often being described as having a wavelength of 1.5418 Å, comprises of a doublet of two unique wavelengths: $K\alpha_1$ at 1.54051 and $K\alpha_2$ at 1.54433 Å. This is caused by the presence of two spin states for 2p electrons which, in turn, each result in slightly different energy emissions on their relaxation [47]. It is possible to isolate the $K\alpha_1$ - radiation through the use of monochromators and this subsequently has a significant impact on the quality of the diffraction pattern acquired. Often, when no monochromator is available diffraction experiments consider the average wavelength of 1.5418 Å.

Other emissions are possible if the core electron removed during the initial interaction between the electron beam and the target is not of the K shell. Ionisation of L and M electrons can be observed but are not as favoured and their resultant transitions and emissions are rarely used as a source X-ray.

2.1.2 Synchrotron Sources

The other principal source of X-rays for use in the analysis of materials, is synchrotron radiation. These synchrotron facilities allow experimenters to access narrow, parallel beams of highly polarised intense X-ray radiation. These parameters are generally grouped and can be described through a single value, brilliance [50].

The existence of synchrotron radiation was first confirmed by Elder *et al.* in 1947 [51]. Synchrotrons have significantly increased in quality in this time: the one used by Elder had a

storage ring energy of 30 MeV and a circumference of 1.8 m compared to Diamond Light Source which has a storage ring energy of 3.0 GeV and a ring circumference of 562 m. This increase in size allows for the generation of the high-energy electrons and subsequent X-rays that are so desired by researchers [52].

There are numerous synchrotron sources around the world which, whilst all having slightly varying layouts and operational methods, generally consists of the following five principal components discussed below and shown in Figure 8:

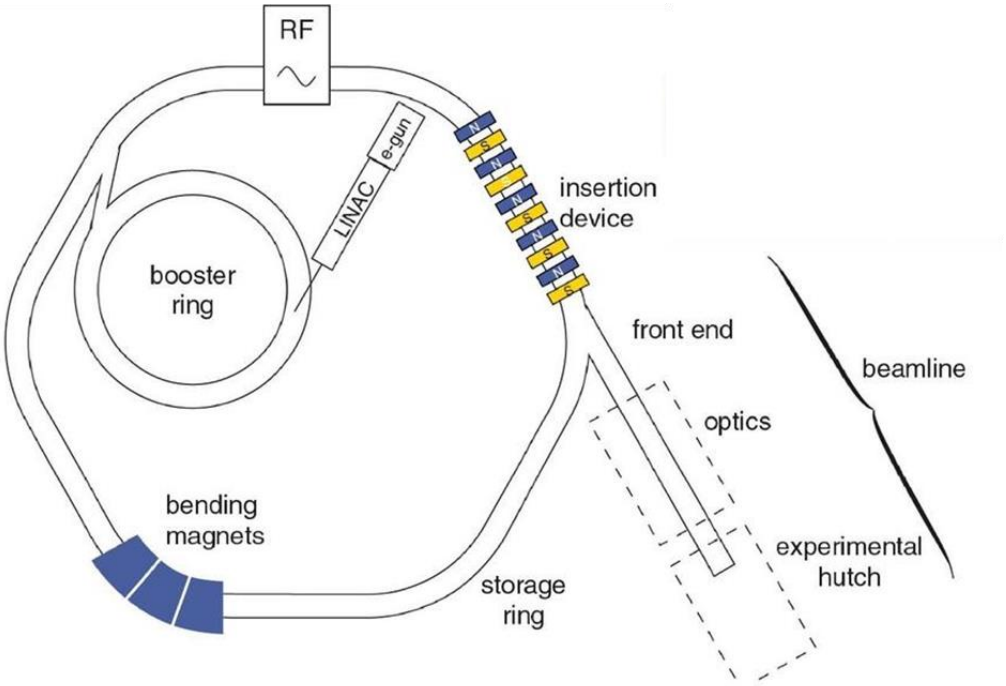

Figure 8: Schematic of a synchrotron facility with key elements highlighted [50].

1. Electron source: Traditionally generated through the thermionic excitement of a filament to liberate electrons, these sources generate electrons which are subsequently injected into a linear accelerator (linac) and accelerated up to 100 MeV.
2. Booster Ring: From the linear accelerator, the electrons are further accelerated in a booster ring. In modern synchrotrons the electrons here are accelerated up to the

energy in the main storage ring. Traditionally this was not achievable, and electrons were accelerated to a lower proportion of this energy. This meant that upon their injection into the storage ring they would need to be once again accelerated to the operational energy and so causing experimental “dead time”. Recent advancements with increasing the size of the booster ring allows for the use of “continuous top up” methods of injection, where when the storage ring current drops by ≈1% of the operational value, an injection of electrons from the booster ring occurs. This consistency of the electron energy allows for continuous operations which is extremely desirable given the demand for modern synchrotron sources.

3. Storage Ring: The storage ring consists of a closed vacuumed system where electrons are continuously circling. Their path is regulated using magnets to either to constrict the beam, in the case of quadrupole and sextupole magnets, or to change the beam direction to achieve a closed approximately circular path, in the case of bending magnets. The straight sections between the dipole bending magnets also allow for the insertion devices which are responsible for the generation of the most intense synchrotron radiation and feed into the beamlines.
4. Radio Frequency Supply: Due to the creation of synchrotron radiation and thus the loss of this energy from the system, the orbiting electrons need to be supplied with extra energy on every orbit else they would spiral into the centre of the storage ring and be lost.
5. Beamlines: Running tangentially to the storage ring, beamlines are where most users contact with synchrotron sources stops and is where experimentation is conducted. The beamline is split into two principal components, the experimental and optics hutch. The experimental hutch is where the samples is placed, and the actual process

of the experiment is performed. This lead lined room is where the sample under experimentation is exposed to the incident X-rays, and contains many detectors and safety systems. The optics hutch controls the incoming photon beam through the use of monochromators and filters to control the wavelength and intensity of the incident beam as it enters the experimental hutch.

2.2 Powder X-ray Diffraction (PXRD)

The regularly repeating structure found in crystalline materials is comparable to that found in diffraction gratings for visible light and as such these systems are capable of diffraction providing the wavelength of the incident X-rays is similar to the interatomic spacings between these layers (approximately 2 – 3 Å) [53]. Upon the interaction of X-rays with atomic lattices the atoms act as secondary point sources and scatter the X-rays in the same way as conventional diffraction grating would for visible light. Two major factors impact the resultant pattern of the diffracted X-rays: the symmetry and size of the unit-cell, which gives the number and position of the peaks; and the positions and type of the atoms within the unit-cell, which influences the intensity of the peaks themselves [54].

Two methods for the interpretation of diffraction data exist, with one being more prevalent: The Laue equations and Bragg's law. Developed first, the Laue equations start with the diffraction caused by a hypothetical one-dimensional row of atoms and obtain the resultant Equation 1 [47]:

Equation 1: A single Laue equation.

$$asin\emptyset = n\lambda$$

Where a is the separation of atoms in a row, $\emptyset$ is the diffraction angle, and λ is the X-ray wavelength. n is simply an integer value. Due to the three-dimensional nature of crystal systems these equations must be duplicated for all three dimensions and as such the three Laue equations are formed:

Equation 2: The full set of Laue equations for a 3-Dimensional structure.

$$a_1 sin\emptyset_1 = n\lambda$$

$$a_2 sin\emptyset_2 = n\lambda$$

$$a_3 sin\emptyset_3 = n\lambda$$

For diffraction to occur all these equations must, simultaneously, be satisfied. The complex nature of these equations means that while the Laue equations are mathematically correct, they are rarely used and instead crystallographers tend to use the more succinct Bragg's law [55].

Bragg's law treats the layers of atoms in a crystalline solid as a series of semi-transparent planes where the angle of incidence is equal to the angle of reflection and is given as θ. The Equation for Bragg's law is given in Equation 3 and is shown visually in Figure 9.

Equation 3: Bragg's Law [55].

$$n\lambda = 2d_{hkl} \sin\theta$$

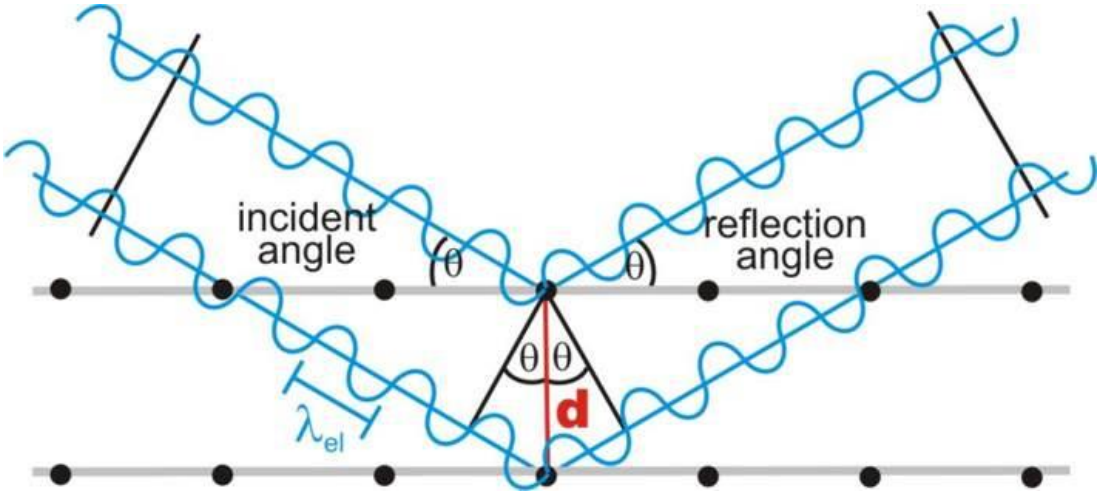

Figure 9: Diagram showing a system that satisfies Bragg's Law, constructive interference is observed in the out-bound X-rays.

Where λ is the wavelength of the incident X-rays, n is the order of reflection and is an integer value, d_{hkl} is the perpendicular lattice plane spacing. Figure 9 shows clearly that constructive

interference will only occur if two incident X-rays remain in phase upon reflection. For this to happen, Bragg's law must be satisfied. Due to the random orientation of crystallites within any powder sample Bragg's law will always be satisfied at some stage and so a diffraction pattern will be observed providing the sample is crystalline [56]. The resultant diffraction pattern can be analysed in a variety of different ways: from simple finger printing to complex Rietveld refinements and structure solution.

The long-range order which allows for the satisfaction of Bragg's law relies on the solid being crystalline. Crystalline solids are solid materials which can be represented with a single arrangement of atoms, a unit-cell. From this unit-cell using only translational symmetry operations along the Cartesian axes, the whole structure can be described, and the long-range order can be generated. These unit-cells are defined by their unit-cell lengths or lattice parameters (the length of the sides of the 3D polyhedron that all the atomic positions inhabit), and the angles between these unit-cell lengths [57]. These seven crystal systems are presented in the Table 1. Each crystal system can be further categorised by which form of centring it exhibits, known as a Bravais lattice. The centring of a unit-cell represents how atomic sites can be distributed within the cell in such a way as to maintain the required symmetry operations that must be present for a unit-cell to belong to any particular crystal system [57]. This is also shown in Table 1.

Not all crystal systems and centring options give rise to a new Bravais lattice type. This is generally due to the ability to describe the combination through another crystal system and centring option which is smaller and simpler [58]. From this selective second level of categorisation the 14 Bravais lattice types can be deduced. These are shown in Table 1.

Table 1: The crystal systems, their essential symmetries, and allowed centring options forming the 14 Bravais lattice types. note the primitive form of the rhombohedral unit-cell is traditionally denoted with the letter R [47, 57, 58].

Crystal System	Unit-cell lengths	Unit-cell angles	Essential Symmetries	Allowed centring
Cubic	a = b = c	α = β = γ = 90°	Four C_3 axes in tetrahedral arrangement	Primitive (P) Body Centred (I) Face Centred (F)
Tetragonal	a = b ≠ c	α = β = γ = 90°	One C_4 axis	Primitive (P) Body Centred (I)
Orthorhombic	a ≠ b ≠ c	α = β = γ = 90°	Three perpendicular C_2 axes	Primitive (P) Side Centred (C) Body Centred (I) Face Centred (F)
Monoclinic	a ≠ b ≠ c	α = γ = 90°, β ≠ 90°	One C_2 axis	Primitive (P) Side Centred (C)
Triclinic	a ≠ b ≠ c	α ≠ β ≠ γ ≠ 90°	None	Primitive (P)
Hexagonal	a = b ≠ c	α = β = 90°, γ = 120°	One C_6 axis	Primitive (P)
Rhombohedral	a = b = c	α = β = γ ≠ 90°	One C_3 axis	Primitive (R)

Whilst the unit-cell describes the smallest repeating unit which describes a system using only translational symmetry alone, the asymmetric unit is smaller still. This asymmetric unit does not simply rely on translational motion to describe the system but on all symmetry operations, which are obtained from the space group of the system. Applying the symmetry operations described by the space group to the asymmetric unit-cell obtains the standard unit-cell which can then be repeated through translational motion to obtain the total structure. There are 230 space groups that describe the transformation from the asymmetric unit-cell to the standard unit-cell. Each can be denoted by a short symbol which contains information on the centring and the symmetry operations they describe [54].

2.2.1 The Rietveld Refinement

Upon the collection of a diffraction pattern, a mathematical refinement of the structure of the sample is often desired to optimise the predicted structural model to the observed data.

These refinements start with an approximated model and key parameters are refined to obtain a more accurate one which fits the experimental data better. The most common, and most suitable for full structure determination, is the Rietveld method. In a Rietveld refinement, the entire content of a diffraction pattern is fitted to a model with refinable parameters. The method of refinement employed is a least-squares refinement. The aim of the least-squares refinement is to minimise the difference between the observed intensity and the calculated intensity originating from the model at all points [59]. This is shown in Equation 4 where the outer summation represents the sum over all points, i, in 2θ. A weighting function, w_i, is also applied.

Equation 4: The process of a least-squares refinement. The difference between the calculated and observed intensity is minimised [59].

$$\sum_i \left(w_i \left(y - y_{calc,i} \right)^2 \right) \rightarrow Min$$

The first stage is the preparation of a calculated diffraction pattern. The intensity of the diffraction pattern, y, at any point, i, is created using the following Equation 5.

Equation 5:The equation used for the determination of calculated intensity, y, at any point, i.

$$y_{calc,i} = \sum_p \left(S_p \sum_{\boldsymbol{s}(p)} \left(\left| F_{calc,\boldsymbol{s},p} \right|^2 \Phi_{\boldsymbol{s},p,i} \, Corr_{\boldsymbol{s},p,i} \right) \right) + Bkg_i$$

Where the outer sum runs over all the crystalline phases, p, which have created Bragg peaks in the pattern and the inner sum is over all reflections, $\boldsymbol{s}$ *=(hkl),* of a phase, p. S_p is a scaling factor, proportional to the weight fraction of the phase, p. $Corr_{\boldsymbol{s},p,i}$ represents a series of correction factors that need to be applied to the intensities $\left| F_{calc,\boldsymbol{s},p} \right|^2$. The profile function is denoted as $\Phi_{\boldsymbol{s},p,i}$. The intensity of the background is defined as Bkg_i.

Hypothetically, perfect Bragg reflection peaks would have a width in 2θ of 0, this is however never observed. This peak broadening, whether caused by instrumental or sample effects, can be represented as one of a series of profiles which are mathematical functions. The most common used is a Thompson-Cox-Hastings function (TCHZ). This is a pseudo-Voigt (PV) function where the Voigt function is a convolution of both the traditional Gaussian and Lorentzian distribution functions. This combination of Gaussian and Lorentzian contributions matches well with most diffraction patterns [60]. The principal advantage of the TCHZ function is the ease with which full width at half maxima (FWHM) can be calculated and reported [61].

Rietveld refinements also offer the ability to determine the absolute weight fraction of multiple phases in a sample. This can be done providing one of the phases is known and crystalline, and the other can be either highly or poorly crystalline. A standard of the unknown or poorly crystalline phase is required. The standard can either be used as an internal standard where a known quantity of the poorly crystalline phase is added to a known quantity of the crystalline phase and a reference measurement is taken, or as an external standard where a separate measurement of the poorly crystalline phase is obtained. Due to the inconsistency of the instrumental parameters from each experiment it is preferable to use an internal standard [61]. The results of a 2-phase Rietveld refinement can be used to determine the degree of a sample's crystallinity. If one phase of the refinement is known to be highly crystalline and the other poorly crystalline then the percentage contribution of the poorly crystalline phase is inversely proportional to the degree of crystallinity [62].

Three values are crucial when quantifying the quality of the fit produced after refinement: the weighted profile factor (R_{wp}) which is a comparison of the calculated pattern and the observed pattern, the expected profile factor (R_{exp}) which estimates the lowest possible value

of the (R_{wp}), and the goodness of fit (*GOF*) also referred to as χ^2. These are calculated from the following equations:

Equation 6: Equation for R_{wp}, where w_m is the weighting given to data point m, $Y_{(OBS,\ M)}$ and $Y_{(CALC,\ M)}$ are the observed and calculated data respectively at data point m [60].

$$R_{wp} = \sqrt{\frac{\sum w_m \left(Y_{obs,m} - Y_{calc,m}\right)^2}{\sum w_m {Y_{obs,m}}^2}}$$

Equation 7: Equation for calculating R_{exp} where the weighting of each data point, m is given by w_m. $Y_{OBS,\ M}$ is the observed data at point m, M is the number of data points, P the total number of parameters [60].

$$R_{exp} = \sqrt{\frac{\sum M - P}{\sum w_m {Y_{obs,m}}^2}}$$

Equation 8: Equation of the relationship of goodness of fit to R_{wp} and R_{exp} [60].

$$GOF = \chi^2 = \frac{R_{wp}}{R_{exp}} = \sqrt{\frac{\sum w_m (Y_{obs,m} - Y_{calc,m})^2}{M - P}}$$

2.2.2 The Pawley Fit

If the structure of a material is unknown a structural independent refinement can be performed. These whole powder pattern fitting (WPPF) methods offer a good preliminary method for the analysis of a diffraction pattern and allow for the determination of such parameters as: lattice parameters, peak positions, peak profiles, and background values alongside offering confirmation of the space group of the structure being studied. Once these values are known then a structure solution or structural Rietveld refinement can be conducted with these values to determine the structural characteristics of the material and their contributions to the diffraction pattern. The Pawley fit [63] is one of the most common methods for performing these structurally independent WPPF refinements. In a Pawley fit, the unit-cell parameters, background-intensity parameters, zero-point errors, and peak-shape parameters are subjected to a least-squares refinement. All reflection intensities

are maximised to fit the observed data set. The result of this is the refinement of a solution to the following set of equations:

Equation 9: The series of equations which are used to represent the calculated intensity of a step wise diffraction pattern at any given step.

$$y_{calc,0} = \sum_{\boldsymbol{s}} \left(I_{\boldsymbol{s}} \cdot \Phi_{\boldsymbol{s},0} \right) + Bkg_1$$

$$y_{calc,1} = \sum_{\boldsymbol{s}} \left(I_{\boldsymbol{s}} \cdot \Phi_{\boldsymbol{s},1} \right) + Bkg_2$$

$$\dots$$

$$y_{calc,N-1} = \sum_{\boldsymbol{s}} \left(I_{\boldsymbol{s}} \cdot \Phi_{\boldsymbol{s},N-1} \right) + Bkg_n$$

Where $y_{calc,i}$ is the calculated intensity at point i. $I_{\boldsymbol{s}}$ is the intensity of the reflection $\boldsymbol{s}$, and $\Phi_{\boldsymbol{s},i}$is the normalised peak shape function of reflection $\boldsymbol{s}$ at position $i \in [0 \dots N-1]$ in the diffraction pattern. Bkg_i is the background term and is generally modelled as a polynomial function.

Principally, Pawley fit refinements are used to determine lattice parameters of structures without requiring information on the atomic positions of the material.

2.2.3 Experimental Setup Used

For the work presented here a Bruker D2-phaser Powder Diffractometer, located at the University of Central Lancashire, was used operating in θ-θ geometry with a copper tube and a Lynxeye Si strip detector. A nickel filter was used to isolate the Kα wavelength, λ = 1.5418 Å. The scans were run on a rotating stage at 30 revolutions per minute between 5 – 120° 2θ to give appropriate range for the subsequent Rietveld refinements. A slit size of 0.2 mm was used to attenuate the beam and a knife edge of 0.1 mm was employed to prevent the beam directly hitting the detector at low values of 2θ and to minimise air scatter. All diffraction patterns were collected under ambient temperature and conditions. Samples were powders

and were placed onto Poly(methyl methacrylate) sample holders manufactured by Bruker. To ensure a flat surface, samples were smoothed with a glass microscope slide. The resulting diffraction patterns were analysed in the Diffrac.Suite Eva software [64]. Rietveld refinements were performed in GSAS through the EXPGUI user interface [65, 66]. Pawley fits and degrees of crystallinity were determined in TOPAS-4 [67].

2.3 Total Scattering Pair Distribution Functions (PDF)

The diffraction of X-rays and subsequent structural characterisation is widely studied and has been discussed in depth in Chapter 2.2, but these sharp Bragg diffraction peaks only occur if the sample being studied displays long-range order. Amorphous materials, disordered states, and largely crystalline samples that contain imperfections have no long-range order and show diffuse scatter. These materials cannot be studied using Bragg peak diffraction alone and are normally not examined using traditional diffraction methods.

The Pair Distribution Function (PDF), obtained from the Fourier transform of X-ray diffraction data, shows the probability of finding any two atoms a specific distance apart [68]. Whilst normal diffraction studies concentrate solely on the Bragg peaks for characterisation, X-ray pair distribution function analysis (XPDF) uses a Fourier transform to extract information from the underlying sinusoidal characteristics of the diffraction data known as diffuse scatter. This information from the diffuse scatter is combined with the Bragg peaks to give an overall pair distribution function. It is for this reason it has the alternative name “Total Scattering”. This total scattering approach allows the identification of imperfections, defects, and dopants in solid crystalline lattices and characterisation of materials that lack long-range order such as glasses and liquids [69]. Whilst non-crystalline materials often have no long-range order, they often display immediate range ordering which does not produce Bragg peaks.

In this most primitive form the PDF, D(r), is a 1-dimensional function which displays the probability of finding two atoms at a distance, r, from one another with each atomic pair being regarded as equal. In reality the intensity of any peak in the PDF is also correlated to the atomic scattering factor of the atoms in the pair for the given scattering probe (X-rays, neutrons, or electrons) and is damped at increasingly high scattering vector (Q) values [70]. For

X-rays this scattering amplitude is proportional to the atomic number of the atom being probed. This reliance upon the scattering amplitude and its subsequent derivation from the atomic number creates a situation where lighter, weak scattering atoms are difficult to study and locate and heavier, strongly scattering atoms are extremely prominent [70]. This situation is not observed in neutron scattering experiments where the scattering amplitude of each atom type is seemingly random due to complex neutron-nuclei interactions. Figure 10 shows the correlation between the atomic number and the X-ray scattering length compared to that of neutrons.

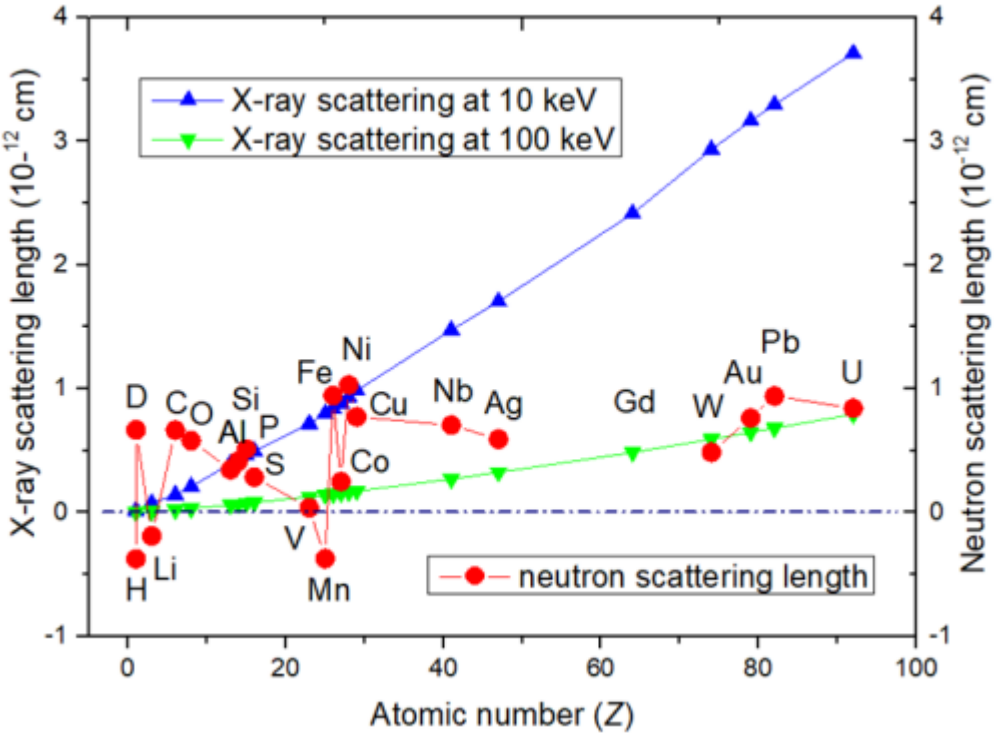

Figure 10: X-ray and neutron scattering length of a selection of elements [71].

The PDF must be reduced from the Radial Distribution Function (RDF) which, due to the ever-increasing number of atoms found at longer contact distances, increases proportionally to the differential of the volume of a sphere and the atomic number density ρ_0: $4\pi^2\rho_0$. The effect of this normalisation is shown below in Figure 11. Whilst other normalisation methods

are available, this method ensures errors from the measurement are approximately constant in r and so can be visually compared across the whole reduced PDF [70].

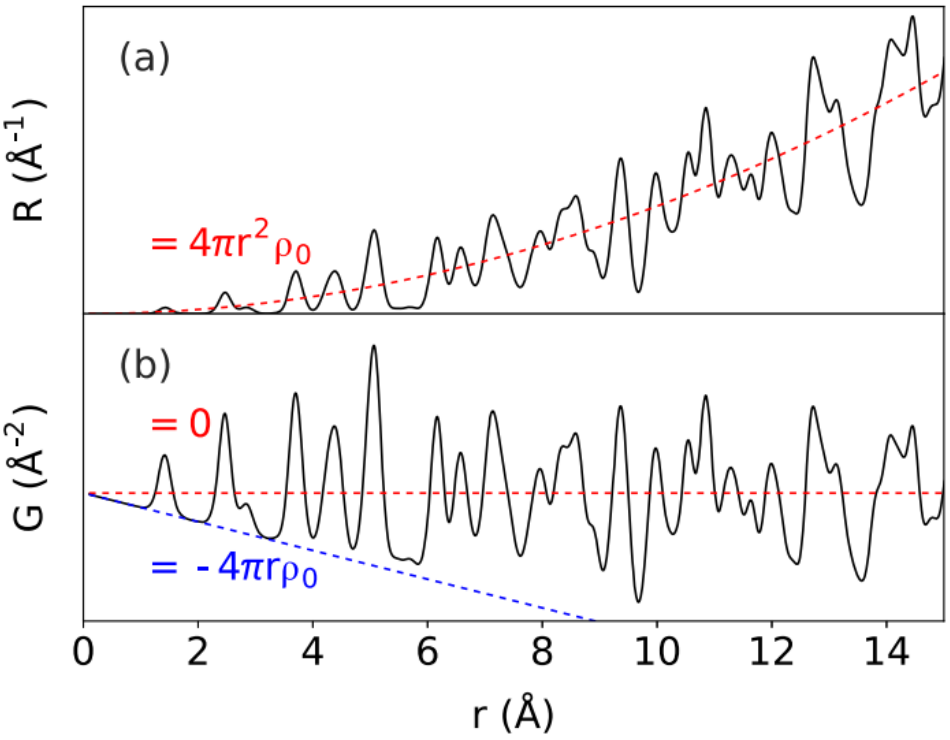

Figure 11: The exponential characteristics of the RDF. a) the RDF (black) is shown with the asymptotic behaviour in red. b) the associated PDF (black) with the asymptotic behaviour in red and a negative sloping baseline in blue [70].

Liquid samples, when studied using XPDF, show broader peaks than their solid counterparts due to the greater range of allowed thermal motion. This broadening is reduced at higher values of r as the PDF transitions from representing the intramolecular forces to representing intermolecular forces. Intramolecular forces are generally very rigid due to the strong bonds which link the atom pairs, either directly or through a few other atoms with limited allowed motion. These strong and well-defined bonds cause correlated motion where the thermal vibrations of one atom in the atomic pair directly effects the other and so the effects of this motion are reduced in the PDF [72-74]. As the PDF increases in r however, the rigidity of the bonding between the atom pairs being studied decreases. This can be caused by the introduction of more atoms linking the two, each introducing a slightly higher degree of

freedom to the system than the last, or the transition from an intramolecular atom pair to an intermolecular atom pair. At the point where intermolecular atomic pairs are being studied, the principal forces between these two atoms are largely intermolecular hydrogen bonding or van der Waals' forces. These weak interactions do not convey the effects of thermal motion of one atom onto the next and so any atomic pair linked by these forces will show peak broadening and a reduction in correlated motion. This combines to lead to the high regions of r in the PDF being dominated by broad and extremely complex features due to many overlapping peaks which are extremely hard to define. These peaks are directly influenced by the conformation and packing of the molecules in the system being studied [70].

These broad features in liquids make resolution of the PDF vitally important as any subtle characteristics can be lost and assumed to be simply caused by the broadness inherent of the material. The resolution of a PDF can be improved by measuring up to as high a scattering vector value (Q) as is possible. Unfortunately, at higher Q values increased intensities are needed due to the fact at high Q values scattering efficiency is suppressed. The scattering vector value, Q, is shown in Equation 10 where θ is the angle of incidence of the beam and λ is the wavelength. Equation 10 clearly shows that to increase the value of Q_{max}, a smaller wavelength (λ) is ideal. It also shows that ideally a large range of θ/2θ values would ideally be collected. It is for this reason that the sample to detector distance should be minimised to offer the highest available range of θ values.

Equation 10: Scattering vector value (Q).

$$Q = |Q| = \frac{2\pi}{d} = \frac{4\pi sin\theta}{\lambda}$$

During the post processing of diffraction data to obtain the PDF, the normalised total structure factor S(Q) is Fourier transformed. This normalised total structure factor is the

measured intensity corrected for background, multiple and Compton scattering, absorption, and other competing interactions. S(Q) can be defined according to Equation 11, where $I(Q)$ is the normalised scattering intensity, atomic concentration is $c_{i,}$ and the atomic form factor is f_i for atom type i which is dependent on Q.

Equation 11: S(Q) defined with respect to I(Q).

$$S(Q) = \frac{I(Q) - \sum c_i |f_i(Q)|^2}{|\sum c_i f_i(Q)|} + 1$$

This, when Fourier transformed, leads to the reduced pair distribution function, D(r), shown in Equation 12, where $\rho(r)$ is the microscopic pair density, the average number density is ρ_0 and the radial distance is r.

Equation 12: D(r) defined in terms of ρ(r).

$$D(r) = \frac{2}{\pi}\int_0^\infty Q[S(Q) - 1]\sin(Qr)\,dQ = 4\pi r[\rho(r) - \rho_0]$$

Due to the inability to calculate the PDF across an infinite Q range, when calculating the D(r), the limits of integration used instead are Q_{min} and Q_{max}. The effects of the inability to achieve a Q_{min} of 0 are widely considered negligible. Most modern instruments achieve a Q_{min} sufficiently small that the terms missing from the transformation are insignificant. This is owed to the fact that the terms of Equation 12 are multiplied by the Q value and as such these contributions are extremely small when compared to the other effects and sources for error in the PDF. The effect of the reduction in the available Q range at high Q values has more pronounced effects. This often results in spurious oscillations and the termination effect of limiting the PDF to Q_{max} causes a convolution of $\rho(r) - \rho_0$ and the broadening function $\sin(Q_{max}\Delta r)/\Delta r$ leading to peak broadening. This can however be overcome with a

sufficiently large enough Q_{max} as this effect becomes dwarfed by thermal parameters and zero point motions which also induce broadening in the PDF [75].

It is for this reason that the great majority of PDF experiments are run at synchrotron sources where wavelengths are low and beam intensities high. It is theoretically possible to run a PDF experiment on a standard laboratory diffractometer, but specialist X-ray sources are required to achieve useable Q ranges, such as silver and tungsten, as can be seen in Table 2. Also due to the low intensities of conventional X-ray sources, experimental times would be extremely long, taking days rather than the several minutes typically required at a synchrotron facility.

Table 2: X-ray energies, wavelengths, an appropriate Q_{max} values for common laboratory X-ray sources and the dedicated XPDF beamlines I15-1 and 28-ID-1 at Diamond Light Source (DLS) and National Synchrotron Light Source (NSLS-II) respectively [52, 69, 76].

Source	*E_0 (KeV)*	*λ (Å)*	*Q_{max} ($Å^{-1}$)*
Cu	8.05	1.538	8.0
Mo	17.48	0.708	17.5
Ag	22.16	0.559	22.0
W	59.32	0.209	59.0
I15-1 DLS	76.60	0.160	78.5
28-ID-1 NSLS-II	75.00 ,117.00	0.165, 0.106	76.2, 118.6

Traditional methods for achieving a useable PDF when high Q data cannot be collected include applying a damping function to reduce the intensity of the highest Q values. This results in broadened features and the effect is analogous to an increase in the temperature and thus the thermal motion parameters. There is no true substitute for the availability of high Q range data collections [75].

The total scattering pair distribution function studies presented here were performed at I15-1 at Diamond Light Source (DLS), Didcot, UK; and 28-ID-1 at National Synchrotron Light Source

(NSLS-II), Brookhaven, New York, USA. The diffraction data obtained was transformed into PDFs with the program GUDRUNX [77] for data obtained from DLS and PDFGETX3 [78] for data obtained from NSLS. To obtain the PDF from the measured diffraction data, first the coherent scattering must be isolated. This requires the removal of the contributions of air, the sample holder, fluorescence effects and incoherent and multiple scattering. From this coherent scattering data, the total scattering structure function, Q[S(Q)-1], can be obtained by dividing the data by the form factor. Whilst this data can be modelled directly, the Fourier transform yields the PDF data D(r) which is real-space data and is used in the modelling process. This process is shown for a data set from the 3-month data collection below in Figure 12.

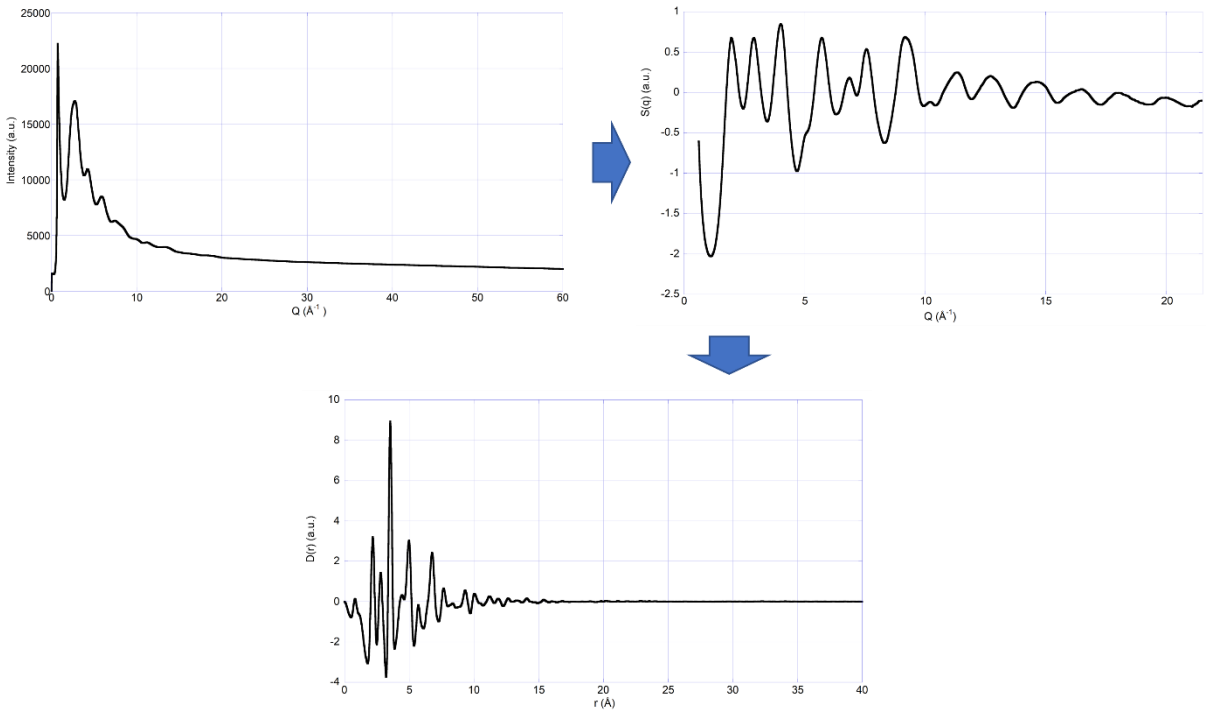

Figure 12: The raw diffraction data, S(q), and D(r) for a sample of zirconium-acetate solution obtained in the 3-month data collection at DLS.

All the generated PDF data were refined in TOPAS-6 [67].

2.3.1 Refinement Techniques

Once collected and processed, PDF data can then be fitted using methods crystallographers will be extremely familiar with. All refinements start with an initial creation of a potential starting model; a representation of what is believed to be present in the sample being studied. From this model a simulated diffraction pattern is calculated, which is subsequently Fourier transformed, in much the same way the data set was, to create a simulated PDF (G_{calc}).

From this, a series of values and parameters, including atomic positions, anisotropic thermal ellipsoids, unit-cell lengths and angles, atomic occupancy, and parameters such as scale and background, can be refined using a least-squares method to optimise the calculated model (G_{calc}) to the observed data set (G_{obs}). This process is similar to that used in a Rietveld refinement using Bragg scattering.

The crucial difference between the traditional Rietveld refinement of a diffraction pattern and a refinement of PDF data is that PDF data refinements are performed in real space as opposed to the reciprocal space conventional diffraction patterns are refined in. This means that structural differences in the sample manifest differently in the PDF to how they would appear in traditional PXRD patterns. This is most notable with thermal parameters and their broadening. Traditional PXRD experiments find it most appropriate to express peak broadening as a pseudo-Voigt function. PDF refinements however must account for correlated motion when modelling peak broadening. This correlated motion, as discussed earlier, is more prevalent at shorter distances of r. The decrease of this correlation, however, can manifest in multiple different ways and so it is essential that the correct shape function of the transition between high correlation at low r and low correlation at high r is correctly

described. An example of some commonly used thermal functions which correlate the effective thermal parameter B to the distance r, are shown below in Figure 13.

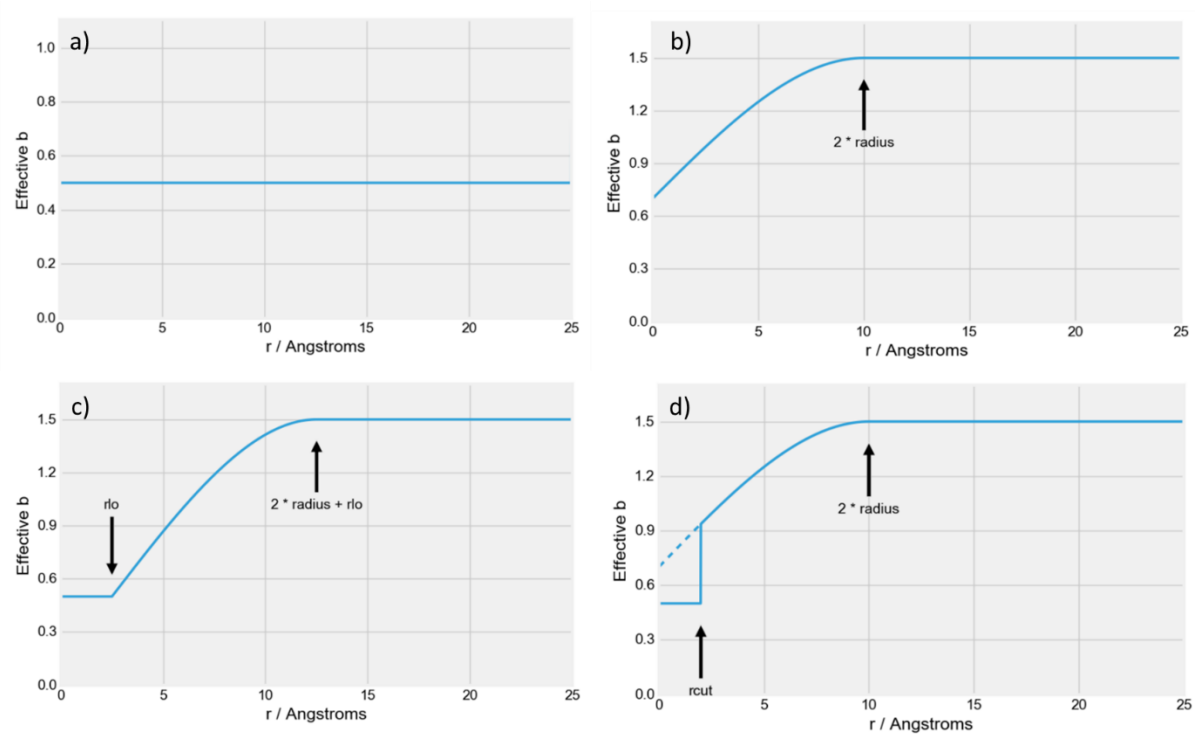

Figure 13: Graphical representations of a series of common thermal parameters used in PDF refinements a) a standard single value B=0.5 b) a spherical function with a gradual rise to low correlated motion c) a spherical system where an immediate range of high correlation which dissipates d) another system of low r bonding which dissipates to a maximum.

Figure 13a represents a single value of B for all distances of r. This is commonly seen in diffraction experiments where the thermal parameters are not correlated to r distances and so a single B value can accurately describe the system. Figure 13b shows a spherical function which starts at an r value of 0 with a low B value and rises to a new higher effective B value at a distance of 2 × ”radius”. Here radius is a refineable parameter. This relationship is good for describing materials which have a gradual dissipation of correlated motion as r increases. Figure 13c describes a function where the values of r and effective B are linked in a similar way to Figure 13b but a low value of B is observed for a fixed distance of r before the relationship gradually increases. This function is optimal for describing systems where there is a gradual dissipation of correlation which is preceded by high levels of correlation at low r

values, such as molecular systems. Figure 13d describes a situation where the relationship between r and the effective B is the same as seen previously with one exception. At low r values a lower effective B value is observed and there is a step function up to the B values seen in the curve. This function is good for describing materials with gradual dissipation of correlated motion but with particularly firm low-r bonding. For the refinements performed within this work the function described in Figure 13c was used.

3.0 Non-Scattering Experimental Techniques

This chapter aims to highlight the non-scattering methods of analysis applied in this research project.

3.1 X-ray Absorption Spectroscopy (XAS)

For the study of liquid, amorphous, or glassy materials, X-ray absorption spectroscopy (XAS) is often employed. This element specific technique does not rely on long- or medium- range order like its scattering counterparts seen earlier in Chapter 2, but allows for the characterisation of the first, second and occasionally third coordination environment around a given element.

A plot of X-ray energy vs attenuation coefficient for a particular element is dominated by a large jump at a specific wavelength. This feature, the absorption edge, is the point where the energy of incident radiation corresponds to the binding energy of a core electron in the sample. At the absorption edge the energy of the incident photon is sufficient to cause the excitation, relaxation, and subsequent emission required for a fluorescence event [79].

The X-ray absorption experiment requires a sample of interest to be bombarded with an incident X-ray beam, of known energy. Upon the interaction of the incident beam with the sample, if the energy is higher than the absorption edge, a photoelectron is ejected. Then a higher energy electron in the atom relaxes to fill this vacancy and this relaxation creates X-ray radiation of a characteristic wavelength in a process called fluorescence. From this point, three unique measurements can be observed. A measure of the comparative intensity of the incident and the transmitted beam, before and after contact with the samples, is said to be a *transmission-mode* experiment. In these experiments the intensity of the X-ray beam

absorbed by the sample is calculated and any decrease in intensity is due to the sample's absorbance. If the fluorescent X-ray itself is measured, then the experiment is said to be run in *fluorescence mode*. In this set up, a detector is placed perpendicular to the sample. When the fluorescence event happens, the resultant X-ray is emitted in an isotropic manner and this side detector can, therefore capture and record some of these potential emissions without detecting any transmission of the incident beam. A third, and less commonly used method of measurements relies on a phenomenon that occurs when instead of emitting a photon, the excited atom relaxes through the release of a high-energy electron, an Auger electron. This electron can then be measured and compared to the incident X-ray beam in what is referred to as an *electron-yield* experiment [79] .

The first photographic measurements of the *K* absorption edges of elements were published in 1920 for elements between Mg and Cr [80]. These early photographic plates were dominated by an intense "white line" which is now understood to be the *K* absorption edge of the element in question. These images showed a fine structure both before and after the absorption edge energy. This marked the discovery of the XAS (X-ray Absorption Spectroscopy). EXAFS (Extended X-ray Absorption Fine Structure) is the study of the region a few electron volts after the absorption edge and XANES (X-ray Absorption Near Edge structure) is the study of the features around the absorption edge itself. These distinct regions are shown in Figure 14.

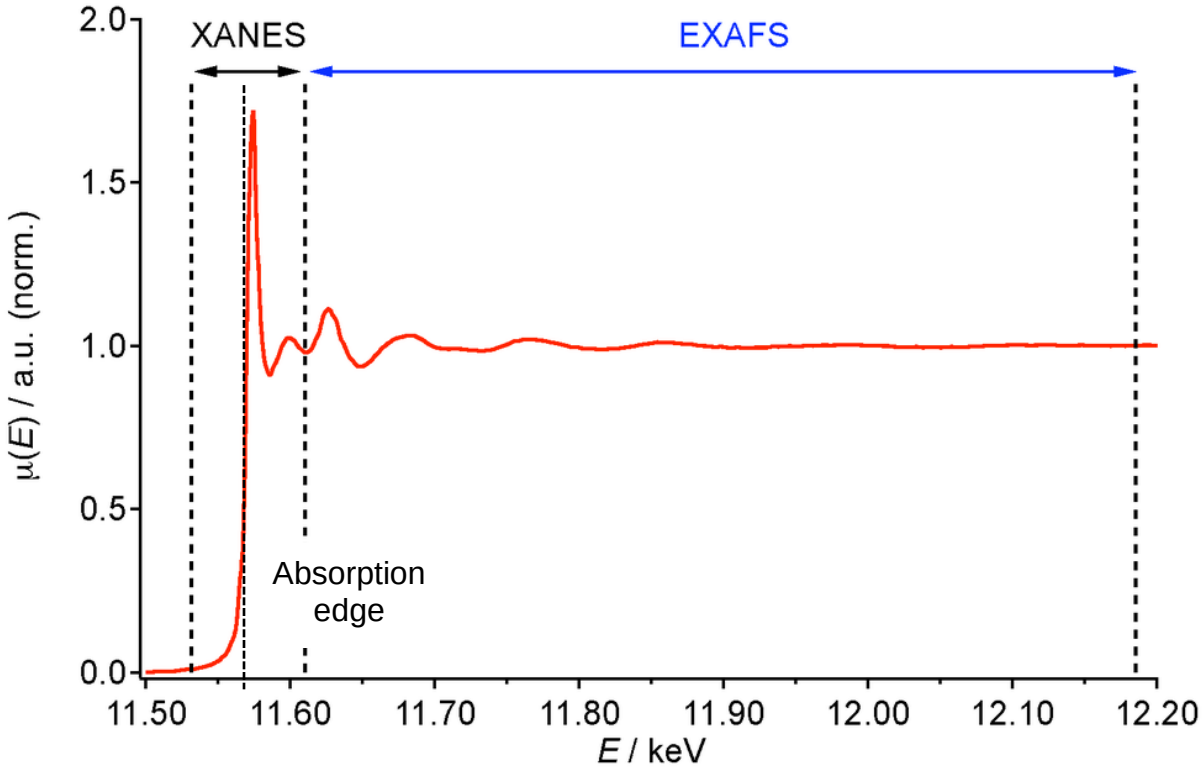

Figure 14: A typical XAS spectra with the XANES and EXAFS regions highlighted [81].

The location of this edge on the energy spectra is characteristic of the element that causes it and as such is chemically of interest. The absorption energy is related to the binding energy of the photo-excited electron and the effective atomic number (Z_{eff}) of its source atom. The Z_{eff} is predominantly influenced by the oxidation number of the absorbing atom as well as its atom type. From this a direct comparison of the edge to a literature source or reference sample can allow for the determination of the type and oxidation state of the absorbing atom. The precise edge location is determined through differentiating the spectrum and locating the highest point on the first differential, thereby mathematically locating the middle of the sharp incline on the original spectrum. Once this edge location is determined it can be compared to standard samples of known oxidation states to compare. Most elements show significant edge shifts with changes in their oxidation state. Study of the pre-edge XANES region can offer insight into the coordination environment of the element being studied and

once again comparison to a known standard through non-quantitative finger printing methods can be used to determine local coordination environments [82].

Figure 14 is not a pure plot; some level of correction has been performed. Had the data presented in Figure 14 been uncorrected, then the pre-edge and post-edge regions would exhibit a general negative gradient, with the average gradient pre-edge being parallel to that post-edge. This negative gradient is a result of the attenuation of X-rays as they interact with matter. The process of absorption attenuates the X-ray flux transmitted through a sample according to Equation 13 where I_0 and I_t are incident and transmitted intensities respectively, μ is the linear absorption coefficient and l is sample length [83].

Equation 13: Attenuation of X-ray flux.

$$\frac{I_t}{I_0} = e^{-\mu l}$$

Providing the sample is suitable (i.e. the element being studied is of sufficient concentration in the sample), most modern XAS experiments are performed in transmission-mode. Here, a reference sample of the element being studied is placed after the second detector to calibrate the equipment. A schematic of this can be seen below in Figure 15. To determine oxidation states of the element in question in samples being studied, the location of the absorption edge can be compared to that of reference samples of the same element with a known oxidation state.

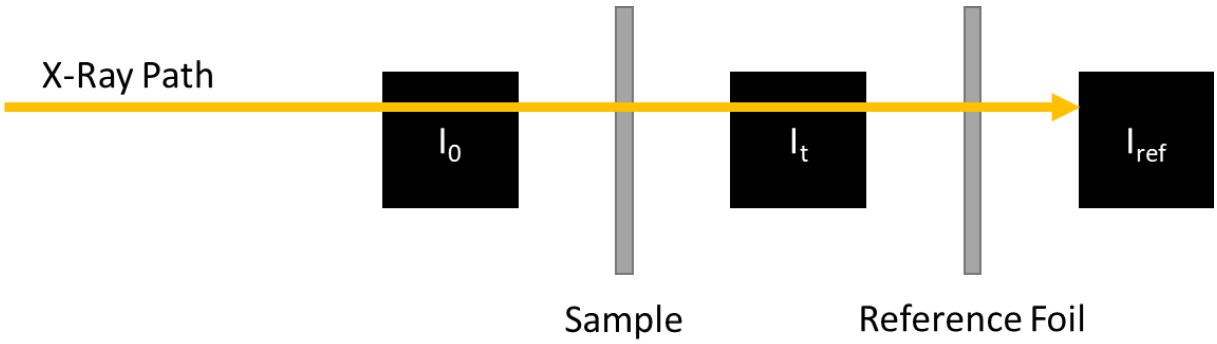

Figure 15: The schematic of a standard XAS experiment in transmission-mode.

As can be seen in Figure 14 the region immediately post edge is not perfect flat but exhibits a series of broad oscillations. These oscillations are not present in the spectra of monoatomic gaseous samples as they are caused by the close proximity of atoms in the sample being studied.

When an X-ray excites an electron from an atom, this electron, often referred to as a photoelectron, propagates from the atom as a spherical wave front. When this wave front subsequently interacts with neighbouring atoms and their electron density, the photoelectric wave is returned to the source atom. This returning wave can have constructive or destructive interference with the source wave. If the waves are in phase, and thus constructive, the electron density around the source atom is increased. This increases the likelihood of finding this state after measurement rather than the state when the photon continues without absorption. For this constructive interference to take place, the photoelectron must travel a whole number of wavelengths from source to return. This is shown in Equation 14 and Figure 16.

Equation 14: Requirement for constructive interference in XAS experiment.

$$2d = n\lambda$$

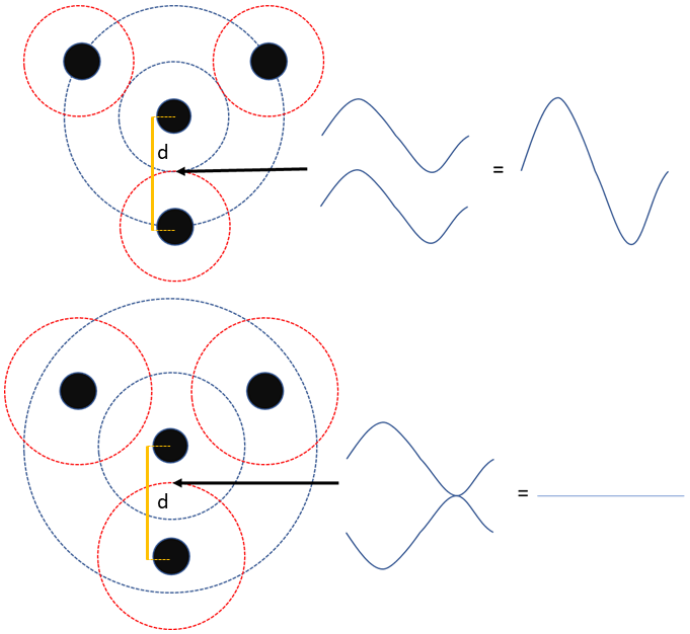

Figure 16: Instances of the relationship between atomic spacing and wavelength (Top) causing constructive interference and (Bottom) causing destructive interference.

Equation 14 shows how the distance between two scattering atoms, d, must be equal to an integer number, n, of wavelengths, λ. The factor of 2 represents both the forward and backward motion of the photoelectron. As the number of potential near neighbour scattering atoms increases, so too does the opportunities for this equation to be satisfied and constructive interference to be present. However, these multiple scattering events, events where the photoelectron is propagated through multiple nearest neighbour atoms, must each have their contributions to the probability of an absorption event occurring calculated and summed.

Equation 15 is commonly known as the EXAFS equation, this equation aims to incorporate all changes in disorder, multiple atoms around the absorber, multiple scattering pathways and phenomena that remove signal from the main pathway.

Equation 15: The EXAFS equation [79].

$$\chi(k) = S_0^2 \sum_i N_i \frac{f_i(k)}{kD_i^2} e^{-\frac{2D_i}{\lambda(k)}} e^{-2k^2\sigma_i^2} \sin 2kD_i + \delta_i(k)$$

Where:

S_0^2 = Amplitude reduction Factor

N = Degeneracy

D = Half path length

σ_i^2 = Mean square relative displacement

λ(k) = Mean free path

Before further structural information can be obtained the plot in k space must first be Fourier transformed into r space. Refinements of EXAFS data happen in r space as this is a visual representation of the contact distances, in r, that are present in the sample. In this way EXAFS is very similar to XPDF but offers element specific contact distances where the atom type of one of the atomic pair can be selected. A potential model is then determined, and a simulated series of contact distances calculated through a FEFF calculation. From this, conclusions about the suitability of the model with respect to the dataset can be deduced [84].

Due to its independence from scattering and Bragg peaks the technique is suitable to study amorphous materials (liquids and glasses) alongside materials which do display long-range order. The element specific nature of EXAFS makes it ideal for studying the environment around elements known to be in the sample being studied.

EXAFS data is traditionally manipulated and fitted using Artemis and Athena in the Demeter suite of programmes and this is the case for the research presented here [85]. All data collections were performed at B18 at Diamond Light Source (DLS), Didcot, UK.

3.2 Synthesis of the Model Compound – Umbite $K_2ZrSi_3O_9 \cdot H_2O$

In an attempt to identify the impact of any structural changes in the zirconium-acetate solutions on their use as a synthesis precursor, samples of a model compound were produced periodically and characterised. The model compound used in this study was umbite. This material was synthesised using a modified synthesis based on that reported by Poojary *et al*. [46]. To a Teflon beaker, 21.5 ml of H_2O, 7.5 g of KOH and 2.0 g of fumed silica were added. The KOH was purchased from Fisher Scientific, and the fumed silica was obtained from Sigma Aldrich. The amount of zirconium-acetate solution added varied based upon its relative concentration, but the molar value of zirconium was standardised to 2.42g an equivalent molar amount of $ZrCl_4$ (0.01 moles Zr) as stated by Poojary *et al*. [46] this led to masses of 9.16g, 5.83g, and 4.28g of solution being required for the 14%, 22%, and 30% solutions respectively [46]. The reagent amounts are detailed below in Table 3. The zirconium-acetate solutions were produced at Luxfer MEL Technologies. The resultant gel was allowed to stir for 2 hours before being transferred into a Teflon lined autoclave and heated to 200 °C for 20 hours. The resultant solid was then removed, washed with 750 ml of water and air dried before being characterised. To confirm the synthesis had been successful, samples were characterised using PXRD.

Table 3: Mass of reagents required for the synthesis of samples of umbite ($K_2ZrSi_3O_9 \cdot H_2O$) showing the difference in the amount of zirconium-acetate solution required based on the solution concentration.

Zirconium-acetate solution concentration (%)	Mass of zirconium-acetate (g)	Mass of H_2O (g)	Mass of KOH (g)	Mass of fumed silica (SiO_2) (g)
14	9.16	21.5	7.5	2.0
22	5.83	21.5	7.5	2.0
30	4.28	21.5	7.5	2.0

3.3 Scanning Electron Microscopy (SEM)

Scanning electron microscopy, much like standard optical microscopy offers the ability to study the physical appearance of a sample but with a greater resolution. Instead of using visible light, with wavelengths approximately 400 – 700 nm, instead electrons are accelerated through up to 200 kV and used as the probe. This offers resolution values up to 100 Å allowing for the study of individual particulates. From this, clear images of the particle morphology and size can be obtained and analysed. Electrons are initially generated through the thermionic emission of a filament. The electrons liberated from this filament are then directed towards the sample under observation through several “magnetic lenses” (Figure 17). These magnetic lenses use the influence magnetic fields have on electrons to direct the electron beam and focus it into as small an area as possible, approximately 50 to 100 Å in diameter. The smaller the achievable focal point, the higher the resolution of the scanning electron microscope. The electron beam scans the sample and interacts with the surface. The reflected electrons are then captured by detectors and an image of the surface of the sample is generated. A schematic of an scanning electron microscope is shown below in Figure 17.

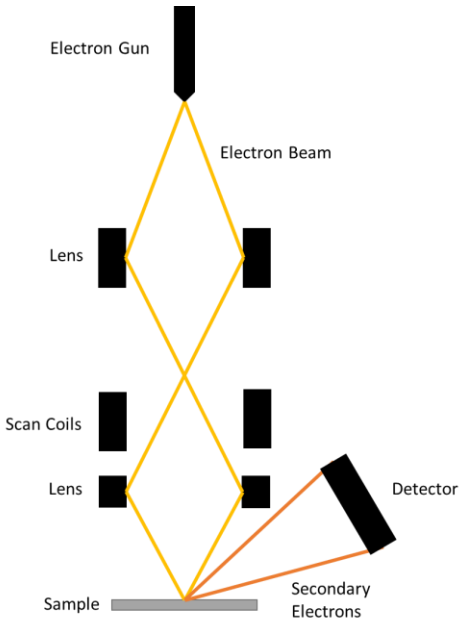

Figure 17: Schematic of a Scanning Electron Microscope. The incident electron beam is denoted in yellow and the secondary electrons which are to be detected are shown in orange.

The bombardment of a sample with high-energy electrons can cause damage to the samples and a build-up of electrons on the surface of the sample. If samples being studied are not conductive of electrons, then it is necessary to coat the samples first in a thin layer of conductive metal. This is most commonly gold although carbon is also used. This coating allows for the dissipation of the electrons and results in better quality images with reduced blurring.

A by-product of the interactions of the electron gun with the sample being studied is the generation of characteristic X-rays of the elements present in the sample, much in the same way X-rays are generated in X-ray tubes and in X-ray fluorescence spectroscopy (XRF). These characteristic wavelengths can then be studied and so an elemental image of the sample can be obtained. This is known as energy dispersive spectroscopy or energy dispersive X-ray (EDS/EDX respectively). It is however advised not to coat the sample in metal if such elemental

analysis is required as this offers no benefits, blurring is not an issue, and can cause false positives results for the presence of gold in the sample. Often, if both methods of analysis are desired, two individual samples are prepared with and without the gold coating.

For the work presented here, a JEOL JCM-6000Plus SEM was used with an accelerating voltage of 15 V. Powder samples of umbite ($K_2ZrSi_3O_9 \cdot H_2O$) held on an aluminium scanning electron microscope stub through a sticky carbon pad. To aid in imaging and to prevent charge build up, samples were sputter-coated with gold to act as an electron dispersion layer. The sputter-coating was performed at The University of Lancaster and the SEM imaging was performed at The University of Central Lancashire.

3.4 Nitrogen Gas Adsorption

Gas adsorption is a technique frequently used in the characterisation of porous materials allowing for the determination of pore size and surface area of a system. Whilst many other adsorptives are available, nitrogen is still the most used due to its small particle size allowing it to measure pores of a variety of sizes, down to a microporous level. Initially a vacuum is created which is subsequently purged with N_2 gas [86]. The rate this gas is adsorbed is plotted against the pressure of the system and from this an isotherm is generated. By extending the process to the point where gas can condense in the pores, the fine pore structure of the system can be evaluated.

The first condensations are observed in the smaller pores, with larger pores following thereafter. The pressure is continually increased, through the addition of adsorptive, until the system is fully saturated. This leads to all the pores of assorted sizes being filled with condensed, liquid nitrogen. Then, the system is incrementally depressurised, and the evaporation of the liquid nitrogen is observed. The characteristics of the isotherm formed from this adsorption and subsequent desorption gives a variety of information regarding the system being studied [57]. The most basic isotherm is the Langmuir isotherm which is based on the following three assumptions:

- Monolayer coverage – a single layer of coverage is achieved only.
- No preference for adsorption sites – adsorption is even over the whole surface with no preference for any area.
- Adsorption is independent of any occupied sites – adsorption can occur anywhere regardless of any locally occupied sites.

When adsorption goes beyond monolayer coverage the Brunauer, Emmett, and Teller (BET) isotherm is more commonly used than the Langmuir isotherm.

The isotherms then generated can be categorised according to the following classification [87]:

Type I: Type I isotherms closely resemble the behaviours seen in a Langmuir isotherm and so shows monolayer formation. However, it can be noted that this may also be indicative of simply the filling of micropores and an extremely small pore diameter. This isotherm property is often seen in systems with extremely small pore sizes such as molecular sieves.

Type II: This isotherm shows an unrestricted monolayer-multilayer adsorption. Because of this it is interpreted not simply by the Langmuir isotherm but also by the Brunauer, Emmett, and Teller (BET) isotherm after monolayer adsorption is achieved. This isotherm is often seen in systems with pore sizes > 500Å.

Type III: This classification of isotherms is extremely rare and, in all cases, shows a weak interaction between the adsorptive and the adsorbent. They can be characterised by their lack of plateau and thus lack of monolayer formation. These isotherms are most often found H_2O adsorption on graphitised carbons.

Type IV: Noted for the presence of a hysteresis. Type IV isotherms are present for systems with narrow (20 – 50Å) pores. This narrow pore size facilitates condensation. This condensation occurs when after the formation of monolayers further adsorptive gas is admitted into the system causing a condensation above the monolayer and within the pores.

Type V: Very similar to type IV, type V isotherms exhibit a hysteresis but are often found in systems where pore size is not well defined.

Type VI: Readily obtained by the adsorption of noble gases onto well-defined systems the type VI isotherm shows a series of steps, each indicative of the first, second, third, etc. monolayer formation.

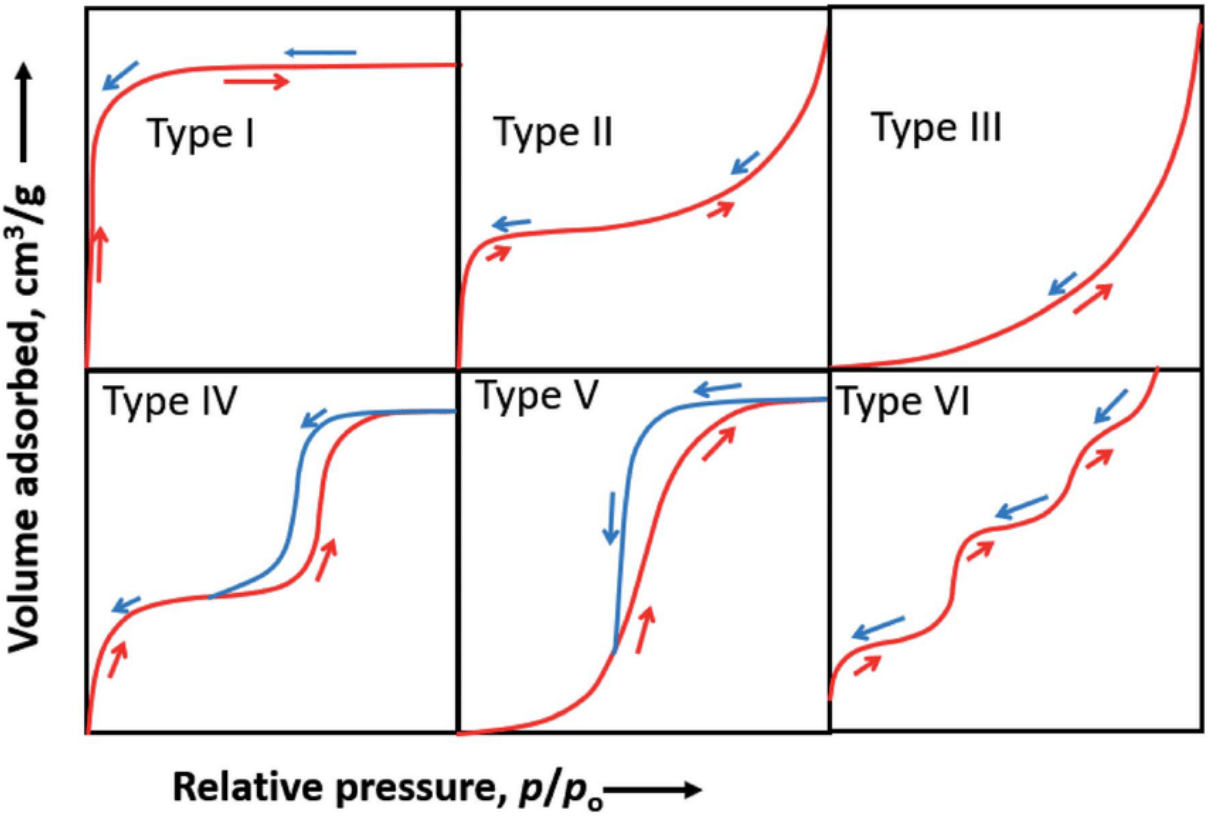

Figure 18: All isotherm types as classified by IUPAC [88].

Nitrogen gas adsorption was used in this project with the aim and intention of determining the total surface area and pore size distribution in the solid-state umbite samples that were synthesised and to see if the changes to the original zirconium-acetate solution used impacted these results. The nitrogen gas adsorption was performed. Nitrogen-gas adsorption was performed at Luxfer MEL Technologies ltd. A Tristar 3020 High Throughput Surface Area and Porosity Analyzer was used with N_2 as a probe gas.

4.0 Zirconium-oxychloride Refinements

The work described in this chapter details the iterative process for developing an acceptable refinement model of the solution species present in zirconium-oxychloride solutions using total scattering methods.

The ability to model aqueous zirconium solutions in the concentrations that this project requires was first developed through the modelling of the XPDF data obtained from solution samples of commercially available 22% zirconium-oxychloride. The zirconium-oxychloride solution was obtained from Luxfer MEL Technologies. Zirconium-oxychloride was chosen as the proof of concept solution as the structure proposed by Clearfield and Vaughn was relatively simple and rigid but no XPDF studies had yet been performed [1]. The structure proposed by Clearfield and Vaughan for the solid material, $ZrOCl_2 \cdot 8H_2O$, would be used as a starting model and its overall suitability would be assessed. If the model was deemed to be appropriate and concordant with the data obtained, selected parameters would be refined to determine the optimal iteration of this structure.

The data used in this chapter were collected on I15-1 at Diamond Light Source, UK. The 22% zirconium-oxychloride sample solution was loaded into bespoke 1.5 mm diameter quartz capillaries which were spun at high speed for 5-minute ambient temperature data collections. Data collections were run at 76 keV for optimal Q range of approximately 40 $Å^{-1}$. I15-1 employs a Perkin Elmer XRD 1611 CP3 area detector as a primary detector.

In summary, this chapter aims to:

- Model the solution species present in aqueous zirconium-oxychloride samples using XPDF data collected at Diamond Light Source.

- Compare these results to those found in literature and determine any differences between the two
- Assess the suitability of XPDF as a method of studying aqueous complex molecular species in solution.

4.1 Preparation of the Refinement Model

Before structural refinements can be performed an appropriate starting model must first be determined. For the refinement of zirconium-oxychloride, the crystallographic information file (CIF) for the Clearfield model [1] was obtained from The Inorganic Crystal Structure Database (ICSD) (collection code 16642) [89].

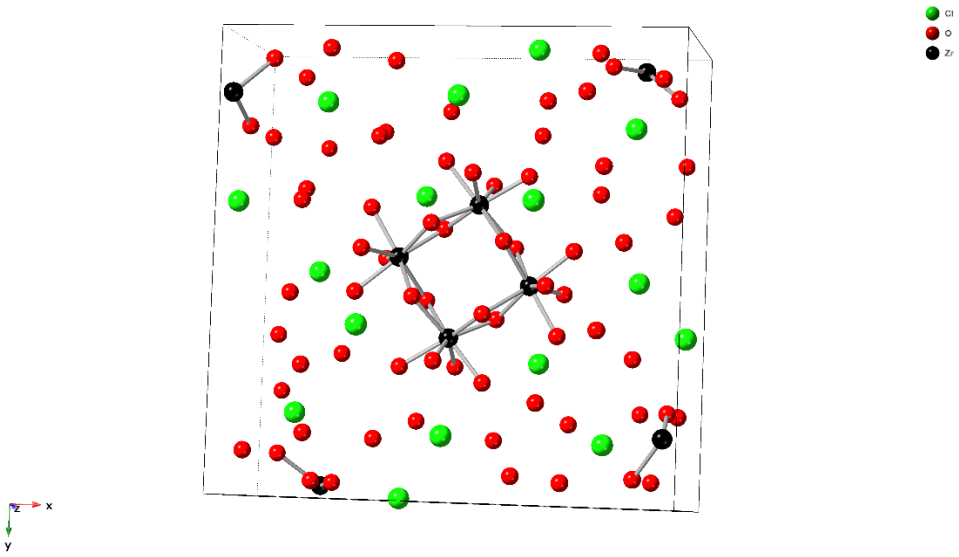

Figure 19: Unit-cell of the Clearfield model of $ZrOCl_2 \cdot 8H_2O$, as viewed down the c axis showing the tetrameric species $[Zr_4(OH)_8(OH_2)_{16}]^{8+}$. Key: Zr–Grey O–Red, Cl–Light Green [1].

Table 4: Space group and lattice parameters of the Clearfield model shown above [1].

Space Group	*a* (Å)	*b* (Å)	*c* (Å)	α = β = γ (°)
P -4 2_1 c	17.08	17.08	7.69	90

As this model is based on solid-phase samples, the long-range order that is implied by the CIF file was not appropriate for these liquid refinements. As such, the symmetry of the unit-cell, $P\,\bar{4}\,2_1c$, was removed and the system was set to have a symmetry of $P1$ using CrystalMaker [90]. This process did require the addition of new atomic positions based upon those obtained from the multiplicity of the sites in the original model. Originally the model could be expressed as just 12 sites (1 zirconium, 2 chlorine, and 9 oxygen) alongside the space group. Upon the removal of the symmetry of the system, the new model contained 96 unique atomic positions. From the newly created model, a single tetrameric unit was isolated. All other atomic positions were discarded and so the file contained just 4 zirconium positions and 24 oxygen positions. This single tetramer unit is shown in Figure 20.

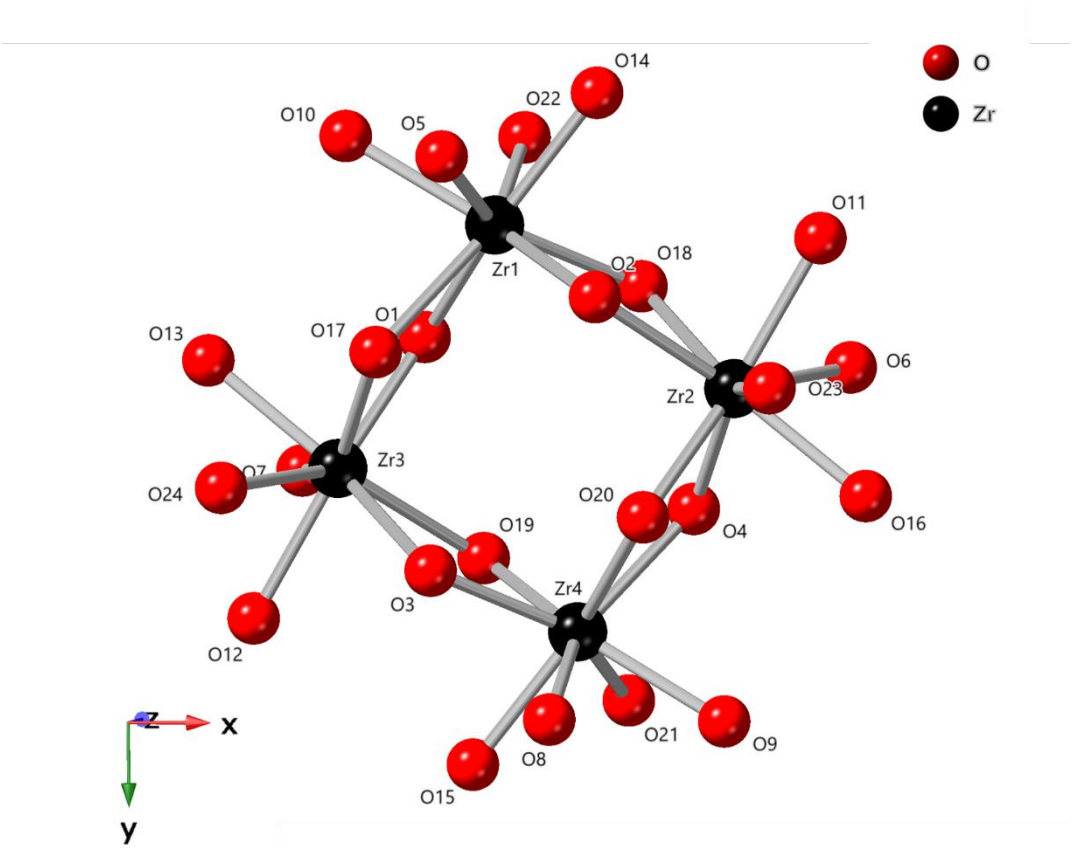

Figure 20: The single isolated tetramer unit ($[Zr_4(OH)_8(OH_2)_{16}]^{8+}$) as seen in the Clearfield model [1]. Key: Zr – Black, O – Red.

The model here obtained still had the lattice parameters of the original model proposed by Clearfield and Vaughn [1]. Any PDF patterns simulated with these lattice parameters would display intercluster interactions from the stacking of the small unit-cells. Therefore, it was crucial that the isolated tetrameric species be isolated in a "supercell". To avoid intercluster interactions, the lattice parameters were required to satisfy the following equation:

Equation 16: Equation of the minimum lattice parameters of a model used for PDF refinement to avoid intercluster interactions.

$$a > (2 \times r_{modelled}) + r_{species}$$

Where a is any lattice parameter, $r_{modelled}$ is the r range over which the modelling will be simulated, and $r_{species}$ is the longest intracluster distance in the species being modelled. For zirconium-oxychloride $r_{species}$ was estimated to be approximately 8.212 Å according to the starting model but structural changes as a result of the refinement process would change this.

The supercell chosen was 6 x 6 x 6 leading to total lattice parameters of *a* = 102.48 Å *b* = 102.48 Å *c* = 46.14 Å. The lattice parameters chosen for this supercell offered the ability to simulate PDF patterns through a broad range of r values up to ≈20 Å.

As it was only the intention to model the tetranuclear cluster, all contributions from the aqueous matrix were to be discarded. This was initially done as part of the data processing, performed in GUDRUNX [91]. The calculated amount of water contained in each sample was removed during the conversion from the 1-dimensional scattering pattern to the Fourier transformed PDF. This was done using a data collection of a sample of water which was deducted from the pattern. It was also through this method that the contribution of the quartz capillary in which the sample was held was removed. The resultant Fourier transformed PDF can be seen in Figure 21.

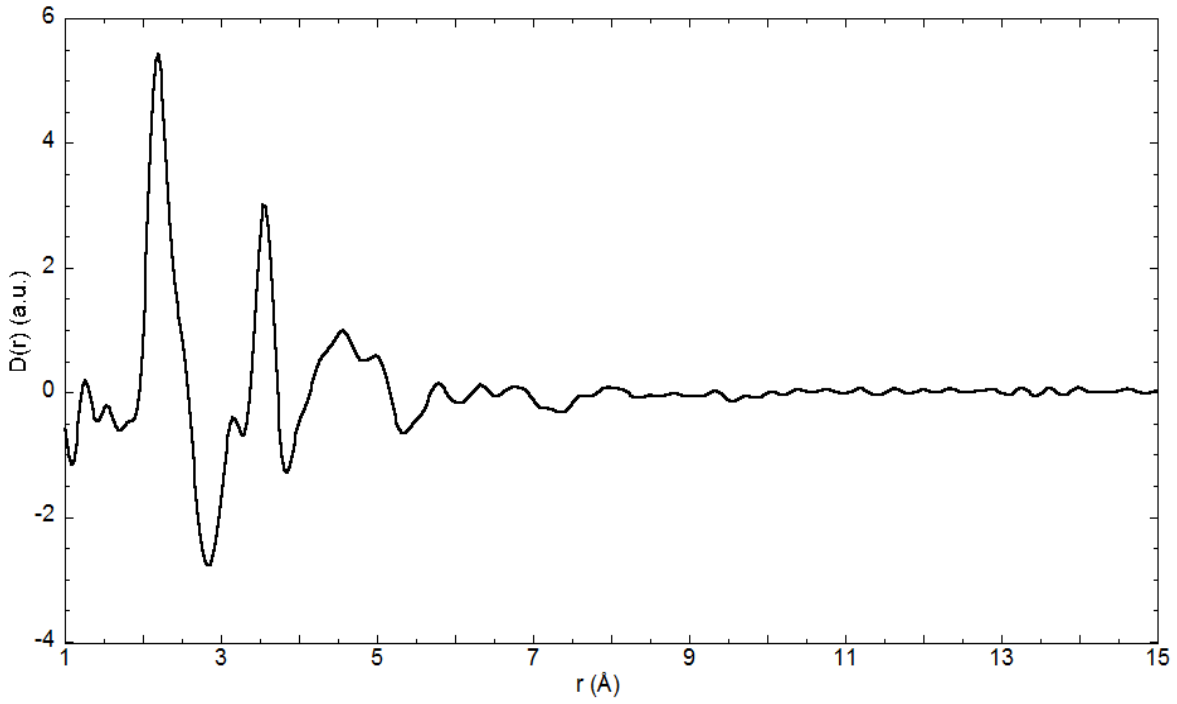

Figure 21: Fourier transformed PDF of zirconium-oxychloride processed using a water filled capillary as a background.

4.2 Refinement Method Iteration 1

Due to the inherent similarity between the two techniques the first iteration of the refinement was performed using a refinement strategy very similar to that involved in a typical Rietveld refinement of powder diffraction data. The three cartesian coordinates which represent each atomic position were each individually refined. To maintain the geometry of the tetrameric cluster, constraints to the atomic positions were applied. This restricted the movement of the atomic site to a factor of the total lattice parameter away from its original position. Initially a value of ± 0.02 of the lattice parameters was used, allowing movement in an anisotropic spheroid of dimensions ≈ 2 Å × 2 Å × 1 Å in the a, b, and c, directions respectively. An additional distance restraint upon the movement of the atomic positions was also applied. This restrained the distance between any pair of bonded atoms to values that were chemically sensible. These values were unique to each individual chemical bond in the cluster species. To represent the correlated motion, which is seen in PDF, simple single value thermal parameters (U_{iso}) are not sufficient. Instead, it is necessary to model the effective thermal parameter of an atomic position as a function of r. This allows for immediate neighbour atomic sites to display correlated motion which is not then modelled at higher r values. A spherical function with a low r plateau was used. This function allows for constant high levels or correlated motion for a low r window, which increases at a refineable value of r to a higher effective U_{iso} value at high r.

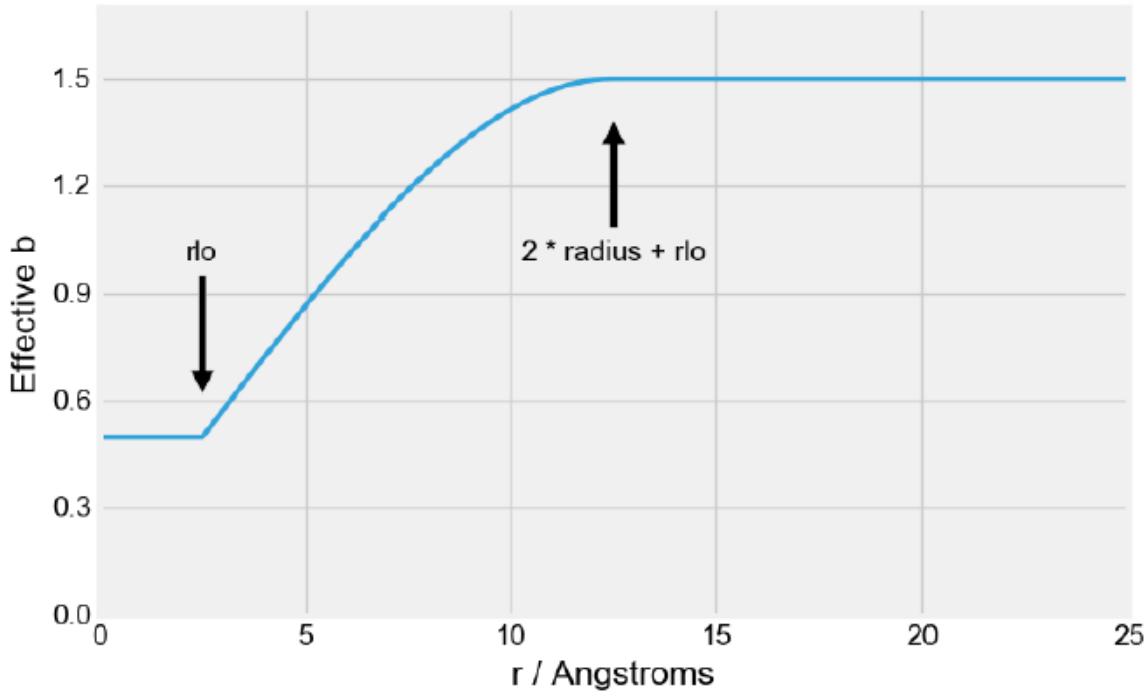

*Figure 22: The function of effective b value with respect to the distance r between an atomic pair. "rlo" the r value at which correlated motion stops being linear, and "2*radius + rlo" the r value at which the correlation again becomes linear are shown.*

The result of this refinement is shown below in Figure 23 and the cluster species is shown in Figure 24. A table of atomic coordinates for this structure is available in Table 1 in the appendix.

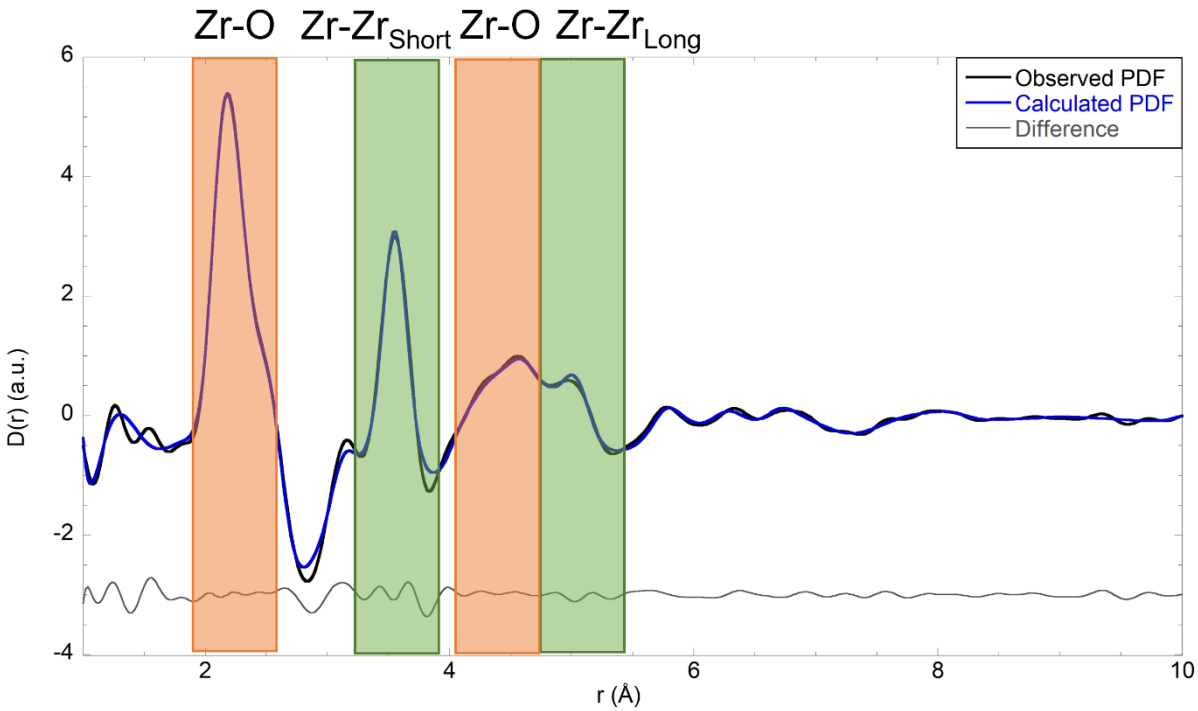

Figure 23: Resultant refinement of PDF data of zirconium-oxychloride using refinement method 1.

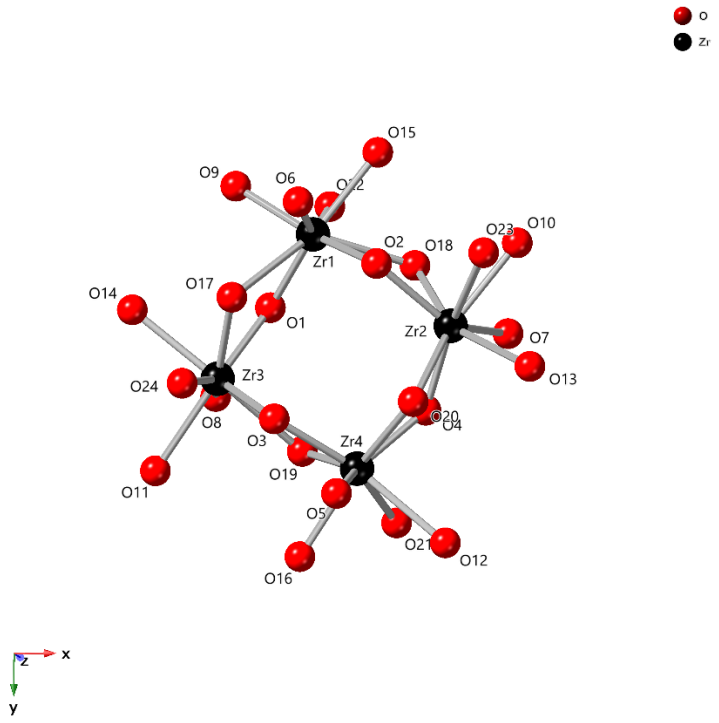

Figure 24: Structure of the resultant model ($[Zr_4(OH)_8(OH_2)_{16}]^{8+}$) of the refinement of zirconium-oxychloride using refinement method 1 Key: Zr – Black, O – Red.

The refinement converged with an R_{wp} of 7.72%. Such a low R_{wp} is considered a sign of good agreement to PDF data and this agreement is visible in the fit shown in Figure 23. It is upon further inspection of the model and its chemical feasibility that issues with this refinement

method become apparent. As is shown in Figure 24, the resultant structure of the tetrameric cluster showed no symmetry. The ability of each individual atomic position to refine almost independently leads to a highly asymmetric system.

The tetrameric cluster contains only Zr-O bonds. When refined, these bonds had distances ranging from 2.08 – 2.62 Å. This broad range of bond lengths in otherwise identical zirconium and oxygen positions is highly unlikely and this is further confirmed by the determination of the resultant oxidation state of the zirconium positions through the use of bond-valence calculations as described by Brown and Altermatt [92]. The Equation used is defined below in Equation 17.

Equation 17: Equation for determining oxidation state of the Zr atom for Zr-O bonds as determined by Brown and Altermatt [92] where r is the bond length and s is the calculated oxidation state of the Zr atom.

$$s = \exp[\ (1.928 - r)/0.37$$

The oxidation states for each of the four zirconium positions are shown below in Table 5.

Table 5: Bond lengths of Zr-O bonds and the resultant oxidation state as derived through bond-valence calculations described by Brown and Altermatt for refinement method 1 [92].

Atomic Site	Zr-$O_{Bridging}$ (Å)	Zr-$O_{in\text{-}plane}$ (Å)	Zr-$O_{Perpendicular}$ (Å)	Calculated oxidation state
Zr_1	2.14	2.22	2.22	3.18
	2.18	2.27	2.33	
	2.40			
	2.53			
Zr_2	2.08	2.23	2.34	3.03
	2.15	2.43	2.60	
	2.29			
	2.44			
Zr_3	2.13	2.29	2.11	3.38
	2.19	2.38	2.30	
	2.21			
	2.54			
Zr_4	2.09	2.21	2.33	3.15
	2.16	2.46	2.54	
	2.16			
	2.54			

The presence of Zr(III) in the cluster is highly unlikely as it is commonly agreed that zirconium prefers to adopt a +4 oxidation state.

It is only when the refined model is directly compared to the original Clearfield model that the two models can truly be judged as presented in Table 6.

Table 6: Bond lengths and angles of the Clearfield model and the model resulting of refinement 1 [1].

	$Zr\text{-}O_{Bridging}$ (Å)		$Zr\text{-}O_{in\text{-}plane}$ (Å)		$Zr\text{-}O_{Perpendicular}$ (Å)	
	Clearfield model [26]	Refined model (Iteration 1)	Clearfield model [26]	Refined model (Iteration 1)	Clearfield model [26]	Refined model (Iteration 1)
Zr_1	2.14	2.14	2.09	2.22	2.36	2.22
	2.21	2.18	2.13	2.27	2.37	2.33
	2.23	2.4				
	2.36	2.53				
Zr_2	2.14	2.08	2.09	2.23	2.36	2.34
	2.21	2.15	2.13	2.43	2.37	2.62
	2.23	2.29				
	2.36	2.44				
Zr_3	2.14	2.13	2.09	2.29	2.36	2.11
	2.21	2.19	2.13	2.38	2.37	2.3
	2.23	2.21				
	2.36	2.54				
Zr_4	2.14	2.09	2.09	2.21	2.36	2.33
	2.21	2.16	2.13	2.46	2.37	2.54
	2.23	2.16				
	2.36	2.54				
	$O\text{-}Zr\text{-}O_{bridging}$ angle (°)		$O\text{-}Zr\text{-}O_{in\text{-}plane}$ angle (°)		$O\text{-}Zr\text{-}O_{Perpendicular}$ angle (°)	
	Clearfield model [26]	Refined model (Iteration 1)	Clearfield model [26]	Refined model (Iteration 1)	Clearfield model [26]	Refined model (Iteration 1)
Zr_1	70.61	69.9	98.32	89.356	132.05	147.97
	75.17	70.34				
Zr_2	70.61	72.39	98.32	85.91	132.05	124.24
	75.17	72.8				
Zr_3	70.61	71.15	98.32	95.23	132.05	155.49
	75.17	75.54				
Zr_4	70.61	70.21	98.32	85.16	132.05	137.02
	75.17	78.44				

	Zr-Zr (Å)					
	Clearfield model [26]	Refined model (Iteration 1)	Clearfield model [26]	Refined model (Iteration 1)		
Zr_1	3.57	3.55	5.05	5.03		
		3.61				
Zr_2	3.57	3.55	5.05	5.06		
		3.56				
Zr_3	3.57	3.54	5.05	5.06		
		3.61				
Zr_4	3.57	3.56	5.05	5.03		
		3.54				

Literature studies indicate that whilst a range of Zr-O bond lengths have been observed in different structures, very rarely do these extend up to values as high as 2.62 Å. More commonly Zr-O bond lengths are found between 2.0 – 2.2 Å [93, 94]. Clearfield reported Zr-O bond lengths as long as 2.36 Å which is slightly beyond this conventional range [1]. Through the use of Shannon radii as determined by Shannon *et al.* [95, 96] conventional Zr-O bond lengths would be expected to be approximately 2.20 Å. Henceforth, 2.2 ± 0.2 Å will be considered a chemically sensible Zr-O bond.

It can be seen from Table 6 that, generally, the range of bond lengths of bridging oxygen positions, Zr-$O_{Bridging}$, are within the same, chemically feasible range. There is however a broadening of the range these values cover, with the largest bond lengths increasing from 2.36 Å to 2.54 Å in the Clearfield and refined models respectively, whilst the smallest bond lengths decrease by a smaller magnitude, from 2.14 Å to 2.08 Å in the Clearfield and refined models, respectively. The bond angles of these bridging oxygen positions remain largely the same although the lack of symmetry in the refined model once again leads each zirconium centre to have its own set of unique bond angles. The range of angles observed moves from 70.61° – 75.12° to a broader 69.90° – 78.44° in the Clearfield and refined models respectively. These differences to the central core bond lengths and angles do not change the structure drastically but do show the presence of some deviation to the highly ordered solid crystalline model.

The terminal oxygen positions show an increase in their bond lengths. The bond lengths of the oxygen positions in line with the plane, Zr-$O_{in\text{-}plane}$, all show increases from the Clearfield model. The smallest distance moves from 2.09 Å in the Clearfield model, to 2.21 Å in the refined model; a substantial change. The longest of these bond lengths moves from 2.13 Å to

2.46 Å which is a change of similar magnitude. The terminal positions which lie perpendicular to the plane, Zr-$O_{Perpendicular}$, show a general broadening of values with the smallest shrinking from 2.36 Å to 2.11 Å whilst the longest increases from 2.37 Å to 2.60 Å in the Clearfield and refined models, respectively.

Analysis of the angles between these terminal oxygen positions shows the most pronounced differences between the Clearfield structure and the result of this refinement. The angles of the "in plane" oxygen positions, O-Zr-$O_{in\text{-}plane}$, decrease from values of 98.32° to a range of unique values spanning 85.16° – 95.23°. The perpendicular positions also show substantial movement from 132.05° to 124.24° – 155.49°.

These changes are substantial and whilst they all support the presence of the tetrameric species in solutions, the structure does show that there is some variation in the terminal oxygen positions and that they do not conform to the rigid structure seen in the solid-state.

The process of removing the contributions of water to the scattering amplitude was also questioned. Removal of water as a background phase during the data processing is a common method when isolating a known phase for solid material PDF. However, the variations in the concentration of water and how this in turn impacts the PDF mean that removing a fixed percentage of water in the Fourier transform stage would not offer the required level of flexibility. This will be assessed in refinement iteration 2.

The refinement method itself was not without issue. The use of cartesian coordinates as the refinement parameters for each atomic position means the total number of parameters required to represent the structure alone is 84; x, y, z, for each of 28 atomic positions. Alongside this the thermal and background parameters lead to over 100 variables being refined from the single data set. Whilst this is well below the number of data points in the

collected data and as such does not statistically invalidate the result, it does cast doubt onto whether the method is reasonable and also whether optimisation can be performed to reduce this number as this could prove detrimental to the use for the method to refine larger systems.

It is due to the asymmetry of the resultant model and variations in otherwise identical bond environments and thus the models overall chemical unfeasibility that, despite the good agreement between the observed and calculated PDF, this model was not deemed valid.

The higher number of parameters meant the refinement process was inefficient and as such, a superior method and resulting model was desired.

4.3 Refinement Method Iteration 2

The previous refinement method removed the contribution of water from the samples PDF prior to refinement during the processing of the PDF. Due to the inflexibility of this method, it was felt that a more accurate approach would be to include the water contributions in the refinement as a separate phase. This allows for the scale of the water removal to be refined and varied to ultimately improving the agreement to the observed PDF. This method would also allow for application in other systems, with little modification, where the water : metal cluster ratio is different or unknown. From the same original diffraction data, a new PDF was generated leaving the contributions from the water in the PDF. As a result of this a new PDF data set was obtained where the only background subtraction used was that of the sample holder and not of the water contribution. The resulting Fourier transformed PDF can be seen below in Figure 25.

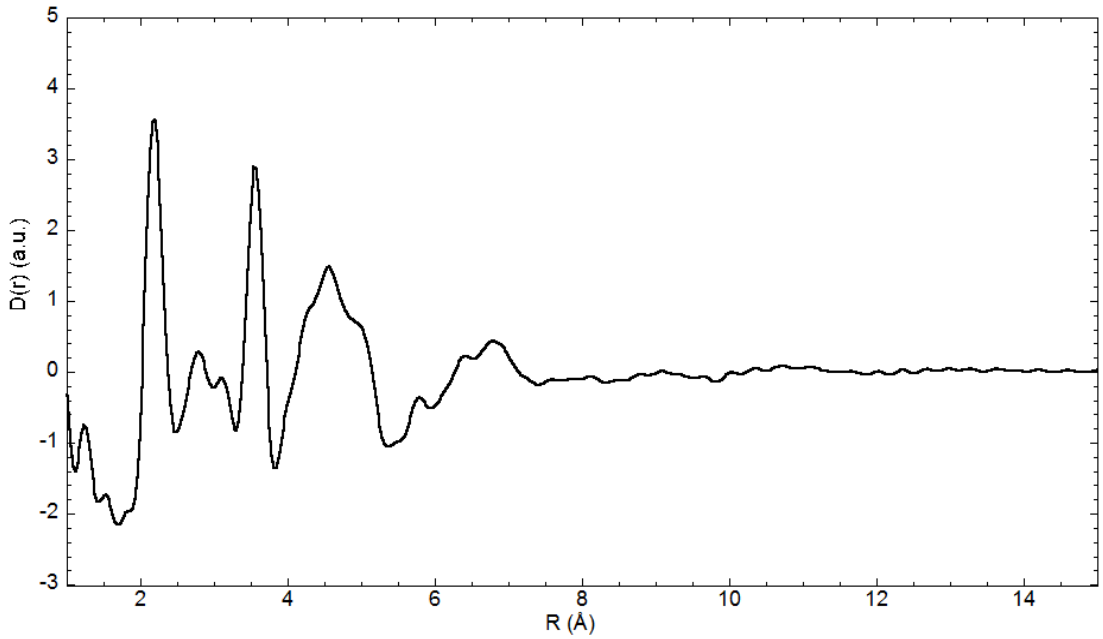

Figure 25: Fourier transformed PDF of zirconium-oxychloride processed using an empty capillary as a background.

In an attempt to reduce the number of parameters involved in the refinement of the model it was decided that it would be ideal to employ a Z-matrix to represent the relationship between atoms in the cluster. A Z-matrix defines every atom in turn with respect to the atoms which have previously been introduced. Beyond the first three atomic sites, each additional site requires a radial distance from a previous site ($site_1 - site_2$), a "bond" angle to a second atomic site through the first ($site_1 - site_2 - site_3$), and a dihedral angle to a third and final atomic site ($site_1 - site_2 - site_3 - site_4$). An example of the first few lines of a Z-matrix definition is shown below in Figure 26.

```
rigid
   z_matrix Xl
   z_matrix X2 Xl 1
   z_matrix X3 Xl 1 X2 90
   z_matrix Zr3 Xl =rXZr; X2   0 X3 90
   z_matrix Zr4 Xl =rXZr; X2  90 X3 90
   z_matrix Zr2 Xl =rXZr; X2 180 X3 90
   z_matrix Zrl Xl =rXZr; X2 270 X3 90
```

Figure 26: The first 8 lines of a Z-matrix used to define the zirconium-oxychloride tetramer showing the definition of the core 4 zirconium positions. This Z-matrix also contains a parameter "=rXZr;" which is used to group common terms.

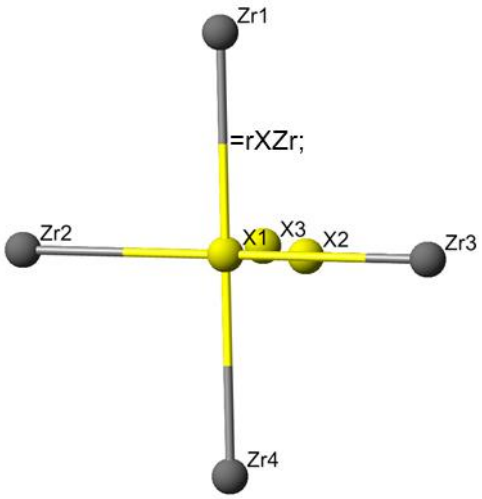

Figure 27: Model resulting from the Z-matrix shown in Figure 26. The core 3 atomic positions (X1, X2 and X3) are shown in yellow and the 4 Zr positions are shown in Grey. The bonds between are representative of the distance =rXZr; from Figure 26.

This allows atoms, not to be defined by their individual locations in 3-dimensional space, but instead to be defined as a relationship to one another. The efficacy of the Z-matrix is amplified when combined with the use of repeating parameters. Each bond distance, angle, and dihedral angle can be grouped into a number of parameters linking similar values. When applied to the zirconium-oxychloride structure this allowed for all Zr-$O_{bridging}$ bonds to be treated equally whilst remaining different to the Zr-$O_{terminal}$ bonds which, in turn, were all treated equally also. This is chemically sensible as it is likely that bonds which exist in identical environments will share common values and characteristics.

The development of a Z-matrix is, however, not without potential for error. The use of parameters to define atomic positions means that in refinements, only these parameters can be refined. As such, the structure must be thoroughly examined and the potential opportunities for movement must be available as refineable parameters. Failure to express a permitted direction of movement as a parameter can lead to refinements entering false minima whereby the true structure remains unachievable with the current Z-matrix. In this way a Z-matrix is not just a description of a structure but also it denotes all chemically sensible movements which must be first assessed during its creation.

Through the development of a Z-matrix for the tetrameric species, the cluster was able to be defined by 7 variables instead of the previous 84.

The background function was also revised in the transition from iteration 1 to iteration 2. Where previously a 20-point Chebyshev background function was used, this was replaced with a linear background with an error function. This more accurately represents the background present in a PDF dataset without overcompensating whilst also reducing the number of refineable background parameters from 20 to 3.

The results of this refinement are presented in Figure 28 and the structure of the cluster species in Figure 29. The atomic coordinates of this model are presented in Table 2 in the appendix.

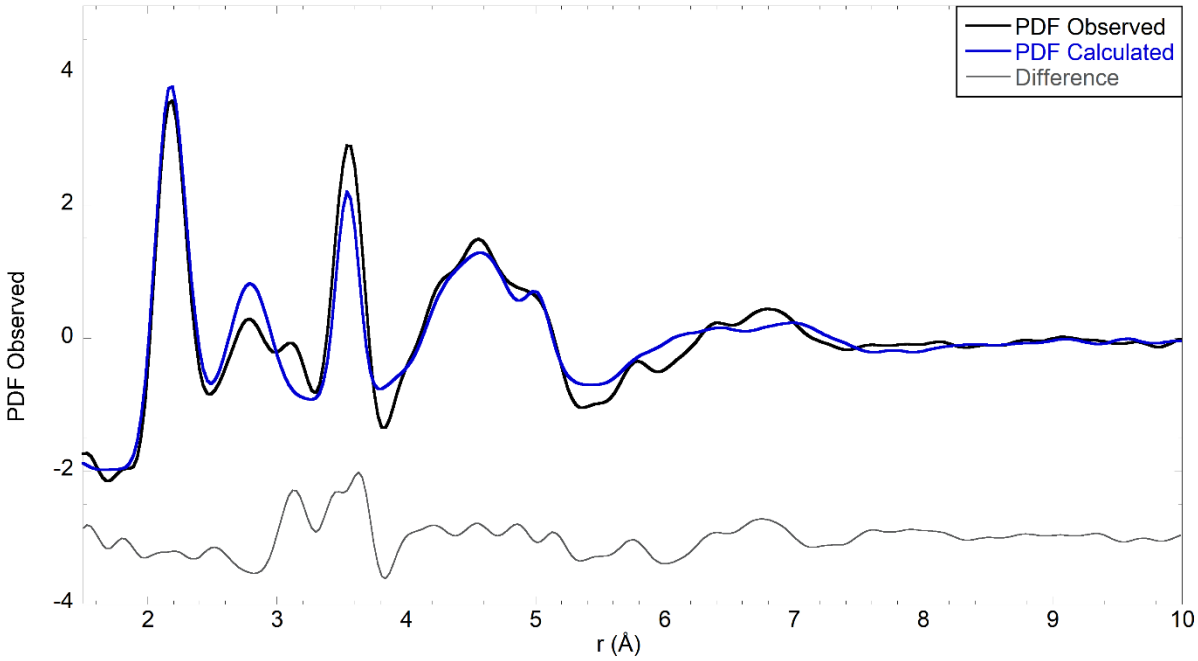

Figure 28: Resultant refinement of PDF data of zirconium-oxychloride using refinement method 2. This refinement iteration modelled the water contribution rather than removing it from the data set as a background measurement.

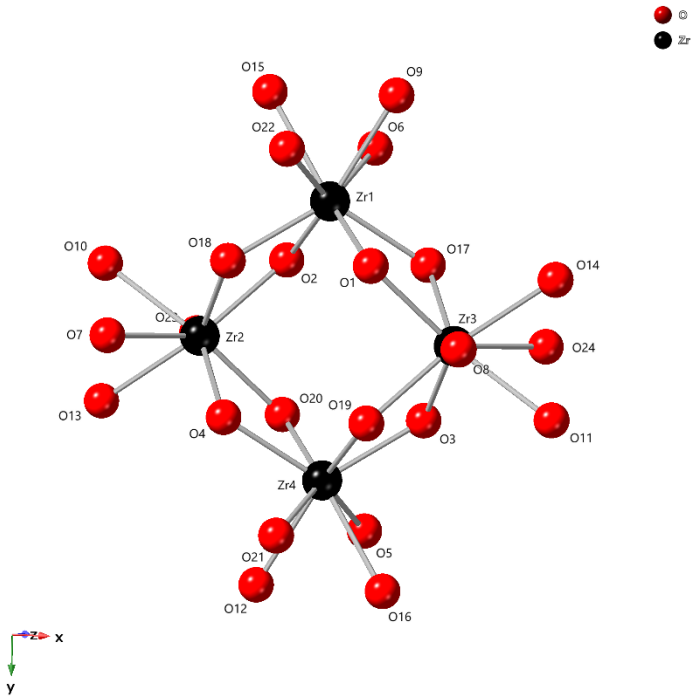

Figure 29: Structure of the resultant model ($[Zr_4(OH)_8(OH_2)_{16}]^{8+}$) of the refinement of zirconium-oxychloride using refinement method 2 Key: Zr – Black, O – Red.

This refinement converged with a higher R_{wp} percentage than refinement iteration 1 at 27.92%. This value is still considered good agreement for PDF data which traditionally obtains

R_{wp} an order of magnitude higher than the best PXRD experiments. The principal peaks of the PDF are fitted with reasonable agreement. There are some differences in the 2.5 – 3.5 Å region where the calculated and observed PDF do not completely agree.

As a test of chemical feasibility, bond-valence sums were used to determine the oxidation state of the zirconium environments. Due to the symmetry imposed by the Z-matrix, each Zr position in the cluster has the same combination of Zr-O bond lengths and as such the same oxidation state. This is shown in Table 7.

Table 7: The resultant oxidation state as derived through bond-valence calculations described by Brown and Altermatt for refinement method 2 [92].

Atomic Site	Zr-$O_{Bridging}$ (Å)	Zr-$O_{in\text{-}plane}$ (Å)	Zr-$O_{Perpendicular}$ (Å)	Calculated oxidation state
$Zr_{1\text{-}4}$	2.18	2.30	2.12	3.94

The resultant calculated oxidation state of approximately 4 is in good agreement with zirconium's preference to the Zr(IV) form and is an improvement from the value of 3.62 seen in the Clearfield single crystal model. The model of the tetramer seems chemically sensible with all Zr-O bonds being within reasonable ranges of values found in literature and determined through the use of Shannon radii [93-96]. The impacts of the refinement can be best seen when the refined model and its values are compared to those of the original solid-state model as proposed by Clearfield and Vaughn [1]. This is shown in Table 8.

Table 8: Bond lengths and angles of the Clearfield model and the model resulting from refinement 2 [1].

$Zr\text{-}O_{Bridging}$ (Å)		$Zr\text{-}O_{in\text{-}plane}$ (Å)		$Zr\text{-}O_{Perpendicular}$ (Å)	
Clearfield model [26]	Refined model (Iteration 2)	Clearfield model [26]	Refined model (Iteration 2)	Clearfield model [26]	Refined model (Iteration 2)
2.23	2.18	2.09	2.3	2.36	2.12
2.36		2.13		2.37	
2.21					
2.14					
$O\text{-}Zr\text{-}O_{bridging}$ angle (°)		$O\text{-}Zr\text{-}O_{in\text{-}plane}$ angle (°)		$O\text{-}Zr\text{-}O_{Perpendicular}$ angle (°)	
Clearfield model [26]	Refined model (Iteration 2)	Clearfield model [26]	Refined model (Iteration 2)	Clearfield model [26]	Refined model (Iteration 2)
70.61	69.99	98.32	65.68	132.05	126.91
75.17					
$Zr\text{-}Zr_{Short}$ (Å)		$Zr\text{-}Zr_{Long}$ (Å)			
Clearfield model [26]	Refined model (Iteration 2)	Clearfield model [26]	Refined model (Iteration 2)		
3.57	3.55	5.05	5.02		

It can be seen that the bond lengths between the two models show good agreement, all being in the same general region. The core $Zr\text{-}O_{bridging}$ bonds are very similar going from a range of values from 2.14 – 2.36 Å to a single value of 2.18 Å in the Clearfield and refined models respectively. The terminal oxygens are where the most variation occurs. The length of the $Zr\text{-}O_{in\text{-}plane}$ bond length in the Clearfield model is similar to that of the $Zr\text{-}O_{Perpendicular}$ in the refined model and vice versa. But it is noted that both sets of bond lengths are in chemically sensible ranges.

The bond angles of the core cluster, like the bond lengths, remain largely unchanged, refining from two values of 70.61° and 75.17°, to a single value of 69.99° which while differing from the latter, is consistent with the former. This agreement combined with that found in the bond lengths is a sign that the core of this tetrameric cluster remains unchanged between the solution and the liquid phases. Once again, the major variations are to be found in the terminal oxygen positions. Here we see a contraction of the angle between the in-plane oxygens, O-Zr-$O_{in\text{-}plane}$, which move from 98.32° to 65.68°. This contraction is coupled with a contraction in the out of plane oxygen bond angles O-Zr-$O_{Perpendicular}$, which show a movement from 132.05° to 126.91°.

This shows that in the transition from the solid-phase to the solution phase, and the subsequent relaxation this incurs, the core structure remains unchanged but the terminal oxygen positions migrate towards the diagonals of the structure. It is believed that this effect is caused by the relaxation induced by the phase change from solid to aqueous, but also by some interaction between the cluster and the free chloride ions which would be in solution. Thus, refinement iteration 3 was designed.

4.4 Refinement Method Iteration 3

Refinement iteration 3 was created with the concern that previous refinement iterations, whilst accurately describing the cluster species were not acknowledging the presence of Cl ions in solution. The Clearfield model explicitly stated that no halide – cluster bonds were found in the solid-state and so previous refinements disregarded the halide ions with the ambition of resolving the structure of the pure cluster [1]. It is however noted that the tetrameric cluster carries an 8+ charge. This net positive charge would need to be balanced to obtain a neutral solution. This charge balancing by the chloride ions infers an ion-dipole interaction and thus a strong correlation and so it was felt prudent to incorporate Cl^- ions into the structural refinement.

To the model, 8 charge-balancing chloride ions were added. These were placed perpendicular to the bridging hydroxyl groups and set just above and below the equatorial plane. These positions are similar to those seen in the solid model of $ZrOCl_2 \cdot 8H_2O$ by Clearfield [1]. This new starting model can be seen in Figure 30.

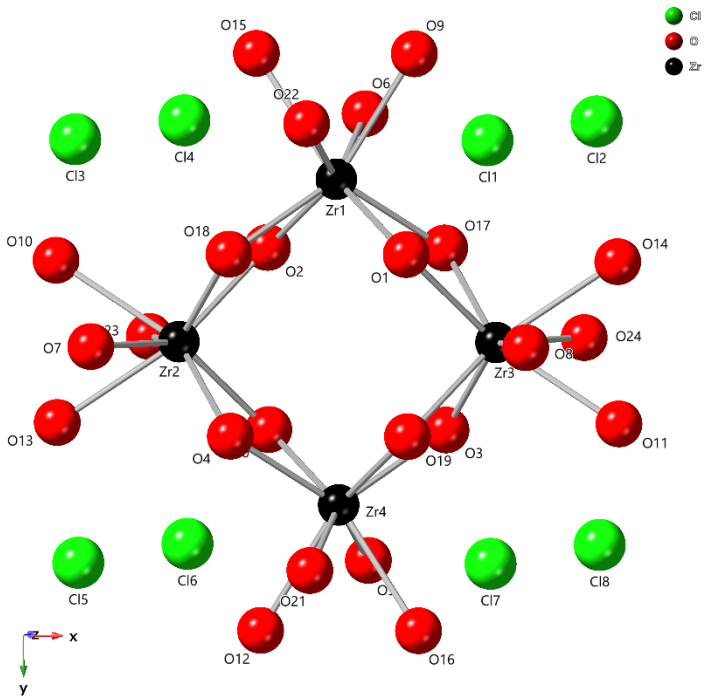

Figure 30: Starting model of refinement iteration 3 showing the location of the chlorine positions. Key: Zr – Black, O – Red, Cl – Lime Green.

This new model was refined against the collected data used in refinement iteration 2 and all other parameters were kept the same. The chlorine positions were defined relative to the centre of the cluster and as such were allowed to change their distance to the cluster and their angle from the equatorial plane. The result of this refinement can be seen in Figure 31 and Figure 32 and the atomic coordinates can be found in the appendix in Table 3.

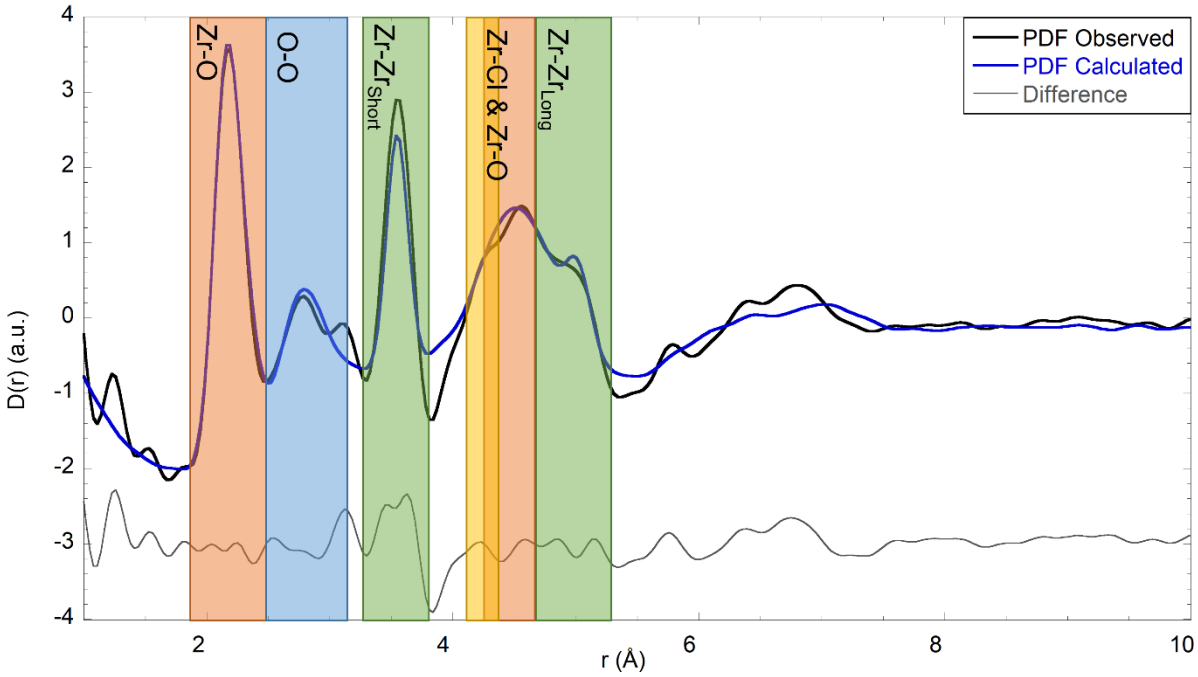

Figure 31: Resultant refinement of PDF data of zirconium-oxychloride using refinement method 3.

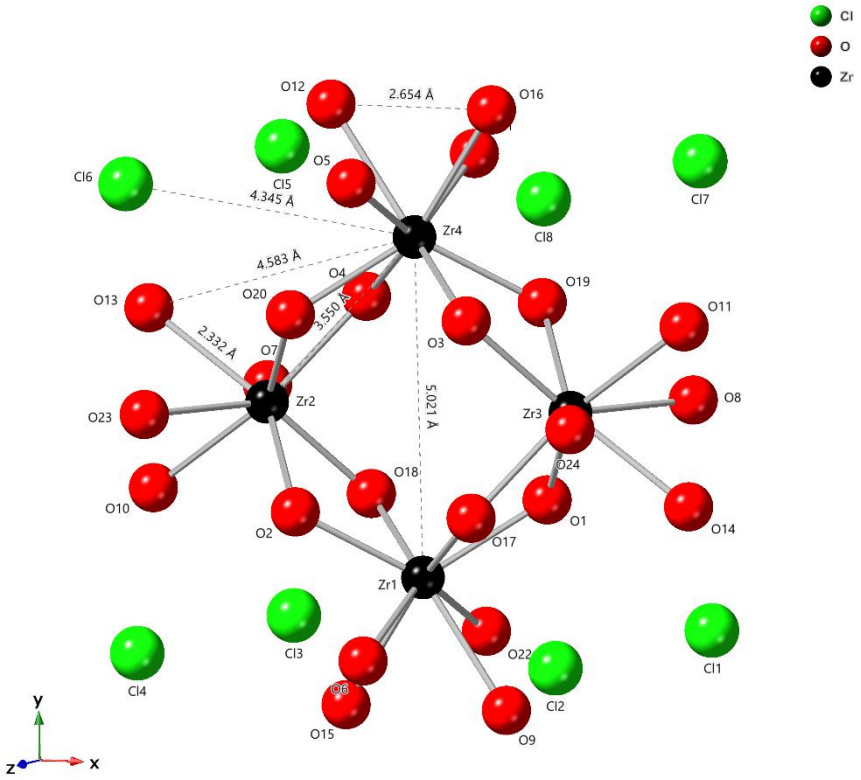

Figure 32: Structure of the resultant model of the refinement of zirconium-oxychloride using refinement method 3 Key: Zr – Black, O – Red, Cl – Lime Green.

This refinement converged with an R_{wp} of 23.12%, a drop of over 4%. The introduction of chlorine positions into the refinement has significantly improved the refinement and this can

be seen from a visual inspection of the region around 2 – 3.5 Å. In this are the first principal peak, that of the Zr-O contact distance is fitted almost perfectly. The smaller peaks between the Zr-O peak and the Zr-Zr peak, at approximately 2.5 Å no longer shows over estimation in the calculated model and whilst the fitting profile is not perfect it is still a marked improvement from the previous refinement iteration. This improvement has been achieved with the introduction of a minimal number of new parameters; only 4, 2 thermal parameters and 2 structural.

To qualitatively analyse this model however, the key parameters of the model must first be analysed to ascertain if they are chemically feasible, and compared to those of the Clearfield model as has been done in previous iterations. These can be seen in Table 9.

Table 9: Bond lengths and angles of the Clearfield model and the model resulting of refinement 3 [1].

$Zr\text{-}O_{Bridging}$ (Å)			$Zr\text{-}O_{in\text{-}plane}$ (Å)			$Zr\text{-}O_{Perpendicular}$ (Å)		
Clearfield model [26]	Refined model (Iteration 2)	Refined model (Iteration 3)	Clearfield model [26]	Refined model (Iteration 2)	Refined model (Iteration 3)	Clearfield model [26]	Refined model (Iteration 2)	Refined model (Iteration 3)
2.23	2.18	2.16	2.09	2.3	2.33	2.36	2.12	2.18
2.36			2.13			2.37		
2.21								
2.14								
O-Zr-$O_{bridging}$ angle (°)			O-Zr-$O_{in\text{-}plane}$ angle (°)			O-Zr-$O_{Perpendicular}$ angle (°)		
Clearfield model [26]	Refined model (Iteration 2)	Refined model (Iteration 3)	Clearfield model [26]	Refined model (Iteration 2)	Refined model (Iteration 3)	Clearfield model [26]	Refined model (Iteration 2)	Refined model (Iteration 3)
70.61	69.99	67.071	98.32	65.68	69.36	132.05	126.91	124.72
75.17								
Cl-$O_{bridging}$ (Å)			Cl-Zr (Å)			Cl angle from plane (°)		
Clearfield model [26]	Refined model (Iteration 2)	Refined model (Iteration 3)	Clearfield model [26]	Refined model (Iteration 2)	Refined model (Iteration 3)	Clearfield model [26]	Refined model (Iteration 2)	Refined model (Iteration 3)
3.18		3.1	4.73		4.35	43.89		53.25
$Zr\text{-}Zr_{Short}$ (Å)			$Zr\text{-}Zr_{Long}$ (Å)					
Clearfield model [26]	Refined model (Iteration 2)	Refined model (Iteration 3)	Clearfield model [26]	Refined model (Iteration 2)	Refined model (Iteration 3)			
3.57	3.55	3.55	5.05	5.02	5.02			

Table 9 clearly shows that the model resulting of refinement iteration 3 is extremely similar to that from iteration 2. The Zr-O bond lengths are in good agreement with maximum variation of 0.05 Å.

The bond angles also showed good levels of agreement. The contraction of the terminal oxygen positions into the diagonal corners of the structure is still present as seen in the previous iteration. This allows room for the newly incorporated chlorine environments which sit perpendicular to the bridging oxygens and thus between the clusters of terminal oxygens.

The newly introduced chlorine positions come with their own set of measurable parameters, and these are also shown in Table 9. The Cl-$O_{bridging}$ distance is the distance between the new chlorine positions and the nearest bridging oxygen position. It was found to be similar to that observed in the solid-state model with the chlorine positions slightly closer, 0.08 Å, to the cluster species in the solution form. In this model each chlorine position had two nearest neighbour Zr positions which were both equidistant. This distance is decreased in the transition from the solid to the liquid model, moving from 4.73 Å to 4.35 Å, a decrease of 0.38 Å. The angle the chlorine atoms sit from the plane was determined to increase from 43.89° to 53.25° showing that the chlorine atoms sit further away from the plane of the cluster in the liquid phase, and closer to the axial region perpendicular to the plane.

All of the zirconium positions in the model refined here display +4 oxidation state, as displayed in Table 10.

Table 10: The resultant oxidation state as derived through bond-valence calculations described by Brown and Altermatt for refinement method 3 [92].

Atomic Site	$Zr\text{-}O_{Bridging}$ (Å)	$Zr\text{-}O_{in\text{-}plane}$ (Å)	$Zr\text{-}O_{Perpendicular}$ (Å)	Calculated oxidation state
$Zr_{1\text{-}4}$	2.156	2.332	2.181	3.84

The visual agreement of this refinement and the high level of chemical sense shown by the model obtained increases the confidence in this refinement iteration. The similarities to a previous model, iteration 2, with the marked improvement of incorporating hydrogen bonded chloride ions, which are known to be in solution, leads to the conclusion that this model is that present in aqueous solutions of zirconium-oxychloride.

Two alternative models which were suggested in literature were also tested [30, 97]. Both were octameric species in slightly differing conformations. These can be seen below in Figure 33.

Figure 33a shows an octameric structure proposed by Tyrsted *et al.* [97]. which is made up of a pair of tetrameric species linked by a pair of dual bridging oxy-hydroxyl groups. Figure 33b shows an alternative octameric species formed by another pair of tetramers stacked on top of one another. This model was described by Singhal *et al.* [30]. For both of these refinements the data set produced in refinement iterations 2 and 3 was used. A Z-Matrix describing the structures was produced with thermal functions like those used in iterations 2 and 3. The refinements were carried out over the same range in r of the PDF.

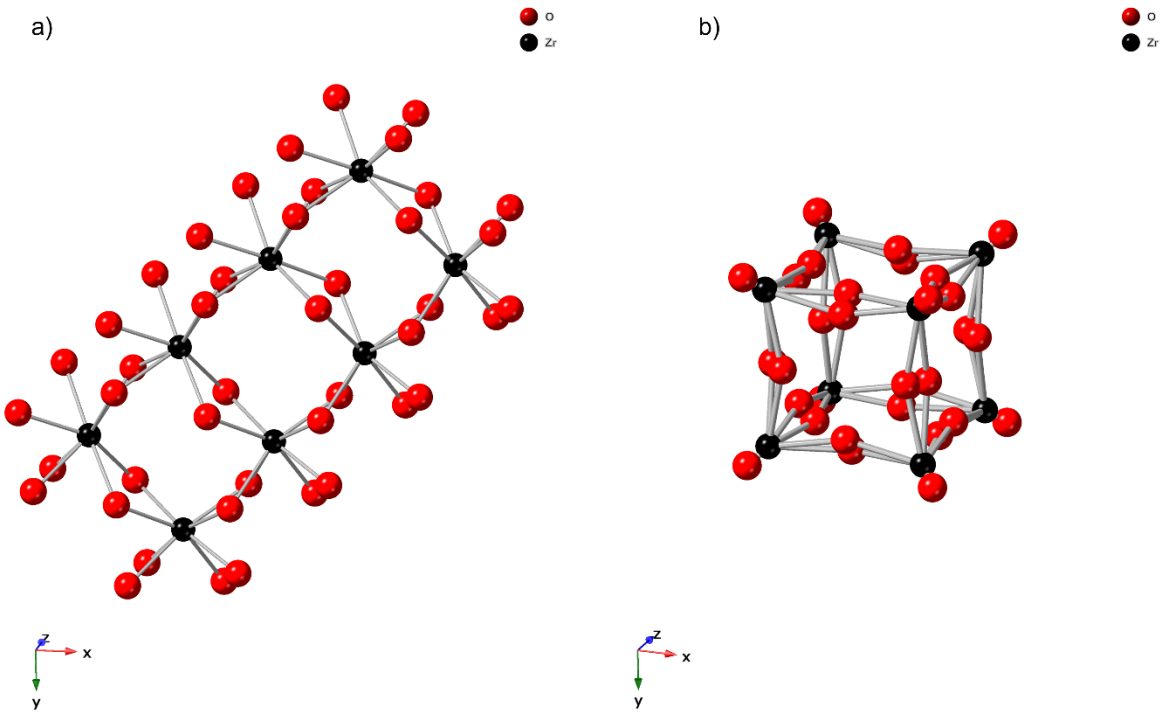

Figure 33: The structures of two alternative models which were assessed in this work. Key: Zr – Black, O – Red.

These refinements converged with high R_{wp} values, 32.76% and 63.59% respectively, and when unrestrained tended towards chemically unfeasible bond lengths and angles. Neither displayed a chemically sensible model with good agreement to the observed data. The refinements can be seen below in Figure 34 and Figure 35, and it can be seen that the observed PDF shows extremely poor agreement to both systems.

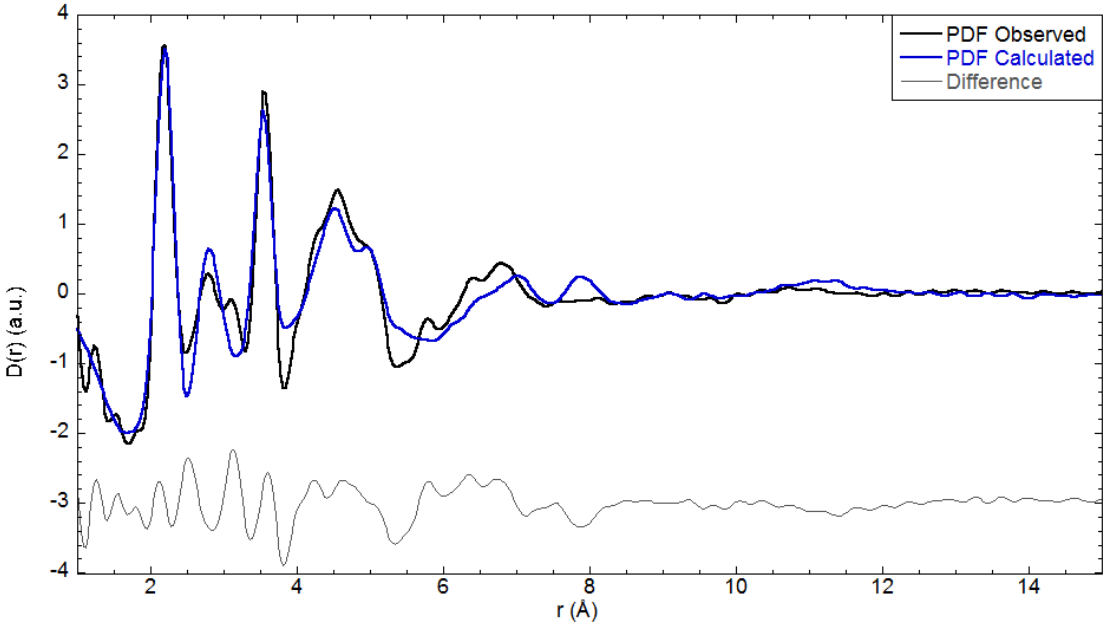

Figure 34: Refinement of PDF data of zirconium-oxychloride using the model shown in Figure 33a.

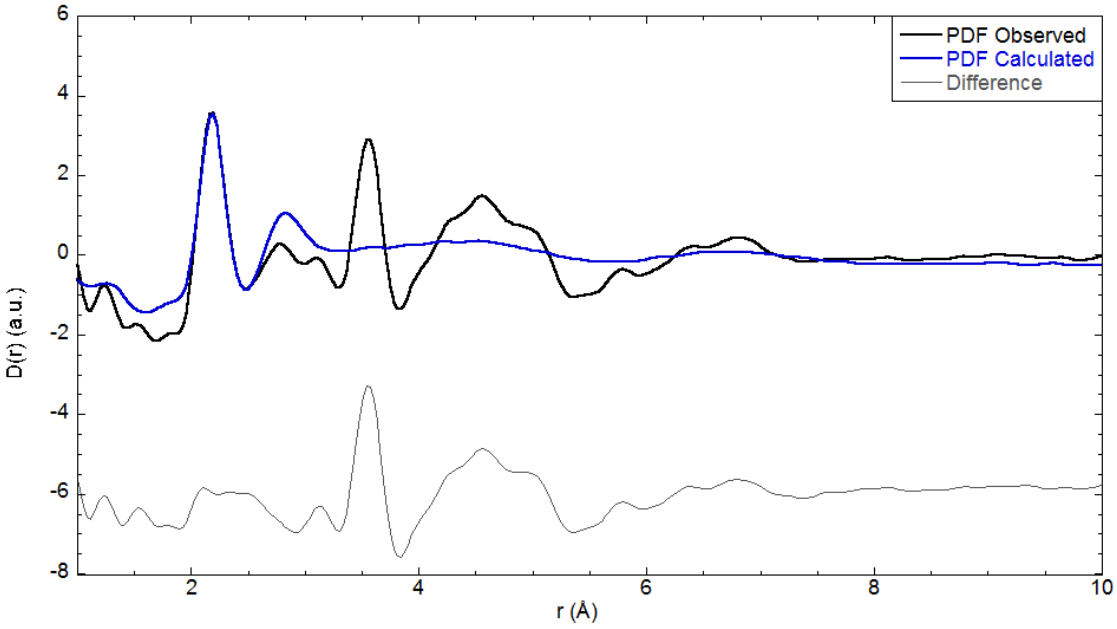

Figure 35: Refinement of PDF data of zirconium-oxychloride using the model shown in Figure 33b.

Figure 34 shows reasonable agreement but the calculated PDF shows features in longer ranges of r than those seen in the observed. Figure 35 shows a much lower level of agreement with no features other than the first Zr-O contact distance being resolved well in the calculated PDF.

The originally proposed Clearfield model has not been rejected and the presence of the tetrameric species and the close association with the chloride ions has been confirmed [1]. The Clearfield model has, however, been refined and the relaxations in the structure, resultant of the transition between the solid and aqueous phase of the sample, have been determined and quantified.

This model also serves to enable the completion of the subsequent portions of this research project. The successful determination of this species has led to the development of the optimal method for the identification and characterisation of the molecular zirconium species present in solutions through the use of PDF data. The method here developed will be applied in subsequent chapters and it is believed that the refinements presented in this chapter have proven the validity of the method therein applied.

5.0 Preliminary Investigation of Commercial Samples

This chapter aims to discuss preliminary investigations into the study of the nature of the zirconium species present in zirconium-acetate solutions. This work was performed prior to the ageing study that makes up the principal component of this project.

These preliminary works aimed to achieve three goals:

- Determine if the EXAFS data observed by Hennig *et al.* [2] was replicable in the context of these commercially available aqueous samples given their differing synthesis routes.
- To determine if EXAFS was a suitable technique for the analysis zirconium-acetate solutions.
- To determine if XPDF could be used as an alternative technique to study zirconium-acetate solutions given the disadvantages commonly incurred through the use of EXAFS, namely a decrease in the measurable range.

It was determined that the optimal way to deduce this information and thus inform whether a broader ageing study would require the use of XPDF, would be to perform a new set of EXAFS measurements on a small range of commercially available zirconium-acetate solutions and see if the results reproduce those seen by Hennig *et al.* [2] Hennig *et al*. had previously studied the nature of the solution species present in solutions of zirconium-oxychloride as acetic acid is added. This work was undertaken using EXAFS and so was repeated to investigate whether the concluding structures, the tetrameric $[Zr_4(OH)_8(OH_2)_{16}]^{8+}$, and the hexameric $Zr_6(O)_4(OH)_4(CH_3COO)_{12}$ were present in these commercially available solutions.

Secondly, XPDF measurements would be taken of the same limited range of zirconium-acetate samples to determine if the materials could be modelled according to the same methodologies as has been previously presented for zirconium-oxychloride, and detailed in Chapter 4. This would subsequently confirm the viability of an ageing study based upon the use of XPDF. The results of these preliminary works are presented herein.

5.1 Zirconium-acetate Zr K-edge EXAFS

Preliminary Zr K-edge EXAFS data were collected at B18 at Diamond Light Source, UK. Three samples of commercially available zirconium-acetate solutions from Luxfer MEL Technologies were studied. The samples consisted of a 30% and two 22% (w/w ZrO_2) samples. All three samples had an acetic acid : zirconium ratio of 1.6. Samples were prepared by saturating a filter paper in the zirconium-acetate solution to be studied for approximately 5 minutes. This wet paper matrix was then suspended in front of the beam and the experiment was performed in transmission-mode. All three samples were normalised to a sample of Zr foil which was scanned for calibration purposes. Three data collections were performed for each sample and the results were averaged. The spectra of three samples studied are shown below in Figure 36 and their respective radial distribution functions (RDFs) in Figure 37.

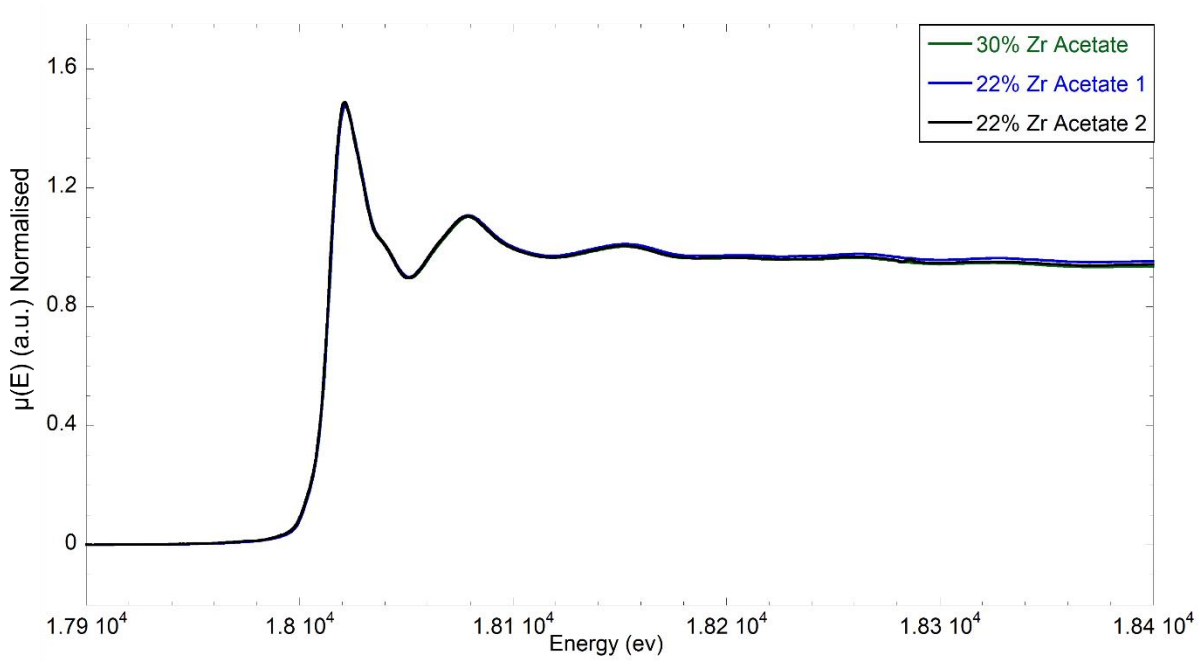

Figure 36: Absorption spectra of three samples of commercially available zirconium-acetate solutions from Luxfer MEL Technologies. All three samples have had their absorption energy normalised to Zr foil which was used as a reference sample.

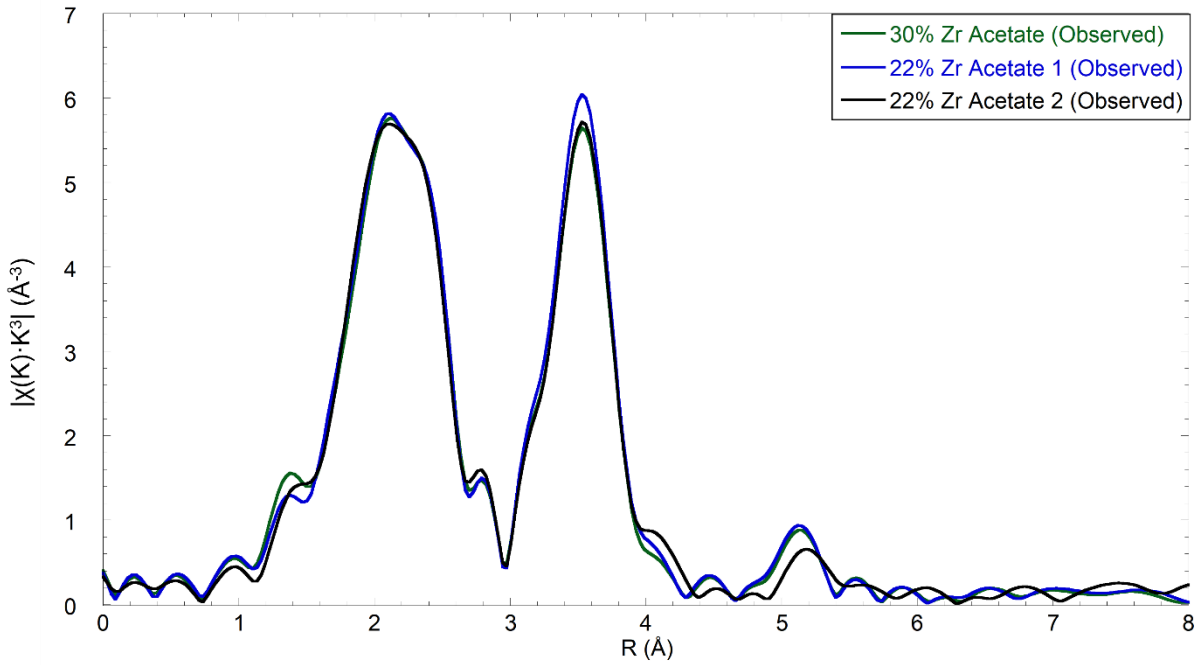

Figure 37: Zr K-edge k^3 weighted EXAFS after Fourier transform.

The post edge features of these spectra are almost identical with the same characteristics being observed indicating there are very few differences between the samples. These spectra were Fourier transformed to obtain the radial distribution function (RDF), χ(r), which could then be viewed and subsequently fitted in real space.

The samples studied here are produced in a different method to those studied by Hennig *et al.* who originally started with 1.0 M zirconium-oxychloride solution and proceeded to measure EXAFS after the addition of differing quantities of acetic acid. These solutions had an equivalent ZrO_2 concentration of 12.4 wt% compared to the 22 wt% and 30 wt% studied here. The solutions studied by Hennig did cover a range of acetic acid : zirconium ratios of 0.0-10.0.

Hennig's work produced two EXAFS spectra for before and after the addition of acetic acid, which can be seen in Figure 38. Before these can be studied it must be noted that the plots displayed below (Figure 38) have been plotted without the phase correction, this shifts the

features of the EXAFS data in the R direction by a refineable factor. This value as refined by Hennig *et al.* for the data presented in Figure 38, is 0.5 Å [2].

On first inspection of Figure 37, it is clear that the RDF's obtained from the commercial samples studied here are substantially different from either of the single-phase systems determined by Hennig *et al.* and seen in Figure 38.

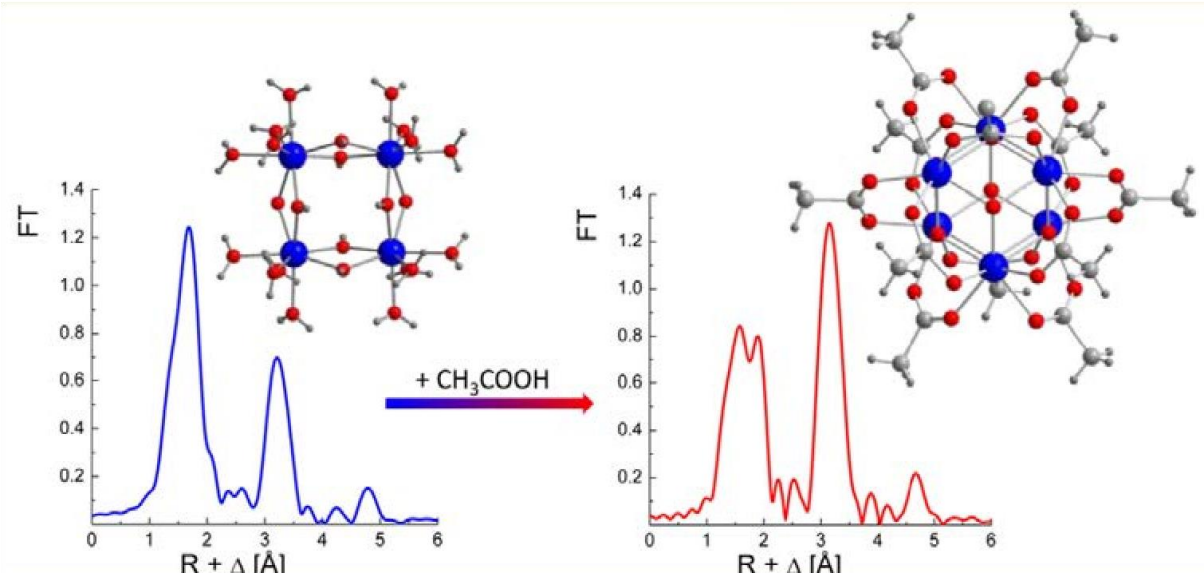

Figure 38: Fourier transformed XAS data of $[Zr_4(OH)_8(OH_2)_{16}]^{8+}$(left) and $Zr_6(O)_4(OH)_4(CH_3COO)_{12}$ (right) as reported by Hennig et al. Key: Zr-Blue, O, Red, C-Grey, H-Grey [2].

These results show two equally large contact distances at 2.1 Å and 3.6 Å, with a smaller peak at approximately 5.1 Å. The results obtained by Hennig *et al.* show a transition from the first peak being the most prominent, to the second becoming the most prominent as the solution moves toward the increased presence of the hexameric species and the concentration of the tetrameric species decreases upon the addition of increasing quantities of acetic acid [2]. Neither of these positions were seen in the EXAFS spectra produced here (Figure 37): two peaks of equal magnitude were observed (2.1 Å and 3.6 Å) with a smaller third peak (5.1 Å). All three peaks seen here are present in the EXAFS data presented by Hennig *et al.* but it is their intensities which are not replicated here. The presence of two equal intensity peaks at

r = 2.1 Å and 3.6 Å, according to Hennig's results, would indicate an equal ratio of hexamer and tetramer which they determined would be present at an acetic acid : zirconium ratio of approximately 0.7. The results presented here show this same phenomenon in samples with an acetic acid : zirconium ratio of 1.6. At such concentrations, and by the results of Hennig *et al.* a higher concentration of the hexameric species than the tetrameric would be expected; approximately 75% : 25% respectively.

The absence of any splitting in the first peak was also noted. Hennig observed splitting of the first peak as the two unique oxygen environments were resolved and whilst the data presented here show broadening of the peak at 2.1 Å, this could not be resolved into two unique peaks.

Contact distances were obtained from the software FEFF9 [85, 98] using the hexameric model proposed by Hennig *et al.* [2] seen in Figure 38. This software simulates all the contact distances possible for the inputted model and returns their potential contribution to an EXAFS spectrum. These contact distances were then used to attempt to model the data collected here. The results of this are seen in Figure 39, 40, and 41. The model proposed by Hennig does show good agreement between all the samples studied with R factors of 0.0086, 0.0075, and 0.0061 for the samples 22% Zr acetate 1, 2, and 30% Zr acetate respectively. This is a good indicator of confidence in the model; Calvin defines any R-factor less than 0.02 as "good enough" [79]. It is however noted that the flexibility of EXAFS means the technique is more suited to the differentiation between alternatives rather than the pursuit of an accurate structural model [79].

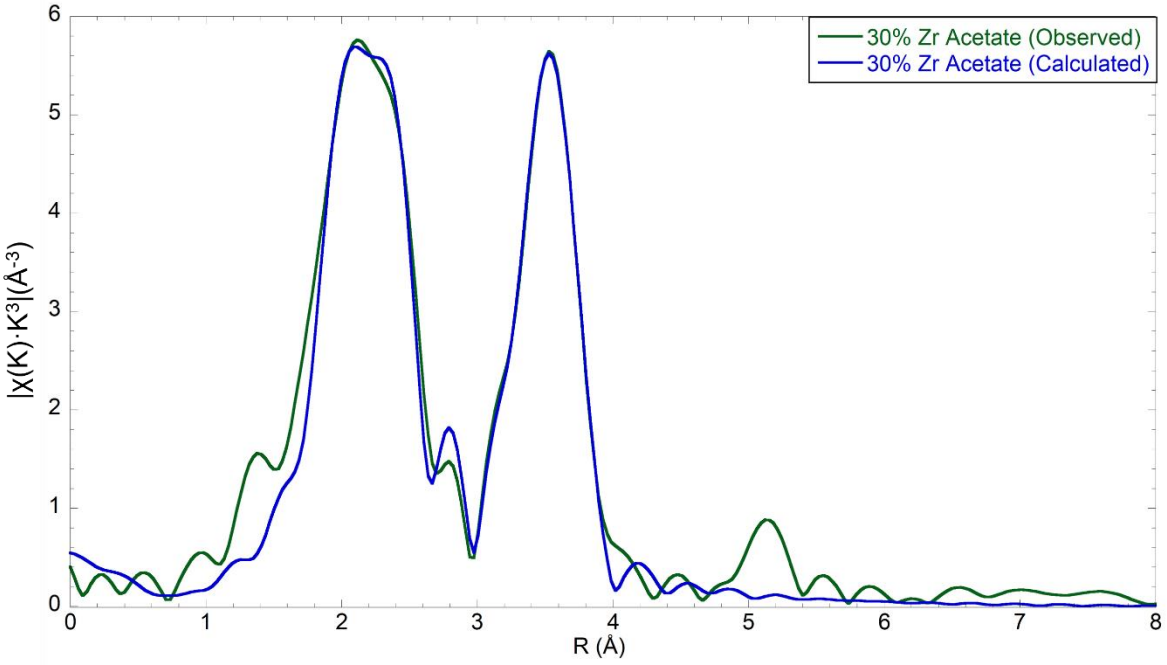

Figure 39: The observed and calculated radial distribution function resulting from the fit of a 30% zirconium-acetate sample to the model proposed by Hennig et al. [2].

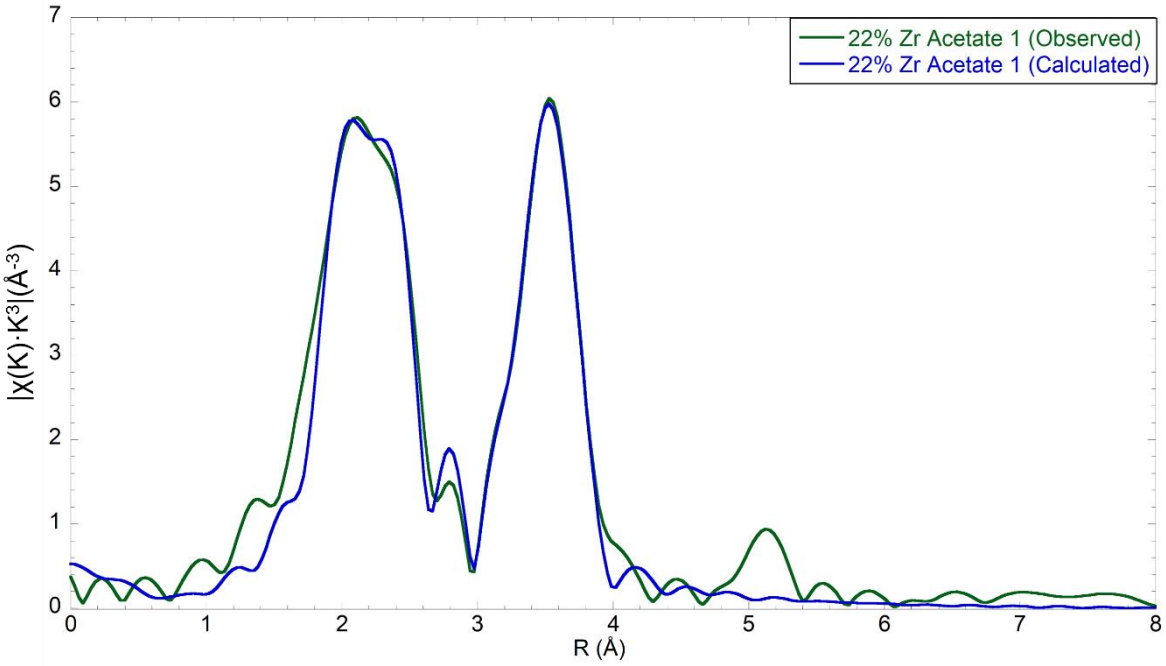

Figure 40: The observed and calculated radial distribution function resulting from the fit of 22% zirconium-acetate sample 1 to the model proposed by Hennig et al. [2].

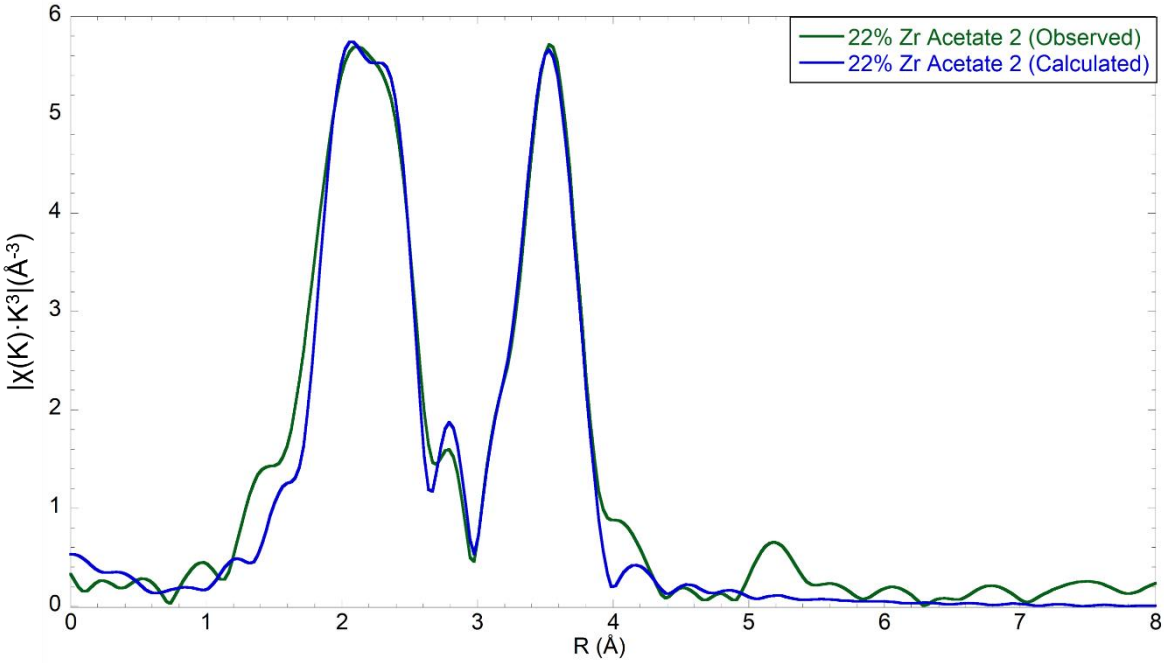

Figure 41: The observed and calculated radial distribution function resulting from the fit of 22% zirconium-acetate sample 2 to the model proposed by Hennig et al. [2].

The contact distances of these three refinements and those performed by Hennig *et al.* are shown below in Table 11.

Table 11: Contact distances from EXAFS refinements of zirconium-acetate solutions compared to those obtained in literature by Hennig et al.[2].

	Hennig Model [2]	30% Zr Acetate (Å)	22% Zr Acetate 1 (Å)	22% Zr Acetate 2 (Å)
Zr – O_1	2.119	2.123	2.123	2.120
Zr – O_2	2.252	2.260	2.260	2.258
Zr – Zr	3.545	3.540	3.536	3.538

It can be seen that despite the visual differences between the data collected that the values obtained from the refinement of the EXAFS data are similar and so, coupled with the refinements R-factors it can be concluded that the samples do contain the hexameric phase. The EXAFS refinements detailed here were single-phase refinements as this is what would be expected for these samples according to the results of Hennig *et al*. as outlined previously.

It is noted however, that the variations observed in the RDFs of these samples between that seen in previous studies was believed to be sufficient to conclude that the commercial samples here studied did not behave in exactly the same was as those synthesised in the laboratory by Hennig, and that further investigation was required. The results presented here however do show one of the key issues with the use of EXAFS for this level of structural refinement. The data obtained is visibly different to that collected by Hennig *et al.* and yet the refinements resolve toward the same structure [2].

It was felt that, due to the natural limitations of EXAFS as a technique, it would not be the most suitable method to study these materials and that XPDF would, instead, offer the best technique to resolve the structure of these samples and deduce why such variations had been observed. The agreement of the EXAFS during fitting to the hexameric species would not be ignored however and the hexameric species would be used as a starting model for all future refinements.

5.2 Zirconium-acetate PDF

Preliminary XPDF analysis of the same commercially acquired samples discussed in Chapter 5.1, were performed at I15-1 at Diamond Light Source, UK using the same experimental procedure described in Chapter 4. The zirconium-acetate solutions were loaded into bespoke 1.5 mm diameter quartz capillaries which were spun at high speed for 5-minute ambient temperature data collections. Data collections were run at 76 keV for optimal Q range of approximately 40 $Å^{-1}$. I15-1 employs a Perkin Elmer XRD 1611 CP3 area detector as a primary detector.

Upon transformation from the raw diffraction patterns to the Pair distribution function, preliminary visual comparisons were made. This method of qualitative analysis allowed for the early determination of the suitability of PDF for the analysis of these solutions and also to identify if any differences between samples could be observed. The resulting PDFs are shown in Figure 42 below.

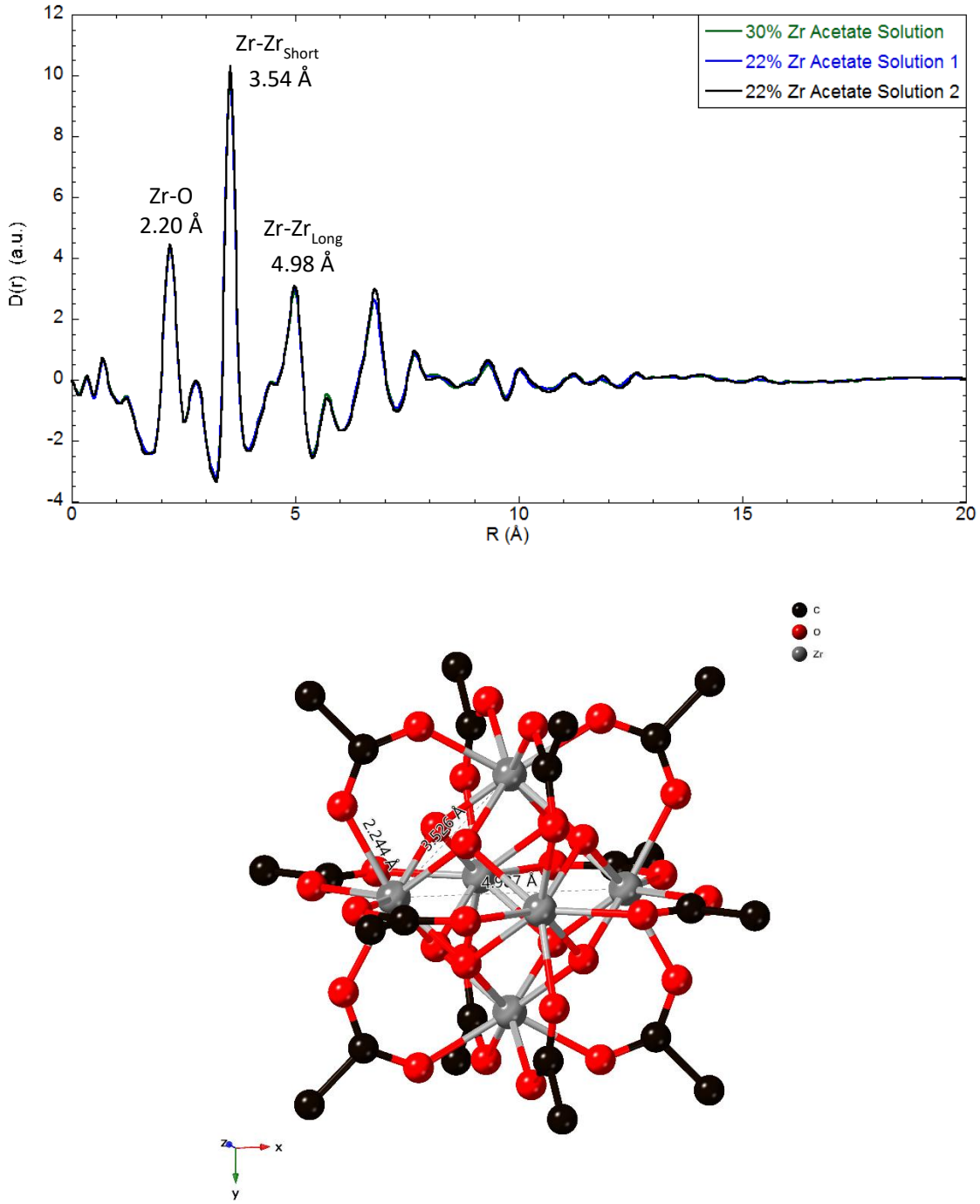

Figure 42: (Top) Overlay of 3 PDFs of zirconium-acetate solutions of 2 different zirconium concentrations collected on I15-1 as part of the preliminary work with some key features labelled. (Bottom) the Hexameric structure, $Zr_6(O)_4(OH)_4(CH_3COO)_{12}$, with the key contact distances labelled.

The PDFs show good agreement between each other up to an r value of approximately 6Å, and the main peaks can be ascribed to some of the principal contact distances from the hexameric structure described by Hennig *et al.* [2] It was noted that some of the principal

contact distances were, whilst of similar lengths, not identical and did vary by up to 0.16 Å; values beyond the margin of error calculated. This comparison can be seen below in Table 12.

Table 12: Comparisons of the literature contact distances of the hexameric cluster and the peak maxima determined from preliminary XPDF.

Contact	Value according to the Hennig hexameric model [2] (Å)	Observed peak maxima (Å)
Zr-O	2.169(2)	2.20
Zr-Zr_{Short}	3.620(3)	3.54
Zr-Zr_{Long}	5.14(1)	4.98

Closer inspection of the PDF, in the range previously unstudied due to the limitations of EXAFS, shows that while the structures show good agreement in the short-range this is not consistent and as the contact distance is increased, the variations in the PDF become larger. This is clear in Figure 43.

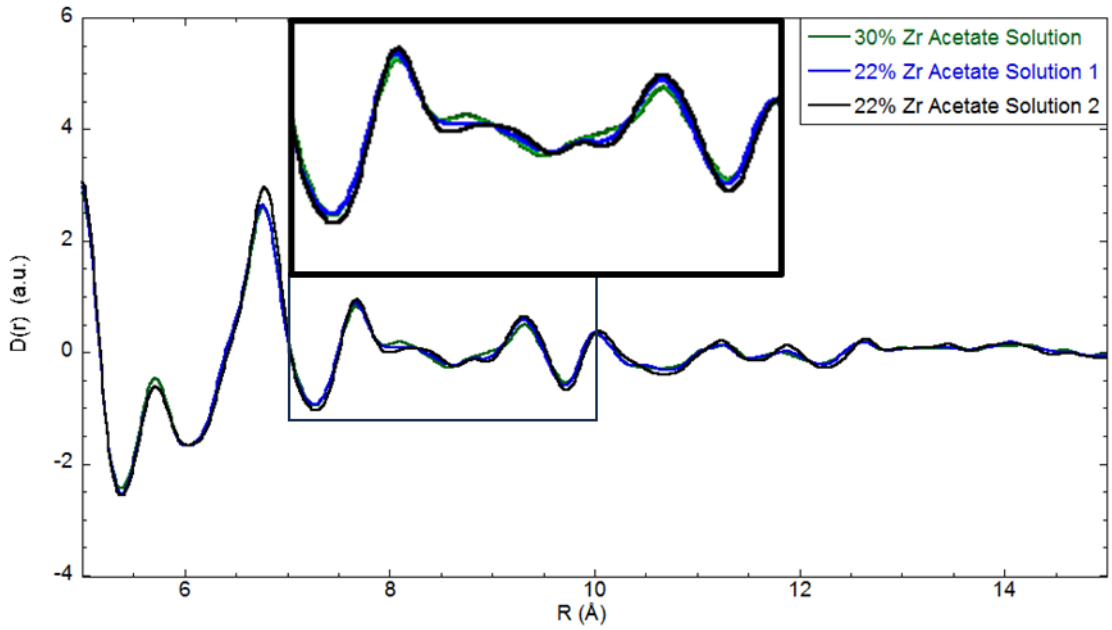

Figure 43: Overlay of 3 PDFs collected on I15-1 focused on the range of 7 – 15 Å.

Here it can be seen that the samples are not perfectly matched, and that variation occurs in the longer range. Whilst XPDF is not element specific, contact distances which involve strongly

scattering atoms, such as zirconium, create stronger peaks. This coupled with the zirconium being towards the centre of the cluster, and so all Zr-Zr contacts will have short distances of r, means that these smaller peaks at longer ranges are most likely to be caused by a zirconium – carbon/oxygen atomic pairing. This presence of the hexameric structure proposed by Hennig *et al.* however did not explain the inconsistencies seen in the EXAFS data collected here [2]. It was felt that the modelling of the whole molecular species would be necessary and using the method developed for the zirconium-oxychloride refinements performed in Chapter 4, this was possible.

6.0 Zirconium-acetate Refinements

Whilst attempts have been made to isolate the complex molecular species present in zirconium-acetate solutions it is not clear if this species remains present and in the same ratios as has been postulated by Hennig *et al.* [2] with the ageing of the solutions. Tosan *et al.*[42] hypothesised a structural evolution over a period of a month and whilst this model is not believed to be present in these systems, no further work has been done to study the evolution of the molecular species present and their ratio over time. To fully understand this, an ageing study must be performed in which samples of various zirconium-acetate solutions with different variables on interest are studied periodically over a prolonged period.

As such this chapter has the following aims:

- To attempt to model the solution species present in aqueous samples of zirconium-acetate solutions through the use of XPDF data collected at Diamond Light Source and National Synchrotron Light Source II.
- Compare the quality of the refinements with the aim of determining the best approach for modelling these solution species with XPDF.
- Identify if this structure is influenced by some key variables describing the solutions including acetic acid : zirconium ratio and the concentration of the solutions (given as equivalent concentration of (ZrO_2).
- Determine the long-term effects on the structure of this molecular species in aqueous solutions through ageing at variable temperatures

6.1 Synthesis of Zirconium-acetate Solutions

For the purpose of this ageing study samples of zirconium-acetate were synthesised by methods which closely resemble those used in full-scale commercial synthesis. The method used was the same as that used industrially by Luxfer MEL Technologies Ltd., but the volumes were scaled down to the requirements of the project. 1500 g of zirconium-acetate was produced for each sample. This allowed each sample to be divided into different storage conditions with enough for regular analysis and sampling.

A range of samples were synthesised with different ZrO_2 concentrations and acetic acid : zirconium ratios. The samples were prepared according to the proprietary method employed by Luxfer MEL Technologies Ltd. which cannot be disclosed here. The method, however differed from that seen in previously published structural studies as it did not employ zirconium-oxychloride as the zirconium source.

The variables studied and the necessary quantities of reagents used can be seen in Table 13 and in the appendix in Table 4 respectively.

Table 13: All zirconium-acetate samples synthesised for the ageing study and their variables.

Sample Name	Feedstock	ZrO_2 weight percentage	Acetic acid : Zr ratio
ZAA1	1	14	1.6
ZAA3	1	14	2.0
ZAA4	1	22	1.6
ZAA6	1	22	2.0
ZAA7	1	30	1.6
ZAA9	1	30	2.0
ZAA10	3	14	1.6
ZAA12	3	14	2.0
ZAA13	3	22	1.6
ZAA15	3	22	2.0
ZAA16	3	30	1.6
ZAA18	3	30	2.0
ZAA19	2	14	1.6
ZAA20	2	22	1.6
ZAA21	2	30	1.6
ZAA22	2	22	2.0
ZAA23	2	30	2.0
ZAA24	1	22	1.3
ZAA25	1	22	5.0
ZAA26	3	22	1.3
ZAA27	3	22	5.0
ZAA29	1	22	5.0
ZAA30	1	22	1.6

The samples synthesised spanned 3 main variables: feedstock, ZrO_2 weight percentage, and molar ratio of acetic acid to zirconium. The feedstock is the source of the zirconium used to create the sample and any variations in these are proprietary. The ZrO_2 weight percentage is the weight : volume percentage of the equivalent concentration of ZrO_2. These values spanned all of those which are commercially available: 14%, 22%, and 30%. The molar ratio of acetic acid to zirconium covered values of 1.3, 1.6, 2.0, and 5.0. Molar ratios of 1.6 and 2.0 are common commercial values and as such would represent the samples most commonly acquired by industrial consumers. 1.3 was determined to be the lowest feasible ratio to which

these samples could be prepared according to the commercial synthesis method. 5.0 was used as a “beyond excess” value.

One 1500g batch of each sample was prepared at Luxfer MEL Technologies and from this, smaller aliquots were prepared and put into storage. The samples were stored in three different controlled temperatures: ambient samples kept at room temperature (approximately 20±3°C), refrigerated samples were stored in a laboratory refrigerator (Porkka Labline LAB300) at approximately 3 °C, and incubated samples were stored in an incubator (SciQuip Incu-80S) at 45 °C. All samples were kept in plastic vials with screw cap lids and plastic Eppendorf’s which were used for the model compound synthesis described in Chapter 7 and for periodic XPDF sampling respectively. This storage method avoids contamination or evaporation.

6.1.1 Physical Observations

As the ageing study proceeded it was noted that a physical change was observed in some of the zirconium-acetate samples. The viscosity of a select range of samples increased to ultimately form a viscous gel after between 9 and 12 months of ageing. This transition into a gelatinous phase was only observed in samples which were kept at the increased temperature (45 °C). The samples which underwent this transition are described below in Table 14.

Table 14: A list of all the zirconium-acetate samples and their phases after 12 months of storage at 45°C. Samples which increased in viscosity are highlighted in orange.

Sample Name	Zr : Acetic Acid Ratio	ZrO_2 Percentage	Feedstock Type	Physical Status
ZAA01	1.6	14	1	Gel
ZAA03	2.0	14	1	Liquid
ZAA04	1.6	22	1	Gel
ZAA06	2.0	22	1	Liquid
ZAA07	1.6	30	1	Viscous Liquid
ZAA09	2.0	30	1	Liquid
ZAA10	1.6	14	3	Gel
ZAA12	2.0	14	3	Liquid
ZAA13	1.6	22	3	Liquid
ZAA15	2.0	22	3	Liquid
ZAA16	1.6	30	3	Liquid
ZAA18	2.0	30	3	Liquid
ZAA19	1.6	14	2	Gel
ZAA20	1.6	22	2	Gel
ZAA21	1.6	30	2	Viscous Liquid
ZAA22	2.0	22	2	Liquid
ZAA23	2.0	30	2	Liquid
ZAA24	1.3	22	1	Gel
ZAA25	5.0	22	1	Liquid
ZAA26	1.3	22	3	Gel
ZAA27	5.0	22	3	Liquid

Table 14 shows that, for samples made of feedstock 1 and 2, the solidification occurred in all samples with an acetic acid : zirconium ratio of <2.0. Samples of feedstock 3 all seemed to resist solidification with the exception of ZAA10. It is not clear at this time what causes this phenomenon in samples of feedstock 3 and investigations into the nature of the feedstocks is beyond the scope of this project. The impact of these physical changes on the studies performed in subsequent chapters will be investigated.

6.2 9-Month Data Collection (March 2020)

For the 9-month data collection only samples from the ambient collection were studied due to beamtime limitations. The samples selected are shown in Table 15 below and all were liquids at this stage. Analysis was performed at I15-1 at Diamond Light Source, UK using the same experimental procedure described in Chapter 4. The zirconium-acetate solutions were loaded into bespoke 1.5 mm diameter quartz capillaries which were spun at high speed for 5-minute ambient temperature data collections. Data collections were run at 76 keV for optimal Q range of approximately 40 $Å^{-1}$. I15-1 employs a Perkin Elmer XRD 1611 CP3 area detector as a primary detector.

All of the Fourier transformed PDF's were obtained from the raw diffraction data using GUDRUNX [91]. The data collected after Fourier transform to generate the PDF is shown below in Figure 44.

Table 15: Details of the zirconium-acetate samples studied in the first data collection in after 9 months ageing.

Sample Name	Feedstock	ZrO_2 weight percentage	Acetic acid : Zr ratio
ZAA1	1	14	1.6
ZAA4	1	22	1.6
ZAA7	1	30	1.6
ZAA10	3	14	1.6
ZAA13	3	22	1.6
ZAA16	3	30	1.6

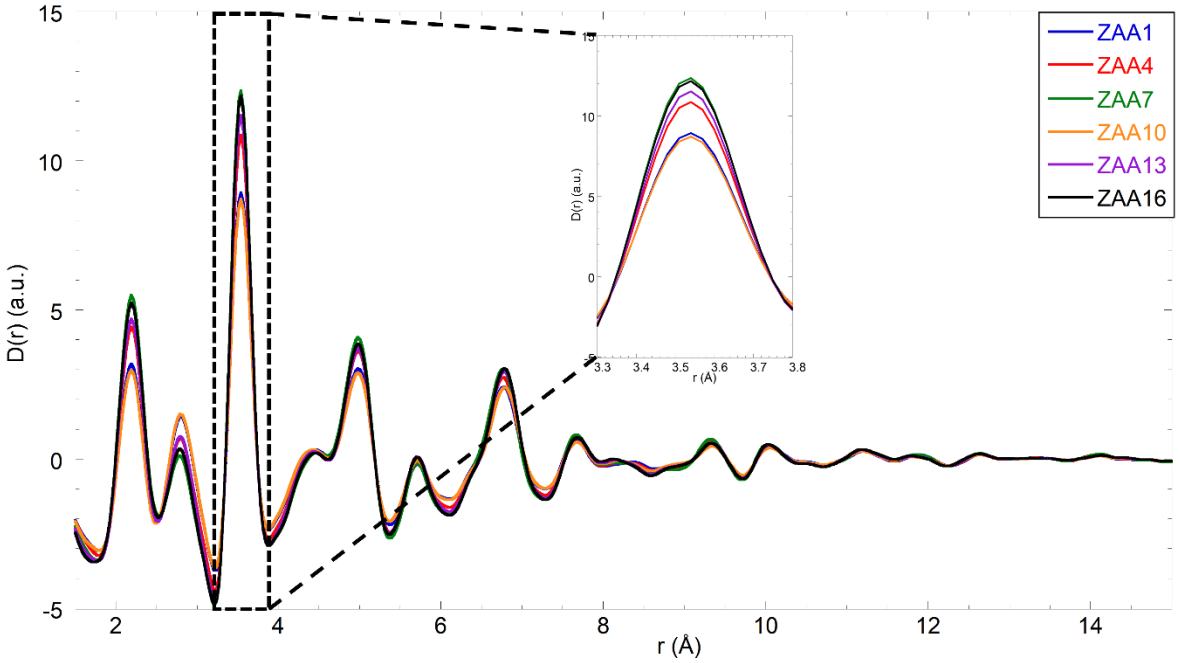

Figure 44: Overlay of the PDFs collected in the 9-month data collection period over an r-range of 0Å < r < 15Å with a zoom in on the largest peak (Inset)

The data presented here in Figure 44 show that the six PDF's form 3 distinct categories with the relative concentration being the main distinction. Samples with a higher concentration show greater magnitude in all of their peaks. This is caused by the increase in the presence of heavier atoms and thus the relative scattering power of the solution being studied. Also, an increase in the concentration of zirconium leads to the presence of more zirconium clusters and as such, more instances of each contact distance.

The immediate short-range region (<1 Å) of the PDF shows variations but these are merely truncation effects from the Fourier transform and will be removed prior to refinement as this region is not structurally relevant and the shortest chemical bonds studied are over 1 Å in length.

6.2.1 Single-phase Refinements

The structural refinement was originally performed with a single molecular species: the hexamer. It was felt that as this was postulated to be the predominant species in these solutions that an attempt to model that phase would fit most if not all of the PDF and its features. The model of the hexamer was obtained in CIF format and was transformed in a similar manner to that developed during the refinement of zirconium-oxychloride (see Chapter 4). Initially the symmetry of the system was removed, converting the space group to P1. New atomic positions were created to account for this loss of information and a super-cell was developed. The resultant model contained 6 unique zirconium positions, 32 unique oxygen positions, and 24 unique carbon positions. Hydrogen positions were omitted for clarity and also due to the extremely weak scattering power of hydrogen with X-rays. It was decided that on visual inspection of the PDF obtained that most discreet features were within the short to medium range in the PDF, with most features appearing at ranges of $r \leq 12$ Å. For that reason, refinements would only be carried out on r values from 1 Å – 15 Å. This led to the creation of a super-cell of dimensions 37.82 Å, 37.82 Å, and 40.88 Å, for lattice parameters *a, b,* and *c* respectively. This offered sufficient range to fit only the intracluster interactions as desired.

An initial model of the hexameric species was generated to be a perfectly symmetrical rhombic dodecahedron, the core zirconium positions forming perfect relative octahedral geometry whilst the bridging oxygen positions were set to be equidistant from all three neighbouring zirconium atoms to which they bonded. Each acetic acid group was to be treated identically and the structure would have 3 identical perpendicular 4-fold rotation axes. The starting model is shown in Figure 45.

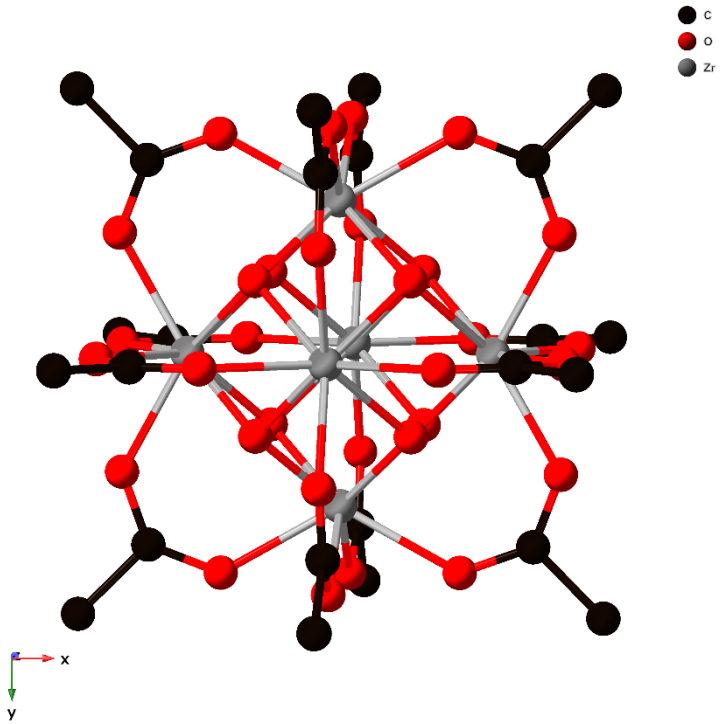

Figure 45: Starting hexameric model showing a symmetrical core used in the first single-phase refinement iteration. Key: Zr – Grey, O – Red, C – Black.

With the use of a Z-matrix to define the structure, the refinements of each data set contained 17 refineable parameters: 7 thermal, 6 structural, and 4 to define the background and scaling. This number is higher than that used for the refinement of zirconium-oxychloride due to the higher complexity of the structure being modelled. The results of the refinements of samples ZAA1, ZAA4, and ZAA7 are displayed below in Figure 46, 47, and 48 respectively and the complete set can be found in Figures 1-6 and Tables 5-10 in the Appendix.

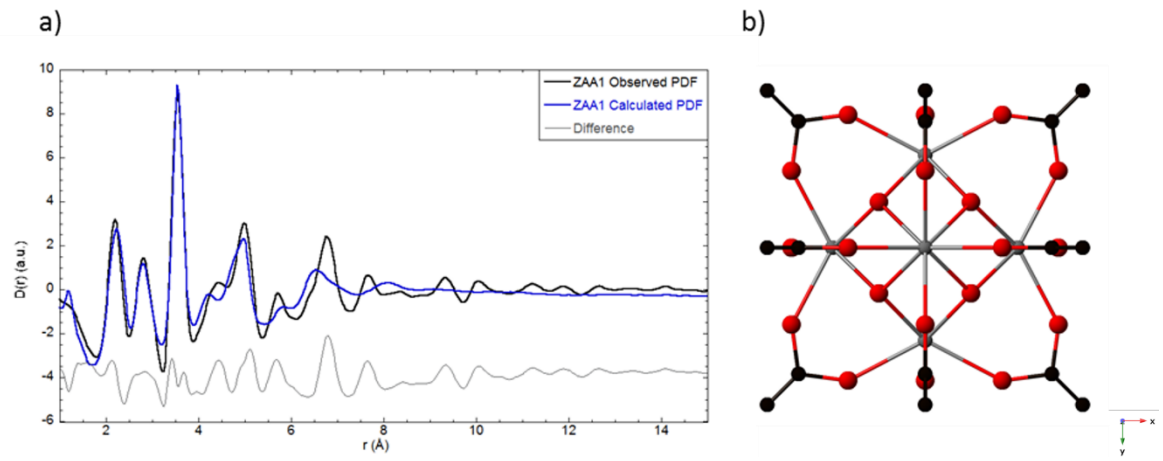

Figure 46: a) Observed (black) and calculated (blue) PDF of the first iteration of the single-phase refinement of sample ZAA1 (14% ZrO_2). b) Resultant model of this refinement. Key: Zr – Grey, O – Red, C – Black. R_{wp} = 34.75%.

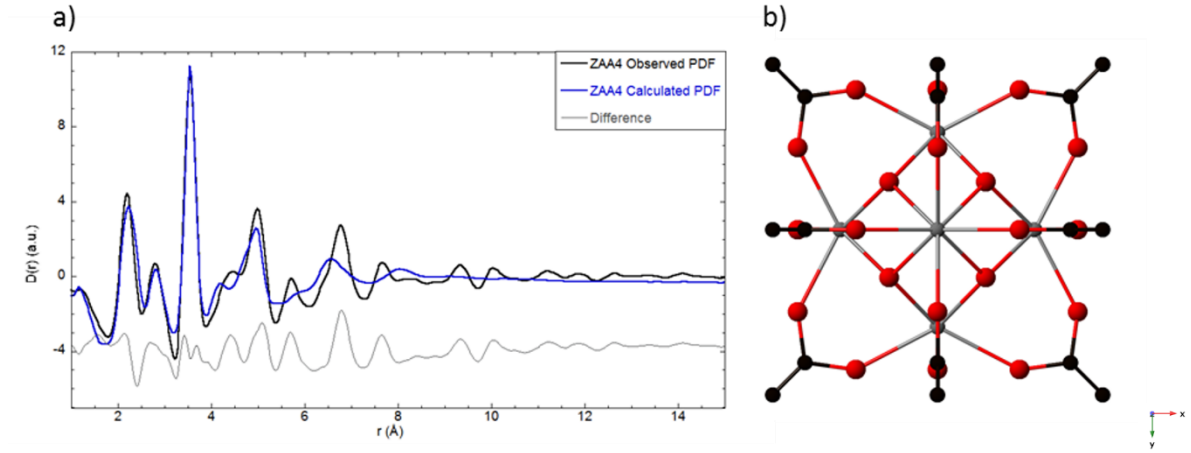

Figure 47: a) Observed (black) and calculated (blue) PDF of the first iteration of the single-phase refinement of sample ZAA4 (22% ZrO_2). b) Resultant model of this refinement. Key: Zr – Grey, O – Red, C – Black. R_{wp} = 34.38%.

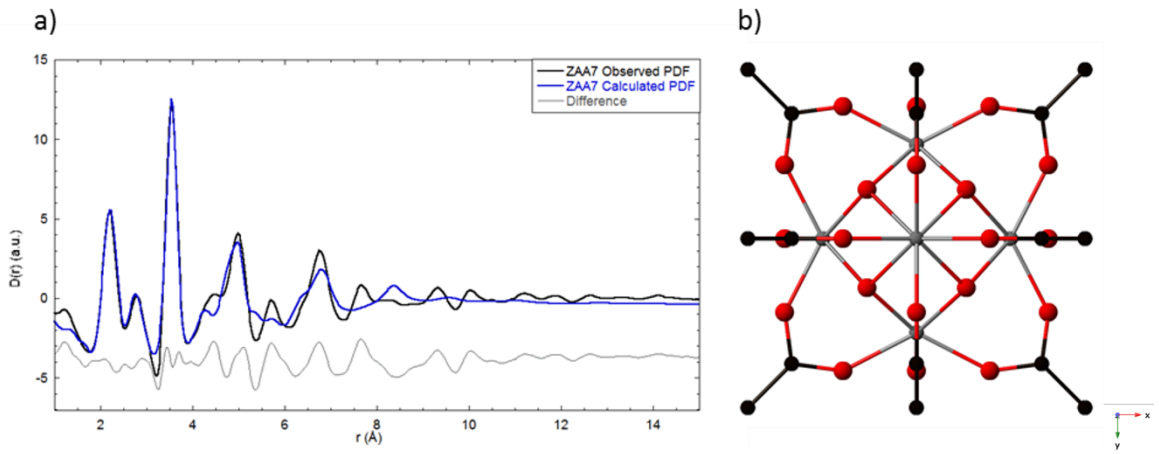

Figure 48: a) Observed (black) and calculated (blue) PDF of the first iteration of the single-phase refinement of sample ZAA7 (30% ZrO_2). b) Resultant model of this refinement. Key: Zr – Grey, O – Red, C – Black. R_{wp} = 29.15%.

The fits presented here show good agreement in the short-range order with the first three peaks being fit relatively well. The first serious discrepancy is visible at 4 Å. The fit subsequently agrees with the peak at 5 Å in the sample ZAA7 but this is not as close an agreement in the samples ZAA1 and ZAA4. The peak at 7 Å is correctly fitted in sample ZAA7 but this is not mirrored in samples ZAA1 or ZAA4. The calculated peak at 8.5 Å has no counterpart in the observed data sets for any sample but is stronger in the calculated PDF of ZAA7. The refinements presented here converged with R_{wp} values of 34.75%, 34.38%, and 29.15% respectively for samples ZAA1, ZAA4, and ZAA7. These values coupled with the visual inspection of the fit are good signs of confidence in the model. It is, however, crucial that the model itself be checked for chemical sense.

It can be seen that all refinements seem to generate similar models, and this is confirmed upon inspection of bond distances and angles that describe the structure. These are shown below in Table 16 together with a comparison with the Hennig model [2].

Table 16: Bond lengths and angles of the Hennig model and the models resulting from the first iteration of the single-phase refinement of samples ZAA1, ZAA4, and ZAA7 [2].

Zr-O $_{Core}$ (Å)				Zr-Zr_{Short} (Å)				Zr-Zr_{Long} (Å)			
Hennig model [2]	ZAA1	ZAA4	ZAA7	Hennig model [2]	ZAA1	ZAA4	ZAA7	Hennig model [2]	ZAA1	ZAA4	ZAA7
2.16	2.16	2.16	2.21	3.54	3.54	3.54	3.56	4.97	5.01	5.01	5.03
2.16				3.53				5.02			
2.18											
Zr-$O_{Acetate}$ (Å)				C-$O_{acetate}$ (Å)				C-$C_{Acetate}$ (Å)			
Hennig model [2]	ZAA1	ZAA4	ZAA7	Hennig model [2]	ZAA1	ZAA4	ZAA7	Hennig model [2]	ZAA1	ZAA4	ZAA7
2.22	2.35	2.38	2.22	1.30	1.35	1.33	1.39	1.63	1.18	1.17	1.66
2.23				1.45							
2.24											
2.25											
Centre of cluster-Zr-$O_{(Acetate)}$ (°)				Zr-O-$C_{(Acetate)}$ (°)				O-C-$C_{(acetate)}$ (°)			
Hennig model [2]	ZAA1	ZAA4	ZAA7	Hennig model [2]	ZAA1	ZAA4	ZAA7	Hennig model [2]	ZAA1	ZAA4	ZAA7
122.04	117.79	117.56	117.27	117.75	144.52	144.55	145.09	105.02	127.32	127.11	127.36
123.99				123.14				111.84			

It is seen that the core of the cluster remains almost identical to that observed by Hennig *et al*. [2] The Zr-$O_{(core)}$ distance is the same for samples ZAA1, ZAA4, and the model proposed by Hennig *et al.* with only a slight deviation appearing in sample ZAA7. The Zr-Zr_{short} and Zr-Zr_{long} distances both match those in the literature model extremely well but this is expected from visual inspection as these peaks are large, well defined, and in the same region as was predicted. The differences between the observed samples and the literature model become more apparent in the region where the bridging acetate groups are modelled (>4 Å). The Zr-$O_{Acetate}$ distance from the core of the cluster to the carboxylate groups are larger in samples ZAA1 and ZAA4 than those seen in the Hennig model. ZAA7 did produce a value in the same range as seen in the model however and visual inspection of the fit shows that in the region of 2.2 Å – 2.3 Å, sample ZAA7 shows the greatest agreement. The carboxylate groups themselves show this pattern continued. The bond distance of the C-C in the carboxylate groups is similar between the samples ZAA1 and ZAA4, 1.17 Å and 1.18 Å, while for ZAA7 and the literature model, the values are 1.63 Å and 1.66 Å respectively. This again shows the sample ZAA7 providing higher levels of agreement to the literature model than the other two samples. This change in the C-C bond length leads to the uniquely superior profile of that peak in the refined ZAA7. This extended bond length leads to greater agreement in this region which is not seen in samples ZAA1 or ZAA4. The refinements for both samples were repeated to exclude local minima with the same results. The C-O contact distance is an exception to the above trend, where instead the values are all in a similar range, but none are identical.

All of these discrepancies in the carboxylate region of the models can be correlated to a visual inspection of the fits themselves. The region below 2.0 Å is poorly matched in the sample

ZAA7 leading to decreased confidence in the results for contact distances in this region, namely C-O and C-C bonds.

It is in the bond angles that a common trend from the samples is observed. For all three principal bond angles presented here, the samples studied show similar values which are all distinctly different from those seen in the literature model. These all combine to form a stretching of the terminal methyl group away from the centre of the cluster species without increasing any bond lengths. The oxygen positions of the carboxylate move closer together and away from those in other carboxylate groups as demonstrated in Figure 49.

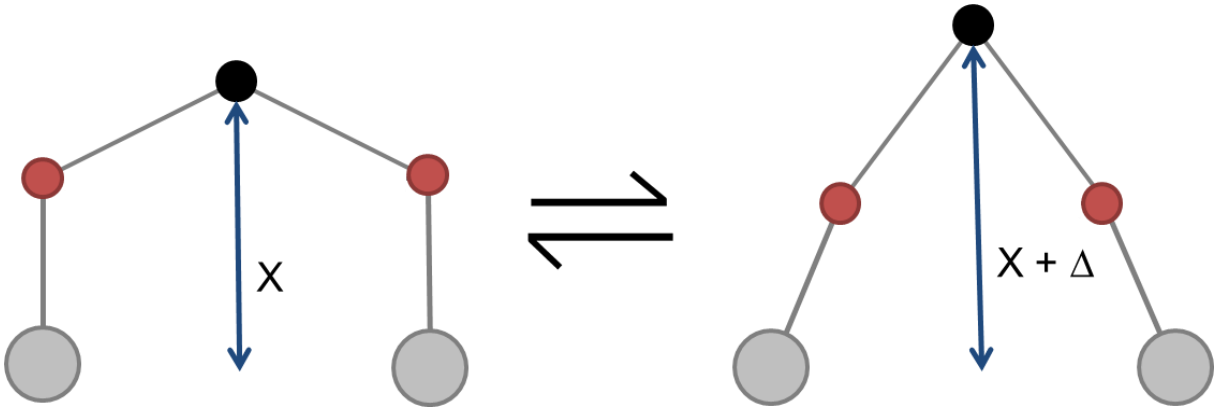

Figure 49: A diagram of the movements seen in the carboxylate groups for the refinements presented herein. The model transfers from that seen on the left to the right with the net effect being a change in the carbon position (Δ). Key: Zr – Grey, O – Red, C – Black.

Overall, the bond distances and angles seen here, with the exception of the variation in the bond angles described above in the carboxylate groups, show reasonable agreement to the model proposed but do show discrepancies between one another. The values all draw the conclusion that the hexameric core in the centre of the cluster is confirmed and that the changes from the literature structure occur in the carboxylate groups which surround it.

The bond lengths and their chemical sensibility cannot be truly assessed until the proposed implication on the oxidation state of the zirconium centres has been compared. These are

determined through the use of the method laid out by Brown and Altermatt [92]. These are shown in Table 17.

Table 17: The resultant oxidation state as derived from the Zr-O bond lengths, through bond-valence calculations described by Brown and Altermatt for the first iteration of the single-phase refinement of samples ZAA1, ZAA4, and ZAA7 [92].

Hennig Model [2]		ZAA1		ZAA4		ZAA7	
Actual value	Rounded value	Actual value	Rounded value	Actual value	Rounded value	Actual value	Rounded value
3.82	4	3.43	3	3.34	3	3.69	4
3.78	4						

From this table it can be seen that the Hennig model displays two unique zirconium environments and thus two unique oxidation states. Both of these oxidation states are very close to 4, the oxidation state zirconium tends to prefer. The refined models however show improbable oxidation states of 3.43, 3.34, and 3.69. Whilst 3.69 could be justifiably rounded up to obtain an integer value of 4, this amount is substantial and so unlikely.

From all of the data presented here it is clear that the models, whilst showing good agreement with the observed data set, do not provide the chemical sense. For this reason, the models obtained are not to be considered viable and further iterations to the refinement procedure were developed.

The table of bond lengths and angles presented previously Table 17 shows that the model used in this first iteration of the refinement process contains single values for some bond lengths and angles when multiple unique values are seen in the literature model. This is due to the fact that the structure proposed by Hennig *et al.* did not exhibit perfect symmetry and was instead distorted with an elongation in one direction, *c* [2]. This distortion leads to multiple values for common distances and angles as seen above.

It was also noted that if the hexameric model was formed from a restructuring of the tetrameric model, previously observed in samples of zirconium-oxychloride, that the four in-plane zirconium atoms would not be truly equivalent to those found in the new axial positions. It was felt that whilst the zirconium positions could reasonably be in the same general orientation, the oxygen atoms would favour those in the equatorial positions due to their previous bonding. For this reason, the oxygen positions in the model were permitted to refine in a way similar to that seen in the previous tetrameric structure. Their distance from the core had previously been parameterised but now a second parameter would also be used to describe their angle relative to the equatorial plane, rather than this being a fixed angle of 35°. This model seen in Figure 50 will hence be referred to as the "Chandelier Model" due to the way the axial zirconium position seems to be suspended above the plane through the bridging carboxylate groups and are beyond conventional bond lengths from the bridging core oxygen positions.

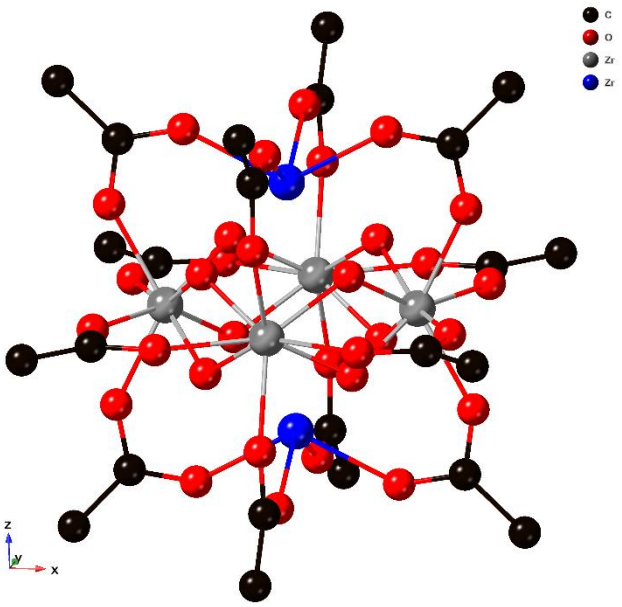

Figure 50: An example of a hexameric cluster displaying the chandelier bonding conformation highlighting the axial zirconium positions. Key: Zr Equatorial – Grey, Zr Axial – Blue, O – Red, C – Black.

Other than this one change all other refineable parameters and degrees of freedom were maintained. The result of a select three of these refinements, ZAA1, ZAA4 and ZAA7, are presented below in Figure 51, Figure 52, and Figure 53 respectively and an exhaustive set can be seen in Figures 7-12 and Tables 11-16 in the appendix.

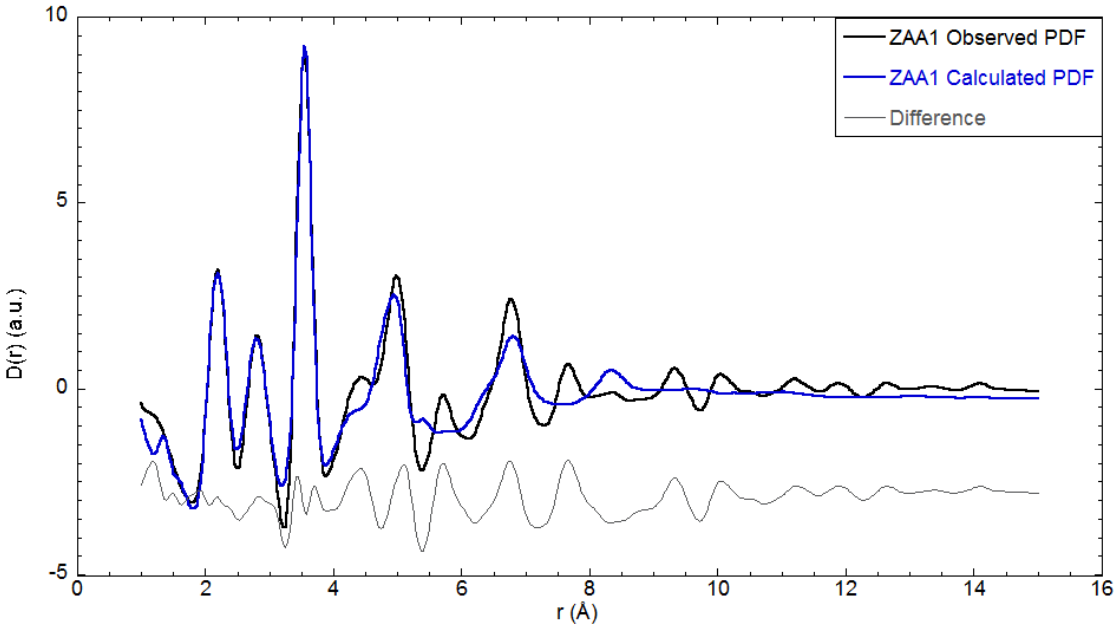

Figure 51: Observed (black) and calculated (blue) PDF of the second iteration of the single-phase refinement of sample ZAA1. R_{wp} = 30.29%.

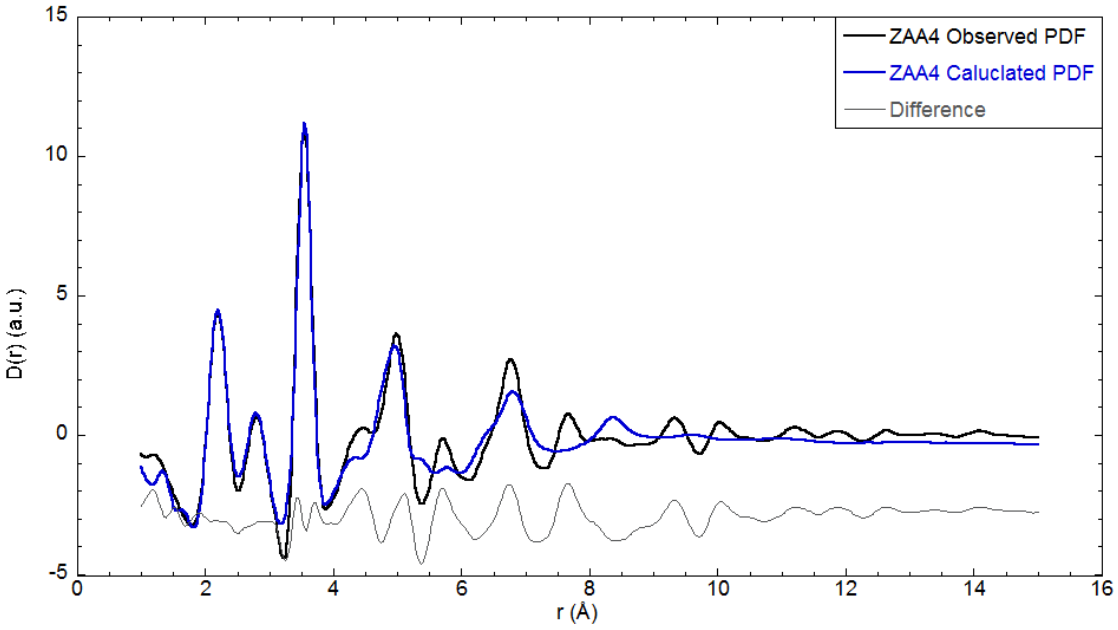

Figure 52: Observed (black) and calculated (blue) PDF of the second iteration of the single-phase refinement of sample ZAA4. R_{wp} = 29.27%.

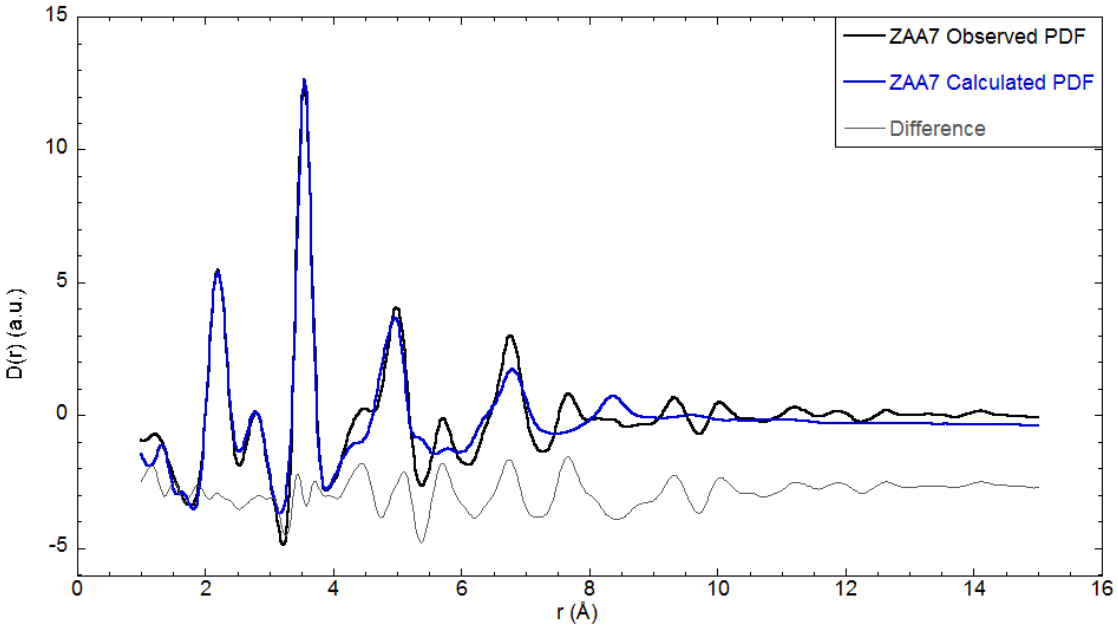

Figure 53: Observed (black) and calculated (blue) PDF of the second iteration of the single-phase refinement of sample ZAA7. R_{wp} = 28.24%.

These refinements converged with R_{wp} values of 30.29%, 29.27%, and 28.24% respectively. These successively higher quality fits all show R_{wp} values lower than their first iteration counterparts which indicates increased confidence in the models obtained. This is shown below in Table 18.

Table 18: R_{wp} values of the two single-phase refinements for samples ZAA1, ZAA4, and ZAA7.

Sample Name	R_{wp} (%)	
	Single-phase first iteration (Fixed-core)	Single-phase second iteration (Chandelier)
ZAA1	34.75	30.29
ZAA4	34.38	29.27
ZAA7	29.15	28.24

The fits themselves show a good indication on the quality of the fit obtained. In all three patterns the quality of fit in values of r < 4 Å is excellent. There is some deviation between the calculated and observed PDF around 4 Å – 5 Å. This feature was also seen in the previous

refinements and so is indication of some element of the samples not being completely modelled using these methods. The region or 6.5 Å < r < 7.0 Å shows substantial improvement compared to the previous refinement iteration. This is caused by all samples in this refinement iteration adopting the longer C-C bond range or ≈1.6 Å.

Once again, a peak at r = 8.5 Å is produced in the calculated PDF which has no counterpart in the observed PDF. The models obtained from these refinements are shown below in Figure 54, 55, and 56, and the corresponding bond lengths and angles can be seen in Table 19. It can be seen from visual inspection of the models that they resolve with high levels of similarity. Many of the variations between the respective models is not apparent by viewing the structures but instead can be obtained from inspecting the values (bond lengths, contact distances, and bond angles) which describe them.

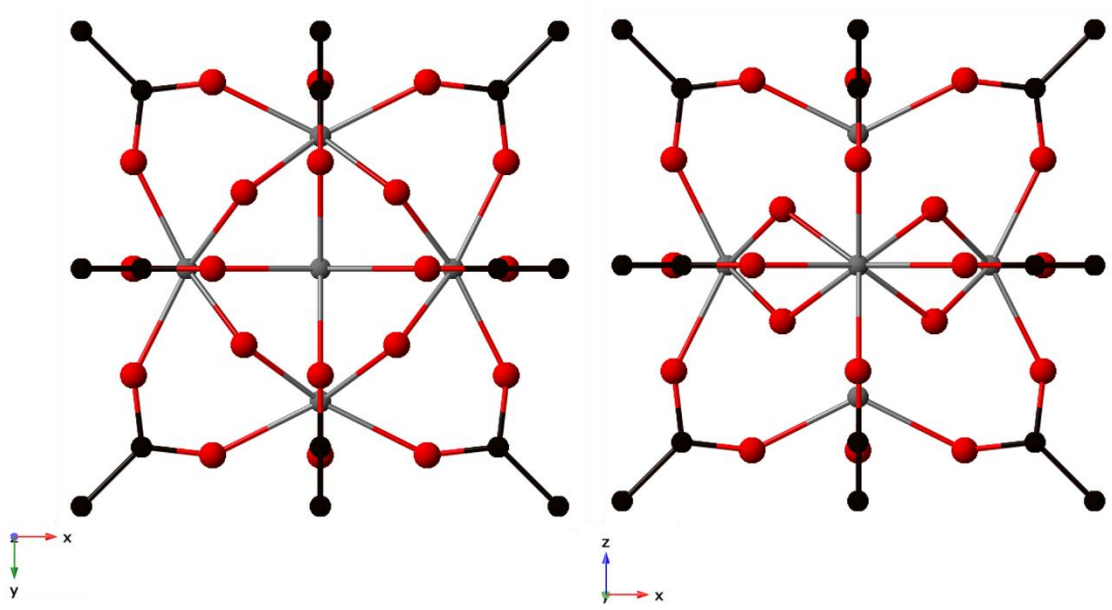

Figure 54: Resultant model of the refinement of data collected on sample ZAA1 using the second iteration single-phase refinement viewed from the axial positions (left) and the equatorial plane (right). Key: Zr – Grey, O – Red, C – Black.

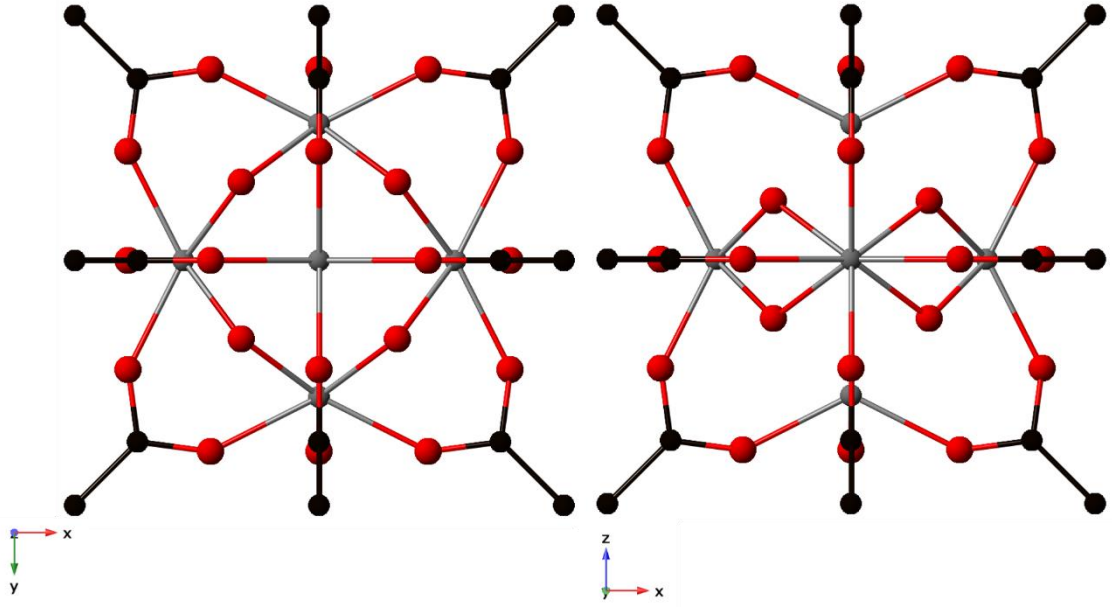

Figure 55: Resultant model of the refinement of data collected on sample ZAA4 using the second iteration single-phase refinement viewed from the axial positions (left) and the equatorial plane (right). Key: Zr – Grey, O – Red, C – Black.

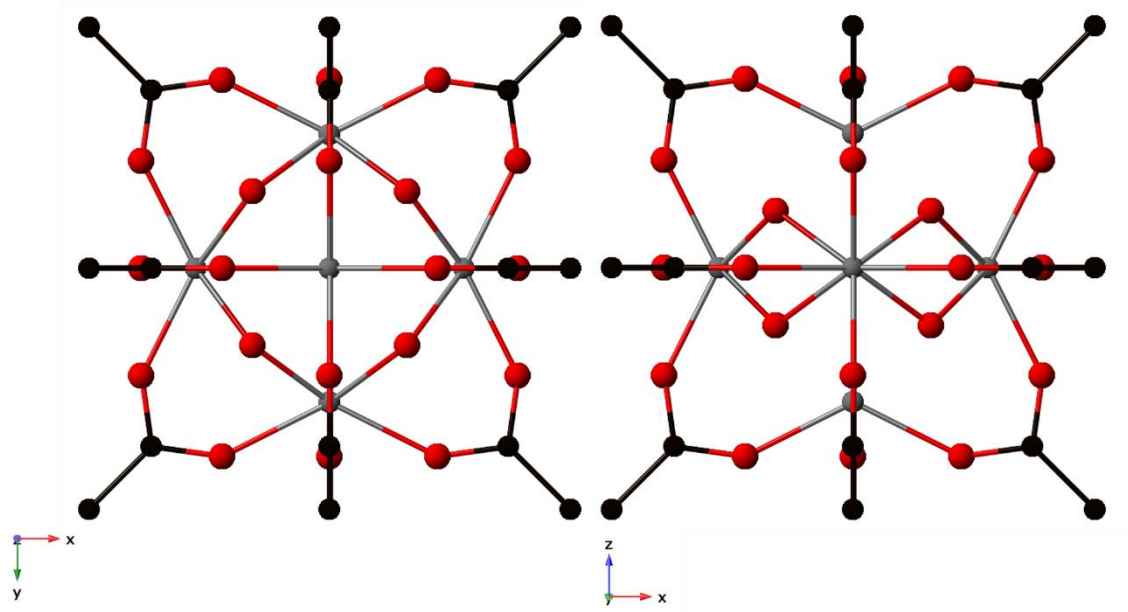

Figure 56: Resultant model of the refinement of data collected on sample ZAA7 using the second iteration single-phase refinement viewed from the axial positions (left) and the equatorial plane (right). Key: Zr – Grey, O – Red, C – Black.

Table 19: Bond lengths and angles of the Hennig model and the models resulting from the second iteration of the single-phase refinement of samples ZAA1, ZAA4, and ZAA7 [2].

Zr-O $_{Core}$ (Å)				Zr-Zr_{Short} (Å)				Zr-Zr_{Long} (Å)			
Hennig model [2]	ZAA1	ZAA4	ZAA7	Hennig model [2]	ZAA1	ZAA4	ZAA7	Hennig model [2]	ZAA1	ZAA4	ZAA7
2.16	2.10	2.10	2.10	3.54	3.56	3.56	3.56	4.97	5.03	5.03	5.03
2.16	2.50	2.49	2.507	3.53				5.02			
2.18											
Zr-$O_{Acetate}$ (Å)				C-$O_{acetate}$ (Å)				C-$C_{Acetate}$ (Å)			
Hennig model [2]	ZAA1	ZAA4	ZAA7	Hennig model [2]	ZAA1	ZAA4	ZAA7	Hennig model [2]	ZAA1	ZAA4	ZAA7
2.22	2.26	2.26	2.26	1.30	1.36	1.35	1.34	1.63	1.60	1.66	1.66
2.23				1.45							
2.24											
2.25											
Centre of cluster-Zr-$O_{(Acetate)}$ (°)				Zr-O-$C_{(Acetate)}$ (°)				O-C-$C_{(acetate)}$ (°)			
Hennig model [2]	ZAA1	ZAA4	ZAA7	Hennig model [2]	ZAA1	ZAA4	ZAA7	Hennig model [2]	ZAA1	ZAA4	ZAA7
122.04	116.59	116.79	116.70	117.75	146.76	145.58	145.37	105.02	128.35	127.37	127.07
123.99				123.14				111.84			

With the exception of the core zirconium oxygen contact distances, of which there are two now reported for the calculated model, all of the bond lengths of the models obtained from these refinements are similar in scale to those in the literature model proposed by Hennig *et al.* and also conventional bond lengths according to literature [2]. This, in turn, means all of them are chemically sensible. The bond angles however show the deviation between this calculated model and that of the literature species. As with the previous refinement iteration, the carboxylate groups are stretched towards the diagonal and thus away from the core of the species. In the Hennig model the distance from the centre of the cluster to the two carbon positions which make up the carboxylate group are 6.07 Å and 4.44 Å for the outer and inner carbon positions respectively. In the models obtained from the refinements presented here, these values are in the range of 6.37 Å – 6.40 Å and 4.74 Å – 4.77 Å respectively an increase of ≈ 0.3 Å for both positions. This is caused by the increase in the Zr-O-$C_{(Acetate)}$ and O-C-$C_{(acetate)}$ bond angles. This phenomenon is seen in the previous refinement iteration.

The alterations made in this refinement iteration led to the creation of two unique zirconium oxygen contact distances. These are approximately 2.10 Å and 2.50 Å. This difference leads to two unique oxidation states for the axial and equatorial zirconium positions. The calculated oxidation states for these models are shown here in Table 20.

Table 20: The resultant oxidation state as derived through bond-valence calculations described by Brown and Altermatt for the second iteration of the single-phase refinement of samples ZAA1, ZAA4, and ZAA7 [92].

Hennig Model [2]		ZAA1		ZAA4		ZAA7	
Actual value	Rounded value	Actual value	Rounded value	Actual value	Rounded value	Actual value	Rounded value
3.82	4	4.15	4	4.14	4	4.17	4
3.78	4	2.47	2	2.52	3	2.46	2

The zirconium positions in the equatorial conformation now have oxidation states in close proximity to 4. It is however on inspection of the axial sites that issues arise. These sites display a calculated oxidation state of 2.46 – 2.52 all of which are both well below the oxidation states commonly reported for zirconium and are also almost exactly equidistant from both 2 and 3 leading to the requirement for a large amount of rounding. This decreases confidence in the model obtained as these oxidation states are both extremely low and not close enough to integer values to be considered viable or chemically sensible.

The results obtained for these two single-phase refinements, whilst being confirmative of the presence of the hexameric cluster as proposed by Hennig *et al.* do still have substantial room for improvement. It is for this reason that two phase refinements were undertaken to introduce another phase to improve the quality of the fit and overall confidence in the models.

6.2.2 Dual-phase Refinements

The previously obtained refinements whilst reasonable in quality do show room for improvement. This coupled with the preliminary EXAFS results (Chapter 5.1) which suggest that there are in fact two phases present led to the testing of two-phase refinements. These refinements would be carried out in the same way as the previously presented single-phase refinements, but instead of containing only a Z-matrix of the hexameric structure there was a second phase of the tetrameric structure as refined previously for zirconium-oxychloride. The chloride positions were removed from the model as it was seen through elemental analysis that no chlorine was present in the samples. Additional parameters were needed to express phase specific values such as scale and thermal parameters. As such the refinements shown here were carried out with 33 and 34 refineable parameters for both the fixed-core and chandelier model refinements respectively.

The first dual-phase refinement performed modelled the core of the hexameric species as a fixed and highly symmetrical rhombic dodecahedron. This is the same model that was used in the first iteration of the single-phase refinements presented previously. The results of these refinements for samples ZAA1, ZAA4, and ZAA7 are presented in Figure 57, Figure 58, and Figure 59,

The complete set of these dual phase refinements can be found in Figures 13-24 and Tables 17-28 in the appendix.

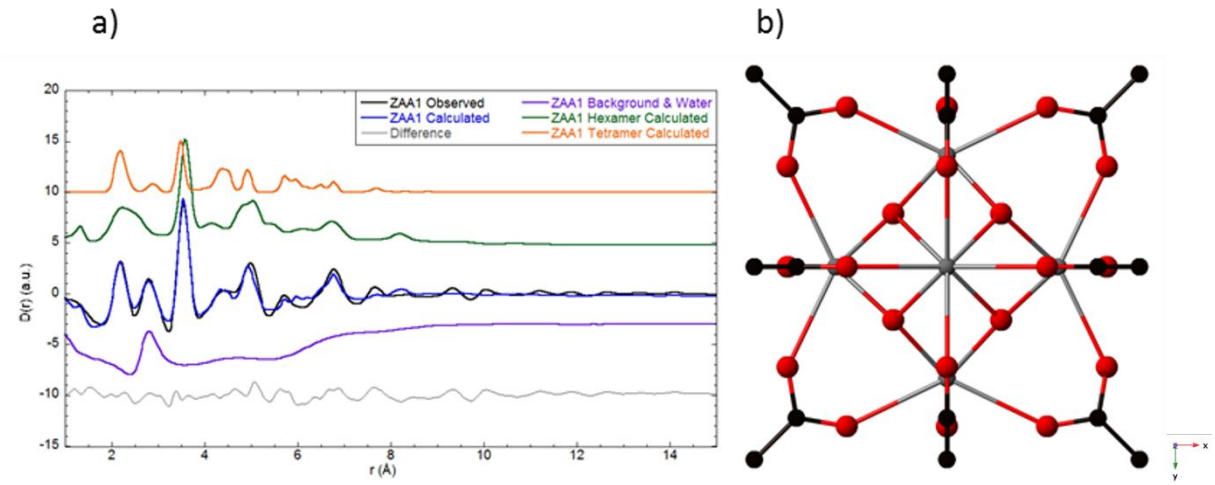

Figure 57: a) Observed (black) and calculated (blue) PDF of the first iteration of the dual-phase refinement of sample ZAA1. Each respective phase has been resolved with the hexameric contribution shown in green, the tetrameric contribution in orange, and the background and water in purple. b) Resultant model of this refinement. Key: Zr – Grey, O – Red, C – Black. R_{wp} = 25.63%.

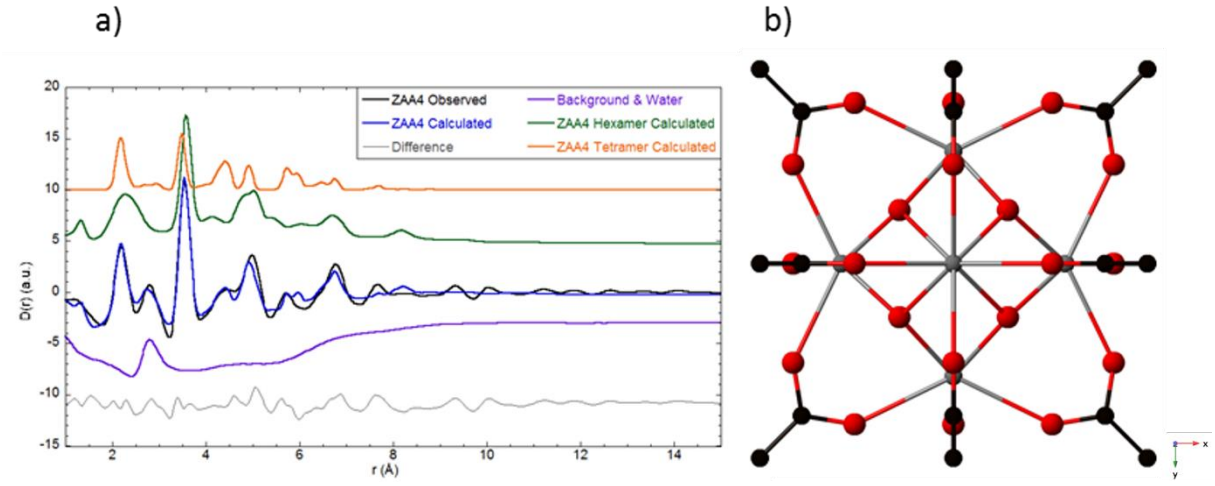

Figure 58: a) Observed (black) and calculated (blue) PDF of the first iteration of the dual-phase refinement of sample ZAA4. Each respective phase has been resolved with the hexameric contribution shown in green, the tetrameric contribution in orange, and the background and water in purple. b) Resultant model of this refinement. Key: Zr – Grey, O – Red, C – Black. R_{wp} = 26.75%.

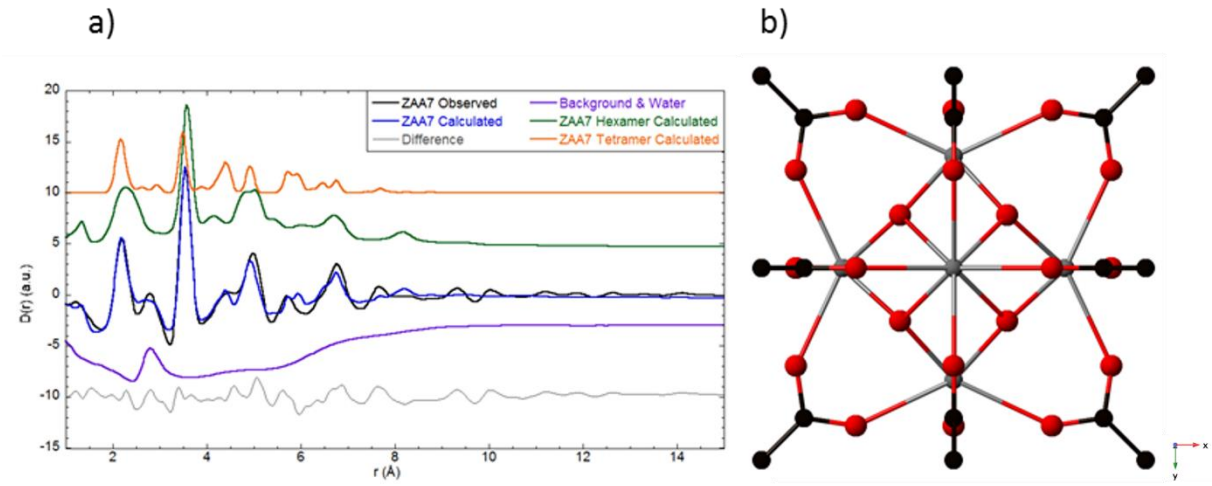

Figure 59: a) Observed (black) and calculated (blue) PDF of the first iteration of the dual-phase refinement of sample ZAA7. Each respective phase has been resolved with the hexameric contribution shown in green, the tetrameric contribution in orange, and the background and water in purple. b) Resultant model of this refinement. Key: Zr – Grey, O – Red, C – Black. R_{wp} = 26.67%.

These refinements converged with R_{wp} scores of 25.63%, 26.75%, and 26.67% for samples ZAA1, ZAA4, and ZAA7 respectively. This is a substantial improvement from the R_{wp} values obtained in previous refinements which is shown in Table 21.

Table 21: R_{wp} values resulting from the two single-phase refinements and the dual-phase refinement.

Sample Name	R_{wp} (%)		
	Single-phase first iteration (Fixed-core)	Single-phase second iteration (Chandelier)	Dual-phase first iteration (Fixed-core)
ZAA1	34.75	30.29	25.63
ZAA4	34.38	29.27	26.75
ZAA7	29.15	28.24	26.67

Comparison of this fixed-core refinement with the single-phase fixed-core refinement presented earlier it is clear that there is an improvement in the agreement between the calculated and observed data. Where previously there was a large discrepancy between the observed and calculated data sets around 5 Å this is improved with the addition of a second

tetrameric phase. The contributions from each phase for each refinement show how the tetrameric phase is responsible for this improvement in the quality of the fit obtained. The tetrameric phase also improves the fit in the region of 6 Å. Where previously the calculated PDF had no contributions which matched this observed feature, now it is clear that a contribution from the tetrameric phase is beneficial to the quality of the refinement.

The key bond lengths and angles are presented in Table 22.

Table 22: Bond lengths and angles of the Hennig model and the hexameric models resulting from the first iteration of the dual-phase refinement of samples ZAA1, ZAA4, and ZAA7 [2].

Zr-O $_{Core}$ (Å)				Zr-Zr_{Short} (Å)				Zr-Zr_{Long} (Å)			
Hennig model [2]	ZAA1	ZAA4	ZAA7	Hennig model [2]	ZAA1	ZAA4	ZAA7	Hennig model [2]	ZAA1	ZAA4	ZAA7
2.16	2.17	2.16	2.16	3.54	3.59	3.59	3.59	4.97	5.07	5.07	5.08
2.16				3.53				5.02			
2.18											
Zr-$O_{Acetate}$ (Å)				C-$O_{acetate}$ (Å)				C-$C_{Acetate}$ (Å)			
Hennig model [2]	ZAA1	ZAA4	ZAA7	Hennig model [2]	ZAA1	ZAA4	ZAA7	Hennig model [2]	ZAA1	ZAA4	ZAA7
2.22	2.54	2.48	2.47	1.30	1.17	1.21	1.19	1.63	1.35	1.34	1.36
2.23				1.45							
2.24											
2.25											
Centre of cluster-Zr-$O_{(Acetate)}$ (°)				Zr-O-$C_{(Acetate)}$ (°)				O-C-$C_{(acetate)}$ (°)			
Hennig model [2]	ZAA1	ZAA4	ZAA7	Hennig model [2]	ZAA1	ZAA4	ZAA7	Hennig model [2]	ZAA1	ZAA4	ZAA7
122.04	115.66	115.98	115.19	117.75	144.65	144.65	146.28	105.02	125.32	125.63	126.47
123.99				123.14				111.84			

From Table 22 it can be seen that once again the refinements have produced results substantially different to those obtained from EXAFS by Hennig *et. al.* The core of the species remains very similar to the literature model but as with previous refinements it is upon closer inspection of the carboxylate groups that differences start to become apparent. The bond distances in these carboxylate groups adopt differing values to those seen in literature. The Zr-$O_{Acetate}$ contact distance is increased from that seen in the Hennig model, from 2.22 Å – 2.25 Å to a value of 2.47 Å – 2.54 Å. These values seen in the calculated model are beyond that which is generally considered reasonable according to previous reports, which generally accepts an average bond distance of around 2.2 ± 0.2 Å [93, 94]. The C-$O_{acetate}$ bonds within the carboxylate group appear shorter in this calculated model than that seen in Hennig's model and is shorter than the typical bond length according to literature which is approximately 1.36 Å for a carboxylate group [99]. The C-$C_{Acetate}$ bonds are also shorter than those seen in the Hennig model and in literature at 1.34 Å – 1.36 Å. Hennig reported values of 1.63 Å and the common literature values are 1.54 Å [99]. The bond angles all show the same patterns that have been reported for previous refinements whereby the methyl group is drawn out toward the diagonal of the structure and the bridging oxygen positions are located closer to the diagonal. This is shown through the decrease in the value of the centre of cluster-Zr-$O_{(Acetate)}$ and also the large increases in the magnitude of the Zr-O-$C_{(Acetate)}$ and O-C-$C_{(acetate)}$ bond angles.

Assessment of the calculated oxidation states through use of the method reported by Brown and Altermatt shows the viability of the zirconium environments proposed and, therefore, by extension the model [92]. These are shown in Table 23.

Table 23: The resultant oxidation state as derived through bond-valence calculations described by Brown and Altermatt for the first iteration of the dual-phase refinement of samples ZAA1, ZAA4, and ZAA7 [92].

Hennig Model [2]		ZAA1		ZAA4		ZAA7	
Actual value	Rounded value	Actual value	Rounded value	Actual value	Rounded value	Actual value	Rounded value
3.82	4	2.87	3	3.00	3	3.05	3
3.78	4						

These values show that the model proposed here from this refinement adopts a zirconium oxidation state of +3, a value uncommon for zirconium.

The two-phase nature of this refinement, however, requires both phases to be assessed for chemical feasibility. As such, the resultant bond lengths, and angles for the tetrameric phases of these refinements are presented in Table 24.

Table 24: Bond lengths and angles of the Clearfield model and the tetrameric models resulting from the first iteration of the dual-phase refinement of samples ZAA1, ZAA4, and ZAA7 [1].

$Zr\text{-}O_{Bridging}$ (Å)				
Clearfield model [1]	ZOC Refined model (Iteration 3)	ZAA1 Dual-phase refinement (Iteration 1)	ZAA4 Dual-phase refinement (Iteration 1)	ZAA7 Dual-phase refinement (Iteration 1)
2.23	2.16	2.12	2.17	2.17
2.36				
2.21				
2.14				
$Zr\text{-}O_{in\text{-}plane}$ (Å)				
Clearfield model [1]	ZOC Refined model (Iteration 3)	ZAA1 Dual-phase refinement (Iteration 1)	ZAA4 Dual-phase refinement (Iteration 1)	ZAA7 Dual-phase refinement (Iteration 1)
2.09	2.33	2.23	2.24	2.22
2.13				
$Zr\text{-}O_{Perpendicular}$ (Å)				
Clearfield model [1]	ZOC Refined model (Iteration 3)	ZAA1 Dual-phase refinement (Iteration 1)	ZAA4 Dual-phase refinement (Iteration 1)	ZAA7 Dual-phase refinement (Iteration 1)
2.36	2.18	2.25	2.12	2.08
2.37				
$O\text{-}Zr\text{-}O_{bridging}$ angle (°)				
Clearfield model [1]	ZOC Refined model (Iteration 3)	ZAA1 Dual-phase refinement (Iteration 1)	ZAA4 Dual-phase refinement (Iteration 1)	ZAA7 Dual-phase refinement (Iteration 1)
70.61	67.07	66.62	71.27	70.63
75.17				
$O\text{-}Zr\text{-}O_{in\text{-}plane}$ angle (°)				
Clearfield model [1]	ZOC Refined model (Iteration 3)	ZAA1 Dual-phase refinement (Iteration 1)	ZAA4 Dual-phase refinement (Iteration 1)	ZAA7 Dual-phase refinement (Iteration 1)
98.32	69.36	81.53	84.12	83.08
$O\text{-}Zr\text{-}O_{Perpendicular}$ angle (°)				
Clearfield model [1]	ZOC Refined model (Iteration 3)	ZAA1 Dual-phase refinement (Iteration 1)	ZAA4 Dual-phase refinement (Iteration 1)	ZAA7 Dual-phase refinement (Iteration 1)
132.05	124.72	147.16	142.41	141.31

Inspection of the values found in Table 24 show that the bond lengths determined for this tetramer in the dual-phase are similar to those found in the zirconium-oxychloride refinements presented earlier. The bond angles however show that the terminal oxygen atoms are no longer found clustered in the diagonal positions. The absence of the chlorine atoms allows for the adoption of a more perfect square antiprism centred on each zirconium centre. This is shown in Figure 60 where the model refined from the sample of zirconium-oxychloride is compared to the tetrameric phase from the refinement of sample ZAA1. In the first instance the angles between the oxygen positions were found at 69.36° and 124.72° respectively for the in-plane and perpendicular terminal oxygen positions but these values were determined to be 81.53° and 147.16° in the tetrameric phase of ZAA1.

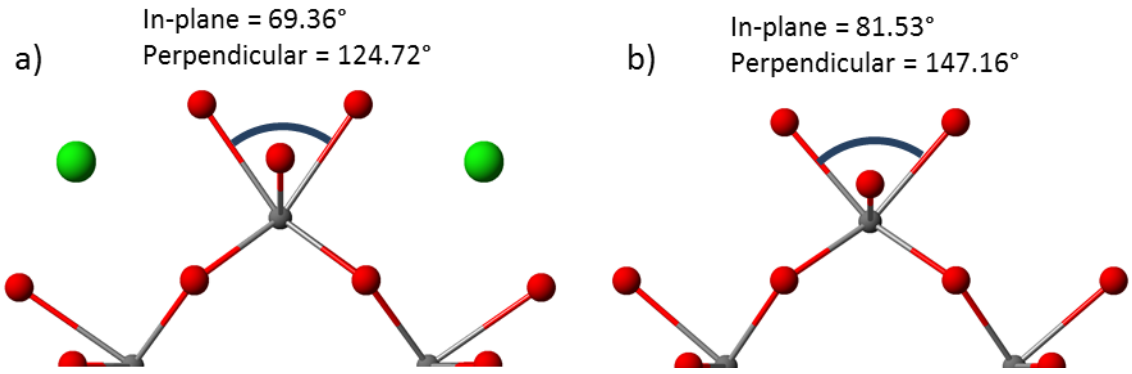

Figure 60: A comparison of a zirconium position and its surrounding oxygen positions for a) the model refined from zirconium-oxychloride and b) the tetrameric phase of the refinement of sample ZAA1 showing the bond angles between both the in plane and perpendicular terminal oxygen positions.

This is indicative of the terminal oxygen atoms filling the vacancy generated by the removal of the chlorine atoms from the model. The calculated oxidation states of the zirconium positions in the tetramer are shown below in Table 25.

Table 25: The resultant oxidation state as derived through bond-valence calculations described by Brown and Altermatt for the tetrameric phase of the first iteration of the dual-phase refinement of samples ZAA1, ZAA4, and ZAA7 [92].

Clearfield Model [1]		ZAA1		ZAA4		ZAA7	
Actual value	Rounded value	Actual value	Rounded value	Actual value	Rounded value	Actual value	Rounded value
3.62	4	4.09	4	4.10	4.0	4.30	4

All the models resolve with zirconium oxidation states equal to 4 which is typical for a zirconium atom. As such this refinement does not contradict the work done previously and confirms the validity of the tetrameric species.

The results presented here have shown that the refinement model does indeed benefit from the addition of a tetrameric phase. The quality of the fit obtained has seen a substantial improvement. The models generated however are not without flaw and the low calculated oxidation states in the hexameric phase and the bond lengths linking the carboxylate groups with the core cluster being beyond those conventionally seen in literature, lead to doubt into the suitability of this model.

A second iteration of the two-phase refinement technique was employed. Much like the single-phase refinements, this second iteration modelled the hexameric species in the chandelier conformation. This refinement was explored with the same justification as the single-phase iteration two refinement. The fits resulting from the refinements are shown below in Figure 61, Figure 62, and Figure 63 for ZAA1, ZAA4, and ZAA7 respectively.

The full set of refinement results and the corresponding tables of atomic coordinates can be found in Figures 25-36 and Tables 29-40 in the appendix.

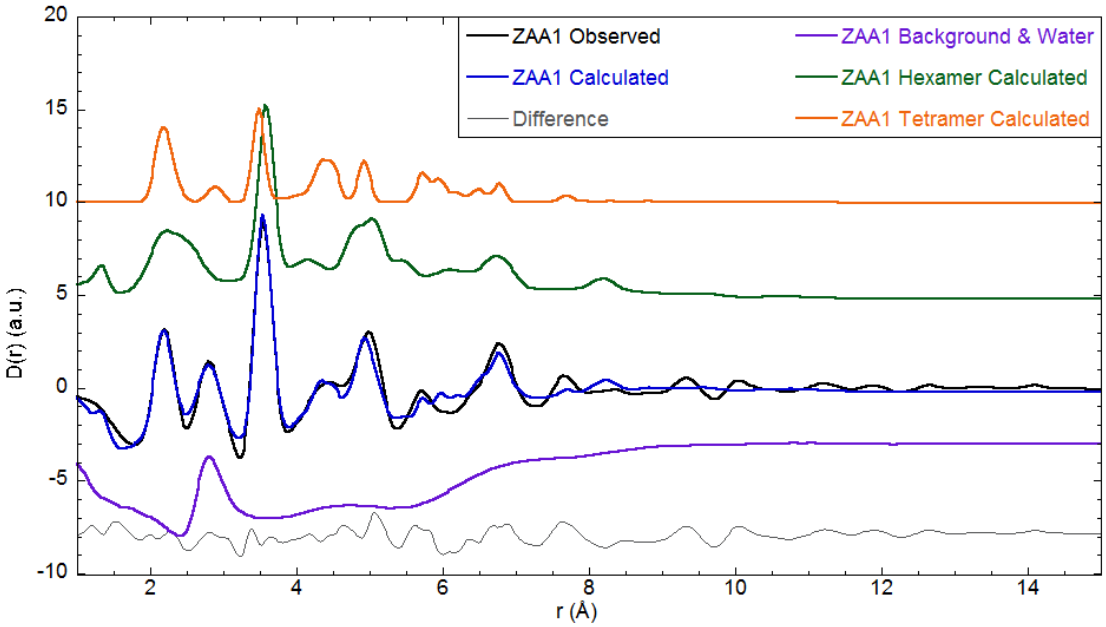

Figure 61: Observed (black) and calculated (blue) PDF of the second iteration of the dual-phase refinement of sample ZAA1. Each respective phase has been resolved with the hexameric contribution shown in green, the tetrameric contribution in orange and the background and water in purple. R_{wp} = 26.07%.

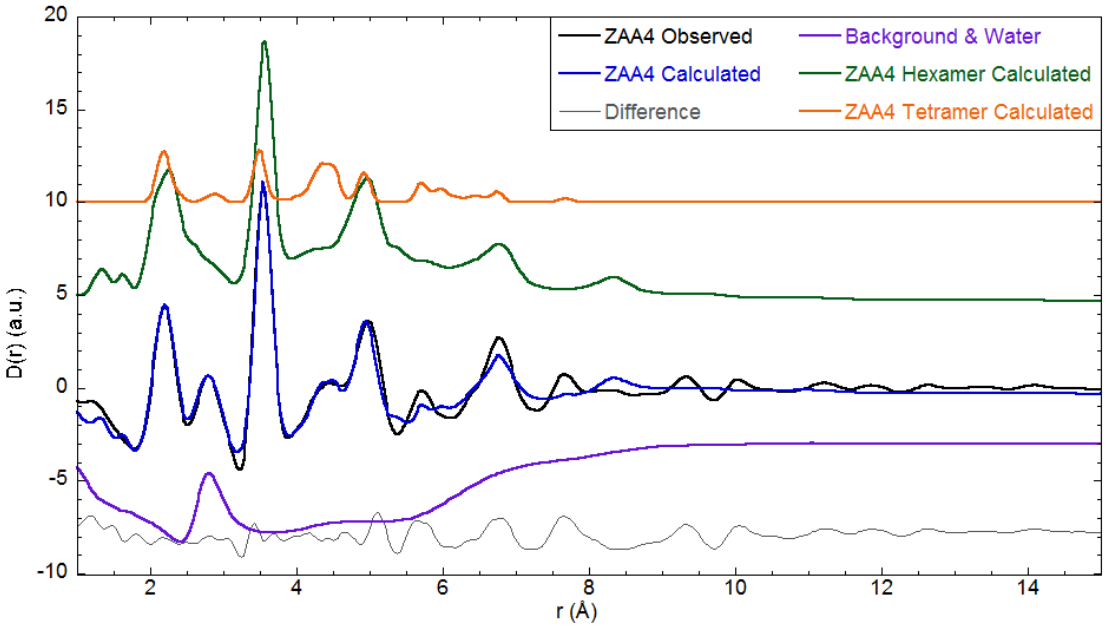

Figure 62: Observed (black) and calculated (blue) PDF of the second iteration of the dual-phase refinement of sample ZAA4. Each respective phase has been resolved with the hexameric contribution shown in green, the tetrameric contribution in orange and the background and water in purple. R_{wp} = 25.25%.

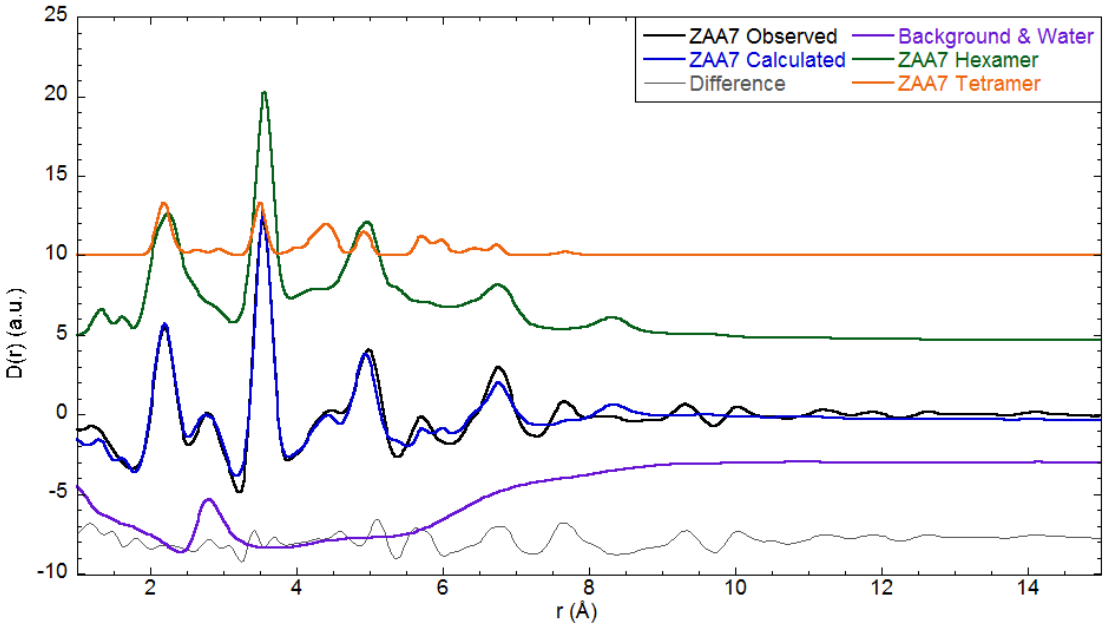

Figure 63: Observed (black) and calculated (blue) PDF of the second iteration of the dual-phase refinement of sample ZAA7. Each respective phase has been resolved with the hexameric contribution shown in green, the tetrameric contribution in orange and the background and water in purple. R_{wp} = 24.84%.

The R_{wp} values of these and all previous fits are shown in Table 26 below.

Table 26: R_{wp} values arising from all the refinements of data from this period data collection.

Sample Name	R_{wp} (%)			
	Single-phase first iteration (Fixed-core)	Single-phase second iteration (Chandelier)	Dual-phase first iteration (Fixed-core)	Dual-phase second iteration (Chandelier)
ZAA1	34.75	30.29	25.63	26.07
ZAA4	34.38	29.27	26.75	25.25
ZAA7	29.15	28.24	26.67	24.84

Visual inspection of the fits shows all refinements show good agreement and this is confirmed by the R_{wp} values shown in Table 26. There is no substantial increase in the quality of the fits against the previous two-phase refinement. All three fits presented here show extremely good agreement with the observed data up to a range of approximately 6 Å, where although the quality of the agreement decreases it is still positive.

A difference in the profile of the tetrameric PDF, within the range 4.5 Å < r < 5.5 Å, can be seen when the sample ZAA1 is compared to samples ZAA4 and ZAA7. ZAA1 shows a broader feature in its calculated tetrameric PDF which is otherwise narrow and well defined in ZAA4 and ZAA7. This is caused by the presence of a significant difference between the two terminal Zr-O bond lengths observed in this tetrameric phase. In ZAA1 these two values are 2.20 and 2.24 Å, whereas in ZAA4 these values are 2.21 and 2.22 Å. This, coupled with the larger O-Zr-O angle found in ZAA1 leads to splitting of this peak and improves the resolution of two unique peaks in the PDF.

Inspections of the models and their key parameters are once again necessary to assess the quality of the refinements presented here. The models obtained are shown below in Figure 64, Figure 65, and Figure 66 for ZAA1, ZAA4, and ZAA7. The images of the structures obtained

from the refinements do not show any substantial variation. instead, the table of key parameters describing them must be consulted. The key bond lengths and angles are presented in Table 27.

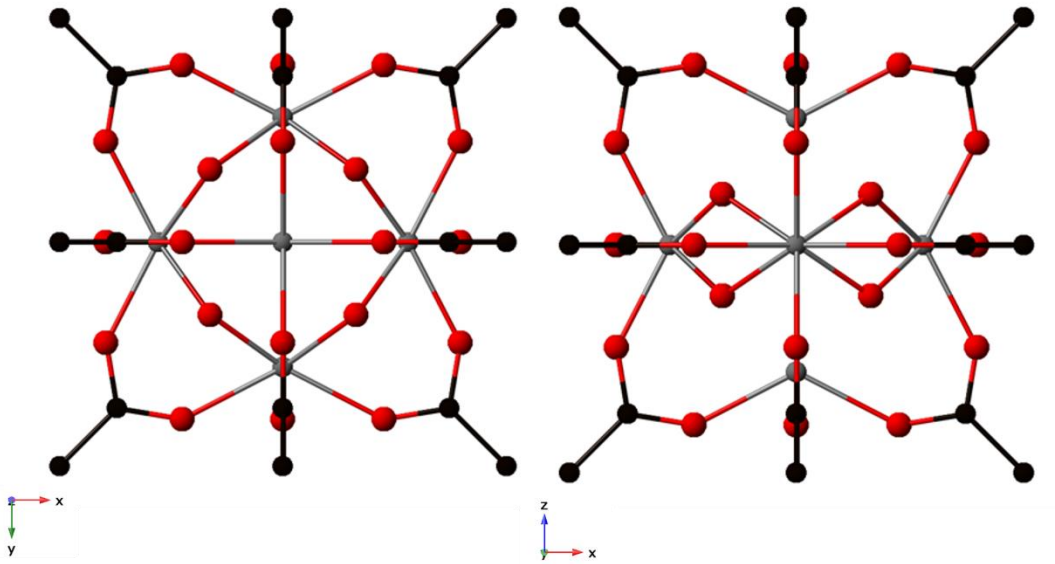

Figure 64: Resultant model of the refinement of data collected on sample ZAA1 using the second iteration dual-phase refinement viewed from the axial positions and the equatorial plane. Key: Zr – Grey, O – Red, C – Black.

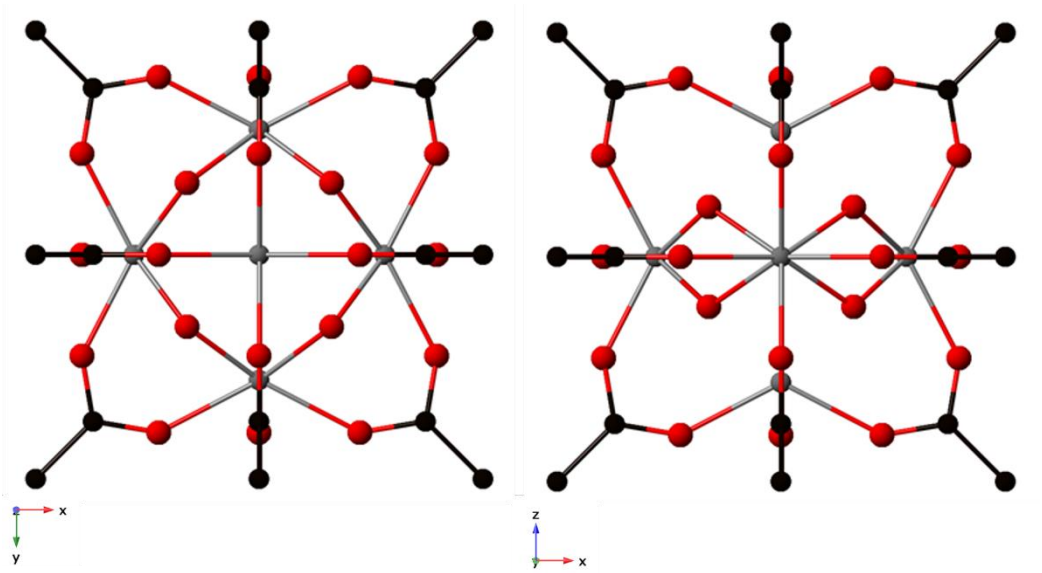

Figure 65: Resultant model of the refinement of data collected on sample ZAA4 using the second iteration dual-phase refinement viewed from the axial positions and the equatorial plane. Key: Zr – Grey, O – Red, C – Black.

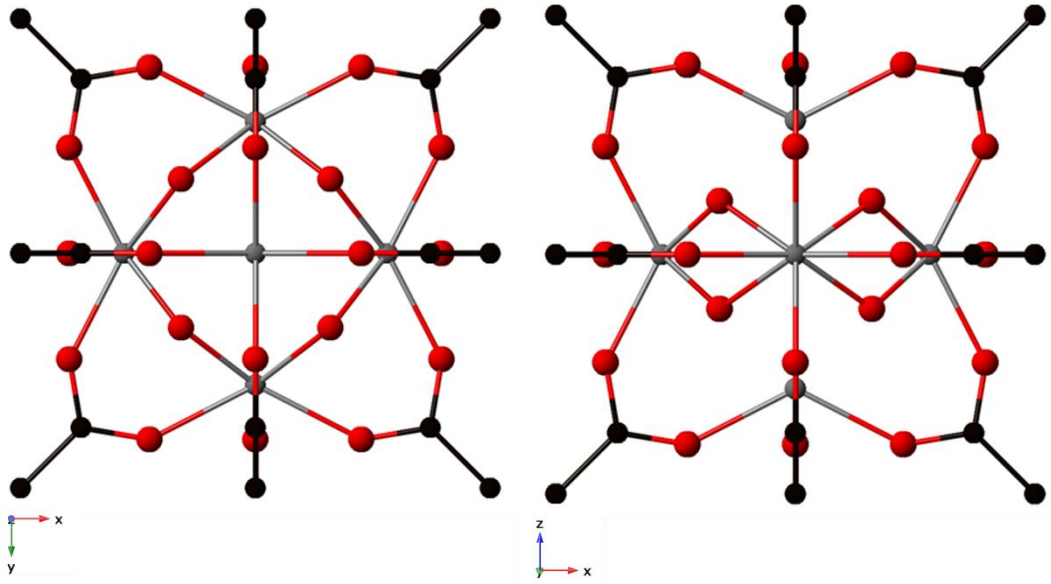

Figure 66: Resultant model of the refinement of data collected on sample ZAA7 using the second iteration dual-phase refinement viewed from the axial positions and the equatorial plane. Key: Zr – Grey, O – Red, C – Black.

Table 27: Bond lengths and angles of the Hennig model and the hexameric models resulting from the second iteration of the dual-phase refinement of samples ZAA1, ZAA4, and ZAA7 [2].

Zr-O $_{Core}$ (Å)				Zr-Zr_{Short} (Å)				Zr-Zr_{Long} (Å)			
Hennig model [2]	ZAA1	ZAA4	ZAA7	Hennig model [2]	ZAA1	ZAA4	ZAA7	Hennig model [2]	ZAA1	ZAA4	ZAA7
2.16	2.07	2.07	2.07	3.538	3.57	3.57	3.57	4.97	5.05	5.05	5.05
2.16	2.58	2.56	2.52	3.526				5.02			
2.18											
Zr-$O_{Acetate}$ (Å)				C-$O_{acetate}$ (Å)				C-$C_{Acetate}$ (Å)			
Hennig model [2]	ZAA1	ZAA4	ZAA7	Hennig model [2]	ZAA1	ZAA4	ZAA7	Hennig model [2]	ZAA1	ZAA4	ZAA7
2.22	2.29	2.29	2.29	1.299	1.34	1.34	1.33	1.63	1.64	1.63	1.63
2.23				1.446							
2.24											
2.25											
Centre of cluster-Zr-$O_{(Acetate)}$ (°)				Zr-O-$C_{(Acetate)}$ (°)				O-C-$C_{(acetate)}$ (°)			
Hennig model [2]	ZAA1	ZAA4	ZAA7	Hennig model [2]	ZAA1	ZAA4	ZAA7	Hennig model [2]	ZAA1	ZAA4	ZAA7
122.04	117.33	117.42	117.21	117.75	143.28	142.96	143.20	105.02	125.61	125.38	125.41
123.99				123.14				111.84			

The introduction of the chandelier model allows for the creation of two unique Zr-O_{Core} distances in the core of the modelled cluster species. One of these has resolved to be shorter than the literature model and the other substantially longer. This longer Zr-O bond of 2.52 – 2.56 Å is substantially longer than literature studies would predict. This is offset by the shorter Zr-O length which is smaller than average although still within the region of literature predictions. The Zr-Zr contact distances are similar to the literature model due to how well defined the peaks are due to the increased scattering power of the zirconium atoms. The Zr-$O_{Acetate}$ distances defined are more reasonable than those seen in the previous two-phase refinement: 2.29 Å is a value within the expected literature threshold. However, the C-$O_{acetate}$ bonds observed are larger than those seen in the previous two phase refinement but within the range of the values seen by Hennig *et al.* and are a good match to expected literature values of 1.36 Å [99]. The C-$C_{Acetate}$ bonds are longer than those seen in previous refinements and those seen in literature but are similar to those seen in the Hennig model. The introduction of the chandelier model has led to decreases in the angle separating the bridging oxygen positions in the cluster as is expected. This can be seen in Figure 67 which compares the core of the hexamer structure in the chandelier and fixed-core refinements. It can be seen that the bridging oxygen positions in the chandelier model are further out than the zirconium positions leading to an increase in the Zr-O contact distance between the bridging oxygen positions and the axial zirconium position.

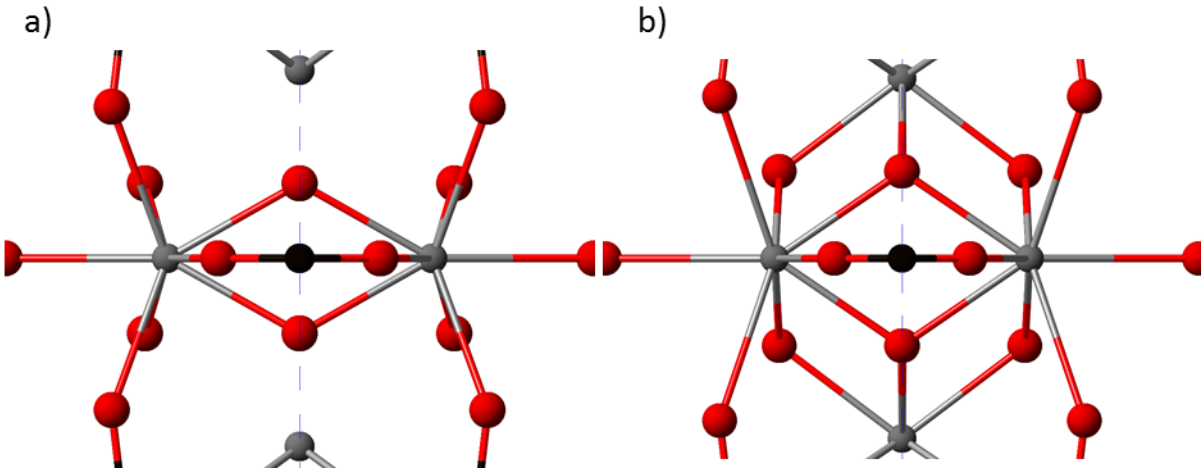

Figure 67: The centre of the hexamer viewed diagonally (110) arising from the a) chandelier model and b) fixed-core model refinements of ZAA1. Key: Zr – Grey, O – Red, C – Black.

The bond angles in the carboxylate group are extremely similar to those seen in previous refinements.

The new models being in the chandelier conformation have two unique zirconium environments and as such two unique oxidation states. These are presented in Table 28 below.

Table 28: The resultant oxidation state as derived through bond-valence calculations described by Brown and Altermatt for the hexameric phase of the second iteration of the dual-phase refinement of samples ZAA1, ZAA4, and ZAA7 [92].

Hennig Model [2]		ZAA1		ZAA4		ZAA7	
Actual value	Rounded value	Actual value	Rounded value	Actual value	Rounded value	Actual value	Rounded value
3.82	4	4.21	4	4.26	4	4.27	4
3.78	4	2.19	2	2.24	2	2.32	2

These values show how the equatorial zirconium positions exhibit a standard +4 oxidation state but those in the axial positions show a substantially decreased value of +2 induced by the increased bond distance between them and the bridging oxygen positions in the core of the cluster.

As the refinement shown here is two phase it is important to assess the chemical sensibility of both phases. As such the key contact distances of the tetrameric phase are presented below in Table 29

Table 29: Bond lengths and angles of the Clearfield model and the tetrameric models resulting from the second iteration of the dual-phase refinement of samples ZAA1, ZAA4, and ZAA7 [1].

$Zr\text{-}O_{Bridging}$ (Å)				
Clearfield model [1]	Refined model (Iteration 3)	ZAA1 Dual-phase refinement (Iteration 1)	ZAA4 Dual-phase refinement (Iteration 1)	ZAA7 Dual-phase refinement (Iteration 1)
2.23	2.16	2.14	2.14	2.19
2.36				
2.21				
2.14				
$Zr\text{-}O_{in\text{-}plane}$ (Å)				
Clearfield model [1]	Refined model (Iteration 3)	ZAA1 Dual-phase refinement (Iteration 1)	ZAA4 Dual-phase refinement (Iteration 1)	ZAA7 Dual-phase refinement (Iteration 1)
2.09	2.33	2.20	2.22	2.21
2.13				
$Zr\text{-}O_{Perpendicular}$ (Å)				
Clearfield model [1]	Refined model (Iteration 3)	ZAA1 Dual-phase refinement (Iteration 1)	ZAA4 Dual-phase refinement (Iteration 1)	ZAA7 Dual-phase refinement (Iteration 1)
2.36	2.18	2.25	2.23	2.11
2.37				
$O\text{-}Zr\text{-}O_{bridging}$ angle (°)				
Clearfield model [1]	Refined model (Iteration 3)	ZAA1 Dual-phase refinement (Iteration 1)	ZAA4 Dual-phase refinement (Iteration 1)	ZAA7 Dual-phase refinement (Iteration 1)
70.61	67.07	67.79	68.42	78.17
75.17				
$O\text{-}Zr\text{-}O_{in\text{-}plane}$ angle (°)				
Clearfield model [1]	Refined model (Iteration 3)	ZAA1 Dual-phase refinement (Iteration 1)	ZAA4 Dual-phase refinement (Iteration 1)	ZAA7 Dual-phase refinement (Iteration 1)
98.32	69.36	85.37	83.89	85.05
$O\text{-}Zr\text{-}O_{Perpendicular}$ angle (°)				
Clearfield model [1]	Refined model (Iteration 3)	ZAA1 Dual-phase refinement (Iteration 1)	ZAA4 Dual-phase refinement (Iteration 1)	ZAA7 Dual-phase refinement (Iteration 1)
132.05	124.72	148.68	145.91	141.21

Once again it can be seen that the tetrameric phase is stable and resolves to be similar to that seen in the original zirconium-oxychloride refinement and also the previous two-phase refinement. The bond angles have, like in the previous two-phase refinements, adapted to the absence of chlorine atoms in the structure and so terminal oxygens are found in positions close to where previously chlorine atoms would be expected. The determined oxidation state of the tetrameric phase for each refinement can be seen in Table 30.

Table 30: The resultant oxidation state as derived through bond-valence calculations described by Brown and Altermatt for the tetrameric phase of the second iteration of the dual-phase refinement of samples ZAA1, ZAA4, and ZAA7 [92].

Clearfield Model [1]		ZAA1		ZAA4		ZAA7	
Actual value	Rounded value	Actual value	Rounded value	Actual value	Rounded value	Actual value	Rounded value
3.62	4	4.07	4	4.07	4.0	4.12	4

Once again, all models show zirconium positions with characteristic +4 oxidation states increasing the chemical viability of the tetramer phase resulting from this refinement.

6.2.3 Summary

The four refinements presented here have all aimed to model the phase composition of zirconium-acetate solutions after 9 months of ageing. It is to be noted that both single-phase refinements resolve with high R_{wp} values and very poor visual fits. The improvement in the quality of fit obtained through the addition of a second phase allows for the conclusion that the solutions studied here all display a ratio of tetrameric and hexameric phases.

The two-phase refinements presented here both show some level of validity whilst also not being without question. The fixed-core method offers the most symmetrical model with all the zirconium positions being treated equally. This would seem more intuitive as all the model lends itself to a high level of symmetry. The results of the bond-valence calculations, however,

describe a common but highly unlikely zirconium position which would exhibit a +3 oxidation state which is generally only seen in unstable complexes and then very rarely. The bond lengths within the cluster for this model are well within those expected within literature with Zr-O contact distances of approximately 2.16 Å, with literature suggesting a bond length of 2.2 Å ± 0.2Å. The bond distances in the carboxylate group however do not agree with those literature would suggest to expect. The Zr-O of the carboxylate is exceptionally large at over 2.50 Å and so is chemically unlikely. These values would only be seen if the carboxylate groups were only weakly associated with the core of the cluster and not exhibiting fully covalent bonding. The chandelier model, whilst overcoming the issues arising from these long Zr-O bonds to the carboxylate groups only shifts the issue to the axial zirconium positions themselves. The four equatorial zirconium positions show great levels of chemical sensibility, but this is not seen when the axial positions are studied. The two distinct environments lead to a dichotomy where the equatorial positions are chemically valid in bond lengths and oxidation states, but the axial positions deviate substantially from expected values. Both models, whilst not being ideal do fit the observed data relatively well and no other non-hexameric model shows any improvement of the refinement result including a modified from of the dual tetrameric model proposed by Tyrsted *et al*. [97].

It is, however, noted that the tetrameric phases for both refinement iterations show high levels of agreement between both each other and also the model determined in Chapter 5.0 increasing the confidence in this derived model. It is hoped that further inspection of the samples, after longer periods of ageing, would give more conclusive results.

6.3 15-Month Data Collection (September 2020)

For the 15-month data collection samples were analysed at I15-1 at Diamond Light Source, UK using the same experimental procedure described in Chapter 4. The zirconium-acetate solutions were loaded into bespoke 1.5 mm diameter quartz capillaries which were spun at high speed for 5-minute ambient temperature data collections. Data collections were run at 76 keV for optimal Q range of approximately 40 $Å^{-1}$. I15-1 employs a Perkin Elmer XRD 1611 CP3 area detector as a primary detector. For the 15-month data collection the samples used were the same capillaries as used in the 9-month data collection interval. These samples were stored, in their capillaries at ambient conditions at I15-1 at Diamond Light Source. As such samples could not be subjected to any controlled temperature conditions in this time. The 15-month data collection was performed on the samples seen below:

Table 31: Details of the samples studied in the second data collection commencing after 15 months of ageing.

Sample Name	Feedstock	ZrO_2 weight percentage	Acetic acid : Zr ratio
ZAA1	1	14	1.6
ZAA4	1	22	1.6
ZAA7	1	30	1.6
ZAA10	3	14	1.6
ZAA13	3	22	1.6
ZAA16	3	30	1.6
ZAA20	2	22	1.6
ZAA24	1	22	1.3
ZAA25	1	22	5.0

Due to the number of samples studied in this data collection, this chapter will concentrate on a select few examples.

The complete set of refinement results originating from this data collection can be found in Figures 37-90 and Tables 41-94 in the appendix.

This chapter will largely focus on the samples ZAA1, ZAA4, and ZAA7, as seen in Chapter 7.2, and also ZAA24, and ZAA25. In these two samples the ratio of acetic acid : zirconium was in the lowest achievable value, 1.3, and a value high in excess of the stoichiometric and charge balancing values (2:1 and 4:1 respectively) of 5.0.

Chapter 6.2 assessed the quality of four different refinement methods: two single-phase and two dual-phase refinements. The single-phase refinements were deemed to be inferior compared to the dual-phase refinements as the quality of the fits were lower. For this reason, whilst the single-phase refinements were carried out for the data presented here, they will not be discussed or presented but may again be found in Figures 43-50 and Tables 47-54 in the Appendix.

An overlay of the 5 PDF patterns to be studied is shown below in Figure 68.

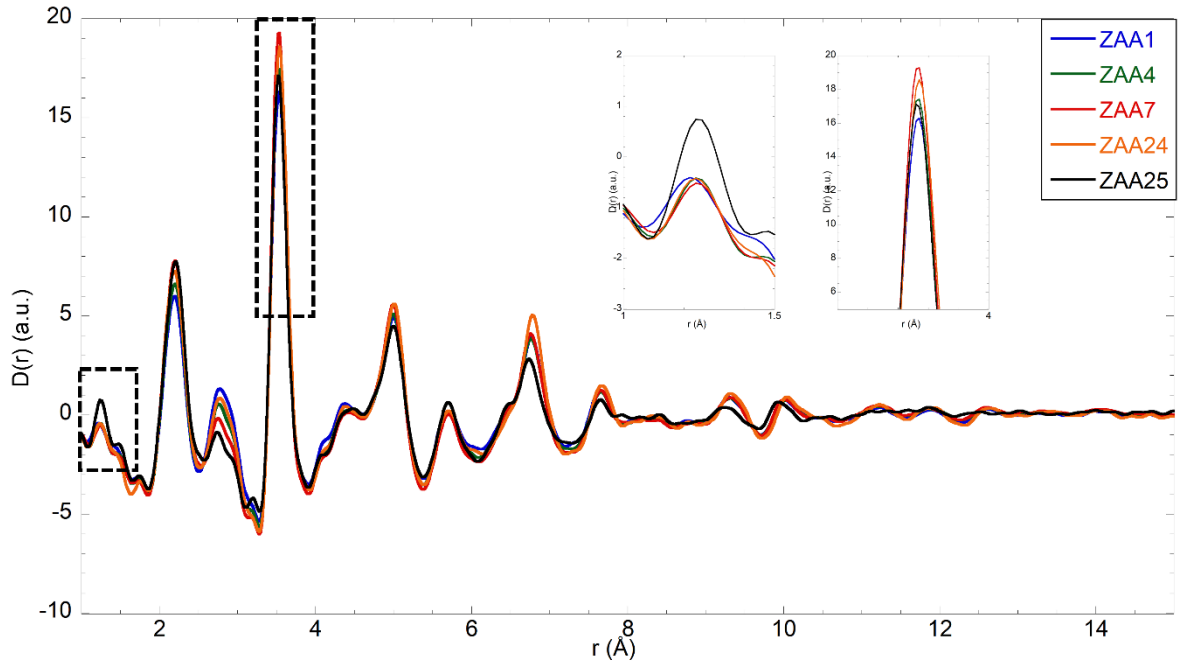

Figure 68: Overlay of the PDFs collected in the 15-month data collection period over an r-range of 0 Å < r < 15 Å.

It can be seen that once again the obtained PDFs all show a similar overall structure. Closer inspection, however, does reveal some deviations. Whilst ZAA24 shows a lower than average

peak intensity in the region of 1.0 – 1.5 Å (previously characterised as C-O and C-C bonds) it shows a higher than average intensity in the principal Zr-Zr peak at 3.5 – 4.0 Å. This implies a reduced concentration of the hexameric phase, where the C-O and C-C bonds are seen exclusively, and a preference for the tetrameric phase. The inverse is also seen for the sample ZAA25. However, these hypotheses can only be confirmed and quantified through the dual-phase refinements and phase ratio analysis presented in Chapter 7.5.

The first dual-phase refinement performed, once again, modelled the core of the hexameric species as a fixed and highly symmetrical rhombic dodecahedron. The results of these refinements can be seen below in Figure 69, 70, 71, 72, and 73.

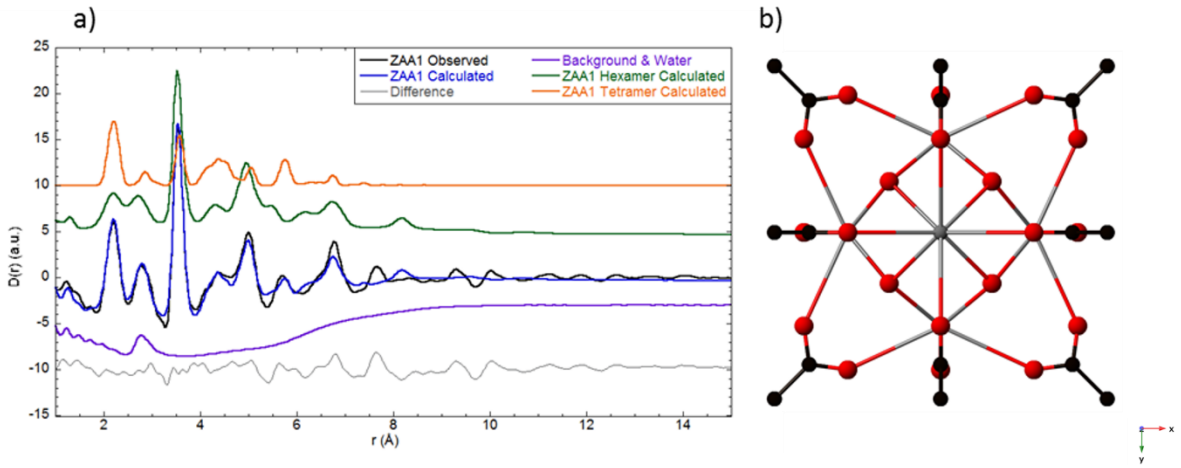

Figure 69: a) Observed (black) and calculated (blue) PDF of the first iteration of the dual-phase refinement of sample ZAA1. Each respective phase has been resolved with the hexameric contribution shown in green, the tetrameric contribution in orange, and the background and water in purple. R_{wp} = 24.77%. b) Resultant model of this refinement. Key: Zr – Grey, O – Red, C – Black.

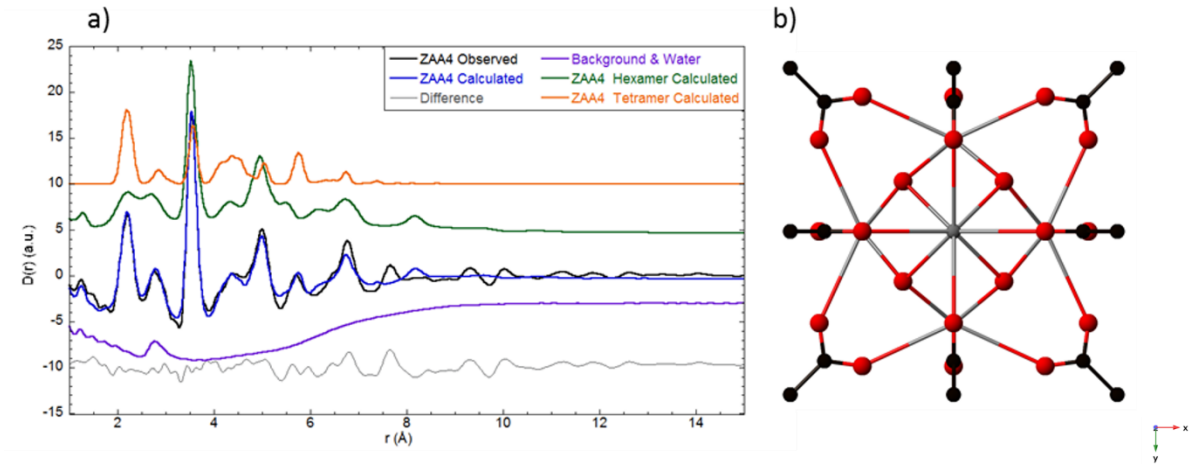

Figure 70: a) Observed (black) and calculated (blue) PDF of the first iteration of the dual-phase refinement of sample ZAA4. Each respective phase has been resolved with the hexameric contribution shown in green, the tetrameric contribution in orange, and the background and water in purple. R_{wp} = 24.38%. b) Resultant model of this refinement. Key: Zr – Grey, O – Red, C – Black.

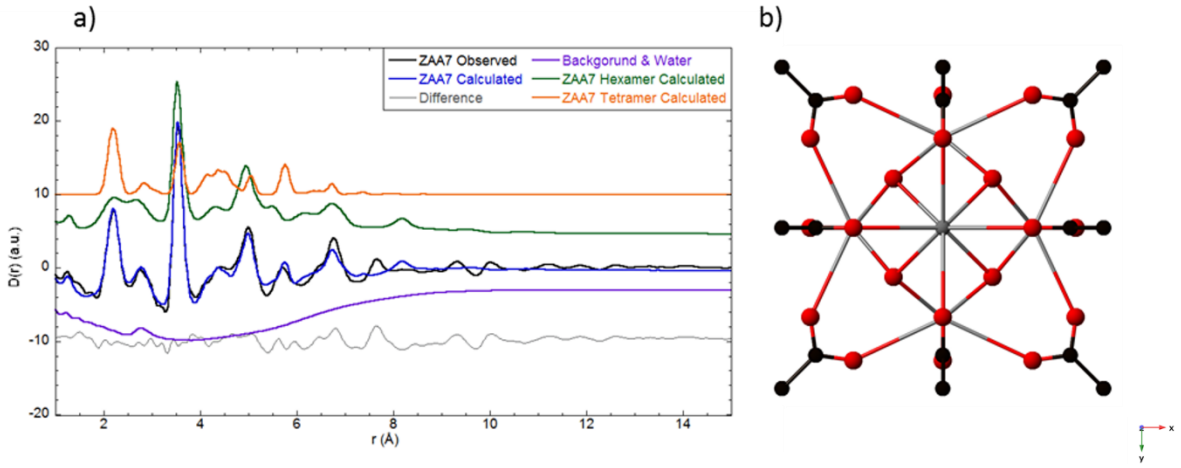

Figure 71: a) Observed (black) and calculated (blue) PDF of the first iteration of the dual-phase refinement of sample ZAA7. Each respective phase has been resolved with the hexameric contribution shown in green, the tetrameric contribution in orange, and the background and water in purple. R_{wp} = 24.17%. b) Resultant model of this refinement. Key: Zr – Grey, O – Red, C – Black.

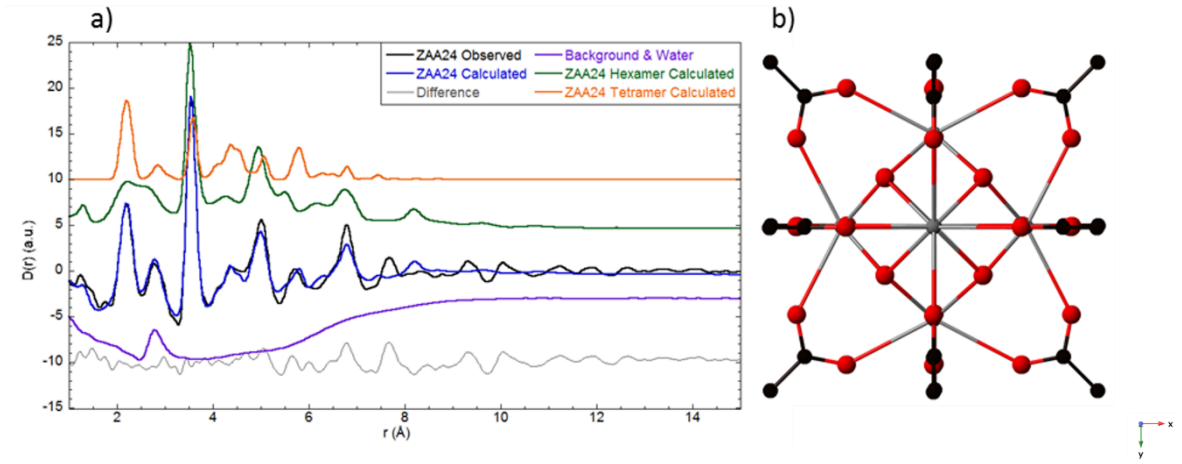

Figure 72: a) Observed (black) and calculated (blue) PDF of the first iteration of the dual-phase refinement of sample ZAA24. Each respective phase has been resolved with the hexameric contribution shown in green, the tetrameric contribution in orange, and the background and water in purple. R_{wp} = 25.53%. b) Resultant model of this refinement. Key: Zr – Grey, O – Red, C – Black.

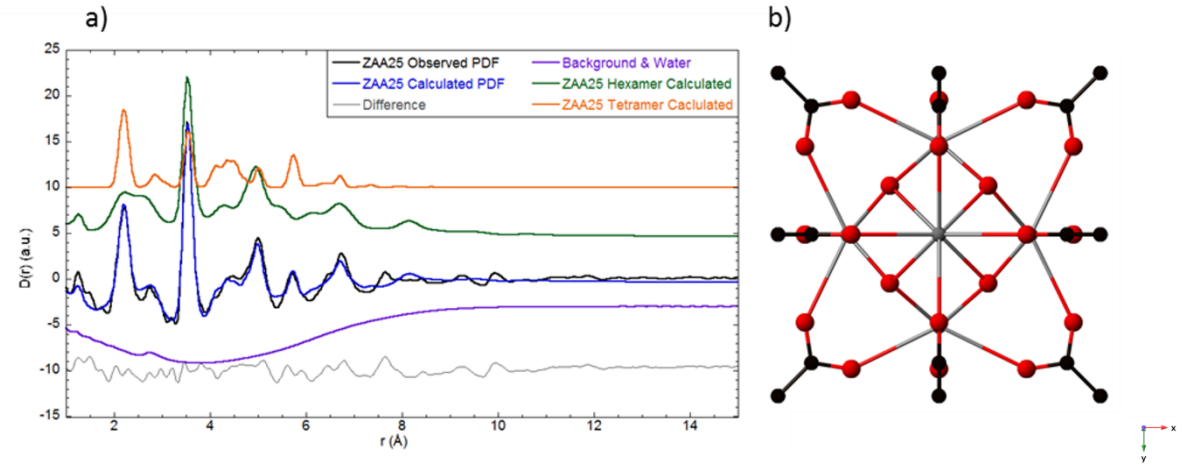

Figure 73: a) Observed (black) and calculated (blue) PDF of the first iteration of the dual-phase refinement of sample ZAA25. Each respective phase has been resolved with the hexameric contribution shown in green, the tetrameric contribution in orange, and the background and water in purple. R_{wp} = 23.06%. b) Resultant model of this refinement. Key: Zr – Grey, O – Red, C – Black.

The refinements shown here converged with R_{wp} values of 24.77%, 24.38%, 24.17%, 25.53%, and 23.06% respectively. These are all very reasonable values and are very similar to those for the fixed-core dual-phase refinements of data collected at the 9-month interval, seen in Chapter 6.2 (25.63%, 26.75%, and 26.67% for ZAA1, ZAA4, and ZAA7 respectively). It is clear

that the refinements' agreement is good, and this is also true when the PDFs are inspected visually. These two facts lead to increased confidence in the models obtained here.

Visually a distinction can be seen in sample ZAA24 in the range 3.5 Å < r < 4.5 Å. ZAA24 shows a higher intensity peak. This increase in intensity is a direct result of the differences between the thermal parameters of this refinement compared to the others. In ZAA24 the radius value (See Figure 22 in Chapter 4) is substantially larger 51.5 Å than that seen in the other samples (ZAA1 radius = 39.1 Å) this represents higher levels of correlated motion at longer r range leading to better defined and thus more intense peaks in the PDF pattern.

In the tetrameric phase of ZAA25 the peak at 5.0 Å shows a broader profile than that seen in the same location for other refinements. This is caused by the subtly shorter Zr-Zr_{short} contact distance seen for this sample (3.543 Å compared to > 3.570 Å seen in others) and the impact this has on other contact distances. Whilst this is not the contact distance with the noticeable change, due to the nature of PDF measurements for molecular systems, subtle variations in one location can have substantive effects in entirely different regions of r. In this instance the Zr-Zr_{long} contact distance which is represented by the peak at 5.0 Å is shifted inducing the variation seen here.

The key bond lengths and angles for the refinements presented here are shown in Table 32.

Table 32: Bond lengths for the hexamer and angles of the Hennig model and the models resulting from the first iteration of the dual-phase refinements of samples ZAA1, ZAA4, ZAA7, ZAA24, and ZAA25 [2].

Zr-O $_{Core}$ (Å)						Zr-Zr_{Short} (Å)						Zr-Zr_{Long} (Å)					
Hennig model [2]	ZAA1	ZAA4	ZAA7	ZAA24	ZAA25	Hennig model [2]	ZAA1	ZAA4	ZAA7	ZAA24	ZAA25	Hennig model [2]	ZAA1	ZAA4	ZAA7	ZAA24	ZAA25
2.16	2.22	2.22	2.22	2.20	2.20	3.54	3.51	3.51	3.51	3.52	3.52	4.97	4.97	4.97	4.96	4.97	4.97
2.16						3.53						5.02					
2.18																	
Zr-$O_{Acetate}$ (Å)						C-$O_{acetate}$ (Å)						C-$C_{Acetate}$ (Å)					
Hennig model [2]	ZAA1	ZAA4	ZAA7	ZAA24	ZAA25	Hennig model [2]	ZAA1	ZAA4	ZAA7	ZAA24	ZAA25	Hennig model [2]	ZAA1	ZAA4	ZAA7	ZAA24	ZAA25
2.22	2.72	2.72	2.71	2.66	2.65	1.30	1.02	1.03	1.05	1.15	1.11	1.63	1.32	1.30	1.30	1.31	1.28
2.23						1.45											
2.24																	
2.25																	
Centre of cluster-Zr-$O_{(Acetate)}$ (°)						Zr-O-$C_{(Acetate)}$ (°)						O-C-$C_{(acetate)}$ (°)					
Hennig model [2]	ZAA1	ZAA4	ZAA7	ZAA24	ZAA25	Hennig model [2]	ZAA1	ZAA4	ZAA7	ZAA24	ZAA25	Hennig model [2]	ZAA1	ZAA4	ZAA7	ZAA24	ZAA25
122	114	114	115	117	115	117	146	147	147	141	145	105	126	127	127	124	127
123						123						111					

Table 32 shows that the refined models obtained here differ greatly from that which is described in literature. The core remains largely intact, as dictated by the geometry of the Z-matrix, with a slight elongation of the Zr-O bonds: from 2.18 to 2.22 Å. Despite this elongation, the Zr-Zr contact distance has decreased slightly from 3.526 – 3.538 Å to 3.51 – 3.52 Å. The Zr-Zr_{long} contact distance remains largely unchanged.

As was described in the previous refinements of the 9-month data set, the fixed-core geometry leads to a stable core cluster at the expense of the carboxylate groups chemical sense. The bond where this is most pronounced is the Zr-$O_{Acetate}$ in which a bond length of 2.65 – 2.72 Å is obtained. This bond is unprecedented in the literature, the common literature values are approximately 2.2 ± 0.2 Å. Whilst the exact values vary, the trends seen in the dual-phase rigid body refinements are also seen here: a contraction of the C-C and C-O bonds and an enlargement of the bond angles seen in the carboxylate groups which largely cancel each other out. This, overall, has the effect of slightly decreasing the distance between opposite methyl groups by approximately 0.3 Å.

Bond-valence calculations to determine the oxidation state of zirconium are presented below in Table 33.

Table 33: The resultant oxidation state as derived through bond-valence calculations described by Brown and Altermatt for the hexameric phase of the first iteration of the dual-phase refinement of samples ZAA1, ZAA4, ZAA7, ZAA24, and ZAA25 [92].

Hennig Model [2]		ZAA1		ZAA4	
Actual value	Rounded value	Actual value	Rounded value	Actual value	Rounded value
3.82	4	2.31	2	2.28	2
3.78	4				
ZAA7		ZAA24		ZAA25	
Actual value	Rounded value	Actual value	Rounded value	Actual value	Rounded value
2.30	2	2.50	3	2.47	2

It can be seen that the values obtained here the models show an incredibly unlikely zirconium oxidation state of +2. This is caused by the extremely long Zr-O bonds linking the core of the cluster to the acetate groups which surround it. These long bonds decrease the calculated oxidation state, and it is unlikely that if the zirconium positions were in this environment that they would be stable.

An inspection of the second, tetrameric, phase of the refinement is necessary and the key bond distances and angles are shown in Table 34 below.

Table 34: Bond lengths and angles of the Clearfield model and the tetrameric models resulting from the first iteration of the dual-phase refinement of samples ZAA1, ZAA4, ZAA7, ZAA24 and ZAA25 [1].

$Zr\text{-}O_{Bridging}$ (Å)						
Clearfield model [1]	Model from ZOC refinement	ZAA1 Tetrameric Phase	ZAA4 Tetrameric Phase	ZAA7 Tetrameric Phase	ZAA24 Tetrameric Phase	ZAA25 Tetrameric Phase
2.23	2.16	2.27	2.27	2.26	2.27	2.26
2.36						
2.21						
2.14						
$Zr\text{-}O_{in\text{-}plane}$ (Å)						
Clearfield model [1]	Model from ZOC refinement	ZAA1 Tetrameric Phase	ZAA4 Tetrameric Phase	ZAA7 Tetrameric Phase	ZAA24 Tetrameric Phase	ZAA25 Tetrameric Phase
2.09	2.33	2.11	2.13	2.14	2.11	2.16
2.13						
$Zr\text{-}O_{Perpendicular}$ (Å)						
Clearfield model [1]	Model from ZOC refinement	ZAA1 Tetrameric Phase	ZAA4 Tetrameric Phase	ZAA7 Tetrameric Phase	ZAA24 Tetrameric Phase	ZAA25 Tetrameric Phase
2.36	2.18	2.17	2.15	2.14	2.16	2.16
2.37						
$O\text{-}Zr\text{-}O_{bridging}$ angle (°)						
Clearfield model [1]	Model from ZOC refinement	ZAA1 Tetrameric Phase	ZAA4 Tetrameric Phase	ZAA7 Tetrameric Phase	ZAA24 Tetrameric Phase	ZAA25 Tetrameric Phase
70.61	67.07	73.04	72.81	72.58	72.36	73.44
75.17						
$O\text{-}Zr\text{-}O_{in\text{-}plane}$ angle (°)						
Clearfield model [1]	Model from ZOC refinement	ZAA1 Tetrameric Phase	ZAA4 Tetrameric Phase	ZAA7 Tetrameric Phase	ZAA24 Tetrameric Phase	ZAA25 Tetrameric Phase
98.32	69.36	85.98	87.49	90.10	82.41	90.45
$O\text{-}Zr\text{-}O_{Perpendicular}$ angle (°)						
Clearfield model [1]	Model from ZOC refinement	ZAA1 Tetrameric Phase	ZAA4 Tetrameric Phase	ZAA7 Tetrameric Phase	ZAA24 Tetrameric Phase	ZAA25 Tetrameric Phase
132.05	124.72	162.41	161.57	161.48	161.42	162.08

Unlike in the refinements resulting from the 9-month data collection period, the tetrameric phase refined here shows more similarity with that proposed by Clearfield *et al.* compared to that isolated from zirconium-oxychloride [1]. It is only the perpendicular bond length which deviates from this by being closer in magnitude to that seen in the zirconium-oxychloride refinements than the Clearfield model. The Zr-O bond distance here is 2.14 Å – 2.17 Å which is closer to the zirconium-oxychloride refined value of 2.18 Å, than the value of 2.36 Å – 2.37 Å which is found in the Clearfield model. The bond angles for the in-plane oxygen positions follow the same trend seen previously in dual-phase refinements, with the bond angle decreasing compared to the Clearfield model (82.41° – 90.45° compared to the Clearfield value of 98.32°) but this contraction and migration towards the diagonal is not as severe as that seen in the model refined from zirconium-oxychloride (69.36°). This trend, however, is not seen in the perpendicular oxygen positions where, instead, the angle between the oxygen positions is substantially increased compared to the Clearfield model (132.05°) and the zirconium-oxychloride model (124.72°) to a range of values between 161.48° – 162.41° [1]. The calculated oxidation states of the zirconium positions are shown below in Table 35.

Table 35: The resultant oxidation state as derived through bond-valence calculations described by Brown and Altermatt for the tetrameric phase of the first iteration of the dual-phase refinement of samples ZAA1, ZAA4, ZAA7, ZAA24, and ZAA25 [92].

Clearfield Model [1]		ZAA1		ZAA4	
Actual value	Rounded value	Actual value	Rounded value	Actual value	Rounded value
3.62	4	3.83	4	3.85	4
ZAA7		ZAA24		ZAA25	
Actual value	Rounded value	Actual value	Rounded value	Actual value	Rounded value
3.86	4	3.88	4	3.75	4

All the zirconium positions shown here exhibit calculated oxidation states of 3.62 – 3.88. These oxidation states are reasonable and round to +4, the value deemed appropriate.

As was seen with the fixed-core refinements from the 9-month data collection, the refinements presented here have a fixed and immoveable Zr core with high levels of chemical sense in both bond angles and distances and the atomic environments this induces. However, this high level of chemical sense breaks down when the carboxylate groups are studied and in particular how these functional groups associate with the hexameric core. Here we see extremely long and chemically insensible Zr-O bonds of over 2.7 Å. This range is unprecedented according to literature sources. The oxidation states of the hexameric phase, resulting from this refinement are exceptionally low, averaging around 2. Values this low are unfeasible and not commonly reported. The tetrameric phase displayed literature supported oxidation states of +4 for all samples.

The second iteration refinements to be performed and examined here employ the use of the chandelier model for the hexamer. This model was employed in the same way as described in previous chapters and the results of the refinements are shown below Figure 74, 75, 76, 77, and 78.

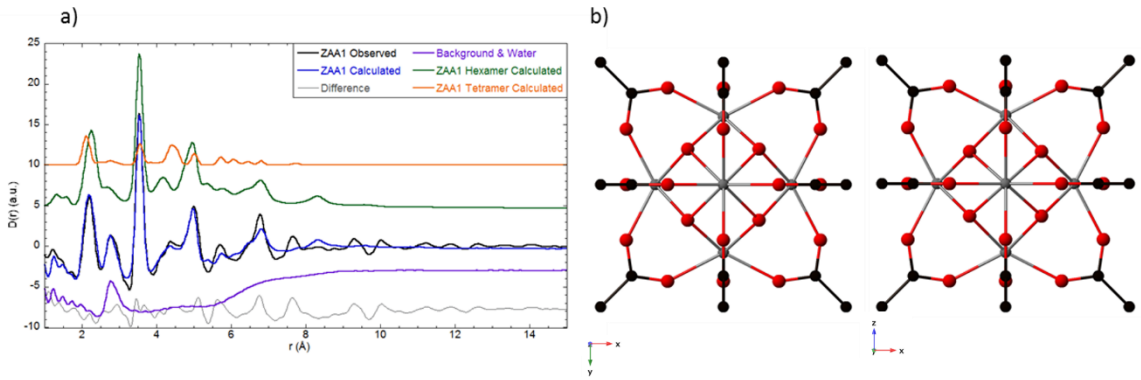

Figure 74: a) Observed (black) and calculated (blue) PDF of the second iteration of the dual-phase refinement of sample ZAA1. Each respective phase has been resolved with the hexameric contribution shown in green, the tetrameric contribution in orange, and the background and water in purple. R_{wp} = 29.36%. b) Resultant model of this refinement. Key: Zr – Grey, O – Red, C – Black.

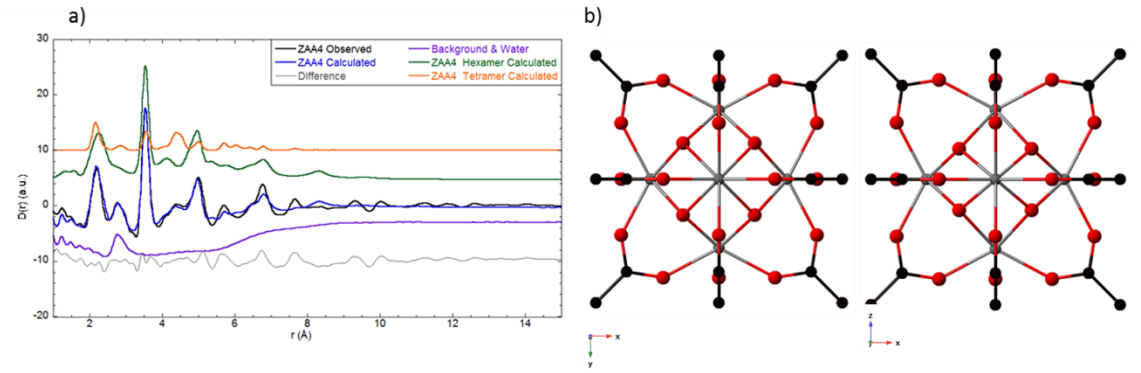

Figure 75: a) Observed (black) and calculated (blue) PDF of the second iteration of the dual-phase refinement of sample ZAA4. Each respective phase has been resolved with the hexameric contribution shown in green, the tetrameric contribution in orange, and the background and water in purple. R_{wp} = 28.34%. b) Resultant model of this refinement. Key: Zr – Grey, O – Red, C – Black.

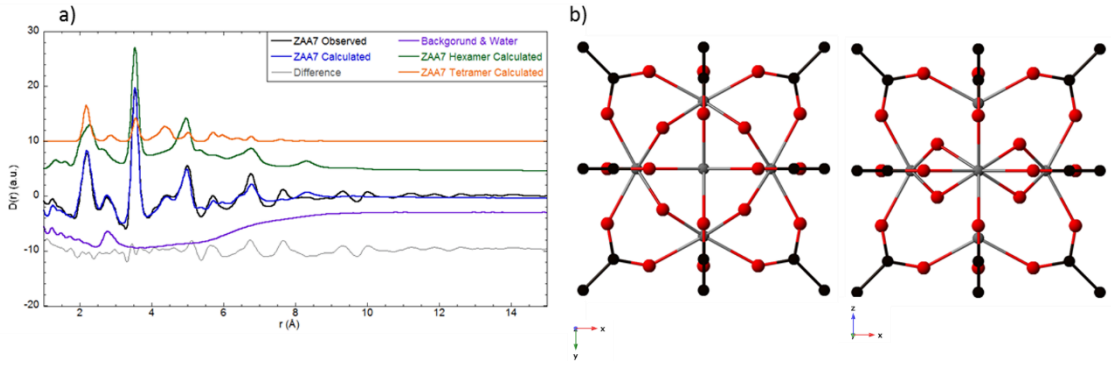

Figure 76: a) Observed (black) and calculated (blue) PDF of the second iteration of the dual-phase refinement of sample ZAA7. Each respective phase has been resolved with the hexameric contribution shown in green, the tetrameric contribution in orange, and the background and water in purple. R_{wp} = 26.59%. b) Resultant model of this refinement. Key: Zr – Grey, O – Red, C – Black.

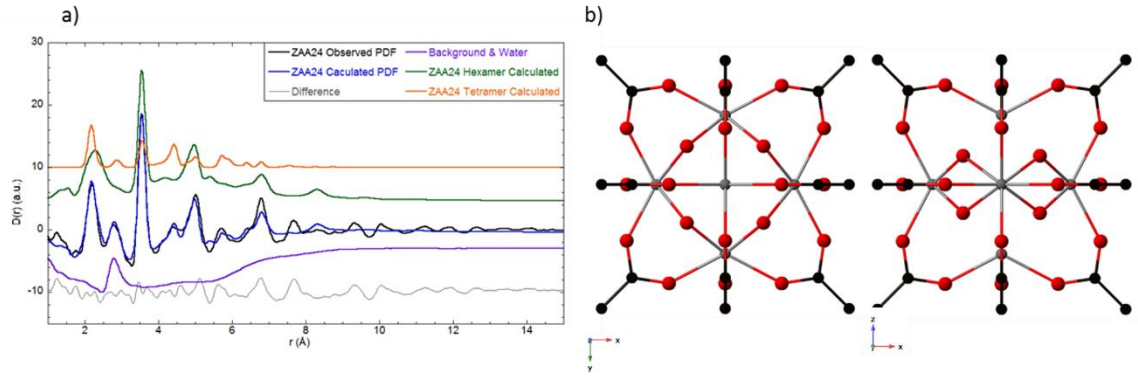

Figure 77: a) Observed (black) and calculated (blue) PDF of the second iteration of the dual-phase refinement of sample ZAA24. Each respective phase has been resolved with the hexameric contribution shown in green, the tetrameric contribution in orange, and the background and water in purple. R_{wp} = 28.51%. b) Resultant model of this refinement. Key: Zr – Grey, O – Red, C – Black.

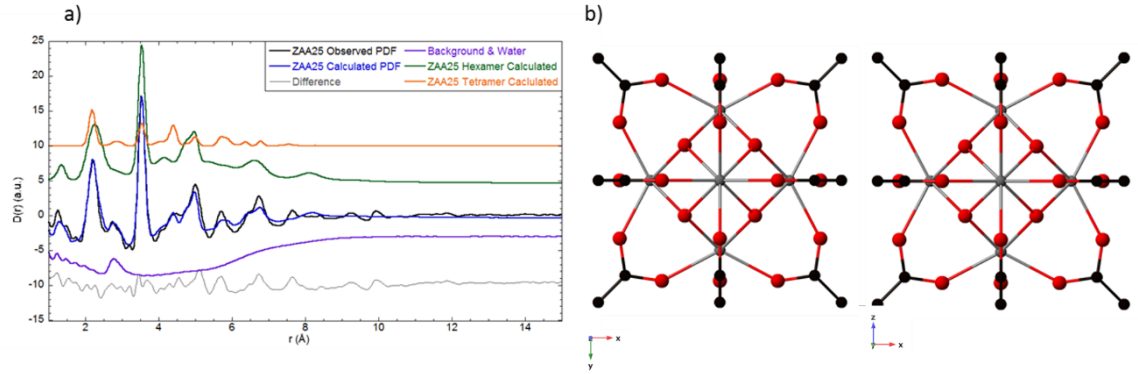

Figure 78: a) Observed (black) and calculated (blue) PDF of the second iteration of the dual-phase refinement of sample ZAA25. Each respective phase has been resolved with the hexameric contribution shown in green, the tetrameric contribution in orange, and the background and water in purple. R_{wp} = 26.72%. b) Resultant model of this refinement. Key: Zr – Grey, O – Red, C – Black.

The refinements seen here converge with R_{wp} values seen below in Table 36.

Table 36: R_{wp} values arising from all the refinements of data from this period data collection.

Sample Name	R_{wp} (%)	
	Dual-phase First Iteration (Fixed-core)	Dual-phase Second Iteration (Chandelier)
ZAA1	24.77	29.36
ZAA4	24.38	28.34
ZAA7	24.17	26.59
ZAA24	25.53	28.51
ZAA25	23.06	26.72

For all samples shown here there was a marked increase in the R_{wp} value from the previous iteration of the refinement. The fixed-core model offered a better quality of fit and thus a higher degree of confidence in the model. However, the degree of confidence offered by the fitting statistics must also be supplemented by confidence in the chemical sense of the model and this is best done through analysis of the key bond lengths and angles which are presented in Table 37.

Table 37: Bond lengths and angles of the Hennig model and the hexamer models resulting from the second iteration of the dual-phase refinements of samples ZAA1, ZAA4, ZAA7, ZAA24, and ZAA25 [2].

Zr-O $_{Core}$ (Å)						Zr-Zr_{Short} (Å)						Zr-Zr_{Long}(Å)					
Hennig model [2]	ZAA1	ZAA4	ZAA7	ZAA24	ZAA25	Hennig model [2]	ZAA1	ZAA4	ZAA7	ZAA24	ZAA25	Hennig model [2]	ZAA1	ZAA4	ZAA7	ZAA24	ZAA25
2.16	2.13	2.09	2.06	2.07	2.15	3.54	3.54	3.54	3.54	3.55	3.54	4.97	5.01	5.01	5.01	5.02	5.00
2.16	2.28	2.32	2.64	2.46	2.19	3.53						5.02					
2.18																	
Zr-$O_{Acetate}$ (Å)						C-$O_{acetate}$ (Å)						C-$C_{Acetate}$ (Å)					
Hennig model [2]	ZAA1	ZAA4	ZAA7	ZAA24	ZAA25	Hennig model [2]	ZAA1	ZAA4	ZAA7	ZAA24	ZAA25	Hennig model [2]	ZAA1	ZAA4	ZAA7	ZAA24	ZAA25
2.22	2.31	2.31	2.31	2.31	2.35	1.30	1.34	1.35	1.35	1.36	1.36	1.63	1.60	1.60	1.62	1.57	1.36
2.23						1.45											
2.24																	
2.25																	
Centre of cluster-Zr-$O_{(Acetate)}$ (°)						Zr-O-$C_{(Acetate)}$ (°)						O-C-$C_{(acetate)}$ (°)					
Hennig model [2]	ZAA1	ZAA4	ZAA7	ZAA24	ZAA25	Hennig model [2]	ZAA1	ZAA4	ZAA7	ZAA24	ZAA25	Hennig model [2]	ZAA1	ZAA4	ZAA7	ZAA24	ZAA25
122.04	117.40	117.82	118.32	117.71	117.78	117.5	144.30	143.42	141.56	143.49	143.72	105.02	126.70	126.23	124.88	126.60	126.50
123.99						123.14						111.84					

The key bond values presented in Table 37 show consistent Zr-Zr contact distances at 3.54 Å and 5.0 Å respectively. The effect of the chandelier model is visible in the presence of two unique Zr-O distances which have remained largely in the realm of bond lengths expected: 2.2 ± 0.2 Å. The bonding from the core to the carboxylate groups is chemically reasonable with Zr-O bonds of approximately 2.3 Å, a chemically sensible value, supported by literature. The C-O bonds seen in the acetic acid groups are precisely where they would be expected and are an improvement toward literature supported values from those seen in Hennig's model [2]. Whilst the degree is not the same, the slight decrease in the C-C bond length also moves towards more acceptable values. The bond angles once again show a migration of the methyl groups of the carboxylate toward the diagonal of the structure, which has been seen before, through the increase in the bond angles. The chemical sense of the zirconium positions can be determined from the calculated oxidation state according to the bond-valence calculations shown below in Table 38.

Table 38: The resultant oxidation state as derived through bond-valence calculations described by Brown and Altermatt for the hexameric phase of the second iteration of the dual-phase refinement of samples ZAA1, ZAA4, ZAA7, ZAA24, and ZAA25 [92].

Hennig Model [2]		ZAA1		ZAA4	
Actual value	Rounded value	Actual value	Rounded value	Actual value	Rounded value
3.815	4	2.99	3	2.80	3
3.781	4	3.75	4	4.01	4
ZAA7		ZAA24		ZAA25	
Actual value	Rounded value	Actual value	Rounded value	Actual value	Rounded value
2.01	2	2.35	2	3.25	3
4.21	4	4.18	4	3.45	3

The values shown here show good support for the chandelier model, with the first two samples, ZAA1 and ZAA4, showing improved oxidation states compared to those seen in

previous refinements. However, samples ZAA7 – ZAA25 show the same pattern seen previously, equatorial positions with almost perfect oxidation states of +4 and axial positions with uncommon oxidation states of +2.

The credibility and chemical sensibility of the tetrameric phase is equally as important as that of the hexameric phase and as the bond lengths and angles are reported below in Table 39.

Table 39: Bond lengths and angles of the Clearfield model and the tetrameric models resulting from the second iteration of the dual-phase refinement of samples ZAA1, ZAA4, ZAA7, ZAA24 and ZAA25 [1].

$Zr\text{-}O_{Bridging}$ (Å)						
Clearfield model [1]	Model from ZOC refinement	ZAA1 Tetrameric Phase	ZAA4 Tetrameric Phase	ZAA7 Tetrameric Phase	ZAA24 Tetrameric Phase	ZAA25 Tetrameric Phase
2.23	2.16	2.08	2.16	2.18	2.17	2.20
2.36						
2.21						
2.14						
$Zr\text{-}O_{in\text{-}plane}$ (Å)						
Clearfield model [1]	Model from ZOC refinement	ZAA1 Tetrameric Phase	ZAA4 Tetrameric Phase	ZAA7 Tetrameric Phase	ZAA24 Tetrameric Phase	ZAA25 Tetrameric Phase
2.09	2.33	2.15	2.14	2.15	2.15	2.13
2.13						
$Zr\text{-}O_{Perpendicular}$ (Å)						
Clearfield model [1]	Model from ZOC refinement	ZAA1 Tetrameric Phase	ZAA4 Tetrameric Phase	ZAA7 Tetrameric Phase	ZAA24 Tetrameric Phase	ZAA25 Tetrameric Phase
2.36	2.18	2.20	2.23	2.23	2.21	2.19
2.37						
$O\text{-}Zr\text{-}O_{bridging}$ angle (°)						
Clearfield model [1]	Model from ZOC refinement	ZAA1 Tetrameric Phase	ZAA4 Tetrameric Phase	ZAA7 Tetrameric Phase	ZAA24 Tetrameric Phase	ZAA25 Tetrameric Phase
70.61	67.07	58.77	66.82	69.20	67.53	70.61
75.17						
$O\text{-}Zr\text{-}O_{in\text{-}plane}$ angle (°)						
Clearfield model [1]	Model from ZOC refinement	ZAA1 Tetrameric Phase	ZAA4 Tetrameric Phase	ZAA7 Tetrameric Phase	ZAA24 Tetrameric Phase	ZAA25 Tetrameric Phase
98.32	69.36	80.39	82.52	85.31	82.75	79.76
$O\text{-}Zr\text{-}O_{Perpendicular}$ angle (°)						
Clearfield model [1]	Model from ZOC refinement	ZAA1 Tetrameric Phase	ZAA4 Tetrameric Phase	ZAA7 Tetrameric Phase	ZAA24 Tetrameric Phase	ZAA25 Tetrameric Phase
132.05	124.72	145.73	149.71	152.42	155.48	155.31

It can be seen that in this iteration of the refinement that the Zr-$O_{Bridging}$ contact distances in the tetrameric phase are similar to those obtained in the zirconium-oxychloride refinements. In the previous dual-phase refinement these bond lengths resolved to be slightly longer than those seen in the zirconium-oxychloride refinements. In the fixed-core refinement of this data set, these values were in the range 2.26 Å – 2.27 Å, here they are seen to be 2.08 Å – 2.18 Å, a value closer to that obtained in the zirconium-oxychloride refinement, 2.16 Å.

The range of bond lengths seen in the in-plane terminal oxygen positions is largely the same as those seen in the previous dual-phase refinements, but the perpendicular positions are slightly extended further from the tetrameric core. Once again, we see a migration of the terminal positions away from the diagonal of the structure compared to that seen when chlorine was present, but not to the extent seen in the Clearfield model [1]. The bond-valence calculations are presented below in Table 40.

Table 40: The resultant oxidation state as derived through bond-valence calculations described by Brown and Altermatt for the tetrameric phase of the second iteration of the dual-phase refinement of samples ZAA1, ZAA4, ZAA7, ZAA24, and ZAA25 [92].

Clearfield Model [1]		ZAA1		ZAA4	
Actual value	Rounded value	Actual value	Rounded value	Actual value	Rounded value
3.62	4	4.75	5	4.17	4
ZAA7		ZAA24		ZAA25	
Actual value	Rounded value	Actual value	Rounded value	Actual value	Rounded value
4.02	4	4.13	4	4.09	4

It can be seen that with the exception of ZAA1 all the zirconium positions exhibit +4 oxidation states. The increase in oxidation state in ZAA1 is induced by the decreased Zr-$O_{Bridging}$ bond length seen in Table 39.

The results of this refinement show good agreement within the core of the structure, with all the core Zr-O contact distances in the hexameric structure being within the range of values reported in literature. The carboxylate groups are chemically sensible and display the same pattern for distorting the bond angles as has been seen in all previous refinements. The bond distances between the Zr positions and the oxygen positions on the carboxylate are also reasonable as has been seen commonly with the chandelier model of refinement but in this instance, this does not come at the cost of the chemical sensibility of the core as it has done previously. The Zr-O bond distances in the core are for the most part within the reasonable window that would be expected; 2.2 ± 0.2 Å. The principal exception to this observation is ZAA7. The oxidation state analysis arising from the bond-valence calculations shows a trend unique to this data collection period. The oxidation states shown for the fixed-core model are exceptionally low, arising from the long Zr-O contact between the core and the carboxylate groups. Those seen in the chandelier model, whilst not achieving the ideal value of +4 universally, do move a great step closer. The equatorial positions all displayed +4 oxidation states whilst most of the axial positions displayed oxidation states of 2 – 3.

6.3.1 Summary

This 15-month data collection has, alongside its 9-month counterpart, served to critically compare the two methods for modelling the hexameric phase in dual-phase refinements. Whilst some of the bond lengths have been seen to be slightly above the expected range, the fixed-core model is felt to be the most likely to represent the hexameric phase present in solution. It is felt that the chandelier model, with its inherent flexibility and its tetramer based core, is not simply representing the hexameric contributions to the PDF pattern but also some of those which should truly be accredited to the tetrameric phase. The low oxidation states of the fixed-core system, induced by the elongated Zr-O bonds from the core to the

carboxylate groups represent the weakened association of the carbonyls to the highly correlated and well bound zirconium – oxygen core. The high level of symmetry offered by the fixed-core model, coupled with its higher level of agreement, shown in the R_{wp} values increases the confidence in this model.

For these reasons it is felt that, despite some faults, the fixed-core model is the superior of the two models and as such the subsequent data collection (18 months, presented in Chapter 6.4) will focus on this fixed-core method of modelling.

6.4 18-Month Data Collection (December 2020)

The data collection presented here represents the broadest range of samples studied in any one data collection in this study and was the first and only XPDF experimental period which was able to assess samples based on storage temperature alongside the physical variables. Data were collected at 28-ID-1 at National Synchrotron Light Source (NSLS-II). Samples were prepared in 1mm Kapton tubing sealed at both ends with epoxy resin. Data were collected under ambient conditions for 1 minute data collections which were repeated an average of 8 times with dark subframes collected between to allow the detector to equilibrate in the dark. A wavelength of 0.1665 Å (74.465 keV) was used.

Whilst 66 samples were studied and underwent structural refinements this chapter will, for brevity, focus on a small subset of these. The sample range selected will cover the full range of acetic acid : zirconium ratios that are included in this study across all three storage temperatures. It was anticipated that the acetic acid : zirconium ratio was the most indicative of changes in the hexamer : tetramer phase ratios (discussed fully in Chapter 6.5) and was of the most interest and relevance to the overall aim of the project. The samples assessed in this chapter are therefore given in Table 41 below.

Table 41: A list of samples studied at NSLS-II as part of the 18 month data collection and the variables that describe them.

Sample Name	Storage Temperature	Acetic Acid : Zirconium Ratio	Concentration (%)	Feedstock
ZAA24C	Chilled	1.3	22	1
ZAA24A	Ambient	1.3	22	1
ZAA24I	Incubated	1.3	22	1
ZAA4C	Chilled	1.6	22	1
ZAA4A	Ambient	1.6	22	1
ZAA4I	Incubated	1.6	22	1
ZAA25C	Chilled	5.0	22	1
ZAA25A	Ambient	5.0	22	1

ZAA25I	Incubated	5.0	22	1

The refinements here are all based on the fixed-core model which, in earlier chapters (Chapter 6.2 – 6.3) was determined to be the superior model. A full set of the refinement results including the chandelier geometry and single-phase refinements can be found in Figures 91-282 and Tables 95-286 in the appendix

A collation of the obtained PDF patterns which will be critically assessed here can be seen below in Figures 79, 80, and 81.

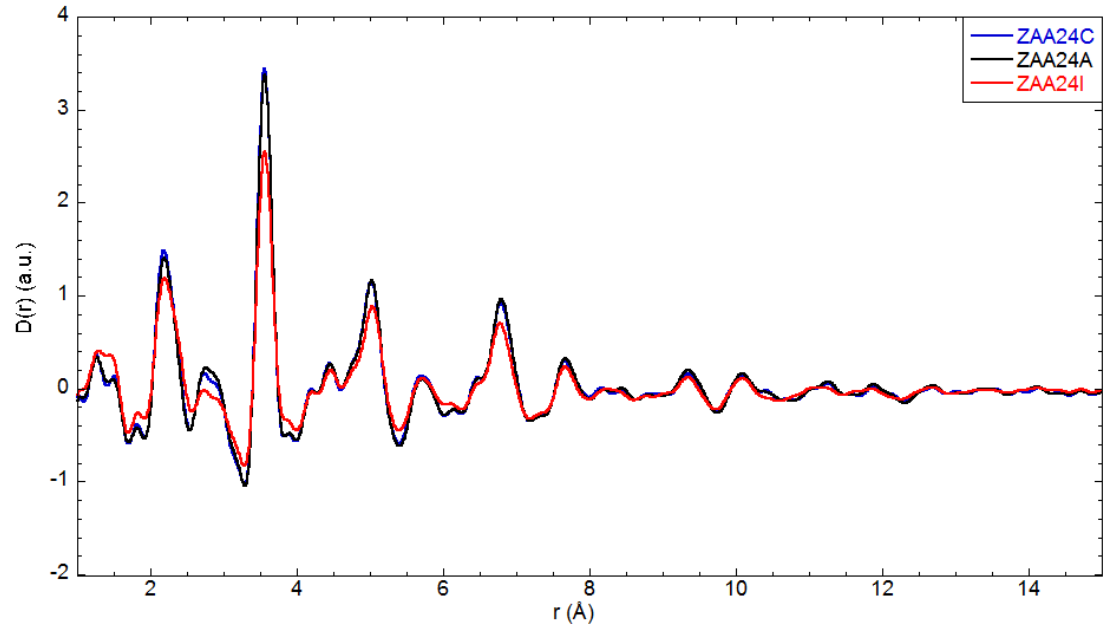

Figure 79: Overlay of the PDFs of samples ZAA24C, ZAA24A, and ZAA24I, collected as part of the 18 month data collection.

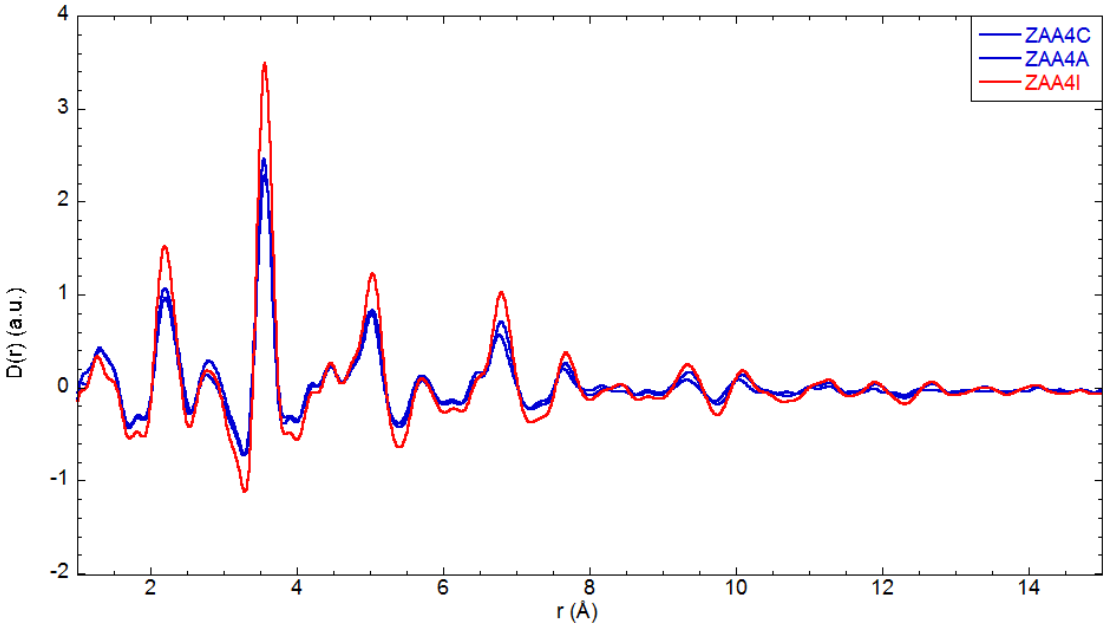

Figure 80: Overlay of the PDFs of samples ZAA4C, ZAA4A, and ZAA4I, collected as part of the 18 month data collection.

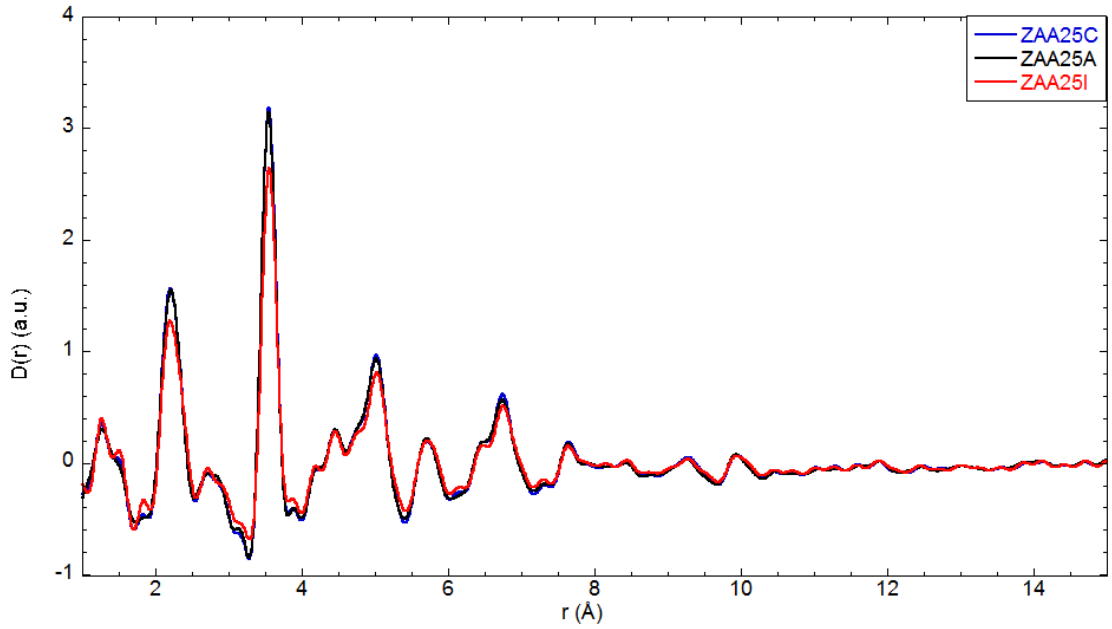

Figure 81: Overlay of the PDFs of samples ZAA25C, ZAA25A, and ZAA25I, collected as part of the 18 month data collection.

It can be seen in the figures above that whilst the obtained PDFs are similar, the storage temperature has a substantive effect on the relative peak intensity. Samples ZAA24 and ZAA4 show distinct differences in the PDF pattern of the incubated samples. For samples ZAA4 this difference manifests over the whole range shown here but in ZAA24 the effect is mitigated at r values r > 8 Å. For both of these, the samples which were stored in the incubator underwent solidification and were a gel like consistency when packed into the capillaries for analysis. It is believed that the solidification has ultimately impacted the relative intensities as this same pattern is not observed in ZAA25, a sample which remained liquid under all storage conditions. Sample ZAA4I shows features in the PDF at high r values. This implies the presence of a longer range of ordering and potentially an aggregation of clusters leading to intracluster contact distances which are not modelled here. The same effect is not noted in ZAA24I, but this may be caused by the reduced intensity seen in the incubated sample countering this effect as the PDF, whilst having lower intensity in low r range, has similar intensities to ZAA24C

and ZAA24A at high r. Sample ZAA25 shows a relatively similar PDF at all three storage temperatures.

The refinements for the sample ZAA24 from all three storage temperatures is shown below.

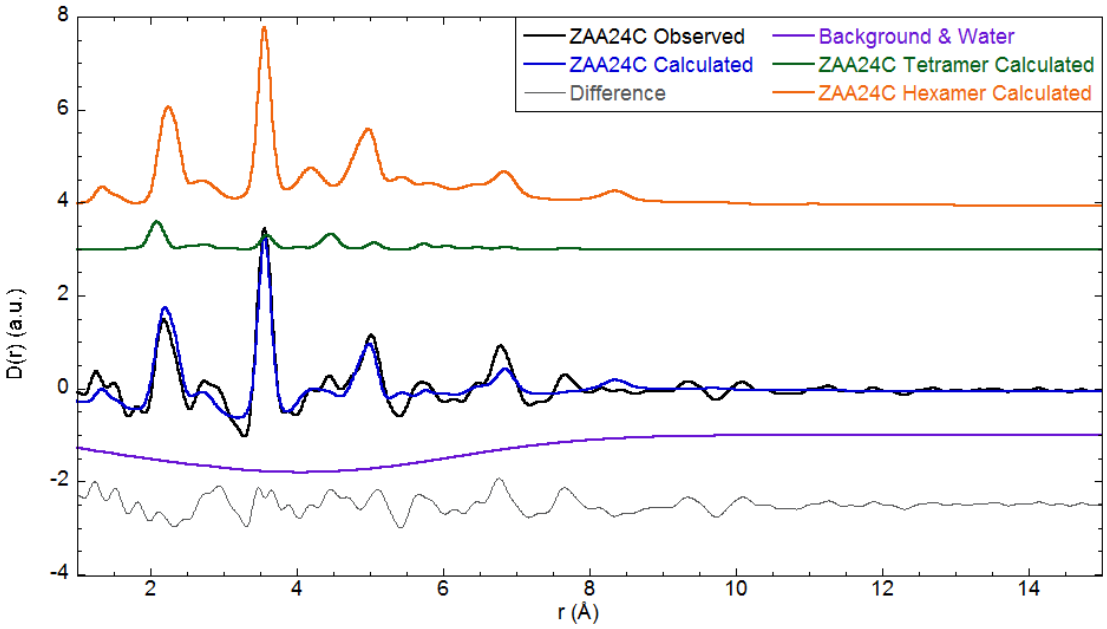

Figure 82: Observed (black) and calculated (blue) PDF of the fixed-core iteration of the dual-phase refinement of sample ZAA24C. Each respective phase has been resolved with the tetrameric contribution shown in green, the hexameric contribution in orange, and the background and water in purple. R_{wp} = 37.13%.

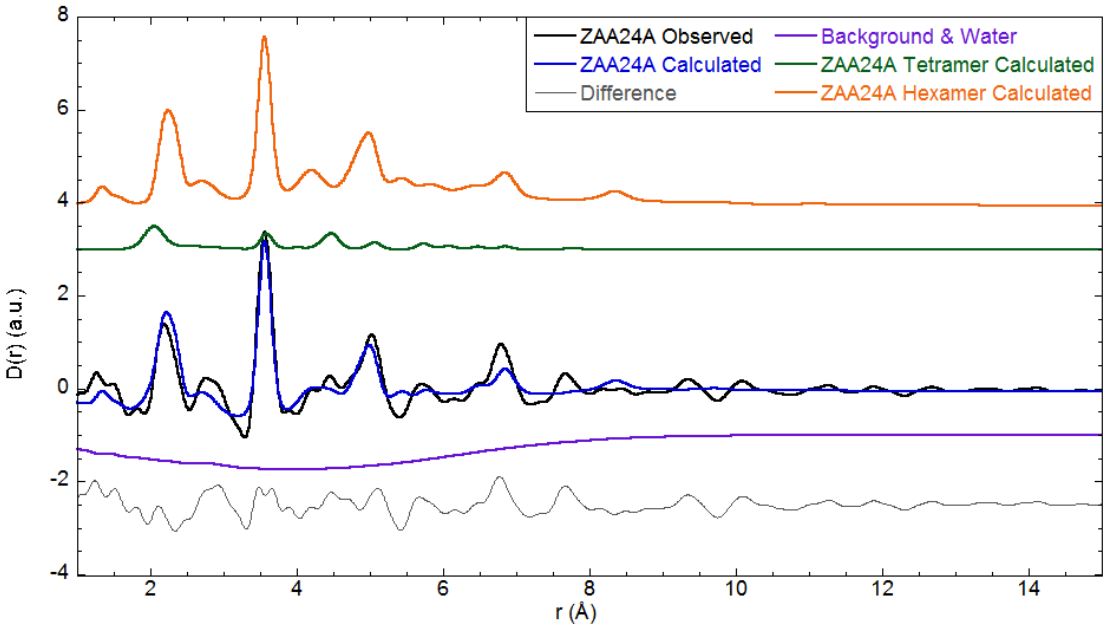

Figure 83: Observed (black) and calculated (blue) PDF of the fixed-core iteration of the dual-phase refinement of sample ZAA24A. Each respective phase has been resolved with the tetrameric contribution shown in green, the hexameric contribution in orange, and the background and water in purple. R_{wp} = 40.55%.

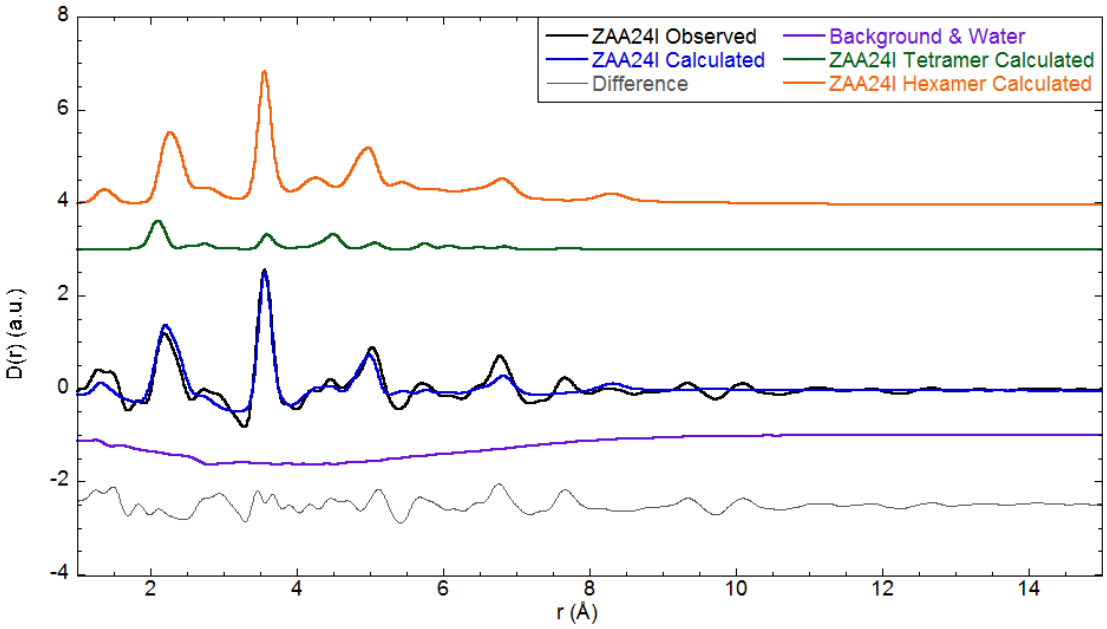

Figure 84: Observed (black) and calculated (blue) PDF of the fixed-core iteration of the dual-phase refinement of sample ZAA24I. Each respective phase has been resolved with the tetrameric contribution shown in green, the hexameric contribution in orange, and the background and water in purple. R_{wp} = 37.37%.

These refinements converged with R_{wp} values of 37.13, 40.55, and 37.37% respectively. It can be seen here that there is very little difference in the fits obtained for these three data sets. The principal difference between the PDF patterns for these samples was in their intensities which is represented in these models as a scale factor. The low r range features, r < 2 Å differ between the three samples with samples ZAA24C and ZAA24A exhibiting decreased intensity at r = 1.50 Å compared to the peak at 1.26 Å. In ZAA24I this difference is not seen, and the peaks are seen with equal intensity. Unfortunately, the refinements do not show the resolution needed to isolate these differences and extract their root cause. The bond distances and angles, shown below (Table 42), confirm that this is true with the only substantive difference being the shortened C-C bond in the incubated sample. This change aims to represent the differences in the short-range of the PDF mentioned previously. The samples show great similarity to the Hennig model with the bond angles being the principal

deviation [2]. Once again, the methyl groups on the carboxylate, migrate away from the cluster through bond angle distortions. This is exacerbated by the elongation of the Zr-O bonds linking the core to the carboxylate groups.

The results of the refinements of the samples ZAA4C-I are shown below (Figures 85 86 87)

Table 42: Bond lengths and angles of the Hennig model and the hexamer models resulting from the fixed-core iteration of the dual-phase refinements of samples ZAA24C, ZAA24A,and ZAA24I [2].

Zr-O $_{Core}$ (Å)				Zr-Zr_{Short} (Å)				Zr-Zr_{Long} (Å)			
Hennig model [2]	ZAA24C	ZAA24A	ZAA24I	Hennig model [2]	ZAA24C	ZAA24A	ZAA24I	Hennig model [2]	ZAA24C	ZAA24A	ZAA24I
2.16	2.18	2.19	2.20	3.538	3.56	3.56	3.56	4.97	5.04	5.03	5.03
2.16				3.526				5.02			
2.18											
Zr-$O_{Acetate}$ (Å)				C-$O_{acetate}$ (Å)				C-$C_{Acetate}$ (Å)			
Hennig model [2]	ZAA24C	ZAA24A	ZAA24I	Hennig model [2]	ZAA24C	ZAA24A	ZAA24I	Hennig model [2]	ZAA24C	ZAA24A	ZAA24I
2.22	2.34	2.34	2.37	1.299	1.35	1.35	1.35	1.63	1.56	1.57	1.49
2.23				1.446							
2.24											
2.25											
Centre of cluster-Zr-$O_{(Acetate)}$ (°)				Zr-O-$C_{(Acetate)}$ (°)				O-C-$C_{(acetate)}$ (°)			
Hennig model [2]	ZAA24C	ZAA24A	ZAA24I	Hennig model [2]	ZAA24C	ZAA24A	ZAA24I	Hennig model [2]	ZAA24C	ZAA24A	ZAA24I
122.04	117.28	117.22	118.19	117.75	145.38	145.22	142.89	105.02	127.66	127.53	126.08
123.99				123.14				111.84			

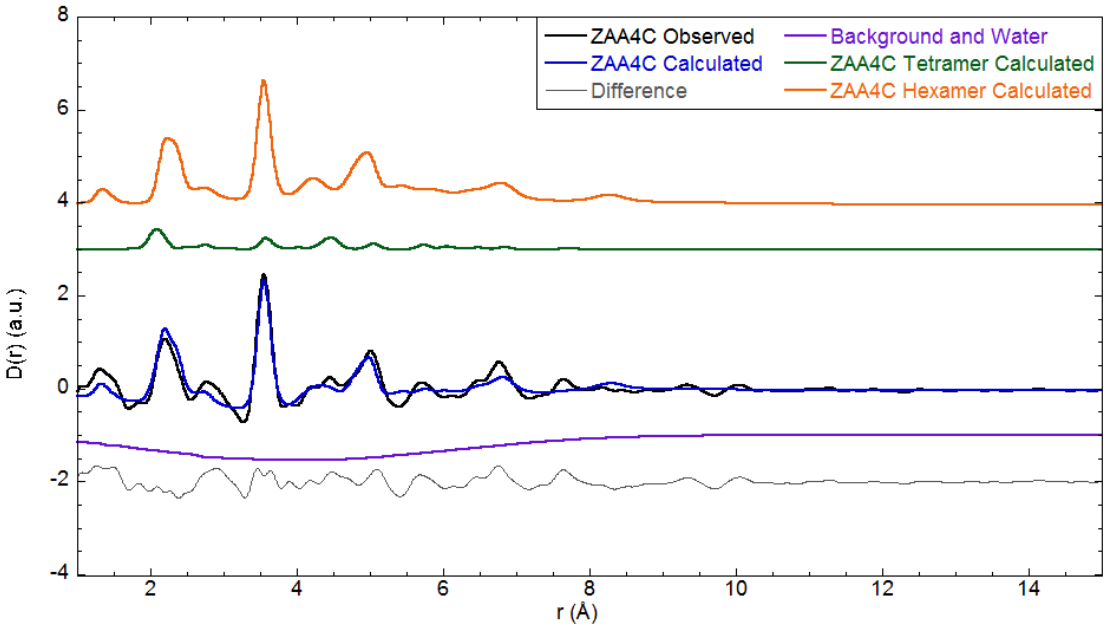

Figure 85: Observed (black) and calculated (blue) PDF of the fixed-core iteration of the dual-phase refinement of sample ZAA4C. Each respective phase has been resolved with the tetrameric contribution shown in green, the hexameric contribution in orange, and the background and water in purple. R_{wp} = 36.90%.

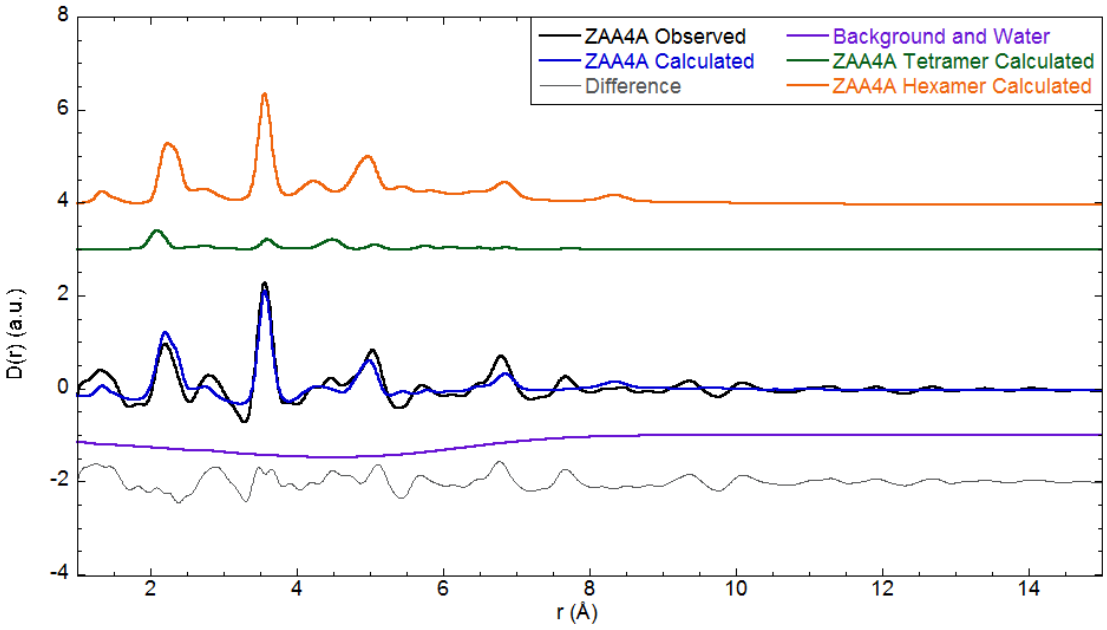

Figure 86: Observed (black) and calculated (blue) PDF of the fixed-core iteration of the dual-phase refinement of sample ZAA4A. Each respective phase has been resolved with the tetrameric contribution shown in green, the hexameric contribution in orange, and the background and water in purple. R_{wp} = 46.09%.

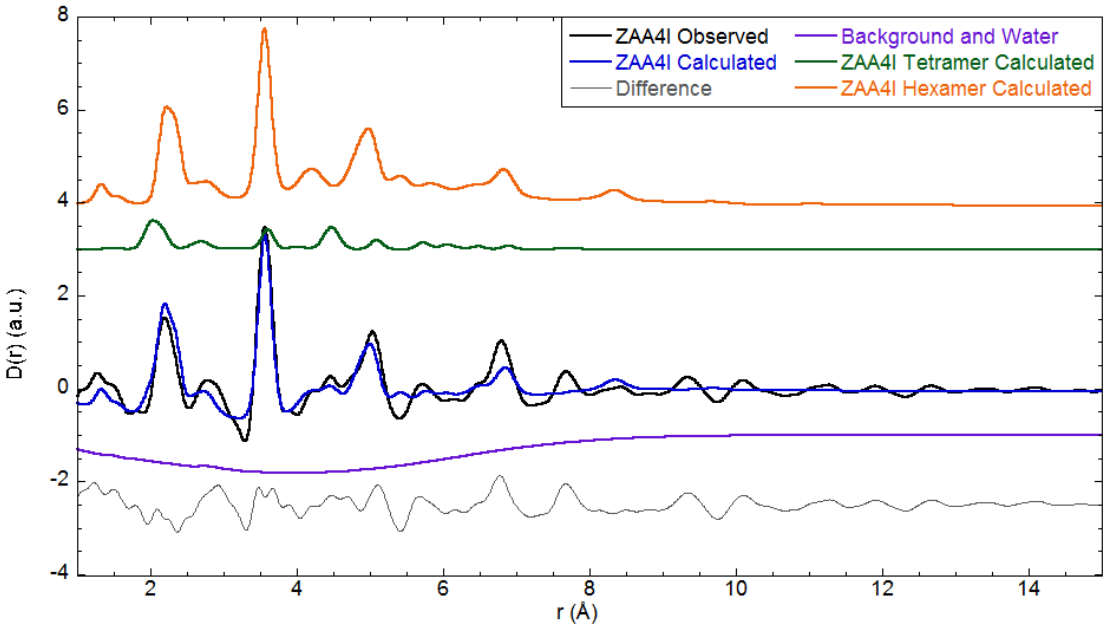

Figure 87: Observed (black) and calculated (blue) PDF of the fixed-core iteration of the dual-phase refinement of sample ZAA4I. Each respective phase has been resolved with the tetrameric contribution shown in green, the hexameric contribution in orange, and the background and water in purple. R_{wp} = 39.89%.

The refinements presented here converged with R_{wp} values of 36.90%, 46.09%, and 39.89%. Once again, the principal difference between these samples is in the peak intensity. The incubated sample displayed greater intensity and this is seen in the refinements where both individual-phases also have greater intensity. The bond lengths and angles show that all three models have high levels of similarity with each other and that the principal difference between them and the Hennig model is once again seen in the bond angles within the carboxylate and its linking to the core. The high level of similarity in the samples ZAA24C-I and ZAA4C-I is unexpected. The solidification that had, by this stage in the ageing process, occurred within these samples does not seem to present any major structural variations to the sample with the only principal difference being an extended range of features but these features were of extremely low intensity suggesting they are made either of weakly scattering atomic pairs or that they are not commonly found.

Table 43: Bond lengths and angles of the Hennig model and the hexamer models resulting from the fixed-core iteration of the dual-phase refinements of samples ZAA4C, ZAA4A,and ZAA4I [2].

Zr-O $_{Core}$ (Å)				Zr-Zr_{Short} (Å)				Zr-Zr_{Long} (Å)			
Hennig model [2]	ZAA4C	ZAA4A	ZAA4I	Hennig model [2]	ZAA4C	ZAA4A	ZAA24I	Hennig model [2]	ZAA4C	ZAA4A	ZAA4I
2.16	2.19	2.20	2.19	3.538	3.55	3.56	3.56	4.97	5.02	5.04	5.04
2.16				3.526				5.02			
2.18											
Zr-$O_{Acetate}$ (Å)				C-$O_{acetate}$ (Å)				C-$C_{Acetate}$ (Å)			
Hennig model [2]	ZAA4C	ZAA4A	ZAA4I	Hennig model [2]	ZAA4C	ZAA4A	ZAA4I	Hennig model [2]	ZAA4C	ZAA4A	ZAA4I
2.22	2.36	2.36	2.35	1.299	1.34	1.35	1.33	1.63	1.49	1.53	1.56
2.23				1.446							
2.24											
2.25											
Centre of cluster-Zr-$O_{(Acetate)}$ (°)				Zr-O-$C_{(Acetate)}$ (°)				O-C-$C_{(acetate)}$ (°)			
Hennig model [2]	ZAA4C	ZAA4A	ZAA4I	Hennig model [2]	ZAA4C	ZAA4A	ZAA4I	Hennig model [2]	ZAA4C	ZAA4A	ZAA4I
122.04	117.47	117.54	117.46	117.75	147.31	144.56	144.00	105.02	129.14	127.09	126.46
123.99				123.14				111.84			

The final set of refinements for this chapter are those from ZAA25C-I and are displayed below in Figures 88 – 90.

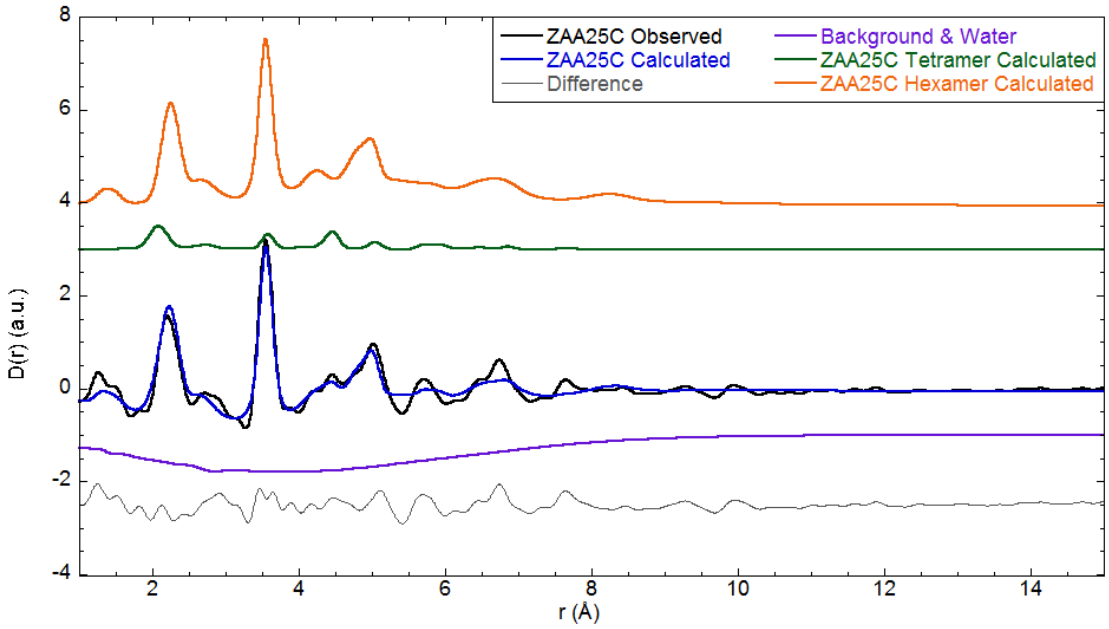

Figure 88: Observed (black) and calculated (blue) PDF of the fixed-core iteration of the dual-phase refinement of sample ZAA25C. Each respective phase has been resolved with the tetrameric contribution shown in green, the hexameric contribution in orange, and the background and water in purple. R_{wp} = 30.14%.

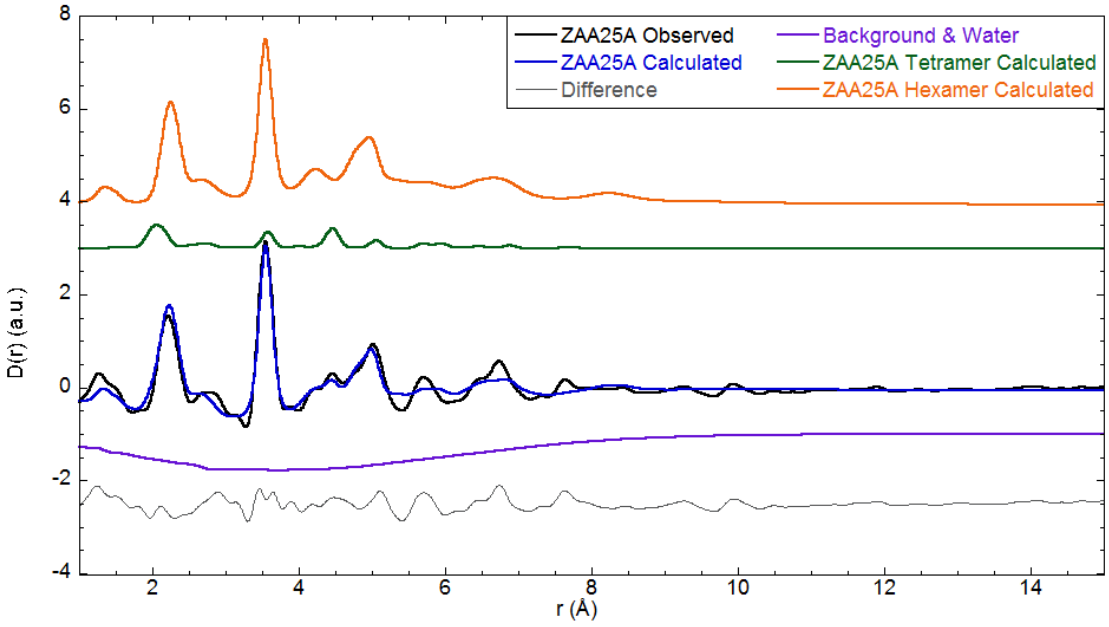

Figure 89: Observed (black) and calculated (blue) PDF of the fixed-core iteration of the dual-phase refinement of sample ZAA25A. Each respective phase has been resolved with the tetrameric contribution shown in green, the hexameric contribution in orange, and the background and water in purple. R_{wp} = 29.31%.

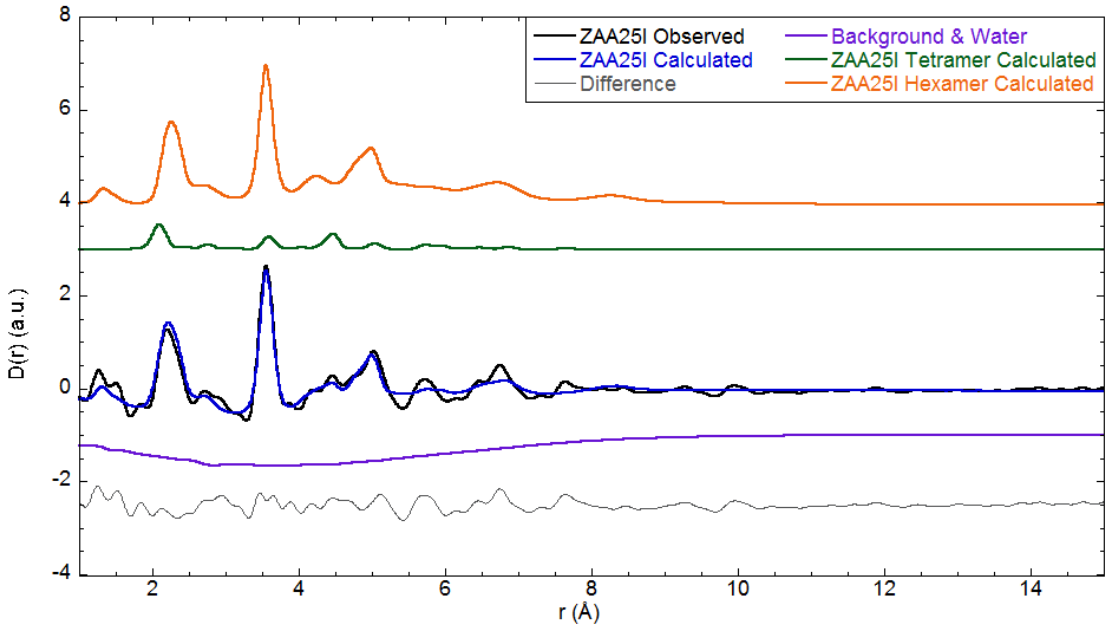

Figure 90: Observed (black) and calculated (blue) PDF of the fixed-core iteration of the dual-phase refinement of sample ZAA25I. Each respective phase has been resolved with the tetrameric contribution shown in green, the hexameric contribution in orange, and the background and water in purple. R_{wp} = 30.79%.

In reference to Figure 81 it was discussed that the relative intensity between the three samples was similar, unlike those of ZAA24C-I and ZAA4C-I seen previously. ZAA25I does however show a slightly lower intensity than seen in its ambient and chilled counterparts and as this sample did not solidify this cannot be ascribed to the physical change of gelling. The refinements shown here have good agreement and converged with R_{wp} values of 30.14%, 29.31%, and 30.79%. These R_{wp} values seen here are substantially lower than those obtained from the other samples from this data collection. This is due to better fitting between the observed and calculated models in the regions of r = 3 Å and r = 7 Å. ZAA25 samples have a larger thermal parameter suggesting lower levels of correlated motion within the cluster species. This manifests in the PDF as peak broadening which, in the case of ZAA25 is more representative of the observed PDF. The bond distance and angles which are shown below (Table 44) show the same patterns as have been described previously although it is noted that

the sample ZAA25I shows a larger than usual Zr-O bond from the core of the cluster to the carboxylate.

Table 44: Bond lengths and angles of the Hennig model and the hexamer models resulting from the fixed-core iteration of the dual-phase refinements of samples ZAA25C, ZAA25A,and ZAA25I [2].

Zr-O $_{Core}$ (Å)				Zr-Zr_{Short} (Å)				Zr-Zr_{Long} (Å)			
Hennig model [2]	ZAA25C	ZAA25A	ZAA25I	Hennig model [2]	ZAA25C	ZAA25A	ZAA25I	Hennig model [2]	ZAA25C	ZAA25A	ZAA25I
2.16	2.21	2.20	2.20	3.538	3.55	3.54	3.55	4.97	5.02	5.01	5.02
2.16				3.526				5.02			
2.18											
Zr-$O_{Acetate}$ (Å)				C-$O_{acetate}$ (Å)				C-$C_{Acetate}$ (Å)			
Hennig model [2]	ZAA25C	ZAA25A	ZAA25I	Hennig model [2]	ZAA25C	ZAA25A	ZAA25I	Hennig model [2]	ZAA25C	ZAA25A	ZAA25I
2.22	2.31	2.32	2.45	1.299	1.36	1.35	1.33	1.63	1.52	1.52	1.51
2.23				1.446							
2.24											
2.25											
Centre of cluster-Zr-$O_{(Acetate)}$ (°)				Zr-O-$C_{(Acetate)}$ (°)				O-C-$C_{(acetate)}$ (°)			
Hennig model [2]	ZAA25C	ZAA25A	ZAA25I	Hennig model [2]	ZAA25C	ZAA25A	ZAA25I	Hennig model [2]	ZAA25C	ZAA25A	ZAA25I
122.04	117.72	117.65	117.42	117.75	144.14	144.04	144.31	105.02	126.86	126.69	126.72
123.99				123.14				111.84			

As the refinements performed here employed the fixed-core model only one zirconium environment is present in each cluster species. This is shown below for both the hexameric phase and the tetrameric phase for each refinement.

Table 45: The resultant oxidation state, as derived through bond-valence calculations described by Brown and Altermatt, for the hexameric phase of the fixed-core iteration of the dual-phase refinement of samples ZAA24C-I, ZAA4C-I, and ZAA25C-I [92].

ZAA24C		ZAA24A		ZAA24I	
Actual value	Rounded value	Actual value	Rounded value	Actual value	Rounded value
3.33	3	3.31	3	3.09	3
ZAA4C		ZAA4A		ZAA4I	
Actual value	Rounded value	Actual value	Rounded value	Actual value	Rounded value
3.20	3	3.18	3	3.27	3
ZAA25C		ZAA25A		ZAA25I	
Actual value	Rounded value	Actual value	Rounded value	Actual value	Rounded value
3.33	3	3.33	3	3.21	3

Table 46: The resultant oxidation state, as derived through bond-valence calculations described by Brown and Altermatt, for the tetrameric phase of the fixed-core iteration of the dual-phase refinement of samples ZAA24C-I, ZAA4C-I, and ZAA25C-I [92].

ZAA24C		ZAA24A		ZAA24I	
Actual value	Rounded value	Actual value	Rounded value	Actual value	Rounded value
5.17	5	5.62	6	4.97	5
ZAA4C		ZAA4A		ZAA4I	
Actual value	Rounded value	Actual value	Rounded value	Actual value	Rounded value
5.08	5	4.99	5	5.51	6
ZAA25C		ZAA25A		ZAA25I	
Actual value	Rounded value	Actual value	Rounded value	Actual value	Rounded value
5.20	5	5.45	5	5.04	5

It can be seen clearly that the hexameric cluster, thanks to the fixed-core model, displays a lower than expected oxidation state of 3. An oxidation state of four is widely regarded as common for zirconium. It is postulated, however that this low oxidation state is a result of the weakly bonded carboxylate groups displaying longer than average bond lengths although this cannot be confirmed at this time. The tetrameric species however displays oxidation states which are extremely high. It is unlikely that zirconium would adopt a +6 oxidation state and this ultimately has a negative impact on the confidence in the results obtained here.

6.4.1 Summary

This data collection has shown that whilst impacting on the overall intensity of a PDF, the storage temperature does not seem to have any overall impact on the structure of the molecular species in solution. As the studies were performed under ambient conditions and not at their respective storage temperatures it is felt that any changes to the structure which are present in temperature controlled samples could potentially be reversed when the samples are returned to ambient conditions. This can be seen through visual inspection of the PDF and so is not dependant on the confidence in the refinement. The oxidation state of the tetrameric species isolated here is cause for concern due to its improbably high value which diminishes the confidence in the structural models obtained. An oxidation state of +5 is very unlikely for zirconium and so further inspection into the cause of these potential false minima is required. Whilst recent work by Somjit *et al.* has proven the possibility of Zr-O bonds as low as 2.15 Å, the Zr-O bonds that lead to these oxidation states are between the ranges 1.99 – 2.19 Å and so are significantly lower than would be expected [100]. It is postulated that there may be a defect in the tetrameric structure which causes a vacancy, lowering the average oxidation state of the zirconium positions whilst maintaining the structure.

Due to PDF only being able to model the atomic positions and not the bonds between them, the bonds which join these Zr-O positions could potentially be double bonds (Zr=O) and so a shorter bond length would be expected. This however must be confirmed through the application of a technique that studies bonding itself within a structure such as X-ray Photoelectron Spectroscopy (XPS).

It is also possible that the geometry of the tetramer in this example is slightly distorted and that samples do not display the eight coordinate, square antiprism geometry based around the zirconium centre. The computer models used here do not offer the flexibility to model this as rigid bodies only allow movement in ways permitted by their design. As discussed in Chapter 4.3, the process of preparing a rigid body means some assumptions must be made to the geometry of the system and which movements of atomic positions are considered reasonable. As such, some potential structural models, such as one which removes this square antiprism geometry cannot be simulated in the models employed here.

6.5 Other Data Collections

After the three periods of data collection that have been described here where completed, a small number of samples of differing ages were analysed in a single experimental session at I15-1 at Diamond Light Source using the same experimental procedure described in Chapter 4. The zirconium-acetate solutions were loaded into bespoke 1.5 mm diameter quartz capillaries which were spun at high speed for 5-minute ambient temperature data collections. Data collections were run at 76 keV for optimal Q range of approximately 40 $Å^{-1}$. I15-1 employs a Perkin Elmer XRD 1611 CP3 area detector as a primary detector. All of the Fourier transformed PDF's were obtained from the raw diffraction data using GUDRUNX [91]. The samples analysed in this session are described below in Table 47.

*Table 47: Details of the samples studied in the final data collection. *Sample ZAA30 was made of a feedstock similar to 1 but not wholly identical.*

Sample Name	Feedstock	ZrO_2 weight percentage	Acetic acid : Zr ratio	Sample Age (months) and conditions
ZAA29	1	22	5.0	0
ZAA30	1*	22	1.6	0
ZAA24	1	22	1.3	36 (Ambient)
ZAA25	1	22	5.0	36 (Ambient)

This data collection allowed for the extremities of ageing to be tested. The two samples with 0 months of ageing would indicate if the postulation by Tosan *et al.* that the solution species is formed over a period of over 1 month from initial sample preparation [42]. The samples with 36 months of ageing, whilst being well beyond the recommended shelf life of any zirconium-acetate solution, serve to see if the effects and patterns observed previously are

continued into the extremes of age. The PDFs resulting from these data collections and the fixed-core refinements of them are shown below in Figures 91 – 94.

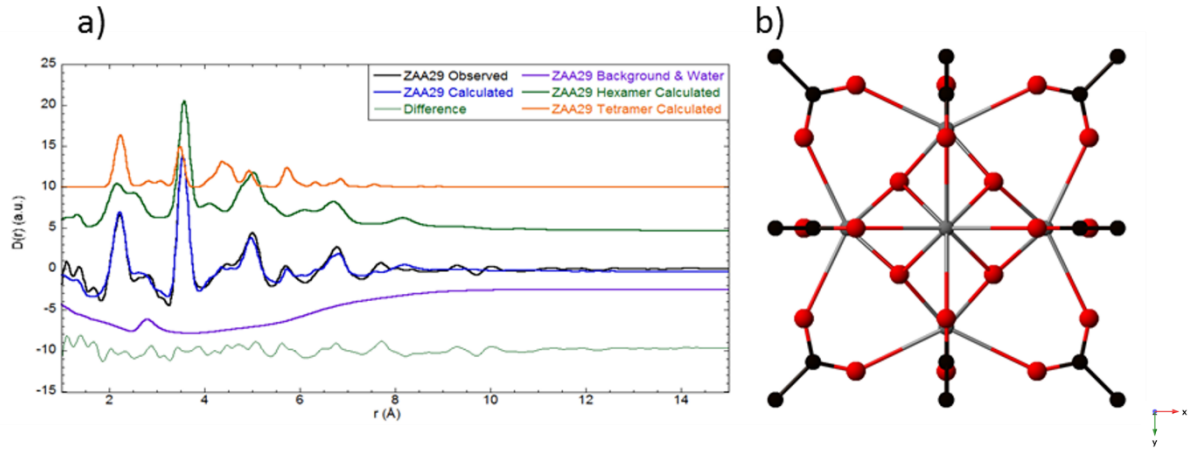

Figure 91: a) Observed (black) and calculated (blue) PDF of the fixed-core iteration of the dual-phase refinement of sample ZAA29. Each respective phase has been resolved with the tetrameric contribution shown in green, the hexameric contribution in orange, and the background and water in purple. R_{wp} = 24.30% b) The model resulting from this refinement. Key: Zr – Grey, O – Red, C – Black.

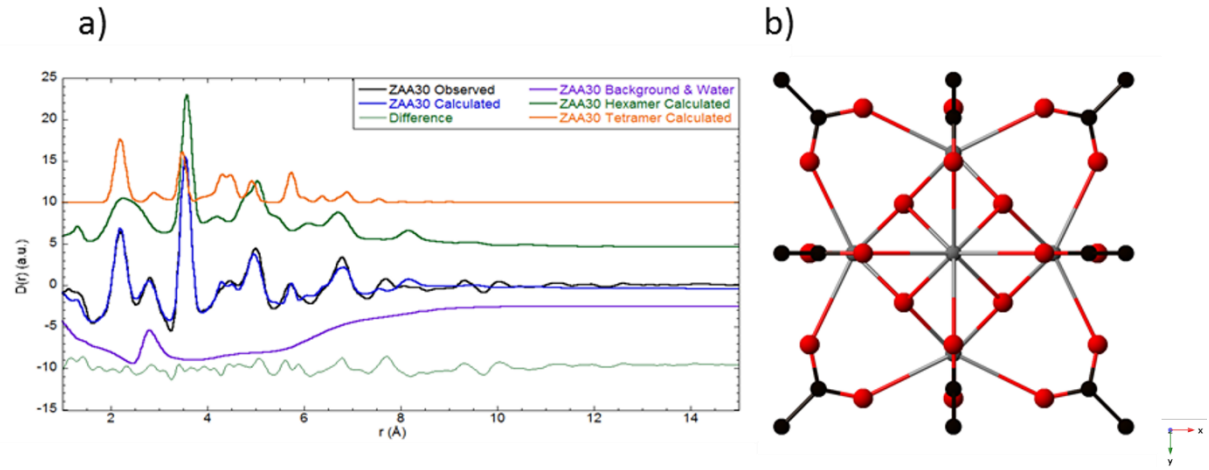

Figure 92: Observed (black) and calculated (blue) PDF of the fixed-core iteration of the dual-phase refinement of sample ZAA30. Each respective phase has been resolved with the tetrameric contribution shown in green, the hexameric contribution in orange, and the background and water in purple. R_{wp} = 22.45% b) The model resulting from this refinement. Key: Zr – Grey, O – Red, C – Black.

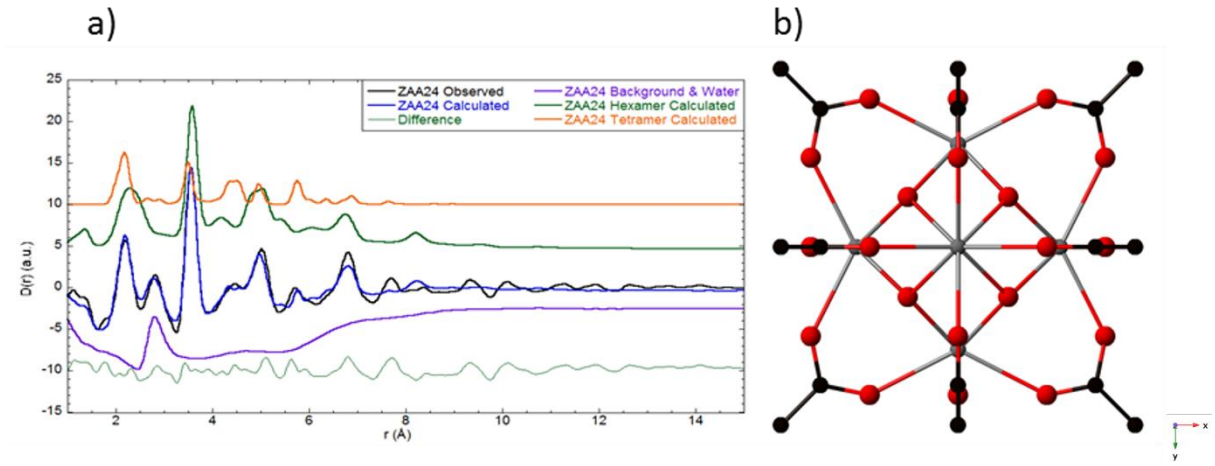

Figure 93: Observed (black) and calculated (blue) PDF of the fixed-core iteration of the dual-phase refinement of sample ZAA24. Each respective phase has been resolved with the tetrameric contribution shown in green, the hexameric contribution in orange, and the background and water in purple. R_{wp} = 26.72% b) The model resulting from this refinement. Key: Zr – Grey, O – Red, C – Black.

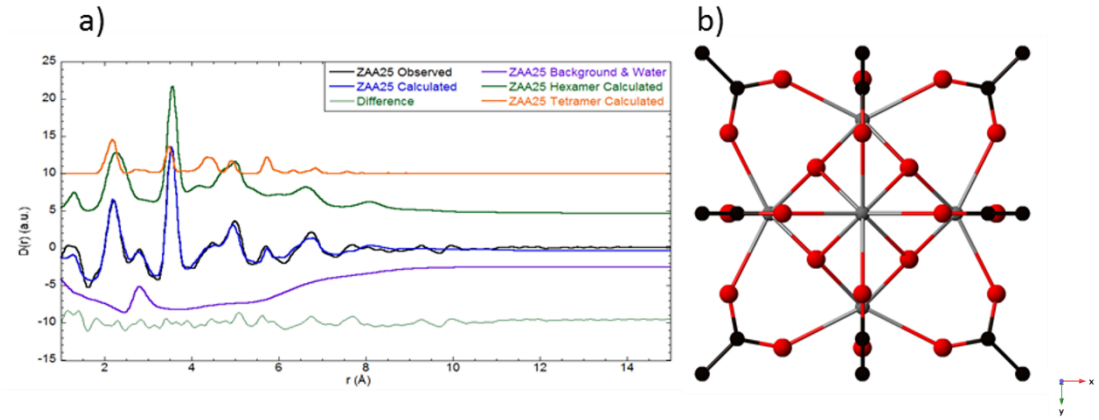

Figure 94: Observed (black) and calculated (blue) PDF of the fixed-core iteration of the dual-phase refinement of sample ZAA25. Each respective phase has been resolved with the tetrameric contribution shown in green, the hexameric contribution in orange, and the background and water in purple. R_{wp} = 22.91% b) The model resulting from this refinement. Key: Zr – Grey, O – Red, C – Black.

All of the refinements presented here show good agreement and converged with R_{wp} values of 24.30%, 22.45%, 26.72%, and 22.91% respectively. The increase in the magnitude of the peaks at 7Å in Figure 92 and Figure 93 which can be seen to be directly influenced by the tetrameric species, indicates a higher level of tetrameric species in these two low acetate samples but this must be confirmed by quantitative phase ratio analysis (Chapter 6.6). The

increase in the range of features observed in Figure 93, indicates some form of aggregation or agglomeration of the cluster species in this sample leading to a longer range of ordering. This effect is less pronounced in Figure 94 which shows an equivalently aged sample with a higher acetic acid : zirconium ratio implying that this feature is not caused simply by age but instead by the acetic acid : zirconium ratio. Analysis of the models and the bond lengths and angles that define them is necessary to fully assess the validity of these refinements. This is shown below in Table 48.

Table 48: Bond lengths and angles of the Hennig model and the hexamer models resulting from the fixed-core iteration of the dual-phase refinements of samples ZAA29, ZAA30, ZAA24, and ZAA25 [2].

Zr-O $_{Core}$ (Å)					Zr-Zr_{Short} (Å)					Zr-Zr_{Long} (Å)				
Hennig model [2]	ZAA29	ZAA30	ZAA24	ZAA25	Hennig model [2]	ZAA29	ZAA30	ZAA24	ZAA25	Hennig model [2]	ZAA29	ZAA30	ZAA24	ZAA25
2.16	2.15	2.18	2.18	2.17	3.54	3.58	3.58	3.59	3.56	4.97	5.06	5.06	5.07	5.04
2.16					3.53					5.02				
2.18														
Zr-$O_{Acetate}$ (Å)					C-$O_{acetate}$ (Å)					C-$C_{Acetate}$ (Å)				
Hennig model [2]	ZAA29	ZAA30	ZAA24	ZAA25	Hennig model [2]	ZAA29	ZAA30	ZAA24	ZAA25	Hennig model [2]	ZAA29	ZAA30	ZAA24	ZAA25
2.22	2.56	2.56	2.47	2.43	1.30	1.13	1.15	1.24	1.24	1.63	1.361	1.33	1.39	1.33
2.23					1.45									
2.24														
2.25														
Centre of cluster-Zr-$O_{(Acetate)}$ (°)					Zr-O-$C_{(Acetate)}$ (°)					O-C-$C_{(acetate)}$ (°)				
Hennig model [2]	ZAA29	ZAA30	ZAA24	ZAA25	Hennig model [2]	ZAA29	ZAA30	ZAA24	ZAA25	Hennig model [2]	ZAA29	ZAA30	ZAA24	ZAA25
122.04	115.73	116.06	116.99	116.83	117.75	142.58	142.51	141.69	142.59	105.02	123.31	123.56	123.68	124.42
123.99					123.14					111.84				

The principal difference between the two sets of aged samples shown above is seen in the Zr-$O_{Acetate}$ bond lengths. The samples which were subjected to 0 months of ageing showed a longer Zr-O bond length, 2.56 Å, against the samples aged for 36 months, 2.43 – 2.47 Å. This can be observed in the resolution of the Zr-O peak in the PDF's in particularly in Figure 91 and also Figure 92 This is indicative of a weaker affinity of the carboxylate groups to the hexameric core of the cluster in the younger samples. The C-$O_{acetate}$ bond lengths however show the inverse effect where age seems to increase the bond length thus showing a migration of the carboxylate oxygens towards the core of the cluster with ageing.

Table 49 describes the bond-valence calculations derived from the models resulting from these refinements. As with previous examples the validity of the model can be assessed by how chemically sensible the bond-valence values are. It can be seen below that all of the refinement models shown here have calculated oxidation states of +3. It is noted that samples ZAA29 and ZAA25 (both samples with a high acetic acid ratio) have a higher calculated oxidation state for the zirconium environments.

Table 49: The resultant oxidation state, as derived through bond-valence calculations described by Brown and Altermatt, for the hexameric phase of the fixed-core iteration of the dual-phase refinement of samples ZAA29, ZAA30, ZAA24, and ZAA25 [92].

Hennig Model [2]		ZAA29		ZAA30	
Actual value	Rounded value	Actual value	Rounded value	Actual value	Rounded value
3.815	4	2.91	3	2.75	3
3.781	4				
ZAA24		ZAA25			
Actual value	Rounded value	Actual value	Rounded value		
2.95	3	3.12	3		

The calculated oxidation states of the tetrameric phases are shown below in Table 50. The only sample that shows an oxidation state that is different to the expected value of +4 is that of ZAA24, the 36 month aged low acetic acid : zirconium ratio sample. Once again this is potentially caused by a vacancy in one of the oxygen positions or possibly the presence of Zr=O bonding but this would require further investigation.

Table 50: The resultant oxidation state, as derived through bond-valence calculations described by Brown and Altermatt, for the tetrameric phase of the fixed-core iteration of the dual-phase refinement of samples ZAA29, ZAA30, ZAA24, and ZAA25 [92].

Hennig Model [2]		ZAA29		ZAA30	
Actual value	Rounded value	Actual value	Rounded value	Actual value	Rounded value
3.815	4	3.52	4	3.98	4
3.781	4				
ZAA24		ZAA25			
Actual value	Rounded value	Actual value	Rounded value		
4.67	5	4.48	4		

It can be seen from this data collection period that the age of the samples, whilst impacting the appearance of the PDF and the features therein, has a minor impact on the structure of the species present. The primary difference seems to be in the movement of the carboxylate oxygen positions towards the cluster with time. It is believed however, that quantitatively evaluating the ratio of the two phases will yield some more insight into the effect of age and the variables studied here. This analysis will be performed in Chapter 6.6

6.6 Phase Ratio Analysis

In the process of undertaking dual-phase refinements, it is possible to calculate the effective molar ratio of the two phases. TOPAS-6 determines a weight percentage ratio but with some basic manipulation this can be converted to a more meaningful molar percentage. This is done using the following equation:

Equation 18: Equation of the formula used to determine the relative molar concentration of the two phases

$$Relative\ molar\ concentration = \frac{N_{Hex}}{N_{Hex} + N_{Tet}}$$

This relative molar concentration accounts for the relative molecular masses of the clusters being assessed and allows for the determination of the dominant molecular species in solution. This calculation was performed for every refinement performed but for brevity, only those that are relevant (i.e. have been discussed in the main body of this thesis or display a unique property) will be discussed herein. General trends however will be discussed.

A comparison of the phase ratios between the hexameric species across all of the synthesis variables studied here shows that the most significant variable with respect to phase ratio is the ratio of acetic acid : zirconium in the sample.

It is noted that the data obtained at the 18-month ageing interval produced phase ratio values in a different region to those collected in all other data collections. Samples collected at NSLS-II (the 18-month data collection) showed hexameric content in the region of 35 – 50% whereas samples collected at DLS (the 9- and 15-month data collections) displayed a lower hexameric content of 20 – 35%.

At this time, it is postulated that this discrepancy arises due to these samples being analysed at a different beamline. All data collections with the exception of those at 18 months were

performed at I15-1, Diamond Light Source. The 18-month collections were collected at NSLS-II. Due to this significant difference samples from each beamline have been separated for the purpose of this phase analysis and so this leads to two figures below. Figure 95 shows the ratio of phases in samples analysed at DLS, whilst Figure 96 shows those from NSLS-II.

Both figures show the same pattern even if the magnitude of the values differs. In both instances the tetrameric species is the dominant species with the hexameric phase never being above 50%. There is an increase in the hexameric content as the acetic acid content of the samples increases, showing that the presence of acetic acid drives the formation of the hexameric phase but even in the 5.0 ratio samples this value never exceeds 50% and so the tetramer is always the dominant species even when the acetic acid content is well in excess of the stoichiometry of the hexamer (2:1). The large error margin shown for samples of 1.6 acetic acid : zirconium ratio in Figure 96 is caused by the increased number of samples of this ratio being studied at NSLS-II.

Previous phase analysis work performed by Hennig *et al.* predicted a tetramer : hexamer phase ratio of 0.05 : 0.95 at an acetic acid : zirconium ratio of 5.0 dropping down to 0.3 : 0.7 at 1.3 [2]. These values were determined from the XAS work performed and no further information was given on how these values were calculated. The results obtained as part of this work have consistently disagreed with these values. This work postulates that the dominant phase is never the hexamer even at values of acetic: zirconium higher than 0.8, the value Hennig *et al.* proposed as the equilibrium point between these two phases. In all of the refinements presented here, throughout the entirety of the ageing study we have consistently found the tetrameric phase to remain the dominant phase comprising 78 – 47% of the samples.

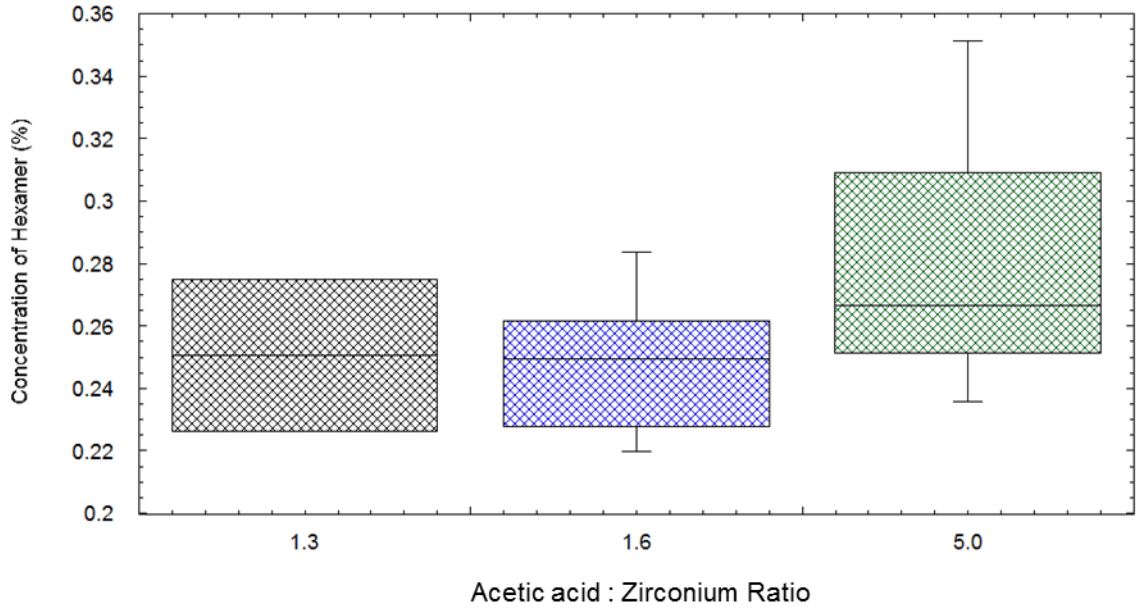

Figure 95: Percentage concentration of hexamer found in samples studied at Diamond Light Source (DLS) distributed by acetic acid : zirconium ratio when refined using the fixed-core model.

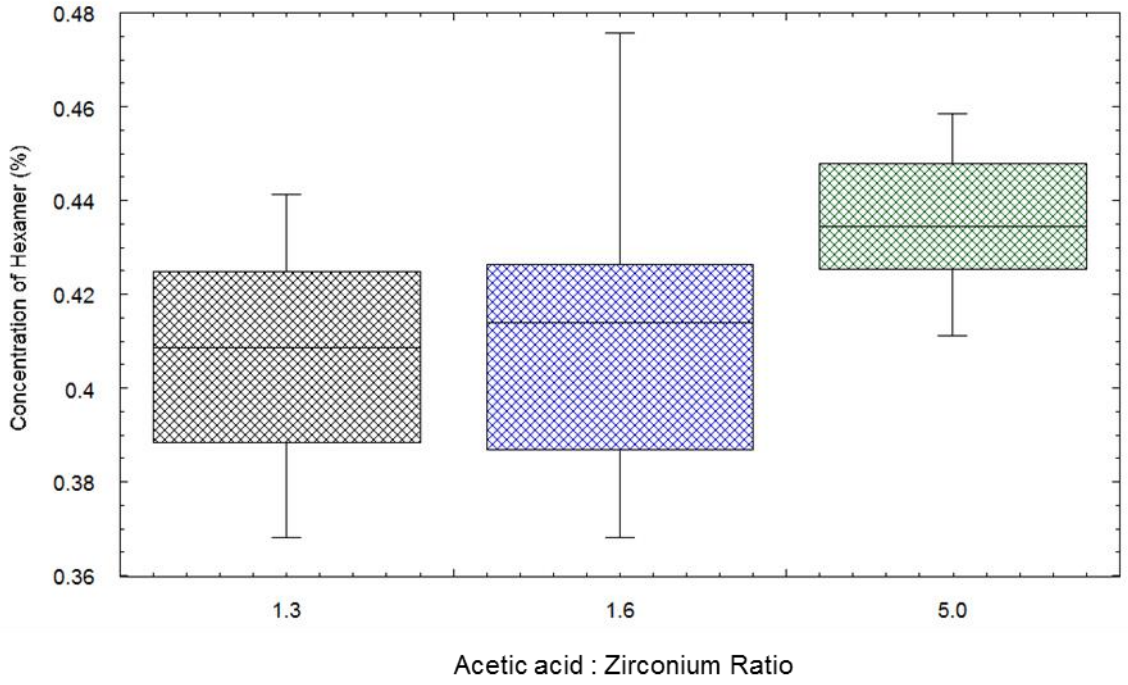

Figure 96: Percentage concentration of hexamer found in samples studied at National Synchrotron Light Source II (NSLS-II) distributed by acetic acid : zirconium ratio when refined using the fixed-core model.

The samples studied in the final data collection aimed to determine if the relationship between the two phases was observed at all sample ages. A direct comparison of two samples with a high acetic acid : zirconium ratio at the extremes of ageing shows no substantial change in the hexameric to tetrameric phase. Both samples contained approximately 30% hexameric species (31.89% and 32.81% for the 0 and 36 month samples respectively). These samples are once again below the 50% hexameric phase ratio showing a dominance of the tetrameric phase at all acetic acid ratios studied here. It is clear from these values that the phase ratio of these materials is not influenced by age and so it is solely the acetic acid : zirconium ratio that impacts the phase ratio of the sample formed.

6.7 Summary of Ageing Study

This ageing study has shown that whilst both the models used in these refinements do not describe the system perfectly, the fixed-core model adequately describes the system with enough accuracy to determine some key information. Firstly, that the system is composed not of one cluster but of two unique clusters, one hexameric and another tetrameric. The hexameric phase whilst not entirely dissimilar to that proposed by Hennig *et al.* does deviate from that ideal model determined from single-crystal X-ray diffraction and XAS analysis [2]. Secondly, no differences were observed in the samples that could be induced by ageing, or storage conditions. Instead, the principal variation between the PDF patterns was caused by the ratio of the two respective phases, induced by the acetic acid : zirconium ratio. And finally, in some samples, longer range features were observed in the PDF patterns but their low intensity implies that these are not the result of polymerisation, as had previously been postulated, but are more likely a result of cluster species agglomeration and an increase in inter-cluster affinity.

It is clear that this ageing study, has shown that these zirconium-acetate samples do not undergo any substantial structural rearrangement over time and are shelf stable for prolonged periods. This information can subsequently inform chemical industries who use these materials as to their stability. Although, it must be noted that a structural study does not rule out any other effects of age or sample composition and so Chapter 7 will assess the use of these materials in a real-world synthesis and how the variables studied impact this.

7.0 Model Compound Analysis

As part of the study of the zirconium-acetate solutions seen in the previous chapter (Chapter 6), a model compound was synthesised from the zirconium-acetate at regular intervals of their ageing. This had the following aims:

- Investigate if, through ageing of the aqueous solutions of zirconium-acetate, the solid compound they are subsequently used to produce is influenced.
- If any variation in quality or quantity of solid product is identified to determine whether this is induced through ageing or the key variables that describe the zirconium-acetate solutions.

The model compound selected for this study was the zirconium silicate, umbite ($K_2ZrSi_3O_9 \cdot H_2O$). The zirconium-acetate samples would be used as the zirconium source for the production of the material, umbite, as described in Chapters 1.6 and 3.2.

These samples would be assessed on the following metrics:

- Percentage yield.
- Rietveld analysis:
    - Characterisation of the umbite phase and detection of any unknown secondary phases.
    - Determination of the degree of crystallinity of the synthetic product.
- Scanning electron microscopy: To characterise variations in the particle morphology.
- Nitrogen gas adsorption: To isolate total pore size and surface area measurements.

7.1 Synthesis of Umbite

The synthesis of umbite was carried out according to the methodology of Poojary *et al.* after slight modification [46]. Samples of the zirconium-acetate solution from the three storage conditions; chilled, ambient, and incubated, were used as the zirconium source. Synthesis was carried out periodically during the ageing study. The details of these ageing intervals can be seen in Table 51.

Table 51: Description of the ageing intervals at which samples were synthesised.

Date of Synthesis Round	Age of Samples
September 2019	3 Months
February 2020	7 Months
September 2020	15 Months
April 2021	22 Months

Whilst not a true time = 0 sample, the synthesis period of September was the first synthesis period due to packing and distribution time. The zirconium acetate samples were prepared in June 2019. For this reason, the September 2019 synthesis was only performed on samples kept ambient and these would be the standard to which other samples would be judged alongside a control sample synthesised from $ZrCl_4$ as is described in the original synthesis by Poojary *et al.* [46]

Due to Government restrictions, the synthesis round commencing in February 2020 is incomplete so, whilst all collected data are presented here, the data set appears incomplete. For September 2020 (15 Months) and April 2021 (22 Months) the synthesis rounds were complete and included all samples stored under all the relevant conditions.

7.2 Yields

The first, and most simple metric of a synthesis employed was a percentage yield calculation. For many commercial users high yield is paramount and so the effect of the zirconium-acetate variables being studied and the storage temperature they were subjected to had on the product yield was determined. Previous work with umbite, synthesised from $ZrCl_4$, by this group has shown a high synthetic yield, ca. 80%. Any deviations from this yield would be potentially problematic in a commercial or industrial setting where consistency is crucial, and quantity is essential. As such for every sample a percentage yield value was determined. This was calculated from the obtained mass of solid umbite. A comprehensive list of these values can be found in Table 287 in the Appendix.

Figure 97 below shows the distribution of the achieved yield against the percentage content of ZrO_2 in the samples across all sample synthesis rounds.

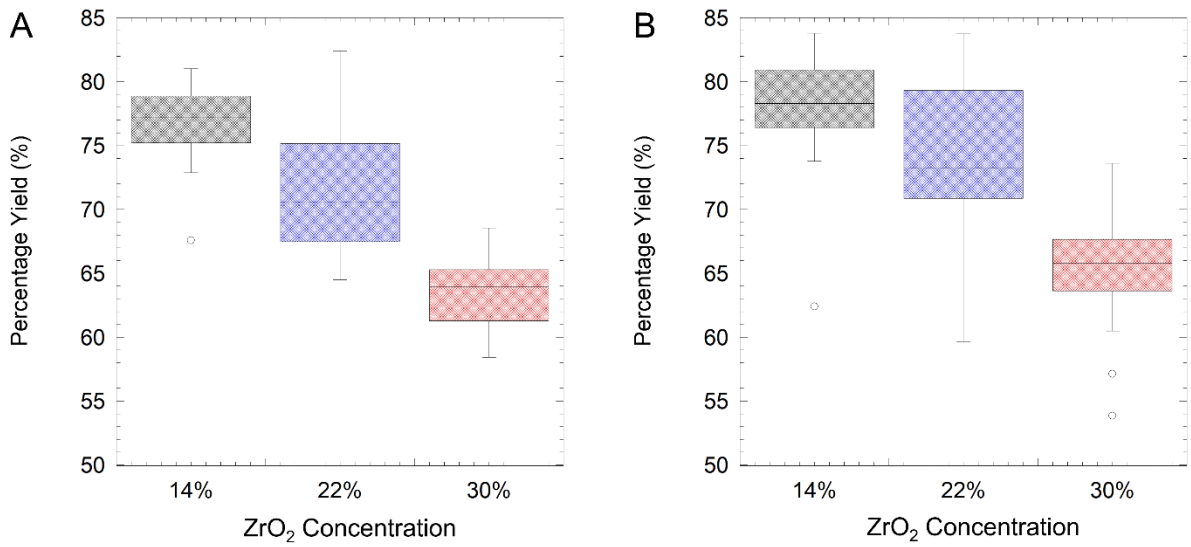

Figure 97: Effect of ZrO_2 concentration on the percentage yield of umbite ($K_2ZrSi_3O_9 \cdot H_2O$) obtained. Samples of feedstock 3 are shown in figure A and both feedstocks 1 and 2 in figure B.

This shows clearly that the for all three feedstocks lower concentration zirconium solutions return higher resultant yields than those obtained with a solution of higher concentration. In each synthesis the volume of zirconium-acetate solution was adapted to account for the concentration differences and standardised to the same molar value. This in turn standardised the amount of acetic acid in the solutions. However, the increased volume required when using 14% ZrO_2 solutions increases the overall pH of the synthesis mixture as $[H^+]$ decreases. This potentially causes the increase in yield for this basic synthesis in samples containing 14% ZrO_2.

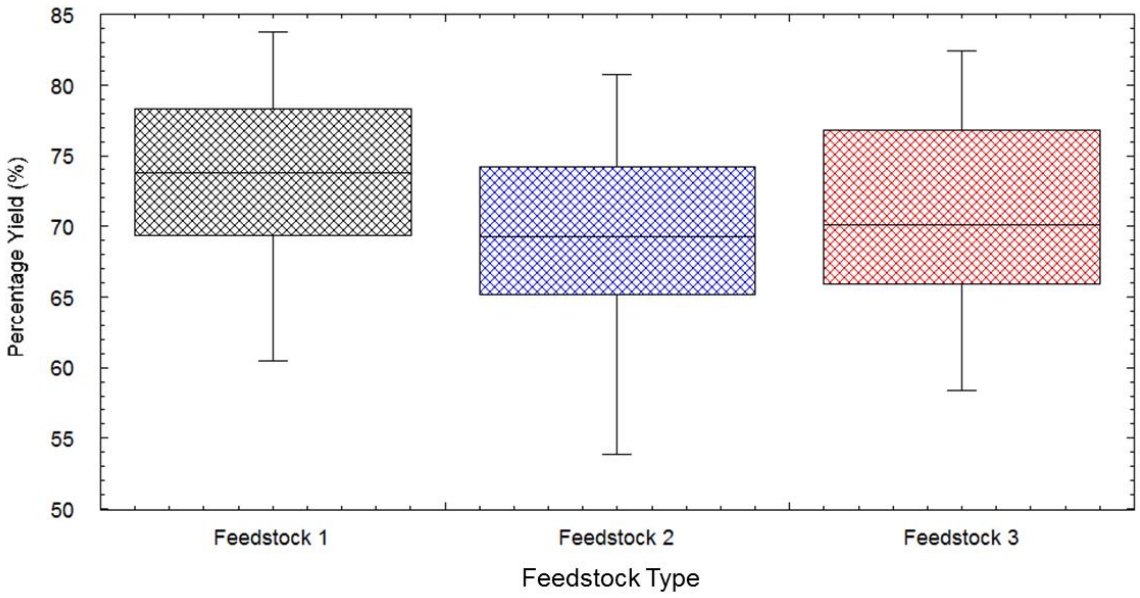

Figure 98: Effect of feedstock concentration on the percentage yield of umbite ($K_2ZrSi_3O_9 \cdot H_2O$) obtained. Plot includes values from all umbite samples synthesised.

Figure 98 shows that the feedstock used in the preparation of the zirconium-acetate samples impacts the yield of model compound. On average, feedstock 1 resulted in a ≈5% higher yield than that seen for samples prepared with feedstock 2 or 3. However, at this stage it is not clear what causes this difference in expected yield as the nature of the feedstock is beyond the scope of this research project.

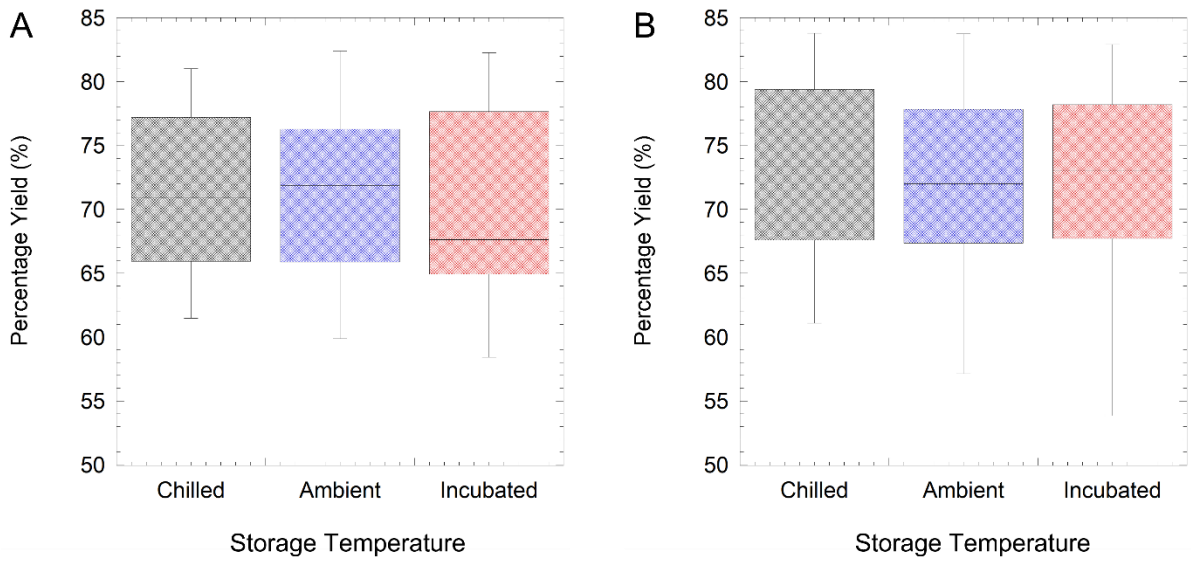

Figure 99: Effect of storage temperature on the percentage yield of umbite ($K_2ZrSi_3O_9 \cdot H_2O$) obtained. Samples of feedstock 3 are shown in figure A and both feedstocks 1 and 2 in figure B.

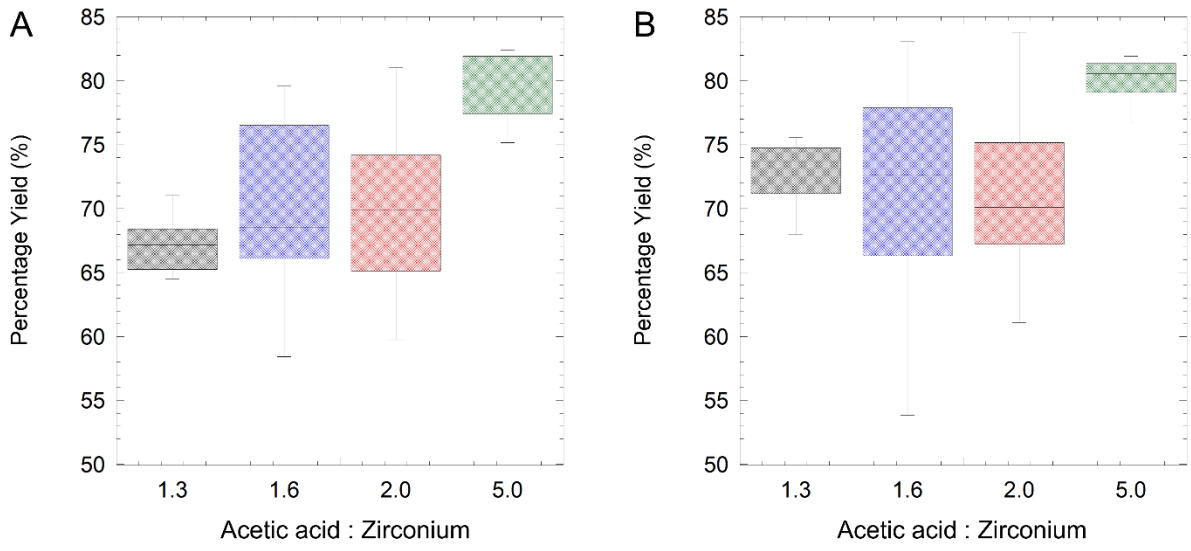

Figure 100: Effect of acetic acid : zirconium ratio on the percentage yield of umbite ($K_2ZrSi_3O_9 \cdot H_2O$) obtained. Samples of feedstock 3 are shown in figure A and both feedstocks 1 and 2 in figure B.

Figure 99 & Figure 100 show how the yield is impacted by the temperature of the storage conditions and the acetic acid : zirconium ratio respectively. It can be seen that the temperature of storage has no significant impact with the average final yield of the model compound with all the storage conditions achieving similar average yields. A broader

distribution of yield was however noted for samples stored in higher temperatures. This was seen for all three feedstocks but is less pronounced in Feedstock 3. Whilst the average yield for incubated samples is generally in line with that seen for the alternative storage conditions, this broader range of obtained values could pose issue for industrial or commercial users where a consistent yield is expected and required.

There is also seemingly a very loose correlation between the ratio of acetic acid : zirconium in the sample and the final yield of the model compound. Feedstock 3 shows this trend more strongly in the average yield achieved but this trend is not well pronounced. It is noted however the significant increased yield in model compounds made from samples of 5.0 : 1, acetic acid : zirconium.

Samples made with an acetic acid : zirconium ratio of 1.3 had pH values >4.0 whereas solutions made with a ratio of 5.0 had pH values of 2.0-2.5. as such, the addition of an excessively acidic zirconium source to a basic synthesis would be expected to increase the internal pH of the reaction and thus obtain lower yields. This however was not observed and instead the shift from 1.3-5.0 produced higher yields (69.9% compared to 79.6%)

This contradicts the previous hypothesis presented from the effect of ZrO_2 concentration on yield as here the yield differences were ascribed to the reaction mixtures pH. Instead, it is possible that the increased volume required in samples with a lower ZrO_2 content leads to a higher volume of reaction mixture which is therefore more dilute. It is postulated then, that the dilute reaction mixture seen in samples made with 14% ZrO_2 is the driving force behind the increased yield.

Figure 101 below shows how the yield of model compound is impacted by sample age. It can be seen that whilst there is no substantial impact on the average yield obtained, the distribution is larger when older samples are used.

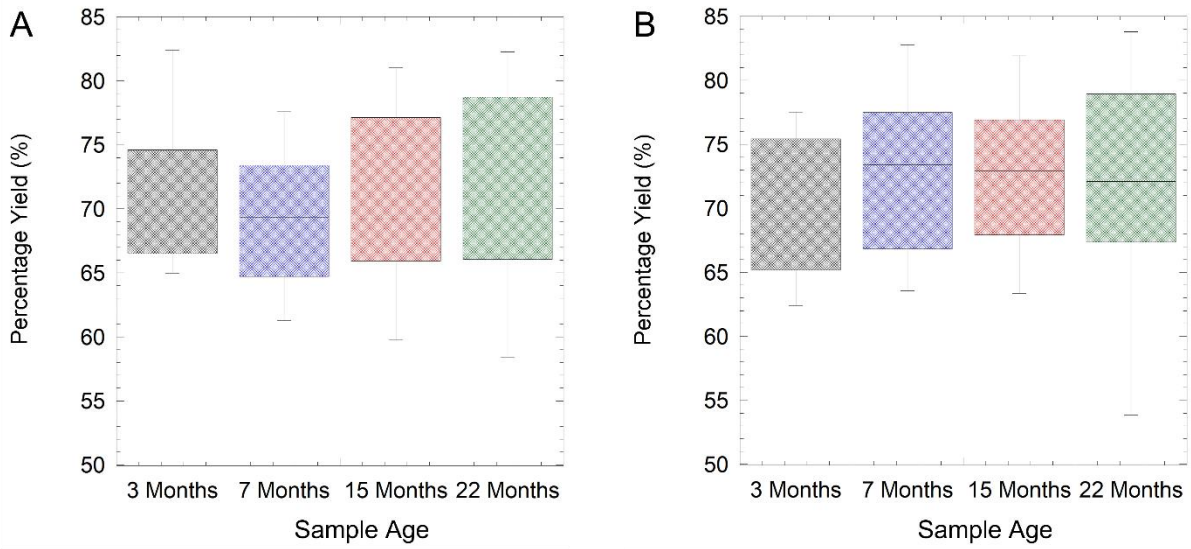

Figure 101: Effect of sample age on the percentage yield of umbite ($K_2ZrSi_3O_9 \cdot H_2O$) obtained. Plot includes values from all umbite samples synthesised.

Samples do seem to have an optimal average yield window at around 15 months, but this period also corresponds with the period where the maximum achieved yield was its lowest. It can be concluded that older samples whilst not directly impacting the yield percentage can impact the reliability of the synthesis.

The information presented here shows that the principal effect on the total yield of a model compound, when made with zirconium-acetate solution, is the relative concentration of the solution. Increases in the relative concentration induce lower yields of model compound and this effect is well pronounced.

Of the other variables studied here, the acetic acid : zirconium ratio (particularly at values beyond excess), and feedstock type impact the expected yield. The high ratio samples result in a higher yield of product and feedstock 2 results in an, on average, lower yield of product.

Whilst it seems that age does not have a major impact on the average yield it is noted that samples from the 22-month-old synthesis round show a substantially broader range of values and as such cause an inconsistent synthesis.

7.3 Rietveld Refinements

After the synthesis of the model compound, each sample was characterised by powder X-ray Diffraction (PXRD) to determine the presence of any impurities or second phases. These collections were performed on a Bruker D2-phaser Powder Diffractometer, located at the University of Central Lancashire, operating in θ-θ geometry with a copper tube and a Lynxeye Si strip detector. A nickel filter was used to isolate the Kα wavelength, λ = 1.5418 Å. Samples were ambient powders and were placed onto Poly(methyl methacrylate) sample holders manufactured by Bruker. To ensure a flat surface, samples were smoothed with a glass microscope slide.

The diffraction patterns were then studied through the use of Rietveld analysis in GSAS and EXPGUI to identify any substantive variations in the structure of the materials. Assessment of the lattice parameters and their variations from the ideal value is an appropriate method to determining the quality of the product formed. An example of one of the Rietveld refinements is shown below in Figure 102 and the resultant table of atomic coordinates is given in Table 52. The structural refinement parameters for this refinement are given in Table 53 and for all others these can be found in Table 291 in the appendix. This refinement converged with a Chi^2 value of 6.773 and all the other refinements for the complete set of 190 samples converged with similar Chi^2 values. The R factors and Chi^2 values for all refinements can be found in Tables 292-295 in the appendix.

The lattice parameters obtained were *a*=10.3079(2) Å, *b*=13.3296(2) Å, and *c*=7.1955(1) Å.

Table 52: Table of atomic coordinates, thermal parameters, multiplicity and fractional occupancy arising from the Rietveld refinement of the umbite synthesised from the zirconium-acetate sample ZAA15 after 3 months of ageing.

Atom Name	*x*	*y*	*z*	U_i/U_e*100 (Å)	Multiplicity	Fractional occupancy
Zr1	0.05132(21)	0.71065(13)	0.2623(4)	3.92(7)	4	1
Si1	0.0325(6)	0.4518(4)	0.2285(12)	3.61(20)	4	1
Si2	0.1716(7)	0.3296(6)	0.5079(10)	3.12(22)	4	1
Si3	0.1399(8)	0.3374(6)	0.9175(12)	4.64(29)	4	1
K1	0.0719(5)	0.57688(31)	0.7187(8)	5.47(18)	4	1
K2	0.2081(6)	0.86924(32)	0.6452(6)	6.72(23)	4	1
O1	0.0846(8)	0.8763(7)	0.2229(17)	0.80(36)	4	1
O2	0.1247(13)	0.2186(14)	0.4125(18)	8.00(69)	4	1
O3	0.0576(15)	0.2449(11)	0.0072(15)	5.11(57)	4	1
O4	0.9819(8)	0.5610(7)	0.2399(22)	1.90(35)	4	1
O5	0.1578(16)	0.4225(11)	0.3680(20)	7.32(63)	4	1
O6	0.2105(13)	0.6872(10)	0.4337(16)	2.10(44)	4	1
O7	0.0882(9)	0.3499(6)	0.6907(14)	0.24(33)	4	1
O8	0.0935(11)	0.4364(10)	0.0208(17)	1.22(43)	4	1
O9	0.1825(12)	0.6941(10)	0.0160(15)	1.76(42)	4	1
O10	0.1910(12)	0.0636(7)	0.6465(15)	2.24(42)	4	1

Table 53: Selected crystallographic data and structure refinement parameters of the umbite synthesised from the zirconium-acetate sample ZAA15 after 3 months of ageing.

Chemical formula	$K_2ZrSi_3O_9{\cdot}H_2$	Radiation type	Cu Kα (1.5418 Å)
Crystal system	Orthorhombic	Collection Range (°)	10 – 120
Space Group	P 2_1 2_1 2_1 (#19)	Step Size (°)	0.02
a (Å)	10.30792(19)	Collection Time (s)	21600
b (Å)	13.32958(22)	Chi^2	6.773
c (Å)	7.19547(13)	R_{wp}	0.0589
α (°)	90	Rp	0.0433
β (°)	90	$R(F^2)$	0.0603
γ (°)	90	Number of observations	5447
Unit Cell Volume ($Å^3$)	988.656(30)	Background	35-point linear interpolation
Z	4	Parameters refined	112

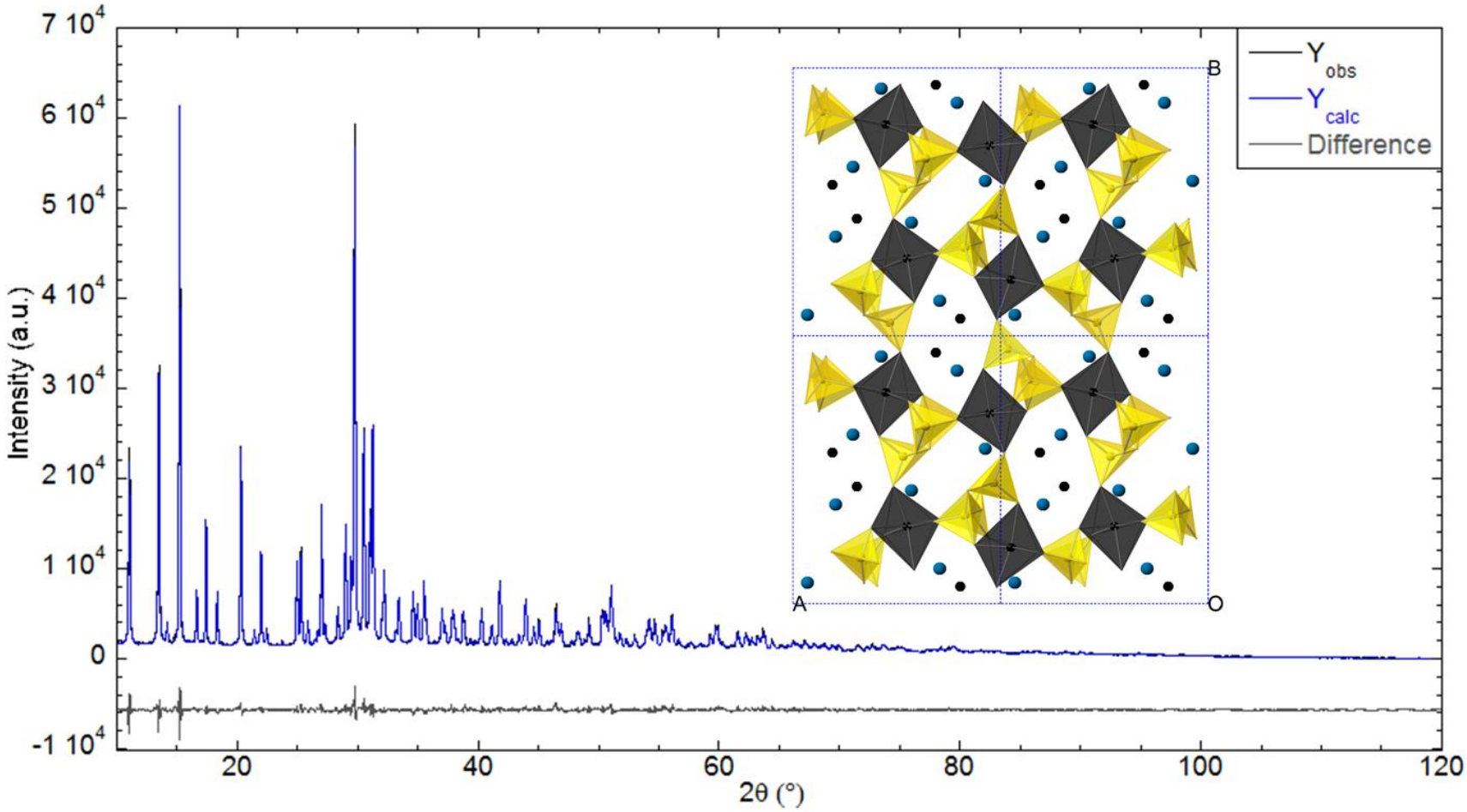

Figure 102: Observed (black), calculated (blue), and difference (grey) diffraction pattern of a sample of umbite synthesised from ZAA15 after 3 months of ageing.The resultant structure of the refined model is displayed (inset). viewed down the c-axis showing the octahedral Zr (Black Polyhedra) and tetrahedral Si (Yellow Polyhedra) of the framework. Within the framework are the counter cations K (Blue Spheres) and the oxygens of the waters of crystallisation (Black Spheres). The unit-cell boundaries are shown in blue dashed lines

The refinement shows good agreement and an almost flat difference curve. The atomic positions are similar to those seen in literature and the bond distances (seen below in Table 54) are also reasonable. The Zr-O bonds are all within expected parameters of 2.2 ± 0.2 Å. The Si-O bonds are all reasonable and around the literature value of 1.60 Å. The K-O bond lengths are slightly long with some being above 3.0 Å but this is likely not bonded K-O pairs but instead caused by the two potassium cations that occupy the elliptical pores. They are the interactions of the potassium cation from one side of the pore interacting with the oxygen at the other.

Table 54: Bond lengths from the refined model of umbite synthesised from zirconium-acetate sample ZAA15.

Atomic Pair	Length (Å)	Atomic Pair	Length (Å)
Zr1_O1	2.252(9)	K1_O3	3.072(14)
Zr1_O2	2.210(15)	K1_O4	3.574(16)
Zr1_O3	2.054(13)	K1_O5	3.374(15)
Zr1_O4	2.125(9)	K1_O5	2.986(16)
Zr1_O6	2.077(13)	K1_O6	2.900(12)
Zr1_O9	2.240(10)	K1_O7	3.036(10)
Si1_O1	1.609(10)	K1_O8	2.877(13)
Si1_O4	1.548(9)	K1_O9	2.884(14)
Si1_O5	1.682(16)	K1_O10	2.883(12)
Si1_O8	1.634(12)	K2_O1	3.296(12)
Si2_O2	1.701(18)	K2_O2	2.836(12)
Si2_O5	1.602(14)	K2_O3	3.383(15)
Si2_O7	1.595(11)	K2_O3	3.023(16)
Si2_O9	1.538(12)	K2_O4	3.085(10)
Si3_O3	1.630(16)	K2_O6	2.865(14)
Si3_O6	1.581(13)	K2_O7	3.284(11)
Si3_O7	1.725(12)	K2_O8	3.448(12)
Si3_O8	1.588(13)	K2_O9	3.554(12)
		K2_O10	2.597(9)

As can be seen in Tables 288-290 in the Appendix and summarised in Table 55, the samples of umbite synthesised here obtained extremely similar lattice parameters with a small range between the highest and lowest values. It is noted that the lattice parameters here all exceed those described in literature, but this phenomenon is witnessed in all syntheses of umbite regardless of zirconium source performed by this group as is demonstrated by the reference value in Table 55. This value was obtained from the Rietveld refinement of a sample of umbite synthesised from $ZrCl_4$.

Table 55: Minimum and maximum lattice parameters and the range between them as determined from the Rietveld refinement of 190 umbite samples. The reference value is obtained from a Rietveld refinement of a sample of umbite synthesised from $ZrCl_4$. The literature values are according to Poojary et al. [46].

	Minimum value (Å)	Maximum value (Å)	Range (Å) (Range as a percentage of literature value)	Reference value (Å)	Literature value (Å)
Lattice Parameter a	10.2916(4)	10.3131(4)	0.051 (0.5%)	10.3108(2)	10.2977(2)
Lattice Parameter b	13.3071(13)	13.3623(2)	0.054 (0.4%)	13.3350(3)	13.2407(3)
Lattice Parameter c	7.1845(3)	7.2107(1)	0.025 (0.3%)	7.1966(2)	7.1956(1)

The range between the highest and lowest achieved lattice parameters represents merely 0.3 – 0.5% of the literature parameters, showing a consistency in the lattice parameters and thus the quality of the product formed. For all the variables in the zirconium-acetate solutions studied here, Rietveld refinement deduced the lattice parameters were well within expected error margins and so it can be inferred that these variables have no impact on the umbite phase of the product formed. Plots of each lattice parameter against the studied variables (Figures 283-291 in the appendix) show no substantial trends.

No secondary crystalline phases were detected during the Rietveld refinements however the presence of an amorphous phase was suspected as diffuse scatter was seen in the diffraction patterns of some samples. The impact of this amorphous phase was quantified in the degree of crystallinity calculations presented in Chapter 7.4.

7.4 Degree of Crystallinity

Whilst the percentage yield obtained in a synthesis is a critical measure, for many users it is imperative that the product obtained is of a high crystallinity. For this reason, the crystallinity of the product synthesised must be quantified. The method used here was to perform a two-phase Rietveld refinement. The primary phase would be that of the model compound, umbite. The second phase was a sample of amorphous umbite which was previously synthesised.

The refinement of the crystalline phase was performed according to conventional methods on the data collections described in Chapter 7.3 [101]. The lattice parameters, atomic positions, peak profile, and scale were all refined to obtain an accurate model of the crystalline phase.

The second phase was obtained from the Rietveld refinement of an lowly-crystalline sample of umbite. In these crystallinity studies, only the scale of the amorphous phase of umbite was refined. As such the diffuse scatter observed in the diffraction patterns was proportionally represented by the amorphous phase, allowing the crystalline phase to refine to the Bragg peaks which were present.

The area beneath the calculated diffraction pattern for each phase is proportional to the contribution of that phase. As such the area beneath the crystalline phase as a percentage of the total area beneath both the crystalline and amorphous phase patterns give rise to the degree of crystallinity. Two refinements which represent the samples with the highest and lowest degrees of crystallinity are shown below. Figure 103 shows a highly crystalline sample with a crystallinity of 88.12% (ZAA21C synthesised at an age of 22 months). This is shown with the extremely low percentage of amorphous phase: the refinement is fully represented by the crystalline phase. Figure 104 shows an extremely amorphous sample with a crystallinity

of 9.80% (ZAA27I synthesised at an age of 15 months). Here a large portion of the diffraction pattern is represented by the amorphous phase which shows a broad and dominant feature at $2\theta = 20° – 40°$. All the other samples synthesised and studied had crystallinity percentage between these two values and most had some contribution of diffuse scatter but to varying different extents.

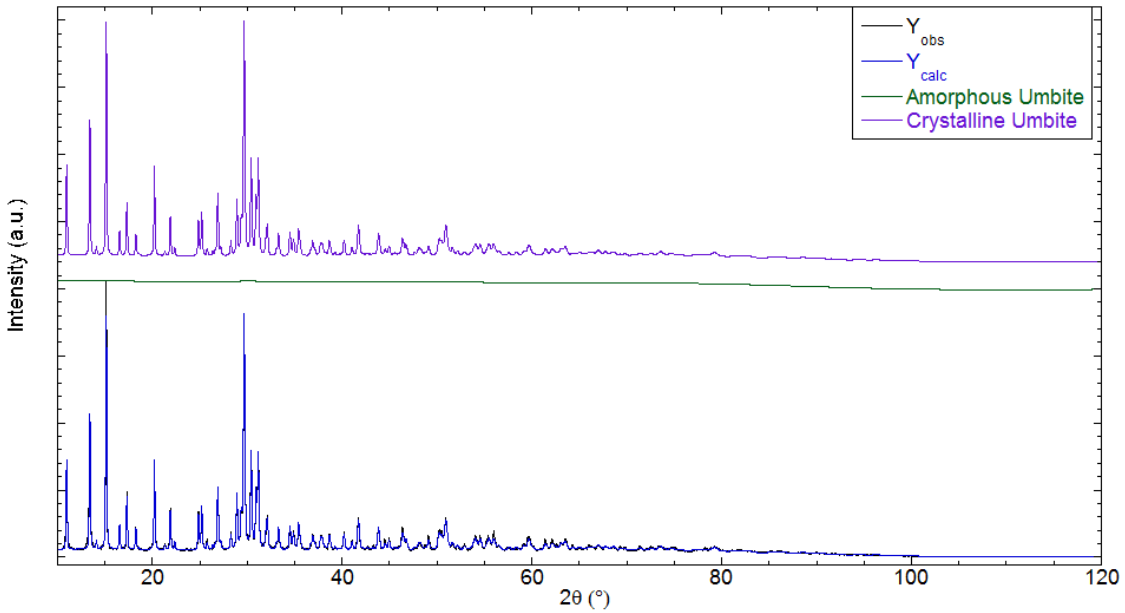

Figure 103: Observed (black) and calculated (blue) diffraction patterns from the crystallinity studies of the sample (sample ZAA21C after 22 months of ageing). The two phases of umbite (amophous in green and crystalline in purple) are displayed above.

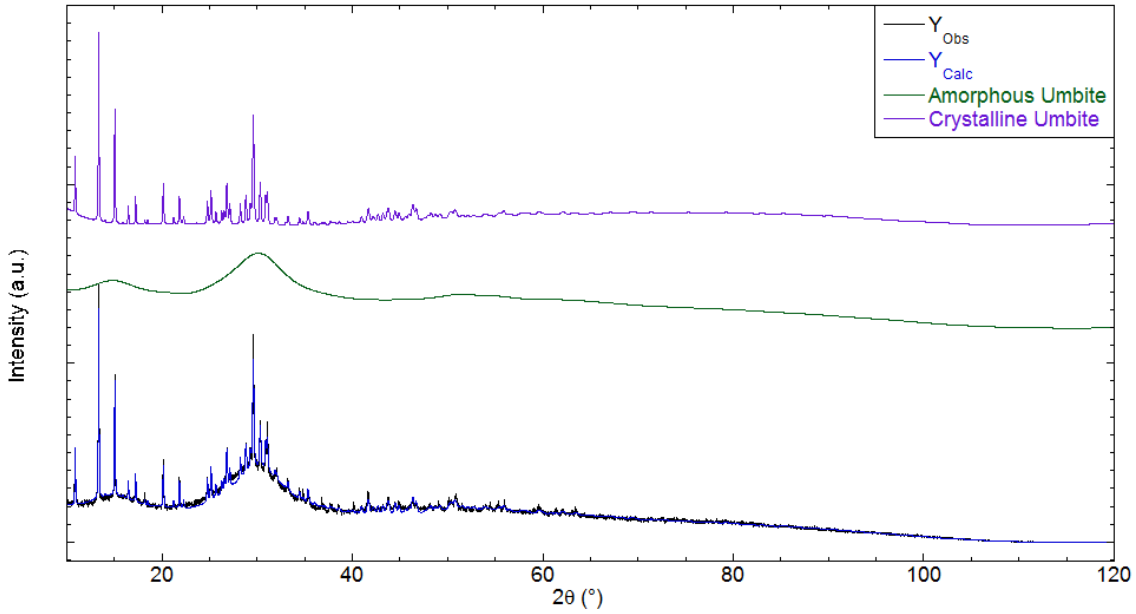

Figure 104: Observed (black) and calculated (blue) diffraction patterns from the crystallinity studies of the sample (sample ZAA27I after 15 months of ageing). The two phases of umbite (amophous in green and crystalline in purple) are displayed above.

Figures 105a, 105b, and 105c below show the impact of storage temperature, ZrO_2 concentration, and feedstock type respectively on the crystallinity of the products obtained.

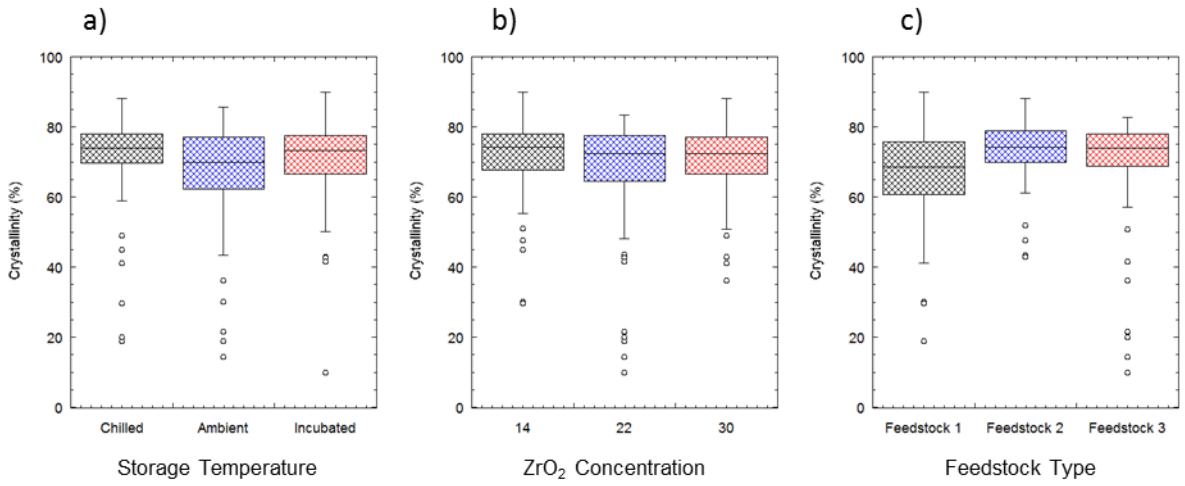

Figure 105: Effect of a) storage temperature, b) ZrO_2 concentration, and c) feedstock type on the percentage degree of crystallinity obtained.

It is noted that there is no strong correlation between the storage temperature or concentration on the crystallinity of the products. Feedstock 2 does show a higher average degree of crystallinity with less below average outliers than seen in the alternative feedstocks, but this difference is minimal.

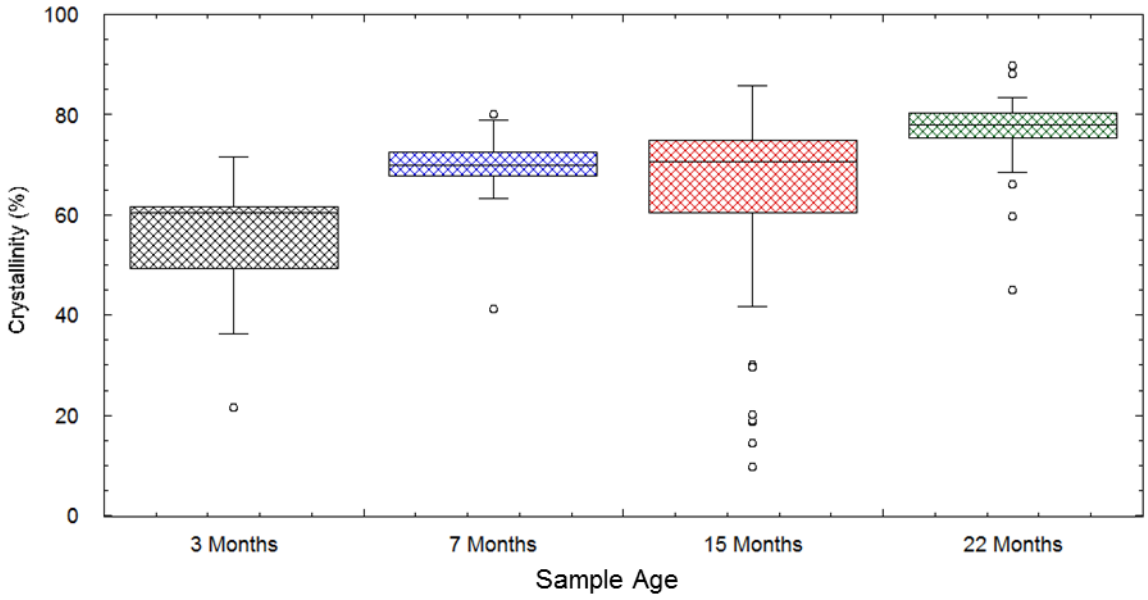

Figure 106: Effect of sample age on the percentage degree of crystallinity obtained.

Figure 106 above shows that over the period of ageing studied here the average crystallinity of the samples of umbite achieved increases. There is a broad range of crystallinity values achieved at the 15-month interval, but it is likely that these are anomalies as is shown by the continuation of the increasing crystallinity in the 22-month sample interval.

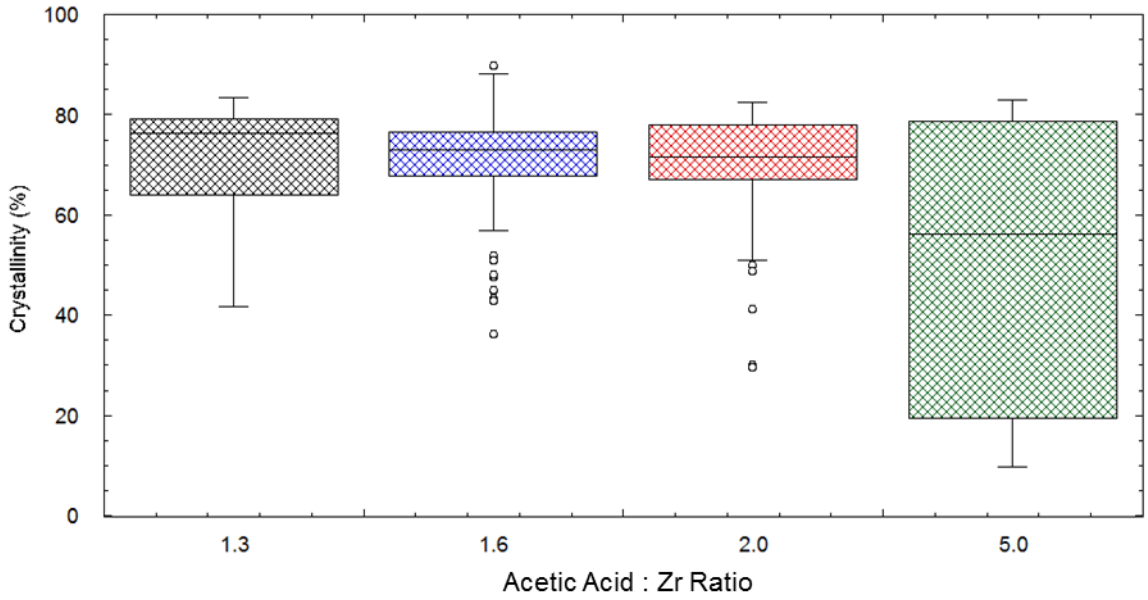

Figure 107: Effect of acetic acid : zirconium ratio on the percentage degree of crystallinity obtained.

Figure 107 shows that whilst the upper limit of crystallinity is not significantly impacted by the ratio of acetic acid : zirconium, the lower limit is. Samples which achieved low levels of crystallinity were largely those where the higher ratio of acetic acid was used, showing that this increased ratio, whilst increasing relative percentage yields (see Figure 100b), has a negative impact on the overall crystallinity of the sample.

7.5 Scanning Electron Microscopy

To Assess the morphology of the umbite powder produced, scanning electron microscopy (SEM) was employed. For this, a JEOL JCM-6000Plus SEM was used with an accelerating voltage of 15 V. Powder samples of umbite ($K_2ZrSi_3O_9 \cdot H_2O$) were held on an aluminium scanning electron microscope stub through a sticky carbon pad under ambient conditions. To aid in imaging and to prevent charge build up, samples were sputter-coated with gold to act as an electron dispersion layer. The sputter-coating was performed at The University of Lancaster and the SEM imaging was performed at The University of Central Lancashire.

SEM imaging was performed on many of the samples of umbite synthesised. The majority of the samples showed good particle morphology. Umbite has a ubiquitous morphology which is easily identifiable and can be seen in the images below.

Figure 108: SEM image of an umbite sample synthesised from ZAA6C after 15 months of ageing showing the characteristic particle morphology.

The distinct combination of small diamond shapes and the larger lamellar square structures make the identification of umbite through SEM imaging straightforward. For this reason, SEM can be easily used as a metric to the quality of the umbite product formed. Samples which display these characteristic formations are high in umbite concentration and any deviations from these formations including surface roughness, or other shapes would indicate the presence of a secondary phase.

Some samples, however, showed poor particle morphology. This manifested as a surface roughness on the surface of the umbite morphology. An example of this is shown below.

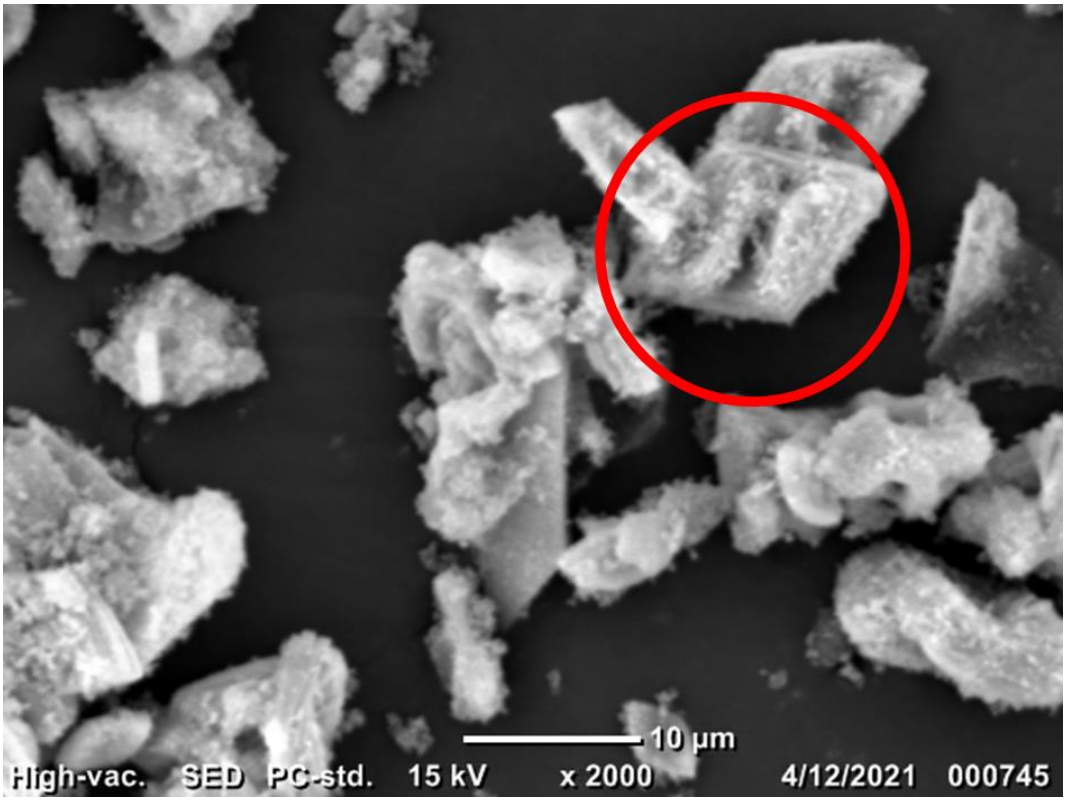

Figure 109: SEM image of an umbite sample synthesised from ZAA25I after 15 months of ageing showing a characteristic morphology which is covered in an amorphous rough surface that is poorly defined.

Figure 109 shows a sample of umbite synthesised from a zirconium-acetate precursor, after 15 months of ageing, that contained high levels of acetic acid. It can be seen in the highlighted region that the original morphology of umbite is present in the sample but that this is covered by a rough layer of another amorphous phase with a poorly defined morphology. This same sample displayed a low crystallinity percentage (42%) and so it is believed that this surface layer is the amorphous layer that is found in the diffraction pattern. This trend was common throughout all samples. Samples with low degrees of crystallinity displayed this same surface phenomena and this can be seen in the figures below.

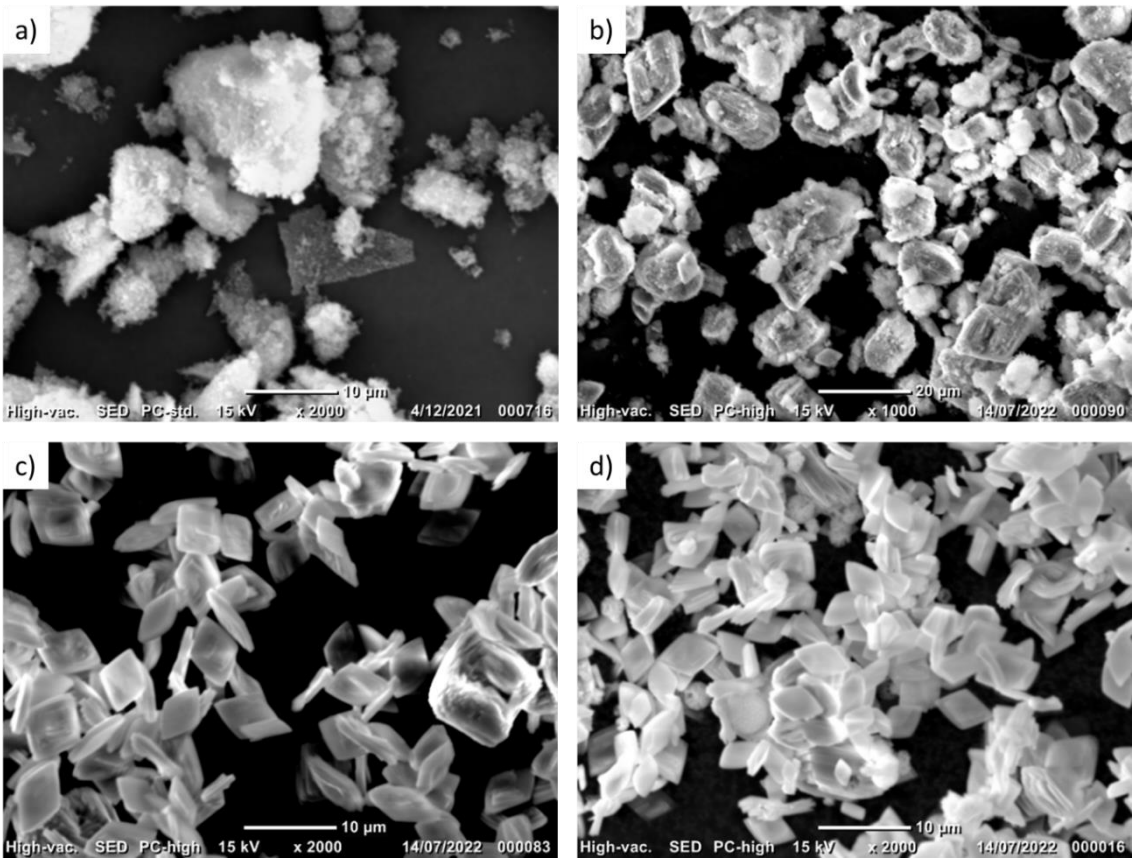

Figure 110: SEM image of an umbite sample synthesised from a) ZAA27I after 15 months of ageing b) ZAA1C after 22 months of ageing c) ZAA10C after 22 months of ageing and d) ZAA1A after 3 months of ageing. Figures a & b show poor surface morphology and c & d show characteristic morphology.

Within Figure 110, Figures a and b are samples with low crystallinity percentages (9.8% and 45% respectively) and Figures c and d have high degrees of crystallinity (79% and 67.8%). This confirms that the degree of crystallinity displayed by the sample has a direct effect on the surface morphology of the particulates.

It was postulated that one of the major influences on the particle morphology was the acetic acid : zirconium ratio. This however was not found to be true in all synthesis rounds. During the synthesis rounds of a sample of high acetic acid content, the particle morphology differed drastically from being characteristic of crystalline umbite, with degrees of crystallinity from the diffraction pattern to support this, to extremely poor morphology. This is seen for sample ZAA25 in Figure 111 below. During the 3 month and 15-month synthesis rounds the sample showed poor morphology but this was not seen in the 7 month or 22-month synthesis round. From this we can conclude that although good morphology is achievable with samples of high acetic acid content, it is inconsistent and so would be unsuitable to any application where an unvarying morphology is regularly required.

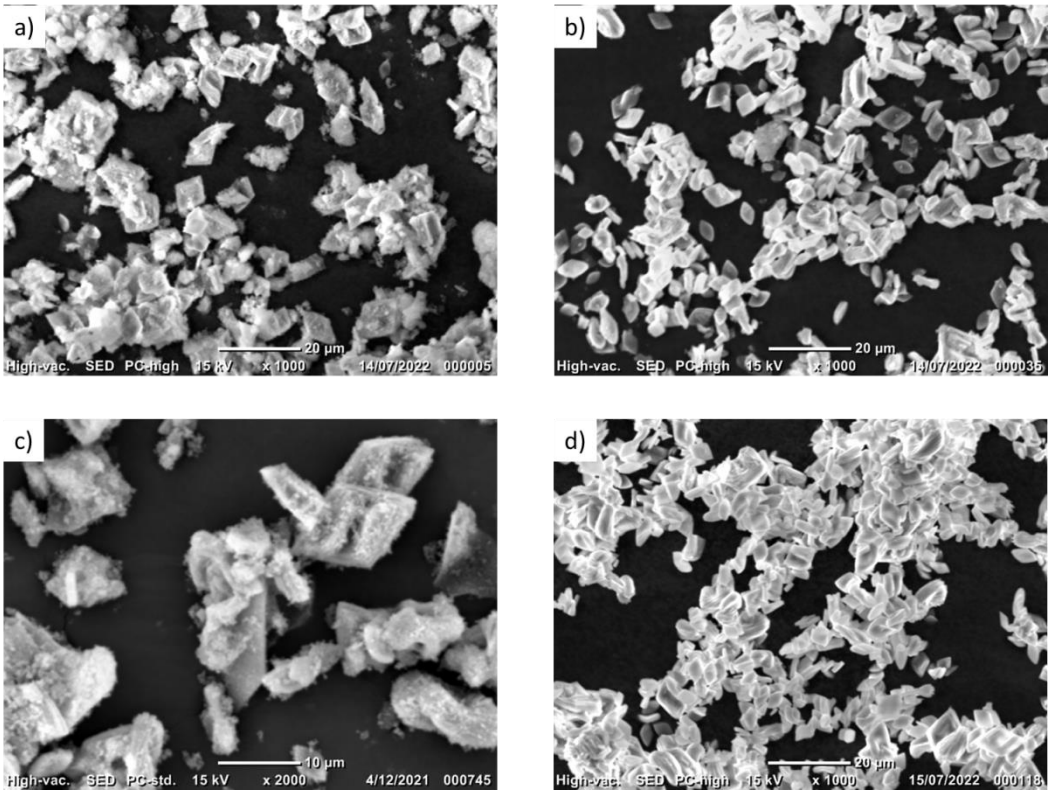

Figure 111: SEM image of umbite synthesised at a) 3 months, b) 7 months, c) 15 months, and d) 22 months from sample ZAA25.

During the 15-month synthesis period 2 samples were seen to display extremely poor particle morphology and degrees of crystallinity. The SEM images for these samples can be seen below in Figure 112.

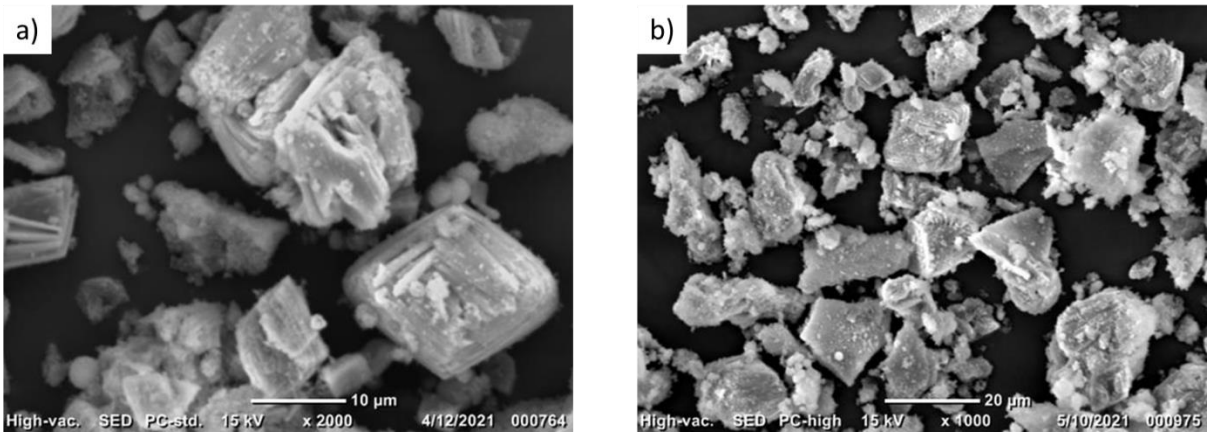

Figure 112: SEM images of umbite synthesised from a) ZAA3C and b) ZAA3A synthesised after 15 months of ageing.

Samples ZAA3C and ZAA3A showed the previously seen characteristic morphology covered in an amorphous layer. These two samples displayed low degrees of crystallinity in the diffraction studies performed: 29.6% and 30.2% respectively. These samples were subsequently analysed by nitrogen gas adsorption (Chapter 7.6) to identify if this difference in crystallinity and morphology manifested in the surface area and total pore volume.

7.6 Nitrogen Gas Adsorption

A select number of samples from the 15-month sample synthesis round were selected for surface area and total pore volume analysis using nitrogen gas adsorption. The samples selected were determined through analysis of the degree of crystallinity calculations seen previously (Chapter 7.4). These included samples with extremely low levels of crystallinity, a sample with the highest observed level of crystallinity, three samples whose morphology was observed to be poor in the SEM studies seen in Chapter 7.5 and three samples to act as controls as the variables which describe them are the most commonly used in commercial synthesis. The degree of crystallinity values for each sample alongside the results of the nitrogen gas adsorption can be seen below in Table 56 and Figure 116. Figures 113, 114, and 115 show the isotherms resulting from the nitrogen gas adsorption.

Table 56: Degree of crystallinity, surface area,and total pore volume for a selection of samples from the 15 month synthesis round. Sample names end with the temperature they were stored at (A=ambient, C=chilled, I=incubated).

Sample Name	Degree of Crystallinity (%)	Surface Area (m^2g^{-1})	Total Pore Volume (cm^3g^{-1})
ZAA3A	30.2	16	0.08
ZAA3C	29.6	39	0.17
ZAA4A	48.2	22	0.11
ZAA4C	67.5	11	0.04
ZAA4I	68.7	7.9	0.02
ZAA7C	73.5	8.5	0.02
ZAA21A	85.7	6.9	0.02
ZAA25A	18.8	67	0.29
ZAA25C	19.0	63	0.25
ZAA25I	42.8	34	0.17
ZAA27A	14.4	79	0.34
ZAA27C	20.1	66	0.28
ZAA27I	9.8	85	0.39

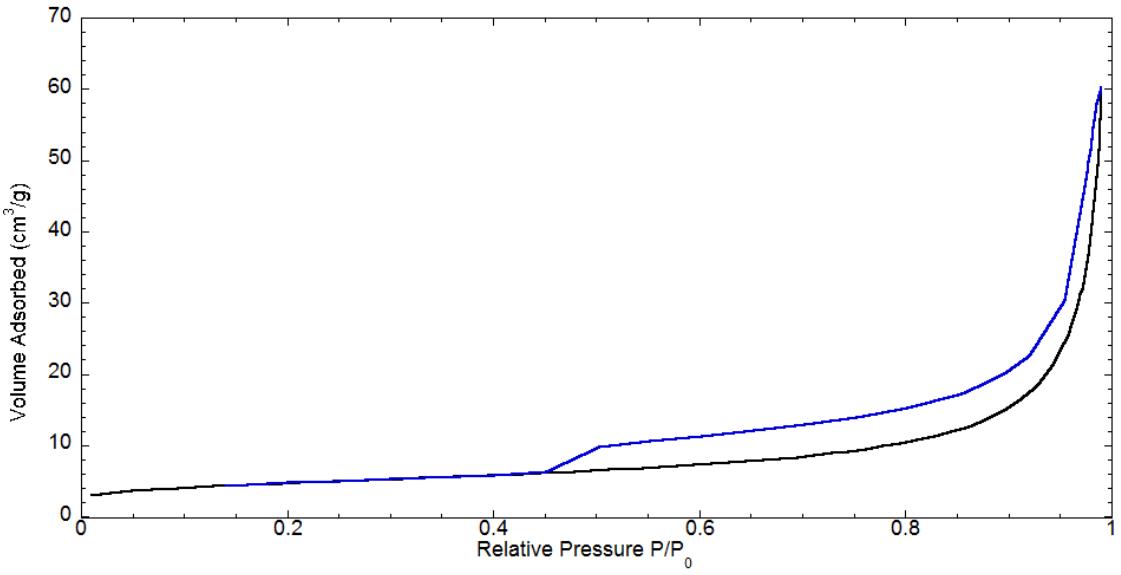

Figure 113: Isotherm resulting from the nitrogen gas adsorption of sample ZAA3A. The adsorption pathway is shown in black and the desorption pathway in blue.

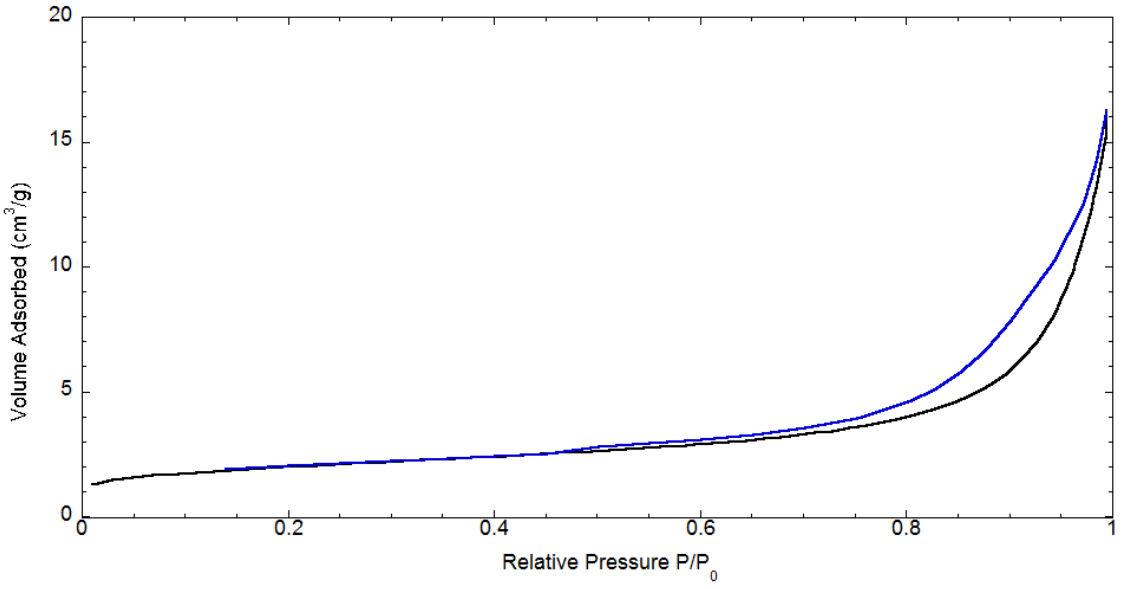

Figure 114: Isotherm resulting from the nitrogen gas adsorption of sample ZAA21A. The adsorption pathway is shown in black and the desorption pathway in blue.

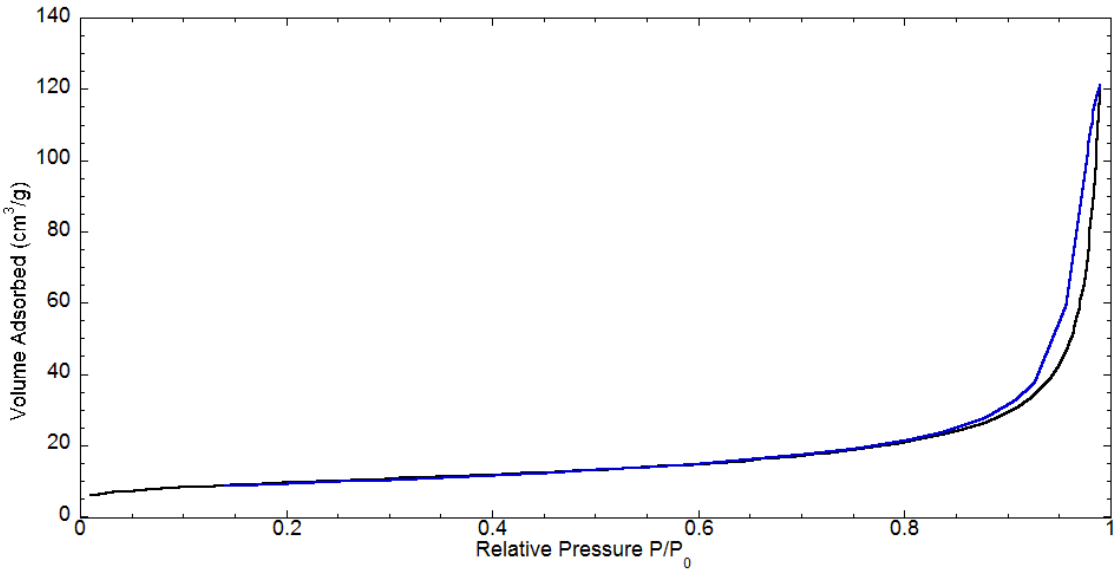

Figure 115: Isotherm resulting from the nitrogen gas adsorption of sample ZAA27I. The adsorption pathway is shown in black and the desorption pathway in blue.

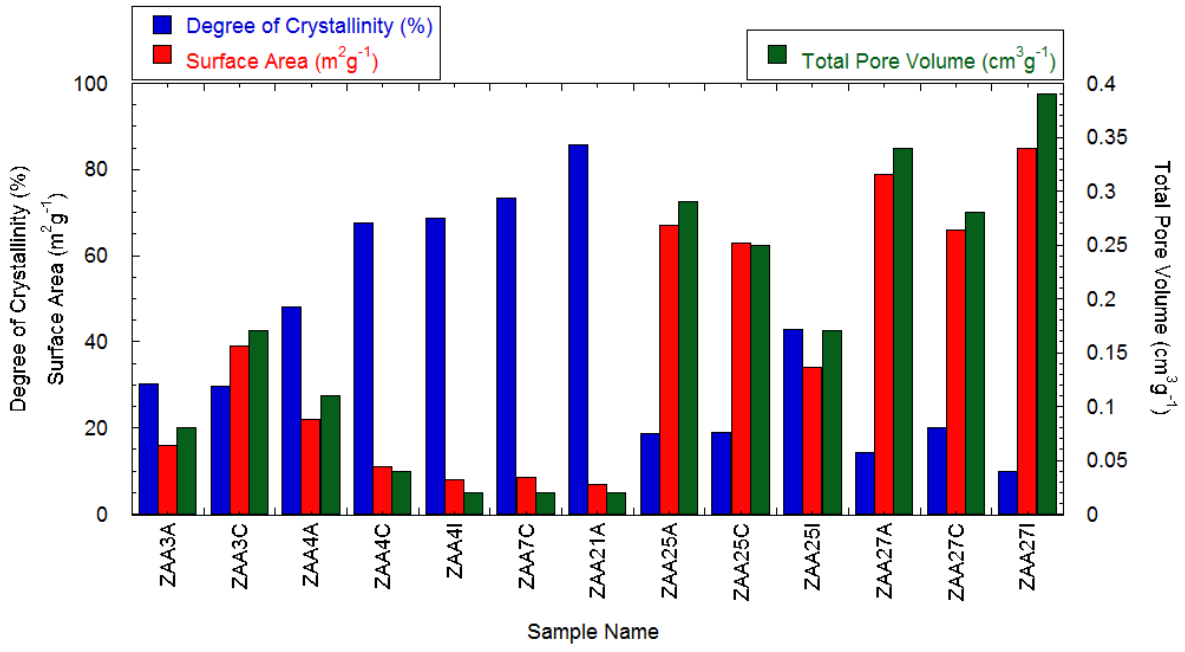

Figure 116: Results of nitrogen gas adsorption studies of a range of samples showing surface area (red) and total pore volume (green) with the degree of crystallintity results.

The three isotherms shown here are all type IV isotherms due to their asymptotic nature at high partial pressures and the presence of a hysteresis. This is indicative of a narrow pore

system with pores of 20-50 Å in which condensation occurs at higher relative pressure. Umbites microporous structure is therefore confirmed here.

From the isotherms it can be seen that sample ZAA21A showed a lower total volume adsorbed compared to ZAA27I showing a smaller total surface area for this more crystalline sample. All three isotherms shown here exhibit loop closing around 0.45 relative pressures. This is the expected region for this phenomenon for systems being studied with nitrogen as a probe molecule at 77 K. This is a result of desorption by evaporation being restricted by tight pore entrances. This in turn causes cavitation and the synonymous sharp drop in adsorbed volume in this region. It is more pronounced in ZAA3A, the sample with the low crystallinity and surface area and so it is likely that the pore entrances in this sample have become restricted in some way. This could potentially inhibit any application which relies on the systems pores being freely accessible.

It is clear from Figure 116 that generally, the total pore volume is directly proportional to the surface area of the material and that these two values are inversely proportional to the calculated degree of crystallinity. This indicates that the highly amorphous samples, such as ZAA25A-C and ZAA27A-C have a higher surface area and total pore volume than their highly crystalline counterparts.

Samples ZAA3A, ZAA3C and ZAA7C were selected due to their poor particle morphology as seen in SEM imaging. Here we can see that whilst ZAA7C follows the trend outlined above, ZAA3A and ZAA3C do not. Instead, here we see both samples have smaller surface area, total pore size, and a lower degree of crystallinity percentage. It is postulated that this caused by the presence of a non-porous yet amorphous secondary phase. This glass-like phase with a

lack of symmetry but well a defined particle boundary can be seen in the SEM images for this sample and is highlighted in Figure 117.

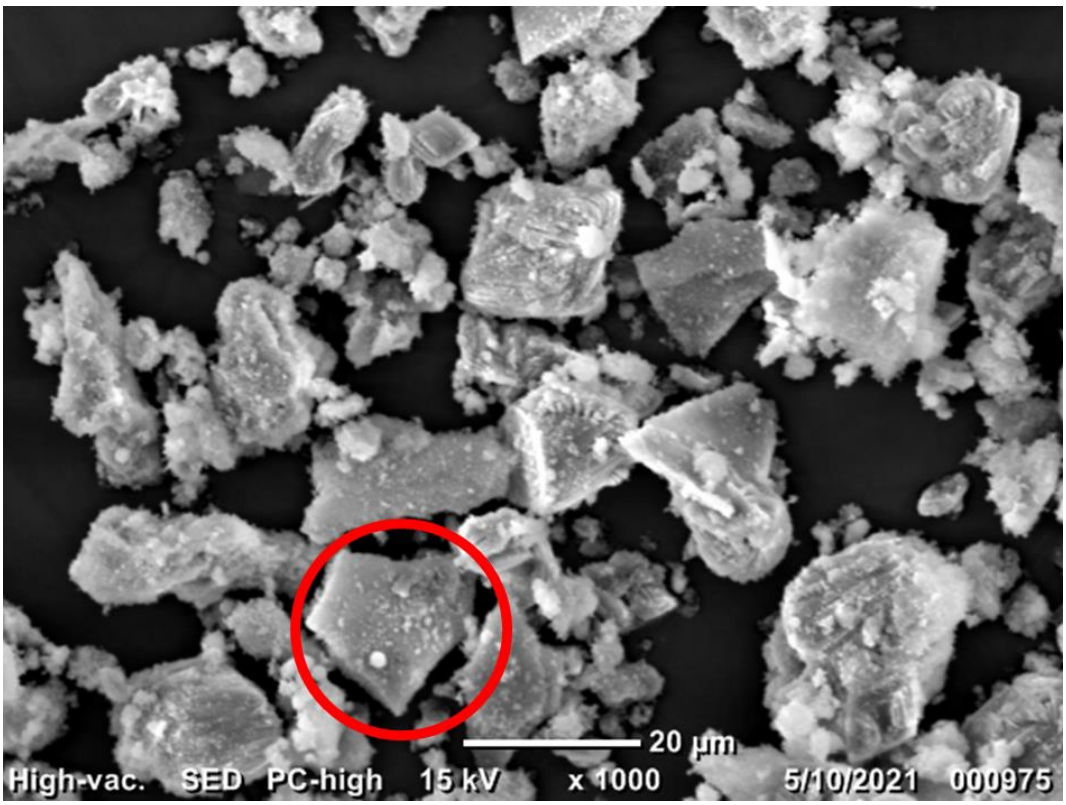

Figure 117: SEM image of sample ZAA3C with the glass-like phase highlighted in red.

This solid-phase does not display the ubiquitous particle morphology that is seen in umbite, and it does not show much surface roughness indicative of many amorphous phases leading to their high surface area. This all together would reduce the surface area and total pore volume whist maintaining a low level of crystallinity as is seen in Figure 116.

The rest of the samples however do follow the trend outlined earlier. This trend is common in the synthesis of solid materials. Samples ZAA27A-C best highlight the impact of the high level of acetic acid in the zirconium-acetate sample on the quality of the basic synthesis subsequently employed. It is felt that the increase in acetic acid substantially shifts the pH of the reaction mixture, negatively impacting the crystallinity of the product formed and leading to larger amounts of an amorphous phase with higher surface area and pore size. This is again

supported in ZAA25A-C although to a smaller extent in the incubated sample implying that there is some influence from the feedstock, but this is beyond the scope of the work presented here.

Overall, it can be concluded that for the samples studied here, with the exception of ZAA3A and ZAA3C that the degree of crystallinity is inversely proportional to the surface are and total pore volume which are increased by the presence of the secondary amorphous phase. The concentration of this amorphous phase is driven by the acid content for this synthesis, and this can be seen in the crystallinity calculations from the XRD analysis, and the nitrogen gas adsorption studies shown here.

7.7 Conclusions of Model Compound Analysis

The relationship between crystallinity and yield will be a critical calculation for all end users and depending on the application each end user will arrive at a different conclusion regarding their own priority. It has been seen here that samples with a higher ratio of acetic acid : zirconium, whilst generating higher yields generated a substandard product in terms of crystallinity. The crystalline phase within these samples was however unchanged and had constantly reasonable lattice parameters. The ratio does not impact the crystalline phase itself. The acetic acid : zirconium ratio only impacts the quantity of crystalline material synthesised. No secondary crystalline phases are introduced.

It seems that sample age has no impact on the lattice parameters and whilst it does seem to induce wider ranges of obtained yields in older samples, this product is often of a higher crystallinity.

In all the metrics studied here, storage temperature seems to have no significant impact on the quantity or quality of the final product formed. Only the physical changes observed in the samples, the gelling (discussed in Chapter 6.1.1) which seems to be accelerated through the addition of heat to the samples, would pose any potential barrier to end users. The synthetic product would be constant and the same, but the processes for their syntheses would need to adapt to the change in state of the sample. In the event that the synthetic route could not be adapted for this change in state i.e. large automated production lines, this gelled sample would have to be disposed of increasing chemical waste. This is against the principles of green chemistry and would incur great cost for end users for both disposal costs and to replace wasted reagents.

The relative ZrO_2 concentration of the sample being used has a significant impact on the final yield of umbite obtained with average yields dropping by 13% a substantial difference when applied to an industrial scale. This reduction in yield did not result in an increase in crystallinity, as was seen when studying the sample acetic acid : zirconium ratio, instead the crystallinity remained constant.

The nature of the zirconium feedstock used in the synthesis of the zirconium-acetate solutions seems to impact the yield and quality of the product obtained with feedstock 2 marginally decreasing yields whilst increasing relative crystallinity.

A direct link has been shown between the surface area, total pore volume, degree of crystallinity and particle morphology and so with the information presented here, from analysis in any one of these ways, predictions can be made regarding any other method.

8.0 Conclusions

The work presented here has sought to complete a set of aims and objectives first described in Chapter 1.2. They were as follows:

- Through the use of EXAFS, determine if the hexameric solution species, $Zr_6(O)_4(OH)_4(CH_3COO)_{12}$, proposed by Hennig *et al.* [2] to be present in laboratory synthesised zirconium-acetate solutions, is present in commercially available zirconium-acetate solutions.
- Develop a method for the study of zirconium-acetate solutions with XPDF using zirconium-oxychloride as a test case.
- Employ the method developed above to a long-term ageing study of commercially available zirconium-acetate solutions covering the effect of storage temperature, relative ZrO_2 concentration, and acetic acid : zirconium ratio, to determine if any structural changes are undergone with time.
- Synthesise the model compound, umbite, periodically through the ageing study using the solutions from the ageing study to determine the impact of the ageing process on the end users of these materials.

Previous structural studies of zirconium-oxychloride have always concentrated on the solid-phase to determine the structure present and then it has always been accepted that the solid-phase material and the liquid phase share the same molecular structure. This work has endeavoured to determine if this assumption is correct. This has been done through the development of a method employing the use of Z-matrices and TOPAS-6 rigid body function to determine from aqueous XPDF data the structure of the molecular species present [62, 67]. It

has been confirmed here through several iterations, that the structure present in aqueous solutions is not wholly unlike that proposed by Clearfield and Vaughan [1]. The model that has been refined shares the same general structure as that proposed from the solid-phase but with refined bond angles and bond lengths. It has also here been proven that the chloride ions, whilst not bonded to the tetrameric structure do have an ionic attraction to the positively charged tetramer, with 8 chloride ions surrounding the 8+ charged tetramer. Their positions are reasonably well defined, and they seem to display high amounts of correlated motion with the cluster species. The presence of these chloride ions in close proximity to the tetrameric phase has never been accounted for in solutions.

Attempts to recreate the work performed by Hennig *et al*. (Chapter 6) returned RDF's significantly different from those seen in literature [2]. For this reason, it was felt that further investigation into the solution species present in zirconium-acetate was necessary. Hennig had proposed the presence of a two-phase system of the tetrameric species previously described by Clearfield *et al*. and a newly proposed hexameric species [1]. Their data suggested an equilibrium point between the two phases at an acetic acid : zirconium ratio of 0.8. The work performed here has suggested that this equilibrium point is, in fact, found at acetic acid : zirconium ratios <5.0 and that the tetrameric phase remained the prevalent phase at values of 1.3-5.

To investigate the root cause of this difference in results, a comprehensive investigation into the nature of the molecular species in zirconium-acetate solutions was undertaken. This would assess the effect of the synthetic variables that describe the sample (concentration, acetic acid : zirconium ratio and feedstock) alongside the storage conditions and the sample age have on the nature of the molecular zirconium species found in solution.

This study has showed that, in agreement with the observations of Hennig *et al*., the solution does not exist as a single-phase but as two phases: a hexamer and tetramer. Two unique descriptions were used to model the hexameric phase: a “fixed-core” and “chandelier”. The XPDF data collections and subsequent refinements confirmed that the fixed-core model, whilst not without its limitations, was the superior method for modelling the solution species, with the chandelier being too close to an “average” structure between the hexamer and tetramer and therefore not fully representing the two unique phases. The fixed-core however offered often more credible bond lengths, and zirconium oxidation states along with higher agreement to the observed data with lower R_{wp} values.

The tetrameric phase used in the refinements was based on that derived from the refinement of zirconium-oxychloride. Some distortions from this structure were seen but it is believed these are induced by the absence of chloride ions from the model: chlorine not being present in the sample’s elemental composition.

The fixed-core model allowed for analysis of the other variables in question, namely storage condition and temperature and the synthesis variations. It was found that whilst XPDF was able to accurately model the phase present and offer refinements to bond lengths it was not able to offer a high enough level of resolution to model some of the smaller differences in the observed PDF. No modellable differences were seen in samples as they aged, or that were induced by the relative storage temperature. It was postulated early on based on work seen by Tyrsted *et al*. that the samples could potentially undergo polymerisation which would manifest in the high r region of the PDF [97]. The presence of this polymerisation would explain the gelling effect observed and described in Chapter 6.1, however, whilst some evidence of aggregation of clusters was detected in the increases in long-range intensity seen in the

18-month data collection, the intensity of these peaks was such that it was unlikely to be induced by Zr-Zr contacts but more likely scattering pairs involving either oxygen or carbon as one or both of the atom types.

XAS is often described as being more suitable for confirming the existence of structures in a qualitative manner and, whilst the methods of modelling PDF applied here do not have quite the necessary level of resolution required to fully describe the structural differences in the solution species, they do offer far more refineable and interesting information on the structure being studied over a longer range than can be seen in XAS.

It was in the phase ratio calculations where the largest discrepancy with the previous literature was seen. The phase ratio seen by Hennig *et al*. is contradicted by the work presented here [2]. At acetic acid : zirconium ratios well in excess of 0.8 (1.3 being the lowest studied) all samples displayed an excess of the tetrameric phase. This was seen up to ratios of 5.0 where still the tetrameric species remained dominant. At these values it has been previously believed the hexamer represents ≈95% of the sample composition but it has been shown here that even at these values the tetramer phase is dominant with the equilibrium point potentially being at an even higher value. Due to the stoichiometry of the hexameric cluster it would not be possible for the equilibrium point to exist below an acetic acid : zirconium ratio of 1.2 as this represents the minimum ratio of acetic acid required to form an equal ratio of hexameric and tetrameric species assuming all carboxylate groups are used to form hexamers.

The results presented here have resolved a value >5 for the ratio of this equilibrium point. This mathematically viable answer assumes that some level of free acetic acid will always

remain in solution and that not all carboxylate ions occupy hexameric species. The equilibrium shown in Equation 19 can therefore be derived.

Equation 19: The equilibrium between the hexameric and tetrameric phase.

$$1.5\ [Zr_4(OH)_8(OH_2)_{16}]^{8+} + 12\ CH_3COOH \rightleftharpoons Zr_6(O)_4(OH)_4(CH_3COO)_{12} + 28\ H_2O + 12H^+$$

The predominance of the tetrameric phase in all samples was seen throughout the ageing period and this was confirmed through analysis of 0 aged and 36-month aged samples alongside those that made the bulk of the ageing study. This discounts the postulation by Tosan *et al.* that the initial rearrangement of the structure of the sample is undergone in the first few months after synthesis. This was not observed in this study.

The synthesis of a model compound and the subsequent solid-phase analysis that was undertaken aimed to investigate the effect that the synthesis variables alongside storage temperature and age had on any end user. Zirconium-acetate solution is often used as a precursor in many syntheses and so any changes in the subsequent synthetic product, induced by the zirconium-acetate must be fully understood.

Analysis of the percentage yield obtained during synthesis determined that the leading influence was the ZrO_2 concentration of the zirconium-acetate solution. At extreme values it was also seen that the acetic acid : zirconium ratio influenced the yield with high ratio samples producing high yields. It was originally hypothesised that the higher pH generated by the 14% samples containing the same amount of acetic acid in a larger volume increased the expected yield but the extremely low pH of the 5.0 acetic acid : zirconium ratio samples and their subsequent high yields seems to contradict this, instead it is postulated that the simple increase in volume is the driving force of the increase in yield. A more dilute solution in which the reagents are more dispersed generates a higher yield. This is potentially caused by a

slower reaction where these reagents migrate in solution before interacting, but this cannot be confirmed at this time. Age was also found to influence the expected yield, but this was seen as an impact not to the average but to the range of values. This inconsistency could be detrimental to end users who expect a consistent yield for economic reasons.

Whilst Rietveld analysis alone determined that any umbite phase synthesised is of the same quality it was found through degree of crystallisation studies that the amount of this crystalline phase was impacted by the age of the sample. As samples aged, the amount of crystalline phase, and thus the degree of crystallinity, increased. On a local level, in a single synthetic round an increase in crystallinity was met with a decrease in the yield of the product but this was not seen over age where the average yield remained fairly constant despite this increase in the degree of crystallinity. No optimum age was identified and instead it is concluded that samples start degradation almost immediately and continue to decrease in performance.

8.1 Future Work

Whilst the project has answered all of the aims it set out to achieve there is still scope for continuation on this project. With regards to the XPDF refinements of zirconium-acetate, whilst the fixed-core model was superior there is potentially another way structural models could be predicted computationally and subsequently compared to the observed data sets. All XPDF modelling seen here has been focused on intracluster interactions and intercluster interactions have not been modelled. There is potential scope for, through the use of a big box modelling approach, studying the arrangement of water molecules around the structure. This potential solvation shell causes features in the XPDF which are not fully explained by the small box modelling employed here. A study of the broader range of features in the PDF could

produce information on the arrangement and potential agglomeration of the clusters studied here which could theoretically be responsible for the gelling observed and described in Chapter 6.1 but this is not clear at this stage. TOPAS-6 employs a small box modelling approach and software such as RMC_POT and EPSR which do use big box modelling often rely on energy minimisation processes to generate the model [102-104]. This is beyond the scope of the work presented here.

The long Zr-O bonds linking the core to the carboxylate groups, found in many of the zirconium-acetate species, raises question and so potential use of X-ray photoelectron spectroscopy (XPS) to determine the binding energy of the zirconium centres of these bonds could potentially be employed as it is felt that the bond lengths revealed here are too long to be considered fully covalent bonds. Also, the introduction of a tetrameric phase with either structural or occupancy defects may potentially resolve the issues seen with the excessive oxidation states in the tetrameric species in samples studied after 18 months. It would also be of interest to apply this method to evermore complex systems of molecular metal clusters, including but not limited to zirconium lactate, zirconium propionate and even non-zirconium carboxylates to determine their structure.

Whilst the work here has concentrated largely on studying the aqueous zirconium-acetate solutions through the use of XPDF recent advancements in scanning transmission electron microscopy (STEM) have yielded the possibility of atomic resolution imaging of solid frameworks and potentially even liquid metal clusters like those seen in this work. The size of the cluster species studied here is within the size range of what is believed to be possible when analysing these molecular metal clusters. This could potentially yield further information on the gelling process that has been observed and which, whilst this study has

looked at the conditions that induce this gelling it has not assessed the true cause. STEM could potentially investigate this by observing cluster density. Investigations could also potentially be made using in-situ XPDF to see in real time the changes induced by gelling.

This work has postulated an equilibrium (Equation 19) at an acetic acid : zirconium ratio greater than 5 but further work would seek to determine a new value based upon the XPDF refinements seen here.

In-situ XPDF could potentially be applied here. Studying the formation of the cluster species during the initial preparation for these samples through the development of a flow cell could confirm that the structural rearrangement is instantaneous as is postulated here. The ability to adjust the acetic acid : zirconium ratio whilst probing the sample would also prove beneficial to study the equilibrium point between the two clusters described here.

Ultimately the work presented here has proven the validity of XPDF to model molecular metal clusters; in particular zirconium-acetate and zirconium-oxychloride, and the four aims outlined at the top of this chapter have been successfully answered.

References

1. A. Clearfield and P. A. Vaughan, *Acta Crystallographica*, 1956, **9**, 555-558.
2. C. Hennig, S. Weiss, W. Kraus, J. Kretzschmar and A. C. Scheinost, *Inorganic Chemistry*, 2017, **56**, 2473-2480.
3. J. H. Cavka, S. Jakobsen, U. Olsbye, N. Guillou, C. Lamberti, S. Bordiga and K. P. Lillerud, *Journal of the American Chemical Society*, 2008, **130**, 13850-13851.
4. A. Dhakshinamoorthy, A. Santiago-Portillo, A. M. Asiri and H. Garcia, *ChemCatChem*, 2019, **11**, 899-923.
5. B. Leonetti, A. Perin, E. K. Ambrosi, G. Sponchia, P. Sgarbossa, A. Castellin, P. Riello and A. Scarso, *Journal of Drug Delivery Science and Technology*, 2021, **61**, 102189-102197.
6. M. F. M. Zwinkels, S. G. Järås, P. G. Menon and T. A. Griffin, *Catalysis Reviews*, 1993, **35**, 319-358.
7. R. Vassen, M. O. Jarligo, T. Steinke, D. E. Mack and D. Stover, *Surface & Coatings Technology*, 2010, **205**, 938-942.
8. D. R. Clarke, M. Oechsner and N. P. Padture, *MRS Bulletin*, 2012, **37**, 891-902.
9. R. Vaßen, D. E. Mack, M. Tandler, Y. J. Sohn, D. Sebold and O. Guillon, *Journal of the American Ceramic Society*, 2021, **104**, 463-471.
10. H. Taimatsu and H. Kaneko, *Analytica Chimica Acta*, 2001, **435**, 247-254.
11. T. Van Gestel, D. Sebold, F. Hauler, W. A. Meulenberg and H.-P. Buchkremer, *Journal of Membrane Science*, 2010, **359**, 64-79.
12. P. D. L. Mercera, J. G. van Ommen, E. B. M. Doesburg, A. J. Burggraaf and J. R. H. Ross, *Applied Catalysis*, 1991, **71**, 363-391.
13. G. K. Chuah, S. Jaenicke, S. A. Cheong and K. S. Chan, *Applied Catalysis A: General*, 1996, **145**, 267-284.
14. M. H. Bocanegra-Bernal and S. D. de la Torre, *Journal of Materials Science*, 2002, **37**, 4947-4971.
15. J. Winarta, B. Shan, S. M. McIntyre, L. Ye, C. Wang, J. Liu and B. Mu, *Crystal Growth & Design*, 2020, **20**, 1347-1362.
16. F. You, *United States Patent and Trademark Office*, 2009, **US 2009/0114390 A1**.
17. E. J. Gonzales, C. M. Welch and J. D. Guthrie, *Textile Research Journal*, 1963, **33**, 600-608.
18. W. B. Blumenthal, *Industrial & Engineering Chemistry*, 1950, **42**, 640-642.
19. M. Forouharshad, M. Montazer, M. B. Moghadam and O. Saligheh, *Thermochimica Acta*, 2011, **520**, 134-138.
20. G. Zhao, C. Dai, Q. You, M. Zhao and J. Zhao, *Journal of Sol-Gel Science and Technology*, 2013, **65**, 392-398.
21. K. De Keukeleere, J. De Roo, P. Lommens, J. C. Martins, P. Van Der Voort and I. Van Driessche, *Inorganic Chemistry*, 2015, **54**, 3469-3476.
22. M. P. Feth, M. Bauer, G. Kickelbick, O. Metelkina, U. Schubert and H. Bertagnolli, *Journal of Non-Crystalline Solids*, 2005, **351**, 432-443.
23. A. C. Geiculescu and H. G. Spencer, *Journal of Sol-Gel Science and Technology*, 2000, **17**, 25-35.
24. M. Bremholm, J. Becker-Christensen and B. B. Iversen, *Advanced Materials*, 2009, **21**, 3572-3575.

25. F. J. Berry, S. J. Skinner, I. M. Bell, R. J. H. Clark and C. B. Ponton, *Journal of Solid State Chemistry*, 1999, **145**, 394-400.
26. G. K. Schweitzer and L. L. Pesterfield, *The Aqueous Chemistry of the Elements*, Oxford University Press, New York, 2010.
27. G. M. Muha and P. A. Vaughan, *The Journal of Chemical Physics*, 1960, **33**, 194-199.
28. T. C. W. Mak, *Canadian Journal of Chemistry*, 1968, **46**, 3491-3497.
29. M. Aaberg, *Acta Chem Scand, Ser A*, 1977, **31**, 171-181.
30. A. Singhal, L. M. Toth, J. S. Lin and K. Affholter, *Journal of the American Chemical Society*, 1996, **118**, 11529-11534.
31. N. Rao, M. N. Holerca, M. L. Klein and V. Pophristic, *The Journal of Physical Chemistry A*, 2007, **111**, 11395-11399.
32. C. B. Messner, T. S. Hofer, B. R. Randolf and B. M. Rode, *Physical Chemistry Chemical Physics*, 2011, **13**, 224-229.
33. Y.-J. Hu, K. E. Knope, S. Skanthakumar, M. G. Kanatzidis, J. F. Mitchell and L. Soderholm, *Journal of the American Chemical Society*, 2013, **135**, 14240-14248.
34. J. A. Sommers, D. C. Hutchison, N. P. Martin, K. Kozma, D. A. Keszler and M. Nyman, *Journal of the American Chemical Society*, 2019, **141**, 16894-16902.
35. H. Xu, S. Sommer, N. L. N. Broge, J. Gao and B. B. Iversen, *Chemistry – A European Journal*, 2019, **25**, 2051-2058.
36. R. D. Stern, R. S. Kingsbury and K. A. Persson, *Inorganic Chemistry*, 2021, **60**, 15456-15466.
37. M. Kløve, R. S. Christensen, I. G. Nielsen, S. Sommer, M. R. V. Jørgensen, A.-C. Dippel and B. B. Iversen, *Chemical Science*, 2022, **13**, 12883-12891.
38. Y. Zhang, F. de Azambuja and T. N. Parac-Vogt, *Coordination Chemistry Reviews*, 2021, **438**, 213886.
39. Z. A. Vladimirova, N. Z. Prozorovskaya and L. N. Komissarova, *Russian Journal of Inorganic Chemistry*, 1973, **18**, 368-370.
40. T. B. Konunova, M. S. Popov and C. Kuang, *Russian Journal of Inorganic Chemistry*, 1956, **14**, 1084-1086.
41. R. Paul, O. Baidya, R. Kumar and R. Kapoor, *Australian Journal of Chemistry*, 1976, **29**, 1605-1607.
42. J.-L. Tosan, B. Durand, M. Roubin, F. Chassagneux and F. Bertin, *Journal of Non-Crystalline Solids*, 1994, **168**, 23-32.
43. M. Bremholm, H. Birkedal, B. B. Iversen and J. S. Pedersen, *The Journal of Physical Chemistry C*, 2015, **119**, 12660-12667.
44. L. Pan, R. Heddy, J. Li, C. Zheng, X.-Y. Huang, X. Tang and L. Kilpatrick, *Inorganic Chemistry*, 2008, **47**, 5537-5539.
45. J. Pascual-Colino, B. Artetxe, G. Beobide, O. Castillo, M. L. Fidalgo-Mayo, A. Isla-López, A. Luque, S. Mena-Gutiérrez and S. Pérez-Yáñez, *Inorganic Chemistry*, 2022, **61**, 4842-4851.
46. D. M. Poojary, A. I. Bortun, L. N. Bortun and A. Clearfield, *Inorganic Chemistry*, 1997, **36**, 3072-3079.
47. A. West, *Basic Solid State Chemistry*, John Wiley & Sons, Chichester, 2 edn., 1999.
48. K. Gibbs, X-Ray Spectra, https://www.schoolphysics.co.uk/age16-19/Atomic%20physics/X%20rays/text/X_ray_spectra/index.html, (accessed 13th October, 2022).

49. V. Pecharsky and P. Zavalij, *Fundamentals of Powder Diffraction*, Springer US, New York, NY, 2 edn., 2009.
50. P. Willmott, in *An Introduction to Synchrotron Radiation*, Wiley, Chichester, 2011, DOI: 10.1002/9781119970958.ch3, pp. 39-86.
51. F. R. Elder, A. M. Gurewitsch, R. V. Langmuir and H. C. Pollock, *Physical Review*, 1947, **71**, 829-830.
52. P. Chater, presented in part at the IUCr 2017, Hyderabad, India, 2017.
53. A. Clearfield, in *Principles and Applications of Powder Diffraction*, John Wiley & Sons, Chichester, 2009, pp. 73-122.
54. Lesley E. Smart and E. A. Moore, *Solid State Chemistry: An Introduction*, CRC Press, Boca Raton, 4 edn., 2012.
55. C. Hammond, *The Basics of Crystallography and Diffraction*, Oxford University Press, Oxford, 2001.
56. C. Housecroft and A. Sharpe, *Inorganic Chemistry*, Pearson, Harlow, 4th edn., 2012.
57. P. W. Atkins and J. De Paula, *Atkins' Physical Chemistry*, Oxford University Press, Oxford, 10th ed. edn., 2014.
58. M. T. Weller, *Inorganic Materials Chemistry*, Oxford University Press, Oxford, 1994.
59. R. B. Von Dreele, in *Powder Diffraction: Theory and Practice*, The Royal Society of Chemistry, 2008, DOI: 10.1039/9781847558237-00266, pp. 266-281.
60. L. B. McCusker, R. B. Von Dreele, D. E. Cox, D. Louer and P. Scardi, *Journal of Applied Crystallography*, 1999, **32**, 36-50.
61. R. E. Dinnebier, A. Leineweber and J. S. O. Evans, *Rietveld Refinement: Practical Powder Diffraction Pattern Analysis using TOPAS*, De Gruyter, 2018.
62. A. Coelho, Topas Academic V6, http;//www.topas-academic.net/, (accessed 13th October, 2022).
63. G. S. Pawley, *Journal of Applied Crystallography*, 1981, **14**, 357-361.
64. Bruker, *Version 4.3*, 2018.
65. B. H. Toby, *Journal of Applied Crystallography*, 2001, **34**, 210-213.
66. A. C. Larson and R. B. Von Dreele, *Los Alamos National Laboratory Report*, 2000, **LAUR**, 86-748.
67. A. A. Coelho, P. A. Chater and A. Kern, *Journal of Applied Crystallography*, 2015, **48**, 869-875.
68. J. L. Billinge Simon, in *International tables of Crystallography*, International union of crystallography, 2019, vol. Vol. H, pp. 649-672.
69. T. Egami and S. J. L. Billinge, *Underneath the Bragg Peaks: Structural Analysis of Complex Materials*, Elsevier Science, 2003.
70. M. W. Terban and S. J. L. Billinge, *Chemical reviews*, 2022, **122**, 1208-1272.
71. Y. Ren and X. Zuo, *Small Methods*, 2018, **2**, 1800064.
72. I. K. Jeong, R. H. Heffner, M. J. Graf and S. J. L. Billinge, *Physical Review B*, 2003, **67**, 104301.
73. I. K. Jeong, T. Proffen, F. Mohiuddin-Jacobs and S. J. L. Billinge, *The Journal of Physical Chemistry A*, 1999, **103**, 921-924.
74. C. L. Farrow, P. Juhas, J. W. Liu, D. Bryndin, E. S. Božin, J. Bloch, T. Proffen and S. J. L. Billinge, *Journal of Physics: Condensed Matter*, 2007, **19**, 335219.
75. B. H. Toby and T. Egami, *Acta Crystallographica Section A*, 1992, **48**, 336-346.
76. M. Abeykoon, 28ID-1(PDF) Pair Distribution Function, https://wiki-nsls2.bnl.gov/beamline28ID1/index.php/Main_Page, (accessed 13th October, 2022).

77. A. K. Soper, *Rutherford Appleton Laboratory Technical Reports*, 2011.
78. P. Juhas, T. Davis, C. L. Farrow and S. J. L. Billinge, *Journal of Applied Crystallography*, 2013, **46**, 560-566.
79. S. Calvin, *XAFS for Everyone*, CRC Press, Boca Raton, 1 edn., 2013.
80. H. Fricke, *Physical Review*, 1920, **16**, 202-215.
81. Quantum Leap XAS, http://www.sigray.com/quantumleap, (accessed 01/07/2020).
82. M. T. Weller and N. A. Young, *Characterisation Methods in Inorganic Chemistry*, Oxford University Press, Oxford, 2017.
83. J. Evans, *X-Ray Absorption Spectroscopy for the Chemical and Materials Sciences*, John Wiley & Sons, Chichester, 2018.
84. S. Hayama, presented in part at the DLS EXAFS Workshop, Diamond Light Source, UK, 2019.
85. B. Ravel and M. Newville, *Journal of Synchrotron Radiation*, 2005, **12**, 537-541.
86. K. Sing, *Colloids and Surfaces A: Physicochemical and Engineering Aspects*, 2001, **187-188**, 3-9.
87. G. Attard and C. Barnes, *Surfaces*, Oxford University Press, Oxford, 1998.
88. V. Kumar, G. Srinivas, B. Wood, K. Ramisetty, A. Stewart, C. Howard, D. J. L. Brett and F. Rodriguez-Reinoso, *Journal of Materials Chemistry A*, 2019, **7**.
89. D. Zagorac, H. Muller, S. Ruehl, J. Zagorac and S. Rehme, *Journal of Applied Crystallography*, 2019, **52**, 918-925.
90. D. C. Palmer, *CrystalMaker Software Ltd, Begbroke, Oxfordshire, England.*, 2014.
91. A. K. Soper and E. R. Barney, *Journal of Applied Crystallography*, 2011, **44**, 714-726.
92. I. D. Brown and D. Altermatt, *Acta Crystallographica Section B*, 1985, **41**, 244-247.
93. S. Øien, D. Wragg, H. Reinsch, S. Svelle, S. Bordiga, C. Lamberti and K. P. Lillerud, *Crystal Growth & Design*, 2014, **14**, 5370-5372.
94. D. K. Smith and W. Newkirk, *Acta Crystallographica*, 1965, **18**, 983-991.
95. R. D. Shannon and C. T. Prewitt, *Acta Crystallographica Section B*, 1969, **25**, 925-946.
96. R. D. Shannon, *Acta Crystallographica Section A*, 1976, **32**, 751-767.
97. C. Tyrsted, N. Lock, K. M. O. Jensen, M. Christensen, E. D. Bojesen, H. Emerich, G. Vaughan, S. J. L. Billinge and B. B. Iversen, *IUCrJ*, 2014, **1**, 165-171.
98. J. J. Rehr, J. J. Kas, M. P. Prange, A. P. Sorini, Y. Takimoto and F. Vila, *Comptes Rendus Physique*, 2009, **10**, 548-559.
99. W. M. Haynes, D. R. Lide and T. J. Bruno, *CRC Handbook of Chemistry and Physics*, CRC Press, Boca Raton, 97 edn., 2016.
100. V. Somjit, P. Thinsoongnoen, T. Pila, B. Boekfa, S. Wannapaiboon and K. Kongpatpanich, *Inorganic Chemistry*, 2022, **61**, 11342-11348.
101. J. S. O. Evans, Tutorial 29: Quantitative Rietveld Refinement, https://topas.webspace.durham.ac.uk/tutorial_quantriet/, (accessed 21/07, 2022).
102. G. Evrard and L. Pusztai, *Journal of Physics: Condensed Matter*, 2005, **17**, S1-S13.
103. A. K. Soper, *Chemical Physics*, 1996, **202**, 295-306.
104. A. K. Soper, *Molecular Physics*, 2001, **99**, 1503-1516.

A Structural Study of the Nature of Molecular Zirconium Species in Aqueous Solution

(Appendices)

By

Joe Rawlinson

A thesis submitted in partial fulfilment for the requirements for the degree of Doctor of Philosophy at the University of Central Lancashire

School of Natural Sciences

2022

10.0 Appendices

Table of Figures

Figure 1: Observed and Calculated PDF from the fixed core refinement of ZAA1 from the 9-month data collection and the resultant model. 314

Figure 2: Observed and Calculated PDF from the fixed core refinement of ZAA4 from the 9-month data collection and the resultant model. 316

Figure 3: Observed and Calculated PDF from the fixed core refinement of ZAA7 from the 9-month data collection and the resultant model. 318

Figure 4: Observed and Calculated PDF from the fixed core refinement of ZAA10 from the 9-month data collection and the resultant model. 320

Figure 5: Observed and Calculated PDF from the fixed core refinement of ZAA13 from the 9-month data collection and the resultant model. 322

Figure 6: Observed and Calculated PDF from the fixed core refinement of ZAA16 from the 9-month data collection and the resultant model. 324

Figure 7: Observed and Calculated PDF from the chandelier core refinement of ZAA1 from the 9-month data collection and the resultant model viewed from the axial (left) and equatorial (right) positions. 326

Figure 8: Observed and Calculated PDF from the chandelier core refinement of ZAA4 from the 9-month data collection and the resultant model viewed from the axial (left) and equatorial (right) positions. 328

Figure 9: Observed and Calculated PDF from the chandelier core refinement of ZAA7 from the 9-month data collection and the resultant model viewed from the axial (left) and equatorial (right) positions. 330

Figure 10: Observed and Calculated PDF from the chandelier core refinement of ZAA10 from the 9-month data collection and the resultant model viewed from the axial (left) and equatorial (right) positions. 332
Figure 11: Observed and Calculated PDF from the chandelier core refinement of ZAA13 from the 9-month data collection and the resultant model viewed from the axial (left) and equatorial (right) positions. 334
Figure 12: Observed and Calculated PDF from the chandelier core refinement of ZAA16 from the 9-month data collection and the resultant model viewed from the axial (left) and equatorial (right) positions. 336
Figure 13: Observed and Calculated PDF from the fixed core refinement of ZAA1 from the 9-month data collection and the resultant model. 338
Figure 14: The tetrameric structure resulting from the fixed core refinement of ZAA1 from the 9-month data collection. 340
Figure 15: Observed and Calculated PDF from the fixed core refinement of ZAA4 from the 9-month data collection and the resultant model. 341
Figure 16: The tetrameric structure resulting from the fixed core refinement of ZAA4 from the 9-month data collection. 343
Figure 17: Observed and Calculated PDF from the fixed core refinement of ZAA7 from the 9-month data collection and the resultant model. 344
Figure 18: The tetrameric structure resulting from the fixed core refinement of ZAA7 from the 9-month data collection. 346
Figure 19: Observed and Calculated PDF from the fixed core refinement of ZAA10 from the 9-month data collection and the resultant model. 347

Figure 20: The tetrameric structure resulting from the fixed core refinement of ZAA10 from the 9-month data collection. 349
Figure 21: Observed and Calculated PDF from the fixed core refinement of ZAA13 from the 9-month data collection and the resultant model. 350
Figure 22: The tetrameric structure resulting from the fixed core refinement of ZAA13 from the 9-month data collection. 352
Figure 23: Observed and Calculated PDF from the fixed core refinement of ZAA16 from the 9-month data collection and the resultant model. 353
Figure 24: The tetrameric structure resulting from the fixed core refinement of ZAA16 from the 9-month data collection. 355
Figure 25: Observed and Calculated PDF from the chandelier core refinement of ZAA1 from the 9-month data collection and the resultant model viewed from the axial (left) and equatorial (right) positions. 356
Figure 26: The tetrameric structure resulting from the chandelier core refinement of ZAA1 from the 9-month data collection. 358
Figure 27: Observed and Calculated PDF from the chandelier core refinement of ZAA4 from the 9-month data collection and the resultant model viewed from the axial (left) and equatorial (right) positions. 359
Figure 28: The tetrameric structure resulting from the chandelier core refinement of ZAA4 from the 9-month data collection. 361
Figure 29: Observed and Calculated PDF from the chandelier core refinement of ZAA7 from the 9-month data collection and the resultant model viewed from the axial (left) and equatorial (right) positions. 362

Figure 30: The tetrameric structure resulting from the chandelier core refinement of ZAA7 from the 9-month data collection. 364
Figure 31: Observed and Calculated PDF from the chandelier core refinement of ZAA10 from the 9-month data collection and the resultant model viewed from the axial (left) and equatorial (right) positions. 365
Figure 32: The tetrameric structure resulting from the chandelier core refinement of ZAA10 from the 9-month data collection. 367
Figure 33: Observed and Calculated PDF from the chandelier core refinement of ZAA13 from the 9-month data collection and the resultant model viewed from the axial (left) and equatorial (right) positions. 368
Figure 34: The tetrameric structure resulting from the chandelier core refinement of ZAA13 from the 9-month data collection. 370
Figure 35: Observed and Calculated PDF from the chandelier core refinement of ZAA16 from the 9-month data collection and the resultant model viewed from the axial (left) and equatorial (right) positions. 371
Figure 36: The tetrameric structure resulting from the chandelier core refinement of ZAA16 from the 9-month data collection. 373
Figure 37: Observed and Calculated PDF from the chandelier core refinement of ZAA1 from the 15-month data collection and the resultant model viewed from the axial (left) and equatorial (right) positions. 374
Figure 38: Observed and Calculated PDF from the fixed core refinement of ZAA1 from the 15-month data collection and the resultant model. 376

Figure 39: Observed and Calculated PDF from the chandelier core refinement of ZAA4 from the 15-month data collection and the resultant model viewed from the axial (left) and equatorial (right) positions. 378

Figure 40: Observed and Calculated PDF from the fixed core refinement of ZAA4 from the 15-month data collection and the resultant model. 380

Figure 41: Observed and Calculated PDF from the chandelier core refinement of ZAA7 from the 15-month data collection and the resultant model viewed from the axial (left) and equatorial (right) positions. 382

Figure 42: Observed and Calculated PDF from the fixed core refinement of ZAA7 from the 15-month data collection and the resultant model. 384

Figure 43: Observed and Calculated PDF from the chandelier core refinement of ZAA10 from the 15-month data collection and the resultant model viewed from the axial (left) and equatorial (right) positions. 386

Figure 44: Observed and Calculated PDF from the fixed core refinement of ZAA10 from the 15-month data collection and the resultant model. 388

Figure 45: Observed and Calculated PDF from the chandelier core refinement of ZAA13 from the 15-month data collection and the resultant model viewed from the axial (left) and equatorial (right) positions. 390

Figure 46: Observed and Calculated PDF from the fixed core refinement of ZAA13 from the 15-month data collection and the resultant model. 392

Figure 47: Observed and Calculated PDF from the chandelier core refinement of ZAA16 from the 15-month data collection and the resultant model viewed from the axial (left) and equatorial (right) positions. 394

Figure 48: Observed and Calculated PDF from the fixed core refinement of ZAA16 from the 15-month data collection and the resultant model. 396
Figure 49: Observed and Calculated PDF from the chandelier core refinement of ZAA20 from the 15-month data collection and the resultant model viewed from the axial (left) and equatorial (right) positions. 398
Figure 50: Observed and Calculated PDF from the fixed core refinement of ZAA20 from the 15-month data collection and the resultant model. 400
Figure 51: Observed and Calculated PDF from the chandelier core refinement of ZAA24 from the 15-month data collection and the resultant model viewed from the axial (left) and equatorial (right) positions. 402
Figure 52: Observed and Calculated PDF from the fixed core refinement of ZAA24 from the 15-month data collection and the resultant model. 404
Figure 53: Observed and Calculated PDF from the chandelier core refinement of ZAA25 from the 15-month data collection and the resultant model viewed from the axial (left) and equatorial (right) positions. 406
Figure 54: Observed and Calculated PDF from the fixed core refinement of ZAA25 from the 15-month data collection and the resultant model. 408
Figure 55: Observed and Calculated PDF from the fixed core refinement of ZAA1 from the 15-month data collection and the resultant model. 410
Figure 56: The tetrameric structure resulting from the fixed core refinement of ZAA1 from the 15-month data collection. 412
Figure 57: Observed and Calculated PDF from the fixed core refinement of ZAA4 from the 15-month data collection and the resultant model. 413

Figure 58: The tetrameric structure resulting from the fixed core refinement of ZAA4 from the 15-month data collection. 415

Figure 59: Observed and Calculated PDF from the fixed core refinement of ZAA7 from the 15-month data collection and the resultant model. 416

Figure 60: The tetrameric structure resulting from the fixed core refinement of ZAA7 from the 15-month data collection. 418

Figure 61: Observed and Calculated PDF from the fixed core refinement of ZAA10 from the 15-month data collection and the resultant model. 419

Figure 62: The tetrameric structure resulting from the fixed core refinement of ZAA10 from the 15-month data collection. 421

Figure 63: Observed and Calculated PDF from the fixed core refinement of ZAA13 from the 15-month data collection and the resultant model. 422

Figure 64: The tetrameric structure resulting from the fixed core refinement of ZAA13 from the 15-month data collection. 424

Figure 65: Observed and Calculated PDF from the fixed core refinement of ZAA16 from the 15-month data collection and the resultant model. 425

Figure 66: The tetrameric structure resulting from the fixed core refinement of ZAA16 from the 15-month data collection. 427

Figure 67: Observed and Calculated PDF from the fixed core refinement of ZAA20 from the 15-month data collection and the resultant model. 428

Figure 68: The tetrameric structure resulting from the fixed core refinement of ZAA20 from the 15-month data collection. 430

Figure 69: Observed and Calculated PDF from the fixed core refinement of ZAA24 from the 15-month data collection and the resultant model. 431

Figure 70: The tetrameric structure resulting from the fixed core refinement of ZAA24 from the 15-month data collection. 433

Figure 71: Observed and Calculated PDF from the fixed core refinement of ZAA25 from the 15-month data collection and the resultant model. 434

Figure 72: The tetrameric structure resulting from the fixed core refinement of ZAA25 from the 15-month data collection. 436

Figure 73: Observed and Calculated PDF from the chandelier core refinement of ZAA1 from the 15-month data collection and the resultant model viewed from the axial (left) and equatorial (right) positions. 437

Figure 74: The tetrameric structure resulting from the chandelier core refinement of ZAA1 from the 15-month data collection. 439

Figure 75: Observed and Calculated PDF from the chandelier core refinement of ZAA4 from the 15-month data collection and the resultant model viewed from the axial (left) and equatorial (right) positions. 441

Figure 76: The tetrameric structure resulting from the chandelier core refinement of ZAA4 from the 15-month data collection. 443

Figure 77: Observed and Calculated PDF from the chandelier core refinement of ZAA7 from the 15-month data collection and the resultant model viewed from the axial (left) and equatorial (right) positions. 445

Figure 78: The tetrameric structure resulting from the chandelier core refinement of ZAA7 from the 15-month data collection. 447

Figure 79: Observed and Calculated PDF from the chandelier core refinement of ZAA10 from the 15-month data collection and the resultant model viewed from the axial (left) and equatorial (right) positions. 449

Figure 80: The tetrameric structure resulting from the chandelier core refinement of ZAA10 from the 15-month data collection. 451
Figure 81: Observed and Calculated PDF from the chandelier core refinement of ZAA13 from the 15-month data collection and the resultant model viewed from the axial (left) and equatorial (right) positions. 453
Figure 82: The tetrameric structure resulting from the chandelier core refinement of ZAA13 from the 15-month data collection. 455
Figure 83: Observed and Calculated PDF from the chandelier core refinement of ZAA16 from the 15-month data collection and the resultant model viewed from the axial (left) and equatorial (right) positions. 457
Figure 84: The tetrameric structure resulting from the chandelier core refinement of ZAA16 from the 15-month data collection. 459
Figure 85: Observed and Calculated PDF from the chandelier core refinement of ZAA20 from the 15-month data collection and the resultant model viewed from the axial (left) and equatorial (right) positions. 461
Figure 86: The tetrameric structure resulting from the chandelier core refinement of ZAA20 from the 15-month data collection. 463
Figure 87: Observed and Calculated PDF from the chandelier core refinement of ZAA24 from the 15-month data collection and the resultant model viewed from the axial (left) and equatorial (right) positions. 465
Figure 88: The tetrameric structure resulting from the chandelier core refinement of ZAA24 from the 15-month data collection. 467

Figure 89: Observed and Calculated PDF from the chandelier core refinement of ZAA25 from the 15-month data collection and the resultant model viewed from the axial (left) and equatorial (right) positions. 469

Figure 90: The tetrameric structure resulting from the chandelier core refinement of ZAA25 from the 15-month data collection. 471

Figure 91: Observed and Calculated PDF from the chandelier core refinement of ZAA1A from the 18-month data collection and the resultant model viewed from the axial (left) and equatorial (right) positions. 473

Figure 92: Observed and Calculated PDF from the fixed core refinement of ZAA1A from the 18-month data collection and the resultant model viewed from the axial (left) and equatorial (right) positions. 475

Figure 93: Observed and Calculated PDF from the chandelier core refinement of ZAA1I from the 18-month data collection and the resultant model viewed from the axial (left) and equatorial (right) positions. 477

Figure 94: Observed and Calculated PDF from the fixed core refinement of ZAA1I from the 18-month data collection and the resultant model viewed from the axial (left) and equatorial (right) positions. 479

Figure 95: Observed and Calculated PDF from the chandelier core refinement of ZAA4A from the 18-month data collection and the resultant model viewed from the axial (left) and equatorial (right) positions. 481

Figure 96: Observed and Calculated PDF from the fixed core refinement of ZAA4A from the 18-month data collection and the resultant model viewed from the axial (left) and equatorial (right) positions. 483

Figure 97: Observed and Calculated PDF from the chandelier core refinement of ZAA4C from the 18-month data collection and the resultant model viewed from the axial (left) and equatorial (right) positions. 485
Figure 98: Observed and Calculated PDF from the fixed core refinement of ZAA4C from the 18-month data collection and the resultant model. 487
Figure 99: Observed and Calculated PDF from the chandelier core refinement of ZAA4I from the 18-month data collection and the resultant model viewed from the axial (left) and equatorial (right) positions. 489
Figure 100: Observed and Calculated PDF from the fixed core refinement of ZAA4I from the 18-month data collection and the resultant model. 491
Figure 101: Observed and Calculated PDF from the chandelier core refinement of ZAA7A from the 18-month data collection and the resultant model viewed from the axial (left) and equatorial (right) positions. 493
Figure 102: Observed and Calculated PDF from the fixed core refinement of ZAA7A from the 18-month data collection and the resultant model. 495
Figure 103: Observed and Calculated PDF from the chandelier core refinement of ZAA7C from the 18-month data collection and the resultant model viewed from the axial (left) and equatorial (right) positions. 497
Figure 104: Observed and Calculated PDF from the fixed core refinement of ZAA7C from the 18-month data collection and the resultant model. 499
Figure 105: Observed and Calculated PDF from the chandelier core refinement of ZAA7I from the 18-month data collection and the resultant model viewed from the axial (left) and equatorial (right) positions. 501

Figure 106: Observed and Calculated PDF from the fixed core refinement of ZAA7I from the 18-month data collection and the resultant model. 503
Figure 107: Observed and Calculated PDF from the chandelier core refinement of ZAA10A from the 18-month data collection and the resultant model viewed from the axial (left) and equatorial (right) positions. 505
Figure 108: Observed and Calculated PDF from the fixed core refinement of ZAA10A from the 18-month data collection and the resultant model. 507
Figure 109: Observed and Calculated PDF from the chandelier core refinement of ZAA10C from the 18-month data collection and the resultant model viewed from the axial (left) and equatorial (right) positions. 509
Figure 110: Observed and Calculated PDF from the fixed core refinement of ZAA10C from the 18-month data collection and the resultant model. 511
Figure 111: Observed and Calculated PDF from the chandelier core refinement of ZAA10I from the 18-month data collection and the resultant model viewed from the axial (left) and equatorial (right) positions. 513
Figure 112: Observed and Calculated PDF from the fixed core refinement of ZAA10I from the 18-month data collection and the resultant model. 515
Figure 113: Observed and Calculated PDF from the chandelier core refinement of ZAA13A from the 18-month data collection and the resultant model viewed from the axial (left) and equatorial (right) positions. 517
Figure 114: Observed and Calculated PDF from the fixed core refinement of ZAA13A from the 18-month data collection and the resultant model. 519

Figure 115: Observed and Calculated PDF from the chandelier core refinement of ZAA13C from the 18-month data collection and the resultant model viewed from the axial (left) and equatorial (right) positions. 521

Figure 116: Observed and Calculated PDF from the fixed core refinement of ZAA13C from the 18-month data collection and the resultant model. 523

Figure 117: Observed and Calculated PDF from the chandelier core refinement of ZAA13I from the 18-month data collection and the resultant model viewed from the axial (left) and equatorial (right) positions. 525

Figure 118: Observed and Calculated PDF from the fixed core refinement of ZAA13I from the 18-month data collection and the resultant model. 527

Figure 119: Observed and Calculated PDF from the chandelier core refinement of ZAA16A from the 18-month data collection and the resultant model viewed from the axial (left) and equatorial (right) positions. 529

Figure 120: Observed and Calculated PDF from the fixed core refinement of ZAA16A from the 18-month data collection and the resultant model. 531

Figure 121: Observed and Calculated PDF from the chandelier core refinement of ZAA16C from the 18-month data collection and the resultant model viewed from the axial (left) and equatorial (right) positions. 533

Figure 122: Observed and Calculated PDF from the fixed core refinement of ZAA16C from the 18-month data collection and the resultant model. 535

Figure 123: Observed and Calculated PDF from the chandelier core refinement of ZAA16I from the 18-month data collection and the resultant model viewed from the axial (left) and equatorial (right) positions. 537

Figure 124: Observed and Calculated PDF from the fixed core refinement of ZAA16I from the 18-month data collection and the resultant model. 539
Figure 125: Observed and Calculated PDF from the chandelier core refinement of ZAA20A from the 18-month data collection and the resultant model viewed from the axial (left) and equatorial (right) positions. 541
Figure 126: Observed and Calculated PDF from the fixed core refinement of ZAA20A from the 18-month data collection and the resultant model. 543
Figure 127: Observed and Calculated PDF from the chandelier core refinement of ZAA20C from the 18-month data collection and the resultant model viewed from the axial (left) and equatorial (right) positions. 545
Figure 128: Observed and Calculated PDF from the fixed core refinement of ZAA20C from the 18-month data collection and the resultant model. 547
Figure 129: Observed and Calculated PDF from the chandelier core refinement of ZAA20I from the 18-month data collection and the resultant model viewed from the axial (left) and equatorial (right) positions. 549
Figure 130: Observed and Calculated PDF from the fixed core refinement of ZAA20I from the 18-month data collection and the resultant model. 551
Figure 131: Observed and Calculated PDF from the chandelier core refinement of ZAA24A from the 18-month data collection and the resultant model viewed from the axial (left) and equatorial (right) positions. 553
Figure 132: Observed and Calculated PDF from the fixed core refinement of ZAA24A from the 18-month data collection and the resultant model. 555

Figure 133: Observed and Calculated PDF from the chandelier core refinement of ZAA24C from the 18-month data collection and the resultant model viewed from the axial (left) and equatorial (right) positions. 557

Figure 134: Observed and Calculated PDF from the fixed core refinement of ZAA24C from the 18-month data collection and the resultant model. 559

Figure 135: Observed and Calculated PDF from the chandelier core refinement of ZAA24I from the 18-month data collection and the resultant model viewed from the axial (left) and equatorial (right) positions. 561

Figure 136: Observed and Calculated PDF from the fixed core refinement of ZAA24I from the 18-month data collection and the resultant model. 563

Figure 137: Observed and Calculated PDF from the chandelier core refinement of ZAA25A from the 18-month data collection and the resultant model viewed from the axial (left) and equatorial (right) positions. 565

Figure 138: Observed and Calculated PDF from the fixed core refinement of ZAA25A from the 18-month data collection and the resultant model. 567

Figure 139: Observed and Calculated PDF from the chandelier core refinement of ZAA25C from the 18-month data collection and the resultant model viewed from the axial (left) and equatorial (right) positions. 569

Figure 140: Observed and Calculated PDF from the fixed core refinement of ZAA25C from the 18-month data collection and the resultant model. 571

Figure 141: Observed and Calculated PDF from the chandelier core refinement of ZAA25I from the 18-month data collection and the resultant model viewed from the axial (left) and equatorial (right) positions. 573

Figure 142: Observed and Calculated PDF from the fixed core refinement of ZAA25I from the 18-month data collection and the resultant model. 575
Figure 143: Observed and Calculated PDF from the chandelier core refinement of ZAA27A from the 18-month data collection and the resultant model viewed from the axial (left) and equatorial (right) positions. 577
Figure 144: Observed and Calculated PDF from the fixed core refinement of ZAA27A from the 18-month data collection and the resultant model. 579
Figure 145: Observed and Calculated PDF from the chandelier core refinement of ZAA27C from the 18-month data collection and the resultant model viewed from the axial (left) and equatorial (right) positions. 581
Figure 146: Observed and Calculated PDF from the fixed core refinement of ZAA27C from the 18-month data collection and the resultant model. 583
Figure 147: Observed and Calculated PDF from the chandelier core refinement of ZAA27I from the 18-month data collection and the resultant model viewed from the axial (left) and equatorial (right) positions. 585
Figure 148: Observed and Calculated PDF from the fixed core refinement of ZAA27I from the 18-month data collection and the resultant model. 587
Figure 149: Observed and Calculated PDF from the chandelier core refinement of ZAA28A from the 18-month data collection and the resultant model viewed from the axial (left) and equatorial (right) positions. 589
Figure 150: Observed and Calculated PDF from the fixed core refinement of ZAA28A from the 18-month data collection and the resultant model. 591

Figure 151: Observed and Calculated PDF from the chandelier core refinement of ZAA28C from the 18-month data collection and the resultant model viewed from the axial (left) and equatorial (right) positions. 593
Figure 152: Observed and Calculated PDF from the fixed core refinement of ZAA28C from the 18-month data collection and the resultant model. 595
Figure 153: Observed and Calculated PDF from the chandelier core refinement of ZAA28I from the 18-month data collection and the resultant model viewed from the axial (left) and equatorial (right) positions. 597
Figure 154: Observed and Calculated PDF from the fixed core refinement of ZAA28I from the 18-month data collection and the resultant model. 599
Figure 155: Observed and Calculated PDF from the fixed core refinement of ZAA1A from the 18-month data collection and the resultant model. 601
Figure 156: The tetrameric structure resulting from the fixed core refinement of ZAA1A from the 18-month data collection. 603
Figure 157: Observed and Calculated PDF from the fixed core refinement of ZAA1I from the 18-month data collection and the resultant model. 604
Figure 158: The tetrameric structure resulting from the fixed core refinement of ZAA1I from the 18-month data collection. 606
Figure 159: Observed and Calculated PDF from the fixed core refinement of ZAA4A from the 18-month data collection and the resultant model. 607
Figure 160: The tetrameric structure resulting from the fixed core refinement of ZAA4A from the 18-month data collection. 609
Figure 161: Observed and Calculated PDF from the fixed core refinement of ZAA4C from the 18-month data collection and the resultant model. 610

Figure 162: The tetrameric structure resulting from the fixed core refinement of ZAA4C from the 18-month data collection. 612

Figure 163: Observed and Calculated PDF from the fixed core refinement of ZAA4I from the 18-month data collection and the resultant model. 613

Figure 164: The tetrameric structure resulting from the fixed core refinement of ZAA4I from the 18-month data collection. 615

Figure 165: Observed and Calculated PDF from the fixed core refinement of ZAA7A from the 18-month data collection and the resultant model. 616

Figure 166: The tetrameric structure resulting from the fixed core refinement of ZAA7A from the 18-month data collection. 618

Figure 167: Observed and Calculated PDF from the fixed core refinement of ZAA7C from the 18-month data collection and the resultant model. 619

Figure 168: The tetrameric structure resulting from the fixed core refinement of ZAA7C from the 18-month data collection. 621

Figure 169: Observed and Calculated PDF from the fixed core refinement of ZAA7I from the 18-month data collection and the resultant model. 622

Figure 170: The tetrameric structure resulting from the fixed core refinement of ZAA7I from the 18-month data collection. 624

Figure 171: Observed and Calculated PDF from the fixed core refinement of ZAA10A from the 18-month data collection and the resultant model. 625

Figure 172: The tetrameric structure resulting from the fixed core refinement of ZAA10A from the 18-month data collection. 627

Figure 173: Observed and Calculated PDF from the fixed core refinement of ZAA10C from the 18-month data collection and the resultant model. 628

Figure 174: The tetrameric structure resulting from the fixed core refinement of ZAA10C from the 18-month data collection. 630

Figure 175: Observed and Calculated PDF from the fixed core refinement of ZAA10I from the 18-month data collection and the resultant model. 631

Figure 176: The tetrameric structure resulting from the fixed core refinement of ZAA10I from the 18-month data collection. 633

Figure 177: Observed and Calculated PDF from the fixed core refinement of ZAA13A from the 18-month data collection and the resultant model. 634

Figure 178: The tetrameric structure resulting from the fixed core refinement of ZAA13A from the 18-month data collection. 636

Figure 179: Observed and Calculated PDF from the fixed core refinement of ZAA13C from the 18-month data collection and the resultant model. 637

Figure 180: The tetrameric structure resulting from the fixed core refinement of ZAA13C from the 18-month data collection. 639

Figure 181: Observed and Calculated PDF from the fixed core refinement of ZAA13I from the 18-month data collection and the resultant model. 640

Figure 182: The tetrameric structure resulting from the fixed core refinement of ZAA13I from the 18-month data collection. 642

Figure 183: Observed and Calculated PDF from the fixed core refinement of ZAA16A from the 18-month data collection and the resultant model. 643

Figure 184: The tetrameric structure resulting from the fixed core refinement of ZAA16A from the 18-month data collection. 645

Figure 185: Observed and Calculated PDF from the fixed core refinement of ZAA16C from the 18-month data collection and the resultant model. 646

Figure 186: The tetrameric structure resulting from the fixed core refinement of ZAA16C from the 18-month data collection. 648

Figure 187: Observed and Calculated PDF from the fixed core refinement of ZAA16I from the 18-month data collection and the resultant model. 649

Figure 188: The tetrameric structure resulting from the fixed core refinement of ZAA16I from the 18-month data collection. 651

Figure 189: Observed and Calculated PDF from the fixed core refinement of ZAA20A from the 18-month data collection and the resultant model. 652

Figure 190: The tetrameric structure resulting from the fixed core refinement of ZAA20A from the 18-month data collection. 654

Figure 191: Observed and Calculated PDF from the fixed core refinement of ZAA20C from the 18-month data collection and the resultant model. 655

Figure 192: The tetrameric structure resulting from the fixed core refinement of ZAA20C from the 18-month data collection. 657

Figure 193: Observed and Calculated PDF from the fixed core refinement of ZAA20I from the 18-month data collection and the resultant model. 658

Figure 194: The tetrameric structure resulting from the fixed core refinement of ZAA20I from the 18-month data collection. 660

Figure 195: Observed and Calculated PDF from the fixed core refinement of ZAA24A from the 18-month data collection and the resultant model. 661

Figure 196: The tetrameric structure resulting from the fixed core refinement of ZAA24A from the 18-month data collection. 663

Figure 197: Observed and Calculated PDF from the fixed core refinement of ZAA24C from the 18-month data collection and the resultant model. 664

Figure 198: The tetrameric structure resulting from the fixed core refinement of ZAA24C from the 18-month data collection. 666

Figure 199: Observed and Calculated PDF from the fixed core refinement of ZAA24I from the 18-month data collection and the resultant model. 667

Figure 200: The tetrameric structure resulting from the fixed core refinement of ZAA24I from the 18-month data collection. 669

Figure 201: Observed and Calculated PDF from the fixed core refinement of ZAA25A from the 18-month data collection and the resultant model. 670

Figure 202: The tetrameric structure resulting from the fixed core refinement of ZAA25A from the 18-month data collection. 672

Figure 203: Observed and Calculated PDF from the fixed core refinement of ZAA25C from the 18-month data collection and the resultant model. 673

Figure 204: The tetrameric structure resulting from the fixed core refinement of ZAA25C from the 18-month data collection. 675

Figure 205: Observed and Calculated PDF from the fixed core refinement of ZAA25I from the 18-month data collection and the resultant model. 676

Figure 206: The tetrameric structure resulting from the fixed core refinement of ZAA25I from the 18-month data collection. 678

Figure 207: Observed and Calculated PDF from the fixed core refinement of ZAA27A from the 18-month data collection and the resultant model. 679

Figure 208: The tetrameric structure resulting from the fixed core refinement of ZAA27A from the 18-month data collection. 681

Figure 209: Observed and Calculated PDF from the fixed core refinement of ZAA27C from the 18-month data collection and the resultant model. 682

Figure 210: The tetrameric structure resulting from the fixed core refinement of ZAA27C from the 18-month data collection. 684

Figure 211: Observed and Calculated PDF from the fixed core refinement of ZAA27I from the 18-month data collection and the resultant model. 685

Figure 212: The tetrameric structure resulting from the fixed core refinement of ZAA27I from the 18-month data collection. 687

Figure 213: Observed and Calculated PDF from the fixed core refinement of ZAA28A from the 18-month data collection and the resultant model. 688

Figure 214: The tetrameric structure resulting from the fixed core refinement of ZAA28A from the 18-month data collection. 690

Figure 215: Observed and Calculated PDF from the fixed core refinement of ZAA28C from the 18-month data collection and the resultant model. 691

Figure 216: The tetrameric structure resulting from the fixed core refinement of ZAA28C from the 18-month data collection. 693

Figure 217: Observed and Calculated PDF from the fixed core refinement of ZAA28I from the 18-month data collection and the resultant model. 694

Figure 218: The tetrameric structure resulting from the fixed core refinement of ZAA28I from the 18-month data collection. 696

Figure 219: Observed and Calculated PDF from the chandelier core refinement of ZAA1A from the 18-month data collection and the resultant model viewed from the axial (left) and equatorial (right) positions. 697

Figure 220: The tetrameric structure resulting from the chandelier core refinement of ZAA1A from the 18-month data collection. 699

Figure 221: Observed and Calculated PDF from the chandelier core refinement of ZAA1I from the 18-month data collection and the resultant model viewed from the axial (left) and equatorial (right) positions. 701

Figure 222: The tetrameric structure resulting from the chandelier core refinement of ZAA1I from the 18-month data collection. 703

Figure 223: Observed and Calculated PDF from the chandelier core refinement of ZAA4A from the 18-month data collection and the resultant model viewed from the axial (left) and equatorial (right) positions. 705

Figure 224: The tetrameric structure resulting from the chandelier core refinement of ZAA4A from the 18-month data collection. 707

Figure 225: Observed and Calculated PDF from the chandelier core refinement of ZAA4C from the 18-month data collection and the resultant model viewed from the axial (left) and equatorial (right) positions. 709

Figure 226: The tetrameric structure resulting from the chandelier core refinement of ZAA4C from the 18-month data collection. 711

Figure 227: Observed and Calculated PDF from the chandelier core refinement of ZAA4I from the 18-month data collection and the resultant model viewed from the axial (left) and equatorial (right) positions. 713

Figure 228: The tetrameric structure resulting from the chandelier core refinement of ZAA4I from the 18-month data collection. 715

Figure 229: Observed and Calculated PDF from the chandelier core refinement of ZAA7A from the 18-month data collection and the resultant model viewed from the axial (left) and equatorial (right) positions. 717

Figure 230: The tetrameric structure resulting from the chandelier core refinement of ZAA7A from the 18-month data collection. 719

Figure 231: Observed and Calculated PDF from the chandelier core refinement of ZAA7C from the 18-month data collection and the resultant model viewed from the axial (left) and equatorial (right) positions. 721

Figure 232: The tetrameric structure resulting from the chandelier core refinement of ZAA7C from the 18-month data collection. 723

Figure 233: Observed and Calculated PDF from the chandelier core refinement of ZAA7I from the 18-month data collection and the resultant model viewed from the axial (left) and equatorial (right) positions. 725

Figure 234: The tetrameric structure resulting from the chandelier core refinement of ZAA7I from the 18-month data collection. 727

Figure 235: Observed and Calculated PDF from the chandelier core refinement of ZAA10A from the 18-month data collection and the resultant model viewed from the axial (left) and equatorial (right) positions. 729

Figure 236: The tetrameric structure resulting from the chandelier core refinement of ZAA10A from the 18-month data collection. 731

Figure 237: Observed and Calculated PDF from the chandelier core refinement of ZAA10C from the 18-month data collection and the resultant model viewed from the axial (left) and equatorial (right) positions. 733

Figure 238: The tetrameric structure resulting from the chandelier core refinement of ZAA10C from the 18-month data collection. 735

Figure 239: Observed and Calculated PDF from the chandelier core refinement of ZAA10I from the 18-month data collection and the resultant model viewed from the axial (left) and equatorial (right) positions. 737

Figure 240: The tetrameric structure resulting from the chandelier core refinement of ZAA10I from the 18-month data collection. 739

Figure 241: Observed and Calculated PDF from the chandelier core refinement of ZAA13A from the 18-month data collection and the resultant model viewed from the axial (left) and equatorial (right) positions. 741

Figure 242: The tetrameric structure resulting from the chandelier core refinement of ZAA13A from the 18-month data collection. 743

Figure 243: Observed and Calculated PDF from the chandelier core refinement of ZAA13C from the 18-month data collection and the resultant model viewed from the axial (left) and equatorial (right) positions. 745

Figure 244: The tetrameric structure resulting from the chandelier core refinement of ZAA13C from the 18-month data collection. 747

Figure 245: Observed and Calculated PDF from the chandelier core refinement of ZAA13I from the 18-month data collection and the resultant model viewed from the axial (left) and equatorial (right) positions. 749

Figure 246: The tetrameric structure resulting from the chandelier core refinement of ZAA13I from the 18-month data collection. 751

Figure 247: Observed and Calculated PDF from the chandelier core refinement of ZAA16A from the 18-month data collection and the resultant model viewed from the axial (left) and equatorial (right) positions. 753

Figure 248: The tetrameric structure resulting from the chandelier core refinement of ZAA16A from the 18-month data collection. 755

Figure 249: Observed and Calculated PDF from the chandelier core refinement of ZAA16C from the 18-month data collection and the resultant model viewed from the axial (left) and equatorial (right) positions. 757

Figure 250: The tetrameric structure resulting from the chandelier core refinement of ZAA16C from the 18-month data collection. 759

Figure 251: Observed and Calculated PDF from the chandelier core refinement of ZAA16I from the 18-month data collection and the resultant model viewed from the axial (left) and equatorial (right) positions. 761

Figure 252: The tetrameric structure resulting from the chandelier core refinement of ZAA16I from the 18-month data collection. 763

Figure 253: Observed and Calculated PDF from the chandelier core refinement of ZAA20A from the 18-month data collection and the resultant model viewed from the axial (left) and equatorial (right) positions. 765

Figure 254: The tetrameric structure resulting from the chandelier core refinement of ZAA20A from the 18-month data collection. 767

Figure 255: Observed and Calculated PDF from the chandelier core refinement of ZAA20C from the 18-month data collection and the resultant model viewed from the axial (left) and equatorial (right) positions. 769

Figure 256: The tetrameric structure resulting from the chandelier core refinement of ZAA20C from the 18-month data collection. 771

Figure 257: Observed and Calculated PDF from the chandelier core refinement of ZAA20I from the 18-month data collection and the resultant model viewed from the axial (left) and equatorial (right) positions. 773

Figure 258: The tetrameric structure resulting from the chandelier core refinement of ZAA20I from the 18-month data collection. 775

Figure 259: Observed and Calculated PDF from the chandelier core refinement of ZAA24A from the 18-month data collection and the resultant model viewed from the axial (left) and equatorial (right) positions. 777

Figure 260: The tetrameric structure resulting from the chandelier core refinement of ZAA24A from the 18-month data collection. 779

Figure 261: Observed and Calculated PDF from the chandelier core refinement of ZAA24C from the 18-month data collection and the resultant model viewed from the axial (left) and equatorial (right) positions. 781

Figure 262: The tetrameric structure resulting from the chandelier core refinement of ZAA24C from the 18-month data collection. 783

Figure 263: Observed and Calculated PDF from the chandelier core refinement of ZAA24I from the 18-month data collection and the resultant model viewed from the axial (left) and equatorial (right) positions. 785

Figure 264: The tetrameric structure resulting from the chandelier core refinement of ZAA24I from the 18-month data collection. 787

Figure 265: Observed and Calculated PDF from the chandelier core refinement of ZAA25A from the 18-month data collection and the resultant model viewed from the axial (left) and equatorial (right) positions. 789

Figure 266: The tetrameric structure resulting from the chandelier core refinement of ZAA25A from the 18-month data collection. 791

Figure 267: Observed and Calculated PDF from the chandelier core refinement of ZAA25C from the 18-month data collection and the resultant model viewed from the axial (left) and equatorial (right) positions. 793

Figure 268: The tetrameric structure resulting from the chandelier core refinement of ZAA25C from the 18-month data collection. 795

Figure 269: Observed and Calculated PDF from the chandelier core refinement of ZAA25I from the 18-month data collection and the resultant model viewed from the axial (left) and equatorial (right) positions. 797

Figure 270: The tetrameric structure resulting from the chandelier core refinement of ZAA25I from the 18-month data collection. 799

Figure 271: Observed and Calculated PDF from the chandelier core refinement of ZAA27A from the 18-month data collection and the resultant model viewed from the axial (left) and equatorial (right) positions. 801

Figure 272: The tetrameric structure resulting from the chandelier core refinement of ZAA27A from the 18-month data collection. 803

Figure 273: Observed and Calculated PDF from the chandelier core refinement of ZAA27C from the 18-month data collection and the resultant model viewed from the axial (left) and equatorial (right) positions. 805

Figure 274: The tetrameric structure resulting from the chandelier core refinement of ZAA27C from the 18-month data collection. 807

Figure 275: Observed and Calculated PDF from the chandelier core refinement of ZAA27I from the 18-month data collection and the resultant model viewed from the axial (left) and equatorial (right) positions. 809
Figure 276: The tetrameric structure resulting from the chandelier core refinement of ZAA27I from the 18-month data collection. 811
Figure 277: Observed and Calculated PDF from the chandelier core refinement of ZAA28A from the 18-month data collection and the resultant model viewed from the axial (left) and equatorial (right) positions. 813
Figure 278: The tetrameric structure resulting from the chandelier core refinement of ZAA28A from the 18-month data collection. 815
Figure 279: Observed and Calculated PDF from the chandelier core refinement of ZAA28C from the 18-month data collection and the resultant model viewed from the axial (left) and equatorial (right) positions. 817
Figure 280: The tetrameric structure resulting from the chandelier core refinement of ZAA28C from the 18-month data collection. 819
Figure 281: Observed and Calculated PDF from the chandelier core refinement of ZAA28I from the 18-month data collection and the resultant model viewed from the axial (left) and equatorial (right) positions. 821
Figure 282: The tetrameric structure resulting from the chandelier core refinement of ZAA28I from the 18-month data collection. 823
Figure 283: Distribution of lattice parameter a resulting from the rietveld refinement of umbite samples synthesised with the zirconium acetate precursor as a function of the feedstock of the zirconium acetate solution 831

Figure 284: Distribution of lattice parameter a resulting from the rietveld refinement of umbite samples synthesised with the zirconium acetate precursor as a function of a) the acetic acid : zirconium ratio and b) the zirconium concentration of the zirconium acetate solution 831
Figure 285: Distribution of lattice parameter a resulting from the rietveld refinement of umbite samples synthesised with the zirconium acetate precursor as a function of a) storage temperature and b) the age of the zirconium acetate solution 832
Figure 286: Distribution of lattice parameter b resulting from the rietveld refinement of umbite samples synthesised with the zirconium acetate precursor as a function of the feedstock of the zirconium acetate solution 832
Figure 287: Distribution of lattice parameter b resulting from the rietveld refinement of umbite samples synthesised with the zirconium acetate precursor as a function of a) the acetic acid : zirconium ratio and b) the zirconium concentration of the zirconium acetate solution 833
Figure 288: Distribution of lattice parameter b resulting from the rietveld refinement of umbite samples synthesised with the zirconium acetate precursor as a function of a) storage temperature and b) the age of the zirconium acetate solution 833
Figure 289: Distribution of lattice parameter c resulting from the rietveld refinement of umbite samples synthesised with the zirconium acetate precursor as a function of the feedstock of the zirconium acetate solution 834
Figure 290: Distribution of lattice parameter c resulting from the rietveld refinement of umbite samples synthesised with the zirconium acetate precursor as a function of a) the acetic acid : zirconium ratio and b) the zirconium concentration of the zirconium acetate solution 834

Figure 291: Distribution of lattice parameter c resulting from the rietveld refinement of umbite samples synthesised with the zirconium acetate precursor as a function of a) storage temperature and b) the age of the zirconium acetate solution 835

Table of Tables

Table 1: Atomic coordinates of the tetrameric model obtained from the first iteration refinement of zirconyl chloride. 310

Table 2: Atomic coordinates of the tetrameric model obtained from the second iteration refinement of zirconyl chloride. 311

Table 3: Atomic coordinates of the tetrameric model obtained from the third iteration refinement of zirconyl chloride. 312

Table 4: All samples studied in the ageing study and the quantity of reagents required for their synthesis. 313

Table 5: The atomic coordinates of the model resulting from the fixed core refinement of ZAA1 from the 9-month data collection. 314

Table 6: The atomic coordinates of the model resulting from the fixed core refinement of ZAA4 from the 9-month data collection. 316

Table 7: The atomic coordinates of the model resulting from the fixed core refinement of ZAA7 from the 9-month data collection. 318

Table 8: The atomic coordinates of the model resulting from the fixed core refinement of ZAA10 from 9-month data collection. 320

Table 9: The atomic coordinates of the model resulting from the fixed core refinement of ZAA13 from the 9-month data collection. 322

Table 10: The atomic coordinates of the model resulting from the fixed core refinement of ZAA16 from the 9-month data collection. 324

Table 11: The atomic coordinates of the model resulting from the chandelier core refinement of ZAA1 from the 9-month data collection. 326

Table 12: The atomic coordinates of the model resulting from the chandelier core refinement of ZAA4 from the 9-month data collection. 328

Table 13: The atomic coordinates of the model resulting from the chandelier core refinement of ZAA7 from the 9-month data collection. 330

Table 14: The atomic coordinates of the model resulting from the chandelier core refinement of ZAA10 from the 9-month data collection. 332

Table 15: The atomic coordinates of the model resulting from the chandelier core refinement of ZAA13 from the 9-month data collection. 334

Table 16: The atomic coordinates of the model resulting from the chandelier core refinement of ZAA16 from the 9-month data collection. 336

Table 17: The atomic coordinates of the model resulting from the fixed core refinement of ZAA1 from the 9-month data collection. 338

Table 18: The atomic coordinates of the tetrameric phase of the fixed core refinement of ZAA1 from the 9-month data collection. 340

Table 19: The atomic coordinates of the model resulting from the fixed core refinement of ZAA4 from the 9-month data collection. 341

Table 20: The atomic coordinates of the tetrameric phase of the fixed core refinement of ZAA4 from the 9-month data collection. 343

Table 21: The atomic coordinates of the model resulting from the fixed core refinement of ZAA7 from the 9-month data collection. 344

Table 22: The atomic coordinates of the tetrameric phase of the fixed core refinement of ZAA7 from the 9-month data collection. 346

Table 23: The atomic coordinates of the model resulting from the fixed core refinement of ZAA10 from the 9-month data collection. 347

Table 24: The atomic coordinates of the tetrameric phase of the fixed core refinement of ZAA10 from the 9-month data collection. 349

Table 25: The atomic coordinates of the model resulting from the fixed core refinement of ZAA13 from the 9-month data collection. 350

Table 26: The atomic coordinates of the tetrameric phase of the fixed core refinement of ZAA13 from the 9-month data collection. 352

Table 27: The atomic coordinates of the model resulting from the fixed core refinement of ZAA16 from the 9-month data collection. 353

Table 28: The atomic coordinates of the tetrameric phase of the fixed core refinement of ZAA16 from the 9-month data collection. 355

Table 29: The atomic coordinates of the model resulting from the chandelier core refinement of ZAA1 from the 9-month data collection. 356

Table 30: The atomic coordinates of the tetrameric phase of the chandelier core refinement of ZAA1 from the 9-month data collection. 358

Table 31: The atomic coordinates of the model resulting from the chandelier core refinement of ZAA4 from the 9-month data collection. 359

Table 32: The atomic coordinates of the tetrameric phase of the chandelier core refinement of ZAA4 from the 9-month data collection. 361

Table 33: The atomic coordinates of the model resulting from the chandelier core refinement of ZAA7 from the 9-month data collection. 362

Table 34: The atomic coordinates of the tetrameric phase of the chandelier core refinement of ZAA7 from the 9-month data collection. 364

Table 35: The atomic coordinates of the model resulting from the chandelier core refinement of ZAA10 from the 9-month data collection. 365

Table 36: The atomic coordinates of the tetrameric phase of the chandelier core refinement of ZAA10 from the 9-month data collection. 367

Table 37: The atomic coordinates of the model resulting from the chandelier core refinement of ZAA13 from the 9-month data collection. 368

Table 38: The atomic coordinates of the tetrameric phase of the chandelier core refinement of ZAA13 from the 9-month data collection. 370

Table 39: The atomic coordinates of the model resulting from the chandelier core refinement of ZAA16 from the 9-month data collection. 371

Table 40: The atomic coordinates of the tetrameric phase of the chandelier core refinement of ZAA16 from the 9-month data collection. 373

Table 41: The atomic coordinates of the model resulting from the chandelier core refinement of ZAA1` from the 15-month data collection. 374

Table 42: The atomic coordinates of the model resulting from the fixed core refinement of ZAA1 from the 15-month data collection. 376

Table 43: The atomic coordinates of the model resulting from the chandelier core refinement of ZAA4 from the 15-month data collection. 378

Table 44: The atomic coordinates of the model resulting from the fixed core refinement of ZAA4 from the 15-month data collection. 380

Table 45: The atomic coordinates of the model resulting from the chandelier core refinement of ZAA7 from the 15-month data collection. 382

Table 46: The atomic coordinates of the model resulting from the fixed core refinement of ZAA7 from the 15-month data collection. 384

Table 47: The atomic coordinates of the model resulting from the chandelier core refinement of ZAA10 from the 15-month data collection. 386

Table 48: The atomic coordinates of the model resulting from the fixed core refinement of ZAA10 from the 15-month data collection. 388

Table 49: The atomic coordinates of the model resulting from the chandelier core refinement of ZAA13 from the 15-month data collection. 390

Table 50: The atomic coordinates of the model resulting from the fixed core refinement of ZAA13 from the 15-month data collection. 392

Table 51: The atomic coordinates of the model resulting from the chandelier core refinement of ZAA16 from the 15-month data collection. 394

Table 52: The atomic coordinates of the model resulting from the fixed core refinement of ZAA16 from the 15-month data collection. 396

Table 53: The atomic coordinates of the model resulting from the chandelier core refinement of ZAA20 from the 15-month data collection. 398

Table 54: The atomic coordinates of the model resulting from the fixed core refinement of ZAA20 from the 15-month data collection. 400

Table 55: The atomic coordinates of the model resulting from the chandelier core refinement of ZAA24 from the 15-month data collection. 402

Table 56: The atomic coordinates of the model resulting from the fixed core refinement of ZAA24 from the 15-month data collection. 404

Table 57: The atomic coordinates of the model resulting from the chandelier core refinement of ZAA25 from the 15-month data collection. 406

Table 58: The atomic coordinates of the model resulting from the fixed core refinement of ZAA25 from the 15-month data collection. 408

Table 59: The atomic coordinates of the model resulting from the fixed core refinement of ZAA1 from the 15-month data collection. 410

Table 60: The atomic coordinates of the tetrameric phase of the fixed core refinement of ZAA1 from the 15-month data collection. 412

Table 61: The atomic coordinates of the model resulting from the fixed core refinement of ZAA4 from the 15-month data collection. 413

Table 62: The atomic coordinates of the tetrameric phase of the fixed core refinement of ZAA4 from the 15-month data collection. 415

Table 63: The atomic coordinates of the model resulting from the fixed core refinement of ZAA7 from the 15-month data collection. 416

Table 64: The atomic coordinates of the tetrameric phase of the fixed core refinement of ZAA7 from the 15-month data collection. 418

Table 65: The atomic coordinates of the model resulting from the fixed core refinement of ZAA10 from the 15-month data collection. 419

Table 66: The atomic coordinates of the tetrameric phase of the fixed core refinement of ZAA10 from the 15-month data collection. 421

Table 67: The atomic coordinates of the model resulting from the fixed core refinement of ZAA13 from the 15-month data collection. 422

Table 68: The atomic coordinates of the tetrameric phase of the fixed core refinement of ZAA13 from the 15-month data collection. 424

Table 69: The atomic coordinates of the model resulting from the fixed core refinement of ZAA16 from the 15-month data collection. 425

Table 70: The atomic coordinates of the tetrameric phase of the fixed core refinement of ZAA16 from the 15-month data collection. 427

Table 71: The atomic coordinates of the model resulting from the fixed core refinement of ZAA20 from the 15-month data collection. 428

Table 72: The atomic coordinates of the tetrameric phase of the fixed core refinement of ZAA20 from the 15-month data collection. 430

Table 73: The atomic coordinates of the model resulting from the fixed core refinement of ZAA24 from the 15-month data collection. 431

Table 74: The atomic coordinates of the tetrameric phase of the fixed core refinement of ZAA24 from the 15-month data collection. 433

Table 75: The atomic coordinates of the model resulting from the fixed core refinement of ZAA25 from the 15-month data collection. 434

Table 76: The atomic coordinates of the tetrameric phase of the fixed core refinement of ZAA25 from the 15-month data collection. 436

Table 77: The atomic coordinates of the model resulting from the chandelier core refinement of ZAA1 from the 15-month data collection. 437

Table 78: The atomic coordinates of the tetrameric phase of the chandelier core refinement of ZAA1 from the15-month data collection. 439

Table 79: The atomic coordinates of the model resulting from the chandelier core refinement of ZAA4 from the 15-month data collection. 441

Table 80: The atomic coordinates of the tetrameric phase of the chandelier core refinement of ZAA4 from 15-month data collection. 443

Table 81: The atomic coordinates of the model resulting from the chandelier core refinement of ZAA7 from the 15-month data collection. 445

Table 82: The atomic coordinates of the tetrameric phase of the chandelier core refinement of ZAA7 from the 15-month data collection. 447

Table 83: The atomic coordinates of the model resulting from the chandelier core refinement of ZAA10 from the 15-month data collection. 449

Table 84: The atomic coordinates of the tetrameric phase of the chandelier core refinement of ZAA10 from the 15-month data collection. 451

Table 85: The atomic coordinates of the model resulting from the chandelier core refinement of ZAA13 from the 15-month data collection. 453

Table 86: The atomic coordinates of the tetrameric phase of the chandelier core refinement of ZAA13 from the 15-month data collection. 455

Table 87: The atomic coordinates of the model resulting from the chandelier core refinement of ZAA16 from the 15-month data collection. 457

Table 88: The atomic coordinates of the tetrameric phase of the chandelier core refinement of ZAA16 from the 15-month data collection. 459

Table 89: The atomic coordinates of the model resulting from the chandelier core refinement of ZAA20 from the 15-month data collection. 461

Table 90: The atomic coordinates of the tetrameric phase of the chandelier core refinement of ZAA20 from the 15-month data collection. 463

Table 91: The atomic coordinates of the model resulting from the chandelier core refinement of ZAA24 from the 15-month data collection. 465

Table 92: The atomic coordinates of the tetrameric phase of the chandelier core refinement of ZAA24 from the 15-month data collection. 467

Table 93: The atomic coordinates of the model resulting from the chandelier core refinement of ZAA25 from the 15-month data collection. 469

Table 94: The atomic coordinates of the tetrameric phase of the chandelier core refinement of ZAA25 from the 15-month data collection. 471

Table 95: The atomic coordinates of the model resulting from the chandelier core refinement of ZAA1A from the 18-month data collection. 473

Table 96: The atomic coordinates of the model resulting from the fixed core refinement of ZAA1A from the 18-month data collection. 475

Table 97: The atomic coordinates of the model resulting from the chandelier core refinement of ZAA1I from the 18-month data collection. 477

Table 98: The atomic coordinates of the model resulting from the fixed core refinement of ZAA1I from the 18-month data collection. 479

Table 99: The atomic coordinates of the model resulting from the chandelier core refinement of ZAA4A from the 18-month data collection. 481

Table 100: The atomic coordinates of the model resulting from the fixed core refinement of ZAA4A from the 18-month data collection. 483

Table 101: The atomic coordinates of the model resulting from the chandelier core refinement of ZAA4C from the 18-month data collection. 485

Table 102: The atomic coordinates of the model resulting from the fixed core refinement of ZAA4C from the 18-month data collection. 487

Table 103: The atomic coordinates of the model resulting from the chandelier core refinement of ZAA4I from the 18-month data collection. 489

Table 104: The atomic coordinates of the model resulting from the fixed core refinement of ZAA4I from the 18-month data collection. 491

Table 105: The atomic coordinates of the model resulting from the chandelier core refinement of ZAA7A from the 18-month data collection. 493

Table 106: The atomic coordinates of the model resulting from the fixed core refinement of ZAA7A from the 18-month data collection. 495

Table 107: The atomic coordinates of the model resulting from the chandelier core refinement of ZAA7C from the 18-month data collection. 497

Table 108: The atomic coordinates of the model resulting from the fixed core refinement of ZAA7C from the 18-month data collection. 499

Table 109: The atomic coordinates of the model resulting from the chandelier core refinement of ZAA7I from the 18-month data collection. 501

Table 110: The atomic coordinates of the model resulting from the fixed core refinement of ZAA7I from the 18-month data collection. 503

Table 111: The atomic coordinates of the model resulting from the chandelier core refinement of ZAA10A from the 18-month data collection. 505

Table 112: The atomic coordinates of the model resulting from the fixed core refinement of ZAA10A from the 18-month data collection. 507

Table 113: The atomic coordinates of the model resulting from the chandelier core refinement of ZAA10C from the 18-month data collection. 509

Table 114: The atomic coordinates of the model resulting from the fixed core refinement of ZAA10C from the 18-month data collection. 511

Table 115: The atomic coordinates of the model resulting from the chandelier core refinement of ZAA10I from the 18-month data collection. 513

Table 116: The atomic coordinates of the model resulting from the fixed core refinement of ZAA10I from the 18-month data collection. 515

Table 117: The atomic coordinates of the model resulting from the chandelier core refinement of ZAA13A from the 18-month data collection. 517

Table 118: The atomic coordinates of the model resulting from the fixed core refinement of ZAA13A from the 18-month data collection. 519

Table 119: The atomic coordinates of the model resulting from the chandelier core refinement of ZAA13C from the 18-month data collection. 521

Table 120: The atomic coordinates of the model resulting from the fixed core refinement of ZAA13C from the 18-month data collection. 523

Table 121: The atomic coordinates of the model resulting from the chandelier core refinement of ZAA13I from the 18-month data collection. 525

Table 122: The atomic coordinates of the model resulting from the fixed core refinement of ZAA13I from the 18-month data collection. 527

Table 123: The atomic coordinates of the model resulting from the chandelier core refinement of ZAA16A from the 18-month data collection. 529

Table 124: The atomic coordinates of the model resulting from the fixed core refinement of ZAA16A from the 18-month data collection. 531

Table 125: The atomic coordinates of the model resulting from the chandelier core refinement of ZAA16C from the 18-month data collection. 533

Table 126: The atomic coordinates of the model resulting from the fixed core refinement of ZAA16C from the 18-month data collection. 535

Table 127: The atomic coordinates of the model resulting from the chandelier core refinement of ZAA16I from the 18-month data collection. 537

Table 128: The atomic coordinates of the model resulting from the fixed core refinement of ZAA16I from the 18-month data collection. 539

Table 129: The atomic coordinates of the model resulting from the chandelier core refinement of ZAA20A from the 18-month data collection. 541

Table 130: The atomic coordinates of the model resulting from the fixed core refinement of ZAA20A from the 18-month data collection. 543

Table 131: The atomic coordinates of the model resulting from the chandelier core refinement of ZAA20C from the 18-month data collection. 545

Table 132: The atomic coordinates of the model resulting from the fixed core refinement of ZAA20C from the 18-month data collection. 547

Table 133: The atomic coordinates of the model resulting from the chandelier core refinement of ZAA20I from the 18-month data collection. 549

Table 134: The atomic coordinates of the model resulting from the fixed core refinement of ZAA20I from the 18-month data collection. 551

Table 135: The atomic coordinates of the model resulting from the chandelier core refinement of ZAA24A from the 18-month data collection. 553

Table 136: The atomic coordinates of the model resulting from the fixed core refinement of ZAA24A from the 18-month data collection. 555

Table 137: The atomic coordinates of the model resulting from the chandelier core refinement of ZAA24C from the 18-month data collection. 557

Table 138: The atomic coordinates of the model resulting from the fixed core refinement of ZAA24C from the 18-month data collection. 559

Table 139: The atomic coordinates of the model resulting from the chandelier core refinement of ZAA24I from the 18-month data collection. 561

Table 140: The atomic coordinates of the model resulting from the fixed core refinement of ZAA24I from the 18-month data collection. 563

Table 141: The atomic coordinates of the model resulting from the chandelier core refinement of ZAA25A from the 18-month data collection. 565

Table 142: The atomic coordinates of the model resulting from the fixed core refinement of ZAA25A from the 18-month data collection. 567

Table 143: The atomic coordinates of the model resulting from the chandelier core refinement of ZAA25C from the 18-month data collection. 569

Table 144: The atomic coordinates of the model resulting from the fixed core refinement of ZAA25C from the 18-month data collection. 571

Table 145: The atomic coordinates of the model resulting from the chandelier core refinement of ZAA25I from the 18-month data collection. 573

Table 146: The atomic coordinates of the model resulting from the fixed core refinement of ZAA25I from the 18-month data collection. 575

Table 147: The atomic coordinates of the model resulting from the chandelier core refinement of ZAA27A from the 18-month data collection. 577

Table 148: The atomic coordinates of the model resulting from the fixed core refinement of ZAA27A from the 18-month data collection. 579

Table 149: The atomic coordinates of the model resulting from the chandelier core refinement of ZAA27C from the 18-month data collection. 581

Table 150: The atomic coordinates of the model resulting from the fixed core refinement of ZAA27C from the 18-month data collection. 583

Table 151: The atomic coordinates of the model resulting from the chandelier core refinement of ZAA27I from the 18-month data collection. 585

Table 152: The atomic coordinates of the model resulting from the fixed core refinement of ZAA27I from the 18-month data collection. 587

Table 153: The atomic coordinates of the model resulting from the chandelier core refinement of ZAA28A from the 18-month data collection. 589

Table 154: The atomic coordinates of the model resulting from the fixed core refinement of ZAA28A from the 18-month data collection. 591

Table 155: The atomic coordinates of the model resulting from the chandelier core refinement of ZAA28C from the 18-month data collection. 593

Table 156: The atomic coordinates of the model resulting from the fixed core refinement of ZAA28C from the 18-month data collection. 595

Table 157: The atomic coordinates of the model resulting from the chandelier core refinement of ZAA28I from the 18-month data collection. 597

Table 158: The atomic coordinates of the model resulting from the fixed core refinement of ZAA28I from the 18-month data collection. 599

Table 159: The atomic coordinates of the model resulting from the fixed core refinement of ZAA1A from the 18-month data collection. 601

Table 160: The atomic coordinates of the tetrameric phase of the fixed core refinement of ZAA1A from 18-month data collection. 603

Table 161: The atomic coordinates of the model resulting from the fixed core refinement of ZAA1I from the 18-month data collection. 604

Table 162: The atomic coordinates of the tetrameric phase of the fixed core refinement of ZAA1I from the 18-month data collection. 606

Table 163: The atomic coordinates of the model resulting from the fixed core refinement of ZAA4A from the 18-month data collection. 607

Table 164: The atomic coordinates of the tetrameric phase of the fixed core refinement of ZAA4A from the 18-month data collection. 609

Table 165: The atomic coordinates of the model resulting from the fixed core refinement of ZAA4C from the 18-month data collection. 610

Table 166: The atomic coordinates of the tetrameric phase of the fixed core refinement of ZAA4C from the 18-month data collection. 612

Table 167: The atomic coordinates of the model resulting from the fixed core refinement of ZAA4I from the 18-month data collection. 613

Table 168: The atomic coordinates of the tetrameric phase of the fixed core refinement of ZAA4I from the 18-month data collection. 615
Table 169: The atomic coordinates of the model resulting from the fixed core refinement of ZAA7A from the 18-month data collection. 616
Table 170: The atomic coordinates of the tetrameric phase of the fixed core refinement of ZAA7A from the 18-month data collection. 618
Table 171: The atomic coordinates of the model resulting from the fixed core refinement of ZAA7C from the 18-month data collection. 619
Table 172: The atomic coordinates of the tetrameric phase of the fixed core refinement of ZAA7C from the 18-month data collection. 621
Table 173: The atomic coordinates of the model resulting from the fixed core refinement of ZAA7I from the 18-month data collection. 622
Table 174: The atomic coordinates of the tetrameric phase of the fixed core refinement of ZAA7I from the 18-month data collection. 624
Table 175: The atomic coordinates of the model resulting from the fixed core refinement of ZAA10A from the 18-month data collection. 625
Table 176: The atomic coordinates of the tetrameric phase of the fixed core refinement of ZAA10A from the 18-month data collection. 627
Table 177: The atomic coordinates of the model resulting from the fixed core refinement of ZAA10C from the 18-month data collection. 628
Table 178: The atomic coordinates of the tetrameric phase of the fixed core refinement of ZAA10C from the 18-month data collection. 630
Table 179: The atomic coordinates of the model resulting from the fixed core refinement of ZAA10I from the 18-month data collection. 631

Table 180: The atomic coordinates of the tetrameric phase of the fixed core refinement of ZAA10I from the 18-month data collection. 633

Table 181: The atomic coordinates of the model resulting from the fixed core refinement of ZAA13A from the 18-month data collection. 634

Table 182: The atomic coordinates of the tetrameric phase of the fixed core refinement of ZAA13A from the 18-month data collection. 636

Table 183: The atomic coordinates of the model resulting from the fixed core refinement of ZAA13C from the 18-month data collection. 637

Table 184: The atomic coordinates of the tetrameric phase of the fixed core refinement of ZAA13C from the 18-month data collection. 639

Table 185: The atomic coordinates of the model resulting from the fixed core refinement of ZAA13I from the 18-month data collection. 640

Table 186: The atomic coordinates of the tetrameric phase of the fixed core refinement of ZAA13I from the 18-month data collection. 642

Table 187: The atomic coordinates of the model resulting from the fixed core refinement of ZAA16A from the 18-month data collection. 643

Table 188: The atomic coordinates of the tetrameric phase of the fixed core refinement of ZAA16A from the 18-month data collection. 645

Table 189: The atomic coordinates of the model resulting from the fixed core refinement of ZAA16C from the 18-month data collection. 646

Table 190: The atomic coordinates of the tetrameric phase of the fixed core refinement of ZAA16C from the 18-month data collection. 648

Table 191: The atomic coordinates of the model resulting from the fixed core refinement of ZAA16I from the 18-month data collection. 649

Table 192: The atomic coordinates of the tetrameric phase of the fixed core refinement of ZAA16I from the 18-month data collection. 651

Table 193: The atomic coordinates of the model resulting from the fixed core refinement of ZAA20A from the 18-month data collection. 652

Table 194: The atomic coordinates of the tetrameric phase of the fixed core refinement of ZAA20A from the 18-month data collection. 654

Table 195: The atomic coordinates of the model resulting from the fixed core refinement of ZAA20C from the 18-month data collection. 655

Table 196: The atomic coordinates of the tetrameric phase of the fixed core refinement of ZAA20C from the 18-month data collection. 657

Table 197: The atomic coordinates of the model resulting from the fixed core refinement of ZAA20I from the 18-month data collection. 658

Table 198: The atomic coordinates of the tetrameric phase of the fixed core refinement of ZAA20I from the 18-month data collection. 660

Table 199: The atomic coordinates of the model resulting from the fixed core refinement of ZAA24A from the 18-month data collection. 661

Table 200: The atomic coordinates of the tetrameric phase of the fixed core refinement of ZAA24A from the 18-month data collection. 663

Table 201: The atomic coordinates of the model resulting from the fixed core refinement of ZAA24C from the 18-month data collection. 664

Table 202: The atomic coordinates of the tetrameric phase of the fixed core refinement of ZAA24C from the 18-month data collection. 666

Table 203: The atomic coordinates of the model resulting from the fixed core refinement of ZAA24I from the 18-month data collection. 667

Table 204: The atomic coordinates of the tetrameric phase of the fixed core refinement of ZAA24I from the 18-month data collection. 669

Table 205: The atomic coordinates of the model resulting from the fixed core refinement of ZAA25A from the 18-month data collection. 670

Table 206: The atomic coordinates of the tetrameric phase of the fixed core refinement of ZAA25A from the 18-month data collection. 672

Table 207: The atomic coordinates of the model resulting from the fixed core refinement of ZAA25C from the 18-month data collection. 673

Table 208: The atomic coordinates of the tetrameric phase of the fixed core refinement of ZAA25C from the 18-month data collection. 675

Table 209: The atomic coordinates of the model resulting from the fixed core refinement of ZAA25I from the 18-month data collection. 676

Table 210: The atomic coordinates of the tetrameric phase of the fixed core refinement of ZAA25I from the 18-month data collection. 678

Table 211: The atomic coordinates of the model resulting from the fixed core refinement of ZAA27A from the 18-month data collection. 679

Table 212: The atomic coordinates of the tetrameric phase of the fixed core refinement of ZAA27A from the 18-month data collection. 681

Table 213: The atomic coordinates of the model resulting from the fixed core refinement of ZAA27C from the 18-month data collection. 682

Table 214: The atomic coordinates of the tetrameric phase of the fixed core refinement of ZAA27C from the 18-month data collection. 684

Table 215: The atomic coordinates of the model resulting from the fixed core refinement of ZAA27I from the 18-month data collection. 685

Table 216: The atomic coordinates of the tetrameric phase of the fixed core refinement of ZAA27I from the 18-month data collection. 687

Table 217: The atomic coordinates of the model resulting from the fixed core refinement of ZAA28A from the 18-month data collection. 688

Table 218: The atomic coordinates of the tetrameric phase of the fixed core refinement of ZAA28A from the 18-month data collection. 690

Table 219: The atomic coordinates of the model resulting from the fixed core refinement of ZAA28C from the 18-month data collection. 691

Table 220: The atomic coordinates of the tetrameric phase of the fixed core refinement of ZAA28C from the 18-month data collection. 693

Table 221: The atomic coordinates of the model resulting from the fixed core refinement of ZAA28I from the 18-month data collection. 694

Table 222: The atomic coordinates of the tetrameric phase of the fixed core refinement of ZAA28I from the 18-month data collection. 696

Table 223: The atomic coordinates of the model resulting from the chandelier core refinement of ZAA1A from the 18-month data collection. 697

Table 224: The atomic coordinates of the tetrameric phase of the chandelier core refinement of ZAA1A from the 18-month data collection. 699

Table 225: The atomic coordinates of the model resulting from the chandelier core refinement of ZAA1I from the 18-month data collection. 701

Table 226: The atomic coordinates of the tetrameric phase of the chandelier core refinement of ZAA1I from the 18-month data collection. 703

Table 227: The atomic coordinates of the model resulting from the chandelier core refinement of ZAA4A from the 18-month data collection. 705

Table 228: The atomic coordinates of the tetrameric phase of the chandelier core refinement of ZAA4A from the 18-month data collection. 707

Table 229: The atomic coordinates of the model resulting from the chandelier core refinement of ZAA4C from the 18-month data collection. 709

Table 230: The atomic coordinates of the tetrameric phase of the chandelier core refinement of ZAA4C from the 18-month data collection. 711

Table 231: The atomic coordinates of the model resulting from the chandelier core refinement of ZAA4I from the 18-month data collection. 713

Table 232: The atomic coordinates of the tetrameric phase of the chandelier core refinement of ZAA4I from the 18-month data collection. 715

Table 233: The atomic coordinates of the model resulting from the chandelier core refinement of ZAA7A from the 18-month data collection. 717

Table 234: The atomic coordinates of the tetrameric phase of the chandelier core refinement of ZAA7A from the 18-month data collection. 719

Table 235: The atomic coordinates of the model resulting from the chandelier core refinement of ZAA7C from the 18-month data collection. 721

Table 236: The atomic coordinates of the tetrameric phase of the chandelier core refinement of ZAA7C from the 18-month data collection. 723

Table 237: The atomic coordinates of the model resulting from the chandelier core refinement of ZAA7I from the 18-month data collection. 725

Table 238: The atomic coordinates of the tetrameric phase of the chandelier core refinement of ZAA7I from the 18-month data collection. 727

Table 239: The atomic coordinates of the model resulting from the chandelier core refinement of ZAA10A from the 18-month data collection. 729

Table 240: The atomic coordinates of the tetrameric phase of the chandelier core refinement of ZAA10A from the 18-month data collection. 731

Table 241: The atomic coordinates of the model resulting from the chandelier core refinement of ZAA10C from the 18-month data collection. 733

Table 242: The atomic coordinates of the tetrameric phase of the chandelier core refinement of ZAA10C from the 18-month data collection. 735

Table 243: The atomic coordinates of the model resulting from the chandelier core refinement of ZAA10I from the 18-month data collection. 737

Table 244: The atomic coordinates of the tetrameric phase of the chandelier core refinement of ZAA10I from the 18-month data collection. 739

Table 245: The atomic coordinates of the model resulting from the chandelier core refinement of ZAA13A from the 18-month data collection. 741

Table 246: The atomic coordinates of the tetrameric phase of the chandelier core refinement of ZAA13A from the 18-month data collection. 743

Table 247: The atomic coordinates of the model resulting from the chandelier core refinement of ZAA13C from the 18-month data collection. 745

Table 248: The atomic coordinates of the tetrameric phase of the chandelier core refinement of ZAA13C from the 18-month data collection. 747

Table 249: The atomic coordinates of the model resulting from the chandelier core refinement of ZAA13I from the 18-month data collection. 749

Table 250: The atomic coordinates of the tetrameric phase of the chandelier core refinement of ZAA13I from the 18-month data collection. 751

Table 251: The atomic coordinates of the model resulting from the chandelier core refinement of ZAA16A from the 18-month data collection. 753

Table 252: The atomic coordinates of the tetrameric phase of the chandelier core refinement of ZAA16A from the 18-month data collection. 755

Table 253: The atomic coordinates of the model resulting from the chandelier core refinement of ZAA16C from the 18-month data collection. 757

Table 254: The atomic coordinates of the tetrameric phase of the chandelier core refinement of ZAA16C from the 18-month data collection. 759

Table 255: The atomic coordinates of the model resulting from the chandelier core refinement of ZAA16I from the 18-month data collection. 761

Table 256: The atomic coordinates of the tetrameric phase of the chandelier core refinement of ZAA16I from the 18-month data collection. 763

Table 257: The atomic coordinates of the model resulting from the chandelier core refinement of ZAA20A from the 18-month data collection. 765

Table 258: The atomic coordinates of the tetrameric phase of the chandelier core refinement of ZAA20A from the 18-month data collection. 767

Table 259: The atomic coordinates of the model resulting from the chandelier core refinement of ZAA20C from the 18-month data collection. 769

Table 260: The atomic coordinates of the tetrameric phase of the chandelier core refinement of ZAA20C from the 18-month data collection. 771

Table 261: The atomic coordinates of the model resulting from the chandelier core refinement of ZAA20I from the 18-month data collection. 773

Table 262: The atomic coordinates of the tetrameric phase of the chandelier core refinement of ZAA20I from the 18-month data collection. 775

Table 263: The atomic coordinates of the model resulting from the chandelier core refinement of ZAA24A from the 18-month data collection. 777

Table 264: The atomic coordinates of the tetrameric phase of the chandelier core refinement of ZAA24A from the 18-month data collection. 779
Table 265: The atomic coordinates of the model resulting from the chandelier core refinement of ZAA24C from the 18-month data collection. 781
Table 266: The atomic coordinates of the tetrameric phase of the chandelier core refinement of ZAA24C from the 18-month data collection. 783
Table 267: The atomic coordinates of the model resulting from the chandelier core refinement of ZAA24I from the 18-month data collection. 785
Table 268: The atomic coordinates of the tetrameric phase of the chandelier core refinement of ZAA24I from the 18-month data collection. 787
Table 269: The atomic coordinates of the model resulting from the chandelier core refinement of ZAA25A from the 18-month data collection. 789
Table 270: The atomic coordinates of the tetrameric phase of the chandelier core refinement of ZAA25A from the 18-month data collection. 791
Table 271: The atomic coordinates of the model resulting from the chandelier core refinement of ZAA25C from the 18-month data collection. 793
Table 272: The atomic coordinates of the tetrameric phase of the chandelier core refinement of ZAA25C from the 18-month data collection. 795
Table 273: The atomic coordinates of the model resulting from the chandelier core refinement of ZAA25I from the 18-month data collection. 797
Table 274: The atomic coordinates of the tetrameric phase of the chandelier core refinement of ZAA25I from the 18-month data collection. 799
Table 275: The atomic coordinates of the model resulting from the chandelier core refinement of ZAA27A from the 18-month data collection. 801

Table 276: The atomic coordinates of the tetrameric phase of the chandelier core refinement of ZAA27A from the 18-month data collection. 803
Table 277: The atomic coordinates of the model resulting from the chandelier core refinement of ZAA27C from the 18-month data collection. 805
Table 278: The atomic coordinates of the tetrameric phase of the chandelier core refinement of ZAA27C from the 18-month data collection. 807
Table 279: The atomic coordinates of the model resulting from the chandelier core refinement of ZAA27I from the 18-month data collection. 809
Table 280: The atomic coordinates of the tetrameric phase of the chandelier core refinement of ZAA27I from the 18-month data collection. 811
Table 281: The atomic coordinates of the model resulting from the chandelier core refinement of ZAA28A from the 18-month data collection. 813
Table 282: The atomic coordinates of the tetrameric phase of the chandelier core refinement of ZAA28A from the 18-month data collection. 815
Table 283: The atomic coordinates of the model resulting from the chandelier core refinement of ZAA28C from the 18-month data collection. 817
Table 284: The atomic coordinates of the tetrameric phase of the chandelier core refinement of ZAA28C from the 18-month data collection. 819
Table 285: The atomic coordinates of the model resulting from the chandelier core refinement of ZAA28I from the 18-month data collection. 821
Table 286: The atomic coordinates of the tetrameric phase of the chandelier core refinement of ZAA28I from the 18-month data collection. 823
Table 287:Percentage yields from the synthesis of a model compound umbite. 824

Table 288:Lattice parameter a values from the rietveld refinement of the umbite samples 825

Table 289: Lattice parameter b values from the rietveld refinement of the umbite samples 827

Table 290: Lattice parameter c values from the rietveld refinement of the umbite samples 829

Table 291: Results of the structural refinements of samples of umbite synthesised from zirconium acetate, common to all samples. 836

Table 292: Structural refinement parameters of samples of umbite synthesised from zirconium acetate solutions aged for 3-months 836

Table 293: Structural refinement parameters of samples of umbite synthesised from zirconium acetate solutions aged for 7 months 837

Table 294: Structural refinement parameters of samples of umbite synthesised from zirconium acetate solutions aged for 15 months 838

Table 295: Structural refinement parameters of samples of umbite synthesised from zirconium acetate solutions aged for 22 months 839

10.1 Zirconium-oxychloride refinements

Table 57: Atomic coordinates of the tetrameric model obtained from the first iteration refinement of zirconyl chloride.

Atom Label	Atom Type	Multiplicity	Fractional X Coordinate	Fractional Y Coordinate	Fractional Z Coordinate	Fractional Occupancy
O1	O	1	0.4839	0.4893	0.5266	1.0000
O2	O	1	0.5107	0.4834	0.4741	1.0000
O3	O	1	0.4897	0.5149	0.4740	1.0000
O4	O	1	0.5167	0.5110	0.5227	1.0000
O5	O	1	0.5051	0.5318	0.4484	1.0000
O6	O	1	0.4962	0.4717	0.4532	1.0000
O7	O	1	0.5315	0.4943	0.5468	1.0000
O8	O	1	0.4707	0.5061	0.5486	1.0000
O9	O	1	0.4774	0.4648	0.5176	1.0000
O10	O	1	0.5368	0.4779	0.5074	1.0000
O11	O	1	0.4618	0.5232	0.5106	1.0000
O12	O	1	0.5230	0.5394	0.5009	1.0000
O13	O	1	0.5425	0.5049	0.4761	1.0000
O14	O	1	0.4589	0.4915	0.4867	1.0000
O15	O	1	0.5074	0.4587	0.5112	1.0000
O16	O	1	0.4923	0.5414	0.5071	1.0000
O17	O	1	0.4812	0.4902	0.4686	1.0000
O18	O	1	0.5135	0.4809	0.5307	1.0000
O19	O	1	0.4902	0.5185	0.5328	1.0000
O20	O	1	0.5194	0.5123	0.4649	1.0000
O21	O	1	0.5087	0.5327	0.5462	1.0000
O22	O	1	0.4941	0.4676	0.5480	1.0000
O23	O	1	0.5345	0.4825	0.4563	1.0000
O24	O	1	0.4723	0.5083	0.4553	1.0000
Zr1	Zr	1	0.4950	0.4758	0.5010	1.0000
Zr2	Zr	1	0.5238	0.4950	0.4998	1.0000
Zr3	Zr	1	0.4755	0.5051	0.4999	1.0000
Zr4	Zr	1	0.5046	0.5239	0.5006	1.0000

Table 58: Atomic coordinates of the tetrameric model obtained from the second iteration refinement of zirconyl chloride.

Atom Label	Atom Type	Multiplicity	Fractional X Coordinate	Fractional Y Coordinate	Fractional Z Coordinate	Fractional Occupancy
O1	O	1	0.5137	0.4863	0.4729	1.0000
O2	O	1	0.4863	0.4863	0.5271	1.0000
O3	O	1	0.5137	0.5137	0.5271	1.0000
O4	O	1	0.4863	0.5137	0.4729	1.0000
O5	O	1	0.5000	0.5339	0.5412	1.0000
O6	O	1	0.5000	0.4661	0.5412	1.0000
O7	O	1	0.4664	0.5000	0.4588	1.0000
O8	O	1	0.5336	0.5000	0.4588	1.0000
O9	O	1	0.5122	0.4566	0.5000	1.0000
O10	O	1	0.4566	0.4878	0.5000	1.0000
O11	O	1	0.5434	0.5122	0.5000	1.0000
O12	O	1	0.4878	0.5434	0.5000	1.0000
O13	O	1	0.4566	0.5122	0.5000	1.0000
O14	O	1	0.5434	0.4878	0.5000	1.0000
O15	O	1	0.4878	0.4566	0.5000	1.0000
O16	O	1	0.5122	0.5434	0.5000	1.0000
O17	O	1	0.5137	0.4863	0.5271	1.0000
O18	O	1	0.4863	0.4863	0.4729	1.0000
O19	O	1	0.5137	0.5137	0.4729	1.0000
O20	O	1	0.4863	0.5137	0.5271	1.0000
O21	O	1	0.5000	0.5336	0.4588	1.0000
O22	O	1	0.5000	0.4664	0.4588	1.0000
O23	O	1	0.4661	0.5000	0.5412	1.0000
O24	O	1	0.5339	0.5000	0.5412	1.0000
Zr1	Zr	1	0.5000	0.4755	0.5000	1.0000
Zr2	Zr	1	0.4755	0.5000	0.5000	1.0000
Zr3	Zr	1	0.5245	0.5000	0.5000	1.0000
Zr4	Zr	1	0.5000	0.5245	0.5000	1.0000

Table 59: Atomic coordinates of the tetrameric model obtained from the third iteration refinement of zirconyl chloride.

Atom Label	Atom Type	Multiplicity	Fractional X Coordinate	Fractional Y Coordinate	Fractional Z Coordinate	Fractional Occupancy
O1	O	1	0.5142	0.4858	0.4742	1.0000
O2	O	1	0.4858	0.4858	0.5258	1.0000
O3	O	1	0.5142	0.5142	0.5258	1.0000
O4	O	1	0.4858	0.5142	0.4742	1.0000
O5	O	1	0.5000	0.5344	0.5419	1.0000
O6	O	1	0.5000	0.4656	0.5419	1.0000
O7	O	1	0.4656	0.5000	0.4581	1.0000
O8	O	1	0.5344	0.5000	0.4581	1.0000
O9	O	1	0.5129	0.4568	0.5000	1.0000
O10	O	1	0.4568	0.4871	0.5000	1.0000
O11	O	1	0.5432	0.5129	0.5000	1.0000
O12	O	1	0.4871	0.5432	0.5000	1.0000
O13	O	1	0.4568	0.5129	0.5000	1.0000
O14	O	1	0.5432	0.4871	0.5000	1.0000
O15	O	1	0.4871	0.4568	0.5000	1.0000
O16	O	1	0.5129	0.5432	0.5000	1.0000
O17	O	1	0.5142	0.4858	0.5258	1.0000
O18	O	1	0.4858	0.4858	0.4742	1.0000
O19	O	1	0.5142	0.5142	0.4742	1.0000
O20	O	1	0.4858	0.5142	0.5258	1.0000
O21	O	1	0.5000	0.5344	0.4581	1.0000
O22	O	1	0.5000	0.4656	0.4581	1.0000
O23	O	1	0.4656	0.5000	0.5419	1.0000
O24	O	1	0.5344	0.5000	0.5419	1.0000
Zr1	Zr	1	0.5000	0.4755	0.5000	1.0000
Zr2	Zr	1	0.4755	0.5000	0.5000	1.0000
Zr3	Zr	1	0.5245	0.5000	0.5000	1.0000
Zr4	Zr	1	0.5000	0.5245	0.5000	1.0000
Cl1	Cl	1	0.5338	0.4662	0.4468	1.0000
Cl2	Cl	1	0.5338	0.4662	0.5532	1.0000
Cl3	Cl	1	0.4662	0.4662	0.4468	1.0000
Cl4	Cl	1	0.4662	0.4662	0.5532	1.0000
Cl5	Cl	1	0.4662	0.5338	0.4468	1.0000
Cl6	Cl	1	0.4662	0.5338	0.5532	1.0000
Cl7	Cl	1	0.5338	0.5338	0.4468	1.0000
Cl8	Cl	1	0.5338	0.5338	0.5532	1.0000

10.2 Zirconium Acetate Synthesis

Table 60: All samples studied in the ageing study and the quantity of reagents required for their synthesis.

Sample Name	Feedstock	ZrO_2 weight percentage	Acetic acid : Zr ratio	ZrO_2 mass percentage in Zr source	Mass of Zr source (g)	Mass of Acetic acid (g)	Mass of Water (g)
ZAA1	1	14	1.6	43.2	485.8	203.3	1086.8
ZAA3	1	14	2.0	43.2	486.1	255.0	1038.5
ZAA4	1	22	1.6	43.2	762.8	319.8	850.9
ZAA6	1	22	2.0	43.2	763.5	399.4	770.1
ZAA7	1	30	1.6	43.2	1041.3	436.7	614.6
ZAA9	1	30	2.0	43.2	1041.0	544.4	505.2
ZAA10	3	14	1.6	40.3	521.3	203.5	1086.8
ZAA12	3	14	2.0	40.3	521.5	253.8	1035.5
ZAA13	3	22	1.6	40.3	818.1	319.1	850.6
ZAA15	3	22	2.0	40.3	818.8	399.1	770.2
ZAA16	3	30	1.6	40.3	1116.1	435.3	614.5
ZAA18	3	30	2.0	40.3	1116.1	544.4	505.7
ZAA19	2	14	1.6	40.8	514.7	203.2	1086.8
ZAA20	2	22	1.6	40.8	808.7	319.4	850.6
ZAA21	2	30	1.6	40.8	1102.3	435.4	614.8
ZAA22	2	22	2.0	40.8	202.3*	99.9*	192.2*
ZAA23	2	30	2.0	40.8	275.0*	136.9*	126.1*
ZAA24	1	22	1.3	43.2	763.8	257.6	912.0
ZAA25	1	22	5.0	43.2	763.8	1005.4	165.1
ZAA26	3	22	1.3	40.3	819.3	258.0	912.2
ZAA27	3	22	5.0	40.3	818.3	1005.6	164.8

10.3 March 2020 Data Collection

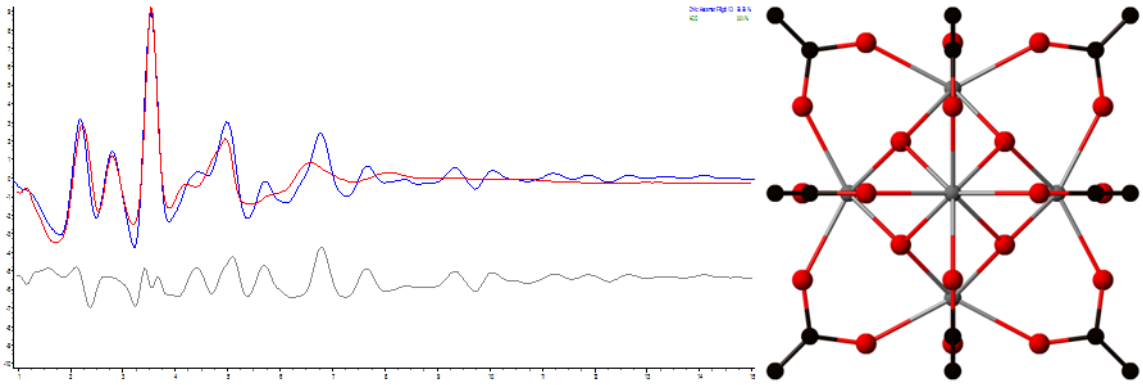

Figure 118: Observed and Calculated PDF from the fixed core refinement of ZAA1 from the 9-month data collection and the resultant model.

Table 61: The atomic coordinates of the model resulting from the fixed core refinement of ZAA1 from the 9-month data collection.

Atom Label	Atom Type	Multiplicity	Fractional X Coordinate	Fractional Y Coordinate	Fractional Z Coordinate	Fractional Occupancy
C1	C	1	0.5900506	0.5000000	0.5833031	1
C2	C	1	0.5000000	0.4099494	0.5833031	1
C3	C	1	0.4099494	0.5000000	0.5833031	1
C4	C	1	0.5000000	0.5900506	0.5833031	1
C5	C	1	0.5900506	0.5000000	0.4166969	1
C6	C	1	0.5000000	0.4099494	0.4166969	1
C7	C	1	0.4099494	0.5000000	0.4166969	1
C8	C	1	0.5000000	0.5900506	0.4166969	1
C9	C	1	0.5900506	0.4099494	0.5000000	1
C10	C	1	0.4099494	0.4099494	0.5000000	1
C11	C	1	0.4099494	0.5900506	0.5000000	1
C12	C	1	0.5900506	0.5900506	0.5000000	1
C13	C	1	0.6126332	0.5000000	0.6041936	1
C14	C	1	0.5000000	0.3873668	0.6041936	1
C15	C	1	0.3873668	0.5000000	0.6041936	1
C16	C	1	0.5000000	0.6126332	0.6041936	1
C17	C	1	0.6126332	0.5000000	0.3958064	1
C18	C	1	0.5000000	0.3873668	0.3958064	1
C19	C	1	0.3873668	0.5000000	0.3958064	1
C20	C	1	0.5000000	0.6126332	0.3958064	1
C21	C	1	0.6126332	0.3873668	0.5000000	1
C22	C	1	0.3873668	0.3873668	0.5000000	1
C23	C	1	0.3873668	0.6126332	0.5000000	1
C24	C	1	0.6126332	0.6126332	0.5000000	1
O1	O	1	0.5332451	0.5329207	0.4692460	1

O2	O	1	0.5332451	0.4670793	0.5307540	1
O3	O	1	0.4667549	0.5329207	0.4692460	1
O4	O	1	0.4667549	0.4670793	0.5307540	1
O5	O	1	0.4667549	0.4670793	0.4692460	1
O6	O	1	0.4667549	0.5329207	0.5307540	1
O7	O	1	0.5332451	0.4670793	0.4692460	1
O8	O	1	0.5332451	0.5329207	0.5307540	1
O9	O	1	0.5955211	0.5000000	0.5497646	1
O10	O	1	0.5955211	0.4462045	0.5000000	1
O11	O	1	0.5955211	0.5000000	0.4502354	1
O12	O	1	0.5955211	0.5537955	0.5000000	1
O13	O	1	0.5000000	0.5955211	0.5497646	1
O14	O	1	0.5537955	0.5955211	0.5000000	1
O15	O	1	0.5000000	0.5955211	0.4502354	1
O16	O	1	0.4462045	0.5955211	0.5000000	1
O17	O	1	0.4044789	0.5000000	0.5497646	1
O18	O	1	0.4044789	0.5537955	0.5000000	1
O19	O	1	0.4044789	0.5000000	0.4502354	1
O20	O	1	0.4044789	0.4462045	0.5000000	1
O21	O	1	0.5000000	0.4044789	0.5497646	1
O22	O	1	0.4462045	0.4044789	0.5000000	1
O23	O	1	0.5000000	0.4044789	0.4502354	1
O24	O	1	0.5537955	0.4044789	0.5000000	1
O25	O	1	0.5537955	0.5000000	0.5883637	1
O26	O	1	0.5000000	0.5537955	0.5883637	1
O27	O	1	0.4462045	0.5000000	0.5883637	1
O28	O	1	0.5000000	0.4462045	0.5883637	1
O29	O	1	0.5537955	0.5000000	0.4116363	1
O30	O	1	0.5000000	0.4462045	0.4116363	1
O31	O	1	0.4462045	0.5000000	0.4116363	1
O32	O	1	0.5000000	0.5537955	0.4116363	1
Zr1	Zr	1	0.5662509	0.5000000	0.5000000	1
Zr2	Zr	1	0.5000000	0.5662509	0.5000000	1
Zr3	Zr	1	0.4337491	0.5000000	0.5000000	1
Zr4	Zr	1	0.5000000	0.4337491	0.5000000	1
Zr5	Zr	1	0.5000000	0.5000000	0.5612867	1
Zr6	Zr	1	0.5000000	0.5000000	0.4387133	1

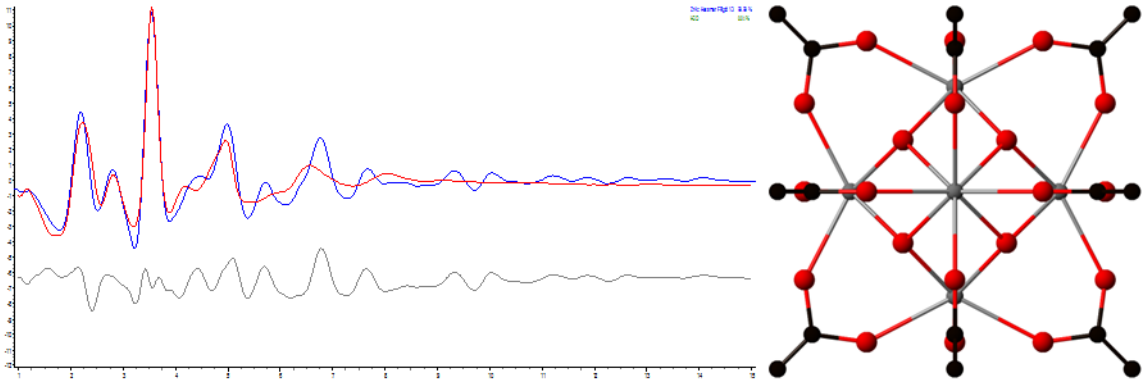

Figure 119: Observed and Calculated PDF from the fixed core refinement of ZAA4 from the 9-month data collection and the resultant model.

Table 62: The atomic coordinates of the model resulting from the fixed core refinement of ZAA4 from the 9-month data collection.

Atom Label	Atom Type	Multiplicity	Fractional X Coordinate	Fractional Y Coordinate	Fractional Z Coordinate	Fractional Occupancy
C1	C	1	0.5904928	0.5000000	0.5837121	1
C2	C	1	0.5000000	0.4095072	0.5837121	1
C3	C	1	0.4095072	0.5000000	0.5837121	1
C4	C	1	0.5000000	0.5904928	0.5837121	1
C5	C	1	0.5904928	0.5000000	0.4162879	1
C6	C	1	0.5000000	0.4095072	0.4162879	1
C7	C	1	0.4095072	0.5000000	0.4162879	1
C8	C	1	0.5000000	0.5904928	0.4162879	1
C9	C	1	0.5904928	0.4095072	0.5000000	1
C10	C	1	0.4095072	0.4095072	0.5000000	1
C11	C	1	0.4095072	0.5904928	0.5000000	1
C12	C	1	0.5904928	0.5904928	0.5000000	1
C13	C	1	0.6123705	0.5000000	0.6039506	1
C14	C	1	0.5000000	0.3876295	0.6039506	1
C15	C	1	0.3876295	0.5000000	0.6039506	1
C16	C	1	0.5000000	0.6123705	0.6039506	1
C17	C	1	0.6123705	0.5000000	0.3960494	1
C18	C	1	0.5000000	0.3876295	0.3960494	1
C19	C	1	0.3876295	0.5000000	0.3960494	1
C20	C	1	0.5000000	0.6123705	0.3960494	1
C21	C	1	0.6123705	0.3876295	0.5000000	1
C22	C	1	0.3876295	0.3876295	0.5000000	1
C23	C	1	0.3876295	0.6123705	0.5000000	1
C24	C	1	0.6123705	0.6123705	0.5000000	1
O1	O	1	0.5328710	0.5325503	0.4695920	1
O2	O	1	0.5328710	0.4674497	0.5304080	1
O3	O	1	0.4671290	0.5325503	0.4695920	1
O4	O	1	0.4671290	0.4674497	0.5304080	1

O5	O	1	0.4671290	0.4674497	0.4695920	1
O6	O	1	0.4671290	0.5325503	0.5304080	1
O7	O	1	0.5328710	0.4674497	0.4695920	1
O8	O	1	0.5328710	0.5325503	0.5304080	1
O9	O	1	0.5953020	0.5000000	0.5516071	1
O10	O	1	0.5953020	0.4442127	0.5000000	1
O11	O	1	0.5953020	0.5000000	0.4483929	1
O12	O	1	0.5953020	0.5557873	0.5000000	1
O13	O	1	0.5000000	0.5953020	0.5516071	1
O14	O	1	0.5557873	0.5953020	0.5000000	1
O15	O	1	0.5000000	0.5953020	0.4483929	1
O16	O	1	0.4442127	0.5953020	0.5000000	1
O17	O	1	0.4046980	0.5000000	0.5516071	1
O18	O	1	0.4046980	0.5557873	0.5000000	1
O19	O	1	0.4046980	0.5000000	0.4483929	1
O20	O	1	0.4046980	0.4442127	0.5000000	1
O21	O	1	0.5000000	0.4046980	0.5516071	1
O22	O	1	0.4442127	0.4046980	0.5000000	1
O23	O	1	0.5000000	0.4046980	0.4483929	1
O24	O	1	0.5557873	0.4046980	0.5000000	1
O25	O	1	0.5557873	0.5000000	0.5881610	1
O26	O	1	0.5000000	0.5557873	0.5881610	1
O27	O	1	0.4442127	0.5000000	0.5881610	1
O28	O	1	0.5000000	0.4442127	0.5881610	1
O29	O	1	0.5557873	0.5000000	0.4118390	1
O30	O	1	0.5000000	0.4442127	0.4118390	1
O31	O	1	0.4442127	0.5000000	0.4118390	1
O32	O	1	0.5000000	0.5557873	0.4118390	1
Zr1	Zr	1	0.5661883	0.5000000	0.5000000	1
Zr2	Zr	1	0.5000000	0.5661883	0.5000000	1
Zr3	Zr	1	0.4338117	0.5000000	0.5000000	1
Zr4	Zr	1	0.5000000	0.4338117	0.5000000	1
Zr5	Zr	1	0.5000000	0.5000000	0.5612288	1
Zr6	Zr	1	0.5000000	0.5000000	0.4387712	1

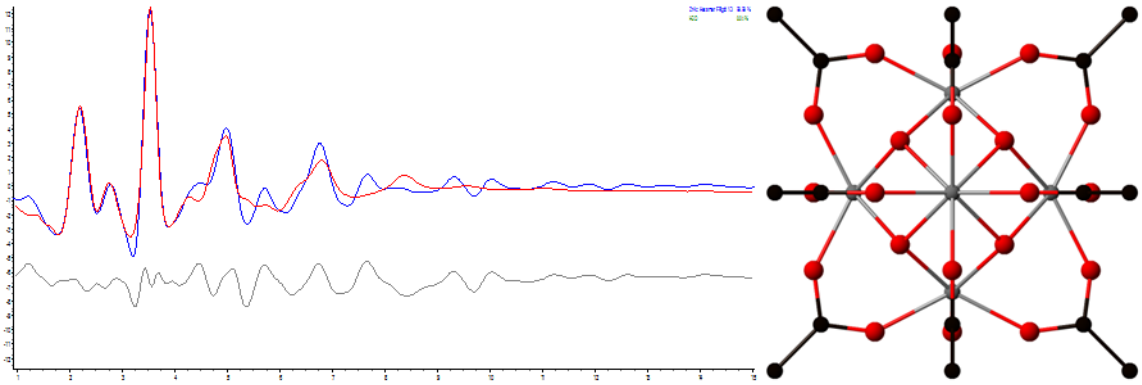

Figure 120: Observed and Calculated PDF from the fixed core refinement of ZAA7 from the 9-month data collection and the resultant model.

Table 63: The atomic coordinates of the model resulting from the fixed core refinement of ZAA7 from the 9-month data collection.

Atom Label	Atom Type	Multiplicity	Fractional X Coordinate	Fractional Y Coordinate	Fractional Z Coordinate	Fractional Occupancy
C1	C	1	0.5884769	0.5000000	0.5818473	1
C2	C	1	0.5000000	0.4115231	0.5818473	1
C3	C	1	0.4115231	0.5000000	0.5818473	1
C4	C	1	0.5000000	0.5884769	0.5818473	1
C5	C	1	0.5884769	0.5000000	0.4181527	1
C6	C	1	0.5000000	0.4115231	0.4181527	1
C7	C	1	0.4115231	0.5000000	0.4181527	1
C8	C	1	0.5000000	0.5884769	0.4181527	1
C9	C	1	0.5884769	0.4115231	0.5000000	1
C10	C	1	0.4115231	0.4115231	0.5000000	1
C11	C	1	0.4115231	0.5884769	0.5000000	1
C12	C	1	0.5884769	0.5884769	0.5000000	1
C13	C	1	0.6194671	0.5000000	0.6105154	1
C14	C	1	0.5000000	0.3805329	0.6105154	1
C15	C	1	0.3805329	0.5000000	0.6105154	1
C16	C	1	0.5000000	0.6194671	0.6105154	1
C17	C	1	0.6194671	0.5000000	0.3894846	1
C18	C	1	0.5000000	0.3805329	0.3894846	1
C19	C	1	0.3805329	0.5000000	0.3894846	1
C20	C	1	0.5000000	0.6194671	0.3894846	1
C21	C	1	0.6194671	0.3805329	0.5000000	1
C22	C	1	0.3805329	0.3805329	0.5000000	1
C23	C	1	0.3805329	0.6194671	0.5000000	1
C24	C	1	0.6194671	0.6194671	0.5000000	1
O1	O	1	0.5351101	0.5347675	0.4675207	1
O2	O	1	0.5351101	0.4652325	0.5324793	1
O3	O	1	0.4648899	0.5347675	0.4675207	1
O4	O	1	0.4648899	0.4652325	0.5324793	1

O5	O	1	0.4648899	0.4652325	0.4675207	1
O6	O	1	0.4648899	0.5347675	0.5324793	1
O7	O	1	0.5351101	0.4652325	0.4675207	1
O8	O	1	0.5351101	0.5347675	0.5324793	1
O9	O	1	0.5933587	0.5000000	0.5481717	1
O10	O	1	0.5933587	0.4479264	0.5000000	1
O11	O	1	0.5933587	0.5000000	0.4518283	1
O12	O	1	0.5933587	0.5520736	0.5000000	1
O13	O	1	0.5000000	0.5933587	0.5481717	1
O14	O	1	0.5520736	0.5933587	0.5000000	1
O15	O	1	0.5000000	0.5933587	0.4518283	1
O16	O	1	0.4479264	0.5933587	0.5000000	1
O17	O	1	0.4066413	0.5000000	0.5481717	1
O18	O	1	0.4066413	0.5520736	0.5000000	1
O19	O	1	0.4066413	0.5000000	0.4518283	1
O20	O	1	0.4066413	0.4479264	0.5000000	1
O21	O	1	0.5000000	0.4066413	0.5481717	1
O22	O	1	0.4479264	0.4066413	0.5000000	1
O23	O	1	0.5000000	0.4066413	0.4518283	1
O24	O	1	0.5520736	0.4066413	0.5000000	1
O25	O	1	0.5520736	0.5000000	0.5863633	1
O26	O	1	0.5000000	0.5520736	0.5863633	1
O27	O	1	0.4479264	0.5000000	0.5863633	1
O28	O	1	0.5000000	0.4479264	0.5863633	1
O29	O	1	0.5520736	0.5000000	0.4136367	1
O30	O	1	0.5000000	0.4479264	0.4136367	1
O31	O	1	0.4479264	0.5000000	0.4136367	1
O32	O	1	0.5000000	0.5520736	0.4136367	1
Zr1	Zr	1	0.5665160	0.5000000	0.5000000	1
Zr2	Zr	1	0.5000000	0.5665160	0.5000000	1
Zr3	Zr	1	0.4334840	0.5000000	0.5000000	1
Zr4	Zr	1	0.5000000	0.4334840	0.5000000	1
Zr5	Zr	1	0.5000000	0.5000000	0.5615319	1
Zr6	Zr	1	0.5000000	0.5000000	0.4384681	1

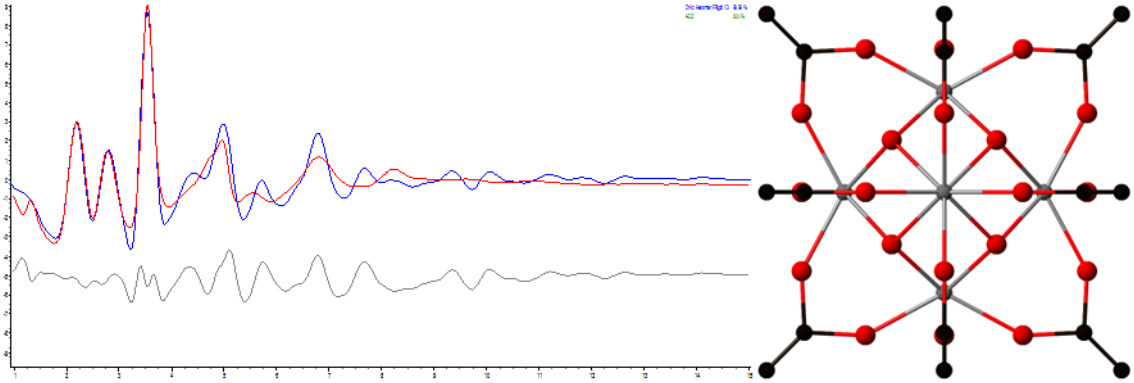

Figure 121: Observed and Calculated PDF from the fixed core refinement of ZAA10 from the 9-month data collection and the resultant model.

Table 64: The atomic coordinates of the model resulting from the fixed core refinement of ZAA10 from 9-month data collection.

Atom Label	Atom Type	Multiplicity	Fractional X Coordinate	Fractional Y Coordinate	Fractional Z Coordinate	Fractional Occupancy
C1	C	1	0.5921384	0.5000000	0.5852344	1
C2	C	1	0.5000000	0.4078616	0.5852344	1
C3	C	1	0.4078616	0.5000000	0.5852344	1
C4	C	1	0.5000000	0.5921384	0.5852344	1
C5	C	1	0.5921384	0.5000000	0.4147656	1
C6	C	1	0.5000000	0.4078616	0.4147656	1
C7	C	1	0.4078616	0.5000000	0.4147656	1
C8	C	1	0.5000000	0.5921384	0.4147656	1
C9	C	1	0.5921384	0.4078616	0.5000000	1
C10	C	1	0.4078616	0.4078616	0.5000000	1
C11	C	1	0.4078616	0.5921384	0.5000000	1
C12	C	1	0.5921384	0.5921384	0.5000000	1
C13	C	1	0.6170442	0.5000000	0.6082740	1
C14	C	1	0.5000000	0.3829558	0.6082740	1
C15	C	1	0.3829558	0.5000000	0.6082740	1
C16	C	1	0.5000000	0.6170442	0.6082740	1
C17	C	1	0.6170442	0.5000000	0.3917260	1
C18	C	1	0.5000000	0.3829558	0.3917260	1
C19	C	1	0.3829558	0.5000000	0.3917260	1
C20	C	1	0.5000000	0.6170442	0.3917260	1
C21	C	1	0.6170442	0.3829558	0.5000000	1
C22	C	1	0.3829558	0.3829558	0.5000000	1
C23	C	1	0.3829558	0.6170442	0.5000000	1
C24	C	1	0.6170442	0.6170442	0.5000000	1
O1	O	1	0.5346473	0.5343092	0.4679488	1
O2	O	1	0.5346473	0.4656908	0.5320512	1
O3	O	1	0.4653527	0.5343092	0.4679488	1
O4	O	1	0.4653527	0.4656908	0.5320512	1

O5	O	1	0.4653527	0.4656908	0.4679488	1
O6	O	1	0.4653527	0.5343092	0.5320512	1
O7	O	1	0.5346473	0.4656908	0.4679488	1
O8	O	1	0.5346473	0.5343092	0.5320512	1
O9	O	1	0.5939216	0.5000000	0.5480123	1
O10	O	1	0.5939216	0.4480987	0.5000000	1
O11	O	1	0.5939216	0.5000000	0.4519877	1
O12	O	1	0.5939216	0.5519013	0.5000000	1
O13	O	1	0.5000000	0.5939216	0.5480123	1
O14	O	1	0.5519013	0.5939216	0.5000000	1
O15	O	1	0.5000000	0.5939216	0.4519877	1
O16	O	1	0.4480987	0.5939216	0.5000000	1
O17	O	1	0.4060784	0.5000000	0.5480123	1
O18	O	1	0.4060784	0.5519013	0.5000000	1
O19	O	1	0.4060784	0.5000000	0.4519877	1
O20	O	1	0.4060784	0.4480987	0.5000000	1
O21	O	1	0.5000000	0.4060784	0.5480123	1
O22	O	1	0.4480987	0.4060784	0.5000000	1
O23	O	1	0.5000000	0.4060784	0.4519877	1
O24	O	1	0.5519013	0.4060784	0.5000000	1
O25	O	1	0.5519013	0.5000000	0.5868841	1
O26	O	1	0.5000000	0.5519013	0.5868841	1
O27	O	1	0.4480987	0.5000000	0.5868841	1
O28	O	1	0.5000000	0.4480987	0.5868841	1
O29	O	1	0.5519013	0.5000000	0.4131159	1
O30	O	1	0.5000000	0.4480987	0.4131159	1
O31	O	1	0.4480987	0.5000000	0.4131159	1
O32	O	1	0.5000000	0.5519013	0.4131159	1
Zr1	Zr	1	0.5660631	0.5000000	0.5000000	1
Zr2	Zr	1	0.5000000	0.5660631	0.5000000	1
Zr3	Zr	1	0.4339369	0.5000000	0.5000000	1
Zr4	Zr	1	0.5000000	0.4339369	0.5000000	1
Zr5	Zr	1	0.5000000	0.5000000	0.5611130	1
Zr6	Zr	1	0.5000000	0.5000000	0.4388870	1

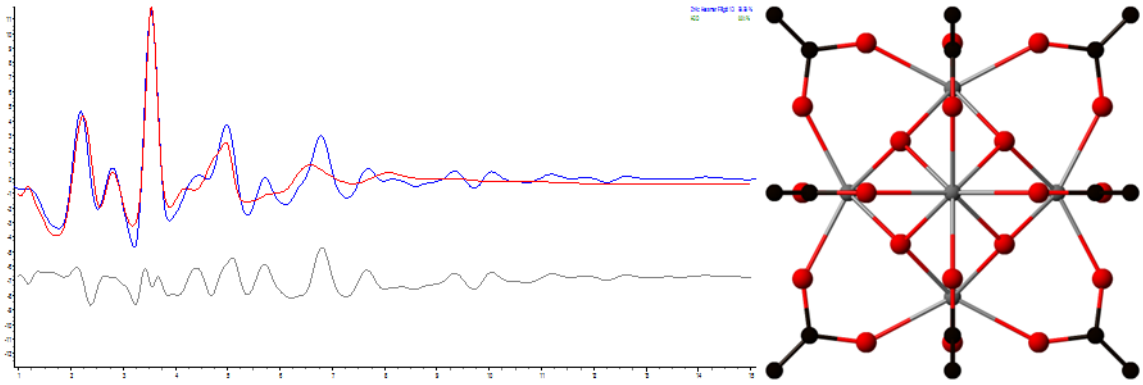

Figure 122: Observed and Calculated PDF from the fixed core refinement of ZAA13 from the 9-month data collection and the resultant model.

Table 65: The atomic coordinates of the model resulting from the fixed core refinement of ZAA13 from the 9-month data collection.

Atom Label	Atom Type	Multiplicity	Fractional X Coordinate	Fractional Y Coordinate	Fractional Z Coordinate	Fractional Occupancy
C1	C	1	0.5898586	0.5000000	0.5831255	1
C2	C	1	0.5000000	0.4101414	0.5831255	1
C3	C	1	0.4101414	0.5000000	0.5831255	1
C4	C	1	0.5000000	0.5898586	0.5831255	1
C5	C	1	0.5898586	0.5000000	0.4168745	1
C6	C	1	0.5000000	0.4101414	0.4168745	1
C7	C	1	0.4101414	0.5000000	0.4168745	1
C8	C	1	0.5000000	0.5898586	0.4168745	1
C9	C	1	0.5898586	0.4101414	0.5000000	1
C10	C	1	0.4101414	0.4101414	0.5000000	1
C11	C	1	0.4101414	0.5898586	0.5000000	1
C12	C	1	0.5898586	0.5898586	0.5000000	1
C13	C	1	0.6130435	0.5000000	0.6045731	1
C14	C	1	0.5000000	0.3869565	0.6045731	1
C15	C	1	0.3869565	0.5000000	0.6045731	1
C16	C	1	0.5000000	0.6130435	0.6045731	1
C17	C	1	0.6130435	0.5000000	0.3954269	1
C18	C	1	0.5000000	0.3869565	0.3954269	1
C19	C	1	0.3869565	0.5000000	0.3954269	1
C20	C	1	0.5000000	0.6130435	0.3954269	1
C21	C	1	0.6130435	0.3869565	0.5000000	1
C22	C	1	0.3869565	0.3869565	0.5000000	1
C23	C	1	0.3869565	0.6130435	0.5000000	1
C24	C	1	0.6130435	0.6130435	0.5000000	1
O1	O	1	0.5337442	0.5334149	0.4687843	1
O2	O	1	0.5337442	0.4665851	0.5312157	1
O3	O	1	0.4662558	0.5334149	0.4687843	1
O4	O	1	0.4662558	0.4665851	0.5312157	1

O5	O	1	0.4662558	0.4665851	0.4687843	1
O6	O	1	0.4662558	0.5334149	0.5312157	1
O7	O	1	0.5337442	0.4665851	0.4687843	1
O8	O	1	0.5337442	0.5334149	0.5312157	1
O9	O	1	0.5955516	0.5000000	0.5483644	1
O10	O	1	0.5955516	0.4477181	0.5000000	1
O11	O	1	0.5955516	0.5000000	0.4516356	1
O12	O	1	0.5955516	0.5522819	0.5000000	1
O13	O	1	0.5000000	0.5955516	0.5483644	1
O14	O	1	0.5522819	0.5955516	0.5000000	1
O15	O	1	0.5000000	0.5955516	0.4516356	1
O16	O	1	0.4477181	0.5955516	0.5000000	1
O17	O	1	0.4044484	0.5000000	0.5483644	1
O18	O	1	0.4044484	0.5522819	0.5000000	1
O19	O	1	0.4044484	0.5000000	0.4516356	1
O20	O	1	0.4044484	0.4477181	0.5000000	1
O21	O	1	0.5000000	0.4044484	0.5483644	1
O22	O	1	0.4477181	0.4044484	0.5000000	1
O23	O	1	0.5000000	0.4044484	0.4516356	1
O24	O	1	0.5522819	0.4044484	0.5000000	1
O25	O	1	0.5522819	0.5000000	0.5883919	1
O26	O	1	0.5000000	0.5522819	0.5883919	1
O27	O	1	0.4477181	0.5000000	0.5883919	1
O28	O	1	0.5000000	0.4477181	0.5883919	1
O29	O	1	0.5522819	0.5000000	0.4116081	1
O30	O	1	0.5000000	0.4477181	0.4116081	1
O31	O	1	0.4477181	0.5000000	0.4116081	1
O32	O	1	0.5000000	0.5522819	0.4116081	1
Zr1	Zr	1	0.5662340	0.5000000	0.5000000	1
Zr2	Zr	1	0.5000000	0.566234	0.5000000	1
Zr3	Zr	1	0.4337660	0.5000000	0.5000000	1
Zr4	Zr	1	0.5000000	0.433766	0.5000000	1
Zr5	Zr	1	0.5000000	0.5000000	0.5612711	1
Zr6	Zr	1	0.5000000	0.5000000	0.4387289	1

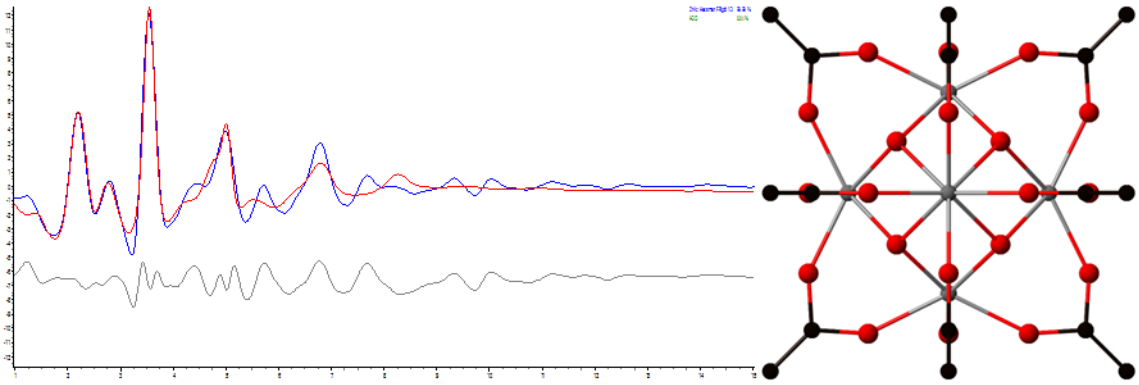

Figure 123: Observed and Calculated PDF from the fixed core refinement of ZAA16 from the 9-month data collection and the resultant model.

Table 66: The atomic coordinates of the model resulting from the fixed core refinement of ZAA16 from the 9-month data collection.

Atom Label	Atom Type	Multiplicity	Fractional X Coordinate	Fractional Y Coordinate	Fractional Z Coordinate	Fractional Occupancy
C1	C	1	0.5903289	0.5000000	0.5835606	1
C2	C	1	0.5000000	0.4096711	0.5835606	1
C3	C	1	0.4096711	0.5000000	0.5835606	1
C4	C	1	0.5000000	0.5903289	0.5835606	1
C5	C	1	0.5903289	0.5000000	0.4164394	1
C6	C	1	0.5000000	0.4096711	0.4164394	1
C7	C	1	0.4096711	0.5000000	0.4164394	1
C8	C	1	0.5000000	0.5903289	0.4164394	1
C9	C	1	0.5903289	0.4096711	0.5000000	1
C10	C	1	0.4096711	0.4096711	0.5000000	1
C11	C	1	0.4096711	0.5903289	0.5000000	1
C12	C	1	0.5903289	0.5903289	0.5000000	1
C13	C	1	0.6176215	0.5000000	0.6088081	1
C14	C	1	0.5000000	0.3823785	0.6088081	1
C15	C	1	0.3823785	0.5000000	0.6088081	1
C16	C	1	0.5000000	0.6176215	0.6088081	1
C17	C	1	0.6176215	0.5000000	0.3911919	1
C18	C	1	0.5000000	0.3823785	0.3911919	1
C19	C	1	0.3823785	0.5000000	0.3911919	1
C20	C	1	0.5000000	0.6176215	0.3911919	1
C21	C	1	0.6176215	0.3823785	0.5000000	1
C22	C	1	0.3823785	0.3823785	0.5000000	1
C23	C	1	0.3823785	0.6176215	0.5000000	1
C24	C	1	0.6176215	0.6176215	0.5000000	1
O1	O	1	0.5342290	0.5338951	0.4683358	1
O2	O	1	0.5342290	0.4661049	0.5316642	1
O3	O	1	0.4657710	0.5338951	0.4683358	1
O4	O	1	0.4657710	0.4661049	0.5316642	1

O5	O	1	0.4657710	0.4661049	0.4683358	1
O6	O	1	0.4657710	0.5338951	0.5316642	1
O7	O	1	0.5342290	0.4661049	0.4683358	1
O8	O	1	0.5342290	0.5338951	0.5316642	1
O9	O	1	0.5926342	0.5000000	0.5491222	1
O10	O	1	0.5926342	0.446899	0.5000000	1
O11	O	1	0.5926342	0.5000000	0.4508778	1
O12	O	1	0.5926342	0.5531010	0.5000000	1
O13	O	1	0.5000000	0.5926342	0.5491222	1
O14	O	1	0.5531010	0.5926342	0.5000000	1
O15	O	1	0.5000000	0.5926342	0.4508778	1
O16	O	1	0.4468990	0.5926342	0.5000000	1
O17	O	1	0.4073658	0.5000000	0.5491222	1
O18	O	1	0.4073658	0.5531010	0.5000000	1
O19	O	1	0.4073658	0.5000000	0.4508778	1
O20	O	1	0.4073658	0.4468990	0.5000000	1
O21	O	1	0.5000000	0.4073658	0.5491222	1
O22	O	1	0.4468990	0.4073658	0.5000000	1
O23	O	1	0.5000000	0.4073658	0.4508778	1
O24	O	1	0.5531010	0.4073658	0.5000000	1
O25	O	1	0.5531010	0.5000000	0.5856931	1
O26	O	1	0.5000000	0.5531010	0.5856931	1
O27	O	1	0.4468990	0.5000000	0.5856931	1
O28	O	1	0.5000000	0.4468990	0.5856931	1
O29	O	1	0.5531010	0.5000000	0.4143069	1
O30	O	1	0.5000000	0.4468990	0.4143069	1
O31	O	1	0.4468990	0.5000000	0.4143069	1
O32	O	1	0.5000000	0.5531010	0.4143069	1
Zr1	Zr	1	0.5663577	0.5000000	0.5000000	1
Zr2	Zr	1	0.5000000	0.5663577	0.5000000	1
Zr3	Zr	1	0.4336423	0.5000000	0.5000000	1
Zr4	Zr	1	0.5000000	0.4336423	0.5000000	1
Zr5	Zr	1	0.5000000	0.5000000	0.5613855	1
Zr6	Zr	1	0.5000000	0.5000000	0.4386145	1

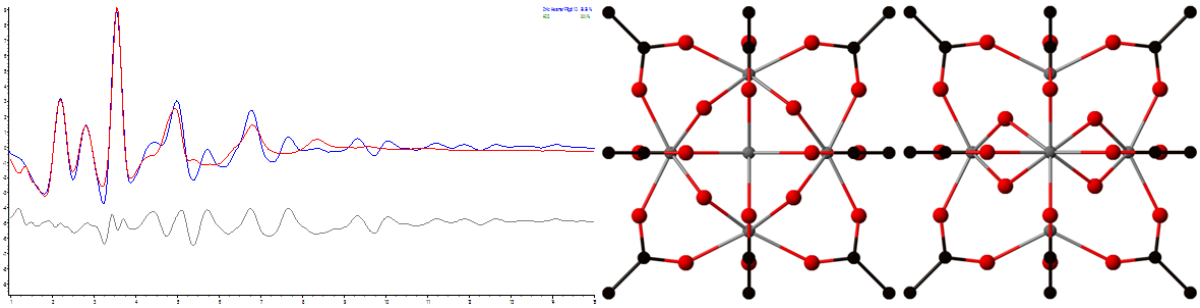

Figure 124: Observed and Calculated PDF from the chandelier core refinement of ZAA1 from the 9-month data collection and the resultant model viewed from the axial (left) and equatorial (right) positions.

Table 67: The atomic coordinates of the model resulting from the chandelier core refinement of ZAA1 from the 9-month data collection.

Atom Label	Atom Type	Multiplicity	Fractional X Coordinate	Fractional Y Coordinate	Fractional Z Coordinate	Fractional Occupancy
C1	C	1	0.5892073	0.5000000	0.5825229	1
C2	C	1	0.5000000	0.4107927	0.5825229	1
C3	C	1	0.4107927	0.5000000	0.5825229	1
C4	C	1	0.5000000	0.5892073	0.5825229	1
C5	C	1	0.5892073	0.5000000	0.4174771	1
C6	C	1	0.5000000	0.4107927	0.4174771	1
C7	C	1	0.4107927	0.5000000	0.4174771	1
C8	C	1	0.5000000	0.5892073	0.4174771	1
C9	C	1	0.5892073	0.4107927	0.5000000	1
C10	C	1	0.4107927	0.4107927	0.5000000	1
C11	C	1	0.4107927	0.5892073	0.5000000	1
C12	C	1	0.5892073	0.5892073	0.5000000	1
C13	C	1	0.6191258	0.5000000	0.6101997	1
C14	C	1	0.5000000	0.3808742	0.6101997	1
C15	C	1	0.3808742	0.5000000	0.6101997	1
C16	C	1	0.5000000	0.6191258	0.6101997	1
C17	C	1	0.6191258	0.5000000	0.3898003	1
C18	C	1	0.5000000	0.3808742	0.3898003	1
C19	C	1	0.3808742	0.5000000	0.3898003	1
C20	C	1	0.5000000	0.6191258	0.3898003	1
C21	C	1	0.6191258	0.3808742	0.5000000	1
C22	C	1	0.3808742	0.3808742	0.5000000	1
C23	C	1	0.3808742	0.6191258	0.5000000	1
C24	C	1	0.6191258	0.6191258	0.5000000	1
O1	O	1	0.5382190	0.4617810	0.4736479	1
O2	O	1	0.5382190	0.4617810	0.5263521	1
O3	O	1	0.4617810	0.4617810	0.4736479	1
O4	O	1	0.4617810	0.4617810	0.5263521	1
O5	O	1	0.4617810	0.5382190	0.4736479	1
O6	O	1	0.4617810	0.5382190	0.5263521	1

O7	O	1	0.5382190	0.5382190	0.4736479	1
O8	O	1	0.5382190	0.5382190	0.5263521	1
O9	O	1	0.5933653	0.5000000	0.5495326	1
O10	O	1	0.5933653	0.4464553	0.5000000	1
O11	O	1	0.5933653	0.5000000	0.4504674	1
O12	O	1	0.5933653	0.5535447	0.5000000	1
O13	O	1	0.5000000	0.5933653	0.5495326	1
O14	O	1	0.5535447	0.5933653	0.5000000	1
O15	O	1	0.5000000	0.5933653	0.4504674	1
O16	O	1	0.4464553	0.5933653	0.5000000	1
O17	O	1	0.4066347	0.5000000	0.5495326	1
O18	O	1	0.4066347	0.5535447	0.5000000	1
O19	O	1	0.4066347	0.5000000	0.4504674	1
O20	O	1	0.4066347	0.4464553	0.5000000	1
O21	O	1	0.5000000	0.4066347	0.5495326	1
O22	O	1	0.4464553	0.4066347	0.5000000	1
O23	O	1	0.5000000	0.4066347	0.4504674	1
O24	O	1	0.5535447	0.4066347	0.5000000	1
O25	O	1	0.5535447	0.5000000	0.5863694	1
O26	O	1	0.5000000	0.5535447	0.5863694	1
O27	O	1	0.4464553	0.5000000	0.5863694	1
O28	O	1	0.5000000	0.4464553	0.5863694	1
O29	O	1	0.5535447	0.5000000	0.4136306	1
O30	O	1	0.5000000	0.4464553	0.4136306	1
O31	O	1	0.4464553	0.5000000	0.4136306	1
O32	O	1	0.5000000	0.5535447	0.4136306	1
Zr1	Zr	1	0.5665638	0.5000000	0.5000000	1
Zr2	Zr	1	0.5000000	0.5665638	0.5000000	1
Zr3	Zr	1	0.4334362	0.5000000	0.5000000	1
Zr4	Zr	1	0.5000000	0.4334362	0.5000000	1
Zr5	Zr	1	0.5000000	0.5000000	0.5615762	1
Zr6	Zr	1	0.5000000	0.5000000	0.4384238	1

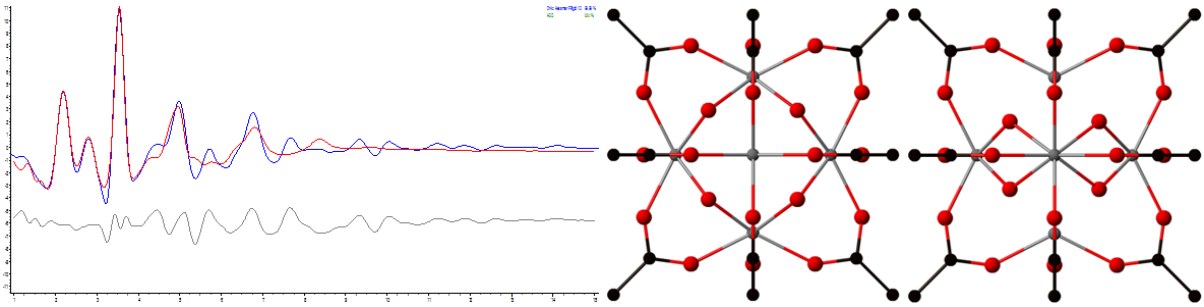

Figure 125: Observed and Calculated PDF from the chandelier core refinement of ZAA4 from the 9-month data collection and the resultant model viewed from the axial (left) and equatorial (right) positions.

Table 68: The atomic coordinates of the model resulting from the chandelier core refinement of ZAA4 from the 9-month data collection.

Atom Label	Atom Type	Multiplicity	Fractional X Coordinate	Fractional Y Coordinate	Fractional Z Coordinate	Fractional Occupancy
C1	C	1	0.5887031	0.5000000	0.5820565	1
C2	C	1	0.5000000	0.4112969	0.5820565	1
C3	C	1	0.4112969	0.5000000	0.5820565	1
C4	C	1	0.5000000	0.5887031	0.5820565	1
C5	C	1	0.5887031	0.5000000	0.4179435	1
C6	C	1	0.5000000	0.4112969	0.4179435	1
C7	C	1	0.4112969	0.5000000	0.4179435	1
C8	C	1	0.5000000	0.5887031	0.4179435	1
C9	C	1	0.5887031	0.4112969	0.5000000	1
C10	C	1	0.4112969	0.4112969	0.5000000	1
C11	C	1	0.4112969	0.5887031	0.5000000	1
C12	C	1	0.5887031	0.5887031	0.5000000	1
C13	C	1	0.6196540	0.5000000	0.6106883	1
C14	C	1	0.5000000	0.3803460	0.6106883	1
C15	C	1	0.3803460	0.5000000	0.6106883	1
C16	C	1	0.5000000	0.6196540	0.6106883	1
C17	C	1	0.6196540	0.5000000	0.3893117	1
C18	C	1	0.5000000	0.3803460	0.3893117	1
C19	C	1	0.3803460	0.5000000	0.3893117	1
C20	C	1	0.5000000	0.6196540	0.3893117	1
C21	C	1	0.6196540	0.3803460	0.5000000	1
C22	C	1	0.3803460	0.3803460	0.5000000	1
C23	C	1	0.3803460	0.6196540	0.5000000	1
C24	C	1	0.6196540	0.6196540	0.5000000	1
O1	O	1	0.5381895	0.4618105	0.4733540	1
O2	O	1	0.5381895	0.4618105	0.5266460	1
O3	O	1	0.4618105	0.4618105	0.4733540	1
O4	O	1	0.4618105	0.4618105	0.5266460	1
O5	O	1	0.4618105	0.5381895	0.4733540	1
O6	O	1	0.4618105	0.5381895	0.5266460	1

O7	O	1	0.5381895	0.5381895	0.4733540	1
O8	O	1	0.5381895	0.5381895	0.5266460	1
O9	O	1	0.5934508	0.5000000	0.5492641	1
O10	O	1	0.5934508	0.4467455	0.5000000	1
O11	O	1	0.5934508	0.5000000	0.4507359	1
O12	O	1	0.5934508	0.5532545	0.5000000	1
O13	O	1	0.5000000	0.5934508	0.5492641	1
O14	O	1	0.5532545	0.5934508	0.5000000	1
O15	O	1	0.5000000	0.5934508	0.4507359	1
O16	O	1	0.4467455	0.5934508	0.5000000	1
O17	O	1	0.4065492	0.5000000	0.5492641	1
O18	O	1	0.4065492	0.5532545	0.5000000	1
O19	O	1	0.4065492	0.5000000	0.4507359	1
O20	O	1	0.4065492	0.4467455	0.5000000	1
O21	O	1	0.5000000	0.4065492	0.5492641	1
O22	O	1	0.4467455	0.4065492	0.5000000	1
O23	O	1	0.5000000	0.4065492	0.4507359	1
O24	O	1	0.5532545	0.4065492	0.5000000	1
O25	O	1	0.5532545	0.5000000	0.5864485	1
O26	O	1	0.5000000	0.5532545	0.5864485	1
O27	O	1	0.4467455	0.5000000	0.5864485	1
O28	O	1	0.5000000	0.4467455	0.5864485	1
O29	O	1	0.5532545	0.5000000	0.4135515	1
O30	O	1	0.5000000	0.4467455	0.4135515	1
O31	O	1	0.4467455	0.5000000	0.4135515	1
O32	O	1	0.5000000	0.5532545	0.4135515	1
Zr1	Zr	1	0.5665569	0.5000000	0.5000000	1
Zr2	Zr	1	0.5000000	0.5665569	0.5000000	1
Zr3	Zr	1	0.4334431	0.5000000	0.5000000	1
Zr4	Zr	1	0.5000000	0.4334431	0.5000000	1
Zr5	Zr	1	0.5000000	0.5000000	0.5615697	1
Zr6	Zr	1	0.5000000	0.5000000	0.4384303	1

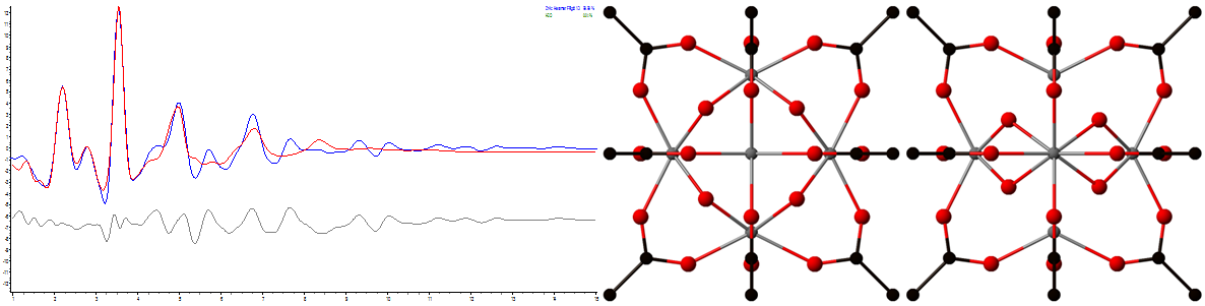

Figure 126: Observed and Calculated PDF from the chandelier core refinement of ZAA7 from the 9-month data collection and the resultant model viewed from the axial (left) and equatorial (right) positions.

Table 69: The atomic coordinates of the model resulting from the chandelier core refinement of ZAA7 from the 9-month data collection.

Atom Label	Atom Type	Multiplicity	Fractional X Coordinate	Fractional Y Coordinate	Fractional Z Coordinate	Fractional Occupancy
C1	C	1	0.5885349	0.5000000	0.5819010	1
C2	C	1	0.5000000	0.4114651	0.5819010	1
C3	C	1	0.4114651	0.5000000	0.5819010	1
C4	C	1	0.5000000	0.5885349	0.5819010	1
C5	C	1	0.5885349	0.5000000	0.4180990	1
C6	C	1	0.5000000	0.4114651	0.4180990	1
C7	C	1	0.4114651	0.5000000	0.4180990	1
C8	C	1	0.5000000	0.5885349	0.4180990	1
C9	C	1	0.5885349	0.4114651	0.5000000	1
C10	C	1	0.4114651	0.4114651	0.5000000	1
C11	C	1	0.4114651	0.5885349	0.5000000	1
C12	C	1	0.5885349	0.5885349	0.5000000	1
C13	C	1	0.6195578	0.5000000	0.6105993	1
C14	C	1	0.5000000	0.3804422	0.6105993	1
C15	C	1	0.3804422	0.5000000	0.6105993	1
C16	C	1	0.5000000	0.6195578	0.6105993	1
C17	C	1	0.6195578	0.5000000	0.3894007	1
C18	C	1	0.5000000	0.3804422	0.3894007	1
C19	C	1	0.3804422	0.5000000	0.3894007	1
C20	C	1	0.5000000	0.6195578	0.3894007	1
C21	C	1	0.6195578	0.3804422	0.5000000	1
C22	C	1	0.3804422	0.3804422	0.5000000	1
C23	C	1	0.3804422	0.6195578	0.5000000	1
C24	C	1	0.6195578	0.6195578	0.5000000	1
O1	O	1	0.5383295	0.4616705	0.4737344	1
O2	O	1	0.5383295	0.4616705	0.5262656	1
O3	O	1	0.4616705	0.4616705	0.4737344	1
O4	O	1	0.4616705	0.4616705	0.5262656	1
O5	O	1	0.4616705	0.5383295	0.4737344	1
O6	O	1	0.4616705	0.5383295	0.5262656	1

O7	O	1	0.5383295	0.5383295	0.4737344	1
O8	O	1	0.5383295	0.5383295	0.5262656	1
O9	O	1	0.5934261	0.5000000	0.5494132	1
O10	O	1	0.5934261	0.4465843	0.5000000	1
O11	O	1	0.5934261	0.5000000	0.4505868	1
O12	O	1	0.5934261	0.5534157	0.5000000	1
O13	O	1	0.5000000	0.5934261	0.5494132	1
O14	O	1	0.5534157	0.5934261	0.5000000	1
O15	O	1	0.5000000	0.5934261	0.4505868	1
O16	O	1	0.4465843	0.5934261	0.5000000	1
O17	O	1	0.4065739	0.5000000	0.5494132	1
O18	O	1	0.4065739	0.5534157	0.5000000	1
O19	O	1	0.4065739	0.5000000	0.4505868	1
O20	O	1	0.4065739	0.4465843	0.5000000	1
O21	O	1	0.5000000	0.4065739	0.5494132	1
O22	O	1	0.4465843	0.4065739	0.5000000	1
O23	O	1	0.5000000	0.4065739	0.4505868	1
O24	O	1	0.5534157	0.4065739	0.5000000	1
O25	O	1	0.5534157	0.5000000	0.5864256	1
O26	O	1	0.5000000	0.5534157	0.5864256	1
O27	O	1	0.4465843	0.5000000	0.5864256	1
O28	O	1	0.5000000	0.4465843	0.5864256	1
O29	O	1	0.5534157	0.5000000	0.4135744	1
O30	O	1	0.5000000	0.4465843	0.4135744	1
O31	O	1	0.4465843	0.5000000	0.4135744	1
O32	O	1	0.5000000	0.5534157	0.4135744	1
Zr1	Zr	1	0.5665601	0.5000000	0.5000000	1
Zr2	Zr	1	0.5000000	0.5665601	0.5000000	1
Zr3	Zr	1	0.4334399	0.5000000	0.5000000	1
Zr4	Zr	1	0.5000000	0.4334399	0.5000000	1
Zr5	Zr	1	0.5000000	0.5000000	0.5615727	1
Zr6	Zr	1	0.5000000	0.5000000	0.4384273	1

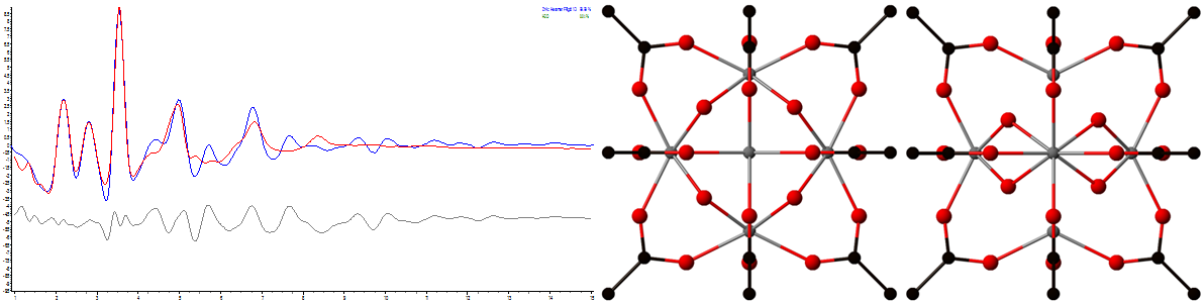

Figure 127: Observed and Calculated PDF from the chandelier core refinement of ZAA10 from the 9-month data collection and the resultant model viewed from the axial (left) and equatorial (right) positions.

Table 70: The atomic coordinates of the model resulting from the chandelier core refinement of ZAA10 from the 9-month data collection.

Atom Label	Atom Type	Multiplicity	Fractional X Coordinate	Fractional Y Coordinate	Fractional Z Coordinate	Fractional Occupancy
C1	C	1	0.5891590	0.5000000	0.5824783	1
C2	C	1	0.5000000	0.4108410	0.5824783	1
C3	C	1	0.4108410	0.5000000	0.5824783	1
C4	C	1	0.5000000	0.5891590	0.5824783	1
C5	C	1	0.5891590	0.5000000	0.4175217	1
C6	C	1	0.5000000	0.4108410	0.4175217	1
C7	C	1	0.4108410	0.5000000	0.4175217	1
C8	C	1	0.5000000	0.5891590	0.4175217	1
C9	C	1	0.5891590	0.4108410	0.5000000	1
C10	C	1	0.4108410	0.4108410	0.5000000	1
C11	C	1	0.4108410	0.5891590	0.5000000	1
C12	C	1	0.5891590	0.5891590	0.5000000	1
C13	C	1	0.6197118	0.5000000	0.6107418	1
C14	C	1	0.5000000	0.3802882	0.6107418	1
C15	C	1	0.3802882	0.5000000	0.6107418	1
C16	C	1	0.5000000	0.6197118	0.6107418	1
C17	C	1	0.6197118	0.5000000	0.3892582	1
C18	C	1	0.5000000	0.3802882	0.3892582	1
C19	C	1	0.3802882	0.5000000	0.3892582	1
C20	C	1	0.5000000	0.6197118	0.3892582	1
C21	C	1	0.6197118	0.3802882	0.5000000	1
C22	C	1	0.3802882	0.3802882	0.5000000	1
C23	C	1	0.3802882	0.6197118	0.5000000	1
C24	C	1	0.6197118	0.6197118	0.5000000	1
O1	O	1	0.5384231	0.4615769	0.4737598	1
O2	O	1	0.5384231	0.4615769	0.5262402	1
O3	O	1	0.4615769	0.4615769	0.4737598	1
O4	O	1	0.4615769	0.4615769	0.5262402	1
O5	O	1	0.4615769	0.5384231	0.4737598	1
O6	O	1	0.4615769	0.5384231	0.5262402	1

O7	O	1	0.5384231	0.5384231	0.4737598	1
O8	O	1	0.5384231	0.5384231	0.5262402	1
O9	O	1	0.5931687	0.5000000	0.5497031	1
O10	O	1	0.5931687	0.4462710	0.5000000	1
O11	O	1	0.5931687	0.5000000	0.4502969	1
O12	O	1	0.5931687	0.5537290	0.5000000	1
O13	O	1	0.5000000	0.5931687	0.5497031	1
O14	O	1	0.5537290	0.5931687	0.5000000	1
O15	O	1	0.5000000	0.5931687	0.4502969	1
O16	O	1	0.4462710	0.5931687	0.5000000	1
O17	O	1	0.4068313	0.5000000	0.5497031	1
O18	O	1	0.4068313	0.5537290	0.5000000	1
O19	O	1	0.4068313	0.5000000	0.4502969	1
O20	O	1	0.4068313	0.4462710	0.5000000	1
O21	O	1	0.5000000	0.4068313	0.5497031	1
O22	O	1	0.4462710	0.4068313	0.5000000	1
O23	O	1	0.5000000	0.4068313	0.4502969	1
O24	O	1	0.5537290	0.4068313	0.5000000	1
O25	O	1	0.5537290	0.5000000	0.5861875	1
O26	O	1	0.5000000	0.5537290	0.5861875	1
O27	O	1	0.4462710	0.5000000	0.5861875	1
O28	O	1	0.5000000	0.4462710	0.5861875	1
O29	O	1	0.5537290	0.5000000	0.4138125	1
O30	O	1	0.5000000	0.4462710	0.4138125	1
O31	O	1	0.4462710	0.5000000	0.4138125	1
O32	O	1	0.5000000	0.5537290	0.4138125	1
Zr1	Zr	1	0.5666025	0.5000000	0.5000000	1
Zr2	Zr	1	0.5000000	0.5666025	0.5000000	1
Zr3	Zr	1	0.4333975	0.5000000	0.5000000	1
Zr4	Zr	1	0.5000000	0.4333975	0.5000000	1
Zr5	Zr	1	0.5000000	0.5000000	0.5616119	1
Zr6	Zr	1	0.5000000	0.5000000	0.4383881	1

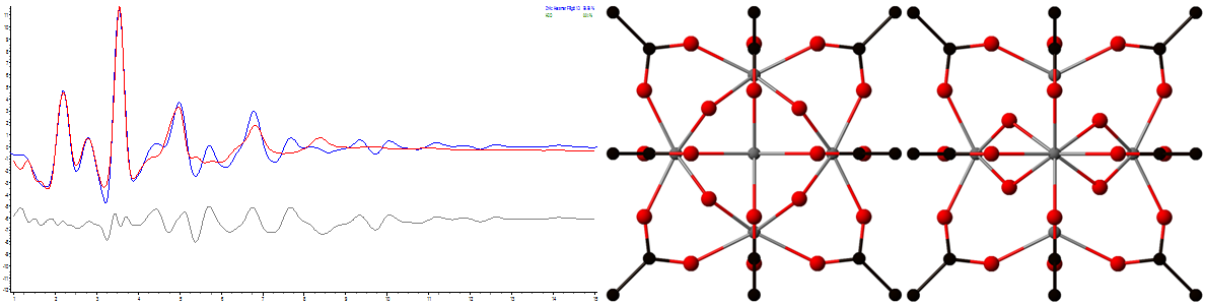

Figure 128: Observed and Calculated PDF from the chandelier core refinement of ZAA13 from the 9-month data collection and the resultant model viewed from the axial (left) and equatorial (right) positions.

Table 71: The atomic coordinates of the model resulting from the chandelier core refinement of ZAA13 from the 9-month data collection.

Atom Label	Atom Type	Multiplicity	Fractional X Coordinate	Fractional Y Coordinate	Fractional Z Coordinate	Fractional Occupancy
C1	C	1	0.5890725	0.5000000	0.5823982	1
C2	C	1	0.5000000	0.4109275	0.5823982	1
C3	C	1	0.4109275	0.5000000	0.5823982	1
C4	C	1	0.5000000	0.5890725	0.5823982	1
C5	C	1	0.5890725	0.5000000	0.4176018	1
C6	C	1	0.5000000	0.4109275	0.4176018	1
C7	C	1	0.4109275	0.5000000	0.4176018	1
C8	C	1	0.5000000	0.5890725	0.4176018	1
C9	C	1	0.5890725	0.4109275	0.5000000	1
C10	C	1	0.4109275	0.4109275	0.5000000	1
C11	C	1	0.4109275	0.5890725	0.5000000	1
C12	C	1	0.5890725	0.5890725	0.5000000	1
C13	C	1	0.6197130	0.5000000	0.6107429	1
C14	C	1	0.5000000	0.3802870	0.6107429	1
C15	C	1	0.3802870	0.5000000	0.6107429	1
C16	C	1	0.5000000	0.6197130	0.6107429	1
C17	C	1	0.6197130	0.5000000	0.3892571	1
C18	C	1	0.5000000	0.3802870	0.3892571	1
C19	C	1	0.3802870	0.5000000	0.3892571	1
C20	C	1	0.5000000	0.6197130	0.3892571	1
C21	C	1	0.6197130	0.3802870	0.5000000	1
C22	C	1	0.3802870	0.3802870	0.5000000	1
C23	C	1	0.3802870	0.6197130	0.5000000	1
C24	C	1	0.6197130	0.6197130	0.5000000	1
O1	O	1	0.5384492	0.4615508	0.4737614	1
O2	O	1	0.5384492	0.4615508	0.5262386	1
O3	O	1	0.4615508	0.4615508	0.4737614	1
O4	O	1	0.4615508	0.4615508	0.5262386	1
O5	O	1	0.4615508	0.5384492	0.4737614	1
O6	O	1	0.4615508	0.5384492	0.5262386	1

O7	O	1	0.5384492	0.5384492	0.4737614	1
O8	O	1	0.5384492	0.5384492	0.5262386	1
O9	O	1	0.5931392	0.5000000	0.5496645	1
O10	O	1	0.5931392	0.4463127	0.5000000	1
O11	O	1	0.5931392	0.5000000	0.4503355	1
O12	O	1	0.5931392	0.5536873	0.5000000	1
O13	O	1	0.5000000	0.5931392	0.5496645	1
O14	O	1	0.5536873	0.5931392	0.5000000	1
O15	O	1	0.5000000	0.5931392	0.4503355	1
O16	O	1	0.4463127	0.5931392	0.5000000	1
O17	O	1	0.4068608	0.5000000	0.5496645	1
O18	O	1	0.4068608	0.5536873	0.5000000	1
O19	O	1	0.4068608	0.5000000	0.4503355	1
O20	O	1	0.4068608	0.4463127	0.5000000	1
O21	O	1	0.5000000	0.4068608	0.5496645	1
O22	O	1	0.4463127	0.4068608	0.5000000	1
O23	O	1	0.5000000	0.4068608	0.4503355	1
O24	O	1	0.5536873	0.4068608	0.5000000	1
O25	O	1	0.5536873	0.5000000	0.5861603	1
O26	O	1	0.5000000	0.5536873	0.5861603	1
O27	O	1	0.4463127	0.5000000	0.5861603	1
O28	O	1	0.5000000	0.4463127	0.5861603	1
O29	O	1	0.5536873	0.5000000	0.4138397	1
O30	O	1	0.5000000	0.4463127	0.4138397	1
O31	O	1	0.4463127	0.5000000	0.4138397	1
O32	O	1	0.5000000	0.5536873	0.4138397	1
Zr1	Zr	1	0.5665839	0.5000000	0.5000000	1
Zr2	Zr	1	0.5000000	0.5665839	0.5000000	1
Zr3	Zr	1	0.4334161	0.5000000	0.5000000	1
Zr4	Zr	1	0.5000000	0.4334161	0.5000000	1
Zr5	Zr	1	0.5000000	0.5000000	0.5615947	1
Zr6	Zr	1	0.5000000	0.5000000	0.4384053	1

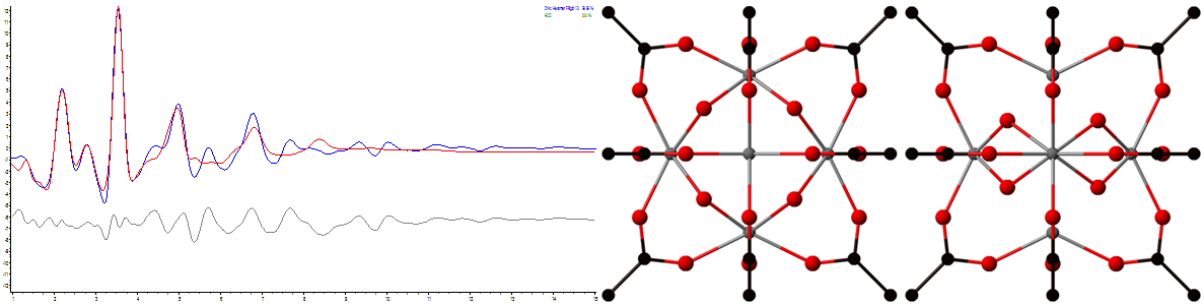

Figure 129: Observed and Calculated PDF from the chandelier core refinement of ZAA16 from the 9-month data collection and the resultant model viewed from the axial (left) and equatorial (right) positions.

Table 72: The atomic coordinates of the model resulting from the chandelier core refinement of ZAA16 from the 9-month data collection.

Atom Label	Atom Type	Multiplicity	Fractional X Coordinate	Fractional Y Coordinate	Fractional Z Coordinate	Fractional Occupancy
C1	C	1	0.5890164	0.5000000	0.5823463	1
C2	C	1	0.5000000	0.4109836	0.5823463	1
C3	C	1	0.4109836	0.5000000	0.5823463	1
C4	C	1	0.5000000	0.5890164	0.5823463	1
C5	C	1	0.5890164	0.5000000	0.4176537	1
C6	C	1	0.5000000	0.4109836	0.4176537	1
C7	C	1	0.4109836	0.5000000	0.4176537	1
C8	C	1	0.5000000	0.5890164	0.4176537	1
C9	C	1	0.5890164	0.4109836	0.5000000	1
C10	C	1	0.4109836	0.4109836	0.5000000	1
C11	C	1	0.4109836	0.5890164	0.5000000	1
C12	C	1	0.5890164	0.5890164	0.5000000	1
C13	C	1	0.6196859	0.5000000	0.6107178	1
C14	C	1	0.5000000	0.3803141	0.6107178	1
C15	C	1	0.3803141	0.5000000	0.6107178	1
C16	C	1	0.5000000	0.6196859	0.6107178	1
C17	C	1	0.6196859	0.5000000	0.3892822	1
C18	C	1	0.5000000	0.3803141	0.3892822	1
C19	C	1	0.3803141	0.5000000	0.3892822	1
C20	C	1	0.5000000	0.6196859	0.3892822	1
C21	C	1	0.6196859	0.3803141	0.5000000	1
C22	C	1	0.3803141	0.3803141	0.5000000	1
C23	C	1	0.3803141	0.6196859	0.5000000	1
C24	C	1	0.6196859	0.6196859	0.5000000	1
O1	O	1	0.5383985	0.4616015	0.4737987	1
O2	O	1	0.5383985	0.4616015	0.5262013	1
O3	O	1	0.4616015	0.4616015	0.4737987	1
O4	O	1	0.4616015	0.4616015	0.5262013	1
O5	O	1	0.4616015	0.5383985	0.4737987	1
O6	O	1	0.4616015	0.5383985	0.5262013	1

O7	O	1	0.5383985	0.5383985	0.4737987	1
O8	O	1	0.5383985	0.5383985	0.5262013	1
O9	O	1	0.5930013	0.5000000	0.5497616	1
O10	O	1	0.5930013	0.4462077	0.5000000	1
O11	O	1	0.5930013	0.5000000	0.4502384	1
O12	O	1	0.5930013	0.5537923	0.5000000	1
O13	O	1	0.5000000	0.5930013	0.5497616	1
O14	O	1	0.5537923	0.5930013	0.5000000	1
O15	O	1	0.5000000	0.5930013	0.4502384	1
O16	O	1	0.4462077	0.5930013	0.5000000	1
O17	O	1	0.4069987	0.5000000	0.5497616	1
O18	O	1	0.4069987	0.5537923	0.5000000	1
O19	O	1	0.4069987	0.5000000	0.4502384	1
O20	O	1	0.4069987	0.4462077	0.5000000	1
O21	O	1	0.5000000	0.4069987	0.5497616	1
O22	O	1	0.4462077	0.4069987	0.5000000	1
O23	O	1	0.5000000	0.4069987	0.4502384	1
O24	O	1	0.5537923	0.4069987	0.5000000	1
O25	O	1	0.5537923	0.5000000	0.5860326	1
O26	O	1	0.5000000	0.5537923	0.5860326	1
O27	O	1	0.4462077	0.5000000	0.5860326	1
O28	O	1	0.5000000	0.4462077	0.5860326	1
O29	O	1	0.5537923	0.5000000	0.4139674	1
O30	O	1	0.5000000	0.4462077	0.4139674	1
O31	O	1	0.4462077	0.5000000	0.4139674	1
O32	O	1	0.5000000	0.5537923	0.4139674	1
Zr1	Zr	1	0.5666035	0.5000000	0.5000000	1
Zr2	Zr	1	0.5000000	0.5666035	0.5000000	1
Zr3	Zr	1	0.4333965	0.5000000	0.5000000	1
Zr4	Zr	1	0.5000000	0.4333965	0.5000000	1
Zr5	Zr	1	0.5000000	0.5000000	0.5616128	1
Zr6	Zr	1	0.5000000	0.5000000	0.4383872	1

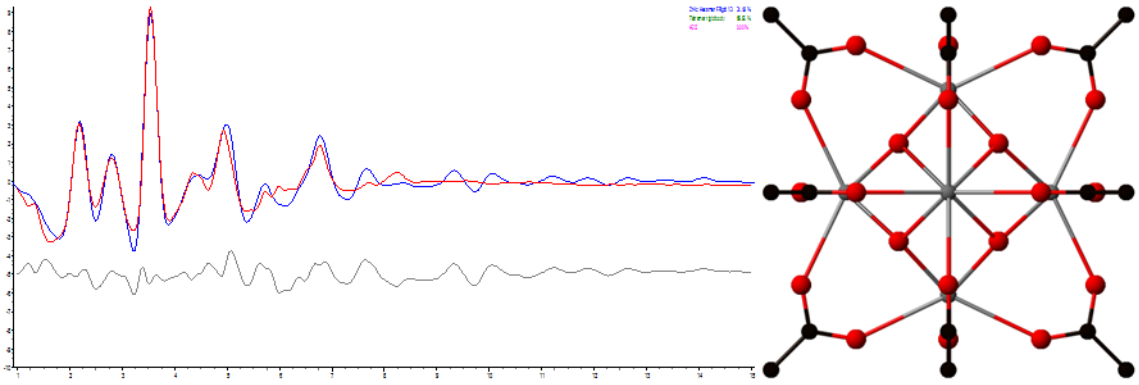

Figure 130: Observed and Calculated PDF from the fixed core refinement of ZAA1 from the 9-month data collection and the resultant model.

Table 73: The atomic coordinates of the model resulting from the fixed core refinement of ZAA1 from the 9-month data collection.

Atom Label	Atom Type	Multiplicity	Fractional X Coordinate	Fractional Y Coordinate	Fractional Z Coordinate	Fractional Occupancy
C1	C	1	0.5909252	0.5000000	0.5841121	1
C2	C	1	0.5000000	0.4090748	0.5841121	1
C3	C	1	0.4090748	0.5000000	0.5841121	1
C4	C	1	0.5000000	0.5909252	0.5841121	1
C5	C	1	0.5909252	0.5000000	0.4158879	1
C6	C	1	0.5000000	0.4090748	0.4158879	1
C7	C	1	0.4090748	0.5000000	0.4158879	1
C8	C	1	0.5000000	0.5909252	0.4158879	1
C9	C	1	0.5909252	0.4090748	0.5000000	1
C10	C	1	0.4090748	0.4090748	0.5000000	1
C11	C	1	0.4090748	0.5909252	0.5000000	1
C12	C	1	0.5909252	0.5909252	0.5000000	1
C13	C	1	0.6160689	0.5000000	0.6073718	1
C14	C	1	0.5000000	0.3839311	0.6073718	1
C15	C	1	0.3839311	0.5000000	0.6073718	1
C16	C	1	0.5000000	0.6160689	0.6073718	1
C17	C	1	0.6160689	0.5000000	0.3926282	1
C18	C	1	0.5000000	0.3839311	0.3926282	1
C19	C	1	0.3839311	0.5000000	0.3926282	1
C20	C	1	0.5000000	0.6160689	0.3926282	1
C21	C	1	0.6160689	0.3839311	0.5000000	1
C22	C	1	0.3839311	0.3839311	0.5000000	1
C23	C	1	0.3839311	0.6160689	0.5000000	1
C24	C	1	0.6160689	0.6160689	0.5000000	1
O1	O	1	0.5324841	0.5321671	0.4699499	1
O2	O	1	0.5324841	0.4678329	0.5300501	1
O3	O	1	0.4675159	0.5321671	0.4699499	1
O4	O	1	0.4675159	0.4678329	0.5300501	1

O5	O	1	0.4675159	0.4678329	0.4699499	1
O6	O	1	0.4675159	0.5321671	0.5300501	1
O7	O	1	0.5324841	0.4678329	0.4699499	1
O8	O	1	0.5324841	0.5321671	0.5300501	1
O9	O	1	0.5961288	0.5000000	0.555905	1
O10	O	1	0.5961288	0.4395668	0.5000000	1
O11	O	1	0.5961288	0.5000000	0.444095	1
O12	O	1	0.5961288	0.5604332	0.5000000	1
O13	O	1	0.5000000	0.5961288	0.555905	1
O14	O	1	0.5604332	0.5961288	0.5000000	1
O15	O	1	0.5000000	0.5961288	0.444095	1
O16	O	1	0.4395668	0.5961288	0.5000000	1
O17	O	1	0.4038712	0.5000000	0.555905	1
O18	O	1	0.4038712	0.5604332	0.5000000	1
O19	O	1	0.4038712	0.5000000	0.444095	1
O20	O	1	0.4038712	0.4395668	0.5000000	1
O21	O	1	0.5000000	0.4038712	0.555905	1
O22	O	1	0.4395668	0.4038712	0.5000000	1
O23	O	1	0.5000000	0.4038712	0.444095	1
O24	O	1	0.5604332	0.4038712	0.5000000	1
O25	O	1	0.5604332	0.5000000	0.5889258	1
O26	O	1	0.5000000	0.5604332	0.5889258	1
O27	O	1	0.4395668	0.5000000	0.5889258	1
O28	O	1	0.5000000	0.4395668	0.5889258	1
O29	O	1	0.5604332	0.5000000	0.4110742	1
O30	O	1	0.5000000	0.4395668	0.4110742	1
O31	O	1	0.4395668	0.5000000	0.4110742	1
O32	O	1	0.5000000	0.5604332	0.4110742	1
Zr1	Zr	1	0.567093	0.5000000	0.5000000	1
Zr2	Zr	1	0.5000000	0.567093	0.5000000	1
Zr3	Zr	1	0.432907	0.5000000	0.5000000	1
Zr4	Zr	1	0.5000000	0.432907	0.5000000	1
Zr5	Zr	1	0.5000000	0.5000000	0.5620657	1
Zr6	Zr	1	0.5000000	0.5000000	0.4379343	1

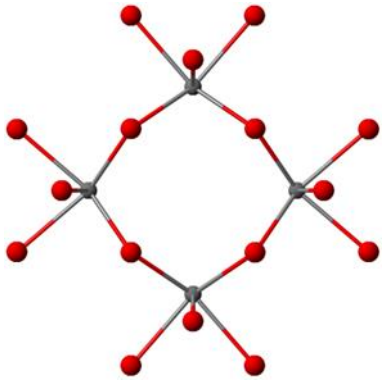

Figure 131: The tetrameric structure resulting from the fixed core refinement of ZAA1 from the 9-month data collection.

Table 74: The atomic coordinates of the tetrameric phase of the fixed core refinement of ZAA1 from the 9-month data collection.

Atom Label	Atom Type	Multiplicity	Fractional X Coordinate	Fractional Y Coordinate	Fractional Z Coordinate	Fractional Occupancy
O1	O	1	0.514304	0.485696	0.4747685	1
O2	O	1	0.485696	0.485696	0.5252315	1
O3	O	1	0.514304	0.514304	0.5252315	1
O4	O	1	0.485696	0.514304	0.4747685	1
O5	O	1	0.5000000	0.5302249	0.5468305	1
O6	O	1	0.5000000	0.4697751	0.5468305	1
O7	O	1	0.4697751	0.5000000	0.4531695	1
O8	O	1	0.5302249	0.5000000	0.4531695	1
O9	O	1	0.5142306	0.4594818	0.5000000	1
O10	O	1	0.4594818	0.4857694	0.5000000	1
O11	O	1	0.5405182	0.5142306	0.5000000	1
O12	O	1	0.4857694	0.5405182	0.5000000	1
O13	O	1	0.4594818	0.5142306	0.5000000	1
O14	O	1	0.5405182	0.4857694	0.5000000	1
O15	O	1	0.4857694	0.4594818	0.5000000	1
O16	O	1	0.5142306	0.5405182	0.5000000	1
O17	O	1	0.514304	0.485696	0.5252315	1
O18	O	1	0.485696	0.485696	0.4747685	1
O19	O	1	0.514304	0.514304	0.4747685	1
O20	O	1	0.485696	0.514304	0.5252315	1
O21	O	1	0.5000000	0.5302249	0.4531695	1
O22	O	1	0.5000000	0.4697751	0.4531695	1
O23	O	1	0.4697751	0.5000000	0.5468305	1
O24	O	1	0.5302249	0.5000000	0.5468305	1
Zr1	Zr	1	0.5000000	0.4759886	0.5000000	1
Zr2	Zr	1	0.4759886	0.5000000	0.5000000	1
Zr3	Zr	1	0.5240114	0.5000000	0.5000000	1
Zr4	Zr	1	0.5000000	0.5240114	0.5000000	1

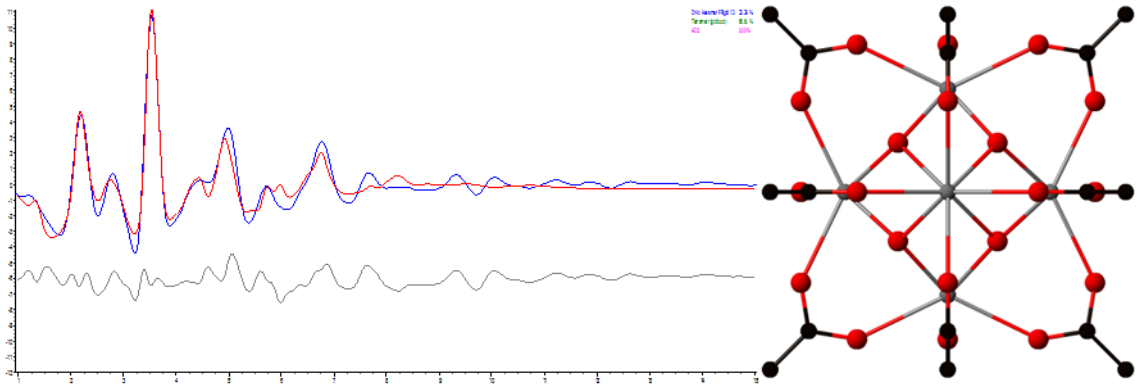

Figure 132: Observed and Calculated PDF from the fixed core refinement of ZAA4 from the 9-month data collection and the resultant model.

Table 75: The atomic coordinates of the model resulting from the fixed core refinement of ZAA4 from the 9-month data collection.

Atom Label	Atom Type	Multiplicity	Fractional X Coordinate	Fractional Y Coordinate	Fractional Z Coordinate	Fractional Occupancy
C1	C	1	0.5906187	0.5000000	0.5838286	1
C2	C	1	0.5000000	0.4093813	0.5838286	1
C3	C	1	0.4093813	0.5000000	0.5838286	1
C4	C	1	0.5000000	0.5906187	0.5838286	1
C5	C	1	0.5906187	0.5000000	0.4161714	1
C6	C	1	0.5000000	0.4093813	0.4161714	1
C7	C	1	0.4093813	0.5000000	0.4161714	1
C8	C	1	0.5000000	0.5906187	0.4161714	1
C9	C	1	0.5906187	0.4093813	0.5000000	1
C10	C	1	0.4093813	0.4093813	0.5000000	1
C11	C	1	0.4093813	0.5906187	0.5000000	1
C12	C	1	0.5906187	0.5906187	0.5000000	1
C13	C	1	0.615742	0.5000000	0.6070695	1
C14	C	1	0.5000000	0.384258	0.6070695	1
C15	C	1	0.384258	0.5000000	0.6070695	1
C16	C	1	0.5000000	0.615742	0.6070695	1
C17	C	1	0.615742	0.5000000	0.3929305	1
C18	C	1	0.5000000	0.384258	0.3929305	1
C19	C	1	0.384258	0.5000000	0.3929305	1
C20	C	1	0.5000000	0.615742	0.3929305	1
C21	C	1	0.615742	0.384258	0.5000000	1
C22	C	1	0.384258	0.384258	0.5000000	1
C23	C	1	0.384258	0.615742	0.5000000	1
C24	C	1	0.615742	0.615742	0.5000000	1
O1	O	1	0.5323338	0.5320183	0.470089	1
O2	O	1	0.5323338	0.4679817	0.529911	1
O3	O	1	0.4676662	0.5320183	0.470089	1
O4	O	1	0.4676662	0.4679817	0.529911	1

O5	O	1	0.4676662	0.4679817	0.470089	1
O6	O	1	0.4676662	0.5320183	0.529911	1
O7	O	1	0.5323338	0.4679817	0.470089	1
O8	O	1	0.5323338	0.5320183	0.529911	1
O9	O	1	0.5958258	0.5000000	0.554638	1
O10	O	1	0.5958258	0.4409363	0.5000000	1
O11	O	1	0.5958258	0.5000000	0.445362	1
O12	O	1	0.5958258	0.5590637	0.5000000	1
O13	O	1	0.5000000	0.5958258	0.554638	1
O14	O	1	0.5590637	0.5958258	0.5000000	1
O15	O	1	0.5000000	0.5958258	0.445362	1
O16	O	1	0.4409363	0.5958258	0.5000000	1
O17	O	1	0.4041742	0.5000000	0.554638	1
O18	O	1	0.4041742	0.5590637	0.5000000	1
O19	O	1	0.4041742	0.5000000	0.445362	1
O20	O	1	0.4041742	0.4409363	0.5000000	1
O21	O	1	0.5000000	0.4041742	0.554638	1
O22	O	1	0.4409363	0.4041742	0.5000000	1
O23	O	1	0.5000000	0.4041742	0.445362	1
O24	O	1	0.5590637	0.4041742	0.5000000	1
O25	O	1	0.5590637	0.5000000	0.5886456	1
O26	O	1	0.5000000	0.5590637	0.5886456	1
O27	O	1	0.4409363	0.5000000	0.5886456	1
O28	O	1	0.5000000	0.4409363	0.5886456	1
O29	O	1	0.5590637	0.5000000	0.4113544	1
O30	O	1	0.5000000	0.4409363	0.4113544	1
O31	O	1	0.4409363	0.5000000	0.4113544	1
O32	O	1	0.5000000	0.5590637	0.4113544	1
Zr1	Zr	1	0.5670444	0.5000000	0.5000000	1
Zr2	Zr	1	0.5000000	0.5670444	0.5000000	1
Zr3	Zr	1	0.4329556	0.5000000	0.5000000	1
Zr4	Zr	1	0.5000000	0.4329556	0.5000000	1
Zr5	Zr	1	0.5000000	0.5000000	0.5620208	1
Zr6	Zr	1	0.5000000	0.5000000	0.4379792	1

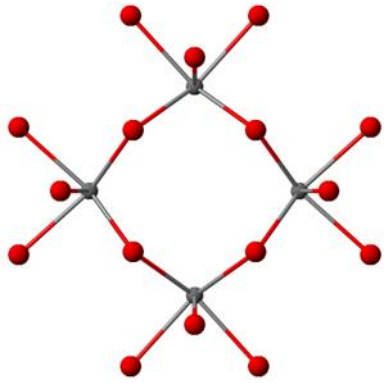

Figure 133: The tetrameric structure resulting from the fixed core refinement of ZAA4 from the 9-month data collection.

Table 76: The atomic coordinates of the tetrameric phase of the fixed core refinement of ZAA4 from the 9-month data collection.

Atom Label	Atom Type	Multiplicity	Fractional X Coordinate	Fractional Y Coordinate	Fractional Z Coordinate	Fractional Occupancy
O1	O	1	0.5140252	0.4859748	0.4725772	1
O2	O	1	0.4859748	0.4859748	0.5274228	1
O3	O	1	0.5140252	0.5140252	0.5274228	1
O4	O	1	0.4859748	0.5140252	0.4725772	1
O5	O	1	0.5000000	0.5307088	0.543634	1
O6	O	1	0.5000000	0.4692912	0.543634	1
O7	O	1	0.4692912	0.5000000	0.456366	1
O8	O	1	0.5307088	0.5000000	0.456366	1
O9	O	1	0.5146466	0.4597431	0.5000000	1
O10	O	1	0.4597431	0.4853534	0.5000000	1
O11	O	1	0.5402569	0.5146466	0.5000000	1
O12	O	1	0.4853534	0.5402569	0.5000000	1
O13	O	1	0.4597431	0.5146466	0.5000000	1
O14	O	1	0.5402569	0.4853534	0.5000000	1
O15	O	1	0.4853534	0.4597431	0.5000000	1
O16	O	1	0.5146466	0.5402569	0.5000000	1
O17	O	1	0.5140252	0.4859748	0.5274228	1
O18	O	1	0.4859748	0.4859748	0.4725772	1
O19	O	1	0.5140252	0.5140252	0.4725772	1
O20	O	1	0.4859748	0.5140252	0.5274228	1
O21	O	1	0.5000000	0.5307088	0.456366	1
O22	O	1	0.5000000	0.4692912	0.456366	1
O23	O	1	0.4692912	0.5000000	0.543634	1
O24	O	1	0.5307088	0.5000000	0.543634	1
Zr1	Zr	1	0.5000000	0.4759777	0.5000000	1
Zr2	Zr	1	0.4759777	0.5000000	0.5000000	1
Zr3	Zr	1	0.5240223	0.5000000	0.5000000	1
Zr4	Zr	1	0.5000000	0.5240223	0.5000000	1

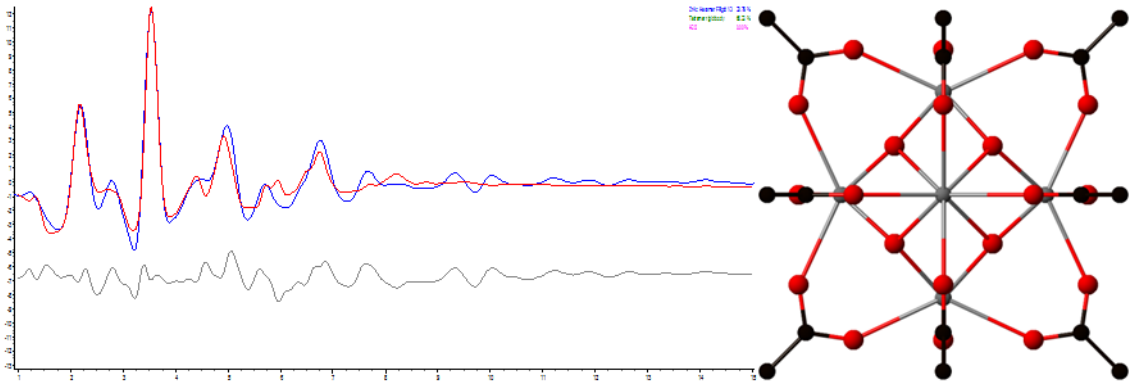

Figure 134: Observed and Calculated PDF from the fixed core refinement of ZAA7 from the 9-month data collection and the resultant model.

Table 77: The atomic coordinates of the model resulting from the fixed core refinement of ZAA7 from the 9-month data collection.

Atom Label	Atom Type	Multiplicity	Fractional X Coordinate	Fractional Y Coordinate	Fractional Z Coordinate	Fractional Occupancy
C1	C	1	0.5901179	0.5000000	0.5833654	1
C2	C	1	0.5000000	0.4098821	0.5833654	1
C3	C	1	0.4098821	0.5000000	0.5833654	1
C4	C	1	0.5000000	0.5901179	0.5833654	1
C5	C	1	0.5901179	0.5000000	0.4166346	1
C6	C	1	0.5000000	0.4098821	0.4166346	1
C7	C	1	0.4098821	0.5000000	0.4166346	1
C8	C	1	0.5000000	0.5901179	0.4166346	1
C9	C	1	0.5901179	0.4098821	0.5000000	1
C10	C	1	0.4098821	0.4098821	0.5000000	1
C11	C	1	0.4098821	0.5901179	0.5000000	1
C12	C	1	0.5901179	0.5901179	0.5000000	1
C13	C	1	0.6155592	0.5000000	0.6069003	1
C14	C	1	0.5000000	0.3844408	0.6069003	1
C15	C	1	0.3844408	0.5000000	0.6069003	1
C16	C	1	0.5000000	0.6155592	0.6069003	1
C17	C	1	0.6155592	0.5000000	0.3930997	1
C18	C	1	0.5000000	0.3844408	0.3930997	1
C19	C	1	0.3844408	0.5000000	0.3930997	1
C20	C	1	0.5000000	0.6155592	0.3930997	1
C21	C	1	0.6155592	0.3844408	0.5000000	1
C22	C	1	0.3844408	0.3844408	0.5000000	1
C23	C	1	0.3844408	0.6155592	0.5000000	1
C24	C	1	0.6155592	0.6155592	0.5000000	1
O1	O	1	0.5322031	0.5318889	0.4702099	1
O2	O	1	0.5322031	0.4681111	0.5297901	1
O3	O	1	0.4677969	0.5318889	0.4702099	1
O4	O	1	0.4677969	0.4681111	0.5297901	1

O5	O	1	0.4677969	0.4681111	0.4702099	1
O6	O	1	0.4677969	0.5318889	0.5297901	1
O7	O	1	0.5322031	0.4681111	0.4702099	1
O8	O	1	0.5322031	0.5318889	0.5297901	1
O9	O	1	0.5948764	0.5000000	0.5544853	1
O10	O	1	0.5948764	0.4411014	0.5000000	1
O11	O	1	0.5948764	0.5000000	0.4455147	1
O12	O	1	0.5948764	0.5588986	0.5000000	1
O13	O	1	0.5000000	0.5948764	0.5544853	1
O14	O	1	0.5588986	0.5948764	0.5000000	1
O15	O	1	0.5000000	0.5948764	0.4455147	1
O16	O	1	0.4411014	0.5948764	0.5000000	1
O17	O	1	0.4051236	0.5000000	0.5544853	1
O18	O	1	0.4051236	0.5588986	0.5000000	1
O19	O	1	0.4051236	0.5000000	0.4455147	1
O20	O	1	0.4051236	0.4411014	0.5000000	1
O21	O	1	0.5000000	0.4051236	0.5544853	1
O22	O	1	0.4411014	0.4051236	0.5000000	1
O23	O	1	0.5000000	0.4051236	0.4455147	1
O24	O	1	0.5588986	0.4051236	0.5000000	1
O25	O	1	0.5588986	0.5000000	0.5877673	1
O26	O	1	0.5000000	0.5588986	0.5877673	1
O27	O	1	0.4411014	0.5000000	0.5877673	1
O28	O	1	0.5000000	0.4411014	0.5877673	1
O29	O	1	0.5588986	0.5000000	0.4122327	1
O30	O	1	0.5000000	0.4411014	0.4122327	1
O31	O	1	0.4411014	0.5000000	0.4122327	1
O32	O	1	0.5000000	0.5588986	0.4122327	1
Zr1	Zr	1	0.5671196	0.5000000	0.5000000	1
Zr2	Zr	1	0.5000000	0.5671196	0.5000000	1
Zr3	Zr	1	0.4328804	0.5000000	0.5000000	1
Zr4	Zr	1	0.5000000	0.4328804	0.5000000	1
Zr5	Zr	1	0.5000000	0.5000000	0.5620903	1
Zr6	Zr	1	0.5000000	0.5000000	0.4379097	1

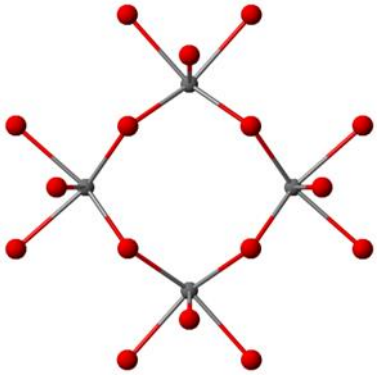

Figure 135: The tetrameric structure resulting from the fixed core refinement of ZAA7 from the 9-month data collection.

Table 78: The atomic coordinates of the tetrameric phase of the fixed core refinement of ZAA7 from the 9-month data collection.

Atom Label	Atom Type	Multiplicity	Fractional X Coordinate	Fractional Y Coordinate	Fractional Z Coordinate	Fractional Occupancy
O1	O	1	0.514264	0.485736	0.472742	1
O2	O	1	0.485736	0.485736	0.527258	1
O3	O	1	0.514264	0.514264	0.527258	1
O4	O	1	0.485736	0.514264	0.472742	1
O5	O	1	0.5000000	0.5307272	0.5426332	1
O6	O	1	0.5000000	0.4692728	0.5426332	1
O7	O	1	0.4692728	0.5000000	0.4573668	1
O8	O	1	0.5307272	0.5000000	0.4573668	1
O9	O	1	0.5143843	0.4596944	0.5000000	1
O10	O	1	0.4596944	0.4856157	0.5000000	1
O11	O	1	0.5403056	0.5143843	0.5000000	1
O12	O	1	0.4856157	0.5403056	0.5000000	1
O13	O	1	0.4596944	0.5143843	0.5000000	1
O14	O	1	0.5403056	0.4856157	0.5000000	1
O15	O	1	0.4856157	0.4596944	0.5000000	1
O16	O	1	0.5143843	0.5403056	0.5000000	1
O17	O	1	0.514264	0.485736	0.527258	1
O18	O	1	0.485736	0.485736	0.472742	1
O19	O	1	0.514264	0.514264	0.472742	1
O20	O	1	0.485736	0.514264	0.527258	1
O21	O	1	0.5000000	0.5307272	0.4573668	1
O22	O	1	0.5000000	0.4692728	0.4573668	1
O23	O	1	0.4692728	0.5000000	0.5426332	1
O24	O	1	0.5307272	0.5000000	0.5426332	1
Zr1	Zr	1	0.5000000	0.4759471	0.5000000	1
Zr2	Zr	1	0.4759471	0.5000000	0.5000000	1
Zr3	Zr	1	0.5240529	0.5000000	0.5000000	1
Zr4	Zr	1	0.5000000	0.5240529	0.5000000	1

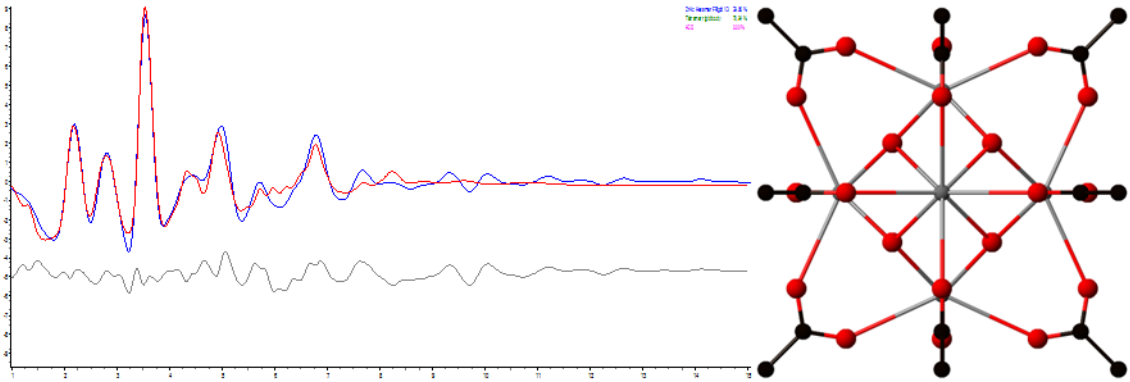

Figure 136: Observed and Calculated PDF from the fixed core refinement of ZAA10 from the 9-month data collection and the resultant model.

Table 79: The atomic coordinates of the model resulting from the fixed core refinement of ZAA10 from the 9-month data collection.

Atom Label	Atom Type	Multiplicity	Fractional X Coordinate	Fractional Y Coordinate	Fractional Z Coordinate	Fractional Occupancy
C1	C	1	0.591527	0.5000000	0.5846689	1
C2	C	1	0.5000000	0.408473	0.5846689	1
C3	C	1	0.408473	0.5000000	0.5846689	1
C4	C	1	0.5000000	0.591527	0.5846689	1
C5	C	1	0.591527	0.5000000	0.4153311	1
C6	C	1	0.5000000	0.408473	0.4153311	1
C7	C	1	0.408473	0.5000000	0.4153311	1
C8	C	1	0.5000000	0.591527	0.4153311	1
C9	C	1	0.591527	0.408473	0.5000000	1
C10	C	1	0.408473	0.408473	0.5000000	1
C11	C	1	0.408473	0.591527	0.5000000	1
C12	C	1	0.591527	0.591527	0.5000000	1
C13	C	1	0.616393	0.5000000	0.6076716	1
C14	C	1	0.5000000	0.383607	0.6076716	1
C15	C	1	0.383607	0.5000000	0.6076716	1
C16	C	1	0.5000000	0.616393	0.6076716	1
C17	C	1	0.616393	0.5000000	0.3923284	1
C18	C	1	0.5000000	0.383607	0.3923284	1
C19	C	1	0.383607	0.5000000	0.3923284	1
C20	C	1	0.5000000	0.616393	0.3923284	1
C21	C	1	0.616393	0.383607	0.5000000	1
C22	C	1	0.383607	0.383607	0.5000000	1
C23	C	1	0.383607	0.616393	0.5000000	1
C24	C	1	0.616393	0.616393	0.5000000	1
O1	O	1	0.533023	0.5327008	0.4694514	1
O2	O	1	0.533023	0.4672992	0.5305486	1
O3	O	1	0.466977	0.5327008	0.4694514	1
O4	O	1	0.466977	0.4672992	0.5305486	1

O5	O	1	0.466977	0.4672992	0.4694514	1
O6	O	1	0.466977	0.5327008	0.5305486	1
O7	O	1	0.533023	0.4672992	0.4694514	1
O8	O	1	0.533023	0.5327008	0.5305486	1
O9	O	1	0.5962043	0.5000000	0.558504	1
O10	O	1	0.5962043	0.4367572	0.5000000	1
O11	O	1	0.5962043	0.5000000	0.441496	1
O12	O	1	0.5962043	0.5632428	0.5000000	1
O13	O	1	0.5000000	0.5962043	0.558504	1
O14	O	1	0.5632428	0.5962043	0.5000000	1
O15	O	1	0.5000000	0.5962043	0.441496	1
O16	O	1	0.4367572	0.5962043	0.5000000	1
O17	O	1	0.4037957	0.5000000	0.558504	1
O18	O	1	0.4037957	0.5632428	0.5000000	1
O19	O	1	0.4037957	0.5000000	0.441496	1
O20	O	1	0.4037957	0.4367572	0.5000000	1
O21	O	1	0.5000000	0.4037957	0.558504	1
O22	O	1	0.4367572	0.4037957	0.5000000	1
O23	O	1	0.5000000	0.4037957	0.441496	1
O24	O	1	0.5632428	0.4037957	0.5000000	1
O25	O	1	0.5632428	0.5000000	0.5889957	1
O26	O	1	0.5000000	0.5632428	0.5889957	1
O27	O	1	0.4367572	0.5000000	0.5889957	1
O28	O	1	0.5000000	0.4367572	0.5889957	1
O29	O	1	0.5632428	0.5000000	0.4110043	1
O30	O	1	0.5000000	0.4367572	0.4110043	1
O31	O	1	0.4367572	0.5000000	0.4110043	1
O32	O	1	0.5000000	0.5632428	0.4110043	1
Zr1	Zr	1	0.5670538	0.5000000	0.5000000	1
Zr2	Zr	1	0.5000000	0.5670538	0.5000000	1
Zr3	Zr	1	0.4329462	0.5000000	0.5000000	1
Zr4	Zr	1	0.5000000	0.4329462	0.5000000	1
Zr5	Zr	1	0.5000000	0.5000000	0.5620294	1
Zr6	Zr	1	0.5000000	0.5000000	0.4379706	1

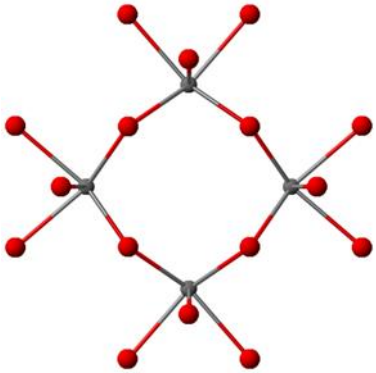

Figure 137: The tetrameric structure resulting from the fixed core refinement of ZAA10 from the 9-month data collection.

Table 80: The atomic coordinates of the tetrameric phase of the fixed core refinement of ZAA10 from the 9-month data collection.

Atom Label	Atom Type	Multiplicity	Fractional X Coordinate	Fractional Y Coordinate	Fractional Z Coordinate	Fractional Occupancy
O1	O	1	0.5142281	0.4857719	0.4744998	1
O2	O	1	0.4857719	0.4857719	0.5255002	1
O3	O	1	0.5142281	0.5142281	0.5255002	1
O4	O	1	0.4857719	0.5142281	0.4744998	1
O5	O	1	0.5000000	0.5300169	0.5478026	1
O6	O	1	0.5000000	0.4699831	0.5478026	1
O7	O	1	0.4699831	0.5000000	0.4521974	1
O8	O	1	0.5300169	0.5000000	0.4521974	1
O9	O	1	0.514306	0.4594109	0.5000000	1
O10	O	1	0.4594109	0.485694	0.5000000	1
O11	O	1	0.5405891	0.514306	0.5000000	1
O12	O	1	0.485694	0.5405891	0.5000000	1
O13	O	1	0.4594109	0.514306	0.5000000	1
O14	O	1	0.5405891	0.485694	0.5000000	1
O15	O	1	0.485694	0.4594109	0.5000000	1
O16	O	1	0.514306	0.5405891	0.5000000	1
O17	O	1	0.5142281	0.4857719	0.5255002	1
O18	O	1	0.4857719	0.4857719	0.4744998	1
O19	O	1	0.5142281	0.5142281	0.4744998	1
O20	O	1	0.4857719	0.5142281	0.5255002	1
O21	O	1	0.5000000	0.5300169	0.4521974	1
O22	O	1	0.5000000	0.4699831	0.4521974	1
O23	O	1	0.4699831	0.5000000	0.5478026	1
O24	O	1	0.5300169	0.5000000	0.5478026	1
Zr1	Zr	1	0.5000000	0.4760034	0.5000000	1
Zr2	Zr	1	0.4760034	0.5000000	0.5000000	1
Zr3	Zr	1	0.5239966	0.5000000	0.5000000	1
Zr4	Zr	1	0.5000000	0.5239966	0.5000000	1

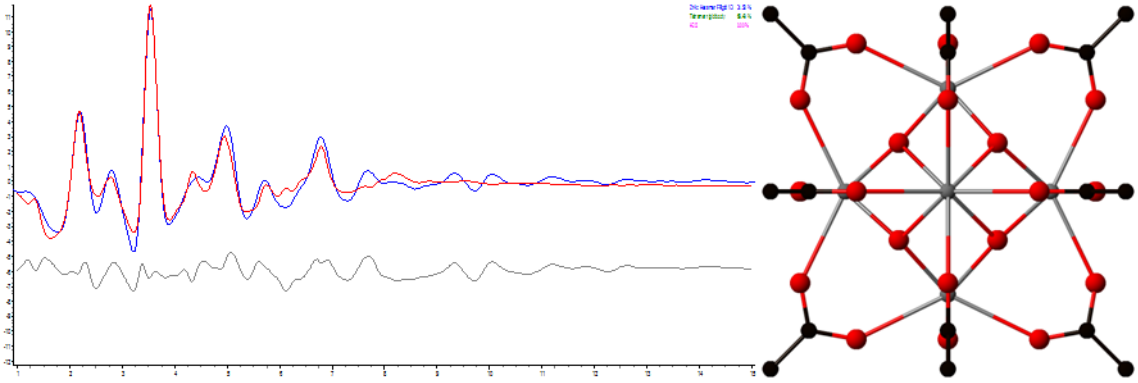

Figure 138: Observed and Calculated PDF from the fixed core refinement of ZAA13 from the 9-month data collection and the resultant model.

Table 81: The atomic coordinates of the model resulting from the fixed core refinement of ZAA13 from the 9-month data collection.

Atom Label	Atom Type	Multiplicity	Fractional X Coordinate	Fractional Y Coordinate	Fractional Z Coordinate	Fractional Occupancy
C1	C	1	0.5907219	0.5000000	0.5839241	1
C2	C	1	0.5000000	0.4092781	0.5839241	1
C3	C	1	0.4092781	0.5000000	0.5839241	1
C4	C	1	0.5000000	0.5907219	0.5839241	1
C5	C	1	0.5907219	0.5000000	0.4160759	1
C6	C	1	0.5000000	0.4092781	0.4160759	1
C7	C	1	0.4092781	0.5000000	0.4160759	1
C8	C	1	0.5000000	0.5907219	0.4160759	1
C9	C	1	0.5907219	0.4092781	0.5000000	1
C10	C	1	0.4092781	0.4092781	0.5000000	1
C11	C	1	0.4092781	0.5907219	0.5000000	1
C12	C	1	0.5907219	0.5907219	0.5000000	1
C13	C	1	0.6158762	0.5000000	0.6071935	1
C14	C	1	0.5000000	0.3841238	0.6071935	1
C15	C	1	0.3841238	0.5000000	0.6071935	1
C16	C	1	0.5000000	0.6158762	0.6071935	1
C17	C	1	0.6158762	0.5000000	0.3928065	1
C18	C	1	0.5000000	0.3841238	0.3928065	1
C19	C	1	0.3841238	0.5000000	0.3928065	1
C20	C	1	0.5000000	0.6158762	0.3928065	1
C21	C	1	0.6158762	0.3841238	0.5000000	1
C22	C	1	0.3841238	0.3841238	0.5000000	1
C23	C	1	0.3841238	0.6158762	0.5000000	1
C24	C	1	0.6158762	0.6158762	0.5000000	1
O1	O	1	0.5321538	0.53184	0.4702555	1
O2	O	1	0.5321538	0.46816	0.5297445	1
O3	O	1	0.4678462	0.53184	0.4702555	1
O4	O	1	0.4678462	0.46816	0.5297445	1

O5	O	1	0.4678462	0.46816	0.4702555	1
O6	O	1	0.4678462	0.53184	0.5297445	1
O7	O	1	0.5321538	0.46816	0.4702555	1
O8	O	1	0.5321538	0.53184	0.5297445	1
O9	O	1	0.5963797	0.5000000	0.5551758	1
O10	O	1	0.5963797	0.440355	0.5000000	1
O11	O	1	0.5963797	0.5000000	0.4448242	1
O12	O	1	0.5963797	0.559645	0.5000000	1
O13	O	1	0.5000000	0.5963797	0.5551758	1
O14	O	1	0.559645	0.5963797	0.5000000	1
O15	O	1	0.5000000	0.5963797	0.4448242	1
O16	O	1	0.440355	0.5963797	0.5000000	1
O17	O	1	0.4036203	0.5000000	0.5551758	1
O18	O	1	0.4036203	0.559645	0.5000000	1
O19	O	1	0.4036203	0.5000000	0.4448242	1
O20	O	1	0.4036203	0.440355	0.5000000	1
O21	O	1	0.5000000	0.4036203	0.5551758	1
O22	O	1	0.440355	0.4036203	0.5000000	1
O23	O	1	0.5000000	0.4036203	0.4448242	1
O24	O	1	0.559645	0.4036203	0.5000000	1
O25	O	1	0.559645	0.5000000	0.5891579	1
O26	O	1	0.5000000	0.559645	0.5891579	1
O27	O	1	0.440355	0.5000000	0.5891579	1
O28	O	1	0.5000000	0.440355	0.5891579	1
O29	O	1	0.559645	0.5000000	0.4108421	1
O30	O	1	0.5000000	0.440355	0.4108421	1
O31	O	1	0.440355	0.5000000	0.4108421	1
O32	O	1	0.5000000	0.559645	0.4108421	1
Zr1	Zr	1	0.5671147	0.5000000	0.5000000	1
Zr2	Zr	1	0.5000000	0.5671147	0.5000000	1
Zr3	Zr	1	0.4328853	0.5000000	0.5000000	1
Zr4	Zr	1	0.5000000	0.4328853	0.5000000	1
Zr5	Zr	1	0.5000000	0.5000000	0.5620857	1
Zr6	Zr	1	0.5000000	0.5000000	0.4379143	1

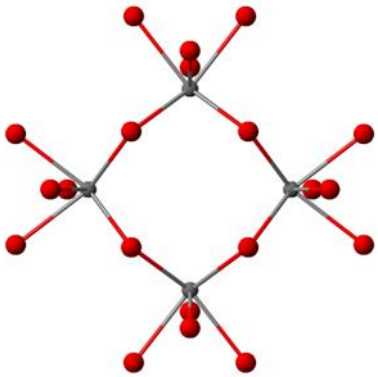

Figure 139: The tetrameric structure resulting from the fixed core refinement of ZAA13 from the 9-month data collection.

Table 82: The atomic coordinates of the tetrameric phase of the fixed core refinement of ZAA13 from the 9-month data collection.

Atom Label	Atom Type	Multiplicity	Fractional X Coordinate	Fractional Y Coordinate	Fractional Z Coordinate	Fractional Occupancy
O1	O	1	0.513789	0.486211	0.4730644	1
O2	O	1	0.486211	0.486211	0.5269356	1
O3	O	1	0.513789	0.513789	0.5269356	1
O4	O	1	0.486211	0.513789	0.4730644	1
O5	O	1	0.5000000	0.5289618	0.5482386	1
O6	O	1	0.5000000	0.4710382	0.5482386	1
O7	O	1	0.4670739	0.5000000	0.4608163	1
O8	O	1	0.5329261	0.5000000	0.4608163	1
O9	O	1	0.5132167	0.4588993	0.5000000	1
O10	O	1	0.4588993	0.4867833	0.5000000	1
O11	O	1	0.5411007	0.5132167	0.5000000	1
O12	O	1	0.4867833	0.5411007	0.5000000	1
O13	O	1	0.4588993	0.5132167	0.5000000	1
O14	O	1	0.5411007	0.4867833	0.5000000	1
O15	O	1	0.4867833	0.4588993	0.5000000	1
O16	O	1	0.5132167	0.5411007	0.5000000	1
O17	O	1	0.513789	0.486211	0.5269356	1
O18	O	1	0.486211	0.486211	0.4730644	1
O19	O	1	0.513789	0.513789	0.4730644	1
O20	O	1	0.486211	0.513789	0.5269356	1
O21	O	1	0.5000000	0.5329261	0.4608163	1
O22	O	1	0.5000000	0.4670739	0.4608163	1
O23	O	1	0.4710382	0.5000000	0.5482386	1
O24	O	1	0.5289618	0.5000000	0.5482386	1
Zr1	Zr	1	0.5000000	0.4760281	0.5000000	1
Zr2	Zr	1	0.4760281	0.5000000	0.5000000	1
Zr3	Zr	1	0.5239719	0.5000000	0.5000000	1
Zr4	Zr	1	0.5000000	0.5239719	0.5000000	1

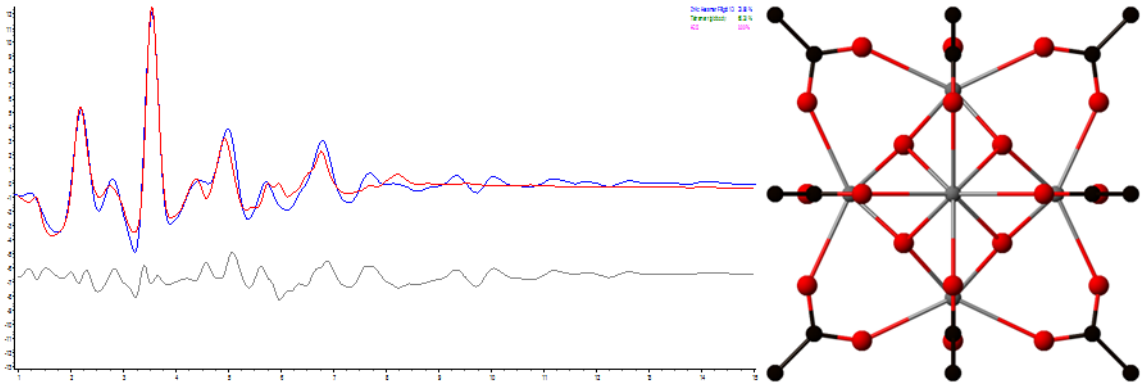

Figure 140: Observed and Calculated PDF from the fixed core refinement of ZAA16 from the 9-month data collection and the resultant model.

Table 83: The atomic coordinates of the model resulting from the fixed core refinement of ZAA16 from the 9-month data collection.

Atom Label	Atom Type	Multiplicity	Fractional X Coordinate	Fractional Y Coordinate	Fractional Z Coordinate	Fractional Occupancy
C1	C	1	0.5907219	0.5000000	0.5839241	1
C2	C	1	0.5000000	0.4092781	0.5839241	1
C3	C	1	0.4092781	0.5000000	0.5839241	1
C4	C	1	0.5000000	0.5907219	0.5839241	1
C5	C	1	0.5907219	0.5000000	0.4160759	1
C6	C	1	0.5000000	0.4092781	0.4160759	1
C7	C	1	0.4092781	0.5000000	0.4160759	1
C8	C	1	0.5000000	0.5907219	0.4160759	1
C9	C	1	0.5907219	0.4092781	0.5000000	1
C10	C	1	0.4092781	0.4092781	0.5000000	1
C11	C	1	0.4092781	0.5907219	0.5000000	1
C12	C	1	0.5907219	0.5907219	0.5000000	1
C13	C	1	0.6158762	0.5000000	0.6071935	1
C14	C	1	0.5000000	0.3841238	0.6071935	1
C15	C	1	0.3841238	0.5000000	0.6071935	1
C16	C	1	0.5000000	0.6158762	0.6071935	1
C17	C	1	0.6158762	0.5000000	0.3928065	1
C18	C	1	0.5000000	0.3841238	0.3928065	1
C19	C	1	0.3841238	0.5000000	0.3928065	1
C20	C	1	0.5000000	0.6158762	0.3928065	1
C21	C	1	0.6158762	0.3841238	0.5000000	1
C22	C	1	0.3841238	0.3841238	0.5000000	1
C23	C	1	0.3841238	0.6158762	0.5000000	1
C24	C	1	0.6158762	0.6158762	0.5000000	1
O1	O	1	0.5321538	0.53184	0.4702555	1
O2	O	1	0.5321538	0.46816	0.5297445	1
O3	O	1	0.4678462	0.53184	0.4702555	1
O4	O	1	0.4678462	0.46816	0.5297445	1

O5	O	1	0.4678462	0.46816	0.4702555	1
O6	O	1	0.4678462	0.53184	0.5297445	1
O7	O	1	0.5321538	0.46816	0.4702555	1
O8	O	1	0.5321538	0.53184	0.5297445	1
O9	O	1	0.5963797	0.5000000	0.5551758	1
O10	O	1	0.5963797	0.440355	0.5000000	1
O11	O	1	0.5963797	0.5000000	0.4448242	1
O12	O	1	0.5963797	0.559645	0.5000000	1
O13	O	1	0.5000000	0.5963797	0.5551758	1
O14	O	1	0.559645	0.5963797	0.5000000	1
O15	O	1	0.5000000	0.5963797	0.4448242	1
O16	O	1	0.440355	0.5963797	0.5000000	1
O17	O	1	0.4036203	0.5000000	0.5551758	1
O18	O	1	0.4036203	0.559645	0.5000000	1
O19	O	1	0.4036203	0.5000000	0.4448242	1
O20	O	1	0.4036203	0.440355	0.5000000	1
O21	O	1	0.5000000	0.4036203	0.5551758	1
O22	O	1	0.440355	0.4036203	0.5000000	1
O23	O	1	0.5000000	0.4036203	0.4448242	1
O24	O	1	0.559645	0.4036203	0.5000000	1
O25	O	1	0.559645	0.5000000	0.5891579	1
O26	O	1	0.5000000	0.559645	0.5891579	1
O27	O	1	0.440355	0.5000000	0.5891579	1
O28	O	1	0.5000000	0.440355	0.5891579	1
O29	O	1	0.559645	0.5000000	0.4108421	1
O30	O	1	0.5000000	0.440355	0.4108421	1
O31	O	1	0.440355	0.5000000	0.4108421	1
O32	O	1	0.5000000	0.559645	0.4108421	1
Zr1	Zr	1	0.5671147	0.5000000	0.5000000	1
Zr2	Zr	1	0.5000000	0.5671147	0.5000000	1
Zr3	Zr	1	0.4328853	0.5000000	0.5000000	1
Zr4	Zr	1	0.5000000	0.4328853	0.5000000	1
Zr5	Zr	1	0.5000000	0.5000000	0.5620857	1
Zr6	Zr	1	0.5000000	0.5000000	0.4379143	1

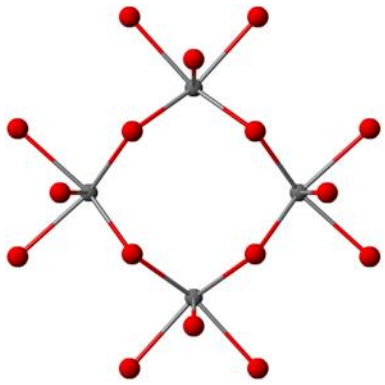

Figure 141: The tetrameric structure resulting from the fixed core refinement of ZAA16 from the 9-month data collection.

Table 84: The atomic coordinates of the tetrameric phase of the fixed core refinement of ZAA16 from the 9-month data collection.

Atom Label	Atom Type	Multiplicity	Fractional X Coordinate	Fractional Y Coordinate	Fractional Z Coordinate	Fractional Occupancy
O1	O	1	0.513789	0.486211	0.4730644	1
O2	O	1	0.486211	0.486211	0.5269356	1
O3	O	1	0.513789	0.513789	0.5269356	1
O4	O	1	0.486211	0.513789	0.4730644	1
O5	O	1	0.5000000	0.5289618	0.5482386	1
O6	O	1	0.5000000	0.4710382	0.5482386	1
O7	O	1	0.4670739	0.5000000	0.4608163	1
O8	O	1	0.5329261	0.5000000	0.4608163	1
O9	O	1	0.5132167	0.4588993	0.5000000	1
O10	O	1	0.4588993	0.4867833	0.5000000	1
O11	O	1	0.5411007	0.5132167	0.5000000	1
O12	O	1	0.4867833	0.5411007	0.5000000	1
O13	O	1	0.4588993	0.5132167	0.5000000	1
O14	O	1	0.5411007	0.4867833	0.5000000	1
O15	O	1	0.4867833	0.4588993	0.5000000	1
O16	O	1	0.5132167	0.5411007	0.5000000	1
O17	O	1	0.513789	0.486211	0.5269356	1
O18	O	1	0.486211	0.486211	0.4730644	1
O19	O	1	0.513789	0.513789	0.4730644	1
O20	O	1	0.486211	0.513789	0.5269356	1
O21	O	1	0.5000000	0.5329261	0.4608163	1
O22	O	1	0.5000000	0.4670739	0.4608163	1
O23	O	1	0.4710382	0.5000000	0.5482386	1
O24	O	1	0.5289618	0.5000000	0.5482386	1
Zr1	Zr	1	0.5000000	0.4760281	0.5000000	1
Zr2	Zr	1	0.4760281	0.5000000	0.5000000	1
Zr3	Zr	1	0.5239719	0.5000000	0.5000000	1
Zr4	Zr	1	0.5000000	0.5239719	0.5000000	1

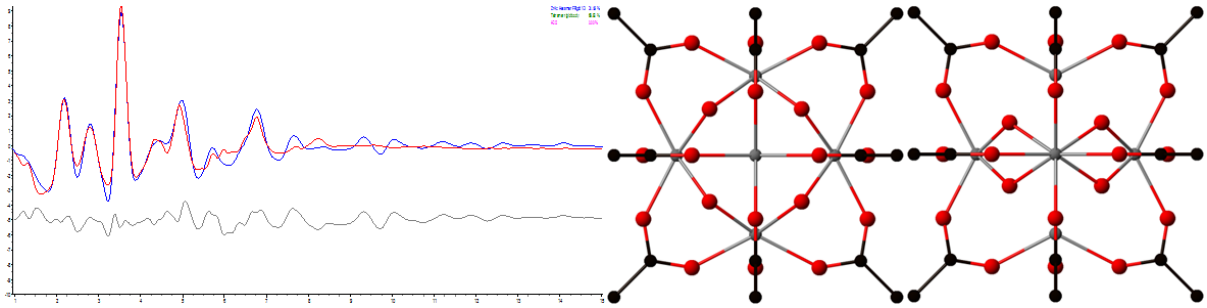

Figure 142: Observed and Calculated PDF from the chandelier core refinement of ZAA1 from the 9-month data collection and the resultant model viewed from the axial (left) and equatorial (right) positions.

Table 85: The atomic coordinates of the model resulting from the chandelier core refinement of ZAA1 from the 9-month data collection.

Atom Label	Atom Type	Multiplicity	Fractional X Coordinate	Fractional Y Coordinate	Fractional Z Coordinate	Fractional Occupancy
C1	C	1	0.5890429	0.5000000	0.5823709	1
C2	C	1	0.5000000	0.4109571	0.5823709	1
C3	C	1	0.4109571	0.5000000	0.5823709	1
C4	C	1	0.5000000	0.5890429	0.5823709	1
C5	C	1	0.5890429	0.5000000	0.4176291	1
C6	C	1	0.5000000	0.4109571	0.4176291	1
C7	C	1	0.4109571	0.5000000	0.4176291	1
C8	C	1	0.5000000	0.5890429	0.4176291	1
C9	C	1	0.5890429	0.4109571	0.5000000	1
C10	C	1	0.4109571	0.4109571	0.5000000	1
C11	C	1	0.4109571	0.5890429	0.5000000	1
C12	C	1	0.5890429	0.5890429	0.5000000	1
C13	C	1	0.6192947	0.5000000	0.6103559	1
C14	C	1	0.5000000	0.3807053	0.6103559	1
C15	C	1	0.3807053	0.5000000	0.6103559	1
C16	C	1	0.5000000	0.6192947	0.6103559	1
C17	C	1	0.6192947	0.5000000	0.3896441	1
C18	C	1	0.5000000	0.3807053	0.3896441	1
C19	C	1	0.3807053	0.5000000	0.3896441	1
C20	C	1	0.5000000	0.6192947	0.3896441	1
C21	C	1	0.6192947	0.3807053	0.5000000	1
C22	C	1	0.3807053	0.3807053	0.5000000	1
C23	C	1	0.3807053	0.6192947	0.5000000	1
C24	C	1	0.6192947	0.6192947	0.5000000	1
O1	O	1	0.5374184	0.4625816	0.4744485	1
O2	O	1	0.5374184	0.4625816	0.5255515	1
O3	O	1	0.4625816	0.4625816	0.4744485	1
O4	O	1	0.4625816	0.4625816	0.5255515	1
O5	O	1	0.4625816	0.5374184	0.4744485	1
O6	O	1	0.4625816	0.5374184	0.5255515	1

O7	O	1	0.5374184	0.5374184	0.4744485	1
O8	O	1	0.5374184	0.5374184	0.5255515	1
O9	O	1	0.5942846	0.5000000	0.5496669	1
O10	O	1	0.5942846	0.4463101	0.5000000	1
O11	O	1	0.5942846	0.5000000	0.4503331	1
O12	O	1	0.5942846	0.5536899	0.5000000	1
O13	O	1	0.5000000	0.5942846	0.5496669	1
O14	O	1	0.5536899	0.5942846	0.5000000	1
O15	O	1	0.5000000	0.5942846	0.4503331	1
O16	O	1	0.4463101	0.5942846	0.5000000	1
O17	O	1	0.4057154	0.5000000	0.5496669	1
O18	O	1	0.4057154	0.5536899	0.5000000	1
O19	O	1	0.4057154	0.5000000	0.4503331	1
O20	O	1	0.4057154	0.4463101	0.5000000	1
O21	O	1	0.5000000	0.4057154	0.5496669	1
O22	O	1	0.4463101	0.4057154	0.5000000	1
O23	O	1	0.5000000	0.4057154	0.4503331	1
O24	O	1	0.5536899	0.4057154	0.5000000	1
O25	O	1	0.5536899	0.5000000	0.5872198	1
O26	O	1	0.5000000	0.5536899	0.5872198	1
O27	O	1	0.4463101	0.5000000	0.5872198	1
O28	O	1	0.5000000	0.4463101	0.5872198	1
O29	O	1	0.5536899	0.5000000	0.4127802	1
O30	O	1	0.5000000	0.4463101	0.4127802	1
O31	O	1	0.4463101	0.5000000	0.4127802	1
O32	O	1	0.5000000	0.5536899	0.4127802	1
Zr1	Zr	1	0.5668612	0.5000000	0.5000000	1
Zr2	Zr	1	0.5000000	0.5668612	0.5000000	1
Zr3	Zr	1	0.4331388	0.5000000	0.5000000	1
Zr4	Zr	1	0.5000000	0.4331388	0.5000000	1
Zr5	Zr	1	0.5000000	0.5000000	0.5618513	1
Zr6	Zr	1	0.5000000	0.5000000	0.4381487	1

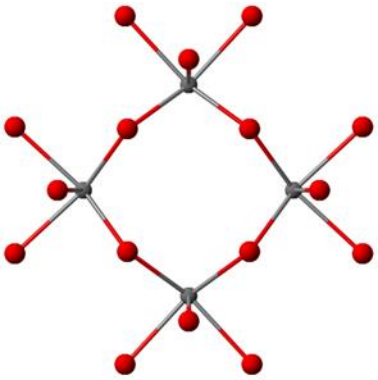

Figure 143: The tetrameric structure resulting from the chandelier core refinement of ZAA1 from the 9-month data collection.

Table 86: The atomic coordinates of the tetrameric phase of the chandelier core refinement of ZAA1 from the 9-month data collection.

Atom Label	Atom Type	Multiplicity	Fractional X Coordinate	Fractional Y Coordinate	Fractional Z Coordinate	Fractional Occupancy
O1	O	1	0.5140296	0.4859704	0.474172	1
O2	O	1	0.4859704	0.4859704	0.525828	1
O3	O	1	0.5140296	0.5140296	0.525828	1
O4	O	1	0.4859704	0.5140296	0.474172	1
O5	O	1	0.5000000	0.5300888	0.5469349	1
O6	O	1	0.5000000	0.4699112	0.5469349	1
O7	O	1	0.4699112	0.5000000	0.4530651	1
O8	O	1	0.5300888	0.5000000	0.4530651	1
O9	O	1	0.5145639	0.4600446	0.5000000	1
O10	O	1	0.4600446	0.4854361	0.5000000	1
O11	O	1	0.5399554	0.5145639	0.5000000	1
O12	O	1	0.4854361	0.5399554	0.5000000	1
O13	O	1	0.4600446	0.5145639	0.5000000	1
O14	O	1	0.5399554	0.4854361	0.5000000	1
O15	O	1	0.4854361	0.4600446	0.5000000	1
O16	O	1	0.5145639	0.5399554	0.5000000	1
O17	O	1	0.5140296	0.4859704	0.525828	1
O18	O	1	0.4859704	0.4859704	0.474172	1
O19	O	1	0.5140296	0.5140296	0.474172	1
O20	O	1	0.4859704	0.5140296	0.525828	1
O21	O	1	0.5000000	0.5300888	0.4530651	1
O22	O	1	0.5000000	0.4699112	0.4530651	1
O23	O	1	0.4699112	0.5000000	0.5469349	1
O24	O	1	0.5300888	0.5000000	0.5469349	1
Zr1	Zr	1	0.5000000	0.4758351	0.5000000	1
Zr2	Zr	1	0.4758351	0.5000000	0.5000000	1
Zr3	Zr	1	0.5241649	0.5000000	0.5000000	1
Zr4	Zr	1	0.5000000	0.5241649	0.5000000	1

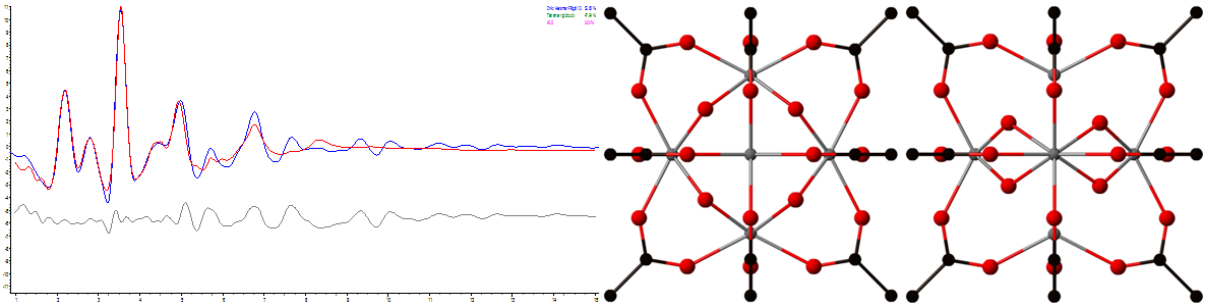

Figure 144: Observed and Calculated PDF from the chandelier core refinement of ZAA4 from the 9-month data collection and the resultant model viewed from the axial (left) and equatorial (right) positions.

Table 87: The atomic coordinates of the model resulting from the chandelier core refinement of ZAA4 from the 9-month data collection.

Atom Label	Atom Type	Multiplicity	Fractional X Coordinate	Fractional Y Coordinate	Fractional Z Coordinate	Fractional Occupancy
C1	C	1	0.5887357	0.5000000	0.5820867	1
C2	C	1	0.5000000	0.4112643	0.5820867	1
C3	C	1	0.4112643	0.5000000	0.5820867	1
C4	C	1	0.5000000	0.5887357	0.5820867	1
C5	C	1	0.5887357	0.5000000	0.4179133	1
C6	C	1	0.5000000	0.4112643	0.4179133	1
C7	C	1	0.4112643	0.5000000	0.4179133	1
C8	C	1	0.5000000	0.5887357	0.4179133	1
C9	C	1	0.5887357	0.4112643	0.5000000	1
C10	C	1	0.4112643	0.4112643	0.5000000	1
C11	C	1	0.4112643	0.5887357	0.5000000	1
C12	C	1	0.5887357	0.5887357	0.5000000	1
C13	C	1	0.6192621	0.5000000	0.6103258	1
C14	C	1	0.5000000	0.3807379	0.6103258	1
C15	C	1	0.3807379	0.5000000	0.6103258	1
C16	C	1	0.5000000	0.6192621	0.6103258	1
C17	C	1	0.6192621	0.5000000	0.3896742	1
C18	C	1	0.5000000	0.3807379	0.3896742	1
C19	C	1	0.3807379	0.5000000	0.3896742	1
C20	C	1	0.5000000	0.6192621	0.3896742	1
C21	C	1	0.6192621	0.3807379	0.5000000	1
C22	C	1	0.3807379	0.3807379	0.5000000	1
C23	C	1	0.3807379	0.6192621	0.5000000	1
C24	C	1	0.6192621	0.6192621	0.5000000	1
O1	O	1	0.5384056	0.4615944	0.4754041	1
O2	O	1	0.5384056	0.4615944	0.5245959	1
O3	O	1	0.4615944	0.4615944	0.4754041	1
O4	O	1	0.4615944	0.4615944	0.5245959	1
O5	O	1	0.4615944	0.5384056	0.4754041	1
O6	O	1	0.4615944	0.5384056	0.5245959	1

O7	O	1	0.5384056	0.5384056	0.4754041	1
O8	O	1	0.5384056	0.5384056	0.5245959	1
O9	O	1	0.5946714	0.5000000	0.5496948	1
O10	O	1	0.5946714	0.4462799	0.5000000	1
O11	O	1	0.5946714	0.5000000	0.4503052	1
O12	O	1	0.5946714	0.5537201	0.5000000	1
O13	O	1	0.5000000	0.5946714	0.5496948	1
O14	O	1	0.5537201	0.5946714	0.5000000	1
O15	O	1	0.5000000	0.5946714	0.4503052	1
O16	O	1	0.4462799	0.5946714	0.5000000	1
O17	O	1	0.4053286	0.5000000	0.5496948	1
O18	O	1	0.4053286	0.5537201	0.5000000	1
O19	O	1	0.4053286	0.5000000	0.4503052	1
O20	O	1	0.4053286	0.4462799	0.5000000	1
O21	O	1	0.5000000	0.4053286	0.5496948	1
O22	O	1	0.4462799	0.4053286	0.5000000	1
O23	O	1	0.5000000	0.4053286	0.4503052	1
O24	O	1	0.5537201	0.4053286	0.5000000	1
O25	O	1	0.5537201	0.5000000	0.5875777	1
O26	O	1	0.5000000	0.5537201	0.5875777	1
O27	O	1	0.4462799	0.5000000	0.5875777	1
O28	O	1	0.5000000	0.4462799	0.5875777	1
O29	O	1	0.5537201	0.5000000	0.4124223	1
O30	O	1	0.5000000	0.4462799	0.4124223	1
O31	O	1	0.4462799	0.5000000	0.4124223	1
O32	O	1	0.5000000	0.5537201	0.4124223	1
Zr1	Zr	1	0.5667972	0.5000000	0.5000000	1
Zr2	Zr	1	0.5000000	0.5667972	0.5000000	1
Zr3	Zr	1	0.4332028	0.5000000	0.5000000	1
Zr4	Zr	1	0.5000000	0.4332028	0.5000000	1
Zr5	Zr	1	0.5000000	0.5000000	0.5617921	1
Zr6	Zr	1	0.5000000	0.5000000	0.4382079	1

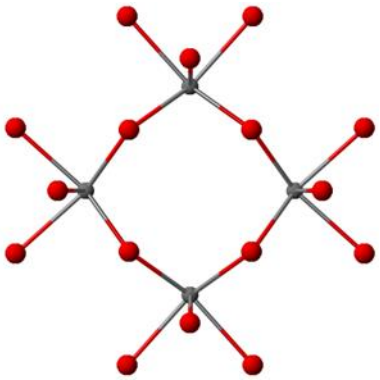

Figure 145: The tetrameric structure resulting from the chandelier core refinement of ZAA4 from the 9-month data collection.

Table 88: The atomic coordinates of the tetrameric phase of the chandelier core refinement of ZAA4 from the 9-month data collection.

Atom Label	Atom Type	Multiplicity	Fractional X Coordinate	Fractional Y Coordinate	Fractional Z Coordinate	Fractional Occupancy
O1	O	1	0.5140777	0.4859223	0.4739234	1
O2	O	1	0.4859223	0.4859223	0.5260766	1
O3	O	1	0.5140777	0.5140777	0.5260766	1
O4	O	1	0.4859223	0.5140777	0.4739234	1
O5	O	1	0.5000000	0.5304456	0.546115	1
O6	O	1	0.5000000	0.4695544	0.546115	1
O7	O	1	0.4695544	0.5000000	0.453885	1
O8	O	1	0.5304456	0.5000000	0.453885	1
O9	O	1	0.5144613	0.4598296	0.5000000	1
O10	O	1	0.4598296	0.4855387	0.5000000	1
O11	O	1	0.5401704	0.5144613	0.5000000	1
O12	O	1	0.4855387	0.5401704	0.5000000	1
O13	O	1	0.4598296	0.5144613	0.5000000	1
O14	O	1	0.5401704	0.4855387	0.5000000	1
O15	O	1	0.4855387	0.4598296	0.5000000	1
O16	O	1	0.5144613	0.5401704	0.5000000	1
O17	O	1	0.5140777	0.4859223	0.5260766	1
O18	O	1	0.4859223	0.4859223	0.4739234	1
O19	O	1	0.5140777	0.5140777	0.4739234	1
O20	O	1	0.4859223	0.5140777	0.5260766	1
O21	O	1	0.5000000	0.5304456	0.453885	1
O22	O	1	0.5000000	0.4695544	0.453885	1
O23	O	1	0.4695544	0.5000000	0.546115	1
O24	O	1	0.5304456	0.5000000	0.546115	1
Zr1	Zr	1	0.5000000	0.4759207	0.5000000	1
Zr2	Zr	1	0.4759207	0.5000000	0.5000000	1
Zr3	Zr	1	0.5240793	0.5000000	0.5000000	1
Zr4	Zr	1	0.5000000	0.5240793	0.5000000	1

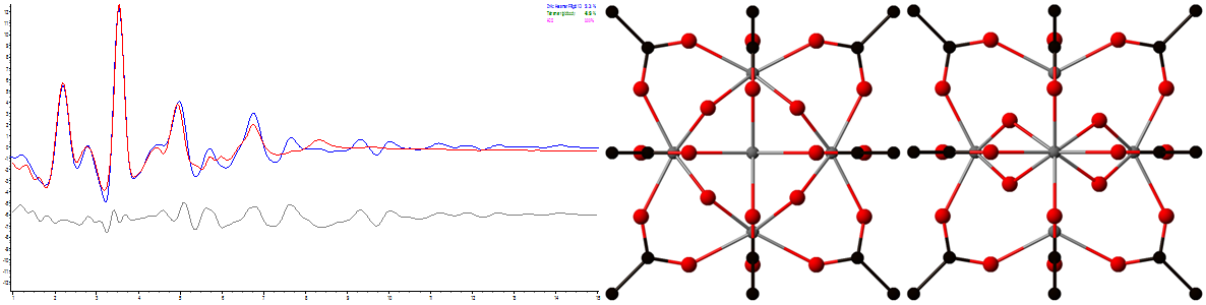

Figure 146: Observed and Calculated PDF from the chandelier core refinement of ZAA7 from the 9-month data collection and the resultant model viewed from the axial (left) and equatorial (right) positions.

Table 89: The atomic coordinates of the model resulting from the chandelier core refinement of ZAA7 from the 9-month data collection.

Atom Label	Atom Type	Multiplicity	Fractional X Coordinate	Fractional Y Coordinate	Fractional Z Coordinate	Fractional Occupancy
C1	C	1	0.5885358	0.5000000	0.5819018	1
C2	C	1	0.5000000	0.4114642	0.5819018	1
C3	C	1	0.4114642	0.5000000	0.5819018	1
C4	C	1	0.5000000	0.5885358	0.5819018	1
C5	C	1	0.5885358	0.5000000	0.4180982	1
C6	C	1	0.5000000	0.4114642	0.4180982	1
C7	C	1	0.4114642	0.5000000	0.4180982	1
C8	C	1	0.5000000	0.5885358	0.4180982	1
C9	C	1	0.5885358	0.4114642	0.5000000	1
C10	C	1	0.4114642	0.4114642	0.5000000	1
C11	C	1	0.4114642	0.5885358	0.5000000	1
C12	C	1	0.5885358	0.5885358	0.5000000	1
C13	C	1	0.6190143	0.5000000	0.6100965	1
C14	C	1	0.5000000	0.3809857	0.6100965	1
C15	C	1	0.3809857	0.5000000	0.6100965	1
C16	C	1	0.5000000	0.6190143	0.6100965	1
C17	C	1	0.6190143	0.5000000	0.3899035	1
C18	C	1	0.5000000	0.3809857	0.3899035	1
C19	C	1	0.3809857	0.5000000	0.3899035	1
C20	C	1	0.5000000	0.6190143	0.3899035	1
C21	C	1	0.6190143	0.3809857	0.5000000	1
C22	C	1	0.3809857	0.3809857	0.5000000	1
C23	C	1	0.3809857	0.6190143	0.5000000	1
C24	C	1	0.6190143	0.6190143	0.5000000	1
O1	O	1	0.5377988	0.4622012	0.4752113	1
O2	O	1	0.5377988	0.4622012	0.5247887	1
O3	O	1	0.4622012	0.4622012	0.4752113	1
O4	O	1	0.4622012	0.4622012	0.5247887	1
O5	O	1	0.4622012	0.5377988	0.4752113	1
O6	O	1	0.4622012	0.5377988	0.5247887	1
O7	O	1	0.5377988	0.5377988	0.4752113	1

O8	O	1	0.5377988	0.5377988	0.5247887	1
O9	O	1	0.5944161	0.5000000	0.5497247	1
O10	O	1	0.5944161	0.4462476	0.5000000	1
O11	O	1	0.5944161	0.5000000	0.4502753	1
O12	O	1	0.5944161	0.5537524	0.5000000	1
O13	O	1	0.5000000	0.5944161	0.5497247	1
O14	O	1	0.5537524	0.5944161	0.5000000	1
O15	O	1	0.5000000	0.5944161	0.4502753	1
O16	O	1	0.4462476	0.5944161	0.5000000	1
O17	O	1	0.4055839	0.5000000	0.5497247	1
O18	O	1	0.4055839	0.5537524	0.5000000	1
O19	O	1	0.4055839	0.5000000	0.4502753	1
O20	O	1	0.4055839	0.4462476	0.5000000	1
O21	O	1	0.5000000	0.4055839	0.5497247	1
O22	O	1	0.4462476	0.4055839	0.5000000	1
O23	O	1	0.5000000	0.4055839	0.4502753	1
O24	O	1	0.5537524	0.4055839	0.5000000	1
O25	O	1	0.5537524	0.5000000	0.5873414	1
O26	O	1	0.5000000	0.5537524	0.5873414	1
O27	O	1	0.4462476	0.5000000	0.5873414	1
O28	O	1	0.5000000	0.4462476	0.5873414	1
O29	O	1	0.5537524	0.5000000	0.4126586	1
O30	O	1	0.5000000	0.4462476	0.4126586	1
O31	O	1	0.4462476	0.5000000	0.4126586	1
O32	O	1	0.5000000	0.5537524	0.4126586	1
Zr1	Zr	1	0.5667796	0.5000000	0.5000000	1
Zr2	Zr	1	0.5000000	0.5667796	0.5000000	1
Zr3	Zr	1	0.4332204	0.5000000	0.5000000	1
Zr4	Zr	1	0.5000000	0.4332204	0.5000000	1
Zr5	Zr	1	0.5000000	0.5000000	0.5617758	1
Zr6	Zr	1	0.5000000	0.5000000	0.4382242	1

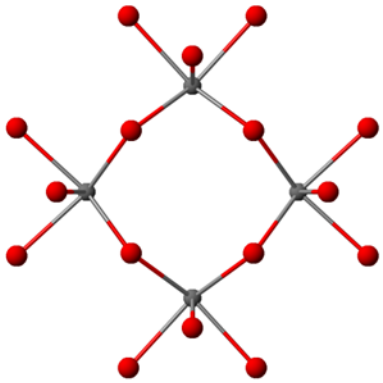

Figure 147: The tetrameric structure resulting from the chandelier core refinement of ZAA7 from the 9-month data collection.

Table 90: The atomic coordinates of the tetrameric phase of the chandelier core refinement of ZAA7 from the 9-month data collection.

Atom Label	Atom Type	Multiplicity	Fractional X Coordinate	Fractional Y Coordinate	Fractional Z Coordinate	Fractional Occupancy
O1	O	1	0.5139679	0.4860321	0.4720352	1
O2	O	1	0.4860321	0.4860321	0.5279648	1
O3	O	1	0.5139679	0.5139679	0.5279648	1
O4	O	1	0.4860321	0.5139679	0.4720352	1
O5	O	1	0.5000000	0.5309578	0.5430604	1
O6	O	1	0.5000000	0.4690422	0.5430604	1
O7	O	1	0.4690422	0.5000000	0.4569396	1
O8	O	1	0.5309578	0.5000000	0.4569396	1
O9	O	1	0.5146	0.4599481	0.5000000	1
O10	O	1	0.4599481	0.4854	0.5000000	1
O11	O	1	0.5400519	0.5146	0.5000000	1
O12	O	1	0.4854	0.5400519	0.5000000	1
O13	O	1	0.4599481	0.5146	0.5000000	1
O14	O	1	0.5400519	0.4854	0.5000000	1
O15	O	1	0.4854	0.4599481	0.5000000	1
O16	O	1	0.5146	0.5400519	0.5000000	1
O17	O	1	0.5139679	0.4860321	0.5279648	1
O18	O	1	0.4860321	0.4860321	0.4720352	1
O19	O	1	0.5139679	0.5139679	0.4720352	1
O20	O	1	0.4860321	0.5139679	0.5279648	1
O21	O	1	0.5000000	0.5309578	0.4569396	1
O22	O	1	0.5000000	0.4690422	0.4569396	1
O23	O	1	0.4690422	0.5000000	0.5430604	1
O24	O	1	0.5309578	0.5000000	0.5430604	1
Zr1	Zr	1	0.5000000	0.4758672	0.5000000	1
Zr2	Zr	1	0.4758672	0.5000000	0.5000000	1
Zr3	Zr	1	0.5241328	0.5000000	0.5000000	1
Zr4	Zr	1	0.5000000	0.5241328	0.5000000	1

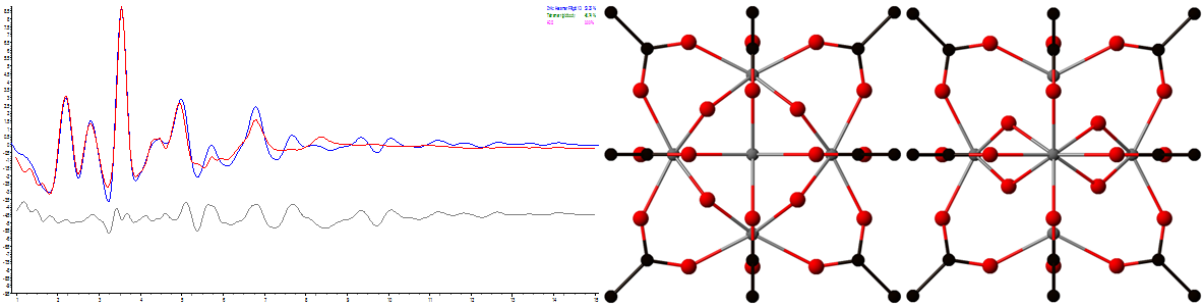

Figure 148: Observed and Calculated PDF from the chandelier core refinement of ZAA10 from the 9-month data collection and the resultant model viewed from the axial (left) and equatorial (right) positions.

Table 91: The atomic coordinates of the model resulting from the chandelier core refinement of ZAA10 from the 9-month data collection.

Atom Label	Atom Type	Multiplicity	Fractional X Coordinate	Fractional Y Coordinate	Fractional Z Coordinate	Fractional Occupancy
C1	C	1	0.5890437	0.5000000	0.5823717	1
C2	C	1	0.5000000	0.4109563	0.5823717	1
C3	C	1	0.4109563	0.5000000	0.5823717	1
C4	C	1	0.5000000	0.5890437	0.5823717	1
C5	C	1	0.5890437	0.5000000	0.4176283	1
C6	C	1	0.5000000	0.4109563	0.4176283	1
C7	C	1	0.4109563	0.5000000	0.4176283	1
C8	C	1	0.5000000	0.5890437	0.4176283	1
C9	C	1	0.5890437	0.4109563	0.5000000	1
C10	C	1	0.4109563	0.4109563	0.5000000	1
C11	C	1	0.4109563	0.5890437	0.5000000	1
C12	C	1	0.5890437	0.5890437	0.5000000	1
C13	C	1	0.6196	0.5000000	0.6106383	1
C14	C	1	0.5000000	0.3804	0.6106383	1
C15	C	1	0.3804	0.5000000	0.6106383	1
C16	C	1	0.5000000	0.6196	0.6106383	1
C17	C	1	0.6196	0.5000000	0.3893617	1
C18	C	1	0.5000000	0.3804	0.3893617	1
C19	C	1	0.3804	0.5000000	0.3893617	1
C20	C	1	0.5000000	0.6196	0.3893617	1
C21	C	1	0.6196	0.3804	0.5000000	1
C22	C	1	0.3804	0.3804	0.5000000	1
C23	C	1	0.3804	0.6196	0.5000000	1
C24	C	1	0.6196	0.6196	0.5000000	1
O1	O	1	0.5381274	0.4618726	0.4752213	1
O2	O	1	0.5381274	0.4618726	0.5247787	1
O3	O	1	0.4618726	0.4618726	0.4752213	1
O4	O	1	0.4618726	0.4618726	0.5247787	1
O5	O	1	0.4618726	0.5381274	0.4752213	1
O6	O	1	0.4618726	0.5381274	0.5247787	1

O7	O	1	0.5381274	0.5381274	0.4752213	1
O8	O	1	0.5381274	0.5381274	0.5247787	1
O9	O	1	0.5943436	0.5000000	0.5498684	1
O10	O	1	0.5943436	0.4460923	0.5000000	1
O11	O	1	0.5943436	0.5000000	0.4501316	1
O12	O	1	0.5943436	0.5539077	0.5000000	1
O13	O	1	0.5000000	0.5943436	0.5498684	1
O14	O	1	0.5539077	0.5943436	0.5000000	1
O15	O	1	0.5000000	0.5943436	0.4501316	1
O16	O	1	0.4460923	0.5943436	0.5000000	1
O17	O	1	0.4056564	0.5000000	0.5498684	1
O18	O	1	0.4056564	0.5539077	0.5000000	1
O19	O	1	0.4056564	0.5000000	0.4501316	1
O20	O	1	0.4056564	0.4460923	0.5000000	1
O21	O	1	0.5000000	0.4056564	0.5498684	1
O22	O	1	0.4460923	0.4056564	0.5000000	1
O23	O	1	0.5000000	0.4056564	0.4501316	1
O24	O	1	0.5539077	0.4056564	0.5000000	1
O25	O	1	0.5539077	0.5000000	0.5872744	1
O26	O	1	0.5000000	0.5539077	0.5872744	1
O27	O	1	0.4460923	0.5000000	0.5872744	1
O28	O	1	0.5000000	0.4460923	0.5872744	1
O29	O	1	0.5539077	0.5000000	0.4127256	1
O30	O	1	0.5000000	0.4460923	0.4127256	1
O31	O	1	0.4460923	0.5000000	0.4127256	1
O32	O	1	0.5000000	0.5539077	0.4127256	1
Zr1	Zr	1	0.5668097	0.5000000	0.5000000	1
Zr2	Zr	1	0.5000000	0.5668097	0.5000000	1
Zr3	Zr	1	0.4331903	0.5000000	0.5000000	1
Zr4	Zr	1	0.5000000	0.4331903	0.5000000	1
Zr5	Zr	1	0.5000000	0.5000000	0.5618036	1
Zr6	Zr	1	0.5000000	0.5000000	0.4381964	1

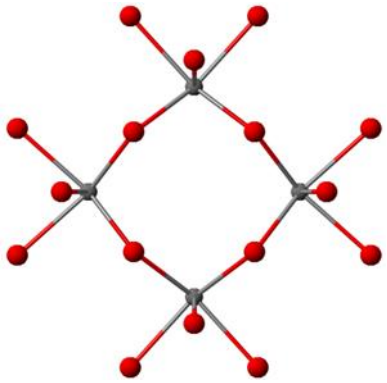

Figure 149: The tetrameric structure resulting from the chandelier core refinement of ZAA10 from the 9-month data collection.

Table 92: The atomic coordinates of the tetrameric phase of the chandelier core refinement of ZAA10 from the 9-month data collection.

Atom Label	Atom Type	Multiplicity	Fractional X Coordinate	Fractional Y Coordinate	Fractional Z Coordinate	Fractional Occupancy
O1	O	1	0.5137177	0.4862823	0.4730845	1
O2	O	1	0.4862823	0.4862823	0.5269155	1
O3	O	1	0.5137177	0.5137177	0.5269155	1
O4	O	1	0.4862823	0.5137177	0.4730845	1
O5	O	1	0.5000000	0.5301797	0.545282	1
O6	O	1	0.5000000	0.4698203	0.545282	1
O7	O	1	0.4698203	0.5000000	0.454718	1
O8	O	1	0.5301797	0.5000000	0.454718	1
O9	O	1	0.514529	0.4597784	0.5000000	1
O10	O	1	0.4597784	0.485471	0.5000000	1
O11	O	1	0.5402216	0.514529	0.5000000	1
O12	O	1	0.485471	0.5402216	0.5000000	1
O13	O	1	0.4597784	0.514529	0.5000000	1
O14	O	1	0.5402216	0.485471	0.5000000	1
O15	O	1	0.485471	0.4597784	0.5000000	1
O16	O	1	0.514529	0.5402216	0.5000000	1
O17	O	1	0.5137177	0.4862823	0.5269155	1
O18	O	1	0.4862823	0.4862823	0.4730845	1
O19	O	1	0.5137177	0.5137177	0.4730845	1
O20	O	1	0.4862823	0.5137177	0.5269155	1
O21	O	1	0.5000000	0.5301797	0.454718	1
O22	O	1	0.5000000	0.4698203	0.454718	1
O23	O	1	0.4698203	0.5000000	0.545282	1
O24	O	1	0.5301797	0.5000000	0.545282	1
Zr1	Zr	1	0.5000000	0.4759205	0.5000000	1
Zr2	Zr	1	0.4759205	0.5000000	0.5000000	1
Zr3	Zr	1	0.5240795	0.5000000	0.5000000	1
Zr4	Zr	1	0.5000000	0.5240795	0.5000000	1

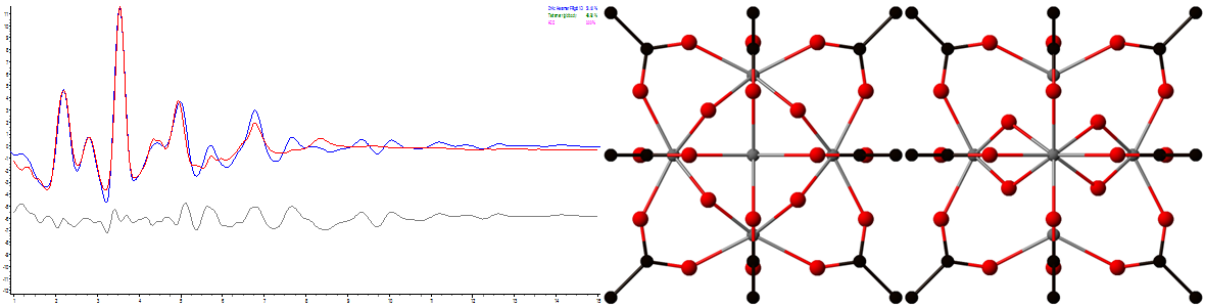

Figure 150: Observed and Calculated PDF from the chandelier core refinement of ZAA13 from the 9-month data collection and the resultant model viewed from the axial (left) and equatorial (right) positions.

Table 93: The atomic coordinates of the model resulting from the chandelier core refinement of ZAA13 from the 9-month data collection.

Atom Label	Atom Type	Multiplicity	Fractional X Coordinate	Fractional Y Coordinate	Fractional Z Coordinate	Fractional Occupancy
C1	C	1	0.5890429	0.5000000	0.5823709	1
C2	C	1	0.5000000	0.4109571	0.5823709	1
C3	C	1	0.4109571	0.5000000	0.5823709	1
C4	C	1	0.5000000	0.5890429	0.5823709	1
C5	C	1	0.5890429	0.5000000	0.4176291	1
C6	C	1	0.5000000	0.4109571	0.4176291	1
C7	C	1	0.4109571	0.5000000	0.4176291	1
C8	C	1	0.5000000	0.5890429	0.4176291	1
C9	C	1	0.5890429	0.4109571	0.5000000	1
C10	C	1	0.4109571	0.4109571	0.5000000	1
C11	C	1	0.4109571	0.5890429	0.5000000	1
C12	C	1	0.5890429	0.5890429	0.5000000	1
C13	C	1	0.6192947	0.5000000	0.6103559	1
C14	C	1	0.5000000	0.3807053	0.6103559	1
C15	C	1	0.3807053	0.5000000	0.6103559	1
C16	C	1	0.5000000	0.6192947	0.6103559	1
C17	C	1	0.6192947	0.5000000	0.3896441	1
C18	C	1	0.5000000	0.3807053	0.3896441	1
C19	C	1	0.3807053	0.5000000	0.3896441	1
C20	C	1	0.5000000	0.6192947	0.3896441	1
C21	C	1	0.6192947	0.3807053	0.5000000	1
C22	C	1	0.3807053	0.3807053	0.5000000	1
C23	C	1	0.3807053	0.6192947	0.5000000	1
C24	C	1	0.6192947	0.6192947	0.5000000	1
O1	O	1	0.5374184	0.4625816	0.4744485	1
O2	O	1	0.5374184	0.4625816	0.5255515	1
O3	O	1	0.4625816	0.4625816	0.4744485	1
O4	O	1	0.4625816	0.4625816	0.5255515	1
O5	O	1	0.4625816	0.5374184	0.4744485	1
O6	O	1	0.4625816	0.5374184	0.5255515	1

O7	O	1	0.5374184	0.5374184	0.4744485	1
O8	O	1	0.5374184	0.5374184	0.5255515	1
O9	O	1	0.5942846	0.5000000	0.5496669	1
O10	O	1	0.5942846	0.4463101	0.5000000	1
O11	O	1	0.5942846	0.5000000	0.4503331	1
O12	O	1	0.5942846	0.5536899	0.5000000	1
O13	O	1	0.5000000	0.5942846	0.5496669	1
O14	O	1	0.5536899	0.5942846	0.5000000	1
O15	O	1	0.5000000	0.5942846	0.4503331	1
O16	O	1	0.4463101	0.5942846	0.5000000	1
O17	O	1	0.4057154	0.5000000	0.5496669	1
O18	O	1	0.4057154	0.5536899	0.5000000	1
O19	O	1	0.4057154	0.5000000	0.4503331	1
O20	O	1	0.4057154	0.4463101	0.5000000	1
O21	O	1	0.5000000	0.4057154	0.5496669	1
O22	O	1	0.4463101	0.4057154	0.5000000	1
O23	O	1	0.5000000	0.4057154	0.4503331	1
O24	O	1	0.5536899	0.4057154	0.5000000	1
O25	O	1	0.5536899	0.5000000	0.5872198	1
O26	O	1	0.5000000	0.5536899	0.5872198	1
O27	O	1	0.4463101	0.5000000	0.5872198	1
O28	O	1	0.5000000	0.4463101	0.5872198	1
O29	O	1	0.5536899	0.5000000	0.4127802	1
O30	O	1	0.5000000	0.4463101	0.4127802	1
O31	O	1	0.4463101	0.5000000	0.4127802	1
O32	O	1	0.5000000	0.5536899	0.4127802	1
Zr1	Zr	1	0.5668612	0.5000000	0.5000000	1
Zr2	Zr	1	0.5000000	0.5668612	0.5000000	1
Zr3	Zr	1	0.4331388	0.5000000	0.5000000	1
Zr4	Zr	1	0.5000000	0.4331388	0.5000000	1
Zr5	Zr	1	0.5000000	0.5000000	0.5618513	1
Zr6	Zr	1	0.5000000	0.5000000	0.4381487	1

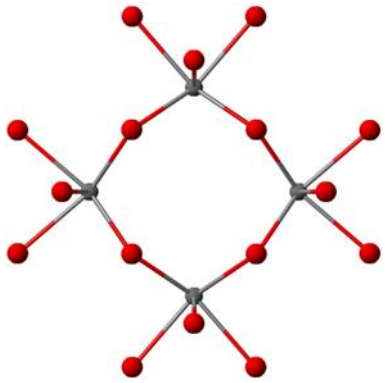

Figure 151: The tetrameric structure resulting from the chandelier core refinement of ZAA13 from the 9-month data collection.

Table 94: The atomic coordinates of the tetrameric phase of the chandelier core refinement of ZAA13 from the 9-month data collection.

Atom Label	Atom Type	Multiplicity	Fractional X Coordinate	Fractional Y Coordinate	Fractional Z Coordinate	Fractional Occupancy
O1	O	1	0.5143363	0.4856637	0.4759523	1
O2	O	1	0.4856637	0.4856637	0.5240477	1
O3	O	1	0.5143363	0.5143363	0.5240477	1
O4	O	1	0.4856637	0.5143363	0.4759523	1
O5	O	1	0.5000000	0.5303569	0.5465889	1
O6	O	1	0.5000000	0.4696431	0.5465889	1
O7	O	1	0.4696431	0.5000000	0.4534111	1
O8	O	1	0.5303569	0.5000000	0.4534111	1
O9	O	1	0.5141517	0.459552	0.5000000	1
O10	O	1	0.459552	0.4858483	0.5000000	1
O11	O	1	0.540448	0.5141517	0.5000000	1
O12	O	1	0.4858483	0.540448	0.5000000	1
O13	O	1	0.459552	0.5141517	0.5000000	1
O14	O	1	0.540448	0.4858483	0.5000000	1
O15	O	1	0.4858483	0.459552	0.5000000	1
O16	O	1	0.5141517	0.540448	0.5000000	1
O17	O	1	0.5143363	0.4856637	0.5240477	1
O18	O	1	0.4856637	0.4856637	0.4759523	1
O19	O	1	0.5143363	0.5143363	0.4759523	1
O20	O	1	0.4856637	0.5143363	0.5240477	1
O21	O	1	0.5000000	0.5303569	0.4534111	1
O22	O	1	0.5000000	0.4696431	0.4534111	1
O23	O	1	0.4696431	0.5000000	0.5465889	1
O24	O	1	0.5303569	0.5000000	0.5465889	1
Zr1	Zr	1	0.5000000	0.4760008	0.5000000	1
Zr2	Zr	1	0.4760008	0.5000000	0.5000000	1
Zr3	Zr	1	0.5239992	0.5000000	0.5000000	1
Zr4	Zr	1	0.5000000	0.5239992	0.5000000	1

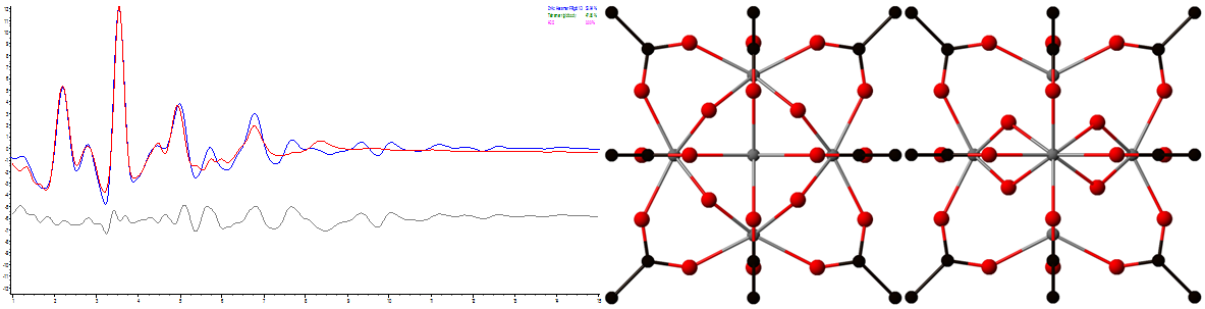

Figure 152: Observed and Calculated PDF from the chandelier core refinement of ZAA16 from the 9-month data collection and the resultant model viewed from the axial (left) and equatorial (right) positions.

Table 95: The atomic coordinates of the model resulting from the chandelier core refinement of ZAA16 from the 9-month data collection.

Atom Label	Atom Type	Multiplicity	Fractional X Coordinate	Fractional Y Coordinate	Fractional Z Coordinate	Fractional Occupancy
C1	C	1	0.5888881	0.5000000	0.5822277	1
C2	C	1	0.5000000	0.4111119	0.5822277	1
C3	C	1	0.4111119	0.5000000	0.5822277	1
C4	C	1	0.5000000	0.5888881	0.5822277	1
C5	C	1	0.5888881	0.5000000	0.4177723	1
C6	C	1	0.5000000	0.4111119	0.4177723	1
C7	C	1	0.4111119	0.5000000	0.4177723	1
C8	C	1	0.5000000	0.5888881	0.4177723	1
C9	C	1	0.5888881	0.4111119	0.5000000	1
C10	C	1	0.4111119	0.4111119	0.5000000	1
C11	C	1	0.4111119	0.5888881	0.5000000	1
C12	C	1	0.5888881	0.5888881	0.5000000	1
C13	C	1	0.6195691	0.5000000	0.6106097	1
C14	C	1	0.5000000	0.3804309	0.6106097	1
C15	C	1	0.3804309	0.5000000	0.6106097	1
C16	C	1	0.5000000	0.6195691	0.6106097	1
C17	C	1	0.6195691	0.5000000	0.3893903	1
C18	C	1	0.5000000	0.3804309	0.3893903	1
C19	C	1	0.3804309	0.5000000	0.3893903	1
C20	C	1	0.5000000	0.6195691	0.3893903	1
C21	C	1	0.6195691	0.3804309	0.5000000	1
C22	C	1	0.3804309	0.3804309	0.5000000	1
C23	C	1	0.3804309	0.6195691	0.5000000	1
C24	C	1	0.6195691	0.6195691	0.5000000	1
O1	O	1	0.537504	0.462496	0.4747413	1
O2	O	1	0.537504	0.462496	0.5252587	1
O3	O	1	0.462496	0.462496	0.4747413	1
O4	O	1	0.462496	0.462496	0.5252587	1
O5	O	1	0.462496	0.537504	0.4747413	1
O6	O	1	0.462496	0.537504	0.5252587	1

O7	O	1	0.537504	0.537504	0.4747413	1
O8	O	1	0.537504	0.537504	0.5252587	1
O9	O	1	0.5941532	0.5000000	0.5497705	1
O10	O	1	0.5941532	0.4461981	0.5000000	1
O11	O	1	0.5941532	0.5000000	0.4502295	1
O12	O	1	0.5941532	0.5538019	0.5000000	1
O13	O	1	0.5000000	0.5941532	0.5497705	1
O14	O	1	0.5538019	0.5941532	0.5000000	1
O15	O	1	0.5000000	0.5941532	0.4502295	1
O16	O	1	0.4461981	0.5941532	0.5000000	1
O17	O	1	0.4058468	0.5000000	0.5497705	1
O18	O	1	0.4058468	0.5538019	0.5000000	1
O19	O	1	0.4058468	0.5000000	0.4502295	1
O20	O	1	0.4058468	0.4461981	0.5000000	1
O21	O	1	0.5000000	0.4058468	0.5497705	1
O22	O	1	0.4461981	0.4058468	0.5000000	1
O23	O	1	0.5000000	0.4058468	0.4502295	1
O24	O	1	0.5538019	0.4058468	0.5000000	1
O25	O	1	0.5538019	0.5000000	0.5870983	1
O26	O	1	0.5000000	0.5538019	0.5870983	1
O27	O	1	0.4461981	0.5000000	0.5870983	1
O28	O	1	0.5000000	0.4461981	0.5870983	1
O29	O	1	0.5538019	0.5000000	0.4129017	1
O30	O	1	0.5000000	0.4461981	0.4129017	1
O31	O	1	0.4461981	0.5000000	0.4129017	1
O32	O	1	0.5000000	0.5538019	0.4129017	1
Zr1	Zr	1	0.566842	0.5000000	0.5000000	1
Zr2	Zr	1	0.5000000	0.566842	0.5000000	1
Zr3	Zr	1	0.433158	0.5000000	0.5000000	1
Zr4	Zr	1	0.5000000	0.433158	0.5000000	1
Zr5	Zr	1	0.5000000	0.5000000	0.5618335	1
Zr6	Zr	1	0.5000000	0.5000000	0.4381665	1

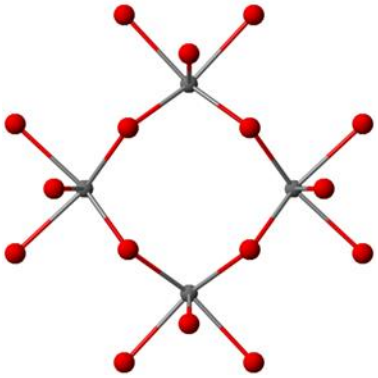

Figure 153: The tetrameric structure resulting from the chandelier core refinement of ZAA16 from the 9-month data collection.

Table 96: The atomic coordinates of the tetrameric phase of the chandelier core refinement of ZAA16 from the 9-month data collection.

Atom Label	Atom Type	Multiplicity	Fractional X Coordinate	Fractional Y Coordinate	Fractional Z Coordinate	Fractional Occupancy
O1	O	1	0.5140296	0.4859704	0.472521	1
O2	O	1	0.4859704	0.4859704	0.527479	1
O3	O	1	0.5140296	0.5140296	0.527479	1
O4	O	1	0.4859704	0.5140296	0.472521	1
O5	O	1	0.5000000	0.5310848	0.5426414	1
O6	O	1	0.5000000	0.4689152	0.5426414	1
O7	O	1	0.4689152	0.5000000	0.4573586	1
O8	O	1	0.5310848	0.5000000	0.4573586	1
O9	O	1	0.514868	0.4599729	0.5000000	1
O10	O	1	0.4599729	0.485132	0.5000000	1
O11	O	1	0.5400271	0.514868	0.5000000	1
O12	O	1	0.485132	0.5400271	0.5000000	1
O13	O	1	0.4599729	0.514868	0.5000000	1
O14	O	1	0.5400271	0.485132	0.5000000	1
O15	O	1	0.485132	0.4599729	0.5000000	1
O16	O	1	0.514868	0.5400271	0.5000000	1
O17	O	1	0.5140296	0.4859704	0.527479	1
O18	O	1	0.4859704	0.4859704	0.472521	1
O19	O	1	0.5140296	0.5140296	0.472521	1
O20	O	1	0.4859704	0.5140296	0.527479	1
O21	O	1	0.5000000	0.5310848	0.4573586	1
O22	O	1	0.5000000	0.4689152	0.4573586	1
O23	O	1	0.4689152	0.5000000	0.5426414	1
O24	O	1	0.5310848	0.5000000	0.5426414	1
Zr1	Zr	1	0.5000000	0.4759565	0.5000000	1
Zr2	Zr	1	0.4759565	0.5000000	0.5000000	1
Zr3	Zr	1	0.5240435	0.5000000	0.5000000	1
Zr4	Zr	1	0.5000000	0.5240435	0.5000000	1

10.4 September 2020 Data Collection

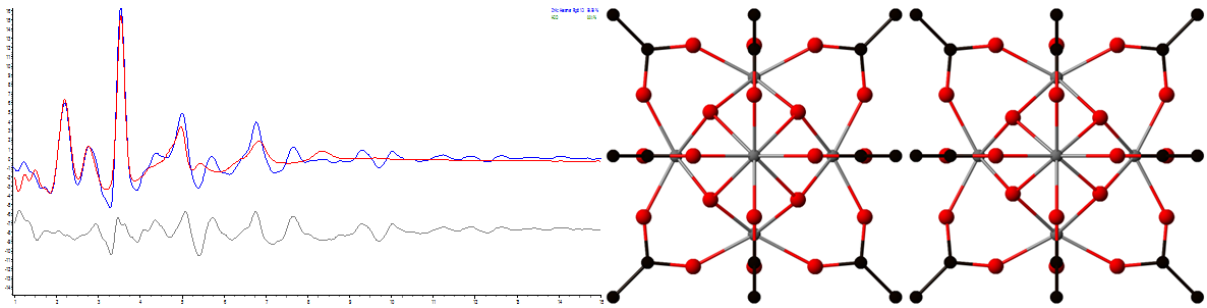

Figure 154: Observed and Calculated PDF from the chandelier core refinement of ZAA1 from the 15-month data collection and the resultant model viewed from the axial (left) and equatorial (right) positions.

Table 97: The atomic coordinates of the model resulting from the chandelier core refinement of ZAA1` from the 15-month data collection.

Atom Label	Atom Type	Multiplicity	Fractional X Coordinate	Fractional Y Coordinate	Fractional Z Coordinate	Fractional Occupancy
C1	C	1	0.5899775	0.5000000	0.5832355	1
C2	C	1	0.5000000	0.4100225	0.5832355	1
C3	C	1	0.4100225	0.5000000	0.5832355	1
C4	C	1	0.5000000	0.5899775	0.5832355	1
C5	C	1	0.5899775	0.5000000	0.4167645	1
C6	C	1	0.5000000	0.4100225	0.4167645	1
C7	C	1	0.4100225	0.5000000	0.4167645	1
C8	C	1	0.5000000	0.5899775	0.4167645	1
C9	C	1	0.5899775	0.4100225	0.5000000	1
C10	C	1	0.4100225	0.4100225	0.5000000	1
C11	C	1	0.4100225	0.5899775	0.5000000	1
C12	C	1	0.5899775	0.5899775	0.5000000	1
C13	C	1	0.6193084	0.5000000	0.6103685	1
C14	C	1	0.5000000	0.3806916	0.6103685	1
C15	C	1	0.3806916	0.5000000	0.6103685	1
C16	C	1	0.5000000	0.6193084	0.6103685	1
C17	C	1	0.6193084	0.5000000	0.3896315	1
C18	C	1	0.5000000	0.3806916	0.3896315	1
C19	C	1	0.3806916	0.5000000	0.3896315	1
C20	C	1	0.5000000	0.6193084	0.3896315	1
C21	C	1	0.6193084	0.3806916	0.5000000	1
C22	C	1	0.3806916	0.3806916	0.5000000	1
C23	C	1	0.3806916	0.6193084	0.5000000	1
C24	C	1	0.6193084	0.6193084	0.5000000	1
O1	O	1	0.5370825	0.4629175	0.4702872	1
O2	O	1	0.5370825	0.4629175	0.5297128	1
O3	O	1	0.4629175	0.4629175	0.4702872	1
O4	O	1	0.4629175	0.4629175	0.5297128	1

O5	O	1	0.4629175	0.5370825	0.4702872	1
O6	O	1	0.4629175	0.5370825	0.5297128	1
O7	O	1	0.5370825	0.5370825	0.4702872	1
O8	O	1	0.5370825	0.5370825	0.5297128	1
O9	O	1	0.5934071	0.5000000	0.5477636	1
O10	O	1	0.5934071	0.4483676	0.5000000	1
O11	O	1	0.5934071	0.5000000	0.4522364	1
O12	O	1	0.5934071	0.5516324	0.5000000	1
O13	O	1	0.5000000	0.5934071	0.5477636	1
O14	O	1	0.5516324	0.5934071	0.5000000	1
O15	O	1	0.5000000	0.5934071	0.4522364	1
O16	O	1	0.4483676	0.5934071	0.5000000	1
O17	O	1	0.4065929	0.5000000	0.5477636	1
O18	O	1	0.4065929	0.5516324	0.5000000	1
O19	O	1	0.4065929	0.5000000	0.4522364	1
O20	O	1	0.4065929	0.4483676	0.5000000	1
O21	O	1	0.5000000	0.4065929	0.5477636	1
O22	O	1	0.4483676	0.4065929	0.5000000	1
O23	O	1	0.5000000	0.4065929	0.4522364	1
O24	O	1	0.5516324	0.4065929	0.5000000	1
O25	O	1	0.5516324	0.5000000	0.586408	1
O26	O	1	0.5000000	0.5516324	0.586408	1
O27	O	1	0.4483676	0.5000000	0.586408	1
O28	O	1	0.5000000	0.4483676	0.586408	1
O29	O	1	0.5516324	0.5000000	0.413592	1
O30	O	1	0.5000000	0.4483676	0.413592	1
O31	O	1	0.4483676	0.5000000	0.413592	1
O32	O	1	0.5000000	0.5516324	0.413592	1
Zr1	Zr	1	0.5662359	0.5000000	0.5000000	1
Zr2	Zr	1	0.5000000	0.5662359	0.5000000	1
Zr3	Zr	1	0.4337641	0.5000000	0.5000000	1
Zr4	Zr	1	0.5000000	0.4337641	0.5000000	1
Zr5	Zr	1	0.5000000	0.5000000	0.5612728	1
Zr6	Zr	1	0.5000000	0.5000000	0.4387272	1

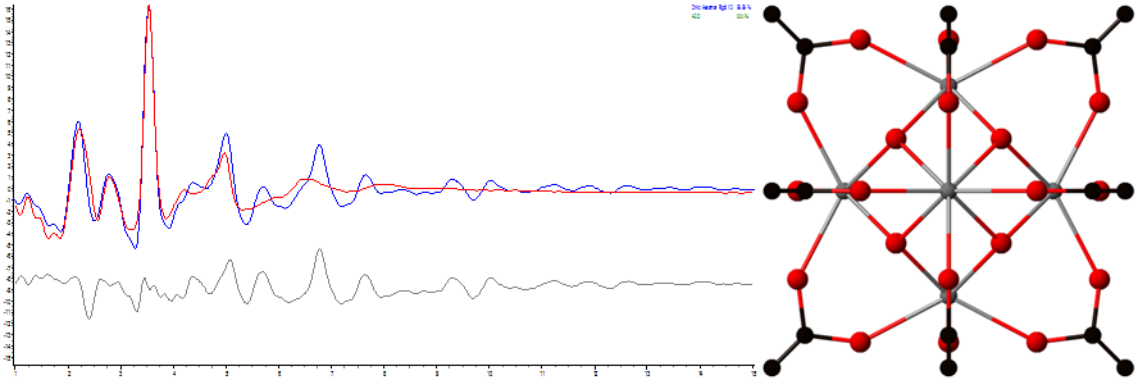

Figure 155: Observed and Calculated PDF from the fixed core refinement of ZAA1 from the 15-month data collection and the resultant model.

Table 98: The atomic coordinates of the model resulting from the fixed core refinement of ZAA1 from the 15-month data collection.

Atom Label	Atom Type	Multiplicity	Fractional X Coordinate	Fractional Y Coordinate	Fractional Z Coordinate	Fractional Occupancy
C1	C	1	0.590628	0.5000000	0.5838372	1
C2	C	1	0.5000000	0.409372	0.5838372	1
C3	C	1	0.409372	0.5000000	0.5838372	1
C4	C	1	0.5000000	0.590628	0.5838372	1
C5	C	1	0.590628	0.5000000	0.4161628	1
C6	C	1	0.5000000	0.409372	0.4161628	1
C7	C	1	0.409372	0.5000000	0.4161628	1
C8	C	1	0.5000000	0.590628	0.4161628	1
C9	C	1	0.590628	0.409372	0.5000000	1
C10	C	1	0.409372	0.409372	0.5000000	1
C11	C	1	0.409372	0.590628	0.5000000	1
C12	C	1	0.590628	0.590628	0.5000000	1
C13	C	1	0.6112167	0.5000000	0.6028832	1
C14	C	1	0.5000000	0.3887833	0.6028832	1
C15	C	1	0.3887833	0.5000000	0.6028832	1
C16	C	1	0.5000000	0.6112167	0.6028832	1
C17	C	1	0.6112167	0.5000000	0.3971168	1
C18	C	1	0.5000000	0.3887833	0.3971168	1
C19	C	1	0.3887833	0.5000000	0.3971168	1
C20	C	1	0.5000000	0.6112167	0.3971168	1
C21	C	1	0.6112167	0.3887833	0.5000000	1
C22	C	1	0.3887833	0.3887833	0.5000000	1
C23	C	1	0.3887833	0.6112167	0.5000000	1
C24	C	1	0.6112167	0.6112167	0.5000000	1
O1	O	1	0.5331046	0.5327816	0.4693759	1
O2	O	1	0.5331046	0.4672184	0.5306241	1
O3	O	1	0.4668954	0.5327816	0.4693759	1
O4	O	1	0.4668954	0.4672184	0.5306241	1
O5	O	1	0.4668954	0.4672184	0.4693759	1

O6	O	1	0.4668954	0.5327816	0.5306241	1
O7	O	1	0.5331046	0.4672184	0.4693759	1
O8	O	1	0.5331046	0.5327816	0.5306241	1
O9	O	1	0.595093	0.5000000	0.5513319	1
O10	O	1	0.595093	0.4445102	0.5000000	1
O11	O	1	0.595093	0.5000000	0.4486681	1
O12	O	1	0.595093	0.5554898	0.5000000	1
O13	O	1	0.5000000	0.595093	0.5513319	1
O14	O	1	0.5554898	0.595093	0.5000000	1
O15	O	1	0.5000000	0.595093	0.4486681	1
O16	O	1	0.4445102	0.595093	0.5000000	1
O17	O	1	0.404907	0.5000000	0.5513319	1
O18	O	1	0.404907	0.5554898	0.5000000	1
O19	O	1	0.404907	0.5000000	0.4486681	1
O20	O	1	0.404907	0.4445102	0.5000000	1
O21	O	1	0.5000000	0.404907	0.5513319	1
O22	O	1	0.4445102	0.404907	0.5000000	1
O23	O	1	0.5000000	0.404907	0.4486681	1
O24	O	1	0.5554898	0.404907	0.5000000	1
O25	O	1	0.5554898	0.5000000	0.5879677	1
O26	O	1	0.5000000	0.5554898	0.5879677	1
O27	O	1	0.4445102	0.5000000	0.5879677	1
O28	O	1	0.5000000	0.4445102	0.5879677	1
O29	O	1	0.5554898	0.5000000	0.4120323	1
O30	O	1	0.5000000	0.4445102	0.4120323	1
O31	O	1	0.4445102	0.5000000	0.4120323	1
O32	O	1	0.5000000	0.5554898	0.4120323	1
Zr1	Zr	1	0.5661193	0.5000000	0.5000000	1
Zr2	Zr	1	0.5000000	0.5661193	0.5000000	1
Zr3	Zr	1	0.4338807	0.5000000	0.5000000	1
Zr4	Zr	1	0.5000000	0.4338807	0.5000000	1
Zr5	Zr	1	0.5000000	0.5000000	0.5611649	1
Zr6	Zr	1	0.5000000	0.5000000	0.4388351	1

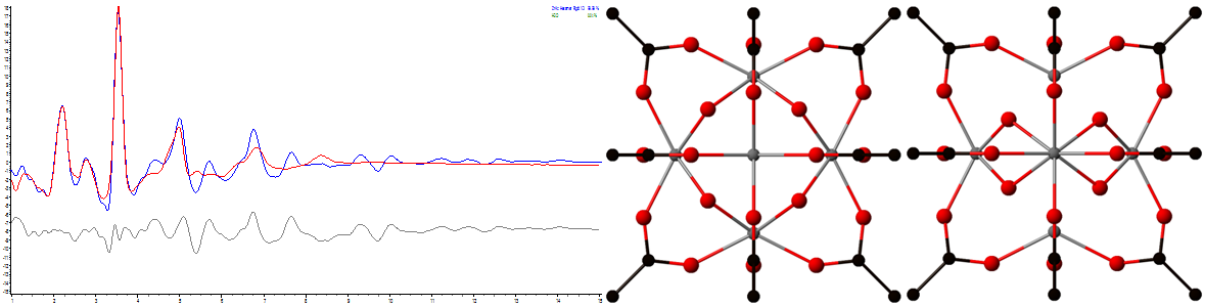

Figure 156: Observed and Calculated PDF from the chandelier core refinement of ZAA4 from the 15-month data collection and the resultant model viewed from the axial (left) and equatorial (right) positions.

Table 99: The atomic coordinates of the model resulting from the chandelier core refinement of ZAA4 from the 15-month data collection.

Atom Label	Atom Type	Multiplicity	Fractional X Coordinate	Fractional Y Coordinate	Fractional Z Coordinate	Fractional Occupancy
C1	C	1	0.5892996	0.5000000	0.5826084	1
C2	C	1	0.5000000	0.4107004	0.5826084	1
C3	C	1	0.4107004	0.5000000	0.5826084	1
C4	C	1	0.5000000	0.5892996	0.5826084	1
C5	C	1	0.5892996	0.5000000	0.4173916	1
C6	C	1	0.5000000	0.4107004	0.4173916	1
C7	C	1	0.4107004	0.5000000	0.4173916	1
C8	C	1	0.5000000	0.5892996	0.4173916	1
C9	C	1	0.5892996	0.4107004	0.5000000	1
C10	C	1	0.4107004	0.4107004	0.5000000	1
C11	C	1	0.4107004	0.5892996	0.5000000	1
C12	C	1	0.5892996	0.5892996	0.5000000	1
C13	C	1	0.6196599	0.5000000	0.6106937	1
C14	C	1	0.5000000	0.3803401	0.6106937	1
C15	C	1	0.3803401	0.5000000	0.6106937	1
C16	C	1	0.5000000	0.6196599	0.6106937	1
C17	C	1	0.6196599	0.5000000	0.3893063	1
C18	C	1	0.5000000	0.3803401	0.3893063	1
C19	C	1	0.3803401	0.5000000	0.3893063	1
C20	C	1	0.5000000	0.6196599	0.3893063	1
C21	C	1	0.6196599	0.3803401	0.5000000	1
C22	C	1	0.3803401	0.3803401	0.5000000	1
C23	C	1	0.3803401	0.6196599	0.5000000	1
C24	C	1	0.6196599	0.6196599	0.5000000	1
O1	O	1	0.538677	0.461323	0.473052	1
O2	O	1	0.538677	0.461323	0.526948	1
O3	O	1	0.461323	0.461323	0.473052	1
O4	O	1	0.461323	0.461323	0.526948	1
O5	O	1	0.461323	0.538677	0.473052	1
O6	O	1	0.461323	0.538677	0.526948	1
O7	O	1	0.538677	0.538677	0.473052	1

O8	O	1	0.538677	0.538677	0.526948	1
O9	O	1	0.5933828	0.5000000	0.5491888	1
O10	O	1	0.5933828	0.446827	0.5000000	1
O11	O	1	0.5933828	0.5000000	0.4508112	1
O12	O	1	0.5933828	0.553173	0.5000000	1
O13	O	1	0.5000000	0.5933828	0.5491888	1
O14	O	1	0.553173	0.5933828	0.5000000	1
O15	O	1	0.5000000	0.5933828	0.4508112	1
O16	O	1	0.446827	0.5933828	0.5000000	1
O17	O	1	0.4066172	0.5000000	0.5491888	1
O18	O	1	0.4066172	0.553173	0.5000000	1
O19	O	1	0.4066172	0.5000000	0.4508112	1
O20	O	1	0.4066172	0.446827	0.5000000	1
O21	O	1	0.5000000	0.4066172	0.5491888	1
O22	O	1	0.446827	0.4066172	0.5000000	1
O23	O	1	0.5000000	0.4066172	0.4508112	1
O24	O	1	0.553173	0.4066172	0.5000000	1
O25	O	1	0.553173	0.5000000	0.5863856	1
O26	O	1	0.5000000	0.553173	0.5863856	1
O27	O	1	0.446827	0.5000000	0.5863856	1
O28	O	1	0.5000000	0.446827	0.5863856	1
O29	O	1	0.553173	0.5000000	0.4136144	1
O30	O	1	0.5000000	0.446827	0.4136144	1
O31	O	1	0.446827	0.5000000	0.4136144	1
O32	O	1	0.5000000	0.553173	0.4136144	1
Zr1	Zr	1	0.5663105	0.5000000	0.5000000	1
Zr2	Zr	1	0.5000000	0.5663105	0.5000000	1
Zr3	Zr	1	0.4336895	0.5000000	0.5000000	1
Zr4	Zr	1	0.5000000	0.4336895	0.5000000	1
Zr5	Zr	1	0.5000000	0.5000000	0.5613418	1
Zr6	Zr	1	0.5000000	0.5000000	0.4386582	1

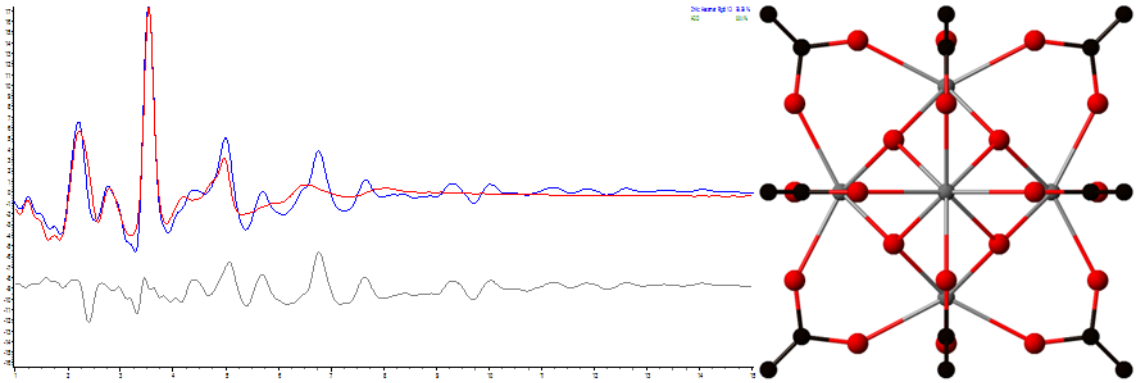

Figure 157: Observed and Calculated PDF from the fixed core refinement of ZAA4 from the 15-month data collection and the resultant model.

Table 100: The atomic coordinates of the model resulting from the fixed core refinement of ZAA4 from the 15-month data collection.

Atom Label	Atom Type	Multiplicity	Fractional X Coordinate	Fractional Y Coordinate	Fractional Z Coordinate	Fractional Occupancy
C1	C	1	0.5907339	0.5000000	0.5839352	1
C2	C	1	0.5000000	0.4092661	0.5839352	1
C3	C	1	0.4092661	0.5000000	0.5839352	1
C4	C	1	0.5000000	0.5907339	0.5839352	1
C5	C	1	0.5907339	0.5000000	0.4160648	1
C6	C	1	0.5000000	0.4092661	0.4160648	1
C7	C	1	0.4092661	0.5000000	0.4160648	1
C8	C	1	0.5000000	0.5907339	0.4160648	1
C9	C	1	0.5907339	0.4092661	0.5000000	1
C10	C	1	0.4092661	0.4092661	0.5000000	1
C11	C	1	0.4092661	0.5907339	0.5000000	1
C12	C	1	0.5907339	0.5907339	0.5000000	1
C13	C	1	0.6113835	0.5000000	0.6030375	1
C14	C	1	0.5000000	0.3886165	0.6030375	1
C15	C	1	0.3886165	0.5000000	0.6030375	1
C16	C	1	0.5000000	0.6113835	0.6030375	1
C17	C	1	0.6113835	0.5000000	0.3969625	1
C18	C	1	0.5000000	0.3886165	0.3969625	1
C19	C	1	0.3886165	0.5000000	0.3969625	1
C20	C	1	0.5000000	0.6113835	0.3969625	1
C21	C	1	0.6113835	0.3886165	0.5000000	1
C22	C	1	0.3886165	0.3886165	0.5000000	1
C23	C	1	0.3886165	0.6113835	0.5000000	1
C24	C	1	0.6113835	0.6113835	0.5000000	1
O1	O	1	0.5330924	0.5327695	0.4693873	1
O2	O	1	0.5330924	0.4672305	0.5306127	1
O3	O	1	0.4669076	0.5327695	0.4693873	1
O4	O	1	0.4669076	0.4672305	0.5306127	1
O5	O	1	0.4669076	0.4672305	0.4693873	1

O6	O	1	0.4669076	0.5327695	0.5306127	1
O7	O	1	0.5330924	0.4672305	0.4693873	1
O8	O	1	0.5330924	0.5327695	0.5306127	1
O9	O	1	0.5950126	0.5000000	0.5513967	1
O10	O	1	0.5950126	0.4444402	0.5000000	1
O11	O	1	0.5950126	0.5000000	0.4486033	1
O12	O	1	0.5950126	0.5555598	0.5000000	1
O13	O	1	0.5000000	0.5950126	0.5513967	1
O14	O	1	0.5555598	0.5950126	0.5000000	1
O15	O	1	0.5000000	0.5950126	0.4486033	1
O16	O	1	0.4444402	0.5950126	0.5000000	1
O17	O	1	0.4049874	0.5000000	0.5513967	1
O18	O	1	0.4049874	0.5555598	0.5000000	1
O19	O	1	0.4049874	0.5000000	0.4486033	1
O20	O	1	0.4049874	0.4444402	0.5000000	1
O21	O	1	0.5000000	0.4049874	0.5513967	1
O22	O	1	0.4444402	0.4049874	0.5000000	1
O23	O	1	0.5000000	0.4049874	0.4486033	1
O24	O	1	0.5555598	0.4049874	0.5000000	1
O25	O	1	0.5555598	0.5000000	0.5878933	1
O26	O	1	0.5000000	0.5555598	0.5878933	1
O27	O	1	0.4444402	0.5000000	0.5878933	1
O28	O	1	0.5000000	0.4444402	0.5878933	1
O29	O	1	0.5555598	0.5000000	0.4121067	1
O30	O	1	0.5000000	0.4444402	0.4121067	1
O31	O	1	0.4444402	0.5000000	0.4121067	1
O32	O	1	0.5000000	0.5555598	0.4121067	1
Zr1	Zr	1	0.5661068	0.5000000	0.5000000	1
Zr2	Zr	1	0.5000000	0.5661068	0.5000000	1
Zr3	Zr	1	0.4338932	0.5000000	0.5000000	1
Zr4	Zr	1	0.5000000	0.4338932	0.5000000	1
Zr5	Zr	1	0.5000000	0.5000000	0.5611534	1
Zr6	Zr	1	0.5000000	0.5000000	0.4388466	1

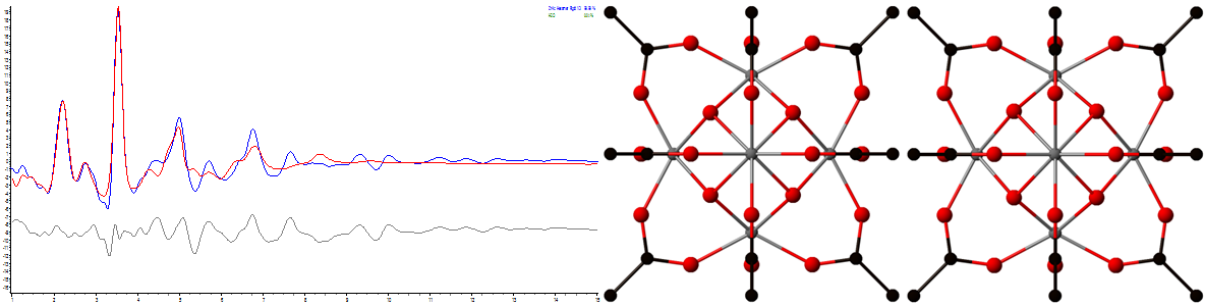

Figure 158: Observed and Calculated PDF from the chandelier core refinement of ZAA7 from the 15-month data collection and the resultant model viewed from the axial (left) and equatorial (right) positions.

Table 101: The atomic coordinates of the model resulting from the chandelier core refinement of ZAA7 from the 15-month data collection.

Atom Label	Atom Type	Multiplicity	Fractional X Coordinate	Fractional Y Coordinate	Fractional Z Coordinate	Fractional Occupancy
C1	C	1	0.5883607	0.5000000	0.5817398	1
C2	C	1	0.5000000	0.4116393	0.5817398	1
C3	C	1	0.4116393	0.5000000	0.5817398	1
C4	C	1	0.5000000	0.5883607	0.5817398	1
C5	C	1	0.5883607	0.5000000	0.4182602	1
C6	C	1	0.5000000	0.4116393	0.4182602	1
C7	C	1	0.4116393	0.5000000	0.4182602	1
C8	C	1	0.5000000	0.5883607	0.4182602	1
C9	C	1	0.5883607	0.4116393	0.5000000	1
C10	C	1	0.4116393	0.4116393	0.5000000	1
C11	C	1	0.4116393	0.5883607	0.5000000	1
C12	C	1	0.5883607	0.5883607	0.5000000	1
C13	C	1	0.6194802	0.5000000	0.6105275	1
C14	C	1	0.5000000	0.3805198	0.6105275	1
C15	C	1	0.3805198	0.5000000	0.6105275	1
C16	C	1	0.5000000	0.6194802	0.6105275	1
C17	C	1	0.6194802	0.5000000	0.3894725	1
C18	C	1	0.5000000	0.3805198	0.3894725	1
C19	C	1	0.3805198	0.5000000	0.3894725	1
C20	C	1	0.5000000	0.6194802	0.3894725	1
C21	C	1	0.6194802	0.3805198	0.5000000	1
C22	C	1	0.3805198	0.3805198	0.5000000	1
C23	C	1	0.3805198	0.6194802	0.5000000	1
C24	C	1	0.6194802	0.6194802	0.5000000	1
O1	O	1	0.5348968	0.4651032	0.4662252	1
O2	O	1	0.5348968	0.4651032	0.5337748	1
O3	O	1	0.4651032	0.4651032	0.4662252	1
O4	O	1	0.4651032	0.4651032	0.5337748	1
O5	O	1	0.4651032	0.5348968	0.4662252	1
O6	O	1	0.4651032	0.5348968	0.5337748	1
O7	O	1	0.5348968	0.5348968	0.4662252	1
O8	O	1	0.5348968	0.5348968	0.5337748	1

O9	O	1	0.5935717	0.5000000	0.5475921	1
O10	O	1	0.5935717	0.448553	0.5000000	1
O11	O	1	0.5935717	0.5000000	0.4524079	1
O12	O	1	0.5935717	0.551447	0.5000000	1
O13	O	1	0.5000000	0.5935717	0.5475921	1
O14	O	1	0.551447	0.5935717	0.5000000	1
O15	O	1	0.5000000	0.5935717	0.4524079	1
O16	O	1	0.448553	0.5935717	0.5000000	1
O17	O	1	0.4064283	0.5000000	0.5475921	1
O18	O	1	0.4064283	0.551447	0.5000000	1
O19	O	1	0.4064283	0.5000000	0.4524079	1
O20	O	1	0.4064283	0.448553	0.5000000	1
O21	O	1	0.5000000	0.4064283	0.5475921	1
O22	O	1	0.448553	0.4064283	0.5000000	1
O23	O	1	0.5000000	0.4064283	0.4524079	1
O24	O	1	0.551447	0.4064283	0.5000000	1
O25	O	1	0.551447	0.5000000	0.5865604	1
O26	O	1	0.5000000	0.551447	0.5865604	1
O27	O	1	0.448553	0.5000000	0.5865604	1
O28	O	1	0.5000000	0.448553	0.5865604	1
O29	O	1	0.551447	0.5000000	0.4134396	1
O30	O	1	0.5000000	0.448553	0.4134396	1
O31	O	1	0.448553	0.5000000	0.4134396	1
O32	O	1	0.5000000	0.551447	0.4134396	1
Zr1	Zr	1	0.566324	0.5000000	0.5000000	1
Zr2	Zr	1	0.5000000	0.566324	0.5000000	1
Zr3	Zr	1	0.433676	0.5000000	0.5000000	1
Zr4	Zr	1	0.5000000	0.433676	0.5000000	1
Zr5	Zr	1	0.5000000	0.5000000	0.5613543	1
Zr6	Zr	1	0.5000000	0.5000000	0.4386457	1

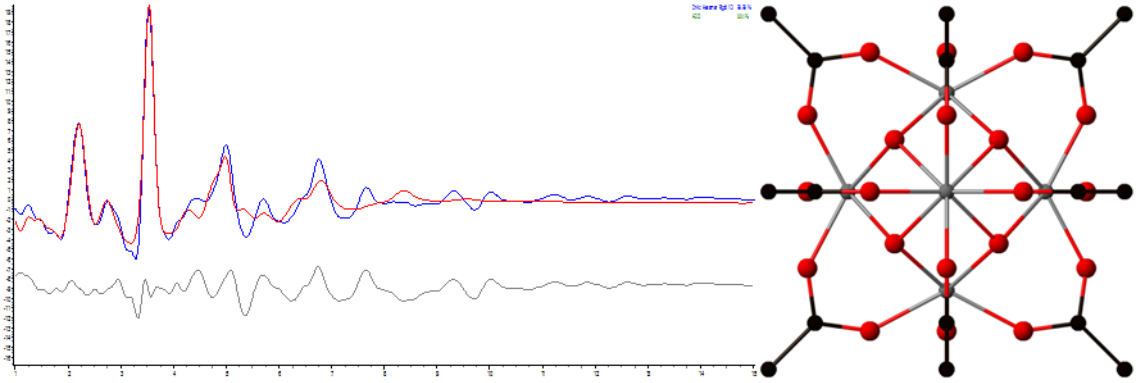

Figure 159: Observed and Calculated PDF from the fixed core refinement of ZAA7 from the 15-month data collection and the resultant model.

Table 102: The atomic coordinates of the model resulting from the fixed core refinement of ZAA7 from the 15-month data collection.

Atom Label	Atom Type	Multiplicity	Fractional X Coordinate	Fractional Y Coordinate	Fractional Z Coordinate	Fractional Occupancy
C1	C	1	0.5883606	0.5000000	0.5817397	1
C2	C	1	0.5000000	0.4116394	0.5817397	1
C3	C	1	0.4116394	0.5000000	0.5817397	1
C4	C	1	0.5000000	0.5883606	0.5817397	1
C5	C	1	0.5883606	0.5000000	0.4182603	1
C6	C	1	0.5000000	0.4116394	0.4182603	1
C7	C	1	0.4116394	0.5000000	0.4182603	1
C8	C	1	0.5000000	0.5883606	0.4182603	1
C9	C	1	0.5883606	0.4116394	0.5000000	1
C10	C	1	0.4116394	0.4116394	0.5000000	1
C11	C	1	0.4116394	0.5883606	0.5000000	1
C12	C	1	0.5883606	0.5883606	0.5000000	1
C13	C	1	0.6194803	0.5000000	0.6105276	1
C14	C	1	0.5000000	0.3805197	0.6105276	1
C15	C	1	0.3805197	0.5000000	0.6105276	1
C16	C	1	0.5000000	0.6194803	0.6105276	1
C17	C	1	0.6194803	0.5000000	0.3894724	1
C18	C	1	0.5000000	0.3805197	0.3894724	1
C19	C	1	0.3805197	0.5000000	0.3894724	1
C20	C	1	0.5000000	0.6194803	0.3894724	1
C21	C	1	0.6194803	0.3805197	0.5000000	1
C22	C	1	0.3805197	0.3805197	0.5000000	1
C23	C	1	0.3805197	0.6194803	0.5000000	1
C24	C	1	0.6194803	0.6194803	0.5000000	1
O1	O	1	0.5348969	0.4651031	0.4662252	1
O2	O	1	0.5348969	0.4651031	0.5337748	1
O3	O	1	0.4651031	0.4651031	0.4662252	1
O4	O	1	0.4651031	0.4651031	0.5337748	1
O5	O	1	0.4651031	0.5348969	0.4662252	1
O6	O	1	0.4651031	0.5348969	0.5337748	1

O7	O	1	0.5348969	0.5348969	0.4662252	1
O8	O	1	0.5348969	0.5348969	0.5337748	1
O9	O	1	0.5935717	0.5000000	0.5475919	1
O10	O	1	0.5935717	0.4485531	0.5000000	1
O11	O	1	0.5935717	0.5000000	0.4524081	1
O12	O	1	0.5935717	0.5514469	0.5000000	1
O13	O	1	0.5000000	0.5935717	0.5475919	1
O14	O	1	0.5514469	0.5935717	0.5000000	1
O15	O	1	0.5000000	0.5935717	0.4524081	1
O16	O	1	0.4485531	0.5935717	0.5000000	1
O17	O	1	0.4064283	0.5000000	0.5475919	1
O18	O	1	0.4064283	0.5514469	0.5000000	1
O19	O	1	0.4064283	0.5000000	0.4524081	1
O20	O	1	0.4064283	0.4485531	0.5000000	1
O21	O	1	0.5000000	0.4064283	0.5475919	1
O22	O	1	0.4485531	0.4064283	0.5000000	1
O23	O	1	0.5000000	0.4064283	0.4524081	1
O24	O	1	0.5514469	0.4064283	0.5000000	1
O25	O	1	0.5514469	0.5000000	0.5865604	1
O26	O	1	0.5000000	0.5514469	0.5865604	1
O27	O	1	0.4485531	0.5000000	0.5865604	1
O28	O	1	0.5000000	0.4485531	0.5865604	1
O29	O	1	0.5514469	0.5000000	0.4134396	1
O30	O	1	0.5000000	0.4485531	0.4134396	1
O31	O	1	0.4485531	0.5000000	0.4134396	1
O32	O	1	0.5000000	0.5514469	0.4134396	1
Zr1	Zr	1	0.566324	0.5000000	0.5000000	1
Zr2	Zr	1	0.5000000	0.566324	0.5000000	1
Zr3	Zr	1	0.433676	0.5000000	0.5000000	1
Zr4	Zr	1	0.5000000	0.433676	0.5000000	1
Zr5	Zr	1	0.5000000	0.5000000	0.5613543	1
Zr6	Zr	1	0.5000000	0.5000000	0.4386457	1

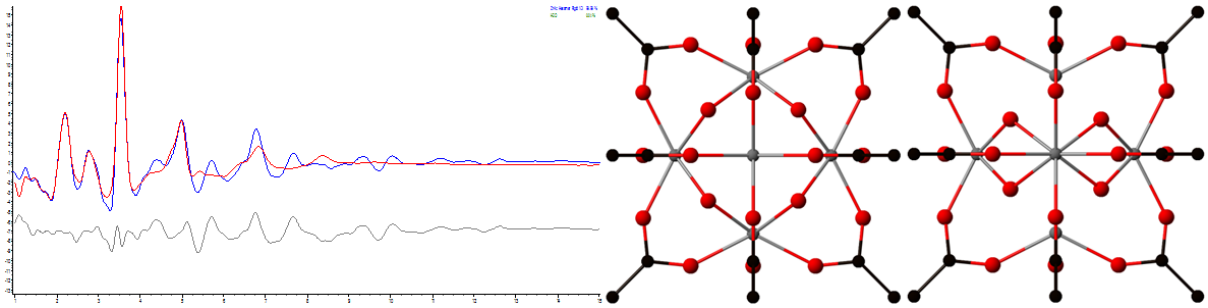

Figure 160: Observed and Calculated PDF from the chandelier core refinement of ZAA10 from the 15-month data collection and the resultant model viewed from the axial (left) and equatorial (right) positions.

Table 103: The atomic coordinates of the model resulting from the chandelier core refinement of ZAA10 from the 15-month data collection.

Atom Label	Atom Type	Multiplicity	Fractional X Coordinate	Fractional Y Coordinate	Fractional Z Coordinate	Fractional Occupancy
C1	C	1	0.5896078	0.5000000	0.5828935	1
C2	C	1	0.5000000	0.4103922	0.5828935	1
C3	C	1	0.4103922	0.5000000	0.5828935	1
C4	C	1	0.5000000	0.5896078	0.5828935	1
C5	C	1	0.5896078	0.5000000	0.4171065	1
C6	C	1	0.5000000	0.4103922	0.4171065	1
C7	C	1	0.4103922	0.5000000	0.4171065	1
C8	C	1	0.5000000	0.5896078	0.4171065	1
C9	C	1	0.5896078	0.4103922	0.5000000	1
C10	C	1	0.4103922	0.4103922	0.5000000	1
C11	C	1	0.4103922	0.5896078	0.5000000	1
C12	C	1	0.5896078	0.5896078	0.5000000	1
C13	C	1	0.6196321	0.5000000	0.610668	1
C14	C	1	0.5000000	0.3803679	0.610668	1
C15	C	1	0.3803679	0.5000000	0.610668	1
C16	C	1	0.5000000	0.6196321	0.610668	1
C17	C	1	0.6196321	0.5000000	0.389332	1
C18	C	1	0.5000000	0.3803679	0.389332	1
C19	C	1	0.3803679	0.5000000	0.389332	1
C20	C	1	0.5000000	0.6196321	0.389332	1
C21	C	1	0.6196321	0.3803679	0.5000000	1
C22	C	1	0.3803679	0.3803679	0.5000000	1
C23	C	1	0.3803679	0.6196321	0.5000000	1
C24	C	1	0.6196321	0.6196321	0.5000000	1
O1	O	1	0.5382863	0.4617137	0.4728705	1
O2	O	1	0.5382863	0.4617137	0.5271295	1
O3	O	1	0.4617137	0.4617137	0.4728705	1
O4	O	1	0.4617137	0.4617137	0.5271295	1
O5	O	1	0.4617137	0.5382863	0.4728705	1
O6	O	1	0.4617137	0.5382863	0.5271295	1
O7	O	1	0.5382863	0.5382863	0.4728705	1
O8	O	1	0.5382863	0.5382863	0.5271295	1

O9	O	1	0.5933122	0.5000000	0.54908	1
O10	O	1	0.5933122	0.4469446	0.5000000	1
O11	O	1	0.5933122	0.5000000	0.45092	1
O12	O	1	0.5933122	0.5530554	0.5000000	1
O13	O	1	0.5000000	0.5933122	0.54908	1
O14	O	1	0.5530554	0.5933122	0.5000000	1
O15	O	1	0.5000000	0.5933122	0.45092	1
O16	O	1	0.4469446	0.5933122	0.5000000	1
O17	O	1	0.4066878	0.5000000	0.54908	1
O18	O	1	0.4066878	0.5530554	0.5000000	1
O19	O	1	0.4066878	0.5000000	0.45092	1
O20	O	1	0.4066878	0.4469446	0.5000000	1
O21	O	1	0.5000000	0.4066878	0.54908	1
O22	O	1	0.4469446	0.4066878	0.5000000	1
O23	O	1	0.5000000	0.4066878	0.45092	1
O24	O	1	0.5530554	0.4066878	0.5000000	1
O25	O	1	0.5530554	0.5000000	0.5863203	1
O26	O	1	0.5000000	0.5530554	0.5863203	1
O27	O	1	0.4469446	0.5000000	0.5863203	1
O28	O	1	0.5000000	0.4469446	0.5863203	1
O29	O	1	0.5530554	0.5000000	0.4136797	1
O30	O	1	0.5000000	0.4469446	0.4136797	1
O31	O	1	0.4469446	0.5000000	0.4136797	1
O32	O	1	0.5000000	0.5530554	0.4136797	1
Zr1	Zr	1	0.5663043	0.5000000	0.5000000	1
Zr2	Zr	1	0.5000000	0.5663043	0.5000000	1
Zr3	Zr	1	0.4336957	0.5000000	0.5000000	1
Zr4	Zr	1	0.5000000	0.4336957	0.5000000	1
Zr5	Zr	1	0.5000000	0.5000000	0.5613361	1
Zr6	Zr	1	0.5000000	0.5000000	0.4386639	1

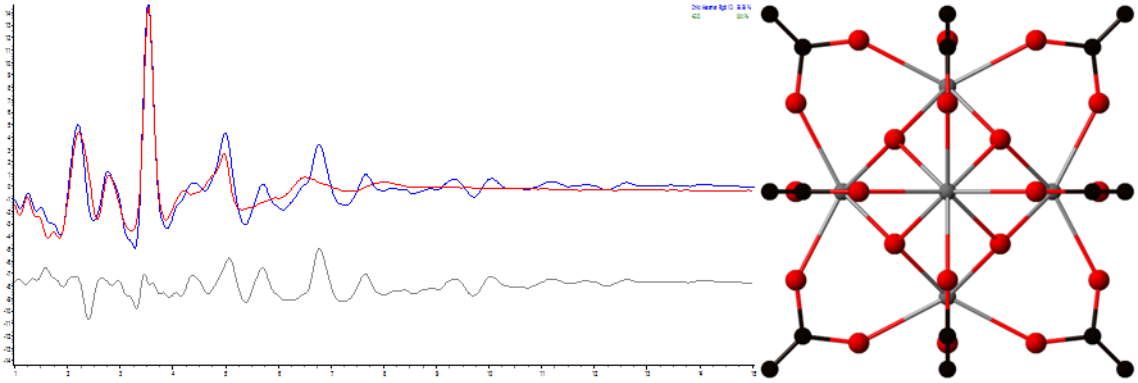

Figure 161: Observed and Calculated PDF from the fixed core refinement of ZAA10 from the 15-month data collection and the resultant model.

Table 104: The atomic coordinates of the model resulting from the fixed core refinement of ZAA10 from the 15-month data collection.

Atom Label	Atom Type	Multiplicity	Fractional X Coordinate	Fractional Y Coordinate	Fractional Z Coordinate	Fractional Occupancy
C1	C	1	0.5908908	0.5000000	0.5840803	1
C2	C	1	0.5000000	0.4091092	0.5840803	1
C3	C	1	0.4091092	0.5000000	0.5840803	1
C4	C	1	0.5000000	0.5908908	0.5840803	1
C5	C	1	0.5908908	0.5000000	0.4159197	1
C6	C	1	0.5000000	0.4091092	0.4159197	1
C7	C	1	0.4091092	0.5000000	0.4159197	1
C8	C	1	0.5000000	0.5908908	0.4159197	1
C9	C	1	0.5908908	0.4091092	0.5000000	1
C10	C	1	0.4091092	0.4091092	0.5000000	1
C11	C	1	0.4091092	0.5908908	0.5000000	1
C12	C	1	0.5908908	0.5908908	0.5000000	1
C13	C	1	0.6114026	0.5000000	0.6030552	1
C14	C	1	0.5000000	0.3885974	0.6030552	1
C15	C	1	0.3885974	0.5000000	0.6030552	1
C16	C	1	0.5000000	0.6114026	0.6030552	1
C17	C	1	0.6114026	0.5000000	0.3969448	1
C18	C	1	0.5000000	0.3885974	0.3969448	1
C19	C	1	0.3885974	0.5000000	0.3969448	1
C20	C	1	0.5000000	0.6114026	0.3969448	1
C21	C	1	0.6114026	0.3885974	0.5000000	1
C22	C	1	0.3885974	0.3885974	0.5000000	1
C23	C	1	0.3885974	0.6114026	0.5000000	1
C24	C	1	0.6114026	0.6114026	0.5000000	1
O1	O	1	0.5331754	0.5328517	0.4693105	1
O2	O	1	0.5331754	0.4671483	0.5306895	1
O3	O	1	0.4668246	0.5328517	0.4693105	1
O4	O	1	0.4668246	0.4671483	0.5306895	1
O5	O	1	0.4668246	0.4671483	0.4693105	1
O6	O	1	0.4668246	0.5328517	0.5306895	1

O7	O	1	0.5331754	0.4671483	0.4693105	1
O8	O	1	0.5331754	0.5328517	0.5306895	1
O9	O	1	0.5950282	0.5000000	0.551453	1
O10	O	1	0.5950282	0.4443793	0.5000000	1
O11	O	1	0.5950282	0.5000000	0.448547	1
O12	O	1	0.5950282	0.5556207	0.5000000	1
O13	O	1	0.5000000	0.5950282	0.551453	1
O14	O	1	0.5556207	0.5950282	0.5000000	1
O15	O	1	0.5000000	0.5950282	0.448547	1
O16	O	1	0.4443793	0.5950282	0.5000000	1
O17	O	1	0.4049718	0.5000000	0.551453	1
O18	O	1	0.4049718	0.5556207	0.5000000	1
O19	O	1	0.4049718	0.5000000	0.448547	1
O20	O	1	0.4049718	0.4443793	0.5000000	1
O21	O	1	0.5000000	0.4049718	0.551453	1
O22	O	1	0.4443793	0.4049718	0.5000000	1
O23	O	1	0.5000000	0.4049718	0.448547	1
O24	O	1	0.5556207	0.4049718	0.5000000	1
O25	O	1	0.5556207	0.5000000	0.5879077	1
O26	O	1	0.5000000	0.5556207	0.5879077	1
O27	O	1	0.4443793	0.5000000	0.5879077	1
O28	O	1	0.5000000	0.4443793	0.5879077	1
O29	O	1	0.5556207	0.5000000	0.4120923	1
O30	O	1	0.5000000	0.4443793	0.4120923	1
O31	O	1	0.4443793	0.5000000	0.4120923	1
O32	O	1	0.5000000	0.5556207	0.4120923	1
Zr1	Zr	1	0.566094	0.5000000	0.5000000	1
Zr2	Zr	1	0.5000000	0.566094	0.5000000	1
Zr3	Zr	1	0.433906	0.5000000	0.5000000	1
Zr4	Zr	1	0.5000000	0.433906	0.5000000	1
Zr5	Zr	1	0.5000000	0.5000000	0.5611415	1
Zr6	Zr	1	0.5000000	0.5000000	0.4388585	1

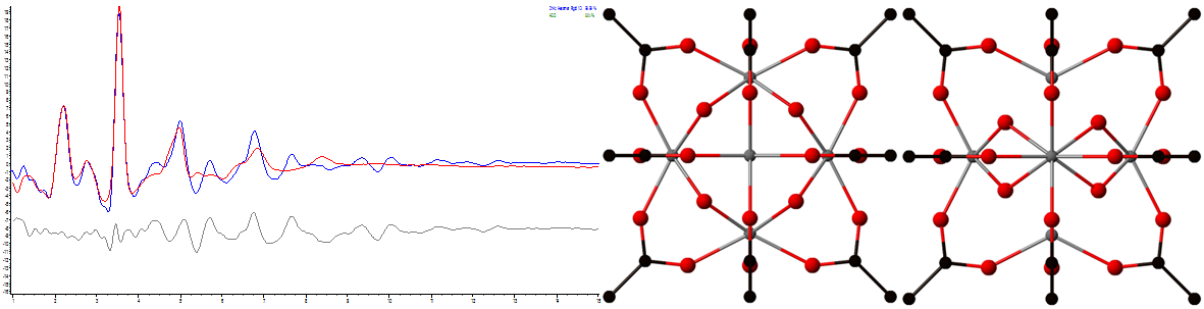

Figure 162: Observed and Calculated PDF from the chandelier core refinement of ZAA13 from the 15-month data collection and the resultant model viewed from the axial (left) and equatorial (right) positions.

Table 105: The atomic coordinates of the model resulting from the chandelier core refinement of ZAA13 from the 15-month data collection.

Atom Label	Atom Type	Multiplicity	Fractional X Coordinate	Fractional Y Coordinate	Fractional Z Coordinate	Fractional Occupancy
C1	C	1	0.5895622	0.5000000	0.5828512	1
C2	C	1	0.5000000	0.4104378	0.5828512	1
C3	C	1	0.4104378	0.5000000	0.5828512	1
C4	C	1	0.5000000	0.5895622	0.5828512	1
C5	C	1	0.5895622	0.5000000	0.4171488	1
C6	C	1	0.5000000	0.4104378	0.4171488	1
C7	C	1	0.4104378	0.5000000	0.4171488	1
C8	C	1	0.5000000	0.5895622	0.4171488	1
C9	C	1	0.5895622	0.4104378	0.5000000	1
C10	C	1	0.4104378	0.4104378	0.5000000	1
C11	C	1	0.4104378	0.5895622	0.5000000	1
C12	C	1	0.5895622	0.5895622	0.5000000	1
C13	C	1	0.6200705	0.5000000	0.6110736	1
C14	C	1	0.5000000	0.3799295	0.6110736	1
C15	C	1	0.3799295	0.5000000	0.6110736	1
C16	C	1	0.5000000	0.6200705	0.6110736	1
C17	C	1	0.6200705	0.5000000	0.3889264	1
C18	C	1	0.5000000	0.3799295	0.3889264	1
C19	C	1	0.3799295	0.5000000	0.3889264	1
C20	C	1	0.5000000	0.6200705	0.3889264	1
C21	C	1	0.6200705	0.3799295	0.5000000	1
C22	C	1	0.3799295	0.3799295	0.5000000	1
C23	C	1	0.3799295	0.6200705	0.5000000	1
C24	C	1	0.6200705	0.6200705	0.5000000	1
O1	O	1	0.5391395	0.4608605	0.4735075	1
O2	O	1	0.5391395	0.4608605	0.5264925	1
O3	O	1	0.4608605	0.4608605	0.4735075	1
O4	O	1	0.4608605	0.4608605	0.5264925	1
O5	O	1	0.4608605	0.5391395	0.4735075	1
O6	O	1	0.4608605	0.5391395	0.5264925	1
O7	O	1	0.5391395	0.5391395	0.4735075	1
O8	O	1	0.5391395	0.5391395	0.5264925	1

O9	O	1	0.59353	0.5000000	0.5492869	1
O10	O	1	0.59353	0.4467208	0.5000000	1
O11	O	1	0.59353	0.5000000	0.4507131	1
O12	O	1	0.59353	0.5532792	0.5000000	1
O13	O	1	0.5000000	0.59353	0.5492869	1
O14	O	1	0.5532792	0.59353	0.5000000	1
O15	O	1	0.5000000	0.59353	0.4507131	1
O16	O	1	0.4467208	0.59353	0.5000000	1
O17	O	1	0.40647	0.5000000	0.5492869	1
O18	O	1	0.40647	0.5532792	0.5000000	1
O19	O	1	0.40647	0.5000000	0.4507131	1
O20	O	1	0.40647	0.4467208	0.5000000	1
O21	O	1	0.5000000	0.40647	0.5492869	1
O22	O	1	0.4467208	0.40647	0.5000000	1
O23	O	1	0.5000000	0.40647	0.4507131	1
O24	O	1	0.5532792	0.40647	0.5000000	1
O25	O	1	0.5532792	0.5000000	0.5865218	1
O26	O	1	0.5000000	0.5532792	0.5865218	1
O27	O	1	0.4467208	0.5000000	0.5865218	1
O28	O	1	0.5000000	0.4467208	0.5865218	1
O29	O	1	0.5532792	0.5000000	0.4134782	1
O30	O	1	0.5000000	0.4467208	0.4134782	1
O31	O	1	0.4467208	0.5000000	0.4134782	1
O32	O	1	0.5000000	0.5532792	0.4134782	1
Zr1	Zr	1	0.566311	0.5000000	0.5000000	1
Zr2	Zr	1	0.5000000	0.566311	0.5000000	1
Zr3	Zr	1	0.433689	0.5000000	0.5000000	1
Zr4	Zr	1	0.5000000	0.433689	0.5000000	1
Zr5	Zr	1	0.5000000	0.5000000	0.5613423	1
Zr6	Zr	1	0.5000000	0.5000000	0.4386577	1

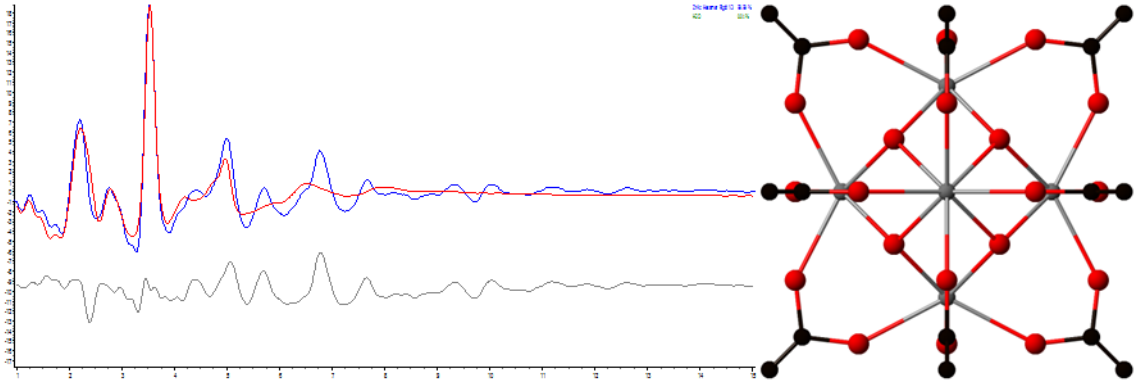

Figure 163: Observed and Calculated PDF from the fixed core refinement of ZAA13 from the 15-month data collection and the resultant model.

Table 106: The atomic coordinates of the model resulting from the fixed core refinement of ZAA13 from the 15-month data collection.

Atom Label	Atom Type	Multiplicity	Fractional X Coordinate	Fractional Y Coordinate	Fractional Z Coordinate	Fractional Occupancy
C1	C	1	0.5907979	0.5000000	0.5839944	1
C2	C	1	0.5000000	0.4092021	0.5839944	1
C3	C	1	0.4092021	0.5000000	0.5839944	1
C4	C	1	0.5000000	0.5907979	0.5839944	1
C5	C	1	0.5907979	0.5000000	0.4160056	1
C6	C	1	0.5000000	0.4092021	0.4160056	1
C7	C	1	0.4092021	0.5000000	0.4160056	1
C8	C	1	0.5000000	0.5907979	0.4160056	1
C9	C	1	0.5907979	0.4092021	0.5000000	1
C10	C	1	0.4092021	0.4092021	0.5000000	1
C11	C	1	0.4092021	0.5907979	0.5000000	1
C12	C	1	0.5907979	0.5907979	0.5000000	1
C13	C	1	0.6113121	0.5000000	0.6029714	1
C14	C	1	0.5000000	0.3886879	0.6029714	1
C15	C	1	0.3886879	0.5000000	0.6029714	1
C16	C	1	0.5000000	0.6113121	0.6029714	1
C17	C	1	0.6113121	0.5000000	0.3970286	1
C18	C	1	0.5000000	0.3886879	0.3970286	1
C19	C	1	0.3886879	0.5000000	0.3970286	1
C20	C	1	0.5000000	0.6113121	0.3970286	1
C21	C	1	0.6113121	0.3886879	0.5000000	1
C22	C	1	0.3886879	0.3886879	0.5000000	1
C23	C	1	0.3886879	0.6113121	0.5000000	1
C24	C	1	0.6113121	0.6113121	0.5000000	1
O1	O	1	0.5330698	0.5327471	0.4694081	1
O2	O	1	0.5330698	0.4672529	0.5305919	1
O3	O	1	0.4669302	0.5327471	0.4694081	1
O4	O	1	0.4669302	0.4672529	0.5305919	1
O5	O	1	0.4669302	0.4672529	0.4694081	1
O6	O	1	0.4669302	0.5327471	0.5305919	1

O7	O	1	0.5330698	0.4672529	0.4694081	1
O8	O	1	0.5330698	0.5327471	0.5305919	1
O9	O	1	0.5950281	0.5000000	0.5512975	1
O10	O	1	0.5950281	0.4445474	0.5000000	1
O11	O	1	0.5950281	0.5000000	0.4487025	1
O12	O	1	0.5950281	0.5554526	0.5000000	1
O13	O	1	0.5000000	0.5950281	0.5512975	1
O14	O	1	0.5554526	0.5950281	0.5000000	1
O15	O	1	0.5000000	0.5950281	0.4487025	1
O16	O	1	0.4445474	0.5950281	0.5000000	1
O17	O	1	0.4049719	0.5000000	0.5512975	1
O18	O	1	0.4049719	0.5554526	0.5000000	1
O19	O	1	0.4049719	0.5000000	0.4487025	1
O20	O	1	0.4049719	0.4445474	0.5000000	1
O21	O	1	0.5000000	0.4049719	0.5512975	1
O22	O	1	0.4445474	0.4049719	0.5000000	1
O23	O	1	0.5000000	0.4049719	0.4487025	1
O24	O	1	0.5554526	0.4049719	0.5000000	1
O25	O	1	0.5554526	0.5000000	0.5879076	1
O26	O	1	0.5000000	0.5554526	0.5879076	1
O27	O	1	0.4445474	0.5000000	0.5879076	1
O28	O	1	0.5000000	0.4445474	0.5879076	1
O29	O	1	0.5554526	0.5000000	0.4120924	1
O30	O	1	0.5000000	0.4445474	0.4120924	1
O31	O	1	0.4445474	0.5000000	0.4120924	1
O32	O	1	0.5000000	0.5554526	0.4120924	1
Zr1	Zr	1	0.5660803	0.5000000	0.5000000	1
Zr2	Zr	1	0.5000000	0.5660803	0.5000000	1
Zr3	Zr	1	0.4339197	0.5000000	0.5000000	1
Zr4	Zr	1	0.5000000	0.4339197	0.5000000	1
Zr5	Zr	1	0.5000000	0.5000000	0.5611289	1
Zr6	Zr	1	0.5000000	0.5000000	0.4388711	1

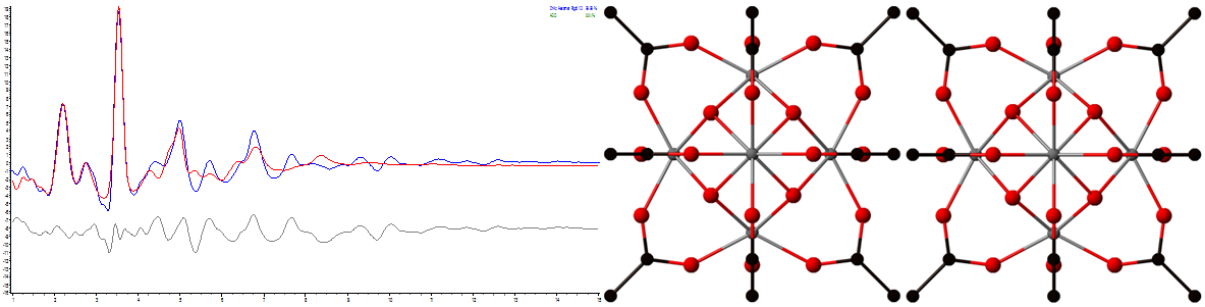

Figure 164: Observed and Calculated PDF from the chandelier core refinement of ZAA16 from the 15-month data collection and the resultant model viewed from the axial (left) and equatorial (right) positions.

Table 107: The atomic coordinates of the model resulting from the chandelier core refinement of ZAA16 from the 15-month data collection.

Atom Label	Atom Type	Multiplicity	Fractional X Coordinate	Fractional Y Coordinate	Fractional Z Coordinate	Fractional Occupancy
C1	C	1	0.5886653	0.5000000	0.5820216	1
C2	C	1	0.5000000	0.4113347	0.5820216	1
C3	C	1	0.4113347	0.5000000	0.5820216	1
C4	C	1	0.5000000	0.5886653	0.5820216	1
C5	C	1	0.5886653	0.5000000	0.4179784	1
C6	C	1	0.5000000	0.4113347	0.4179784	1
C7	C	1	0.4113347	0.5000000	0.4179784	1
C8	C	1	0.5000000	0.5886653	0.4179784	1
C9	C	1	0.5886653	0.4113347	0.5000000	1
C10	C	1	0.4113347	0.4113347	0.5000000	1
C11	C	1	0.4113347	0.5886653	0.5000000	1
C12	C	1	0.5886653	0.5886653	0.5000000	1
C13	C	1	0.6195676	0.5000000	0.6106084	1
C14	C	1	0.5000000	0.3804324	0.6106084	1
C15	C	1	0.3804324	0.5000000	0.6106084	1
C16	C	1	0.5000000	0.6195676	0.6106084	1
C17	C	1	0.6195676	0.5000000	0.3893916	1
C18	C	1	0.5000000	0.3804324	0.3893916	1
C19	C	1	0.3804324	0.5000000	0.3893916	1
C20	C	1	0.5000000	0.6195676	0.3893916	1
C21	C	1	0.6195676	0.3804324	0.5000000	1
C22	C	1	0.3804324	0.3804324	0.5000000	1
C23	C	1	0.3804324	0.6195676	0.5000000	1
C24	C	1	0.6195676	0.6195676	0.5000000	1
O1	O	1	0.5348366	0.4651634	0.4662993	1
O2	O	1	0.5348366	0.4651634	0.5337007	1
O3	O	1	0.4651634	0.4651634	0.4662993	1
O4	O	1	0.4651634	0.4651634	0.5337007	1
O5	O	1	0.4651634	0.5348366	0.4662993	1
O6	O	1	0.4651634	0.5348366	0.5337007	1
O7	O	1	0.5348366	0.5348366	0.4662993	1
O8	O	1	0.5348366	0.5348366	0.5337007	1

O9	O	1	0.5934783	0.5000000	0.5477553	1
O10	O	1	0.5934783	0.4483766	0.5000000	1
O11	O	1	0.5934783	0.5000000	0.4522447	1
O12	O	1	0.5934783	0.5516234	0.5000000	1
O13	O	1	0.5000000	0.5934783	0.5477553	1
O14	O	1	0.5516234	0.5934783	0.5000000	1
O15	O	1	0.5000000	0.5934783	0.4522447	1
O16	O	1	0.4483766	0.5934783	0.5000000	1
O17	O	1	0.4065217	0.5000000	0.5477553	1
O18	O	1	0.4065217	0.5516234	0.5000000	1
O19	O	1	0.4065217	0.5000000	0.4522447	1
O20	O	1	0.4065217	0.4483766	0.5000000	1
O21	O	1	0.5000000	0.4065217	0.5477553	1
O22	O	1	0.4483766	0.4065217	0.5000000	1
O23	O	1	0.5000000	0.4065217	0.4522447	1
O24	O	1	0.5516234	0.4065217	0.5000000	1
O25	O	1	0.5516234	0.5000000	0.586474	1
O26	O	1	0.5000000	0.5516234	0.586474	1
O27	O	1	0.4483766	0.5000000	0.586474	1
O28	O	1	0.5000000	0.4483766	0.586474	1
O29	O	1	0.5516234	0.5000000	0.413526	1
O30	O	1	0.5000000	0.4483766	0.413526	1
O31	O	1	0.4483766	0.5000000	0.413526	1
O32	O	1	0.5000000	0.5516234	0.413526	1
Zr1	Zr	1	0.5663209	0.5000000	0.5000000	1
Zr2	Zr	1	0.5000000	0.5663209	0.5000000	1
Zr3	Zr	1	0.4336791	0.5000000	0.5000000	1
Zr4	Zr	1	0.5000000	0.4336791	0.5000000	1
Zr5	Zr	1	0.5000000	0.5000000	0.5613515	1
Zr6	Zr	1	0.5000000	0.5000000	0.4386485	1

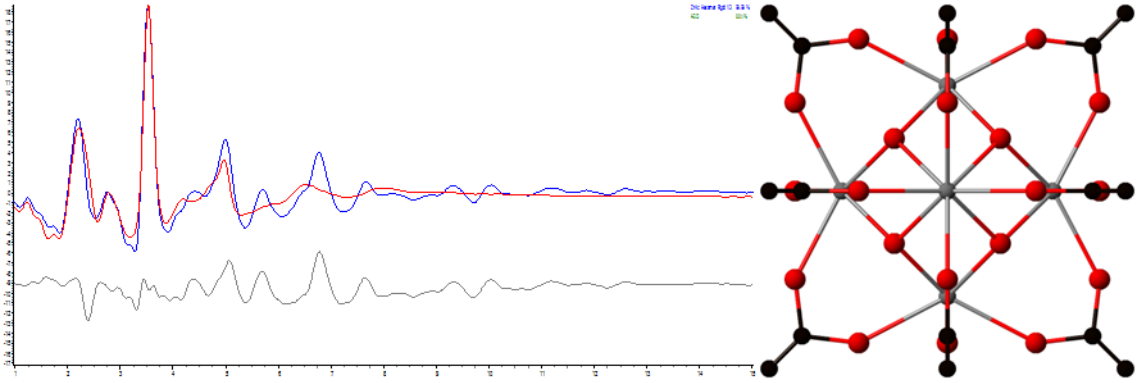

Figure 165: Observed and Calculated PDF from the fixed core refinement of ZAA16 from the 15-month data collection and the resultant model.

Table 108: The atomic coordinates of the model resulting from the fixed core refinement of ZAA16 from the 15-month data collection.

Atom Label	Atom Type	Multiplicity	Fractional X Coordinate	Fractional Y Coordinate	Fractional Z Coordinate	Fractional Occupancy
C1	C	1	0.5907554	0.5000000	0.5839551	1
C2	C	1	0.5000000	0.4092446	0.5839551	1
C3	C	1	0.4092446	0.5000000	0.5839551	1
C4	C	1	0.5000000	0.5907554	0.5839551	1
C5	C	1	0.5907554	0.5000000	0.4160449	1
C6	C	1	0.5000000	0.4092446	0.4160449	1
C7	C	1	0.4092446	0.5000000	0.4160449	1
C8	C	1	0.5000000	0.5907554	0.4160449	1
C9	C	1	0.5907554	0.4092446	0.5000000	1
C10	C	1	0.4092446	0.4092446	0.5000000	1
C11	C	1	0.4092446	0.5907554	0.5000000	1
C12	C	1	0.5907554	0.5907554	0.5000000	1
C13	C	1	0.6112969	0.5000000	0.6029574	1
C14	C	1	0.5000000	0.3887031	0.6029574	1
C15	C	1	0.3887031	0.5000000	0.6029574	1
C16	C	1	0.5000000	0.6112969	0.6029574	1
C17	C	1	0.6112969	0.5000000	0.3970426	1
C18	C	1	0.5000000	0.3887031	0.3970426	1
C19	C	1	0.3887031	0.5000000	0.3970426	1
C20	C	1	0.5000000	0.6112969	0.3970426	1
C21	C	1	0.6112969	0.3887031	0.5000000	1
C22	C	1	0.3887031	0.3887031	0.5000000	1
C23	C	1	0.3887031	0.6112969	0.5000000	1
C24	C	1	0.6112969	0.6112969	0.5000000	1
O1	O	1	0.5330362	0.5327139	0.4694392	1
O2	O	1	0.5330362	0.4672861	0.5305608	1
O3	O	1	0.4669638	0.5327139	0.4694392	1
O4	O	1	0.4669638	0.4672861	0.5305608	1
O5	O	1	0.4669638	0.4672861	0.4694392	1
O6	O	1	0.4669638	0.5327139	0.5305608	1

O7	O	1	0.5330362	0.4672861	0.4694392	1
O8	O	1	0.5330362	0.5327139	0.5305608	1
O9	O	1	0.5950343	0.5000000	0.551243	1
O10	O	1	0.5950343	0.4446063	0.5000000	1
O11	O	1	0.5950343	0.5000000	0.448757	1
O12	O	1	0.5950343	0.5553937	0.5000000	1
O13	O	1	0.5000000	0.5950343	0.551243	1
O14	O	1	0.5553937	0.5950343	0.5000000	1
O15	O	1	0.5000000	0.5950343	0.448757	1
O16	O	1	0.4446063	0.5950343	0.5000000	1
O17	O	1	0.4049657	0.5000000	0.551243	1
O18	O	1	0.4049657	0.5553937	0.5000000	1
O19	O	1	0.4049657	0.5000000	0.448757	1
O20	O	1	0.4049657	0.4446063	0.5000000	1
O21	O	1	0.5000000	0.4049657	0.551243	1
O22	O	1	0.4446063	0.4049657	0.5000000	1
O23	O	1	0.5000000	0.4049657	0.448757	1
O24	O	1	0.5553937	0.4049657	0.5000000	1
O25	O	1	0.5553937	0.5000000	0.5879134	1
O26	O	1	0.5000000	0.5553937	0.5879134	1
O27	O	1	0.4446063	0.5000000	0.5879134	1
O28	O	1	0.5000000	0.4446063	0.5879134	1
O29	O	1	0.5553937	0.5000000	0.4120866	1
O30	O	1	0.5000000	0.4446063	0.4120866	1
O31	O	1	0.4446063	0.5000000	0.4120866	1
O32	O	1	0.5000000	0.5553937	0.4120866	1
Zr1	Zr	1	0.5660636	0.5000000	0.5000000	1
Zr2	Zr	1	0.5000000	0.5660636	0.5000000	1
Zr3	Zr	1	0.4339364	0.5000000	0.5000000	1
Zr4	Zr	1	0.5000000	0.4339364	0.5000000	1
Zr5	Zr	1	0.5000000	0.5000000	0.5611134	1
Zr6	Zr	1	0.5000000	0.5000000	0.4388866	1

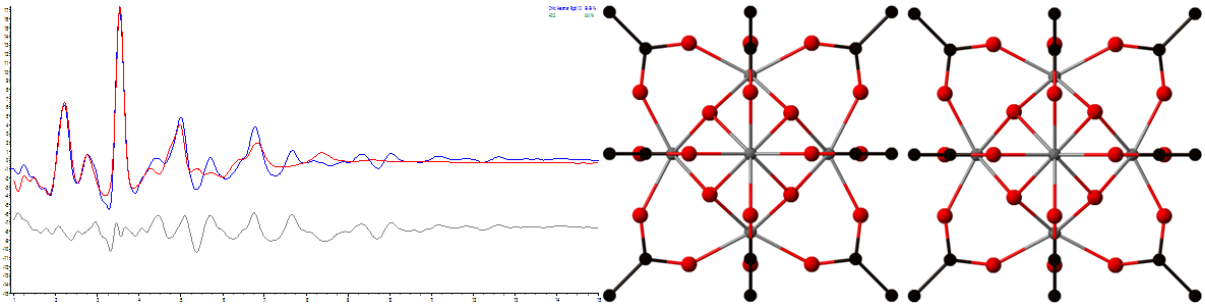

Figure 166: Observed and Calculated PDF from the chandelier core refinement of ZAA20 from the 15-month data collection and the resultant model viewed from the axial (left) and equatorial (right) positions.

Table 109: The atomic coordinates of the model resulting from the chandelier core refinement of ZAA20 from the 15-month data collection.

Atom Label	Atom Type	Multiplicity	Fractional X Coordinate	Fractional Y Coordinate	Fractional Z Coordinate	Fractional Occupancy
C1	C	1	0.5890778	0.5000000	0.5824031	1
C2	C	1	0.5000000	0.4109222	0.5824031	1
C3	C	1	0.4109222	0.5000000	0.5824031	1
C4	C	1	0.5000000	0.5890778	0.5824031	1
C5	C	1	0.5890778	0.5000000	0.4175969	1
C6	C	1	0.5000000	0.4109222	0.4175969	1
C7	C	1	0.4109222	0.5000000	0.4175969	1
C8	C	1	0.5000000	0.5890778	0.4175969	1
C9	C	1	0.5890778	0.4109222	0.5000000	1
C10	C	1	0.4109222	0.4109222	0.5000000	1
C11	C	1	0.4109222	0.5890778	0.5000000	1
C12	C	1	0.5890778	0.5890778	0.5000000	1
C13	C	1	0.6196745	0.5000000	0.6107073	1
C14	C	1	0.5000000	0.3803255	0.6107073	1
C15	C	1	0.3803255	0.5000000	0.6107073	1
C16	C	1	0.5000000	0.6196745	0.6107073	1
C17	C	1	0.6196745	0.5000000	0.3892927	1
C18	C	1	0.5000000	0.3803255	0.3892927	1
C19	C	1	0.3803255	0.5000000	0.3892927	1
C20	C	1	0.5000000	0.6196745	0.3892927	1
C21	C	1	0.6196745	0.3803255	0.5000000	1
C22	C	1	0.3803255	0.3803255	0.5000000	1
C23	C	1	0.3803255	0.6196745	0.5000000	1
C24	C	1	0.6196745	0.6196745	0.5000000	1
O1	O	1	0.5345241	0.4654759	0.4663878	1
O2	O	1	0.5345241	0.4654759	0.5336122	1
O3	O	1	0.4654759	0.4654759	0.4663878	1
O4	O	1	0.4654759	0.4654759	0.5336122	1
O5	O	1	0.4654759	0.5345241	0.4663878	1
O6	O	1	0.4654759	0.5345241	0.5336122	1
O7	O	1	0.5345241	0.5345241	0.4663878	1
O8	O	1	0.5345241	0.5345241	0.5336122	1

O9	O	1	0.5935523	0.5000000	0.5480396	1
O10	O	1	0.5935523	0.4480693	0.5000000	1
O11	O	1	0.5935523	0.5000000	0.4519604	1
O12	O	1	0.5935523	0.5519307	0.5000000	1
O13	O	1	0.5000000	0.5935523	0.5480396	1
O14	O	1	0.5519307	0.5935523	0.5000000	1
O15	O	1	0.5000000	0.5935523	0.4519604	1
O16	O	1	0.4480693	0.5935523	0.5000000	1
O17	O	1	0.4064477	0.5000000	0.5480396	1
O18	O	1	0.4064477	0.5519307	0.5000000	1
O19	O	1	0.4064477	0.5000000	0.4519604	1
O20	O	1	0.4064477	0.4480693	0.5000000	1
O21	O	1	0.5000000	0.4064477	0.5480396	1
O22	O	1	0.4480693	0.4064477	0.5000000	1
O23	O	1	0.5000000	0.4064477	0.4519604	1
O24	O	1	0.5519307	0.4064477	0.5000000	1
O25	O	1	0.5519307	0.5000000	0.5865424	1
O26	O	1	0.5000000	0.5519307	0.5865424	1
O27	O	1	0.4480693	0.5000000	0.5865424	1
O28	O	1	0.5000000	0.4480693	0.5865424	1
O29	O	1	0.5519307	0.5000000	0.4134576	1
O30	O	1	0.5000000	0.4480693	0.4134576	1
O31	O	1	0.4480693	0.5000000	0.4134576	1
O32	O	1	0.5000000	0.5519307	0.4134576	1
Zr1	Zr	1	0.5663195	0.5000000	0.5000000	1
Zr2	Zr	1	0.5000000	0.5663195	0.5000000	1
Zr3	Zr	1	0.4336805	0.5000000	0.5000000	1
Zr4	Zr	1	0.5000000	0.4336805	0.5000000	1
Zr5	Zr	1	0.5000000	0.5000000	0.5613502	1
Zr6	Zr	1	0.5000000	0.5000000	0.4386498	1

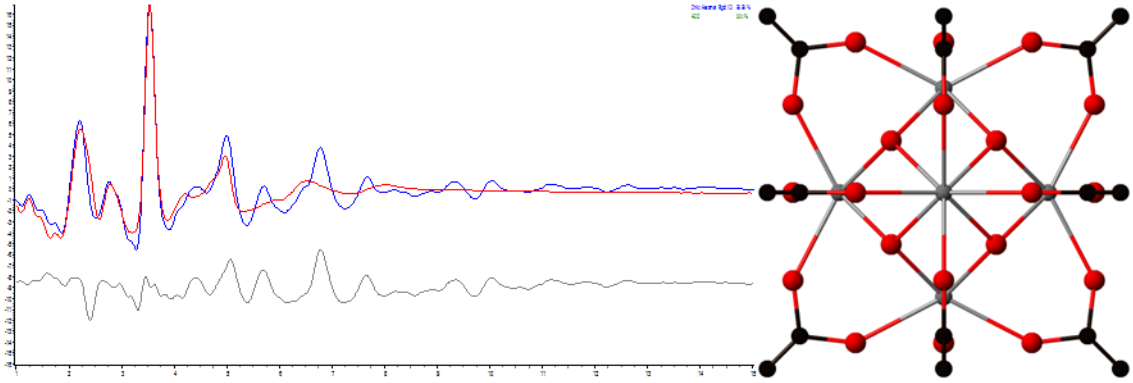

Figure 167: Observed and Calculated PDF from the fixed core refinement of ZAA20 from the 15-month data collection and the resultant model.

Table 110: The atomic coordinates of the model resulting from the fixed core refinement of ZAA20 from the 15-month data collection.

Atom Label	Atom Type	Multiplicity	Fractional X Coordinate	Fractional Y Coordinate	Fractional Z Coordinate	Fractional Occupancy
C1	C	1	0.5908178	0.5000000	0.5840128	1
C2	C	1	0.5000000	0.4091822	0.5840128	1
C3	C	1	0.4091822	0.5000000	0.5840128	1
C4	C	1	0.5000000	0.5908178	0.5840128	1
C5	C	1	0.5908178	0.5000000	0.4159872	1
C6	C	1	0.5000000	0.4091822	0.4159872	1
C7	C	1	0.4091822	0.5000000	0.4159872	1
C8	C	1	0.5000000	0.5908178	0.4159872	1
C9	C	1	0.5908178	0.4091822	0.5000000	1
C10	C	1	0.4091822	0.4091822	0.5000000	1
C11	C	1	0.4091822	0.5908178	0.5000000	1
C12	C	1	0.5908178	0.5908178	0.5000000	1
C13	C	1	0.6113762	0.5000000	0.6030308	1
C14	C	1	0.5000000	0.3886238	0.6030308	1
C15	C	1	0.3886238	0.5000000	0.6030308	1
C16	C	1	0.5000000	0.6113762	0.6030308	1
C17	C	1	0.6113762	0.5000000	0.3969692	1
C18	C	1	0.5000000	0.3886238	0.3969692	1
C19	C	1	0.3886238	0.5000000	0.3969692	1
C20	C	1	0.5000000	0.6113762	0.3969692	1
C21	C	1	0.6113762	0.3886238	0.5000000	1
C22	C	1	0.3886238	0.3886238	0.5000000	1
C23	C	1	0.3886238	0.6113762	0.5000000	1
C24	C	1	0.6113762	0.6113762	0.5000000	1
O1	O	1	0.5331159	0.5327928	0.4693654	1
O2	O	1	0.5331159	0.4672072	0.5306346	1
O3	O	1	0.4668841	0.5327928	0.4693654	1
O4	O	1	0.4668841	0.4672072	0.5306346	1
O5	O	1	0.4668841	0.4672072	0.4693654	1
O6	O	1	0.4668841	0.5327928	0.5306346	1

O7	O	1	0.5331159	0.4672072	0.4693654	1
O8	O	1	0.5331159	0.5327928	0.5306346	1
O9	O	1	0.5950505	0.5000000	0.5514002	1
O10	O	1	0.5950505	0.4444364	0.5000000	1
O11	O	1	0.5950505	0.5000000	0.4485998	1
O12	O	1	0.5950505	0.5555636	0.5000000	1
O13	O	1	0.5000000	0.5950505	0.5514002	1
O14	O	1	0.5555636	0.5950505	0.5000000	1
O15	O	1	0.5000000	0.5950505	0.4485998	1
O16	O	1	0.4444364	0.5950505	0.5000000	1
O17	O	1	0.4049495	0.5000000	0.5514002	1
O18	O	1	0.4049495	0.5555636	0.5000000	1
O19	O	1	0.4049495	0.5000000	0.4485998	1
O20	O	1	0.4049495	0.4444364	0.5000000	1
O21	O	1	0.5000000	0.4049495	0.5514002	1
O22	O	1	0.4444364	0.4049495	0.5000000	1
O23	O	1	0.5000000	0.4049495	0.4485998	1
O24	O	1	0.5555636	0.4049495	0.5000000	1
O25	O	1	0.5555636	0.5000000	0.5879283	1
O26	O	1	0.5000000	0.5555636	0.5879283	1
O27	O	1	0.4444364	0.5000000	0.5879283	1
O28	O	1	0.5000000	0.4444364	0.5879283	1
O29	O	1	0.5555636	0.5000000	0.4120717	1
O30	O	1	0.5000000	0.4444364	0.4120717	1
O31	O	1	0.4444364	0.5000000	0.4120717	1
O32	O	1	0.5000000	0.5555636	0.4120717	1
Zr1	Zr	1	0.5660910	0.5000000	0.5000000	1
Zr2	Zr	1	0.5000000	0.5660910	0.5000000	1
Zr3	Zr	1	0.4339090	0.5000000	0.5000000	1
Zr4	Zr	1	0.5000000	0.4339090	0.5000000	1
Zr5	Zr	1	0.5000000	0.5000000	0.5611388	1
Zr6	Zr	1	0.5000000	0.5000000	0.4388612	1

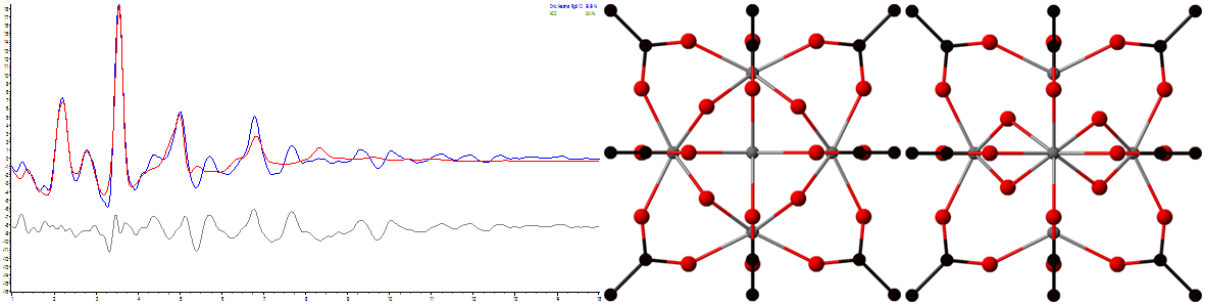

Figure 168: Observed and Calculated PDF from the chandelier core refinement of ZAA24 from the 15-month data collection and the resultant model viewed from the axial (left) and equatorial (right) positions.

Table 111: The atomic coordinates of the model resulting from the chandelier core refinement of ZAA24 from the 15-month data collection.

Atom Label	Atom Type	Multiplicity	Fractional X Coordinate	Fractional Y Coordinate	Fractional Z Coordinate	Fractional Occupancy
C1	C	1	0.5895171	0.5000000	0.5828096	1
C2	C	1	0.5000000	0.4104829	0.5828096	1
C3	C	1	0.4104829	0.5000000	0.5828096	1
C4	C	1	0.5000000	0.5895171	0.5828096	1
C5	C	1	0.5895171	0.5000000	0.4171904	1
C6	C	1	0.5000000	0.4104829	0.4171904	1
C7	C	1	0.4104829	0.5000000	0.4171904	1
C8	C	1	0.5000000	0.5895171	0.4171904	1
C9	C	1	0.5895171	0.4104829	0.5000000	1
C10	C	1	0.4104829	0.4104829	0.5000000	1
C11	C	1	0.4104829	0.5895171	0.5000000	1
C12	C	1	0.5895171	0.5895171	0.5000000	1
C13	C	1	0.6189814	0.5000000	0.6100661	1
C14	C	1	0.5000000	0.3810186	0.6100661	1
C15	C	1	0.3810186	0.5000000	0.6100661	1
C16	C	1	0.5000000	0.6189814	0.6100661	1
C17	C	1	0.6189814	0.5000000	0.3899339	1
C18	C	1	0.5000000	0.3810186	0.3899339	1
C19	C	1	0.3810186	0.5000000	0.3899339	1
C20	C	1	0.5000000	0.6189814	0.3899339	1
C21	C	1	0.6189814	0.3810186	0.5000000	1
C22	C	1	0.3810186	0.3810186	0.5000000	1
C23	C	1	0.3810186	0.6189814	0.5000000	1
C24	C	1	0.6189814	0.6189814	0.5000000	1
O1	O	1	0.5383277	0.4616723	0.4733796	1
O2	O	1	0.5383277	0.4616723	0.5266204	1
O3	O	1	0.4616723	0.4616723	0.4733796	1
O4	O	1	0.4616723	0.4616723	0.5266204	1
O5	O	1	0.4616723	0.5383277	0.4733796	1
O6	O	1	0.4616723	0.5383277	0.5266204	1
O7	O	1	0.5383277	0.5383277	0.4733796	1
O8	O	1	0.5383277	0.5383277	0.5266204	1

O9	O	1	0.5930414	0.5000000	0.5494606	1
O10	O	1	0.5930414	0.4465331	0.5000000	1
O11	O	1	0.5930414	0.5000000	0.4505394	1
O12	O	1	0.5930414	0.5534669	0.5000000	1
O13	O	1	0.5000000	0.5930414	0.5494606	1
O14	O	1	0.5534669	0.5930414	0.5000000	1
O15	O	1	0.5000000	0.5930414	0.4505394	1
O16	O	1	0.4465331	0.5930414	0.5000000	1
O17	O	1	0.4069586	0.5000000	0.5494606	1
O18	O	1	0.4069586	0.5534669	0.5000000	1
O19	O	1	0.4069586	0.5000000	0.4505394	1
O20	O	1	0.4069586	0.4465331	0.5000000	1
O21	O	1	0.5000000	0.4069586	0.5494606	1
O22	O	1	0.4465331	0.4069586	0.5000000	1
O23	O	1	0.5000000	0.4069586	0.4505394	1
O24	O	1	0.5534669	0.4069586	0.5000000	1
O25	O	1	0.5534669	0.5000000	0.5860697	1
O26	O	1	0.5000000	0.5534669	0.5860697	1
O27	O	1	0.4465331	0.5000000	0.5860697	1
O28	O	1	0.5000000	0.4465331	0.5860697	1
O29	O	1	0.5534669	0.5000000	0.4139303	1
O30	O	1	0.5000000	0.4465331	0.4139303	1
O31	O	1	0.4465331	0.5000000	0.4139303	1
O32	O	1	0.5000000	0.5534669	0.4139303	1
Zr1	Zr	1	0.5665367	0.5000000	0.5000000	1
Zr2	Zr	1	0.5000000	0.5665367	0.5000000	1
Zr3	Zr	1	0.4334633	0.5000000	0.5000000	1
Zr4	Zr	1	0.5000000	0.4334633	0.5000000	1
Zr5	Zr	1	0.5000000	0.5000000	0.5615511	1
Zr6	Zr	1	0.5000000	0.5000000	0.4384489	1

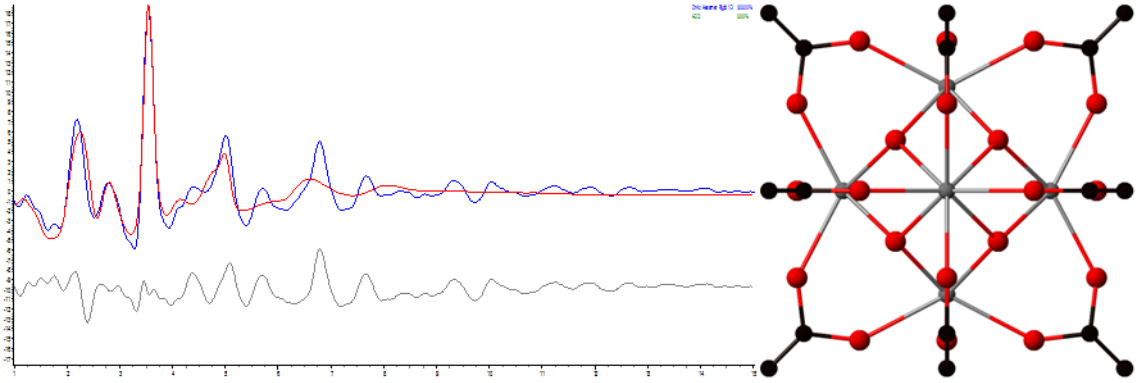

Figure 169: Observed and Calculated PDF from the fixed core refinement of ZAA24 from the 15-month data collection and the resultant model.

Table 112: The atomic coordinates of the model resulting from the fixed core refinement of ZAA24 from the 15-month data collection.

Atom Label	Atom Type	Multiplicity	Fractional X Coordinate	Fractional Y Coordinate	Fractional Z Coordinate	Fractional Occupancy
C1	C	1	0.5909815	0.5000000	0.5841642	1
C2	C	1	0.5000000	0.4090185	0.5841642	1
C3	C	1	0.4090185	0.5000000	0.5841642	1
C4	C	1	0.5000000	0.5909815	0.5841642	1
C5	C	1	0.5909815	0.5000000	0.4158358	1
C6	C	1	0.5000000	0.4090185	0.4158358	1
C7	C	1	0.4090185	0.5000000	0.4158358	1
C8	C	1	0.5000000	0.5909815	0.4158358	1
C9	C	1	0.5909815	0.4090185	0.5000000	1
C10	C	1	0.4090185	0.4090185	0.5000000	1
C11	C	1	0.4090185	0.5909815	0.5000000	1
C12	C	1	0.5909815	0.5909815	0.5000000	1
C13	C	1	0.6132073	0.5000000	0.6047247	1
C14	C	1	0.5000000	0.3867927	0.6047247	1
C15	C	1	0.3867927	0.5000000	0.6047247	1
C16	C	1	0.5000000	0.6132073	0.6047247	1
C17	C	1	0.6132073	0.5000000	0.3952753	1
C18	C	1	0.5000000	0.3867927	0.3952753	1
C19	C	1	0.3867927	0.5000000	0.3952753	1
C20	C	1	0.5000000	0.6132073	0.3952753	1
C21	C	1	0.6132073	0.3867927	0.5000000	1
C22	C	1	0.3867927	0.3867927	0.5000000	1
C23	C	1	0.3867927	0.6132073	0.5000000	1
C24	C	1	0.6132073	0.6132073	0.5000000	1
O1	O	1	0.5325611	0.5322434	0.4698787	1
O2	O	1	0.5325611	0.4677566	0.5301213	1
O3	O	1	0.4674389	0.5322434	0.4698787	1
O4	O	1	0.4674389	0.4677566	0.5301213	1
O5	O	1	0.4674389	0.4677566	0.4698787	1
O6	O	1	0.4674389	0.5322434	0.5301213	1

O7	O	1	0.5325611	0.4677566	0.4698787	1
O8	O	1	0.5325611	0.5322434	0.5301213	1
O9	O	1	0.5952794	0.5000000	0.5511942	1
O10	O	1	0.5952794	0.4446591	0.5000000	1
O11	O	1	0.5952794	0.5000000	0.4488058	1
O12	O	1	0.5952794	0.5553409	0.5000000	1
O13	O	1	0.5000000	0.5952794	0.5511942	1
O14	O	1	0.5553409	0.5952794	0.5000000	1
O15	O	1	0.5000000	0.5952794	0.4488058	1
O16	O	1	0.4446591	0.5952794	0.5000000	1
O17	O	1	0.4047206	0.5000000	0.5511942	1
O18	O	1	0.4047206	0.5553409	0.5000000	1
O19	O	1	0.4047206	0.5000000	0.4488058	1
O20	O	1	0.4047206	0.4446591	0.5000000	1
O21	O	1	0.5000000	0.4047206	0.5511942	1
O22	O	1	0.4446591	0.4047206	0.5000000	1
O23	O	1	0.5000000	0.4047206	0.4488058	1
O24	O	1	0.5553409	0.4047206	0.5000000	1
O25	O	1	0.5553409	0.5000000	0.5881401	1
O26	O	1	0.5000000	0.5553409	0.5881401	1
O27	O	1	0.4446591	0.5000000	0.5881401	1
O28	O	1	0.5000000	0.4446591	0.5881401	1
O29	O	1	0.5553409	0.5000000	0.4118599	1
O30	O	1	0.5000000	0.4446591	0.4118599	1
O31	O	1	0.4446591	0.5000000	0.4118599	1
O32	O	1	0.5000000	0.5553409	0.4118599	1
Zr1	Zr	1	0.5662428	0.5000000	0.5000000	1
Zr2	Zr	1	0.5000000	0.5662428	0.5000000	1
Zr3	Zr	1	0.4337572	0.5000000	0.5000000	1
Zr4	Zr	1	0.5000000	0.4337572	0.5000000	1
Zr5	Zr	1	0.5000000	0.5000000	0.5612792	1
Zr6	Zr	1	0.5000000	0.5000000	0.4387208	1

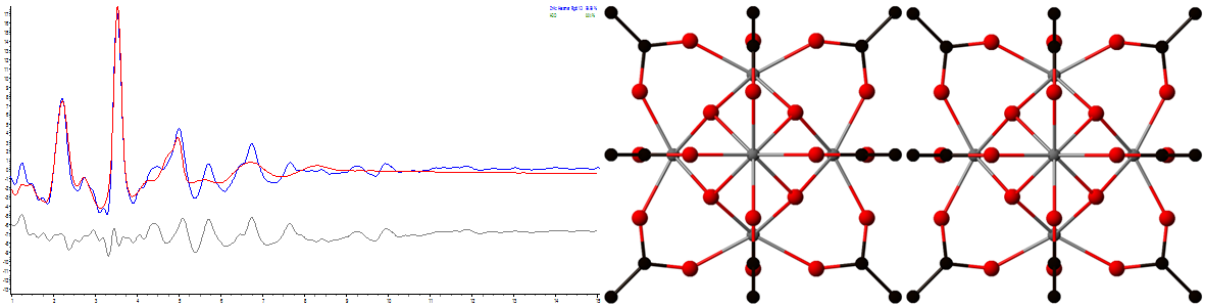

Figure 170: Observed and Calculated PDF from the chandelier core refinement of ZAA25 from the 15-month data collection and the resultant model viewed from the axial (left) and equatorial (right) positions.

Table 113: The atomic coordinates of the model resulting from the chandelier core refinement of ZAA25 from the 15-month data collection.

Atom Label	Atom Type	Multiplicity	Fractional X Coordinate	Fractional Y Coordinate	Fractional Z Coordinate	Fractional Occupancy
C1	C	1	0.5898109	0.5000000	0.5830813	1
C2	C	1	0.5000000	0.4101891	0.5830813	1
C3	C	1	0.4101891	0.5000000	0.5830813	1
C4	C	1	0.5000000	0.5898109	0.5830813	1
C5	C	1	0.5898109	0.5000000	0.4169187	1
C6	C	1	0.5000000	0.4101891	0.4169187	1
C7	C	1	0.4101891	0.5000000	0.4169187	1
C8	C	1	0.5000000	0.5898109	0.4169187	1
C9	C	1	0.5898109	0.4101891	0.5000000	1
C10	C	1	0.4101891	0.4101891	0.5000000	1
C11	C	1	0.4101891	0.5898109	0.5000000	1
C12	C	1	0.5898109	0.5898109	0.5000000	1
C13	C	1	0.6173716	0.5000000	0.6085769	1
C14	C	1	0.5000000	0.3826284	0.6085769	1
C15	C	1	0.3826284	0.5000000	0.6085769	1
C16	C	1	0.5000000	0.6173716	0.6085769	1
C17	C	1	0.6173716	0.5000000	0.3914231	1
C18	C	1	0.5000000	0.3826284	0.3914231	1
C19	C	1	0.3826284	0.5000000	0.3914231	1
C20	C	1	0.5000000	0.6173716	0.3914231	1
C21	C	1	0.6173716	0.3826284	0.5000000	1
C22	C	1	0.3826284	0.3826284	0.5000000	1
C23	C	1	0.3826284	0.6173716	0.5000000	1
C24	C	1	0.6173716	0.6173716	0.5000000	1
O1	O	1	0.5348497	0.4651503	0.4680136	1
O2	O	1	0.5348497	0.4651503	0.5319864	1
O3	O	1	0.4651503	0.4651503	0.4680136	1
O4	O	1	0.4651503	0.4651503	0.5319864	1
O5	O	1	0.4651503	0.5348497	0.4680136	1
O6	O	1	0.4651503	0.5348497	0.5319864	1
O7	O	1	0.5348497	0.5348497	0.4680136	1
O8	O	1	0.5348497	0.5348497	0.5319864	1

O9	O	1	0.5938833	0.5000000	0.5483382	1
O10	O	1	0.5938833	0.4477464	0.5000000	1
O11	O	1	0.5938833	0.5000000	0.4516618	1
O12	O	1	0.5938833	0.5522536	0.5000000	1
O13	O	1	0.5000000	0.5938833	0.5483382	1
O14	O	1	0.5522536	0.5938833	0.5000000	1
O15	O	1	0.5000000	0.5938833	0.4516618	1
O16	O	1	0.4477464	0.5938833	0.5000000	1
O17	O	1	0.4061167	0.5000000	0.5483382	1
O18	O	1	0.4061167	0.5522536	0.5000000	1
O19	O	1	0.4061167	0.5000000	0.4516618	1
O20	O	1	0.4061167	0.4477464	0.5000000	1
O21	O	1	0.5000000	0.4061167	0.5483382	1
O22	O	1	0.4477464	0.4061167	0.5000000	1
O23	O	1	0.5000000	0.4061167	0.4516618	1
O24	O	1	0.5522536	0.4061167	0.5000000	1
O25	O	1	0.5522536	0.5000000	0.5868486	1
O26	O	1	0.5000000	0.5522536	0.5868486	1
O27	O	1	0.4477464	0.5000000	0.5868486	1
O28	O	1	0.5000000	0.4477464	0.5868486	1
O29	O	1	0.5522536	0.5000000	0.4131514	1
O30	O	1	0.5000000	0.4477464	0.4131514	1
O31	O	1	0.4477464	0.5000000	0.4131514	1
O32	O	1	0.5000000	0.5522536	0.4131514	1
Zr1	Zr	1	0.5661125	0.5000000	0.5000000	1
Zr2	Zr	1	0.5000000	0.5661125	0.5000000	1
Zr3	Zr	1	0.4338875	0.5000000	0.5000000	1
Zr4	Zr	1	0.5000000	0.4338875	0.5000000	1
Zr5	Zr	1	0.5000000	0.5000000	0.5611587	1
Zr6	Zr	1	0.5000000	0.5000000	0.4388413	1

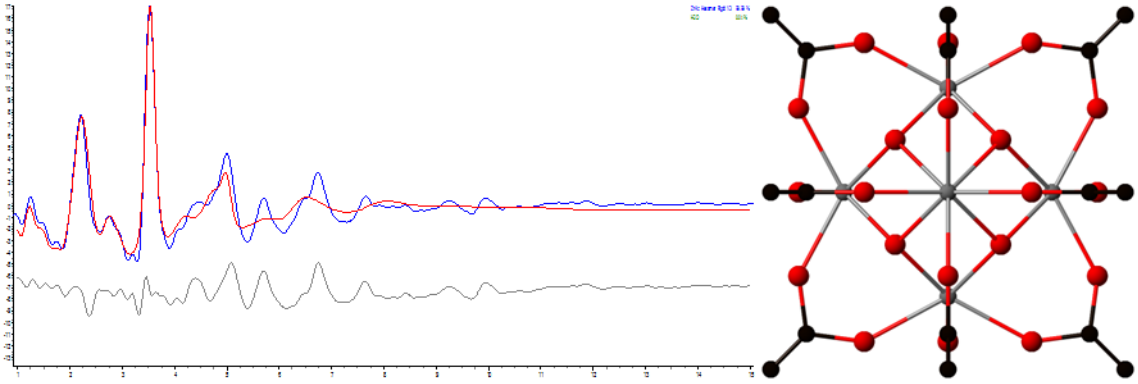

Figure 171: Observed and Calculated PDF from the fixed core refinement of ZAA25 from the 15-month data collection and the resultant model.

Table 114: The atomic coordinates of the model resulting from the fixed core refinement of ZAA25 from the 15-month data collection.

Atom Label	Atom Type	Multiplicity	Fractional X Coordinate	Fractional Y Coordinate	Fractional Z Coordinate	Fractional Occupancy
C1	C	1	0.5897859	0.5000000	0.5830582	1
C2	C	1	0.5000000	0.4102141	0.5830582	1
C3	C	1	0.4102141	0.5000000	0.5830582	1
C4	C	1	0.5000000	0.5897859	0.5830582	1
C5	C	1	0.5897859	0.5000000	0.4169418	1
C6	C	1	0.5000000	0.4102141	0.4169418	1
C7	C	1	0.4102141	0.5000000	0.4169418	1
C8	C	1	0.5000000	0.5897859	0.4169418	1
C9	C	1	0.5897859	0.4102141	0.5000000	1
C10	C	1	0.4102141	0.4102141	0.5000000	1
C11	C	1	0.4102141	0.5897859	0.5000000	1
C12	C	1	0.5897859	0.5897859	0.5000000	1
C13	C	1	0.6124103	0.5000000	0.6039874	1
C14	C	1	0.5000000	0.3875897	0.6039874	1
C15	C	1	0.3875897	0.5000000	0.6039874	1
C16	C	1	0.5000000	0.6124103	0.6039874	1
C17	C	1	0.6124103	0.5000000	0.3960126	1
C18	C	1	0.5000000	0.3875897	0.3960126	1
C19	C	1	0.3875897	0.5000000	0.3960126	1
C20	C	1	0.5000000	0.6124103	0.3960126	1
C21	C	1	0.6124103	0.3875897	0.5000000	1
C22	C	1	0.3875897	0.3875897	0.5000000	1
C23	C	1	0.3875897	0.6124103	0.5000000	1
C24	C	1	0.6124103	0.6124103	0.5000000	1
O1	O	1	0.5335278	0.5332007	0.4689844	1
O2	O	1	0.5335278	0.4667993	0.5310156	1
O3	O	1	0.4664722	0.5332007	0.4689844	1
O4	O	1	0.4664722	0.4667993	0.5310156	1
O5	O	1	0.4664722	0.4667993	0.4689844	1
O6	O	1	0.4664722	0.5332007	0.5310156	1

O7	O	1	0.5335278	0.4667993	0.4689844	1
O8	O	1	0.5335278	0.5332007	0.5310156	1
O9	O	1	0.5947944	0.5000000	0.5491183	1
O10	O	1	0.5947944	0.4469031	0.5000000	1
O11	O	1	0.5947944	0.5000000	0.4508817	1
O12	O	1	0.5947944	0.5530969	0.5000000	1
O13	O	1	0.5000000	0.5947944	0.5491183	1
O14	O	1	0.5530969	0.5947944	0.5000000	1
O15	O	1	0.5000000	0.5947944	0.4508817	1
O16	O	1	0.4469031	0.5947944	0.5000000	1
O17	O	1	0.4052056	0.5000000	0.5491183	1
O18	O	1	0.4052056	0.5530969	0.5000000	1
O19	O	1	0.4052056	0.5000000	0.4508817	1
O20	O	1	0.4052056	0.4469031	0.5000000	1
O21	O	1	0.5000000	0.4052056	0.5491183	1
O22	O	1	0.4469031	0.4052056	0.5000000	1
O23	O	1	0.5000000	0.4052056	0.4508817	1
O24	O	1	0.5530969	0.4052056	0.5000000	1
O25	O	1	0.5530969	0.5000000	0.5876915	1
O26	O	1	0.5000000	0.5530969	0.5876915	1
O27	O	1	0.4469031	0.5000000	0.5876915	1
O28	O	1	0.5000000	0.4469031	0.5876915	1
O29	O	1	0.5530969	0.5000000	0.4123085	1
O30	O	1	0.5000000	0.4469031	0.4123085	1
O31	O	1	0.4469031	0.5000000	0.4123085	1
O32	O	1	0.5000000	0.5530969	0.4123085	1
Zr1	Zr	1	0.5660959	0.5000000	0.5000000	1
Zr2	Zr	1	0.5000000	0.5660959	0.5000000	1
Zr3	Zr	1	0.4339041	0.5000000	0.5000000	1
Zr4	Zr	1	0.5000000	0.4339041	0.5000000	1
Zr5	Zr	1	0.5000000	0.5000000	0.5611433	1
Zr6	Zr	1	0.5000000	0.5000000	0.4388567	1

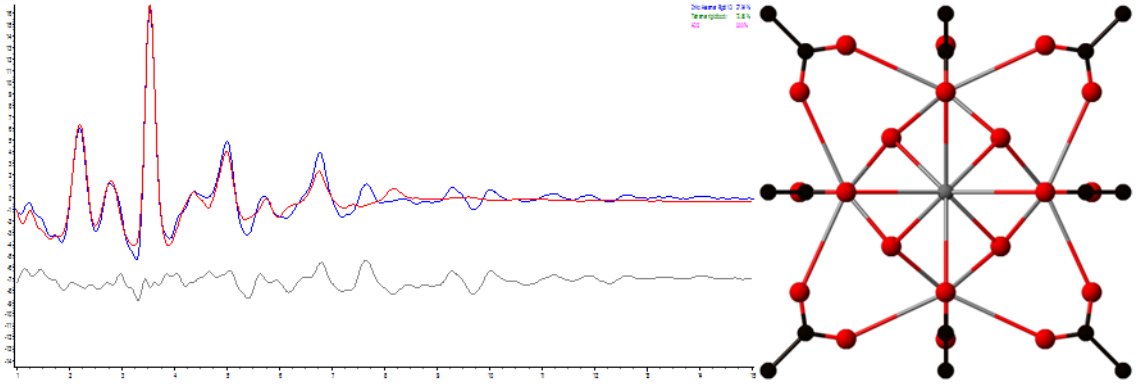

Figure 172: Observed and Calculated PDF from the fixed core refinement of ZAA1 from the 15-month data collection and the resultant model.

Table 115: The atomic coordinates of the model resulting from the fixed core refinement of ZAA1 from the 15-month data collection.

Atom Label	Atom Type	Multiplicity	Fractional X Coordinate	Fractional Y Coordinate	Fractional Z Coordinate	Fractional Occupancy
C1	C	1	0.5919291	0.5000000	0.5850408	1
C2	C	1	0.5000000	0.4080709	0.5850408	1
C3	C	1	0.4080709	0.5000000	0.5850408	1
C4	C	1	0.5000000	0.5919291	0.5850408	1
C5	C	1	0.5919291	0.5000000	0.4149592	1
C6	C	1	0.5000000	0.4080709	0.4149592	1
C7	C	1	0.4080709	0.5000000	0.4149592	1
C8	C	1	0.5000000	0.5919291	0.4149592	1
C9	C	1	0.5919291	0.4080709	0.5000000	1
C10	C	1	0.4080709	0.4080709	0.5000000	1
C11	C	1	0.4080709	0.5919291	0.5000000	1
C12	C	1	0.5919291	0.5919291	0.5000000	1
C13	C	1	0.6165111	0.5000000	0.6077809	1
C14	C	1	0.5000000	0.3834889	0.6077809	1
C15	C	1	0.3834889	0.5000000	0.6077809	1
C16	C	1	0.5000000	0.6165111	0.6077809	1
C17	C	1	0.6165111	0.5000000	0.3922191	1
C18	C	1	0.5000000	0.3834889	0.3922191	1
C19	C	1	0.3834889	0.5000000	0.3922191	1
C20	C	1	0.5000000	0.6165111	0.3922191	1
C21	C	1	0.6165111	0.3834889	0.5000000	1
C22	C	1	0.3834889	0.3834889	0.5000000	1
C23	C	1	0.3834889	0.6165111	0.5000000	1
C24	C	1	0.6165111	0.6165111	0.5000000	1
O1	O	1	0.5358083	0.5354589	0.4668748	1
O2	O	1	0.5358083	0.4645411	0.5331252	1
O3	O	1	0.4641917	0.5354589	0.4668748	1
O4	O	1	0.4641917	0.4645411	0.5331252	1
O5	O	1	0.4641917	0.4645411	0.4668748	1
O6	O	1	0.4641917	0.5354589	0.5331252	1

O7	O	1	0.5358083	0.4645411	0.4668748	1
O8	O	1	0.5358083	0.5354589	0.5331252	1
O9	O	1	0.5958881	0.5000000	0.5604255	1
O10	O	1	0.5958881	0.4346801	0.5000000	1
O11	O	1	0.5958881	0.5000000	0.4395745	1
O12	O	1	0.5958881	0.5653199	0.5000000	1
O13	O	1	0.5000000	0.5958881	0.5604255	1
O14	O	1	0.5653199	0.5958881	0.5000000	1
O15	O	1	0.5000000	0.5958881	0.4395745	1
O16	O	1	0.4346801	0.5958881	0.5000000	1
O17	O	1	0.4041119	0.5000000	0.5604255	1
O18	O	1	0.4041119	0.5653199	0.5000000	1
O19	O	1	0.4041119	0.5000000	0.4395745	1
O20	O	1	0.4041119	0.4346801	0.5000000	1
O21	O	1	0.5000000	0.4041119	0.5604255	1
O22	O	1	0.4346801	0.4041119	0.5000000	1
O23	O	1	0.5000000	0.4041119	0.4395745	1
O24	O	1	0.5653199	0.4041119	0.5000000	1
O25	O	1	0.5653199	0.5000000	0.5887032	1
O26	O	1	0.5000000	0.5653199	0.5887032	1
O27	O	1	0.4346801	0.5000000	0.5887032	1
O28	O	1	0.5000000	0.4346801	0.5887032	1
O29	O	1	0.5653199	0.5000000	0.4112968	1
O30	O	1	0.5000000	0.4346801	0.4112968	1
O31	O	1	0.4346801	0.5000000	0.4112968	1
O32	O	1	0.5000000	0.5653199	0.4112968	1
Zr1	Zr	1	0.5656546	0.5000000	0.5000000	1
Zr2	Zr	1	0.5000000	0.5656546	0.5000000	1
Zr3	Zr	1	0.4343454	0.5000000	0.5000000	1
Zr4	Zr	1	0.5000000	0.4343454	0.5000000	1
Zr5	Zr	1	0.5000000	0.5000000	0.5607351	1
Zr6	Zr	1	0.5000000	0.5000000	0.4392649	1

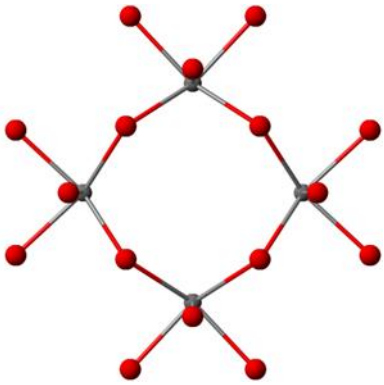

Figure 173: The tetrameric structure resulting from the fixed core refinement of ZAA1 from the 15-month data collection.

Table 116: The atomic coordinates of the tetrameric phase of the fixed core refinement of ZAA1 from the 15-month data collection.

Atom Label	Atom Type	Multiplicity	Fractional X Coordinate	Fractional Y Coordinate	Fractional Z Coordinate	Fractional Occupancy
O1	O	1	0.5150141	0.4849859	0.4706739	1
O2	O	1	0.4849859	0.4849859	0.5293261	1
O3	O	1	0.5150141	0.5150141	0.5293261	1
O4	O	1	0.4849859	0.5150141	0.4706739	1
O5	O	1	0.5000000	0.5278721	0.5464579	1
O6	O	1	0.5000000	0.4721279	0.5464579	1
O7	O	1	0.4721279	0.5000000	0.4535421	1
O8	O	1	0.5278721	0.5000000	0.4535421	1
O9	O	1	0.5140461	0.4602953	0.5000000	1
O10	O	1	0.4602953	0.4859539	0.5000000	1
O11	O	1	0.5397047	0.5140461	0.5000000	1
O12	O	1	0.4859539	0.5397047	0.5000000	1
O13	O	1	0.4602953	0.5140461	0.5000000	1
O14	O	1	0.5397047	0.4859539	0.5000000	1
O15	O	1	0.4859539	0.4602953	0.5000000	1
O16	O	1	0.5140461	0.5397047	0.5000000	1
O17	O	1	0.5150141	0.4849859	0.5293261	1
O18	O	1	0.4849859	0.4849859	0.4706739	1
O19	O	1	0.5150141	0.5150141	0.4706739	1
O20	O	1	0.4849859	0.5150141	0.5293261	1
O21	O	1	0.5000000	0.5278721	0.4535421	1
O22	O	1	0.5000000	0.4721279	0.4535421	1
O23	O	1	0.4721279	0.5000000	0.5464579	1
O24	O	1	0.5278721	0.5000000	0.5464579	1
Zr1	Zr	1	0.5000000	0.4753646	0.5000000	1
Zr2	Zr	1	0.4753646	0.5000000	0.5000000	1
Zr3	Zr	1	0.5246354	0.5000000	0.5000000	1
Zr4	Zr	1	0.5000000	0.5246354	0.5000000	1

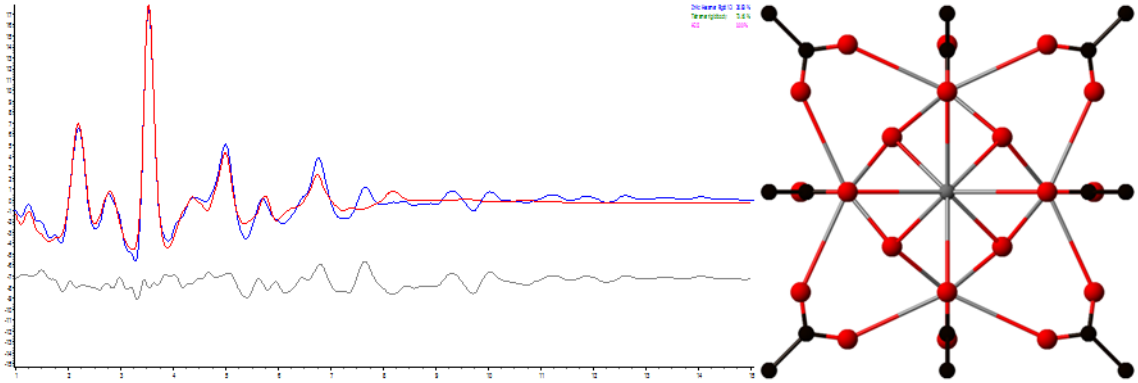

Figure 174: Observed and Calculated PDF from the fixed core refinement of ZAA4 from the 15-month data collection and the resultant model.

Table 117: The atomic coordinates of the model resulting from the fixed core refinement of ZAA4 from the 15-month data collection.

Atom Label	Atom Type	Multiplicity	Fractional X Coordinate	Fractional Y Coordinate	Fractional Z Coordinate	Fractional Occupancy
C1	C	1	0.5922728	0.5000000	0.5853588	1
C2	C	1	0.5000000	0.4077272	0.5853588	1
C3	C	1	0.4077272	0.5000000	0.5853588	1
C4	C	1	0.5000000	0.5922728	0.5853588	1
C5	C	1	0.5922728	0.5000000	0.4146412	1
C6	C	1	0.5000000	0.4077272	0.4146412	1
C7	C	1	0.4077272	0.5000000	0.4146412	1
C8	C	1	0.5000000	0.5922728	0.4146412	1
C9	C	1	0.5922728	0.4077272	0.5000000	1
C10	C	1	0.4077272	0.4077272	0.5000000	1
C11	C	1	0.4077272	0.5922728	0.5000000	1
C12	C	1	0.5922728	0.5922728	0.5000000	1
C13	C	1	0.6164895	0.5000000	0.6077609	1
C14	C	1	0.5000000	0.3835105	0.6077609	1
C15	C	1	0.3835105	0.5000000	0.6077609	1
C16	C	1	0.5000000	0.6164895	0.6077609	1
C17	C	1	0.6164895	0.5000000	0.3922391	1
C18	C	1	0.5000000	0.3835105	0.3922391	1
C19	C	1	0.3835105	0.5000000	0.3922391	1
C20	C	1	0.5000000	0.6164895	0.3922391	1
C21	C	1	0.6164895	0.3835105	0.5000000	1
C22	C	1	0.3835105	0.3835105	0.5000000	1
C23	C	1	0.3835105	0.6164895	0.5000000	1
C24	C	1	0.6164895	0.6164895	0.5000000	1
O1	O	1	0.5360875	0.5357353	0.4666166	1
O2	O	1	0.5360875	0.4642647	0.5333834	1
O3	O	1	0.4639125	0.5357353	0.4666166	1
O4	O	1	0.4639125	0.4642647	0.5333834	1
O5	O	1	0.4639125	0.4642647	0.4666166	1
O6	O	1	0.4639125	0.5357353	0.5333834	1

O7	O	1	0.5360875	0.4642647	0.4666166	1
O8	O	1	0.5360875	0.5357353	0.5333834	1
O9	O	1	0.5959621	0.5000000	0.5603378	1
O10	O	1	0.5959621	0.4347749	0.5000000	1
O11	O	1	0.5959621	0.5000000	0.4396622	1
O12	O	1	0.5959621	0.5652251	0.5000000	1
O13	O	1	0.5000000	0.5959621	0.5603378	1
O14	O	1	0.5652251	0.5959621	0.5000000	1
O15	O	1	0.5000000	0.5959621	0.4396622	1
O16	O	1	0.4347749	0.5959621	0.5000000	1
O17	O	1	0.4040379	0.5000000	0.5603378	1
O18	O	1	0.4040379	0.5652251	0.5000000	1
O19	O	1	0.4040379	0.5000000	0.4396622	1
O20	O	1	0.4040379	0.4347749	0.5000000	1
O21	O	1	0.5000000	0.4040379	0.5603378	1
O22	O	1	0.4347749	0.4040379	0.5000000	1
O23	O	1	0.5000000	0.4040379	0.4396622	1
O24	O	1	0.5652251	0.4040379	0.5000000	1
O25	O	1	0.5652251	0.5000000	0.5887716	1
O26	O	1	0.5000000	0.5652251	0.5887716	1
O27	O	1	0.4347749	0.5000000	0.5887716	1
O28	O	1	0.5000000	0.4347749	0.5887716	1
O29	O	1	0.5652251	0.5000000	0.4112284	1
O30	O	1	0.5000000	0.4347749	0.4112284	1
O31	O	1	0.4347749	0.5000000	0.4112284	1
O32	O	1	0.5000000	0.5652251	0.4112284	1
Zr1	Zr	1	0.565649	0.5000000	0.5000000	1
Zr2	Zr	1	0.5000000	0.565649	0.5000000	1
Zr3	Zr	1	0.434351	0.5000000	0.5000000	1
Zr4	Zr	1	0.5000000	0.434351	0.5000000	1
Zr5	Zr	1	0.5000000	0.5000000	0.5607299	1
Zr6	Zr	1	0.5000000	0.5000000	0.4392701	1

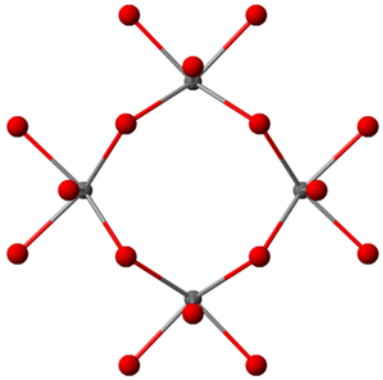

Figure 175: The tetrameric structure resulting from the fixed core refinement of ZAA4 from the 15-month data collection.

Table 118: The atomic coordinates of the tetrameric phase of the fixed core refinement of ZAA4 from the 15-month data collection.

Atom Label	Atom Type	Multiplicity	Fractional X Coordinate	Fractional Y Coordinate	Fractional Z Coordinate	Fractional Occupancy
O1	O	1	0.515025	0.484975	0.4708246	1
O2	O	1	0.484975	0.484975	0.5291754	1
O3	O	1	0.515025	0.515025	0.5291754	1
O4	O	1	0.484975	0.515025	0.4708246	1
O5	O	1	0.5000000	0.5279603	0.5460565	1
O6	O	1	0.5000000	0.4720397	0.5460565	1
O7	O	1	0.4720397	0.5000000	0.4539435	1
O8	O	1	0.5279603	0.5000000	0.4539435	1
O9	O	1	0.514351	0.4604094	0.5000000	1
O10	O	1	0.4604094	0.485649	0.5000000	1
O11	O	1	0.5395906	0.514351	0.5000000	1
O12	O	1	0.485649	0.5395906	0.5000000	1
O13	O	1	0.4604094	0.514351	0.5000000	1
O14	O	1	0.5395906	0.485649	0.5000000	1
O15	O	1	0.485649	0.4604094	0.5000000	1
O16	O	1	0.514351	0.5395906	0.5000000	1
O17	O	1	0.515025	0.484975	0.5291754	1
O18	O	1	0.484975	0.484975	0.4708246	1
O19	O	1	0.515025	0.515025	0.4708246	1
O20	O	1	0.484975	0.515025	0.5291754	1
O21	O	1	0.5000000	0.5279603	0.4539435	1
O22	O	1	0.5000000	0.4720397	0.4539435	1
O23	O	1	0.4720397	0.5000000	0.5460565	1
O24	O	1	0.5279603	0.5000000	0.5460565	1
Zr1	Zr	1	0.5000000	0.4754038	0.5000000	1
Zr2	Zr	1	0.4754038	0.5000000	0.5000000	1
Zr3	Zr	1	0.5245962	0.5000000	0.5000000	1
Zr4	Zr	1	0.5000000	0.5245962	0.5000000	1

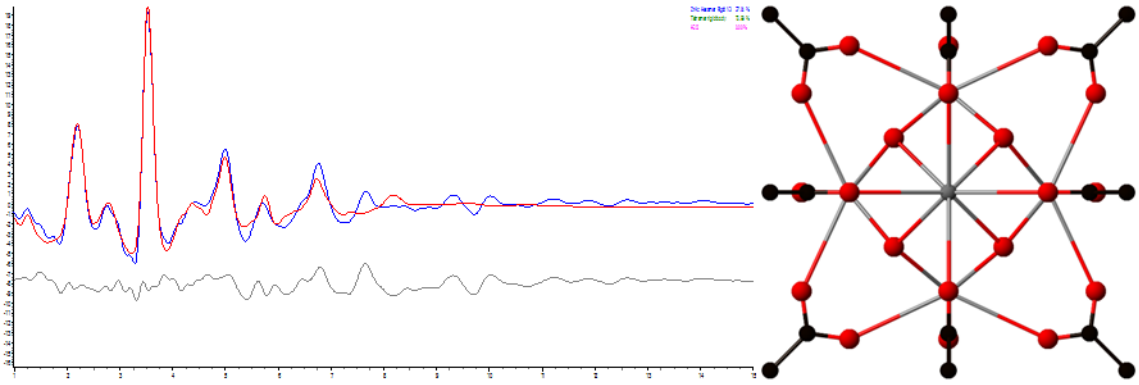

Figure 176: Observed and Calculated PDF from the fixed core refinement of ZAA7 from the 15-month data collection and the resultant model.

Table 119: The atomic coordinates of the model resulting from the fixed core refinement of ZAA7 from the 15-month data collection.

Atom Label	Atom Type	Multiplicity	Fractional X Coordinate	Fractional Y Coordinate	Fractional Z Coordinate	Fractional Occupancy
C1	C	1	0.5922913	0.5000000	0.5853759	1
C2	C	1	0.5000000	0.4077087	0.5853759	1
C3	C	1	0.4077087	0.5000000	0.5853759	1
C4	C	1	0.5000000	0.5922913	0.5853759	1
C5	C	1	0.5922913	0.5000000	0.4146241	1
C6	C	1	0.5000000	0.4077087	0.4146241	1
C7	C	1	0.4077087	0.5000000	0.4146241	1
C8	C	1	0.5000000	0.5922913	0.4146241	1
C9	C	1	0.5922913	0.4077087	0.5000000	1
C10	C	1	0.4077087	0.4077087	0.5000000	1
C11	C	1	0.4077087	0.5922913	0.5000000	1
C12	C	1	0.5922913	0.5922913	0.5000000	1
C13	C	1	0.6165536	0.5000000	0.6078202	1
C14	C	1	0.5000000	0.3834464	0.6078202	1
C15	C	1	0.3834464	0.5000000	0.6078202	1
C16	C	1	0.5000000	0.6165536	0.6078202	1
C17	C	1	0.6165536	0.5000000	0.3921798	1
C18	C	1	0.5000000	0.3834464	0.3921798	1
C19	C	1	0.3834464	0.5000000	0.3921798	1
C20	C	1	0.5000000	0.6165536	0.3921798	1
C21	C	1	0.6165536	0.3834464	0.5000000	1
C22	C	1	0.3834464	0.3834464	0.5000000	1
C23	C	1	0.3834464	0.6165536	0.5000000	1
C24	C	1	0.6165536	0.6165536	0.5000000	1
O1	O	1	0.5359665	0.5356155	0.4667285	1
O2	O	1	0.5359665	0.4643845	0.5332715	1
O3	O	1	0.4640335	0.5356155	0.4667285	1
O4	O	1	0.4640335	0.4643845	0.5332715	1
O5	O	1	0.4640335	0.4643845	0.4667285	1
O6	O	1	0.4640335	0.5356155	0.5332715	1

O7	O	1	0.5359665	0.4643845	0.4667285	1
O8	O	1	0.5359665	0.5356155	0.5332715	1
O9	O	1	0.5961321	0.5000000	0.5600037	1
O10	O	1	0.5961321	0.4351361	0.5000000	1
O11	O	1	0.5961321	0.5000000	0.4399963	1
O12	O	1	0.5961321	0.5648639	0.5000000	1
O13	O	1	0.5000000	0.5961321	0.5600037	1
O14	O	1	0.5648639	0.5961321	0.5000000	1
O15	O	1	0.5000000	0.5961321	0.4399963	1
O16	O	1	0.4351361	0.5961321	0.5000000	1
O17	O	1	0.4038679	0.5000000	0.5600037	1
O18	O	1	0.4038679	0.5648639	0.5000000	1
O19	O	1	0.4038679	0.5000000	0.4399963	1
O20	O	1	0.4038679	0.4351361	0.5000000	1
O21	O	1	0.5000000	0.4038679	0.5600037	1
O22	O	1	0.4351361	0.4038679	0.5000000	1
O23	O	1	0.5000000	0.4038679	0.4399963	1
O24	O	1	0.5648639	0.4038679	0.5000000	1
O25	O	1	0.5648639	0.5000000	0.5889289	1
O26	O	1	0.5000000	0.5648639	0.5889289	1
O27	O	1	0.4351361	0.5000000	0.5889289	1
O28	O	1	0.5000000	0.4351361	0.5889289	1
O29	O	1	0.5648639	0.5000000	0.4110711	1
O30	O	1	0.5000000	0.4351361	0.4110711	1
O31	O	1	0.4351361	0.5000000	0.4110711	1
O32	O	1	0.5000000	0.5648639	0.4110711	1
Zr1	Zr	1	0.5656282	0.5000000	0.5000000	1
Zr2	Zr	1	0.5000000	0.5656282	0.5000000	1
Zr3	Zr	1	0.4343718	0.5000000	0.5000000	1
Zr4	Zr	1	0.5000000	0.4343718	0.5000000	1
Zr5	Zr	1	0.5000000	0.5000000	0.5607106	1
Zr6	Zr	1	0.5000000	0.5000000	0.4392894	1

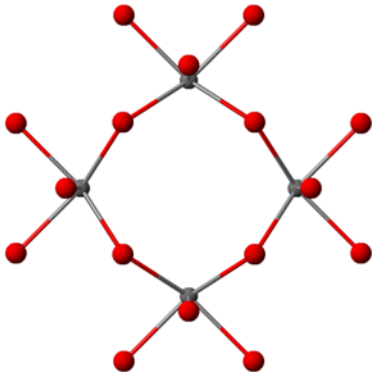

Figure 177: The tetrameric structure resulting from the fixed core refinement of ZAA7 from the 15-month data collection.

Table 120: The atomic coordinates of the tetrameric phase of the fixed core refinement of ZAA7 from the 15-month data collection.

Atom Label	Atom Type	Multiplicity	Fractional X Coordinate	Fractional Y Coordinate	Fractional Z Coordinate	Fractional Occupancy
O1	O	1	0.5149969	0.4850031	0.4709553	1
O2	O	1	0.4850031	0.4850031	0.5290447	1
O3	O	1	0.5149969	0.5149969	0.5290447	1
O4	O	1	0.4850031	0.5149969	0.4709553	1
O5	O	1	0.5000000	0.527962	0.545785	1
O6	O	1	0.5000000	0.472038	0.545785	1
O7	O	1	0.472038	0.5000000	0.454215	1
O8	O	1	0.527962	0.5000000	0.454215	1
O9	O	1	0.5148002	0.4606248	0.5000000	1
O10	O	1	0.4606248	0.4851998	0.5000000	1
O11	O	1	0.5393752	0.5148002	0.5000000	1
O12	O	1	0.4851998	0.5393752	0.5000000	1
O13	O	1	0.4606248	0.5148002	0.5000000	1
O14	O	1	0.5393752	0.4851998	0.5000000	1
O15	O	1	0.4851998	0.4606248	0.5000000	1
O16	O	1	0.5148002	0.5393752	0.5000000	1
O17	O	1	0.5149969	0.4850031	0.5290447	1
O18	O	1	0.4850031	0.4850031	0.4709553	1
O19	O	1	0.5149969	0.5149969	0.4709553	1
O20	O	1	0.4850031	0.5149969	0.5290447	1
O21	O	1	0.5000000	0.527962	0.454215	1
O22	O	1	0.5000000	0.472038	0.454215	1
O23	O	1	0.472038	0.5000000	0.545785	1
O24	O	1	0.527962	0.5000000	0.545785	1
Zr1	Zr	1	0.5000000	0.4753988	0.5000000	1
Zr2	Zr	1	0.4753988	0.5000000	0.5000000	1
Zr3	Zr	1	0.5246012	0.5000000	0.5000000	1
Zr4	Zr	1	0.5000000	0.5246012	0.5000000	1

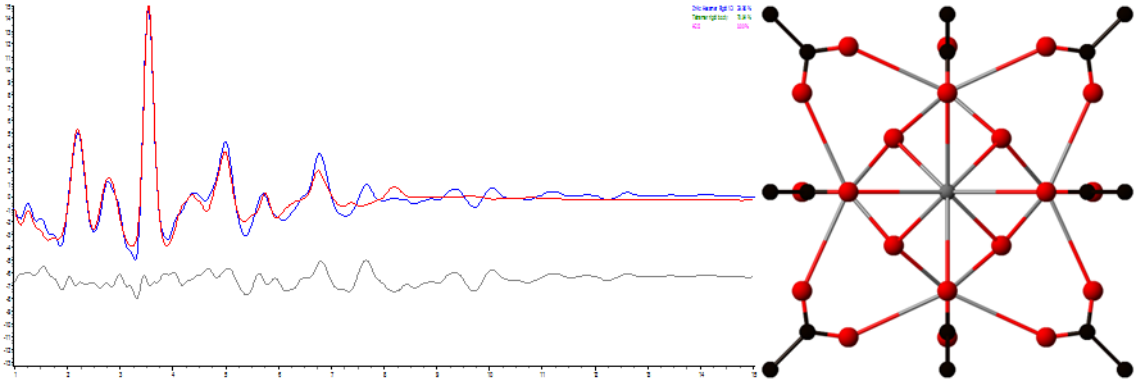

Figure 178: Observed and Calculated PDF from the fixed core refinement of ZAA10 from the 15-month data collection and the resultant model.

Table 121: The atomic coordinates of the model resulting from the fixed core refinement of ZAA10 from the 15-month data collection.

Atom Label	Atom Type	Multiplicity	Fractional X Coordinate	Fractional Y Coordinate	Fractional Z Coordinate	Fractional Occupancy
C1	C	1	0.5920433	0.5000000	0.5851465	1
C2	C	1	0.5000000	0.4079567	0.5851465	1
C3	C	1	0.4079567	0.5000000	0.5851465	1
C4	C	1	0.5000000	0.5920433	0.5851465	1
C5	C	1	0.5920433	0.5000000	0.4148535	1
C6	C	1	0.5000000	0.4079567	0.4148535	1
C7	C	1	0.4079567	0.5000000	0.4148535	1
C8	C	1	0.5000000	0.5920433	0.4148535	1
C9	C	1	0.5920433	0.4079567	0.5000000	1
C10	C	1	0.4079567	0.4079567	0.5000000	1
C11	C	1	0.4079567	0.5920433	0.5000000	1
C12	C	1	0.5920433	0.5920433	0.5000000	1
C13	C	1	0.6167961	0.5000000	0.6080445	1
C14	C	1	0.5000000	0.3832039	0.6080445	1
C15	C	1	0.3832039	0.5000000	0.6080445	1
C16	C	1	0.5000000	0.6167961	0.6080445	1
C17	C	1	0.6167961	0.5000000	0.3919555	1
C18	C	1	0.5000000	0.3832039	0.3919555	1
C19	C	1	0.3832039	0.5000000	0.3919555	1
C20	C	1	0.5000000	0.6167961	0.3919555	1
C21	C	1	0.6167961	0.3832039	0.5000000	1
C22	C	1	0.3832039	0.3832039	0.5000000	1
C23	C	1	0.3832039	0.6167961	0.5000000	1
C24	C	1	0.6167961	0.6167961	0.5000000	1
O1	O	1	0.5354614	0.5351154	0.4671957	1
O2	O	1	0.5354614	0.4648846	0.5328043	1
O3	O	1	0.4645386	0.5351154	0.4671957	1
O4	O	1	0.4645386	0.4648846	0.5328043	1
O5	O	1	0.4645386	0.4648846	0.4671957	1
O6	O	1	0.4645386	0.5351154	0.5328043	1

O7	O	1	0.5354614	0.4648846	0.4671957	1
O8	O	1	0.5354614	0.5351154	0.5328043	1
O9	O	1	0.5957073	0.5000000	0.5602799	1
O10	O	1	0.5957073	0.4348374	0.5000000	1
O11	O	1	0.5957073	0.5000000	0.4397201	1
O12	O	1	0.5957073	0.5651626	0.5000000	1
O13	O	1	0.5000000	0.5957073	0.5602799	1
O14	O	1	0.5651626	0.5957073	0.5000000	1
O15	O	1	0.5000000	0.5957073	0.4397201	1
O16	O	1	0.4348374	0.5957073	0.5000000	1
O17	O	1	0.4042927	0.5000000	0.5602799	1
O18	O	1	0.4042927	0.5651626	0.5000000	1
O19	O	1	0.4042927	0.5000000	0.4397201	1
O20	O	1	0.4042927	0.4348374	0.5000000	1
O21	O	1	0.5000000	0.4042927	0.5602799	1
O22	O	1	0.4348374	0.4042927	0.5000000	1
O23	O	1	0.5000000	0.4042927	0.4397201	1
O24	O	1	0.5651626	0.4042927	0.5000000	1
O25	O	1	0.5651626	0.5000000	0.588536	1
O26	O	1	0.5000000	0.5651626	0.588536	1
O27	O	1	0.4348374	0.5000000	0.588536	1
O28	O	1	0.5000000	0.4348374	0.588536	1
O29	O	1	0.5651626	0.5000000	0.411464	1
O30	O	1	0.5000000	0.4348374	0.411464	1
O31	O	1	0.4348374	0.5000000	0.411464	1
O32	O	1	0.5000000	0.5651626	0.411464	1
Zr1	Zr	1	0.5657013	0.5000000	0.5000000	1
Zr2	Zr	1	0.5000000	0.5657013	0.5000000	1
Zr3	Zr	1	0.4342987	0.5000000	0.5000000	1
Zr4	Zr	1	0.5000000	0.4342987	0.5000000	1
Zr5	Zr	1	0.5000000	0.5000000	0.5607783	1
Zr6	Zr	1	0.5000000	0.5000000	0.4392217	1

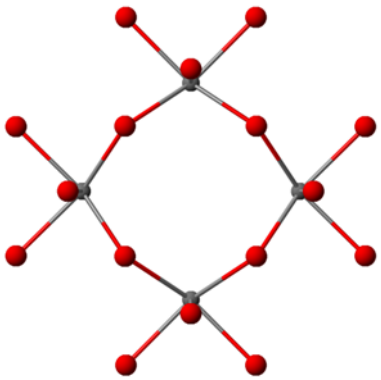

Figure 179: The tetrameric structure resulting from the fixed core refinement of ZAA10 from the 15-month data collection.

Table 122: The atomic coordinates of the tetrameric phase of the fixed core refinement of ZAA10 from the 15-month data collection.

Atom Label	Atom Type	Multiplicity	Fractional X Coordinate	Fractional Y Coordinate	Fractional Z Coordinate	Fractional Occupancy
O1	O	1	0.5148091	0.4851909	0.470068	1
O2	O	1	0.4851909	0.4851909	0.529932	1
O3	O	1	0.5148091	0.5148091	0.529932	1
O4	O	1	0.4851909	0.5148091	0.470068	1
O5	O	1	0.5000000	0.5277524	0.5462582	1
O6	O	1	0.5000000	0.4722476	0.5462582	1
O7	O	1	0.4722476	0.5000000	0.4537418	1
O8	O	1	0.5277524	0.5000000	0.4537418	1
O9	O	1	0.5146714	0.4605387	0.5000000	1
O10	O	1	0.4605387	0.4853286	0.5000000	1
O11	O	1	0.5394613	0.5146714	0.5000000	1
O12	O	1	0.4853286	0.5394613	0.5000000	1
O13	O	1	0.4605387	0.5146714	0.5000000	1
O14	O	1	0.5394613	0.4853286	0.5000000	1
O15	O	1	0.4853286	0.4605387	0.5000000	1
O16	O	1	0.5146714	0.5394613	0.5000000	1
O17	O	1	0.5148091	0.4851909	0.529932	1
O18	O	1	0.4851909	0.4851909	0.470068	1
O19	O	1	0.5148091	0.5148091	0.470068	1
O20	O	1	0.4851909	0.5148091	0.529932	1
O21	O	1	0.5000000	0.5277524	0.4537418	1
O22	O	1	0.5000000	0.4722476	0.4537418	1
O23	O	1	0.4722476	0.5000000	0.5462582	1
O24	O	1	0.5277524	0.5000000	0.5462582	1
Zr1	Zr	1	0.5000000	0.4753997	0.5000000	1
Zr2	Zr	1	0.4753997	0.5000000	0.5000000	1
Zr3	Zr	1	0.5246003	0.5000000	0.5000000	1
Zr4	Zr	1	0.5000000	0.5246003	0.5000000	1

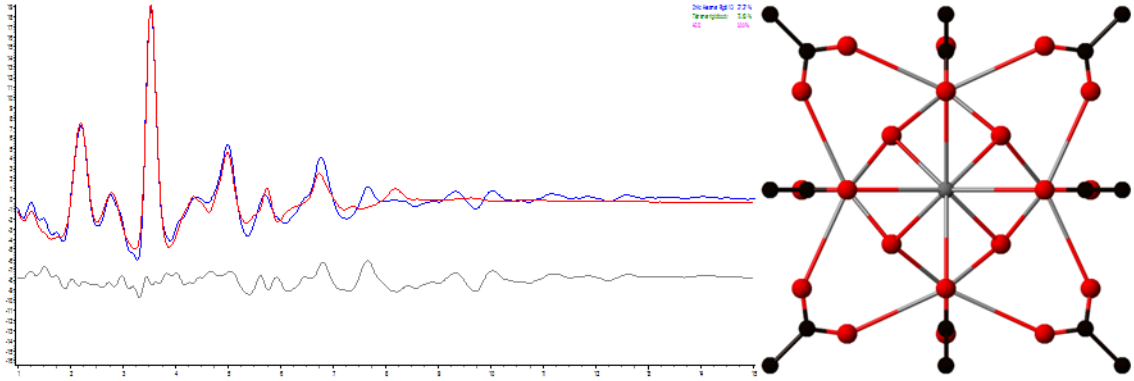

Figure 180: Observed and Calculated PDF from the fixed core refinement of ZAA13 from the 15-month data collection and the resultant model.

Table 123: The atomic coordinates of the model resulting from the fixed core refinement of ZAA13 from the 15-month data collection.

Atom Label	Atom Type	Multiplicity	Fractional X Coordinate	Fractional Y Coordinate	Fractional Z Coordinate	Fractional Occupancy
C1	C	1	0.5922737	0.5000000	0.5853596	1
C2	C	1	0.5000000	0.4077263	0.5853596	1
C3	C	1	0.4077263	0.5000000	0.5853596	1
C4	C	1	0.5000000	0.5922737	0.5853596	1
C5	C	1	0.5922737	0.5000000	0.4146404	1
C6	C	1	0.5000000	0.4077263	0.4146404	1
C7	C	1	0.4077263	0.5000000	0.4146404	1
C8	C	1	0.5000000	0.5922737	0.4146404	1
C9	C	1	0.5922737	0.4077263	0.5000000	1
C10	C	1	0.4077263	0.4077263	0.5000000	1
C11	C	1	0.4077263	0.5922737	0.5000000	1
C12	C	1	0.5922737	0.5922737	0.5000000	1
C13	C	1	0.616692	0.5000000	0.6079482	1
C14	C	1	0.5000000	0.383308	0.6079482	1
C15	C	1	0.383308	0.5000000	0.6079482	1
C16	C	1	0.5000000	0.616692	0.6079482	1
C17	C	1	0.616692	0.5000000	0.3920518	1
C18	C	1	0.5000000	0.383308	0.3920518	1
C19	C	1	0.383308	0.5000000	0.3920518	1
C20	C	1	0.5000000	0.616692	0.3920518	1
C21	C	1	0.616692	0.383308	0.5000000	1
C22	C	1	0.383308	0.383308	0.5000000	1
C23	C	1	0.383308	0.616692	0.5000000	1
C24	C	1	0.616692	0.616692	0.5000000	1
O1	O	1	0.5363526	0.5359979	0.4663714	1
O2	O	1	0.5363526	0.4640021	0.5336286	1
O3	O	1	0.4636474	0.5359979	0.4663714	1
O4	O	1	0.4636474	0.4640021	0.5336286	1
O5	O	1	0.4636474	0.4640021	0.4663714	1
O6	O	1	0.4636474	0.5359979	0.5336286	1

O7	O	1	0.5363526	0.4640021	0.4663714	1
O8	O	1	0.5363526	0.5359979	0.5336286	1
O9	O	1	0.5957704	0.5000000	0.5605278	1
O10	O	1	0.5957704	0.4345695	0.5000000	1
O11	O	1	0.5957704	0.5000000	0.4394722	1
O12	O	1	0.5957704	0.5654305	0.5000000	1
O13	O	1	0.5000000	0.5957704	0.5605278	1
O14	O	1	0.5654305	0.5957704	0.5000000	1
O15	O	1	0.5000000	0.5957704	0.4394722	1
O16	O	1	0.4345695	0.5957704	0.5000000	1
O17	O	1	0.4042296	0.5000000	0.5605278	1
O18	O	1	0.4042296	0.5654305	0.5000000	1
O19	O	1	0.4042296	0.5000000	0.4394722	1
O20	O	1	0.4042296	0.4345695	0.5000000	1
O21	O	1	0.5000000	0.4042296	0.5605278	1
O22	O	1	0.4345695	0.4042296	0.5000000	1
O23	O	1	0.5000000	0.4042296	0.4394722	1
O24	O	1	0.5654305	0.4042296	0.5000000	1
O25	O	1	0.5654305	0.5000000	0.5885943	1
O26	O	1	0.5000000	0.5654305	0.5885943	1
O27	O	1	0.4345695	0.5000000	0.5885943	1
O28	O	1	0.5000000	0.4345695	0.5885943	1
O29	O	1	0.5654305	0.5000000	0.4114057	1
O30	O	1	0.5000000	0.4345695	0.4114057	1
O31	O	1	0.4345695	0.5000000	0.4114057	1
O32	O	1	0.5000000	0.5654305	0.4114057	1
Zr1	Zr	1	0.5656414	0.5000000	0.5000000	1
Zr2	Zr	1	0.5000000	0.5656414	0.5000000	1
Zr3	Zr	1	0.4343586	0.5000000	0.5000000	1
Zr4	Zr	1	0.5000000	0.4343586	0.5000000	1
Zr5	Zr	1	0.5000000	0.5000000	0.5607229	1
Zr6	Zr	1	0.5000000	0.5000000	0.4392771	1

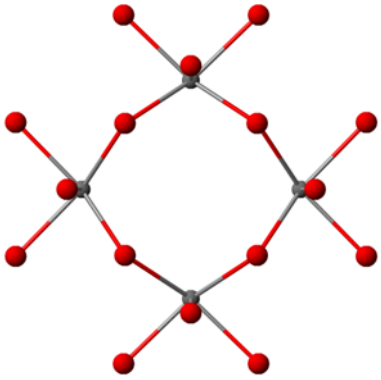

Figure 181: The tetrameric structure resulting from the fixed core refinement of ZAA13 from the 15-month data collection.

Table 124: The atomic coordinates of the tetrameric phase of the fixed core refinement of ZAA13 from the 15-month data collection.

Atom Label	Atom Type	Multiplicity	Fractional X Coordinate	Fractional Y Coordinate	Fractional Z Coordinate	Fractional Occupancy
O1	O	1	0.5148534	0.4851466	0.4707196	1
O2	O	1	0.4851466	0.4851466	0.5292804	1
O3	O	1	0.5148534	0.5148534	0.5292804	1
O4	O	1	0.4851466	0.5148534	0.4707196	1
O5	O	1	0.5000000	0.5278624	0.5452361	1
O6	O	1	0.5000000	0.4721376	0.5452361	1
O7	O	1	0.4721376	0.5000000	0.4547639	1
O8	O	1	0.5278624	0.5000000	0.4547639	1
O9	O	1	0.5151376	0.4606839	0.5000000	1
O10	O	1	0.4606839	0.4848624	0.5000000	1
O11	O	1	0.5393161	0.5151376	0.5000000	1
O12	O	1	0.4848624	0.5393161	0.5000000	1
O13	O	1	0.4606839	0.5151376	0.5000000	1
O14	O	1	0.5393161	0.4848624	0.5000000	1
O15	O	1	0.4848624	0.4606839	0.5000000	1
O16	O	1	0.5151376	0.5393161	0.5000000	1
O17	O	1	0.5148534	0.4851466	0.5292804	1
O18	O	1	0.4851466	0.4851466	0.4707196	1
O19	O	1	0.5148534	0.5148534	0.4707196	1
O20	O	1	0.4851466	0.5148534	0.5292804	1
O21	O	1	0.5000000	0.5278624	0.4547639	1
O22	O	1	0.5000000	0.4721376	0.4547639	1
O23	O	1	0.4721376	0.5000000	0.5452361	1
O24	O	1	0.5278624	0.5000000	0.5452361	1
Zr1	Zr	1	0.5000000	0.4754001	0.5000000	1
Zr2	Zr	1	0.4754001	0.5000000	0.5000000	1
Zr3	Zr	1	0.5245999	0.5000000	0.5000000	1
Zr4	Zr	1	0.5000000	0.5245999	0.5000000	1

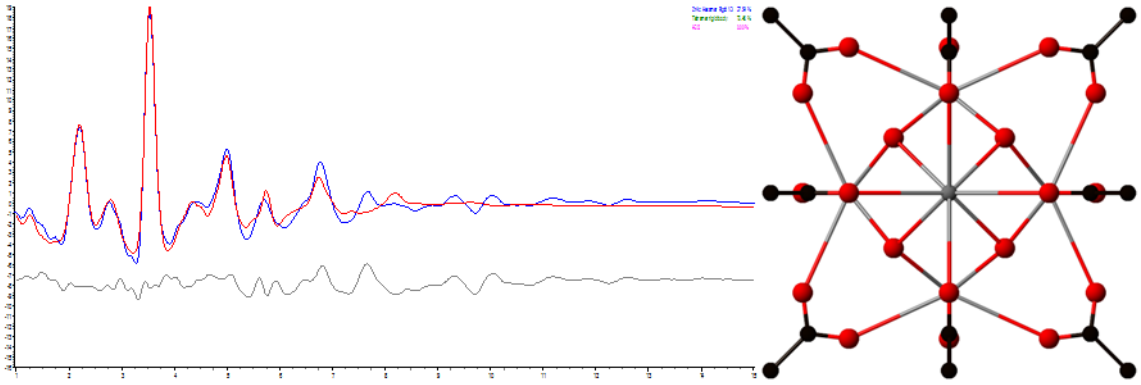

Figure 182: Observed and Calculated PDF from the fixed core refinement of ZAA16 from the 15-month data collection and the resultant model.

Table 125: The atomic coordinates of the model resulting from the fixed core refinement of ZAA16 from the 15-month data collection.

Atom Label	Atom Type	Multiplicity	Fractional X Coordinate	Fractional Y Coordinate	Fractional Z Coordinate	Fractional Occupancy
C1	C	1	0.5923038	0.5000000	0.5853875	1
C2	C	1	0.5000000	0.4076962	0.5853875	1
C3	C	1	0.4076962	0.5000000	0.5853875	1
C4	C	1	0.5000000	0.5923038	0.5853875	1
C5	C	1	0.5923038	0.5000000	0.4146125	1
C6	C	1	0.5000000	0.4076962	0.4146125	1
C7	C	1	0.4076962	0.5000000	0.4146125	1
C8	C	1	0.5000000	0.5923038	0.4146125	1
C9	C	1	0.5923038	0.4076962	0.5000000	1
C10	C	1	0.4076962	0.4076962	0.5000000	1
C11	C	1	0.4076962	0.5923038	0.5000000	1
C12	C	1	0.5923038	0.5923038	0.5000000	1
C13	C	1	0.6166887	0.5000000	0.6079452	1
C14	C	1	0.5000000	0.3833113	0.6079452	1
C15	C	1	0.3833113	0.5000000	0.6079452	1
C16	C	1	0.5000000	0.6166887	0.6079452	1
C17	C	1	0.6166887	0.5000000	0.3920548	1
C18	C	1	0.5000000	0.3833113	0.3920548	1
C19	C	1	0.3833113	0.5000000	0.3920548	1
C20	C	1	0.5000000	0.6166887	0.3920548	1
C21	C	1	0.6166887	0.3833113	0.5000000	1
C22	C	1	0.3833113	0.3833113	0.5000000	1
C23	C	1	0.3833113	0.6166887	0.5000000	1
C24	C	1	0.6166887	0.6166887	0.5000000	1
O1	O	1	0.5364087	0.5360534	0.4663194	1
O2	O	1	0.5364087	0.4639466	0.5336806	1
O3	O	1	0.4635913	0.5360534	0.4663194	1
O4	O	1	0.4635913	0.4639466	0.5336806	1
O5	O	1	0.4635913	0.4639466	0.4663194	1
O6	O	1	0.4635913	0.5360534	0.5336806	1

O7	O	1	0.5364087	0.4639466	0.4663194	1
O8	O	1	0.5364087	0.5360534	0.5336806	1
O9	O	1	0.5957144	0.5000000	0.5604945	1
O10	O	1	0.5957144	0.4346055	0.5000000	1
O11	O	1	0.5957144	0.5000000	0.4395055	1
O12	O	1	0.5957144	0.5653945	0.5000000	1
O13	O	1	0.5000000	0.5957144	0.5604945	1
O14	O	1	0.5653945	0.5957144	0.5000000	1
O15	O	1	0.5000000	0.5957144	0.4395055	1
O16	O	1	0.4346055	0.5957144	0.5000000	1
O17	O	1	0.4042856	0.5000000	0.5604945	1
O18	O	1	0.4042856	0.5653945	0.5000000	1
O19	O	1	0.4042856	0.5000000	0.4395055	1
O20	O	1	0.4042856	0.4346055	0.5000000	1
O21	O	1	0.5000000	0.4042856	0.5604945	1
O22	O	1	0.4346055	0.4042856	0.5000000	1
O23	O	1	0.5000000	0.4042856	0.4395055	1
O24	O	1	0.5653945	0.4042856	0.5000000	1
O25	O	1	0.5653945	0.5000000	0.5885425	1
O26	O	1	0.5000000	0.5653945	0.5885425	1
O27	O	1	0.4346055	0.5000000	0.5885425	1
O28	O	1	0.5000000	0.4346055	0.5885425	1
O29	O	1	0.5653945	0.5000000	0.4114575	1
O30	O	1	0.5000000	0.4346055	0.4114575	1
O31	O	1	0.4346055	0.5000000	0.4114575	1
O32	O	1	0.5000000	0.5653945	0.4114575	1
Zr1	Zr	1	0.5656077	0.5000000	0.5000000	1
Zr2	Zr	1	0.5000000	0.5656077	0.5000000	1
Zr3	Zr	1	0.4343923	0.5000000	0.5000000	1
Zr4	Zr	1	0.5000000	0.4343923	0.5000000	1
Zr5	Zr	1	0.5000000	0.5000000	0.5606917	1
Zr6	Zr	1	0.5000000	0.5000000	0.4393083	1

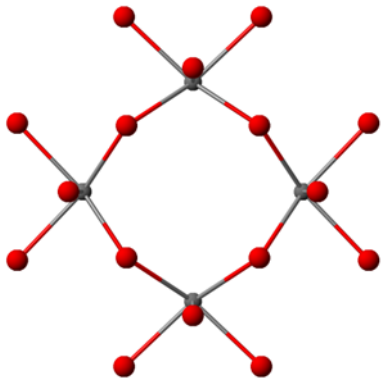

Figure 183: The tetrameric structure resulting from the fixed core refinement of ZAA16 from the 15-month data collection.

Table 126: The atomic coordinates of the tetrameric phase of the fixed core refinement of ZAA16 from the 15-month data collection.

Atom Label	Atom Type	Multiplicity	Fractional X Coordinate	Fractional Y Coordinate	Fractional Z Coordinate	Fractional Occupancy
O1	O	1	0.5148415	0.4851585	0.470911	1
O2	O	1	0.4851585	0.4851585	0.529089	1
O3	O	1	0.5148415	0.5148415	0.529089	1
O4	O	1	0.4851585	0.5148415	0.470911	1
O5	O	1	0.5000000	0.5278238	0.5450111	1
O6	O	1	0.5000000	0.4721762	0.5450111	1
O7	O	1	0.4721762	0.5000000	0.4549889	1
O8	O	1	0.5278238	0.5000000	0.4549889	1
O9	O	1	0.5153671	0.4607305	0.5000000	1
O10	O	1	0.4607305	0.4846329	0.5000000	1
O11	O	1	0.5392695	0.5153671	0.5000000	1
O12	O	1	0.4846329	0.5392695	0.5000000	1
O13	O	1	0.4607305	0.5153671	0.5000000	1
O14	O	1	0.5392695	0.4846329	0.5000000	1
O15	O	1	0.4846329	0.4607305	0.5000000	1
O16	O	1	0.5153671	0.5392695	0.5000000	1
O17	O	1	0.5148415	0.4851585	0.529089	1
O18	O	1	0.4851585	0.4851585	0.470911	1
O19	O	1	0.5148415	0.5148415	0.470911	1
O20	O	1	0.4851585	0.5148415	0.529089	1
O21	O	1	0.5000000	0.5278238	0.4549889	1
O22	O	1	0.5000000	0.4721762	0.4549889	1
O23	O	1	0.4721762	0.5000000	0.5450111	1
O24	O	1	0.5278238	0.5000000	0.5450111	1
Zr1	Zr	1	0.5000000	0.4753847	0.5000000	1
Zr2	Zr	1	0.4753847	0.5000000	0.5000000	1
Zr3	Zr	1	0.5246153	0.5000000	0.5000000	1
Zr4	Zr	1	0.5000000	0.5246153	0.5000000	1

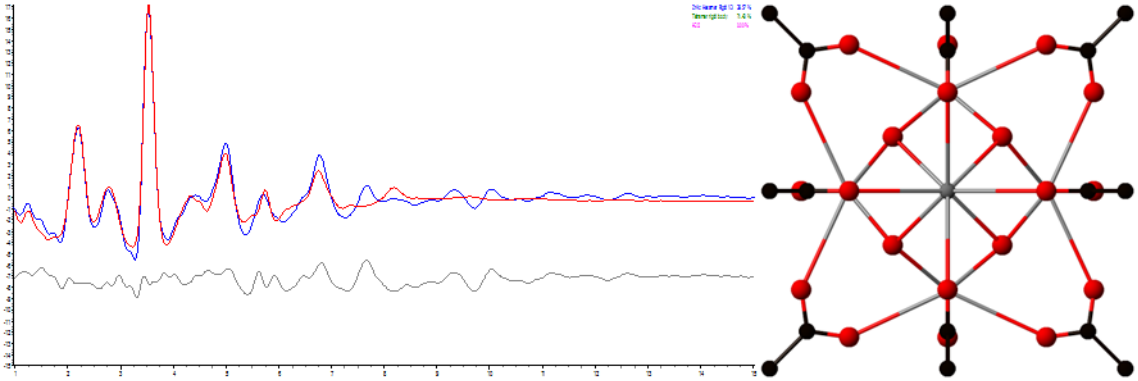

Figure 184: Observed and Calculated PDF from the fixed core refinement of ZAA20 from the 15-month data collection and the resultant model.

Table 127: The atomic coordinates of the model resulting from the fixed core refinement of ZAA20 from the 15-month data collection.

Atom Label	Atom Type	Multiplicity	Fractional X Coordinate	Fractional Y Coordinate	Fractional Z Coordinate	Fractional Occupancy
C1	C	1	0.5920278	0.5000000	0.5851321	1
C2	C	1	0.5000000	0.4079722	0.5851321	1
C3	C	1	0.4079722	0.5000000	0.5851321	1
C4	C	1	0.5000000	0.5920278	0.5851321	1
C5	C	1	0.5920278	0.5000000	0.4148679	1
C6	C	1	0.5000000	0.4079722	0.4148679	1
C7	C	1	0.4079722	0.5000000	0.4148679	1
C8	C	1	0.5000000	0.5920278	0.4148679	1
C9	C	1	0.5920278	0.4079722	0.5000000	1
C10	C	1	0.4079722	0.4079722	0.5000000	1
C11	C	1	0.4079722	0.5920278	0.5000000	1
C12	C	1	0.5920278	0.5920278	0.5000000	1
C13	C	1	0.6166279	0.5000000	0.6078889	1
C14	C	1	0.5000000	0.3833721	0.6078889	1
C15	C	1	0.3833721	0.5000000	0.6078889	1
C16	C	1	0.5000000	0.6166279	0.6078889	1
C17	C	1	0.6166279	0.5000000	0.3921111	1
C18	C	1	0.5000000	0.3833721	0.3921111	1
C19	C	1	0.3833721	0.5000000	0.3921111	1
C20	C	1	0.5000000	0.6166279	0.3921111	1
C21	C	1	0.6166279	0.3833721	0.5000000	1
C22	C	1	0.3833721	0.3833721	0.5000000	1
C23	C	1	0.3833721	0.6166279	0.5000000	1
C24	C	1	0.6166279	0.6166279	0.5000000	1
O1	O	1	0.5359135	0.5355631	0.4667775	1
O2	O	1	0.5359135	0.4644369	0.5332225	1
O3	O	1	0.4640865	0.5355631	0.4667775	1
O4	O	1	0.4640865	0.4644369	0.5332225	1
O5	O	1	0.4640865	0.4644369	0.4667775	1
O6	O	1	0.4640865	0.5355631	0.5332225	1

O7	O	1	0.5359135	0.4644369	0.4667775	1
O8	O	1	0.5359135	0.5355631	0.5332225	1
O9	O	1	0.5959666	0.5000000	0.5598384	1
O10	O	1	0.5959666	0.4353147	0.5000000	1
O11	O	1	0.5959666	0.5000000	0.4401616	1
O12	O	1	0.5959666	0.5646853	0.5000000	1
O13	O	1	0.5000000	0.5959666	0.5598384	1
O14	O	1	0.5646853	0.5959666	0.5000000	1
O15	O	1	0.5000000	0.5959666	0.4401616	1
O16	O	1	0.4353147	0.5959666	0.5000000	1
O17	O	1	0.4040334	0.5000000	0.5598384	1
O18	O	1	0.4040334	0.5646853	0.5000000	1
O19	O	1	0.4040334	0.5000000	0.4401616	1
O20	O	1	0.4040334	0.4353147	0.5000000	1
O21	O	1	0.5000000	0.4040334	0.5598384	1
O22	O	1	0.4353147	0.4040334	0.5000000	1
O23	O	1	0.5000000	0.4040334	0.4401616	1
O24	O	1	0.5646853	0.4040334	0.5000000	1
O25	O	1	0.5646853	0.5000000	0.5887758	1
O26	O	1	0.5000000	0.5646853	0.5887758	1
O27	O	1	0.4353147	0.5000000	0.5887758	1
O28	O	1	0.5000000	0.4353147	0.5887758	1
O29	O	1	0.5646853	0.5000000	0.4112242	1
O30	O	1	0.5000000	0.4353147	0.4112242	1
O31	O	1	0.4353147	0.5000000	0.4112242	1
O32	O	1	0.5000000	0.5646853	0.4112242	1
Zr1	Zr	1	0.5656438	0.5000000	0.5000000	1
Zr2	Zr	1	0.5000000	0.5656438	0.5000000	1
Zr3	Zr	1	0.4343562	0.5000000	0.5000000	1
Zr4	Zr	1	0.5000000	0.4343562	0.5000000	1
Zr5	Zr	1	0.5000000	0.5000000	0.5607251	1
Zr6	Zr	1	0.5000000	0.5000000	0.4392749	1

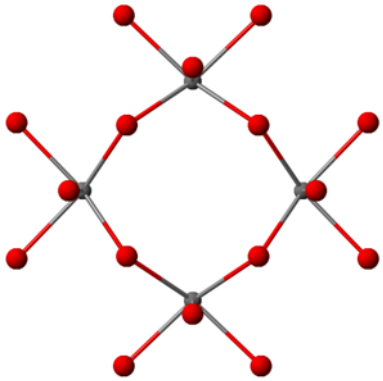

Figure 185: The tetrameric structure resulting from the fixed core refinement of ZAA20 from the 15-month data collection.

Table 128: The atomic coordinates of the tetrameric phase of the fixed core refinement of ZAA20 from the 15-month data collection.

Atom Label	Atom Type	Multiplicity	Fractional X Coordinate	Fractional Y Coordinate	Fractional Z Coordinate	Fractional Occupancy
O1	O	1	0.5147561	0.4852439	0.4706079	1
O2	O	1	0.4852439	0.4852439	0.5293921	1
O3	O	1	0.5147561	0.5147561	0.5293921	1
O4	O	1	0.4852439	0.5147561	0.4706079	1
O5	O	1	0.5000000	0.5276845	0.5453139	1
O6	O	1	0.5000000	0.4723155	0.5453139	1
O7	O	1	0.4723155	0.5000000	0.4546861	1
O8	O	1	0.5276845	0.5000000	0.4546861	1
O9	O	1	0.5153164	0.4606509	0.5000000	1
O10	O	1	0.4606509	0.4846836	0.5000000	1
O11	O	1	0.5393491	0.5153164	0.5000000	1
O12	O	1	0.4846836	0.5393491	0.5000000	1
O13	O	1	0.4606509	0.5153164	0.5000000	1
O14	O	1	0.5393491	0.4846836	0.5000000	1
O15	O	1	0.4846836	0.4606509	0.5000000	1
O16	O	1	0.5153164	0.5393491	0.5000000	1
O17	O	1	0.5147561	0.4852439	0.5293921	1
O18	O	1	0.4852439	0.4852439	0.4706079	1
O19	O	1	0.5147561	0.5147561	0.4706079	1
O20	O	1	0.4852439	0.5147561	0.5293921	1
O21	O	1	0.5000000	0.5276845	0.4546861	1
O22	O	1	0.5000000	0.4723155	0.4546861	1
O23	O	1	0.4723155	0.5000000	0.5453139	1
O24	O	1	0.5276845	0.5000000	0.5453139	1
Zr1	Zr	1	0.5000000	0.4753633	0.5000000	1
Zr2	Zr	1	0.4753633	0.5000000	0.5000000	1
Zr3	Zr	1	0.5246367	0.5000000	0.5000000	1
Zr4	Zr	1	0.5000000	0.5246367	0.5000000	1

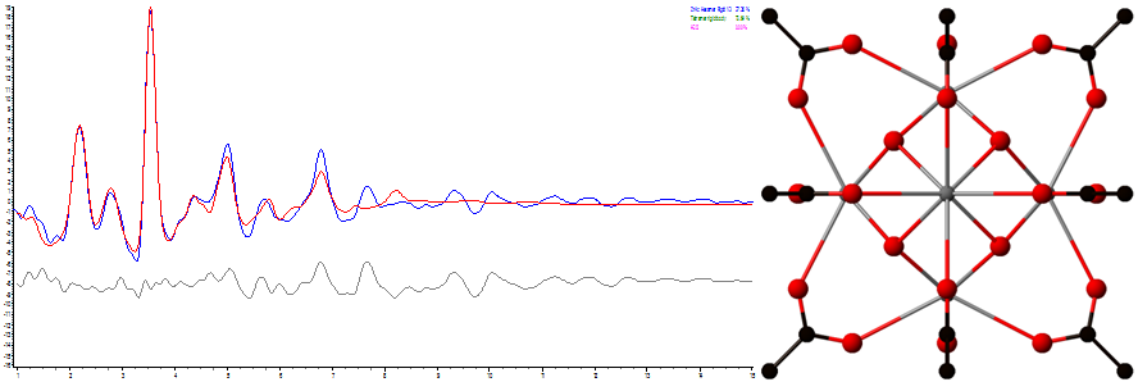

Figure 186: Observed and Calculated PDF from the fixed core refinement of ZAA24 from the 15-month data collection and the resultant model.

Table 129: The atomic coordinates of the model resulting from the fixed core refinement of ZAA24 from the 15-month data collection.

Atom Label	Atom Type	Multiplicity	Fractional X Coordinate	Fractional Y Coordinate	Fractional Z Coordinate	Fractional Occupancy
C1	C	1	0.5922902	0.5000000	0.5853749	1
C2	C	1	0.5000000	0.4077098	0.5853749	1
C3	C	1	0.4077098	0.5000000	0.5853749	1
C4	C	1	0.5000000	0.5922902	0.5853749	1
C5	C	1	0.5922902	0.5000000	0.4146251	1
C6	C	1	0.5000000	0.4077098	0.4146251	1
C7	C	1	0.4077098	0.5000000	0.4146251	1
C8	C	1	0.5000000	0.5922902	0.4146251	1
C9	C	1	0.5922902	0.4077098	0.5000000	1
C10	C	1	0.4077098	0.4077098	0.5000000	1
C11	C	1	0.4077098	0.5922902	0.5000000	1
C12	C	1	0.5922902	0.5922902	0.5000000	1
C13	C	1	0.6167138	0.5000000	0.6079684	1
C14	C	1	0.5000000	0.3832862	0.6079684	1
C15	C	1	0.3832862	0.5000000	0.6079684	1
C16	C	1	0.5000000	0.6167138	0.6079684	1
C17	C	1	0.6167138	0.5000000	0.3920316	1
C18	C	1	0.5000000	0.3832862	0.3920316	1
C19	C	1	0.3832862	0.5000000	0.3920316	1
C20	C	1	0.5000000	0.6167138	0.3920316	1
C21	C	1	0.6167138	0.3832862	0.5000000	1
C22	C	1	0.3832862	0.3832862	0.5000000	1
C23	C	1	0.3832862	0.6167138	0.5000000	1
C24	C	1	0.6167138	0.6167138	0.5000000	1
O1	O	1	0.5349976	0.5346561	0.4676248	1
O2	O	1	0.5349976	0.4653439	0.5323752	1
O3	O	1	0.4650024	0.5346561	0.4676248	1
O4	O	1	0.4650024	0.4653439	0.5323752	1
O5	O	1	0.4650024	0.4653439	0.4676248	1
O6	O	1	0.4650024	0.5346561	0.5323752	1

O7	O	1	0.5349976	0.4653439	0.4676248	1
O8	O	1	0.5349976	0.5346561	0.5323752	1
O9	O	1	0.5980484	0.5000000	0.5577867	1
O10	O	1	0.5980484	0.4375326	0.5000000	1
O11	O	1	0.5980484	0.5000000	0.4422133	1
O12	O	1	0.5980484	0.5624674	0.5000000	1
O13	O	1	0.5000000	0.5980484	0.5577867	1
O14	O	1	0.5624674	0.5980484	0.5000000	1
O15	O	1	0.5000000	0.5980484	0.4422133	1
O16	O	1	0.4375326	0.5980484	0.5000000	1
O17	O	1	0.4019516	0.5000000	0.5577867	1
O18	O	1	0.4019516	0.5624674	0.5000000	1
O19	O	1	0.4019516	0.5000000	0.4422133	1
O20	O	1	0.4019516	0.4375326	0.5000000	1
O21	O	1	0.5000000	0.4019516	0.5577867	1
O22	O	1	0.4375326	0.4019516	0.5000000	1
O23	O	1	0.5000000	0.4019516	0.4422133	1
O24	O	1	0.5624674	0.4019516	0.5000000	1
O25	O	1	0.5624674	0.5000000	0.5907016	1
O26	O	1	0.5000000	0.5624674	0.5907016	1
O27	O	1	0.4375326	0.5000000	0.5907016	1
O28	O	1	0.5000000	0.4375326	0.5907016	1
O29	O	1	0.5624674	0.5000000	0.4092984	1
O30	O	1	0.5000000	0.4375326	0.4092984	1
O31	O	1	0.4375326	0.5000000	0.4092984	1
O32	O	1	0.5000000	0.5624674	0.4092984	1
Zr1	Zr	1	0.5657191	0.5000000	0.5000000	1
Zr2	Zr	1	0.5000000	0.5657191	0.5000000	1
Zr3	Zr	1	0.4342809	0.5000000	0.5000000	1
Zr4	Zr	1	0.5000000	0.4342809	0.5000000	1
Zr5	Zr	1	0.5000000	0.5000000	0.5607948	1
Zr6	Zr	1	0.5000000	0.5000000	0.4392052	1

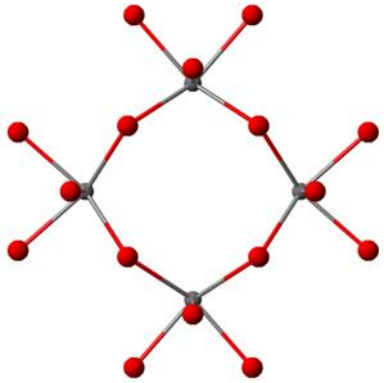

Figure 187: The tetrameric structure resulting from the fixed core refinement of ZAA24 from the 15-month data collection.

Table 130: The atomic coordinates of the tetrameric phase of the fixed core refinement of ZAA24 from the 15-month data collection.

Atom Label	Atom Type	Multiplicity	Fractional X Coordinate	Fractional Y Coordinate	Fractional Z Coordinate	Fractional Occupancy
O1	O	1	0.5150429	0.4849571	0.4709543	1
O2	O	1	0.4849571	0.4849571	0.5290457	1
O3	O	1	0.5150429	0.5150429	0.5290457	1
O4	O	1	0.4849571	0.5150429	0.4709543	1
O5	O	1	0.5000000	0.5281079	0.5461522	1
O6	O	1	0.5000000	0.4718921	0.5461522	1
O7	O	1	0.4718921	0.5000000	0.4538478	1
O8	O	1	0.5281079	0.5000000	0.4538478	1
O9	O	1	0.5135673	0.4597945	0.5000000	1
O10	O	1	0.4597945	0.4864327	0.5000000	1
O11	O	1	0.5402055	0.5135673	0.5000000	1
O12	O	1	0.4864327	0.5402055	0.5000000	1
O13	O	1	0.4597945	0.5135673	0.5000000	1
O14	O	1	0.5402055	0.4864327	0.5000000	1
O15	O	1	0.4864327	0.4597945	0.5000000	1
O16	O	1	0.5135673	0.5402055	0.5000000	1
O17	O	1	0.5150429	0.4849571	0.5290457	1
O18	O	1	0.4849571	0.4849571	0.4709543	1
O19	O	1	0.5150429	0.5150429	0.4709543	1
O20	O	1	0.4849571	0.5150429	0.5290457	1
O21	O	1	0.5000000	0.5281079	0.4538478	1
O22	O	1	0.5000000	0.4718921	0.4538478	1
O23	O	1	0.4718921	0.5000000	0.5461522	1
O24	O	1	0.5281079	0.5000000	0.5461522	1
Zr1	Zr	1	0.5000000	0.4752909	0.5000000	1
Zr2	Zr	1	0.4752909	0.5000000	0.5000000	1
Zr3	Zr	1	0.5247091	0.5000000	0.5000000	1
Zr4	Zr	1	0.5000000	0.5247091	0.5000000	1

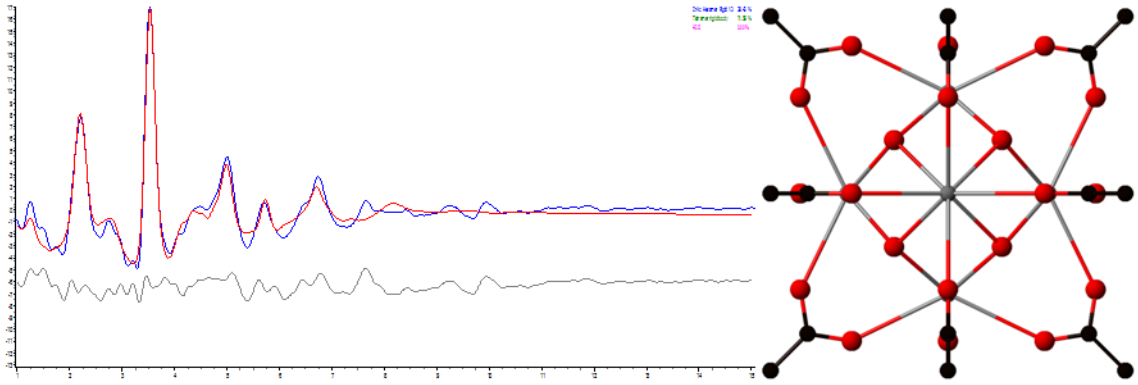

Figure 188: Observed and Calculated PDF from the fixed core refinement of ZAA25 from the 15-month data collection and the resultant model.

Table 131: The atomic coordinates of the model resulting from the fixed core refinement of ZAA25 from the 15-month data collection.

Atom Label	Atom Type	Multiplicity	Fractional X Coordinate	Fractional Y Coordinate	Fractional Z Coordinate	Fractional Occupancy
C1	C	1	0.5919502	0.5000000	0.5850603	1
C2	C	1	0.5000000	0.4080498	0.5850603	1
C3	C	1	0.4080498	0.5000000	0.5850603	1
C4	C	1	0.5000000	0.5919502	0.5850603	1
C5	C	1	0.5919502	0.5000000	0.4149397	1
C6	C	1	0.5000000	0.4080498	0.4149397	1
C7	C	1	0.4080498	0.5000000	0.4149397	1
C8	C	1	0.5000000	0.5919502	0.4149397	1
C9	C	1	0.5919502	0.4080498	0.5000000	1
C10	C	1	0.4080498	0.4080498	0.5000000	1
C11	C	1	0.4080498	0.5919502	0.5000000	1
C12	C	1	0.5919502	0.5919502	0.5000000	1
C13	C	1	0.6158524	0.5000000	0.6071716	1
C14	C	1	0.5000000	0.3841476	0.6071716	1
C15	C	1	0.3841476	0.5000000	0.6071716	1
C16	C	1	0.5000000	0.6158524	0.6071716	1
C17	C	1	0.6158524	0.5000000	0.3928284	1
C18	C	1	0.5000000	0.3841476	0.3928284	1
C19	C	1	0.3841476	0.5000000	0.3928284	1
C20	C	1	0.5000000	0.6158524	0.3928284	1
C21	C	1	0.6158524	0.3841476	0.5000000	1
C22	C	1	0.3841476	0.3841476	0.5000000	1
C23	C	1	0.3841476	0.6158524	0.5000000	1
C24	C	1	0.6158524	0.6158524	0.5000000	1
O1	O	1	0.5352812	0.5349369	0.4673625	1
O2	O	1	0.5352812	0.4650631	0.5326375	1
O3	O	1	0.4647188	0.5349369	0.4673625	1
O4	O	1	0.4647188	0.4650631	0.5326375	1
O5	O	1	0.4647188	0.4650631	0.4673625	1
O6	O	1	0.4647188	0.5349369	0.5326375	1

O7	O	1	0.5352812	0.4650631	0.4673625	1
O8	O	1	0.5352812	0.5349369	0.5326375	1
O9	O	1	0.5964791	0.5000000	0.5583188	1
O10	O	1	0.5964791	0.4369574	0.5000000	1
O11	O	1	0.5964791	0.5000000	0.4416812	1
O12	O	1	0.5964791	0.5630426	0.5000000	1
O13	O	1	0.5000000	0.5964791	0.5583188	1
O14	O	1	0.5630426	0.5964791	0.5000000	1
O15	O	1	0.5000000	0.5964791	0.4416812	1
O16	O	1	0.4369574	0.5964791	0.5000000	1
O17	O	1	0.4035209	0.5000000	0.5583188	1
O18	O	1	0.4035209	0.5630426	0.5000000	1
O19	O	1	0.4035209	0.5000000	0.4416812	1
O20	O	1	0.4035209	0.4369574	0.5000000	1
O21	O	1	0.5000000	0.4035209	0.5583188	1
O22	O	1	0.4369574	0.4035209	0.5000000	1
O23	O	1	0.5000000	0.4035209	0.4416812	1
O24	O	1	0.5630426	0.4035209	0.5000000	1
O25	O	1	0.5630426	0.5000000	0.5892499	1
O26	O	1	0.5000000	0.5630426	0.5892499	1
O27	O	1	0.4369574	0.5000000	0.5892499	1
O28	O	1	0.5000000	0.4369574	0.5892499	1
O29	O	1	0.5630426	0.5000000	0.4107501	1
O30	O	1	0.5000000	0.4369574	0.4107501	1
O31	O	1	0.4369574	0.5000000	0.4107501	1
O32	O	1	0.5000000	0.5630426	0.4107501	1
Zr1	Zr	1	0.5657675	0.5000000	0.5000000	1
Zr2	Zr	1	0.5000000	0.5657675	0.5000000	1
Zr3	Zr	1	0.4342325	0.5000000	0.5000000	1
Zr4	Zr	1	0.5000000	0.4342325	0.5000000	1
Zr5	Zr	1	0.5000000	0.5000000	0.5608395	1
Zr6	Zr	1	0.5000000	0.5000000	0.4391605	1

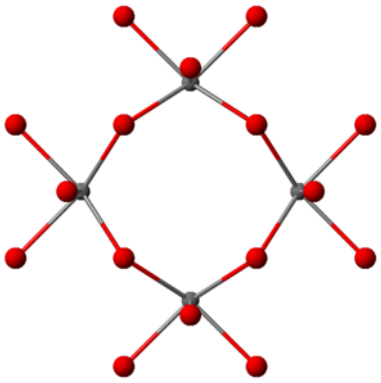

Figure 189: The tetrameric structure resulting from the fixed core refinement of ZAA25 from the 15-month data collection.

Table 132: The atomic coordinates of the tetrameric phase of the fixed core refinement of ZAA25 from the 15-month data collection.

Atom Label	Atom Type	Multiplicity	Fractional X Coordinate	Fractional Y Coordinate	Fractional Z Coordinate	Fractional Occupancy
O1	O	1	0.5149313	0.4850687	0.470665	1
O2	O	1	0.4850687	0.4850687	0.529335	1
O3	O	1	0.5149313	0.5149313	0.529335	1
O4	O	1	0.4850687	0.5149313	0.470665	1
O5	O	1	0.5000000	0.5277351	0.546288	1
O6	O	1	0.5000000	0.4722649	0.546288	1
O7	O	1	0.4722649	0.5000000	0.453712	1
O8	O	1	0.5277351	0.5000000	0.453712	1
O9	O	1	0.5149401	0.4607266	0.5000000	1
O10	O	1	0.4607266	0.4850599	0.5000000	1
O11	O	1	0.5392734	0.5149401	0.5000000	1
O12	O	1	0.4850599	0.5392734	0.5000000	1
O13	O	1	0.4607266	0.5149401	0.5000000	1
O14	O	1	0.5392734	0.4850599	0.5000000	1
O15	O	1	0.4850599	0.4607266	0.5000000	1
O16	O	1	0.5149401	0.5392734	0.5000000	1
O17	O	1	0.5149313	0.4850687	0.529335	1
O18	O	1	0.4850687	0.4850687	0.470665	1
O19	O	1	0.5149313	0.5149313	0.470665	1
O20	O	1	0.4850687	0.5149313	0.529335	1
O21	O	1	0.5000000	0.5277351	0.453712	1
O22	O	1	0.5000000	0.4722649	0.453712	1
O23	O	1	0.4722649	0.5000000	0.546288	1
O24	O	1	0.5277351	0.5000000	0.546288	1
Zr1	Zr	1	0.5000000	0.4755501	0.5000000	1
Zr2	Zr	1	0.4755501	0.5000000	0.5000000	1
Zr3	Zr	1	0.5244499	0.5000000	0.5000000	1
Zr4	Zr	1	0.5000000	0.5244499	0.5000000	1

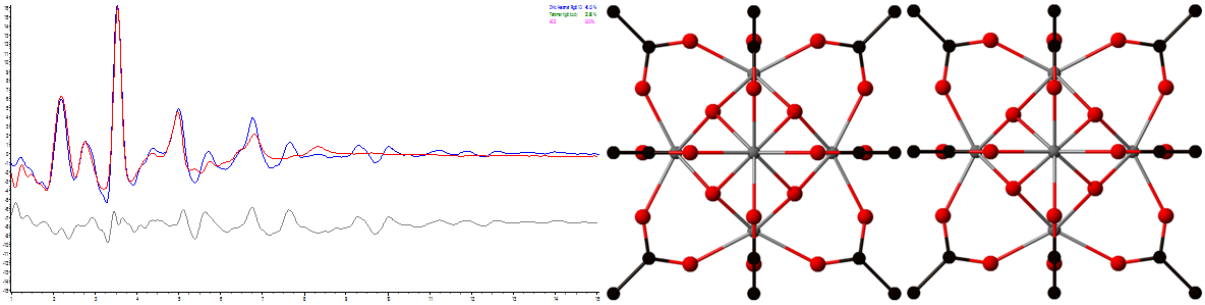

Figure 190: Observed and Calculated PDF from the chandelier core refinement of ZAA1 from the 15-month data collection and the resultant model viewed from the axial (left) and equatorial (right) positions.

Table 133: The atomic coordinates of the model resulting from the chandelier core refinement of ZAA1 from the 15-month data collection.

Atom Label	Atom Type	Multiplicity	Fractional X Coordinate	Fractional Y Coordinate	Fractional Z Coordinate	Fractional Occupancy
C1	C	1	0.5892378	0.5000000	0.5825512	1
C2	C	1	0.5000000	0.4107622	0.5825512	1
C3	C	1	0.4107622	0.5000000	0.5825512	1
C4	C	1	0.5000000	0.5892378	0.5825512	1
C5	C	1	0.5892378	0.5000000	0.4174488	1
C6	C	1	0.5000000	0.4107622	0.4174488	1
C7	C	1	0.4107622	0.5000000	0.4174488	1
C8	C	1	0.5000000	0.5892378	0.4174488	1
C9	C	1	0.5892378	0.4107622	0.5000000	1
C10	C	1	0.4107622	0.4107622	0.5000000	1
C11	C	1	0.4107622	0.5892378	0.5000000	1
C12	C	1	0.5892378	0.5892378	0.5000000	1
C13	C	1	0.6191974	0.5000000	0.6102659	1
C14	C	1	0.5000000	0.3808026	0.6102659	1
C15	C	1	0.3808026	0.5000000	0.6102659	1
C16	C	1	0.5000000	0.6191974	0.6102659	1
C17	C	1	0.6191974	0.5000000	0.3897341	1
C18	C	1	0.5000000	0.3808026	0.3897341	1
C19	C	1	0.3808026	0.5000000	0.3897341	1
C20	C	1	0.5000000	0.6191974	0.3897341	1
C21	C	1	0.6191974	0.3808026	0.5000000	1
C22	C	1	0.3808026	0.3808026	0.5000000	1
C23	C	1	0.3808026	0.6191974	0.5000000	1
C24	C	1	0.6191974	0.6191974	0.5000000	1
O1	O	1	0.5346573	0.4653427	0.471116	1
O2	O	1	0.5346573	0.4653427	0.528884	1
O3	O	1	0.4653427	0.4653427	0.471116	1
O4	O	1	0.4653427	0.4653427	0.528884	1
O5	O	1	0.4653427	0.5346573	0.471116	1
O6	O	1	0.4653427	0.5346573	0.528884	1
O7	O	1	0.5346573	0.5346573	0.471116	1
O8	O	1	0.5346573	0.5346573	0.528884	1

O9	O	1	0.5943533	0.5000000	0.550106	1
O10	O	1	0.5943533	0.4458355	0.5000000	1
O11	O	1	0.5943533	0.5000000	0.449894	1
O12	O	1	0.5943533	0.5541645	0.5000000	1
O13	O	1	0.5000000	0.5943533	0.550106	1
O14	O	1	0.5541645	0.5943533	0.5000000	1
O15	O	1	0.5000000	0.5943533	0.449894	1
O16	O	1	0.4458355	0.5943533	0.5000000	1
O17	O	1	0.4056467	0.5000000	0.550106	1
O18	O	1	0.4056467	0.5541645	0.5000000	1
O19	O	1	0.4056467	0.5000000	0.449894	1
O20	O	1	0.4056467	0.4458355	0.5000000	1
O21	O	1	0.5000000	0.4056467	0.550106	1
O22	O	1	0.4458355	0.4056467	0.5000000	1
O23	O	1	0.5000000	0.4056467	0.449894	1
O24	O	1	0.5541645	0.4056467	0.5000000	1
O25	O	1	0.5541645	0.5000000	0.5872834	1
O26	O	1	0.5000000	0.5541645	0.5872834	1
O27	O	1	0.4458355	0.5000000	0.5872834	1
O28	O	1	0.5000000	0.4458355	0.5872834	1
O29	O	1	0.5541645	0.5000000	0.4127166	1
O30	O	1	0.5000000	0.4458355	0.4127166	1
O31	O	1	0.4458355	0.5000000	0.4127166	1
O32	O	1	0.5000000	0.5541645	0.4127166	1
Zr1	Zr	1	0.5662718	0.5000000	0.5000000	1
Zr2	Zr	1	0.5000000	0.5662718	0.5000000	1
Zr3	Zr	1	0.4337282	0.5000000	0.5000000	1
Zr4	Zr	1	0.5000000	0.4337282	0.5000000	1
Zr5	Zr	1	0.5000000	0.5000000	0.561306	1
Zr6	Zr	1	0.5000000	0.5000000	0.438694	1

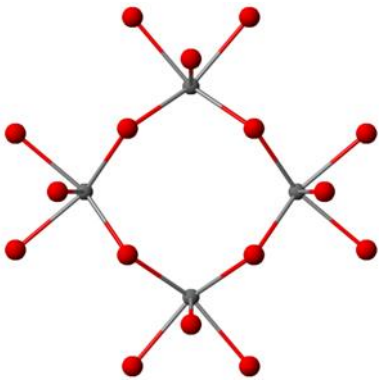

Figure 191: The tetrameric structure resulting from the chandelier core refinement of ZAA1 from the 15-month data collection.

Table 134: The atomic coordinates of the tetrameric phase of the chandelier core refinement of ZAA1 from the15-month data collection.

Atom Label	Atom Type	Multiplicity	Fractional X Coordinate	Fractional Y Coordinate	Fractional Z Coordinate	Fractional Occupancy
O1	O	1	0.5146281	0.4853719	0.4779024	1
O2	O	1	0.4853719	0.4853719	0.5220976	1
O3	O	1	0.5146281	0.5146281	0.5220976	1
O4	O	1	0.4853719	0.5146281	0.4779024	1
O5	O	1	0.5000000	0.5308467	0.5454631	1
O6	O	1	0.5000000	0.4691533	0.5454631	1
O7	O	1	0.4691533	0.5000000	0.4545369	1
O8	O	1	0.5308467	0.5000000	0.4545369	1
O9	O	1	0.5135232	0.4594568	0.5000000	1
O10	O	1	0.4594568	0.4864768	0.5000000	1
O11	O	1	0.5405432	0.5135232	0.5000000	1
O12	O	1	0.4864768	0.5405432	0.5000000	1
O13	O	1	0.4594568	0.5135232	0.5000000	1
O14	O	1	0.5405432	0.4864768	0.5000000	1
O15	O	1	0.4864768	0.4594568	0.5000000	1
O16	O	1	0.5135232	0.5405432	0.5000000	1
O17	O	1	0.5146281	0.4853719	0.5220976	1
O18	O	1	0.4853719	0.4853719	0.4779024	1
O19	O	1	0.5146281	0.5146281	0.4779024	1
O20	O	1	0.4853719	0.5146281	0.5220976	1
O21	O	1	0.5000000	0.5308467	0.4545369	1
O22	O	1	0.5000000	0.4691533	0.4545369	1
O23	O	1	0.4691533	0.5000000	0.5454631	1
O24	O	1	0.5308467	0.5000000	0.5454631	1
Zr1	Zr	1	0.5000000	0.4754633	0.5000000	1
Zr2	Zr	1	0.4754633	0.5000000	0.5000000	1
Zr3	Zr	1	0.5245367	0.5000000	0.5000000	1
Zr4	Zr	1	0.5000000	0.5245367	0.5000000	1

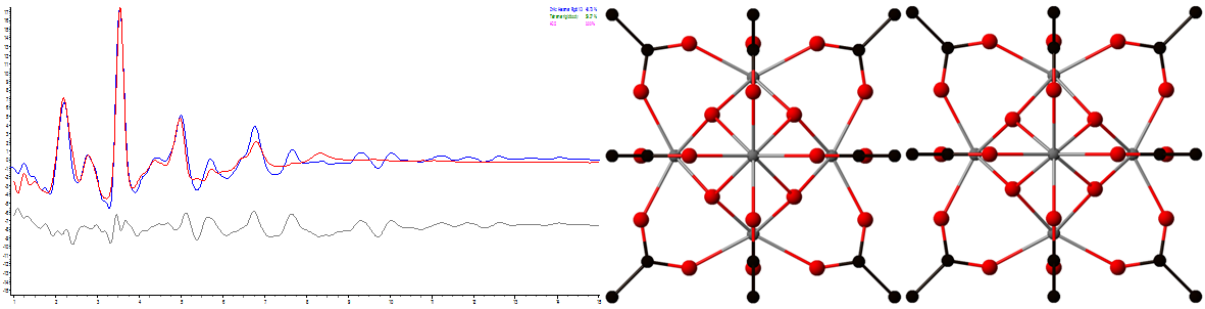

Figure 192: Observed and Calculated PDF from the chandelier core refinement of ZAA4 from the 15-month data collection and the resultant model viewed from the axial (left) and equatorial (right) positions.

Table 135: The atomic coordinates of the model resulting from the chandelier core refinement of ZAA4 from the 15-month data collection.

Atom Label	Atom Type	Multiplicity	Fractional X Coordinate	Fractional Y Coordinate	Fractional Z Coordinate	Fractional Occupancy
C1	C	1	0.5892932	0.5000000	0.5826024	1
C2	C	1	0.5000000	0.4107068	0.5826024	1
C3	C	1	0.4107068	0.5000000	0.5826024	1
C4	C	1	0.5000000	0.5892932	0.5826024	1
C5	C	1	0.5892932	0.5000000	0.4173976	1
C6	C	1	0.5000000	0.4107068	0.4173976	1
C7	C	1	0.4107068	0.5000000	0.4173976	1
C8	C	1	0.5000000	0.5892932	0.4173976	1
C9	C	1	0.5892932	0.4107068	0.5000000	1
C10	C	1	0.4107068	0.4107068	0.5000000	1
C11	C	1	0.4107068	0.5892932	0.5000000	1
C12	C	1	0.5892932	0.5892932	0.5000000	1
C13	C	1	0.6192175	0.5000000	0.6102845	1
C14	C	1	0.5000000	0.3807825	0.6102845	1
C15	C	1	0.3807825	0.5000000	0.6102845	1
C16	C	1	0.5000000	0.6192175	0.6102845	1
C17	C	1	0.6192175	0.5000000	0.3897155	1
C18	C	1	0.5000000	0.3807825	0.3897155	1
C19	C	1	0.3807825	0.5000000	0.3897155	1
C20	C	1	0.5000000	0.6192175	0.3897155	1
C21	C	1	0.6192175	0.3807825	0.5000000	1
C22	C	1	0.3807825	0.3807825	0.5000000	1
C23	C	1	0.3807825	0.6192175	0.5000000	1
C24	C	1	0.6192175	0.6192175	0.5000000	1
O1	O	1	0.5346951	0.4653049	0.4729379	1
O2	O	1	0.5346951	0.4653049	0.5270621	1
O3	O	1	0.4653049	0.4653049	0.4729379	1
O4	O	1	0.4653049	0.4653049	0.5270621	1
O5	O	1	0.4653049	0.5346951	0.4729379	1
O6	O	1	0.4653049	0.5346951	0.5270621	1
O7	O	1	0.5346951	0.5346951	0.4729379	1
O8	O	1	0.5346951	0.5346951	0.5270621	1

O9	O	1	0.5947276	0.5000000	0.5500126	1
O10	O	1	0.5947276	0.4459364	0.5000000	1
O11	O	1	0.5947276	0.5000000	0.4499874	1
O12	O	1	0.5947276	0.5540636	0.5000000	1
O13	O	1	0.5000000	0.5947276	0.5500126	1
O14	O	1	0.5540636	0.5947276	0.5000000	1
O15	O	1	0.5000000	0.5947276	0.4499874	1
O16	O	1	0.4459364	0.5947276	0.5000000	1
O17	O	1	0.4052724	0.5000000	0.5500126	1
O18	O	1	0.4052724	0.5540636	0.5000000	1
O19	O	1	0.4052724	0.5000000	0.4499874	1
O20	O	1	0.4052724	0.4459364	0.5000000	1
O21	O	1	0.5000000	0.4052724	0.5500126	1
O22	O	1	0.4459364	0.4052724	0.5000000	1
O23	O	1	0.5000000	0.4052724	0.4499874	1
O24	O	1	0.5540636	0.4052724	0.5000000	1
O25	O	1	0.5540636	0.5000000	0.5876296	1
O26	O	1	0.5000000	0.5540636	0.5876296	1
O27	O	1	0.4459364	0.5000000	0.5876296	1
O28	O	1	0.5000000	0.4459364	0.5876296	1
O29	O	1	0.5540636	0.5000000	0.4123704	1
O30	O	1	0.5000000	0.4459364	0.4123704	1
O31	O	1	0.4459364	0.5000000	0.4123704	1
O32	O	1	0.5000000	0.5540636	0.4123704	1
Zr1	Zr	1	0.5662053	0.5000000	0.5000000	1
Zr2	Zr	1	0.5000000	0.5662053	0.5000000	1
Zr3	Zr	1	0.4337947	0.5000000	0.5000000	1
Zr4	Zr	1	0.5000000	0.4337947	0.5000000	1
Zr5	Zr	1	0.5000000	0.5000000	0.5612446	1
Zr6	Zr	1	0.5000000	0.5000000	0.4387554	1

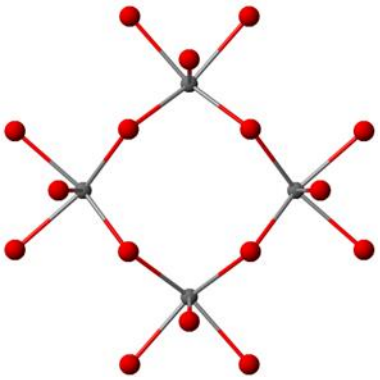

Figure 193: The tetrameric structure resulting from the chandelier core refinement of ZAA4 from the 15-month data collection.

Table 136: The atomic coordinates of the tetrameric phase of the chandelier core refinement of ZAA4 from 15-month data collection.

Atom Label	Atom Type	Multiplicity	Fractional X Coordinate	Fractional Y Coordinate	Fractional Z Coordinate	Fractional Occupancy
O1	O	1	0.5141446	0.4858554	0.4742437	1
O2	O	1	0.4858554	0.4858554	0.5257563	1
O3	O	1	0.5141446	0.5141446	0.5257563	1
O4	O	1	0.4858554	0.5141446	0.4742437	1
O5	O	1	0.5000000	0.5302796	0.5467183	1
O6	O	1	0.5000000	0.4697204	0.5467183	1
O7	O	1	0.4697204	0.5000000	0.4532817	1
O8	O	1	0.5302796	0.5000000	0.4532817	1
O9	O	1	0.5137461	0.4597454	0.5000000	1
O10	O	1	0.4597454	0.4862539	0.5000000	1
O11	O	1	0.5402546	0.5137461	0.5000000	1
O12	O	1	0.4862539	0.5402546	0.5000000	1
O13	O	1	0.4597454	0.5137461	0.5000000	1
O14	O	1	0.5402546	0.4862539	0.5000000	1
O15	O	1	0.4862539	0.4597454	0.5000000	1
O16	O	1	0.5137461	0.5402546	0.5000000	1
O17	O	1	0.5141446	0.4858554	0.5257563	1
O18	O	1	0.4858554	0.4858554	0.4742437	1
O19	O	1	0.5141446	0.5141446	0.4742437	1
O20	O	1	0.4858554	0.5141446	0.5257563	1
O21	O	1	0.5000000	0.5302796	0.4532817	1
O22	O	1	0.5000000	0.4697204	0.4532817	1
O23	O	1	0.4697204	0.5000000	0.5467183	1
O24	O	1	0.5302796	0.5000000	0.5467183	1
Zr1	Zr	1	0.5000000	0.4754144	0.5000000	1
Zr2	Zr	1	0.4754144	0.5000000	0.5000000	1
Zr3	Zr	1	0.5245856	0.5000000	0.5000000	1
Zr4	Zr	1	0.5000000	0.5245856	0.5000000	1

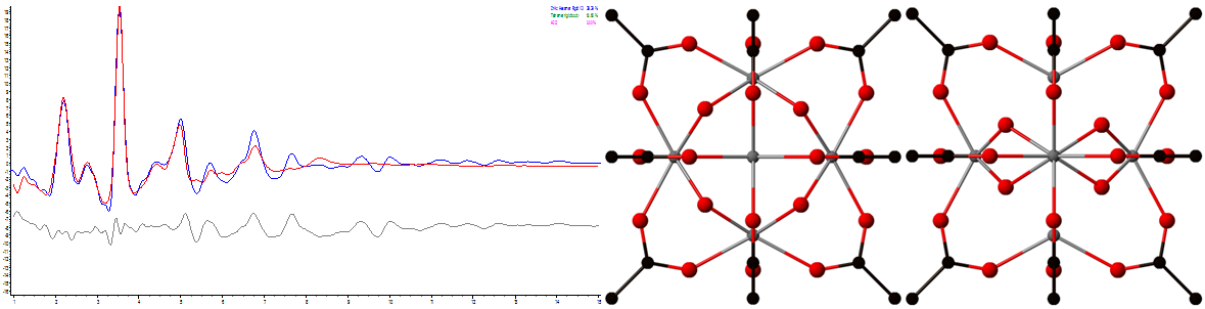

Figure 194: Observed and Calculated PDF from the chandelier core refinement of ZAA7 from the 15-month data collection and the resultant model viewed from the axial (left) and equatorial (right) positions.

Table 137: The atomic coordinates of the model resulting from the chandelier core refinement of ZAA7 from the 15-month data collection.

Atom Label	Atom Type	Multiplicity	Fractional X Coordinate	Fractional Y Coordinate	Fractional Z Coordinate	Fractional Occupancy
C1	C	1	0.5889239	0.5000000	0.5822608	1
C2	C	1	0.5000000	0.4110761	0.5822608	1
C3	C	1	0.4110761	0.5000000	0.5822608	1
C4	C	1	0.5000000	0.5889239	0.5822608	1
C5	C	1	0.5889239	0.5000000	0.4177392	1
C6	C	1	0.5000000	0.4110761	0.4177392	1
C7	C	1	0.4110761	0.5000000	0.4177392	1
C8	C	1	0.5000000	0.5889239	0.4177392	1
C9	C	1	0.5889239	0.4110761	0.5000000	1
C10	C	1	0.4110761	0.4110761	0.5000000	1
C11	C	1	0.4110761	0.5889239	0.5000000	1
C12	C	1	0.5889239	0.5889239	0.5000000	1
C13	C	1	0.6191839	0.5000000	0.6102534	1
C14	C	1	0.5000000	0.3808161	0.6102534	1
C15	C	1	0.3808161	0.5000000	0.6102534	1
C16	C	1	0.5000000	0.6191839	0.6102534	1
C17	C	1	0.6191839	0.5000000	0.3897466	1
C18	C	1	0.5000000	0.3808161	0.3897466	1
C19	C	1	0.3808161	0.5000000	0.3897466	1
C20	C	1	0.5000000	0.6191839	0.3897466	1
C21	C	1	0.6191839	0.3808161	0.5000000	1
C22	C	1	0.3808161	0.3808161	0.5000000	1
C23	C	1	0.3808161	0.6191839	0.5000000	1
C24	C	1	0.6191839	0.6191839	0.5000000	1
O1	O	1	0.5403018	0.4596982	0.4759639	1
O2	O	1	0.5403018	0.4596982	0.5240361	1
O3	O	1	0.4596982	0.4596982	0.4759639	1
O4	O	1	0.4596982	0.4596982	0.5240361	1
O5	O	1	0.4596982	0.5403018	0.4759639	1
O6	O	1	0.4596982	0.5403018	0.5240361	1
O7	O	1	0.5403018	0.5403018	0.4759639	1
O8	O	1	0.5403018	0.5403018	0.5240361	1

O9	O	1	0.5951898	0.5000000	0.5497898	1
O10	O	1	0.5951898	0.4461773	0.5000000	1
O11	O	1	0.5951898	0.5000000	0.4502102	1
O12	O	1	0.5951898	0.5538227	0.5000000	1
O13	O	1	0.5000000	0.5951898	0.5497898	1
O14	O	1	0.5538227	0.5951898	0.5000000	1
O15	O	1	0.5000000	0.5951898	0.4502102	1
O16	O	1	0.4461773	0.5951898	0.5000000	1
O17	O	1	0.4048102	0.5000000	0.5497898	1
O18	O	1	0.4048102	0.5538227	0.5000000	1
O19	O	1	0.4048102	0.5000000	0.4502102	1
O20	O	1	0.4048102	0.4461773	0.5000000	1
O21	O	1	0.5000000	0.4048102	0.5497898	1
O22	O	1	0.4461773	0.4048102	0.5000000	1
O23	O	1	0.5000000	0.4048102	0.4502102	1
O24	O	1	0.5538227	0.4048102	0.5000000	1
O25	O	1	0.5538227	0.5000000	0.5880572	1
O26	O	1	0.5000000	0.5538227	0.5880572	1
O27	O	1	0.4461773	0.5000000	0.5880572	1
O28	O	1	0.5000000	0.4461773	0.5880572	1
O29	O	1	0.5538227	0.5000000	0.4119428	1
O30	O	1	0.5000000	0.4461773	0.4119428	1
O31	O	1	0.4461773	0.5000000	0.4119428	1
O32	O	1	0.5000000	0.5538227	0.4119428	1
Zr1	Zr	1	0.5661804	0.5000000	0.5000000	1
Zr2	Zr	1	0.5000000	0.5661804	0.5000000	1
Zr3	Zr	1	0.4338196	0.5000000	0.5000000	1
Zr4	Zr	1	0.5000000	0.4338196	0.5000000	1
Zr5	Zr	1	0.5000000	0.5000000	0.5612215	1
Zr6	Zr	1	0.5000000	0.5000000	0.4387785	1

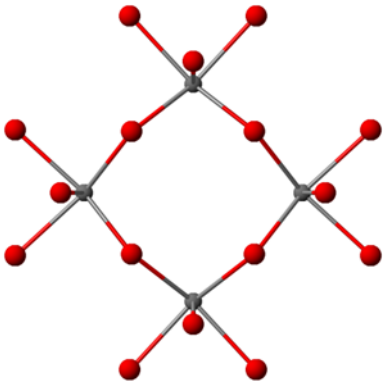

Figure 195: The tetrameric structure resulting from the chandelier core refinement of ZAA7 from the 15-month data collection.

Table 138: The atomic coordinates of the tetrameric phase of the chandelier core refinement of ZAA7 from the 15-month data collection.

Atom Label	Atom Type	Multiplicity	Fractional X Coordinate	Fractional Y Coordinate	Fractional Z Coordinate	Fractional Occupancy
O1	O	1	0.5138291	0.4861709	0.4731901	1
O2	O	1	0.4861709	0.4861709	0.5268099	1
O3	O	1	0.5138291	0.5138291	0.5268099	1
O4	O	1	0.4861709	0.5138291	0.4731901	1
O5	O	1	0.5000000	0.5297351	0.5469244	1
O6	O	1	0.5000000	0.4702649	0.5469244	1
O7	O	1	0.4702649	0.5000000	0.4530756	1
O8	O	1	0.5297351	0.5000000	0.4530756	1
O9	O	1	0.514223	0.4600121	0.5000000	1
O10	O	1	0.4600121	0.485777	0.5000000	1
O11	O	1	0.5399879	0.514223	0.5000000	1
O12	O	1	0.485777	0.5399879	0.5000000	1
O13	O	1	0.4600121	0.514223	0.5000000	1
O14	O	1	0.5399879	0.485777	0.5000000	1
O15	O	1	0.485777	0.4600121	0.5000000	1
O16	O	1	0.514223	0.5399879	0.5000000	1
O17	O	1	0.5138291	0.4861709	0.5268099	1
O18	O	1	0.4861709	0.4861709	0.4731901	1
O19	O	1	0.5138291	0.5138291	0.4731901	1
O20	O	1	0.4861709	0.5138291	0.5268099	1
O21	O	1	0.5000000	0.5297351	0.4530756	1
O22	O	1	0.5000000	0.4702649	0.4530756	1
O23	O	1	0.4702649	0.5000000	0.5469244	1
O24	O	1	0.5297351	0.5000000	0.5469244	1
Zr1	Zr	1	0.5000000	0.4754496	0.5000000	1
Zr2	Zr	1	0.4754496	0.5000000	0.5000000	1
Zr3	Zr	1	0.5245504	0.5000000	0.5000000	1
Zr4	Zr	1	0.5000000	0.5245504	0.5000000	1

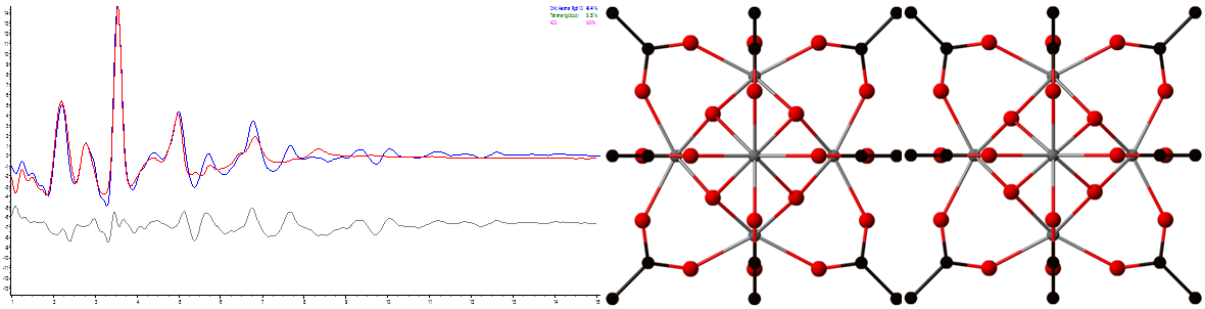

Figure 196: Observed and Calculated PDF from the chandelier core refinement of ZAA10 from the 15-month data collection and the resultant model viewed from the axial (left) and equatorial (right) positions.

Table 139: The atomic coordinates of the model resulting from the chandelier core refinement of ZAA10 from the 15-month data collection.

Atom Label	Atom Type	Multiplicity	Fractional X Coordinate	Fractional Y Coordinate	Fractional Z Coordinate	Fractional Occupancy
C1	C	1	0.5895235	0.5000000	0.5828155	1
C2	C	1	0.5000000	0.4104765	0.5828155	1
C3	C	1	0.4104765	0.5000000	0.5828155	1
C4	C	1	0.5000000	0.5895235	0.5828155	1
C5	C	1	0.5895235	0.5000000	0.4171845	1
C6	C	1	0.5000000	0.4104765	0.4171845	1
C7	C	1	0.4104765	0.5000000	0.4171845	1
C8	C	1	0.5000000	0.5895235	0.4171845	1
C9	C	1	0.5895235	0.4104765	0.5000000	1
C10	C	1	0.4104765	0.4104765	0.5000000	1
C11	C	1	0.4104765	0.5895235	0.5000000	1
C12	C	1	0.5895235	0.5895235	0.5000000	1
C13	C	1	0.6193913	0.5000000	0.6104453	1
C14	C	1	0.5000000	0.3806087	0.6104453	1
C15	C	1	0.3806087	0.5000000	0.6104453	1
C16	C	1	0.5000000	0.6193913	0.6104453	1
C17	C	1	0.6193913	0.5000000	0.3895547	1
C18	C	1	0.5000000	0.3806087	0.3895547	1
C19	C	1	0.3806087	0.5000000	0.3895547	1
C20	C	1	0.5000000	0.6193913	0.3895547	1
C21	C	1	0.6193913	0.3806087	0.5000000	1
C22	C	1	0.3806087	0.3806087	0.5000000	1
C23	C	1	0.3806087	0.6193913	0.5000000	1
C24	C	1	0.6193913	0.6193913	0.5000000	1
O1	O	1	0.5350473	0.4649527	0.4715748	1
O2	O	1	0.5350473	0.4649527	0.5284252	1
O3	O	1	0.4649527	0.4649527	0.4715748	1
O4	O	1	0.4649527	0.4649527	0.5284252	1
O5	O	1	0.4649527	0.5350473	0.4715748	1
O6	O	1	0.4649527	0.5350473	0.5284252	1
O7	O	1	0.5350473	0.5350473	0.4715748	1
O8	O	1	0.5350473	0.5350473	0.5284252	1

O9	O	1	0.5943072	0.5000000	0.5498717	1
O10	O	1	0.5943072	0.4460887	0.5000000	1
O11	O	1	0.5943072	0.5000000	0.4501283	1
O12	O	1	0.5943072	0.5539113	0.5000000	1
O13	O	1	0.5000000	0.5943072	0.5498717	1
O14	O	1	0.5539113	0.5943072	0.5000000	1
O15	O	1	0.5000000	0.5943072	0.4501283	1
O16	O	1	0.4460887	0.5943072	0.5000000	1
O17	O	1	0.4056928	0.5000000	0.5498717	1
O18	O	1	0.4056928	0.5539113	0.5000000	1
O19	O	1	0.4056928	0.5000000	0.4501283	1
O20	O	1	0.4056928	0.4460887	0.5000000	1
O21	O	1	0.5000000	0.4056928	0.5498717	1
O22	O	1	0.4460887	0.4056928	0.5000000	1
O23	O	1	0.5000000	0.4056928	0.4501283	1
O24	O	1	0.5539113	0.4056928	0.5000000	1
O25	O	1	0.5539113	0.5000000	0.5872407	1
O26	O	1	0.5000000	0.5539113	0.5872407	1
O27	O	1	0.4460887	0.5000000	0.5872407	1
O28	O	1	0.5000000	0.4460887	0.5872407	1
O29	O	1	0.5539113	0.5000000	0.4127593	1
O30	O	1	0.5000000	0.4460887	0.4127593	1
O31	O	1	0.4460887	0.5000000	0.4127593	1
O32	O	1	0.5000000	0.5539113	0.4127593	1
Zr1	Zr	1	0.5662118	0.5000000	0.5000000	1
Zr2	Zr	1	0.5000000	0.5662118	0.5000000	1
Zr3	Zr	1	0.4337882	0.5000000	0.5000000	1
Zr4	Zr	1	0.5000000	0.4337882	0.5000000	1
Zr5	Zr	1	0.5000000	0.5000000	0.5612505	1
Zr6	Zr	1	0.5000000	0.5000000	0.4387495	1

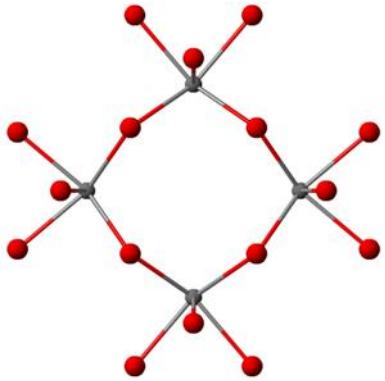

Figure 197: The tetrameric structure resulting from the chandelier core refinement of ZAA10 from the 15-month data collection.

Table 140: The atomic coordinates of the tetrameric phase of the chandelier core refinement of ZAA10 from the 15-month data collection.

Atom Label	Atom Type	Multiplicity	Fractional X Coordinate	Fractional Y Coordinate	Fractional Z Coordinate	Fractional Occupancy
O1	O	1	0.5145595	0.4854405	0.4771955	1
O2	O	1	0.4854405	0.4854405	0.5228045	1
O3	O	1	0.5145595	0.5145595	0.5228045	1
O4	O	1	0.4854405	0.5145595	0.4771955	1
O5	O	1	0.5000000	0.5306354	0.5457628	1
O6	O	1	0.5000000	0.4693646	0.5457628	1
O7	O	1	0.4693646	0.5000000	0.4542372	1
O8	O	1	0.5306354	0.5000000	0.4542372	1
O9	O	1	0.5135019	0.4594525	0.5000000	1
O10	O	1	0.4594525	0.4864981	0.5000000	1
O11	O	1	0.5405475	0.5135019	0.5000000	1
O12	O	1	0.4864981	0.5405475	0.5000000	1
O13	O	1	0.4594525	0.5135019	0.5000000	1
O14	O	1	0.5405475	0.4864981	0.5000000	1
O15	O	1	0.4864981	0.4594525	0.5000000	1
O16	O	1	0.5135019	0.5405475	0.5000000	1
O17	O	1	0.5145595	0.4854405	0.5228045	1
O18	O	1	0.4854405	0.4854405	0.4771955	1
O19	O	1	0.5145595	0.5145595	0.4771955	1
O20	O	1	0.4854405	0.5145595	0.5228045	1
O21	O	1	0.5000000	0.5306354	0.4542372	1
O22	O	1	0.5000000	0.4693646	0.4542372	1
O23	O	1	0.4693646	0.5000000	0.5457628	1
O24	O	1	0.5306354	0.5000000	0.5457628	1
Zr1	Zr	1	0.5000000	0.4754215	0.5000000	1
Zr2	Zr	1	0.4754215	0.5000000	0.5000000	1
Zr3	Zr	1	0.5245785	0.5000000	0.5000000	1
Zr4	Zr	1	0.5000000	0.5245785	0.5000000	1

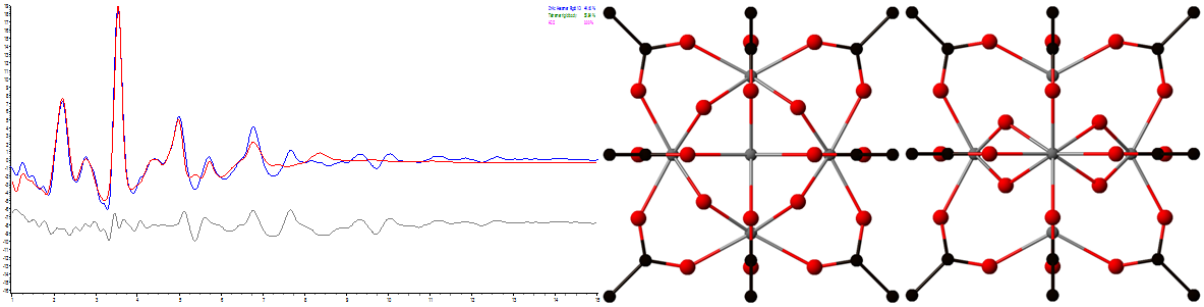

Figure 198: Observed and Calculated PDF from the chandelier core refinement of ZAA13 from the 15-month data collection and the resultant model viewed from the axial (left) and equatorial (right) positions.

Table 141: The atomic coordinates of the model resulting from the chandelier core refinement of ZAA13 from the 15-month data collection.

Atom Label	Atom Type	Multiplicity	Fractional X Coordinate	Fractional Y Coordinate	Fractional Z Coordinate	Fractional Occupancy
C1	C	1	0.5891194	0.5000000	0.5824417	1
C2	C	1	0.5000000	0.4108806	0.5824417	1
C3	C	1	0.4108806	0.5000000	0.5824417	1
C4	C	1	0.5000000	0.5891194	0.5824417	1
C5	C	1	0.5891194	0.5000000	0.4175583	1
C6	C	1	0.5000000	0.4108806	0.4175583	1
C7	C	1	0.4108806	0.5000000	0.4175583	1
C8	C	1	0.5000000	0.5891194	0.4175583	1
C9	C	1	0.5891194	0.4108806	0.5000000	1
C10	C	1	0.4108806	0.4108806	0.5000000	1
C11	C	1	0.4108806	0.5891194	0.5000000	1
C12	C	1	0.5891194	0.5891194	0.5000000	1
C13	C	1	0.61961	0.5000000	0.6106476	1
C14	C	1	0.5000000	0.38039	0.6106476	1
C15	C	1	0.38039	0.5000000	0.6106476	1
C16	C	1	0.5000000	0.61961	0.6106476	1
C17	C	1	0.61961	0.5000000	0.3893524	1
C18	C	1	0.5000000	0.38039	0.3893524	1
C19	C	1	0.38039	0.5000000	0.3893524	1
C20	C	1	0.5000000	0.61961	0.3893524	1
C21	C	1	0.61961	0.38039	0.5000000	1
C22	C	1	0.38039	0.38039	0.5000000	1
C23	C	1	0.38039	0.61961	0.5000000	1
C24	C	1	0.61961	0.61961	0.5000000	1
O1	O	1	0.5397862	0.4602138	0.4752097	1
O2	O	1	0.5397862	0.4602138	0.5247903	1
O3	O	1	0.4602138	0.4602138	0.4752097	1
O4	O	1	0.4602138	0.4602138	0.5247903	1
O5	O	1	0.4602138	0.5397862	0.4752097	1
O6	O	1	0.4602138	0.5397862	0.5247903	1
O7	O	1	0.5397862	0.5397862	0.4752097	1
O8	O	1	0.5397862	0.5397862	0.5247903	1

O9	O	1	0.5950925	0.5000000	0.5496479	1
O10	O	1	0.5950925	0.4463306	0.5000000	1
O11	O	1	0.5950925	0.5000000	0.4503521	1
O12	O	1	0.5950925	0.5536694	0.5000000	1
O13	O	1	0.5000000	0.5950925	0.5496479	1
O14	O	1	0.5536694	0.5950925	0.5000000	1
O15	O	1	0.5000000	0.5950925	0.4503521	1
O16	O	1	0.4463306	0.5950925	0.5000000	1
O17	O	1	0.4049075	0.5000000	0.5496479	1
O18	O	1	0.4049075	0.5536694	0.5000000	1
O19	O	1	0.4049075	0.5000000	0.4503521	1
O20	O	1	0.4049075	0.4463306	0.5000000	1
O21	O	1	0.5000000	0.4049075	0.5496479	1
O22	O	1	0.4463306	0.4049075	0.5000000	1
O23	O	1	0.5000000	0.4049075	0.4503521	1
O24	O	1	0.5536694	0.4049075	0.5000000	1
O25	O	1	0.5536694	0.5000000	0.5879672	1
O26	O	1	0.5000000	0.5536694	0.5879672	1
O27	O	1	0.4463306	0.5000000	0.5879672	1
O28	O	1	0.5000000	0.4463306	0.5879672	1
O29	O	1	0.5536694	0.5000000	0.4120328	1
O30	O	1	0.5000000	0.4463306	0.4120328	1
O31	O	1	0.4463306	0.5000000	0.4120328	1
O32	O	1	0.5000000	0.5536694	0.4120328	1
Zr1	Zr	1	0.5663224	0.5000000	0.5000000	1
Zr2	Zr	1	0.5000000	0.5663224	0.5000000	1
Zr3	Zr	1	0.4336776	0.5000000	0.5000000	1
Zr4	Zr	1	0.5000000	0.4336776	0.5000000	1
Zr5	Zr	1	0.5000000	0.5000000	0.5613529	1
Zr6	Zr	1	0.5000000	0.5000000	0.4386471	1

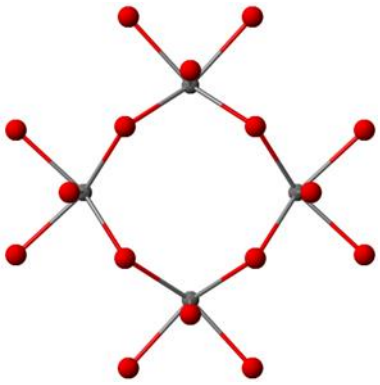

Figure 199: The tetrameric structure resulting from the chandelier core refinement of ZAA13 from the 15-month data collection.

Table 142: The atomic coordinates of the tetrameric phase of the chandelier core refinement of ZAA13 from the 15-month data collection.

Atom Label	Atom Type	Multiplicity	Fractional X Coordinate	Fractional Y Coordinate	Fractional Z Coordinate	Fractional Occupancy
O1	O	1	0.5149107	0.4850893	0.4719672	1
O2	O	1	0.4850893	0.4850893	0.5280328	1
O3	O	1	0.5149107	0.5149107	0.5280328	1
O4	O	1	0.4850893	0.5149107	0.4719672	1
O5	O	1	0.5000000	0.5275951	0.5461964	1
O6	O	1	0.5000000	0.4724049	0.5461964	1
O7	O	1	0.4724049	0.5000000	0.4538036	1
O8	O	1	0.5275951	0.5000000	0.4538036	1
O9	O	1	0.5141438	0.4602185	0.5000000	1
O10	O	1	0.4602185	0.4858562	0.5000000	1
O11	O	1	0.5397815	0.5141438	0.5000000	1
O12	O	1	0.4858562	0.5397815	0.5000000	1
O13	O	1	0.4602185	0.5141438	0.5000000	1
O14	O	1	0.5397815	0.4858562	0.5000000	1
O15	O	1	0.4858562	0.4602185	0.5000000	1
O16	O	1	0.5141438	0.5397815	0.5000000	1
O17	O	1	0.5149107	0.4850893	0.5280328	1
O18	O	1	0.4850893	0.4850893	0.4719672	1
O19	O	1	0.5149107	0.5149107	0.4719672	1
O20	O	1	0.4850893	0.5149107	0.5280328	1
O21	O	1	0.5000000	0.5275951	0.4538036	1
O22	O	1	0.5000000	0.4724049	0.4538036	1
O23	O	1	0.4724049	0.5000000	0.5461964	1
O24	O	1	0.5275951	0.5000000	0.5461964	1
Zr1	Zr	1	0.5000000	0.4756279	0.5000000	1
Zr2	Zr	1	0.4756279	0.5000000	0.5000000	1
Zr3	Zr	1	0.5243721	0.5000000	0.5000000	1
Zr4	Zr	1	0.5000000	0.5243721	0.5000000	1

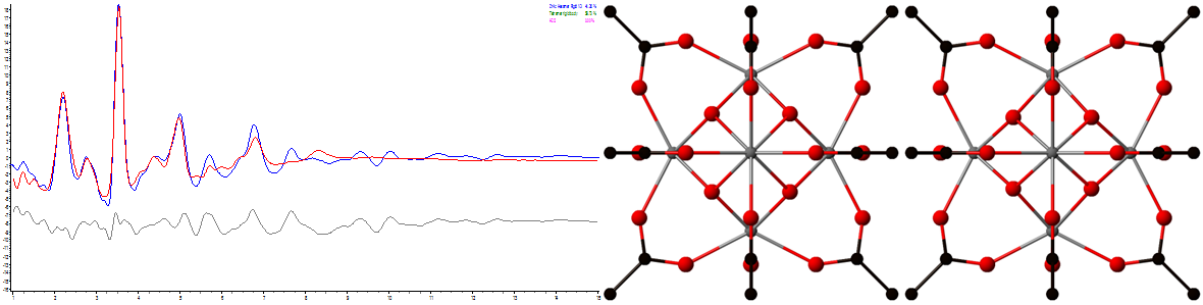

Figure 200: Observed and Calculated PDF from the chandelier core refinement of ZAA16 from the 15-month data collection and the resultant model viewed from the axial (left) and equatorial (right) positions.

Table 143: The atomic coordinates of the model resulting from the chandelier core refinement of ZAA16 from the 15-month data collection.

Atom Label	Atom Type	Multiplicity	Fractional X Coordinate	Fractional Y Coordinate	Fractional Z Coordinate	Fractional Occupancy
C1	C	1	0.5896586	0.5000000	0.5829405	1
C2	C	1	0.5000000	0.4103414	0.5829405	1
C3	C	1	0.4103414	0.5000000	0.5829405	1
C4	C	1	0.5000000	0.5896586	0.5829405	1
C5	C	1	0.5896586	0.5000000	0.4170595	1
C6	C	1	0.5000000	0.4103414	0.4170595	1
C7	C	1	0.4103414	0.5000000	0.4170595	1
C8	C	1	0.5000000	0.5896586	0.4170595	1
C9	C	1	0.5896586	0.4103414	0.5000000	1
C10	C	1	0.4103414	0.4103414	0.5000000	1
C11	C	1	0.4103414	0.5896586	0.5000000	1
C12	C	1	0.5896586	0.5896586	0.5000000	1
C13	C	1	0.6192858	0.5000000	0.6103477	1
C14	C	1	0.5000000	0.3807142	0.6103477	1
C15	C	1	0.3807142	0.5000000	0.6103477	1
C16	C	1	0.5000000	0.6192858	0.6103477	1
C17	C	1	0.6192858	0.5000000	0.3896523	1
C18	C	1	0.5000000	0.3807142	0.3896523	1
C19	C	1	0.3807142	0.5000000	0.3896523	1
C20	C	1	0.5000000	0.6192858	0.3896523	1
C21	C	1	0.6192858	0.3807142	0.5000000	1
C22	C	1	0.3807142	0.3807142	0.5000000	1
C23	C	1	0.3807142	0.6192858	0.5000000	1
C24	C	1	0.6192858	0.6192858	0.5000000	1
O1	O	1	0.5330572	0.4669428	0.4721208	1
O2	O	1	0.5330572	0.4669428	0.5278792	1
O3	O	1	0.4669428	0.4669428	0.4721208	1
O4	O	1	0.4669428	0.4669428	0.5278792	1
O5	O	1	0.4669428	0.5330572	0.4721208	1
O6	O	1	0.4669428	0.5330572	0.5278792	1
O7	O	1	0.5330572	0.5330572	0.4721208	1
O8	O	1	0.5330572	0.5330572	0.5278792	1

O9	O	1	0.594439	0.5000000	0.550952	1
O10	O	1	0.594439	0.4449209	0.5000000	1
O11	O	1	0.594439	0.5000000	0.449048	1
O12	O	1	0.594439	0.5550791	0.5000000	1
O13	O	1	0.5000000	0.594439	0.550952	1
O14	O	1	0.5550791	0.594439	0.5000000	1
O15	O	1	0.5000000	0.594439	0.449048	1
O16	O	1	0.4449209	0.594439	0.5000000	1
O17	O	1	0.405561	0.5000000	0.550952	1
O18	O	1	0.405561	0.5550791	0.5000000	1
O19	O	1	0.405561	0.5000000	0.449048	1
O20	O	1	0.405561	0.4449209	0.5000000	1
O21	O	1	0.5000000	0.405561	0.550952	1
O22	O	1	0.4449209	0.405561	0.5000000	1
O23	O	1	0.5000000	0.405561	0.449048	1
O24	O	1	0.5550791	0.405561	0.5000000	1
O25	O	1	0.5550791	0.5000000	0.5873626	1
O26	O	1	0.5000000	0.5550791	0.5873626	1
O27	O	1	0.4449209	0.5000000	0.5873626	1
O28	O	1	0.5000000	0.4449209	0.5873626	1
O29	O	1	0.5550791	0.5000000	0.4126374	1
O30	O	1	0.5000000	0.4449209	0.4126374	1
O31	O	1	0.4449209	0.5000000	0.4126374	1
O32	O	1	0.5000000	0.5550791	0.4126374	1
Zr1	Zr	1	0.5660718	0.5000000	0.5000000	1
Zr2	Zr	1	0.5000000	0.5660718	0.5000000	1
Zr3	Zr	1	0.4339282	0.5000000	0.5000000	1
Zr4	Zr	1	0.5000000	0.4339282	0.5000000	1
Zr5	Zr	1	0.5000000	0.5000000	0.561121	1
Zr6	Zr	1	0.5000000	0.5000000	0.438879	1

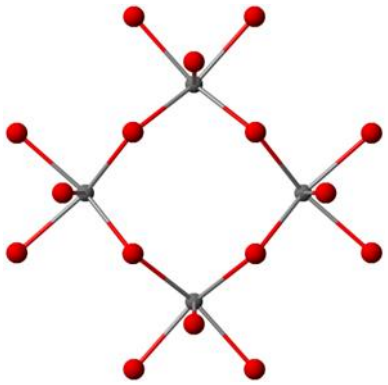

Figure 201: The tetrameric structure resulting from the chandelier core refinement of ZAA16 from the 15-month data collection.

Table 144: The atomic coordinates of the tetrameric phase of the chandelier core refinement of ZAA16 from the 15-month data collection.

Atom Label	Atom Type	Multiplicity	Fractional X Coordinate	Fractional Y Coordinate	Fractional Z Coordinate	Fractional Occupancy
O1	O	1	0.5138634	0.4861366	0.4730597	1
O2	O	1	0.4861366	0.4861366	0.5269403	1
O3	O	1	0.5138634	0.5138634	0.5269403	1
O4	O	1	0.4861366	0.5138634	0.4730597	1
O5	O	1	0.5000000	0.5298234	0.5467311	1
O6	O	1	0.5000000	0.4701766	0.5467311	1
O7	O	1	0.4701766	0.5000000	0.4532689	1
O8	O	1	0.5298234	0.5000000	0.4532689	1
O9	O	1	0.5136691	0.4598139	0.5000000	1
O10	O	1	0.4598139	0.4863309	0.5000000	1
O11	O	1	0.5401861	0.5136691	0.5000000	1
O12	O	1	0.4863309	0.5401861	0.5000000	1
O13	O	1	0.4598139	0.5136691	0.5000000	1
O14	O	1	0.5401861	0.4863309	0.5000000	1
O15	O	1	0.4863309	0.4598139	0.5000000	1
O16	O	1	0.5136691	0.5401861	0.5000000	1
O17	O	1	0.5138634	0.4861366	0.5269403	1
O18	O	1	0.4861366	0.4861366	0.4730597	1
O19	O	1	0.5138634	0.5138634	0.4730597	1
O20	O	1	0.4861366	0.5138634	0.5269403	1
O21	O	1	0.5000000	0.5298234	0.4532689	1
O22	O	1	0.5000000	0.4701766	0.4532689	1
O23	O	1	0.4701766	0.5000000	0.5467311	1
O24	O	1	0.5298234	0.5000000	0.5467311	1
Zr1	Zr	1	0.5000000	0.4752909	0.5000000	1
Zr2	Zr	1	0.4752909	0.5000000	0.5000000	1
Zr3	Zr	1	0.5247091	0.5000000	0.5000000	1
Zr4	Zr	1	0.5000000	0.5247091	0.5000000	1

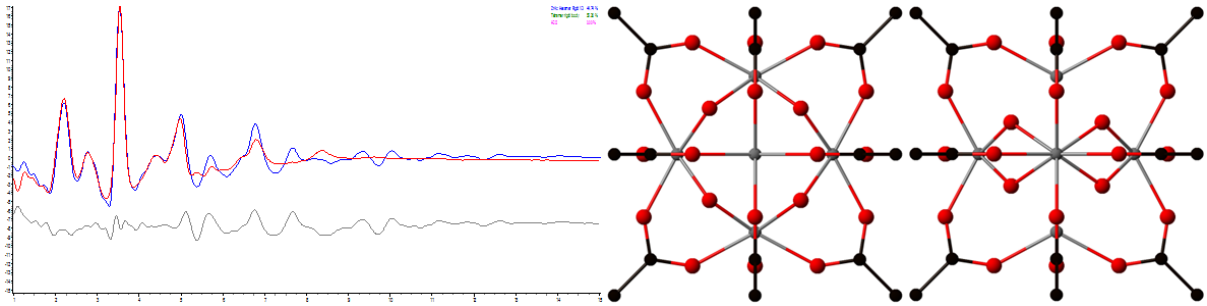

Figure 202: Observed and Calculated PDF from the chandelier core refinement of ZAA20 from the 15-month data collection and the resultant model viewed from the axial (left) and equatorial (right) positions.

Table 145: The atomic coordinates of the model resulting from the chandelier core refinement of ZAA20 from the 15-month data collection.

Atom Label	Atom Type	Multiplicity	Fractional X Coordinate	Fractional Y Coordinate	Fractional Z Coordinate	Fractional Occupancy
C1	C	1	0.5891027	0.5000000	0.5824262	1
C2	C	1	0.5000000	0.4108973	0.5824262	1
C3	C	1	0.4108973	0.5000000	0.5824262	1
C4	C	1	0.5000000	0.5891027	0.5824262	1
C5	C	1	0.5891027	0.5000000	0.4175738	1
C6	C	1	0.5000000	0.4108973	0.4175738	1
C7	C	1	0.4108973	0.5000000	0.4175738	1
C8	C	1	0.5000000	0.5891027	0.4175738	1
C9	C	1	0.5891027	0.4108973	0.5000000	1
C10	C	1	0.4108973	0.4108973	0.5000000	1
C11	C	1	0.4108973	0.5891027	0.5000000	1
C12	C	1	0.5891027	0.5891027	0.5000000	1
C13	C	1	0.6198277	0.5000000	0.610849	1
C14	C	1	0.5000000	0.3801723	0.610849	1
C15	C	1	0.3801723	0.5000000	0.610849	1
C16	C	1	0.5000000	0.6198277	0.610849	1
C17	C	1	0.6198277	0.5000000	0.389151	1
C18	C	1	0.5000000	0.3801723	0.389151	1
C19	C	1	0.3801723	0.5000000	0.389151	1
C20	C	1	0.5000000	0.6198277	0.389151	1
C21	C	1	0.6198277	0.3801723	0.5000000	1
C22	C	1	0.3801723	0.3801723	0.5000000	1
C23	C	1	0.3801723	0.6198277	0.5000000	1
C24	C	1	0.6198277	0.6198277	0.5000000	1
O1	O	1	0.5388929	0.4611071	0.4750345	1
O2	O	1	0.5388929	0.4611071	0.5249655	1
O3	O	1	0.4611071	0.4611071	0.4750345	1
O4	O	1	0.4611071	0.4611071	0.5249655	1
O5	O	1	0.4611071	0.5388929	0.4750345	1
O6	O	1	0.4611071	0.5388929	0.5249655	1
O7	O	1	0.5388929	0.5388929	0.4750345	1
O8	O	1	0.5388929	0.5388929	0.5249655	1

O9	O	1	0.5947806	0.5000000	0.5493057	1
O10	O	1	0.5947806	0.4467005	0.5000000	1
O11	O	1	0.5947806	0.5000000	0.4506943	1
O12	O	1	0.5947806	0.5532995	0.5000000	1
O13	O	1	0.5000000	0.5947806	0.5493057	1
O14	O	1	0.5532995	0.5947806	0.5000000	1
O15	O	1	0.5000000	0.5947806	0.4506943	1
O16	O	1	0.4467005	0.5947806	0.5000000	1
O17	O	1	0.4052194	0.5000000	0.5493057	1
O18	O	1	0.4052194	0.5532995	0.5000000	1
O19	O	1	0.4052194	0.5000000	0.4506943	1
O20	O	1	0.4052194	0.4467005	0.5000000	1
O21	O	1	0.5000000	0.4052194	0.5493057	1
O22	O	1	0.4467005	0.4052194	0.5000000	1
O23	O	1	0.5000000	0.4052194	0.4506943	1
O24	O	1	0.5532995	0.4052194	0.5000000	1
O25	O	1	0.5532995	0.5000000	0.5876787	1
O26	O	1	0.5000000	0.5532995	0.5876787	1
O27	O	1	0.4467005	0.5000000	0.5876787	1
O28	O	1	0.5000000	0.4467005	0.5876787	1
O29	O	1	0.5532995	0.5000000	0.4123213	1
O30	O	1	0.5000000	0.4467005	0.4123213	1
O31	O	1	0.4467005	0.5000000	0.4123213	1
O32	O	1	0.5000000	0.5532995	0.4123213	1
Zr1	Zr	1	0.5661803	0.5000000	0.5000000	1
Zr2	Zr	1	0.5000000	0.5661803	0.5000000	1
Zr3	Zr	1	0.4338197	0.5000000	0.5000000	1
Zr4	Zr	1	0.5000000	0.4338197	0.5000000	1
Zr5	Zr	1	0.5000000	0.5000000	0.5612214	1
Zr6	Zr	1	0.5000000	0.5000000	0.4387786	1

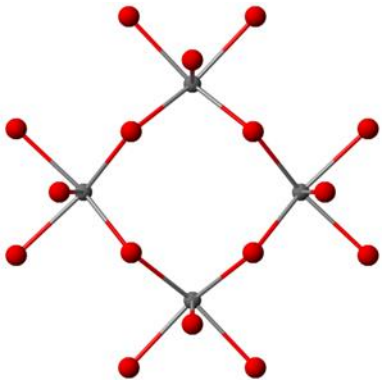

Figure 203: The tetrameric structure resulting from the chandelier core refinement of ZAA20 from the 15-month data collection.

Table 146: The atomic coordinates of the tetrameric phase of the chandelier core refinement of ZAA20 from the 15-month data collection.

Atom Label	Atom Type	Multiplicity	Fractional X Coordinate	Fractional Y Coordinate	Fractional Z Coordinate	Fractional Occupancy
O1	O	1	0.5137824	0.4862176	0.473036	1
O2	O	1	0.4862176	0.4862176	0.526964	1
O3	O	1	0.5137824	0.5137824	0.526964	1
O4	O	1	0.4862176	0.5137824	0.473036	1
O5	O	1	0.5000000	0.5300821	0.5461147	1
O6	O	1	0.5000000	0.4699179	0.5461147	1
O7	O	1	0.4699179	0.5000000	0.4538853	1
O8	O	1	0.5300821	0.5000000	0.4538853	1
O9	O	1	0.514377	0.4601216	0.5000000	1
O10	O	1	0.4601216	0.485623	0.5000000	1
O11	O	1	0.5398784	0.514377	0.5000000	1
O12	O	1	0.485623	0.5398784	0.5000000	1
O13	O	1	0.4601216	0.514377	0.5000000	1
O14	O	1	0.5398784	0.485623	0.5000000	1
O15	O	1	0.485623	0.4601216	0.5000000	1
O16	O	1	0.514377	0.5398784	0.5000000	1
O17	O	1	0.5137824	0.4862176	0.526964	1
O18	O	1	0.4862176	0.4862176	0.473036	1
O19	O	1	0.5137824	0.5137824	0.473036	1
O20	O	1	0.4862176	0.5137824	0.526964	1
O21	O	1	0.5000000	0.5300821	0.4538853	1
O22	O	1	0.5000000	0.4699179	0.4538853	1
O23	O	1	0.4699179	0.5000000	0.5461147	1
O24	O	1	0.5300821	0.5000000	0.5461147	1
Zr1	Zr	1	0.5000000	0.4753785	0.5000000	1
Zr2	Zr	1	0.4753785	0.5000000	0.5000000	1
Zr3	Zr	1	0.5246215	0.5000000	0.5000000	1
Zr4	Zr	1	0.5000000	0.5246215	0.5000000	1

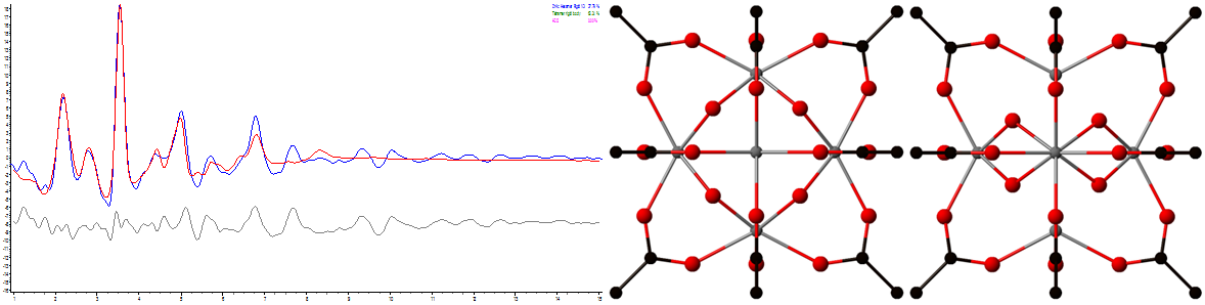

Figure 204: Observed and Calculated PDF from the chandelier core refinement of ZAA24 from the 15-month data collection and the resultant model viewed from the axial (left) and equatorial (right) positions.

Table 147: The atomic coordinates of the model resulting from the chandelier core refinement of ZAA24 from the 15-month data collection.

Atom Label	Atom Type	Multiplicity	Fractional X Coordinate	Fractional Y Coordinate	Fractional Z Coordinate	Fractional Occupancy
C1	C	1	0.58962	0.5000000	0.5829048	1
C2	C	1	0.5000000	0.41038	0.5829048	1
C3	C	1	0.41038	0.5000000	0.5829048	1
C4	C	1	0.5000000	0.58962	0.5829048	1
C5	C	1	0.58962	0.5000000	0.4170952	1
C6	C	1	0.5000000	0.41038	0.4170952	1
C7	C	1	0.41038	0.5000000	0.4170952	1
C8	C	1	0.5000000	0.58962	0.4170952	1
C9	C	1	0.58962	0.41038	0.5000000	1
C10	C	1	0.41038	0.41038	0.5000000	1
C11	C	1	0.41038	0.58962	0.5000000	1
C12	C	1	0.58962	0.58962	0.5000000	1
C13	C	1	0.6189832	0.5000000	0.6100677	1
C14	C	1	0.5000000	0.3810168	0.6100677	1
C15	C	1	0.3810168	0.5000000	0.6100677	1
C16	C	1	0.5000000	0.6189832	0.6100677	1
C17	C	1	0.6189832	0.5000000	0.3899323	1
C18	C	1	0.5000000	0.3810168	0.3899323	1
C19	C	1	0.3810168	0.5000000	0.3899323	1
C20	C	1	0.5000000	0.6189832	0.3899323	1
C21	C	1	0.6189832	0.3810168	0.5000000	1
C22	C	1	0.3810168	0.3810168	0.5000000	1
C23	C	1	0.3810168	0.6189832	0.5000000	1
C24	C	1	0.6189832	0.6189832	0.5000000	1
O1	O	1	0.536872	0.463128	0.4746879	1
O2	O	1	0.536872	0.463128	0.5253121	1
O3	O	1	0.463128	0.463128	0.4746879	1
O4	O	1	0.463128	0.463128	0.5253121	1
O5	O	1	0.463128	0.536872	0.4746879	1
O6	O	1	0.463128	0.536872	0.5253121	1
O7	O	1	0.536872	0.536872	0.4746879	1
O8	O	1	0.536872	0.536872	0.5253121	1

O9	O	1	0.5948563	0.5000000	0.5500944	1
O10	O	1	0.5948563	0.4458479	0.5000000	1
O11	O	1	0.5948563	0.5000000	0.4499056	1
O12	O	1	0.5948563	0.5541521	0.5000000	1
O13	O	1	0.5000000	0.5948563	0.5500944	1
O14	O	1	0.5541521	0.5948563	0.5000000	1
O15	O	1	0.5000000	0.5948563	0.4499056	1
O16	O	1	0.4458479	0.5948563	0.5000000	1
O17	O	1	0.4051437	0.5000000	0.5500944	1
O18	O	1	0.4051437	0.5541521	0.5000000	1
O19	O	1	0.4051437	0.5000000	0.4499056	1
O20	O	1	0.4051437	0.4458479	0.5000000	1
O21	O	1	0.5000000	0.4051437	0.5500944	1
O22	O	1	0.4458479	0.4051437	0.5000000	1
O23	O	1	0.5000000	0.4051437	0.4499056	1
O24	O	1	0.5541521	0.4051437	0.5000000	1
O25	O	1	0.5541521	0.5000000	0.5877487	1
O26	O	1	0.5000000	0.5541521	0.5877487	1
O27	O	1	0.4458479	0.5000000	0.5877487	1
O28	O	1	0.5000000	0.4458479	0.5877487	1
O29	O	1	0.5541521	0.5000000	0.4122513	1
O30	O	1	0.5000000	0.4458479	0.4122513	1
O31	O	1	0.4458479	0.5000000	0.4122513	1
O32	O	1	0.5000000	0.5541521	0.4122513	1
Zr1	Zr	1	0.5664152	0.5000000	0.5000000	1
Zr2	Zr	1	0.5000000	0.5664152	0.5000000	1
Zr3	Zr	1	0.4335848	0.5000000	0.5000000	1
Zr4	Zr	1	0.5000000	0.4335848	0.5000000	1
Zr5	Zr	1	0.5000000	0.5000000	0.5614387	1
Zr6	Zr	1	0.5000000	0.5000000	0.4385613	1

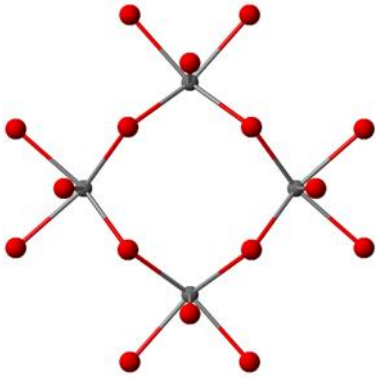

Figure 205: The tetrameric structure resulting from the chandelier core refinement of ZAA24 from the 15-month data collection.

Table 148: The atomic coordinates of the tetrameric phase of the chandelier core refinement of ZAA24 from the 15-month data collection.

Atom Label	Atom Type	Multiplicity	Fractional X Coordinate	Fractional Y Coordinate	Fractional Z Coordinate	Fractional Occupancy
O1	O	1	0.5142723	0.4857277	0.4738754	1
O2	O	1	0.4857277	0.4857277	0.5261246	1
O3	O	1	0.5142723	0.5142723	0.5261246	1
O4	O	1	0.4857277	0.5142723	0.4738754	1
O5	O	1	0.5000000	0.5291323	0.5467623	1
O6	O	1	0.5000000	0.4708677	0.5467623	1
O7	O	1	0.4708677	0.5000000	0.4532377	1
O8	O	1	0.5291323	0.5000000	0.4532377	1
O9	O	1	0.5138392	0.4597308	0.5000000	1
O10	O	1	0.4597308	0.4861608	0.5000000	1
O11	O	1	0.5402692	0.5138392	0.5000000	1
O12	O	1	0.4861608	0.5402692	0.5000000	1
O13	O	1	0.4597308	0.5138392	0.5000000	1
O14	O	1	0.5402692	0.4861608	0.5000000	1
O15	O	1	0.4861608	0.4597308	0.5000000	1
O16	O	1	0.5138392	0.5402692	0.5000000	1
O17	O	1	0.5142723	0.4857277	0.5261246	1
O18	O	1	0.4857277	0.4857277	0.4738754	1
O19	O	1	0.5142723	0.5142723	0.4738754	1
O20	O	1	0.4857277	0.5142723	0.5261246	1
O21	O	1	0.5000000	0.5291323	0.4532377	1
O22	O	1	0.5000000	0.4708677	0.4532377	1
O23	O	1	0.4708677	0.5000000	0.5467623	1
O24	O	1	0.5291323	0.5000000	0.5467623	1
Zr1	Zr	1	0.5000000	0.4754416	0.5000000	1
Zr2	Zr	1	0.4754416	0.5000000	0.5000000	1
Zr3	Zr	1	0.5245584	0.5000000	0.5000000	1
Zr4	Zr	1	0.5000000	0.5245584	0.5000000	1

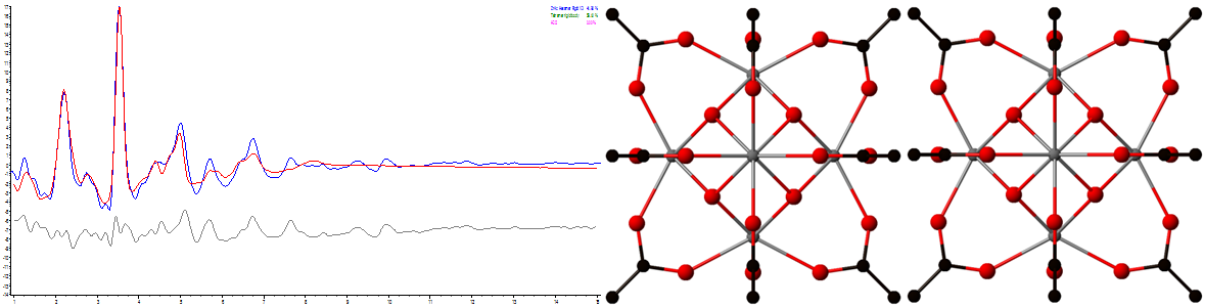

Figure 206: Observed and Calculated PDF from the chandelier core refinement of ZAA25 from the 15-month data collection and the resultant model viewed from the axial (left) and equatorial (right) positions.

Table 149: The atomic coordinates of the model resulting from the chandelier core refinement of ZAA25 from the 15-month data collection.

Atom Label	Atom Type	Multiplicity	Fractional X Coordinate	Fractional Y Coordinate	Fractional Z Coordinate	Fractional Occupancy
C1	C	1	0.5898644	0.5000000	0.5831309	1
C2	C	1	0.5000000	0.4101356	0.5831309	1
C3	C	1	0.4101356	0.5000000	0.5831309	1
C4	C	1	0.5000000	0.5898644	0.5831309	1
C5	C	1	0.5898644	0.5000000	0.4168691	1
C6	C	1	0.5000000	0.4101356	0.4168691	1
C7	C	1	0.4101356	0.5000000	0.4168691	1
C8	C	1	0.5000000	0.5898644	0.4168691	1
C9	C	1	0.5898644	0.4101356	0.5000000	1
C10	C	1	0.4101356	0.4101356	0.5000000	1
C11	C	1	0.4101356	0.5898644	0.5000000	1
C12	C	1	0.5898644	0.5898644	0.5000000	1
C13	C	1	0.6153021	0.5000000	0.6066624	1
C14	C	1	0.5000000	0.3846979	0.6066624	1
C15	C	1	0.3846979	0.5000000	0.6066624	1
C16	C	1	0.5000000	0.6153021	0.6066624	1
C17	C	1	0.6153021	0.5000000	0.3933376	1
C18	C	1	0.5000000	0.3846979	0.3933376	1
C19	C	1	0.3846979	0.5000000	0.3933376	1
C20	C	1	0.5000000	0.6153021	0.3933376	1
C21	C	1	0.6153021	0.3846979	0.5000000	1
C22	C	1	0.3846979	0.3846979	0.5000000	1
C23	C	1	0.3846979	0.6153021	0.5000000	1
C24	C	1	0.6153021	0.6153021	0.5000000	1
O1	O	1	0.5333475	0.4666525	0.4698951	1
O2	O	1	0.5333475	0.4666525	0.5301049	1
O3	O	1	0.4666525	0.4666525	0.4698951	1
O4	O	1	0.4666525	0.4666525	0.5301049	1
O5	O	1	0.4666525	0.5333475	0.4698951	1
O6	O	1	0.4666525	0.5333475	0.5301049	1
O7	O	1	0.5333475	0.5333475	0.4698951	1
O8	O	1	0.5333475	0.5333475	0.5301049	1

O9	O	1	0.5950757	0.5000000	0.5508879	1
O10	O	1	0.5950757	0.4449902	0.5000000	1
O11	O	1	0.5950757	0.5000000	0.4491121	1
O12	O	1	0.5950757	0.5550098	0.5000000	1
O13	O	1	0.5000000	0.5950757	0.5508879	1
O14	O	1	0.5550098	0.5950757	0.5000000	1
O15	O	1	0.5000000	0.5950757	0.4491121	1
O16	O	1	0.4449902	0.5950757	0.5000000	1
O17	O	1	0.4049243	0.5000000	0.5508879	1
O18	O	1	0.4049243	0.5550098	0.5000000	1
O19	O	1	0.4049243	0.5000000	0.4491121	1
O20	O	1	0.4049243	0.4449902	0.5000000	1
O21	O	1	0.5000000	0.4049243	0.5508879	1
O22	O	1	0.4449902	0.4049243	0.5000000	1
O23	O	1	0.5000000	0.4049243	0.4491121	1
O24	O	1	0.5550098	0.4049243	0.5000000	1
O25	O	1	0.5550098	0.5000000	0.5879517	1
O26	O	1	0.5000000	0.5550098	0.5879517	1
O27	O	1	0.4449902	0.5000000	0.5879517	1
O28	O	1	0.5000000	0.4449902	0.5879517	1
O29	O	1	0.5550098	0.5000000	0.4120483	1
O30	O	1	0.5000000	0.4449902	0.4120483	1
O31	O	1	0.4449902	0.5000000	0.4120483	1
O32	O	1	0.5000000	0.5550098	0.4120483	1
Zr1	Zr	1	0.5661032	0.5000000	0.5000000	1
Zr2	Zr	1	0.5000000	0.5661032	0.5000000	1
Zr3	Zr	1	0.4338968	0.5000000	0.5000000	1
Zr4	Zr	1	0.5000000	0.4338968	0.5000000	1
Zr5	Zr	1	0.5000000	0.5000000	0.5611501	1
Zr6	Zr	1	0.5000000	0.5000000	0.4388499	1

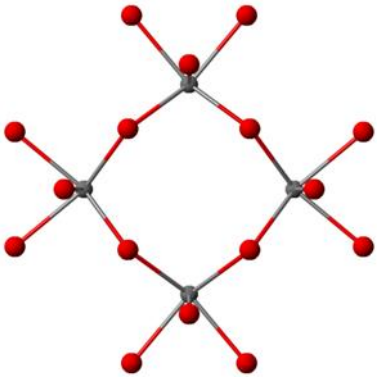

Figure 207: The tetrameric structure resulting from the chandelier core refinement of ZAA25 from the 15-month data collection.

Table 150: The atomic coordinates of the tetrameric phase of the chandelier core refinement of ZAA25 from the 15-month data collection.

Atom Label	Atom Type	Multiplicity	Fractional X Coordinate	Fractional Y Coordinate	Fractional Z Coordinate	Fractional Occupancy
O1	O	1	0.5149313	0.4850687	0.470665	1
O2	O	1	0.4850687	0.4850687	0.529335	1
O3	O	1	0.5149313	0.5149313	0.529335	1
O4	O	1	0.4850687	0.5149313	0.470665	1
O5	O	1	0.5000000	0.5277351	0.546288	1
O6	O	1	0.5000000	0.4722649	0.546288	1
O7	O	1	0.4722649	0.5000000	0.453712	1
O8	O	1	0.5277351	0.5000000	0.453712	1
O9	O	1	0.5149401	0.4607266	0.5000000	1
O10	O	1	0.4607266	0.4850599	0.5000000	1
O11	O	1	0.5392734	0.5149401	0.5000000	1
O12	O	1	0.4850599	0.5392734	0.5000000	1
O13	O	1	0.4607266	0.5149401	0.5000000	1
O14	O	1	0.5392734	0.4850599	0.5000000	1
O15	O	1	0.4850599	0.4607266	0.5000000	1
O16	O	1	0.5149401	0.5392734	0.5000000	1
O17	O	1	0.5149313	0.4850687	0.529335	1
O18	O	1	0.4850687	0.4850687	0.470665	1
O19	O	1	0.5149313	0.5149313	0.470665	1
O20	O	1	0.4850687	0.5149313	0.529335	1
O21	O	1	0.5000000	0.5277351	0.453712	1
O22	O	1	0.5000000	0.4722649	0.453712	1
O23	O	1	0.4722649	0.5000000	0.546288	1
O24	O	1	0.5277351	0.5000000	0.546288	1
Zr1	Zr	1	0.5000000	0.4755501	0.5000000	1
Zr2	Zr	1	0.4755501	0.5000000	0.5000000	1
Zr3	Zr	1	0.5244499	0.5000000	0.5000000	1
Zr4	Zr	1	0.5000000	0.5244499	0.5000000	1

10.5 December 2020 Data Collection

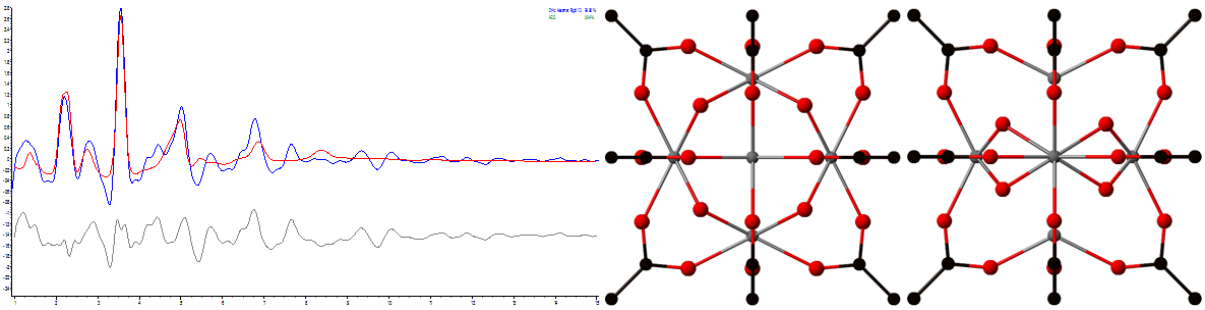

Figure 208: Observed and Calculated PDF from the chandelier core refinement of ZAA1A from the 18-month data collection and the resultant model viewed from the axial (left) and equatorial (right) positions.

Table 151: The atomic coordinates of the model resulting from the chandelier core refinement of ZAA1A from the 18-month data collection.

Atom Label	Atom Type	Multiplicity	Fractional X Coordinate	Fractional Y Coordinate	Fractional Z Coordinate	Fractional Occupancy
C1	C	1	0.5904865	0.5000000	0.5837063	1
C2	C	1	0.5000000	0.4095135	0.5837063	1
C3	C	1	0.4095135	0.5000000	0.5837063	1
C4	C	1	0.5000000	0.5904865	0.5837063	1
C5	C	1	0.5904865	0.5000000	0.4162937	1
C6	C	1	0.5000000	0.4095135	0.4162937	1
C7	C	1	0.4095135	0.5000000	0.4162937	1
C8	C	1	0.5000000	0.5904865	0.4162937	1
C9	C	1	0.5904865	0.4095135	0.5000000	1
C10	C	1	0.4095135	0.4095135	0.5000000	1
C11	C	1	0.4095135	0.5904865	0.5000000	1
C12	C	1	0.5904865	0.5904865	0.5000000	1
C13	C	1	0.619792	0.5000000	0.610816	1
C14	C	1	0.5000000	0.380208	0.610816	1
C15	C	1	0.380208	0.5000000	0.610816	1
C16	C	1	0.5000000	0.619792	0.610816	1
C17	C	1	0.619792	0.5000000	0.389184	1
C18	C	1	0.5000000	0.380208	0.389184	1
C19	C	1	0.380208	0.5000000	0.389184	1
C20	C	1	0.5000000	0.619792	0.389184	1
C21	C	1	0.619792	0.380208	0.5000000	1
C22	C	1	0.380208	0.380208	0.5000000	1
C23	C	1	0.380208	0.619792	0.5000000	1
C24	C	1	0.619792	0.619792	0.5000000	1
O1	O	1	0.5441182	0.4558818	0.4746718	1
O2	O	1	0.5441182	0.4558818	0.5253282	1
O3	O	1	0.4558818	0.4558818	0.4746718	1
O4	O	1	0.4558818	0.4558818	0.5253282	1
O5	O	1	0.4558818	0.5441182	0.4746718	1

O6	O	1	0.4558818	0.5441182	0.5253282	1
O7	O	1	0.5441182	0.5441182	0.4746718	1
O8	O	1	0.5441182	0.5441182	0.5253282	1
O9	O	1	0.5938332	0.5000000	0.5503637	1
O10	O	1	0.5938332	0.4455569	0.5000000	1
O11	O	1	0.5938332	0.5000000	0.4496363	1
O12	O	1	0.5938332	0.5544431	0.5000000	1
O13	O	1	0.5000000	0.5938332	0.5503637	1
O14	O	1	0.5544431	0.5938332	0.5000000	1
O15	O	1	0.5000000	0.5938332	0.4496363	1
O16	O	1	0.4455569	0.5938332	0.5000000	1
O17	O	1	0.4061668	0.5000000	0.5503637	1
O18	O	1	0.4061668	0.5544431	0.5000000	1
O19	O	1	0.4061668	0.5000000	0.4496363	1
O20	O	1	0.4061668	0.4455569	0.5000000	1
O21	O	1	0.5000000	0.4061668	0.5503637	1
O22	O	1	0.4455569	0.4061668	0.5000000	1
O23	O	1	0.5000000	0.4061668	0.4496363	1
O24	O	1	0.5544431	0.4061668	0.5000000	1
O25	O	1	0.5544431	0.5000000	0.5868022	1
O26	O	1	0.5000000	0.5544431	0.5868022	1
O27	O	1	0.4455569	0.5000000	0.5868022	1
O28	O	1	0.5000000	0.4455569	0.5868022	1
O29	O	1	0.5544431	0.5000000	0.4131978	1
O30	O	1	0.5000000	0.4455569	0.4131978	1
O31	O	1	0.4455569	0.5000000	0.4131978	1
O32	O	1	0.5000000	0.5544431	0.4131978	1
Zr1	Zr	1	0.5665743	0.5000000	0.5000000	1
Zr2	Zr	1	0.5000000	0.5665743	0.5000000	1
Zr3	Zr	1	0.4334257	0.5000000	0.5000000	1
Zr4	Zr	1	0.5000000	0.4334257	0.5000000	1
Zr5	Zr	1	0.5000000	0.5000000	0.5615859	1
Zr6	Zr	1	0.5000000	0.5000000	0.4384141	1

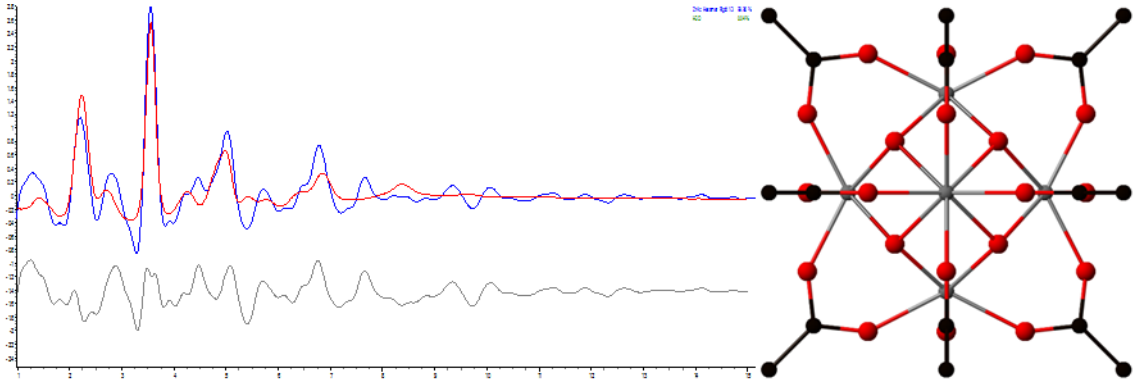

Figure 209: Observed and Calculated PDF from the fixed core refinement of ZAA1A from the 18-month data collection and the resultant model viewed from the axial (left) and equatorial (right) positions.

Table 152: The atomic coordinates of the model resulting from the fixed core refinement of ZAA1A from the 18-month data collection.

Atom Label	Atom Type	Multiplicity	Fractional X Coordinate	Fractional Y Coordinate	Fractional Z Coordinate	Fractional Occupancy
C1	C	1	0.589803	0.5000000	0.5830741	1
C2	C	1	0.5000000	0.410197	0.5830741	1
C3	C	1	0.410197	0.5000000	0.5830741	1
C4	C	1	0.5000000	0.589803	0.5830741	1
C5	C	1	0.589803	0.5000000	0.4169259	1
C6	C	1	0.5000000	0.410197	0.4169259	1
C7	C	1	0.410197	0.5000000	0.4169259	1
C8	C	1	0.5000000	0.589803	0.4169259	1
C9	C	1	0.589803	0.410197	0.5000000	1
C10	C	1	0.410197	0.410197	0.5000000	1
C11	C	1	0.410197	0.589803	0.5000000	1
C12	C	1	0.589803	0.589803	0.5000000	1
C13	C	1	0.6196839	0.5000000	0.610716	1
C14	C	1	0.5000000	0.3803161	0.610716	1
C15	C	1	0.3803161	0.5000000	0.610716	1
C16	C	1	0.5000000	0.6196839	0.610716	1
C17	C	1	0.6196839	0.5000000	0.389284	1
C18	C	1	0.5000000	0.3803161	0.389284	1
C19	C	1	0.3803161	0.5000000	0.389284	1
C20	C	1	0.5000000	0.6196839	0.389284	1
C21	C	1	0.6196839	0.3803161	0.5000000	1
C22	C	1	0.3803161	0.3803161	0.5000000	1
C23	C	1	0.3803161	0.6196839	0.5000000	1
C24	C	1	0.6196839	0.6196839	0.5000000	1
O1	O	1	0.5350087	0.5346671	0.4676145	1
O2	O	1	0.5350087	0.4653329	0.5323855	1
O3	O	1	0.4649913	0.5346671	0.4676145	1
O4	O	1	0.4649913	0.4653329	0.5323855	1
O5	O	1	0.4649913	0.4653329	0.4676145	1
O6	O	1	0.4649913	0.5346671	0.5323855	1

O7	O	1	0.5350087	0.4653329	0.4676145	1
O8	O	1	0.5350087	0.5346671	0.5323855	1
O9	O	1	0.5939613	0.5000000	0.5491125	1
O10	O	1	0.5939613	0.4469094	0.5000000	1
O11	O	1	0.5939613	0.5000000	0.4508875	1
O12	O	1	0.5939613	0.5530906	0.5000000	1
O13	O	1	0.5000000	0.5939613	0.5491125	1
O14	O	1	0.5530906	0.5939613	0.5000000	1
O15	O	1	0.5000000	0.5939613	0.4508875	1
O16	O	1	0.4469094	0.5939613	0.5000000	1
O17	O	1	0.4060387	0.5000000	0.5491125	1
O18	O	1	0.4060387	0.5530906	0.5000000	1
O19	O	1	0.4060387	0.5000000	0.4508875	1
O20	O	1	0.4060387	0.4469094	0.5000000	1
O21	O	1	0.5000000	0.4060387	0.5491125	1
O22	O	1	0.4469094	0.4060387	0.5000000	1
O23	O	1	0.5000000	0.4060387	0.4508875	1
O24	O	1	0.5530906	0.4060387	0.5000000	1
O25	O	1	0.5530906	0.5000000	0.5869208	1
O26	O	1	0.5000000	0.5530906	0.5869208	1
O27	O	1	0.4469094	0.5000000	0.5869208	1
O28	O	1	0.5000000	0.4469094	0.5869208	1
O29	O	1	0.5530906	0.5000000	0.4130792	1
O30	O	1	0.5000000	0.4469094	0.4130792	1
O31	O	1	0.4469094	0.5000000	0.4130792	1
O32	O	1	0.5000000	0.5530906	0.4130792	1
Zr1	Zr	1	0.566611	0.5000000	0.5000000	1
Zr2	Zr	1	0.5000000	0.566611	0.5000000	1
Zr3	Zr	1	0.433389	0.5000000	0.5000000	1
Zr4	Zr	1	0.5000000	0.433389	0.5000000	1
Zr5	Zr	1	0.5000000	0.5000000	0.5616198	1
Zr6	Zr	1	0.5000000	0.5000000	0.4383802	1

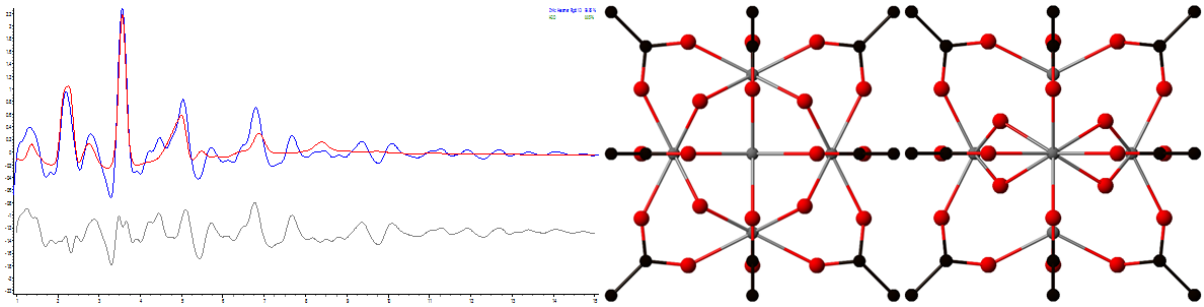

Figure 210: Observed and Calculated PDF from the chandelier core refinement of ZAA1I from the 18-month data collection and the resultant model viewed from the axial (left) and equatorial (right) positions.

Table 153: The atomic coordinates of the model resulting from the chandelier core refinement of ZAA1I from the 18-month data collection.

Atom Label	Atom Type	Multiplicity	Fractional X Coordinate	Fractional Y Coordinate	Fractional Z Coordinate	Fractional Occupancy
C1	C	1	0.5906433	0.5000000	0.5838514	1
C2	C	1	0.5000000	0.4093567	0.5838514	1
C3	C	1	0.4093567	0.5000000	0.5838514	1
C4	C	1	0.5000000	0.5906433	0.5838514	1
C5	C	1	0.5906433	0.5000000	0.4161486	1
C6	C	1	0.5000000	0.4093567	0.4161486	1
C7	C	1	0.4093567	0.5000000	0.4161486	1
C8	C	1	0.5000000	0.5906433	0.4161486	1
C9	C	1	0.5906433	0.4093567	0.5000000	1
C10	C	1	0.4093567	0.4093567	0.5000000	1
C11	C	1	0.4093567	0.5906433	0.5000000	1
C12	C	1	0.5906433	0.5906433	0.5000000	1
C13	C	1	0.6197913	0.5000000	0.6108153	1
C14	C	1	0.5000000	0.3802087	0.6108153	1
C15	C	1	0.3802087	0.5000000	0.6108153	1
C16	C	1	0.5000000	0.6197913	0.6108153	1
C17	C	1	0.6197913	0.5000000	0.3891847	1
C18	C	1	0.5000000	0.3802087	0.3891847	1
C19	C	1	0.3802087	0.5000000	0.3891847	1
C20	C	1	0.5000000	0.6197913	0.3891847	1
C21	C	1	0.6197913	0.3802087	0.5000000	1
C22	C	1	0.3802087	0.3802087	0.5000000	1
C23	C	1	0.3802087	0.6197913	0.5000000	1
C24	C	1	0.6197913	0.6197913	0.5000000	1
O1	O	1	0.5443285	0.4556715	0.474642	1
O2	O	1	0.5443285	0.4556715	0.525358	1
O3	O	1	0.4556715	0.4556715	0.474642	1
O4	O	1	0.4556715	0.4556715	0.525358	1
O5	O	1	0.4556715	0.5443285	0.474642	1
O6	O	1	0.4556715	0.5443285	0.525358	1
O7	O	1	0.5443285	0.5443285	0.474642	1
O8	O	1	0.5443285	0.5443285	0.525358	1

O9	O	1	0.5942871	0.5000000	0.5504694	1
O10	O	1	0.5942871	0.4454426	0.5000000	1
O11	O	1	0.5942871	0.5000000	0.4495306	1
O12	O	1	0.5942871	0.5545574	0.5000000	1
O13	O	1	0.5000000	0.5942871	0.5504694	1
O14	O	1	0.5545574	0.5942871	0.5000000	1
O15	O	1	0.5000000	0.5942871	0.4495306	1
O16	O	1	0.4454426	0.5942871	0.5000000	1
O17	O	1	0.4057129	0.5000000	0.5504694	1
O18	O	1	0.4057129	0.5545574	0.5000000	1
O19	O	1	0.4057129	0.5000000	0.4495306	1
O20	O	1	0.4057129	0.4454426	0.5000000	1
O21	O	1	0.5000000	0.4057129	0.5504694	1
O22	O	1	0.4454426	0.4057129	0.5000000	1
O23	O	1	0.5000000	0.4057129	0.4495306	1
O24	O	1	0.5545574	0.4057129	0.5000000	1
O25	O	1	0.5545574	0.5000000	0.5872221	1
O26	O	1	0.5000000	0.5545574	0.5872221	1
O27	O	1	0.4454426	0.5000000	0.5872221	1
O28	O	1	0.5000000	0.4454426	0.5872221	1
O29	O	1	0.5545574	0.5000000	0.4127779	1
O30	O	1	0.5000000	0.4454426	0.4127779	1
O31	O	1	0.4454426	0.5000000	0.4127779	1
O32	O	1	0.5000000	0.5545574	0.4127779	1
Zr1	Zr	1	0.5667941	0.5000000	0.5000000	1
Zr2	Zr	1	0.5000000	0.5667941	0.5000000	1
Zr3	Zr	1	0.4332059	0.5000000	0.5000000	1
Zr4	Zr	1	0.5000000	0.4332059	0.5000000	1
Zr5	Zr	1	0.5000000	0.5000000	0.5617892	1
Zr6	Zr	1	0.5000000	0.5000000	0.4382108	1

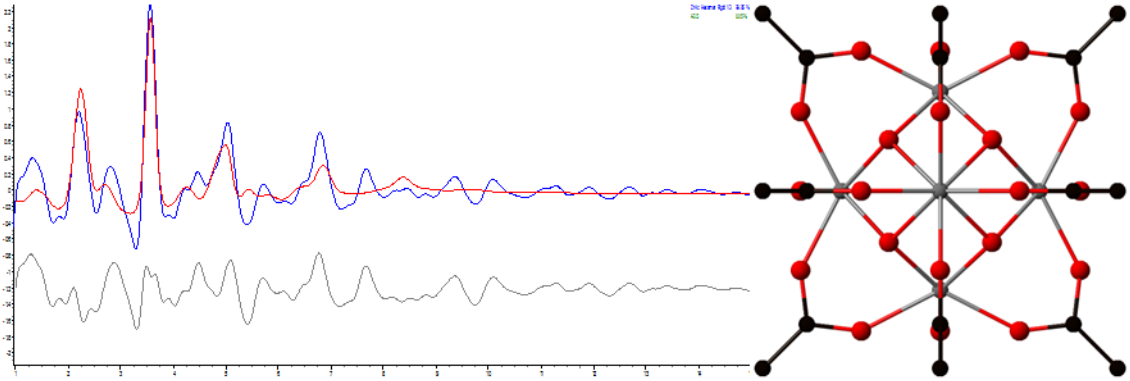

Figure 211: Observed and Calculated PDF from the fixed core refinement of ZAA1I from the 18-month data collection and the resultant model viewed from the axial (left) and equatorial (right) positions.

Table 154: The atomic coordinates of the model resulting from the fixed core refinement of ZAA1I from the 18-month data collection.

Atom Label	Atom Type	Multiplicity	Fractional X Coordinate	Fractional Y Coordinate	Fractional Z Coordinate	Fractional Occupancy
C1	C	1	0.5899878	0.5000000	0.583245	1
C2	C	1	0.5000000	0.4100122	0.583245	1
C3	C	1	0.4100122	0.5000000	0.583245	1
C4	C	1	0.5000000	0.5899878	0.583245	1
C5	C	1	0.5899878	0.5000000	0.416755	1
C6	C	1	0.5000000	0.4100122	0.416755	1
C7	C	1	0.4100122	0.5000000	0.416755	1
C8	C	1	0.5000000	0.5899878	0.416755	1
C9	C	1	0.5899878	0.4100122	0.5000000	1
C10	C	1	0.4100122	0.4100122	0.5000000	1
C11	C	1	0.4100122	0.5899878	0.5000000	1
C12	C	1	0.5899878	0.5899878	0.5000000	1
C13	C	1	0.6197203	0.5000000	0.6107496	1
C14	C	1	0.5000000	0.3802797	0.6107496	1
C15	C	1	0.3802797	0.5000000	0.6107496	1
C16	C	1	0.5000000	0.6197203	0.6107496	1
C17	C	1	0.6197203	0.5000000	0.3892504	1
C18	C	1	0.5000000	0.3802797	0.3892504	1
C19	C	1	0.3802797	0.5000000	0.3892504	1
C20	C	1	0.5000000	0.6197203	0.3892504	1
C21	C	1	0.6197203	0.3802797	0.5000000	1
C22	C	1	0.3802797	0.3802797	0.5000000	1
C23	C	1	0.3802797	0.6197203	0.5000000	1
C24	C	1	0.6197203	0.6197203	0.5000000	1
O1	O	1	0.5349199	0.5345792	0.4676967	1
O2	O	1	0.5349199	0.4654208	0.5323033	1
O3	O	1	0.4650801	0.5345792	0.4676967	1
O4	O	1	0.4650801	0.4654208	0.5323033	1
O5	O	1	0.4650801	0.4654208	0.4676967	1
O6	O	1	0.4650801	0.5345792	0.5323033	1

O7	O	1	0.5349199	0.4654208	0.4676967	1
O8	O	1	0.5349199	0.5345792	0.5323033	1
O9	O	1	0.5944224	0.5000000	0.5494418	1
O10	O	1	0.5944224	0.4465534	0.5000000	1
O11	O	1	0.5944224	0.5000000	0.4505582	1
O12	O	1	0.5944224	0.5534466	0.5000000	1
O13	O	1	0.5000000	0.5944224	0.5494418	1
O14	O	1	0.5534466	0.5944224	0.5000000	1
O15	O	1	0.5000000	0.5944224	0.4505582	1
O16	O	1	0.4465534	0.5944224	0.5000000	1
O17	O	1	0.4055776	0.5000000	0.5494418	1
O18	O	1	0.4055776	0.5534466	0.5000000	1
O19	O	1	0.4055776	0.5000000	0.4505582	1
O20	O	1	0.4055776	0.4465534	0.5000000	1
O21	O	1	0.5000000	0.4055776	0.5494418	1
O22	O	1	0.4465534	0.4055776	0.5000000	1
O23	O	1	0.5000000	0.4055776	0.4505582	1
O24	O	1	0.5534466	0.4055776	0.5000000	1
O25	O	1	0.5534466	0.5000000	0.5873473	1
O26	O	1	0.5000000	0.5534466	0.5873473	1
O27	O	1	0.4465534	0.5000000	0.5873473	1
O28	O	1	0.5000000	0.4465534	0.5873473	1
O29	O	1	0.5534466	0.5000000	0.4126527	1
O30	O	1	0.5000000	0.4465534	0.4126527	1
O31	O	1	0.4465534	0.5000000	0.4126527	1
O32	O	1	0.5000000	0.5534466	0.4126527	1
Zr1	Zr	1	0.5668547	0.5000000	0.5000000	1
Zr2	Zr	1	0.5000000	0.5668547	0.5000000	1
Zr3	Zr	1	0.4331453	0.5000000	0.5000000	1
Zr4	Zr	1	0.5000000	0.4331453	0.5000000	1
Zr5	Zr	1	0.5000000	0.5000000	0.5618452	1
Zr6	Zr	1	0.5000000	0.5000000	0.4381548	1

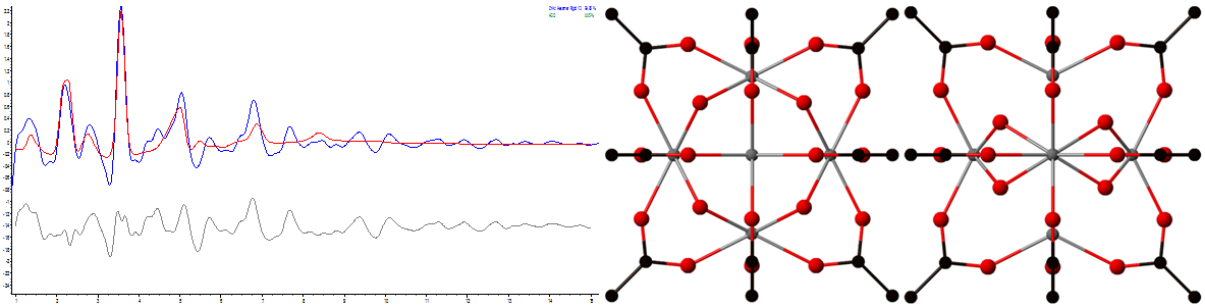

Figure 212: Observed and Calculated PDF from the chandelier core refinement of ZAA4A from the 18-month data collection and the resultant model viewed from the axial (left) and equatorial (right) positions.

Table 155: The atomic coordinates of the model resulting from the chandelier core refinement of ZAA4A from the 18-month data collection.

Atom Label	Atom Type	Multiplicity	Fractional X Coordinate	Fractional Y Coordinate	Fractional Z Coordinate	Fractional Occupancy
C1	C	1	0.5906433	0.5000000	0.5838514	1
C2	C	1	0.5000000	0.4093567	0.5838514	1
C3	C	1	0.4093567	0.5000000	0.5838514	1
C4	C	1	0.5000000	0.5906433	0.5838514	1
C5	C	1	0.5906433	0.5000000	0.4161486	1
C6	C	1	0.5000000	0.4093567	0.4161486	1
C7	C	1	0.4093567	0.5000000	0.4161486	1
C8	C	1	0.5000000	0.5906433	0.4161486	1
C9	C	1	0.5906433	0.4093567	0.5000000	1
C10	C	1	0.4093567	0.4093567	0.5000000	1
C11	C	1	0.4093567	0.5906433	0.5000000	1
C12	C	1	0.5906433	0.5906433	0.5000000	1
C13	C	1	0.6197913	0.5000000	0.6108153	1
C14	C	1	0.5000000	0.3802087	0.6108153	1
C15	C	1	0.3802087	0.5000000	0.6108153	1
C16	C	1	0.5000000	0.6197913	0.6108153	1
C17	C	1	0.6197913	0.5000000	0.3891847	1
C18	C	1	0.5000000	0.3802087	0.3891847	1
C19	C	1	0.3802087	0.5000000	0.3891847	1
C20	C	1	0.5000000	0.6197913	0.3891847	1
C21	C	1	0.6197913	0.3802087	0.5000000	1
C22	C	1	0.3802087	0.3802087	0.5000000	1
C23	C	1	0.3802087	0.6197913	0.5000000	1
C24	C	1	0.6197913	0.6197913	0.5000000	1
O1	O	1	0.5443285	0.4556715	0.474642	1
O2	O	1	0.5443285	0.4556715	0.525358	1
O3	O	1	0.4556715	0.4556715	0.474642	1
O4	O	1	0.4556715	0.4556715	0.525358	1
O5	O	1	0.4556715	0.5443285	0.474642	1
O6	O	1	0.4556715	0.5443285	0.525358	1
O7	O	1	0.5443285	0.5443285	0.474642	1
O8	O	1	0.5443285	0.5443285	0.525358	1

O9	O	1	0.5942871	0.5000000	0.5504694	1
O10	O	1	0.5942871	0.4454426	0.5000000	1
O11	O	1	0.5942871	0.5000000	0.4495306	1
O12	O	1	0.5942871	0.5545574	0.5000000	1
O13	O	1	0.5000000	0.5942871	0.5504694	1
O14	O	1	0.5545574	0.5942871	0.5000000	1
O15	O	1	0.5000000	0.5942871	0.4495306	1
O16	O	1	0.4454426	0.5942871	0.5000000	1
O17	O	1	0.4057129	0.5000000	0.5504694	1
O18	O	1	0.4057129	0.5545574	0.5000000	1
O19	O	1	0.4057129	0.5000000	0.4495306	1
O20	O	1	0.4057129	0.4454426	0.5000000	1
O21	O	1	0.5000000	0.4057129	0.5504694	1
O22	O	1	0.4454426	0.4057129	0.5000000	1
O23	O	1	0.5000000	0.4057129	0.4495306	1
O24	O	1	0.5545574	0.4057129	0.5000000	1
O25	O	1	0.5545574	0.5000000	0.5872221	1
O26	O	1	0.5000000	0.5545574	0.5872221	1
O27	O	1	0.4454426	0.5000000	0.5872221	1
O28	O	1	0.5000000	0.4454426	0.5872221	1
O29	O	1	0.5545574	0.5000000	0.4127779	1
O30	O	1	0.5000000	0.4454426	0.4127779	1
O31	O	1	0.4454426	0.5000000	0.4127779	1
O32	O	1	0.5000000	0.5545574	0.4127779	1
Zr1	Zr	1	0.5667941	0.5000000	0.5000000	1
Zr2	Zr	1	0.5000000	0.5667941	0.5000000	1
Zr3	Zr	1	0.4332059	0.5000000	0.5000000	1
Zr4	Zr	1	0.5000000	0.4332059	0.5000000	1
Zr5	Zr	1	0.5000000	0.5000000	0.5617892	1
Zr6	Zr	1	0.5000000	0.5000000	0.4382108	1

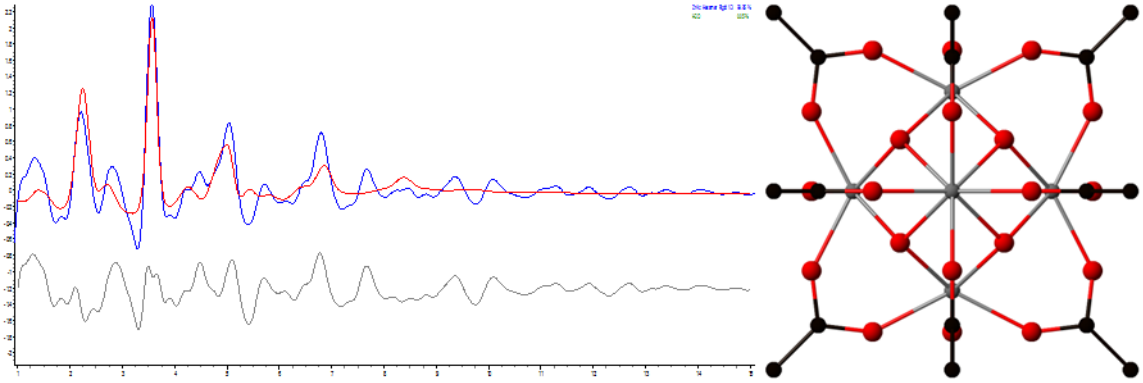

Figure 213: Observed and Calculated PDF from the fixed core refinement of ZAA4A from the 18-month data collection and the resultant model viewed from the axial (left) and equatorial (right) positions.

Table 156: The atomic coordinates of the model resulting from the fixed core refinement of ZAA4A from the 18-month data collection.

Atom Label	Atom Type	Multiplicity	Fractional X Coordinate	Fractional Y Coordinate	Fractional Z Coordinate	Fractional Occupancy
C1	C	1	0.5899878	0.5000000	0.583245	1
C2	C	1	0.5000000	0.4100122	0.583245	1
C3	C	1	0.4100122	0.5000000	0.583245	1
C4	C	1	0.5000000	0.5899878	0.583245	1
C5	C	1	0.5899878	0.5000000	0.416755	1
C6	C	1	0.5000000	0.4100122	0.416755	1
C7	C	1	0.4100122	0.5000000	0.416755	1
C8	C	1	0.5000000	0.5899878	0.416755	1
C9	C	1	0.5899878	0.4100122	0.5000000	1
C10	C	1	0.4100122	0.4100122	0.5000000	1
C11	C	1	0.4100122	0.5899878	0.5000000	1
C12	C	1	0.5899878	0.5899878	0.5000000	1
C13	C	1	0.6197203	0.5000000	0.6107496	1
C14	C	1	0.5000000	0.3802797	0.6107496	1
C15	C	1	0.3802797	0.5000000	0.6107496	1
C16	C	1	0.5000000	0.6197203	0.6107496	1
C17	C	1	0.6197203	0.5000000	0.3892504	1
C18	C	1	0.5000000	0.3802797	0.3892504	1
C19	C	1	0.3802797	0.5000000	0.3892504	1
C20	C	1	0.5000000	0.6197203	0.3892504	1
C21	C	1	0.6197203	0.3802797	0.5000000	1
C22	C	1	0.3802797	0.3802797	0.5000000	1
C23	C	1	0.3802797	0.6197203	0.5000000	1
C24	C	1	0.6197203	0.6197203	0.5000000	1
O1	O	1	0.5349199	0.5345792	0.4676967	1
O2	O	1	0.5349199	0.4654208	0.5323033	1
O3	O	1	0.4650801	0.5345792	0.4676967	1
O4	O	1	0.4650801	0.4654208	0.5323033	1
O5	O	1	0.4650801	0.4654208	0.4676967	1
O6	O	1	0.4650801	0.5345792	0.5323033	1

O7	O	1	0.5349199	0.4654208	0.4676967	1
O8	O	1	0.5349199	0.5345792	0.5323033	1
O9	O	1	0.5944224	0.5000000	0.5494418	1
O10	O	1	0.5944224	0.4465534	0.5000000	1
O11	O	1	0.5944224	0.5000000	0.4505582	1
O12	O	1	0.5944224	0.5534466	0.5000000	1
O13	O	1	0.5000000	0.5944224	0.5494418	1
O14	O	1	0.5534466	0.5944224	0.5000000	1
O15	O	1	0.5000000	0.5944224	0.4505582	1
O16	O	1	0.4465534	0.5944224	0.5000000	1
O17	O	1	0.4055776	0.5000000	0.5494418	1
O18	O	1	0.4055776	0.5534466	0.5000000	1
O19	O	1	0.4055776	0.5000000	0.4505582	1
O20	O	1	0.4055776	0.4465534	0.5000000	1
O21	O	1	0.5000000	0.4055776	0.5494418	1
O22	O	1	0.4465534	0.4055776	0.5000000	1
O23	O	1	0.5000000	0.4055776	0.4505582	1
O24	O	1	0.5534466	0.4055776	0.5000000	1
O25	O	1	0.5534466	0.5000000	0.5873473	1
O26	O	1	0.5000000	0.5534466	0.5873473	1
O27	O	1	0.4465534	0.5000000	0.5873473	1
O28	O	1	0.5000000	0.4465534	0.5873473	1
O29	O	1	0.5534466	0.5000000	0.4126527	1
O30	O	1	0.5000000	0.4465534	0.4126527	1
O31	O	1	0.4465534	0.5000000	0.4126527	1
O32	O	1	0.5000000	0.5534466	0.4126527	1
Zr1	Zr	1	0.5668547	0.5000000	0.5000000	1
Zr2	Zr	1	0.5000000	0.5668547	0.5000000	1
Zr3	Zr	1	0.4331453	0.5000000	0.5000000	1
Zr4	Zr	1	0.5000000	0.4331453	0.5000000	1
Zr5	Zr	1	0.5000000	0.5000000	0.5618452	1
Zr6	Zr	1	0.5000000	0.5000000	0.4381548	1

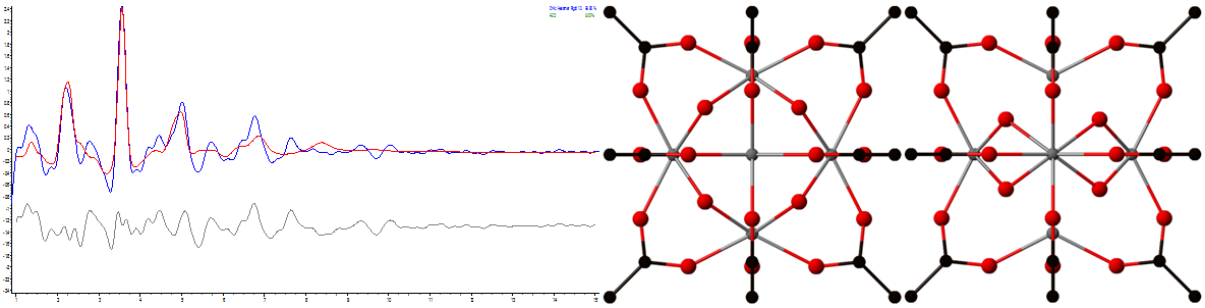

Figure 214: Observed and Calculated PDF from the chandelier core refinement of ZAA4C from the 18-month data collection and the resultant model viewed from the axial (left) and equatorial (right) positions.

Table 157: The atomic coordinates of the model resulting from the chandelier core refinement of ZAA4C from the 18-month data collection.

Atom Label	Atom Type	Multiplicity	Fractional X Coordinate	Fractional Y Coordinate	Fractional Z Coordinate	Fractional Occupancy
C1	C	1	0.5901243	0.5000000	0.5833712	1
C2	C	1	0.5000000	0.4098757	0.5833712	1
C3	C	1	0.4098757	0.5000000	0.5833712	1
C4	C	1	0.5000000	0.5901243	0.5833712	1
C5	C	1	0.5901243	0.5000000	0.4166288	1
C6	C	1	0.5000000	0.4098757	0.4166288	1
C7	C	1	0.4098757	0.5000000	0.4166288	1
C8	C	1	0.5000000	0.5901243	0.4166288	1
C9	C	1	0.5901243	0.4098757	0.5000000	1
C10	C	1	0.4098757	0.4098757	0.5000000	1
C11	C	1	0.4098757	0.5901243	0.5000000	1
C12	C	1	0.5901243	0.5901243	0.5000000	1
C13	C	1	0.6197597	0.5000000	0.6107861	1
C14	C	1	0.5000000	0.3802403	0.6107861	1
C15	C	1	0.3802403	0.5000000	0.6107861	1
C16	C	1	0.5000000	0.6197597	0.6107861	1
C17	C	1	0.6197597	0.5000000	0.3892139	1
C18	C	1	0.5000000	0.3802403	0.3892139	1
C19	C	1	0.3802403	0.5000000	0.3892139	1
C20	C	1	0.5000000	0.6197597	0.3892139	1
C21	C	1	0.6197597	0.3802403	0.5000000	1
C22	C	1	0.3802403	0.3802403	0.5000000	1
C23	C	1	0.3802403	0.6197597	0.5000000	1
C24	C	1	0.6197597	0.6197597	0.5000000	1
O1	O	1	0.5395779	0.4604221	0.4727339	1
O2	O	1	0.5395779	0.4604221	0.5272661	1
O3	O	1	0.4604221	0.4604221	0.4727339	1
O4	O	1	0.4604221	0.4604221	0.5272661	1
O5	O	1	0.4604221	0.5395779	0.4727339	1
O6	O	1	0.4604221	0.5395779	0.5272661	1
O7	O	1	0.5395779	0.5395779	0.4727339	1
O8	O	1	0.5395779	0.5395779	0.5272661	1

O9	O	1	0.5939983	0.5000000	0.5498183	1
O10	O	1	0.5939983	0.4461464	0.5000000	1
O11	O	1	0.5939983	0.5000000	0.4501817	1
O12	O	1	0.5939983	0.5538536	0.5000000	1
O13	O	1	0.5000000	0.5939983	0.5498183	1
O14	O	1	0.5538536	0.5939983	0.5000000	1
O15	O	1	0.5000000	0.5939983	0.4501817	1
O16	O	1	0.4461464	0.5939983	0.5000000	1
O17	O	1	0.4060017	0.5000000	0.5498183	1
O18	O	1	0.4060017	0.5538536	0.5000000	1
O19	O	1	0.4060017	0.5000000	0.4501817	1
O20	O	1	0.4060017	0.4461464	0.5000000	1
O21	O	1	0.5000000	0.4060017	0.5498183	1
O22	O	1	0.4461464	0.4060017	0.5000000	1
O23	O	1	0.5000000	0.4060017	0.4501817	1
O24	O	1	0.5538536	0.4060017	0.5000000	1
O25	O	1	0.5538536	0.5000000	0.586955	1
O26	O	1	0.5000000	0.5538536	0.586955	1
O27	O	1	0.4461464	0.5000000	0.586955	1
O28	O	1	0.5000000	0.4461464	0.586955	1
O29	O	1	0.5538536	0.5000000	0.413045	1
O30	O	1	0.5000000	0.4461464	0.413045	1
O31	O	1	0.4461464	0.5000000	0.413045	1
O32	O	1	0.5000000	0.5538536	0.413045	1
Zr1	Zr	1	0.5665337	0.5000000	0.5000000	1
Zr2	Zr	1	0.5000000	0.5665337	0.5000000	1
Zr3	Zr	1	0.4334663	0.5000000	0.5000000	1
Zr4	Zr	1	0.5000000	0.4334663	0.5000000	1
Zr5	Zr	1	0.5000000	0.5000000	0.5615483	1
Zr6	Zr	1	0.5000000	0.5000000	0.4384517	1

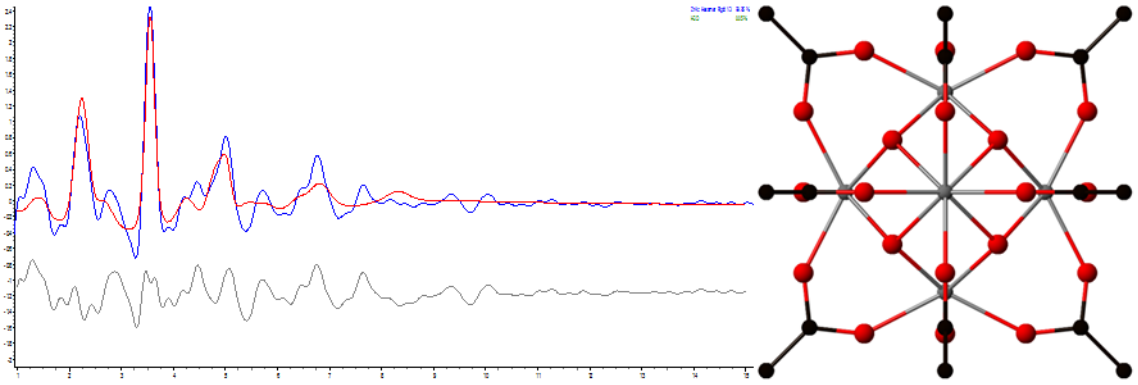

Figure 215: Observed and Calculated PDF from the fixed core refinement of ZAA4C from the 18-month data collection and the resultant model.

Table 158: The atomic coordinates of the model resulting from the fixed core refinement of ZAA4C from the 18-month data collection.

Atom Label	Atom Type	Multiplicity	Fractional X Coordinate	Fractional Y Coordinate	Fractional Z Coordinate	Fractional Occupancy
C1	C	1	0.5901081	0.5000000	0.5833562	1
C2	C	1	0.5000000	0.4098919	0.5833562	1
C3	C	1	0.4098919	0.5000000	0.5833562	1
C4	C	1	0.5000000	0.5901081	0.5833562	1
C5	C	1	0.5901081	0.5000000	0.4166438	1
C6	C	1	0.5000000	0.4098919	0.4166438	1
C7	C	1	0.4098919	0.5000000	0.4166438	1
C8	C	1	0.5000000	0.5901081	0.4166438	1
C9	C	1	0.5901081	0.4098919	0.5000000	1
C10	C	1	0.4098919	0.4098919	0.5000000	1
C11	C	1	0.4098919	0.5901081	0.5000000	1
C12	C	1	0.5901081	0.5901081	0.5000000	1
C13	C	1	0.6186975	0.5000000	0.6098035	1
C14	C	1	0.5000000	0.3813025	0.6098035	1
C15	C	1	0.3813025	0.5000000	0.6098035	1
C16	C	1	0.5000000	0.6186975	0.6098035	1
C17	C	1	0.6186975	0.5000000	0.3901965	1
C18	C	1	0.5000000	0.3813025	0.3901965	1
C19	C	1	0.3813025	0.5000000	0.3901965	1
C20	C	1	0.5000000	0.6186975	0.3901965	1
C21	C	1	0.6186975	0.3813025	0.5000000	1
C22	C	1	0.3813025	0.3813025	0.5000000	1
C23	C	1	0.3813025	0.6186975	0.5000000	1
C24	C	1	0.6186975	0.6186975	0.5000000	1
O1	O	1	0.5350741	0.5347319	0.467554	1
O2	O	1	0.5350741	0.4652681	0.532446	1
O3	O	1	0.4649259	0.5347319	0.467554	1
O4	O	1	0.4649259	0.4652681	0.532446	1
O5	O	1	0.4649259	0.4652681	0.467554	1
O6	O	1	0.4649259	0.5347319	0.532446	1

O7	O	1	0.5350741	0.4652681	0.467554	1
O8	O	1	0.5350741	0.5347319	0.532446	1
O9	O	1	0.5941623	0.5000000	0.5496527	1
O10	O	1	0.5941623	0.4463254	0.5000000	1
O11	O	1	0.5941623	0.5000000	0.4503473	1
O12	O	1	0.5941623	0.5536746	0.5000000	1
O13	O	1	0.5000000	0.5941623	0.5496527	1
O14	O	1	0.5536746	0.5941623	0.5000000	1
O15	O	1	0.5000000	0.5941623	0.4503473	1
O16	O	1	0.4463254	0.5941623	0.5000000	1
O17	O	1	0.4058377	0.5000000	0.5496527	1
O18	O	1	0.4058377	0.5536746	0.5000000	1
O19	O	1	0.4058377	0.5000000	0.4503473	1
O20	O	1	0.4058377	0.4463254	0.5000000	1
O21	O	1	0.5000000	0.4058377	0.5496527	1
O22	O	1	0.4463254	0.4058377	0.5000000	1
O23	O	1	0.5000000	0.4058377	0.4503473	1
O24	O	1	0.5536746	0.4058377	0.5000000	1
O25	O	1	0.5536746	0.5000000	0.5871067	1
O26	O	1	0.5000000	0.5536746	0.5871067	1
O27	O	1	0.4463254	0.5000000	0.5871067	1
O28	O	1	0.5000000	0.4463254	0.5871067	1
O29	O	1	0.5536746	0.5000000	0.4128933	1
O30	O	1	0.5000000	0.4463254	0.4128933	1
O31	O	1	0.4463254	0.5000000	0.4128933	1
O32	O	1	0.5000000	0.5536746	0.4128933	1
Zr1	Zr	1	0.566499	0.5000000	0.5000000	1
Zr2	Zr	1	0.5000000	0.566499	0.5000000	1
Zr3	Zr	1	0.433501	0.5000000	0.5000000	1
Zr4	Zr	1	0.5000000	0.433501	0.5000000	1
Zr5	Zr	1	0.5000000	0.5000000	0.5615162	1
Zr6	Zr	1	0.5000000	0.5000000	0.4384838	1

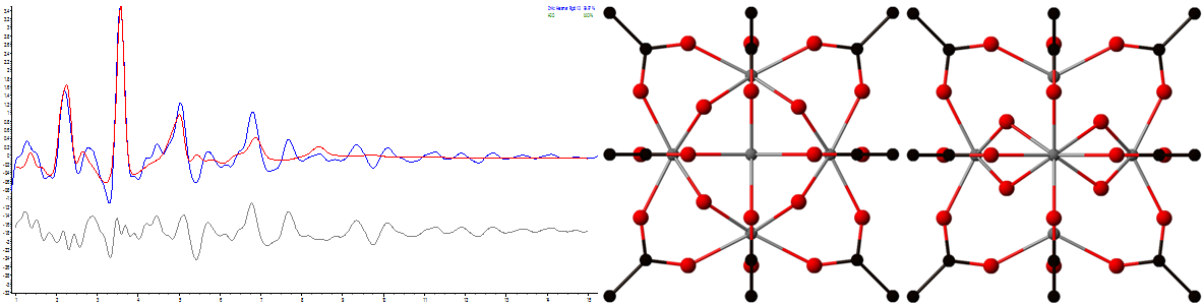

Figure 216: Observed and Calculated PDF from the chandelier core refinement of ZAA4I from the 18-month data collection and the resultant model viewed from the axial (left) and equatorial (right) positions.

Table 159: The atomic coordinates of the model resulting from the chandelier core refinement of ZAA4I from the 18-month data collection.

Atom Label	Atom Type	Multiplicity	Fractional X Coordinate	Fractional Y Coordinate	Fractional Z Coordinate	Fractional Occupancy
C1	C	1	0.5898395	0.5000000	0.5831078	1
C2	C	1	0.5000000	0.4101605	0.5831078	1
C3	C	1	0.4101605	0.5000000	0.5831078	1
C4	C	1	0.5000000	0.5898395	0.5831078	1
C5	C	1	0.5898395	0.5000000	0.4168922	1
C6	C	1	0.5000000	0.4101605	0.4168922	1
C7	C	1	0.4101605	0.5000000	0.4168922	1
C8	C	1	0.5000000	0.5898395	0.4168922	1
C9	C	1	0.5898395	0.4101605	0.5000000	1
C10	C	1	0.4101605	0.4101605	0.5000000	1
C11	C	1	0.4101605	0.5898395	0.5000000	1
C12	C	1	0.5898395	0.5898395	0.5000000	1
C13	C	1	0.620353	0.5000000	0.611335	1
C14	C	1	0.5000000	0.379647	0.611335	1
C15	C	1	0.379647	0.5000000	0.611335	1
C16	C	1	0.5000000	0.620353	0.611335	1
C17	C	1	0.620353	0.5000000	0.388665	1
C18	C	1	0.5000000	0.379647	0.388665	1
C19	C	1	0.379647	0.5000000	0.388665	1
C20	C	1	0.5000000	0.620353	0.388665	1
C21	C	1	0.620353	0.379647	0.5000000	1
C22	C	1	0.379647	0.379647	0.5000000	1
C23	C	1	0.379647	0.620353	0.5000000	1
C24	C	1	0.620353	0.620353	0.5000000	1
O1	O	1	0.5402856	0.4597144	0.4738453	1
O2	O	1	0.5402856	0.4597144	0.5261547	1
O3	O	1	0.4597144	0.4597144	0.4738453	1
O4	O	1	0.4597144	0.4597144	0.5261547	1
O5	O	1	0.4597144	0.5402856	0.4738453	1
O6	O	1	0.4597144	0.5402856	0.5261547	1
O7	O	1	0.5402856	0.5402856	0.4738453	1
O8	O	1	0.5402856	0.5402856	0.5261547	1

O9	O	1	0.5943067	0.5000000	0.5497298	1
O10	O	1	0.5943067	0.4462421	0.5000000	1
O11	O	1	0.5943067	0.5000000	0.4502702	1
O12	O	1	0.5943067	0.5537579	0.5000000	1
O13	O	1	0.5000000	0.5943067	0.5497298	1
O14	O	1	0.5537579	0.5943067	0.5000000	1
O15	O	1	0.5000000	0.5943067	0.4502702	1
O16	O	1	0.4462421	0.5943067	0.5000000	1
O17	O	1	0.4056933	0.5000000	0.5497298	1
O18	O	1	0.4056933	0.5537579	0.5000000	1
O19	O	1	0.4056933	0.5000000	0.4502702	1
O20	O	1	0.4056933	0.4462421	0.5000000	1
O21	O	1	0.5000000	0.4056933	0.5497298	1
O22	O	1	0.4462421	0.4056933	0.5000000	1
O23	O	1	0.5000000	0.4056933	0.4502702	1
O24	O	1	0.5537579	0.4056933	0.5000000	1
O25	O	1	0.5537579	0.5000000	0.5872403	1
O26	O	1	0.5000000	0.5537579	0.5872403	1
O27	O	1	0.4462421	0.5000000	0.5872403	1
O28	O	1	0.5000000	0.4462421	0.5872403	1
O29	O	1	0.5537579	0.5000000	0.4127597	1
O30	O	1	0.5000000	0.4462421	0.4127597	1
O31	O	1	0.4462421	0.5000000	0.4127597	1
O32	O	1	0.5000000	0.5537579	0.4127597	1
Zr1	Zr	1	0.5668925	0.5000000	0.5000000	1
Zr2	Zr	1	0.5000000	0.5668925	0.5000000	1
Zr3	Zr	1	0.4331075	0.5000000	0.5000000	1
Zr4	Zr	1	0.5000000	0.4331075	0.5000000	1
Zr5	Zr	1	0.5000000	0.5000000	0.5618802	1
Zr6	Zr	1	0.5000000	0.5000000	0.4381198	1

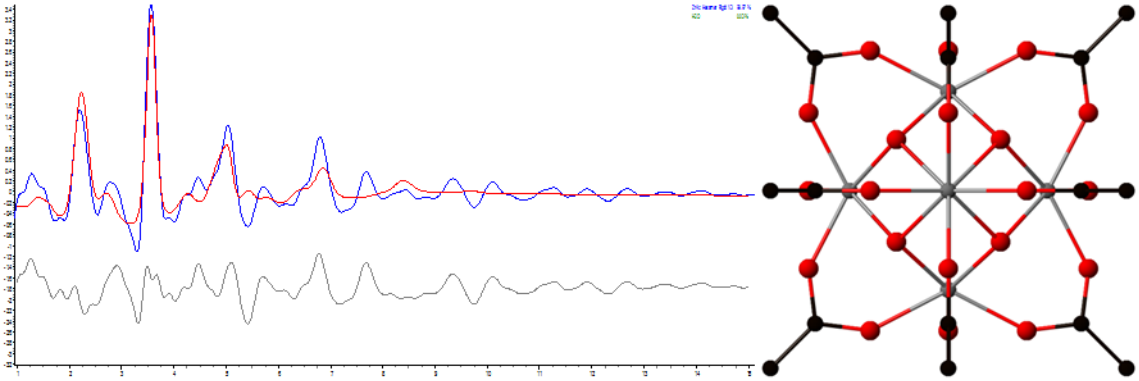

Figure 217: Observed and Calculated PDF from the fixed core refinement of ZAA4I from the 18-month data collection and the resultant model.

Table 160: The atomic coordinates of the model resulting from the fixed core refinement of ZAA4I from the 18-month data collection.

Atom Label	Atom Type	Multiplicity	Fractional X Coordinate	Fractional Y Coordinate	Fractional Z Coordinate	Fractional Occupancy
C1	C	1	0.5897236	0.5000000	0.5830006	1
C2	C	1	0.5000000	0.4102764	0.5830006	1
C3	C	1	0.4102764	0.5000000	0.5830006	1
C4	C	1	0.5000000	0.5897236	0.5830006	1
C5	C	1	0.5897236	0.5000000	0.4169994	1
C6	C	1	0.5000000	0.4102764	0.4169994	1
C7	C	1	0.4102764	0.5000000	0.4169994	1
C8	C	1	0.5000000	0.5897236	0.4169994	1
C9	C	1	0.5897236	0.4102764	0.5000000	1
C10	C	1	0.4102764	0.4102764	0.5000000	1
C11	C	1	0.4102764	0.5897236	0.5000000	1
C12	C	1	0.5897236	0.5897236	0.5000000	1
C13	C	1	0.619945	0.5000000	0.6109575	1
C14	C	1	0.5000000	0.380055	0.6109575	1
C15	C	1	0.380055	0.5000000	0.6109575	1
C16	C	1	0.5000000	0.619945	0.6109575	1
C17	C	1	0.619945	0.5000000	0.3890425	1
C18	C	1	0.5000000	0.380055	0.3890425	1
C19	C	1	0.380055	0.5000000	0.3890425	1
C20	C	1	0.5000000	0.619945	0.3890425	1
C21	C	1	0.619945	0.380055	0.5000000	1
C22	C	1	0.380055	0.380055	0.5000000	1
C23	C	1	0.380055	0.619945	0.5000000	1
C24	C	1	0.619945	0.619945	0.5000000	1
O1	O	1	0.5350309	0.5346891	0.467594	1
O2	O	1	0.5350309	0.4653109	0.532406	1
O3	O	1	0.4649691	0.5346891	0.467594	1
O4	O	1	0.4649691	0.4653109	0.532406	1
O5	O	1	0.4649691	0.4653109	0.467594	1
O6	O	1	0.4649691	0.5346891	0.532406	1

O7	O	1	0.5350309	0.4653109	0.467594	1
O8	O	1	0.5350309	0.5346891	0.532406	1
O9	O	1	0.5943662	0.5000000	0.5487156	1
O10	O	1	0.5943662	0.4473384	0.5000000	1
O11	O	1	0.5943662	0.5000000	0.4512844	1
O12	O	1	0.5943662	0.5526616	0.5000000	1
O13	O	1	0.5000000	0.5943662	0.5487156	1
O14	O	1	0.5526616	0.5943662	0.5000000	1
O15	O	1	0.5000000	0.5943662	0.4512844	1
O16	O	1	0.4473384	0.5943662	0.5000000	1
O17	O	1	0.4056338	0.5000000	0.5487156	1
O18	O	1	0.4056338	0.5526616	0.5000000	1
O19	O	1	0.4056338	0.5000000	0.4512844	1
O20	O	1	0.4056338	0.4473384	0.5000000	1
O21	O	1	0.5000000	0.4056338	0.5487156	1
O22	O	1	0.4473384	0.4056338	0.5000000	1
O23	O	1	0.5000000	0.4056338	0.4512844	1
O24	O	1	0.5526616	0.4056338	0.5000000	1
O25	O	1	0.5526616	0.5000000	0.5872953	1
O26	O	1	0.5000000	0.5526616	0.5872953	1
O27	O	1	0.4473384	0.5000000	0.5872953	1
O28	O	1	0.5000000	0.4473384	0.5872953	1
O29	O	1	0.5526616	0.5000000	0.4127047	1
O30	O	1	0.5000000	0.4473384	0.4127047	1
O31	O	1	0.4473384	0.5000000	0.4127047	1
O32	O	1	0.5000000	0.5526616	0.4127047	1
Zr1	Zr	1	0.5668679	0.5000000	0.5000000	1
Zr2	Zr	1	0.5000000	0.5668679	0.5000000	1
Zr3	Zr	1	0.4331321	0.5000000	0.5000000	1
Zr4	Zr	1	0.5000000	0.4331321	0.5000000	1
Zr5	Zr	1	0.5000000	0.5000000	0.5618575	1
Zr6	Zr	1	0.5000000	0.5000000	0.4381425	1

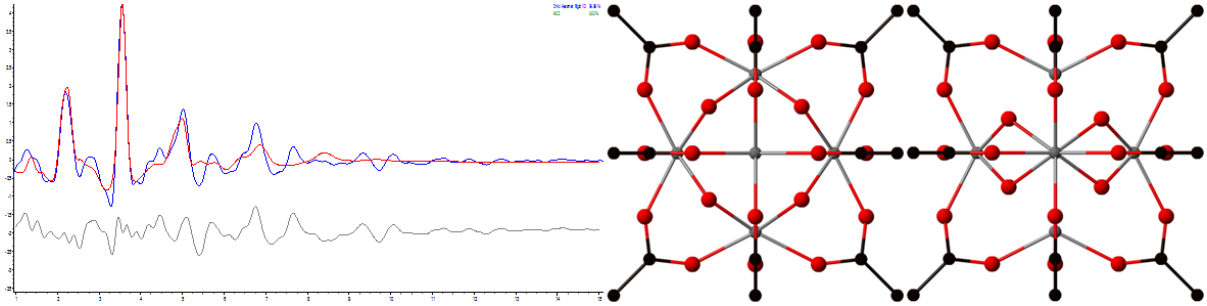

Figure 218: Observed and Calculated PDF from the chandelier core refinement of ZAA7A from the 18-month data collection and the resultant model viewed from the axial (left) and equatorial (right) positions.

Table 161: The atomic coordinates of the model resulting from the chandelier core refinement of ZAA7A from the 18-month data collection.

Atom Label	Atom Type	Multiplicity	Fractional X Coordinate	Fractional Y Coordinate	Fractional Z Coordinate	Fractional Occupancy
C1	C	1	0.589709	0.5000000	0.5829871	1
C2	C	1	0.5000000	0.410291	0.5829871	1
C3	C	1	0.410291	0.5000000	0.5829871	1
C4	C	1	0.5000000	0.589709	0.5829871	1
C5	C	1	0.589709	0.5000000	0.4170129	1
C6	C	1	0.5000000	0.410291	0.4170129	1
C7	C	1	0.410291	0.5000000	0.4170129	1
C8	C	1	0.5000000	0.589709	0.4170129	1
C9	C	1	0.589709	0.410291	0.5000000	1
C10	C	1	0.410291	0.410291	0.5000000	1
C11	C	1	0.410291	0.589709	0.5000000	1
C12	C	1	0.589709	0.589709	0.5000000	1
C13	C	1	0.6202937	0.5000000	0.6112801	1
C14	C	1	0.5000000	0.3797063	0.6112801	1
C15	C	1	0.3797063	0.5000000	0.6112801	1
C16	C	1	0.5000000	0.6202937	0.6112801	1
C17	C	1	0.6202937	0.5000000	0.3887199	1
C18	C	1	0.5000000	0.3797063	0.3887199	1
C19	C	1	0.3797063	0.5000000	0.3887199	1
C20	C	1	0.5000000	0.6202937	0.3887199	1
C21	C	1	0.6202937	0.3797063	0.5000000	1
C22	C	1	0.3797063	0.3797063	0.5000000	1
C23	C	1	0.3797063	0.6202937	0.5000000	1
C24	C	1	0.6202937	0.6202937	0.5000000	1
O1	O	1	0.5394017	0.4605983	0.4733129	1
O2	O	1	0.5394017	0.4605983	0.5266871	1
O3	O	1	0.4605983	0.4605983	0.4733129	1
O4	O	1	0.4605983	0.4605983	0.5266871	1
O5	O	1	0.4605983	0.5394017	0.4733129	1
O6	O	1	0.4605983	0.5394017	0.5266871	1
O7	O	1	0.5394017	0.5394017	0.4733129	1
O8	O	1	0.5394017	0.5394017	0.5266871	1

O9	O	1	0.5939042	0.5000000	0.5495482	1
O10	O	1	0.5939042	0.4464384	0.5000000	1
O11	O	1	0.5939042	0.5000000	0.4504518	1
O12	O	1	0.5939042	0.5535616	0.5000000	1
O13	O	1	0.5000000	0.5939042	0.5495482	1
O14	O	1	0.5535616	0.5939042	0.5000000	1
O15	O	1	0.5000000	0.5939042	0.4504518	1
O16	O	1	0.4464384	0.5939042	0.5000000	1
O17	O	1	0.4060958	0.5000000	0.5495482	1
O18	O	1	0.4060958	0.5535616	0.5000000	1
O19	O	1	0.4060958	0.5000000	0.4504518	1
O20	O	1	0.4060958	0.4464384	0.5000000	1
O21	O	1	0.5000000	0.4060958	0.5495482	1
O22	O	1	0.4464384	0.4060958	0.5000000	1
O23	O	1	0.5000000	0.4060958	0.4504518	1
O24	O	1	0.5535616	0.4060958	0.5000000	1
O25	O	1	0.5535616	0.5000000	0.586868	1
O26	O	1	0.5000000	0.5535616	0.586868	1
O27	O	1	0.4464384	0.5000000	0.586868	1
O28	O	1	0.5000000	0.4464384	0.586868	1
O29	O	1	0.5535616	0.5000000	0.413132	1
O30	O	1	0.5000000	0.4464384	0.413132	1
O31	O	1	0.4464384	0.5000000	0.413132	1
O32	O	1	0.5000000	0.5535616	0.413132	1
Zr1	Zr	1	0.5666126	0.5000000	0.5000000	1
Zr2	Zr	1	0.5000000	0.5666126	0.5000000	1
Zr3	Zr	1	0.4333874	0.5000000	0.5000000	1
Zr4	Zr	1	0.5000000	0.4333874	0.5000000	1
Zr5	Zr	1	0.5000000	0.5000000	0.5616213	1
Zr6	Zr	1	0.5000000	0.5000000	0.4383787	1

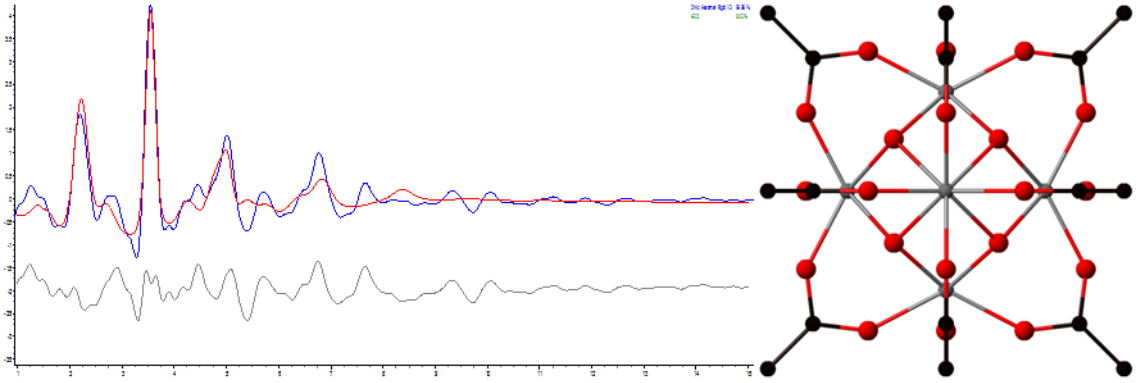

Figure 219: Observed and Calculated PDF from the fixed core refinement of ZAA7A from the 18-month data collection and the resultant model.

Table 162: The atomic coordinates of the model resulting from the fixed core refinement of ZAA7A from the 18-month data collection.

Atom Label	Atom Type	Multiplicity	Fractional X Coordinate	Fractional Y Coordinate	Fractional Z Coordinate	Fractional Occupancy
C1	C	1	0.5894779	0.5000000	0.5827733	1
C2	C	1	0.5000000	0.4105221	0.5827733	1
C3	C	1	0.4105221	0.5000000	0.5827733	1
C4	C	1	0.5000000	0.5894779	0.5827733	1
C5	C	1	0.5894779	0.5000000	0.4172267	1
C6	C	1	0.5000000	0.4105221	0.4172267	1
C7	C	1	0.4105221	0.5000000	0.4172267	1
C8	C	1	0.5000000	0.5894779	0.4172267	1
C9	C	1	0.5894779	0.4105221	0.5000000	1
C10	C	1	0.4105221	0.4105221	0.5000000	1
C11	C	1	0.4105221	0.5894779	0.5000000	1
C12	C	1	0.5894779	0.5894779	0.5000000	1
C13	C	1	0.6197273	0.5000000	0.6107561	1
C14	C	1	0.5000000	0.3802727	0.6107561	1
C15	C	1	0.3802727	0.5000000	0.6107561	1
C16	C	1	0.5000000	0.6197273	0.6107561	1
C17	C	1	0.6197273	0.5000000	0.3892439	1
C18	C	1	0.5000000	0.3802727	0.3892439	1
C19	C	1	0.3802727	0.5000000	0.3892439	1
C20	C	1	0.5000000	0.6197273	0.3892439	1
C21	C	1	0.6197273	0.3802727	0.5000000	1
C22	C	1	0.3802727	0.3802727	0.5000000	1
C23	C	1	0.3802727	0.6197273	0.5000000	1
C24	C	1	0.6197273	0.6197273	0.5000000	1
O1	O	1	0.5352659	0.5349218	0.4673766	1
O2	O	1	0.5352659	0.4650782	0.5326234	1
O3	O	1	0.4647341	0.5349218	0.4673766	1
O4	O	1	0.4647341	0.4650782	0.5326234	1
O5	O	1	0.4647341	0.4650782	0.4673766	1
O6	O	1	0.4647341	0.5349218	0.5326234	1

O7	O	1	0.5352659	0.4650782	0.4673766	1
O8	O	1	0.5352659	0.5349218	0.5326234	1
O9	O	1	0.5940423	0.5000000	0.5486203	1
O10	O	1	0.5940423	0.4474414	0.5000000	1
O11	O	1	0.5940423	0.5000000	0.4513797	1
O12	O	1	0.5940423	0.5525586	0.5000000	1
O13	O	1	0.5000000	0.5940423	0.5486203	1
O14	O	1	0.5525586	0.5940423	0.5000000	1
O15	O	1	0.5000000	0.5940423	0.4513797	1
O16	O	1	0.4474414	0.5940423	0.5000000	1
O17	O	1	0.4059577	0.5000000	0.5486203	1
O18	O	1	0.4059577	0.5525586	0.5000000	1
O19	O	1	0.4059577	0.5000000	0.4513797	1
O20	O	1	0.4059577	0.4474414	0.5000000	1
O21	O	1	0.5000000	0.4059577	0.5486203	1
O22	O	1	0.4474414	0.4059577	0.5000000	1
O23	O	1	0.5000000	0.4059577	0.4513797	1
O24	O	1	0.5525586	0.4059577	0.5000000	1
O25	O	1	0.5525586	0.5000000	0.5869956	1
O26	O	1	0.5000000	0.5525586	0.5869956	1
O27	O	1	0.4474414	0.5000000	0.5869956	1
O28	O	1	0.5000000	0.4474414	0.5869956	1
O29	O	1	0.5525586	0.5000000	0.4130044	1
O30	O	1	0.5000000	0.4474414	0.4130044	1
O31	O	1	0.4474414	0.5000000	0.4130044	1
O32	O	1	0.5000000	0.5525586	0.4130044	1
Zr1	Zr	1	0.5665864	0.5000000	0.5000000	1
Zr2	Zr	1	0.5000000	0.5665864	0.5000000	1
Zr3	Zr	1	0.4334136	0.5000000	0.5000000	1
Zr4	Zr	1	0.5000000	0.4334136	0.5000000	1
Zr5	Zr	1	0.5000000	0.5000000	0.561597	1
Zr6	Zr	1	0.5000000	0.5000000	0.438403	1

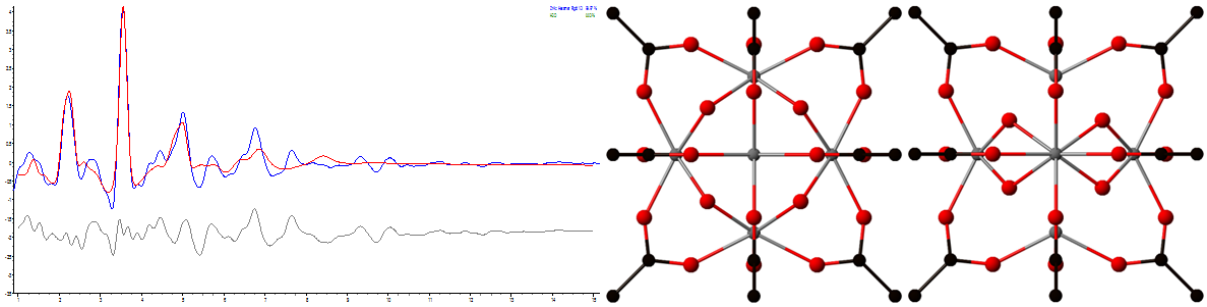

Figure 220: Observed and Calculated PDF from the chandelier core refinement of ZAA7C from the 18-month data collection and the resultant model viewed from the axial (left) and equatorial (right) positions.

Table 163: The atomic coordinates of the model resulting from the chandelier core refinement of ZAA7C from the 18-month data collection.

Atom Label	Atom Type	Multiplicity	Fractional X Coordinate	Fractional Y Coordinate	Fractional Z Coordinate	Fractional Occupancy
C1	C	1	0.5898547	0.5000000	0.5831218	1
C2	C	1	0.5000000	0.4101453	0.5831218	1
C3	C	1	0.4101453	0.5000000	0.5831218	1
C4	C	1	0.5000000	0.5898547	0.5831218	1
C5	C	1	0.5898547	0.5000000	0.4168782	1
C6	C	1	0.5000000	0.4101453	0.4168782	1
C7	C	1	0.4101453	0.5000000	0.4168782	1
C8	C	1	0.5000000	0.5898547	0.4168782	1
C9	C	1	0.5898547	0.4101453	0.5000000	1
C10	C	1	0.4101453	0.4101453	0.5000000	1
C11	C	1	0.4101453	0.5898547	0.5000000	1
C12	C	1	0.5898547	0.5898547	0.5000000	1
C13	C	1	0.6203782	0.5000000	0.6113582	1
C14	C	1	0.5000000	0.3796218	0.6113582	1
C15	C	1	0.3796218	0.5000000	0.6113582	1
C16	C	1	0.5000000	0.6203782	0.6113582	1
C17	C	1	0.6203782	0.5000000	0.3886418	1
C18	C	1	0.5000000	0.3796218	0.3886418	1
C19	C	1	0.3796218	0.5000000	0.3886418	1
C20	C	1	0.5000000	0.6203782	0.3886418	1
C21	C	1	0.6203782	0.3796218	0.5000000	1
C22	C	1	0.3796218	0.3796218	0.5000000	1
C23	C	1	0.3796218	0.6203782	0.5000000	1
C24	C	1	0.6203782	0.6203782	0.5000000	1
O1	O	1	0.5397986	0.4602014	0.4733557	1
O2	O	1	0.5397986	0.4602014	0.5266443	1
O3	O	1	0.4602014	0.4602014	0.4733557	1
O4	O	1	0.4602014	0.4602014	0.5266443	1
O5	O	1	0.4602014	0.5397986	0.4733557	1
O6	O	1	0.4602014	0.5397986	0.5266443	1
O7	O	1	0.5397986	0.5397986	0.4733557	1
O8	O	1	0.5397986	0.5397986	0.5266443	1

O9	O	1	0.5937531	0.5000000	0.549699	1
O10	O	1	0.5937531	0.4462754	0.5000000	1
O11	O	1	0.5937531	0.5000000	0.450301	1
O12	O	1	0.5937531	0.5537246	0.5000000	1
O13	O	1	0.5000000	0.5937531	0.549699	1
O14	O	1	0.5537246	0.5937531	0.5000000	1
O15	O	1	0.5000000	0.5937531	0.450301	1
O16	O	1	0.4462754	0.5937531	0.5000000	1
O17	O	1	0.4062469	0.5000000	0.549699	1
O18	O	1	0.4062469	0.5537246	0.5000000	1
O19	O	1	0.4062469	0.5000000	0.450301	1
O20	O	1	0.4062469	0.4462754	0.5000000	1
O21	O	1	0.5000000	0.4062469	0.549699	1
O22	O	1	0.4462754	0.4062469	0.5000000	1
O23	O	1	0.5000000	0.4062469	0.450301	1
O24	O	1	0.5537246	0.4062469	0.5000000	1
O25	O	1	0.5537246	0.5000000	0.5867282	1
O26	O	1	0.5000000	0.5537246	0.5867282	1
O27	O	1	0.4462754	0.5000000	0.5867282	1
O28	O	1	0.5000000	0.4462754	0.5867282	1
O29	O	1	0.5537246	0.5000000	0.4132718	1
O30	O	1	0.5000000	0.4462754	0.4132718	1
O31	O	1	0.4462754	0.5000000	0.4132718	1
O32	O	1	0.5000000	0.5537246	0.4132718	1
Zr1	Zr	1	0.566529	0.5000000	0.5000000	1
Zr2	Zr	1	0.5000000	0.566529	0.5000000	1
Zr3	Zr	1	0.433471	0.5000000	0.5000000	1
Zr4	Zr	1	0.5000000	0.433471	0.5000000	1
Zr5	Zr	1	0.5000000	0.5000000	0.5615439	1
Zr6	Zr	1	0.5000000	0.5000000	0.4384561	1

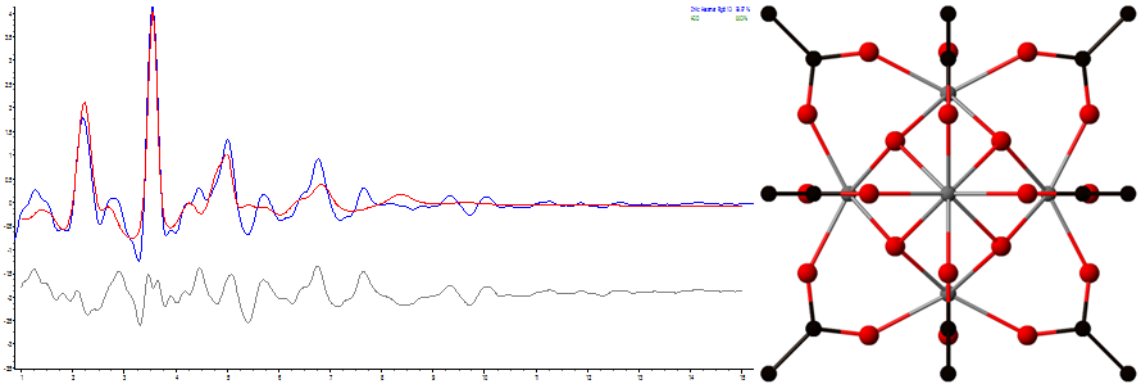

Figure 221: Observed and Calculated PDF from the fixed core refinement of ZAA7C from the 18-month data collection and the resultant model.

Table 164: The atomic coordinates of the model resulting from the fixed core refinement of ZAA7C from the 18-month data collection.

Atom Label	Atom Type	Multiplicity	Fractional X Coordinate	Fractional Y Coordinate	Fractional Z Coordinate	Fractional Occupancy
C1	C	1	0.5895704	0.5000000	0.5828588	1
C2	C	1	0.5000000	0.4104296	0.5828588	1
C3	C	1	0.4104296	0.5000000	0.5828588	1
C4	C	1	0.5000000	0.5895704	0.5828588	1
C5	C	1	0.5895704	0.5000000	0.4171412	1
C6	C	1	0.5000000	0.4104296	0.4171412	1
C7	C	1	0.4104296	0.5000000	0.4171412	1
C8	C	1	0.5000000	0.5895704	0.4171412	1
C9	C	1	0.5895704	0.4104296	0.5000000	1
C10	C	1	0.4104296	0.4104296	0.5000000	1
C11	C	1	0.4104296	0.5895704	0.5000000	1
C12	C	1	0.5895704	0.5895704	0.5000000	1
C13	C	1	0.6195851	0.5000000	0.6106246	1
C14	C	1	0.5000000	0.3804149	0.6106246	1
C15	C	1	0.3804149	0.5000000	0.6106246	1
C16	C	1	0.5000000	0.6195851	0.6106246	1
C17	C	1	0.6195851	0.5000000	0.3893754	1
C18	C	1	0.5000000	0.3804149	0.3893754	1
C19	C	1	0.3804149	0.5000000	0.3893754	1
C20	C	1	0.5000000	0.6195851	0.3893754	1
C21	C	1	0.6195851	0.3804149	0.5000000	1
C22	C	1	0.3804149	0.3804149	0.5000000	1
C23	C	1	0.3804149	0.6195851	0.5000000	1
C24	C	1	0.6195851	0.6195851	0.5000000	1
O1	O	1	0.5352006	0.5348572	0.467437	1
O2	O	1	0.5352006	0.4651428	0.532563	1
O3	O	1	0.4647994	0.5348572	0.467437	1
O4	O	1	0.4647994	0.4651428	0.532563	1
O5	O	1	0.4647994	0.4651428	0.467437	1
O6	O	1	0.4647994	0.5348572	0.532563	1

O7	O	1	0.5352006	0.4651428	0.467437	1
O8	O	1	0.5352006	0.5348572	0.532563	1
O9	O	1	0.5939155	0.5000000	0.5487803	1
O10	O	1	0.5939155	0.4472685	0.5000000	1
O11	O	1	0.5939155	0.5000000	0.4512197	1
O12	O	1	0.5939155	0.5527315	0.5000000	1
O13	O	1	0.5000000	0.5939155	0.5487803	1
O14	O	1	0.5527315	0.5939155	0.5000000	1
O15	O	1	0.5000000	0.5939155	0.4512197	1
O16	O	1	0.4472685	0.5939155	0.5000000	1
O17	O	1	0.4060845	0.5000000	0.5487803	1
O18	O	1	0.4060845	0.5527315	0.5000000	1
O19	O	1	0.4060845	0.5000000	0.4512197	1
O20	O	1	0.4060845	0.4472685	0.5000000	1
O21	O	1	0.5000000	0.4060845	0.5487803	1
O22	O	1	0.4472685	0.4060845	0.5000000	1
O23	O	1	0.5000000	0.4060845	0.4512197	1
O24	O	1	0.5527315	0.4060845	0.5000000	1
O25	O	1	0.5527315	0.5000000	0.5868784	1
O26	O	1	0.5000000	0.5527315	0.5868784	1
O27	O	1	0.4472685	0.5000000	0.5868784	1
O28	O	1	0.5000000	0.4472685	0.5868784	1
O29	O	1	0.5527315	0.5000000	0.4131216	1
O30	O	1	0.5000000	0.4472685	0.4131216	1
O31	O	1	0.4472685	0.5000000	0.4131216	1
O32	O	1	0.5000000	0.5527315	0.4131216	1
Zr1	Zr	1	0.5665181	0.5000000	0.5000000	1
Zr2	Zr	1	0.5000000	0.5665181	0.5000000	1
Zr3	Zr	1	0.4334819	0.5000000	0.5000000	1
Zr4	Zr	1	0.5000000	0.4334819	0.5000000	1
Zr5	Zr	1	0.5000000	0.5000000	0.5615339	1
Zr6	Zr	1	0.5000000	0.5000000	0.4384661	1

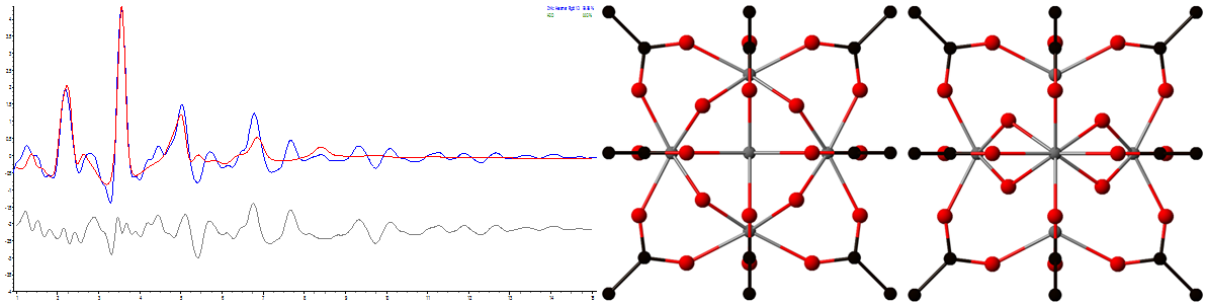

Figure 222: Observed and Calculated PDF from the chandelier core refinement of ZAA7I from the 18-month data collection and the resultant model viewed from the axial (left) and equatorial (right) positions.

Table 165: The atomic coordinates of the model resulting from the chandelier core refinement of ZAA7I from the 18-month data collection.

Atom Label	Atom Type	Multiplicity	Fractional X Coordinate	Fractional Y Coordinate	Fractional Z Coordinate	Fractional Occupancy
C1	C	1	0.5896921	0.5000000	0.5829714	1
C2	C	1	0.5000000	0.4103079	0.5829714	1
C3	C	1	0.4103079	0.5000000	0.5829714	1
C4	C	1	0.5000000	0.5896921	0.5829714	1
C5	C	1	0.5896921	0.5000000	0.4170286	1
C6	C	1	0.5000000	0.4103079	0.4170286	1
C7	C	1	0.4103079	0.5000000	0.4170286	1
C8	C	1	0.5000000	0.5896921	0.4170286	1
C9	C	1	0.5896921	0.4103079	0.5000000	1
C10	C	1	0.4103079	0.4103079	0.5000000	1
C11	C	1	0.4103079	0.5896921	0.5000000	1
C12	C	1	0.5896921	0.5896921	0.5000000	1
C13	C	1	0.6202921	0.5000000	0.6112785	1
C14	C	1	0.5000000	0.3797079	0.6112785	1
C15	C	1	0.3797079	0.5000000	0.6112785	1
C16	C	1	0.5000000	0.6202921	0.6112785	1
C17	C	1	0.6202921	0.5000000	0.3887215	1
C18	C	1	0.5000000	0.3797079	0.3887215	1
C19	C	1	0.3797079	0.5000000	0.3887215	1
C20	C	1	0.5000000	0.6202921	0.3887215	1
C21	C	1	0.6202921	0.3797079	0.5000000	1
C22	C	1	0.3797079	0.3797079	0.5000000	1
C23	C	1	0.3797079	0.6202921	0.5000000	1
C24	C	1	0.6202921	0.6202921	0.5000000	1
O1	O	1	0.5401795	0.4598205	0.4738903	1
O2	O	1	0.5401795	0.4598205	0.5261097	1
O3	O	1	0.4598205	0.4598205	0.4738903	1
O4	O	1	0.4598205	0.4598205	0.5261097	1
O5	O	1	0.4598205	0.5401795	0.4738903	1
O6	O	1	0.4598205	0.5401795	0.5261097	1
O7	O	1	0.5401795	0.5401795	0.4738903	1
O8	O	1	0.5401795	0.5401795	0.5261097	1

O9	O	1	0.5942764	0.5000000	0.5495197	1
O10	O	1	0.5942764	0.4464693	0.5000000	1
O11	O	1	0.5942764	0.5000000	0.4504803	1
O12	O	1	0.5942764	0.5535307	0.5000000	1
O13	O	1	0.5000000	0.5942764	0.5495197	1
O14	O	1	0.5535307	0.5942764	0.5000000	1
O15	O	1	0.5000000	0.5942764	0.4504803	1
O16	O	1	0.4464693	0.5942764	0.5000000	1
O17	O	1	0.4057236	0.5000000	0.5495197	1
O18	O	1	0.4057236	0.5535307	0.5000000	1
O19	O	1	0.4057236	0.5000000	0.4504803	1
O20	O	1	0.4057236	0.4464693	0.5000000	1
O21	O	1	0.5000000	0.4057236	0.5495197	1
O22	O	1	0.4464693	0.4057236	0.5000000	1
O23	O	1	0.5000000	0.4057236	0.4504803	1
O24	O	1	0.5535307	0.4057236	0.5000000	1
O25	O	1	0.5535307	0.5000000	0.5872122	1
O26	O	1	0.5000000	0.5535307	0.5872122	1
O27	O	1	0.4464693	0.5000000	0.5872122	1
O28	O	1	0.5000000	0.4464693	0.5872122	1
O29	O	1	0.5535307	0.5000000	0.4127878	1
O30	O	1	0.5000000	0.4464693	0.4127878	1
O31	O	1	0.4464693	0.5000000	0.4127878	1
O32	O	1	0.5000000	0.5535307	0.4127878	1
Zr1	Zr	1	0.5667868	0.5000000	0.5000000	1
Zr2	Zr	1	0.5000000	0.5667868	0.5000000	1
Zr3	Zr	1	0.4332132	0.5000000	0.5000000	1
Zr4	Zr	1	0.5000000	0.4332132	0.5000000	1
Zr5	Zr	1	0.5000000	0.5000000	0.5617825	1
Zr6	Zr	1	0.5000000	0.5000000	0.4382175	1

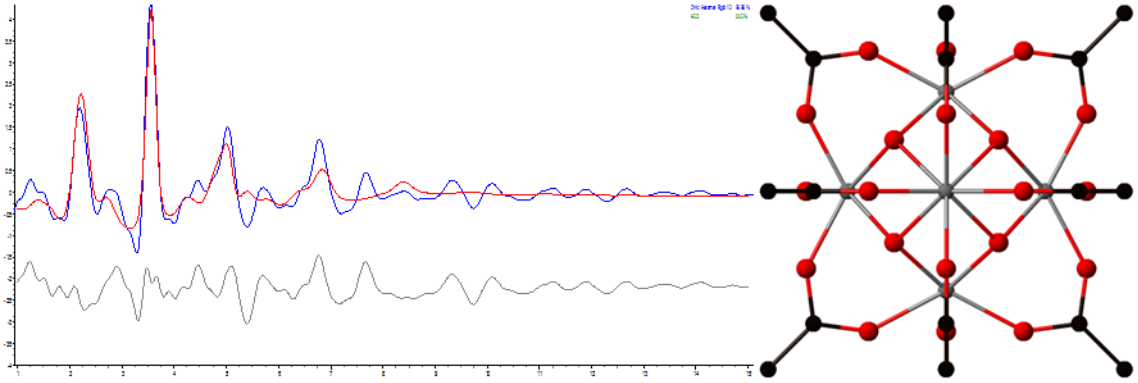

Figure 223: Observed and Calculated PDF from the fixed core refinement of ZAA7I from the 18-month data collection and the resultant model.

Table 166: The atomic coordinates of the model resulting from the fixed core refinement of ZAA7I from the 18-month data collection.

Atom Label	Atom Type	Multiplicity	Fractional X Coordinate	Fractional Y Coordinate	Fractional Z Coordinate	Fractional Occupancy
C1	C	1	0.5893628	0.5000000	0.5826668	1
C2	C	1	0.5000000	0.4106372	0.5826668	1
C3	C	1	0.4106372	0.5000000	0.5826668	1
C4	C	1	0.5000000	0.5893628	0.5826668	1
C5	C	1	0.5893628	0.5000000	0.4173332	1
C6	C	1	0.5000000	0.4106372	0.4173332	1
C7	C	1	0.4106372	0.5000000	0.4173332	1
C8	C	1	0.5000000	0.5893628	0.4173332	1
C9	C	1	0.5893628	0.4106372	0.5000000	1
C10	C	1	0.4106372	0.4106372	0.5000000	1
C11	C	1	0.4106372	0.5893628	0.5000000	1
C12	C	1	0.5893628	0.5893628	0.5000000	1
C13	C	1	0.619945	0.5000000	0.6109575	1
C14	C	1	0.5000000	0.380055	0.6109575	1
C15	C	1	0.380055	0.5000000	0.6109575	1
C16	C	1	0.5000000	0.619945	0.6109575	1
C17	C	1	0.619945	0.5000000	0.3890425	1
C18	C	1	0.5000000	0.380055	0.3890425	1
C19	C	1	0.380055	0.5000000	0.3890425	1
C20	C	1	0.5000000	0.619945	0.3890425	1
C21	C	1	0.619945	0.380055	0.5000000	1
C22	C	1	0.380055	0.380055	0.5000000	1
C23	C	1	0.380055	0.619945	0.5000000	1
C24	C	1	0.619945	0.619945	0.5000000	1
O1	O	1	0.5351379	0.534795	0.467495	1
O2	O	1	0.5351379	0.465205	0.532505	1
O3	O	1	0.4648621	0.534795	0.467495	1
O4	O	1	0.4648621	0.465205	0.532505	1
O5	O	1	0.4648621	0.465205	0.467495	1
O6	O	1	0.4648621	0.534795	0.532505	1

O7	O	1	0.5351379	0.465205	0.467495	1
O8	O	1	0.5351379	0.534795	0.532505	1
O9	O	1	0.5944071	0.5000000	0.54829	1
O10	O	1	0.5944071	0.4477986	0.5000000	1
O11	O	1	0.5944071	0.5000000	0.45171	1
O12	O	1	0.5944071	0.5522014	0.5000000	1
O13	O	1	0.5000000	0.5944071	0.54829	1
O14	O	1	0.5522014	0.5944071	0.5000000	1
O15	O	1	0.5000000	0.5944071	0.45171	1
O16	O	1	0.4477986	0.5944071	0.5000000	1
O17	O	1	0.4055929	0.5000000	0.54829	1
O18	O	1	0.4055929	0.5522014	0.5000000	1
O19	O	1	0.4055929	0.5000000	0.45171	1
O20	O	1	0.4055929	0.4477986	0.5000000	1
O21	O	1	0.5000000	0.4055929	0.54829	1
O22	O	1	0.4477986	0.4055929	0.5000000	1
O23	O	1	0.5000000	0.4055929	0.45171	1
O24	O	1	0.5522014	0.4055929	0.5000000	1
O25	O	1	0.5522014	0.5000000	0.5873332	1
O26	O	1	0.5000000	0.5522014	0.5873332	1
O27	O	1	0.4477986	0.5000000	0.5873332	1
O28	O	1	0.5000000	0.4477986	0.5873332	1
O29	O	1	0.5522014	0.5000000	0.4126668	1
O30	O	1	0.5000000	0.4477986	0.4126668	1
O31	O	1	0.4477986	0.5000000	0.4126668	1
O32	O	1	0.5000000	0.5522014	0.4126668	1
Zr1	Zr	1	0.5667895	0.5000000	0.5000000	1
Zr2	Zr	1	0.5000000	0.5667895	0.5000000	1
Zr3	Zr	1	0.4332105	0.5000000	0.5000000	1
Zr4	Zr	1	0.5000000	0.4332105	0.5000000	1
Zr5	Zr	1	0.5000000	0.5000000	0.561785	1
Zr6	Zr	1	0.5000000	0.5000000	0.438215	1

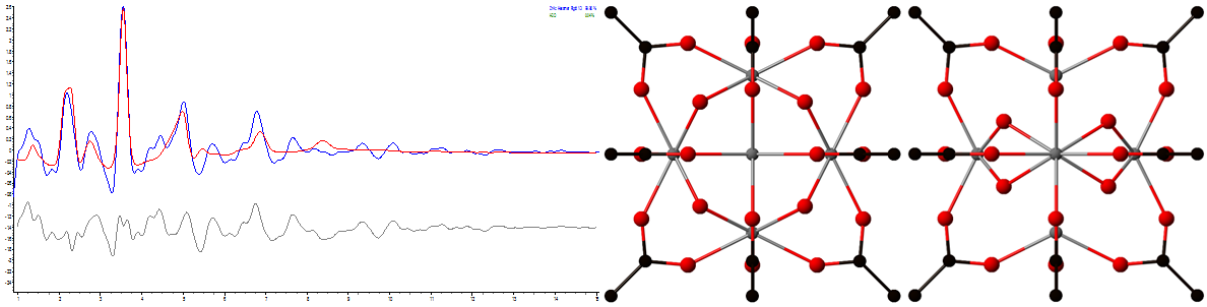

Figure 224: Observed and Calculated PDF from the chandelier core refinement of ZAA10A from the 18-month data collection and the resultant model viewed from the axial (left) and equatorial (right) positions.

Table 167: The atomic coordinates of the model resulting from the chandelier core refinement of ZAA10A from the 18-month data collection.

Atom Label	Atom Type	Multiplicity	Fractional X Coordinate	Fractional Y Coordinate	Fractional Z Coordinate	Fractional Occupancy
C1	C	1	0.5905877	0.5000000	0.5837999	1
C2	C	1	0.5000000	0.4094123	0.5837999	1
C3	C	1	0.4094123	0.5000000	0.5837999	1
C4	C	1	0.5000000	0.5905877	0.5837999	1
C5	C	1	0.5905877	0.5000000	0.4162001	1
C6	C	1	0.5000000	0.4094123	0.4162001	1
C7	C	1	0.4094123	0.5000000	0.4162001	1
C8	C	1	0.5000000	0.5905877	0.4162001	1
C9	C	1	0.5905877	0.4094123	0.5000000	1
C10	C	1	0.4094123	0.4094123	0.5000000	1
C11	C	1	0.4094123	0.5905877	0.5000000	1
C12	C	1	0.5905877	0.5905877	0.5000000	1
C13	C	1	0.6198102	0.5000000	0.6108328	1
C14	C	1	0.5000000	0.3801898	0.6108328	1
C15	C	1	0.3801898	0.5000000	0.6108328	1
C16	C	1	0.5000000	0.6198102	0.6108328	1
C17	C	1	0.6198102	0.5000000	0.3891672	1
C18	C	1	0.5000000	0.3801898	0.3891672	1
C19	C	1	0.3801898	0.5000000	0.3891672	1
C20	C	1	0.5000000	0.6198102	0.3891672	1
C21	C	1	0.6198102	0.3801898	0.5000000	1
C22	C	1	0.3801898	0.3801898	0.5000000	1
C23	C	1	0.3801898	0.6198102	0.5000000	1
C24	C	1	0.6198102	0.6198102	0.5000000	1
O1	O	1	0.5442317	0.4557683	0.4746175	1
O2	O	1	0.5442317	0.4557683	0.5253825	1
O3	O	1	0.4557683	0.4557683	0.4746175	1
O4	O	1	0.4557683	0.4557683	0.5253825	1
O5	O	1	0.4557683	0.5442317	0.4746175	1
O6	O	1	0.4557683	0.5442317	0.5253825	1
O7	O	1	0.5442317	0.5442317	0.4746175	1
O8	O	1	0.5442317	0.5442317	0.5253825	1

O9	O	1	0.5937504	0.5000000	0.5505544	1
O10	O	1	0.5937504	0.4453507	0.5000000	1
O11	O	1	0.5937504	0.5000000	0.4494456	1
O12	O	1	0.5937504	0.5546493	0.5000000	1
O13	O	1	0.5000000	0.5937504	0.5505544	1
O14	O	1	0.5546493	0.5937504	0.5000000	1
O15	O	1	0.5000000	0.5937504	0.4494456	1
O16	O	1	0.4453507	0.5937504	0.5000000	1
O17	O	1	0.4062496	0.5000000	0.5505544	1
O18	O	1	0.4062496	0.5546493	0.5000000	1
O19	O	1	0.4062496	0.5000000	0.4494456	1
O20	O	1	0.4062496	0.4453507	0.5000000	1
O21	O	1	0.5000000	0.4062496	0.5505544	1
O22	O	1	0.4453507	0.4062496	0.5000000	1
O23	O	1	0.5000000	0.4062496	0.4494456	1
O24	O	1	0.5546493	0.4062496	0.5000000	1
O25	O	1	0.5546493	0.5000000	0.5867257	1
O26	O	1	0.5000000	0.5546493	0.5867257	1
O27	O	1	0.4453507	0.5000000	0.5867257	1
O28	O	1	0.5000000	0.4453507	0.5867257	1
O29	O	1	0.5546493	0.5000000	0.4132743	1
O30	O	1	0.5000000	0.4453507	0.4132743	1
O31	O	1	0.4453507	0.5000000	0.4132743	1
O32	O	1	0.5000000	0.5546493	0.4132743	1
Zr1	Zr	1	0.5665305	0.5000000	0.5000000	1
Zr2	Zr	1	0.5000000	0.5665305	0.5000000	1
Zr3	Zr	1	0.4334695	0.5000000	0.5000000	1
Zr4	Zr	1	0.5000000	0.4334695	0.5000000	1
Zr5	Zr	1	0.5000000	0.5000000	0.5615454	1
Zr6	Zr	1	0.5000000	0.5000000	0.4384546	1

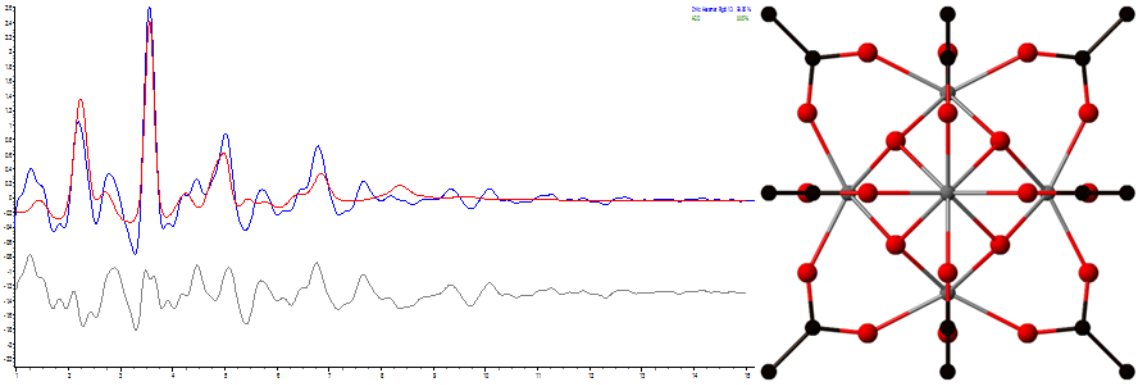

Figure 225: Observed and Calculated PDF from the fixed core refinement of ZAA10A from the 18-month data collection and the resultant model.

Table 168: The atomic coordinates of the model resulting from the fixed core refinement of ZAA10A from the 18-month data collection.

Atom Label	Atom Type	Multiplicity	Fractional X Coordinate	Fractional Y Coordinate	Fractional Z Coordinate	Fractional Occupancy
C1	C	1	0.5900374	0.5000000	0.5832909	1
C2	C	1	0.5000000	0.4099626	0.5832909	1
C3	C	1	0.4099626	0.5000000	0.5832909	1
C4	C	1	0.5000000	0.5900374	0.5832909	1
C5	C	1	0.5900374	0.5000000	0.4167091	1
C6	C	1	0.5000000	0.4099626	0.4167091	1
C7	C	1	0.4099626	0.5000000	0.4167091	1
C8	C	1	0.5000000	0.5900374	0.4167091	1
C9	C	1	0.5900374	0.4099626	0.5000000	1
C10	C	1	0.4099626	0.4099626	0.5000000	1
C11	C	1	0.4099626	0.5900374	0.5000000	1
C12	C	1	0.5900374	0.5900374	0.5000000	1
C13	C	1	0.6195095	0.5000000	0.6105546	1
C14	C	1	0.5000000	0.3804905	0.6105546	1
C15	C	1	0.3804905	0.5000000	0.6105546	1
C16	C	1	0.5000000	0.6195095	0.6105546	1
C17	C	1	0.6195095	0.5000000	0.3894454	1
C18	C	1	0.5000000	0.3804905	0.3894454	1
C19	C	1	0.3804905	0.5000000	0.3894454	1
C20	C	1	0.5000000	0.6195095	0.3894454	1
C21	C	1	0.6195095	0.3804905	0.5000000	1
C22	C	1	0.3804905	0.3804905	0.5000000	1
C23	C	1	0.3804905	0.6195095	0.5000000	1
C24	C	1	0.6195095	0.6195095	0.5000000	1
O1	O	1	0.5349037	0.5345631	0.4677117	1
O2	O	1	0.5349037	0.4654369	0.5322883	1
O3	O	1	0.4650963	0.5345631	0.4677117	1
O4	O	1	0.4650963	0.4654369	0.5322883	1
O5	O	1	0.4650963	0.4654369	0.4677117	1
O6	O	1	0.4650963	0.5345631	0.5322883	1

O7	O	1	0.5349037	0.4654369	0.4677117	1
O8	O	1	0.5349037	0.5345631	0.5322883	1
O9	O	1	0.5937923	0.5000000	0.5493852	1
O10	O	1	0.5937923	0.4466146	0.5000000	1
O11	O	1	0.5937923	0.5000000	0.4506148	1
O12	O	1	0.5937923	0.5533854	0.5000000	1
O13	O	1	0.5000000	0.5937923	0.5493852	1
O14	O	1	0.5533854	0.5937923	0.5000000	1
O15	O	1	0.5000000	0.5937923	0.4506148	1
O16	O	1	0.4466146	0.5937923	0.5000000	1
O17	O	1	0.4062077	0.5000000	0.5493852	1
O18	O	1	0.4062077	0.5533854	0.5000000	1
O19	O	1	0.4062077	0.5000000	0.4506148	1
O20	O	1	0.4062077	0.4466146	0.5000000	1
O21	O	1	0.5000000	0.4062077	0.5493852	1
O22	O	1	0.4466146	0.4062077	0.5000000	1
O23	O	1	0.5000000	0.4062077	0.4506148	1
O24	O	1	0.5533854	0.4062077	0.5000000	1
O25	O	1	0.5533854	0.5000000	0.5867644	1
O26	O	1	0.5000000	0.5533854	0.5867644	1
O27	O	1	0.4466146	0.5000000	0.5867644	1
O28	O	1	0.5000000	0.4466146	0.5867644	1
O29	O	1	0.5533854	0.5000000	0.4132356	1
O30	O	1	0.5000000	0.4466146	0.4132356	1
O31	O	1	0.4466146	0.5000000	0.4132356	1
O32	O	1	0.5000000	0.5533854	0.4132356	1
Zr1	Zr	1	0.5665737	0.5000000	0.5000000	1
Zr2	Zr	1	0.5000000	0.5665737	0.5000000	1
Zr3	Zr	1	0.4334263	0.5000000	0.5000000	1
Zr4	Zr	1	0.5000000	0.4334263	0.5000000	1
Zr5	Zr	1	0.5000000	0.5000000	0.5615853	1
Zr6	Zr	1	0.5000000	0.5000000	0.4384147	1

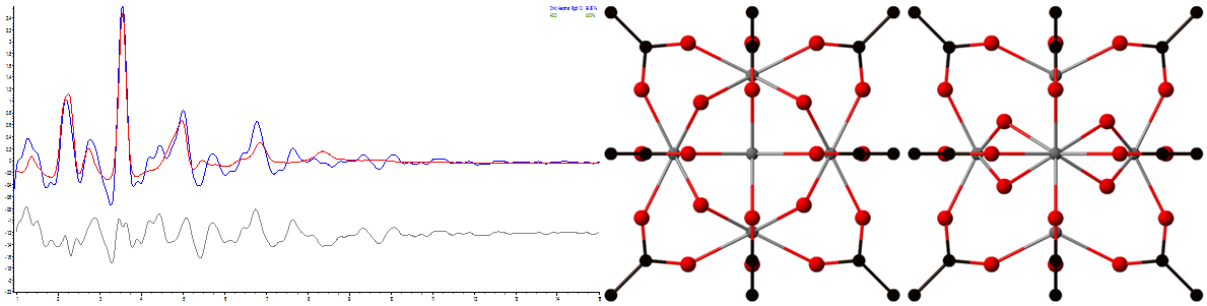

Figure 226: Observed and Calculated PDF from the chandelier core refinement of ZAA10C from the 18-month data collection and the resultant model viewed from the axial (left) and equatorial (right) positions.

Table 169: The atomic coordinates of the model resulting from the chandelier core refinement of ZAA10C from the 18-month data collection.

Atom Label	Atom Type	Multiplicity	Fractional X Coordinate	Fractional Y Coordinate	Fractional Z Coordinate	Fractional Occupancy
C1	C	1	0.5903733	0.5000000	0.5836016	1
C2	C	1	0.5000000	0.4096267	0.5836016	1
C3	C	1	0.4096267	0.5000000	0.5836016	1
C4	C	1	0.5000000	0.5903733	0.5836016	1
C5	C	1	0.5903733	0.5000000	0.4163984	1
C6	C	1	0.5000000	0.4096267	0.4163984	1
C7	C	1	0.4096267	0.5000000	0.4163984	1
C8	C	1	0.5000000	0.5903733	0.4163984	1
C9	C	1	0.5903733	0.4096267	0.5000000	1
C10	C	1	0.4096267	0.4096267	0.5000000	1
C11	C	1	0.4096267	0.5903733	0.5000000	1
C12	C	1	0.5903733	0.5903733	0.5000000	1
C13	C	1	0.6197018	0.5000000	0.6107325	1
C14	C	1	0.5000000	0.3802982	0.6107325	1
C15	C	1	0.3802982	0.5000000	0.6107325	1
C16	C	1	0.5000000	0.6197018	0.6107325	1
C17	C	1	0.6197018	0.5000000	0.3892675	1
C18	C	1	0.5000000	0.3802982	0.3892675	1
C19	C	1	0.3802982	0.5000000	0.3892675	1
C20	C	1	0.5000000	0.6197018	0.3892675	1
C21	C	1	0.6197018	0.3802982	0.5000000	1
C22	C	1	0.3802982	0.3802982	0.5000000	1
C23	C	1	0.3802982	0.6197018	0.5000000	1
C24	C	1	0.6197018	0.6197018	0.5000000	1
O1	O	1	0.5436086	0.4563914	0.4745485	1
O2	O	1	0.5436086	0.4563914	0.5254515	1
O3	O	1	0.4563914	0.4563914	0.4745485	1
O4	O	1	0.4563914	0.4563914	0.5254515	1
O5	O	1	0.4563914	0.5436086	0.4745485	1
O6	O	1	0.4563914	0.5436086	0.5254515	1
O7	O	1	0.5436086	0.5436086	0.4745485	1
O8	O	1	0.5436086	0.5436086	0.5254515	1

O9	O	1	0.5936433	0.5000000	0.5503856	1
O10	O	1	0.5936433	0.4455332	0.5000000	1
O11	O	1	0.5936433	0.5000000	0.4496144	1
O12	O	1	0.5936433	0.5544668	0.5000000	1
O13	O	1	0.5000000	0.5936433	0.5503856	1
O14	O	1	0.5544668	0.5936433	0.5000000	1
O15	O	1	0.5000000	0.5936433	0.4496144	1
O16	O	1	0.4455332	0.5936433	0.5000000	1
O17	O	1	0.4063567	0.5000000	0.5503856	1
O18	O	1	0.4063567	0.5544668	0.5000000	1
O19	O	1	0.4063567	0.5000000	0.4496144	1
O20	O	1	0.4063567	0.4455332	0.5000000	1
O21	O	1	0.5000000	0.4063567	0.5503856	1
O22	O	1	0.4455332	0.4063567	0.5000000	1
O23	O	1	0.5000000	0.4063567	0.4496144	1
O24	O	1	0.5544668	0.4063567	0.5000000	1
O25	O	1	0.5544668	0.5000000	0.5866266	1
O26	O	1	0.5000000	0.5544668	0.5866266	1
O27	O	1	0.4455332	0.5000000	0.5866266	1
O28	O	1	0.5000000	0.4455332	0.5866266	1
O29	O	1	0.5544668	0.5000000	0.4133734	1
O30	O	1	0.5000000	0.4455332	0.4133734	1
O31	O	1	0.4455332	0.5000000	0.4133734	1
O32	O	1	0.5000000	0.5544668	0.4133734	1
Zr1	Zr	1	0.5664672	0.5000000	0.5000000	1
Zr2	Zr	1	0.5000000	0.5664672	0.5000000	1
Zr3	Zr	1	0.4335328	0.5000000	0.5000000	1
Zr4	Zr	1	0.5000000	0.4335328	0.5000000	1
Zr5	Zr	1	0.5000000	0.5000000	0.5614868	1
Zr6	Zr	1	0.5000000	0.5000000	0.4385132	1

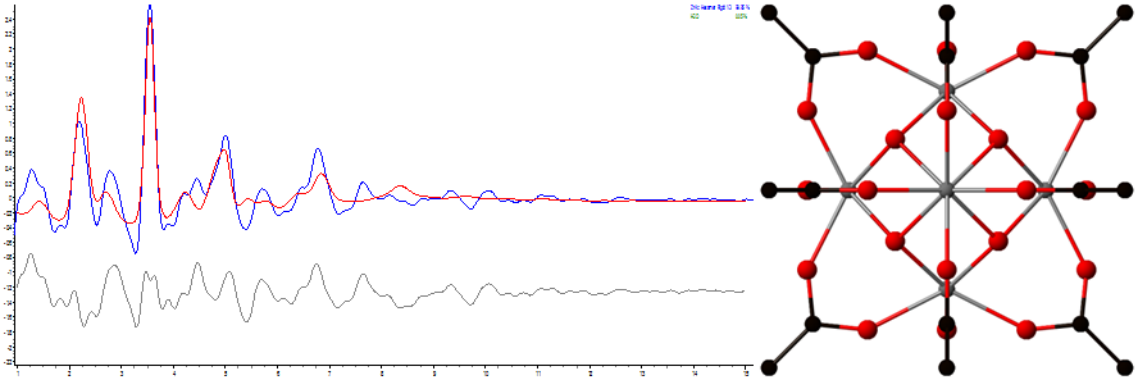

Figure 227: Observed and Calculated PDF from the fixed core refinement of ZAA10C from the 18-month data collection and the resultant model.

Table 170: The atomic coordinates of the model resulting from the fixed core refinement of ZAA10C from the 18-month data collection.

Atom Label	Atom Type	Multiplicity	Fractional X Coordinate	Fractional Y Coordinate	Fractional Z Coordinate	Fractional Occupancy
C1	C	1	0.5900219	0.5000000	0.5832765	1
C2	C	1	0.5000000	0.4099781	0.5832765	1
C3	C	1	0.4099781	0.5000000	0.5832765	1
C4	C	1	0.5000000	0.5900219	0.5832765	1
C5	C	1	0.5900219	0.5000000	0.4167235	1
C6	C	1	0.5000000	0.4099781	0.4167235	1
C7	C	1	0.4099781	0.5000000	0.4167235	1
C8	C	1	0.5000000	0.5900219	0.4167235	1
C9	C	1	0.5900219	0.4099781	0.5000000	1
C10	C	1	0.4099781	0.4099781	0.5000000	1
C11	C	1	0.4099781	0.5900219	0.5000000	1
C12	C	1	0.5900219	0.5900219	0.5000000	1
C13	C	1	0.6195722	0.5000000	0.6106126	1
C14	C	1	0.5000000	0.3804278	0.6106126	1
C15	C	1	0.3804278	0.5000000	0.6106126	1
C16	C	1	0.5000000	0.6195722	0.6106126	1
C17	C	1	0.6195722	0.5000000	0.3893874	1
C18	C	1	0.5000000	0.3804278	0.3893874	1
C19	C	1	0.3804278	0.5000000	0.3893874	1
C20	C	1	0.5000000	0.6195722	0.3893874	1
C21	C	1	0.6195722	0.3804278	0.5000000	1
C22	C	1	0.3804278	0.3804278	0.5000000	1
C23	C	1	0.3804278	0.6195722	0.5000000	1
C24	C	1	0.6195722	0.6195722	0.5000000	1
O1	O	1	0.5346935	0.534355	0.4679061	1
O2	O	1	0.5346935	0.465645	0.5320939	1
O3	O	1	0.4653065	0.534355	0.4679061	1
O4	O	1	0.4653065	0.465645	0.5320939	1
O5	O	1	0.4653065	0.465645	0.4679061	1
O6	O	1	0.4653065	0.534355	0.5320939	1

O7	O	1	0.5346935	0.465645	0.4679061	1
O8	O	1	0.5346935	0.534355	0.5320939	1
O9	O	1	0.5938075	0.5000000	0.549476	1
O10	O	1	0.5938075	0.4465165	0.5000000	1
O11	O	1	0.5938075	0.5000000	0.450524	1
O12	O	1	0.5938075	0.5534835	0.5000000	1
O13	O	1	0.5000000	0.5938075	0.549476	1
O14	O	1	0.5534835	0.5938075	0.5000000	1
O15	O	1	0.5000000	0.5938075	0.450524	1
O16	O	1	0.4465165	0.5938075	0.5000000	1
O17	O	1	0.4061925	0.5000000	0.549476	1
O18	O	1	0.4061925	0.5534835	0.5000000	1
O19	O	1	0.4061925	0.5000000	0.450524	1
O20	O	1	0.4061925	0.4465165	0.5000000	1
O21	O	1	0.5000000	0.4061925	0.549476	1
O22	O	1	0.4465165	0.4061925	0.5000000	1
O23	O	1	0.5000000	0.4061925	0.450524	1
O24	O	1	0.5534835	0.4061925	0.5000000	1
O25	O	1	0.5534835	0.5000000	0.5867785	1
O26	O	1	0.5000000	0.5534835	0.5867785	1
O27	O	1	0.4465165	0.5000000	0.5867785	1
O28	O	1	0.5000000	0.4465165	0.5867785	1
O29	O	1	0.5534835	0.5000000	0.4132215	1
O30	O	1	0.5000000	0.4465165	0.4132215	1
O31	O	1	0.4465165	0.5000000	0.4132215	1
O32	O	1	0.5000000	0.5534835	0.4132215	1
Zr1	Zr	1	0.5664645	0.5000000	0.5000000	1
Zr2	Zr	1	0.5000000	0.5664645	0.5000000	1
Zr3	Zr	1	0.4335355	0.5000000	0.5000000	1
Zr4	Zr	1	0.5000000	0.4335355	0.5000000	1
Zr5	Zr	1	0.5000000	0.5000000	0.5614843	1
Zr6	Zr	1	0.5000000	0.5000000	0.4385157	1

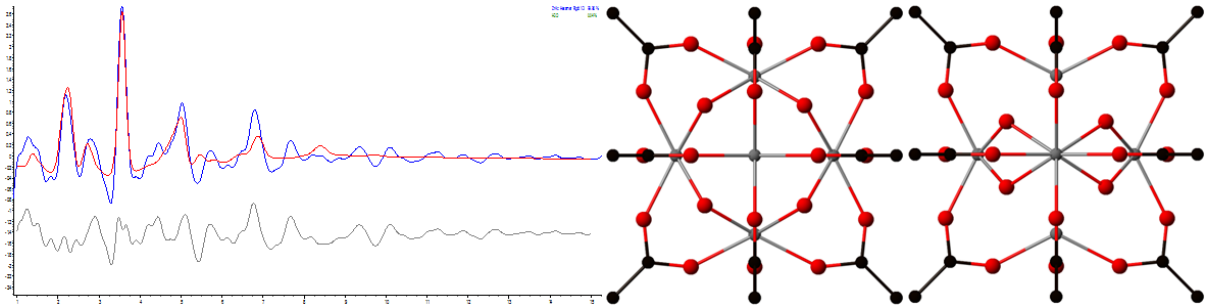

Figure 228: Observed and Calculated PDF from the chandelier core refinement of ZAA10I from the 18-month data collection and the resultant model viewed from the axial (left) and equatorial (right) positions.

Table 171: The atomic coordinates of the model resulting from the chandelier core refinement of ZAA10I from the 18-month data collection.

Atom Label	Atom Type	Multiplicity	Fractional X Coordinate	Fractional Y Coordinate	Fractional Z Coordinate	Fractional Occupancy
C1	C	1	0.5903174	0.5000000	0.5835499	1
C2	C	1	0.5000000	0.4096826	0.5835499	1
C3	C	1	0.4096826	0.5000000	0.5835499	1
C4	C	1	0.5000000	0.5903174	0.5835499	1
C5	C	1	0.5903174	0.5000000	0.4164501	1
C6	C	1	0.5000000	0.4096826	0.4164501	1
C7	C	1	0.4096826	0.5000000	0.4164501	1
C8	C	1	0.5000000	0.5903174	0.4164501	1
C9	C	1	0.5903174	0.4096826	0.5000000	1
C10	C	1	0.4096826	0.4096826	0.5000000	1
C11	C	1	0.4096826	0.5903174	0.5000000	1
C12	C	1	0.5903174	0.5903174	0.5000000	1
C13	C	1	0.6200664	0.5000000	0.6110698	1
C14	C	1	0.5000000	0.3799336	0.6110698	1
C15	C	1	0.3799336	0.5000000	0.6110698	1
C16	C	1	0.5000000	0.6200664	0.6110698	1
C17	C	1	0.6200664	0.5000000	0.3889302	1
C18	C	1	0.5000000	0.3799336	0.3889302	1
C19	C	1	0.3799336	0.5000000	0.3889302	1
C20	C	1	0.5000000	0.6200664	0.3889302	1
C21	C	1	0.6200664	0.3799336	0.5000000	1
C22	C	1	0.3799336	0.3799336	0.5000000	1
C23	C	1	0.3799336	0.6200664	0.5000000	1
C24	C	1	0.6200664	0.6200664	0.5000000	1
O1	O	1	0.5423246	0.4576754	0.4744093	1
O2	O	1	0.5423246	0.4576754	0.5255907	1
O3	O	1	0.4576754	0.4576754	0.4744093	1
O4	O	1	0.4576754	0.4576754	0.5255907	1
O5	O	1	0.4576754	0.5423246	0.4744093	1
O6	O	1	0.4576754	0.5423246	0.5255907	1
O7	O	1	0.5423246	0.5423246	0.4744093	1
O8	O	1	0.5423246	0.5423246	0.5255907	1

O9	O	1	0.5941205	0.5000000	0.5498933	1
O10	O	1	0.5941205	0.4460653	0.5000000	1
O11	O	1	0.5941205	0.5000000	0.4501067	1
O12	O	1	0.5941205	0.5539347	0.5000000	1
O13	O	1	0.5000000	0.5941205	0.5498933	1
O14	O	1	0.5539347	0.5941205	0.5000000	1
O15	O	1	0.5000000	0.5941205	0.4501067	1
O16	O	1	0.4460653	0.5941205	0.5000000	1
O17	O	1	0.4058795	0.5000000	0.5498933	1
O18	O	1	0.4058795	0.5539347	0.5000000	1
O19	O	1	0.4058795	0.5000000	0.4501067	1
O20	O	1	0.4058795	0.4460653	0.5000000	1
O21	O	1	0.5000000	0.4058795	0.5498933	1
O22	O	1	0.4460653	0.4058795	0.5000000	1
O23	O	1	0.5000000	0.4058795	0.4501067	1
O24	O	1	0.5539347	0.4058795	0.5000000	1
O25	O	1	0.5539347	0.5000000	0.587068	1
O26	O	1	0.5000000	0.5539347	0.587068	1
O27	O	1	0.4460653	0.5000000	0.587068	1
O28	O	1	0.5000000	0.4460653	0.587068	1
O29	O	1	0.5539347	0.5000000	0.412932	1
O30	O	1	0.5000000	0.4460653	0.412932	1
O31	O	1	0.4460653	0.5000000	0.412932	1
O32	O	1	0.5000000	0.5539347	0.412932	1
Zr1	Zr	1	0.5667751	0.5000000	0.5000000	1
Zr2	Zr	1	0.5000000	0.5667751	0.5000000	1
Zr3	Zr	1	0.4332249	0.5000000	0.5000000	1
Zr4	Zr	1	0.5000000	0.4332249	0.5000000	1
Zr5	Zr	1	0.5000000	0.5000000	0.5617716	1
Zr6	Zr	1	0.5000000	0.5000000	0.4382284	1

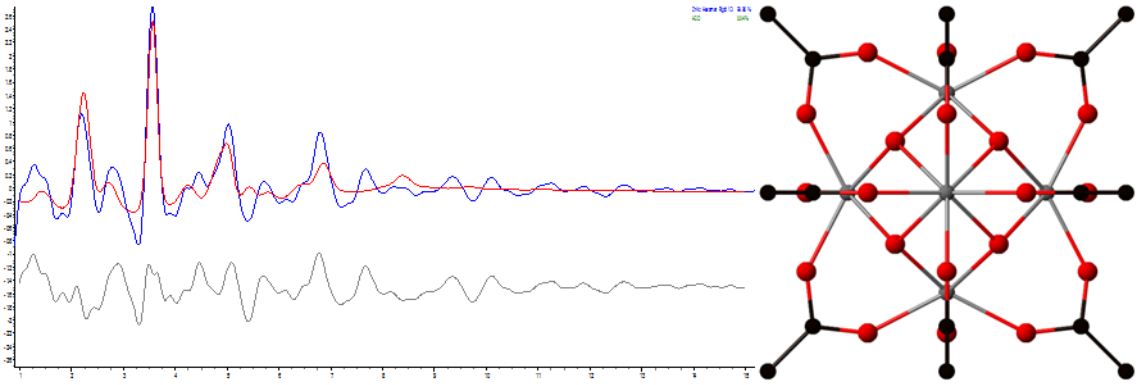

Figure 229: Observed and Calculated PDF from the fixed core refinement of ZAA10I from the 18-month data collection and the resultant model.

Table 172: The atomic coordinates of the model resulting from the fixed core refinement of ZAA10I from the 18-month data collection.

Atom Label	Atom Type	Multiplicity	Fractional X Coordinate	Fractional Y Coordinate	Fractional Z Coordinate	Fractional Occupancy
C1	C	1	0.5898988	0.5000000	0.5831626	1
C2	C	1	0.5000000	0.4101012	0.5831626	1
C3	C	1	0.4101012	0.5000000	0.5831626	1
C4	C	1	0.5000000	0.5898988	0.5831626	1
C5	C	1	0.5898988	0.5000000	0.4168374	1
C6	C	1	0.5000000	0.4101012	0.4168374	1
C7	C	1	0.4101012	0.5000000	0.4168374	1
C8	C	1	0.5000000	0.5898988	0.4168374	1
C9	C	1	0.5898988	0.4101012	0.5000000	1
C10	C	1	0.4101012	0.4101012	0.5000000	1
C11	C	1	0.4101012	0.5898988	0.5000000	1
C12	C	1	0.5898988	0.5898988	0.5000000	1
C13	C	1	0.6199203	0.5000000	0.6109347	1
C14	C	1	0.5000000	0.3800797	0.6109347	1
C15	C	1	0.3800797	0.5000000	0.6109347	1
C16	C	1	0.5000000	0.6199203	0.6109347	1
C17	C	1	0.6199203	0.5000000	0.3890653	1
C18	C	1	0.5000000	0.3800797	0.3890653	1
C19	C	1	0.3800797	0.5000000	0.3890653	1
C20	C	1	0.5000000	0.6199203	0.3890653	1
C21	C	1	0.6199203	0.3800797	0.5000000	1
C22	C	1	0.3800797	0.3800797	0.5000000	1
C23	C	1	0.3800797	0.6199203	0.5000000	1
C24	C	1	0.6199203	0.6199203	0.5000000	1
O1	O	1	0.53483	0.5344902	0.4677798	1
O2	O	1	0.53483	0.4655098	0.5322202	1
O3	O	1	0.46517	0.5344902	0.4677798	1
O4	O	1	0.46517	0.4655098	0.5322202	1
O5	O	1	0.46517	0.4655098	0.4677798	1
O6	O	1	0.46517	0.5344902	0.5322202	1

O7	O	1	0.53483	0.4655098	0.4677798	1
O8	O	1	0.53483	0.5344902	0.5322202	1
O9	O	1	0.5942053	0.5000000	0.5490848	1
O10	O	1	0.5942053	0.4469394	0.5000000	1
O11	O	1	0.5942053	0.5000000	0.4509152	1
O12	O	1	0.5942053	0.5530606	0.5000000	1
O13	O	1	0.5000000	0.5942053	0.5490848	1
O14	O	1	0.5530606	0.5942053	0.5000000	1
O15	O	1	0.5000000	0.5942053	0.4509152	1
O16	O	1	0.4469394	0.5942053	0.5000000	1
O17	O	1	0.4057947	0.5000000	0.5490848	1
O18	O	1	0.4057947	0.5530606	0.5000000	1
O19	O	1	0.4057947	0.5000000	0.4509152	1
O20	O	1	0.4057947	0.4469394	0.5000000	1
O21	O	1	0.5000000	0.4057947	0.5490848	1
O22	O	1	0.4469394	0.4057947	0.5000000	1
O23	O	1	0.5000000	0.4057947	0.4509152	1
O24	O	1	0.5530606	0.4057947	0.5000000	1
O25	O	1	0.5530606	0.5000000	0.5871465	1
O26	O	1	0.5000000	0.5530606	0.5871465	1
O27	O	1	0.4469394	0.5000000	0.5871465	1
O28	O	1	0.5000000	0.4469394	0.5871465	1
O29	O	1	0.5530606	0.5000000	0.4128535	1
O30	O	1	0.5000000	0.4469394	0.4128535	1
O31	O	1	0.4469394	0.5000000	0.4128535	1
O32	O	1	0.5000000	0.5530606	0.4128535	1
Zr1	Zr	1	0.5667943	0.5000000	0.5000000	1
Zr2	Zr	1	0.5000000	0.5667943	0.5000000	1
Zr3	Zr	1	0.4332057	0.5000000	0.5000000	1
Zr4	Zr	1	0.5000000	0.4332057	0.5000000	1
Zr5	Zr	1	0.5000000	0.5000000	0.5617894	1
Zr6	Zr	1	0.5000000	0.5000000	0.4382106	1

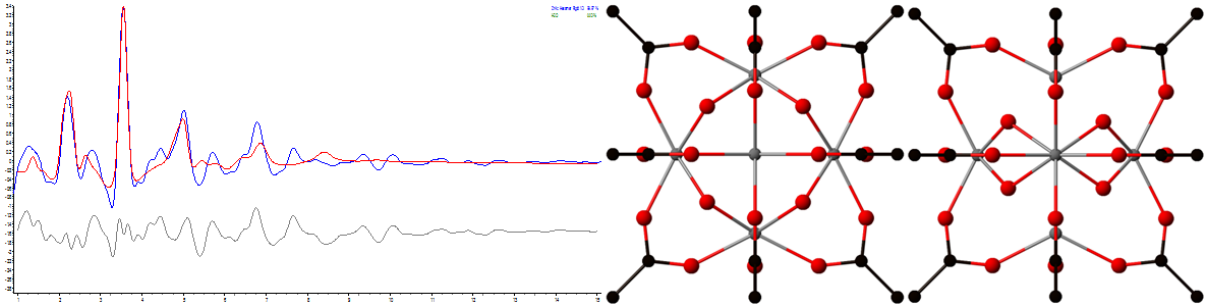

Figure 230: Observed and Calculated PDF from the chandelier core refinement of ZAA13A from the 18-month data collection and the resultant model viewed from the axial (left) and equatorial (right) positions.

Table 173: The atomic coordinates of the model resulting from the chandelier core refinement of ZAA13A from the 18-month data collection.

Atom Label	Atom Type	Multiplicity	Fractional X Coordinate	Fractional Y Coordinate	Fractional Z Coordinate	Fractional Occupancy
C1	C	1	0.5899387	0.5000000	0.5831996	1
C2	C	1	0.5000000	0.4100613	0.5831996	1
C3	C	1	0.4100613	0.5000000	0.5831996	1
C4	C	1	0.5000000	0.5899387	0.5831996	1
C5	C	1	0.5899387	0.5000000	0.4168004	1
C6	C	1	0.5000000	0.4100613	0.4168004	1
C7	C	1	0.4100613	0.5000000	0.4168004	1
C8	C	1	0.5000000	0.5899387	0.4168004	1
C9	C	1	0.5899387	0.4100613	0.5000000	1
C10	C	1	0.4100613	0.4100613	0.5000000	1
C11	C	1	0.4100613	0.5899387	0.5000000	1
C12	C	1	0.5899387	0.5899387	0.5000000	1
C13	C	1	0.6202256	0.5000000	0.611217	1
C14	C	1	0.5000000	0.3797744	0.611217	1
C15	C	1	0.3797744	0.5000000	0.611217	1
C16	C	1	0.5000000	0.6202256	0.611217	1
C17	C	1	0.6202256	0.5000000	0.388783	1
C18	C	1	0.5000000	0.3797744	0.388783	1
C19	C	1	0.3797744	0.5000000	0.388783	1
C20	C	1	0.5000000	0.6202256	0.388783	1
C21	C	1	0.6202256	0.3797744	0.5000000	1
C22	C	1	0.3797744	0.3797744	0.5000000	1
C23	C	1	0.3797744	0.6202256	0.5000000	1
C24	C	1	0.6202256	0.6202256	0.5000000	1
O1	O	1	0.5404863	0.4595137	0.4738046	1
O2	O	1	0.5404863	0.4595137	0.5261954	1
O3	O	1	0.4595137	0.4595137	0.4738046	1
O4	O	1	0.4595137	0.4595137	0.5261954	1
O5	O	1	0.4595137	0.5404863	0.4738046	1
O6	O	1	0.4595137	0.5404863	0.5261954	1
O7	O	1	0.5404863	0.5404863	0.4738046	1
O8	O	1	0.5404863	0.5404863	0.5261954	1

O9	O	1	0.5938878	0.5000000	0.5497648	1
O10	O	1	0.5938878	0.4462042	0.5000000	1
O11	O	1	0.5938878	0.5000000	0.4502352	1
O12	O	1	0.5938878	0.5537958	0.5000000	1
O13	O	1	0.5000000	0.5938878	0.5497648	1
O14	O	1	0.5537958	0.5938878	0.5000000	1
O15	O	1	0.5000000	0.5938878	0.4502352	1
O16	O	1	0.4462042	0.5938878	0.5000000	1
O17	O	1	0.4061122	0.5000000	0.5497648	1
O18	O	1	0.4061122	0.5537958	0.5000000	1
O19	O	1	0.4061122	0.5000000	0.4502352	1
O20	O	1	0.4061122	0.4462042	0.5000000	1
O21	O	1	0.5000000	0.4061122	0.5497648	1
O22	O	1	0.4462042	0.4061122	0.5000000	1
O23	O	1	0.5000000	0.4061122	0.4502352	1
O24	O	1	0.5537958	0.4061122	0.5000000	1
O25	O	1	0.5537958	0.5000000	0.5868528	1
O26	O	1	0.5000000	0.5537958	0.5868528	1
O27	O	1	0.4462042	0.5000000	0.5868528	1
O28	O	1	0.5000000	0.4462042	0.5868528	1
O29	O	1	0.5537958	0.5000000	0.4131472	1
O30	O	1	0.5000000	0.4462042	0.4131472	1
O31	O	1	0.4462042	0.5000000	0.4131472	1
O32	O	1	0.5000000	0.5537958	0.4131472	1
Zr1	Zr	1	0.566576	0.5000000	0.5000000	1
Zr2	Zr	1	0.5000000	0.566576	0.5000000	1
Zr3	Zr	1	0.433424	0.5000000	0.5000000	1
Zr4	Zr	1	0.5000000	0.433424	0.5000000	1
Zr5	Zr	1	0.5000000	0.5000000	0.5615874	1
Zr6	Zr	1	0.5000000	0.5000000	0.4384126	1

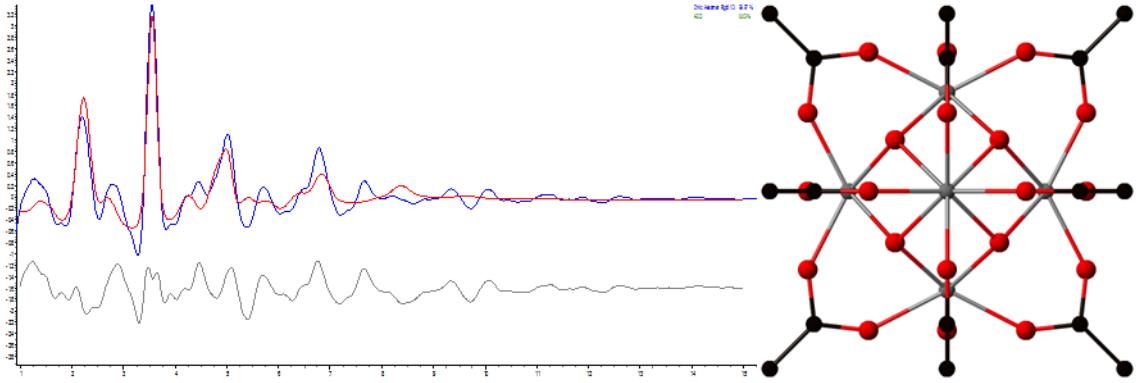

Figure 231: Observed and Calculated PDF from the fixed core refinement of ZAA13A from the 18-month data collection and the resultant model.

Table 174: The atomic coordinates of the model resulting from the fixed core refinement of ZAA13A from the 18-month data collection.

Atom Label	Atom Type	Multiplicity	Fractional X Coordinate	Fractional Y Coordinate	Fractional Z Coordinate	Fractional Occupancy
C1	C	1	0.5896386	0.5000000	0.5829219	1
C2	C	1	0.5000000	0.4103614	0.5829219	1
C3	C	1	0.4103614	0.5000000	0.5829219	1
C4	C	1	0.5000000	0.5896386	0.5829219	1
C5	C	1	0.5896386	0.5000000	0.4170781	1
C6	C	1	0.5000000	0.4103614	0.4170781	1
C7	C	1	0.4103614	0.5000000	0.4170781	1
C8	C	1	0.5000000	0.5896386	0.4170781	1
C9	C	1	0.5896386	0.4103614	0.5000000	1
C10	C	1	0.4103614	0.4103614	0.5000000	1
C11	C	1	0.4103614	0.5896386	0.5000000	1
C12	C	1	0.5896386	0.5896386	0.5000000	1
C13	C	1	0.6196645	0.5000000	0.610698	1
C14	C	1	0.5000000	0.3803355	0.610698	1
C15	C	1	0.3803355	0.5000000	0.610698	1
C16	C	1	0.5000000	0.6196645	0.610698	1
C17	C	1	0.6196645	0.5000000	0.389302	1
C18	C	1	0.5000000	0.3803355	0.389302	1
C19	C	1	0.3803355	0.5000000	0.389302	1
C20	C	1	0.5000000	0.6196645	0.389302	1
C21	C	1	0.6196645	0.3803355	0.5000000	1
C22	C	1	0.3803355	0.3803355	0.5000000	1
C23	C	1	0.3803355	0.6196645	0.5000000	1
C24	C	1	0.6196645	0.6196645	0.5000000	1
O1	O	1	0.5351	0.5347575	0.4675301	1
O2	O	1	0.5351	0.4652425	0.5324699	1
O3	O	1	0.4649	0.5347575	0.4675301	1
O4	O	1	0.4649	0.4652425	0.5324699	1
O5	O	1	0.4649	0.4652425	0.4675301	1
O6	O	1	0.4649	0.5347575	0.5324699	1

O7	O	1	0.5351	0.4652425	0.4675301	1
O8	O	1	0.5351	0.5347575	0.5324699	1
O9	O	1	0.5938476	0.5000000	0.5489975	1
O10	O	1	0.5938476	0.4470338	0.5000000	1
O11	O	1	0.5938476	0.5000000	0.4510025	1
O12	O	1	0.5938476	0.5529662	0.5000000	1
O13	O	1	0.5000000	0.5938476	0.5489975	1
O14	O	1	0.5529662	0.5938476	0.5000000	1
O15	O	1	0.5000000	0.5938476	0.4510025	1
O16	O	1	0.4470338	0.5938476	0.5000000	1
O17	O	1	0.4061524	0.5000000	0.5489975	1
O18	O	1	0.4061524	0.5529662	0.5000000	1
O19	O	1	0.4061524	0.5000000	0.4510025	1
O20	O	1	0.4061524	0.4470338	0.5000000	1
O21	O	1	0.5000000	0.4061524	0.5489975	1
O22	O	1	0.4470338	0.4061524	0.5000000	1
O23	O	1	0.5000000	0.4061524	0.4510025	1
O24	O	1	0.5529662	0.4061524	0.5000000	1
O25	O	1	0.5529662	0.5000000	0.5868156	1
O26	O	1	0.5000000	0.5529662	0.5868156	1
O27	O	1	0.4470338	0.5000000	0.5868156	1
O28	O	1	0.5000000	0.4470338	0.5868156	1
O29	O	1	0.5529662	0.5000000	0.4131844	1
O30	O	1	0.5000000	0.4470338	0.4131844	1
O31	O	1	0.4470338	0.5000000	0.4131844	1
O32	O	1	0.5000000	0.5529662	0.4131844	1
Zr1	Zr	1	0.5665863	0.5000000	0.5000000	1
Zr2	Zr	1	0.5000000	0.5665863	0.5000000	1
Zr3	Zr	1	0.4334137	0.5000000	0.5000000	1
Zr4	Zr	1	0.5000000	0.4334137	0.5000000	1
Zr5	Zr	1	0.5000000	0.5000000	0.561597	1
Zr6	Zr	1	0.5000000	0.5000000	0.438403	1

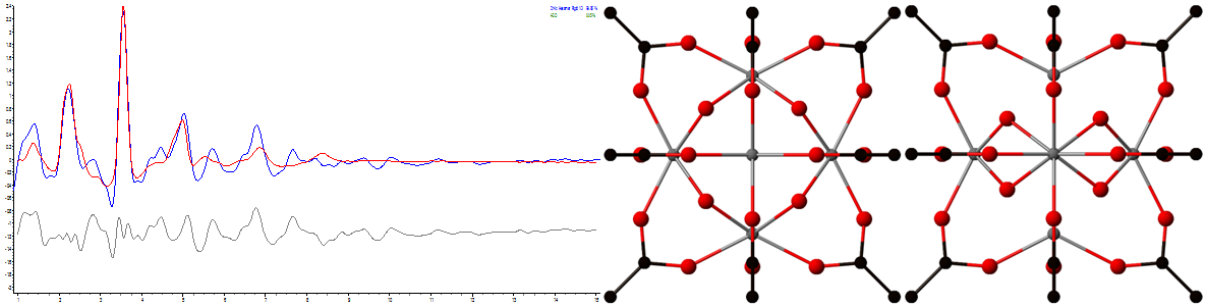

Figure 232: Observed and Calculated PDF from the chandelier core refinement of ZAA13C from the 18-month data collection and the resultant model viewed from the axial (left) and equatorial (right) positions.

Table 175: The atomic coordinates of the model resulting from the chandelier core refinement of ZAA13C from the 18-month data collection.

Atom Label	Atom Type	Multiplicity	Fractional X Coordinate	Fractional Y Coordinate	Fractional Z Coordinate	Fractional Occupancy
C1	C	1	0.5908389	0.5000000	0.5840323	1
C2	C	1	0.5000000	0.4091611	0.5840323	1
C3	C	1	0.4091611	0.5000000	0.5840323	1
C4	C	1	0.5000000	0.5908389	0.5840323	1
C5	C	1	0.5908389	0.5000000	0.4159677	1
C6	C	1	0.5000000	0.4091611	0.4159677	1
C7	C	1	0.4091611	0.5000000	0.4159677	1
C8	C	1	0.5000000	0.5908389	0.4159677	1
C9	C	1	0.5908389	0.4091611	0.5000000	1
C10	C	1	0.4091611	0.4091611	0.5000000	1
C11	C	1	0.4091611	0.5908389	0.5000000	1
C12	C	1	0.5908389	0.5908389	0.5000000	1
C13	C	1	0.6194032	0.5000000	0.6104563	1
C14	C	1	0.5000000	0.3805968	0.6104563	1
C15	C	1	0.3805968	0.5000000	0.6104563	1
C16	C	1	0.5000000	0.6194032	0.6104563	1
C17	C	1	0.6194032	0.5000000	0.3895437	1
C18	C	1	0.5000000	0.3805968	0.3895437	1
C19	C	1	0.3805968	0.5000000	0.3895437	1
C20	C	1	0.5000000	0.6194032	0.3895437	1
C21	C	1	0.6194032	0.3805968	0.5000000	1
C22	C	1	0.3805968	0.3805968	0.5000000	1
C23	C	1	0.3805968	0.6194032	0.5000000	1
C24	C	1	0.6194032	0.6194032	0.5000000	1
O1	O	1	0.5390998	0.4609002	0.4724809	1
O2	O	1	0.5390998	0.4609002	0.5275191	1
O3	O	1	0.4609002	0.4609002	0.4724809	1
O4	O	1	0.4609002	0.4609002	0.5275191	1
O5	O	1	0.4609002	0.5390998	0.4724809	1
O6	O	1	0.4609002	0.5390998	0.5275191	1
O7	O	1	0.5390998	0.5390998	0.4724809	1
O8	O	1	0.5390998	0.5390998	0.5275191	1

O9	O	1	0.5939641	0.5000000	0.5498988	1
O10	O	1	0.5939641	0.4460594	0.5000000	1
O11	O	1	0.5939641	0.5000000	0.4501012	1
O12	O	1	0.5939641	0.5539406	0.5000000	1
O13	O	1	0.5000000	0.5939641	0.5498988	1
O14	O	1	0.5539406	0.5939641	0.5000000	1
O15	O	1	0.5000000	0.5939641	0.4501012	1
O16	O	1	0.4460594	0.5939641	0.5000000	1
O17	O	1	0.4060359	0.5000000	0.5498988	1
O18	O	1	0.4060359	0.5539406	0.5000000	1
O19	O	1	0.4060359	0.5000000	0.4501012	1
O20	O	1	0.4060359	0.4460594	0.5000000	1
O21	O	1	0.5000000	0.4060359	0.5498988	1
O22	O	1	0.4460594	0.4060359	0.5000000	1
O23	O	1	0.5000000	0.4060359	0.4501012	1
O24	O	1	0.5539406	0.4060359	0.5000000	1
O25	O	1	0.5539406	0.5000000	0.5869234	1
O26	O	1	0.5000000	0.5539406	0.5869234	1
O27	O	1	0.4460594	0.5000000	0.5869234	1
O28	O	1	0.5000000	0.4460594	0.5869234	1
O29	O	1	0.5539406	0.5000000	0.4130766	1
O30	O	1	0.5000000	0.4460594	0.4130766	1
O31	O	1	0.4460594	0.5000000	0.4130766	1
O32	O	1	0.5000000	0.5539406	0.4130766	1
Zr1	Zr	1	0.5665244	0.5000000	0.5000000	1
Zr2	Zr	1	0.5000000	0.5665244	0.5000000	1
Zr3	Zr	1	0.4334756	0.5000000	0.5000000	1
Zr4	Zr	1	0.5000000	0.4334756	0.5000000	1
Zr5	Zr	1	0.5000000	0.5000000	0.5615397	1
Zr6	Zr	1	0.5000000	0.5000000	0.4384603	1

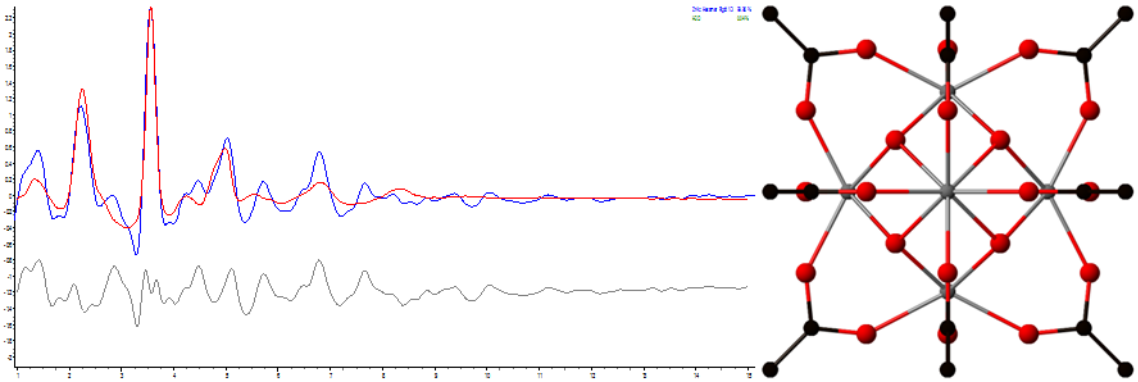

Figure 233: Observed and Calculated PDF from the fixed core refinement of ZAA13C from the 18-month data collection and the resultant model.

Table 176: The atomic coordinates of the model resulting from the fixed core refinement of ZAA13C from the 18-month data collection.

Atom Label	Atom Type	Multiplicity	Fractional X Coordinate	Fractional Y Coordinate	Fractional Z Coordinate	Fractional Occupancy
C1	C	1	0.5907142	0.5000000	0.5839169	1
C2	C	1	0.5000000	0.4092858	0.5839169	1
C3	C	1	0.4092858	0.5000000	0.5839169	1
C4	C	1	0.5000000	0.5907142	0.5839169	1
C5	C	1	0.5907142	0.5000000	0.4160831	1
C6	C	1	0.5000000	0.4092858	0.4160831	1
C7	C	1	0.4092858	0.5000000	0.4160831	1
C8	C	1	0.5000000	0.5907142	0.4160831	1
C9	C	1	0.5907142	0.4092858	0.5000000	1
C10	C	1	0.4092858	0.4092858	0.5000000	1
C11	C	1	0.4092858	0.5907142	0.5000000	1
C12	C	1	0.5907142	0.5907142	0.5000000	1
C13	C	1	0.6183102	0.5000000	0.6094452	1
C14	C	1	0.5000000	0.3816898	0.6094452	1
C15	C	1	0.3816898	0.5000000	0.6094452	1
C16	C	1	0.5000000	0.6183102	0.6094452	1
C17	C	1	0.6183102	0.5000000	0.3905548	1
C18	C	1	0.5000000	0.3816898	0.3905548	1
C19	C	1	0.3816898	0.5000000	0.3905548	1
C20	C	1	0.5000000	0.6183102	0.3905548	1
C21	C	1	0.6183102	0.3816898	0.5000000	1
C22	C	1	0.3816898	0.3816898	0.5000000	1
C23	C	1	0.3816898	0.6183102	0.5000000	1
C24	C	1	0.6183102	0.6183102	0.5000000	1
O1	O	1	0.5348233	0.5344835	0.467786	1
O2	O	1	0.5348233	0.4655165	0.532214	1
O3	O	1	0.4651767	0.5344835	0.467786	1
O4	O	1	0.4651767	0.4655165	0.532214	1
O5	O	1	0.4651767	0.4655165	0.467786	1
O6	O	1	0.4651767	0.5344835	0.532214	1

O7	O	1	0.5348233	0.4655165	0.467786	1
O8	O	1	0.5348233	0.5344835	0.532214	1
O9	O	1	0.5945718	0.5000000	0.5499959	1
O10	O	1	0.5945718	0.4459545	0.5000000	1
O11	O	1	0.5945718	0.5000000	0.4500041	1
O12	O	1	0.5945718	0.5540455	0.5000000	1
O13	O	1	0.5000000	0.5945718	0.5499959	1
O14	O	1	0.5540455	0.5945718	0.5000000	1
O15	O	1	0.5000000	0.5945718	0.4500041	1
O16	O	1	0.4459545	0.5945718	0.5000000	1
O17	O	1	0.4054282	0.5000000	0.5499959	1
O18	O	1	0.4054282	0.5540455	0.5000000	1
O19	O	1	0.4054282	0.5000000	0.4500041	1
O20	O	1	0.4054282	0.4459545	0.5000000	1
O21	O	1	0.5000000	0.4054282	0.5499959	1
O22	O	1	0.4459545	0.4054282	0.5000000	1
O23	O	1	0.5000000	0.4054282	0.4500041	1
O24	O	1	0.5540455	0.4054282	0.5000000	1
O25	O	1	0.5540455	0.5000000	0.5874856	1
O26	O	1	0.5000000	0.5540455	0.5874856	1
O27	O	1	0.4459545	0.5000000	0.5874856	1
O28	O	1	0.5000000	0.4459545	0.5874856	1
O29	O	1	0.5540455	0.5000000	0.4125144	1
O30	O	1	0.5000000	0.4459545	0.4125144	1
O31	O	1	0.4459545	0.5000000	0.4125144	1
O32	O	1	0.5000000	0.5540455	0.4125144	1
Zr1	Zr	1	0.5665326	0.5000000	0.5000000	1
Zr2	Zr	1	0.5000000	0.5665326	0.5000000	1
Zr3	Zr	1	0.4334674	0.5000000	0.5000000	1
Zr4	Zr	1	0.5000000	0.4334674	0.5000000	1
Zr5	Zr	1	0.5000000	0.5000000	0.5615473	1
Zr6	Zr	1	0.5000000	0.5000000	0.4384527	1

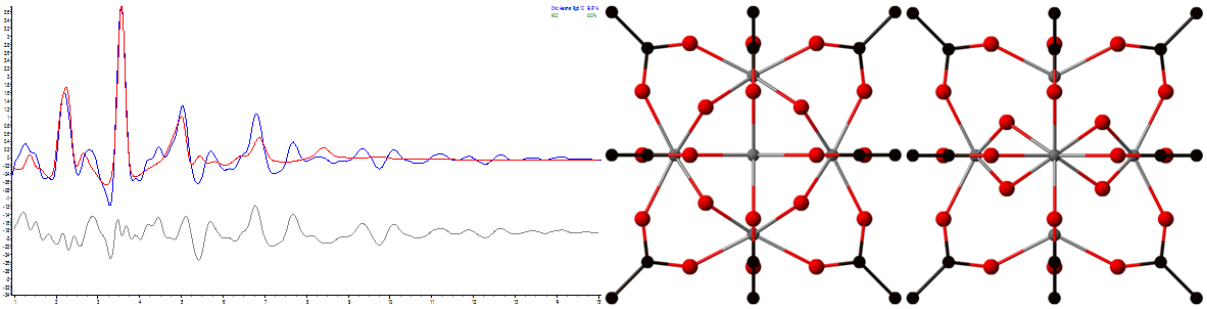

Figure 234: Observed and Calculated PDF from the chandelier core refinement of ZAA13I from the 18-month data collection and the resultant model viewed from the axial (left) and equatorial (right) positions.

Table 177: The atomic coordinates of the model resulting from the chandelier core refinement of ZAA13I from the 18-month data collection.

Atom Label	Atom Type	Multiplicity	Fractional X Coordinate	Fractional Y Coordinate	Fractional Z Coordinate	Fractional Occupancy
C1	C	1	0.589887	0.5000000	0.5831517	1
C2	C	1	0.5000000	0.410113	0.5831517	1
C3	C	1	0.410113	0.5000000	0.5831517	1
C4	C	1	0.5000000	0.589887	0.5831517	1
C5	C	1	0.589887	0.5000000	0.4168483	1
C6	C	1	0.5000000	0.410113	0.4168483	1
C7	C	1	0.410113	0.5000000	0.4168483	1
C8	C	1	0.5000000	0.589887	0.4168483	1
C9	C	1	0.589887	0.410113	0.5000000	1
C10	C	1	0.410113	0.410113	0.5000000	1
C11	C	1	0.410113	0.589887	0.5000000	1
C12	C	1	0.589887	0.589887	0.5000000	1
C13	C	1	0.6202452	0.5000000	0.6112352	1
C14	C	1	0.5000000	0.3797548	0.6112352	1
C15	C	1	0.3797548	0.5000000	0.6112352	1
C16	C	1	0.5000000	0.6202452	0.6112352	1
C17	C	1	0.6202452	0.5000000	0.3887648	1
C18	C	1	0.5000000	0.3797548	0.3887648	1
C19	C	1	0.3797548	0.5000000	0.3887648	1
C20	C	1	0.5000000	0.6202452	0.3887648	1
C21	C	1	0.6202452	0.3797548	0.5000000	1
C22	C	1	0.3797548	0.3797548	0.5000000	1
C23	C	1	0.3797548	0.6202452	0.5000000	1
C24	C	1	0.6202452	0.6202452	0.5000000	1
O1	O	1	0.5404453	0.4595547	0.4740022	1
O2	O	1	0.5404453	0.4595547	0.5259978	1
O3	O	1	0.4595547	0.4595547	0.4740022	1
O4	O	1	0.4595547	0.4595547	0.5259978	1
O5	O	1	0.4595547	0.5404453	0.4740022	1
O6	O	1	0.4595547	0.5404453	0.5259978	1
O7	O	1	0.5404453	0.5404453	0.4740022	1
O8	O	1	0.5404453	0.5404453	0.5259978	1

O9	O	1	0.5941299	0.5000000	0.5496963	1
O10	O	1	0.5941299	0.4462783	0.5000000	1
O11	O	1	0.5941299	0.5000000	0.4503037	1
O12	O	1	0.5941299	0.5537217	0.5000000	1
O13	O	1	0.5000000	0.5941299	0.5496963	1
O14	O	1	0.5537217	0.5941299	0.5000000	1
O15	O	1	0.5000000	0.5941299	0.4503037	1
O16	O	1	0.4462783	0.5941299	0.5000000	1
O17	O	1	0.4058701	0.5000000	0.5496963	1
O18	O	1	0.4058701	0.5537217	0.5000000	1
O19	O	1	0.4058701	0.5000000	0.4503037	1
O20	O	1	0.4058701	0.4462783	0.5000000	1
O21	O	1	0.5000000	0.4058701	0.5496963	1
O22	O	1	0.4462783	0.4058701	0.5000000	1
O23	O	1	0.5000000	0.4058701	0.4503037	1
O24	O	1	0.5537217	0.4058701	0.5000000	1
O25	O	1	0.5537217	0.5000000	0.5870767	1
O26	O	1	0.5000000	0.5537217	0.5870767	1
O27	O	1	0.4462783	0.5000000	0.5870767	1
O28	O	1	0.5000000	0.4462783	0.5870767	1
O29	O	1	0.5537217	0.5000000	0.4129233	1
O30	O	1	0.5000000	0.4462783	0.4129233	1
O31	O	1	0.4462783	0.5000000	0.4129233	1
O32	O	1	0.5000000	0.5537217	0.4129233	1
Zr1	Zr	1	0.5668095	0.5000000	0.5000000	1
Zr2	Zr	1	0.5000000	0.5668095	0.5000000	1
Zr3	Zr	1	0.4331905	0.5000000	0.5000000	1
Zr4	Zr	1	0.5000000	0.4331905	0.5000000	1
Zr5	Zr	1	0.5000000	0.5000000	0.5618034	1
Zr6	Zr	1	0.5000000	0.5000000	0.4381966	1

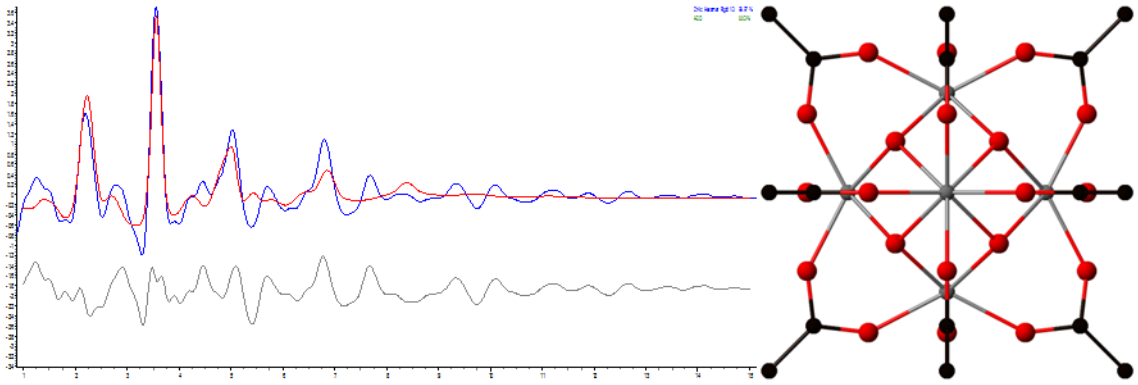

Figure 235: Observed and Calculated PDF from the fixed core refinement of ZAA13I from the 18-month data collection and the resultant model.

Table 178: The atomic coordinates of the model resulting from the fixed core refinement of ZAA13I from the 18-month data collection.

Atom Label	Atom Type	Multiplicity	Fractional X Coordinate	Fractional Y Coordinate	Fractional Z Coordinate	Fractional Occupancy
C1	C	1	0.5898165	0.5000000	0.5830865	1
C2	C	1	0.5000000	0.4101835	0.5830865	1
C3	C	1	0.4101835	0.5000000	0.5830865	1
C4	C	1	0.5000000	0.5898165	0.5830865	1
C5	C	1	0.5898165	0.5000000	0.4169135	1
C6	C	1	0.5000000	0.4101835	0.4169135	1
C7	C	1	0.4101835	0.5000000	0.4169135	1
C8	C	1	0.5000000	0.5898165	0.4169135	1
C9	C	1	0.5898165	0.4101835	0.5000000	1
C10	C	1	0.4101835	0.4101835	0.5000000	1
C11	C	1	0.4101835	0.5898165	0.5000000	1
C12	C	1	0.5898165	0.5898165	0.5000000	1
C13	C	1	0.6199602	0.5000000	0.6109716	1
C14	C	1	0.5000000	0.3800398	0.6109716	1
C15	C	1	0.3800398	0.5000000	0.6109716	1
C16	C	1	0.5000000	0.6199602	0.6109716	1
C17	C	1	0.6199602	0.5000000	0.3890284	1
C18	C	1	0.5000000	0.3800398	0.3890284	1
C19	C	1	0.3800398	0.5000000	0.3890284	1
C20	C	1	0.5000000	0.6199602	0.3890284	1
C21	C	1	0.6199602	0.3800398	0.5000000	1
C22	C	1	0.3800398	0.3800398	0.5000000	1
C23	C	1	0.3800398	0.6199602	0.5000000	1
C24	C	1	0.6199602	0.6199602	0.5000000	1
O1	O	1	0.5348021	0.5344625	0.4678056	1
O2	O	1	0.5348021	0.4655375	0.5321944	1
O3	O	1	0.4651979	0.5344625	0.4678056	1
O4	O	1	0.4651979	0.4655375	0.5321944	1
O5	O	1	0.4651979	0.4655375	0.4678056	1
O6	O	1	0.4651979	0.5344625	0.5321944	1

O7	O	1	0.5348021	0.4655375	0.4678056	1
O8	O	1	0.5348021	0.5344625	0.5321944	1
O9	O	1	0.5942346	0.5000000	0.5488531	1
O10	O	1	0.5942346	0.4471898	0.5000000	1
O11	O	1	0.5942346	0.5000000	0.4511469	1
O12	O	1	0.5942346	0.5528102	0.5000000	1
O13	O	1	0.5000000	0.5942346	0.5488531	1
O14	O	1	0.5528102	0.5942346	0.5000000	1
O15	O	1	0.5000000	0.5942346	0.4511469	1
O16	O	1	0.4471898	0.5942346	0.5000000	1
O17	O	1	0.4057654	0.5000000	0.5488531	1
O18	O	1	0.4057654	0.5528102	0.5000000	1
O19	O	1	0.4057654	0.5000000	0.4511469	1
O20	O	1	0.4057654	0.4471898	0.5000000	1
O21	O	1	0.5000000	0.4057654	0.5488531	1
O22	O	1	0.4471898	0.4057654	0.5000000	1
O23	O	1	0.5000000	0.4057654	0.4511469	1
O24	O	1	0.5528102	0.4057654	0.5000000	1
O25	O	1	0.5528102	0.5000000	0.5871736	1
O26	O	1	0.5000000	0.5528102	0.5871736	1
O27	O	1	0.4471898	0.5000000	0.5871736	1
O28	O	1	0.5000000	0.4471898	0.5871736	1
O29	O	1	0.5528102	0.5000000	0.4128264	1
O30	O	1	0.5000000	0.4471898	0.4128264	1
O31	O	1	0.4471898	0.5000000	0.4128264	1
O32	O	1	0.5000000	0.5528102	0.4128264	1
Zr1	Zr	1	0.5667885	0.5000000	0.5000000	1
Zr2	Zr	1	0.5000000	0.5667885	0.5000000	1
Zr3	Zr	1	0.4332115	0.5000000	0.5000000	1
Zr4	Zr	1	0.5000000	0.4332115	0.5000000	1
Zr5	Zr	1	0.5000000	0.5000000	0.561784	1
Zr6	Zr	1	0.5000000	0.5000000	0.438216	1

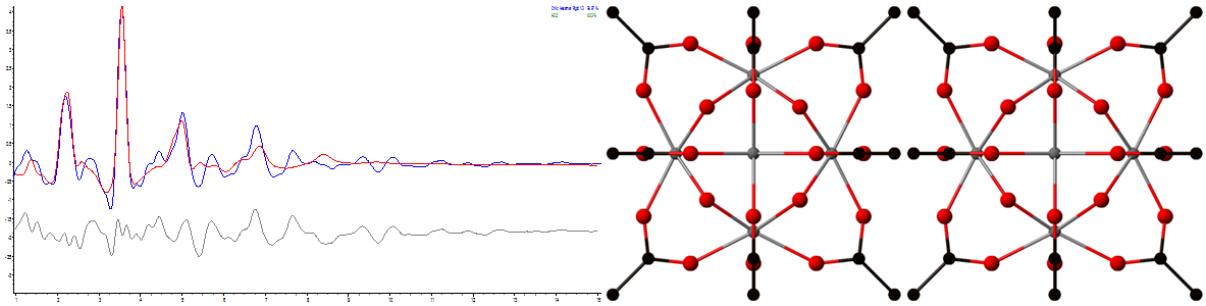

Figure 236: Observed and Calculated PDF from the chandelier core refinement of ZAA16A from the 18-month data collection and the resultant model viewed from the axial (left) and equatorial (right) positions.

Table 179: The atomic coordinates of the model resulting from the chandelier core refinement of ZAA16A from the 18-month data collection.

Atom Label	Atom Type	Multiplicity	Fractional X Coordinate	Fractional Y Coordinate	Fractional Z Coordinate	Fractional Occupancy
C1	C	1	0.5898336	0.5000000	0.5831024	1
C2	C	1	0.5000000	0.4101664	0.5831024	1
C3	C	1	0.4101664	0.5000000	0.5831024	1
C4	C	1	0.5000000	0.5898336	0.5831024	1
C5	C	1	0.5898336	0.5000000	0.4168976	1
C6	C	1	0.5000000	0.4101664	0.4168976	1
C7	C	1	0.4101664	0.5000000	0.4168976	1
C8	C	1	0.5000000	0.5898336	0.4168976	1
C9	C	1	0.5898336	0.4101664	0.5000000	1
C10	C	1	0.4101664	0.4101664	0.5000000	1
C11	C	1	0.4101664	0.5898336	0.5000000	1
C12	C	1	0.5898336	0.5898336	0.5000000	1
C13	C	1	0.6203143	0.5000000	0.6112991	1
C14	C	1	0.5000000	0.3796857	0.6112991	1
C15	C	1	0.3796857	0.5000000	0.6112991	1
C16	C	1	0.5000000	0.6203143	0.6112991	1
C17	C	1	0.6203143	0.5000000	0.3887009	1
C18	C	1	0.5000000	0.3796857	0.3887009	1
C19	C	1	0.3796857	0.5000000	0.3887009	1
C20	C	1	0.5000000	0.6203143	0.3887009	1
C21	C	1	0.6203143	0.3796857	0.5000000	1
C22	C	1	0.3796857	0.3796857	0.5000000	1
C23	C	1	0.3796857	0.6203143	0.5000000	1
C24	C	1	0.6203143	0.6203143	0.5000000	1
O1	O	1	0.5397076	0.4602924	0.4734902	1
O2	O	1	0.5397076	0.4602924	0.5265098	1
O3	O	1	0.4602924	0.4602924	0.4734902	1
O4	O	1	0.4602924	0.4602924	0.5265098	1
O5	O	1	0.4602924	0.5397076	0.4734902	1
O6	O	1	0.4602924	0.5397076	0.5265098	1
O7	O	1	0.5397076	0.5397076	0.4734902	1
O8	O	1	0.5397076	0.5397076	0.5265098	1

O9	O	1	0.5938381	0.5000000	0.5496586	1
O10	O	1	0.5938381	0.4463191	0.5000000	1
O11	O	1	0.5938381	0.5000000	0.4503414	1
O12	O	1	0.5938381	0.5536809	0.5000000	1
O13	O	1	0.5000000	0.5938381	0.5496586	1
O14	O	1	0.5536809	0.5938381	0.5000000	1
O15	O	1	0.5000000	0.5938381	0.4503414	1
O16	O	1	0.4463191	0.5938381	0.5000000	1
O17	O	1	0.4061619	0.5000000	0.5496586	1
O18	O	1	0.4061619	0.5536809	0.5000000	1
O19	O	1	0.4061619	0.5000000	0.4503414	1
O20	O	1	0.4061619	0.4463191	0.5000000	1
O21	O	1	0.5000000	0.4061619	0.5496586	1
O22	O	1	0.4463191	0.4061619	0.5000000	1
O23	O	1	0.5000000	0.4061619	0.4503414	1
O24	O	1	0.5536809	0.4061619	0.5000000	1
O25	O	1	0.5536809	0.5000000	0.5868068	1
O26	O	1	0.5000000	0.5536809	0.5868068	1
O27	O	1	0.4463191	0.5000000	0.5868068	1
O28	O	1	0.5000000	0.4463191	0.5868068	1
O29	O	1	0.5536809	0.5000000	0.4131932	1
O30	O	1	0.5000000	0.4463191	0.4131932	1
O31	O	1	0.4463191	0.5000000	0.4131932	1
O32	O	1	0.5000000	0.5536809	0.4131932	1
Zr1	Zr	1	0.5666213	0.5000000	0.5000000	1
Zr2	Zr	1	0.5000000	0.5666213	0.5000000	1
Zr3	Zr	1	0.4333787	0.5000000	0.5000000	1
Zr4	Zr	1	0.5000000	0.4333787	0.5000000	1
Zr5	Zr	1	0.5000000	0.5000000	0.5616293	1
Zr6	Zr	1	0.5000000	0.5000000	0.4383707	1

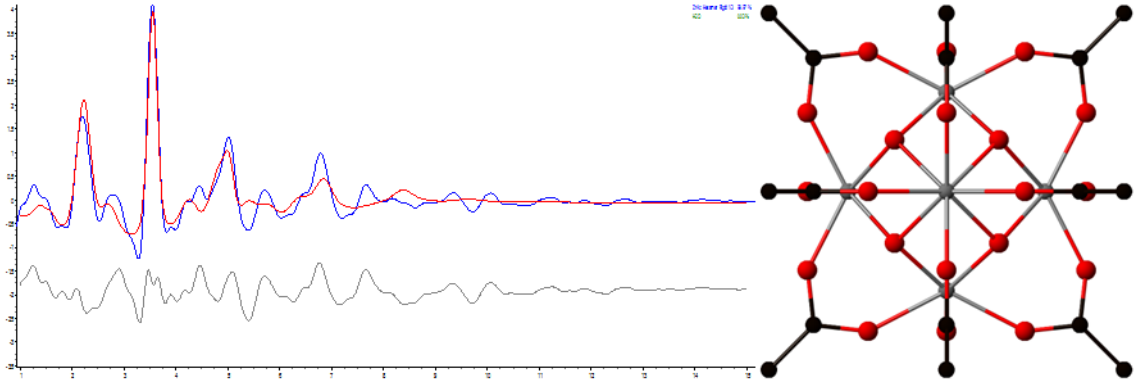

Figure 237: Observed and Calculated PDF from the fixed core refinement of ZAA16A from the 18-month data collection and the resultant model.

Table 180: The atomic coordinates of the model resulting from the fixed core refinement of ZAA16A from the 18-month data collection.

Atom Label	Atom Type	Multiplicity	Fractional X Coordinate	Fractional Y Coordinate	Fractional Z Coordinate	Fractional Occupancy
C1	C	1	0.589731	0.5000000	0.5830074	1
C2	C	1	0.5000000	0.410269	0.5830074	1
C3	C	1	0.410269	0.5000000	0.5830074	1
C4	C	1	0.5000000	0.589731	0.5830074	1
C5	C	1	0.589731	0.5000000	0.4169926	1
C6	C	1	0.5000000	0.410269	0.4169926	1
C7	C	1	0.410269	0.5000000	0.4169926	1
C8	C	1	0.5000000	0.589731	0.4169926	1
C9	C	1	0.589731	0.410269	0.5000000	1
C10	C	1	0.410269	0.410269	0.5000000	1
C11	C	1	0.410269	0.589731	0.5000000	1
C12	C	1	0.589731	0.589731	0.5000000	1
C13	C	1	0.6198093	0.5000000	0.6108319	1
C14	C	1	0.5000000	0.3801907	0.6108319	1
C15	C	1	0.3801907	0.5000000	0.6108319	1
C16	C	1	0.5000000	0.6198093	0.6108319	1
C17	C	1	0.6198093	0.5000000	0.3891681	1
C18	C	1	0.5000000	0.3801907	0.3891681	1
C19	C	1	0.3801907	0.5000000	0.3891681	1
C20	C	1	0.5000000	0.6198093	0.3891681	1
C21	C	1	0.6198093	0.3801907	0.5000000	1
C22	C	1	0.3801907	0.3801907	0.5000000	1
C23	C	1	0.3801907	0.6198093	0.5000000	1
C24	C	1	0.6198093	0.6198093	0.5000000	1
O1	O	1	0.5351122	0.5347696	0.4675187	1
O2	O	1	0.5351122	0.4652304	0.5324813	1
O3	O	1	0.4648878	0.5347696	0.4675187	1
O4	O	1	0.4648878	0.4652304	0.5324813	1
O5	O	1	0.4648878	0.4652304	0.4675187	1
O6	O	1	0.4648878	0.5347696	0.5324813	1

O7	O	1	0.5351122	0.4652304	0.4675187	1
O8	O	1	0.5351122	0.5347696	0.5324813	1
O9	O	1	0.5939364	0.5000000	0.5488678	1
O10	O	1	0.5939364	0.4471739	0.5000000	1
O11	O	1	0.5939364	0.5000000	0.4511322	1
O12	O	1	0.5939364	0.5528261	0.5000000	1
O13	O	1	0.5000000	0.5939364	0.5488678	1
O14	O	1	0.5528261	0.5939364	0.5000000	1
O15	O	1	0.5000000	0.5939364	0.4511322	1
O16	O	1	0.4471739	0.5939364	0.5000000	1
O17	O	1	0.4060636	0.5000000	0.5488678	1
O18	O	1	0.4060636	0.5528261	0.5000000	1
O19	O	1	0.4060636	0.5000000	0.4511322	1
O20	O	1	0.4060636	0.4471739	0.5000000	1
O21	O	1	0.5000000	0.4060636	0.5488678	1
O22	O	1	0.4471739	0.4060636	0.5000000	1
O23	O	1	0.5000000	0.4060636	0.4511322	1
O24	O	1	0.5528261	0.4060636	0.5000000	1
O25	O	1	0.5528261	0.5000000	0.5868977	1
O26	O	1	0.5000000	0.5528261	0.5868977	1
O27	O	1	0.4471739	0.5000000	0.5868977	1
O28	O	1	0.5000000	0.4471739	0.5868977	1
O29	O	1	0.5528261	0.5000000	0.4131023	1
O30	O	1	0.5000000	0.4471739	0.4131023	1
O31	O	1	0.4471739	0.5000000	0.4131023	1
O32	O	1	0.5000000	0.5528261	0.4131023	1
Zr1	Zr	1	0.5665997	0.5000000	0.5000000	1
Zr2	Zr	1	0.5000000	0.5665997	0.5000000	1
Zr3	Zr	1	0.4334003	0.5000000	0.5000000	1
Zr4	Zr	1	0.5000000	0.4334003	0.5000000	1
Zr5	Zr	1	0.5000000	0.5000000	0.5616094	1
Zr6	Zr	1	0.5000000	0.5000000	0.4383906	1

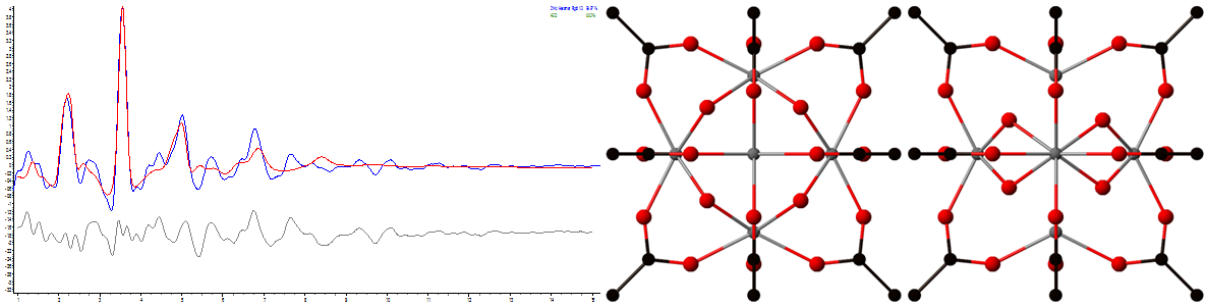

Figure 238: Observed and Calculated PDF from the chandelier core refinement of ZAA16C from the 18-month data collection and the resultant model viewed from the axial (left) and equatorial (right) positions.

Table 181: The atomic coordinates of the model resulting from the chandelier core refinement of ZAA16C from the 18-month data collection.

Atom Label	Atom Type	Multiplicity	Fractional X Coordinate	Fractional Y Coordinate	Fractional Z Coordinate	Fractional Occupancy
C1	C	1	0.5898388	0.5000000	0.5831072	1
C2	C	1	0.5000000	0.4101612	0.5831072	1
C3	C	1	0.4101612	0.5000000	0.5831072	1
C4	C	1	0.5000000	0.5898388	0.5831072	1
C5	C	1	0.5898388	0.5000000	0.4168928	1
C6	C	1	0.5000000	0.4101612	0.4168928	1
C7	C	1	0.4101612	0.5000000	0.4168928	1
C8	C	1	0.5000000	0.5898388	0.4168928	1
C9	C	1	0.5898388	0.4101612	0.5000000	1
C10	C	1	0.4101612	0.4101612	0.5000000	1
C11	C	1	0.4101612	0.5898388	0.5000000	1
C12	C	1	0.5898388	0.5898388	0.5000000	1
C13	C	1	0.6202296	0.5000000	0.6112208	1
C14	C	1	0.5000000	0.3797704	0.6112208	1
C15	C	1	0.3797704	0.5000000	0.6112208	1
C16	C	1	0.5000000	0.6202296	0.6112208	1
C17	C	1	0.6202296	0.5000000	0.3887792	1
C18	C	1	0.5000000	0.3797704	0.3887792	1
C19	C	1	0.3797704	0.5000000	0.3887792	1
C20	C	1	0.5000000	0.6202296	0.3887792	1
C21	C	1	0.6202296	0.3797704	0.5000000	1
C22	C	1	0.3797704	0.3797704	0.5000000	1
C23	C	1	0.3797704	0.6202296	0.5000000	1
C24	C	1	0.6202296	0.6202296	0.5000000	1
O1	O	1	0.5397921	0.4602079	0.47351	1
O2	O	1	0.5397921	0.4602079	0.52649	1
O3	O	1	0.4602079	0.4602079	0.47351	1
O4	O	1	0.4602079	0.4602079	0.52649	1
O5	O	1	0.4602079	0.5397921	0.47351	1
O6	O	1	0.4602079	0.5397921	0.52649	1
O7	O	1	0.5397921	0.5397921	0.47351	1
O8	O	1	0.5397921	0.5397921	0.52649	1

O9	O	1	0.5937293	0.5000000	0.5497077	1
O10	O	1	0.5937293	0.446266	0.5000000	1
O11	O	1	0.5937293	0.5000000	0.4502923	1
O12	O	1	0.5937293	0.553734	0.5000000	1
O13	O	1	0.5000000	0.5937293	0.5497077	1
O14	O	1	0.553734	0.5937293	0.5000000	1
O15	O	1	0.5000000	0.5937293	0.4502923	1
O16	O	1	0.446266	0.5937293	0.5000000	1
O17	O	1	0.4062707	0.5000000	0.5497077	1
O18	O	1	0.4062707	0.553734	0.5000000	1
O19	O	1	0.4062707	0.5000000	0.4502923	1
O20	O	1	0.4062707	0.446266	0.5000000	1
O21	O	1	0.5000000	0.4062707	0.5497077	1
O22	O	1	0.446266	0.4062707	0.5000000	1
O23	O	1	0.5000000	0.4062707	0.4502923	1
O24	O	1	0.553734	0.4062707	0.5000000	1
O25	O	1	0.553734	0.5000000	0.5867062	1
O26	O	1	0.5000000	0.553734	0.5867062	1
O27	O	1	0.446266	0.5000000	0.5867062	1
O28	O	1	0.5000000	0.446266	0.5867062	1
O29	O	1	0.553734	0.5000000	0.4132938	1
O30	O	1	0.5000000	0.446266	0.4132938	1
O31	O	1	0.446266	0.5000000	0.4132938	1
O32	O	1	0.5000000	0.553734	0.4132938	1
Zr1	Zr	1	0.5665907	0.5000000	0.5000000	1
Zr2	Zr	1	0.5000000	0.5665907	0.5000000	1
Zr3	Zr	1	0.4334093	0.5000000	0.5000000	1
Zr4	Zr	1	0.5000000	0.4334093	0.5000000	1
Zr5	Zr	1	0.5000000	0.5000000	0.561601	1
Zr6	Zr	1	0.5000000	0.5000000	0.438399	1

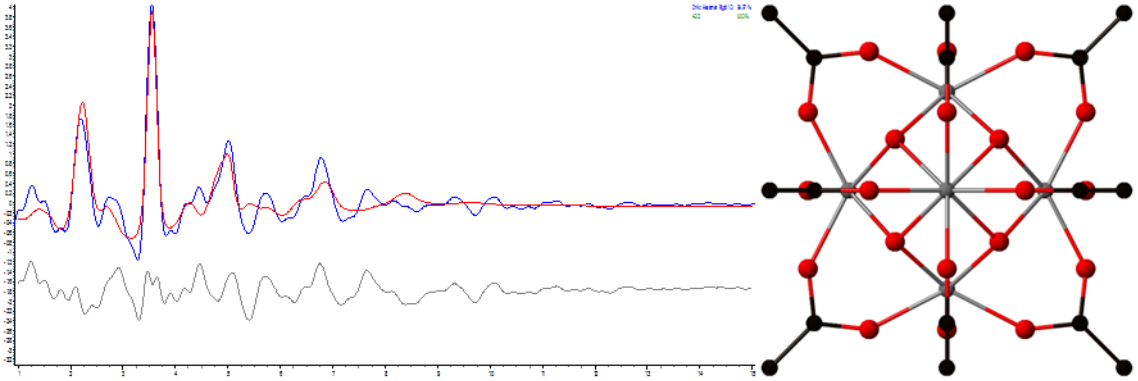

Figure 239: Observed and Calculated PDF from the fixed core refinement of ZAA16C from the 18-month data collection and the resultant model.

Table 182: The atomic coordinates of the model resulting from the fixed core refinement of ZAA16C from the 18-month data collection.

Atom Label	Atom Type	Multiplicity	Fractional X Coordinate	Fractional Y Coordinate	Fractional Z Coordinate	Fractional Occupancy
C1	C	1	0.5897274	0.5000000	0.5830041	1
C2	C	1	0.5000000	0.4102726	0.5830041	1
C3	C	1	0.4102726	0.5000000	0.5830041	1
C4	C	1	0.5000000	0.5897274	0.5830041	1
C5	C	1	0.5897274	0.5000000	0.4169959	1
C6	C	1	0.5000000	0.4102726	0.4169959	1
C7	C	1	0.4102726	0.5000000	0.4169959	1
C8	C	1	0.5000000	0.5897274	0.4169959	1
C9	C	1	0.5897274	0.4102726	0.5000000	1
C10	C	1	0.4102726	0.4102726	0.5000000	1
C11	C	1	0.4102726	0.5897274	0.5000000	1
C12	C	1	0.5897274	0.5897274	0.5000000	1
C13	C	1	0.6197686	0.5000000	0.6107943	1
C14	C	1	0.5000000	0.3802314	0.6107943	1
C15	C	1	0.3802314	0.5000000	0.6107943	1
C16	C	1	0.5000000	0.6197686	0.6107943	1
C17	C	1	0.6197686	0.5000000	0.3892057	1
C18	C	1	0.5000000	0.3802314	0.3892057	1
C19	C	1	0.3802314	0.5000000	0.3892057	1
C20	C	1	0.5000000	0.6197686	0.3892057	1
C21	C	1	0.6197686	0.3802314	0.5000000	1
C22	C	1	0.3802314	0.3802314	0.5000000	1
C23	C	1	0.3802314	0.6197686	0.5000000	1
C24	C	1	0.6197686	0.6197686	0.5000000	1
O1	O	1	0.5351759	0.5348327	0.4674598	1
O2	O	1	0.5351759	0.4651673	0.5325402	1
O3	O	1	0.4648241	0.5348327	0.4674598	1
O4	O	1	0.4648241	0.4651673	0.5325402	1
O5	O	1	0.4648241	0.4651673	0.4674598	1
O6	O	1	0.4648241	0.5348327	0.5325402	1

O7	O	1	0.5351759	0.4651673	0.4674598	1
O8	O	1	0.5351759	0.5348327	0.5325402	1
O9	O	1	0.5938198	0.5000000	0.5488263	1
O10	O	1	0.5938198	0.4472188	0.5000000	1
O11	O	1	0.5938198	0.5000000	0.4511737	1
O12	O	1	0.5938198	0.5527812	0.5000000	1
O13	O	1	0.5000000	0.5938198	0.5488263	1
O14	O	1	0.5527812	0.5938198	0.5000000	1
O15	O	1	0.5000000	0.5938198	0.4511737	1
O16	O	1	0.4472188	0.5938198	0.5000000	1
O17	O	1	0.4061802	0.5000000	0.5488263	1
O18	O	1	0.4061802	0.5527812	0.5000000	1
O19	O	1	0.4061802	0.5000000	0.4511737	1
O20	O	1	0.4061802	0.4472188	0.5000000	1
O21	O	1	0.5000000	0.4061802	0.5488263	1
O22	O	1	0.4472188	0.4061802	0.5000000	1
O23	O	1	0.5000000	0.4061802	0.4511737	1
O24	O	1	0.5527812	0.4061802	0.5000000	1
O25	O	1	0.5527812	0.5000000	0.5867899	1
O26	O	1	0.5000000	0.5527812	0.5867899	1
O27	O	1	0.4472188	0.5000000	0.5867899	1
O28	O	1	0.5000000	0.4472188	0.5867899	1
O29	O	1	0.5527812	0.5000000	0.4132101	1
O30	O	1	0.5000000	0.4472188	0.4132101	1
O31	O	1	0.4472188	0.5000000	0.4132101	1
O32	O	1	0.5000000	0.5527812	0.4132101	1
Zr1	Zr	1	0.566562	0.5000000	0.5000000	1
Zr2	Zr	1	0.5000000	0.566562	0.5000000	1
Zr3	Zr	1	0.433438	0.5000000	0.5000000	1
Zr4	Zr	1	0.5000000	0.433438	0.5000000	1
Zr5	Zr	1	0.5000000	0.5000000	0.5615745	1
Zr6	Zr	1	0.5000000	0.5000000	0.4384255	1

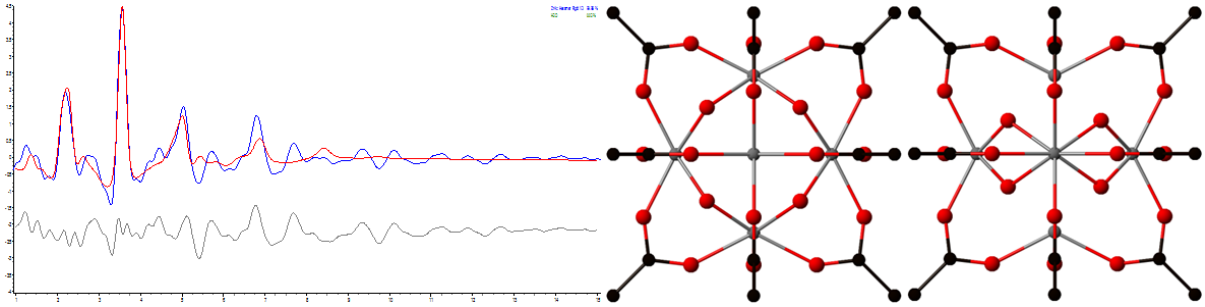

Figure 240: Observed and Calculated PDF from the chandelier core refinement of ZAA16I from the 18-month data collection and the resultant model viewed from the axial (left) and equatorial (right) positions.

Table 183: The atomic coordinates of the model resulting from the chandelier core refinement of ZAA16I from the 18-month data collection.

Atom Label	Atom Type	Multiplicity	Fractional X Coordinate	Fractional Y Coordinate	Fractional Z Coordinate	Fractional Occupancy
C1	C	1	0.5899121	0.5000000	0.5831749	1
C2	C	1	0.5000000	0.4100879	0.5831749	1
C3	C	1	0.4100879	0.5000000	0.5831749	1
C4	C	1	0.5000000	0.5899121	0.5831749	1
C5	C	1	0.5899121	0.5000000	0.4168251	1
C6	C	1	0.5000000	0.4100879	0.4168251	1
C7	C	1	0.4100879	0.5000000	0.4168251	1
C8	C	1	0.5000000	0.5899121	0.4168251	1
C9	C	1	0.5899121	0.4100879	0.5000000	1
C10	C	1	0.4100879	0.4100879	0.5000000	1
C11	C	1	0.4100879	0.5899121	0.5000000	1
C12	C	1	0.5899121	0.5899121	0.5000000	1
C13	C	1	0.6203867	0.5000000	0.6113661	1
C14	C	1	0.5000000	0.3796133	0.6113661	1
C15	C	1	0.3796133	0.5000000	0.6113661	1
C16	C	1	0.5000000	0.6203867	0.6113661	1
C17	C	1	0.6203867	0.5000000	0.3886339	1
C18	C	1	0.5000000	0.3796133	0.3886339	1
C19	C	1	0.3796133	0.5000000	0.3886339	1
C20	C	1	0.5000000	0.6203867	0.3886339	1
C21	C	1	0.6203867	0.3796133	0.5000000	1
C22	C	1	0.3796133	0.3796133	0.5000000	1
C23	C	1	0.3796133	0.6203867	0.5000000	1
C24	C	1	0.6203867	0.6203867	0.5000000	1
O1	O	1	0.5399633	0.4600367	0.4737936	1
O2	O	1	0.5399633	0.4600367	0.5262064	1
O3	O	1	0.4600367	0.4600367	0.4737936	1
O4	O	1	0.4600367	0.4600367	0.5262064	1
O5	O	1	0.4600367	0.5399633	0.4737936	1
O6	O	1	0.4600367	0.5399633	0.5262064	1
O7	O	1	0.5399633	0.5399633	0.4737936	1
O8	O	1	0.5399633	0.5399633	0.5262064	1

O9	O	1	0.5942593	0.5000000	0.5496367	1
O10	O	1	0.5942593	0.4463427	0.5000000	1
O11	O	1	0.5942593	0.5000000	0.4503633	1
O12	O	1	0.5942593	0.5536573	0.5000000	1
O13	O	1	0.5000000	0.5942593	0.5496367	1
O14	O	1	0.5536573	0.5942593	0.5000000	1
O15	O	1	0.5000000	0.5942593	0.4503633	1
O16	O	1	0.4463427	0.5942593	0.5000000	1
O17	O	1	0.4057407	0.5000000	0.5496367	1
O18	O	1	0.4057407	0.5536573	0.5000000	1
O19	O	1	0.4057407	0.5000000	0.4503633	1
O20	O	1	0.4057407	0.4463427	0.5000000	1
O21	O	1	0.5000000	0.4057407	0.5496367	1
O22	O	1	0.4463427	0.4057407	0.5000000	1
O23	O	1	0.5000000	0.4057407	0.4503633	1
O24	O	1	0.5536573	0.4057407	0.5000000	1
O25	O	1	0.5536573	0.5000000	0.5871964	1
O26	O	1	0.5000000	0.5536573	0.5871964	1
O27	O	1	0.4463427	0.5000000	0.5871964	1
O28	O	1	0.5000000	0.4463427	0.5871964	1
O29	O	1	0.5536573	0.5000000	0.4128036	1
O30	O	1	0.5000000	0.4463427	0.4128036	1
O31	O	1	0.4463427	0.5000000	0.4128036	1
O32	O	1	0.5000000	0.5536573	0.4128036	1
Zr1	Zr	1	0.5668452	0.5000000	0.5000000	1
Zr2	Zr	1	0.5000000	0.5668452	0.5000000	1
Zr3	Zr	1	0.4331548	0.5000000	0.5000000	1
Zr4	Zr	1	0.5000000	0.4331548	0.5000000	1
Zr5	Zr	1	0.5000000	0.5000000	0.5618365	1
Zr6	Zr	1	0.5000000	0.5000000	0.4381635	1

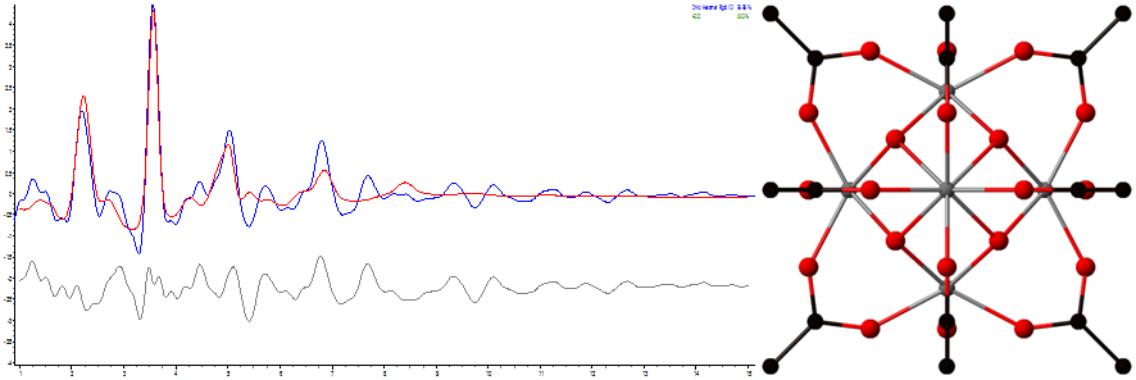

Figure 241: Observed and Calculated PDF from the fixed core refinement of ZAA16I from the 18-month data collection and the resultant model.

Table 184: The atomic coordinates of the model resulting from the fixed core refinement of ZAA16I from the 18-month data collection.

Atom Label	Atom Type	Multiplicity	Fractional X Coordinate	Fractional Y Coordinate	Fractional Z Coordinate	Fractional Occupancy
C1	C	1	0.5896771	0.5000000	0.5829576	1
C2	C	1	0.5000000	0.4103229	0.5829576	1
C3	C	1	0.4103229	0.5000000	0.5829576	1
C4	C	1	0.5000000	0.5896771	0.5829576	1
C5	C	1	0.5896771	0.5000000	0.4170424	1
C6	C	1	0.5000000	0.4103229	0.4170424	1
C7	C	1	0.4103229	0.5000000	0.4170424	1
C8	C	1	0.5000000	0.5896771	0.4170424	1
C9	C	1	0.5896771	0.4103229	0.5000000	1
C10	C	1	0.4103229	0.4103229	0.5000000	1
C11	C	1	0.4103229	0.5896771	0.5000000	1
C12	C	1	0.5896771	0.5896771	0.5000000	1
C13	C	1	0.6200864	0.5000000	0.6110883	1
C14	C	1	0.5000000	0.3799136	0.6110883	1
C15	C	1	0.3799136	0.5000000	0.6110883	1
C16	C	1	0.5000000	0.6200864	0.6110883	1
C17	C	1	0.6200864	0.5000000	0.3889117	1
C18	C	1	0.5000000	0.3799136	0.3889117	1
C19	C	1	0.3799136	0.5000000	0.3889117	1
C20	C	1	0.5000000	0.6200864	0.3889117	1
C21	C	1	0.6200864	0.3799136	0.5000000	1
C22	C	1	0.3799136	0.3799136	0.5000000	1
C23	C	1	0.3799136	0.6200864	0.5000000	1
C24	C	1	0.6200864	0.6200864	0.5000000	1
O1	O	1	0.5351408	0.5347979	0.4674923	1
O2	O	1	0.5351408	0.4652021	0.5325077	1
O3	O	1	0.4648592	0.5347979	0.4674923	1
O4	O	1	0.4648592	0.4652021	0.5325077	1
O5	O	1	0.4648592	0.4652021	0.4674923	1
O6	O	1	0.4648592	0.5347979	0.5325077	1

O7	O	1	0.5351408	0.4652021	0.4674923	1
O8	O	1	0.5351408	0.5347979	0.5325077	1
O9	O	1	0.5943929	0.5000000	0.5485229	1
O10	O	1	0.5943929	0.4475468	0.5000000	1
O11	O	1	0.5943929	0.5000000	0.4514771	1
O12	O	1	0.5943929	0.5524532	0.5000000	1
O13	O	1	0.5000000	0.5943929	0.5485229	1
O14	O	1	0.5524532	0.5943929	0.5000000	1
O15	O	1	0.5000000	0.5943929	0.4514771	1
O16	O	1	0.4475468	0.5943929	0.5000000	1
O17	O	1	0.4056071	0.5000000	0.5485229	1
O18	O	1	0.4056071	0.5524532	0.5000000	1
O19	O	1	0.4056071	0.5000000	0.4514771	1
O20	O	1	0.4056071	0.4475468	0.5000000	1
O21	O	1	0.5000000	0.4056071	0.5485229	1
O22	O	1	0.4475468	0.4056071	0.5000000	1
O23	O	1	0.5000000	0.4056071	0.4514771	1
O24	O	1	0.5524532	0.4056071	0.5000000	1
O25	O	1	0.5524532	0.5000000	0.58732	1
O26	O	1	0.5000000	0.5524532	0.58732	1
O27	O	1	0.4475468	0.5000000	0.58732	1
O28	O	1	0.5000000	0.4475468	0.58732	1
O29	O	1	0.5524532	0.5000000	0.41268	1
O30	O	1	0.5000000	0.4475468	0.41268	1
O31	O	1	0.4475468	0.5000000	0.41268	1
O32	O	1	0.5000000	0.5524532	0.41268	1
Zr1	Zr	1	0.5668491	0.5000000	0.5000000	1
Zr2	Zr	1	0.5000000	0.5668491	0.5000000	1
Zr3	Zr	1	0.4331509	0.5000000	0.5000000	1
Zr4	Zr	1	0.5000000	0.4331509	0.5000000	1
Zr5	Zr	1	0.5000000	0.5000000	0.56184	1
Zr6	Zr	1	0.5000000	0.5000000	0.43816	1

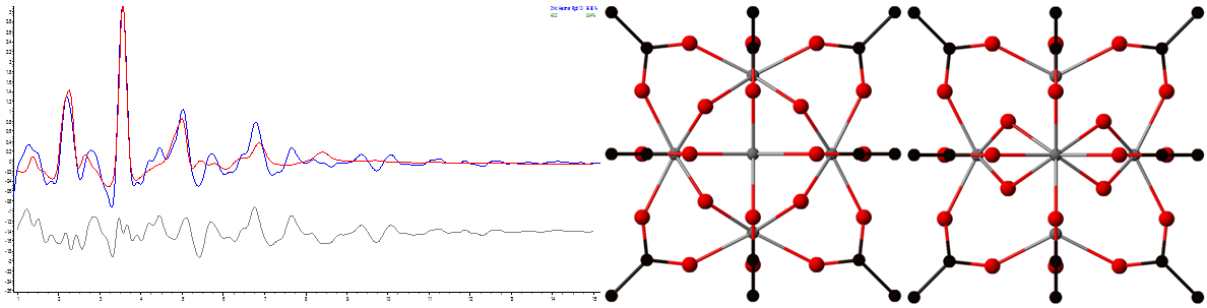

Figure 242: Observed and Calculated PDF from the chandelier core refinement of ZAA20A from the 18-month data collection and the resultant model viewed from the axial (left) and equatorial (right) positions.

Table 185: The atomic coordinates of the model resulting from the chandelier core refinement of ZAA20A from the 18-month data collection.

Atom Label	Atom Type	Multiplicity	Fractional X Coordinate	Fractional Y Coordinate	Fractional Z Coordinate	Fractional Occupancy
C1	C	1	0.5900268	0.5000000	0.5832811	1
C2	C	1	0.5000000	0.4099732	0.5832811	1
C3	C	1	0.4099732	0.5000000	0.5832811	1
C4	C	1	0.5000000	0.5900268	0.5832811	1
C5	C	1	0.5900268	0.5000000	0.4167189	1
C6	C	1	0.5000000	0.4099732	0.4167189	1
C7	C	1	0.4099732	0.5000000	0.4167189	1
C8	C	1	0.5000000	0.5900268	0.4167189	1
C9	C	1	0.5900268	0.4099732	0.5000000	1
C10	C	1	0.4099732	0.4099732	0.5000000	1
C11	C	1	0.4099732	0.5900268	0.5000000	1
C12	C	1	0.5900268	0.5900268	0.5000000	1
C13	C	1	0.6203172	0.5000000	0.6113018	1
C14	C	1	0.5000000	0.3796828	0.6113018	1
C15	C	1	0.3796828	0.5000000	0.6113018	1
C16	C	1	0.5000000	0.6203172	0.6113018	1
C17	C	1	0.6203172	0.5000000	0.3886982	1
C18	C	1	0.5000000	0.3796828	0.3886982	1
C19	C	1	0.3796828	0.5000000	0.3886982	1
C20	C	1	0.5000000	0.6203172	0.3886982	1
C21	C	1	0.6203172	0.3796828	0.5000000	1
C22	C	1	0.3796828	0.3796828	0.5000000	1
C23	C	1	0.3796828	0.6203172	0.5000000	1
C24	C	1	0.6203172	0.6203172	0.5000000	1
O1	O	1	0.5404722	0.4595278	0.4737192	1
O2	O	1	0.5404722	0.4595278	0.5262808	1
O3	O	1	0.4595278	0.4595278	0.4737192	1
O4	O	1	0.4595278	0.4595278	0.5262808	1
O5	O	1	0.4595278	0.5404722	0.4737192	1
O6	O	1	0.4595278	0.5404722	0.5262808	1
O7	O	1	0.5404722	0.5404722	0.4737192	1
O8	O	1	0.5404722	0.5404722	0.5262808	1

O9	O	1	0.5939845	0.5000000	0.5497736	1
O10	O	1	0.5939845	0.4461948	0.5000000	1
O11	O	1	0.5939845	0.5000000	0.4502264	1
O12	O	1	0.5939845	0.5538052	0.5000000	1
O13	O	1	0.5000000	0.5939845	0.5497736	1
O14	O	1	0.5538052	0.5939845	0.5000000	1
O15	O	1	0.5000000	0.5939845	0.4502264	1
O16	O	1	0.4461948	0.5939845	0.5000000	1
O17	O	1	0.4060155	0.5000000	0.5497736	1
O18	O	1	0.4060155	0.5538052	0.5000000	1
O19	O	1	0.4060155	0.5000000	0.4502264	1
O20	O	1	0.4060155	0.4461948	0.5000000	1
O21	O	1	0.5000000	0.4060155	0.5497736	1
O22	O	1	0.4461948	0.4060155	0.5000000	1
O23	O	1	0.5000000	0.4060155	0.4502264	1
O24	O	1	0.5538052	0.4060155	0.5000000	1
O25	O	1	0.5538052	0.5000000	0.5869422	1
O26	O	1	0.5000000	0.5538052	0.5869422	1
O27	O	1	0.4461948	0.5000000	0.5869422	1
O28	O	1	0.5000000	0.4461948	0.5869422	1
O29	O	1	0.5538052	0.5000000	0.4130578	1
O30	O	1	0.5000000	0.4461948	0.4130578	1
O31	O	1	0.4461948	0.5000000	0.4130578	1
O32	O	1	0.5000000	0.5538052	0.4130578	1
Zr1	Zr	1	0.5666151	0.5000000	0.5000000	1
Zr2	Zr	1	0.5000000	0.5666151	0.5000000	1
Zr3	Zr	1	0.4333849	0.5000000	0.5000000	1
Zr4	Zr	1	0.5000000	0.4333849	0.5000000	1
Zr5	Zr	1	0.5000000	0.5000000	0.5616237	1
Zr6	Zr	1	0.5000000	0.5000000	0.4383763	1

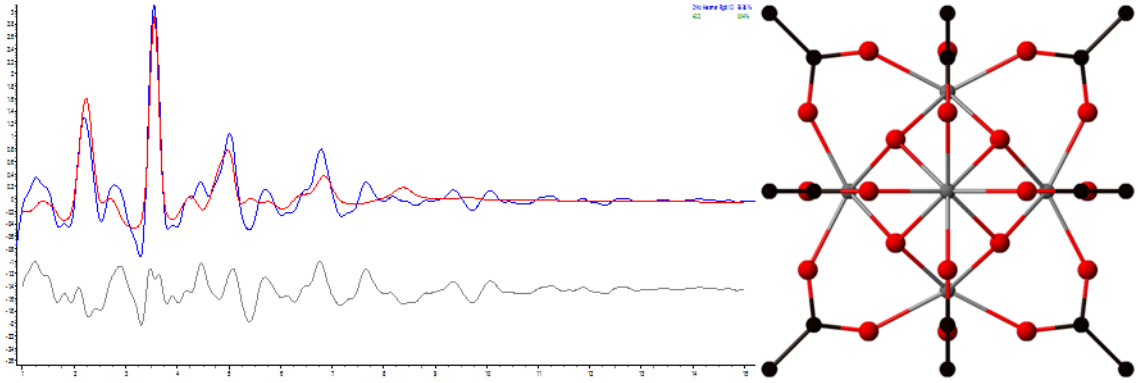

Figure 243: Observed and Calculated PDF from the fixed core refinement of ZAA20A from the 18-month data collection and the resultant model.

Table 186: The atomic coordinates of the model resulting from the fixed core refinement of ZAA20A from the 18-month data collection.

Atom Label	Atom Type	Multiplicity	Fractional X Coordinate	Fractional Y Coordinate	Fractional Z Coordinate	Fractional Occupancy
C1	C	1	0.5898144	0.5000000	0.5830846	1
C2	C	1	0.5000000	0.4101856	0.5830846	1
C3	C	1	0.4101856	0.5000000	0.5830846	1
C4	C	1	0.5000000	0.5898144	0.5830846	1
C5	C	1	0.5898144	0.5000000	0.4169154	1
C6	C	1	0.5000000	0.4101856	0.4169154	1
C7	C	1	0.4101856	0.5000000	0.4169154	1
C8	C	1	0.5000000	0.5898144	0.4169154	1
C9	C	1	0.5898144	0.4101856	0.5000000	1
C10	C	1	0.4101856	0.4101856	0.5000000	1
C11	C	1	0.4101856	0.5898144	0.5000000	1
C12	C	1	0.5898144	0.5898144	0.5000000	1
C13	C	1	0.6197767	0.5000000	0.6108018	1
C14	C	1	0.5000000	0.3802233	0.6108018	1
C15	C	1	0.3802233	0.5000000	0.6108018	1
C16	C	1	0.5000000	0.6197767	0.6108018	1
C17	C	1	0.6197767	0.5000000	0.3891982	1
C18	C	1	0.5000000	0.3802233	0.3891982	1
C19	C	1	0.3802233	0.5000000	0.3891982	1
C20	C	1	0.5000000	0.6197767	0.3891982	1
C21	C	1	0.6197767	0.3802233	0.5000000	1
C22	C	1	0.3802233	0.3802233	0.5000000	1
C23	C	1	0.3802233	0.6197767	0.5000000	1
C24	C	1	0.6197767	0.6197767	0.5000000	1
O1	O	1	0.5350346	0.5346928	0.4675905	1
O2	O	1	0.5350346	0.4653072	0.5324095	1
O3	O	1	0.4649654	0.5346928	0.4675905	1
O4	O	1	0.4649654	0.4653072	0.5324095	1
O5	O	1	0.4649654	0.4653072	0.4675905	1
O6	O	1	0.4649654	0.5346928	0.5324095	1

O7	O	1	0.5350346	0.4653072	0.4675905	1
O8	O	1	0.5350346	0.5346928	0.5324095	1
O9	O	1	0.5940283	0.5000000	0.5490976	1
O10	O	1	0.5940283	0.4469255	0.5000000	1
O11	O	1	0.5940283	0.5000000	0.4509024	1
O12	O	1	0.5940283	0.5530745	0.5000000	1
O13	O	1	0.5000000	0.5940283	0.5490976	1
O14	O	1	0.5530745	0.5940283	0.5000000	1
O15	O	1	0.5000000	0.5940283	0.4509024	1
O16	O	1	0.4469255	0.5940283	0.5000000	1
O17	O	1	0.4059717	0.5000000	0.5490976	1
O18	O	1	0.4059717	0.5530745	0.5000000	1
O19	O	1	0.4059717	0.5000000	0.4509024	1
O20	O	1	0.4059717	0.4469255	0.5000000	1
O21	O	1	0.5000000	0.4059717	0.5490976	1
O22	O	1	0.4469255	0.4059717	0.5000000	1
O23	O	1	0.5000000	0.4059717	0.4509024	1
O24	O	1	0.5530745	0.4059717	0.5000000	1
O25	O	1	0.5530745	0.5000000	0.5869828	1
O26	O	1	0.5000000	0.5530745	0.5869828	1
O27	O	1	0.4469255	0.5000000	0.5869828	1
O28	O	1	0.5000000	0.4469255	0.5869828	1
O29	O	1	0.5530745	0.5000000	0.4130172	1
O30	O	1	0.5000000	0.4469255	0.4130172	1
O31	O	1	0.4469255	0.5000000	0.4130172	1
O32	O	1	0.5000000	0.5530745	0.4130172	1
Zr1	Zr	1	0.5665998	0.5000000	0.5000000	1
Zr2	Zr	1	0.5000000	0.5665998	0.5000000	1
Zr3	Zr	1	0.4334002	0.5000000	0.5000000	1
Zr4	Zr	1	0.5000000	0.4334002	0.5000000	1
Zr5	Zr	1	0.5000000	0.5000000	0.5616094	1
Zr6	Zr	1	0.5000000	0.5000000	0.4383906	1

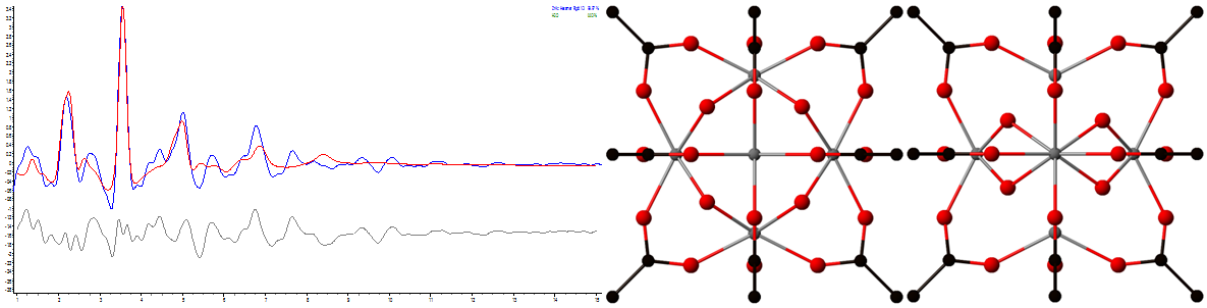

Figure 244: Observed and Calculated PDF from the chandelier core refinement of ZAA20C from the 18-month data collection and the resultant model viewed from the axial (left) and equatorial (right) positions.

Table 187: The atomic coordinates of the model resulting from the chandelier core refinement of ZAA20C from the 18-month data collection.

Atom Label	Atom Type	Multiplicity	Fractional X Coordinate	Fractional Y Coordinate	Fractional Z Coordinate	Fractional Occupancy
C1	C	1	0.5899251	0.5000000	0.583187	1
C2	C	1	0.5000000	0.4100749	0.583187	1
C3	C	1	0.4100749	0.5000000	0.583187	1
C4	C	1	0.5000000	0.5899251	0.583187	1
C5	C	1	0.5899251	0.5000000	0.416813	1
C6	C	1	0.5000000	0.4100749	0.416813	1
C7	C	1	0.4100749	0.5000000	0.416813	1
C8	C	1	0.5000000	0.5899251	0.416813	1
C9	C	1	0.5899251	0.4100749	0.5000000	1
C10	C	1	0.4100749	0.4100749	0.5000000	1
C11	C	1	0.4100749	0.5899251	0.5000000	1
C12	C	1	0.5899251	0.5899251	0.5000000	1
C13	C	1	0.6202645	0.5000000	0.611253	1
C14	C	1	0.5000000	0.3797355	0.611253	1
C15	C	1	0.3797355	0.5000000	0.611253	1
C16	C	1	0.5000000	0.6202645	0.611253	1
C17	C	1	0.6202645	0.5000000	0.388747	1
C18	C	1	0.5000000	0.3797355	0.388747	1
C19	C	1	0.3797355	0.5000000	0.388747	1
C20	C	1	0.5000000	0.6202645	0.388747	1
C21	C	1	0.6202645	0.3797355	0.5000000	1
C22	C	1	0.3797355	0.3797355	0.5000000	1
C23	C	1	0.3797355	0.6202645	0.5000000	1
C24	C	1	0.6202645	0.6202645	0.5000000	1
O1	O	1	0.5401963	0.4598037	0.4736357	1
O2	O	1	0.5401963	0.4598037	0.5263643	1
O3	O	1	0.4598037	0.4598037	0.4736357	1
O4	O	1	0.4598037	0.4598037	0.5263643	1
O5	O	1	0.4598037	0.5401963	0.4736357	1
O6	O	1	0.4598037	0.5401963	0.5263643	1
O7	O	1	0.5401963	0.5401963	0.4736357	1
O8	O	1	0.5401963	0.5401963	0.5263643	1

O9	O	1	0.593839	0.5000000	0.5497244	1
O10	O	1	0.593839	0.446248	0.5000000	1
O11	O	1	0.593839	0.5000000	0.4502756	1
O12	O	1	0.593839	0.553752	0.5000000	1
O13	O	1	0.5000000	0.593839	0.5497244	1
O14	O	1	0.553752	0.593839	0.5000000	1
O15	O	1	0.5000000	0.593839	0.4502756	1
O16	O	1	0.446248	0.593839	0.5000000	1
O17	O	1	0.406161	0.5000000	0.5497244	1
O18	O	1	0.406161	0.553752	0.5000000	1
O19	O	1	0.406161	0.5000000	0.4502756	1
O20	O	1	0.406161	0.446248	0.5000000	1
O21	O	1	0.5000000	0.406161	0.5497244	1
O22	O	1	0.446248	0.406161	0.5000000	1
O23	O	1	0.5000000	0.406161	0.4502756	1
O24	O	1	0.553752	0.406161	0.5000000	1
O25	O	1	0.553752	0.5000000	0.5868076	1
O26	O	1	0.5000000	0.553752	0.5868076	1
O27	O	1	0.446248	0.5000000	0.5868076	1
O28	O	1	0.5000000	0.446248	0.5868076	1
O29	O	1	0.553752	0.5000000	0.4131924	1
O30	O	1	0.5000000	0.446248	0.4131924	1
O31	O	1	0.446248	0.5000000	0.4131924	1
O32	O	1	0.5000000	0.553752	0.4131924	1
Zr1	Zr	1	0.5665564	0.5000000	0.5000000	1
Zr2	Zr	1	0.5000000	0.5665564	0.5000000	1
Zr3	Zr	1	0.4334436	0.5000000	0.5000000	1
Zr4	Zr	1	0.5000000	0.4334436	0.5000000	1
Zr5	Zr	1	0.5000000	0.5000000	0.5615693	1
Zr6	Zr	1	0.5000000	0.5000000	0.4384307	1

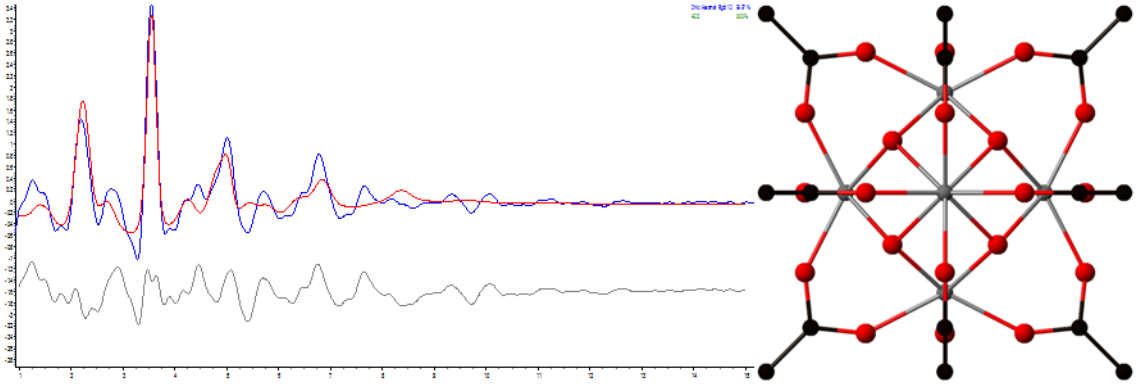

Figure 245: Observed and Calculated PDF from the fixed core refinement of ZAA20C from the 18-month data collection and the resultant model.

Table 188: The atomic coordinates of the model resulting from the fixed core refinement of ZAA20C from the 18-month data collection.

Atom Label	Atom Type	Multiplicity	Fractional X Coordinate	Fractional Y Coordinate	Fractional Z Coordinate	Fractional Occupancy
C1	C	1	0.589887	0.5000000	0.5831517	1
C2	C	1	0.5000000	0.410113	0.5831517	1
C3	C	1	0.410113	0.5000000	0.5831517	1
C4	C	1	0.5000000	0.589887	0.5831517	1
C5	C	1	0.589887	0.5000000	0.4168483	1
C6	C	1	0.5000000	0.410113	0.4168483	1
C7	C	1	0.410113	0.5000000	0.4168483	1
C8	C	1	0.5000000	0.589887	0.4168483	1
C9	C	1	0.589887	0.410113	0.5000000	1
C10	C	1	0.410113	0.410113	0.5000000	1
C11	C	1	0.410113	0.589887	0.5000000	1
C12	C	1	0.589887	0.589887	0.5000000	1
C13	C	1	0.6195031	0.5000000	0.6105487	1
C14	C	1	0.5000000	0.3804969	0.6105487	1
C15	C	1	0.3804969	0.5000000	0.6105487	1
C16	C	1	0.5000000	0.6195031	0.6105487	1
C17	C	1	0.6195031	0.5000000	0.3894513	1
C18	C	1	0.5000000	0.3804969	0.3894513	1
C19	C	1	0.3804969	0.5000000	0.3894513	1
C20	C	1	0.5000000	0.6195031	0.3894513	1
C21	C	1	0.6195031	0.3804969	0.5000000	1
C22	C	1	0.3804969	0.3804969	0.5000000	1
C23	C	1	0.3804969	0.6195031	0.5000000	1
C24	C	1	0.6195031	0.6195031	0.5000000	1
O1	O	1	0.5350766	0.5347343	0.4675517	1
O2	O	1	0.5350766	0.4652657	0.5324483	1
O3	O	1	0.4649234	0.5347343	0.4675517	1
O4	O	1	0.4649234	0.4652657	0.5324483	1
O5	O	1	0.4649234	0.4652657	0.4675517	1
O6	O	1	0.4649234	0.5347343	0.5324483	1

O7	O	1	0.5350766	0.4652657	0.4675517	1
O8	O	1	0.5350766	0.5347343	0.5324483	1
O9	O	1	0.5937561	0.5000000	0.5490792	1
O10	O	1	0.5937561	0.4469454	0.5000000	1
O11	O	1	0.5937561	0.5000000	0.4509208	1
O12	O	1	0.5937561	0.5530546	0.5000000	1
O13	O	1	0.5000000	0.5937561	0.5490792	1
O14	O	1	0.5530546	0.5937561	0.5000000	1
O15	O	1	0.5000000	0.5937561	0.4509208	1
O16	O	1	0.4469454	0.5937561	0.5000000	1
O17	O	1	0.4062439	0.5000000	0.5490792	1
O18	O	1	0.4062439	0.5530546	0.5000000	1
O19	O	1	0.4062439	0.5000000	0.4509208	1
O20	O	1	0.4062439	0.4469454	0.5000000	1
O21	O	1	0.5000000	0.4062439	0.5490792	1
O22	O	1	0.4469454	0.4062439	0.5000000	1
O23	O	1	0.5000000	0.4062439	0.4509208	1
O24	O	1	0.5530546	0.4062439	0.5000000	1
O25	O	1	0.5530546	0.5000000	0.5867309	1
O26	O	1	0.5000000	0.5530546	0.5867309	1
O27	O	1	0.4469454	0.5000000	0.5867309	1
O28	O	1	0.5000000	0.4469454	0.5867309	1
O29	O	1	0.5530546	0.5000000	0.4132691	1
O30	O	1	0.5000000	0.4469454	0.4132691	1
O31	O	1	0.4469454	0.5000000	0.4132691	1
O32	O	1	0.5000000	0.5530546	0.4132691	1
Zr1	Zr	1	0.5665449	0.5000000	0.5000000	1
Zr2	Zr	1	0.5000000	0.5665449	0.5000000	1
Zr3	Zr	1	0.4334551	0.5000000	0.5000000	1
Zr4	Zr	1	0.5000000	0.4334551	0.5000000	1
Zr5	Zr	1	0.5000000	0.5000000	0.5615587	1
Zr6	Zr	1	0.5000000	0.5000000	0.4384413	1

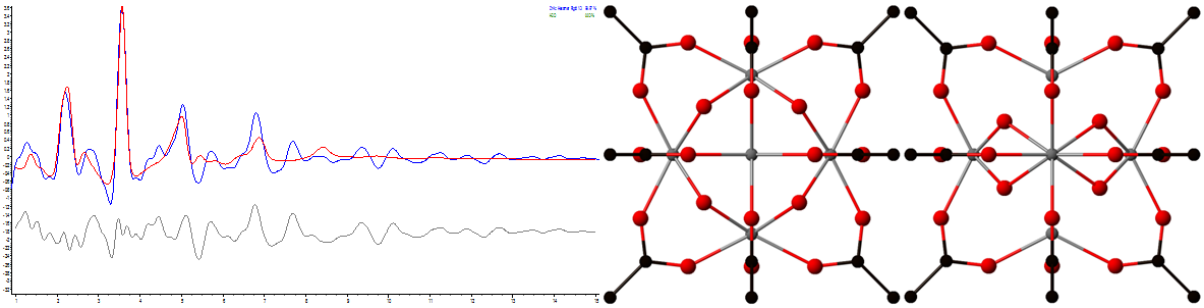

Figure 246: Observed and Calculated PDF from the chandelier core refinement of ZAA20I from the 18-month data collection and the resultant model viewed from the axial (left) and equatorial (right) positions.

Table 189: The atomic coordinates of the model resulting from the chandelier core refinement of ZAA20I from the 18-month data collection.

Atom Label	Atom Type	Multiplicity	Fractional X Coordinate	Fractional Y Coordinate	Fractional Z Coordinate	Fractional Occupancy
C1	C	1	0.5899716	0.5000000	0.58323	1
C2	C	1	0.5000000	0.4100284	0.58323	1
C3	C	1	0.4100284	0.5000000	0.58323	1
C4	C	1	0.5000000	0.5899716	0.58323	1
C5	C	1	0.5899716	0.5000000	0.41677	1
C6	C	1	0.5000000	0.4100284	0.41677	1
C7	C	1	0.4100284	0.5000000	0.41677	1
C8	C	1	0.5000000	0.5899716	0.41677	1
C9	C	1	0.5899716	0.4100284	0.5000000	1
C10	C	1	0.4100284	0.4100284	0.5000000	1
C11	C	1	0.4100284	0.5899716	0.5000000	1
C12	C	1	0.5899716	0.5899716	0.5000000	1
C13	C	1	0.6202695	0.5000000	0.6112577	1
C14	C	1	0.5000000	0.3797305	0.6112577	1
C15	C	1	0.3797305	0.5000000	0.6112577	1
C16	C	1	0.5000000	0.6202695	0.6112577	1
C17	C	1	0.6202695	0.5000000	0.3887423	1
C18	C	1	0.5000000	0.3797305	0.3887423	1
C19	C	1	0.3797305	0.5000000	0.3887423	1
C20	C	1	0.5000000	0.6202695	0.3887423	1
C21	C	1	0.6202695	0.3797305	0.5000000	1
C22	C	1	0.3797305	0.3797305	0.5000000	1
C23	C	1	0.3797305	0.6202695	0.5000000	1
C24	C	1	0.6202695	0.6202695	0.5000000	1
O1	O	1	0.540418	0.459582	0.4739243	1
O2	O	1	0.540418	0.459582	0.5260757	1
O3	O	1	0.459582	0.459582	0.4739243	1
O4	O	1	0.459582	0.459582	0.5260757	1
O5	O	1	0.459582	0.540418	0.4739243	1
O6	O	1	0.459582	0.540418	0.5260757	1
O7	O	1	0.540418	0.540418	0.4739243	1
O8	O	1	0.540418	0.540418	0.5260757	1

O9	O	1	0.5941902	0.5000000	0.5497742	1
O10	O	1	0.5941902	0.4461941	0.5000000	1
O11	O	1	0.5941902	0.5000000	0.4502258	1
O12	O	1	0.5941902	0.5538059	0.5000000	1
O13	O	1	0.5000000	0.5941902	0.5497742	1
O14	O	1	0.5538059	0.5941902	0.5000000	1
O15	O	1	0.5000000	0.5941902	0.4502258	1
O16	O	1	0.4461941	0.5941902	0.5000000	1
O17	O	1	0.4058098	0.5000000	0.5497742	1
O18	O	1	0.4058098	0.5538059	0.5000000	1
O19	O	1	0.4058098	0.5000000	0.4502258	1
O20	O	1	0.4058098	0.4461941	0.5000000	1
O21	O	1	0.5000000	0.4058098	0.5497742	1
O22	O	1	0.4461941	0.4058098	0.5000000	1
O23	O	1	0.5000000	0.4058098	0.4502258	1
O24	O	1	0.5538059	0.4058098	0.5000000	1
O25	O	1	0.5538059	0.5000000	0.5871325	1
O26	O	1	0.5000000	0.5538059	0.5871325	1
O27	O	1	0.4461941	0.5000000	0.5871325	1
O28	O	1	0.5000000	0.4461941	0.5871325	1
O29	O	1	0.5538059	0.5000000	0.4128675	1
O30	O	1	0.5000000	0.4461941	0.4128675	1
O31	O	1	0.4461941	0.5000000	0.4128675	1
O32	O	1	0.5000000	0.5538059	0.4128675	1
Zr1	Zr	1	0.5668856	0.5000000	0.5000000	1
Zr2	Zr	1	0.5000000	0.5668856	0.5000000	1
Zr3	Zr	1	0.4331144	0.5000000	0.5000000	1
Zr4	Zr	1	0.5000000	0.4331144	0.5000000	1
Zr5	Zr	1	0.5000000	0.5000000	0.5618738	1
Zr6	Zr	1	0.5000000	0.5000000	0.4381262	1

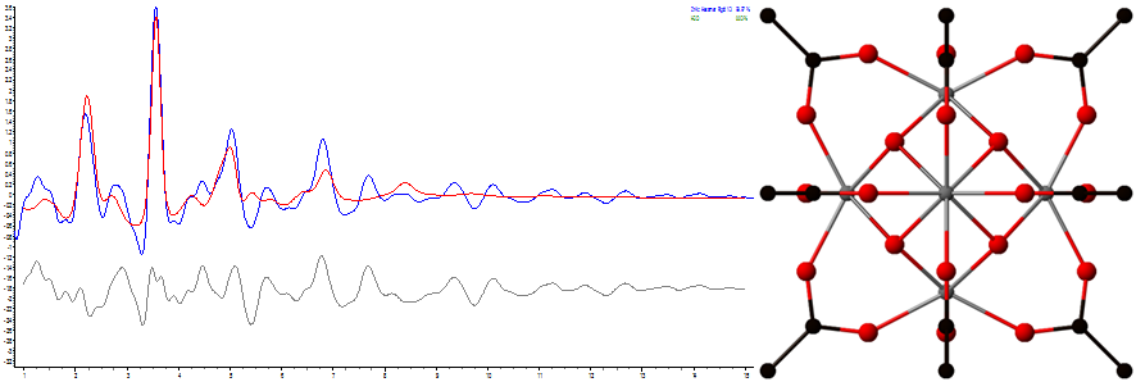

Figure 247: Observed and Calculated PDF from the fixed core refinement of ZAA20I from the 18-month data collection and the resultant model.

Table 190: The atomic coordinates of the model resulting from the fixed core refinement of ZAA20I from the 18-month data collection.

Atom Label	Atom Type	Multiplicity	Fractional X Coordinate	Fractional Y Coordinate	Fractional Z Coordinate	Fractional Occupancy
C1	C	1	0.5898523	0.5000000	0.5831197	1
C2	C	1	0.5000000	0.4101477	0.5831197	1
C3	C	1	0.4101477	0.5000000	0.5831197	1
C4	C	1	0.5000000	0.5898523	0.5831197	1
C5	C	1	0.5898523	0.5000000	0.4168803	1
C6	C	1	0.5000000	0.4101477	0.4168803	1
C7	C	1	0.4101477	0.5000000	0.4168803	1
C8	C	1	0.5000000	0.5898523	0.4168803	1
C9	C	1	0.5898523	0.4101477	0.5000000	1
C10	C	1	0.4101477	0.4101477	0.5000000	1
C11	C	1	0.4101477	0.5898523	0.5000000	1
C12	C	1	0.5898523	0.5898523	0.5000000	1
C13	C	1	0.620064	0.5000000	0.6110676	1
C14	C	1	0.5000000	0.379936	0.6110676	1
C15	C	1	0.379936	0.5000000	0.6110676	1
C16	C	1	0.5000000	0.620064	0.6110676	1
C17	C	1	0.620064	0.5000000	0.3889324	1
C18	C	1	0.5000000	0.379936	0.3889324	1
C19	C	1	0.379936	0.5000000	0.3889324	1
C20	C	1	0.5000000	0.620064	0.3889324	1
C21	C	1	0.620064	0.379936	0.5000000	1
C22	C	1	0.379936	0.379936	0.5000000	1
C23	C	1	0.379936	0.620064	0.5000000	1
C24	C	1	0.620064	0.620064	0.5000000	1
O1	O	1	0.5349082	0.5345676	0.4677075	1
O2	O	1	0.5349082	0.4654324	0.5322925	1
O3	O	1	0.4650918	0.5345676	0.4677075	1
O4	O	1	0.4650918	0.4654324	0.5322925	1
O5	O	1	0.4650918	0.4654324	0.4677075	1
O6	O	1	0.4650918	0.5345676	0.5322925	1

O7	O	1	0.5349082	0.4654324	0.4677075	1
O8	O	1	0.5349082	0.5345676	0.5322925	1
O9	O	1	0.5943491	0.5000000	0.5488168	1
O10	O	1	0.5943491	0.4472291	0.5000000	1
O11	O	1	0.5943491	0.5000000	0.4511832	1
O12	O	1	0.5943491	0.5527709	0.5000000	1
O13	O	1	0.5000000	0.5943491	0.5488168	1
O14	O	1	0.5527709	0.5943491	0.5000000	1
O15	O	1	0.5000000	0.5943491	0.4511832	1
O16	O	1	0.4472291	0.5943491	0.5000000	1
O17	O	1	0.4056509	0.5000000	0.5488168	1
O18	O	1	0.4056509	0.5527709	0.5000000	1
O19	O	1	0.4056509	0.5000000	0.4511832	1
O20	O	1	0.4056509	0.4472291	0.5000000	1
O21	O	1	0.5000000	0.4056509	0.5488168	1
O22	O	1	0.4472291	0.4056509	0.5000000	1
O23	O	1	0.5000000	0.4056509	0.4511832	1
O24	O	1	0.5527709	0.4056509	0.5000000	1
O25	O	1	0.5527709	0.5000000	0.5872795	1
O26	O	1	0.5000000	0.5527709	0.5872795	1
O27	O	1	0.4472291	0.5000000	0.5872795	1
O28	O	1	0.5000000	0.4472291	0.5872795	1
O29	O	1	0.5527709	0.5000000	0.4127205	1
O30	O	1	0.5000000	0.4472291	0.4127205	1
O31	O	1	0.4472291	0.5000000	0.4127205	1
O32	O	1	0.5000000	0.5527709	0.4127205	1
Zr1	Zr	1	0.5668578	0.5000000	0.5000000	1
Zr2	Zr	1	0.5000000	0.5668578	0.5000000	1
Zr3	Zr	1	0.4331422	0.5000000	0.5000000	1
Zr4	Zr	1	0.5000000	0.4331422	0.5000000	1
Zr5	Zr	1	0.5000000	0.5000000	0.5618481	1
Zr6	Zr	1	0.5000000	0.5000000	0.4381519	1

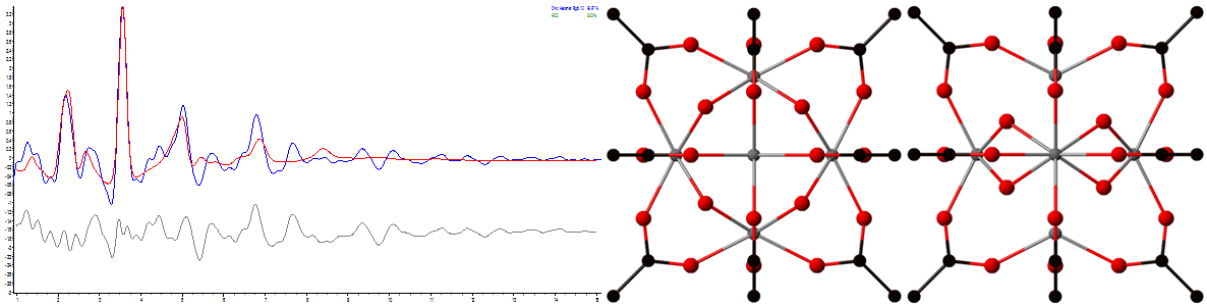

Figure 248: Observed and Calculated PDF from the chandelier core refinement of ZAA24A from the 18-month data collection and the resultant model viewed from the axial (left) and equatorial (right) positions.

Table 191: The atomic coordinates of the model resulting from the chandelier core refinement of ZAA24A from the 18-month data collection.

Atom Label	Atom Type	Multiplicity	Fractional X Coordinate	Fractional Y Coordinate	Fractional Z Coordinate	Fractional Occupancy
C1	C	1	0.5901672	0.5000000	0.5834109	1
C2	C	1	0.5000000	0.4098328	0.5834109	1
C3	C	1	0.4098328	0.5000000	0.5834109	1
C4	C	1	0.5000000	0.5901672	0.5834109	1
C5	C	1	0.5901672	0.5000000	0.4165891	1
C6	C	1	0.5000000	0.4098328	0.4165891	1
C7	C	1	0.4098328	0.5000000	0.4165891	1
C8	C	1	0.5000000	0.5901672	0.4165891	1
C9	C	1	0.5901672	0.4098328	0.5000000	1
C10	C	1	0.4098328	0.4098328	0.5000000	1
C11	C	1	0.4098328	0.5901672	0.5000000	1
C12	C	1	0.5901672	0.5901672	0.5000000	1
C13	C	1	0.6201487	0.5000000	0.6111459	1
C14	C	1	0.5000000	0.3798513	0.6111459	1
C15	C	1	0.3798513	0.5000000	0.6111459	1
C16	C	1	0.5000000	0.6201487	0.6111459	1
C17	C	1	0.6201487	0.5000000	0.3888541	1
C18	C	1	0.5000000	0.3798513	0.3888541	1
C19	C	1	0.3798513	0.5000000	0.3888541	1
C20	C	1	0.5000000	0.6201487	0.3888541	1
C21	C	1	0.6201487	0.3798513	0.5000000	1
C22	C	1	0.3798513	0.3798513	0.5000000	1
C23	C	1	0.3798513	0.6201487	0.5000000	1
C24	C	1	0.6201487	0.6201487	0.5000000	1
O1	O	1	0.5412046	0.4587954	0.4740908	1
O2	O	1	0.5412046	0.4587954	0.5259092	1
O3	O	1	0.4587954	0.4587954	0.4740908	1
O4	O	1	0.4587954	0.4587954	0.5259092	1
O5	O	1	0.4587954	0.5412046	0.4740908	1
O6	O	1	0.4587954	0.5412046	0.5259092	1
O7	O	1	0.5412046	0.5412046	0.4740908	1
O8	O	1	0.5412046	0.5412046	0.5259092	1

O9	O	1	0.5941169	0.5000000	0.549966	1
O10	O	1	0.5941169	0.4459868	0.5000000	1
O11	O	1	0.5941169	0.5000000	0.450034	1
O12	O	1	0.5941169	0.5540132	0.5000000	1
O13	O	1	0.5000000	0.5941169	0.549966	1
O14	O	1	0.5540132	0.5941169	0.5000000	1
O15	O	1	0.5000000	0.5941169	0.450034	1
O16	O	1	0.4459868	0.5941169	0.5000000	1
O17	O	1	0.4058831	0.5000000	0.549966	1
O18	O	1	0.4058831	0.5540132	0.5000000	1
O19	O	1	0.4058831	0.5000000	0.450034	1
O20	O	1	0.4058831	0.4459868	0.5000000	1
O21	O	1	0.5000000	0.4058831	0.549966	1
O22	O	1	0.4459868	0.4058831	0.5000000	1
O23	O	1	0.5000000	0.4058831	0.450034	1
O24	O	1	0.5540132	0.4058831	0.5000000	1
O25	O	1	0.5540132	0.5000000	0.5870647	1
O26	O	1	0.5000000	0.5540132	0.5870647	1
O27	O	1	0.4459868	0.5000000	0.5870647	1
O28	O	1	0.5000000	0.4459868	0.5870647	1
O29	O	1	0.5540132	0.5000000	0.4129353	1
O30	O	1	0.5000000	0.4459868	0.4129353	1
O31	O	1	0.4459868	0.5000000	0.4129353	1
O32	O	1	0.5000000	0.5540132	0.4129353	1
Zr1	Zr	1	0.5668104	0.5000000	0.5000000	1
Zr2	Zr	1	0.5000000	0.5668104	0.5000000	1
Zr3	Zr	1	0.4331896	0.5000000	0.5000000	1
Zr4	Zr	1	0.5000000	0.4331896	0.5000000	1
Zr5	Zr	1	0.5000000	0.5000000	0.5618043	1
Zr6	Zr	1	0.5000000	0.5000000	0.4381957	1

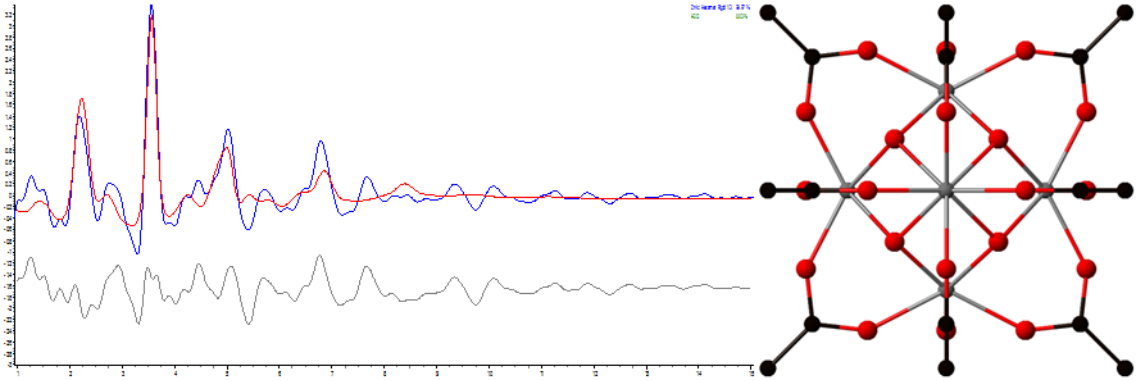

Figure 249: Observed and Calculated PDF from the fixed core refinement of ZAA24A from the 18-month data collection and the resultant model.

Table 192: The atomic coordinates of the model resulting from the fixed core refinement of ZAA24A from the 18-month data collection.

Atom Label	Atom Type	Multiplicity	Fractional X Coordinate	Fractional Y Coordinate	Fractional Z Coordinate	Fractional Occupancy
C1	C	1	0.5899499	0.5000000	0.5832099	1
C2	C	1	0.5000000	0.4100501	0.5832099	1
C3	C	1	0.4100501	0.5000000	0.5832099	1
C4	C	1	0.5000000	0.5899499	0.5832099	1
C5	C	1	0.5899499	0.5000000	0.4167901	1
C6	C	1	0.5000000	0.4100501	0.4167901	1
C7	C	1	0.4100501	0.5000000	0.4167901	1
C8	C	1	0.5000000	0.5899499	0.4167901	1
C9	C	1	0.5899499	0.4100501	0.5000000	1
C10	C	1	0.4100501	0.4100501	0.5000000	1
C11	C	1	0.4100501	0.5899499	0.5000000	1
C12	C	1	0.5899499	0.5899499	0.5000000	1
C13	C	1	0.6198916	0.5000000	0.6109081	1
C14	C	1	0.5000000	0.3801084	0.6109081	1
C15	C	1	0.3801084	0.5000000	0.6109081	1
C16	C	1	0.5000000	0.6198916	0.6109081	1
C17	C	1	0.6198916	0.5000000	0.3890919	1
C18	C	1	0.5000000	0.3801084	0.3890919	1
C19	C	1	0.3801084	0.5000000	0.3890919	1
C20	C	1	0.5000000	0.6198916	0.3890919	1
C21	C	1	0.6198916	0.3801084	0.5000000	1
C22	C	1	0.3801084	0.3801084	0.5000000	1
C23	C	1	0.3801084	0.6198916	0.5000000	1
C24	C	1	0.6198916	0.6198916	0.5000000	1
O1	O	1	0.5348747	0.5345344	0.4677385	1
O2	O	1	0.5348747	0.4654656	0.5322615	1
O3	O	1	0.4651253	0.5345344	0.4677385	1
O4	O	1	0.4651253	0.4654656	0.5322615	1
O5	O	1	0.4651253	0.4654656	0.4677385	1
O6	O	1	0.4651253	0.5345344	0.5322615	1

O7	O	1	0.5348747	0.4654656	0.4677385	1
O8	O	1	0.5348747	0.5345344	0.5322615	1
O9	O	1	0.5942255	0.5000000	0.5490109	1
O10	O	1	0.5942255	0.4470192	0.5000000	1
O11	O	1	0.5942255	0.5000000	0.4509891	1
O12	O	1	0.5942255	0.5529808	0.5000000	1
O13	O	1	0.5000000	0.5942255	0.5490109	1
O14	O	1	0.5529808	0.5942255	0.5000000	1
O15	O	1	0.5000000	0.5942255	0.4509891	1
O16	O	1	0.4470192	0.5942255	0.5000000	1
O17	O	1	0.4057745	0.5000000	0.5490109	1
O18	O	1	0.4057745	0.5529808	0.5000000	1
O19	O	1	0.4057745	0.5000000	0.4509891	1
O20	O	1	0.4057745	0.4470192	0.5000000	1
O21	O	1	0.5000000	0.4057745	0.5490109	1
O22	O	1	0.4470192	0.4057745	0.5000000	1
O23	O	1	0.5000000	0.4057745	0.4509891	1
O24	O	1	0.5529808	0.4057745	0.5000000	1
O25	O	1	0.5529808	0.5000000	0.5871651	1
O26	O	1	0.5000000	0.5529808	0.5871651	1
O27	O	1	0.4470192	0.5000000	0.5871651	1
O28	O	1	0.5000000	0.4470192	0.5871651	1
O29	O	1	0.5529808	0.5000000	0.4128349	1
O30	O	1	0.5000000	0.4470192	0.4128349	1
O31	O	1	0.4470192	0.5000000	0.4128349	1
O32	O	1	0.5000000	0.5529808	0.4128349	1
Zr1	Zr	1	0.5667979	0.5000000	0.5000000	1
Zr2	Zr	1	0.5000000	0.5667979	0.5000000	1
Zr3	Zr	1	0.4332021	0.5000000	0.5000000	1
Zr4	Zr	1	0.5000000	0.4332021	0.5000000	1
Zr5	Zr	1	0.5000000	0.5000000	0.5617927	1
Zr6	Zr	1	0.5000000	0.5000000	0.4382073	1

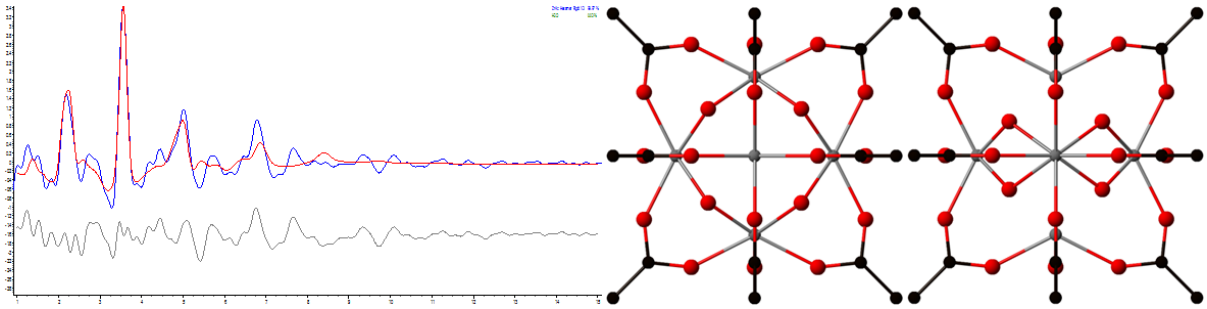

Figure 250: Observed and Calculated PDF from the chandelier core refinement of ZAA24C from the 18-month data collection and the resultant model viewed from the axial (left) and equatorial (right) positions.

Table 193: The atomic coordinates of the model resulting from the chandelier core refinement of ZAA24C from the 18-month data collection.

Atom Label	Atom Type	Multiplicity	Fractional X Coordinate	Fractional Y Coordinate	Fractional Z Coordinate	Fractional Occupancy
C1	C	1	0.5900293	0.5000000	0.5832833	1
C2	C	1	0.5000000	0.4099707	0.5832833	1
C3	C	1	0.4099707	0.5000000	0.5832833	1
C4	C	1	0.5000000	0.5900293	0.5832833	1
C5	C	1	0.5900293	0.5000000	0.4167167	1
C6	C	1	0.5000000	0.4099707	0.4167167	1
C7	C	1	0.4099707	0.5000000	0.4167167	1
C8	C	1	0.5000000	0.5900293	0.4167167	1
C9	C	1	0.5900293	0.4099707	0.5000000	1
C10	C	1	0.4099707	0.4099707	0.5000000	1
C11	C	1	0.4099707	0.5900293	0.5000000	1
C12	C	1	0.5900293	0.5900293	0.5000000	1
C13	C	1	0.6201354	0.5000000	0.6111336	1
C14	C	1	0.5000000	0.3798646	0.6111336	1
C15	C	1	0.3798646	0.5000000	0.6111336	1
C16	C	1	0.5000000	0.6201354	0.6111336	1
C17	C	1	0.6201354	0.5000000	0.3888664	1
C18	C	1	0.5000000	0.3798646	0.3888664	1
C19	C	1	0.3798646	0.5000000	0.3888664	1
C20	C	1	0.5000000	0.6201354	0.3888664	1
C21	C	1	0.6201354	0.3798646	0.5000000	1
C22	C	1	0.3798646	0.3798646	0.5000000	1
C23	C	1	0.3798646	0.6201354	0.5000000	1
C24	C	1	0.6201354	0.6201354	0.5000000	1
O1	O	1	0.5395945	0.4604055	0.4734392	1
O2	O	1	0.5395945	0.4604055	0.5265608	1
O3	O	1	0.4604055	0.4604055	0.4734392	1
O4	O	1	0.4604055	0.4604055	0.5265608	1
O5	O	1	0.4604055	0.5395945	0.4734392	1
O6	O	1	0.4604055	0.5395945	0.5265608	1
O7	O	1	0.5395945	0.5395945	0.4734392	1
O8	O	1	0.5395945	0.5395945	0.5265608	1

O9	O	1	0.593963	0.5000000	0.5496695	1
O10	O	1	0.593963	0.4463073	0.5000000	1
O11	O	1	0.593963	0.5000000	0.4503305	1
O12	O	1	0.593963	0.5536927	0.5000000	1
O13	O	1	0.5000000	0.593963	0.5496695	1
O14	O	1	0.5536927	0.593963	0.5000000	1
O15	O	1	0.5000000	0.593963	0.4503305	1
O16	O	1	0.4463073	0.593963	0.5000000	1
O17	O	1	0.406037	0.5000000	0.5496695	1
O18	O	1	0.406037	0.5536927	0.5000000	1
O19	O	1	0.406037	0.5000000	0.4503305	1
O20	O	1	0.406037	0.4463073	0.5000000	1
O21	O	1	0.5000000	0.406037	0.5496695	1
O22	O	1	0.4463073	0.406037	0.5000000	1
O23	O	1	0.5000000	0.406037	0.4503305	1
O24	O	1	0.5536927	0.406037	0.5000000	1
O25	O	1	0.5536927	0.5000000	0.5869224	1
O26	O	1	0.5000000	0.5536927	0.5869224	1
O27	O	1	0.4463073	0.5000000	0.5869224	1
O28	O	1	0.5000000	0.4463073	0.5869224	1
O29	O	1	0.5536927	0.5000000	0.4130776	1
O30	O	1	0.5000000	0.4463073	0.4130776	1
O31	O	1	0.4463073	0.5000000	0.4130776	1
O32	O	1	0.5000000	0.5536927	0.4130776	1
Zr1	Zr	1	0.5667426	0.5000000	0.5000000	1
Zr2	Zr	1	0.5000000	0.5667426	0.5000000	1
Zr3	Zr	1	0.4332574	0.5000000	0.5000000	1
Zr4	Zr	1	0.5000000	0.4332574	0.5000000	1
Zr5	Zr	1	0.5000000	0.5000000	0.5617415	1
Zr6	Zr	1	0.5000000	0.5000000	0.4382585	1

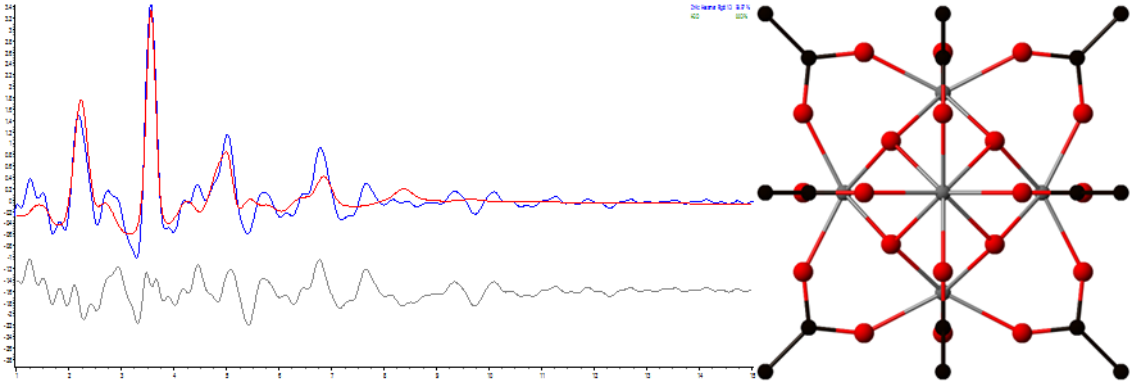

Figure 251: Observed and Calculated PDF from the fixed core refinement of ZAA24C from the 18-month data collection and the resultant model.

Table 194: The atomic coordinates of the model resulting from the fixed core refinement of ZAA24C from the 18-month data collection.

Atom Label	Atom Type	Multiplicity	Fractional X Coordinate	Fractional Y Coordinate	Fractional Z Coordinate	Fractional Occupancy
C1	C	1	0.5900972	0.5000000	0.5833462	1
C2	C	1	0.5000000	0.4099028	0.5833462	1
C3	C	1	0.4099028	0.5000000	0.5833462	1
C4	C	1	0.5000000	0.5900972	0.5833462	1
C5	C	1	0.5900972	0.5000000	0.4166538	1
C6	C	1	0.5000000	0.4099028	0.4166538	1
C7	C	1	0.4099028	0.5000000	0.4166538	1
C8	C	1	0.5000000	0.5900972	0.4166538	1
C9	C	1	0.5900972	0.4099028	0.5000000	1
C10	C	1	0.4099028	0.4099028	0.5000000	1
C11	C	1	0.4099028	0.5900972	0.5000000	1
C12	C	1	0.5900972	0.5900972	0.5000000	1
C13	C	1	0.6195848	0.5000000	0.6106243	1
C14	C	1	0.5000000	0.3804152	0.6106243	1
C15	C	1	0.3804152	0.5000000	0.6106243	1
C16	C	1	0.5000000	0.6195848	0.6106243	1
C17	C	1	0.6195848	0.5000000	0.3893757	1
C18	C	1	0.5000000	0.3804152	0.3893757	1
C19	C	1	0.3804152	0.5000000	0.3893757	1
C20	C	1	0.5000000	0.6195848	0.3893757	1
C21	C	1	0.6195848	0.3804152	0.5000000	1
C22	C	1	0.3804152	0.3804152	0.5000000	1
C23	C	1	0.3804152	0.6195848	0.5000000	1
C24	C	1	0.6195848	0.6195848	0.5000000	1
O1	O	1	0.5349016	0.534561	0.4677136	1
O2	O	1	0.5349016	0.465439	0.5322864	1
O3	O	1	0.4650984	0.534561	0.4677136	1
O4	O	1	0.4650984	0.465439	0.5322864	1
O5	O	1	0.4650984	0.465439	0.4677136	1
O6	O	1	0.4650984	0.534561	0.5322864	1

O7	O	1	0.5349016	0.465439	0.4677136	1
O8	O	1	0.5349016	0.534561	0.5322864	1
O9	O	1	0.5939871	0.5000000	0.5490584	1
O10	O	1	0.5939871	0.4469679	0.5000000	1
O11	O	1	0.5939871	0.5000000	0.4509416	1
O12	O	1	0.5939871	0.5530321	0.5000000	1
O13	O	1	0.5000000	0.5939871	0.5490584	1
O14	O	1	0.5530321	0.5939871	0.5000000	1
O15	O	1	0.5000000	0.5939871	0.4509416	1
O16	O	1	0.4469679	0.5939871	0.5000000	1
O17	O	1	0.4060129	0.5000000	0.5490584	1
O18	O	1	0.4060129	0.5530321	0.5000000	1
O19	O	1	0.4060129	0.5000000	0.4509416	1
O20	O	1	0.4060129	0.4469679	0.5000000	1
O21	O	1	0.5000000	0.4060129	0.5490584	1
O22	O	1	0.4469679	0.4060129	0.5000000	1
O23	O	1	0.5000000	0.4060129	0.4509416	1
O24	O	1	0.5530321	0.4060129	0.5000000	1
O25	O	1	0.5530321	0.5000000	0.5869446	1
O26	O	1	0.5000000	0.5530321	0.5869446	1
O27	O	1	0.4469679	0.5000000	0.5869446	1
O28	O	1	0.5000000	0.4469679	0.5869446	1
O29	O	1	0.5530321	0.5000000	0.4130554	1
O30	O	1	0.5000000	0.4469679	0.4130554	1
O31	O	1	0.4469679	0.5000000	0.4130554	1
O32	O	1	0.5000000	0.5530321	0.4130554	1
Zr1	Zr	1	0.566711	0.5000000	0.5000000	1
Zr2	Zr	1	0.5000000	0.566711	0.5000000	1
Zr3	Zr	1	0.433289	0.5000000	0.5000000	1
Zr4	Zr	1	0.5000000	0.433289	0.5000000	1
Zr5	Zr	1	0.5000000	0.5000000	0.5617123	1
Zr6	Zr	1	0.5000000	0.5000000	0.4382877	1

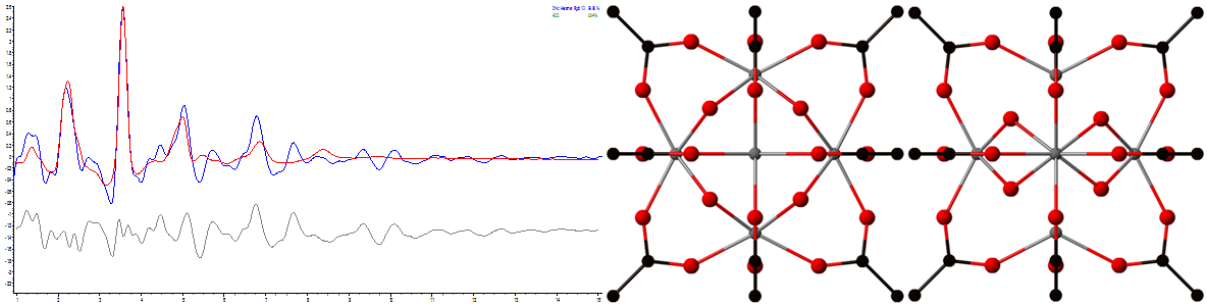

Figure 252: Observed and Calculated PDF from the chandelier core refinement of ZAA24I from the 18-month data collection and the resultant model viewed from the axial (left) and equatorial (right) positions.

Table 195: The atomic coordinates of the model resulting from the chandelier core refinement of ZAA24I from the 18-month data collection.

Atom Label	Atom Type	Multiplicity	Fractional X Coordinate	Fractional Y Coordinate	Fractional Z Coordinate	Fractional Occupancy
C1	C	1	0.5902746	0.5000000	0.5835103	1
C2	C	1	0.5000000	0.4097254	0.5835103	1
C3	C	1	0.4097254	0.5000000	0.5835103	1
C4	C	1	0.5000000	0.5902746	0.5835103	1
C5	C	1	0.5902746	0.5000000	0.4164897	1
C6	C	1	0.5000000	0.4097254	0.4164897	1
C7	C	1	0.4097254	0.5000000	0.4164897	1
C8	C	1	0.5000000	0.5902746	0.4164897	1
C9	C	1	0.5902746	0.4097254	0.5000000	1
C10	C	1	0.4097254	0.4097254	0.5000000	1
C11	C	1	0.4097254	0.5902746	0.5000000	1
C12	C	1	0.5902746	0.5902746	0.5000000	1
C13	C	1	0.6196203	0.5000000	0.6106571	1
C14	C	1	0.5000000	0.3803797	0.6106571	1
C15	C	1	0.3803797	0.5000000	0.6106571	1
C16	C	1	0.5000000	0.6196203	0.6106571	1
C17	C	1	0.6196203	0.5000000	0.3893429	1
C18	C	1	0.5000000	0.3803797	0.3893429	1
C19	C	1	0.3803797	0.5000000	0.3893429	1
C20	C	1	0.5000000	0.6196203	0.3893429	1
C21	C	1	0.6196203	0.3803797	0.5000000	1
C22	C	1	0.3803797	0.3803797	0.5000000	1
C23	C	1	0.3803797	0.6196203	0.5000000	1
C24	C	1	0.6196203	0.6196203	0.5000000	1
O1	O	1	0.5381977	0.4618023	0.4725696	1
O2	O	1	0.5381977	0.4618023	0.5274304	1
O3	O	1	0.4618023	0.4618023	0.4725696	1
O4	O	1	0.4618023	0.4618023	0.5274304	1
O5	O	1	0.4618023	0.5381977	0.4725696	1
O6	O	1	0.4618023	0.5381977	0.5274304	1
O7	O	1	0.5381977	0.5381977	0.4725696	1
O8	O	1	0.5381977	0.5381977	0.5274304	1

O9	O	1	0.5944479	0.5000000	0.5496361	1
O10	O	1	0.5944479	0.4463434	0.5000000	1
O11	O	1	0.5944479	0.5000000	0.4503639	1
O12	O	1	0.5944479	0.5536566	0.5000000	1
O13	O	1	0.5000000	0.5944479	0.5496361	1
O14	O	1	0.5536566	0.5944479	0.5000000	1
O15	O	1	0.5000000	0.5944479	0.4503639	1
O16	O	1	0.4463434	0.5944479	0.5000000	1
O17	O	1	0.4055521	0.5000000	0.5496361	1
O18	O	1	0.4055521	0.5536566	0.5000000	1
O19	O	1	0.4055521	0.5000000	0.4503639	1
O20	O	1	0.4055521	0.4463434	0.5000000	1
O21	O	1	0.5000000	0.4055521	0.5496361	1
O22	O	1	0.4463434	0.4055521	0.5000000	1
O23	O	1	0.5000000	0.4055521	0.4503639	1
O24	O	1	0.5536566	0.4055521	0.5000000	1
O25	O	1	0.5536566	0.5000000	0.5873709	1
O26	O	1	0.5000000	0.5536566	0.5873709	1
O27	O	1	0.4463434	0.5000000	0.5873709	1
O28	O	1	0.5000000	0.4463434	0.5873709	1
O29	O	1	0.5536566	0.5000000	0.4126291	1
O30	O	1	0.5000000	0.4463434	0.4126291	1
O31	O	1	0.4463434	0.5000000	0.4126291	1
O32	O	1	0.5000000	0.5536566	0.4126291	1
Zr1	Zr	1	0.5667705	0.5000000	0.5000000	1
Zr2	Zr	1	0.5000000	0.5667705	0.5000000	1
Zr3	Zr	1	0.4332295	0.5000000	0.5000000	1
Zr4	Zr	1	0.5000000	0.4332295	0.5000000	1
Zr5	Zr	1	0.5000000	0.5000000	0.5617674	1
Zr6	Zr	1	0.5000000	0.5000000	0.4382326	1

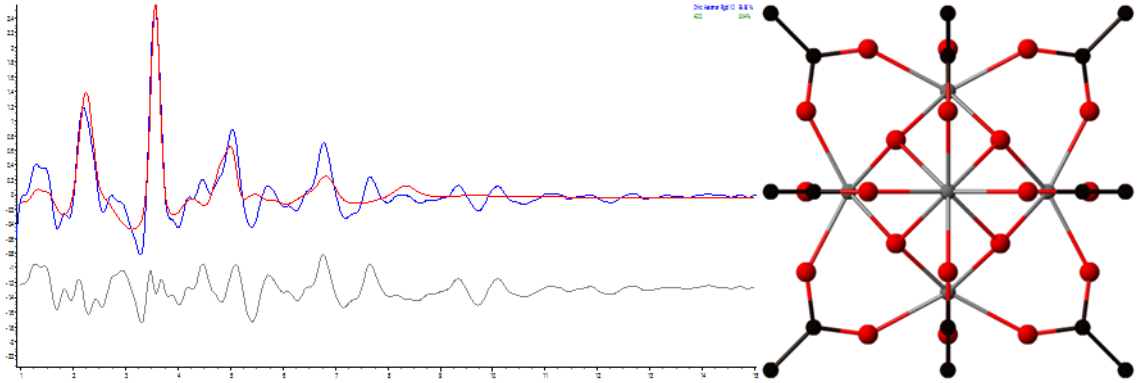

Figure 253: Observed and Calculated PDF from the fixed core refinement of ZAA24I from the 18-month data collection and the resultant model.

Table 196: The atomic coordinates of the model resulting from the fixed core refinement of ZAA24I from the 18-month data collection.

Atom Label	Atom Type	Multiplicity	Fractional X Coordinate	Fractional Y Coordinate	Fractional Z Coordinate	Fractional Occupancy
C1	C	1	0.5901318	0.5000000	0.5833782	1
C2	C	1	0.5000000	0.4098682	0.5833782	1
C3	C	1	0.4098682	0.5000000	0.5833782	1
C4	C	1	0.5000000	0.5901318	0.5833782	1
C5	C	1	0.5901318	0.5000000	0.4166218	1
C6	C	1	0.5000000	0.4098682	0.4166218	1
C7	C	1	0.4098682	0.5000000	0.4166218	1
C8	C	1	0.5000000	0.5901318	0.4166218	1
C9	C	1	0.5901318	0.4098682	0.5000000	1
C10	C	1	0.4098682	0.4098682	0.5000000	1
C11	C	1	0.4098682	0.5901318	0.5000000	1
C12	C	1	0.5901318	0.5901318	0.5000000	1
C13	C	1	0.6188446	0.5000000	0.6099395	1
C14	C	1	0.5000000	0.3811554	0.6099395	1
C15	C	1	0.3811554	0.5000000	0.6099395	1
C16	C	1	0.5000000	0.6188446	0.6099395	1
C17	C	1	0.6188446	0.5000000	0.3900605	1
C18	C	1	0.5000000	0.3811554	0.3900605	1
C19	C	1	0.3811554	0.5000000	0.3900605	1
C20	C	1	0.5000000	0.6188446	0.3900605	1
C21	C	1	0.6188446	0.3811554	0.5000000	1
C22	C	1	0.3811554	0.3811554	0.5000000	1
C23	C	1	0.3811554	0.6188446	0.5000000	1
C24	C	1	0.6188446	0.6188446	0.5000000	1
O1	O	1	0.5348708	0.5345305	0.4677421	1
O2	O	1	0.5348708	0.4654695	0.5322579	1
O3	O	1	0.4651292	0.5345305	0.4677421	1
O4	O	1	0.4651292	0.4654695	0.5322579	1
O5	O	1	0.4651292	0.4654695	0.4677421	1
O6	O	1	0.4651292	0.5345305	0.5322579	1

O7	O	1	0.5348708	0.4654695	0.4677421	1
O8	O	1	0.5348708	0.5345305	0.5322579	1
O9	O	1	0.5950058	0.5000000	0.5494387	1
O10	O	1	0.5950058	0.4465568	0.5000000	1
O11	O	1	0.5950058	0.5000000	0.4505613	1
O12	O	1	0.5950058	0.5534432	0.5000000	1
O13	O	1	0.5000000	0.5950058	0.5494387	1
O14	O	1	0.5534432	0.5950058	0.5000000	1
O15	O	1	0.5000000	0.5950058	0.4505613	1
O16	O	1	0.4465568	0.5950058	0.5000000	1
O17	O	1	0.4049942	0.5000000	0.5494387	1
O18	O	1	0.4049942	0.5534432	0.5000000	1
O19	O	1	0.4049942	0.5000000	0.4505613	1
O20	O	1	0.4049942	0.4465568	0.5000000	1
O21	O	1	0.5000000	0.4049942	0.5494387	1
O22	O	1	0.4465568	0.4049942	0.5000000	1
O23	O	1	0.5000000	0.4049942	0.4505613	1
O24	O	1	0.5534432	0.4049942	0.5000000	1
O25	O	1	0.5534432	0.5000000	0.587887	1
O26	O	1	0.5000000	0.5534432	0.587887	1
O27	O	1	0.4465568	0.5000000	0.587887	1
O28	O	1	0.5000000	0.4465568	0.587887	1
O29	O	1	0.5534432	0.5000000	0.412113	1
O30	O	1	0.5000000	0.4465568	0.412113	1
O31	O	1	0.4465568	0.5000000	0.412113	1
O32	O	1	0.5000000	0.5534432	0.412113	1
Zr1	Zr	1	0.5667593	0.5000000	0.5000000	1
Zr2	Zr	1	0.5000000	0.5667593	0.5000000	1
Zr3	Zr	1	0.4332407	0.5000000	0.5000000	1
Zr4	Zr	1	0.5000000	0.4332407	0.5000000	1
Zr5	Zr	1	0.5000000	0.5000000	0.561757	1
Zr6	Zr	1	0.5000000	0.5000000	0.438243	1

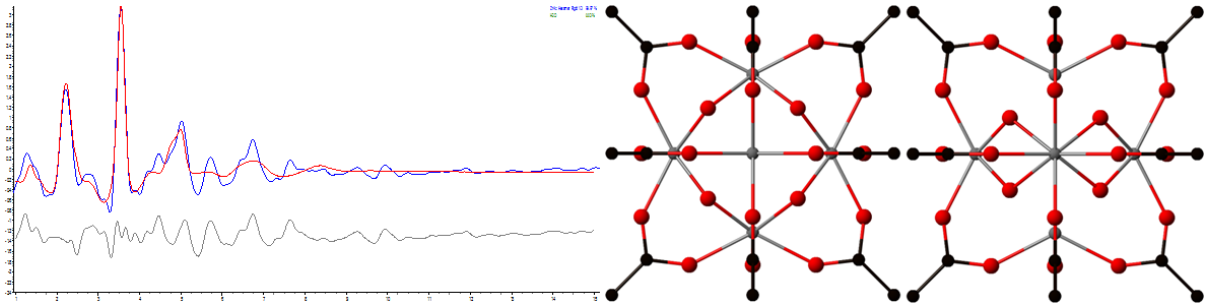

Figure 254: Observed and Calculated PDF from the chandelier core refinement of ZAA25A from the 18-month data collection and the resultant model viewed from the axial (left) and equatorial (right) positions.

Table 197: The atomic coordinates of the model resulting from the chandelier core refinement of ZAA25A from the 18-month data collection.

Atom Label	Atom Type	Multiplicity	Fractional X Coordinate	Fractional Y Coordinate	Fractional Z Coordinate	Fractional Occupancy
C1	C	1	0.5893976	0.5000000	0.582699	1
C2	C	1	0.5000000	0.4106024	0.582699	1
C3	C	1	0.4106024	0.5000000	0.582699	1
C4	C	1	0.5000000	0.5893976	0.582699	1
C5	C	1	0.5893976	0.5000000	0.417301	1
C6	C	1	0.5000000	0.4106024	0.417301	1
C7	C	1	0.4106024	0.5000000	0.417301	1
C8	C	1	0.5000000	0.5893976	0.417301	1
C9	C	1	0.5893976	0.4106024	0.5000000	1
C10	C	1	0.4106024	0.4106024	0.5000000	1
C11	C	1	0.4106024	0.5893976	0.5000000	1
C12	C	1	0.5893976	0.5893976	0.5000000	1
C13	C	1	0.6189635	0.5000000	0.6100495	1
C14	C	1	0.5000000	0.3810365	0.6100495	1
C15	C	1	0.3810365	0.5000000	0.6100495	1
C16	C	1	0.5000000	0.6189635	0.6100495	1
C17	C	1	0.6189635	0.5000000	0.3899505	1
C18	C	1	0.5000000	0.3810365	0.3899505	1
C19	C	1	0.3810365	0.5000000	0.3899505	1
C20	C	1	0.5000000	0.6189635	0.3899505	1
C21	C	1	0.6189635	0.3810365	0.5000000	1
C22	C	1	0.3810365	0.3810365	0.5000000	1
C23	C	1	0.3810365	0.6189635	0.5000000	1
C24	C	1	0.6189635	0.6189635	0.5000000	1
O1	O	1	0.5379149	0.4620851	0.4719676	1
O2	O	1	0.5379149	0.4620851	0.5280324	1
O3	O	1	0.4620851	0.4620851	0.4719676	1
O4	O	1	0.4620851	0.4620851	0.5280324	1
O5	O	1	0.4620851	0.5379149	0.4719676	1
O6	O	1	0.4620851	0.5379149	0.5280324	1
O7	O	1	0.5379149	0.5379149	0.4719676	1
O8	O	1	0.5379149	0.5379149	0.5280324	1

O9	O	1	0.5937606	0.5000000	0.5493167	1
O10	O	1	0.5937606	0.4466887	0.5000000	1
O11	O	1	0.5937606	0.5000000	0.4506833	1
O12	O	1	0.5937606	0.5533113	0.5000000	1
O13	O	1	0.5000000	0.5937606	0.5493167	1
O14	O	1	0.5533113	0.5937606	0.5000000	1
O15	O	1	0.5000000	0.5937606	0.4506833	1
O16	O	1	0.4466887	0.5937606	0.5000000	1
O17	O	1	0.4062394	0.5000000	0.5493167	1
O18	O	1	0.4062394	0.5533113	0.5000000	1
O19	O	1	0.4062394	0.5000000	0.4506833	1
O20	O	1	0.4062394	0.4466887	0.5000000	1
O21	O	1	0.5000000	0.4062394	0.5493167	1
O22	O	1	0.4466887	0.4062394	0.5000000	1
O23	O	1	0.5000000	0.4062394	0.4506833	1
O24	O	1	0.5533113	0.4062394	0.5000000	1
O25	O	1	0.5533113	0.5000000	0.5867351	1
O26	O	1	0.5000000	0.5533113	0.5867351	1
O27	O	1	0.4466887	0.5000000	0.5867351	1
O28	O	1	0.5000000	0.4466887	0.5867351	1
O29	O	1	0.5533113	0.5000000	0.4132649	1
O30	O	1	0.5000000	0.4466887	0.4132649	1
O31	O	1	0.4466887	0.5000000	0.4132649	1
O32	O	1	0.5000000	0.5533113	0.4132649	1
Zr1	Zr	1	0.5664208	0.5000000	0.5000000	1
Zr2	Zr	1	0.5000000	0.5664208	0.5000000	1
Zr3	Zr	1	0.4335792	0.5000000	0.5000000	1
Zr4	Zr	1	0.5000000	0.4335792	0.5000000	1
Zr5	Zr	1	0.5000000	0.5000000	0.5614439	1
Zr6	Zr	1	0.5000000	0.5000000	0.4385561	1

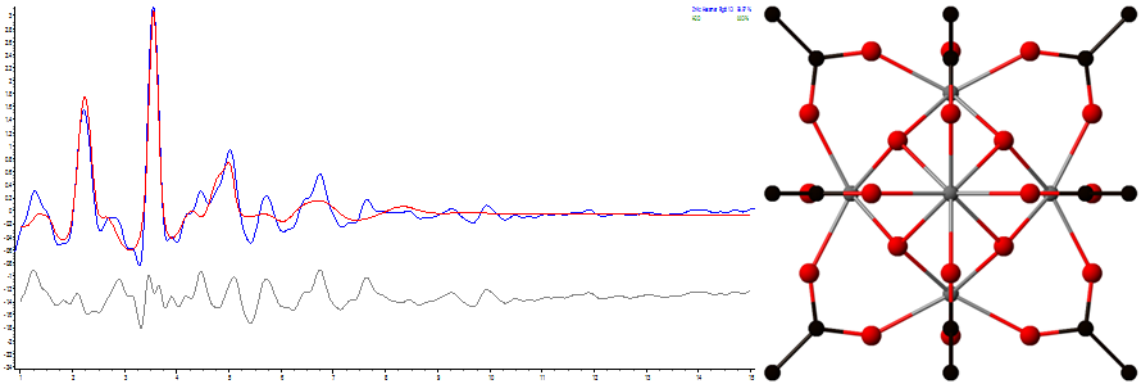

Figure 255: Observed and Calculated PDF from the fixed core refinement of ZAA25A from the 18-month data collection and the resultant model.

Table 198: The atomic coordinates of the model resulting from the fixed core refinement of ZAA25A from the 18-month data collection.

Atom Label	Atom Type	Multiplicity	Fractional X Coordinate	Fractional Y Coordinate	Fractional Z Coordinate	Fractional Occupancy
C1	C	1	0.5893893	0.5000000	0.5826913	1
C2	C	1	0.5000000	0.4106107	0.5826913	1
C3	C	1	0.4106107	0.5000000	0.5826913	1
C4	C	1	0.5000000	0.5893893	0.5826913	1
C5	C	1	0.5893893	0.5000000	0.4173087	1
C6	C	1	0.5000000	0.4106107	0.4173087	1
C7	C	1	0.4106107	0.5000000	0.4173087	1
C8	C	1	0.5000000	0.5893893	0.4173087	1
C9	C	1	0.5893893	0.4106107	0.5000000	1
C10	C	1	0.4106107	0.4106107	0.5000000	1
C11	C	1	0.4106107	0.5893893	0.5000000	1
C12	C	1	0.5893893	0.5893893	0.5000000	1
C13	C	1	0.6184014	0.5000000	0.6095296	1
C14	C	1	0.5000000	0.3815986	0.6095296	1
C15	C	1	0.3815986	0.5000000	0.6095296	1
C16	C	1	0.5000000	0.6184014	0.6095296	1
C17	C	1	0.6184014	0.5000000	0.3904704	1
C18	C	1	0.5000000	0.3815986	0.3904704	1
C19	C	1	0.3815986	0.5000000	0.3904704	1
C20	C	1	0.5000000	0.6184014	0.3904704	1
C21	C	1	0.6184014	0.3815986	0.5000000	1
C22	C	1	0.3815986	0.3815986	0.5000000	1
C23	C	1	0.3815986	0.6184014	0.5000000	1
C24	C	1	0.6184014	0.6184014	0.5000000	1
O1	O	1	0.5353427	0.5349979	0.4673055	1
O2	O	1	0.5353427	0.4650021	0.5326945	1
O3	O	1	0.4646573	0.5349979	0.4673055	1
O4	O	1	0.4646573	0.4650021	0.5326945	1
O5	O	1	0.4646573	0.4650021	0.4673055	1
O6	O	1	0.4646573	0.5349979	0.5326945	1

O7	O	1	0.5353427	0.4650021	0.4673055	1
O8	O	1	0.5353427	0.5349979	0.5326945	1
O9	O	1	0.5939526	0.5000000	0.5488581	1
O10	O	1	0.5939526	0.4471844	0.5000000	1
O11	O	1	0.5939526	0.5000000	0.4511419	1
O12	O	1	0.5939526	0.5528156	0.5000000	1
O13	O	1	0.5000000	0.5939526	0.5488581	1
O14	O	1	0.5528156	0.5939526	0.5000000	1
O15	O	1	0.5000000	0.5939526	0.4511419	1
O16	O	1	0.4471844	0.5939526	0.5000000	1
O17	O	1	0.4060474	0.5000000	0.5488581	1
O18	O	1	0.4060474	0.5528156	0.5000000	1
O19	O	1	0.4060474	0.5000000	0.4511419	1
O20	O	1	0.4060474	0.4471844	0.5000000	1
O21	O	1	0.5000000	0.4060474	0.5488581	1
O22	O	1	0.4471844	0.4060474	0.5000000	1
O23	O	1	0.5000000	0.4060474	0.4511419	1
O24	O	1	0.5528156	0.4060474	0.5000000	1
O25	O	1	0.5528156	0.5000000	0.5869127	1
O26	O	1	0.5000000	0.5528156	0.5869127	1
O27	O	1	0.4471844	0.5000000	0.5869127	1
O28	O	1	0.5000000	0.4471844	0.5869127	1
O29	O	1	0.5528156	0.5000000	0.4130873	1
O30	O	1	0.5000000	0.4471844	0.4130873	1
O31	O	1	0.4471844	0.5000000	0.4130873	1
O32	O	1	0.5000000	0.5528156	0.4130873	1
Zr1	Zr	1	0.566415	0.5000000	0.5000000	1
Zr2	Zr	1	0.5000000	0.566415	0.5000000	1
Zr3	Zr	1	0.433585	0.5000000	0.5000000	1
Zr4	Zr	1	0.5000000	0.433585	0.5000000	1
Zr5	Zr	1	0.5000000	0.5000000	0.5614385	1
Zr6	Zr	1	0.5000000	0.5000000	0.4385615	1

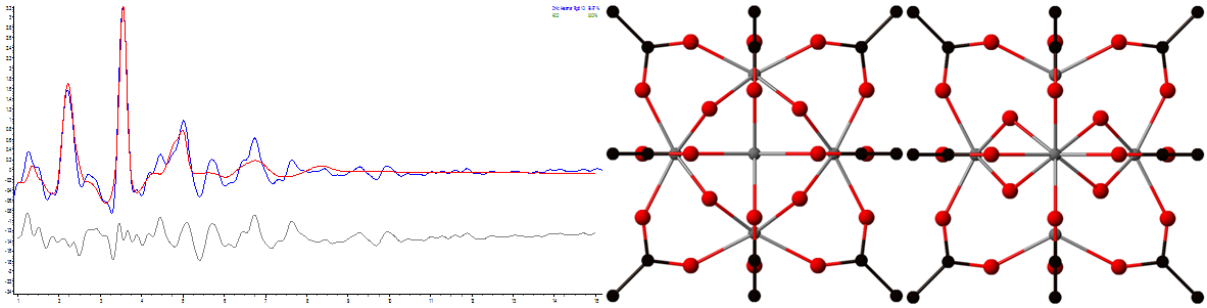

Figure 256: Observed and Calculated PDF from the chandelier core refinement of ZAA25C from the 18-month data collection and the resultant model viewed from the axial (left) and equatorial (right) positions.

Table 199: The atomic coordinates of the model resulting from the chandelier core refinement of ZAA25C from the 18-month data collection.

Atom Label	Atom Type	Multiplicity	Fractional X Coordinate	Fractional Y Coordinate	Fractional Z Coordinate	Fractional Occupancy
C1	C	1	0.5894631	0.5000000	0.5827596	1
C2	C	1	0.5000000	0.4105369	0.5827596	1
C3	C	1	0.4105369	0.5000000	0.5827596	1
C4	C	1	0.5000000	0.5894631	0.5827596	1
C5	C	1	0.5894631	0.5000000	0.4172404	1
C6	C	1	0.5000000	0.4105369	0.4172404	1
C7	C	1	0.4105369	0.5000000	0.4172404	1
C8	C	1	0.5000000	0.5894631	0.4172404	1
C9	C	1	0.5894631	0.4105369	0.5000000	1
C10	C	1	0.4105369	0.4105369	0.5000000	1
C11	C	1	0.4105369	0.5894631	0.5000000	1
C12	C	1	0.5894631	0.5894631	0.5000000	1
C13	C	1	0.6189112	0.5000000	0.6100011	1
C14	C	1	0.5000000	0.3810888	0.6100011	1
C15	C	1	0.3810888	0.5000000	0.6100011	1
C16	C	1	0.5000000	0.6189112	0.6100011	1
C17	C	1	0.6189112	0.5000000	0.3899989	1
C18	C	1	0.5000000	0.3810888	0.3899989	1
C19	C	1	0.3810888	0.5000000	0.3899989	1
C20	C	1	0.5000000	0.6189112	0.3899989	1
C21	C	1	0.6189112	0.3810888	0.5000000	1
C22	C	1	0.3810888	0.3810888	0.5000000	1
C23	C	1	0.3810888	0.6189112	0.5000000	1
C24	C	1	0.6189112	0.6189112	0.5000000	1
O1	O	1	0.5378496	0.4621504	0.4719957	1
O2	O	1	0.5378496	0.4621504	0.5280043	1
O3	O	1	0.4621504	0.4621504	0.4719957	1
O4	O	1	0.4621504	0.4621504	0.5280043	1
O5	O	1	0.4621504	0.5378496	0.4719957	1
O6	O	1	0.4621504	0.5378496	0.5280043	1
O7	O	1	0.5378496	0.5378496	0.4719957	1
O8	O	1	0.5378496	0.5378496	0.5280043	1

O9	O	1	0.5938005	0.5000000	0.5493544	1
O10	O	1	0.5938005	0.446648	0.5000000	1
O11	O	1	0.5938005	0.5000000	0.4506456	1
O12	O	1	0.5938005	0.553352	0.5000000	1
O13	O	1	0.5000000	0.5938005	0.5493544	1
O14	O	1	0.553352	0.5938005	0.5000000	1
O15	O	1	0.5000000	0.5938005	0.4506456	1
O16	O	1	0.446648	0.5938005	0.5000000	1
O17	O	1	0.4061995	0.5000000	0.5493544	1
O18	O	1	0.4061995	0.553352	0.5000000	1
O19	O	1	0.4061995	0.5000000	0.4506456	1
O20	O	1	0.4061995	0.446648	0.5000000	1
O21	O	1	0.5000000	0.4061995	0.5493544	1
O22	O	1	0.446648	0.4061995	0.5000000	1
O23	O	1	0.5000000	0.4061995	0.4506456	1
O24	O	1	0.553352	0.4061995	0.5000000	1
O25	O	1	0.553352	0.5000000	0.586772	1
O26	O	1	0.5000000	0.553352	0.586772	1
O27	O	1	0.446648	0.5000000	0.586772	1
O28	O	1	0.5000000	0.446648	0.586772	1
O29	O	1	0.553352	0.5000000	0.413228	1
O30	O	1	0.5000000	0.446648	0.413228	1
O31	O	1	0.446648	0.5000000	0.413228	1
O32	O	1	0.5000000	0.553352	0.413228	1
Zr1	Zr	1	0.566488	0.5000000	0.5000000	1
Zr2	Zr	1	0.5000000	0.566488	0.5000000	1
Zr3	Zr	1	0.433512	0.5000000	0.5000000	1
Zr4	Zr	1	0.5000000	0.433512	0.5000000	1
Zr5	Zr	1	0.5000000	0.5000000	0.5615061	1
Zr6	Zr	1	0.5000000	0.5000000	0.4384939	1

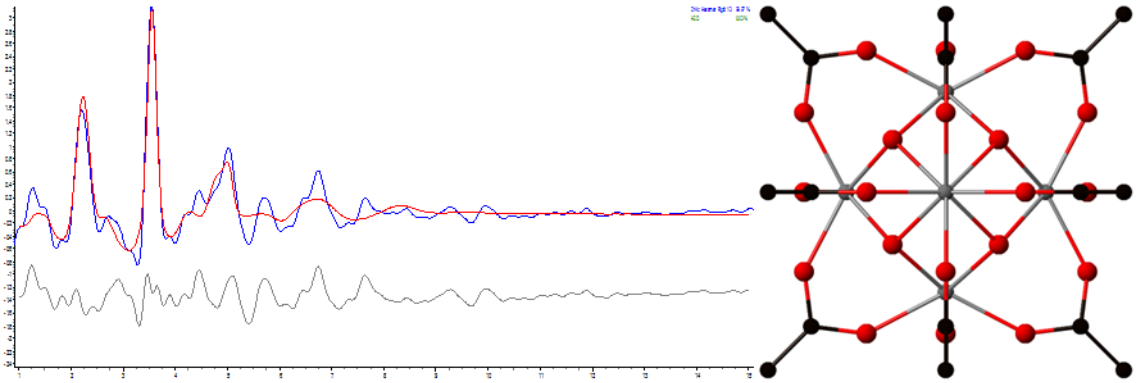

Figure 257: Observed and Calculated PDF from the fixed core refinement of ZAA25C from the 18-month data collection and the resultant model.

Table 200: The atomic coordinates of the model resulting from the fixed core refinement of ZAA25C from the 18-month data collection.

Atom Label	Atom Type	Multiplicity	Fractional X Coordinate	Fractional Y Coordinate	Fractional Z Coordinate	Fractional Occupancy
C1	C	1	0.5894245	0.5000000	0.5827239	1
C2	C	1	0.5000000	0.4105755	0.5827239	1
C3	C	1	0.4105755	0.5000000	0.5827239	1
C4	C	1	0.5000000	0.5894245	0.5827239	1
C5	C	1	0.5894245	0.5000000	0.4172761	1
C6	C	1	0.5000000	0.4105755	0.4172761	1
C7	C	1	0.4105755	0.5000000	0.4172761	1
C8	C	1	0.5000000	0.5894245	0.4172761	1
C9	C	1	0.5894245	0.4105755	0.5000000	1
C10	C	1	0.4105755	0.4105755	0.5000000	1
C11	C	1	0.4105755	0.5894245	0.5000000	1
C12	C	1	0.5894245	0.5894245	0.5000000	1
C13	C	1	0.6183516	0.5000000	0.6094835	1
C14	C	1	0.5000000	0.3816484	0.6094835	1
C15	C	1	0.3816484	0.5000000	0.6094835	1
C16	C	1	0.5000000	0.6183516	0.6094835	1
C17	C	1	0.6183516	0.5000000	0.3905165	1
C18	C	1	0.5000000	0.3816484	0.3905165	1
C19	C	1	0.3816484	0.5000000	0.3905165	1
C20	C	1	0.5000000	0.6183516	0.3905165	1
C21	C	1	0.6183516	0.3816484	0.5000000	1
C22	C	1	0.3816484	0.3816484	0.5000000	1
C23	C	1	0.3816484	0.6183516	0.5000000	1
C24	C	1	0.6183516	0.6183516	0.5000000	1
O1	O	1	0.5352811	0.5349369	0.4673625	1
O2	O	1	0.5352811	0.4650631	0.5326375	1
O3	O	1	0.4647189	0.5349369	0.4673625	1
O4	O	1	0.4647189	0.4650631	0.5326375	1
O5	O	1	0.4647189	0.4650631	0.4673625	1
O6	O	1	0.4647189	0.5349369	0.5326375	1

O7	O	1	0.5352811	0.4650631	0.4673625	1
O8	O	1	0.5352811	0.5349369	0.5326375	1
O9	O	1	0.594131	0.5000000	0.5488552	1
O10	O	1	0.594131	0.4471876	0.5000000	1
O11	O	1	0.594131	0.5000000	0.4511448	1
O12	O	1	0.594131	0.5528124	0.5000000	1
O13	O	1	0.5000000	0.594131	0.5488552	1
O14	O	1	0.5528124	0.594131	0.5000000	1
O15	O	1	0.5000000	0.594131	0.4511448	1
O16	O	1	0.4471876	0.594131	0.5000000	1
O17	O	1	0.405869	0.5000000	0.5488552	1
O18	O	1	0.405869	0.5528124	0.5000000	1
O19	O	1	0.405869	0.5000000	0.4511448	1
O20	O	1	0.405869	0.4471876	0.5000000	1
O21	O	1	0.5000000	0.405869	0.5488552	1
O22	O	1	0.4471876	0.405869	0.5000000	1
O23	O	1	0.5000000	0.405869	0.4511448	1
O24	O	1	0.5528124	0.405869	0.5000000	1
O25	O	1	0.5528124	0.5000000	0.5870778	1
O26	O	1	0.5000000	0.5528124	0.5870778	1
O27	O	1	0.4471876	0.5000000	0.5870778	1
O28	O	1	0.5000000	0.4471876	0.5870778	1
O29	O	1	0.5528124	0.5000000	0.4129222	1
O30	O	1	0.5000000	0.4471876	0.4129222	1
O31	O	1	0.4471876	0.5000000	0.4129222	1
O32	O	1	0.5000000	0.5528124	0.4129222	1
Zr1	Zr	1	0.56648	0.5000000	0.5000000	1
Zr2	Zr	1	0.5000000	0.56648	0.5000000	1
Zr3	Zr	1	0.43352	0.5000000	0.5000000	1
Zr4	Zr	1	0.5000000	0.43352	0.5000000	1
Zr5	Zr	1	0.5000000	0.5000000	0.5614986	1
Zr6	Zr	1	0.5000000	0.5000000	0.4385014	1

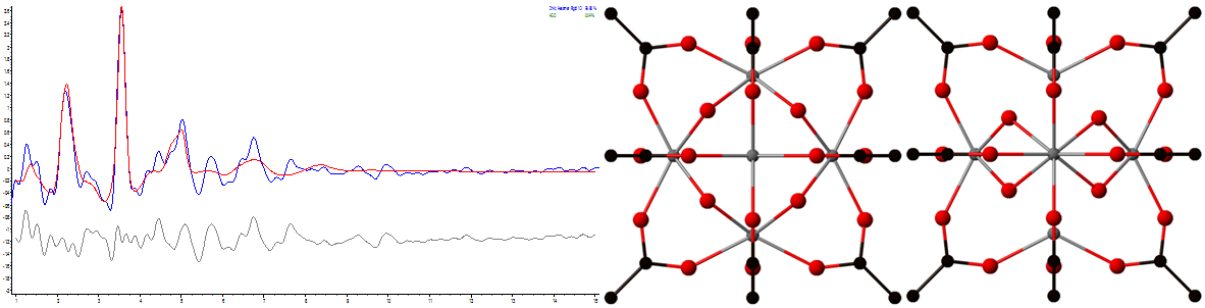

Figure 258: Observed and Calculated PDF from the chandelier core refinement of ZAA25I from the 18-month data collection and the resultant model viewed from the axial (left) and equatorial (right) positions.

Table 201: The atomic coordinates of the model resulting from the chandelier core refinement of ZAA25I from the 18-month data collection.

Atom Label	Atom Type	Multiplicity	Fractional X Coordinate	Fractional Y Coordinate	Fractional Z Coordinate	Fractional Occupancy
C1	C	1	0.5897493	0.5000000	0.5830243	1
C2	C	1	0.5000000	0.4102507	0.5830243	1
C3	C	1	0.4102507	0.5000000	0.5830243	1
C4	C	1	0.5000000	0.5897493	0.5830243	1
C5	C	1	0.5897493	0.5000000	0.4169757	1
C6	C	1	0.5000000	0.4102507	0.4169757	1
C7	C	1	0.4102507	0.5000000	0.4169757	1
C8	C	1	0.5000000	0.5897493	0.4169757	1
C9	C	1	0.5897493	0.4102507	0.5000000	1
C10	C	1	0.4102507	0.4102507	0.5000000	1
C11	C	1	0.4102507	0.5897493	0.5000000	1
C12	C	1	0.5897493	0.5897493	0.5000000	1
C13	C	1	0.6189033	0.5000000	0.6099938	1
C14	C	1	0.5000000	0.3810967	0.6099938	1
C15	C	1	0.3810967	0.5000000	0.6099938	1
C16	C	1	0.5000000	0.6189033	0.6099938	1
C17	C	1	0.6189033	0.5000000	0.3900062	1
C18	C	1	0.5000000	0.3810967	0.3900062	1
C19	C	1	0.3810967	0.5000000	0.3900062	1
C20	C	1	0.5000000	0.6189033	0.3900062	1
C21	C	1	0.6189033	0.3810967	0.5000000	1
C22	C	1	0.3810967	0.3810967	0.5000000	1
C23	C	1	0.3810967	0.6189033	0.5000000	1
C24	C	1	0.6189033	0.6189033	0.5000000	1
O1	O	1	0.5378916	0.4621084	0.4717473	1
O2	O	1	0.5378916	0.4621084	0.5282527	1
O3	O	1	0.4621084	0.4621084	0.4717473	1
O4	O	1	0.4621084	0.4621084	0.5282527	1
O5	O	1	0.4621084	0.5378916	0.4717473	1
O6	O	1	0.4621084	0.5378916	0.5282527	1
O7	O	1	0.5378916	0.5378916	0.4717473	1
O8	O	1	0.5378916	0.5378916	0.5282527	1

O9	O	1	0.5938341	0.5000000	0.5496203	1
O10	O	1	0.5938341	0.4463605	0.5000000	1
O11	O	1	0.5938341	0.5000000	0.4503797	1
O12	O	1	0.5938341	0.5536395	0.5000000	1
O13	O	1	0.5000000	0.5938341	0.5496203	1
O14	O	1	0.5536395	0.5938341	0.5000000	1
O15	O	1	0.5000000	0.5938341	0.4503797	1
O16	O	1	0.4463605	0.5938341	0.5000000	1
O17	O	1	0.4061659	0.5000000	0.5496203	1
O18	O	1	0.4061659	0.5536395	0.5000000	1
O19	O	1	0.4061659	0.5000000	0.4503797	1
O20	O	1	0.4061659	0.4463605	0.5000000	1
O21	O	1	0.5000000	0.4061659	0.5496203	1
O22	O	1	0.4463605	0.4061659	0.5000000	1
O23	O	1	0.5000000	0.4061659	0.4503797	1
O24	O	1	0.5536395	0.4061659	0.5000000	1
O25	O	1	0.5536395	0.5000000	0.5868031	1
O26	O	1	0.5000000	0.5536395	0.5868031	1
O27	O	1	0.4463605	0.5000000	0.5868031	1
O28	O	1	0.5000000	0.4463605	0.5868031	1
O29	O	1	0.5536395	0.5000000	0.4131969	1
O30	O	1	0.5000000	0.4463605	0.4131969	1
O31	O	1	0.4463605	0.5000000	0.4131969	1
O32	O	1	0.5000000	0.5536395	0.4131969	1
Zr1	Zr	1	0.566596	0.5000000	0.5000000	1
Zr2	Zr	1	0.5000000	0.566596	0.5000000	1
Zr3	Zr	1	0.433404	0.5000000	0.5000000	1
Zr4	Zr	1	0.5000000	0.433404	0.5000000	1
Zr5	Zr	1	0.5000000	0.5000000	0.561606	1
Zr6	Zr	1	0.5000000	0.5000000	0.438394	1

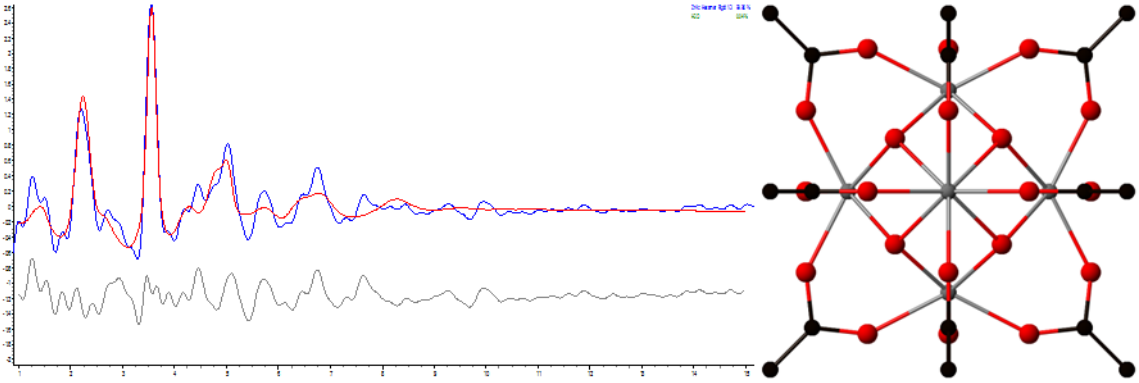

Figure 259: Observed and Calculated PDF from the fixed core refinement of ZAA25I from the 18-month data collection and the resultant model.

Table 202: The atomic coordinates of the model resulting from the fixed core refinement of ZAA25I from the 18-month data collection.

Atom Label	Atom Type	Multiplicity	Fractional X Coordinate	Fractional Y Coordinate	Fractional Z Coordinate	Fractional Occupancy
C1	C	1	0.5898753	0.5000000	0.5831409	1
C2	C	1	0.5000000	0.4101247	0.5831409	1
C3	C	1	0.4101247	0.5000000	0.5831409	1
C4	C	1	0.5000000	0.5898753	0.5831409	1
C5	C	1	0.5898753	0.5000000	0.4168591	1
C6	C	1	0.5000000	0.4101247	0.4168591	1
C7	C	1	0.4101247	0.5000000	0.4168591	1
C8	C	1	0.5000000	0.5898753	0.4168591	1
C9	C	1	0.5898753	0.4101247	0.5000000	1
C10	C	1	0.4101247	0.4101247	0.5000000	1
C11	C	1	0.4101247	0.5898753	0.5000000	1
C12	C	1	0.5898753	0.5898753	0.5000000	1
C13	C	1	0.6176542	0.5000000	0.6088383	1
C14	C	1	0.5000000	0.3823458	0.6088383	1
C15	C	1	0.3823458	0.5000000	0.6088383	1
C16	C	1	0.5000000	0.6176542	0.6088383	1
C17	C	1	0.6176542	0.5000000	0.3911617	1
C18	C	1	0.5000000	0.3823458	0.3911617	1
C19	C	1	0.3823458	0.5000000	0.3911617	1
C20	C	1	0.5000000	0.6176542	0.3911617	1
C21	C	1	0.6176542	0.3823458	0.5000000	1
C22	C	1	0.3823458	0.3823458	0.5000000	1
C23	C	1	0.3823458	0.6176542	0.5000000	1
C24	C	1	0.6176542	0.6176542	0.5000000	1
O1	O	1	0.535223	0.5348793	0.4674163	1
O2	O	1	0.535223	0.4651207	0.5325837	1
O3	O	1	0.464777	0.5348793	0.4674163	1
O4	O	1	0.464777	0.4651207	0.5325837	1
O5	O	1	0.464777	0.4651207	0.4674163	1
O6	O	1	0.464777	0.5348793	0.5325837	1

O7	O	1	0.535223	0.4651207	0.4674163	1
O8	O	1	0.535223	0.5348793	0.5325837	1
O9	O	1	0.5940471	0.5000000	0.5493191	1
O10	O	1	0.5940471	0.4466861	0.5000000	1
O11	O	1	0.5940471	0.5000000	0.4506809	1
O12	O	1	0.5940471	0.5533139	0.5000000	1
O13	O	1	0.5000000	0.5940471	0.5493191	1
O14	O	1	0.5533139	0.5940471	0.5000000	1
O15	O	1	0.5000000	0.5940471	0.4506809	1
O16	O	1	0.4466861	0.5940471	0.5000000	1
O17	O	1	0.4059529	0.5000000	0.5493191	1
O18	O	1	0.4059529	0.5533139	0.5000000	1
O19	O	1	0.4059529	0.5000000	0.4506809	1
O20	O	1	0.4059529	0.4466861	0.5000000	1
O21	O	1	0.5000000	0.4059529	0.5493191	1
O22	O	1	0.4466861	0.4059529	0.5000000	1
O23	O	1	0.5000000	0.4059529	0.4506809	1
O24	O	1	0.5533139	0.4059529	0.5000000	1
O25	O	1	0.5533139	0.5000000	0.5870001	1
O26	O	1	0.5000000	0.5533139	0.5870001	1
O27	O	1	0.4466861	0.5000000	0.5870001	1
O28	O	1	0.5000000	0.4466861	0.5870001	1
O29	O	1	0.5533139	0.5000000	0.4129999	1
O30	O	1	0.5000000	0.4466861	0.4129999	1
O31	O	1	0.4466861	0.5000000	0.4129999	1
O32	O	1	0.5000000	0.5533139	0.4129999	1
Zr1	Zr	1	0.5665545	0.5000000	0.5000000	1
Zr2	Zr	1	0.5000000	0.5665545	0.5000000	1
Zr3	Zr	1	0.4334455	0.5000000	0.5000000	1
Zr4	Zr	1	0.5000000	0.4334455	0.5000000	1
Zr5	Zr	1	0.5000000	0.5000000	0.5615675	1
Zr6	Zr	1	0.5000000	0.5000000	0.4384325	1

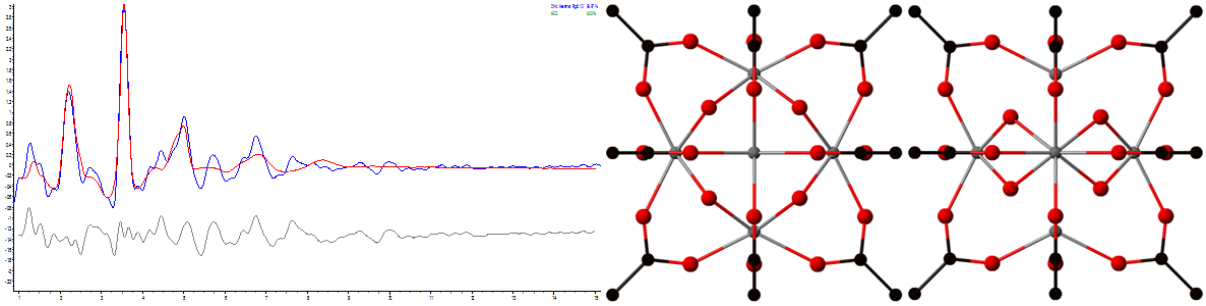

Figure 260: Observed and Calculated PDF from the chandelier core refinement of ZAA27A from the 18-month data collection and the resultant model viewed from the axial (left) and equatorial (right) positions.

Table 203: The atomic coordinates of the model resulting from the chandelier core refinement of ZAA27A from the 18-month data collection.

Atom Label	Atom Type	Multiplicity	Fractional X Coordinate	Fractional Y Coordinate	Fractional Z Coordinate	Fractional Occupancy
C1	C	1	0.5897855	0.5000000	0.5830579	1
C2	C	1	0.5000000	0.4102145	0.5830579	1
C3	C	1	0.4102145	0.5000000	0.5830579	1
C4	C	1	0.5000000	0.5897855	0.5830579	1
C5	C	1	0.5897855	0.5000000	0.4169421	1
C6	C	1	0.5000000	0.4102145	0.4169421	1
C7	C	1	0.4102145	0.5000000	0.4169421	1
C8	C	1	0.5000000	0.5897855	0.4169421	1
C9	C	1	0.5897855	0.4102145	0.5000000	1
C10	C	1	0.4102145	0.4102145	0.5000000	1
C11	C	1	0.4102145	0.5897855	0.5000000	1
C12	C	1	0.5897855	0.5897855	0.5000000	1
C13	C	1	0.6194293	0.5000000	0.6104805	1
C14	C	1	0.5000000	0.3805707	0.6104805	1
C15	C	1	0.3805707	0.5000000	0.6104805	1
C16	C	1	0.5000000	0.6194293	0.6104805	1
C17	C	1	0.6194293	0.5000000	0.3895195	1
C18	C	1	0.5000000	0.3805707	0.3895195	1
C19	C	1	0.3805707	0.5000000	0.3895195	1
C20	C	1	0.5000000	0.6194293	0.3895195	1
C21	C	1	0.6194293	0.3805707	0.5000000	1
C22	C	1	0.3805707	0.3805707	0.5000000	1
C23	C	1	0.3805707	0.6194293	0.5000000	1
C24	C	1	0.6194293	0.6194293	0.5000000	1
O1	O	1	0.5382144	0.4617856	0.4719915	1
O2	O	1	0.5382144	0.4617856	0.5280085	1
O3	O	1	0.4617856	0.4617856	0.4719915	1
O4	O	1	0.4617856	0.4617856	0.5280085	1
O5	O	1	0.4617856	0.5382144	0.4719915	1
O6	O	1	0.4617856	0.5382144	0.5280085	1
O7	O	1	0.5382144	0.5382144	0.4719915	1
O8	O	1	0.5382144	0.5382144	0.5280085	1

O9	O	1	0.5936052	0.5000000	0.5496705	1
O10	O	1	0.5936052	0.4463062	0.5000000	1
O11	O	1	0.5936052	0.5000000	0.4503295	1
O12	O	1	0.5936052	0.5536938	0.5000000	1
O13	O	1	0.5000000	0.5936052	0.5496705	1
O14	O	1	0.5536938	0.5936052	0.5000000	1
O15	O	1	0.5000000	0.5936052	0.4503295	1
O16	O	1	0.4463062	0.5936052	0.5000000	1
O17	O	1	0.4063948	0.5000000	0.5496705	1
O18	O	1	0.4063948	0.5536938	0.5000000	1
O19	O	1	0.4063948	0.5000000	0.4503295	1
O20	O	1	0.4063948	0.4463062	0.5000000	1
O21	O	1	0.5000000	0.4063948	0.5496705	1
O22	O	1	0.4463062	0.4063948	0.5000000	1
O23	O	1	0.5000000	0.4063948	0.4503295	1
O24	O	1	0.5536938	0.4063948	0.5000000	1
O25	O	1	0.5536938	0.5000000	0.5865914	1
O26	O	1	0.5000000	0.5536938	0.5865914	1
O27	O	1	0.4463062	0.5000000	0.5865914	1
O28	O	1	0.5000000	0.4463062	0.5865914	1
O29	O	1	0.5536938	0.5000000	0.4134086	1
O30	O	1	0.5000000	0.4463062	0.4134086	1
O31	O	1	0.4463062	0.5000000	0.4134086	1
O32	O	1	0.5000000	0.5536938	0.4134086	1
Zr1	Zr	1	0.5665327	0.5000000	0.5000000	1
Zr2	Zr	1	0.5000000	0.5665327	0.5000000	1
Zr3	Zr	1	0.4334673	0.5000000	0.5000000	1
Zr4	Zr	1	0.5000000	0.4334673	0.5000000	1
Zr5	Zr	1	0.5000000	0.5000000	0.5615474	1
Zr6	Zr	1	0.5000000	0.5000000	0.4384526	1

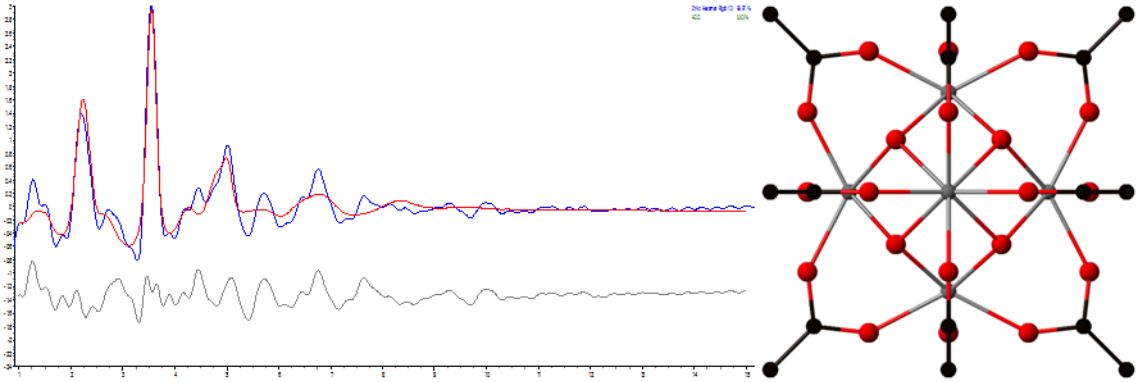

Figure 261: Observed and Calculated PDF from the fixed core refinement of ZAA27A from the 18-month data collection and the resultant model.

Table 204: The atomic coordinates of the model resulting from the fixed core refinement of ZAA27A from the 18-month data collection.

Atom Label	Atom Type	Multiplicity	Fractional X Coordinate	Fractional Y Coordinate	Fractional Z Coordinate	Fractional Occupancy
C1	C	1	0.5898293	0.5000000	0.5830984	1
C2	C	1	0.5000000	0.4101707	0.5830984	1
C3	C	1	0.4101707	0.5000000	0.5830984	1
C4	C	1	0.5000000	0.5898293	0.5830984	1
C5	C	1	0.5898293	0.5000000	0.4169016	1
C6	C	1	0.5000000	0.4101707	0.4169016	1
C7	C	1	0.4101707	0.5000000	0.4169016	1
C8	C	1	0.5000000	0.5898293	0.4169016	1
C9	C	1	0.5898293	0.4101707	0.5000000	1
C10	C	1	0.4101707	0.4101707	0.5000000	1
C11	C	1	0.4101707	0.5898293	0.5000000	1
C12	C	1	0.5898293	0.5898293	0.5000000	1
C13	C	1	0.6187928	0.5000000	0.6098916	1
C14	C	1	0.5000000	0.3812072	0.6098916	1
C15	C	1	0.3812072	0.5000000	0.6098916	1
C16	C	1	0.5000000	0.6187928	0.6098916	1
C17	C	1	0.6187928	0.5000000	0.3901084	1
C18	C	1	0.5000000	0.3812072	0.3901084	1
C19	C	1	0.3812072	0.5000000	0.3901084	1
C20	C	1	0.5000000	0.6187928	0.3901084	1
C21	C	1	0.6187928	0.3812072	0.5000000	1
C22	C	1	0.3812072	0.3812072	0.5000000	1
C23	C	1	0.3812072	0.6187928	0.5000000	1
C24	C	1	0.6187928	0.6187928	0.5000000	1
O1	O	1	0.53522	0.5348763	0.4674191	1
O2	O	1	0.53522	0.4651237	0.5325809	1
O3	O	1	0.46478	0.5348763	0.4674191	1
O4	O	1	0.46478	0.4651237	0.5325809	1
O5	O	1	0.46478	0.4651237	0.4674191	1
O6	O	1	0.46478	0.5348763	0.5325809	1

O7	O	1	0.53522	0.4651237	0.4674191	1
O8	O	1	0.53522	0.5348763	0.5325809	1
O9	O	1	0.594034	0.5000000	0.5492719	1
O10	O	1	0.594034	0.4467371	0.5000000	1
O11	O	1	0.594034	0.5000000	0.4507281	1
O12	O	1	0.594034	0.5532629	0.5000000	1
O13	O	1	0.5000000	0.594034	0.5492719	1
O14	O	1	0.5532629	0.594034	0.5000000	1
O15	O	1	0.5000000	0.594034	0.4507281	1
O16	O	1	0.4467371	0.594034	0.5000000	1
O17	O	1	0.405966	0.5000000	0.5492719	1
O18	O	1	0.405966	0.5532629	0.5000000	1
O19	O	1	0.405966	0.5000000	0.4507281	1
O20	O	1	0.405966	0.4467371	0.5000000	1
O21	O	1	0.5000000	0.405966	0.5492719	1
O22	O	1	0.4467371	0.405966	0.5000000	1
O23	O	1	0.5000000	0.405966	0.4507281	1
O24	O	1	0.5532629	0.405966	0.5000000	1
O25	O	1	0.5532629	0.5000000	0.586988	1
O26	O	1	0.5000000	0.5532629	0.586988	1
O27	O	1	0.4467371	0.5000000	0.586988	1
O28	O	1	0.5000000	0.4467371	0.586988	1
O29	O	1	0.5532629	0.5000000	0.413012	1
O30	O	1	0.5000000	0.4467371	0.413012	1
O31	O	1	0.4467371	0.5000000	0.413012	1
O32	O	1	0.5000000	0.5532629	0.413012	1
Zr1	Zr	1	0.5664885	0.5000000	0.5000000	1
Zr2	Zr	1	0.5000000	0.5664885	0.5000000	1
Zr3	Zr	1	0.4335115	0.5000000	0.5000000	1
Zr4	Zr	1	0.5000000	0.4335115	0.5000000	1
Zr5	Zr	1	0.5000000	0.5000000	0.5615065	1
Zr6	Zr	1	0.5000000	0.5000000	0.4384935	1

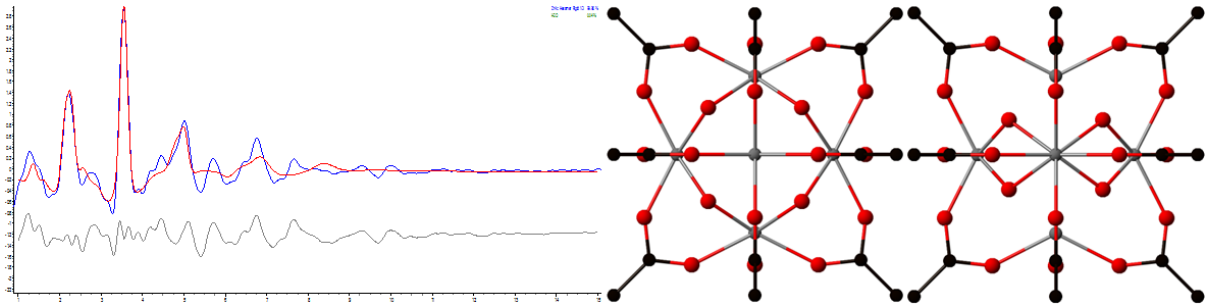

Figure 262: Observed and Calculated PDF from the chandelier core refinement of ZAA27C from the 18-month data collection and the resultant model viewed from the axial (left) and equatorial (right) positions.

Table 205: The atomic coordinates of the model resulting from the chandelier core refinement of ZAA27C from the 18-month data collection.

Atom Label	Atom Type	Multiplicity	Fractional X Coordinate	Fractional Y Coordinate	Fractional Z Coordinate	Fractional Occupancy
C1	C	1	0.5897585	0.5000000	0.5830329	1
C2	C	1	0.5000000	0.4102415	0.5830329	1
C3	C	1	0.4102415	0.5000000	0.5830329	1
C4	C	1	0.5000000	0.5897585	0.5830329	1
C5	C	1	0.5897585	0.5000000	0.4169671	1
C6	C	1	0.5000000	0.4102415	0.4169671	1
C7	C	1	0.4102415	0.5000000	0.4169671	1
C8	C	1	0.5000000	0.5897585	0.4169671	1
C9	C	1	0.5897585	0.4102415	0.5000000	1
C10	C	1	0.4102415	0.4102415	0.5000000	1
C11	C	1	0.4102415	0.5897585	0.5000000	1
C12	C	1	0.5897585	0.5897585	0.5000000	1
C13	C	1	0.6198627	0.5000000	0.6108813	1
C14	C	1	0.5000000	0.3801373	0.6108813	1
C15	C	1	0.3801373	0.5000000	0.6108813	1
C16	C	1	0.5000000	0.6198627	0.6108813	1
C17	C	1	0.6198627	0.5000000	0.3891187	1
C18	C	1	0.5000000	0.3801373	0.3891187	1
C19	C	1	0.3801373	0.5000000	0.3891187	1
C20	C	1	0.5000000	0.6198627	0.3891187	1
C21	C	1	0.6198627	0.3801373	0.5000000	1
C22	C	1	0.3801373	0.3801373	0.5000000	1
C23	C	1	0.3801373	0.6198627	0.5000000	1
C24	C	1	0.6198627	0.6198627	0.5000000	1
O1	O	1	0.5398059	0.4601941	0.4728639	1
O2	O	1	0.5398059	0.4601941	0.5271361	1
O3	O	1	0.4601941	0.4601941	0.4728639	1
O4	O	1	0.4601941	0.4601941	0.5271361	1
O5	O	1	0.4601941	0.5398059	0.4728639	1
O6	O	1	0.4601941	0.5398059	0.5271361	1
O7	O	1	0.5398059	0.5398059	0.4728639	1
O8	O	1	0.5398059	0.5398059	0.5271361	1

O9	O	1	0.5938289	0.5000000	0.5496589	1
O10	O	1	0.5938289	0.4463188	0.5000000	1
O11	O	1	0.5938289	0.5000000	0.4503411	1
O12	O	1	0.5938289	0.5536812	0.5000000	1
O13	O	1	0.5000000	0.5938289	0.5496589	1
O14	O	1	0.5536812	0.5938289	0.5000000	1
O15	O	1	0.5000000	0.5938289	0.4503411	1
O16	O	1	0.4463188	0.5938289	0.5000000	1
O17	O	1	0.4061711	0.5000000	0.5496589	1
O18	O	1	0.4061711	0.5536812	0.5000000	1
O19	O	1	0.4061711	0.5000000	0.4503411	1
O20	O	1	0.4061711	0.4463188	0.5000000	1
O21	O	1	0.5000000	0.4061711	0.5496589	1
O22	O	1	0.4463188	0.4061711	0.5000000	1
O23	O	1	0.5000000	0.4061711	0.4503411	1
O24	O	1	0.5536812	0.4061711	0.5000000	1
O25	O	1	0.5536812	0.5000000	0.5867983	1
O26	O	1	0.5000000	0.5536812	0.5867983	1
O27	O	1	0.4463188	0.5000000	0.5867983	1
O28	O	1	0.5000000	0.4463188	0.5867983	1
O29	O	1	0.5536812	0.5000000	0.4132017	1
O30	O	1	0.5000000	0.4463188	0.4132017	1
O31	O	1	0.4463188	0.5000000	0.4132017	1
O32	O	1	0.5000000	0.5536812	0.4132017	1
Zr1	Zr	1	0.5664347	0.5000000	0.5000000	1
Zr2	Zr	1	0.5000000	0.5664347	0.5000000	1
Zr3	Zr	1	0.4335653	0.5000000	0.5000000	1
Zr4	Zr	1	0.5000000	0.4335653	0.5000000	1
Zr5	Zr	1	0.5000000	0.5000000	0.5614567	1
Zr6	Zr	1	0.5000000	0.5000000	0.4385433	1

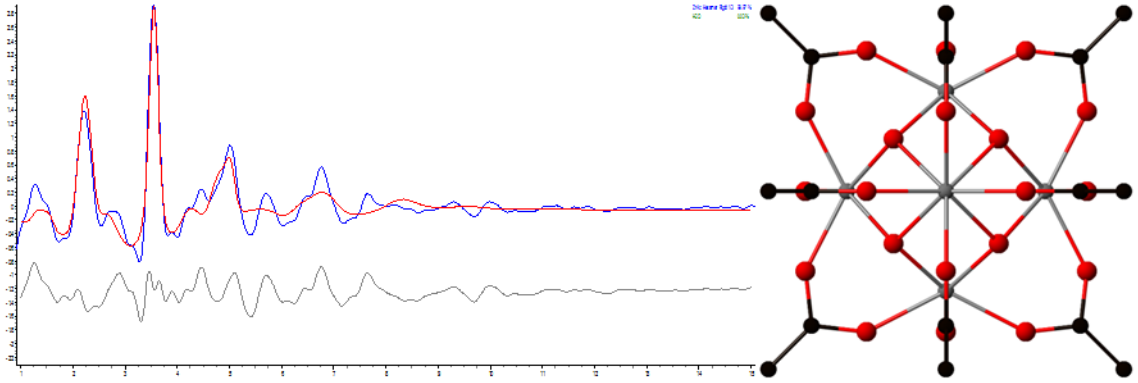

Figure 263: Observed and Calculated PDF from the fixed core refinement of ZAA27C from the 18-month data collection and the resultant model.

Table 206: The atomic coordinates of the model resulting from the fixed core refinement of ZAA27C from the 18-month data collection.

Atom Label	Atom Type	Multiplicity	Fractional X Coordinate	Fractional Y Coordinate	Fractional Z Coordinate	Fractional Occupancy
C1	C	1	0.5896907	0.5000000	0.5829702	1
C2	C	1	0.5000000	0.4103093	0.5829702	1
C3	C	1	0.4103093	0.5000000	0.5829702	1
C4	C	1	0.5000000	0.5896907	0.5829702	1
C5	C	1	0.5896907	0.5000000	0.4170298	1
C6	C	1	0.5000000	0.4103093	0.4170298	1
C7	C	1	0.4103093	0.5000000	0.4170298	1
C8	C	1	0.5000000	0.5896907	0.4170298	1
C9	C	1	0.5896907	0.4103093	0.5000000	1
C10	C	1	0.4103093	0.4103093	0.5000000	1
C11	C	1	0.4103093	0.5896907	0.5000000	1
C12	C	1	0.5896907	0.5896907	0.5000000	1
C13	C	1	0.6186657	0.5000000	0.609774	1
C14	C	1	0.5000000	0.3813343	0.609774	1
C15	C	1	0.3813343	0.5000000	0.609774	1
C16	C	1	0.5000000	0.6186657	0.609774	1
C17	C	1	0.6186657	0.5000000	0.390226	1
C18	C	1	0.5000000	0.3813343	0.390226	1
C19	C	1	0.3813343	0.5000000	0.390226	1
C20	C	1	0.5000000	0.6186657	0.390226	1
C21	C	1	0.6186657	0.3813343	0.5000000	1
C22	C	1	0.3813343	0.3813343	0.5000000	1
C23	C	1	0.3813343	0.6186657	0.5000000	1
C24	C	1	0.6186657	0.6186657	0.5000000	1
O1	O	1	0.5351237	0.534781	0.4675082	1
O2	O	1	0.5351237	0.465219	0.5324918	1
O3	O	1	0.4648763	0.534781	0.4675082	1
O4	O	1	0.4648763	0.465219	0.5324918	1
O5	O	1	0.4648763	0.465219	0.4675082	1
O6	O	1	0.4648763	0.534781	0.5324918	1

O7	O	1	0.5351237	0.465219	0.4675082	1
O8	O	1	0.5351237	0.534781	0.5324918	1
O9	O	1	0.5938996	0.5000000	0.5491695	1
O10	O	1	0.5938996	0.4468478	0.5000000	1
O11	O	1	0.5938996	0.5000000	0.4508305	1
O12	O	1	0.5938996	0.5531522	0.5000000	1
O13	O	1	0.5000000	0.5938996	0.5491695	1
O14	O	1	0.5531522	0.5938996	0.5000000	1
O15	O	1	0.5000000	0.5938996	0.4508305	1
O16	O	1	0.4468478	0.5938996	0.5000000	1
O17	O	1	0.4061004	0.5000000	0.5491695	1
O18	O	1	0.4061004	0.5531522	0.5000000	1
O19	O	1	0.4061004	0.5000000	0.4508305	1
O20	O	1	0.4061004	0.4468478	0.5000000	1
O21	O	1	0.5000000	0.4061004	0.5491695	1
O22	O	1	0.4468478	0.4061004	0.5000000	1
O23	O	1	0.5000000	0.4061004	0.4508305	1
O24	O	1	0.5531522	0.4061004	0.5000000	1
O25	O	1	0.5531522	0.5000000	0.5868637	1
O26	O	1	0.5000000	0.5531522	0.5868637	1
O27	O	1	0.4468478	0.5000000	0.5868637	1
O28	O	1	0.5000000	0.4468478	0.5868637	1
O29	O	1	0.5531522	0.5000000	0.4131363	1
O30	O	1	0.5000000	0.4468478	0.4131363	1
O31	O	1	0.4468478	0.5000000	0.4131363	1
O32	O	1	0.5000000	0.5531522	0.4131363	1
Zr1	Zr	1	0.566434	0.5000000	0.5000000	1
Zr2	Zr	1	0.5000000	0.566434	0.5000000	1
Zr3	Zr	1	0.433566	0.5000000	0.5000000	1
Zr4	Zr	1	0.5000000	0.433566	0.5000000	1
Zr5	Zr	1	0.5000000	0.5000000	0.5614561	1
Zr6	Zr	1	0.5000000	0.5000000	0.4385439	1

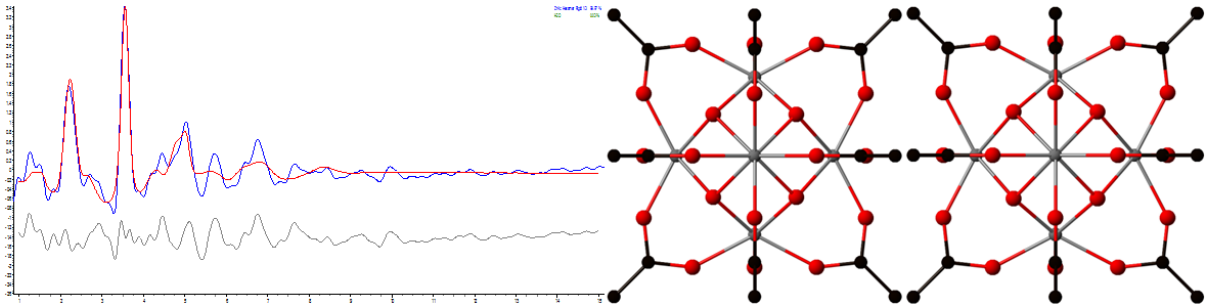

Figure 264: Observed and Calculated PDF from the chandelier core refinement of ZAA27I from the 18-month data collection and the resultant model viewed from the axial (left) and equatorial (right) positions.

Table 207: The atomic coordinates of the model resulting from the chandelier core refinement of ZAA27I from the 18-month data collection.

Atom Label	Atom Type	Multiplicity	Fractional X Coordinate	Fractional Y Coordinate	Fractional Z Coordinate	Fractional Occupancy
C1	C	1	0.5899503	0.5000000	0.5832103	1
C2	C	1	0.5000000	0.4100497	0.5832103	1
C3	C	1	0.4100497	0.5000000	0.5832103	1
C4	C	1	0.5000000	0.5899503	0.5832103	1
C5	C	1	0.5899503	0.5000000	0.4167897	1
C6	C	1	0.5000000	0.4100497	0.4167897	1
C7	C	1	0.4100497	0.5000000	0.4167897	1
C8	C	1	0.5000000	0.5899503	0.4167897	1
C9	C	1	0.5899503	0.4100497	0.5000000	1
C10	C	1	0.4100497	0.4100497	0.5000000	1
C11	C	1	0.4100497	0.5899503	0.5000000	1
C12	C	1	0.5899503	0.5899503	0.5000000	1
C13	C	1	0.6190673	0.5000000	0.6101456	1
C14	C	1	0.5000000	0.3809327	0.6101456	1
C15	C	1	0.3809327	0.5000000	0.6101456	1
C16	C	1	0.5000000	0.6190673	0.6101456	1
C17	C	1	0.6190673	0.5000000	0.3898544	1
C18	C	1	0.5000000	0.3809327	0.3898544	1
C19	C	1	0.3809327	0.5000000	0.3898544	1
C20	C	1	0.5000000	0.6190673	0.3898544	1
C21	C	1	0.6190673	0.3809327	0.5000000	1
C22	C	1	0.3809327	0.3809327	0.5000000	1
C23	C	1	0.3809327	0.6190673	0.5000000	1
C24	C	1	0.6190673	0.6190673	0.5000000	1
O1	O	1	0.5351189	0.4648811	0.4663417	1
O2	O	1	0.5351189	0.4648811	0.5336583	1
O3	O	1	0.4648811	0.4648811	0.4663417	1
O4	O	1	0.4648811	0.4648811	0.5336583	1
O5	O	1	0.4648811	0.5351189	0.4663417	1
O6	O	1	0.4648811	0.5351189	0.5336583	1
O7	O	1	0.5351189	0.5351189	0.4663417	1
O8	O	1	0.5351189	0.5351189	0.5336583	1

O9	O	1	0.5941365	0.5000000	0.5485911	1
O10	O	1	0.5941365	0.447473	0.5000000	1
O11	O	1	0.5941365	0.5000000	0.4514089	1
O12	O	1	0.5941365	0.552527	0.5000000	1
O13	O	1	0.5000000	0.5941365	0.5485911	1
O14	O	1	0.552527	0.5941365	0.5000000	1
O15	O	1	0.5000000	0.5941365	0.4514089	1
O16	O	1	0.447473	0.5941365	0.5000000	1
O17	O	1	0.4058635	0.5000000	0.5485911	1
O18	O	1	0.4058635	0.552527	0.5000000	1
O19	O	1	0.4058635	0.5000000	0.4514089	1
O20	O	1	0.4058635	0.447473	0.5000000	1
O21	O	1	0.5000000	0.4058635	0.5485911	1
O22	O	1	0.447473	0.4058635	0.5000000	1
O23	O	1	0.5000000	0.4058635	0.4514089	1
O24	O	1	0.552527	0.4058635	0.5000000	1
O25	O	1	0.552527	0.5000000	0.5870829	1
O26	O	1	0.5000000	0.552527	0.5870829	1
O27	O	1	0.447473	0.5000000	0.5870829	1
O28	O	1	0.5000000	0.447473	0.5870829	1
O29	O	1	0.552527	0.5000000	0.4129171	1
O30	O	1	0.5000000	0.447473	0.4129171	1
O31	O	1	0.447473	0.5000000	0.4129171	1
O32	O	1	0.5000000	0.552527	0.4129171	1
Zr1	Zr	1	0.5666409	0.5000000	0.5000000	1
Zr2	Zr	1	0.5000000	0.5666409	0.5000000	1
Zr3	Zr	1	0.4333591	0.5000000	0.5000000	1
Zr4	Zr	1	0.5000000	0.4333591	0.5000000	1
Zr5	Zr	1	0.5000000	0.5000000	0.5616475	1
Zr6	Zr	1	0.5000000	0.5000000	0.4383525	1

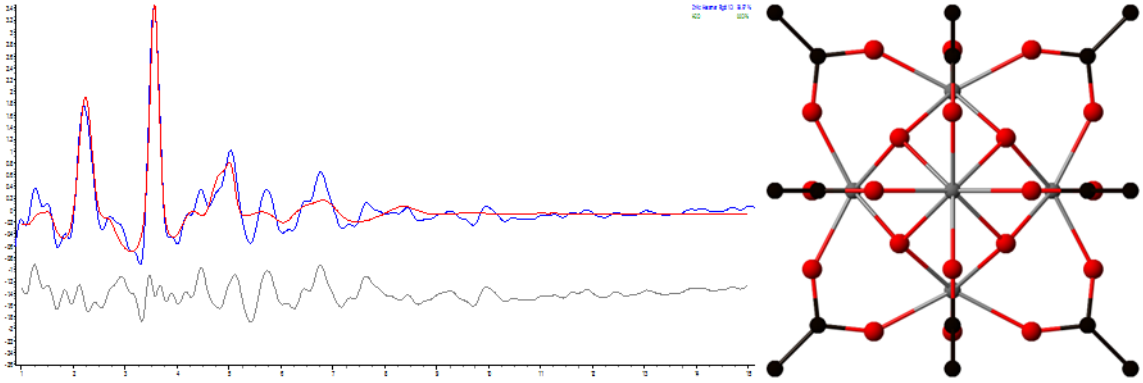

Figure 265: Observed and Calculated PDF from the fixed core refinement of ZAA27I from the 18-month data collection and the resultant model.

Table 208: The atomic coordinates of the model resulting from the fixed core refinement of ZAA27I from the 18-month data collection.

Atom Label	Atom Type	Multiplicity	Fractional X Coordinate	Fractional Y Coordinate	Fractional Z Coordinate	Fractional Occupancy
C1	C	1	0.5900968	0.5000000	0.5833458	1
C2	C	1	0.5000000	0.4099032	0.5833458	1
C3	C	1	0.4099032	0.5000000	0.5833458	1
C4	C	1	0.5000000	0.5900968	0.5833458	1
C5	C	1	0.5900968	0.5000000	0.4166542	1
C6	C	1	0.5000000	0.4099032	0.4166542	1
C7	C	1	0.4099032	0.5000000	0.4166542	1
C8	C	1	0.5000000	0.5900968	0.4166542	1
C9	C	1	0.5900968	0.4099032	0.5000000	1
C10	C	1	0.4099032	0.4099032	0.5000000	1
C11	C	1	0.4099032	0.5900968	0.5000000	1
C12	C	1	0.5900968	0.5900968	0.5000000	1
C13	C	1	0.6189109	0.5000000	0.6100009	1
C14	C	1	0.5000000	0.3810891	0.6100009	1
C15	C	1	0.3810891	0.5000000	0.6100009	1
C16	C	1	0.5000000	0.6189109	0.6100009	1
C17	C	1	0.6189109	0.5000000	0.3899991	1
C18	C	1	0.5000000	0.3810891	0.3899991	1
C19	C	1	0.3810891	0.5000000	0.3899991	1
C20	C	1	0.5000000	0.6189109	0.3899991	1
C21	C	1	0.6189109	0.3810891	0.5000000	1
C22	C	1	0.3810891	0.3810891	0.5000000	1
C23	C	1	0.3810891	0.6189109	0.5000000	1
C24	C	1	0.6189109	0.6189109	0.5000000	1
O1	O	1	0.5355988	0.5352515	0.4670686	1
O2	O	1	0.5355988	0.4647485	0.5329314	1
O3	O	1	0.4644012	0.5352515	0.4670686	1
O4	O	1	0.4644012	0.4647485	0.5329314	1
O5	O	1	0.4644012	0.4647485	0.4670686	1
O6	O	1	0.4644012	0.5352515	0.5329314	1

O7	O	1	0.5355988	0.4647485	0.4670686	1
O8	O	1	0.5355988	0.5352515	0.5329314	1
O9	O	1	0.5941036	0.5000000	0.5486549	1
O10	O	1	0.5941036	0.4474041	0.5000000	1
O11	O	1	0.5941036	0.5000000	0.4513451	1
O12	O	1	0.5941036	0.5525959	0.5000000	1
O13	O	1	0.5000000	0.5941036	0.5486549	1
O14	O	1	0.5525959	0.5941036	0.5000000	1
O15	O	1	0.5000000	0.5941036	0.4513451	1
O16	O	1	0.4474041	0.5941036	0.5000000	1
O17	O	1	0.4058964	0.5000000	0.5486549	1
O18	O	1	0.4058964	0.5525959	0.5000000	1
O19	O	1	0.4058964	0.5000000	0.4513451	1
O20	O	1	0.4058964	0.4474041	0.5000000	1
O21	O	1	0.5000000	0.4058964	0.5486549	1
O22	O	1	0.4474041	0.4058964	0.5000000	1
O23	O	1	0.5000000	0.4058964	0.4513451	1
O24	O	1	0.5525959	0.4058964	0.5000000	1
O25	O	1	0.5525959	0.5000000	0.5870524	1
O26	O	1	0.5000000	0.5525959	0.5870524	1
O27	O	1	0.4474041	0.5000000	0.5870524	1
O28	O	1	0.5000000	0.4474041	0.5870524	1
O29	O	1	0.5525959	0.5000000	0.4129476	1
O30	O	1	0.5000000	0.4474041	0.4129476	1
O31	O	1	0.4474041	0.5000000	0.4129476	1
O32	O	1	0.5000000	0.5525959	0.4129476	1
Zr1	Zr	1	0.5666246	0.5000000	0.5000000	1
Zr2	Zr	1	0.5000000	0.5666246	0.5000000	1
Zr3	Zr	1	0.4333754	0.5000000	0.5000000	1
Zr4	Zr	1	0.5000000	0.4333754	0.5000000	1
Zr5	Zr	1	0.5000000	0.5000000	0.5616324	1
Zr6	Zr	1	0.5000000	0.5000000	0.4383676	1

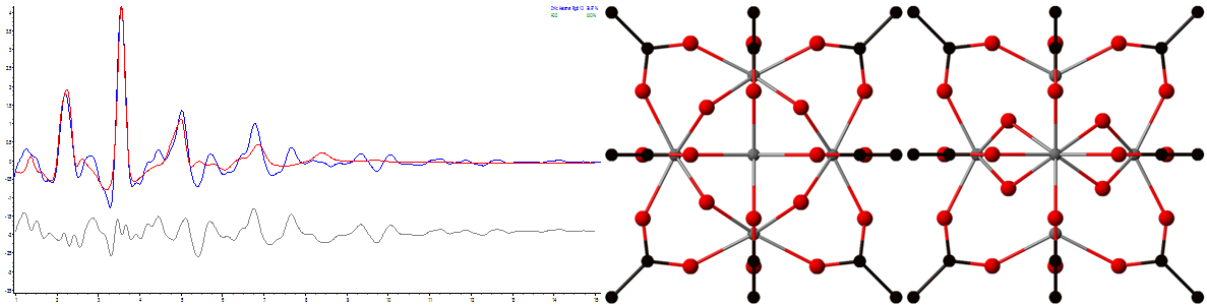

Figure 266: Observed and Calculated PDF from the chandelier core refinement of ZAA28A from the 18-month data collection and the resultant model viewed from the axial (left) and equatorial (right) positions.

Table 209: The atomic coordinates of the model resulting from the chandelier core refinement of ZAA28A from the 18-month data collection.

Atom Label	Atom Type	Multiplicity	Fractional X Coordinate	Fractional Y Coordinate	Fractional Z Coordinate	Fractional Occupancy
C1	C	1	0.5896729	0.5000000	0.5829537	1
C2	C	1	0.5000000	0.4103271	0.5829537	1
C3	C	1	0.4103271	0.5000000	0.5829537	1
C4	C	1	0.5000000	0.5896729	0.5829537	1
C5	C	1	0.5896729	0.5000000	0.4170463	1
C6	C	1	0.5000000	0.4103271	0.4170463	1
C7	C	1	0.4103271	0.5000000	0.4170463	1
C8	C	1	0.5000000	0.5896729	0.4170463	1
C9	C	1	0.5896729	0.4103271	0.5000000	1
C10	C	1	0.4103271	0.4103271	0.5000000	1
C11	C	1	0.4103271	0.5896729	0.5000000	1
C12	C	1	0.5896729	0.5896729	0.5000000	1
C13	C	1	0.6201748	0.5000000	0.6111701	1
C14	C	1	0.5000000	0.3798252	0.6111701	1
C15	C	1	0.3798252	0.5000000	0.6111701	1
C16	C	1	0.5000000	0.6201748	0.6111701	1
C17	C	1	0.6201748	0.5000000	0.3888299	1
C18	C	1	0.5000000	0.3798252	0.3888299	1
C19	C	1	0.3798252	0.5000000	0.3888299	1
C20	C	1	0.5000000	0.6201748	0.3888299	1
C21	C	1	0.6201748	0.3798252	0.5000000	1
C22	C	1	0.3798252	0.3798252	0.5000000	1
C23	C	1	0.3798252	0.6201748	0.5000000	1
C24	C	1	0.6201748	0.6201748	0.5000000	1
O1	O	1	0.5398886	0.4601114	0.4736785	1
O2	O	1	0.5398886	0.4601114	0.5263215	1
O3	O	1	0.4601114	0.4601114	0.4736785	1
O4	O	1	0.4601114	0.4601114	0.5263215	1
O5	O	1	0.4601114	0.5398886	0.4736785	1
O6	O	1	0.4601114	0.5398886	0.5263215	1
O7	O	1	0.5398886	0.5398886	0.4736785	1
O8	O	1	0.5398886	0.5398886	0.5263215	1

O9	O	1	0.5938925	0.5000000	0.5495614	1
O10	O	1	0.5938925	0.4464241	0.5000000	1
O11	O	1	0.5938925	0.5000000	0.4504386	1
O12	O	1	0.5938925	0.5535759	0.5000000	1
O13	O	1	0.5000000	0.5938925	0.5495614	1
O14	O	1	0.5535759	0.5938925	0.5000000	1
O15	O	1	0.5000000	0.5938925	0.4504386	1
O16	O	1	0.4464241	0.5938925	0.5000000	1
O17	O	1	0.4061075	0.5000000	0.5495614	1
O18	O	1	0.4061075	0.5535759	0.5000000	1
O19	O	1	0.4061075	0.5000000	0.4504386	1
O20	O	1	0.4061075	0.4464241	0.5000000	1
O21	O	1	0.5000000	0.4061075	0.5495614	1
O22	O	1	0.4464241	0.4061075	0.5000000	1
O23	O	1	0.5000000	0.4061075	0.4504386	1
O24	O	1	0.5535759	0.4061075	0.5000000	1
O25	O	1	0.5535759	0.5000000	0.5868571	1
O26	O	1	0.5000000	0.5535759	0.5868571	1
O27	O	1	0.4464241	0.5000000	0.5868571	1
O28	O	1	0.5000000	0.4464241	0.5868571	1
O29	O	1	0.5535759	0.5000000	0.4131429	1
O30	O	1	0.5000000	0.4464241	0.4131429	1
O31	O	1	0.4464241	0.5000000	0.4131429	1
O32	O	1	0.5000000	0.5535759	0.4131429	1
Zr1	Zr	1	0.5665519	0.5000000	0.5000000	1
Zr2	Zr	1	0.5000000	0.5665519	0.5000000	1
Zr3	Zr	1	0.4334481	0.5000000	0.5000000	1
Zr4	Zr	1	0.5000000	0.4334481	0.5000000	1
Zr5	Zr	1	0.5000000	0.5000000	0.5615652	1
Zr6	Zr	1	0.5000000	0.5000000	0.4384348	1

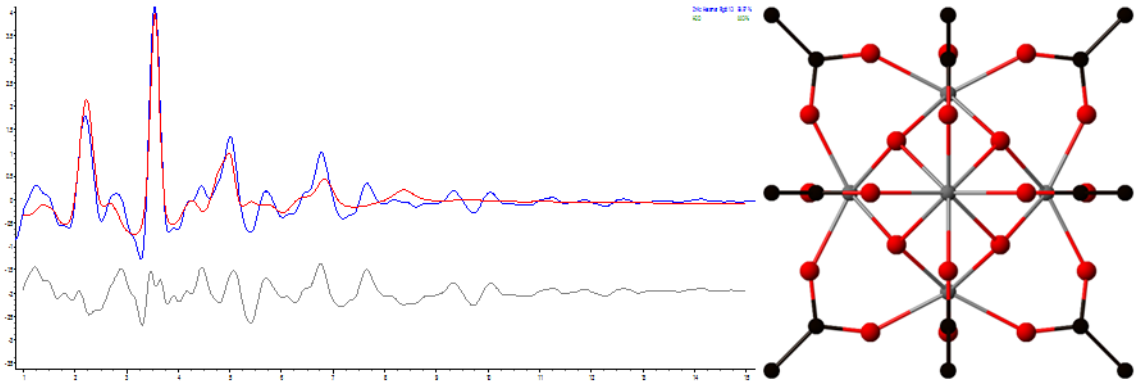

Figure 267: Observed and Calculated PDF from the fixed core refinement of ZAA28A from the 18-month data collection and the resultant model.

Table 210: The atomic coordinates of the model resulting from the fixed core refinement of ZAA28A from the 18-month data collection.

Atom Label	Atom Type	Multiplicity	Fractional X Coordinate	Fractional Y Coordinate	Fractional Z Coordinate	Fractional Occupancy
C1	C	1	0.5895789	0.5000000	0.5828667	1
C2	C	1	0.5000000	0.4104211	0.5828667	1
C3	C	1	0.4104211	0.5000000	0.5828667	1
C4	C	1	0.5000000	0.5895789	0.5828667	1
C5	C	1	0.5895789	0.5000000	0.4171333	1
C6	C	1	0.5000000	0.4104211	0.4171333	1
C7	C	1	0.4104211	0.5000000	0.4171333	1
C8	C	1	0.5000000	0.5895789	0.4171333	1
C9	C	1	0.5895789	0.4104211	0.5000000	1
C10	C	1	0.4104211	0.4104211	0.5000000	1
C11	C	1	0.4104211	0.5895789	0.5000000	1
C12	C	1	0.5895789	0.5895789	0.5000000	1
C13	C	1	0.6195515	0.5000000	0.6105935	1
C14	C	1	0.5000000	0.3804485	0.6105935	1
C15	C	1	0.3804485	0.5000000	0.6105935	1
C16	C	1	0.5000000	0.6195515	0.6105935	1
C17	C	1	0.6195515	0.5000000	0.3894065	1
C18	C	1	0.5000000	0.3804485	0.3894065	1
C19	C	1	0.3804485	0.5000000	0.3894065	1
C20	C	1	0.5000000	0.6195515	0.3894065	1
C21	C	1	0.6195515	0.3804485	0.5000000	1
C22	C	1	0.3804485	0.3804485	0.5000000	1
C23	C	1	0.3804485	0.6195515	0.5000000	1
C24	C	1	0.6195515	0.6195515	0.5000000	1
O1	O	1	0.5351725	0.5348294	0.467463	1
O2	O	1	0.5351725	0.4651706	0.532537	1
O3	O	1	0.4648275	0.5348294	0.467463	1
O4	O	1	0.4648275	0.4651706	0.532537	1
O5	O	1	0.4648275	0.4651706	0.467463	1
O6	O	1	0.4648275	0.5348294	0.532537	1

O7	O	1	0.5351725	0.4651706	0.467463	1
O8	O	1	0.5351725	0.5348294	0.532537	1
O9	O	1	0.593738	0.5000000	0.5487559	1
O10	O	1	0.593738	0.4472949	0.5000000	1
O11	O	1	0.593738	0.5000000	0.4512441	1
O12	O	1	0.593738	0.5527051	0.5000000	1
O13	O	1	0.5000000	0.593738	0.5487559	1
O14	O	1	0.5527051	0.593738	0.5000000	1
O15	O	1	0.5000000	0.593738	0.4512441	1
O16	O	1	0.4472949	0.593738	0.5000000	1
O17	O	1	0.406262	0.5000000	0.5487559	1
O18	O	1	0.406262	0.5527051	0.5000000	1
O19	O	1	0.406262	0.5000000	0.4512441	1
O20	O	1	0.406262	0.4472949	0.5000000	1
O21	O	1	0.5000000	0.406262	0.5487559	1
O22	O	1	0.4472949	0.406262	0.5000000	1
O23	O	1	0.5000000	0.406262	0.4512441	1
O24	O	1	0.5527051	0.406262	0.5000000	1
O25	O	1	0.5527051	0.5000000	0.5867142	1
O26	O	1	0.5000000	0.5527051	0.5867142	1
O27	O	1	0.4472949	0.5000000	0.5867142	1
O28	O	1	0.5000000	0.4472949	0.5867142	1
O29	O	1	0.5527051	0.5000000	0.4132858	1
O30	O	1	0.5000000	0.4472949	0.4132858	1
O31	O	1	0.4472949	0.5000000	0.4132858	1
O32	O	1	0.5000000	0.5527051	0.4132858	1
Zr1	Zr	1	0.566564	0.5000000	0.5000000	1
Zr2	Zr	1	0.5000000	0.566564	0.5000000	1
Zr3	Zr	1	0.433436	0.5000000	0.5000000	1
Zr4	Zr	1	0.5000000	0.433436	0.5000000	1
Zr5	Zr	1	0.5000000	0.5000000	0.5615763	1
Zr6	Zr	1	0.5000000	0.5000000	0.4384237	1

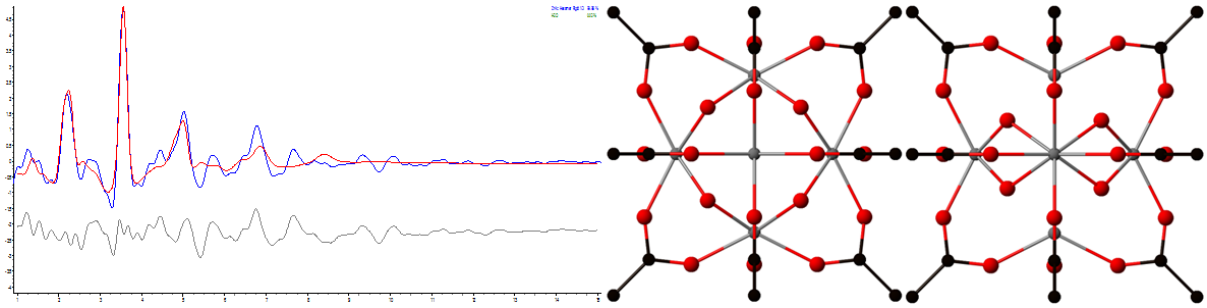

Figure 268: Observed and Calculated PDF from the chandelier core refinement of ZAA28C from the 18-month data collection and the resultant model viewed from the axial (left) and equatorial (right) positions.

Table 211: The atomic coordinates of the model resulting from the chandelier core refinement of ZAA28C from the 18-month data collection.

Atom Label	Atom Type	Multiplicity	Fractional X Coordinate	Fractional Y Coordinate	Fractional Z Coordinate	Fractional Occupancy
C1	C	1	0.5898226	0.5000000	0.5830921	1
C2	C	1	0.5000000	0.4101774	0.5830921	1
C3	C	1	0.4101774	0.5000000	0.5830921	1
C4	C	1	0.5000000	0.5898226	0.5830921	1
C5	C	1	0.5898226	0.5000000	0.4169079	1
C6	C	1	0.5000000	0.4101774	0.4169079	1
C7	C	1	0.4101774	0.5000000	0.4169079	1
C8	C	1	0.5000000	0.5898226	0.4169079	1
C9	C	1	0.5898226	0.4101774	0.5000000	1
C10	C	1	0.4101774	0.4101774	0.5000000	1
C11	C	1	0.4101774	0.5898226	0.5000000	1
C12	C	1	0.5898226	0.5898226	0.5000000	1
C13	C	1	0.6202678	0.5000000	0.6112561	1
C14	C	1	0.5000000	0.3797322	0.6112561	1
C15	C	1	0.3797322	0.5000000	0.6112561	1
C16	C	1	0.5000000	0.6202678	0.6112561	1
C17	C	1	0.6202678	0.5000000	0.3887439	1
C18	C	1	0.5000000	0.3797322	0.3887439	1
C19	C	1	0.3797322	0.5000000	0.3887439	1
C20	C	1	0.5000000	0.6202678	0.3887439	1
C21	C	1	0.6202678	0.3797322	0.5000000	1
C22	C	1	0.3797322	0.3797322	0.5000000	1
C23	C	1	0.3797322	0.6202678	0.5000000	1
C24	C	1	0.6202678	0.6202678	0.5000000	1
O1	O	1	0.5396257	0.4603743	0.4734515	1
O2	O	1	0.5396257	0.4603743	0.5265485	1
O3	O	1	0.4603743	0.4603743	0.4734515	1
O4	O	1	0.4603743	0.4603743	0.5265485	1
O5	O	1	0.4603743	0.5396257	0.4734515	1
O6	O	1	0.4603743	0.5396257	0.5265485	1
O7	O	1	0.5396257	0.5396257	0.4734515	1
O8	O	1	0.5396257	0.5396257	0.5265485	1

O9	O	1	0.5938973	0.5000000	0.5496228	1
O10	O	1	0.5938973	0.4463578	0.5000000	1
O11	O	1	0.5938973	0.5000000	0.4503772	1
O12	O	1	0.5938973	0.5536422	0.5000000	1
O13	O	1	0.5000000	0.5938973	0.5496228	1
O14	O	1	0.5536422	0.5938973	0.5000000	1
O15	O	1	0.5000000	0.5938973	0.4503772	1
O16	O	1	0.4463578	0.5938973	0.5000000	1
O17	O	1	0.4061027	0.5000000	0.5496228	1
O18	O	1	0.4061027	0.5536422	0.5000000	1
O19	O	1	0.4061027	0.5000000	0.4503772	1
O20	O	1	0.4061027	0.4463578	0.5000000	1
O21	O	1	0.5000000	0.4061027	0.5496228	1
O22	O	1	0.4463578	0.4061027	0.5000000	1
O23	O	1	0.5000000	0.4061027	0.4503772	1
O24	O	1	0.5536422	0.4061027	0.5000000	1
O25	O	1	0.5536422	0.5000000	0.5868615	1
O26	O	1	0.5000000	0.5536422	0.5868615	1
O27	O	1	0.4463578	0.5000000	0.5868615	1
O28	O	1	0.5000000	0.4463578	0.5868615	1
O29	O	1	0.5536422	0.5000000	0.4131385	1
O30	O	1	0.5000000	0.4463578	0.4131385	1
O31	O	1	0.4463578	0.5000000	0.4131385	1
O32	O	1	0.5000000	0.5536422	0.4131385	1
Zr1	Zr	1	0.5666506	0.5000000	0.5000000	1
Zr2	Zr	1	0.5000000	0.5666506	0.5000000	1
Zr3	Zr	1	0.4333494	0.5000000	0.5000000	1
Zr4	Zr	1	0.5000000	0.4333494	0.5000000	1
Zr5	Zr	1	0.5000000	0.5000000	0.5616565	1
Zr6	Zr	1	0.5000000	0.5000000	0.4383435	1

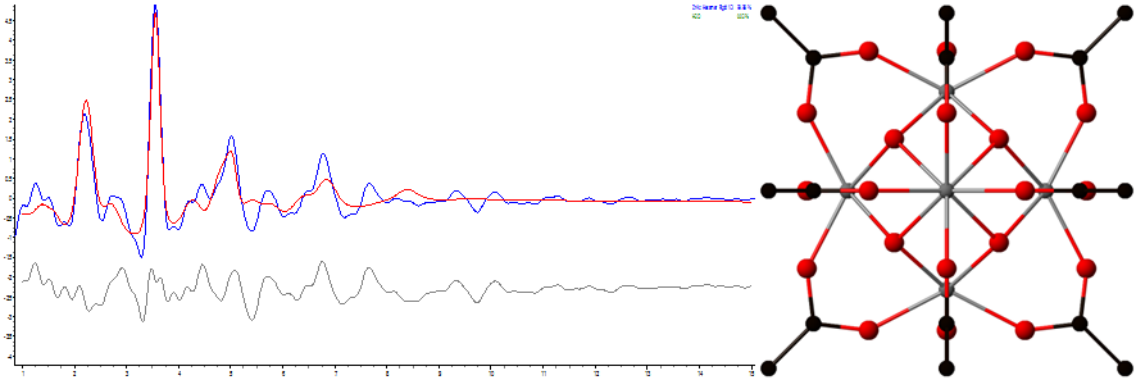

Figure 269: Observed and Calculated PDF from the fixed core refinement of ZAA28C from the 18-month data collection and the resultant model.

Table 212: The atomic coordinates of the model resulting from the fixed core refinement of ZAA28C from the 18-month data collection.

Atom Label	Atom Type	Multiplicity	Fractional X Coordinate	Fractional Y Coordinate	Fractional Z Coordinate	Fractional Occupancy
C1	C	1	0.5896188	0.5000000	0.5829036	1
C2	C	1	0.5000000	0.4103812	0.5829036	1
C3	C	1	0.4103812	0.5000000	0.5829036	1
C4	C	1	0.5000000	0.5896188	0.5829036	1
C5	C	1	0.5896188	0.5000000	0.4170964	1
C6	C	1	0.5000000	0.4103812	0.4170964	1
C7	C	1	0.4103812	0.5000000	0.4170964	1
C8	C	1	0.5000000	0.5896188	0.4170964	1
C9	C	1	0.5896188	0.4103812	0.5000000	1
C10	C	1	0.4103812	0.4103812	0.5000000	1
C11	C	1	0.4103812	0.5896188	0.5000000	1
C12	C	1	0.5896188	0.5896188	0.5000000	1
C13	C	1	0.6198994	0.5000000	0.6109153	1
C14	C	1	0.5000000	0.3801006	0.6109153	1
C15	C	1	0.3801006	0.5000000	0.6109153	1
C16	C	1	0.5000000	0.6198994	0.6109153	1
C17	C	1	0.6198994	0.5000000	0.3890847	1
C18	C	1	0.5000000	0.3801006	0.3890847	1
C19	C	1	0.3801006	0.5000000	0.3890847	1
C20	C	1	0.5000000	0.6198994	0.3890847	1
C21	C	1	0.6198994	0.3801006	0.5000000	1
C22	C	1	0.3801006	0.3801006	0.5000000	1
C23	C	1	0.3801006	0.6198994	0.5000000	1
C24	C	1	0.6198994	0.6198994	0.5000000	1
O1	O	1	0.5352156	0.534872	0.4674231	1
O2	O	1	0.5352156	0.465128	0.5325769	1
O3	O	1	0.4647844	0.534872	0.4674231	1
O4	O	1	0.4647844	0.465128	0.5325769	1
O5	O	1	0.4647844	0.465128	0.4674231	1
O6	O	1	0.4647844	0.534872	0.5325769	1

O7	O	1	0.5352156	0.465128	0.4674231	1
O8	O	1	0.5352156	0.534872	0.5325769	1
O9	O	1	0.5940729	0.5000000	0.5486252	1
O10	O	1	0.5940729	0.4474361	0.5000000	1
O11	O	1	0.5940729	0.5000000	0.4513748	1
O12	O	1	0.5940729	0.5525639	0.5000000	1
O13	O	1	0.5000000	0.5940729	0.5486252	1
O14	O	1	0.5525639	0.5940729	0.5000000	1
O15	O	1	0.5000000	0.5940729	0.4513748	1
O16	O	1	0.4474361	0.5940729	0.5000000	1
O17	O	1	0.4059271	0.5000000	0.5486252	1
O18	O	1	0.4059271	0.5525639	0.5000000	1
O19	O	1	0.4059271	0.5000000	0.4513748	1
O20	O	1	0.4059271	0.4474361	0.5000000	1
O21	O	1	0.5000000	0.4059271	0.5486252	1
O22	O	1	0.4474361	0.4059271	0.5000000	1
O23	O	1	0.5000000	0.4059271	0.4513748	1
O24	O	1	0.5525639	0.4059271	0.5000000	1
O25	O	1	0.5525639	0.5000000	0.587024	1
O26	O	1	0.5000000	0.5525639	0.587024	1
O27	O	1	0.4474361	0.5000000	0.587024	1
O28	O	1	0.5000000	0.4474361	0.587024	1
O29	O	1	0.5525639	0.5000000	0.412976	1
O30	O	1	0.5000000	0.4474361	0.412976	1
O31	O	1	0.4474361	0.5000000	0.412976	1
O32	O	1	0.5000000	0.5525639	0.412976	1
Zr1	Zr	1	0.5666461	0.5000000	0.5000000	1
Zr2	Zr	1	0.5000000	0.5666461	0.5000000	1
Zr3	Zr	1	0.4333539	0.5000000	0.5000000	1
Zr4	Zr	1	0.5000000	0.4333539	0.5000000	1
Zr5	Zr	1	0.5000000	0.5000000	0.5616523	1
Zr6	Zr	1	0.5000000	0.5000000	0.4383477	1

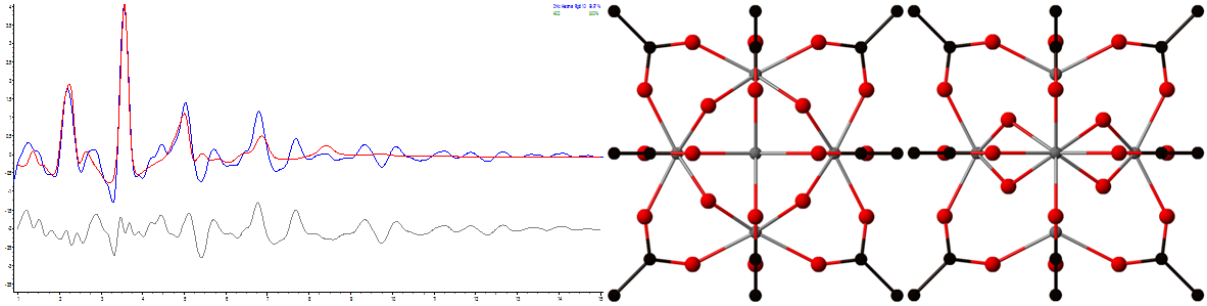

Figure 270: Observed and Calculated PDF from the chandelier core refinement of ZAA28I from the 18-month data collection and the resultant model viewed from the axial (left) and equatorial (right) positions.

Table 213: The atomic coordinates of the model resulting from the chandelier core refinement of ZAA28I from the 18-month data collection.

Atom Label	Atom Type	Multiplicity	Fractional X Coordinate	Fractional Y Coordinate	Fractional Z Coordinate	Fractional Occupancy
C1	C	1	0.5897713	0.5000000	0.5830447	1
C2	C	1	0.5000000	0.4102287	0.5830447	1
C3	C	1	0.4102287	0.5000000	0.5830447	1
C4	C	1	0.5000000	0.5897713	0.5830447	1
C5	C	1	0.5897713	0.5000000	0.4169553	1
C6	C	1	0.5000000	0.4102287	0.4169553	1
C7	C	1	0.4102287	0.5000000	0.4169553	1
C8	C	1	0.5000000	0.5897713	0.4169553	1
C9	C	1	0.5897713	0.4102287	0.5000000	1
C10	C	1	0.4102287	0.4102287	0.5000000	1
C11	C	1	0.4102287	0.5897713	0.5000000	1
C12	C	1	0.5897713	0.5897713	0.5000000	1
C13	C	1	0.6202597	0.5000000	0.6112486	1
C14	C	1	0.5000000	0.3797403	0.6112486	1
C15	C	1	0.3797403	0.5000000	0.6112486	1
C16	C	1	0.5000000	0.6202597	0.6112486	1
C17	C	1	0.6202597	0.5000000	0.3887514	1
C18	C	1	0.5000000	0.3797403	0.3887514	1
C19	C	1	0.3797403	0.5000000	0.3887514	1
C20	C	1	0.5000000	0.6202597	0.3887514	1
C21	C	1	0.6202597	0.3797403	0.5000000	1
C22	C	1	0.3797403	0.3797403	0.5000000	1
C23	C	1	0.3797403	0.6202597	0.5000000	1
C24	C	1	0.6202597	0.6202597	0.5000000	1
O1	O	1	0.5402276	0.4597724	0.4739869	1
O2	O	1	0.5402276	0.4597724	0.5260131	1
O3	O	1	0.4597724	0.4597724	0.4739869	1
O4	O	1	0.4597724	0.4597724	0.5260131	1
O5	O	1	0.4597724	0.5402276	0.4739869	1
O6	O	1	0.4597724	0.5402276	0.5260131	1
O7	O	1	0.5402276	0.5402276	0.4739869	1
O8	O	1	0.5402276	0.5402276	0.5260131	1

O9	O	1	0.5941985	0.5000000	0.5495947	1
O10	O	1	0.5941985	0.4463881	0.5000000	1
O11	O	1	0.5941985	0.5000000	0.4504053	1
O12	O	1	0.5941985	0.5536119	0.5000000	1
O13	O	1	0.5000000	0.5941985	0.5495947	1
O14	O	1	0.5536119	0.5941985	0.5000000	1
O15	O	1	0.5000000	0.5941985	0.4504053	1
O16	O	1	0.4463881	0.5941985	0.5000000	1
O17	O	1	0.4058015	0.5000000	0.5495947	1
O18	O	1	0.4058015	0.5536119	0.5000000	1
O19	O	1	0.4058015	0.5000000	0.4504053	1
O20	O	1	0.4058015	0.4463881	0.5000000	1
O21	O	1	0.5000000	0.4058015	0.5495947	1
O22	O	1	0.4463881	0.4058015	0.5000000	1
O23	O	1	0.5000000	0.4058015	0.4504053	1
O24	O	1	0.5536119	0.4058015	0.5000000	1
O25	O	1	0.5536119	0.5000000	0.5871402	1
O26	O	1	0.5000000	0.5536119	0.5871402	1
O27	O	1	0.4463881	0.5000000	0.5871402	1
O28	O	1	0.5000000	0.4463881	0.5871402	1
O29	O	1	0.5536119	0.5000000	0.4128598	1
O30	O	1	0.5000000	0.4463881	0.4128598	1
O31	O	1	0.4463881	0.5000000	0.4128598	1
O32	O	1	0.5000000	0.5536119	0.4128598	1
Zr1	Zr	1	0.566798	0.5000000	0.5000000	1
Zr2	Zr	1	0.5000000	0.566798	0.5000000	1
Zr3	Zr	1	0.433202	0.5000000	0.5000000	1
Zr4	Zr	1	0.5000000	0.433202	0.5000000	1
Zr5	Zr	1	0.5000000	0.5000000	0.5617929	1
Zr6	Zr	1	0.5000000	0.5000000	0.4382071	1

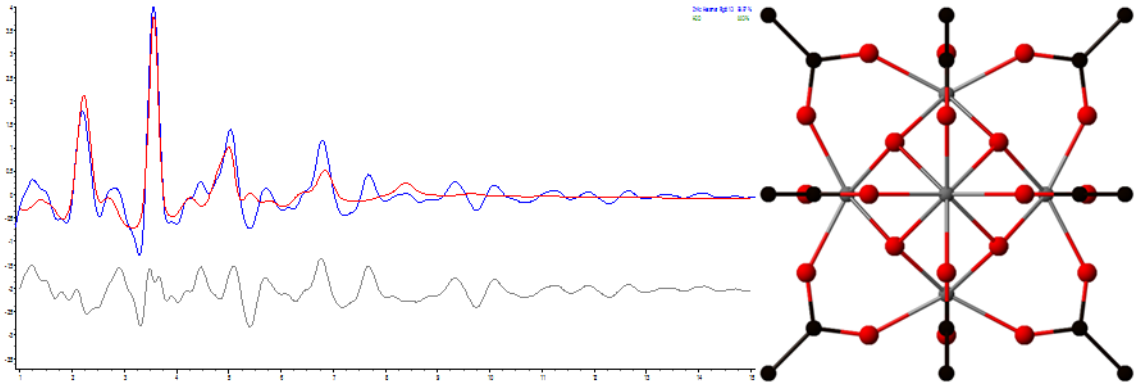

Figure 271: Observed and Calculated PDF from the fixed core refinement of ZAA28I from the 18-month data collection and the resultant model.

Table 214: The atomic coordinates of the model resulting from the fixed core refinement of ZAA28I from the 18-month data collection.

Atom Label	Atom Type	Multiplicity	Fractional X Coordinate	Fractional Y Coordinate	Fractional Z Coordinate	Fractional Occupancy
C1	C	1	0.5895122	0.5000000	0.5828051	1
C2	C	1	0.5000000	0.4104878	0.5828051	1
C3	C	1	0.4104878	0.5000000	0.5828051	1
C4	C	1	0.5000000	0.5895122	0.5828051	1
C5	C	1	0.5895122	0.5000000	0.4171949	1
C6	C	1	0.5000000	0.4104878	0.4171949	1
C7	C	1	0.4104878	0.5000000	0.4171949	1
C8	C	1	0.5000000	0.5895122	0.4171949	1
C9	C	1	0.5895122	0.4104878	0.5000000	1
C10	C	1	0.4104878	0.4104878	0.5000000	1
C11	C	1	0.4104878	0.5895122	0.5000000	1
C12	C	1	0.5895122	0.5895122	0.5000000	1
C13	C	1	0.6198796	0.5000000	0.610897	1
C14	C	1	0.5000000	0.3801204	0.610897	1
C15	C	1	0.3801204	0.5000000	0.610897	1
C16	C	1	0.5000000	0.6198796	0.610897	1
C17	C	1	0.6198796	0.5000000	0.389103	1
C18	C	1	0.5000000	0.3801204	0.389103	1
C19	C	1	0.3801204	0.5000000	0.389103	1
C20	C	1	0.5000000	0.6198796	0.389103	1
C21	C	1	0.6198796	0.3801204	0.5000000	1
C22	C	1	0.3801204	0.3801204	0.5000000	1
C23	C	1	0.3801204	0.6198796	0.5000000	1
C24	C	1	0.6198796	0.6198796	0.5000000	1
O1	O	1	0.5350162	0.5346745	0.4676076	1
O2	O	1	0.5350162	0.4653255	0.5323924	1
O3	O	1	0.4649838	0.5346745	0.4676076	1
O4	O	1	0.4649838	0.4653255	0.5323924	1
O5	O	1	0.4649838	0.4653255	0.4676076	1
O6	O	1	0.4649838	0.5346745	0.5323924	1

O7	O	1	0.5350162	0.4653255	0.4676076	1
O8	O	1	0.5350162	0.5346745	0.5323924	1
O9	O	1	0.5942769	0.5000000	0.5485257	1
O10	O	1	0.5942769	0.4475437	0.5000000	1
O11	O	1	0.5942769	0.5000000	0.4514743	1
O12	O	1	0.5942769	0.5524563	0.5000000	1
O13	O	1	0.5000000	0.5942769	0.5485257	1
O14	O	1	0.5524563	0.5942769	0.5000000	1
O15	O	1	0.5000000	0.5942769	0.4514743	1
O16	O	1	0.4475437	0.5942769	0.5000000	1
O17	O	1	0.4057231	0.5000000	0.5485257	1
O18	O	1	0.4057231	0.5524563	0.5000000	1
O19	O	1	0.4057231	0.5000000	0.4514743	1
O20	O	1	0.4057231	0.4475437	0.5000000	1
O21	O	1	0.5000000	0.4057231	0.5485257	1
O22	O	1	0.4475437	0.4057231	0.5000000	1
O23	O	1	0.5000000	0.4057231	0.4514743	1
O24	O	1	0.5524563	0.4057231	0.5000000	1
O25	O	1	0.5524563	0.5000000	0.5872127	1
O26	O	1	0.5000000	0.5524563	0.5872127	1
O27	O	1	0.4475437	0.5000000	0.5872127	1
O28	O	1	0.5000000	0.4475437	0.5872127	1
O29	O	1	0.5524563	0.5000000	0.4127873	1
O30	O	1	0.5000000	0.4475437	0.4127873	1
O31	O	1	0.4475437	0.5000000	0.4127873	1
O32	O	1	0.5000000	0.5524563	0.4127873	1
Zr1	Zr	1	0.5667889	0.5000000	0.5000000	1
Zr2	Zr	1	0.5000000	0.5667889	0.5000000	1
Zr3	Zr	1	0.4332111	0.5000000	0.5000000	1
Zr4	Zr	1	0.5000000	0.4332111	0.5000000	1
Zr5	Zr	1	0.5000000	0.5000000	0.5617844	1
Zr6	Zr	1	0.5000000	0.5000000	0.4382156	1

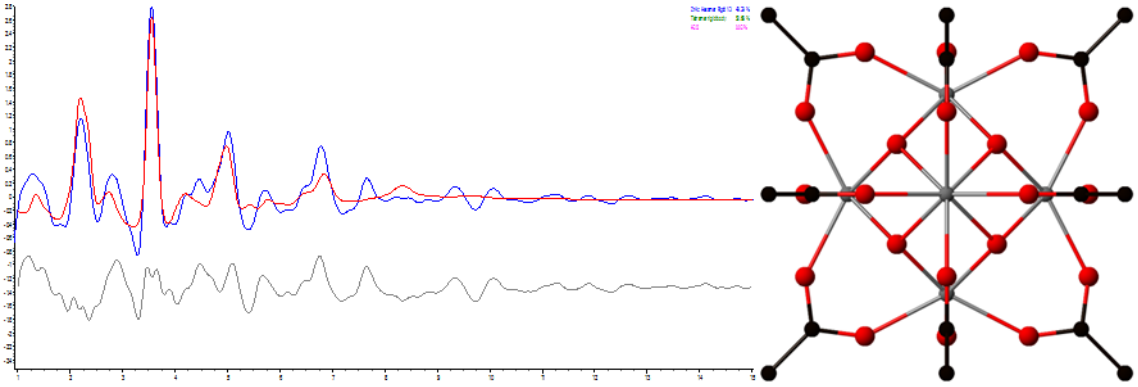

Figure 272: Observed and Calculated PDF from the fixed core refinement of ZAA1A from the 18-month data collection and the resultant model.

Table 215: The atomic coordinates of the model resulting from the fixed core refinement of ZAA1A from the 18-month data collection.

Atom Label	Atom Type	Multiplicity	Fractional X Coordinate	Fractional Y Coordinate	Fractional Z Coordinate	Fractional Occupancy
C1	C	1	0.5901193	0.5000000	0.5833666	1
C2	C	1	0.5000000	0.4098807	0.5833666	1
C3	C	1	0.4098807	0.5000000	0.5833666	1
C4	C	1	0.5000000	0.5901193	0.5833666	1
C5	C	1	0.5901193	0.5000000	0.4166334	1
C6	C	1	0.5000000	0.4098807	0.4166334	1
C7	C	1	0.4098807	0.5000000	0.4166334	1
C8	C	1	0.5000000	0.5901193	0.4166334	1
C9	C	1	0.5901193	0.4098807	0.5000000	1
C10	C	1	0.4098807	0.4098807	0.5000000	1
C11	C	1	0.4098807	0.5901193	0.5000000	1
C12	C	1	0.5901193	0.5901193	0.5000000	1
C13	C	1	0.619318	0.5000000	0.6103774	1
C14	C	1	0.5000000	0.380682	0.6103774	1
C15	C	1	0.380682	0.5000000	0.6103774	1
C16	C	1	0.5000000	0.619318	0.6103774	1
C17	C	1	0.619318	0.5000000	0.3896226	1
C18	C	1	0.5000000	0.380682	0.3896226	1
C19	C	1	0.380682	0.5000000	0.3896226	1
C20	C	1	0.5000000	0.619318	0.3896226	1
C21	C	1	0.619318	0.380682	0.5000000	1
C22	C	1	0.380682	0.380682	0.5000000	1
C23	C	1	0.380682	0.619318	0.5000000	1
C24	C	1	0.619318	0.619318	0.5000000	1
O1	O	1	0.5335579	0.5332304	0.4689566	1
O2	O	1	0.5335579	0.4667696	0.5310434	1
O3	O	1	0.4664421	0.5332304	0.4689566	1
O4	O	1	0.4664421	0.4667696	0.5310434	1
O5	O	1	0.4664421	0.4667696	0.4689566	1
O6	O	1	0.4664421	0.5332304	0.5310434	1

O7	O	1	0.5335579	0.4667696	0.4689566	1
O8	O	1	0.5335579	0.5332304	0.5310434	1
O9	O	1	0.5948089	0.5000000	0.5507915	1
O10	O	1	0.5948089	0.4450944	0.5000000	1
O11	O	1	0.5948089	0.5000000	0.4492085	1
O12	O	1	0.5948089	0.5549056	0.5000000	1
O13	O	1	0.5000000	0.5948089	0.5507915	1
O14	O	1	0.5549056	0.5948089	0.5000000	1
O15	O	1	0.5000000	0.5948089	0.4492085	1
O16	O	1	0.4450944	0.5948089	0.5000000	1
O17	O	1	0.4051911	0.5000000	0.5507915	1
O18	O	1	0.4051911	0.5549056	0.5000000	1
O19	O	1	0.4051911	0.5000000	0.4492085	1
O20	O	1	0.4051911	0.4450944	0.5000000	1
O21	O	1	0.5000000	0.4051911	0.5507915	1
O22	O	1	0.4450944	0.4051911	0.5000000	1
O23	O	1	0.5000000	0.4051911	0.4492085	1
O24	O	1	0.5549056	0.4051911	0.5000000	1
O25	O	1	0.5549056	0.5000000	0.5877049	1
O26	O	1	0.5000000	0.5549056	0.5877049	1
O27	O	1	0.4450944	0.5000000	0.5877049	1
O28	O	1	0.5000000	0.4450944	0.5877049	1
O29	O	1	0.5549056	0.5000000	0.4122951	1
O30	O	1	0.5000000	0.4450944	0.4122951	1
O31	O	1	0.4450944	0.5000000	0.4122951	1
O32	O	1	0.5000000	0.5549056	0.4122951	1
Zr1	Zr	1	0.5663948	0.5000000	0.5000000	1
Zr2	Zr	1	0.5000000	0.5663948	0.5000000	1
Zr3	Zr	1	0.4336052	0.5000000	0.5000000	1
Zr4	Zr	1	0.5000000	0.4336052	0.5000000	1
Zr5	Zr	1	0.5000000	0.5000000	0.5614198	1
Zr6	Zr	1	0.5000000	0.5000000	0.4385802	1

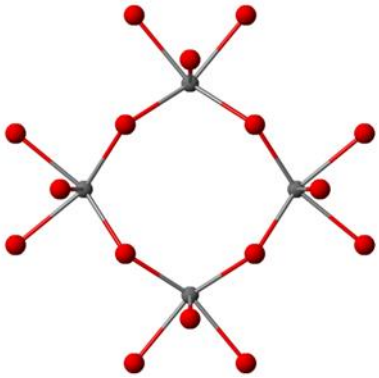

Figure 273: The tetrameric structure resulting from the fixed core refinement of ZAA1A from the 18-month data collection.

Table 216: The atomic coordinates of the tetrameric phase of the fixed core refinement of ZAA1A from 18-month data collection.

Atom Label	Atom Type	Multiplicity	Fractional X Coordinate	Fractional Y Coordinate	Fractional Z Coordinate	Fractional Occupancy
O1	O	1	0.5151851	0.4848149	0.4839685	1
O2	O	1	0.4848149	0.4848149	0.5160315	1
O3	O	1	0.5151851	0.5151851	0.5160315	1
O4	O	1	0.4848149	0.5151851	0.4839685	1
O5	O	1	0.5000000	0.5304846	0.5459481	1
O6	O	1	0.5000000	0.4695154	0.5459481	1
O7	O	1	0.4695154	0.5000000	0.4540519	1
O8	O	1	0.5304846	0.5000000	0.4540519	1
O9	O	1	0.5131279	0.4591648	0.5000000	1
O10	O	1	0.4591648	0.4868721	0.5000000	1
O11	O	1	0.5408352	0.5131279	0.5000000	1
O12	O	1	0.4868721	0.5408352	0.5000000	1
O13	O	1	0.4591648	0.5131279	0.5000000	1
O14	O	1	0.5408352	0.4868721	0.5000000	1
O15	O	1	0.4868721	0.4591648	0.5000000	1
O16	O	1	0.5131279	0.5408352	0.5000000	1
O17	O	1	0.5151851	0.4848149	0.5160315	1
O18	O	1	0.4848149	0.4848149	0.4839685	1
O19	O	1	0.5151851	0.5151851	0.4839685	1
O20	O	1	0.4848149	0.5151851	0.5160315	1
O21	O	1	0.5000000	0.5304846	0.4540519	1
O22	O	1	0.5000000	0.4695154	0.4540519	1
O23	O	1	0.4695154	0.5000000	0.5459481	1
O24	O	1	0.5304846	0.5000000	0.5459481	1
Zr1	Zr	1	0.5000000	0.4751417	0.5000000	1
Zr2	Zr	1	0.4751417	0.5000000	0.5000000	1
Zr3	Zr	1	0.5248583	0.5000000	0.5000000	1
Zr4	Zr	1	0.5000000	0.5248583	0.5000000	1

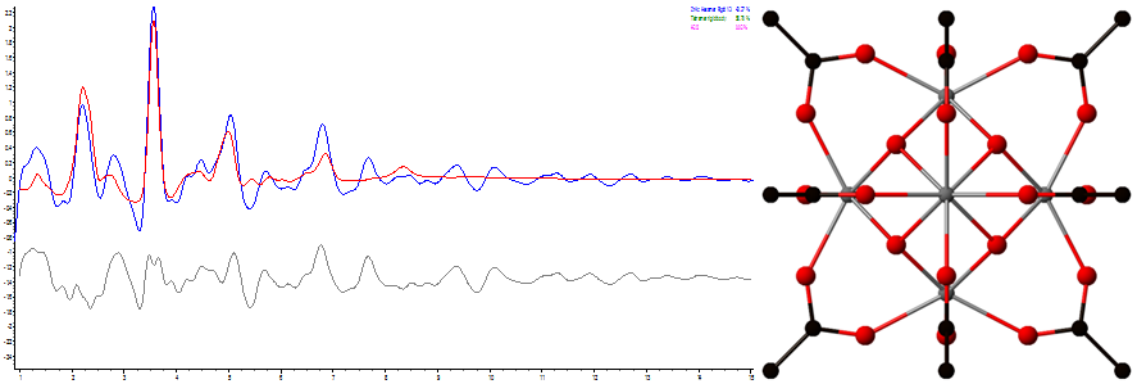

Figure 274: Observed and Calculated PDF from the fixed core refinement of ZAA1I from the 18-month data collection and the resultant model.

Table 217: The atomic coordinates of the model resulting from the fixed core refinement of ZAA1I from the 18-month data collection.

Atom Label	Atom Type	Multiplicity	Fractional X Coordinate	Fractional Y Coordinate	Fractional Z Coordinate	Fractional Occupancy
C1	C	1	0.5903031	0.5000000	0.5835367	1
C2	C	1	0.5000000	0.4096969	0.5835367	1
C3	C	1	0.4096969	0.5000000	0.5835367	1
C4	C	1	0.5000000	0.5903031	0.5835367	1
C5	C	1	0.5903031	0.5000000	0.4164633	1
C6	C	1	0.5000000	0.4096969	0.4164633	1
C7	C	1	0.4096969	0.5000000	0.4164633	1
C8	C	1	0.5000000	0.5903031	0.4164633	1
C9	C	1	0.5903031	0.4096969	0.5000000	1
C10	C	1	0.4096969	0.4096969	0.5000000	1
C11	C	1	0.4096969	0.5903031	0.5000000	1
C12	C	1	0.5903031	0.5903031	0.5000000	1
C13	C	1	0.6191353	0.5000000	0.6102085	1
C14	C	1	0.5000000	0.3808647	0.6102085	1
C15	C	1	0.3808647	0.5000000	0.6102085	1
C16	C	1	0.5000000	0.6191353	0.6102085	1
C17	C	1	0.6191353	0.5000000	0.3897915	1
C18	C	1	0.5000000	0.3808647	0.3897915	1
C19	C	1	0.3808647	0.5000000	0.3897915	1
C20	C	1	0.5000000	0.6191353	0.3897915	1
C21	C	1	0.6191353	0.3808647	0.5000000	1
C22	C	1	0.3808647	0.3808647	0.5000000	1
C23	C	1	0.3808647	0.6191353	0.5000000	1
C24	C	1	0.6191353	0.6191353	0.5000000	1
O1	O	1	0.5342424	0.5339083	0.4683234	1
O2	O	1	0.5342424	0.4660917	0.5316766	1
O3	O	1	0.4657576	0.5339083	0.4683234	1
O4	O	1	0.4657576	0.4660917	0.5316766	1
O5	O	1	0.4657576	0.4660917	0.4683234	1
O6	O	1	0.4657576	0.5339083	0.5316766	1

O7	O	1	0.5342424	0.4660917	0.4683234	1
O8	O	1	0.5342424	0.5339083	0.5316766	1
O9	O	1	0.5953079	0.5000000	0.5509936	1
O10	O	1	0.5953079	0.4448759	0.5000000	1
O11	O	1	0.5953079	0.5000000	0.4490064	1
O12	O	1	0.5953079	0.5551241	0.5000000	1
O13	O	1	0.5000000	0.5953079	0.5509936	1
O14	O	1	0.5551241	0.5953079	0.5000000	1
O15	O	1	0.5000000	0.5953079	0.4490064	1
O16	O	1	0.4448759	0.5953079	0.5000000	1
O17	O	1	0.4046921	0.5000000	0.5509936	1
O18	O	1	0.4046921	0.5551241	0.5000000	1
O19	O	1	0.4046921	0.5000000	0.4490064	1
O20	O	1	0.4046921	0.4448759	0.5000000	1
O21	O	1	0.5000000	0.4046921	0.5509936	1
O22	O	1	0.4448759	0.4046921	0.5000000	1
O23	O	1	0.5000000	0.4046921	0.4490064	1
O24	O	1	0.5551241	0.4046921	0.5000000	1
O25	O	1	0.5551241	0.5000000	0.5881664	1
O26	O	1	0.5000000	0.5551241	0.5881664	1
O27	O	1	0.4448759	0.5000000	0.5881664	1
O28	O	1	0.5000000	0.4448759	0.5881664	1
O29	O	1	0.5551241	0.5000000	0.4118336	1
O30	O	1	0.5000000	0.4448759	0.4118336	1
O31	O	1	0.4448759	0.5000000	0.4118336	1
O32	O	1	0.5000000	0.5551241	0.4118336	1
Zr1	Zr	1	0.5666196	0.5000000	0.5000000	1
Zr2	Zr	1	0.5000000	0.5666196	0.5000000	1
Zr3	Zr	1	0.4333804	0.5000000	0.5000000	1
Zr4	Zr	1	0.5000000	0.4333804	0.5000000	1
Zr5	Zr	1	0.5000000	0.5000000	0.5616278	1
Zr6	Zr	1	0.5000000	0.5000000	0.4383722	1

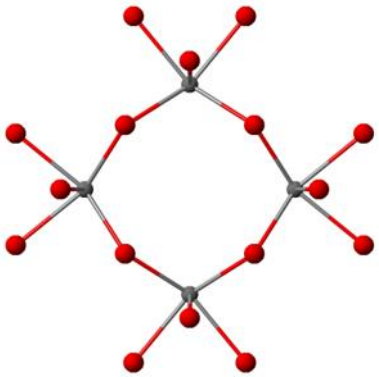

Figure 275: The tetrameric structure resulting from the fixed core refinement of ZAA1I from the 18-month data collection.

Table 218: The atomic coordinates of the tetrameric phase of the fixed core refinement of ZAA1I from the 18-month data collection.

Atom Label	Atom Type	Multiplicity	Fractional X Coordinate	Fractional Y Coordinate	Fractional Z Coordinate	Fractional Occupancy
O1	O	1	0.5152158	0.4847842	0.4822028	1
O2	O	1	0.4847842	0.4847842	0.5177972	1
O3	O	1	0.5152158	0.5152158	0.5177972	1
O4	O	1	0.4847842	0.5152158	0.4822028	1
O5	O	1	0.5000000	0.5304769	0.5455239	1
O6	O	1	0.5000000	0.4695231	0.5455239	1
O7	O	1	0.4695231	0.5000000	0.4544761	1
O8	O	1	0.5304769	0.5000000	0.4544761	1
O9	O	1	0.5132442	0.4589711	0.5000000	1
O10	O	1	0.4589711	0.4867558	0.5000000	1
O11	O	1	0.5410289	0.5132442	0.5000000	1
O12	O	1	0.4867558	0.5410289	0.5000000	1
O13	O	1	0.4589711	0.5132442	0.5000000	1
O14	O	1	0.5410289	0.4867558	0.5000000	1
O15	O	1	0.4867558	0.4589711	0.5000000	1
O16	O	1	0.5132442	0.5410289	0.5000000	1
O17	O	1	0.5152158	0.4847842	0.5177972	1
O18	O	1	0.4847842	0.4847842	0.4822028	1
O19	O	1	0.5152158	0.5152158	0.4822028	1
O20	O	1	0.4847842	0.5152158	0.5177972	1
O21	O	1	0.5000000	0.5304769	0.4544761	1
O22	O	1	0.5000000	0.4695231	0.4544761	1
O23	O	1	0.4695231	0.5000000	0.5455239	1
O24	O	1	0.5304769	0.5000000	0.5455239	1
Zr1	Zr	1	0.5000000	0.4751862	0.5000000	1
Zr2	Zr	1	0.4751862	0.5000000	0.5000000	1
Zr3	Zr	1	0.5248138	0.5000000	0.5000000	1
Zr4	Zr	1	0.5000000	0.5248138	0.5000000	1

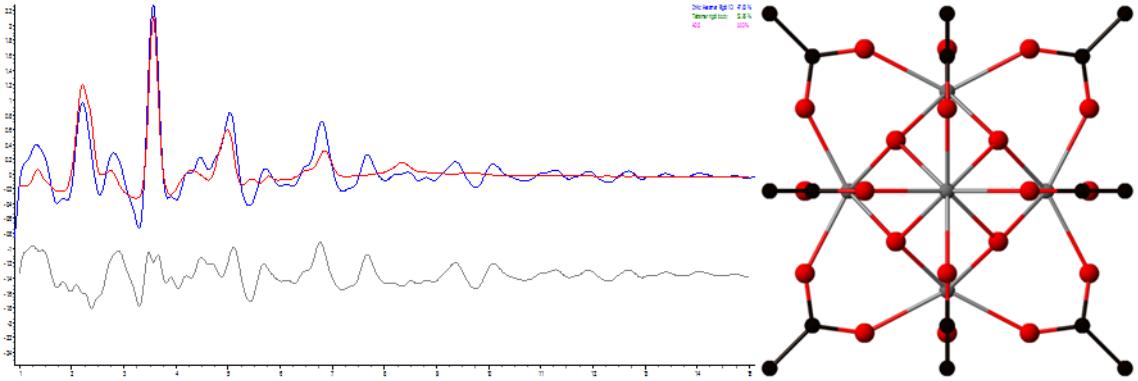

Figure 276: Observed and Calculated PDF from the fixed core refinement of ZAA4A from the 18-month data collection and the resultant model.

Table 219: The atomic coordinates of the model resulting from the fixed core refinement of ZAA4A from the 18-month data collection.

Atom Label	Atom Type	Multiplicity	Fractional X Coordinate	Fractional Y Coordinate	Fractional Z Coordinate	Fractional Occupancy
C1	C	1	0.5905386	0.5000000	0.5837546	1
C2	C	1	0.5000000	0.4094614	0.5837546	1
C3	C	1	0.4094614	0.5000000	0.5837546	1
C4	C	1	0.5000000	0.5905386	0.5837546	1
C5	C	1	0.5905386	0.5000000	0.4162454	1
C6	C	1	0.5000000	0.4094614	0.4162454	1
C7	C	1	0.4094614	0.5000000	0.4162454	1
C8	C	1	0.5000000	0.5905386	0.4162454	1
C9	C	1	0.5905386	0.4094614	0.5000000	1
C10	C	1	0.4094614	0.4094614	0.5000000	1
C11	C	1	0.4094614	0.5905386	0.5000000	1
C12	C	1	0.5905386	0.5905386	0.5000000	1
C13	C	1	0.6192182	0.5000000	0.6102851	1
C14	C	1	0.5000000	0.3807818	0.6102851	1
C15	C	1	0.3807818	0.5000000	0.6102851	1
C16	C	1	0.5000000	0.6192182	0.6102851	1
C17	C	1	0.6192182	0.5000000	0.3897149	1
C18	C	1	0.5000000	0.3807818	0.3897149	1
C19	C	1	0.3807818	0.5000000	0.3897149	1
C20	C	1	0.5000000	0.6192182	0.3897149	1
C21	C	1	0.6192182	0.3807818	0.5000000	1
C22	C	1	0.3807818	0.3807818	0.5000000	1
C23	C	1	0.3807818	0.6192182	0.5000000	1
C24	C	1	0.6192182	0.6192182	0.5000000	1
O1	O	1	0.5343455	0.5340104	0.468228	1
O2	O	1	0.5343455	0.4659896	0.531772	1
O3	O	1	0.4656545	0.5340104	0.468228	1
O4	O	1	0.4656545	0.4659896	0.531772	1
O5	O	1	0.4656545	0.4659896	0.468228	1
O6	O	1	0.4656545	0.5340104	0.531772	1

O7	O	1	0.5343455	0.4659896	0.468228	1
O8	O	1	0.5343455	0.5340104	0.531772	1
O9	O	1	0.5954294	0.5000000	0.5511766	1
O10	O	1	0.5954294	0.4446781	0.5000000	1
O11	O	1	0.5954294	0.5000000	0.4488234	1
O12	O	1	0.5954294	0.5553219	0.5000000	1
O13	O	1	0.5000000	0.5954294	0.5511766	1
O14	O	1	0.5553219	0.5954294	0.5000000	1
O15	O	1	0.5000000	0.5954294	0.4488234	1
O16	O	1	0.4446781	0.5954294	0.5000000	1
O17	O	1	0.4045706	0.5000000	0.5511766	1
O18	O	1	0.4045706	0.5553219	0.5000000	1
O19	O	1	0.4045706	0.5000000	0.4488234	1
O20	O	1	0.4045706	0.4446781	0.5000000	1
O21	O	1	0.5000000	0.4045706	0.5511766	1
O22	O	1	0.4446781	0.4045706	0.5000000	1
O23	O	1	0.5000000	0.4045706	0.4488234	1
O24	O	1	0.5553219	0.4045706	0.5000000	1
O25	O	1	0.5553219	0.5000000	0.5882789	1
O26	O	1	0.5000000	0.5553219	0.5882789	1
O27	O	1	0.4446781	0.5000000	0.5882789	1
O28	O	1	0.5000000	0.4446781	0.5882789	1
O29	O	1	0.5553219	0.5000000	0.4117211	1
O30	O	1	0.5000000	0.4446781	0.4117211	1
O31	O	1	0.4446781	0.5000000	0.4117211	1
O32	O	1	0.5000000	0.5553219	0.4117211	1
Zr1	Zr	1	0.5665864	0.5000000	0.5000000	1
Zr2	Zr	1	0.5000000	0.5665864	0.5000000	1
Zr3	Zr	1	0.4334136	0.5000000	0.5000000	1
Zr4	Zr	1	0.5000000	0.4334136	0.5000000	1
Zr5	Zr	1	0.5000000	0.5000000	0.5615971	1
Zr6	Zr	1	0.5000000	0.5000000	0.4384029	1

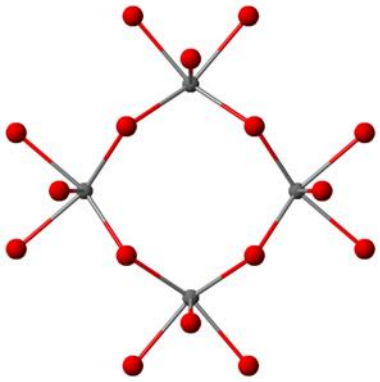

Figure 277: The tetrameric structure resulting from the fixed core refinement of ZAA4A from the 18-month data collection.

Table 220: The atomic coordinates of the tetrameric phase of the fixed core refinement of ZAA4A from the 18-month data collection.

Atom Label	Atom Type	Multiplicity	Fractional X Coordinate	Fractional Y Coordinate	Fractional Z Coordinate	Fractional Occupancy
O1	O	1	0.5149852	0.4850148	0.4803096	1
O2	O	1	0.4850148	0.4850148	0.5196904	1
O3	O	1	0.5149852	0.5149852	0.5196904	1
O4	O	1	0.4850148	0.5149852	0.4803096	1
O5	O	1	0.5000000	0.530756	0.5456649	1
O6	O	1	0.5000000	0.469244	0.5456649	1
O7	O	1	0.469244	0.5000000	0.4543351	1
O8	O	1	0.530756	0.5000000	0.4543351	1
O9	O	1	0.5135047	0.4592865	0.5000000	1
O10	O	1	0.4592865	0.4864953	0.5000000	1
O11	O	1	0.5407135	0.5135047	0.5000000	1
O12	O	1	0.4864953	0.5407135	0.5000000	1
O13	O	1	0.4592865	0.5135047	0.5000000	1
O14	O	1	0.5407135	0.4864953	0.5000000	1
O15	O	1	0.4864953	0.4592865	0.5000000	1
O16	O	1	0.5135047	0.5407135	0.5000000	1
O17	O	1	0.5149852	0.4850148	0.5196904	1
O18	O	1	0.4850148	0.4850148	0.4803096	1
O19	O	1	0.5149852	0.5149852	0.4803096	1
O20	O	1	0.4850148	0.5149852	0.5196904	1
O21	O	1	0.5000000	0.530756	0.4543351	1
O22	O	1	0.5000000	0.469244	0.4543351	1
O23	O	1	0.469244	0.5000000	0.5456649	1
O24	O	1	0.530756	0.5000000	0.5456649	1
Zr1	Zr	1	0.5000000	0.4751768	0.5000000	1
Zr2	Zr	1	0.4751768	0.5000000	0.5000000	1
Zr3	Zr	1	0.5248232	0.5000000	0.5000000	1
Zr4	Zr	1	0.5000000	0.5248232	0.5000000	1

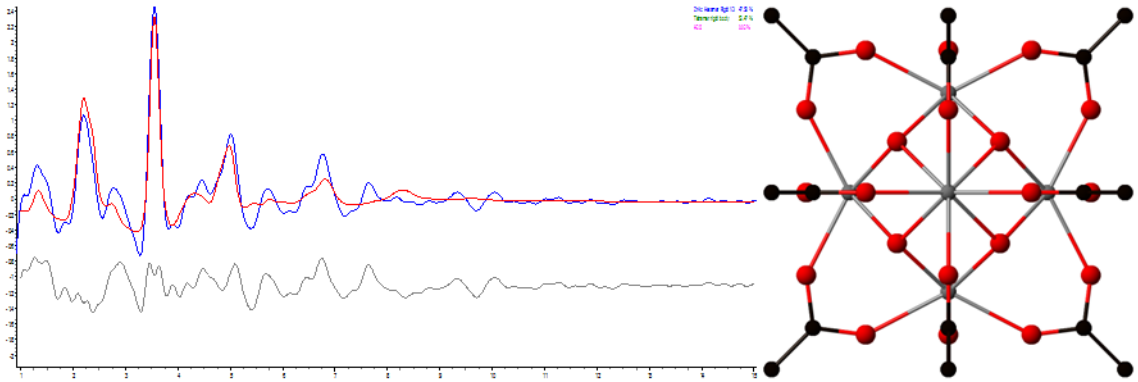

Figure 278: Observed and Calculated PDF from the fixed core refinement of ZAA4C from the 18-month data collection and the resultant model.

Table 221: The atomic coordinates of the model resulting from the fixed core refinement of ZAA4C from the 18-month data collection.

Atom Label	Atom Type	Multiplicity	Fractional X Coordinate	Fractional Y Coordinate	Fractional Z Coordinate	Fractional Occupancy
C1	C	1	0.5904445	0.5000000	0.5836675	1
C2	C	1	0.5000000	0.4095555	0.5836675	1
C3	C	1	0.4095555	0.5000000	0.5836675	1
C4	C	1	0.5000000	0.5904445	0.5836675	1
C5	C	1	0.5904445	0.5000000	0.4163325	1
C6	C	1	0.5000000	0.4095555	0.4163325	1
C7	C	1	0.4095555	0.5000000	0.4163325	1
C8	C	1	0.5000000	0.5904445	0.4163325	1
C9	C	1	0.5904445	0.4095555	0.5000000	1
C10	C	1	0.4095555	0.4095555	0.5000000	1
C11	C	1	0.4095555	0.5904445	0.5000000	1
C12	C	1	0.5904445	0.5904445	0.5000000	1
C13	C	1	0.6182238	0.5000000	0.6093653	1
C14	C	1	0.5000000	0.3817762	0.6093653	1
C15	C	1	0.3817762	0.5000000	0.6093653	1
C16	C	1	0.5000000	0.6182238	0.6093653	1
C17	C	1	0.6182238	0.5000000	0.3906347	1
C18	C	1	0.5000000	0.3817762	0.3906347	1
C19	C	1	0.3817762	0.5000000	0.3906347	1
C20	C	1	0.5000000	0.6182238	0.3906347	1
C21	C	1	0.6182238	0.3817762	0.5000000	1
C22	C	1	0.3817762	0.3817762	0.5000000	1
C23	C	1	0.3817762	0.6182238	0.5000000	1
C24	C	1	0.6182238	0.6182238	0.5000000	1
O1	O	1	0.5344456	0.5341095	0.4681354	1
O2	O	1	0.5344456	0.4658905	0.5318646	1
O3	O	1	0.4655544	0.5341095	0.4681354	1
O4	O	1	0.4655544	0.4658905	0.5318646	1
O5	O	1	0.4655544	0.4658905	0.4681354	1
O6	O	1	0.4655544	0.5341095	0.5318646	1

O7	O	1	0.5344456	0.4658905	0.4681354	1
O8	O	1	0.5344456	0.5341095	0.5318646	1
O9	O	1	0.5950853	0.5000000	0.5512253	1
O10	O	1	0.5950853	0.4446254	0.5000000	1
O11	O	1	0.5950853	0.5000000	0.4487747	1
O12	O	1	0.5950853	0.5553746	0.5000000	1
O13	O	1	0.5000000	0.5950853	0.5512253	1
O14	O	1	0.5553746	0.5950853	0.5000000	1
O15	O	1	0.5000000	0.5950853	0.4487747	1
O16	O	1	0.4446254	0.5950853	0.5000000	1
O17	O	1	0.4049147	0.5000000	0.5512253	1
O18	O	1	0.4049147	0.5553746	0.5000000	1
O19	O	1	0.4049147	0.5000000	0.4487747	1
O20	O	1	0.4049147	0.4446254	0.5000000	1
O21	O	1	0.5000000	0.4049147	0.5512253	1
O22	O	1	0.4446254	0.4049147	0.5000000	1
O23	O	1	0.5000000	0.4049147	0.4487747	1
O24	O	1	0.5553746	0.4049147	0.5000000	1
O25	O	1	0.5553746	0.5000000	0.5879605	1
O26	O	1	0.5000000	0.5553746	0.5879605	1
O27	O	1	0.4446254	0.5000000	0.5879605	1
O28	O	1	0.5000000	0.4446254	0.5879605	1
O29	O	1	0.5553746	0.5000000	0.4120395	1
O30	O	1	0.5000000	0.4446254	0.4120395	1
O31	O	1	0.4446254	0.5000000	0.4120395	1
O32	O	1	0.5000000	0.5553746	0.4120395	1
Zr1	Zr	1	0.5662978	0.5000000	0.5000000	1
Zr2	Zr	1	0.5000000	0.5662978	0.5000000	1
Zr3	Zr	1	0.4337022	0.5000000	0.5000000	1
Zr4	Zr	1	0.5000000	0.4337022	0.5000000	1
Zr5	Zr	1	0.5000000	0.5000000	0.56133	1
Zr6	Zr	1	0.5000000	0.5000000	0.43867	1

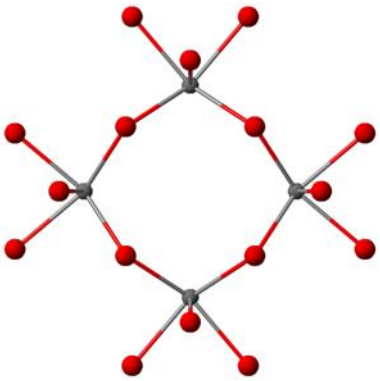

Figure 279: The tetrameric structure resulting from the fixed core refinement of ZAA4C from the 18-month data collection.

Table 222: The atomic coordinates of the tetrameric phase of the fixed core refinement of ZAA4C from the 18-month data collection.

Atom Label	Atom Type	Multiplicity	Fractional X Coordinate	Fractional Y Coordinate	Fractional Z Coordinate	Fractional Occupancy
O1	O	1	0.514989	0.485011	0.4805518	1
O2	O	1	0.485011	0.485011	0.5194482	1
O3	O	1	0.514989	0.514989	0.5194482	1
O4	O	1	0.485011	0.514989	0.4805518	1
O5	O	1	0.5000000	0.5304985	0.5455748	1
O6	O	1	0.5000000	0.4695015	0.5455748	1
O7	O	1	0.4695015	0.5000000	0.4544252	1
O8	O	1	0.5304985	0.5000000	0.4544252	1
O9	O	1	0.5134889	0.4593224	0.5000000	1
O10	O	1	0.4593224	0.4865111	0.5000000	1
O11	O	1	0.5406776	0.5134889	0.5000000	1
O12	O	1	0.4865111	0.5406776	0.5000000	1
O13	O	1	0.4593224	0.5134889	0.5000000	1
O14	O	1	0.5406776	0.4865111	0.5000000	1
O15	O	1	0.4865111	0.4593224	0.5000000	1
O16	O	1	0.5134889	0.5406776	0.5000000	1
O17	O	1	0.514989	0.485011	0.5194482	1
O18	O	1	0.485011	0.485011	0.4805518	1
O19	O	1	0.514989	0.514989	0.4805518	1
O20	O	1	0.485011	0.514989	0.5194482	1
O21	O	1	0.5000000	0.5304985	0.4544252	1
O22	O	1	0.5000000	0.4695015	0.4544252	1
O23	O	1	0.4695015	0.5000000	0.5455748	1
O24	O	1	0.5304985	0.5000000	0.5455748	1
Zr1	Zr	1	0.5000000	0.4752958	0.5000000	1
Zr2	Zr	1	0.4752958	0.5000000	0.5000000	1
Zr3	Zr	1	0.5247042	0.5000000	0.5000000	1
Zr4	Zr	1	0.5000000	0.5247042	0.5000000	1

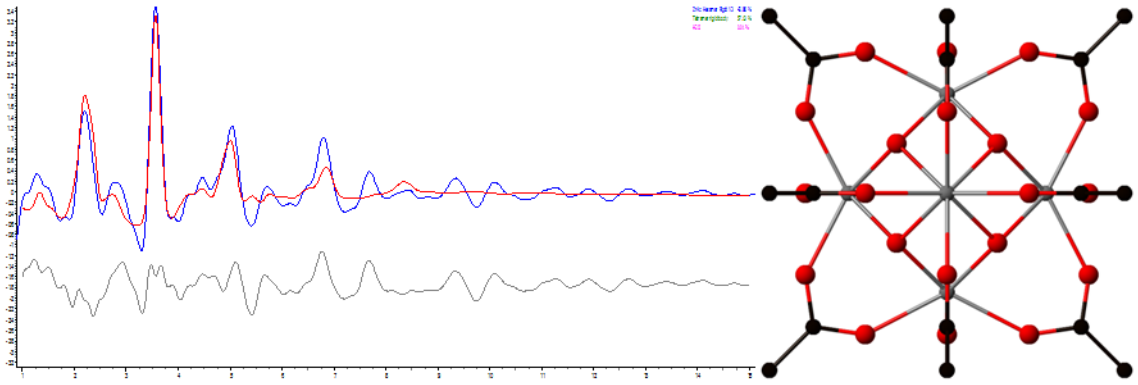

Figure 280: Observed and Calculated PDF from the fixed core refinement of ZAA4I from the 18-month data collection and the resultant model.

Table 223: The atomic coordinates of the model resulting from the fixed core refinement of ZAA4I from the 18-month data collection.

Atom Label	Atom Type	Multiplicity	Fractional X Coordinate	Fractional Y Coordinate	Fractional Z Coordinate	Fractional Occupancy
C1	C	1	0.5900179	0.5000000	0.5832729	1
C2	C	1	0.5000000	0.4099821	0.5832729	1
C3	C	1	0.4099821	0.5000000	0.5832729	1
C4	C	1	0.5000000	0.5900179	0.5832729	1
C5	C	1	0.5900179	0.5000000	0.4167271	1
C6	C	1	0.5000000	0.4099821	0.4167271	1
C7	C	1	0.4099821	0.5000000	0.4167271	1
C8	C	1	0.5000000	0.5900179	0.4167271	1
C9	C	1	0.5900179	0.4099821	0.5000000	1
C10	C	1	0.4099821	0.4099821	0.5000000	1
C11	C	1	0.4099821	0.5900179	0.5000000	1
C12	C	1	0.5900179	0.5900179	0.5000000	1
C13	C	1	0.6193294	0.5000000	0.610388	1
C14	C	1	0.5000000	0.3806706	0.610388	1
C15	C	1	0.3806706	0.5000000	0.610388	1
C16	C	1	0.5000000	0.6193294	0.610388	1
C17	C	1	0.6193294	0.5000000	0.389612	1
C18	C	1	0.5000000	0.3806706	0.389612	1
C19	C	1	0.3806706	0.5000000	0.389612	1
C20	C	1	0.5000000	0.6193294	0.389612	1
C21	C	1	0.6193294	0.3806706	0.5000000	1
C22	C	1	0.3806706	0.3806706	0.5000000	1
C23	C	1	0.3806706	0.6193294	0.5000000	1
C24	C	1	0.6193294	0.6193294	0.5000000	1
O1	O	1	0.5338462	0.5335159	0.4686899	1
O2	O	1	0.5338462	0.4664841	0.5313101	1
O3	O	1	0.4661538	0.5335159	0.4686899	1
O4	O	1	0.4661538	0.4664841	0.5313101	1
O5	O	1	0.4661538	0.4664841	0.4686899	1
O6	O	1	0.4661538	0.5335159	0.5313101	1

O7	O	1	0.5338462	0.4664841	0.4686899	1
O8	O	1	0.5338462	0.5335159	0.5313101	1
O9	O	1	0.5952614	0.5000000	0.5509921	1
O10	O	1	0.5952614	0.4448775	0.5000000	1
O11	O	1	0.5952614	0.5000000	0.4490079	1
O12	O	1	0.5952614	0.5551225	0.5000000	1
O13	O	1	0.5000000	0.5952614	0.5509921	1
O14	O	1	0.5551225	0.5952614	0.5000000	1
O15	O	1	0.5000000	0.5952614	0.4490079	1
O16	O	1	0.4448775	0.5952614	0.5000000	1
O17	O	1	0.4047386	0.5000000	0.5509921	1
O18	O	1	0.4047386	0.5551225	0.5000000	1
O19	O	1	0.4047386	0.5000000	0.4490079	1
O20	O	1	0.4047386	0.4448775	0.5000000	1
O21	O	1	0.5000000	0.4047386	0.5509921	1
O22	O	1	0.4448775	0.4047386	0.5000000	1
O23	O	1	0.5000000	0.4047386	0.4490079	1
O24	O	1	0.5551225	0.4047386	0.5000000	1
O25	O	1	0.5551225	0.5000000	0.5881234	1
O26	O	1	0.5000000	0.5551225	0.5881234	1
O27	O	1	0.4448775	0.5000000	0.5881234	1
O28	O	1	0.5000000	0.4448775	0.5881234	1
O29	O	1	0.5551225	0.5000000	0.4118766	1
O30	O	1	0.5000000	0.4448775	0.4118766	1
O31	O	1	0.4448775	0.5000000	0.4118766	1
O32	O	1	0.5000000	0.5551225	0.4118766	1
Zr1	Zr	1	0.5666156	0.5000000	0.5000000	1
Zr2	Zr	1	0.5000000	0.5666156	0.5000000	1
Zr3	Zr	1	0.4333844	0.5000000	0.5000000	1
Zr4	Zr	1	0.5000000	0.4333844	0.5000000	1
Zr5	Zr	1	0.5000000	0.5000000	0.5616241	1
Zr6	Zr	1	0.5000000	0.5000000	0.4383759	1

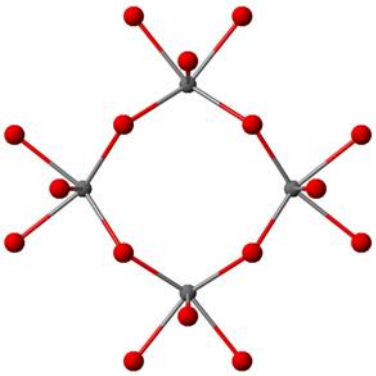

Figure 281: The tetrameric structure resulting from the fixed core refinement of ZAA4I from the 18-month data collection.

Table 224: The atomic coordinates of the tetrameric phase of the fixed core refinement of ZAA4I from the 18-month data collection.

Atom Label	Atom Type	Multiplicity	Fractional X Coordinate	Fractional Y Coordinate	Fractional Z Coordinate	Fractional Occupancy
O1	O	1	0.515244	0.484756	0.4837488	1
O2	O	1	0.484756	0.484756	0.5162512	1
O3	O	1	0.515244	0.515244	0.5162512	1
O4	O	1	0.484756	0.515244	0.4837488	1
O5	O	1	0.5000000	0.5303906	0.5458782	1
O6	O	1	0.5000000	0.4696094	0.5458782	1
O7	O	1	0.4696094	0.5000000	0.4541218	1
O8	O	1	0.5303906	0.5000000	0.4541218	1
O9	O	1	0.5128559	0.4588891	0.5000000	1
O10	O	1	0.4588891	0.4871441	0.5000000	1
O11	O	1	0.5411109	0.5128559	0.5000000	1
O12	O	1	0.4871441	0.5411109	0.5000000	1
O13	O	1	0.4588891	0.5128559	0.5000000	1
O14	O	1	0.5411109	0.4871441	0.5000000	1
O15	O	1	0.4871441	0.4588891	0.5000000	1
O16	O	1	0.5128559	0.5411109	0.5000000	1
O17	O	1	0.515244	0.484756	0.5162512	1
O18	O	1	0.484756	0.484756	0.4837488	1
O19	O	1	0.515244	0.515244	0.4837488	1
O20	O	1	0.484756	0.515244	0.5162512	1
O21	O	1	0.5000000	0.5303906	0.4541218	1
O22	O	1	0.5000000	0.4696094	0.4541218	1
O23	O	1	0.4696094	0.5000000	0.5458782	1
O24	O	1	0.5303906	0.5000000	0.5458782	1
Zr1	Zr	1	0.5000000	0.4751046	0.5000000	1
Zr2	Zr	1	0.4751046	0.5000000	0.5000000	1
Zr3	Zr	1	0.5248954	0.5000000	0.5000000	1
Zr4	Zr	1	0.5000000	0.5248954	0.5000000	1

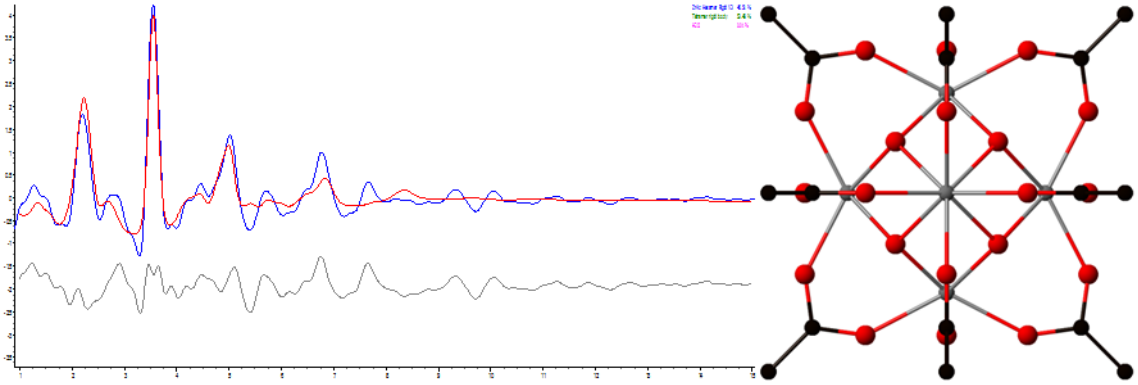

Figure 282: Observed and Calculated PDF from the fixed core refinement of ZAA7A from the 18-month data collection and the resultant model.

Table 225: The atomic coordinates of the model resulting from the fixed core refinement of ZAA7A from the 18-month data collection.

Atom Label	Atom Type	Multiplicity	Fractional X Coordinate	Fractional Y Coordinate	Fractional Z Coordinate	Fractional Occupancy
C1	C	1	0.589811	0.5000000	0.5830814	1
C2	C	1	0.5000000	0.410189	0.5830814	1
C3	C	1	0.410189	0.5000000	0.5830814	1
C4	C	1	0.5000000	0.589811	0.5830814	1
C5	C	1	0.589811	0.5000000	0.4169186	1
C6	C	1	0.5000000	0.410189	0.4169186	1
C7	C	1	0.410189	0.5000000	0.4169186	1
C8	C	1	0.5000000	0.589811	0.4169186	1
C9	C	1	0.589811	0.410189	0.5000000	1
C10	C	1	0.410189	0.410189	0.5000000	1
C11	C	1	0.410189	0.589811	0.5000000	1
C12	C	1	0.589811	0.589811	0.5000000	1
C13	C	1	0.6192131	0.5000000	0.6102804	1
C14	C	1	0.5000000	0.3807869	0.6102804	1
C15	C	1	0.3807869	0.5000000	0.6102804	1
C16	C	1	0.5000000	0.6192131	0.6102804	1
C17	C	1	0.6192131	0.5000000	0.3897196	1
C18	C	1	0.5000000	0.3807869	0.3897196	1
C19	C	1	0.3807869	0.5000000	0.3897196	1
C20	C	1	0.5000000	0.6192131	0.3897196	1
C21	C	1	0.6192131	0.3807869	0.5000000	1
C22	C	1	0.3807869	0.3807869	0.5000000	1
C23	C	1	0.3807869	0.6192131	0.5000000	1
C24	C	1	0.6192131	0.6192131	0.5000000	1
O1	O	1	0.5343641	0.5340288	0.4682108	1
O2	O	1	0.5343641	0.4659712	0.5317892	1
O3	O	1	0.4656359	0.5340288	0.4682108	1
O4	O	1	0.4656359	0.4659712	0.5317892	1
O5	O	1	0.4656359	0.4659712	0.4682108	1
O6	O	1	0.4656359	0.5340288	0.5317892	1

O7	O	1	0.5343641	0.4659712	0.4682108	1
O8	O	1	0.5343641	0.5340288	0.5317892	1
O9	O	1	0.5947731	0.5000000	0.5502649	1
O10	O	1	0.5947731	0.4456636	0.5000000	1
O11	O	1	0.5947731	0.5000000	0.4497351	1
O12	O	1	0.5947731	0.5543364	0.5000000	1
O13	O	1	0.5000000	0.5947731	0.5502649	1
O14	O	1	0.5543364	0.5947731	0.5000000	1
O15	O	1	0.5000000	0.5947731	0.4497351	1
O16	O	1	0.4456636	0.5947731	0.5000000	1
O17	O	1	0.4052269	0.5000000	0.5502649	1
O18	O	1	0.4052269	0.5543364	0.5000000	1
O19	O	1	0.4052269	0.5000000	0.4497351	1
O20	O	1	0.4052269	0.4456636	0.5000000	1
O21	O	1	0.5000000	0.4052269	0.5502649	1
O22	O	1	0.4456636	0.4052269	0.5000000	1
O23	O	1	0.5000000	0.4052269	0.4497351	1
O24	O	1	0.5543364	0.4052269	0.5000000	1
O25	O	1	0.5543364	0.5000000	0.5876717	1
O26	O	1	0.5000000	0.5543364	0.5876717	1
O27	O	1	0.4456636	0.5000000	0.5876717	1
O28	O	1	0.5000000	0.4456636	0.5876717	1
O29	O	1	0.5543364	0.5000000	0.4123283	1
O30	O	1	0.5000000	0.4456636	0.4123283	1
O31	O	1	0.4456636	0.5000000	0.4123283	1
O32	O	1	0.5000000	0.5543364	0.4123283	1
Zr1	Zr	1	0.5664046	0.5000000	0.5000000	1
Zr2	Zr	1	0.5000000	0.5664046	0.5000000	1
Zr3	Zr	1	0.4335954	0.5000000	0.5000000	1
Zr4	Zr	1	0.5000000	0.4335954	0.5000000	1
Zr5	Zr	1	0.5000000	0.5000000	0.5614289	1
Zr6	Zr	1	0.5000000	0.5000000	0.4385711	1

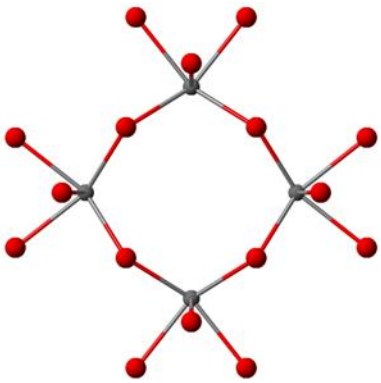

Figure 283: The tetrameric structure resulting from the fixed core refinement of ZAA7A from the 18-month data collection.

Table 226: The atomic coordinates of the tetrameric phase of the fixed core refinement of ZAA7A from the 18-month data collection.

Atom Label	Atom Type	Multiplicity	Fractional X Coordinate	Fractional Y Coordinate	Fractional Z Coordinate	Fractional Occupancy
O1	O	1	0.5152714	0.4847286	0.4830265	1
O2	O	1	0.4847286	0.4847286	0.5169735	1
O3	O	1	0.5152714	0.5152714	0.5169735	1
O4	O	1	0.4847286	0.5152714	0.4830265	1
O5	O	1	0.5000000	0.5302716	0.5451958	1
O6	O	1	0.5000000	0.4697284	0.5451958	1
O7	O	1	0.4697284	0.5000000	0.4548042	1
O8	O	1	0.5302716	0.5000000	0.4548042	1
O9	O	1	0.5128917	0.458919	0.5000000	1
O10	O	1	0.458919	0.4871083	0.5000000	1
O11	O	1	0.541081	0.5128917	0.5000000	1
O12	O	1	0.4871083	0.541081	0.5000000	1
O13	O	1	0.458919	0.5128917	0.5000000	1
O14	O	1	0.541081	0.4871083	0.5000000	1
O15	O	1	0.4871083	0.458919	0.5000000	1
O16	O	1	0.5128917	0.541081	0.5000000	1
O17	O	1	0.5152714	0.4847286	0.5169735	1
O18	O	1	0.4847286	0.4847286	0.4830265	1
O19	O	1	0.5152714	0.5152714	0.4830265	1
O20	O	1	0.4847286	0.5152714	0.5169735	1
O21	O	1	0.5000000	0.5302716	0.4548042	1
O22	O	1	0.5000000	0.4697284	0.4548042	1
O23	O	1	0.4697284	0.5000000	0.5451958	1
O24	O	1	0.5302716	0.5000000	0.5451958	1
Zr1	Zr	1	0.5000000	0.475262	0.5000000	1
Zr2	Zr	1	0.475262	0.5000000	0.5000000	1
Zr3	Zr	1	0.524738	0.5000000	0.5000000	1
Zr4	Zr	1	0.5000000	0.524738	0.5000000	1

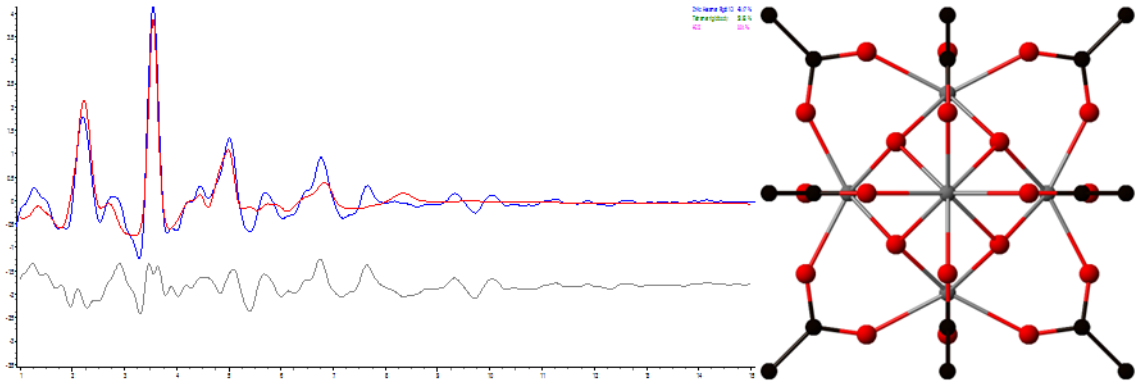

Figure 284: Observed and Calculated PDF from the fixed core refinement of ZAA7C from the 18-month data collection and the resultant model.

Table 227: The atomic coordinates of the model resulting from the fixed core refinement of ZAA7C from the 18-month data collection.

Atom Label	Atom Type	Multiplicity	Fractional X Coordinate	Fractional Y Coordinate	Fractional Z Coordinate	Fractional Occupancy
C1	C	1	0.589516	0.5000000	0.5828086	1
C2	C	1	0.5000000	0.410484	0.5828086	1
C3	C	1	0.410484	0.5000000	0.5828086	1
C4	C	1	0.5000000	0.589516	0.5828086	1
C5	C	1	0.589516	0.5000000	0.4171914	1
C6	C	1	0.5000000	0.410484	0.4171914	1
C7	C	1	0.410484	0.5000000	0.4171914	1
C8	C	1	0.5000000	0.589516	0.4171914	1
C9	C	1	0.589516	0.410484	0.5000000	1
C10	C	1	0.410484	0.410484	0.5000000	1
C11	C	1	0.410484	0.589516	0.5000000	1
C12	C	1	0.589516	0.589516	0.5000000	1
C13	C	1	0.619036	0.5000000	0.6101166	1
C14	C	1	0.5000000	0.380964	0.6101166	1
C15	C	1	0.380964	0.5000000	0.6101166	1
C16	C	1	0.5000000	0.619036	0.6101166	1
C17	C	1	0.619036	0.5000000	0.3898834	1
C18	C	1	0.5000000	0.380964	0.3898834	1
C19	C	1	0.380964	0.5000000	0.3898834	1
C20	C	1	0.5000000	0.619036	0.3898834	1
C21	C	1	0.619036	0.380964	0.5000000	1
C22	C	1	0.380964	0.380964	0.5000000	1
C23	C	1	0.380964	0.619036	0.5000000	1
C24	C	1	0.619036	0.619036	0.5000000	1
O1	O	1	0.5345479	0.5342108	0.4680408	1
O2	O	1	0.5345479	0.4657892	0.5319592	1
O3	O	1	0.4654521	0.5342108	0.4680408	1
O4	O	1	0.4654521	0.4657892	0.5319592	1
O5	O	1	0.4654521	0.4657892	0.4680408	1
O6	O	1	0.4654521	0.5342108	0.5319592	1

O7	O	1	0.5345479	0.4657892	0.4680408	1
O8	O	1	0.5345479	0.5342108	0.5319592	1
O9	O	1	0.5945656	0.5000000	0.5500313	1
O10	O	1	0.5945656	0.4459162	0.5000000	1
O11	O	1	0.5945656	0.5000000	0.4499687	1
O12	O	1	0.5945656	0.5540838	0.5000000	1
O13	O	1	0.5000000	0.5945656	0.5500313	1
O14	O	1	0.5540838	0.5945656	0.5000000	1
O15	O	1	0.5000000	0.5945656	0.4499687	1
O16	O	1	0.4459162	0.5945656	0.5000000	1
O17	O	1	0.4054344	0.5000000	0.5500313	1
O18	O	1	0.4054344	0.5540838	0.5000000	1
O19	O	1	0.4054344	0.5000000	0.4499687	1
O20	O	1	0.4054344	0.4459162	0.5000000	1
O21	O	1	0.5000000	0.4054344	0.5500313	1
O22	O	1	0.4459162	0.4054344	0.5000000	1
O23	O	1	0.5000000	0.4054344	0.4499687	1
O24	O	1	0.5540838	0.4054344	0.5000000	1
O25	O	1	0.5540838	0.5000000	0.5874797	1
O26	O	1	0.5000000	0.5540838	0.5874797	1
O27	O	1	0.4459162	0.5000000	0.5874797	1
O28	O	1	0.5000000	0.4459162	0.5874797	1
O29	O	1	0.5540838	0.5000000	0.4125203	1
O30	O	1	0.5000000	0.4459162	0.4125203	1
O31	O	1	0.4459162	0.5000000	0.4125203	1
O32	O	1	0.5000000	0.5540838	0.4125203	1
Zr1	Zr	1	0.5664023	0.5000000	0.5000000	1
Zr2	Zr	1	0.5000000	0.5664023	0.5000000	1
Zr3	Zr	1	0.4335977	0.5000000	0.5000000	1
Zr4	Zr	1	0.5000000	0.4335977	0.5000000	1
Zr5	Zr	1	0.5000000	0.5000000	0.5614268	1
Zr6	Zr	1	0.5000000	0.5000000	0.4385732	1

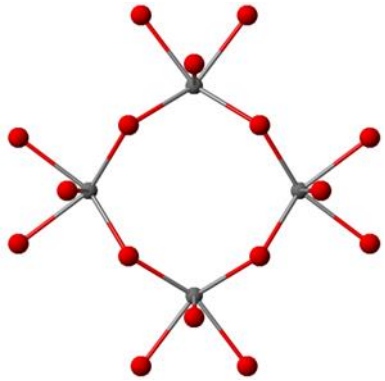

Figure 285: The tetrameric structure resulting from the fixed core refinement of ZAA7C from the 18-month data collection.

Table 228: The atomic coordinates of the tetrameric phase of the fixed core refinement of ZAA7C from the 18-month data collection.

Atom Label	Atom Type	Multiplicity	Fractional X Coordinate	Fractional Y Coordinate	Fractional Z Coordinate	Fractional Occupancy
O1	O	1	0.5153968	0.4846032	0.4837292	1
O2	O	1	0.4846032	0.4846032	0.5162708	1
O3	O	1	0.5153968	0.5153968	0.5162708	1
O4	O	1	0.4846032	0.5153968	0.4837292	1
O5	O	1	0.5000000	0.5297685	0.5456887	1
O6	O	1	0.5000000	0.4702315	0.5456887	1
O7	O	1	0.4702315	0.5000000	0.4543113	1
O8	O	1	0.5297685	0.5000000	0.4543113	1
O9	O	1	0.512521	0.4587046	0.5000000	1
O10	O	1	0.4587046	0.487479	0.5000000	1
O11	O	1	0.5412954	0.512521	0.5000000	1
O12	O	1	0.487479	0.5412954	0.5000000	1
O13	O	1	0.4587046	0.512521	0.5000000	1
O14	O	1	0.5412954	0.487479	0.5000000	1
O15	O	1	0.487479	0.4587046	0.5000000	1
O16	O	1	0.512521	0.5412954	0.5000000	1
O17	O	1	0.5153968	0.4846032	0.5162708	1
O18	O	1	0.4846032	0.4846032	0.4837292	1
O19	O	1	0.5153968	0.5153968	0.4837292	1
O20	O	1	0.4846032	0.5153968	0.5162708	1
O21	O	1	0.5000000	0.5297685	0.4543113	1
O22	O	1	0.5000000	0.4702315	0.4543113	1
O23	O	1	0.4702315	0.5000000	0.5456887	1
O24	O	1	0.5297685	0.5000000	0.5456887	1
Zr1	Zr	1	0.5000000	0.4752844	0.5000000	1
Zr2	Zr	1	0.4752844	0.5000000	0.5000000	1
Zr3	Zr	1	0.5247156	0.5000000	0.5000000	1
Zr4	Zr	1	0.5000000	0.5247156	0.5000000	1

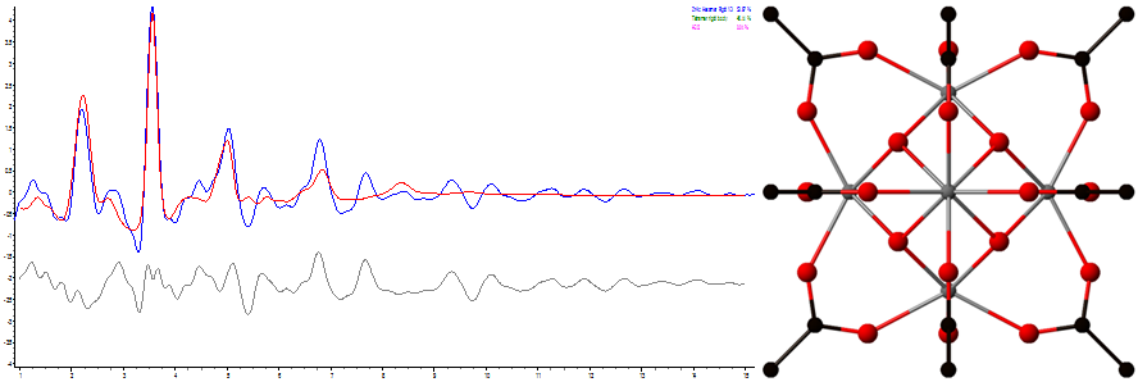

Figure 286: Observed and Calculated PDF from the fixed core refinement of ZAA7I from the 18-month data collection and the resultant model.

Table 229: The atomic coordinates of the model resulting from the fixed core refinement of ZAA7I from the 18-month data collection.

Atom Label	Atom Type	Multiplicity	Fractional X Coordinate	Fractional Y Coordinate	Fractional Z Coordinate	Fractional Occupancy
C1	C	1	0.5897379	0.5000000	0.5830138	1
C2	C	1	0.5000000	0.4102621	0.5830138	1
C3	C	1	0.4102621	0.5000000	0.5830138	1
C4	C	1	0.5000000	0.5897379	0.5830138	1
C5	C	1	0.5897379	0.5000000	0.4169862	1
C6	C	1	0.5000000	0.4102621	0.4169862	1
C7	C	1	0.4102621	0.5000000	0.4169862	1
C8	C	1	0.5000000	0.5897379	0.4169862	1
C9	C	1	0.5897379	0.4102621	0.5000000	1
C10	C	1	0.4102621	0.4102621	0.5000000	1
C11	C	1	0.4102621	0.5897379	0.5000000	1
C12	C	1	0.5897379	0.5897379	0.5000000	1
C13	C	1	0.6195557	0.5000000	0.6105974	1
C14	C	1	0.5000000	0.3804443	0.6105974	1
C15	C	1	0.3804443	0.5000000	0.6105974	1
C16	C	1	0.5000000	0.6195557	0.6105974	1
C17	C	1	0.6195557	0.5000000	0.3894026	1
C18	C	1	0.5000000	0.3804443	0.3894026	1
C19	C	1	0.3804443	0.5000000	0.3894026	1
C20	C	1	0.5000000	0.6195557	0.3894026	1
C21	C	1	0.6195557	0.3804443	0.5000000	1
C22	C	1	0.3804443	0.3804443	0.5000000	1
C23	C	1	0.3804443	0.6195557	0.5000000	1
C24	C	1	0.6195557	0.6195557	0.5000000	1
O1	O	1	0.5338835	0.5335529	0.4686554	1
O2	O	1	0.5338835	0.4664471	0.5313446	1
O3	O	1	0.4661165	0.5335529	0.4686554	1
O4	O	1	0.4661165	0.4664471	0.5313446	1
O5	O	1	0.4661165	0.4664471	0.4686554	1
O6	O	1	0.4661165	0.5335529	0.5313446	1

O7	O	1	0.5338835	0.4664471	0.4686554	1
O8	O	1	0.5338835	0.5335529	0.5313446	1
O9	O	1	0.5951266	0.5000000	0.5500802	1
O10	O	1	0.5951266	0.4458633	0.5000000	1
O11	O	1	0.5951266	0.5000000	0.4499198	1
O12	O	1	0.5951266	0.5541367	0.5000000	1
O13	O	1	0.5000000	0.5951266	0.5500802	1
O14	O	1	0.5541367	0.5951266	0.5000000	1
O15	O	1	0.5000000	0.5951266	0.4499198	1
O16	O	1	0.4458633	0.5951266	0.5000000	1
O17	O	1	0.4048734	0.5000000	0.5500802	1
O18	O	1	0.4048734	0.5541367	0.5000000	1
O19	O	1	0.4048734	0.5000000	0.4499198	1
O20	O	1	0.4048734	0.4458633	0.5000000	1
O21	O	1	0.5000000	0.4048734	0.5500802	1
O22	O	1	0.4458633	0.4048734	0.5000000	1
O23	O	1	0.5000000	0.4048734	0.4499198	1
O24	O	1	0.5541367	0.4048734	0.5000000	1
O25	O	1	0.5541367	0.5000000	0.5879987	1
O26	O	1	0.5000000	0.5541367	0.5879987	1
O27	O	1	0.4458633	0.5000000	0.5879987	1
O28	O	1	0.5000000	0.4458633	0.5879987	1
O29	O	1	0.5541367	0.5000000	0.4120013	1
O30	O	1	0.5000000	0.4458633	0.4120013	1
O31	O	1	0.4458633	0.5000000	0.4120013	1
O32	O	1	0.5000000	0.5541367	0.4120013	1
Zr1	Zr	1	0.5666375	0.5000000	0.5000000	1
Zr2	Zr	1	0.5000000	0.5666375	0.5000000	1
Zr3	Zr	1	0.4333625	0.5000000	0.5000000	1
Zr4	Zr	1	0.5000000	0.4333625	0.5000000	1
Zr5	Zr	1	0.5000000	0.5000000	0.5616443	1
Zr6	Zr	1	0.5000000	0.5000000	0.4383557	1

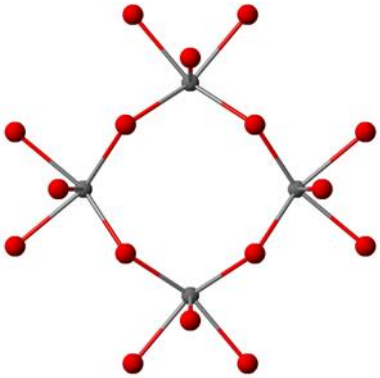

Figure 287: The tetrameric structure resulting from the fixed core refinement of ZAA7I from the 18-month data collection.

Table 230: The atomic coordinates of the tetrameric phase of the fixed core refinement of ZAA7I from the 18-month data collection.

Atom Label	Atom Type	Multiplicity	Fractional X Coordinate	Fractional Y Coordinate	Fractional Z Coordinate	Fractional Occupancy
O1	O	1	0.5150493	0.4849507	0.4820318	1
O2	O	1	0.4849507	0.4849507	0.5179682	1
O3	O	1	0.5150493	0.5150493	0.5179682	1
O4	O	1	0.4849507	0.5150493	0.4820318	1
O5	O	1	0.5000000	0.5307285	0.5447182	1
O6	O	1	0.5000000	0.4692715	0.5447182	1
O7	O	1	0.4692715	0.5000000	0.4552818	1
O8	O	1	0.5307285	0.5000000	0.4552818	1
O9	O	1	0.5133398	0.4592069	0.5000000	1
O10	O	1	0.4592069	0.4866602	0.5000000	1
O11	O	1	0.5407931	0.5133398	0.5000000	1
O12	O	1	0.4866602	0.5407931	0.5000000	1
O13	O	1	0.4592069	0.5133398	0.5000000	1
O14	O	1	0.5407931	0.4866602	0.5000000	1
O15	O	1	0.4866602	0.4592069	0.5000000	1
O16	O	1	0.5133398	0.5407931	0.5000000	1
O17	O	1	0.5150493	0.4849507	0.5179682	1
O18	O	1	0.4849507	0.4849507	0.4820318	1
O19	O	1	0.5150493	0.5150493	0.4820318	1
O20	O	1	0.4849507	0.5150493	0.5179682	1
O21	O	1	0.5000000	0.5307285	0.4552818	1
O22	O	1	0.5000000	0.4692715	0.4552818	1
O23	O	1	0.4692715	0.5000000	0.5447182	1
O24	O	1	0.5307285	0.5000000	0.5447182	1
Zr1	Zr	1	0.5000000	0.4751823	0.5000000	1
Zr2	Zr	1	0.4751823	0.5000000	0.5000000	1
Zr3	Zr	1	0.5248177	0.5000000	0.5000000	1
Zr4	Zr	1	0.5000000	0.5248177	0.5000000	1

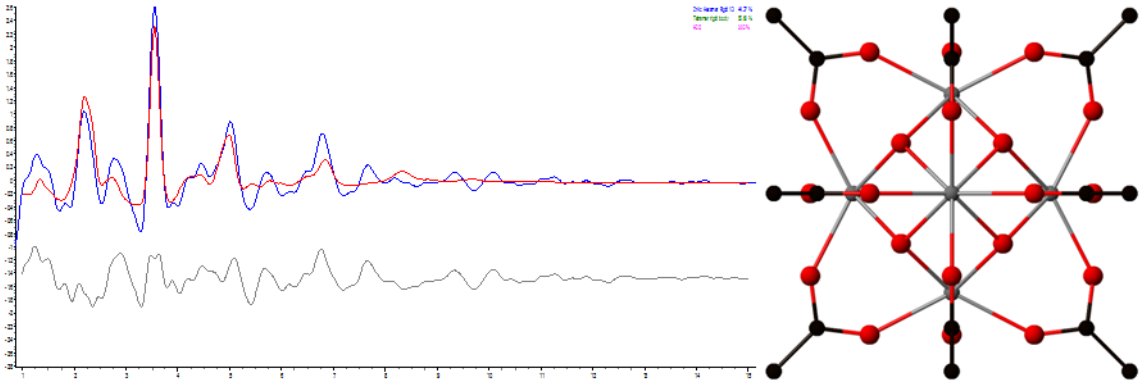

Figure 288: Observed and Calculated PDF from the fixed core refinement of ZAA10A from the 18-month data collection and the resultant model.

Table 231: The atomic coordinates of the model resulting from the fixed core refinement of ZAA10A from the 18-month data collection.

Atom Label	Atom Type	Multiplicity	Fractional X Coordinate	Fractional Y Coordinate	Fractional Z Coordinate	Fractional Occupancy
C1	C	1	0.59024	0.5000000	0.5834783	1
C2	C	1	0.5000000	0.40976	0.5834783	1
C3	C	1	0.40976	0.5000000	0.5834783	1
C4	C	1	0.5000000	0.59024	0.5834783	1
C5	C	1	0.59024	0.5000000	0.4165217	1
C6	C	1	0.5000000	0.40976	0.4165217	1
C7	C	1	0.40976	0.5000000	0.4165217	1
C8	C	1	0.5000000	0.59024	0.4165217	1
C9	C	1	0.59024	0.40976	0.5000000	1
C10	C	1	0.40976	0.40976	0.5000000	1
C11	C	1	0.40976	0.59024	0.5000000	1
C12	C	1	0.59024	0.59024	0.5000000	1
C13	C	1	0.6190312	0.5000000	0.6101121	1
C14	C	1	0.5000000	0.3809688	0.6101121	1
C15	C	1	0.3809688	0.5000000	0.6101121	1
C16	C	1	0.5000000	0.6190312	0.6101121	1
C17	C	1	0.6190312	0.5000000	0.3898879	1
C18	C	1	0.5000000	0.3809688	0.3898879	1
C19	C	1	0.3809688	0.5000000	0.3898879	1
C20	C	1	0.5000000	0.6190312	0.3898879	1
C21	C	1	0.6190312	0.3809688	0.5000000	1
C22	C	1	0.3809688	0.3809688	0.5000000	1
C23	C	1	0.3809688	0.6190312	0.5000000	1
C24	C	1	0.6190312	0.6190312	0.5000000	1
O1	O	1	0.5340764	0.5337439	0.4684769	1
O2	O	1	0.5340764	0.4662561	0.5315231	1
O3	O	1	0.4659236	0.5337439	0.4684769	1
O4	O	1	0.4659236	0.4662561	0.5315231	1
O5	O	1	0.4659236	0.4662561	0.4684769	1
O6	O	1	0.4659236	0.5337439	0.5315231	1

O7	O	1	0.5340764	0.4662561	0.4684769	1
O8	O	1	0.5340764	0.5337439	0.5315231	1
O9	O	1	0.5947361	0.5000000	0.5510065	1
O10	O	1	0.5947361	0.444862	0.5000000	1
O11	O	1	0.5947361	0.5000000	0.4489935	1
O12	O	1	0.5947361	0.555138	0.5000000	1
O13	O	1	0.5000000	0.5947361	0.5510065	1
O14	O	1	0.555138	0.5947361	0.5000000	1
O15	O	1	0.5000000	0.5947361	0.4489935	1
O16	O	1	0.444862	0.5947361	0.5000000	1
O17	O	1	0.4052639	0.5000000	0.5510065	1
O18	O	1	0.4052639	0.555138	0.5000000	1
O19	O	1	0.4052639	0.5000000	0.4489935	1
O20	O	1	0.4052639	0.444862	0.5000000	1
O21	O	1	0.5000000	0.4052639	0.5510065	1
O22	O	1	0.444862	0.4052639	0.5000000	1
O23	O	1	0.5000000	0.4052639	0.4489935	1
O24	O	1	0.555138	0.4052639	0.5000000	1
O25	O	1	0.555138	0.5000000	0.5876375	1
O26	O	1	0.5000000	0.555138	0.5876375	1
O27	O	1	0.444862	0.5000000	0.5876375	1
O28	O	1	0.5000000	0.444862	0.5876375	1
O29	O	1	0.555138	0.5000000	0.4123625	1
O30	O	1	0.5000000	0.444862	0.4123625	1
O31	O	1	0.444862	0.5000000	0.4123625	1
O32	O	1	0.5000000	0.555138	0.4123625	1
Zr1	Zr	1	0.5663343	0.5000000	0.5000000	1
Zr2	Zr	1	0.5000000	0.5663343	0.5000000	1
Zr3	Zr	1	0.4336657	0.5000000	0.5000000	1
Zr4	Zr	1	0.5000000	0.4336657	0.5000000	1
Zr5	Zr	1	0.5000000	0.5000000	0.5613639	1
Zr6	Zr	1	0.5000000	0.5000000	0.4386361	1

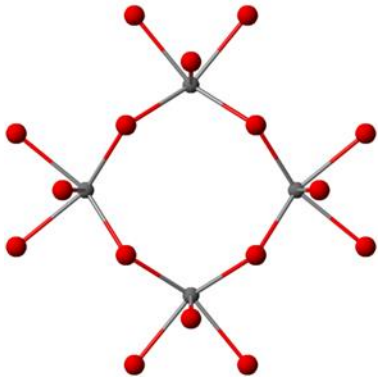

Figure 289: The tetrameric structure resulting from the fixed core refinement of ZAA10A from the 18-month data collection.

Table 232: The atomic coordinates of the tetrameric phase of the fixed core refinement of ZAA10A from the 18-month data collection.

Atom Label	Atom Type	Multiplicity	Fractional X Coordinate	Fractional Y Coordinate	Fractional Z Coordinate	Fractional Occupancy
O1	O	1	0.5152265	0.4847735	0.4829751	1
O2	O	1	0.4847735	0.4847735	0.5170249	1
O3	O	1	0.5152265	0.5152265	0.5170249	1
O4	O	1	0.4847735	0.5152265	0.4829751	1
O5	O	1	0.5000000	0.5301824	0.545695	1
O6	O	1	0.5000000	0.4698176	0.545695	1
O7	O	1	0.4698176	0.5000000	0.454305	1
O8	O	1	0.5301824	0.5000000	0.454305	1
O9	O	1	0.5132813	0.4589692	0.5000000	1
O10	O	1	0.4589692	0.4867187	0.5000000	1
O11	O	1	0.5410308	0.5132813	0.5000000	1
O12	O	1	0.4867187	0.5410308	0.5000000	1
O13	O	1	0.4589692	0.5132813	0.5000000	1
O14	O	1	0.5410308	0.4867187	0.5000000	1
O15	O	1	0.4867187	0.4589692	0.5000000	1
O16	O	1	0.5132813	0.5410308	0.5000000	1
O17	O	1	0.5152265	0.4847735	0.5170249	1
O18	O	1	0.4847735	0.4847735	0.4829751	1
O19	O	1	0.5152265	0.5152265	0.4829751	1
O20	O	1	0.4847735	0.5152265	0.5170249	1
O21	O	1	0.5000000	0.5301824	0.454305	1
O22	O	1	0.5000000	0.4698176	0.454305	1
O23	O	1	0.4698176	0.5000000	0.545695	1
O24	O	1	0.5301824	0.5000000	0.545695	1
Zr1	Zr	1	0.5000000	0.4752629	0.5000000	1
Zr2	Zr	1	0.4752629	0.5000000	0.5000000	1
Zr3	Zr	1	0.5247371	0.5000000	0.5000000	1
Zr4	Zr	1	0.5000000	0.5247371	0.5000000	1

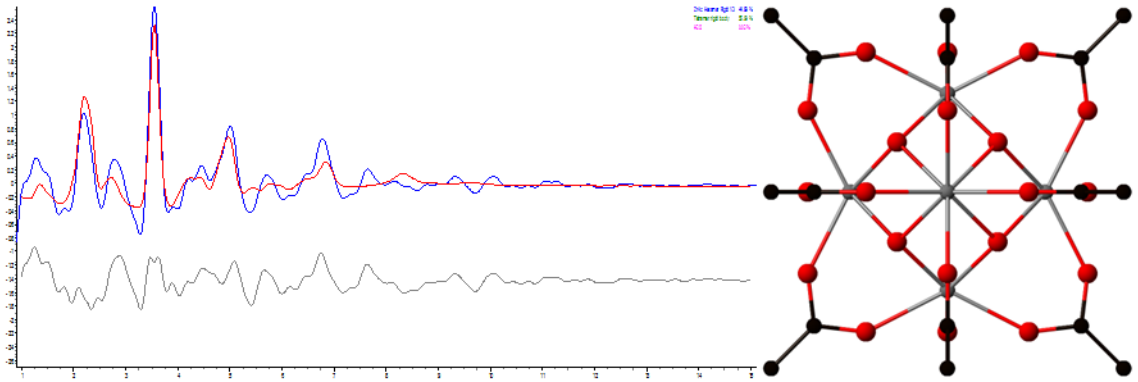

Figure 290: Observed and Calculated PDF from the fixed core refinement of ZAA10C from the 18-month data collection and the resultant model.

Table 233: The atomic coordinates of the model resulting from the fixed core refinement of ZAA10C from the 18-month data collection.

Atom Label	Atom Type	Multiplicity	Fractional X Coordinate	Fractional Y Coordinate	Fractional Z Coordinate	Fractional Occupancy
C1	C	1	0.5902177	0.5000000	0.5834577	1
C2	C	1	0.5000000	0.4097823	0.5834577	1
C3	C	1	0.4097823	0.5000000	0.5834577	1
C4	C	1	0.5000000	0.5902177	0.5834577	1
C5	C	1	0.5902177	0.5000000	0.4165423	1
C6	C	1	0.5000000	0.4097823	0.4165423	1
C7	C	1	0.4097823	0.5000000	0.4165423	1
C8	C	1	0.5000000	0.5902177	0.4165423	1
C9	C	1	0.5902177	0.4097823	0.5000000	1
C10	C	1	0.4097823	0.4097823	0.5000000	1
C11	C	1	0.4097823	0.5902177	0.5000000	1
C12	C	1	0.5902177	0.5902177	0.5000000	1
C13	C	1	0.6190884	0.5000000	0.6101651	1
C14	C	1	0.5000000	0.3809116	0.6101651	1
C15	C	1	0.3809116	0.5000000	0.6101651	1
C16	C	1	0.5000000	0.6190884	0.6101651	1
C17	C	1	0.6190884	0.5000000	0.3898349	1
C18	C	1	0.5000000	0.3809116	0.3898349	1
C19	C	1	0.3809116	0.5000000	0.3898349	1
C20	C	1	0.5000000	0.6190884	0.3898349	1
C21	C	1	0.6190884	0.3809116	0.5000000	1
C22	C	1	0.3809116	0.3809116	0.5000000	1
C23	C	1	0.3809116	0.6190884	0.5000000	1
C24	C	1	0.6190884	0.6190884	0.5000000	1
O1	O	1	0.5340877	0.5337551	0.4684665	1
O2	O	1	0.5340877	0.4662449	0.5315335	1
O3	O	1	0.4659123	0.5337551	0.4684665	1
O4	O	1	0.4659123	0.4662449	0.5315335	1
O5	O	1	0.4659123	0.4662449	0.4684665	1
O6	O	1	0.4659123	0.5337551	0.5315335	1

O7	O	1	0.5340877	0.4662449	0.4684665	1
O8	O	1	0.5340877	0.5337551	0.5315335	1
O9	O	1	0.5944615	0.5000000	0.5508591	1
O10	O	1	0.5944615	0.4450214	0.5000000	1
O11	O	1	0.5944615	0.5000000	0.4491409	1
O12	O	1	0.5944615	0.5549786	0.5000000	1
O13	O	1	0.5000000	0.5944615	0.5508591	1
O14	O	1	0.5549786	0.5944615	0.5000000	1
O15	O	1	0.5000000	0.5944615	0.4491409	1
O16	O	1	0.4450214	0.5944615	0.5000000	1
O17	O	1	0.4055385	0.5000000	0.5508591	1
O18	O	1	0.4055385	0.5549786	0.5000000	1
O19	O	1	0.4055385	0.5000000	0.4491409	1
O20	O	1	0.4055385	0.4450214	0.5000000	1
O21	O	1	0.5000000	0.4055385	0.5508591	1
O22	O	1	0.4450214	0.4055385	0.5000000	1
O23	O	1	0.5000000	0.4055385	0.4491409	1
O24	O	1	0.5549786	0.4055385	0.5000000	1
O25	O	1	0.5549786	0.5000000	0.5873835	1
O26	O	1	0.5000000	0.5549786	0.5873835	1
O27	O	1	0.4450214	0.5000000	0.5873835	1
O28	O	1	0.5000000	0.4450214	0.5873835	1
O29	O	1	0.5549786	0.5000000	0.4126165	1
O30	O	1	0.5000000	0.4450214	0.4126165	1
O31	O	1	0.4450214	0.5000000	0.4126165	1
O32	O	1	0.5000000	0.5549786	0.4126165	1
Zr1	Zr	1	0.5662624	0.5000000	0.5000000	1
Zr2	Zr	1	0.5000000	0.5662624	0.5000000	1
Zr3	Zr	1	0.4337376	0.5000000	0.5000000	1
Zr4	Zr	1	0.5000000	0.4337376	0.5000000	1
Zr5	Zr	1	0.5000000	0.5000000	0.5612973	1
Zr6	Zr	1	0.5000000	0.5000000	0.4387027	1

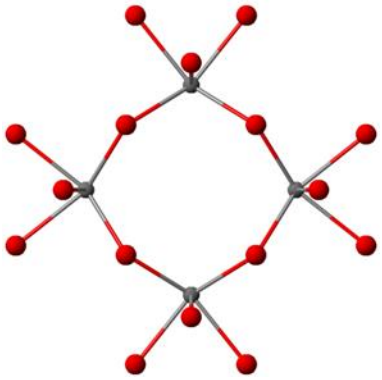

Figure 291: The tetrameric structure resulting from the fixed core refinement of ZAA10C from the 18-month data collection.

Table 234: The atomic coordinates of the tetrameric phase of the fixed core refinement of ZAA10C from the 18-month data collection.

Atom Label	Atom Type	Multiplicity	Fractional X Coordinate	Fractional Y Coordinate	Fractional Z Coordinate	Fractional Occupancy
O1	O	1	0.5152813	0.4847187	0.4824937	1
O2	O	1	0.4847187	0.4847187	0.5175063	1
O3	O	1	0.5152813	0.5152813	0.5175063	1
O4	O	1	0.4847187	0.5152813	0.4824937	1
O5	O	1	0.5000000	0.5300149	0.545337	1
O6	O	1	0.5000000	0.4699851	0.545337	1
O7	O	1	0.4699851	0.5000000	0.454663	1
O8	O	1	0.5300149	0.5000000	0.454663	1
O9	O	1	0.5130757	0.4588508	0.5000000	1
O10	O	1	0.4588508	0.4869243	0.5000000	1
O11	O	1	0.5411492	0.5130757	0.5000000	1
O12	O	1	0.4869243	0.5411492	0.5000000	1
O13	O	1	0.4588508	0.5130757	0.5000000	1
O14	O	1	0.5411492	0.4869243	0.5000000	1
O15	O	1	0.4869243	0.4588508	0.5000000	1
O16	O	1	0.5130757	0.5411492	0.5000000	1
O17	O	1	0.5152813	0.4847187	0.5175063	1
O18	O	1	0.4847187	0.4847187	0.4824937	1
O19	O	1	0.5152813	0.5152813	0.4824937	1
O20	O	1	0.4847187	0.5152813	0.5175063	1
O21	O	1	0.5000000	0.5300149	0.454663	1
O22	O	1	0.5000000	0.4699851	0.454663	1
O23	O	1	0.4699851	0.5000000	0.545337	1
O24	O	1	0.5300149	0.5000000	0.545337	1
Zr1	Zr	1	0.5000000	0.4753075	0.5000000	1
Zr2	Zr	1	0.4753075	0.5000000	0.5000000	1
Zr3	Zr	1	0.5246925	0.5000000	0.5000000	1
Zr4	Zr	1	0.5000000	0.5246925	0.5000000	1

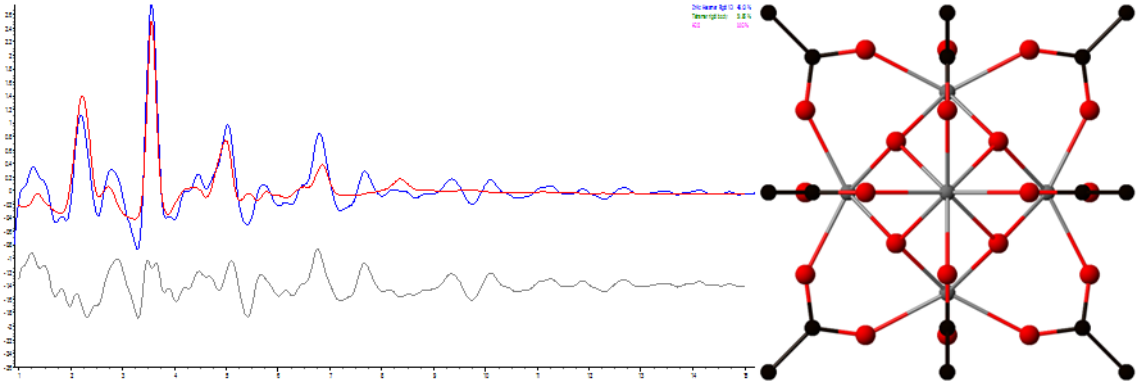

Figure 292: Observed and Calculated PDF from the fixed core refinement of ZAA10I from the 18-month data collection and the resultant model.

Table 235: The atomic coordinates of the model resulting from the fixed core refinement of ZAA10I from the 18-month data collection.

Atom Label	Atom Type	Multiplicity	Fractional X Coordinate	Fractional Y Coordinate	Fractional Z Coordinate	Fractional Occupancy
C1	C	1	0.5901303	0.5000000	0.5833768	1
C2	C	1	0.5000000	0.4098697	0.5833768	1
C3	C	1	0.4098697	0.5000000	0.5833768	1
C4	C	1	0.5000000	0.5901303	0.5833768	1
C5	C	1	0.5901303	0.5000000	0.4166232	1
C6	C	1	0.5000000	0.4098697	0.4166232	1
C7	C	1	0.4098697	0.5000000	0.4166232	1
C8	C	1	0.5000000	0.5901303	0.4166232	1
C9	C	1	0.5901303	0.4098697	0.5000000	1
C10	C	1	0.4098697	0.4098697	0.5000000	1
C11	C	1	0.4098697	0.5901303	0.5000000	1
C12	C	1	0.5901303	0.5901303	0.5000000	1
C13	C	1	0.6195045	0.5000000	0.61055	1
C14	C	1	0.5000000	0.3804955	0.61055	1
C15	C	1	0.3804955	0.5000000	0.61055	1
C16	C	1	0.5000000	0.6195045	0.61055	1
C17	C	1	0.6195045	0.5000000	0.38945	1
C18	C	1	0.5000000	0.3804955	0.38945	1
C19	C	1	0.3804955	0.5000000	0.38945	1
C20	C	1	0.5000000	0.6195045	0.38945	1
C21	C	1	0.6195045	0.3804955	0.5000000	1
C22	C	1	0.3804955	0.3804955	0.5000000	1
C23	C	1	0.3804955	0.6195045	0.5000000	1
C24	C	1	0.6195045	0.6195045	0.5000000	1
O1	O	1	0.5341587	0.5338254	0.4684008	1
O2	O	1	0.5341587	0.4661746	0.5315992	1
O3	O	1	0.4658413	0.5338254	0.4684008	1
O4	O	1	0.4658413	0.4661746	0.5315992	1
O5	O	1	0.4658413	0.4661746	0.4684008	1
O6	O	1	0.4658413	0.5338254	0.5315992	1

O7	O	1	0.5341587	0.4661746	0.4684008	1
O8	O	1	0.5341587	0.5338254	0.5315992	1
O9	O	1	0.5949297	0.5000000	0.5506211	1
O10	O	1	0.5949297	0.4452786	0.5000000	1
O11	O	1	0.5949297	0.5000000	0.4493789	1
O12	O	1	0.5949297	0.5547214	0.5000000	1
O13	O	1	0.5000000	0.5949297	0.5506211	1
O14	O	1	0.5547214	0.5949297	0.5000000	1
O15	O	1	0.5000000	0.5949297	0.4493789	1
O16	O	1	0.4452786	0.5949297	0.5000000	1
O17	O	1	0.4050703	0.5000000	0.5506211	1
O18	O	1	0.4050703	0.5547214	0.5000000	1
O19	O	1	0.4050703	0.5000000	0.4493789	1
O20	O	1	0.4050703	0.4452786	0.5000000	1
O21	O	1	0.5000000	0.4050703	0.5506211	1
O22	O	1	0.4452786	0.4050703	0.5000000	1
O23	O	1	0.5000000	0.4050703	0.4493789	1
O24	O	1	0.5547214	0.4050703	0.5000000	1
O25	O	1	0.5547214	0.5000000	0.5878166	1
O26	O	1	0.5000000	0.5547214	0.5878166	1
O27	O	1	0.4452786	0.5000000	0.5878166	1
O28	O	1	0.5000000	0.4452786	0.5878166	1
O29	O	1	0.5547214	0.5000000	0.4121834	1
O30	O	1	0.5000000	0.4452786	0.4121834	1
O31	O	1	0.4452786	0.5000000	0.4121834	1
O32	O	1	0.5000000	0.5547214	0.4121834	1
Zr1	Zr	1	0.5665762	0.5000000	0.5000000	1
Zr2	Zr	1	0.5000000	0.5665762	0.5000000	1
Zr3	Zr	1	0.4334238	0.5000000	0.5000000	1
Zr4	Zr	1	0.5000000	0.4334238	0.5000000	1
Zr5	Zr	1	0.5000000	0.5000000	0.5615876	1
Zr6	Zr	1	0.5000000	0.5000000	0.4384124	1

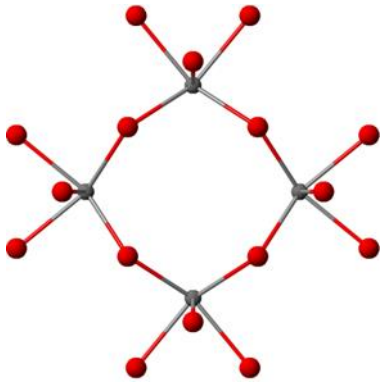

Figure 293: The tetrameric structure resulting from the fixed core refinement of ZAA10I from the 18-month data collection.

Table 236: The atomic coordinates of the tetrameric phase of the fixed core refinement of ZAA10I from the 18-month data collection.

Atom Label	Atom Type	Multiplicity	Fractional X Coordinate	Fractional Y Coordinate	Fractional Z Coordinate	Fractional Occupancy
O1	O	1	0.5150899	0.4849101	0.4813862	1
O2	O	1	0.4849101	0.4849101	0.5186138	1
O3	O	1	0.5150899	0.5150899	0.5186138	1
O4	O	1	0.4849101	0.5150899	0.4813862	1
O5	O	1	0.5000000	0.5303672	0.5451693	1
O6	O	1	0.5000000	0.4696328	0.5451693	1
O7	O	1	0.4696328	0.5000000	0.4548307	1
O8	O	1	0.5303672	0.5000000	0.4548307	1
O9	O	1	0.5132304	0.4590515	0.5000000	1
O10	O	1	0.4590515	0.4867696	0.5000000	1
O11	O	1	0.5409485	0.5132304	0.5000000	1
O12	O	1	0.4867696	0.5409485	0.5000000	1
O13	O	1	0.4590515	0.5132304	0.5000000	1
O14	O	1	0.5409485	0.4867696	0.5000000	1
O15	O	1	0.4867696	0.4590515	0.5000000	1
O16	O	1	0.5132304	0.5409485	0.5000000	1
O17	O	1	0.5150899	0.4849101	0.5186138	1
O18	O	1	0.4849101	0.4849101	0.4813862	1
O19	O	1	0.5150899	0.5150899	0.4813862	1
O20	O	1	0.4849101	0.5150899	0.5186138	1
O21	O	1	0.5000000	0.5303672	0.4548307	1
O22	O	1	0.5000000	0.4696328	0.4548307	1
O23	O	1	0.4696328	0.5000000	0.5451693	1
O24	O	1	0.5303672	0.5000000	0.5451693	1
Zr1	Zr	1	0.5000000	0.475177	0.5000000	1
Zr2	Zr	1	0.475177	0.5000000	0.5000000	1
Zr3	Zr	1	0.524823	0.5000000	0.5000000	1
Zr4	Zr	1	0.5000000	0.524823	0.5000000	1

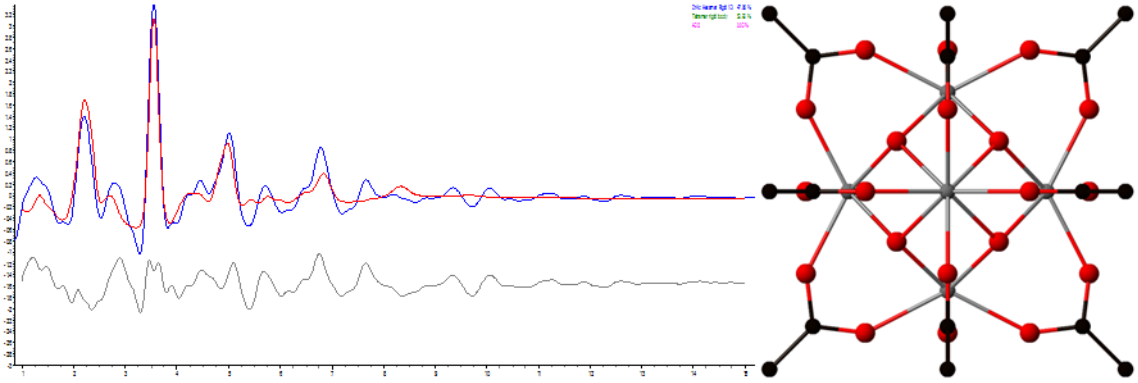

Figure 294: Observed and Calculated PDF from the fixed core refinement of ZAA13A from the 18-month data collection and the resultant model.

Table 237: The atomic coordinates of the model resulting from the fixed core refinement of ZAA13A from the 18-month data collection.

Atom Label	Atom Type	Multiplicity	Fractional X Coordinate	Fractional Y Coordinate	Fractional Z Coordinate	Fractional Occupancy
C1	C	1	0.5902574	0.5000000	0.5834944	1
C2	C	1	0.5000000	0.4097426	0.5834944	1
C3	C	1	0.4097426	0.5000000	0.5834944	1
C4	C	1	0.5000000	0.5902574	0.5834944	1
C5	C	1	0.5902574	0.5000000	0.4165056	1
C6	C	1	0.5000000	0.4097426	0.4165056	1
C7	C	1	0.4097426	0.5000000	0.4165056	1
C8	C	1	0.5000000	0.5902574	0.4165056	1
C9	C	1	0.5902574	0.4097426	0.5000000	1
C10	C	1	0.4097426	0.4097426	0.5000000	1
C11	C	1	0.4097426	0.5902574	0.5000000	1
C12	C	1	0.5902574	0.5902574	0.5000000	1
C13	C	1	0.6191309	0.5000000	0.6102044	1
C14	C	1	0.5000000	0.3808691	0.6102044	1
C15	C	1	0.3808691	0.5000000	0.6102044	1
C16	C	1	0.5000000	0.6191309	0.6102044	1
C17	C	1	0.6191309	0.5000000	0.3897956	1
C18	C	1	0.5000000	0.3808691	0.3897956	1
C19	C	1	0.3808691	0.5000000	0.3897956	1
C20	C	1	0.5000000	0.6191309	0.3897956	1
C21	C	1	0.6191309	0.3808691	0.5000000	1
C22	C	1	0.3808691	0.3808691	0.5000000	1
C23	C	1	0.3808691	0.6191309	0.5000000	1
C24	C	1	0.6191309	0.6191309	0.5000000	1
O1	O	1	0.5341047	0.533772	0.4684507	1
O2	O	1	0.5341047	0.466228	0.5315493	1
O3	O	1	0.4658953	0.533772	0.4684507	1
O4	O	1	0.4658953	0.466228	0.5315493	1
O5	O	1	0.4658953	0.466228	0.4684507	1
O6	O	1	0.4658953	0.533772	0.5315493	1

O7	O	1	0.5341047	0.466228	0.4684507	1
O8	O	1	0.5341047	0.533772	0.5315493	1
O9	O	1	0.5946637	0.5000000	0.5508423	1
O10	O	1	0.5946637	0.4450395	0.5000000	1
O11	O	1	0.5946637	0.5000000	0.4491577	1
O12	O	1	0.5946637	0.5549605	0.5000000	1
O13	O	1	0.5000000	0.5946637	0.5508423	1
O14	O	1	0.5549605	0.5946637	0.5000000	1
O15	O	1	0.5000000	0.5946637	0.4491577	1
O16	O	1	0.4450395	0.5946637	0.5000000	1
O17	O	1	0.4053363	0.5000000	0.5508423	1
O18	O	1	0.4053363	0.5549605	0.5000000	1
O19	O	1	0.4053363	0.5000000	0.4491577	1
O20	O	1	0.4053363	0.4450395	0.5000000	1
O21	O	1	0.5000000	0.4053363	0.5508423	1
O22	O	1	0.4450395	0.4053363	0.5000000	1
O23	O	1	0.5000000	0.4053363	0.4491577	1
O24	O	1	0.5549605	0.4053363	0.5000000	1
O25	O	1	0.5549605	0.5000000	0.5875705	1
O26	O	1	0.5000000	0.5549605	0.5875705	1
O27	O	1	0.4450395	0.5000000	0.5875705	1
O28	O	1	0.5000000	0.4450395	0.5875705	1
O29	O	1	0.5549605	0.5000000	0.4124295	1
O30	O	1	0.5000000	0.4450395	0.4124295	1
O31	O	1	0.4450395	0.5000000	0.4124295	1
O32	O	1	0.5000000	0.5549605	0.4124295	1
Zr1	Zr	1	0.5663323	0.5000000	0.5000000	1
Zr2	Zr	1	0.5000000	0.5663323	0.5000000	1
Zr3	Zr	1	0.4336677	0.5000000	0.5000000	1
Zr4	Zr	1	0.5000000	0.4336677	0.5000000	1
Zr5	Zr	1	0.5000000	0.5000000	0.561362	1
Zr6	Zr	1	0.5000000	0.5000000	0.438638	1

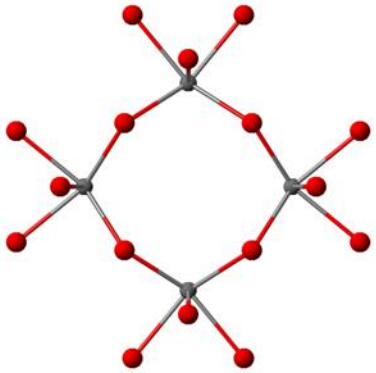

Figure 295: The tetrameric structure resulting from the fixed core refinement of ZAA13A from the 18-month data collection.

Table 238: The atomic coordinates of the tetrameric phase of the fixed core refinement of ZAA13A from the 18-month data collection.

Atom Label	Atom Type	Multiplicity	Fractional X Coordinate	Fractional Y Coordinate	Fractional Z Coordinate	Fractional Occupancy
O1	O	1	0.5151531	0.4848469	0.4825343	1
O2	O	1	0.4848469	0.4848469	0.5174657	1
O3	O	1	0.5151531	0.5151531	0.5174657	1
O4	O	1	0.4848469	0.5151531	0.4825343	1
O5	O	1	0.5000000	0.5304141	0.5453134	1
O6	O	1	0.5000000	0.4695859	0.5453134	1
O7	O	1	0.4695859	0.5000000	0.4546866	1
O8	O	1	0.5304141	0.5000000	0.4546866	1
O9	O	1	0.5132118	0.4590908	0.5000000	1
O10	O	1	0.4590908	0.4867882	0.5000000	1
O11	O	1	0.5409092	0.5132118	0.5000000	1
O12	O	1	0.4867882	0.5409092	0.5000000	1
O13	O	1	0.4590908	0.5132118	0.5000000	1
O14	O	1	0.5409092	0.4867882	0.5000000	1
O15	O	1	0.4867882	0.4590908	0.5000000	1
O16	O	1	0.5132118	0.5409092	0.5000000	1
O17	O	1	0.5151531	0.4848469	0.5174657	1
O18	O	1	0.4848469	0.4848469	0.4825343	1
O19	O	1	0.5151531	0.5151531	0.4825343	1
O20	O	1	0.4848469	0.5151531	0.5174657	1
O21	O	1	0.5000000	0.5304141	0.4546866	1
O22	O	1	0.5000000	0.4695859	0.4546866	1
O23	O	1	0.4695859	0.5000000	0.5453134	1
O24	O	1	0.5304141	0.5000000	0.5453134	1
Zr1	Zr	1	0.5000000	0.4752378	0.5000000	1
Zr2	Zr	1	0.4752378	0.5000000	0.5000000	1
Zr3	Zr	1	0.5247622	0.5000000	0.5000000	1
Zr4	Zr	1	0.5000000	0.5247622	0.5000000	1

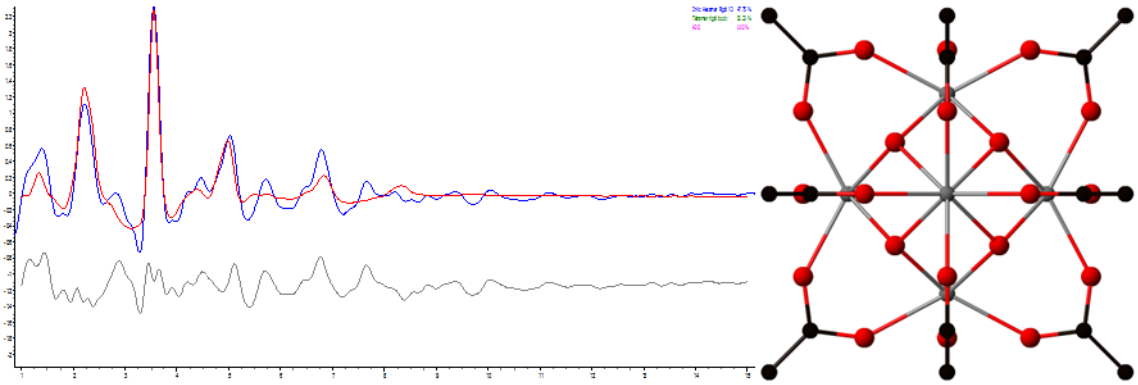

Figure 296: Observed and Calculated PDF from the fixed core refinement of ZAA13C from the 18-month data collection and the resultant model.

Table 239: The atomic coordinates of the model resulting from the fixed core refinement of ZAA13C from the 18-month data collection.

Atom Label	Atom Type	Multiplicity	Fractional X Coordinate	Fractional Y Coordinate	Fractional Z Coordinate	Fractional Occupancy
C1	C	1	0.590902	0.5000000	0.5840907	1
C2	C	1	0.5000000	0.409098	0.5840907	1
C3	C	1	0.409098	0.5000000	0.5840907	1
C4	C	1	0.5000000	0.590902	0.5840907	1
C5	C	1	0.590902	0.5000000	0.4159093	1
C6	C	1	0.5000000	0.409098	0.4159093	1
C7	C	1	0.409098	0.5000000	0.4159093	1
C8	C	1	0.5000000	0.590902	0.4159093	1
C9	C	1	0.590902	0.409098	0.5000000	1
C10	C	1	0.409098	0.409098	0.5000000	1
C11	C	1	0.409098	0.590902	0.5000000	1
C12	C	1	0.590902	0.590902	0.5000000	1
C13	C	1	0.6183472	0.5000000	0.6094794	1
C14	C	1	0.5000000	0.3816528	0.6094794	1
C15	C	1	0.3816528	0.5000000	0.6094794	1
C16	C	1	0.5000000	0.6183472	0.6094794	1
C17	C	1	0.6183472	0.5000000	0.3905206	1
C18	C	1	0.5000000	0.3816528	0.3905206	1
C19	C	1	0.3816528	0.5000000	0.3905206	1
C20	C	1	0.5000000	0.6183472	0.3905206	1
C21	C	1	0.6183472	0.3816528	0.5000000	1
C22	C	1	0.3816528	0.3816528	0.5000000	1
C23	C	1	0.3816528	0.6183472	0.5000000	1
C24	C	1	0.6183472	0.6183472	0.5000000	1
O1	O	1	0.5345694	0.5342321	0.4680209	1
O2	O	1	0.5345694	0.4657679	0.5319791	1
O3	O	1	0.4654306	0.5342321	0.4680209	1
O4	O	1	0.4654306	0.4657679	0.5319791	1
O5	O	1	0.4654306	0.4657679	0.4680209	1
O6	O	1	0.4654306	0.5342321	0.5319791	1

O7	O	1	0.5345694	0.4657679	0.4680209	1
O8	O	1	0.5345694	0.5342321	0.5319791	1
O9	O	1	0.5955838	0.5000000	0.5509633	1
O10	O	1	0.5955838	0.4449087	0.5000000	1
O11	O	1	0.5955838	0.5000000	0.4490367	1
O12	O	1	0.5955838	0.5550913	0.5000000	1
O13	O	1	0.5000000	0.5955838	0.5509633	1
O14	O	1	0.5550913	0.5955838	0.5000000	1
O15	O	1	0.5000000	0.5955838	0.4490367	1
O16	O	1	0.4449087	0.5955838	0.5000000	1
O17	O	1	0.4044162	0.5000000	0.5509633	1
O18	O	1	0.4044162	0.5550913	0.5000000	1
O19	O	1	0.4044162	0.5000000	0.4490367	1
O20	O	1	0.4044162	0.4449087	0.5000000	1
O21	O	1	0.5000000	0.4044162	0.5509633	1
O22	O	1	0.4449087	0.4044162	0.5000000	1
O23	O	1	0.5000000	0.4044162	0.4490367	1
O24	O	1	0.5550913	0.4044162	0.5000000	1
O25	O	1	0.5550913	0.5000000	0.5884217	1
O26	O	1	0.5000000	0.5550913	0.5884217	1
O27	O	1	0.4449087	0.5000000	0.5884217	1
O28	O	1	0.5000000	0.4449087	0.5884217	1
O29	O	1	0.5550913	0.5000000	0.4115783	1
O30	O	1	0.5000000	0.4449087	0.4115783	1
O31	O	1	0.4449087	0.5000000	0.4115783	1
O32	O	1	0.5000000	0.5550913	0.4115783	1
Zr1	Zr	1	0.5662772	0.5000000	0.5000000	1
Zr2	Zr	1	0.5000000	0.5662772	0.5000000	1
Zr3	Zr	1	0.4337228	0.5000000	0.5000000	1
Zr4	Zr	1	0.5000000	0.4337228	0.5000000	1
Zr5	Zr	1	0.5000000	0.5000000	0.5613111	1
Zr6	Zr	1	0.5000000	0.5000000	0.4386889	1

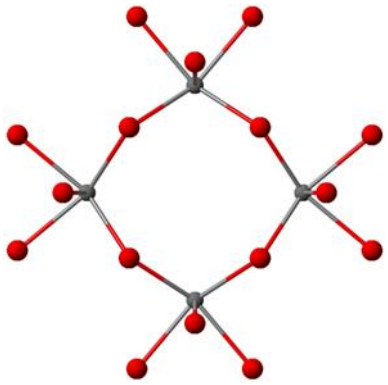

Figure 297: The tetrameric structure resulting from the fixed core refinement of ZAA13C from the 18-month data collection.

Table 240: The atomic coordinates of the tetrameric phase of the fixed core refinement of ZAA13C from the 18-month data collection.

Atom Label	Atom Type	Multiplicity	Fractional X Coordinate	Fractional Y Coordinate	Fractional Z Coordinate	Fractional Occupancy
O1	O	1	0.5150979	0.4849021	0.4825698	1
O2	O	1	0.4849021	0.4849021	0.5174302	1
O3	O	1	0.5150979	0.5150979	0.5174302	1
O4	O	1	0.4849021	0.5150979	0.4825698	1
O5	O	1	0.5000000	0.5303546	0.5458573	1
O6	O	1	0.5000000	0.4696454	0.5458573	1
O7	O	1	0.4696454	0.5000000	0.4541427	1
O8	O	1	0.5303546	0.5000000	0.4541427	1
O9	O	1	0.5133566	0.459162	0.5000000	1
O10	O	1	0.459162	0.4866434	0.5000000	1
O11	O	1	0.540838	0.5133566	0.5000000	1
O12	O	1	0.4866434	0.540838	0.5000000	1
O13	O	1	0.459162	0.5133566	0.5000000	1
O14	O	1	0.540838	0.4866434	0.5000000	1
O15	O	1	0.4866434	0.459162	0.5000000	1
O16	O	1	0.5133566	0.540838	0.5000000	1
O17	O	1	0.5150979	0.4849021	0.5174302	1
O18	O	1	0.4849021	0.4849021	0.4825698	1
O19	O	1	0.5150979	0.5150979	0.4825698	1
O20	O	1	0.4849021	0.5150979	0.5174302	1
O21	O	1	0.5000000	0.5303546	0.4541427	1
O22	O	1	0.5000000	0.4696454	0.4541427	1
O23	O	1	0.4696454	0.5000000	0.5458573	1
O24	O	1	0.5303546	0.5000000	0.5458573	1
Zr1	Zr	1	0.5000000	0.4751275	0.5000000	1
Zr2	Zr	1	0.4751275	0.5000000	0.5000000	1
Zr3	Zr	1	0.5248725	0.5000000	0.5000000	1
Zr4	Zr	1	0.5000000	0.5248725	0.5000000	1

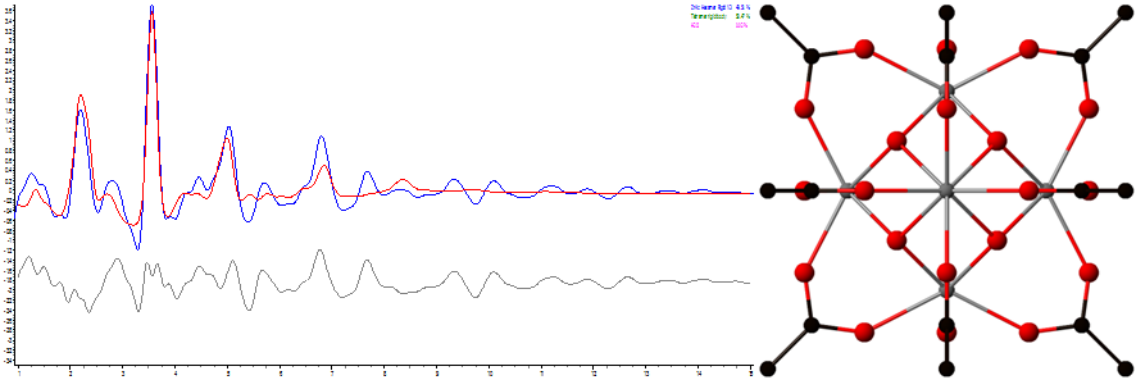

Figure 298: Observed and Calculated PDF from the fixed core refinement of ZAA13I from the 18-month data collection and the resultant model.

Table 241: The atomic coordinates of the model resulting from the fixed core refinement of ZAA13I from the 18-month data collection.

Atom Label	Atom Type	Multiplicity	Fractional X Coordinate	Fractional Y Coordinate	Fractional Z Coordinate	Fractional Occupancy
C1	C	1	0.5901578	0.5000000	0.5834022	1
C2	C	1	0.5000000	0.4098422	0.5834022	1
C3	C	1	0.4098422	0.5000000	0.5834022	1
C4	C	1	0.5000000	0.5901578	0.5834022	1
C5	C	1	0.5901578	0.5000000	0.4165978	1
C6	C	1	0.5000000	0.4098422	0.4165978	1
C7	C	1	0.4098422	0.5000000	0.4165978	1
C8	C	1	0.5000000	0.5901578	0.4165978	1
C9	C	1	0.5901578	0.4098422	0.5000000	1
C10	C	1	0.4098422	0.4098422	0.5000000	1
C11	C	1	0.4098422	0.5901578	0.5000000	1
C12	C	1	0.5901578	0.5901578	0.5000000	1
C13	C	1	0.6194994	0.5000000	0.6105453	1
C14	C	1	0.5000000	0.3805006	0.6105453	1
C15	C	1	0.3805006	0.5000000	0.6105453	1
C16	C	1	0.5000000	0.6194994	0.6105453	1
C17	C	1	0.6194994	0.5000000	0.3894547	1
C18	C	1	0.5000000	0.3805006	0.3894547	1
C19	C	1	0.3805006	0.5000000	0.3894547	1
C20	C	1	0.5000000	0.6194994	0.3894547	1
C21	C	1	0.6194994	0.3805006	0.5000000	1
C22	C	1	0.3805006	0.3805006	0.5000000	1
C23	C	1	0.3805006	0.6194994	0.5000000	1
C24	C	1	0.6194994	0.6194994	0.5000000	1
O1	O	1	0.5335245	0.5331974	0.4689875	1
O2	O	1	0.5335245	0.4668026	0.5310125	1
O3	O	1	0.4664755	0.5331974	0.4689875	1
O4	O	1	0.4664755	0.4668026	0.5310125	1
O5	O	1	0.4664755	0.4668026	0.4689875	1
O6	O	1	0.4664755	0.5331974	0.5310125	1

O7	O	1	0.5335245	0.4668026	0.4689875	1
O8	O	1	0.5335245	0.5331974	0.5310125	1
O9	O	1	0.5949966	0.5000000	0.5508303	1
O10	O	1	0.5949966	0.4450524	0.5000000	1
O11	O	1	0.5949966	0.5000000	0.4491697	1
O12	O	1	0.5949966	0.5549476	0.5000000	1
O13	O	1	0.5000000	0.5949966	0.5508303	1
O14	O	1	0.5549476	0.5949966	0.5000000	1
O15	O	1	0.5000000	0.5949966	0.4491697	1
O16	O	1	0.4450524	0.5949966	0.5000000	1
O17	O	1	0.4050034	0.5000000	0.5508303	1
O18	O	1	0.4050034	0.5549476	0.5000000	1
O19	O	1	0.4050034	0.5000000	0.4491697	1
O20	O	1	0.4050034	0.4450524	0.5000000	1
O21	O	1	0.5000000	0.4050034	0.5508303	1
O22	O	1	0.4450524	0.4050034	0.5000000	1
O23	O	1	0.5000000	0.4050034	0.4491697	1
O24	O	1	0.5549476	0.4050034	0.5000000	1
O25	O	1	0.5549476	0.5000000	0.5878785	1
O26	O	1	0.5000000	0.5549476	0.5878785	1
O27	O	1	0.4450524	0.5000000	0.5878785	1
O28	O	1	0.5000000	0.4450524	0.5878785	1
O29	O	1	0.5549476	0.5000000	0.4121215	1
O30	O	1	0.5000000	0.4450524	0.4121215	1
O31	O	1	0.4450524	0.5000000	0.4121215	1
O32	O	1	0.5000000	0.5549476	0.4121215	1
Zr1	Zr	1	0.5665623	0.5000000	0.5000000	1
Zr2	Zr	1	0.5000000	0.5665623	0.5000000	1
Zr3	Zr	1	0.4334377	0.5000000	0.5000000	1
Zr4	Zr	1	0.5000000	0.4334377	0.5000000	1
Zr5	Zr	1	0.5000000	0.5000000	0.5615748	1
Zr6	Zr	1	0.5000000	0.5000000	0.4384252	1

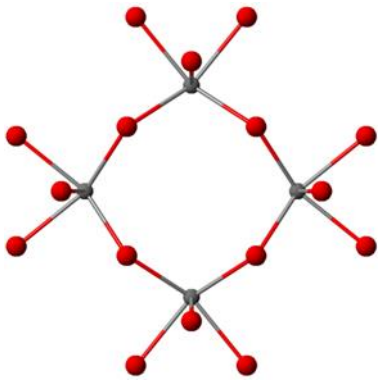

Figure 299: The tetrameric structure resulting from the fixed core refinement of ZAA13I from the 18-month data collection.

Table 242: The atomic coordinates of the tetrameric phase of the fixed core refinement of ZAA13I from the 18-month data collection.

Atom Label	Atom Type	Multiplicity	Fractional X Coordinate	Fractional Y Coordinate	Fractional Z Coordinate	Fractional Occupancy
O1	O	1	0.5151243	0.4848757	0.4835586	1
O2	O	1	0.4848757	0.4848757	0.5164414	1
O3	O	1	0.5151243	0.5151243	0.5164414	1
O4	O	1	0.4848757	0.5151243	0.4835586	1
O5	O	1	0.5000000	0.5304796	0.5454831	1
O6	O	1	0.5000000	0.4695204	0.5454831	1
O7	O	1	0.4695204	0.5000000	0.4545169	1
O8	O	1	0.5304796	0.5000000	0.4545169	1
O9	O	1	0.5129901	0.4590595	0.5000000	1
O10	O	1	0.4590595	0.4870099	0.5000000	1
O11	O	1	0.5409405	0.5129901	0.5000000	1
O12	O	1	0.4870099	0.5409405	0.5000000	1
O13	O	1	0.4590595	0.5129901	0.5000000	1
O14	O	1	0.5409405	0.4870099	0.5000000	1
O15	O	1	0.4870099	0.4590595	0.5000000	1
O16	O	1	0.5129901	0.5409405	0.5000000	1
O17	O	1	0.5151243	0.4848757	0.5164414	1
O18	O	1	0.4848757	0.4848757	0.4835586	1
O19	O	1	0.5151243	0.5151243	0.4835586	1
O20	O	1	0.4848757	0.5151243	0.5164414	1
O21	O	1	0.5000000	0.5304796	0.4545169	1
O22	O	1	0.5000000	0.4695204	0.4545169	1
O23	O	1	0.4695204	0.5000000	0.5454831	1
O24	O	1	0.5304796	0.5000000	0.5454831	1
Zr1	Zr	1	0.5000000	0.4751164	0.5000000	1
Zr2	Zr	1	0.4751164	0.5000000	0.5000000	1
Zr3	Zr	1	0.5248836	0.5000000	0.5000000	1
Zr4	Zr	1	0.5000000	0.5248836	0.5000000	1

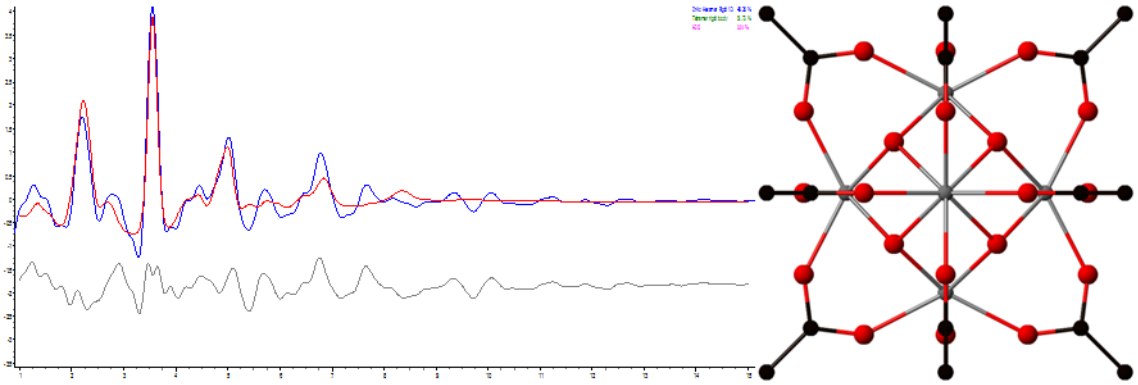

Figure 300: Observed and Calculated PDF from the fixed core refinement of ZAA16A from the 18-month data collection and the resultant model.

Table 243: The atomic coordinates of the model resulting from the fixed core refinement of ZAA16A from the 18-month data collection.

Atom Label	Atom Type	Multiplicity	Fractional X Coordinate	Fractional Y Coordinate	Fractional Z Coordinate	Fractional Occupancy
C1	C	1	0.5899682	0.5000000	0.5832269	1
C2	C	1	0.5000000	0.4100318	0.5832269	1
C3	C	1	0.4100318	0.5000000	0.5832269	1
C4	C	1	0.5000000	0.5899682	0.5832269	1
C5	C	1	0.5899682	0.5000000	0.4167731	1
C6	C	1	0.5000000	0.4100318	0.4167731	1
C7	C	1	0.4100318	0.5000000	0.4167731	1
C8	C	1	0.5000000	0.5899682	0.4167731	1
C9	C	1	0.5899682	0.4100318	0.5000000	1
C10	C	1	0.4100318	0.4100318	0.5000000	1
C11	C	1	0.4100318	0.5899682	0.5000000	1
C12	C	1	0.5899682	0.5899682	0.5000000	1
C13	C	1	0.6193119	0.5000000	0.6103718	1
C14	C	1	0.5000000	0.3806881	0.6103718	1
C15	C	1	0.3806881	0.5000000	0.6103718	1
C16	C	1	0.5000000	0.6193119	0.6103718	1
C17	C	1	0.6193119	0.5000000	0.3896282	1
C18	C	1	0.5000000	0.3806881	0.3896282	1
C19	C	1	0.3806881	0.5000000	0.3896282	1
C20	C	1	0.5000000	0.6193119	0.3896282	1
C21	C	1	0.6193119	0.3806881	0.5000000	1
C22	C	1	0.3806881	0.3806881	0.5000000	1
C23	C	1	0.3806881	0.6193119	0.5000000	1
C24	C	1	0.6193119	0.6193119	0.5000000	1
O1	O	1	0.534361	0.5340257	0.4682137	1
O2	O	1	0.534361	0.4659743	0.5317863	1
O3	O	1	0.465639	0.5340257	0.4682137	1
O4	O	1	0.465639	0.4659743	0.5317863	1
O5	O	1	0.465639	0.4659743	0.4682137	1
O6	O	1	0.465639	0.5340257	0.5317863	1

O7	O	1	0.534361	0.4659743	0.4682137	1
O8	O	1	0.534361	0.5340257	0.5317863	1
O9	O	1	0.5945151	0.5000000	0.5503905	1
O10	O	1	0.5945151	0.4455278	0.5000000	1
O11	O	1	0.5945151	0.5000000	0.4496095	1
O12	O	1	0.5945151	0.5544722	0.5000000	1
O13	O	1	0.5000000	0.5945151	0.5503905	1
O14	O	1	0.5544722	0.5945151	0.5000000	1
O15	O	1	0.5000000	0.5945151	0.4496095	1
O16	O	1	0.4455278	0.5945151	0.5000000	1
O17	O	1	0.4054849	0.5000000	0.5503905	1
O18	O	1	0.4054849	0.5544722	0.5000000	1
O19	O	1	0.4054849	0.5000000	0.4496095	1
O20	O	1	0.4054849	0.4455278	0.5000000	1
O21	O	1	0.5000000	0.4054849	0.5503905	1
O22	O	1	0.4455278	0.4054849	0.5000000	1
O23	O	1	0.5000000	0.4054849	0.4496095	1
O24	O	1	0.5544722	0.4054849	0.5000000	1
O25	O	1	0.5544722	0.5000000	0.5874331	1
O26	O	1	0.5000000	0.5544722	0.5874331	1
O27	O	1	0.4455278	0.5000000	0.5874331	1
O28	O	1	0.5000000	0.4455278	0.5874331	1
O29	O	1	0.5544722	0.5000000	0.4125669	1
O30	O	1	0.5000000	0.4455278	0.4125669	1
O31	O	1	0.4455278	0.5000000	0.4125669	1
O32	O	1	0.5000000	0.5544722	0.4125669	1
Zr1	Zr	1	0.5664377	0.5000000	0.5000000	1
Zr2	Zr	1	0.5000000	0.5664377	0.5000000	1
Zr3	Zr	1	0.4335623	0.5000000	0.5000000	1
Zr4	Zr	1	0.5000000	0.4335623	0.5000000	1
Zr5	Zr	1	0.5000000	0.5000000	0.5614595	1
Zr6	Zr	1	0.5000000	0.5000000	0.4385405	1

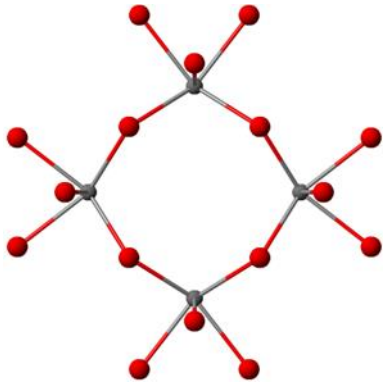

Figure 301: The tetrameric structure resulting from the fixed core refinement of ZAA16A from the 18-month data collection.

Table 244: The atomic coordinates of the tetrameric phase of the fixed core refinement of ZAA16A from the 18-month data collection.

Atom Label	Atom Type	Multiplicity	Fractional X Coordinate	Fractional Y Coordinate	Fractional Z Coordinate	Fractional Occupancy
O1	O	1	0.5152425	0.4847575	0.482572	1
O2	O	1	0.4847575	0.4847575	0.517428	1
O3	O	1	0.5152425	0.5152425	0.517428	1
O4	O	1	0.4847575	0.5152425	0.482572	1
O5	O	1	0.5000000	0.5300748	0.545286	1
O6	O	1	0.5000000	0.4699252	0.545286	1
O7	O	1	0.4699252	0.5000000	0.454714	1
O8	O	1	0.5300748	0.5000000	0.454714	1
O9	O	1	0.5127427	0.4588057	0.5000000	1
O10	O	1	0.4588057	0.4872573	0.5000000	1
O11	O	1	0.5411943	0.5127427	0.5000000	1
O12	O	1	0.4872573	0.5411943	0.5000000	1
O13	O	1	0.4588057	0.5127427	0.5000000	1
O14	O	1	0.5411943	0.4872573	0.5000000	1
O15	O	1	0.4872573	0.4588057	0.5000000	1
O16	O	1	0.5127427	0.5411943	0.5000000	1
O17	O	1	0.5152425	0.4847575	0.517428	1
O18	O	1	0.4847575	0.4847575	0.482572	1
O19	O	1	0.5152425	0.5152425	0.482572	1
O20	O	1	0.4847575	0.5152425	0.517428	1
O21	O	1	0.5000000	0.5300748	0.454714	1
O22	O	1	0.5000000	0.4699252	0.454714	1
O23	O	1	0.4699252	0.5000000	0.545286	1
O24	O	1	0.5300748	0.5000000	0.545286	1
Zr1	Zr	1	0.5000000	0.4752608	0.5000000	1
Zr2	Zr	1	0.4752608	0.5000000	0.5000000	1
Zr3	Zr	1	0.5247392	0.5000000	0.5000000	1
Zr4	Zr	1	0.5000000	0.5247392	0.5000000	1

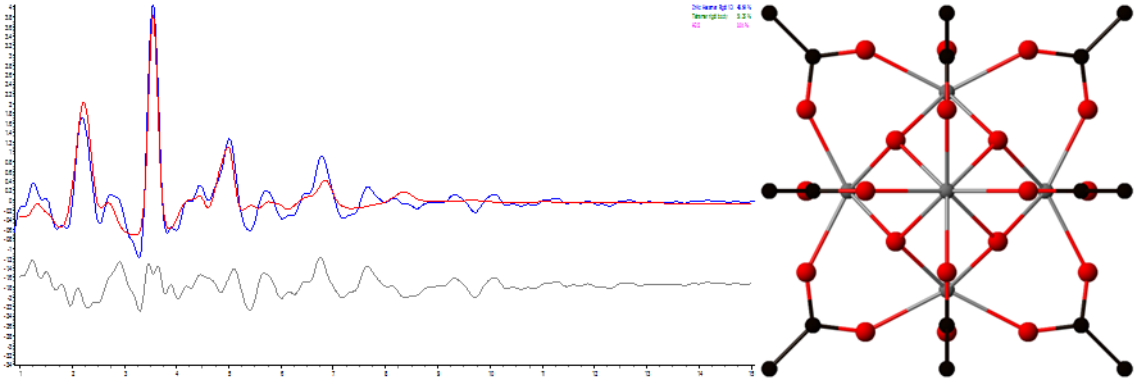

Figure 302: Observed and Calculated PDF from the fixed core refinement of ZAA16C from the 18-month data collection and the resultant model.

Table 245: The atomic coordinates of the model resulting from the fixed core refinement of ZAA16C from the 18-month data collection.

Atom Label	Atom Type	Multiplicity	Fractional X Coordinate	Fractional Y Coordinate	Fractional Z Coordinate	Fractional Occupancy
C1	C	1	0.5901016	0.5000000	0.5833503	1
C2	C	1	0.5000000	0.4098984	0.5833503	1
C3	C	1	0.4098984	0.5000000	0.5833503	1
C4	C	1	0.5000000	0.5901016	0.5833503	1
C5	C	1	0.5901016	0.5000000	0.4166497	1
C6	C	1	0.5000000	0.4098984	0.4166497	1
C7	C	1	0.4098984	0.5000000	0.4166497	1
C8	C	1	0.5000000	0.5901016	0.4166497	1
C9	C	1	0.5901016	0.4098984	0.5000000	1
C10	C	1	0.4098984	0.4098984	0.5000000	1
C11	C	1	0.4098984	0.5901016	0.5000000	1
C12	C	1	0.5901016	0.5901016	0.5000000	1
C13	C	1	0.6193008	0.5000000	0.6103616	1
C14	C	1	0.5000000	0.3806992	0.6103616	1
C15	C	1	0.3806992	0.5000000	0.6103616	1
C16	C	1	0.5000000	0.6193008	0.6103616	1
C17	C	1	0.6193008	0.5000000	0.3896384	1
C18	C	1	0.5000000	0.3806992	0.3896384	1
C19	C	1	0.3806992	0.5000000	0.3896384	1
C20	C	1	0.5000000	0.6193008	0.3896384	1
C21	C	1	0.6193008	0.3806992	0.5000000	1
C22	C	1	0.3806992	0.3806992	0.5000000	1
C23	C	1	0.3806992	0.6193008	0.5000000	1
C24	C	1	0.6193008	0.6193008	0.5000000	1
O1	O	1	0.5342738	0.5339394	0.4682943	1
O2	O	1	0.5342738	0.4660606	0.5317057	1
O3	O	1	0.4657262	0.5339394	0.4682943	1
O4	O	1	0.4657262	0.4660606	0.5317057	1
O5	O	1	0.4657262	0.4660606	0.4682943	1
O6	O	1	0.4657262	0.5339394	0.5317057	1

O7	O	1	0.5342738	0.4660606	0.4682943	1
O8	O	1	0.5342738	0.5339394	0.5317057	1
O9	O	1	0.594534	0.5000000	0.5505827	1
O10	O	1	0.594534	0.4453201	0.5000000	1
O11	O	1	0.594534	0.5000000	0.4494173	1
O12	O	1	0.594534	0.5546799	0.5000000	1
O13	O	1	0.5000000	0.594534	0.5505827	1
O14	O	1	0.5546799	0.594534	0.5000000	1
O15	O	1	0.5000000	0.594534	0.4494173	1
O16	O	1	0.4453201	0.594534	0.5000000	1
O17	O	1	0.405466	0.5000000	0.5505827	1
O18	O	1	0.405466	0.5546799	0.5000000	1
O19	O	1	0.405466	0.5000000	0.4494173	1
O20	O	1	0.405466	0.4453201	0.5000000	1
O21	O	1	0.5000000	0.405466	0.5505827	1
O22	O	1	0.4453201	0.405466	0.5000000	1
O23	O	1	0.5000000	0.405466	0.4494173	1
O24	O	1	0.5546799	0.405466	0.5000000	1
O25	O	1	0.5546799	0.5000000	0.5874505	1
O26	O	1	0.5000000	0.5546799	0.5874505	1
O27	O	1	0.4453201	0.5000000	0.5874505	1
O28	O	1	0.5000000	0.4453201	0.5874505	1
O29	O	1	0.5546799	0.5000000	0.4125495	1
O30	O	1	0.5000000	0.4453201	0.4125495	1
O31	O	1	0.4453201	0.5000000	0.4125495	1
O32	O	1	0.5000000	0.5546799	0.4125495	1
Zr1	Zr	1	0.5663805	0.5000000	0.5000000	1
Zr2	Zr	1	0.5000000	0.5663805	0.5000000	1
Zr3	Zr	1	0.4336195	0.5000000	0.5000000	1
Zr4	Zr	1	0.5000000	0.4336195	0.5000000	1
Zr5	Zr	1	0.5000000	0.5000000	0.5614066	1
Zr6	Zr	1	0.5000000	0.5000000	0.4385934	1

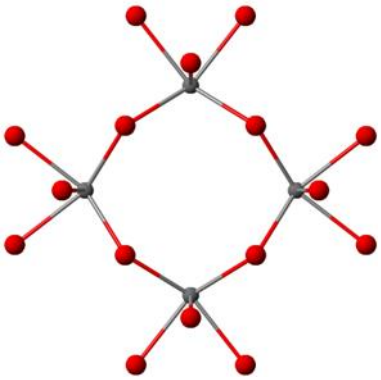

Figure 303: The tetrameric structure resulting from the fixed core refinement of ZAA16C from the 18-month data collection.

Table 246: The atomic coordinates of the tetrameric phase of the fixed core refinement of ZAA16C from the 18-month data collection.

Atom Label	Atom Type	Multiplicity	Fractional X Coordinate	Fractional Y Coordinate	Fractional Z Coordinate	Fractional Occupancy
O1	O	1	0.5153002	0.4846998	0.4826551	1
O2	O	1	0.4846998	0.4846998	0.5173449	1
O3	O	1	0.5153002	0.5153002	0.5173449	1
O4	O	1	0.4846998	0.5153002	0.4826551	1
O5	O	1	0.5000000	0.5300707	0.5453053	1
O6	O	1	0.5000000	0.4699293	0.5453053	1
O7	O	1	0.4699293	0.5000000	0.4546947	1
O8	O	1	0.5300707	0.5000000	0.4546947	1
O9	O	1	0.5128382	0.4588204	0.5000000	1
O10	O	1	0.4588204	0.4871618	0.5000000	1
O11	O	1	0.5411796	0.5128382	0.5000000	1
O12	O	1	0.4871618	0.5411796	0.5000000	1
O13	O	1	0.4588204	0.5128382	0.5000000	1
O14	O	1	0.5411796	0.4871618	0.5000000	1
O15	O	1	0.4871618	0.4588204	0.5000000	1
O16	O	1	0.5128382	0.5411796	0.5000000	1
O17	O	1	0.5153002	0.4846998	0.5173449	1
O18	O	1	0.4846998	0.4846998	0.4826551	1
O19	O	1	0.5153002	0.5153002	0.4826551	1
O20	O	1	0.4846998	0.5153002	0.5173449	1
O21	O	1	0.5000000	0.5300707	0.4546947	1
O22	O	1	0.5000000	0.4699293	0.4546947	1
O23	O	1	0.4699293	0.5000000	0.5453053	1
O24	O	1	0.5300707	0.5000000	0.5453053	1
Zr1	Zr	1	0.5000000	0.475285	0.5000000	1
Zr2	Zr	1	0.475285	0.5000000	0.5000000	1
Zr3	Zr	1	0.524715	0.5000000	0.5000000	1
Zr4	Zr	1	0.5000000	0.524715	0.5000000	1

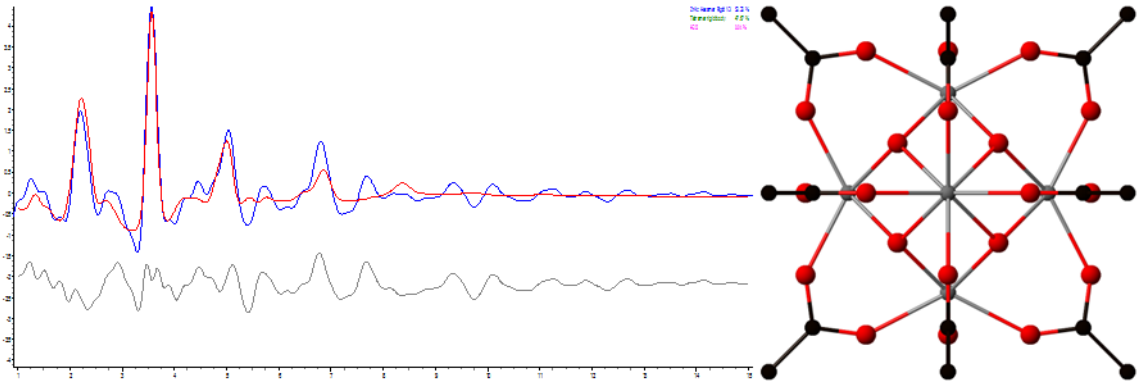

Figure 304: Observed and Calculated PDF from the fixed core refinement of ZAA16I from the 18-month data collection and the resultant model.

Table 247: The atomic coordinates of the model resulting from the fixed core refinement of ZAA16I from the 18-month data collection.

Atom Label	Atom Type	Multiplicity	Fractional X Coordinate	Fractional Y Coordinate	Fractional Z Coordinate	Fractional Occupancy
C1	C	1	0.590193	0.5000000	0.5834348	1
C2	C	1	0.5000000	0.409807	0.5834348	1
C3	C	1	0.409807	0.5000000	0.5834348	1
C4	C	1	0.5000000	0.590193	0.5834348	1
C5	C	1	0.590193	0.5000000	0.4165652	1
C6	C	1	0.5000000	0.409807	0.4165652	1
C7	C	1	0.409807	0.5000000	0.4165652	1
C8	C	1	0.5000000	0.590193	0.4165652	1
C9	C	1	0.590193	0.409807	0.5000000	1
C10	C	1	0.409807	0.409807	0.5000000	1
C11	C	1	0.409807	0.590193	0.5000000	1
C12	C	1	0.590193	0.590193	0.5000000	1
C13	C	1	0.6195918	0.5000000	0.6106307	1
C14	C	1	0.5000000	0.3804082	0.6106307	1
C15	C	1	0.3804082	0.5000000	0.6106307	1
C16	C	1	0.5000000	0.6195918	0.6106307	1
C17	C	1	0.6195918	0.5000000	0.3893693	1
C18	C	1	0.5000000	0.3804082	0.3893693	1
C19	C	1	0.3804082	0.5000000	0.3893693	1
C20	C	1	0.5000000	0.6195918	0.3893693	1
C21	C	1	0.6195918	0.3804082	0.5000000	1
C22	C	1	0.3804082	0.3804082	0.5000000	1
C23	C	1	0.3804082	0.6195918	0.5000000	1
C24	C	1	0.6195918	0.6195918	0.5000000	1
O1	O	1	0.5336893	0.5333606	0.468835	1
O2	O	1	0.5336893	0.4666394	0.531165	1
O3	O	1	0.4663107	0.5333606	0.468835	1
O4	O	1	0.4663107	0.4666394	0.531165	1
O5	O	1	0.4663107	0.4666394	0.468835	1
O6	O	1	0.4663107	0.5333606	0.531165	1

O7	O	1	0.5336893	0.4666394	0.468835	1
O8	O	1	0.5336893	0.5333606	0.531165	1
O9	O	1	0.59512	0.5000000	0.5507408	1
O10	O	1	0.59512	0.4451492	0.5000000	1
O11	O	1	0.59512	0.5000000	0.4492592	1
O12	O	1	0.59512	0.5548508	0.5000000	1
O13	O	1	0.5000000	0.59512	0.5507408	1
O14	O	1	0.5548508	0.59512	0.5000000	1
O15	O	1	0.5000000	0.59512	0.4492592	1
O16	O	1	0.4451492	0.59512	0.5000000	1
O17	O	1	0.40488	0.5000000	0.5507408	1
O18	O	1	0.40488	0.5548508	0.5000000	1
O19	O	1	0.40488	0.5000000	0.4492592	1
O20	O	1	0.40488	0.4451492	0.5000000	1
O21	O	1	0.5000000	0.40488	0.5507408	1
O22	O	1	0.4451492	0.40488	0.5000000	1
O23	O	1	0.5000000	0.40488	0.4492592	1
O24	O	1	0.5548508	0.40488	0.5000000	1
O25	O	1	0.5548508	0.5000000	0.5879927	1
O26	O	1	0.5000000	0.5548508	0.5879927	1
O27	O	1	0.4451492	0.5000000	0.5879927	1
O28	O	1	0.5000000	0.4451492	0.5879927	1
O29	O	1	0.5548508	0.5000000	0.4120073	1
O30	O	1	0.5000000	0.4451492	0.4120073	1
O31	O	1	0.4451492	0.5000000	0.4120073	1
O32	O	1	0.5000000	0.5548508	0.4120073	1
Zr1	Zr	1	0.5666541	0.5000000	0.5000000	1
Zr2	Zr	1	0.5000000	0.5666541	0.5000000	1
Zr3	Zr	1	0.4333459	0.5000000	0.5000000	1
Zr4	Zr	1	0.5000000	0.4333459	0.5000000	1
Zr5	Zr	1	0.5000000	0.5000000	0.5616597	1
Zr6	Zr	1	0.5000000	0.5000000	0.4383403	1

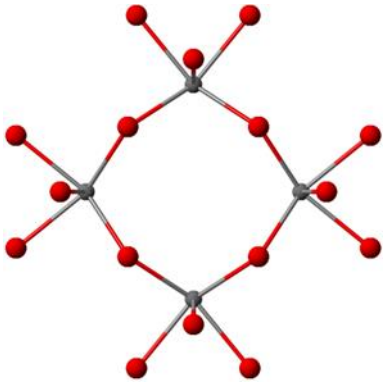

Figure 305: The tetrameric structure resulting from the fixed core refinement of ZAA16I from the 18-month data collection.

Table 248: The atomic coordinates of the tetrameric phase of the fixed core refinement of ZAA16I from the 18-month data collection.

Atom Label	Atom Type	Multiplicity	Fractional X Coordinate	Fractional Y Coordinate	Fractional Z Coordinate	Fractional Occupancy
O1	O	1	0.5150749	0.4849251	0.4826171	1
O2	O	1	0.4849251	0.4849251	0.5173829	1
O3	O	1	0.5150749	0.5150749	0.5173829	1
O4	O	1	0.4849251	0.5150749	0.4826171	1
O5	O	1	0.5000000	0.5307445	0.5448751	1
O6	O	1	0.5000000	0.4692555	0.5448751	1
O7	O	1	0.4692555	0.5000000	0.4551249	1
O8	O	1	0.5307445	0.5000000	0.4551249	1
O9	O	1	0.513085	0.4590694	0.5000000	1
O10	O	1	0.4590694	0.486915	0.5000000	1
O11	O	1	0.5409306	0.513085	0.5000000	1
O12	O	1	0.486915	0.5409306	0.5000000	1
O13	O	1	0.4590694	0.513085	0.5000000	1
O14	O	1	0.5409306	0.486915	0.5000000	1
O15	O	1	0.486915	0.4590694	0.5000000	1
O16	O	1	0.513085	0.5409306	0.5000000	1
O17	O	1	0.5150749	0.4849251	0.5173829	1
O18	O	1	0.4849251	0.4849251	0.4826171	1
O19	O	1	0.5150749	0.5150749	0.4826171	1
O20	O	1	0.4849251	0.5150749	0.5173829	1
O21	O	1	0.5000000	0.5307445	0.4551249	1
O22	O	1	0.5000000	0.4692555	0.4551249	1
O23	O	1	0.4692555	0.5000000	0.5448751	1
O24	O	1	0.5307445	0.5000000	0.5448751	1
Zr1	Zr	1	0.5000000	0.4751432	0.5000000	1
Zr2	Zr	1	0.4751432	0.5000000	0.5000000	1
Zr3	Zr	1	0.5248568	0.5000000	0.5000000	1
Zr4	Zr	1	0.5000000	0.5248568	0.5000000	1

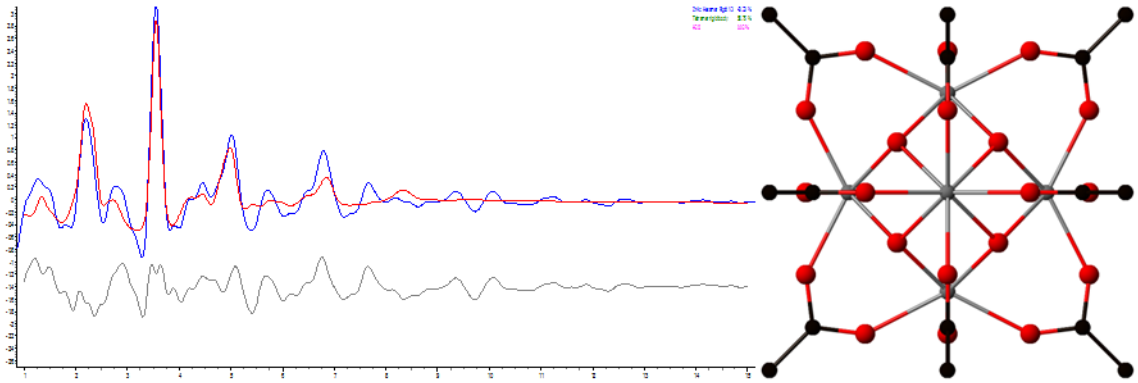

Figure 306: Observed and Calculated PDF from the fixed core refinement of ZAA20A from the 18-month data collection and the resultant model.

Table 249: The atomic coordinates of the model resulting from the fixed core refinement of ZAA20A from the 18-month data collection.

Atom Label	Atom Type	Multiplicity	Fractional X Coordinate	Fractional Y Coordinate	Fractional Z Coordinate	Fractional Occupancy
C1	C	1	0.5902442	0.5000000	0.5834822	1
C2	C	1	0.5000000	0.4097558	0.5834822	1
C3	C	1	0.4097558	0.5000000	0.5834822	1
C4	C	1	0.5000000	0.5902442	0.5834822	1
C5	C	1	0.5902442	0.5000000	0.4165178	1
C6	C	1	0.5000000	0.4097558	0.4165178	1
C7	C	1	0.4097558	0.5000000	0.4165178	1
C8	C	1	0.5000000	0.5902442	0.4165178	1
C9	C	1	0.5902442	0.4097558	0.5000000	1
C10	C	1	0.4097558	0.4097558	0.5000000	1
C11	C	1	0.4097558	0.5902442	0.5000000	1
C12	C	1	0.5902442	0.5902442	0.5000000	1
C13	C	1	0.61904	0.5000000	0.6101203	1
C14	C	1	0.5000000	0.38096	0.6101203	1
C15	C	1	0.38096	0.5000000	0.6101203	1
C16	C	1	0.5000000	0.61904	0.6101203	1
C17	C	1	0.61904	0.5000000	0.3898797	1
C18	C	1	0.5000000	0.38096	0.3898797	1
C19	C	1	0.38096	0.5000000	0.3898797	1
C20	C	1	0.5000000	0.61904	0.3898797	1
C21	C	1	0.61904	0.38096	0.5000000	1
C22	C	1	0.38096	0.38096	0.5000000	1
C23	C	1	0.38096	0.61904	0.5000000	1
C24	C	1	0.61904	0.61904	0.5000000	1
O1	O	1	0.5339253	0.5335943	0.4686167	1
O2	O	1	0.5339253	0.4664057	0.5313833	1
O3	O	1	0.4660747	0.5335943	0.4686167	1
O4	O	1	0.4660747	0.4664057	0.5313833	1
O5	O	1	0.4660747	0.4664057	0.4686167	1
O6	O	1	0.4660747	0.5335943	0.5313833	1

O7	O	1	0.5339253	0.4664057	0.4686167	1
O8	O	1	0.5339253	0.5335943	0.5313833	1
O9	O	1	0.5947607	0.5000000	0.5510077	1
O10	O	1	0.5947607	0.4448608	0.5000000	1
O11	O	1	0.5947607	0.5000000	0.4489923	1
O12	O	1	0.5947607	0.5551392	0.5000000	1
O13	O	1	0.5000000	0.5947607	0.5510077	1
O14	O	1	0.5551392	0.5947607	0.5000000	1
O15	O	1	0.5000000	0.5947607	0.4489923	1
O16	O	1	0.4448608	0.5947607	0.5000000	1
O17	O	1	0.4052393	0.5000000	0.5510077	1
O18	O	1	0.4052393	0.5551392	0.5000000	1
O19	O	1	0.4052393	0.5000000	0.4489923	1
O20	O	1	0.4052393	0.4448608	0.5000000	1
O21	O	1	0.5000000	0.4052393	0.5510077	1
O22	O	1	0.4448608	0.4052393	0.5000000	1
O23	O	1	0.5000000	0.4052393	0.4489923	1
O24	O	1	0.5551392	0.4052393	0.5000000	1
O25	O	1	0.5551392	0.5000000	0.5876602	1
O26	O	1	0.5000000	0.5551392	0.5876602	1
O27	O	1	0.4448608	0.5000000	0.5876602	1
O28	O	1	0.5000000	0.4448608	0.5876602	1
O29	O	1	0.5551392	0.5000000	0.4123398	1
O30	O	1	0.5000000	0.4448608	0.4123398	1
O31	O	1	0.4448608	0.5000000	0.4123398	1
O32	O	1	0.5000000	0.5551392	0.4123398	1
Zr1	Zr	1	0.5663778	0.5000000	0.5000000	1
Zr2	Zr	1	0.5000000	0.5663778	0.5000000	1
Zr3	Zr	1	0.4336222	0.5000000	0.5000000	1
Zr4	Zr	1	0.5000000	0.4336222	0.5000000	1
Zr5	Zr	1	0.5000000	0.5000000	0.5614041	1
Zr6	Zr	1	0.5000000	0.5000000	0.4385959	1

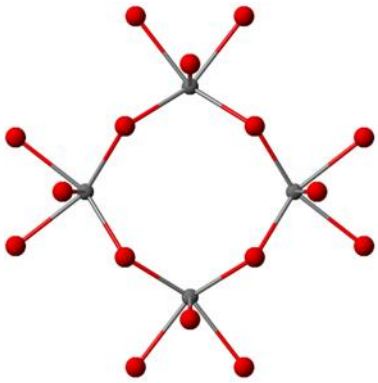

Figure 307: The tetrameric structure resulting from the fixed core refinement of ZAA20A from the 18-month data collection.

Table 250: The atomic coordinates of the tetrameric phase of the fixed core refinement of ZAA20A from the 18-month data collection.

Atom Label	Atom Type	Multiplicity	Fractional X Coordinate	Fractional Y Coordinate	Fractional Z Coordinate	Fractional Occupancy
O1	O	1	0.515374	0.484626	0.4842757	1
O2	O	1	0.484626	0.484626	0.5157243	1
O3	O	1	0.515374	0.515374	0.5157243	1
O4	O	1	0.484626	0.515374	0.4842757	1
O5	O	1	0.5000000	0.5300604	0.5460406	1
O6	O	1	0.5000000	0.4699396	0.5460406	1
O7	O	1	0.4699396	0.5000000	0.4539594	1
O8	O	1	0.5300604	0.5000000	0.4539594	1
O9	O	1	0.5127843	0.4587894	0.5000000	1
O10	O	1	0.4587894	0.4872157	0.5000000	1
O11	O	1	0.5412106	0.5127843	0.5000000	1
O12	O	1	0.4872157	0.5412106	0.5000000	1
O13	O	1	0.4587894	0.5127843	0.5000000	1
O14	O	1	0.5412106	0.4872157	0.5000000	1
O15	O	1	0.4872157	0.4587894	0.5000000	1
O16	O	1	0.5127843	0.5412106	0.5000000	1
O17	O	1	0.515374	0.484626	0.5157243	1
O18	O	1	0.484626	0.484626	0.4842757	1
O19	O	1	0.515374	0.515374	0.4842757	1
O20	O	1	0.484626	0.515374	0.5157243	1
O21	O	1	0.5000000	0.5300604	0.4539594	1
O22	O	1	0.5000000	0.4699396	0.4539594	1
O23	O	1	0.4699396	0.5000000	0.5460406	1
O24	O	1	0.5300604	0.5000000	0.5460406	1
Zr1	Zr	1	0.5000000	0.4752617	0.5000000	1
Zr2	Zr	1	0.4752617	0.5000000	0.5000000	1
Zr3	Zr	1	0.5247383	0.5000000	0.5000000	1
Zr4	Zr	1	0.5000000	0.5247383	0.5000000	1

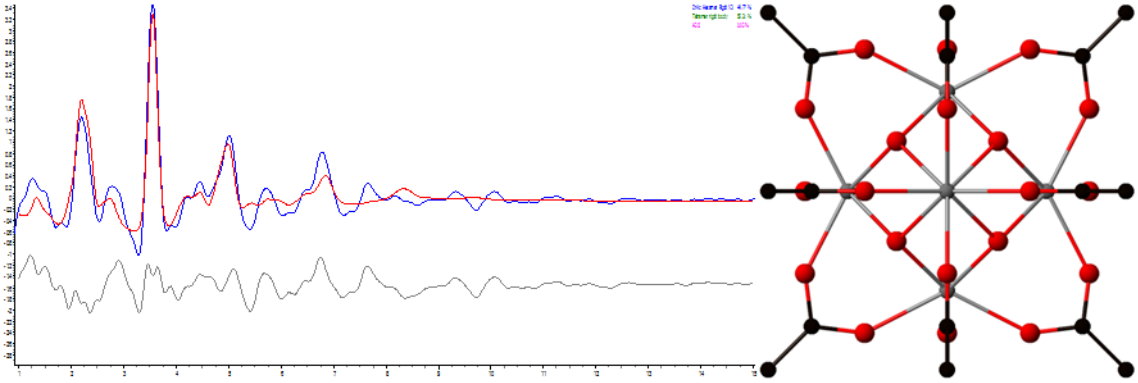

Figure 308: Observed and Calculated PDF from the fixed core refinement of ZAA20C from the 18-month data collection and the resultant model.

Table 251: The atomic coordinates of the model resulting from the fixed core refinement of ZAA20C from the 18-month data collection.

Atom Label	Atom Type	Multiplicity	Fractional X Coordinate	Fractional Y Coordinate	Fractional Z Coordinate	Fractional Occupancy
C1	C	1	0.5901903	0.5000000	0.5834323	1
C2	C	1	0.5000000	0.4098097	0.5834323	1
C3	C	1	0.4098097	0.5000000	0.5834323	1
C4	C	1	0.5000000	0.5901903	0.5834323	1
C5	C	1	0.5901903	0.5000000	0.4165677	1
C6	C	1	0.5000000	0.4098097	0.4165677	1
C7	C	1	0.4098097	0.5000000	0.4165677	1
C8	C	1	0.5000000	0.5901903	0.4165677	1
C9	C	1	0.5901903	0.4098097	0.5000000	1
C10	C	1	0.4098097	0.4098097	0.5000000	1
C11	C	1	0.4098097	0.5901903	0.5000000	1
C12	C	1	0.5901903	0.5901903	0.5000000	1
C13	C	1	0.6191803	0.5000000	0.6102501	1
C14	C	1	0.5000000	0.3808197	0.6102501	1
C15	C	1	0.3808197	0.5000000	0.6102501	1
C16	C	1	0.5000000	0.6191803	0.6102501	1
C17	C	1	0.6191803	0.5000000	0.3897499	1
C18	C	1	0.5000000	0.3808197	0.3897499	1
C19	C	1	0.3808197	0.5000000	0.3897499	1
C20	C	1	0.5000000	0.6191803	0.3897499	1
C21	C	1	0.6191803	0.3808197	0.5000000	1
C22	C	1	0.3808197	0.3808197	0.5000000	1
C23	C	1	0.3808197	0.6191803	0.5000000	1
C24	C	1	0.6191803	0.6191803	0.5000000	1
O1	O	1	0.5338132	0.5334833	0.4687205	1
O2	O	1	0.5338132	0.4665167	0.5312795	1
O3	O	1	0.4661868	0.5334833	0.4687205	1
O4	O	1	0.4661868	0.4665167	0.5312795	1
O5	O	1	0.4661868	0.4665167	0.4687205	1
O6	O	1	0.4661868	0.5334833	0.5312795	1

O7	O	1	0.5338132	0.4665167	0.4687205	1
O8	O	1	0.5338132	0.5334833	0.5312795	1
O9	O	1	0.5946447	0.5000000	0.5509786	1
O10	O	1	0.5946447	0.4448921	0.5000000	1
O11	O	1	0.5946447	0.5000000	0.4490214	1
O12	O	1	0.5946447	0.5551079	0.5000000	1
O13	O	1	0.5000000	0.5946447	0.5509786	1
O14	O	1	0.5551079	0.5946447	0.5000000	1
O15	O	1	0.5000000	0.5946447	0.4490214	1
O16	O	1	0.4448921	0.5946447	0.5000000	1
O17	O	1	0.4053553	0.5000000	0.5509786	1
O18	O	1	0.4053553	0.5551079	0.5000000	1
O19	O	1	0.4053553	0.5000000	0.4490214	1
O20	O	1	0.4053553	0.4448921	0.5000000	1
O21	O	1	0.5000000	0.4053553	0.5509786	1
O22	O	1	0.4448921	0.4053553	0.5000000	1
O23	O	1	0.5000000	0.4053553	0.4490214	1
O24	O	1	0.5551079	0.4053553	0.5000000	1
O25	O	1	0.5551079	0.5000000	0.5875529	1
O26	O	1	0.5000000	0.5551079	0.5875529	1
O27	O	1	0.4448921	0.5000000	0.5875529	1
O28	O	1	0.5000000	0.4448921	0.5875529	1
O29	O	1	0.5551079	0.5000000	0.4124471	1
O30	O	1	0.5000000	0.4448921	0.4124471	1
O31	O	1	0.4448921	0.5000000	0.4124471	1
O32	O	1	0.5000000	0.5551079	0.4124471	1
Zr1	Zr	1	0.5663455	0.5000000	0.5000000	1
Zr2	Zr	1	0.5000000	0.5663455	0.5000000	1
Zr3	Zr	1	0.4336545	0.5000000	0.5000000	1
Zr4	Zr	1	0.5000000	0.4336545	0.5000000	1
Zr5	Zr	1	0.5000000	0.5000000	0.5613743	1
Zr6	Zr	1	0.5000000	0.5000000	0.4386257	1

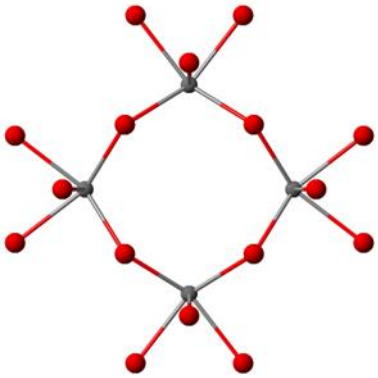

Figure 309: The tetrameric structure resulting from the fixed core refinement of ZAA20C from the 18-month data collection.

Table 252: The atomic coordinates of the tetrameric phase of the fixed core refinement of ZAA20C from the 18-month data collection.

Atom Label	Atom Type	Multiplicity	Fractional X Coordinate	Fractional Y Coordinate	Fractional Z Coordinate	Fractional Occupancy
O1	O	1	0.5152942	0.4847058	0.4839147	1
O2	O	1	0.4847058	0.4847058	0.5160853	1
O3	O	1	0.5152942	0.5152942	0.5160853	1
O4	O	1	0.4847058	0.5152942	0.4839147	1
O5	O	1	0.5000000	0.5299953	0.5459798	1
O6	O	1	0.5000000	0.4700047	0.5459798	1
O7	O	1	0.4700047	0.5000000	0.4540202	1
O8	O	1	0.5299953	0.5000000	0.4540202	1
O9	O	1	0.5126927	0.4587839	0.5000000	1
O10	O	1	0.4587839	0.4873073	0.5000000	1
O11	O	1	0.5412161	0.5126927	0.5000000	1
O12	O	1	0.4873073	0.5412161	0.5000000	1
O13	O	1	0.4587839	0.5126927	0.5000000	1
O14	O	1	0.5412161	0.4873073	0.5000000	1
O15	O	1	0.4873073	0.4587839	0.5000000	1
O16	O	1	0.5126927	0.5412161	0.5000000	1
O17	O	1	0.5152942	0.4847058	0.5160853	1
O18	O	1	0.4847058	0.4847058	0.4839147	1
O19	O	1	0.5152942	0.5152942	0.4839147	1
O20	O	1	0.4847058	0.5152942	0.5160853	1
O21	O	1	0.5000000	0.5299953	0.4540202	1
O22	O	1	0.5000000	0.4700047	0.4540202	1
O23	O	1	0.4700047	0.5000000	0.5459798	1
O24	O	1	0.5299953	0.5000000	0.5459798	1
Zr1	Zr	1	0.5000000	0.4752722	0.5000000	1
Zr2	Zr	1	0.4752722	0.5000000	0.5000000	1
Zr3	Zr	1	0.5247278	0.5000000	0.5000000	1
Zr4	Zr	1	0.5000000	0.5247278	0.5000000	1

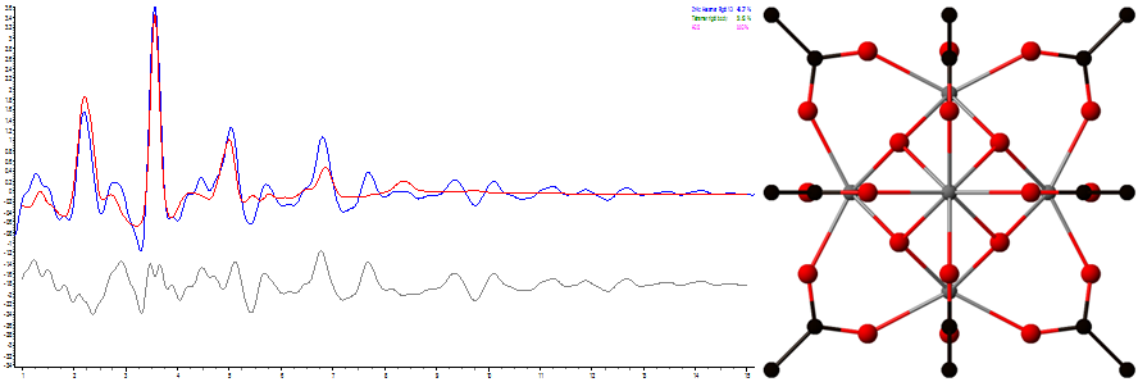

Figure 310: Observed and Calculated PDF from the fixed core refinement of ZAA20I from the 18-month data collection and the resultant model.

Table 253: The atomic coordinates of the model resulting from the fixed core refinement of ZAA20I from the 18-month data collection.

Atom Label	Atom Type	Multiplicity	Fractional X Coordinate	Fractional Y Coordinate	Fractional Z Coordinate	Fractional Occupancy
C1	C	1	0.5904473	0.5000000	0.58367	1
C2	C	1	0.5000000	0.4095527	0.58367	1
C3	C	1	0.4095527	0.5000000	0.58367	1
C4	C	1	0.5000000	0.5904473	0.58367	1
C5	C	1	0.5904473	0.5000000	0.41633	1
C6	C	1	0.5000000	0.4095527	0.41633	1
C7	C	1	0.4095527	0.5000000	0.41633	1
C8	C	1	0.5000000	0.5904473	0.41633	1
C9	C	1	0.5904473	0.4095527	0.5000000	1
C10	C	1	0.4095527	0.4095527	0.5000000	1
C11	C	1	0.4095527	0.5904473	0.5000000	1
C12	C	1	0.5904473	0.5904473	0.5000000	1
C13	C	1	0.619695	0.5000000	0.6107263	1
C14	C	1	0.5000000	0.380305	0.6107263	1
C15	C	1	0.380305	0.5000000	0.6107263	1
C16	C	1	0.5000000	0.619695	0.6107263	1
C17	C	1	0.619695	0.5000000	0.3892737	1
C18	C	1	0.5000000	0.380305	0.3892737	1
C19	C	1	0.380305	0.5000000	0.3892737	1
C20	C	1	0.5000000	0.619695	0.3892737	1
C21	C	1	0.619695	0.380305	0.5000000	1
C22	C	1	0.380305	0.380305	0.5000000	1
C23	C	1	0.380305	0.619695	0.5000000	1
C24	C	1	0.619695	0.619695	0.5000000	1
O1	O	1	0.5338475	0.5335172	0.4686887	1
O2	O	1	0.5338475	0.4664828	0.5313113	1
O3	O	1	0.4661525	0.5335172	0.4686887	1
O4	O	1	0.4661525	0.4664828	0.5313113	1
O5	O	1	0.4661525	0.4664828	0.4686887	1
O6	O	1	0.4661525	0.5335172	0.5313113	1

O7	O	1	0.5338475	0.4664828	0.4686887	1
O8	O	1	0.5338475	0.5335172	0.5313113	1
O9	O	1	0.5952273	0.5000000	0.5508865	1
O10	O	1	0.5952273	0.4449917	0.5000000	1
O11	O	1	0.5952273	0.5000000	0.4491135	1
O12	O	1	0.5952273	0.5550083	0.5000000	1
O13	O	1	0.5000000	0.5952273	0.5508865	1
O14	O	1	0.5550083	0.5952273	0.5000000	1
O15	O	1	0.5000000	0.5952273	0.4491135	1
O16	O	1	0.4449917	0.5952273	0.5000000	1
O17	O	1	0.4047727	0.5000000	0.5508865	1
O18	O	1	0.4047727	0.5550083	0.5000000	1
O19	O	1	0.4047727	0.5000000	0.4491135	1
O20	O	1	0.4047727	0.4449917	0.5000000	1
O21	O	1	0.5000000	0.4047727	0.5508865	1
O22	O	1	0.4449917	0.4047727	0.5000000	1
O23	O	1	0.5000000	0.4047727	0.4491135	1
O24	O	1	0.5550083	0.4047727	0.5000000	1
O25	O	1	0.5550083	0.5000000	0.5880919	1
O26	O	1	0.5000000	0.5550083	0.5880919	1
O27	O	1	0.4449917	0.5000000	0.5880919	1
O28	O	1	0.5000000	0.4449917	0.5880919	1
O29	O	1	0.5550083	0.5000000	0.4119081	1
O30	O	1	0.5000000	0.4449917	0.4119081	1
O31	O	1	0.4449917	0.5000000	0.4119081	1
O32	O	1	0.5000000	0.5550083	0.4119081	1
Zr1	Zr	1	0.5665768	0.5000000	0.5000000	1
Zr2	Zr	1	0.5000000	0.5665768	0.5000000	1
Zr3	Zr	1	0.4334232	0.5000000	0.5000000	1
Zr4	Zr	1	0.5000000	0.4334232	0.5000000	1
Zr5	Zr	1	0.5000000	0.5000000	0.5615882	1
Zr6	Zr	1	0.5000000	0.5000000	0.4384118	1

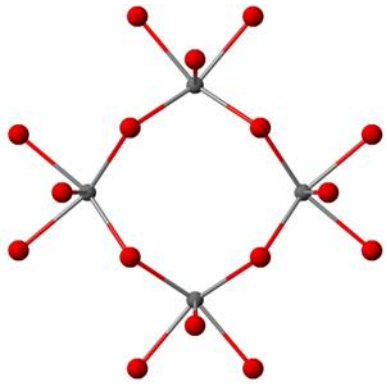

Figure 311: The tetrameric structure resulting from the fixed core refinement of ZAA20I from the 18-month data collection.

Table 254: The atomic coordinates of the tetrameric phase of the fixed core refinement of ZAA20I from the 18-month data collection.

Atom Label	Atom Type	Multiplicity	Fractional X Coordinate	Fractional Y Coordinate	Fractional Z Coordinate	Fractional Occupancy
O1	O	1	0.5150056	0.4849944	0.4816137	1
O2	O	1	0.4849944	0.4849944	0.5183863	1
O3	O	1	0.5150056	0.5150056	0.5183863	1
O4	O	1	0.4849944	0.5150056	0.4816137	1
O5	O	1	0.5000000	0.5307873	0.5452296	1
O6	O	1	0.5000000	0.4692127	0.5452296	1
O7	O	1	0.4692127	0.5000000	0.4547704	1
O8	O	1	0.5307873	0.5000000	0.4547704	1
O9	O	1	0.51337	0.4592223	0.5000000	1
O10	O	1	0.4592223	0.48663	0.5000000	1
O11	O	1	0.5407777	0.51337	0.5000000	1
O12	O	1	0.48663	0.5407777	0.5000000	1
O13	O	1	0.4592223	0.51337	0.5000000	1
O14	O	1	0.5407777	0.48663	0.5000000	1
O15	O	1	0.48663	0.4592223	0.5000000	1
O16	O	1	0.51337	0.5407777	0.5000000	1
O17	O	1	0.5150056	0.4849944	0.5183863	1
O18	O	1	0.4849944	0.4849944	0.4816137	1
O19	O	1	0.5150056	0.5150056	0.4816137	1
O20	O	1	0.4849944	0.5150056	0.5183863	1
O21	O	1	0.5000000	0.5307873	0.4547704	1
O22	O	1	0.5000000	0.4692127	0.4547704	1
O23	O	1	0.4692127	0.5000000	0.5452296	1
O24	O	1	0.5307873	0.5000000	0.5452296	1
Zr1	Zr	1	0.5000000	0.4751336	0.5000000	1
Zr2	Zr	1	0.4751336	0.5000000	0.5000000	1
Zr3	Zr	1	0.5248664	0.5000000	0.5000000	1
Zr4	Zr	1	0.5000000	0.5248664	0.5000000	1

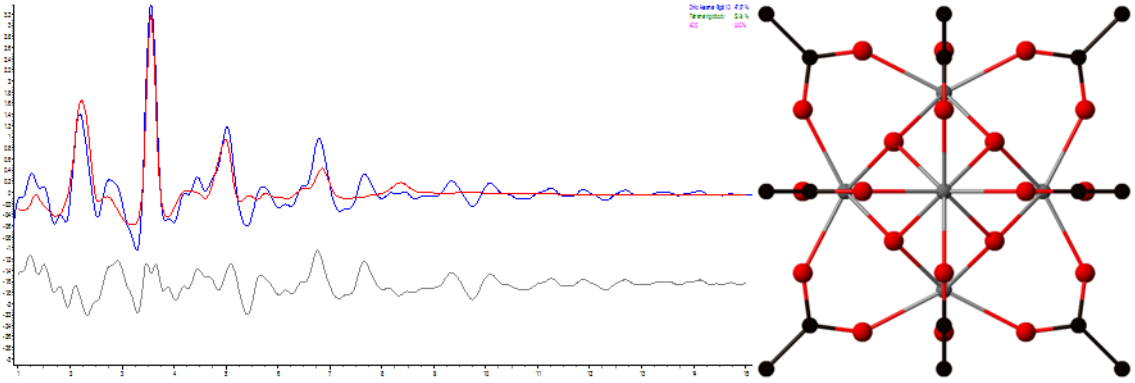

Figure 312: Observed and Calculated PDF from the fixed core refinement of ZAA24A from the 18-month data collection and the resultant model.

Table 255: The atomic coordinates of the model resulting from the fixed core refinement of ZAA24A from the 18-month data collection.

Atom Label	Atom Type	Multiplicity	Fractional X Coordinate	Fractional Y Coordinate	Fractional Z Coordinate	Fractional Occupancy
C1	C	1	0.5903369	0.5000000	0.5835679	1
C2	C	1	0.5000000	0.4096631	0.5835679	1
C3	C	1	0.4096631	0.5000000	0.5835679	1
C4	C	1	0.5000000	0.5903369	0.5835679	1
C5	C	1	0.5903369	0.5000000	0.4164321	1
C6	C	1	0.5000000	0.4096631	0.4164321	1
C7	C	1	0.4096631	0.5000000	0.4164321	1
C8	C	1	0.5000000	0.5903369	0.4164321	1
C9	C	1	0.5903369	0.4096631	0.5000000	1
C10	C	1	0.4096631	0.4096631	0.5000000	1
C11	C	1	0.4096631	0.5903369	0.5000000	1
C12	C	1	0.5903369	0.5903369	0.5000000	1
C13	C	1	0.6196152	0.5000000	0.6106524	1
C14	C	1	0.5000000	0.3803848	0.6106524	1
C15	C	1	0.3803848	0.5000000	0.6106524	1
C16	C	1	0.5000000	0.6196152	0.6106524	1
C17	C	1	0.6196152	0.5000000	0.3893476	1
C18	C	1	0.5000000	0.3803848	0.3893476	1
C19	C	1	0.3803848	0.5000000	0.3893476	1
C20	C	1	0.5000000	0.6196152	0.3893476	1
C21	C	1	0.6196152	0.3803848	0.5000000	1
C22	C	1	0.3803848	0.3803848	0.5000000	1
C23	C	1	0.3803848	0.6196152	0.5000000	1
C24	C	1	0.6196152	0.6196152	0.5000000	1
O1	O	1	0.5338867	0.5335561	0.4686524	1
O2	O	1	0.5338867	0.4664439	0.5313476	1
O3	O	1	0.4661133	0.5335561	0.4686524	1
O4	O	1	0.4661133	0.4664439	0.5313476	1
O5	O	1	0.4661133	0.4664439	0.4686524	1
O6	O	1	0.4661133	0.5335561	0.5313476	1

O7	O	1	0.5338867	0.4664439	0.4686524	1
O8	O	1	0.5338867	0.5335561	0.5313476	1
O9	O	1	0.5949718	0.5000000	0.5508646	1
O10	O	1	0.5949718	0.4450154	0.5000000	1
O11	O	1	0.5949718	0.5000000	0.4491354	1
O12	O	1	0.5949718	0.5549846	0.5000000	1
O13	O	1	0.5000000	0.5949718	0.5508646	1
O14	O	1	0.5549846	0.5949718	0.5000000	1
O15	O	1	0.5000000	0.5949718	0.4491354	1
O16	O	1	0.4450154	0.5949718	0.5000000	1
O17	O	1	0.4050282	0.5000000	0.5508646	1
O18	O	1	0.4050282	0.5549846	0.5000000	1
O19	O	1	0.4050282	0.5000000	0.4491354	1
O20	O	1	0.4050282	0.4450154	0.5000000	1
O21	O	1	0.5000000	0.4050282	0.5508646	1
O22	O	1	0.4450154	0.4050282	0.5000000	1
O23	O	1	0.5000000	0.4050282	0.4491354	1
O24	O	1	0.5549846	0.4050282	0.5000000	1
O25	O	1	0.5549846	0.5000000	0.5878556	1
O26	O	1	0.5000000	0.5549846	0.5878556	1
O27	O	1	0.4450154	0.5000000	0.5878556	1
O28	O	1	0.5000000	0.4450154	0.5878556	1
O29	O	1	0.5549846	0.5000000	0.4121444	1
O30	O	1	0.5000000	0.4450154	0.4121444	1
O31	O	1	0.4450154	0.5000000	0.4121444	1
O32	O	1	0.5000000	0.5549846	0.4121444	1
Zr1	Zr	1	0.5665806	0.5000000	0.5000000	1
Zr2	Zr	1	0.5000000	0.5665806	0.5000000	1
Zr3	Zr	1	0.4334194	0.5000000	0.5000000	1
Zr4	Zr	1	0.5000000	0.4334194	0.5000000	1
Zr5	Zr	1	0.5000000	0.5000000	0.5615917	1
Zr6	Zr	1	0.5000000	0.5000000	0.4384083	1

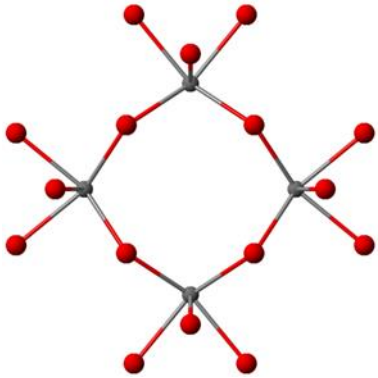

Figure 313: The tetrameric structure resulting from the fixed core refinement of ZAA24A from the 18-month data collection.

Table 256: The atomic coordinates of the tetrameric phase of the fixed core refinement of ZAA24A from the 18-month data collection.

Atom Label	Atom Type	Multiplicity	Fractional X Coordinate	Fractional Y Coordinate	Fractional Z Coordinate	Fractional Occupancy
O1	O	1	0.514965	0.485035	0.4794992	1
O2	O	1	0.485035	0.485035	0.5205008	1
O3	O	1	0.514965	0.514965	0.5205008	1
O4	O	1	0.485035	0.514965	0.4794992	1
O5	O	1	0.5000000	0.5316249	0.5404388	1
O6	O	1	0.5000000	0.4683751	0.5404388	1
O7	O	1	0.4683751	0.5000000	0.4595612	1
O8	O	1	0.5316249	0.5000000	0.4595612	1
O9	O	1	0.5131592	0.4592027	0.5000000	1
O10	O	1	0.4592027	0.4868408	0.5000000	1
O11	O	1	0.5407973	0.5131592	0.5000000	1
O12	O	1	0.4868408	0.5407973	0.5000000	1
O13	O	1	0.4592027	0.5131592	0.5000000	1
O14	O	1	0.5407973	0.4868408	0.5000000	1
O15	O	1	0.4868408	0.4592027	0.5000000	1
O16	O	1	0.5131592	0.5407973	0.5000000	1
O17	O	1	0.514965	0.485035	0.5205008	1
O18	O	1	0.485035	0.485035	0.4794992	1
O19	O	1	0.514965	0.514965	0.4794992	1
O20	O	1	0.485035	0.514965	0.5205008	1
O21	O	1	0.5000000	0.5316249	0.4595612	1
O22	O	1	0.5000000	0.4683751	0.4595612	1
O23	O	1	0.4683751	0.5000000	0.5404388	1
O24	O	1	0.5316249	0.5000000	0.5404388	1
Zr1	Zr	1	0.5000000	0.4752469	0.5000000	1
Zr2	Zr	1	0.4752469	0.5000000	0.5000000	1
Zr3	Zr	1	0.5247531	0.5000000	0.5000000	1
Zr4	Zr	1	0.5000000	0.5247531	0.5000000	1

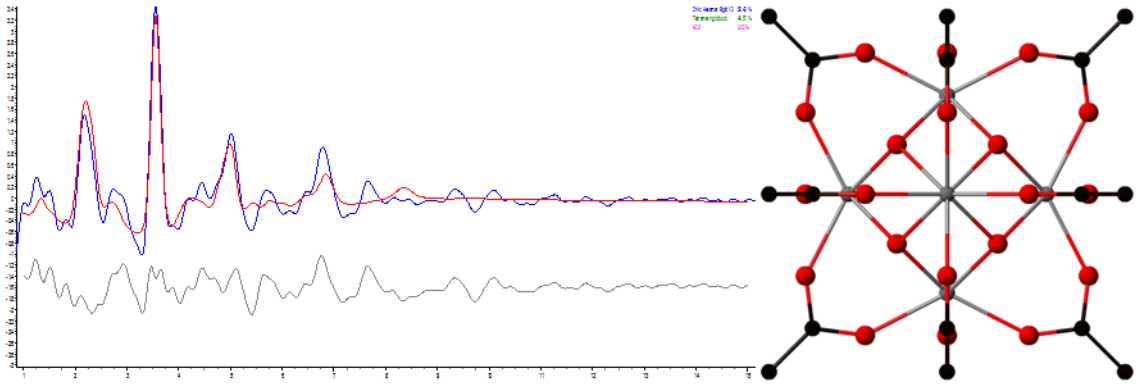

Figure 314: Observed and Calculated PDF from the fixed core refinement of ZAA24C from the 18-month data collection and the resultant model.

Table 257: The atomic coordinates of the model resulting from the fixed core refinement of ZAA24C from the 18-month data collection.

Atom Label	Atom Type	Multiplicity	Fractional X Coordinate	Fractional Y Coordinate	Fractional Z Coordinate	Fractional Occupancy
C1	C	1	0.5903313	0.5000000	0.5835628	1
C2	C	1	0.5000000	0.4096687	0.5835628	1
C3	C	1	0.4096687	0.5000000	0.5835628	1
C4	C	1	0.5000000	0.5903313	0.5835628	1
C5	C	1	0.5903313	0.5000000	0.4164372	1
C6	C	1	0.5000000	0.4096687	0.4164372	1
C7	C	1	0.4096687	0.5000000	0.4164372	1
C8	C	1	0.5000000	0.5903313	0.4164372	1
C9	C	1	0.5903313	0.4096687	0.5000000	1
C10	C	1	0.4096687	0.4096687	0.5000000	1
C11	C	1	0.4096687	0.5903313	0.5000000	1
C12	C	1	0.5903313	0.5903313	0.5000000	1
C13	C	1	0.6195111	0.5000000	0.6105561	1
C14	C	1	0.5000000	0.3804889	0.6105561	1
C15	C	1	0.3804889	0.5000000	0.6105561	1
C16	C	1	0.5000000	0.6195111	0.6105561	1
C17	C	1	0.6195111	0.5000000	0.3894439	1
C18	C	1	0.5000000	0.3804889	0.3894439	1
C19	C	1	0.3804889	0.5000000	0.3894439	1
C20	C	1	0.5000000	0.6195111	0.3894439	1
C21	C	1	0.6195111	0.3804889	0.5000000	1
C22	C	1	0.3804889	0.3804889	0.5000000	1
C23	C	1	0.3804889	0.6195111	0.5000000	1
C24	C	1	0.6195111	0.6195111	0.5000000	1
O1	O	1	0.5337896	0.5334599	0.4687423	1
O2	O	1	0.5337896	0.4665401	0.5312577	1
O3	O	1	0.4662104	0.5334599	0.4687423	1
O4	O	1	0.4662104	0.4665401	0.5312577	1
O5	O	1	0.4662104	0.4665401	0.4687423	1
O6	O	1	0.4662104	0.5334599	0.5312577	1

O7	O	1	0.5337896	0.4665401	0.4687423	1
O8	O	1	0.5337896	0.5334599	0.5312577	1
O9	O	1	0.5948854	0.5000000	0.5508555	1
O10	O	1	0.5948854	0.4450253	0.5000000	1
O11	O	1	0.5948854	0.5000000	0.4491445	1
O12	O	1	0.5948854	0.5549747	0.5000000	1
O13	O	1	0.5000000	0.5948854	0.5508555	1
O14	O	1	0.5549747	0.5948854	0.5000000	1
O15	O	1	0.5000000	0.5948854	0.4491445	1
O16	O	1	0.4450253	0.5948854	0.5000000	1
O17	O	1	0.4051146	0.5000000	0.5508555	1
O18	O	1	0.4051146	0.5549747	0.5000000	1
O19	O	1	0.4051146	0.5000000	0.4491445	1
O20	O	1	0.4051146	0.4450253	0.5000000	1
O21	O	1	0.5000000	0.4051146	0.5508555	1
O22	O	1	0.4450253	0.4051146	0.5000000	1
O23	O	1	0.5000000	0.4051146	0.4491445	1
O24	O	1	0.5549747	0.4051146	0.5000000	1
O25	O	1	0.5549747	0.5000000	0.5877756	1
O26	O	1	0.5000000	0.5549747	0.5877756	1
O27	O	1	0.4450253	0.5000000	0.5877756	1
O28	O	1	0.5000000	0.4450253	0.5877756	1
O29	O	1	0.5549747	0.5000000	0.4122244	1
O30	O	1	0.5000000	0.4450253	0.4122244	1
O31	O	1	0.4450253	0.5000000	0.4122244	1
O32	O	1	0.5000000	0.5549747	0.4122244	1
Zr1	Zr	1	0.5665322	0.5000000	0.5000000	1
Zr2	Zr	1	0.5000000	0.5665322	0.5000000	1
Zr3	Zr	1	0.4334678	0.5000000	0.5000000	1
Zr4	Zr	1	0.5000000	0.4334678	0.5000000	1
Zr5	Zr	1	0.5000000	0.5000000	0.5615469	1
Zr6	Zr	1	0.5000000	0.5000000	0.4384531	1

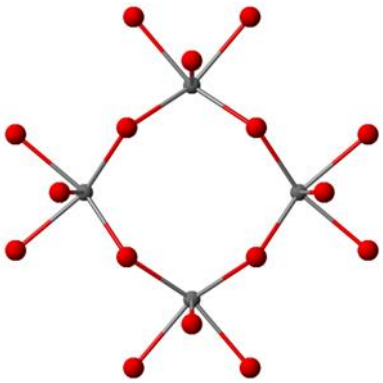

Figure 315: The tetrameric structure resulting from the fixed core refinement of ZAA24C from the 18-month data collection.

Table 258: The atomic coordinates of the tetrameric phase of the fixed core refinement of ZAA24C from the 18-month data collection.

Atom Label	Atom Type	Multiplicity	Fractional X Coordinate	Fractional Y Coordinate	Fractional Z Coordinate	Fractional Occupancy
O1	O	1	0.5149506	0.4850494	0.4805666	1
O2	O	1	0.4850494	0.4850494	0.5194334	1
O3	O	1	0.5149506	0.5149506	0.5194334	1
O4	O	1	0.4850494	0.5149506	0.4805666	1
O5	O	1	0.5000000	0.5305539	0.5448563	1
O6	O	1	0.5000000	0.4694461	0.5448563	1
O7	O	1	0.4694461	0.5000000	0.4551437	1
O8	O	1	0.5305539	0.5000000	0.4551437	1
O9	O	1	0.5134736	0.4592847	0.5000000	1
O10	O	1	0.4592847	0.4865264	0.5000000	1
O11	O	1	0.5407153	0.5134736	0.5000000	1
O12	O	1	0.4865264	0.5407153	0.5000000	1
O13	O	1	0.4592847	0.5134736	0.5000000	1
O14	O	1	0.5407153	0.4865264	0.5000000	1
O15	O	1	0.4865264	0.4592847	0.5000000	1
O16	O	1	0.5134736	0.5407153	0.5000000	1
O17	O	1	0.5149506	0.4850494	0.5194334	1
O18	O	1	0.4850494	0.4850494	0.4805666	1
O19	O	1	0.5149506	0.5149506	0.4805666	1
O20	O	1	0.4850494	0.5149506	0.5194334	1
O21	O	1	0.5000000	0.5305539	0.4551437	1
O22	O	1	0.5000000	0.4694461	0.4551437	1
O23	O	1	0.4694461	0.5000000	0.5448563	1
O24	O	1	0.5305539	0.5000000	0.5448563	1
Zr1	Zr	1	0.5000000	0.475221	0.5000000	1
Zr2	Zr	1	0.475221	0.5000000	0.5000000	1
Zr3	Zr	1	0.524779	0.5000000	0.5000000	1
Zr4	Zr	1	0.5000000	0.524779	0.5000000	1

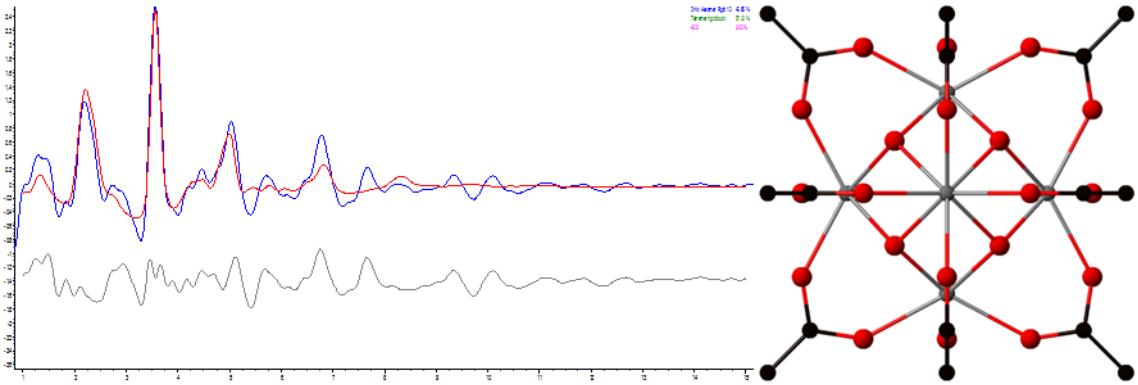

Figure 316: Observed and Calculated PDF from the fixed core refinement of ZAA24I from the 18-month data collection and the resultant model.

Table 259: The atomic coordinates of the model resulting from the fixed core refinement of ZAA24I from the 18-month data collection.

Atom Label	Atom Type	Multiplicity	Fractional X Coordinate	Fractional Y Coordinate	Fractional Z Coordinate	Fractional Occupancy
C1	C	1	0.5905838	0.5000000	0.5837964	1
C2	C	1	0.5000000	0.4094162	0.5837964	1
C3	C	1	0.4094162	0.5000000	0.5837964	1
C4	C	1	0.5000000	0.5905838	0.5837964	1
C5	C	1	0.5905838	0.5000000	0.4162036	1
C6	C	1	0.5000000	0.4094162	0.4162036	1
C7	C	1	0.4094162	0.5000000	0.4162036	1
C8	C	1	0.5000000	0.5905838	0.4162036	1
C9	C	1	0.5905838	0.4094162	0.5000000	1
C10	C	1	0.4094162	0.4094162	0.5000000	1
C11	C	1	0.4094162	0.5905838	0.5000000	1
C12	C	1	0.5905838	0.5905838	0.5000000	1
C13	C	1	0.618527	0.5000000	0.6096457	1
C14	C	1	0.5000000	0.381473	0.6096457	1
C15	C	1	0.381473	0.5000000	0.6096457	1
C16	C	1	0.5000000	0.618527	0.6096457	1
C17	C	1	0.618527	0.5000000	0.3903543	1
C18	C	1	0.5000000	0.381473	0.3903543	1
C19	C	1	0.381473	0.5000000	0.3903543	1
C20	C	1	0.5000000	0.618527	0.3903543	1
C21	C	1	0.618527	0.381473	0.5000000	1
C22	C	1	0.381473	0.381473	0.5000000	1
C23	C	1	0.381473	0.618527	0.5000000	1
C24	C	1	0.618527	0.618527	0.5000000	1
O1	O	1	0.5348372	0.5344973	0.4677732	1
O2	O	1	0.5348372	0.4655027	0.5322268	1
O3	O	1	0.4651628	0.5344973	0.4677732	1
O4	O	1	0.4651628	0.4655027	0.5322268	1
O5	O	1	0.4651628	0.4655027	0.4677732	1
O6	O	1	0.4651628	0.5344973	0.5322268	1

O7	O	1	0.5348372	0.4655027	0.4677732	1
O8	O	1	0.5348372	0.5344973	0.5322268	1
O9	O	1	0.5961275	0.5000000	0.5511319	1
O10	O	1	0.5961275	0.4447265	0.5000000	1
O11	O	1	0.5961275	0.5000000	0.4488681	1
O12	O	1	0.5961275	0.5552735	0.5000000	1
O13	O	1	0.5000000	0.5961275	0.5511319	1
O14	O	1	0.5552735	0.5961275	0.5000000	1
O15	O	1	0.5000000	0.5961275	0.4488681	1
O16	O	1	0.4447265	0.5961275	0.5000000	1
O17	O	1	0.4038725	0.5000000	0.5511319	1
O18	O	1	0.4038725	0.5552735	0.5000000	1
O19	O	1	0.4038725	0.5000000	0.4488681	1
O20	O	1	0.4038725	0.4447265	0.5000000	1
O21	O	1	0.5000000	0.4038725	0.5511319	1
O22	O	1	0.4447265	0.4038725	0.5000000	1
O23	O	1	0.5000000	0.4038725	0.4488681	1
O24	O	1	0.5552735	0.4038725	0.5000000	1
O25	O	1	0.5552735	0.5000000	0.5889247	1
O26	O	1	0.5000000	0.5552735	0.5889247	1
O27	O	1	0.4447265	0.5000000	0.5889247	1
O28	O	1	0.5000000	0.4447265	0.5889247	1
O29	O	1	0.5552735	0.5000000	0.4110753	1
O30	O	1	0.5000000	0.4447265	0.4110753	1
O31	O	1	0.4447265	0.5000000	0.4110753	1
O32	O	1	0.5000000	0.5552735	0.4110753	1
Zr1	Zr	1	0.5665067	0.5000000	0.5000000	1
Zr2	Zr	1	0.5000000	0.5665067	0.5000000	1
Zr3	Zr	1	0.4334933	0.5000000	0.5000000	1
Zr4	Zr	1	0.5000000	0.4334933	0.5000000	1
Zr5	Zr	1	0.5000000	0.5000000	0.5615234	1
Zr6	Zr	1	0.5000000	0.5000000	0.4384766	1

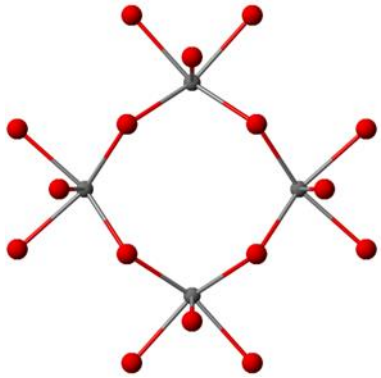

Figure 317: The tetrameric structure resulting from the fixed core refinement of ZAA24I from the 18-month data collection.

Table 260: The atomic coordinates of the tetrameric phase of the fixed core refinement of ZAA24I from the 18-month data collection.

Atom Label	Atom Type	Multiplicity	Fractional X Coordinate	Fractional Y Coordinate	Fractional Z Coordinate	Fractional Occupancy
O1	O	1	0.5150409	0.4849591	0.4800258	1
O2	O	1	0.4849591	0.4849591	0.5199742	1
O3	O	1	0.5150409	0.5150409	0.5199742	1
O4	O	1	0.4849591	0.5150409	0.4800258	1
O5	O	1	0.5000000	0.5307479	0.5452153	1
O6	O	1	0.5000000	0.4692521	0.5452153	1
O7	O	1	0.4692521	0.5000000	0.4547847	1
O8	O	1	0.5307479	0.5000000	0.4547847	1
O9	O	1	0.5139594	0.4595667	0.5000000	1
O10	O	1	0.4595667	0.4860406	0.5000000	1
O11	O	1	0.5404333	0.5139594	0.5000000	1
O12	O	1	0.4860406	0.5404333	0.5000000	1
O13	O	1	0.4595667	0.5139594	0.5000000	1
O14	O	1	0.5404333	0.4860406	0.5000000	1
O15	O	1	0.4860406	0.4595667	0.5000000	1
O16	O	1	0.5139594	0.5404333	0.5000000	1
O17	O	1	0.5150409	0.4849591	0.5199742	1
O18	O	1	0.4849591	0.4849591	0.4800258	1
O19	O	1	0.5150409	0.5150409	0.4800258	1
O20	O	1	0.4849591	0.5150409	0.5199742	1
O21	O	1	0.5000000	0.5307479	0.4547847	1
O22	O	1	0.5000000	0.4692521	0.4547847	1
O23	O	1	0.4692521	0.5000000	0.5452153	1
O24	O	1	0.5307479	0.5000000	0.5452153	1
Zr1	Zr	1	0.5000000	0.4751949	0.5000000	1
Zr2	Zr	1	0.4751949	0.5000000	0.5000000	1
Zr3	Zr	1	0.5248051	0.5000000	0.5000000	1
Zr4	Zr	1	0.5000000	0.5248051	0.5000000	1

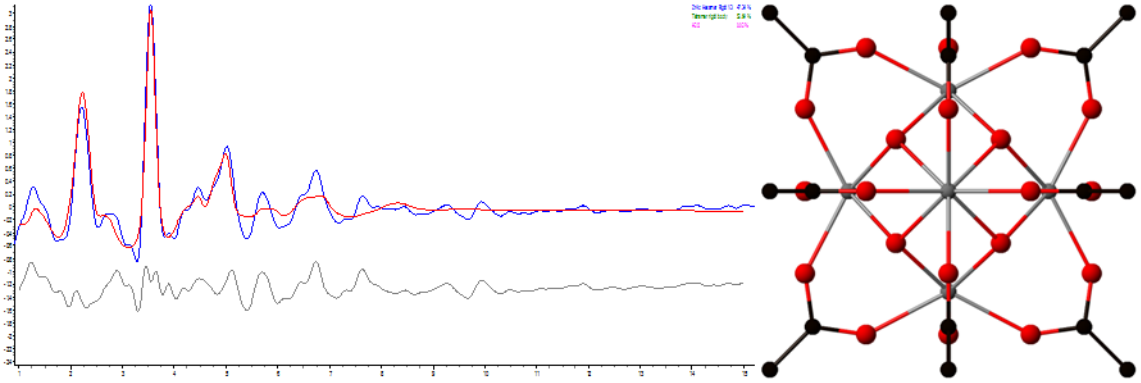

Figure 318: Observed and Calculated PDF from the fixed core refinement of ZAA25A from the 18-month data collection and the resultant model.

Table 261: The atomic coordinates of the model resulting from the fixed core refinement of ZAA25A from the 18-month data collection.

Atom Label	Atom Type	Multiplicity	Fractional X Coordinate	Fractional Y Coordinate	Fractional Z Coordinate	Fractional Occupancy
C1	C	1	0.5895643	0.5000000	0.5828533	1
C2	C	1	0.5000000	0.4104357	0.5828533	1
C3	C	1	0.4104357	0.5000000	0.5828533	1
C4	C	1	0.5000000	0.5895643	0.5828533	1
C5	C	1	0.5895643	0.5000000	0.4171467	1
C6	C	1	0.5000000	0.4104357	0.4171467	1
C7	C	1	0.4104357	0.5000000	0.4171467	1
C8	C	1	0.5000000	0.5895643	0.4171467	1
C9	C	1	0.5895643	0.4104357	0.5000000	1
C10	C	1	0.4104357	0.4104357	0.5000000	1
C11	C	1	0.4104357	0.5895643	0.5000000	1
C12	C	1	0.5895643	0.5895643	0.5000000	1
C13	C	1	0.6179425	0.5000000	0.6091051	1
C14	C	1	0.5000000	0.3820575	0.6091051	1
C15	C	1	0.3820575	0.5000000	0.6091051	1
C16	C	1	0.5000000	0.6179425	0.6091051	1
C17	C	1	0.6179425	0.5000000	0.3908949	1
C18	C	1	0.5000000	0.3820575	0.3908949	1
C19	C	1	0.3820575	0.5000000	0.3908949	1
C20	C	1	0.5000000	0.6179425	0.3908949	1
C21	C	1	0.6179425	0.3820575	0.5000000	1
C22	C	1	0.3820575	0.3820575	0.5000000	1
C23	C	1	0.3820575	0.6179425	0.5000000	1
C24	C	1	0.6179425	0.6179425	0.5000000	1
O1	O	1	0.5345859	0.5342485	0.4680056	1
O2	O	1	0.5345859	0.4657515	0.5319944	1
O3	O	1	0.4654141	0.5342485	0.4680056	1
O4	O	1	0.4654141	0.4657515	0.5319944	1
O5	O	1	0.4654141	0.4657515	0.4680056	1
O6	O	1	0.4654141	0.5342485	0.5319944	1

O7	O	1	0.5345859	0.4657515	0.4680056	1
O8	O	1	0.5345859	0.5342485	0.5319944	1
O9	O	1	0.5947119	0.5000000	0.5502362	1
O10	O	1	0.5947119	0.4456946	0.5000000	1
O11	O	1	0.5947119	0.5000000	0.4497638	1
O12	O	1	0.5947119	0.5543054	0.5000000	1
O13	O	1	0.5000000	0.5947119	0.5502362	1
O14	O	1	0.5543054	0.5947119	0.5000000	1
O15	O	1	0.5000000	0.5947119	0.4497638	1
O16	O	1	0.4456946	0.5947119	0.5000000	1
O17	O	1	0.4052881	0.5000000	0.5502362	1
O18	O	1	0.4052881	0.5543054	0.5000000	1
O19	O	1	0.4052881	0.5000000	0.4497638	1
O20	O	1	0.4052881	0.4456946	0.5000000	1
O21	O	1	0.5000000	0.4052881	0.5502362	1
O22	O	1	0.4456946	0.4052881	0.5000000	1
O23	O	1	0.5000000	0.4052881	0.4497638	1
O24	O	1	0.5543054	0.4052881	0.5000000	1
O25	O	1	0.5543054	0.5000000	0.5876152	1
O26	O	1	0.5000000	0.5543054	0.5876152	1
O27	O	1	0.4456946	0.5000000	0.5876152	1
O28	O	1	0.5000000	0.4456946	0.5876152	1
O29	O	1	0.5543054	0.5000000	0.4123848	1
O30	O	1	0.5000000	0.4456946	0.4123848	1
O31	O	1	0.4456946	0.5000000	0.4123848	1
O32	O	1	0.5000000	0.5543054	0.4123848	1
Zr1	Zr	1	0.5662592	0.5000000	0.5000000	1
Zr2	Zr	1	0.5000000	0.5662592	0.5000000	1
Zr3	Zr	1	0.4337408	0.5000000	0.5000000	1
Zr4	Zr	1	0.5000000	0.4337408	0.5000000	1
Zr5	Zr	1	0.5000000	0.5000000	0.5612943	1
Zr6	Zr	1	0.5000000	0.5000000	0.4387057	1

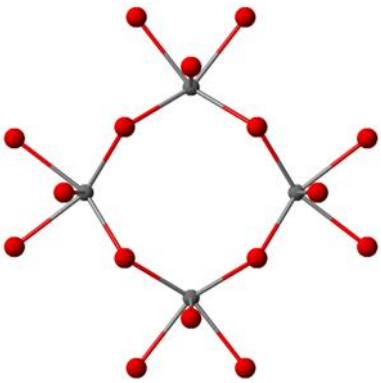

Figure 319: The tetrameric structure resulting from the fixed core refinement of ZAA25A from the 18-month data collection.

Table 262: The atomic coordinates of the tetrameric phase of the fixed core refinement of ZAA25A from the 18-month data collection.

Atom Label	Atom Type	Multiplicity	Fractional X Coordinate	Fractional Y Coordinate	Fractional Z Coordinate	Fractional Occupancy
O1	O	1	0.5154495	0.4845505	0.4831725	1
O2	O	1	0.4845505	0.4845505	0.5168275	1
O3	O	1	0.5154495	0.5154495	0.5168275	1
O4	O	1	0.4845505	0.5154495	0.4831725	1
O5	O	1	0.5000000	0.5296391	0.545764	1
O6	O	1	0.5000000	0.4703609	0.545764	1
O7	O	1	0.4703609	0.5000000	0.454236	1
O8	O	1	0.5296391	0.5000000	0.454236	1
O9	O	1	0.5127317	0.4587794	0.5000000	1
O10	O	1	0.4587794	0.4872683	0.5000000	1
O11	O	1	0.5412206	0.5127317	0.5000000	1
O12	O	1	0.4872683	0.5412206	0.5000000	1
O13	O	1	0.4587794	0.5127317	0.5000000	1
O14	O	1	0.5412206	0.4872683	0.5000000	1
O15	O	1	0.4872683	0.4587794	0.5000000	1
O16	O	1	0.5127317	0.5412206	0.5000000	1
O17	O	1	0.5154495	0.4845505	0.5168275	1
O18	O	1	0.4845505	0.4845505	0.4831725	1
O19	O	1	0.5154495	0.5154495	0.4831725	1
O20	O	1	0.4845505	0.5154495	0.5168275	1
O21	O	1	0.5000000	0.5296391	0.454236	1
O22	O	1	0.5000000	0.4703609	0.454236	1
O23	O	1	0.4703609	0.5000000	0.545764	1
O24	O	1	0.5296391	0.5000000	0.545764	1
Zr1	Zr	1	0.5000000	0.4752923	0.5000000	1
Zr2	Zr	1	0.4752923	0.5000000	0.5000000	1
Zr3	Zr	1	0.5247077	0.5000000	0.5000000	1
Zr4	Zr	1	0.5000000	0.5247077	0.5000000	1

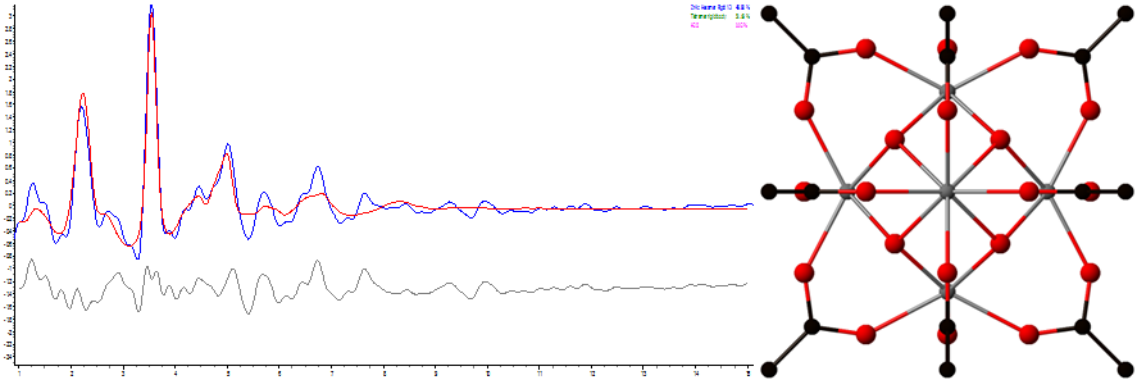

Figure 320: Observed and Calculated PDF from the fixed core refinement of ZAA25C from the 18-month data collection and the resultant model.

Table 263: The atomic coordinates of the model resulting from the fixed core refinement of ZAA25C from the 18-month data collection.

Atom Label	Atom Type	Multiplicity	Fractional X Coordinate	Fractional Y Coordinate	Fractional Z Coordinate	Fractional Occupancy
C1	C	1	0.5896023	0.5000000	0.5828884	1
C2	C	1	0.5000000	0.4103977	0.5828884	1
C3	C	1	0.4103977	0.5000000	0.5828884	1
C4	C	1	0.5000000	0.5896023	0.5828884	1
C5	C	1	0.5896023	0.5000000	0.4171116	1
C6	C	1	0.5000000	0.4103977	0.4171116	1
C7	C	1	0.4103977	0.5000000	0.4171116	1
C8	C	1	0.5000000	0.5896023	0.4171116	1
C9	C	1	0.5896023	0.4103977	0.5000000	1
C10	C	1	0.4103977	0.4103977	0.5000000	1
C11	C	1	0.4103977	0.5896023	0.5000000	1
C12	C	1	0.5896023	0.5896023	0.5000000	1
C13	C	1	0.6180478	0.5000000	0.6092025	1
C14	C	1	0.5000000	0.3819522	0.6092025	1
C15	C	1	0.3819522	0.5000000	0.6092025	1
C16	C	1	0.5000000	0.6180478	0.6092025	1
C17	C	1	0.6180478	0.5000000	0.3907975	1
C18	C	1	0.5000000	0.3819522	0.3907975	1
C19	C	1	0.3819522	0.5000000	0.3907975	1
C20	C	1	0.5000000	0.6180478	0.3907975	1
C21	C	1	0.6180478	0.3819522	0.5000000	1
C22	C	1	0.3819522	0.3819522	0.5000000	1
C23	C	1	0.3819522	0.6180478	0.5000000	1
C24	C	1	0.6180478	0.6180478	0.5000000	1
O1	O	1	0.5349225	0.5345818	0.4676942	1
O2	O	1	0.5349225	0.4654182	0.5323058	1
O3	O	1	0.4650775	0.5345818	0.4676942	1
O4	O	1	0.4650775	0.4654182	0.5323058	1
O5	O	1	0.4650775	0.4654182	0.4676942	1
O6	O	1	0.4650775	0.5345818	0.5323058	1

O7	O	1	0.5349225	0.4654182	0.4676942	1
O8	O	1	0.5349225	0.5345818	0.5323058	1
O9	O	1	0.5946966	0.5000000	0.5499389	1
O10	O	1	0.5946966	0.4460161	0.5000000	1
O11	O	1	0.5946966	0.5000000	0.4500611	1
O12	O	1	0.5946966	0.5539839	0.5000000	1
O13	O	1	0.5000000	0.5946966	0.5499389	1
O14	O	1	0.5539839	0.5946966	0.5000000	1
O15	O	1	0.5000000	0.5946966	0.4500611	1
O16	O	1	0.4460161	0.5946966	0.5000000	1
O17	O	1	0.4053034	0.5000000	0.5499389	1
O18	O	1	0.4053034	0.5539839	0.5000000	1
O19	O	1	0.4053034	0.5000000	0.4500611	1
O20	O	1	0.4053034	0.4460161	0.5000000	1
O21	O	1	0.5000000	0.4053034	0.5499389	1
O22	O	1	0.4460161	0.4053034	0.5000000	1
O23	O	1	0.5000000	0.4053034	0.4500611	1
O24	O	1	0.5539839	0.4053034	0.5000000	1
O25	O	1	0.5539839	0.5000000	0.587601	1
O26	O	1	0.5000000	0.5539839	0.587601	1
O27	O	1	0.4460161	0.5000000	0.587601	1
O28	O	1	0.5000000	0.4460161	0.587601	1
O29	O	1	0.5539839	0.5000000	0.412399	1
O30	O	1	0.5000000	0.4460161	0.412399	1
O31	O	1	0.4460161	0.5000000	0.412399	1
O32	O	1	0.5000000	0.5539839	0.412399	1
Zr1	Zr	1	0.566334	0.5000000	0.5000000	1
Zr2	Zr	1	0.5000000	0.566334	0.5000000	1
Zr3	Zr	1	0.433666	0.5000000	0.5000000	1
Zr4	Zr	1	0.5000000	0.433666	0.5000000	1
Zr5	Zr	1	0.5000000	0.5000000	0.5613636	1
Zr6	Zr	1	0.5000000	0.5000000	0.4386364	1

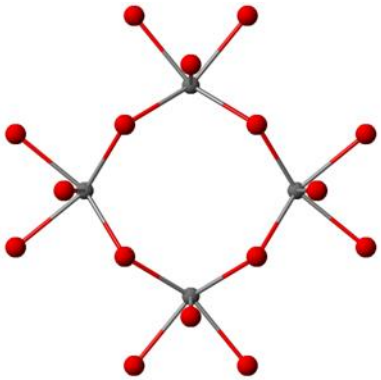

Figure 321: The tetrameric structure resulting from the fixed core refinement of ZAA25C from the 18-month data collection.

Table 264: The atomic coordinates of the tetrameric phase of the fixed core refinement of ZAA25C from the 18-month data collection.

Atom Label	Atom Type	Multiplicity	Fractional X Coordinate	Fractional Y Coordinate	Fractional Z Coordinate	Fractional Occupancy
O1	O	1	0.515414	0.484586	0.481603	1
O2	O	1	0.484586	0.484586	0.518397	1
O3	O	1	0.515414	0.515414	0.518397	1
O4	O	1	0.484586	0.515414	0.481603	1
O5	O	1	0.5000000	0.5295277	0.5457562	1
O6	O	1	0.5000000	0.4704723	0.5457562	1
O7	O	1	0.4704723	0.5000000	0.4542438	1
O8	O	1	0.5295277	0.5000000	0.4542438	1
O9	O	1	0.5132532	0.4590979	0.5000000	1
O10	O	1	0.4590979	0.4867468	0.5000000	1
O11	O	1	0.5409021	0.5132532	0.5000000	1
O12	O	1	0.4867468	0.5409021	0.5000000	1
O13	O	1	0.4590979	0.5132532	0.5000000	1
O14	O	1	0.5409021	0.4867468	0.5000000	1
O15	O	1	0.4867468	0.4590979	0.5000000	1
O16	O	1	0.5132532	0.5409021	0.5000000	1
O17	O	1	0.515414	0.484586	0.518397	1
O18	O	1	0.484586	0.484586	0.481603	1
O19	O	1	0.515414	0.515414	0.481603	1
O20	O	1	0.484586	0.515414	0.518397	1
O21	O	1	0.5000000	0.5295277	0.4542438	1
O22	O	1	0.5000000	0.4704723	0.4542438	1
O23	O	1	0.4704723	0.5000000	0.5457562	1
O24	O	1	0.5295277	0.5000000	0.5457562	1
Zr1	Zr	1	0.5000000	0.4753141	0.5000000	1
Zr2	Zr	1	0.4753141	0.5000000	0.5000000	1
Zr3	Zr	1	0.5246859	0.5000000	0.5000000	1
Zr4	Zr	1	0.5000000	0.5246859	0.5000000	1

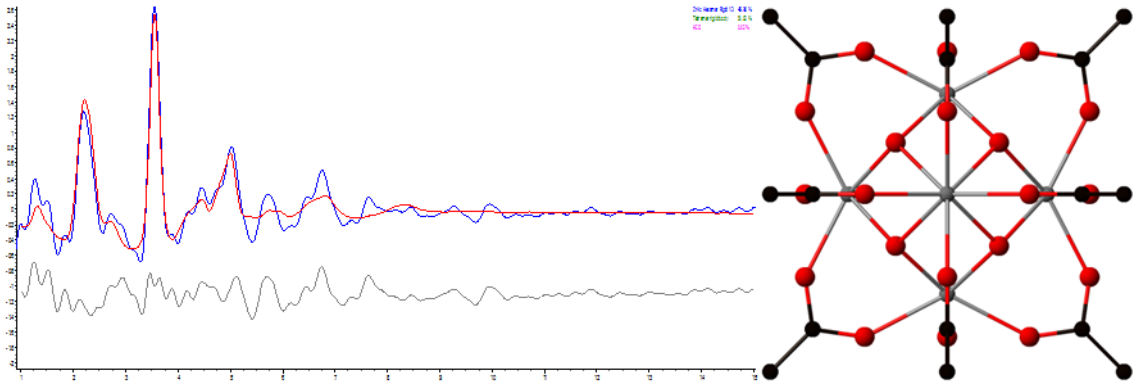

Figure 322: Observed and Calculated PDF from the fixed core refinement of ZAA25I from the 18-month data collection and the resultant model.

Table 265: The atomic coordinates of the model resulting from the fixed core refinement of ZAA25I from the 18-month data collection.

Atom Label	Atom Type	Multiplicity	Fractional X Coordinate	Fractional Y Coordinate	Fractional Z Coordinate	Fractional Occupancy
C1	C	1	0.5899386	0.5000000	0.5831995	1
C2	C	1	0.5000000	0.4100614	0.5831995	1
C3	C	1	0.4100614	0.5000000	0.5831995	1
C4	C	1	0.5000000	0.5899386	0.5831995	1
C5	C	1	0.5899386	0.5000000	0.4168005	1
C6	C	1	0.5000000	0.4100614	0.4168005	1
C7	C	1	0.4100614	0.5000000	0.4168005	1
C8	C	1	0.5000000	0.5899386	0.4168005	1
C9	C	1	0.5899386	0.4100614	0.5000000	1
C10	C	1	0.4100614	0.4100614	0.5000000	1
C11	C	1	0.4100614	0.5899386	0.5000000	1
C12	C	1	0.5899386	0.5899386	0.5000000	1
C13	C	1	0.6182102	0.5000000	0.6093526	1
C14	C	1	0.5000000	0.3817898	0.6093526	1
C15	C	1	0.3817898	0.5000000	0.6093526	1
C16	C	1	0.5000000	0.6182102	0.6093526	1
C17	C	1	0.6182102	0.5000000	0.3906474	1
C18	C	1	0.5000000	0.3817898	0.3906474	1
C19	C	1	0.3817898	0.5000000	0.3906474	1
C20	C	1	0.5000000	0.6182102	0.3906474	1
C21	C	1	0.6182102	0.3817898	0.5000000	1
C22	C	1	0.3817898	0.3817898	0.5000000	1
C23	C	1	0.3817898	0.6182102	0.5000000	1
C24	C	1	0.6182102	0.6182102	0.5000000	1
O1	O	1	0.5345811	0.5342437	0.4680101	1
O2	O	1	0.5345811	0.4657563	0.5319899	1
O3	O	1	0.4654189	0.5342437	0.4680101	1
O4	O	1	0.4654189	0.4657563	0.5319899	1
O5	O	1	0.4654189	0.4657563	0.4680101	1
O6	O	1	0.4654189	0.5342437	0.5319899	1

O7	O	1	0.5345811	0.4657563	0.4680101	1
O8	O	1	0.5345811	0.5342437	0.5319899	1
O9	O	1	0.5950055	0.5000000	0.5509766	1
O10	O	1	0.5950055	0.4448944	0.5000000	1
O11	O	1	0.5950055	0.5000000	0.4490234	1
O12	O	1	0.5950055	0.5551056	0.5000000	1
O13	O	1	0.5000000	0.5950055	0.5509766	1
O14	O	1	0.5551056	0.5950055	0.5000000	1
O15	O	1	0.5000000	0.5950055	0.4490234	1
O16	O	1	0.4448944	0.5950055	0.5000000	1
O17	O	1	0.4049945	0.5000000	0.5509766	1
O18	O	1	0.4049945	0.5551056	0.5000000	1
O19	O	1	0.4049945	0.5000000	0.4490234	1
O20	O	1	0.4049945	0.4448944	0.5000000	1
O21	O	1	0.5000000	0.4049945	0.5509766	1
O22	O	1	0.4448944	0.4049945	0.5000000	1
O23	O	1	0.5000000	0.4049945	0.4490234	1
O24	O	1	0.5551056	0.4049945	0.5000000	1
O25	O	1	0.5551056	0.5000000	0.5878867	1
O26	O	1	0.5000000	0.5551056	0.5878867	1
O27	O	1	0.4448944	0.5000000	0.5878867	1
O28	O	1	0.5000000	0.4448944	0.5878867	1
O29	O	1	0.5551056	0.5000000	0.4121133	1
O30	O	1	0.5000000	0.4448944	0.4121133	1
O31	O	1	0.4448944	0.5000000	0.4121133	1
O32	O	1	0.5000000	0.5551056	0.4121133	1
Zr1	Zr	1	0.56642	0.5000000	0.5000000	1
Zr2	Zr	1	0.5000000	0.56642	0.5000000	1
Zr3	Zr	1	0.43358	0.5000000	0.5000000	1
Zr4	Zr	1	0.5000000	0.43358	0.5000000	1
Zr5	Zr	1	0.5000000	0.5000000	0.5614432	1
Zr6	Zr	1	0.5000000	0.5000000	0.4385568	1

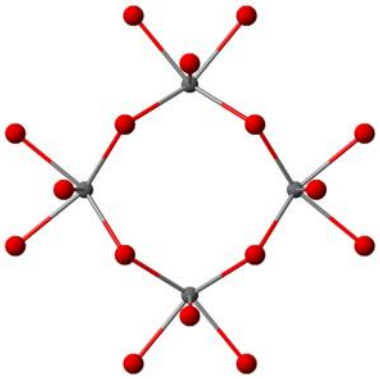

Figure 323: The tetrameric structure resulting from the fixed core refinement of ZAA25I from the 18-month data collection.

Table 266: The atomic coordinates of the tetrameric phase of the fixed core refinement of ZAA25I from the 18-month data collection.

Atom Label	Atom Type	Multiplicity	Fractional X Coordinate	Fractional Y Coordinate	Fractional Z Coordinate	Fractional Occupancy
O1	O	1	0.5152974	0.4847026	0.4802085	1
O2	O	1	0.4847026	0.4847026	0.5197915	1
O3	O	1	0.5152974	0.5152974	0.5197915	1
O4	O	1	0.4847026	0.5152974	0.4802085	1
O5	O	1	0.5000000	0.5296354	0.5453778	1
O6	O	1	0.5000000	0.4703646	0.5453778	1
O7	O	1	0.4703646	0.5000000	0.4546222	1
O8	O	1	0.5296354	0.5000000	0.4546222	1
O9	O	1	0.5132389	0.459079	0.5000000	1
O10	O	1	0.459079	0.4867611	0.5000000	1
O11	O	1	0.540921	0.5132389	0.5000000	1
O12	O	1	0.4867611	0.540921	0.5000000	1
O13	O	1	0.459079	0.5132389	0.5000000	1
O14	O	1	0.540921	0.4867611	0.5000000	1
O15	O	1	0.4867611	0.459079	0.5000000	1
O16	O	1	0.5132389	0.540921	0.5000000	1
O17	O	1	0.5152974	0.4847026	0.5197915	1
O18	O	1	0.4847026	0.4847026	0.4802085	1
O19	O	1	0.5152974	0.5152974	0.4802085	1
O20	O	1	0.4847026	0.5152974	0.5197915	1
O21	O	1	0.5000000	0.5296354	0.4546222	1
O22	O	1	0.5000000	0.4703646	0.4546222	1
O23	O	1	0.4703646	0.5000000	0.5453778	1
O24	O	1	0.5296354	0.5000000	0.5453778	1
Zr1	Zr	1	0.5000000	0.4752709	0.5000000	1
Zr2	Zr	1	0.4752709	0.5000000	0.5000000	1
Zr3	Zr	1	0.5247291	0.5000000	0.5000000	1
Zr4	Zr	1	0.5000000	0.5247291	0.5000000	1

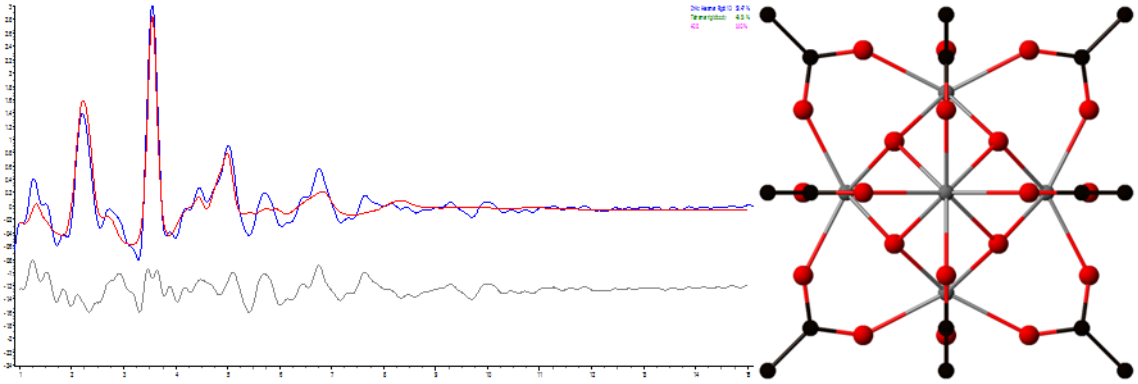

Figure 324: Observed and Calculated PDF from the fixed core refinement of ZAA27A from the 18-month data collection and the resultant model.

Table 267: The atomic coordinates of the model resulting from the fixed core refinement of ZAA27A from the 18-month data collection.

Atom Label	Atom Type	Multiplicity	Fractional X Coordinate	Fractional Y Coordinate	Fractional Z Coordinate	Fractional Occupancy
C1	C	1	0.5898889	0.5000000	0.5831535	1
C2	C	1	0.5000000	0.4101111	0.5831535	1
C3	C	1	0.4101111	0.5000000	0.5831535	1
C4	C	1	0.5000000	0.5898889	0.5831535	1
C5	C	1	0.5898889	0.5000000	0.4168465	1
C6	C	1	0.5000000	0.4101111	0.4168465	1
C7	C	1	0.4101111	0.5000000	0.4168465	1
C8	C	1	0.5000000	0.5898889	0.4168465	1
C9	C	1	0.5898889	0.4101111	0.5000000	1
C10	C	1	0.4101111	0.4101111	0.5000000	1
C11	C	1	0.4101111	0.5898889	0.5000000	1
C12	C	1	0.5898889	0.5898889	0.5000000	1
C13	C	1	0.6183094	0.5000000	0.6094445	1
C14	C	1	0.5000000	0.3816906	0.6094445	1
C15	C	1	0.3816906	0.5000000	0.6094445	1
C16	C	1	0.5000000	0.6183094	0.6094445	1
C17	C	1	0.6183094	0.5000000	0.3905555	1
C18	C	1	0.5000000	0.3816906	0.3905555	1
C19	C	1	0.3816906	0.5000000	0.3905555	1
C20	C	1	0.5000000	0.6183094	0.3905555	1
C21	C	1	0.6183094	0.3816906	0.5000000	1
C22	C	1	0.3816906	0.3816906	0.5000000	1
C23	C	1	0.3816906	0.6183094	0.5000000	1
C24	C	1	0.6183094	0.6183094	0.5000000	1
O1	O	1	0.5344714	0.5341351	0.4681115	1
O2	O	1	0.5344714	0.4658649	0.5318885	1
O3	O	1	0.4655286	0.5341351	0.4681115	1
O4	O	1	0.4655286	0.4658649	0.5318885	1
O5	O	1	0.4655286	0.4658649	0.4681115	1
O6	O	1	0.4655286	0.5341351	0.5318885	1

O7	O	1	0.5344714	0.4658649	0.4681115	1
O8	O	1	0.5344714	0.5341351	0.5318885	1
O9	O	1	0.5946613	0.5000000	0.5509106	1
O10	O	1	0.5946613	0.4449657	0.5000000	1
O11	O	1	0.5946613	0.5000000	0.4490894	1
O12	O	1	0.5946613	0.5550343	0.5000000	1
O13	O	1	0.5000000	0.5946613	0.5509106	1
O14	O	1	0.5550343	0.5946613	0.5000000	1
O15	O	1	0.5000000	0.5946613	0.4490894	1
O16	O	1	0.4449657	0.5946613	0.5000000	1
O17	O	1	0.4053387	0.5000000	0.5509106	1
O18	O	1	0.4053387	0.5550343	0.5000000	1
O19	O	1	0.4053387	0.5000000	0.4490894	1
O20	O	1	0.4053387	0.4449657	0.5000000	1
O21	O	1	0.5000000	0.4053387	0.5509106	1
O22	O	1	0.4449657	0.4053387	0.5000000	1
O23	O	1	0.5000000	0.4053387	0.4490894	1
O24	O	1	0.5550343	0.4053387	0.5000000	1
O25	O	1	0.5550343	0.5000000	0.5875683	1
O26	O	1	0.5000000	0.5550343	0.5875683	1
O27	O	1	0.4449657	0.5000000	0.5875683	1
O28	O	1	0.5000000	0.4449657	0.5875683	1
O29	O	1	0.5550343	0.5000000	0.4124317	1
O30	O	1	0.5000000	0.4449657	0.4124317	1
O31	O	1	0.4449657	0.5000000	0.4124317	1
O32	O	1	0.5000000	0.5550343	0.4124317	1
Zr1	Zr	1	0.5663407	0.5000000	0.5000000	1
Zr2	Zr	1	0.5000000	0.5663407	0.5000000	1
Zr3	Zr	1	0.4336593	0.5000000	0.5000000	1
Zr4	Zr	1	0.5000000	0.4336593	0.5000000	1
Zr5	Zr	1	0.5000000	0.5000000	0.5613698	1
Zr6	Zr	1	0.5000000	0.5000000	0.4386302	1

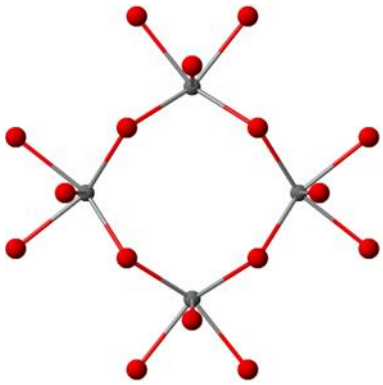

Figure 325: The tetrameric structure resulting from the fixed core refinement of ZAA27A from the 18-month data collection.

Table 268: The atomic coordinates of the tetrameric phase of the fixed core refinement of ZAA27A from the 18-month data collection.

Atom Label	Atom Type	Multiplicity	Fractional X Coordinate	Fractional Y Coordinate	Fractional Z Coordinate	Fractional Occupancy
O1	O	1	0.5152282	0.4847718	0.4811496	1
O2	O	1	0.4847718	0.4847718	0.5188504	1
O3	O	1	0.5152282	0.5152282	0.5188504	1
O4	O	1	0.4847718	0.5152282	0.4811496	1
O5	O	1	0.5000000	0.5296252	0.5453231	1
O6	O	1	0.5000000	0.4703748	0.5453231	1
O7	O	1	0.4703748	0.5000000	0.4546769	1
O8	O	1	0.5296252	0.5000000	0.4546769	1
O9	O	1	0.5129465	0.4588541	0.5000000	1
O10	O	1	0.4588541	0.4870535	0.5000000	1
O11	O	1	0.5411459	0.5129465	0.5000000	1
O12	O	1	0.4870535	0.5411459	0.5000000	1
O13	O	1	0.4588541	0.5129465	0.5000000	1
O14	O	1	0.5411459	0.4870535	0.5000000	1
O15	O	1	0.4870535	0.4588541	0.5000000	1
O16	O	1	0.5129465	0.5411459	0.5000000	1
O17	O	1	0.5152282	0.4847718	0.5188504	1
O18	O	1	0.4847718	0.4847718	0.4811496	1
O19	O	1	0.5152282	0.5152282	0.4811496	1
O20	O	1	0.4847718	0.5152282	0.5188504	1
O21	O	1	0.5000000	0.5296252	0.4546769	1
O22	O	1	0.5000000	0.4703748	0.4546769	1
O23	O	1	0.4703748	0.5000000	0.5453231	1
O24	O	1	0.5296252	0.5000000	0.5453231	1
Zr1	Zr	1	0.5000000	0.4752523	0.5000000	1
Zr2	Zr	1	0.4752523	0.5000000	0.5000000	1
Zr3	Zr	1	0.5247477	0.5000000	0.5000000	1
Zr4	Zr	1	0.5000000	0.5247477	0.5000000	1

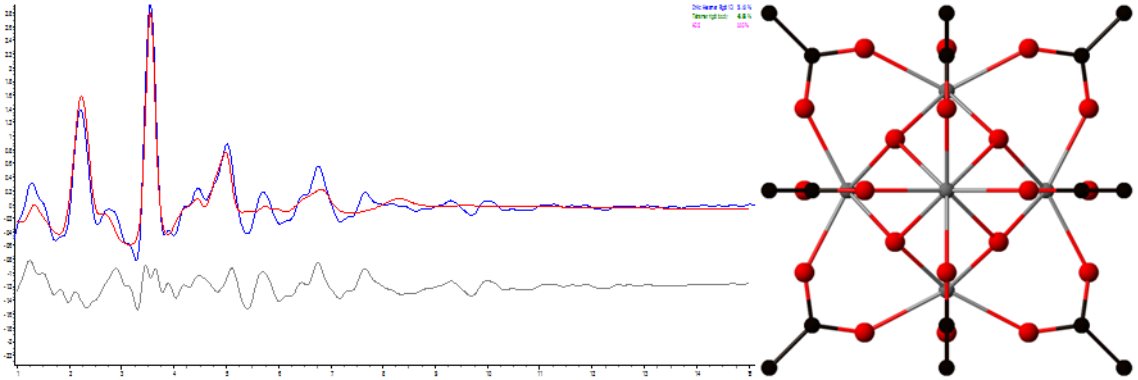

Figure 326: Observed and Calculated PDF from the fixed core refinement of ZAA27C from the 18-month data collection and the resultant model.

Table 269: The atomic coordinates of the model resulting from the fixed core refinement of ZAA27C from the 18-month data collection.

Atom Label	Atom Type	Multiplicity	Fractional X Coordinate	Fractional Y Coordinate	Fractional Z Coordinate	Fractional Occupancy
C1	C	1	0.5897783	0.5000000	0.5830511	1
C2	C	1	0.5000000	0.4102217	0.5830511	1
C3	C	1	0.4102217	0.5000000	0.5830511	1
C4	C	1	0.5000000	0.5897783	0.5830511	1
C5	C	1	0.5897783	0.5000000	0.4169489	1
C6	C	1	0.5000000	0.4102217	0.4169489	1
C7	C	1	0.4102217	0.5000000	0.4169489	1
C8	C	1	0.5000000	0.5897783	0.4169489	1
C9	C	1	0.5897783	0.4102217	0.5000000	1
C10	C	1	0.4102217	0.4102217	0.5000000	1
C11	C	1	0.4102217	0.5897783	0.5000000	1
C12	C	1	0.5897783	0.5897783	0.5000000	1
C13	C	1	0.6182289	0.5000000	0.60937	1
C14	C	1	0.5000000	0.3817711	0.60937	1
C15	C	1	0.3817711	0.5000000	0.60937	1
C16	C	1	0.5000000	0.6182289	0.60937	1
C17	C	1	0.6182289	0.5000000	0.39063	1
C18	C	1	0.5000000	0.3817711	0.39063	1
C19	C	1	0.3817711	0.5000000	0.39063	1
C20	C	1	0.5000000	0.6182289	0.39063	1
C21	C	1	0.6182289	0.3817711	0.5000000	1
C22	C	1	0.3817711	0.3817711	0.5000000	1
C23	C	1	0.3817711	0.6182289	0.5000000	1
C24	C	1	0.6182289	0.6182289	0.5000000	1
O1	O	1	0.534494	0.5341575	0.4680906	1
O2	O	1	0.534494	0.4658425	0.5319094	1
O3	O	1	0.465506	0.5341575	0.4680906	1
O4	O	1	0.465506	0.4658425	0.5319094	1
O5	O	1	0.465506	0.4658425	0.4680906	1
O6	O	1	0.465506	0.5341575	0.5319094	1

O7	O	1	0.534494	0.4658425	0.4680906	1
O8	O	1	0.534494	0.5341575	0.5319094	1
O9	O	1	0.5946891	0.5000000	0.550536	1
O10	O	1	0.5946891	0.4453707	0.5000000	1
O11	O	1	0.5946891	0.5000000	0.449464	1
O12	O	1	0.5946891	0.5546293	0.5000000	1
O13	O	1	0.5000000	0.5946891	0.550536	1
O14	O	1	0.5546293	0.5946891	0.5000000	1
O15	O	1	0.5000000	0.5946891	0.449464	1
O16	O	1	0.4453707	0.5946891	0.5000000	1
O17	O	1	0.4053109	0.5000000	0.550536	1
O18	O	1	0.4053109	0.5546293	0.5000000	1
O19	O	1	0.4053109	0.5000000	0.449464	1
O20	O	1	0.4053109	0.4453707	0.5000000	1
O21	O	1	0.5000000	0.4053109	0.550536	1
O22	O	1	0.4453707	0.4053109	0.5000000	1
O23	O	1	0.5000000	0.4053109	0.449464	1
O24	O	1	0.5546293	0.4053109	0.5000000	1
O25	O	1	0.5546293	0.5000000	0.587594	1
O26	O	1	0.5000000	0.5546293	0.587594	1
O27	O	1	0.4453707	0.5000000	0.587594	1
O28	O	1	0.5000000	0.4453707	0.587594	1
O29	O	1	0.5546293	0.5000000	0.412406	1
O30	O	1	0.5000000	0.4453707	0.412406	1
O31	O	1	0.4453707	0.5000000	0.412406	1
O32	O	1	0.5000000	0.5546293	0.412406	1
Zr1	Zr	1	0.5662557	0.5000000	0.5000000	1
Zr2	Zr	1	0.5000000	0.5662557	0.5000000	1
Zr3	Zr	1	0.4337443	0.5000000	0.5000000	1
Zr4	Zr	1	0.5000000	0.4337443	0.5000000	1
Zr5	Zr	1	0.5000000	0.5000000	0.5612911	1
Zr6	Zr	1	0.5000000	0.5000000	0.4387089	1

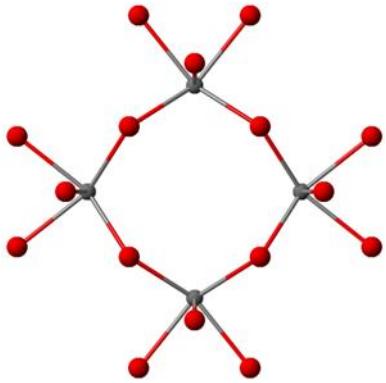

Figure 327: The tetrameric structure resulting from the fixed core refinement of ZAA27C from the 18-month data collection.

Table 270: The atomic coordinates of the tetrameric phase of the fixed core refinement of ZAA27C from the 18-month data collection.

Atom Label	Atom Type	Multiplicity	Fractional X Coordinate	Fractional Y Coordinate	Fractional Z Coordinate	Fractional Occupancy
O1	O	1	0.5151761	0.4848239	0.4821754	1
O2	O	1	0.4848239	0.4848239	0.5178246	1
O3	O	1	0.5151761	0.5151761	0.5178246	1
O4	O	1	0.4848239	0.5151761	0.4821754	1
O5	O	1	0.5000000	0.5299157	0.545353	1
O6	O	1	0.5000000	0.4700843	0.545353	1
O7	O	1	0.4700843	0.5000000	0.454647	1
O8	O	1	0.5299157	0.5000000	0.454647	1
O9	O	1	0.512927	0.4589298	0.5000000	1
O10	O	1	0.4589298	0.487073	0.5000000	1
O11	O	1	0.5410702	0.512927	0.5000000	1
O12	O	1	0.487073	0.5410702	0.5000000	1
O13	O	1	0.4589298	0.512927	0.5000000	1
O14	O	1	0.5410702	0.487073	0.5000000	1
O15	O	1	0.487073	0.4589298	0.5000000	1
O16	O	1	0.512927	0.5410702	0.5000000	1
O17	O	1	0.5151761	0.4848239	0.5178246	1
O18	O	1	0.4848239	0.4848239	0.4821754	1
O19	O	1	0.5151761	0.5151761	0.4821754	1
O20	O	1	0.4848239	0.5151761	0.5178246	1
O21	O	1	0.5000000	0.5299157	0.454647	1
O22	O	1	0.5000000	0.4700843	0.454647	1
O23	O	1	0.4700843	0.5000000	0.545353	1
O24	O	1	0.5299157	0.5000000	0.545353	1
Zr1	Zr	1	0.5000000	0.4751901	0.5000000	1
Zr2	Zr	1	0.4751901	0.5000000	0.5000000	1
Zr3	Zr	1	0.5248099	0.5000000	0.5000000	1
Zr4	Zr	1	0.5000000	0.5248099	0.5000000	1

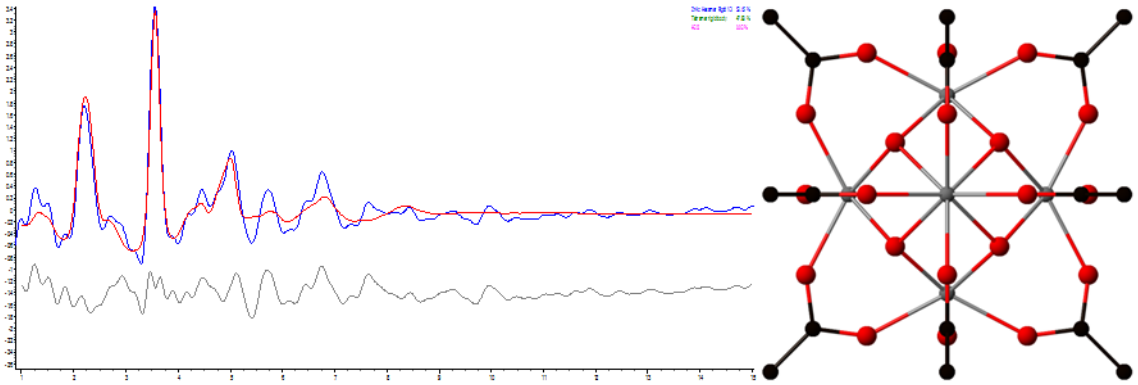

Figure 328: Observed and Calculated PDF from the fixed core refinement of ZAA27I from the 18-month data collection and the resultant model.

Table 271: The atomic coordinates of the model resulting from the fixed core refinement of ZAA27I from the 18-month data collection.

Atom Label	Atom Type	Multiplicity	Fractional X Coordinate	Fractional Y Coordinate	Fractional Z Coordinate	Fractional Occupancy
C1	C	1	0.5901401	0.5000000	0.5833859	1
C2	C	1	0.5000000	0.4098599	0.5833859	1
C3	C	1	0.4098599	0.5000000	0.5833859	1
C4	C	1	0.5000000	0.5901401	0.5833859	1
C5	C	1	0.5901401	0.5000000	0.4166141	1
C6	C	1	0.5000000	0.4098599	0.4166141	1
C7	C	1	0.4098599	0.5000000	0.4166141	1
C8	C	1	0.5000000	0.5901401	0.4166141	1
C9	C	1	0.5901401	0.4098599	0.5000000	1
C10	C	1	0.4098599	0.4098599	0.5000000	1
C11	C	1	0.4098599	0.5901401	0.5000000	1
C12	C	1	0.5901401	0.5901401	0.5000000	1
C13	C	1	0.6189748	0.5000000	0.61006	1
C14	C	1	0.5000000	0.3810252	0.61006	1
C15	C	1	0.3810252	0.5000000	0.61006	1
C16	C	1	0.5000000	0.6189748	0.61006	1
C17	C	1	0.6189748	0.5000000	0.38994	1
C18	C	1	0.5000000	0.3810252	0.38994	1
C19	C	1	0.3810252	0.5000000	0.38994	1
C20	C	1	0.5000000	0.6189748	0.38994	1
C21	C	1	0.6189748	0.3810252	0.5000000	1
C22	C	1	0.3810252	0.3810252	0.5000000	1
C23	C	1	0.3810252	0.6189748	0.5000000	1
C24	C	1	0.6189748	0.6189748	0.5000000	1
O1	O	1	0.5351385	0.5347957	0.4674944	1
O2	O	1	0.5351385	0.4652043	0.5325056	1
O3	O	1	0.4648615	0.5347957	0.4674944	1
O4	O	1	0.4648615	0.4652043	0.5325056	1
O5	O	1	0.4648615	0.4652043	0.4674944	1
O6	O	1	0.4648615	0.5347957	0.5325056	1

O7	O	1	0.5351385	0.4652043	0.4674944	1
O8	O	1	0.5351385	0.5347957	0.5325056	1
O9	O	1	0.5950137	0.5000000	0.5499584	1
O10	O	1	0.5950137	0.445995	0.5000000	1
O11	O	1	0.5950137	0.5000000	0.4500416	1
O12	O	1	0.5950137	0.554005	0.5000000	1
O13	O	1	0.5000000	0.5950137	0.5499584	1
O14	O	1	0.554005	0.5950137	0.5000000	1
O15	O	1	0.5000000	0.5950137	0.4500416	1
O16	O	1	0.445995	0.5950137	0.5000000	1
O17	O	1	0.4049863	0.5000000	0.5499584	1
O18	O	1	0.4049863	0.554005	0.5000000	1
O19	O	1	0.4049863	0.5000000	0.4500416	1
O20	O	1	0.4049863	0.445995	0.5000000	1
O21	O	1	0.5000000	0.4049863	0.5499584	1
O22	O	1	0.445995	0.4049863	0.5000000	1
O23	O	1	0.5000000	0.4049863	0.4500416	1
O24	O	1	0.554005	0.4049863	0.5000000	1
O25	O	1	0.554005	0.5000000	0.5878943	1
O26	O	1	0.5000000	0.554005	0.5878943	1
O27	O	1	0.445995	0.5000000	0.5878943	1
O28	O	1	0.5000000	0.445995	0.5878943	1
O29	O	1	0.554005	0.5000000	0.4121057	1
O30	O	1	0.5000000	0.445995	0.4121057	1
O31	O	1	0.445995	0.5000000	0.4121057	1
O32	O	1	0.5000000	0.554005	0.4121057	1
Zr1	Zr	1	0.5664871	0.5000000	0.5000000	1
Zr2	Zr	1	0.5000000	0.5664871	0.5000000	1
Zr3	Zr	1	0.4335129	0.5000000	0.5000000	1
Zr4	Zr	1	0.5000000	0.4335129	0.5000000	1
Zr5	Zr	1	0.5000000	0.5000000	0.5615052	1
Zr6	Zr	1	0.5000000	0.5000000	0.4384948	1

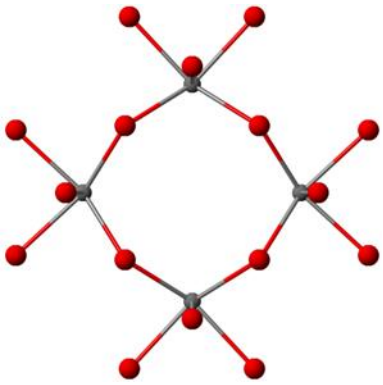

Figure 329: The tetrameric structure resulting from the fixed core refinement of ZAA27I from the 18-month data collection.

Table 272: The atomic coordinates of the tetrameric phase of the fixed core refinement of ZAA27I from the 18-month data collection.

Atom Label	Atom Type	Multiplicity	Fractional X Coordinate	Fractional Y Coordinate	Fractional Z Coordinate	Fractional Occupancy
O1	O	1	0.5152874	0.4847126	0.4795312	1
O2	O	1	0.4847126	0.4847126	0.5204688	1
O3	O	1	0.5152874	0.5152874	0.5204688	1
O4	O	1	0.4847126	0.5152874	0.4795312	1
O5	O	1	0.5000000	0.5287928	0.5456656	1
O6	O	1	0.5000000	0.4712072	0.5456656	1
O7	O	1	0.4712072	0.5000000	0.4543344	1
O8	O	1	0.5287928	0.5000000	0.4543344	1
O9	O	1	0.5142537	0.4598345	0.5000000	1
O10	O	1	0.4598345	0.4857463	0.5000000	1
O11	O	1	0.5401655	0.5142537	0.5000000	1
O12	O	1	0.4857463	0.5401655	0.5000000	1
O13	O	1	0.4598345	0.5142537	0.5000000	1
O14	O	1	0.5401655	0.4857463	0.5000000	1
O15	O	1	0.4857463	0.4598345	0.5000000	1
O16	O	1	0.5142537	0.5401655	0.5000000	1
O17	O	1	0.5152874	0.4847126	0.5204688	1
O18	O	1	0.4847126	0.4847126	0.4795312	1
O19	O	1	0.5152874	0.5152874	0.4795312	1
O20	O	1	0.4847126	0.5152874	0.5204688	1
O21	O	1	0.5000000	0.5287928	0.4543344	1
O22	O	1	0.5000000	0.4712072	0.4543344	1
O23	O	1	0.4712072	0.5000000	0.5456656	1
O24	O	1	0.5287928	0.5000000	0.5456656	1
Zr1	Zr	1	0.5000000	0.4752148	0.5000000	1
Zr2	Zr	1	0.4752148	0.5000000	0.5000000	1
Zr3	Zr	1	0.5247852	0.5000000	0.5000000	1
Zr4	Zr	1	0.5000000	0.5247852	0.5000000	1

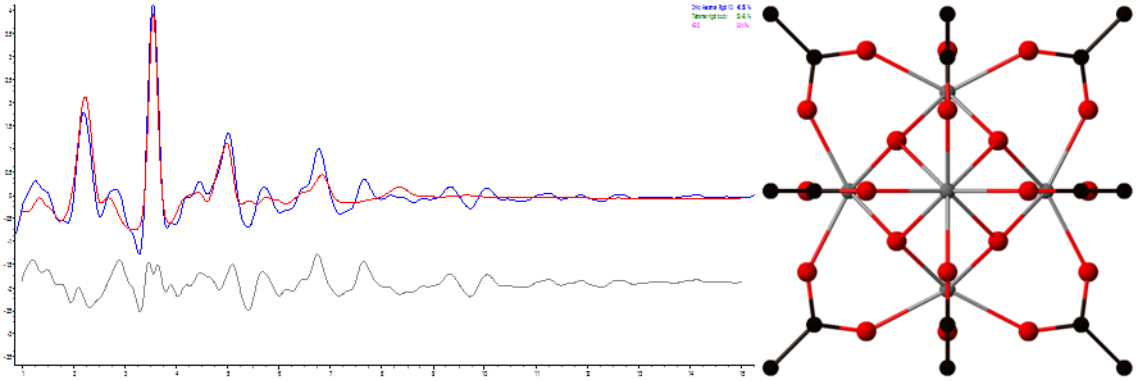

Figure 330: Observed and Calculated PDF from the fixed core refinement of ZAA28A from the 18-month data collection and the resultant model.

Table 273: The atomic coordinates of the model resulting from the fixed core refinement of ZAA28A from the 18-month data collection.

Atom Label	Atom Type	Multiplicity	Fractional X Coordinate	Fractional Y Coordinate	Fractional Z Coordinate	Fractional Occupancy
C1	C	1	0.5898924	0.5000000	0.5831568	1
C2	C	1	0.5000000	0.4101076	0.5831568	1
C3	C	1	0.4101076	0.5000000	0.5831568	1
C4	C	1	0.5000000	0.5898924	0.5831568	1
C5	C	1	0.5898924	0.5000000	0.4168432	1
C6	C	1	0.5000000	0.4101076	0.4168432	1
C7	C	1	0.4101076	0.5000000	0.4168432	1
C8	C	1	0.5000000	0.5898924	0.4168432	1
C9	C	1	0.5898924	0.4101076	0.5000000	1
C10	C	1	0.4101076	0.4101076	0.5000000	1
C11	C	1	0.4101076	0.5898924	0.5000000	1
C12	C	1	0.5898924	0.5898924	0.5000000	1
C13	C	1	0.6191417	0.5000000	0.6102144	1
C14	C	1	0.5000000	0.3808583	0.6102144	1
C15	C	1	0.3808583	0.5000000	0.6102144	1
C16	C	1	0.5000000	0.6191417	0.6102144	1
C17	C	1	0.6191417	0.5000000	0.3897856	1
C18	C	1	0.5000000	0.3808583	0.3897856	1
C19	C	1	0.3808583	0.5000000	0.3897856	1
C20	C	1	0.5000000	0.6191417	0.3897856	1
C21	C	1	0.6191417	0.3808583	0.5000000	1
C22	C	1	0.3808583	0.3808583	0.5000000	1
C23	C	1	0.3808583	0.6191417	0.5000000	1
C24	C	1	0.6191417	0.6191417	0.5000000	1
O1	O	1	0.5341487	0.5338155	0.4684101	1
O2	O	1	0.5341487	0.4661845	0.5315899	1
O3	O	1	0.4658513	0.5338155	0.4684101	1
O4	O	1	0.4658513	0.4661845	0.5315899	1
O5	O	1	0.4658513	0.4661845	0.4684101	1
O6	O	1	0.4658513	0.5338155	0.5315899	1

O7	O	1	0.5341487	0.4661845	0.4684101	1
O8	O	1	0.5341487	0.5338155	0.5315899	1
O9	O	1	0.5945913	0.5000000	0.5504672	1
O10	O	1	0.5945913	0.445445	0.5000000	1
O11	O	1	0.5945913	0.5000000	0.4495328	1
O12	O	1	0.5945913	0.554555	0.5000000	1
O13	O	1	0.5000000	0.5945913	0.5504672	1
O14	O	1	0.554555	0.5945913	0.5000000	1
O15	O	1	0.5000000	0.5945913	0.4495328	1
O16	O	1	0.445445	0.5945913	0.5000000	1
O17	O	1	0.4054087	0.5000000	0.5504672	1
O18	O	1	0.4054087	0.554555	0.5000000	1
O19	O	1	0.4054087	0.5000000	0.4495328	1
O20	O	1	0.4054087	0.445445	0.5000000	1
O21	O	1	0.5000000	0.4054087	0.5504672	1
O22	O	1	0.445445	0.4054087	0.5000000	1
O23	O	1	0.5000000	0.4054087	0.4495328	1
O24	O	1	0.554555	0.4054087	0.5000000	1
O25	O	1	0.554555	0.5000000	0.5875036	1
O26	O	1	0.5000000	0.554555	0.5875036	1
O27	O	1	0.445445	0.5000000	0.5875036	1
O28	O	1	0.5000000	0.445445	0.5875036	1
O29	O	1	0.554555	0.5000000	0.4124964	1
O30	O	1	0.5000000	0.445445	0.4124964	1
O31	O	1	0.445445	0.5000000	0.4124964	1
O32	O	1	0.5000000	0.554555	0.4124964	1
Zr1	Zr	1	0.5663583	0.5000000	0.5000000	1
Zr2	Zr	1	0.5000000	0.5663583	0.5000000	1
Zr3	Zr	1	0.4336417	0.5000000	0.5000000	1
Zr4	Zr	1	0.5000000	0.4336417	0.5000000	1
Zr5	Zr	1	0.5000000	0.5000000	0.561386	1
Zr6	Zr	1	0.5000000	0.5000000	0.438614	1

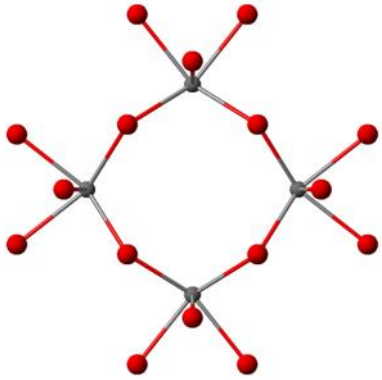

Figure 331: The tetrameric structure resulting from the fixed core refinement of ZAA28A from the 18-month data collection.

Table 274: The atomic coordinates of the tetrameric phase of the fixed core refinement of ZAA28A from the 18-month data collection.

Atom Label	Atom Type	Multiplicity	Fractional X Coordinate	Fractional Y Coordinate	Fractional Z Coordinate	Fractional Occupancy
O1	O	1	0.5152566	0.4847434	0.4832648	1
O2	O	1	0.4847434	0.4847434	0.5167352	1
O3	O	1	0.5152566	0.5152566	0.5167352	1
O4	O	1	0.4847434	0.5152566	0.4832648	1
O5	O	1	0.5000000	0.5301601	0.5453424	1
O6	O	1	0.5000000	0.4698399	0.5453424	1
O7	O	1	0.4698399	0.5000000	0.4546576	1
O8	O	1	0.5301601	0.5000000	0.4546576	1
O9	O	1	0.5128951	0.4589222	0.5000000	1
O10	O	1	0.4589222	0.4871049	0.5000000	1
O11	O	1	0.5410778	0.5128951	0.5000000	1
O12	O	1	0.4871049	0.5410778	0.5000000	1
O13	O	1	0.4589222	0.5128951	0.5000000	1
O14	O	1	0.5410778	0.4871049	0.5000000	1
O15	O	1	0.4871049	0.4589222	0.5000000	1
O16	O	1	0.5128951	0.5410778	0.5000000	1
O17	O	1	0.5152566	0.4847434	0.5167352	1
O18	O	1	0.4847434	0.4847434	0.4832648	1
O19	O	1	0.5152566	0.5152566	0.4832648	1
O20	O	1	0.4847434	0.5152566	0.5167352	1
O21	O	1	0.5000000	0.5301601	0.4546576	1
O22	O	1	0.5000000	0.4698399	0.4546576	1
O23	O	1	0.4698399	0.5000000	0.5453424	1
O24	O	1	0.5301601	0.5000000	0.5453424	1
Zr1	Zr	1	0.5000000	0.4752676	0.5000000	1
Zr2	Zr	1	0.4752676	0.5000000	0.5000000	1
Zr3	Zr	1	0.5247324	0.5000000	0.5000000	1
Zr4	Zr	1	0.5000000	0.5247324	0.5000000	1

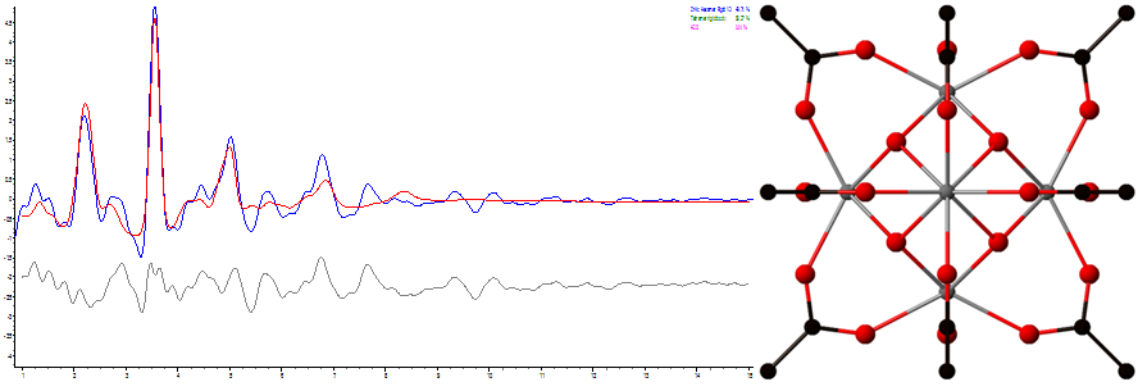

Figure 332: Observed and Calculated PDF from the fixed core refinement of ZAA28C from the 18-month data collection and the resultant model.

Table 275: The atomic coordinates of the model resulting from the fixed core refinement of ZAA28C from the 18-month data collection.

Atom Label	Atom Type	Multiplicity	Fractional X Coordinate	Fractional Y Coordinate	Fractional Z Coordinate	Fractional Occupancy
C1	C	1	0.5899926	0.5000000	0.5832495	1
C2	C	1	0.5000000	0.4100074	0.5832495	1
C3	C	1	0.4100074	0.5000000	0.5832495	1
C4	C	1	0.5000000	0.5899926	0.5832495	1
C5	C	1	0.5899926	0.5000000	0.4167505	1
C6	C	1	0.5000000	0.4100074	0.4167505	1
C7	C	1	0.4100074	0.5000000	0.4167505	1
C8	C	1	0.5000000	0.5899926	0.4167505	1
C9	C	1	0.5899926	0.4100074	0.5000000	1
C10	C	1	0.4100074	0.4100074	0.5000000	1
C11	C	1	0.4100074	0.5899926	0.5000000	1
C12	C	1	0.5899926	0.5899926	0.5000000	1
C13	C	1	0.6193507	0.5000000	0.6104077	1
C14	C	1	0.5000000	0.3806493	0.6104077	1
C15	C	1	0.3806493	0.5000000	0.6104077	1
C16	C	1	0.5000000	0.6193507	0.6104077	1
C17	C	1	0.6193507	0.5000000	0.3895923	1
C18	C	1	0.5000000	0.3806493	0.3895923	1
C19	C	1	0.3806493	0.5000000	0.3895923	1
C20	C	1	0.5000000	0.6193507	0.3895923	1
C21	C	1	0.6193507	0.3806493	0.5000000	1
C22	C	1	0.3806493	0.3806493	0.5000000	1
C23	C	1	0.3806493	0.6193507	0.5000000	1
C24	C	1	0.6193507	0.6193507	0.5000000	1
O1	O	1	0.5339545	0.5336232	0.4685898	1
O2	O	1	0.5339545	0.4663768	0.5314102	1
O3	O	1	0.4660455	0.5336232	0.4685898	1
O4	O	1	0.4660455	0.4663768	0.5314102	1
O5	O	1	0.4660455	0.4663768	0.4685898	1
O6	O	1	0.4660455	0.5336232	0.5314102	1

O7	O	1	0.5339545	0.4663768	0.4685898	1
O8	O	1	0.5339545	0.5336232	0.5314102	1
O9	O	1	0.5947428	0.5000000	0.550624	1
O10	O	1	0.5947428	0.4452755	0.5000000	1
O11	O	1	0.5947428	0.5000000	0.449376	1
O12	O	1	0.5947428	0.5547245	0.5000000	1
O13	O	1	0.5000000	0.5947428	0.550624	1
O14	O	1	0.5547245	0.5947428	0.5000000	1
O15	O	1	0.5000000	0.5947428	0.449376	1
O16	O	1	0.4452755	0.5947428	0.5000000	1
O17	O	1	0.4052572	0.5000000	0.550624	1
O18	O	1	0.4052572	0.5547245	0.5000000	1
O19	O	1	0.4052572	0.5000000	0.449376	1
O20	O	1	0.4052572	0.4452755	0.5000000	1
O21	O	1	0.5000000	0.4052572	0.550624	1
O22	O	1	0.4452755	0.4052572	0.5000000	1
O23	O	1	0.5000000	0.4052572	0.449376	1
O24	O	1	0.5547245	0.4052572	0.5000000	1
O25	O	1	0.5547245	0.5000000	0.5876437	1
O26	O	1	0.5000000	0.5547245	0.5876437	1
O27	O	1	0.4452755	0.5000000	0.5876437	1
O28	O	1	0.5000000	0.4452755	0.5876437	1
O29	O	1	0.5547245	0.5000000	0.4123563	1
O30	O	1	0.5000000	0.4452755	0.4123563	1
O31	O	1	0.4452755	0.5000000	0.4123563	1
O32	O	1	0.5000000	0.5547245	0.4123563	1
Zr1	Zr	1	0.5664815	0.5000000	0.5000000	1
Zr2	Zr	1	0.5000000	0.5664815	0.5000000	1
Zr3	Zr	1	0.4335185	0.5000000	0.5000000	1
Zr4	Zr	1	0.5000000	0.4335185	0.5000000	1
Zr5	Zr	1	0.5000000	0.5000000	0.5615	1
Zr6	Zr	1	0.5000000	0.5000000	0.4385	1

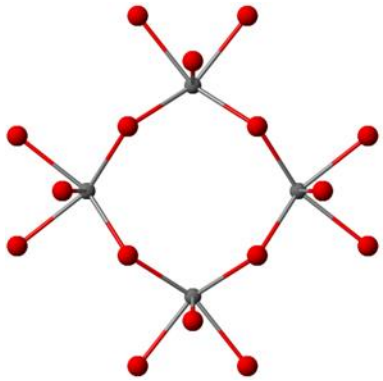

Figure 333: The tetrameric structure resulting from the fixed core refinement of ZAA28C from the 18-month data collection.

Table 276: The atomic coordinates of the tetrameric phase of the fixed core refinement of ZAA28C from the 18-month data collection.

Atom Label	Atom Type	Multiplicity	Fractional X Coordinate	Fractional Y Coordinate	Fractional Z Coordinate	Fractional Occupancy
O1	O	1	0.5151408	0.4848592	0.4821747	1
O2	O	1	0.4848592	0.4848592	0.5178253	1
O3	O	1	0.5151408	0.5151408	0.5178253	1
O4	O	1	0.4848592	0.5151408	0.4821747	1
O5	O	1	0.5000000	0.5304707	0.5450787	1
O6	O	1	0.5000000	0.4695293	0.5450787	1
O7	O	1	0.4695293	0.5000000	0.4549213	1
O8	O	1	0.5304707	0.5000000	0.4549213	1
O9	O	1	0.5128654	0.4589314	0.5000000	1
O10	O	1	0.4589314	0.4871346	0.5000000	1
O11	O	1	0.5410686	0.5128654	0.5000000	1
O12	O	1	0.4871346	0.5410686	0.5000000	1
O13	O	1	0.4589314	0.5128654	0.5000000	1
O14	O	1	0.5410686	0.4871346	0.5000000	1
O15	O	1	0.4871346	0.4589314	0.5000000	1
O16	O	1	0.5128654	0.5410686	0.5000000	1
O17	O	1	0.5151408	0.4848592	0.5178253	1
O18	O	1	0.4848592	0.4848592	0.4821747	1
O19	O	1	0.5151408	0.5151408	0.4821747	1
O20	O	1	0.4848592	0.5151408	0.5178253	1
O21	O	1	0.5000000	0.5304707	0.4549213	1
O22	O	1	0.5000000	0.4695293	0.4549213	1
O23	O	1	0.4695293	0.5000000	0.5450787	1
O24	O	1	0.5304707	0.5000000	0.5450787	1
Zr1	Zr	1	0.5000000	0.4752653	0.5000000	1
Zr2	Zr	1	0.4752653	0.5000000	0.5000000	1
Zr3	Zr	1	0.5247347	0.5000000	0.5000000	1
Zr4	Zr	1	0.5000000	0.5247347	0.5000000	1

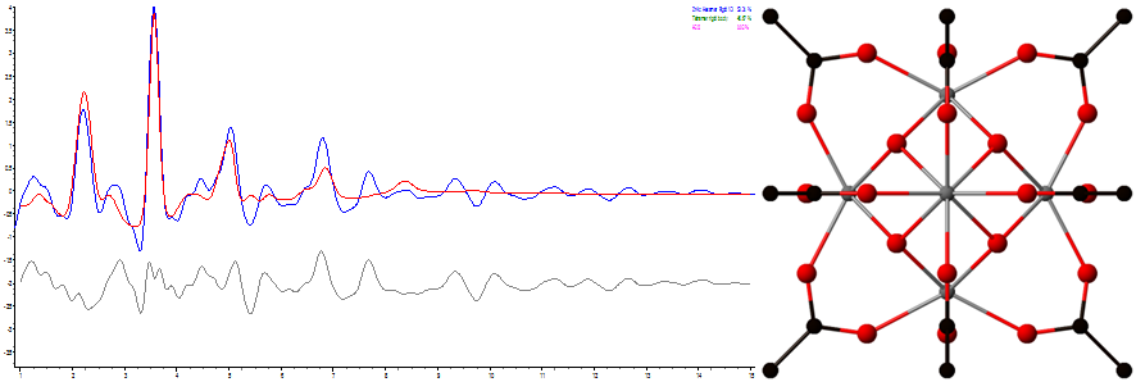

Figure 334: Observed and Calculated PDF from the fixed core refinement of ZAA28I from the 18-month data collection and the resultant model.

Table 277: The atomic coordinates of the model resulting from the fixed core refinement of ZAA28I from the 18-month data collection.

Atom Label	Atom Type	Multiplicity	Fractional X Coordinate	Fractional Y Coordinate	Fractional Z Coordinate	Fractional Occupancy
C1	C	1	0.5899347	0.5000000	0.5831958	1
C2	C	1	0.5000000	0.4100653	0.5831958	1
C3	C	1	0.4100653	0.5000000	0.5831958	1
C4	C	1	0.5000000	0.5899347	0.5831958	1
C5	C	1	0.5899347	0.5000000	0.4168042	1
C6	C	1	0.5000000	0.4100653	0.4168042	1
C7	C	1	0.4100653	0.5000000	0.4168042	1
C8	C	1	0.5000000	0.5899347	0.4168042	1
C9	C	1	0.5899347	0.4100653	0.5000000	1
C10	C	1	0.4100653	0.4100653	0.5000000	1
C11	C	1	0.4100653	0.5899347	0.5000000	1
C12	C	1	0.5899347	0.5899347	0.5000000	1
C13	C	1	0.6196117	0.5000000	0.6106491	1
C14	C	1	0.5000000	0.3803883	0.6106491	1
C15	C	1	0.3803883	0.5000000	0.6106491	1
C16	C	1	0.5000000	0.6196117	0.6106491	1
C17	C	1	0.6196117	0.5000000	0.3893509	1
C18	C	1	0.5000000	0.3803883	0.3893509	1
C19	C	1	0.3803883	0.5000000	0.3893509	1
C20	C	1	0.5000000	0.6196117	0.3893509	1
C21	C	1	0.6196117	0.3803883	0.5000000	1
C22	C	1	0.3803883	0.3803883	0.5000000	1
C23	C	1	0.3803883	0.6196117	0.5000000	1
C24	C	1	0.6196117	0.6196117	0.5000000	1
O1	O	1	0.5340646	0.5337323	0.4684878	1
O2	O	1	0.5340646	0.4662677	0.5315122	1
O3	O	1	0.4659354	0.5337323	0.4684878	1
O4	O	1	0.4659354	0.4662677	0.5315122	1
O5	O	1	0.4659354	0.4662677	0.4684878	1
O6	O	1	0.4659354	0.5337323	0.5315122	1

O7	O	1	0.5340646	0.4662677	0.4684878	1
O8	O	1	0.5340646	0.5337323	0.5315122	1
O9	O	1	0.5949676	0.5000000	0.5500499	1
O10	O	1	0.5949676	0.4458961	0.5000000	1
O11	O	1	0.5949676	0.5000000	0.4499501	1
O12	O	1	0.5949676	0.5541039	0.5000000	1
O13	O	1	0.5000000	0.5949676	0.5500499	1
O14	O	1	0.5541039	0.5949676	0.5000000	1
O15	O	1	0.5000000	0.5949676	0.4499501	1
O16	O	1	0.4458961	0.5949676	0.5000000	1
O17	O	1	0.4050324	0.5000000	0.5500499	1
O18	O	1	0.4050324	0.5541039	0.5000000	1
O19	O	1	0.4050324	0.5000000	0.4499501	1
O20	O	1	0.4050324	0.4458961	0.5000000	1
O21	O	1	0.5000000	0.4050324	0.5500499	1
O22	O	1	0.4458961	0.4050324	0.5000000	1
O23	O	1	0.5000000	0.4050324	0.4499501	1
O24	O	1	0.5541039	0.4050324	0.5000000	1
O25	O	1	0.5541039	0.5000000	0.5878516	1
O26	O	1	0.5000000	0.5541039	0.5878516	1
O27	O	1	0.4458961	0.5000000	0.5878516	1
O28	O	1	0.5000000	0.4458961	0.5878516	1
O29	O	1	0.5541039	0.5000000	0.4121484	1
O30	O	1	0.5000000	0.4458961	0.4121484	1
O31	O	1	0.4458961	0.5000000	0.4121484	1
O32	O	1	0.5000000	0.5541039	0.4121484	1
Zr1	Zr	1	0.5666505	0.5000000	0.5000000	1
Zr2	Zr	1	0.5000000	0.5666505	0.5000000	1
Zr3	Zr	1	0.4333495	0.5000000	0.5000000	1
Zr4	Zr	1	0.5000000	0.4333495	0.5000000	1
Zr5	Zr	1	0.5000000	0.5000000	0.5616564	1
Zr6	Zr	1	0.5000000	0.5000000	0.4383436	1

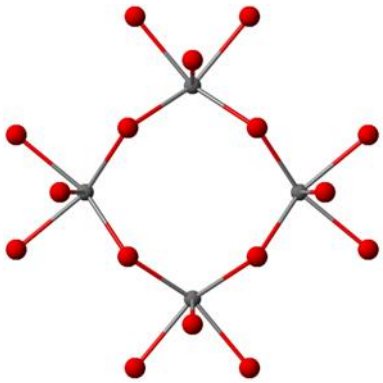

Figure 335: The tetrameric structure resulting from the fixed core refinement of ZAA28I from the 18-month data collection.

Table 278: The atomic coordinates of the tetrameric phase of the fixed core refinement of ZAA28I from the 18-month data collection.

Atom Label	Atom Type	Multiplicity	Fractional X Coordinate	Fractional Y Coordinate	Fractional Z Coordinate	Fractional Occupancy
O1	O	1	0.5149774	0.4850226	0.4811336	1
O2	O	1	0.4850226	0.4850226	0.5188664	1
O3	O	1	0.5149774	0.5149774	0.5188664	1
O4	O	1	0.4850226	0.5149774	0.4811336	1
O5	O	1	0.5000000	0.5306835	0.5449081	1
O6	O	1	0.5000000	0.4693165	0.5449081	1
O7	O	1	0.4693165	0.5000000	0.4550919	1
O8	O	1	0.5306835	0.5000000	0.4550919	1
O9	O	1	0.5132663	0.4592105	0.5000000	1
O10	O	1	0.4592105	0.4867337	0.5000000	1
O11	O	1	0.5407895	0.5132663	0.5000000	1
O12	O	1	0.4867337	0.5407895	0.5000000	1
O13	O	1	0.4592105	0.5132663	0.5000000	1
O14	O	1	0.5407895	0.4867337	0.5000000	1
O15	O	1	0.4867337	0.4592105	0.5000000	1
O16	O	1	0.5132663	0.5407895	0.5000000	1
O17	O	1	0.5149774	0.4850226	0.5188664	1
O18	O	1	0.4850226	0.4850226	0.4811336	1
O19	O	1	0.5149774	0.5149774	0.4811336	1
O20	O	1	0.4850226	0.5149774	0.5188664	1
O21	O	1	0.5000000	0.5306835	0.4550919	1
O22	O	1	0.5000000	0.4693165	0.4550919	1
O23	O	1	0.4693165	0.5000000	0.5449081	1
O24	O	1	0.5306835	0.5000000	0.5449081	1
Zr1	Zr	1	0.5000000	0.475225	0.5000000	1
Zr2	Zr	1	0.475225	0.5000000	0.5000000	1
Zr3	Zr	1	0.524775	0.5000000	0.5000000	1
Zr4	Zr	1	0.5000000	0.524775	0.5000000	1

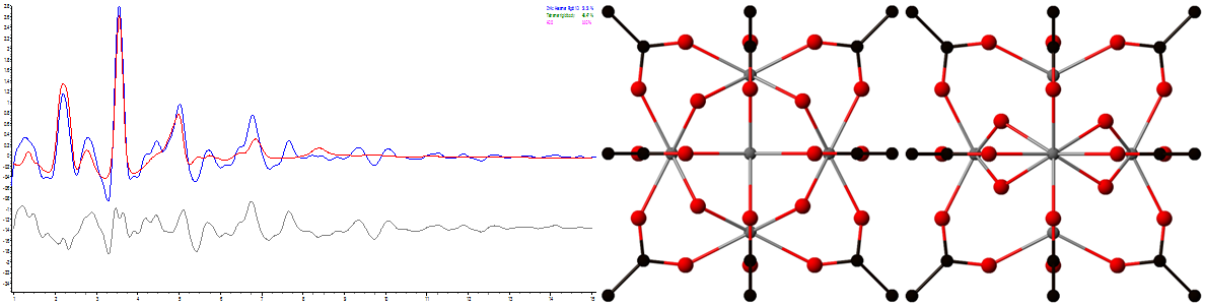

Figure 336: Observed and Calculated PDF from the chandelier core refinement of ZAA1A from the 18-month data collection and the resultant model viewed from the axial (left) and equatorial (right) positions.

Table 279: The atomic coordinates of the model resulting from the chandelier core refinement of ZAA1A from the 18-month data collection.

Atom Label	Atom Type	Multiplicity	Fractional X Coordinate	Fractional Y Coordinate	Fractional Z Coordinate	Fractional Occupancy
C1	C	1	0.5904231	0.5000000	0.5836476	1
C2	C	1	0.5000000	0.4095769	0.5836476	1
C3	C	1	0.4095769	0.5000000	0.5836476	1
C4	C	1	0.5000000	0.5904231	0.5836476	1
C5	C	1	0.5904231	0.5000000	0.4163524	1
C6	C	1	0.5000000	0.4095769	0.4163524	1
C7	C	1	0.4095769	0.5000000	0.4163524	1
C8	C	1	0.5000000	0.5904231	0.4163524	1
C9	C	1	0.5904231	0.4095769	0.5000000	1
C10	C	1	0.4095769	0.4095769	0.5000000	1
C11	C	1	0.4095769	0.5904231	0.5000000	1
C12	C	1	0.5904231	0.5904231	0.5000000	1
C13	C	1	0.6200231	0.5000000	0.6110298	1
C14	C	1	0.5000000	0.3799769	0.6110298	1
C15	C	1	0.3799769	0.5000000	0.6110298	1
C16	C	1	0.5000000	0.6200231	0.6110298	1
C17	C	1	0.6200231	0.5000000	0.3889702	1
C18	C	1	0.5000000	0.3799769	0.3889702	1
C19	C	1	0.3799769	0.5000000	0.3889702	1
C20	C	1	0.5000000	0.6200231	0.3889702	1
C21	C	1	0.6200231	0.3799769	0.5000000	1
C22	C	1	0.3799769	0.3799769	0.5000000	1
C23	C	1	0.3799769	0.6200231	0.5000000	1
C24	C	1	0.6200231	0.6200231	0.5000000	1
O1	O	1	0.5443148	0.4556852	0.4742353	1
O2	O	1	0.5443148	0.4556852	0.5257647	1
O3	O	1	0.4556852	0.4556852	0.4742353	1
O4	O	1	0.4556852	0.4556852	0.5257647	1
O5	O	1	0.4556852	0.5443148	0.4742353	1
O6	O	1	0.4556852	0.5443148	0.5257647	1
O7	O	1	0.5443148	0.5443148	0.4742353	1
O8	O	1	0.5443148	0.5443148	0.5257647	1

O9	O	1	0.5943226	0.5000000	0.5505445	1
O10	O	1	0.5943226	0.4453614	0.5000000	1
O11	O	1	0.5943226	0.5000000	0.4494555	1
O12	O	1	0.5943226	0.5546386	0.5000000	1
O13	O	1	0.5000000	0.5943226	0.5505445	1
O14	O	1	0.5546386	0.5943226	0.5000000	1
O15	O	1	0.5000000	0.5943226	0.4494555	1
O16	O	1	0.4453614	0.5943226	0.5000000	1
O17	O	1	0.4056774	0.5000000	0.5505445	1
O18	O	1	0.4056774	0.5546386	0.5000000	1
O19	O	1	0.4056774	0.5000000	0.4494555	1
O20	O	1	0.4056774	0.4453614	0.5000000	1
O21	O	1	0.5000000	0.4056774	0.5505445	1
O22	O	1	0.4453614	0.4056774	0.5000000	1
O23	O	1	0.5000000	0.4056774	0.4494555	1
O24	O	1	0.5546386	0.4056774	0.5000000	1
O25	O	1	0.5546386	0.5000000	0.587255	1
O26	O	1	0.5000000	0.5546386	0.587255	1
O27	O	1	0.4453614	0.5000000	0.587255	1
O28	O	1	0.5000000	0.4453614	0.587255	1
O29	O	1	0.5546386	0.5000000	0.412745	1
O30	O	1	0.5000000	0.4453614	0.412745	1
O31	O	1	0.4453614	0.5000000	0.412745	1
O32	O	1	0.5000000	0.5546386	0.412745	1
Zr1	Zr	1	0.5665406	0.5000000	0.5000000	1
Zr2	Zr	1	0.5000000	0.5665406	0.5000000	1
Zr3	Zr	1	0.4334594	0.5000000	0.5000000	1
Zr4	Zr	1	0.5000000	0.4334594	0.5000000	1
Zr5	Zr	1	0.5000000	0.5000000	0.5615547	1
Zr6	Zr	1	0.5000000	0.5000000	0.4384453	1

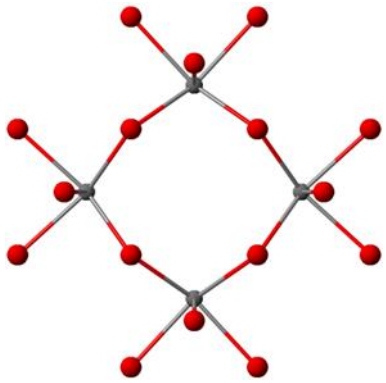

Figure 337: The tetrameric structure resulting from the chandelier core refinement of ZAA1A from the 18-month data collection.

Table 280: The atomic coordinates of the tetrameric phase of the chandelier core refinement of ZAA1A from the 18-month data collection.

Atom Label	Atom Type	Multiplicity	Fractional X Coordinate	Fractional Y Coordinate	Fractional Z Coordinate	Fractional Occupancy
O1	O	1	0.5144626	0.4855374	0.4777671	1
O2	O	1	0.4855374	0.4855374	0.5222329	1
O3	O	1	0.5144626	0.5144626	0.5222329	1
O4	O	1	0.4855374	0.5144626	0.4777671	1
O5	O	1	0.5000000	0.5296264	0.5473344	1
O6	O	1	0.5000000	0.4703736	0.5473344	1
O7	O	1	0.4703736	0.5000000	0.4526656	1
O8	O	1	0.5296264	0.5000000	0.4526656	1
O9	O	1	0.5144338	0.4597394	0.5000000	1
O10	O	1	0.4597394	0.4855662	0.5000000	1
O11	O	1	0.5402606	0.5144338	0.5000000	1
O12	O	1	0.4855662	0.5402606	0.5000000	1
O13	O	1	0.4597394	0.5144338	0.5000000	1
O14	O	1	0.5402606	0.4855662	0.5000000	1
O15	O	1	0.4855662	0.4597394	0.5000000	1
O16	O	1	0.5144338	0.5402606	0.5000000	1
O17	O	1	0.5144626	0.4855374	0.5222329	1
O18	O	1	0.4855374	0.4855374	0.4777671	1
O19	O	1	0.5144626	0.5144626	0.4777671	1
O20	O	1	0.4855374	0.5144626	0.5222329	1
O21	O	1	0.5000000	0.5296264	0.4526656	1
O22	O	1	0.5000000	0.4703736	0.4526656	1
O23	O	1	0.4703736	0.5000000	0.5473344	1
O24	O	1	0.5296264	0.5000000	0.5473344	1
Zr1	Zr	1	0.5000000	0.4754731	0.5000000	1
Zr2	Zr	1	0.4754731	0.5000000	0.5000000	1
Zr3	Zr	1	0.5245269	0.5000000	0.5000000	1
Zr4	Zr	1	0.5000000	0.5245269	0.5000000	1

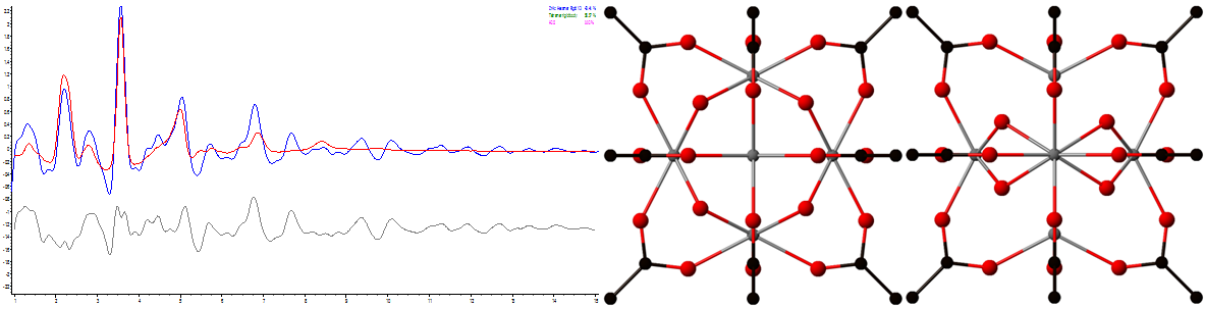

Figure 338: Observed and Calculated PDF from the chandelier core refinement of ZAA1I from the 18-month data collection and the resultant model viewed from the axial (left) and equatorial (right) positions.

Table 281: The atomic coordinates of the model resulting from the chandelier core refinement of ZAA1I from the 18-month data collection.

Atom Label	Atom Type	Multiplicity	Fractional X Coordinate	Fractional Y Coordinate	Fractional Z Coordinate	Fractional Occupancy
C1	C	1	0.590706	0.5000000	0.5839094	1
C2	C	1	0.5000000	0.409294	0.5839094	1
C3	C	1	0.409294	0.5000000	0.5839094	1
C4	C	1	0.5000000	0.590706	0.5839094	1
C5	C	1	0.590706	0.5000000	0.4160906	1
C6	C	1	0.5000000	0.409294	0.4160906	1
C7	C	1	0.409294	0.5000000	0.4160906	1
C8	C	1	0.5000000	0.590706	0.4160906	1
C9	C	1	0.590706	0.409294	0.5000000	1
C10	C	1	0.409294	0.409294	0.5000000	1
C11	C	1	0.409294	0.590706	0.5000000	1
C12	C	1	0.590706	0.590706	0.5000000	1
C13	C	1	0.620112	0.5000000	0.611112	1
C14	C	1	0.5000000	0.379888	0.611112	1
C15	C	1	0.379888	0.5000000	0.611112	1
C16	C	1	0.5000000	0.620112	0.611112	1
C17	C	1	0.620112	0.5000000	0.388888	1
C18	C	1	0.5000000	0.379888	0.388888	1
C19	C	1	0.379888	0.5000000	0.388888	1
C20	C	1	0.5000000	0.620112	0.388888	1
C21	C	1	0.620112	0.379888	0.5000000	1
C22	C	1	0.379888	0.379888	0.5000000	1
C23	C	1	0.379888	0.620112	0.5000000	1
C24	C	1	0.620112	0.620112	0.5000000	1
O1	O	1	0.5443232	0.4556768	0.4742057	1
O2	O	1	0.5443232	0.4556768	0.5257943	1
O3	O	1	0.4556768	0.4556768	0.4742057	1
O4	O	1	0.4556768	0.4556768	0.5257943	1
O5	O	1	0.4556768	0.5443232	0.4742057	1
O6	O	1	0.4556768	0.5443232	0.5257943	1
O7	O	1	0.5443232	0.5443232	0.4742057	1
O8	O	1	0.5443232	0.5443232	0.5257943	1

O9	O	1	0.594964	0.5000000	0.5505801	1
O10	O	1	0.594964	0.4453229	0.5000000	1
O11	O	1	0.594964	0.5000000	0.4494199	1
O12	O	1	0.594964	0.5546771	0.5000000	1
O13	O	1	0.5000000	0.594964	0.5505801	1
O14	O	1	0.5546771	0.594964	0.5000000	1
O15	O	1	0.5000000	0.594964	0.4494199	1
O16	O	1	0.4453229	0.594964	0.5000000	1
O17	O	1	0.405036	0.5000000	0.5505801	1
O18	O	1	0.405036	0.5546771	0.5000000	1
O19	O	1	0.405036	0.5000000	0.4494199	1
O20	O	1	0.405036	0.4453229	0.5000000	1
O21	O	1	0.5000000	0.405036	0.5505801	1
O22	O	1	0.4453229	0.405036	0.5000000	1
O23	O	1	0.5000000	0.405036	0.4494199	1
O24	O	1	0.5546771	0.405036	0.5000000	1
O25	O	1	0.5546771	0.5000000	0.5878483	1
O26	O	1	0.5000000	0.5546771	0.5878483	1
O27	O	1	0.4453229	0.5000000	0.5878483	1
O28	O	1	0.5000000	0.4453229	0.5878483	1
O29	O	1	0.5546771	0.5000000	0.4121517	1
O30	O	1	0.5000000	0.4453229	0.4121517	1
O31	O	1	0.4453229	0.5000000	0.4121517	1
O32	O	1	0.5000000	0.5546771	0.4121517	1
Zr1	Zr	1	0.5667375	0.5000000	0.5000000	1
Zr2	Zr	1	0.5000000	0.5667375	0.5000000	1
Zr3	Zr	1	0.4332625	0.5000000	0.5000000	1
Zr4	Zr	1	0.5000000	0.4332625	0.5000000	1
Zr5	Zr	1	0.5000000	0.5000000	0.5617368	1
Zr6	Zr	1	0.5000000	0.5000000	0.4382632	1

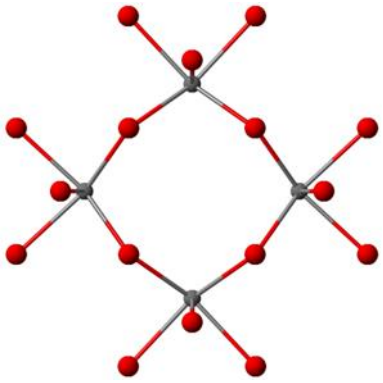

Figure 339: The tetrameric structure resulting from the chandelier core refinement of ZAA1I from the 18-month data collection.

Table 282: The atomic coordinates of the tetrameric phase of the chandelier core refinement of ZAA1I from the 18-month data collection.

Atom Label	Atom Type	Multiplicity	Fractional X Coordinate	Fractional Y Coordinate	Fractional Z Coordinate	Fractional Occupancy
O1	O	1	0.514487	0.485513	0.4766265	1
O2	O	1	0.485513	0.485513	0.5233735	1
O3	O	1	0.514487	0.514487	0.5233735	1
O4	O	1	0.485513	0.514487	0.4766265	1
O5	O	1	0.5000000	0.530134	0.547737	1
O6	O	1	0.5000000	0.469866	0.547737	1
O7	O	1	0.469866	0.5000000	0.452263	1
O8	O	1	0.530134	0.5000000	0.452263	1
O9	O	1	0.5145428	0.4597648	0.5000000	1
O10	O	1	0.4597648	0.4854572	0.5000000	1
O11	O	1	0.5402352	0.5145428	0.5000000	1
O12	O	1	0.4854572	0.5402352	0.5000000	1
O13	O	1	0.4597648	0.5145428	0.5000000	1
O14	O	1	0.5402352	0.4854572	0.5000000	1
O15	O	1	0.4854572	0.4597648	0.5000000	1
O16	O	1	0.5145428	0.5402352	0.5000000	1
O17	O	1	0.514487	0.485513	0.5233735	1
O18	O	1	0.485513	0.485513	0.4766265	1
O19	O	1	0.514487	0.514487	0.4766265	1
O20	O	1	0.485513	0.514487	0.5233735	1
O21	O	1	0.5000000	0.530134	0.452263	1
O22	O	1	0.5000000	0.469866	0.452263	1
O23	O	1	0.469866	0.5000000	0.547737	1
O24	O	1	0.530134	0.5000000	0.547737	1
Zr1	Zr	1	0.5000000	0.4753959	0.5000000	1
Zr2	Zr	1	0.4753959	0.5000000	0.5000000	1
Zr3	Zr	1	0.5246041	0.5000000	0.5000000	1
Zr4	Zr	1	0.5000000	0.5246041	0.5000000	1

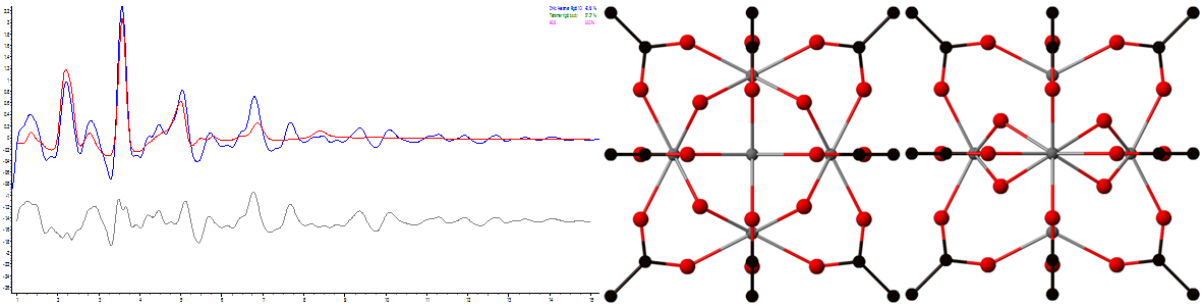

Figure 340: Observed and Calculated PDF from the chandelier core refinement of ZAA4A from the 18-month data collection and the resultant model viewed from the axial (left) and equatorial (right) positions.

Table 283: The atomic coordinates of the model resulting from the chandelier core refinement of ZAA4A from the 18-month data collection.

Atom Label	Atom Type	Multiplicity	Fractional X Coordinate	Fractional Y Coordinate	Fractional Z Coordinate	Fractional Occupancy
C1	C	1	0.5907703	0.5000000	0.5839689	1
C2	C	1	0.5000000	0.4092297	0.5839689	1
C3	C	1	0.4092297	0.5000000	0.5839689	1
C4	C	1	0.5000000	0.5907703	0.5839689	1
C5	C	1	0.5907703	0.5000000	0.4160311	1
C6	C	1	0.5000000	0.4092297	0.4160311	1
C7	C	1	0.4092297	0.5000000	0.4160311	1
C8	C	1	0.5000000	0.5907703	0.4160311	1
C9	C	1	0.5907703	0.4092297	0.5000000	1
C10	C	1	0.4092297	0.4092297	0.5000000	1
C11	C	1	0.4092297	0.5907703	0.5000000	1
C12	C	1	0.5907703	0.5907703	0.5000000	1
C13	C	1	0.6200606	0.5000000	0.6110644	1
C14	C	1	0.5000000	0.3799394	0.6110644	1
C15	C	1	0.3799394	0.5000000	0.6110644	1
C16	C	1	0.5000000	0.6200606	0.6110644	1
C17	C	1	0.6200606	0.5000000	0.3889356	1
C18	C	1	0.5000000	0.3799394	0.3889356	1
C19	C	1	0.3799394	0.5000000	0.3889356	1
C20	C	1	0.5000000	0.6200606	0.3889356	1
C21	C	1	0.6200606	0.3799394	0.5000000	1
C22	C	1	0.3799394	0.3799394	0.5000000	1
C23	C	1	0.3799394	0.6200606	0.5000000	1
C24	C	1	0.6200606	0.6200606	0.5000000	1
O1	O	1	0.544217	0.455783	0.4741114	1
O2	O	1	0.544217	0.455783	0.5258886	1
O3	O	1	0.455783	0.455783	0.4741114	1
O4	O	1	0.455783	0.455783	0.5258886	1
O5	O	1	0.455783	0.544217	0.4741114	1
O6	O	1	0.455783	0.544217	0.5258886	1
O7	O	1	0.544217	0.544217	0.4741114	1
O8	O	1	0.544217	0.544217	0.5258886	1

O9	O	1	0.594844	0.5000000	0.5507865	1
O10	O	1	0.594844	0.4450998	0.5000000	1
O11	O	1	0.594844	0.5000000	0.4492135	1
O12	O	1	0.594844	0.5549002	0.5000000	1
O13	O	1	0.5000000	0.594844	0.5507865	1
O14	O	1	0.5549002	0.594844	0.5000000	1
O15	O	1	0.5000000	0.594844	0.4492135	1
O16	O	1	0.4450998	0.594844	0.5000000	1
O17	O	1	0.405156	0.5000000	0.5507865	1
O18	O	1	0.405156	0.5549002	0.5000000	1
O19	O	1	0.405156	0.5000000	0.4492135	1
O20	O	1	0.405156	0.4450998	0.5000000	1
O21	O	1	0.5000000	0.405156	0.5507865	1
O22	O	1	0.4450998	0.405156	0.5000000	1
O23	O	1	0.5000000	0.405156	0.4492135	1
O24	O	1	0.5549002	0.405156	0.5000000	1
O25	O	1	0.5549002	0.5000000	0.5877373	1
O26	O	1	0.5000000	0.5549002	0.5877373	1
O27	O	1	0.4450998	0.5000000	0.5877373	1
O28	O	1	0.5000000	0.4450998	0.5877373	1
O29	O	1	0.5549002	0.5000000	0.4122627	1
O30	O	1	0.5000000	0.4450998	0.4122627	1
O31	O	1	0.4450998	0.5000000	0.4122627	1
O32	O	1	0.5000000	0.5549002	0.4122627	1
Zr1	Zr	1	0.5667816	0.5000000	0.5000000	1
Zr2	Zr	1	0.5000000	0.5667816	0.5000000	1
Zr3	Zr	1	0.4332184	0.5000000	0.5000000	1
Zr4	Zr	1	0.5000000	0.4332184	0.5000000	1
Zr5	Zr	1	0.5000000	0.5000000	0.5617777	1
Zr6	Zr	1	0.5000000	0.5000000	0.4382223	1

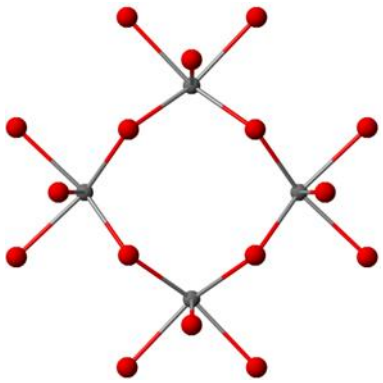

Figure 341: The tetrameric structure resulting from the chandelier core refinement of ZAA4A from the 18-month data collection.

Table 284: The atomic coordinates of the tetrameric phase of the chandelier core refinement of ZAA4A from the 18-month data collection.

Atom Label	Atom Type	Multiplicity	Fractional X Coordinate	Fractional Y Coordinate	Fractional Z Coordinate	Fractional Occupancy
O1	O	1	0.5144836	0.4855164	0.4765632	1
O2	O	1	0.4855164	0.4855164	0.5234368	1
O3	O	1	0.5144836	0.5144836	0.5234368	1
O4	O	1	0.4855164	0.5144836	0.4765632	1
O5	O	1	0.5000000	0.5305173	0.5465295	1
O6	O	1	0.5000000	0.4694827	0.5465295	1
O7	O	1	0.4694827	0.5000000	0.4534705	1
O8	O	1	0.5305173	0.5000000	0.4534705	1
O9	O	1	0.5148786	0.4597705	0.5000000	1
O10	O	1	0.4597705	0.4851214	0.5000000	1
O11	O	1	0.5402295	0.5148786	0.5000000	1
O12	O	1	0.4851214	0.5402295	0.5000000	1
O13	O	1	0.4597705	0.5148786	0.5000000	1
O14	O	1	0.5402295	0.4851214	0.5000000	1
O15	O	1	0.4851214	0.4597705	0.5000000	1
O16	O	1	0.5148786	0.5402295	0.5000000	1
O17	O	1	0.5144836	0.4855164	0.5234368	1
O18	O	1	0.4855164	0.4855164	0.4765632	1
O19	O	1	0.5144836	0.5144836	0.4765632	1
O20	O	1	0.4855164	0.5144836	0.5234368	1
O21	O	1	0.5000000	0.5305173	0.4534705	1
O22	O	1	0.5000000	0.4694827	0.4534705	1
O23	O	1	0.4694827	0.5000000	0.5465295	1
O24	O	1	0.5305173	0.5000000	0.5465295	1
Zr1	Zr	1	0.5000000	0.4754513	0.5000000	1
Zr2	Zr	1	0.4754513	0.5000000	0.5000000	1
Zr3	Zr	1	0.5245487	0.5000000	0.5000000	1
Zr4	Zr	1	0.5000000	0.5245487	0.5000000	1

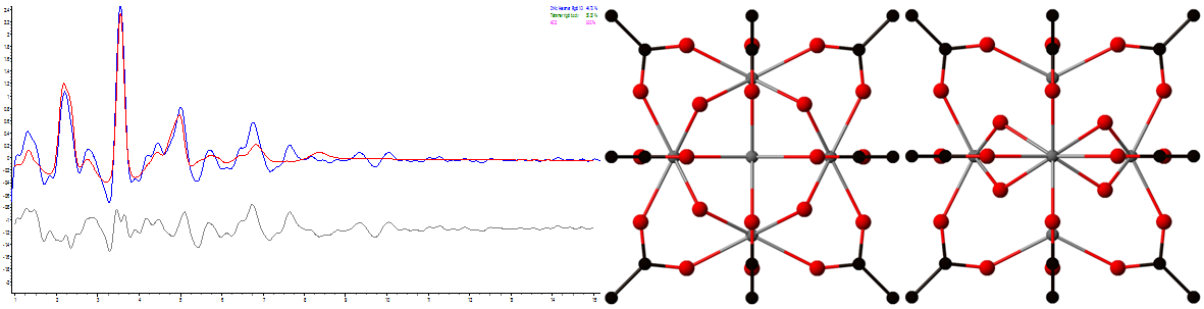

Figure 342: Observed and Calculated PDF from the chandelier core refinement of ZAA4C from the 18-month data collection and the resultant model viewed from the axial (left) and equatorial (right) positions.

Table 285: The atomic coordinates of the model resulting from the chandelier core refinement of ZAA4C from the 18-month data collection.

Atom Label	Atom Type	Multiplicity	Fractional X Coordinate	Fractional Y Coordinate	Fractional Z Coordinate	Fractional Occupancy
C1	C	1	0.5908237	0.5000000	0.5840182	1
C2	C	1	0.5000000	0.4091763	0.5840182	1
C3	C	1	0.4091763	0.5000000	0.5840182	1
C4	C	1	0.5000000	0.5908237	0.5840182	1
C5	C	1	0.5908237	0.5000000	0.4159818	1
C6	C	1	0.5000000	0.4091763	0.4159818	1
C7	C	1	0.4091763	0.5000000	0.4159818	1
C8	C	1	0.5000000	0.5908237	0.4159818	1
C9	C	1	0.5908237	0.4091763	0.5000000	1
C10	C	1	0.4091763	0.4091763	0.5000000	1
C11	C	1	0.4091763	0.5908237	0.5000000	1
C12	C	1	0.5908237	0.5908237	0.5000000	1
C13	C	1	0.6193831	0.5000000	0.6104377	1
C14	C	1	0.5000000	0.3806169	0.6104377	1
C15	C	1	0.3806169	0.5000000	0.6104377	1
C16	C	1	0.5000000	0.6193831	0.6104377	1
C17	C	1	0.6193831	0.5000000	0.3895623	1
C18	C	1	0.5000000	0.3806169	0.3895623	1
C19	C	1	0.3806169	0.5000000	0.3895623	1
C20	C	1	0.5000000	0.6193831	0.3895623	1
C21	C	1	0.6193831	0.3806169	0.5000000	1
C22	C	1	0.3806169	0.3806169	0.5000000	1
C23	C	1	0.3806169	0.6193831	0.5000000	1
C24	C	1	0.6193831	0.6193831	0.5000000	1
O1	O	1	0.5443396	0.4556604	0.4735403	1
O2	O	1	0.5443396	0.4556604	0.5264597	1
O3	O	1	0.4556604	0.4556604	0.4735403	1
O4	O	1	0.4556604	0.4556604	0.5264597	1
O5	O	1	0.4556604	0.5443396	0.4735403	1
O6	O	1	0.4556604	0.5443396	0.5264597	1
O7	O	1	0.5443396	0.5443396	0.4735403	1
O8	O	1	0.5443396	0.5443396	0.5264597	1

O9	O	1	0.5944559	0.5000000	0.551283	1
O10	O	1	0.5944559	0.4445631	0.5000000	1
O11	O	1	0.5944559	0.5000000	0.448717	1
O12	O	1	0.5944559	0.5554369	0.5000000	1
O13	O	1	0.5000000	0.5944559	0.551283	1
O14	O	1	0.5554369	0.5944559	0.5000000	1
O15	O	1	0.5000000	0.5944559	0.448717	1
O16	O	1	0.4445631	0.5944559	0.5000000	1
O17	O	1	0.4055441	0.5000000	0.551283	1
O18	O	1	0.4055441	0.5554369	0.5000000	1
O19	O	1	0.4055441	0.5000000	0.448717	1
O20	O	1	0.4055441	0.4445631	0.5000000	1
O21	O	1	0.5000000	0.4055441	0.551283	1
O22	O	1	0.4445631	0.4055441	0.5000000	1
O23	O	1	0.5000000	0.4055441	0.448717	1
O24	O	1	0.5554369	0.4055441	0.5000000	1
O25	O	1	0.5554369	0.5000000	0.5873783	1
O26	O	1	0.5000000	0.5554369	0.5873783	1
O27	O	1	0.4445631	0.5000000	0.5873783	1
O28	O	1	0.5000000	0.4445631	0.5873783	1
O29	O	1	0.5554369	0.5000000	0.4126217	1
O30	O	1	0.5000000	0.4445631	0.4126217	1
O31	O	1	0.4445631	0.5000000	0.4126217	1
O32	O	1	0.5000000	0.5554369	0.4126217	1
Zr1	Zr	1	0.5664218	0.5000000	0.5000000	1
Zr2	Zr	1	0.5000000	0.5664218	0.5000000	1
Zr3	Zr	1	0.4335782	0.5000000	0.5000000	1
Zr4	Zr	1	0.5000000	0.4335782	0.5000000	1
Zr5	Zr	1	0.5000000	0.5000000	0.5614448	1
Zr6	Zr	1	0.5000000	0.5000000	0.4385552	1

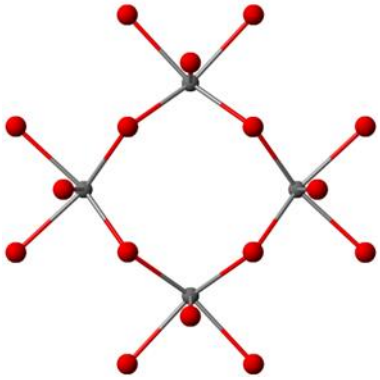

Figure 343: The tetrameric structure resulting from the chandelier core refinement of ZAA4C from the 18-month data collection.

Table 286: The atomic coordinates of the tetrameric phase of the chandelier core refinement of ZAA4C from the 18-month data collection.

Atom Label	Atom Type	Multiplicity	Fractional X Coordinate	Fractional Y Coordinate	Fractional Z Coordinate	Fractional Occupancy
O1	O	1	0.5144134	0.4855866	0.4762393	1
O2	O	1	0.4855866	0.4855866	0.5237607	1
O3	O	1	0.5144134	0.5144134	0.5237607	1
O4	O	1	0.4855866	0.5144134	0.4762393	1
O5	O	1	0.5000000	0.5292253	0.5468777	1
O6	O	1	0.5000000	0.4707747	0.5468777	1
O7	O	1	0.4707747	0.5000000	0.4531223	1
O8	O	1	0.5292253	0.5000000	0.4531223	1
O9	O	1	0.5145195	0.4598162	0.5000000	1
O10	O	1	0.4598162	0.4854805	0.5000000	1
O11	O	1	0.5401838	0.5145195	0.5000000	1
O12	O	1	0.4854805	0.5401838	0.5000000	1
O13	O	1	0.4598162	0.5145195	0.5000000	1
O14	O	1	0.5401838	0.4854805	0.5000000	1
O15	O	1	0.4854805	0.4598162	0.5000000	1
O16	O	1	0.5145195	0.5401838	0.5000000	1
O17	O	1	0.5144134	0.4855866	0.5237607	1
O18	O	1	0.4855866	0.4855866	0.4762393	1
O19	O	1	0.5144134	0.5144134	0.4762393	1
O20	O	1	0.4855866	0.5144134	0.5237607	1
O21	O	1	0.5000000	0.5292253	0.4531223	1
O22	O	1	0.5000000	0.4707747	0.4531223	1
O23	O	1	0.4707747	0.5000000	0.5468777	1
O24	O	1	0.5292253	0.5000000	0.5468777	1
Zr1	Zr	1	0.5000000	0.4754913	0.5000000	1
Zr2	Zr	1	0.4754913	0.5000000	0.5000000	1
Zr3	Zr	1	0.5245087	0.5000000	0.5000000	1
Zr4	Zr	1	0.5000000	0.5245087	0.5000000	1

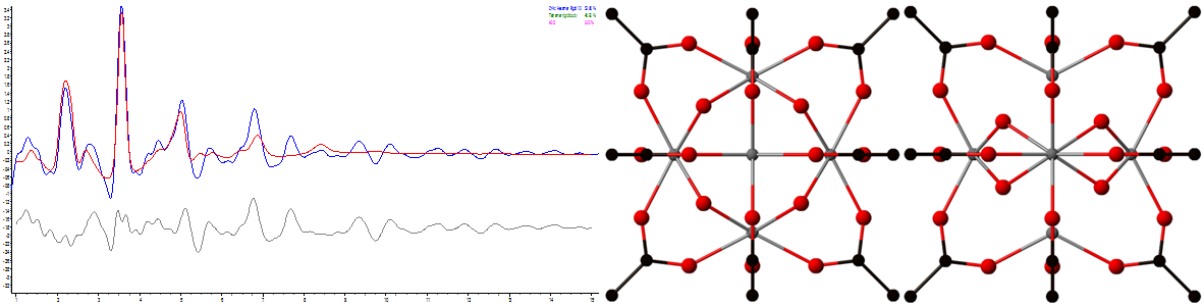

Figure 344: Observed and Calculated PDF from the chandelier core refinement of ZAA4I from the 18-month data collection and the resultant model viewed from the axial (left) and equatorial (right) positions.

Table 287: The atomic coordinates of the model resulting from the chandelier core refinement of ZAA4I from the 18-month data collection.

Atom Label	Atom Type	Multiplicity	Fractional X Coordinate	Fractional Y Coordinate	Fractional Z Coordinate	Fractional Occupancy
C1	C	1	0.5904591	0.5000000	0.583681	1
C2	C	1	0.5000000	0.4095409	0.583681	1
C3	C	1	0.4095409	0.5000000	0.583681	1
C4	C	1	0.5000000	0.5904591	0.583681	1
C5	C	1	0.5904591	0.5000000	0.416319	1
C6	C	1	0.5000000	0.4095409	0.416319	1
C7	C	1	0.4095409	0.5000000	0.416319	1
C8	C	1	0.5000000	0.5904591	0.416319	1
C9	C	1	0.5904591	0.4095409	0.5000000	1
C10	C	1	0.4095409	0.4095409	0.5000000	1
C11	C	1	0.4095409	0.5904591	0.5000000	1
C12	C	1	0.5904591	0.5904591	0.5000000	1
C13	C	1	0.6203183	0.5000000	0.6113028	1
C14	C	1	0.5000000	0.3796817	0.6113028	1
C15	C	1	0.3796817	0.5000000	0.6113028	1
C16	C	1	0.5000000	0.6203183	0.6113028	1
C17	C	1	0.6203183	0.5000000	0.3886972	1
C18	C	1	0.5000000	0.3796817	0.3886972	1
C19	C	1	0.3796817	0.5000000	0.3886972	1
C20	C	1	0.5000000	0.6203183	0.3886972	1
C21	C	1	0.6203183	0.3796817	0.5000000	1
C22	C	1	0.3796817	0.3796817	0.5000000	1
C23	C	1	0.3796817	0.6203183	0.5000000	1
C24	C	1	0.6203183	0.6203183	0.5000000	1
O1	O	1	0.541725	0.458275	0.4742861	1
O2	O	1	0.541725	0.458275	0.5257139	1
O3	O	1	0.458275	0.458275	0.4742861	1
O4	O	1	0.458275	0.458275	0.5257139	1
O5	O	1	0.458275	0.541725	0.4742861	1
O6	O	1	0.458275	0.541725	0.5257139	1
O7	O	1	0.541725	0.541725	0.4742861	1
O8	O	1	0.541725	0.541725	0.5257139	1

O9	O	1	0.594941	0.5000000	0.5501169	1
O10	O	1	0.594941	0.4458236	0.5000000	1
O11	O	1	0.594941	0.5000000	0.4498831	1
O12	O	1	0.594941	0.5541764	0.5000000	1
O13	O	1	0.5000000	0.594941	0.5501169	1
O14	O	1	0.5541764	0.594941	0.5000000	1
O15	O	1	0.5000000	0.594941	0.4498831	1
O16	O	1	0.4458236	0.594941	0.5000000	1
O17	O	1	0.405059	0.5000000	0.5501169	1
O18	O	1	0.405059	0.5541764	0.5000000	1
O19	O	1	0.405059	0.5000000	0.4498831	1
O20	O	1	0.405059	0.4458236	0.5000000	1
O21	O	1	0.5000000	0.405059	0.5501169	1
O22	O	1	0.4458236	0.405059	0.5000000	1
O23	O	1	0.5000000	0.405059	0.4498831	1
O24	O	1	0.5541764	0.405059	0.5000000	1
O25	O	1	0.5541764	0.5000000	0.5878271	1
O26	O	1	0.5000000	0.5541764	0.5878271	1
O27	O	1	0.4458236	0.5000000	0.5878271	1
O28	O	1	0.5000000	0.4458236	0.5878271	1
O29	O	1	0.5541764	0.5000000	0.4121729	1
O30	O	1	0.5000000	0.4458236	0.4121729	1
O31	O	1	0.4458236	0.5000000	0.4121729	1
O32	O	1	0.5000000	0.5541764	0.4121729	1
Zr1	Zr	1	0.5667022	0.5000000	0.5000000	1
Zr2	Zr	1	0.5000000	0.5667022	0.5000000	1
Zr3	Zr	1	0.4332978	0.5000000	0.5000000	1
Zr4	Zr	1	0.5000000	0.4332978	0.5000000	1
Zr5	Zr	1	0.5000000	0.5000000	0.5617042	1
Zr6	Zr	1	0.5000000	0.5000000	0.4382958	1

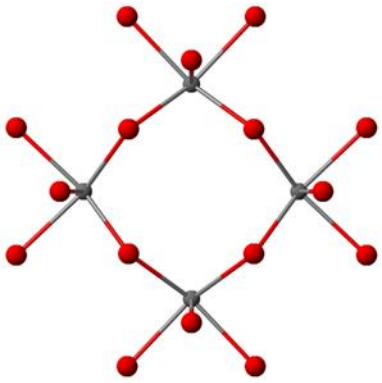

Figure 345: The tetrameric structure resulting from the chandelier core refinement of ZAA4I from the 18-month data collection.

Table 288: The atomic coordinates of the tetrameric phase of the chandelier core refinement of ZAA4I from the 18-month data collection.

Atom Label	Atom Type	Multiplicity	Fractional X Coordinate	Fractional Y Coordinate	Fractional Z Coordinate	Fractional Occupancy
O1	O	1	0.5143221	0.4856779	0.4754612	1
O2	O	1	0.4856779	0.4856779	0.5245388	1
O3	O	1	0.5143221	0.5143221	0.5245388	1
O4	O	1	0.4856779	0.5143221	0.4754612	1
O5	O	1	0.5000000	0.5301636	0.5462521	1
O6	O	1	0.5000000	0.4698364	0.5462521	1
O7	O	1	0.4698364	0.5000000	0.4537479	1
O8	O	1	0.5301636	0.5000000	0.4537479	1
O9	O	1	0.5146875	0.4598283	0.5000000	1
O10	O	1	0.4598283	0.4853125	0.5000000	1
O11	O	1	0.5401717	0.5146875	0.5000000	1
O12	O	1	0.4853125	0.5401717	0.5000000	1
O13	O	1	0.4598283	0.5146875	0.5000000	1
O14	O	1	0.5401717	0.4853125	0.5000000	1
O15	O	1	0.4853125	0.4598283	0.5000000	1
O16	O	1	0.5146875	0.5401717	0.5000000	1
O17	O	1	0.5143221	0.4856779	0.5245388	1
O18	O	1	0.4856779	0.4856779	0.4754612	1
O19	O	1	0.5143221	0.5143221	0.4754612	1
O20	O	1	0.4856779	0.5143221	0.5245388	1
O21	O	1	0.5000000	0.5301636	0.4537479	1
O22	O	1	0.5000000	0.4698364	0.4537479	1
O23	O	1	0.4698364	0.5000000	0.5462521	1
O24	O	1	0.5301636	0.5000000	0.5462521	1
Zr1	Zr	1	0.5000000	0.4753186	0.5000000	1
Zr2	Zr	1	0.4753186	0.5000000	0.5000000	1
Zr3	Zr	1	0.5246814	0.5000000	0.5000000	1
Zr4	Zr	1	0.5000000	0.5246814	0.5000000	1

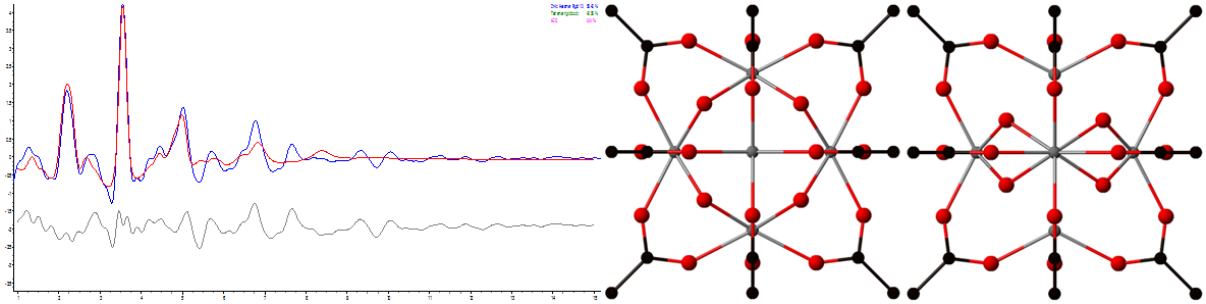

Figure 346: Observed and Calculated PDF from the chandelier core refinement of ZAA7A from the 18-month data collection and the resultant model viewed from the axial (left) and equatorial (right) positions.

Table 289: The atomic coordinates of the model resulting from the chandelier core refinement of ZAA7A from the 18-month data collection.

Atom Label	Atom Type	Multiplicity	Fractional X Coordinate	Fractional Y Coordinate	Fractional Z Coordinate	Fractional Occupancy
C1	C	1	0.5899395	0.5000000	0.5832003	1
C2	C	1	0.5000000	0.4100605	0.5832003	1
C3	C	1	0.4100605	0.5000000	0.5832003	1
C4	C	1	0.5000000	0.5899395	0.5832003	1
C5	C	1	0.5899395	0.5000000	0.4167997	1
C6	C	1	0.5000000	0.4100605	0.4167997	1
C7	C	1	0.4100605	0.5000000	0.4167997	1
C8	C	1	0.5000000	0.5899395	0.4167997	1
C9	C	1	0.5899395	0.4100605	0.5000000	1
C10	C	1	0.4100605	0.4100605	0.5000000	1
C11	C	1	0.4100605	0.5899395	0.5000000	1
C12	C	1	0.5899395	0.5899395	0.5000000	1
C13	C	1	0.6200396	0.5000000	0.611045	1
C14	C	1	0.5000000	0.3799604	0.611045	1
C15	C	1	0.3799604	0.5000000	0.611045	1
C16	C	1	0.5000000	0.6200396	0.611045	1
C17	C	1	0.6200396	0.5000000	0.388955	1
C18	C	1	0.5000000	0.3799604	0.388955	1
C19	C	1	0.3799604	0.5000000	0.388955	1
C20	C	1	0.5000000	0.6200396	0.388955	1
C21	C	1	0.6200396	0.3799604	0.5000000	1
C22	C	1	0.3799604	0.3799604	0.5000000	1
C23	C	1	0.3799604	0.6200396	0.5000000	1
C24	C	1	0.6200396	0.6200396	0.5000000	1
O1	O	1	0.5411225	0.4588775	0.4745569	1
O2	O	1	0.5411225	0.4588775	0.5254431	1
O3	O	1	0.4588775	0.4588775	0.4745569	1
O4	O	1	0.4588775	0.4588775	0.5254431	1
O5	O	1	0.4588775	0.5411225	0.4745569	1
O6	O	1	0.4588775	0.5411225	0.5254431	1
O7	O	1	0.5411225	0.5411225	0.4745569	1
O8	O	1	0.5411225	0.5411225	0.5254431	1

O9	O	1	0.5944722	0.5000000	0.5501001	1
O10	O	1	0.5944722	0.4458418	0.5000000	1
O11	O	1	0.5944722	0.5000000	0.4498999	1
O12	O	1	0.5944722	0.5541582	0.5000000	1
O13	O	1	0.5000000	0.5944722	0.5501001	1
O14	O	1	0.5541582	0.5944722	0.5000000	1
O15	O	1	0.5000000	0.5944722	0.4498999	1
O16	O	1	0.4458418	0.5944722	0.5000000	1
O17	O	1	0.4055278	0.5000000	0.5501001	1
O18	O	1	0.4055278	0.5541582	0.5000000	1
O19	O	1	0.4055278	0.5000000	0.4498999	1
O20	O	1	0.4055278	0.4458418	0.5000000	1
O21	O	1	0.5000000	0.4055278	0.5501001	1
O22	O	1	0.4458418	0.4055278	0.5000000	1
O23	O	1	0.5000000	0.4055278	0.4498999	1
O24	O	1	0.5541582	0.4055278	0.5000000	1
O25	O	1	0.5541582	0.5000000	0.5873933	1
O26	O	1	0.5000000	0.5541582	0.5873933	1
O27	O	1	0.4458418	0.5000000	0.5873933	1
O28	O	1	0.5000000	0.4458418	0.5873933	1
O29	O	1	0.5541582	0.5000000	0.4126067	1
O30	O	1	0.5000000	0.4458418	0.4126067	1
O31	O	1	0.4458418	0.5000000	0.4126067	1
O32	O	1	0.5000000	0.5541582	0.4126067	1
Zr1	Zr	1	0.5665389	0.5000000	0.5000000	1
Zr2	Zr	1	0.5000000	0.5665389	0.5000000	1
Zr3	Zr	1	0.4334611	0.5000000	0.5000000	1
Zr4	Zr	1	0.5000000	0.4334611	0.5000000	1
Zr5	Zr	1	0.5000000	0.5000000	0.5615531	1
Zr6	Zr	1	0.5000000	0.5000000	0.4384469	1

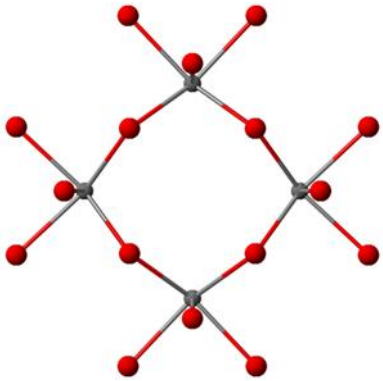

Figure 347: The tetrameric structure resulting from the chandelier core refinement of ZAA7A from the 18-month data collection.

Table 290: The atomic coordinates of the tetrameric phase of the chandelier core refinement of ZAA7A from the 18-month data collection.

Atom Label	Atom Type	Multiplicity	Fractional X Coordinate	Fractional Y Coordinate	Fractional Z Coordinate	Fractional Occupancy
O1	O	1	0.5142995	0.4857005	0.4737372	1
O2	O	1	0.4857005	0.4857005	0.5262628	1
O3	O	1	0.5142995	0.5142995	0.5262628	1
O4	O	1	0.4857005	0.5142995	0.4737372	1
O5	O	1	0.5000000	0.5291674	0.5463425	1
O6	O	1	0.5000000	0.4708326	0.5463425	1
O7	O	1	0.4708326	0.5000000	0.4536575	1
O8	O	1	0.5291674	0.5000000	0.4536575	1
O9	O	1	0.5146112	0.459937	0.5000000	1
O10	O	1	0.459937	0.4853888	0.5000000	1
O11	O	1	0.540063	0.5146112	0.5000000	1
O12	O	1	0.4853888	0.540063	0.5000000	1
O13	O	1	0.459937	0.5146112	0.5000000	1
O14	O	1	0.540063	0.4853888	0.5000000	1
O15	O	1	0.4853888	0.459937	0.5000000	1
O16	O	1	0.5146112	0.540063	0.5000000	1
O17	O	1	0.5142995	0.4857005	0.5262628	1
O18	O	1	0.4857005	0.4857005	0.4737372	1
O19	O	1	0.5142995	0.5142995	0.4737372	1
O20	O	1	0.4857005	0.5142995	0.5262628	1
O21	O	1	0.5000000	0.5291674	0.4536575	1
O22	O	1	0.5000000	0.4708326	0.4536575	1
O23	O	1	0.4708326	0.5000000	0.5463425	1
O24	O	1	0.5291674	0.5000000	0.5463425	1
Zr1	Zr	1	0.5000000	0.4754832	0.5000000	1
Zr2	Zr	1	0.4754832	0.5000000	0.5000000	1
Zr3	Zr	1	0.5245168	0.5000000	0.5000000	1
Zr4	Zr	1	0.5000000	0.5245168	0.5000000	1

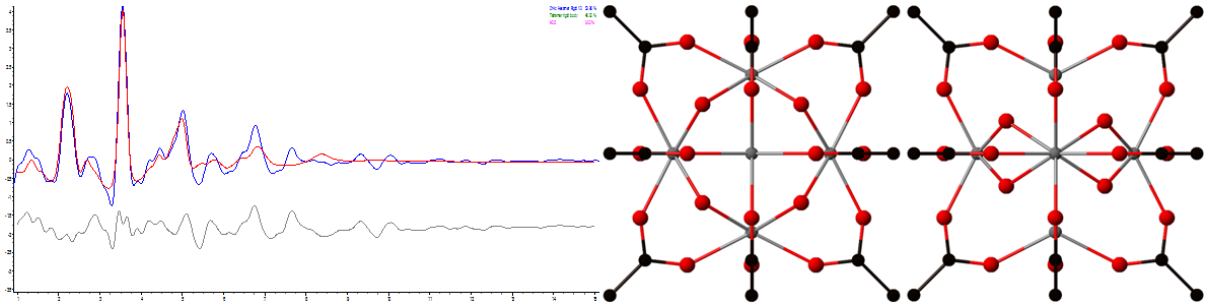

Figure 348: Observed and Calculated PDF from the chandelier core refinement of ZAA7C from the 18-month data collection and the resultant model viewed from the axial (left) and equatorial (right) positions.

Table 291: The atomic coordinates of the model resulting from the chandelier core refinement of ZAA7C from the 18-month data collection.

Atom Label	Atom Type	Multiplicity	Fractional X Coordinate	Fractional Y Coordinate	Fractional Z Coordinate	Fractional Occupancy
C1	C	1	0.5900613	0.5000000	0.5833129	1
C2	C	1	0.5000000	0.4099387	0.5833129	1
C3	C	1	0.4099387	0.5000000	0.5833129	1
C4	C	1	0.5000000	0.5900613	0.5833129	1
C5	C	1	0.5900613	0.5000000	0.4166871	1
C6	C	1	0.5000000	0.4099387	0.4166871	1
C7	C	1	0.4099387	0.5000000	0.4166871	1
C8	C	1	0.5000000	0.5900613	0.4166871	1
C9	C	1	0.5900613	0.4099387	0.5000000	1
C10	C	1	0.4099387	0.4099387	0.5000000	1
C11	C	1	0.4099387	0.5900613	0.5000000	1
C12	C	1	0.5900613	0.5900613	0.5000000	1
C13	C	1	0.6198589	0.5000000	0.6108779	1
C14	C	1	0.5000000	0.3801411	0.6108779	1
C15	C	1	0.3801411	0.5000000	0.6108779	1
C16	C	1	0.5000000	0.6198589	0.6108779	1
C17	C	1	0.6198589	0.5000000	0.3891221	1
C18	C	1	0.5000000	0.3801411	0.3891221	1
C19	C	1	0.3801411	0.5000000	0.3891221	1
C20	C	1	0.5000000	0.6198589	0.3891221	1
C21	C	1	0.6198589	0.3801411	0.5000000	1
C22	C	1	0.3801411	0.3801411	0.5000000	1
C23	C	1	0.3801411	0.6198589	0.5000000	1
C24	C	1	0.6198589	0.6198589	0.5000000	1
O1	O	1	0.5416315	0.4583685	0.4745263	1
O2	O	1	0.5416315	0.4583685	0.5254737	1
O3	O	1	0.4583685	0.4583685	0.4745263	1
O4	O	1	0.4583685	0.4583685	0.5254737	1
O5	O	1	0.4583685	0.5416315	0.4745263	1
O6	O	1	0.4583685	0.5416315	0.5254737	1
O7	O	1	0.5416315	0.5416315	0.4745263	1
O8	O	1	0.5416315	0.5416315	0.5254737	1

O9	O	1	0.5942613	0.5000000	0.5503626	1
O10	O	1	0.5942613	0.445558	0.5000000	1
O11	O	1	0.5942613	0.5000000	0.4496374	1
O12	O	1	0.5942613	0.554442	0.5000000	1
O13	O	1	0.5000000	0.5942613	0.5503626	1
O14	O	1	0.554442	0.5942613	0.5000000	1
O15	O	1	0.5000000	0.5942613	0.4496374	1
O16	O	1	0.445558	0.5942613	0.5000000	1
O17	O	1	0.4057387	0.5000000	0.5503626	1
O18	O	1	0.4057387	0.554442	0.5000000	1
O19	O	1	0.4057387	0.5000000	0.4496374	1
O20	O	1	0.4057387	0.445558	0.5000000	1
O21	O	1	0.5000000	0.4057387	0.5503626	1
O22	O	1	0.445558	0.4057387	0.5000000	1
O23	O	1	0.5000000	0.4057387	0.4496374	1
O24	O	1	0.554442	0.4057387	0.5000000	1
O25	O	1	0.554442	0.5000000	0.5871983	1
O26	O	1	0.5000000	0.554442	0.5871983	1
O27	O	1	0.445558	0.5000000	0.5871983	1
O28	O	1	0.5000000	0.445558	0.5871983	1
O29	O	1	0.554442	0.5000000	0.4128017	1
O30	O	1	0.5000000	0.445558	0.4128017	1
O31	O	1	0.445558	0.5000000	0.4128017	1
O32	O	1	0.5000000	0.554442	0.4128017	1
Zr1	Zr	1	0.566488	0.5000000	0.5000000	1
Zr2	Zr	1	0.5000000	0.566488	0.5000000	1
Zr3	Zr	1	0.433512	0.5000000	0.5000000	1
Zr4	Zr	1	0.5000000	0.433512	0.5000000	1
Zr5	Zr	1	0.5000000	0.5000000	0.561506	1
Zr6	Zr	1	0.5000000	0.5000000	0.438494	1

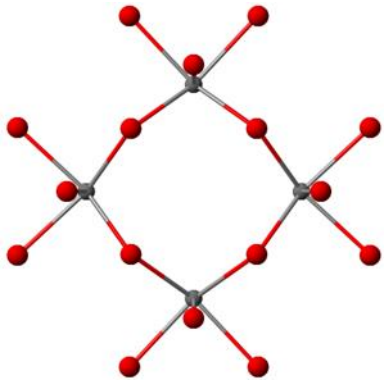

Figure 349: The tetrameric structure resulting from the chandelier core refinement of ZAA7C from the 18-month data collection.

Table 292: The atomic coordinates of the tetrameric phase of the chandelier core refinement of ZAA7C from the 18-month data collection.

Atom Label	Atom Type	Multiplicity	Fractional X Coordinate	Fractional Y Coordinate	Fractional Z Coordinate	Fractional Occupancy
O1	O	1	0.5143234	0.4856766	0.4736985	1
O2	O	1	0.4856766	0.4856766	0.5263015	1
O3	O	1	0.5143234	0.5143234	0.5263015	1
O4	O	1	0.4856766	0.5143234	0.4736985	1
O5	O	1	0.5000000	0.5289056	0.5466018	1
O6	O	1	0.5000000	0.4710944	0.5466018	1
O7	O	1	0.4710944	0.5000000	0.4533982	1
O8	O	1	0.5289056	0.5000000	0.4533982	1
O9	O	1	0.5145691	0.4599496	0.5000000	1
O10	O	1	0.4599496	0.4854309	0.5000000	1
O11	O	1	0.5400504	0.5145691	0.5000000	1
O12	O	1	0.4854309	0.5400504	0.5000000	1
O13	O	1	0.4599496	0.5145691	0.5000000	1
O14	O	1	0.5400504	0.4854309	0.5000000	1
O15	O	1	0.4854309	0.4599496	0.5000000	1
O16	O	1	0.5145691	0.5400504	0.5000000	1
O17	O	1	0.5143234	0.4856766	0.5263015	1
O18	O	1	0.4856766	0.4856766	0.4736985	1
O19	O	1	0.5143234	0.5143234	0.4736985	1
O20	O	1	0.4856766	0.5143234	0.5263015	1
O21	O	1	0.5000000	0.5289056	0.4533982	1
O22	O	1	0.5000000	0.4710944	0.4533982	1
O23	O	1	0.4710944	0.5000000	0.5466018	1
O24	O	1	0.5289056	0.5000000	0.5466018	1
Zr1	Zr	1	0.5000000	0.4755497	0.5000000	1
Zr2	Zr	1	0.4755497	0.5000000	0.5000000	1
Zr3	Zr	1	0.5244503	0.5000000	0.5000000	1
Zr4	Zr	1	0.5000000	0.5244503	0.5000000	1

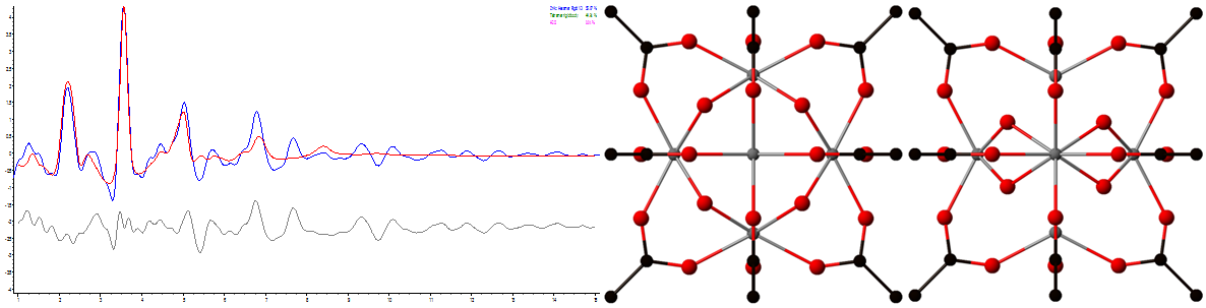

Figure 350: Observed and Calculated PDF from the chandelier core refinement of ZAA7I from the 18-month data collection and the resultant model viewed from the axial (left) and equatorial (right) positions.

Table 293: The atomic coordinates of the model resulting from the chandelier core refinement of ZAA7I from the 18-month data collection.

Atom Label	Atom Type	Multiplicity	Fractional X Coordinate	Fractional Y Coordinate	Fractional Z Coordinate	Fractional Occupancy
C1	C	1	0.5898481	0.5000000	0.5831158	1
C2	C	1	0.5000000	0.4101519	0.5831158	1
C3	C	1	0.4101519	0.5000000	0.5831158	1
C4	C	1	0.5000000	0.5898481	0.5831158	1
C5	C	1	0.5898481	0.5000000	0.4168842	1
C6	C	1	0.5000000	0.4101519	0.4168842	1
C7	C	1	0.4101519	0.5000000	0.4168842	1
C8	C	1	0.5000000	0.5898481	0.4168842	1
C9	C	1	0.5898481	0.4101519	0.5000000	1
C10	C	1	0.4101519	0.4101519	0.5000000	1
C11	C	1	0.4101519	0.5898481	0.5000000	1
C12	C	1	0.5898481	0.5898481	0.5000000	1
C13	C	1	0.6202109	0.5000000	0.6112034	1
C14	C	1	0.5000000	0.3797891	0.6112034	1
C15	C	1	0.3797891	0.5000000	0.6112034	1
C16	C	1	0.5000000	0.6202109	0.6112034	1
C17	C	1	0.6202109	0.5000000	0.3887966	1
C18	C	1	0.5000000	0.3797891	0.3887966	1
C19	C	1	0.3797891	0.5000000	0.3887966	1
C20	C	1	0.5000000	0.6202109	0.3887966	1
C21	C	1	0.6202109	0.3797891	0.5000000	1
C22	C	1	0.3797891	0.3797891	0.5000000	1
C23	C	1	0.3797891	0.6202109	0.5000000	1
C24	C	1	0.6202109	0.6202109	0.5000000	1
O1	O	1	0.5411763	0.4588237	0.4745858	1
O2	O	1	0.5411763	0.4588237	0.5254142	1
O3	O	1	0.4588237	0.4588237	0.4745858	1
O4	O	1	0.4588237	0.4588237	0.5254142	1
O5	O	1	0.4588237	0.5411763	0.4745858	1
O6	O	1	0.4588237	0.5411763	0.5254142	1
O7	O	1	0.5411763	0.5411763	0.4745858	1
O8	O	1	0.5411763	0.5411763	0.5254142	1

O9	O	1	0.5948549	0.5000000	0.5499427	1
O10	O	1	0.5948549	0.446012	0.5000000	1
O11	O	1	0.5948549	0.5000000	0.4500573	1
O12	O	1	0.5948549	0.553988	0.5000000	1
O13	O	1	0.5000000	0.5948549	0.5499427	1
O14	O	1	0.553988	0.5948549	0.5000000	1
O15	O	1	0.5000000	0.5948549	0.4500573	1
O16	O	1	0.446012	0.5948549	0.5000000	1
O17	O	1	0.4051451	0.5000000	0.5499427	1
O18	O	1	0.4051451	0.553988	0.5000000	1
O19	O	1	0.4051451	0.5000000	0.4500573	1
O20	O	1	0.4051451	0.446012	0.5000000	1
O21	O	1	0.5000000	0.4051451	0.5499427	1
O22	O	1	0.446012	0.4051451	0.5000000	1
O23	O	1	0.5000000	0.4051451	0.4500573	1
O24	O	1	0.553988	0.4051451	0.5000000	1
O25	O	1	0.553988	0.5000000	0.5877474	1
O26	O	1	0.5000000	0.553988	0.5877474	1
O27	O	1	0.446012	0.5000000	0.5877474	1
O28	O	1	0.5000000	0.446012	0.5877474	1
O29	O	1	0.553988	0.5000000	0.4122526	1
O30	O	1	0.5000000	0.446012	0.4122526	1
O31	O	1	0.446012	0.5000000	0.4122526	1
O32	O	1	0.5000000	0.553988	0.4122526	1
Zr1	Zr	1	0.5667392	0.5000000	0.5000000	1
Zr2	Zr	1	0.5000000	0.5667392	0.5000000	1
Zr3	Zr	1	0.4332608	0.5000000	0.5000000	1
Zr4	Zr	1	0.5000000	0.4332608	0.5000000	1
Zr5	Zr	1	0.5000000	0.5000000	0.5617384	1
Zr6	Zr	1	0.5000000	0.5000000	0.4382616	1

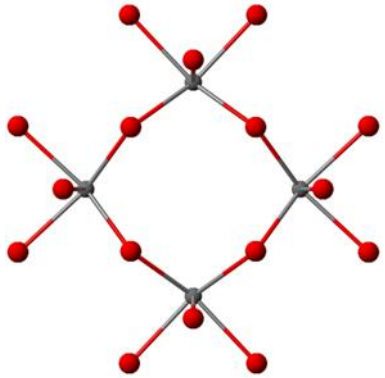

Figure 351: The tetrameric structure resulting from the chandelier core refinement of ZAA7I from the 18-month data collection.

Table 294: The atomic coordinates of the tetrameric phase of the chandelier core refinement of ZAA7I from the 18-month data collection.

Atom Label	Atom Type	Multiplicity	Fractional X Coordinate	Fractional Y Coordinate	Fractional Z Coordinate	Fractional Occupancy
O1	O	1	0.5143074	0.4856926	0.4750423	1
O2	O	1	0.4856926	0.4856926	0.5249577	1
O3	O	1	0.5143074	0.5143074	0.5249577	1
O4	O	1	0.4856926	0.5143074	0.4750423	1
O5	O	1	0.5000000	0.5297724	0.5463577	1
O6	O	1	0.5000000	0.4702276	0.5463577	1
O7	O	1	0.4702276	0.5000000	0.4536423	1
O8	O	1	0.5297724	0.5000000	0.4536423	1
O9	O	1	0.5145547	0.459852	0.5000000	1
O10	O	1	0.459852	0.4854453	0.5000000	1
O11	O	1	0.540148	0.5145547	0.5000000	1
O12	O	1	0.4854453	0.540148	0.5000000	1
O13	O	1	0.459852	0.5145547	0.5000000	1
O14	O	1	0.540148	0.4854453	0.5000000	1
O15	O	1	0.4854453	0.459852	0.5000000	1
O16	O	1	0.5145547	0.540148	0.5000000	1
O17	O	1	0.5143074	0.4856926	0.5249577	1
O18	O	1	0.4856926	0.4856926	0.4750423	1
O19	O	1	0.5143074	0.5143074	0.4750423	1
O20	O	1	0.4856926	0.5143074	0.5249577	1
O21	O	1	0.5000000	0.5297724	0.4536423	1
O22	O	1	0.5000000	0.4702276	0.4536423	1
O23	O	1	0.4702276	0.5000000	0.5463577	1
O24	O	1	0.5297724	0.5000000	0.5463577	1
Zr1	Zr	1	0.5000000	0.4754067	0.5000000	1
Zr2	Zr	1	0.4754067	0.5000000	0.5000000	1
Zr3	Zr	1	0.5245933	0.5000000	0.5000000	1
Zr4	Zr	1	0.5000000	0.5245933	0.5000000	1

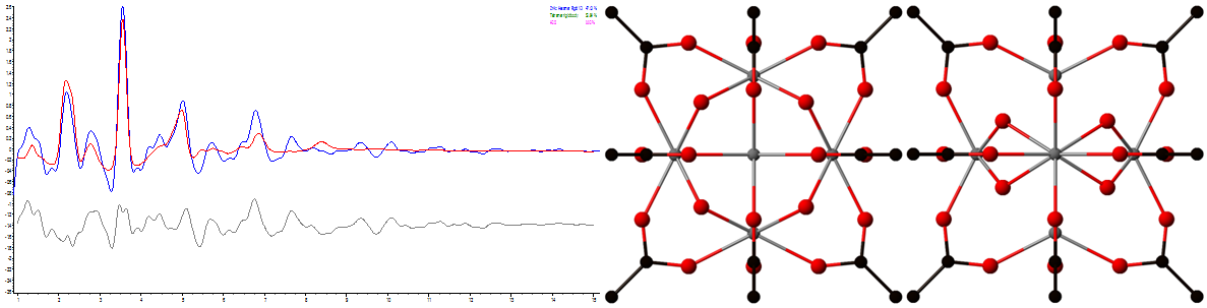

Figure 352: Observed and Calculated PDF from the chandelier core refinement of ZAA10A from the 18-month data collection and the resultant model viewed from the axial (left) and equatorial (right) positions.

Table 295: The atomic coordinates of the model resulting from the chandelier core refinement of ZAA10A from the 18-month data collection.

Atom Label	Atom Type	Multiplicity	Fractional X Coordinate	Fractional Y Coordinate	Fractional Z Coordinate	Fractional Occupancy
C1	C	1	0.590596	0.5000000	0.5838076	1
C2	C	1	0.5000000	0.409404	0.5838076	1
C3	C	1	0.409404	0.5000000	0.5838076	1
C4	C	1	0.5000000	0.590596	0.5838076	1
C5	C	1	0.590596	0.5000000	0.4161924	1
C6	C	1	0.5000000	0.409404	0.4161924	1
C7	C	1	0.409404	0.5000000	0.4161924	1
C8	C	1	0.5000000	0.590596	0.4161924	1
C9	C	1	0.590596	0.409404	0.5000000	1
C10	C	1	0.409404	0.409404	0.5000000	1
C11	C	1	0.409404	0.590596	0.5000000	1
C12	C	1	0.590596	0.590596	0.5000000	1
C13	C	1	0.6200268	0.5000000	0.6110332	1
C14	C	1	0.5000000	0.3799732	0.6110332	1
C15	C	1	0.3799732	0.5000000	0.6110332	1
C16	C	1	0.5000000	0.6200268	0.6110332	1
C17	C	1	0.6200268	0.5000000	0.3889668	1
C18	C	1	0.5000000	0.3799732	0.3889668	1
C19	C	1	0.3799732	0.5000000	0.3889668	1
C20	C	1	0.5000000	0.6200268	0.3889668	1
C21	C	1	0.6200268	0.3799732	0.5000000	1
C22	C	1	0.3799732	0.3799732	0.5000000	1
C23	C	1	0.3799732	0.6200268	0.5000000	1
C24	C	1	0.6200268	0.6200268	0.5000000	1
O1	O	1	0.5443716	0.4556284	0.4740465	1
O2	O	1	0.5443716	0.4556284	0.5259535	1
O3	O	1	0.4556284	0.4556284	0.4740465	1
O4	O	1	0.4556284	0.4556284	0.5259535	1
O5	O	1	0.4556284	0.5443716	0.4740465	1
O6	O	1	0.4556284	0.5443716	0.5259535	1
O7	O	1	0.5443716	0.5443716	0.4740465	1
O8	O	1	0.5443716	0.5443716	0.5259535	1

O9	O	1	0.5942405	0.5000000	0.5507946	1
O10	O	1	0.5942405	0.4450911	0.5000000	1
O11	O	1	0.5942405	0.5000000	0.4492054	1
O12	O	1	0.5942405	0.5549089	0.5000000	1
O13	O	1	0.5000000	0.5942405	0.5507946	1
O14	O	1	0.5549089	0.5942405	0.5000000	1
O15	O	1	0.5000000	0.5942405	0.4492054	1
O16	O	1	0.4450911	0.5942405	0.5000000	1
O17	O	1	0.4057595	0.5000000	0.5507946	1
O18	O	1	0.4057595	0.5549089	0.5000000	1
O19	O	1	0.4057595	0.5000000	0.4492054	1
O20	O	1	0.4057595	0.4450911	0.5000000	1
O21	O	1	0.5000000	0.4057595	0.5507946	1
O22	O	1	0.4450911	0.4057595	0.5000000	1
O23	O	1	0.5000000	0.4057595	0.4492054	1
O24	O	1	0.5549089	0.4057595	0.5000000	1
O25	O	1	0.5549089	0.5000000	0.5871791	1
O26	O	1	0.5000000	0.5549089	0.5871791	1
O27	O	1	0.4450911	0.5000000	0.5871791	1
O28	O	1	0.5000000	0.4450911	0.5871791	1
O29	O	1	0.5549089	0.5000000	0.4128209	1
O30	O	1	0.5000000	0.4450911	0.4128209	1
O31	O	1	0.4450911	0.5000000	0.4128209	1
O32	O	1	0.5000000	0.5549089	0.4128209	1
Zr1	Zr	1	0.5664638	0.5000000	0.5000000	1
Zr2	Zr	1	0.5000000	0.5664638	0.5000000	1
Zr3	Zr	1	0.4335362	0.5000000	0.5000000	1
Zr4	Zr	1	0.5000000	0.4335362	0.5000000	1
Zr5	Zr	1	0.5000000	0.5000000	0.5614837	1
Zr6	Zr	1	0.5000000	0.5000000	0.4385163	1

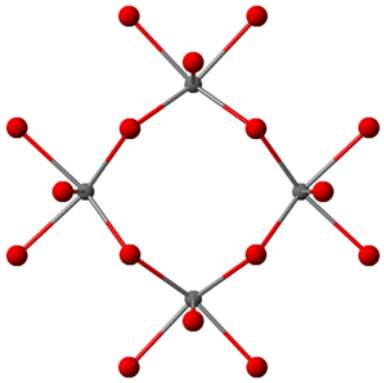

Figure 353: The tetrameric structure resulting from the chandelier core refinement of ZAA10A from the 18-month data collection.

Table 296: The atomic coordinates of the tetrameric phase of the chandelier core refinement of ZAA10A from the 18-month data collection.

Atom Label	Atom Type	Multiplicity	Fractional X Coordinate	Fractional Y Coordinate	Fractional Z Coordinate	Fractional Occupancy
O1	O	1	0.5143787	0.4856213	0.4770819	1
O2	O	1	0.4856213	0.4856213	0.5229181	1
O3	O	1	0.5143787	0.5143787	0.5229181	1
O4	O	1	0.4856213	0.5143787	0.4770819	1
O5	O	1	0.5000000	0.529628	0.5469645	1
O6	O	1	0.5000000	0.470372	0.5469645	1
O7	O	1	0.470372	0.5000000	0.4530355	1
O8	O	1	0.529628	0.5000000	0.4530355	1
O9	O	1	0.5145869	0.4598699	0.5000000	1
O10	O	1	0.4598699	0.4854131	0.5000000	1
O11	O	1	0.5401301	0.5145869	0.5000000	1
O12	O	1	0.4854131	0.5401301	0.5000000	1
O13	O	1	0.4598699	0.5145869	0.5000000	1
O14	O	1	0.5401301	0.4854131	0.5000000	1
O15	O	1	0.4854131	0.4598699	0.5000000	1
O16	O	1	0.5145869	0.5401301	0.5000000	1
O17	O	1	0.5143787	0.4856213	0.5229181	1
O18	O	1	0.4856213	0.4856213	0.4770819	1
O19	O	1	0.5143787	0.5143787	0.4770819	1
O20	O	1	0.4856213	0.5143787	0.5229181	1
O21	O	1	0.5000000	0.529628	0.4530355	1
O22	O	1	0.5000000	0.470372	0.4530355	1
O23	O	1	0.470372	0.5000000	0.5469645	1
O24	O	1	0.529628	0.5000000	0.5469645	1
Zr1	Zr	1	0.5000000	0.4754536	0.5000000	1
Zr2	Zr	1	0.4754536	0.5000000	0.5000000	1
Zr3	Zr	1	0.5245464	0.5000000	0.5000000	1
Zr4	Zr	1	0.5000000	0.5245464	0.5000000	1

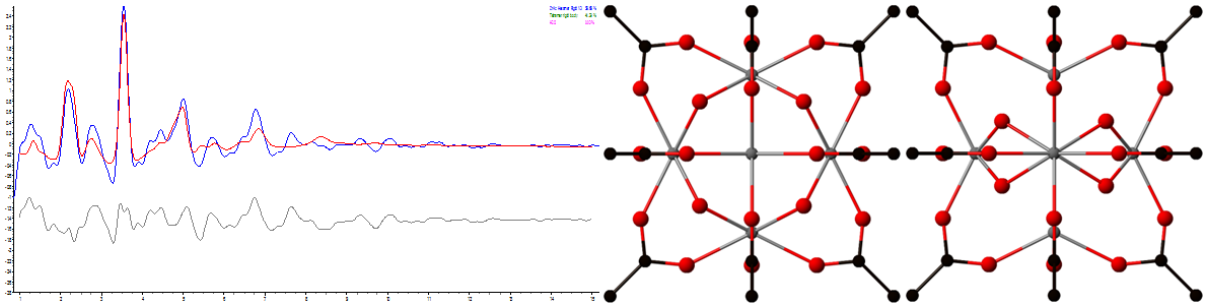

Figure 354: Observed and Calculated PDF from the chandelier core refinement of ZAA10C from the 18-month data collection and the resultant model viewed from the axial (left) and equatorial (right) positions.

Table 297: The atomic coordinates of the model resulting from the chandelier core refinement of ZAA10C from the 18-month data collection.

Atom Label	Atom Type	Multiplicity	Fractional X Coordinate	Fractional Y Coordinate	Fractional Z Coordinate	Fractional Occupancy
C1	C	1	0.5903479	0.5000000	0.5835781	1
C2	C	1	0.5000000	0.4096521	0.5835781	1
C3	C	1	0.4096521	0.5000000	0.5835781	1
C4	C	1	0.5000000	0.5903479	0.5835781	1
C5	C	1	0.5903479	0.5000000	0.4164219	1
C6	C	1	0.5000000	0.4096521	0.4164219	1
C7	C	1	0.4096521	0.5000000	0.4164219	1
C8	C	1	0.5000000	0.5903479	0.4164219	1
C9	C	1	0.5903479	0.4096521	0.5000000	1
C10	C	1	0.4096521	0.4096521	0.5000000	1
C11	C	1	0.4096521	0.5903479	0.5000000	1
C12	C	1	0.5903479	0.5903479	0.5000000	1
C13	C	1	0.6198515	0.5000000	0.610871	1
C14	C	1	0.5000000	0.3801485	0.610871	1
C15	C	1	0.3801485	0.5000000	0.610871	1
C16	C	1	0.5000000	0.6198515	0.610871	1
C17	C	1	0.6198515	0.5000000	0.389129	1
C18	C	1	0.5000000	0.3801485	0.389129	1
C19	C	1	0.3801485	0.5000000	0.389129	1
C20	C	1	0.5000000	0.6198515	0.389129	1
C21	C	1	0.6198515	0.3801485	0.5000000	1
C22	C	1	0.3801485	0.3801485	0.5000000	1
C23	C	1	0.3801485	0.6198515	0.5000000	1
C24	C	1	0.6198515	0.6198515	0.5000000	1
O1	O	1	0.5438413	0.4561587	0.4747581	1
O2	O	1	0.5438413	0.4561587	0.5252419	1
O3	O	1	0.4561587	0.4561587	0.4747581	1
O4	O	1	0.4561587	0.4561587	0.5252419	1
O5	O	1	0.4561587	0.5438413	0.4747581	1
O6	O	1	0.4561587	0.5438413	0.5252419	1
O7	O	1	0.5438413	0.5438413	0.4747581	1
O8	O	1	0.5438413	0.5438413	0.5252419	1

O9	O	1	0.5938949	0.5000000	0.5508979	1
O10	O	1	0.5938949	0.4449794	0.5000000	1
O11	O	1	0.5938949	0.5000000	0.4491021	1
O12	O	1	0.5938949	0.5550206	0.5000000	1
O13	O	1	0.5000000	0.5938949	0.5508979	1
O14	O	1	0.5550206	0.5938949	0.5000000	1
O15	O	1	0.5000000	0.5938949	0.4491021	1
O16	O	1	0.4449794	0.5938949	0.5000000	1
O17	O	1	0.4061051	0.5000000	0.5508979	1
O18	O	1	0.4061051	0.5550206	0.5000000	1
O19	O	1	0.4061051	0.5000000	0.4491021	1
O20	O	1	0.4061051	0.4449794	0.5000000	1
O21	O	1	0.5000000	0.4061051	0.5508979	1
O22	O	1	0.4449794	0.4061051	0.5000000	1
O23	O	1	0.5000000	0.4061051	0.4491021	1
O24	O	1	0.5550206	0.4061051	0.5000000	1
O25	O	1	0.5550206	0.5000000	0.5868594	1
O26	O	1	0.5000000	0.5550206	0.5868594	1
O27	O	1	0.4449794	0.5000000	0.5868594	1
O28	O	1	0.5000000	0.4449794	0.5868594	1
O29	O	1	0.5550206	0.5000000	0.4131406	1
O30	O	1	0.5000000	0.4449794	0.4131406	1
O31	O	1	0.4449794	0.5000000	0.4131406	1
O32	O	1	0.5000000	0.5550206	0.4131406	1
Zr1	Zr	1	0.56648	0.5000000	0.5000000	1
Zr2	Zr	1	0.5000000	0.56648	0.5000000	1
Zr3	Zr	1	0.43352	0.5000000	0.5000000	1
Zr4	Zr	1	0.5000000	0.43352	0.5000000	1
Zr5	Zr	1	0.5000000	0.5000000	0.5614986	1
Zr6	Zr	1	0.5000000	0.5000000	0.4385014	1

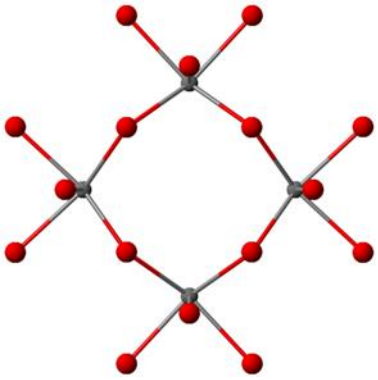

Figure 355: The tetrameric structure resulting from the chandelier core refinement of ZAA10C from the 18-month data collection.

Table 298: The atomic coordinates of the tetrameric phase of the chandelier core refinement of ZAA10C from the 18-month data collection.

Atom Label	Atom Type	Multiplicity	Fractional X Coordinate	Fractional Y Coordinate	Fractional Z Coordinate	Fractional Occupancy
O1	O	1	0.5143796	0.4856204	0.4725256	1
O2	O	1	0.4856204	0.4856204	0.5274744	1
O3	O	1	0.5143796	0.5143796	0.5274744	1
O4	O	1	0.4856204	0.5143796	0.4725256	1
O5	O	1	0.5000000	0.5285046	0.5460537	1
O6	O	1	0.5000000	0.4714954	0.5460537	1
O7	O	1	0.4714954	0.5000000	0.4539463	1
O8	O	1	0.5285046	0.5000000	0.4539463	1
O9	O	1	0.5144385	0.4599915	0.5000000	1
O10	O	1	0.4599915	0.4855615	0.5000000	1
O11	O	1	0.5400085	0.5144385	0.5000000	1
O12	O	1	0.4855615	0.5400085	0.5000000	1
O13	O	1	0.4599915	0.5144385	0.5000000	1
O14	O	1	0.5400085	0.4855615	0.5000000	1
O15	O	1	0.4855615	0.4599915	0.5000000	1
O16	O	1	0.5144385	0.5400085	0.5000000	1
O17	O	1	0.5143796	0.4856204	0.5274744	1
O18	O	1	0.4856204	0.4856204	0.4725256	1
O19	O	1	0.5143796	0.5143796	0.4725256	1
O20	O	1	0.4856204	0.5143796	0.5274744	1
O21	O	1	0.5000000	0.5285046	0.4539463	1
O22	O	1	0.5000000	0.4714954	0.4539463	1
O23	O	1	0.4714954	0.5000000	0.5460537	1
O24	O	1	0.5285046	0.5000000	0.5460537	1
Zr1	Zr	1	0.5000000	0.4755515	0.5000000	1
Zr2	Zr	1	0.4755515	0.5000000	0.5000000	1
Zr3	Zr	1	0.5244485	0.5000000	0.5000000	1
Zr4	Zr	1	0.5000000	0.5244485	0.5000000	1

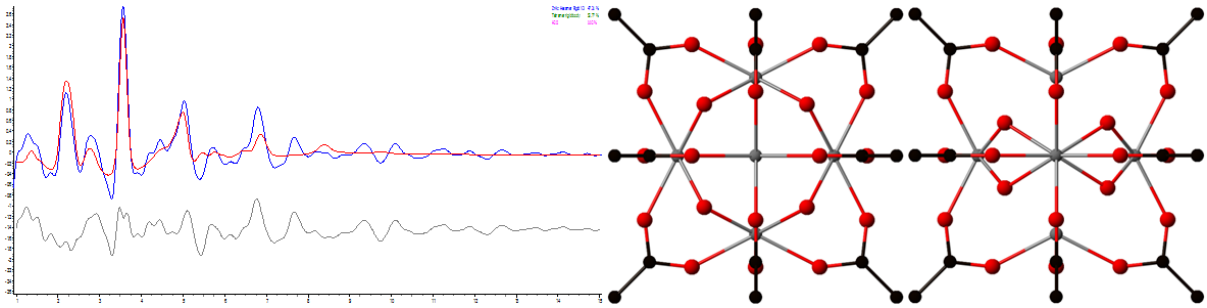

Figure 356: Observed and Calculated PDF from the chandelier core refinement of ZAA10I from the 18-month data collection and the resultant model viewed from the axial (left) and equatorial (right) positions.

Table 299: The atomic coordinates of the model resulting from the chandelier core refinement of ZAA10I from the 18-month data collection.

Atom Label	Atom Type	Multiplicity	Fractional X Coordinate	Fractional Y Coordinate	Fractional Z Coordinate	Fractional Occupancy
C1	C	1	0.5904655	0.5000000	0.5836869	1
C2	C	1	0.5000000	0.4095345	0.5836869	1
C3	C	1	0.4095345	0.5000000	0.5836869	1
C4	C	1	0.5000000	0.5904655	0.5836869	1
C5	C	1	0.5904655	0.5000000	0.4163131	1
C6	C	1	0.5000000	0.4095345	0.4163131	1
C7	C	1	0.4095345	0.5000000	0.4163131	1
C8	C	1	0.5000000	0.5904655	0.4163131	1
C9	C	1	0.5904655	0.4095345	0.5000000	1
C10	C	1	0.4095345	0.4095345	0.5000000	1
C11	C	1	0.4095345	0.5904655	0.5000000	1
C12	C	1	0.5904655	0.5904655	0.5000000	1
C13	C	1	0.6201302	0.5000000	0.6111288	1
C14	C	1	0.5000000	0.3798698	0.6111288	1
C15	C	1	0.3798698	0.5000000	0.6111288	1
C16	C	1	0.5000000	0.6201302	0.6111288	1
C17	C	1	0.6201302	0.5000000	0.3888712	1
C18	C	1	0.5000000	0.3798698	0.3888712	1
C19	C	1	0.3798698	0.5000000	0.3888712	1
C20	C	1	0.5000000	0.6201302	0.3888712	1
C21	C	1	0.6201302	0.3798698	0.5000000	1
C22	C	1	0.3798698	0.3798698	0.5000000	1
C23	C	1	0.3798698	0.6201302	0.5000000	1
C24	C	1	0.6201302	0.6201302	0.5000000	1
O1	O	1	0.5437845	0.4562155	0.4743092	1
O2	O	1	0.5437845	0.4562155	0.5256908	1
O3	O	1	0.4562155	0.4562155	0.4743092	1
O4	O	1	0.4562155	0.4562155	0.5256908	1
O5	O	1	0.4562155	0.5437845	0.4743092	1
O6	O	1	0.4562155	0.5437845	0.5256908	1
O7	O	1	0.5437845	0.5437845	0.4743092	1
O8	O	1	0.5437845	0.5437845	0.5256908	1

O9	O	1	0.5946123	0.5000000	0.5503937	1
O10	O	1	0.5946123	0.4455244	0.5000000	1
O11	O	1	0.5946123	0.5000000	0.4496063	1
O12	O	1	0.5946123	0.5544756	0.5000000	1
O13	O	1	0.5000000	0.5946123	0.5503937	1
O14	O	1	0.5544756	0.5946123	0.5000000	1
O15	O	1	0.5000000	0.5946123	0.4496063	1
O16	O	1	0.4455244	0.5946123	0.5000000	1
O17	O	1	0.4053877	0.5000000	0.5503937	1
O18	O	1	0.4053877	0.5544756	0.5000000	1
O19	O	1	0.4053877	0.5000000	0.4496063	1
O20	O	1	0.4053877	0.4455244	0.5000000	1
O21	O	1	0.5000000	0.4053877	0.5503937	1
O22	O	1	0.4455244	0.4053877	0.5000000	1
O23	O	1	0.5000000	0.4053877	0.4496063	1
O24	O	1	0.5544756	0.4053877	0.5000000	1
O25	O	1	0.5544756	0.5000000	0.587523	1
O26	O	1	0.5000000	0.5544756	0.587523	1
O27	O	1	0.4455244	0.5000000	0.587523	1
O28	O	1	0.5000000	0.4455244	0.587523	1
O29	O	1	0.5544756	0.5000000	0.412477	1
O30	O	1	0.5000000	0.4455244	0.412477	1
O31	O	1	0.4455244	0.5000000	0.412477	1
O32	O	1	0.5000000	0.5544756	0.412477	1
Zr1	Zr	1	0.5666943	0.5000000	0.5000000	1
Zr2	Zr	1	0.5000000	0.5666943	0.5000000	1
Zr3	Zr	1	0.4333057	0.5000000	0.5000000	1
Zr4	Zr	1	0.5000000	0.4333057	0.5000000	1
Zr5	Zr	1	0.5000000	0.5000000	0.5616969	1
Zr6	Zr	1	0.5000000	0.5000000	0.4383031	1

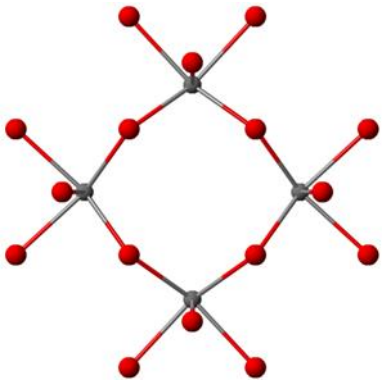

Figure 357: The tetrameric structure resulting from the chandelier core refinement of ZAA10I from the 18-month data collection.

Table 300: The atomic coordinates of the tetrameric phase of the chandelier core refinement of ZAA10I from the 18-month data collection.

Atom Label	Atom Type	Multiplicity	Fractional X Coordinate	Fractional Y Coordinate	Fractional Z Coordinate	Fractional Occupancy
O1	O	1	0.5144048	0.4855952	0.4769007	1
O2	O	1	0.4855952	0.4855952	0.5230993	1
O3	O	1	0.5144048	0.5144048	0.5230993	1
O4	O	1	0.4855952	0.5144048	0.4769007	1
O5	O	1	0.5000000	0.5297165	0.5475429	1
O6	O	1	0.5000000	0.4702835	0.5475429	1
O7	O	1	0.4702835	0.5000000	0.4524571	1
O8	O	1	0.5297165	0.5000000	0.4524571	1
O9	O	1	0.5144393	0.4597754	0.5000000	1
O10	O	1	0.4597754	0.4855607	0.5000000	1
O11	O	1	0.5402246	0.5144393	0.5000000	1
O12	O	1	0.4855607	0.5402246	0.5000000	1
O13	O	1	0.4597754	0.5144393	0.5000000	1
O14	O	1	0.5402246	0.4855607	0.5000000	1
O15	O	1	0.4855607	0.4597754	0.5000000	1
O16	O	1	0.5144393	0.5402246	0.5000000	1
O17	O	1	0.5144048	0.4855952	0.5230993	1
O18	O	1	0.4855952	0.4855952	0.4769007	1
O19	O	1	0.5144048	0.5144048	0.4769007	1
O20	O	1	0.4855952	0.5144048	0.5230993	1
O21	O	1	0.5000000	0.5297165	0.4524571	1
O22	O	1	0.5000000	0.4702835	0.4524571	1
O23	O	1	0.4702835	0.5000000	0.5475429	1
O24	O	1	0.5297165	0.5000000	0.5475429	1
Zr1	Zr	1	0.5000000	0.4754105	0.5000000	1
Zr2	Zr	1	0.4754105	0.5000000	0.5000000	1
Zr3	Zr	1	0.5245895	0.5000000	0.5000000	1
Zr4	Zr	1	0.5000000	0.5245895	0.5000000	1

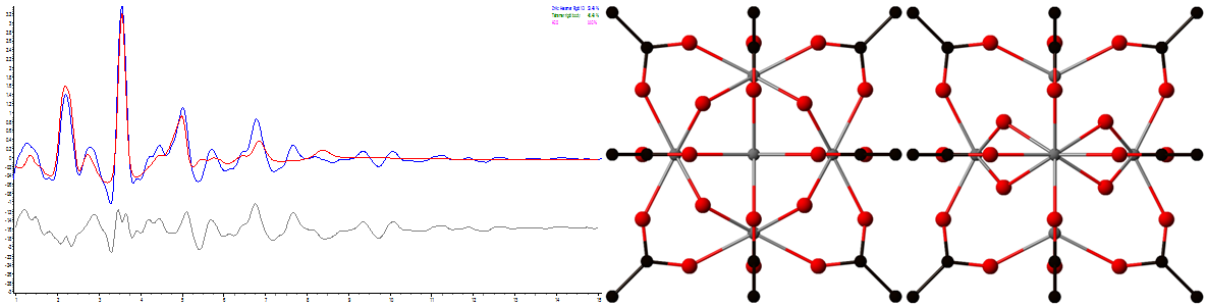

Figure 358: Observed and Calculated PDF from the chandelier core refinement of ZAA13A from the 18-month data collection and the resultant model viewed from the axial (left) and equatorial (right) positions.

Table 301: The atomic coordinates of the model resulting from the chandelier core refinement of ZAA13A from the 18-month data collection.

Atom Label	Atom Type	Multiplicity	Fractional X Coordinate	Fractional Y Coordinate	Fractional Z Coordinate	Fractional Occupancy
C1	C	1	0.5904418	0.5000000	0.583665	1
C2	C	1	0.5000000	0.4095582	0.583665	1
C3	C	1	0.4095582	0.5000000	0.583665	1
C4	C	1	0.5000000	0.5904418	0.583665	1
C5	C	1	0.5904418	0.5000000	0.416335	1
C6	C	1	0.5000000	0.4095582	0.416335	1
C7	C	1	0.4095582	0.5000000	0.416335	1
C8	C	1	0.5000000	0.5904418	0.416335	1
C9	C	1	0.5904418	0.4095582	0.5000000	1
C10	C	1	0.4095582	0.4095582	0.5000000	1
C11	C	1	0.4095582	0.5904418	0.5000000	1
C12	C	1	0.5904418	0.5904418	0.5000000	1
C13	C	1	0.619946	0.5000000	0.6109584	1
C14	C	1	0.5000000	0.380054	0.6109584	1
C15	C	1	0.380054	0.5000000	0.6109584	1
C16	C	1	0.5000000	0.619946	0.6109584	1
C17	C	1	0.619946	0.5000000	0.3890416	1
C18	C	1	0.5000000	0.380054	0.3890416	1
C19	C	1	0.380054	0.5000000	0.3890416	1
C20	C	1	0.5000000	0.619946	0.3890416	1
C21	C	1	0.619946	0.380054	0.5000000	1
C22	C	1	0.380054	0.380054	0.5000000	1
C23	C	1	0.380054	0.619946	0.5000000	1
C24	C	1	0.619946	0.619946	0.5000000	1
O1	O	1	0.5430583	0.4569417	0.4743339	1
O2	O	1	0.5430583	0.4569417	0.5256661	1
O3	O	1	0.4569417	0.4569417	0.4743339	1
O4	O	1	0.4569417	0.4569417	0.5256661	1
O5	O	1	0.4569417	0.5430583	0.4743339	1
O6	O	1	0.4569417	0.5430583	0.5256661	1
O7	O	1	0.5430583	0.5430583	0.4743339	1
O8	O	1	0.5430583	0.5430583	0.5256661	1

O9	O	1	0.5942959	0.5000000	0.5505018	1
O10	O	1	0.5942959	0.4454075	0.5000000	1
O11	O	1	0.5942959	0.5000000	0.4494982	1
O12	O	1	0.5942959	0.5545925	0.5000000	1
O13	O	1	0.5000000	0.5942959	0.5505018	1
O14	O	1	0.5545925	0.5942959	0.5000000	1
O15	O	1	0.5000000	0.5942959	0.4494982	1
O16	O	1	0.4454075	0.5942959	0.5000000	1
O17	O	1	0.4057041	0.5000000	0.5505018	1
O18	O	1	0.4057041	0.5545925	0.5000000	1
O19	O	1	0.4057041	0.5000000	0.4494982	1
O20	O	1	0.4057041	0.4454075	0.5000000	1
O21	O	1	0.5000000	0.4057041	0.5505018	1
O22	O	1	0.4454075	0.4057041	0.5000000	1
O23	O	1	0.5000000	0.4057041	0.4494982	1
O24	O	1	0.5545925	0.4057041	0.5000000	1
O25	O	1	0.5545925	0.5000000	0.5872302	1
O26	O	1	0.5000000	0.5545925	0.5872302	1
O27	O	1	0.4454075	0.5000000	0.5872302	1
O28	O	1	0.5000000	0.4454075	0.5872302	1
O29	O	1	0.5545925	0.5000000	0.4127698	1
O30	O	1	0.5000000	0.4454075	0.4127698	1
O31	O	1	0.4454075	0.5000000	0.4127698	1
O32	O	1	0.5000000	0.5545925	0.4127698	1
Zr1	Zr	1	0.5664597	0.5000000	0.5000000	1
Zr2	Zr	1	0.5000000	0.5664597	0.5000000	1
Zr3	Zr	1	0.4335403	0.5000000	0.5000000	1
Zr4	Zr	1	0.5000000	0.4335403	0.5000000	1
Zr5	Zr	1	0.5000000	0.5000000	0.5614799	1
Zr6	Zr	1	0.5000000	0.5000000	0.4385201	1

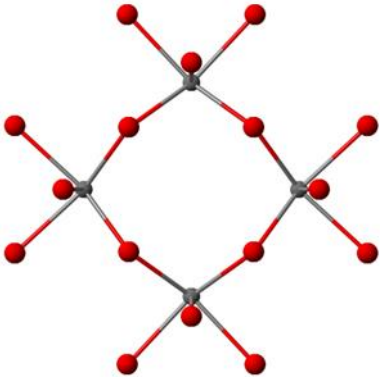

Figure 359: The tetrameric structure resulting from the chandelier core refinement of ZAA13A from the 18-month data collection.

Table 302: The atomic coordinates of the tetrameric phase of the chandelier core refinement of ZAA13A from the 18-month data collection.

Atom Label	Atom Type	Multiplicity	Fractional X Coordinate	Fractional Y Coordinate	Fractional Z Coordinate	Fractional Occupancy
O1	O	1	0.5142797	0.4857203	0.4760905	1
O2	O	1	0.4857203	0.4857203	0.5239095	1
O3	O	1	0.5142797	0.5142797	0.5239095	1
O4	O	1	0.4857203	0.5142797	0.4760905	1
O5	O	1	0.5000000	0.5292073	0.5469759	1
O6	O	1	0.5000000	0.4707927	0.5469759	1
O7	O	1	0.4707927	0.5000000	0.4530241	1
O8	O	1	0.5292073	0.5000000	0.4530241	1
O9	O	1	0.5145806	0.4597996	0.5000000	1
O10	O	1	0.4597996	0.4854194	0.5000000	1
O11	O	1	0.5402004	0.5145806	0.5000000	1
O12	O	1	0.4854194	0.5402004	0.5000000	1
O13	O	1	0.4597996	0.5145806	0.5000000	1
O14	O	1	0.5402004	0.4854194	0.5000000	1
O15	O	1	0.4854194	0.4597996	0.5000000	1
O16	O	1	0.5145806	0.5402004	0.5000000	1
O17	O	1	0.5142797	0.4857203	0.5239095	1
O18	O	1	0.4857203	0.4857203	0.4760905	1
O19	O	1	0.5142797	0.5142797	0.4760905	1
O20	O	1	0.4857203	0.5142797	0.5239095	1
O21	O	1	0.5000000	0.5292073	0.4530241	1
O22	O	1	0.5000000	0.4707927	0.4530241	1
O23	O	1	0.4707927	0.5000000	0.5469759	1
O24	O	1	0.5292073	0.5000000	0.5469759	1
Zr1	Zr	1	0.5000000	0.4754563	0.5000000	1
Zr2	Zr	1	0.4754563	0.5000000	0.5000000	1
Zr3	Zr	1	0.5245437	0.5000000	0.5000000	1
Zr4	Zr	1	0.5000000	0.5245437	0.5000000	1

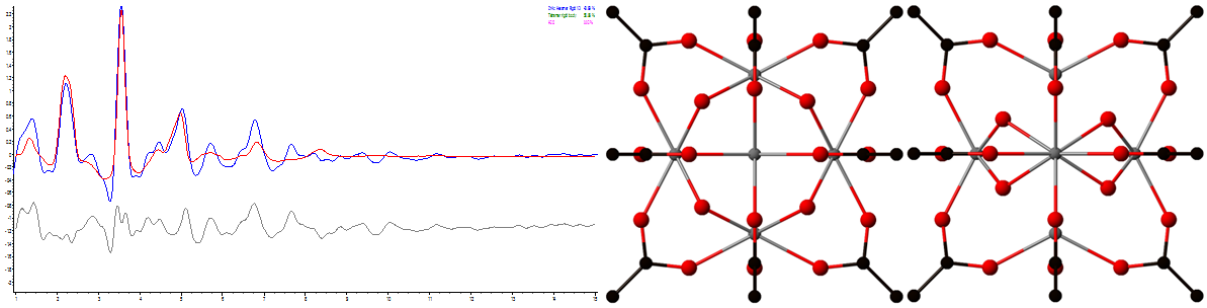

Figure 360: Observed and Calculated PDF from the chandelier core refinement of ZAA13C from the 18-month data collection and the resultant model viewed from the axial (left) and equatorial (right) positions.

Table 303: The atomic coordinates of the model resulting from the chandelier core refinement of ZAA13C from the 18-month data collection.

Atom Label	Atom Type	Multiplicity	Fractional X Coordinate	Fractional Y Coordinate	Fractional Z Coordinate	Fractional Occupancy
C1	C	1	0.5910749	0.5000000	0.5842506	1
C2	C	1	0.5000000	0.4089251	0.5842506	1
C3	C	1	0.4089251	0.5000000	0.5842506	1
C4	C	1	0.5000000	0.5910749	0.5842506	1
C5	C	1	0.5910749	0.5000000	0.4157494	1
C6	C	1	0.5000000	0.4089251	0.4157494	1
C7	C	1	0.4089251	0.5000000	0.4157494	1
C8	C	1	0.5000000	0.5910749	0.4157494	1
C9	C	1	0.5910749	0.4089251	0.5000000	1
C10	C	1	0.4089251	0.4089251	0.5000000	1
C11	C	1	0.4089251	0.5910749	0.5000000	1
C12	C	1	0.5910749	0.5910749	0.5000000	1
C13	C	1	0.6188191	0.5000000	0.609916	1
C14	C	1	0.5000000	0.3811809	0.609916	1
C15	C	1	0.3811809	0.5000000	0.609916	1
C16	C	1	0.5000000	0.6188191	0.609916	1
C17	C	1	0.6188191	0.5000000	0.390084	1
C18	C	1	0.5000000	0.3811809	0.390084	1
C19	C	1	0.3811809	0.5000000	0.390084	1
C20	C	1	0.5000000	0.6188191	0.390084	1
C21	C	1	0.6188191	0.3811809	0.5000000	1
C22	C	1	0.3811809	0.3811809	0.5000000	1
C23	C	1	0.3811809	0.6188191	0.5000000	1
C24	C	1	0.6188191	0.6188191	0.5000000	1
O1	O	1	0.5441352	0.4558648	0.4733574	1
O2	O	1	0.5441352	0.4558648	0.5266426	1
O3	O	1	0.4558648	0.4558648	0.4733574	1
O4	O	1	0.4558648	0.4558648	0.5266426	1
O5	O	1	0.4558648	0.5441352	0.4733574	1
O6	O	1	0.4558648	0.5441352	0.5266426	1
O7	O	1	0.5441352	0.5441352	0.4733574	1
O8	O	1	0.5441352	0.5441352	0.5266426	1

O9	O	1	0.5950338	0.5000000	0.5508774	1
O10	O	1	0.5950338	0.4450016	0.5000000	1
O11	O	1	0.5950338	0.5000000	0.4491226	1
O12	O	1	0.5950338	0.5549984	0.5000000	1
O13	O	1	0.5000000	0.5950338	0.5508774	1
O14	O	1	0.5549984	0.5950338	0.5000000	1
O15	O	1	0.5000000	0.5950338	0.4491226	1
O16	O	1	0.4450016	0.5950338	0.5000000	1
O17	O	1	0.4049662	0.5000000	0.5508774	1
O18	O	1	0.4049662	0.5549984	0.5000000	1
O19	O	1	0.4049662	0.5000000	0.4491226	1
O20	O	1	0.4049662	0.4450016	0.5000000	1
O21	O	1	0.5000000	0.4049662	0.5508774	1
O22	O	1	0.4450016	0.4049662	0.5000000	1
O23	O	1	0.5000000	0.4049662	0.4491226	1
O24	O	1	0.5549984	0.4049662	0.5000000	1
O25	O	1	0.5549984	0.5000000	0.5879129	1
O26	O	1	0.5000000	0.5549984	0.5879129	1
O27	O	1	0.4450016	0.5000000	0.5879129	1
O28	O	1	0.5000000	0.4450016	0.5879129	1
O29	O	1	0.5549984	0.5000000	0.4120871	1
O30	O	1	0.5000000	0.4450016	0.4120871	1
O31	O	1	0.4450016	0.5000000	0.4120871	1
O32	O	1	0.5000000	0.5549984	0.4120871	1
Zr1	Zr	1	0.5664831	0.5000000	0.5000000	1
Zr2	Zr	1	0.5000000	0.5664831	0.5000000	1
Zr3	Zr	1	0.4335169	0.5000000	0.5000000	1
Zr4	Zr	1	0.5000000	0.4335169	0.5000000	1
Zr5	Zr	1	0.5000000	0.5000000	0.5615015	1
Zr6	Zr	1	0.5000000	0.5000000	0.4384985	1

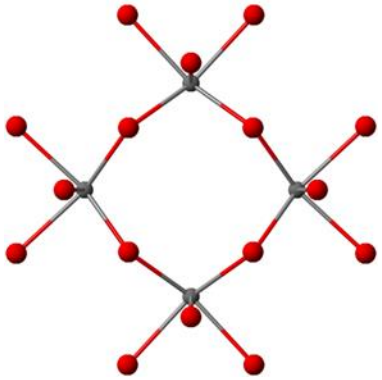

Figure 361: The tetrameric structure resulting from the chandelier core refinement of ZAA13C from the 18-month data collection.

Table 304: The atomic coordinates of the tetrameric phase of the chandelier core refinement of ZAA13C from the 18-month data collection.

Atom Label	Atom Type	Multiplicity	Fractional X Coordinate	Fractional Y Coordinate	Fractional Z Coordinate	Fractional Occupancy
O1	O	1	0.5143382	0.4856618	0.4773589	1
O2	O	1	0.4856618	0.4856618	0.5226411	1
O3	O	1	0.5143382	0.5143382	0.5226411	1
O4	O	1	0.4856618	0.5143382	0.4773589	1
O5	O	1	0.5000000	0.5292482	0.5476034	1
O6	O	1	0.5000000	0.4707518	0.5476034	1
O7	O	1	0.4707518	0.5000000	0.4523966	1
O8	O	1	0.5292482	0.5000000	0.4523966	1
O9	O	1	0.5146082	0.4597309	0.5000000	1
O10	O	1	0.4597309	0.4853918	0.5000000	1
O11	O	1	0.5402691	0.5146082	0.5000000	1
O12	O	1	0.4853918	0.5402691	0.5000000	1
O13	O	1	0.4597309	0.5146082	0.5000000	1
O14	O	1	0.5402691	0.4853918	0.5000000	1
O15	O	1	0.4853918	0.4597309	0.5000000	1
O16	O	1	0.5146082	0.5402691	0.5000000	1
O17	O	1	0.5143382	0.4856618	0.5226411	1
O18	O	1	0.4856618	0.4856618	0.4773589	1
O19	O	1	0.5143382	0.5143382	0.4773589	1
O20	O	1	0.4856618	0.5143382	0.5226411	1
O21	O	1	0.5000000	0.5292482	0.4523966	1
O22	O	1	0.5000000	0.4707518	0.4523966	1
O23	O	1	0.4707518	0.5000000	0.5476034	1
O24	O	1	0.5292482	0.5000000	0.5476034	1
Zr1	Zr	1	0.5000000	0.4755119	0.5000000	1
Zr2	Zr	1	0.4755119	0.5000000	0.5000000	1
Zr3	Zr	1	0.5244881	0.5000000	0.5000000	1
Zr4	Zr	1	0.5000000	0.5244881	0.5000000	1

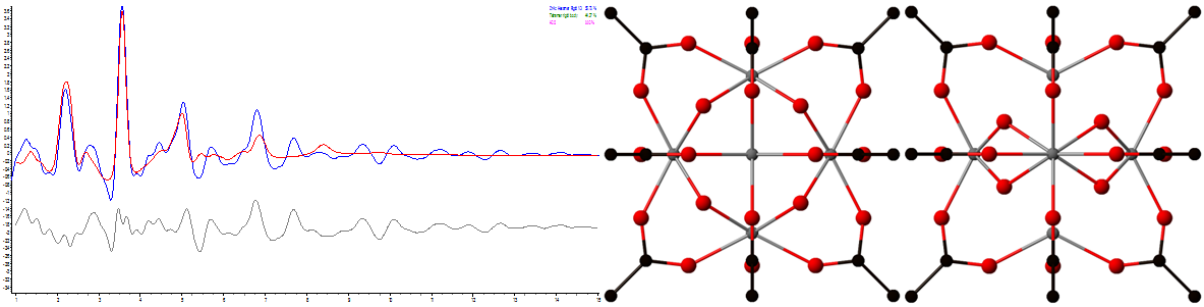

Figure 362: Observed and Calculated PDF from the chandelier core refinement of ZAA13I from the 18-month data collection and the resultant model viewed from the axial (left) and equatorial (right) positions.

Table 305: The atomic coordinates of the model resulting from the chandelier core refinement of ZAA13I from the 18-month data collection.

Atom Label	Atom Type	Multiplicity	Fractional X Coordinate	Fractional Y Coordinate	Fractional Z Coordinate	Fractional Occupancy
C1	C	1	0.5902176	0.5000000	0.5834575	1
C2	C	1	0.5000000	0.4097824	0.5834575	1
C3	C	1	0.4097824	0.5000000	0.5834575	1
C4	C	1	0.5000000	0.5902176	0.5834575	1
C5	C	1	0.5902176	0.5000000	0.4165425	1
C6	C	1	0.5000000	0.4097824	0.4165425	1
C7	C	1	0.4097824	0.5000000	0.4165425	1
C8	C	1	0.5000000	0.5902176	0.4165425	1
C9	C	1	0.5902176	0.4097824	0.5000000	1
C10	C	1	0.4097824	0.4097824	0.5000000	1
C11	C	1	0.4097824	0.5902176	0.5000000	1
C12	C	1	0.5902176	0.5902176	0.5000000	1
C13	C	1	0.6201473	0.5000000	0.6111447	1
C14	C	1	0.5000000	0.3798527	0.6111447	1
C15	C	1	0.3798527	0.5000000	0.6111447	1
C16	C	1	0.5000000	0.6201473	0.6111447	1
C17	C	1	0.6201473	0.5000000	0.3888553	1
C18	C	1	0.5000000	0.3798527	0.3888553	1
C19	C	1	0.3798527	0.5000000	0.3888553	1
C20	C	1	0.5000000	0.6201473	0.3888553	1
C21	C	1	0.6201473	0.3798527	0.5000000	1
C22	C	1	0.3798527	0.3798527	0.5000000	1
C23	C	1	0.3798527	0.6201473	0.5000000	1
C24	C	1	0.6201473	0.6201473	0.5000000	1
O1	O	1	0.5412954	0.4587046	0.4746546	1
O2	O	1	0.5412954	0.4587046	0.5253454	1
O3	O	1	0.4587046	0.4587046	0.4746546	1
O4	O	1	0.4587046	0.4587046	0.5253454	1
O5	O	1	0.4587046	0.5412954	0.4746546	1
O6	O	1	0.4587046	0.5412954	0.5253454	1
O7	O	1	0.5412954	0.5412954	0.4746546	1
O8	O	1	0.5412954	0.5412954	0.5253454	1

O9	O	1	0.5944625	0.5000000	0.5498816	1
O10	O	1	0.5944625	0.446078	0.5000000	1
O11	O	1	0.5944625	0.5000000	0.4501184	1
O12	O	1	0.5944625	0.553922	0.5000000	1
O13	O	1	0.5000000	0.5944625	0.5498816	1
O14	O	1	0.553922	0.5944625	0.5000000	1
O15	O	1	0.5000000	0.5944625	0.4501184	1
O16	O	1	0.446078	0.5944625	0.5000000	1
O17	O	1	0.4055375	0.5000000	0.5498816	1
O18	O	1	0.4055375	0.553922	0.5000000	1
O19	O	1	0.4055375	0.5000000	0.4501184	1
O20	O	1	0.4055375	0.446078	0.5000000	1
O21	O	1	0.5000000	0.4055375	0.5498816	1
O22	O	1	0.446078	0.4055375	0.5000000	1
O23	O	1	0.5000000	0.4055375	0.4501184	1
O24	O	1	0.553922	0.4055375	0.5000000	1
O25	O	1	0.553922	0.5000000	0.5873844	1
O26	O	1	0.5000000	0.553922	0.5873844	1
O27	O	1	0.446078	0.5000000	0.5873844	1
O28	O	1	0.5000000	0.446078	0.5873844	1
O29	O	1	0.553922	0.5000000	0.4126156	1
O30	O	1	0.5000000	0.446078	0.4126156	1
O31	O	1	0.446078	0.5000000	0.4126156	1
O32	O	1	0.5000000	0.553922	0.4126156	1
Zr1	Zr	1	0.5667734	0.5000000	0.5000000	1
Zr2	Zr	1	0.5000000	0.5667734	0.5000000	1
Zr3	Zr	1	0.4332266	0.5000000	0.5000000	1
Zr4	Zr	1	0.5000000	0.4332266	0.5000000	1
Zr5	Zr	1	0.5000000	0.5000000	0.5617701	1
Zr6	Zr	1	0.5000000	0.5000000	0.4382299	1

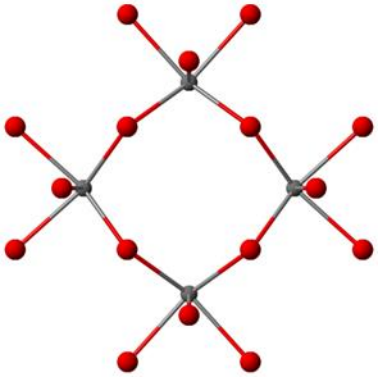

Figure 363: The tetrameric structure resulting from the chandelier core refinement of ZAA13I from the 18-month data collection.

Table 306: The atomic coordinates of the tetrameric phase of the chandelier core refinement of ZAA13I from the 18-month data collection.

Atom Label	Atom Type	Multiplicity	Fractional X Coordinate	Fractional Y Coordinate	Fractional Z Coordinate	Fractional Occupancy
O1	O	1	0.5142775	0.4857225	0.474573	1
O2	O	1	0.4857225	0.4857225	0.525427	1
O3	O	1	0.5142775	0.5142775	0.525427	1
O4	O	1	0.4857225	0.5142775	0.474573	1
O5	O	1	0.5000000	0.5294489	0.5482931	1
O6	O	1	0.5000000	0.4705511	0.5482931	1
O7	O	1	0.4705511	0.5000000	0.4517069	1
O8	O	1	0.5294489	0.5000000	0.4517069	1
O9	O	1	0.5142138	0.4597345	0.5000000	1
O10	O	1	0.4597345	0.4857862	0.5000000	1
O11	O	1	0.5402655	0.5142138	0.5000000	1
O12	O	1	0.4857862	0.5402655	0.5000000	1
O13	O	1	0.4597345	0.5142138	0.5000000	1
O14	O	1	0.5402655	0.4857862	0.5000000	1
O15	O	1	0.4857862	0.4597345	0.5000000	1
O16	O	1	0.5142138	0.5402655	0.5000000	1
O17	O	1	0.5142775	0.4857225	0.525427	1
O18	O	1	0.4857225	0.4857225	0.474573	1
O19	O	1	0.5142775	0.5142775	0.474573	1
O20	O	1	0.4857225	0.5142775	0.525427	1
O21	O	1	0.5000000	0.5294489	0.4517069	1
O22	O	1	0.5000000	0.4705511	0.4517069	1
O23	O	1	0.4705511	0.5000000	0.5482931	1
O24	O	1	0.5294489	0.5000000	0.5482931	1
Zr1	Zr	1	0.5000000	0.4754959	0.5000000	1
Zr2	Zr	1	0.4754959	0.5000000	0.5000000	1
Zr3	Zr	1	0.5245041	0.5000000	0.5000000	1
Zr4	Zr	1	0.5000000	0.5245041	0.5000000	1

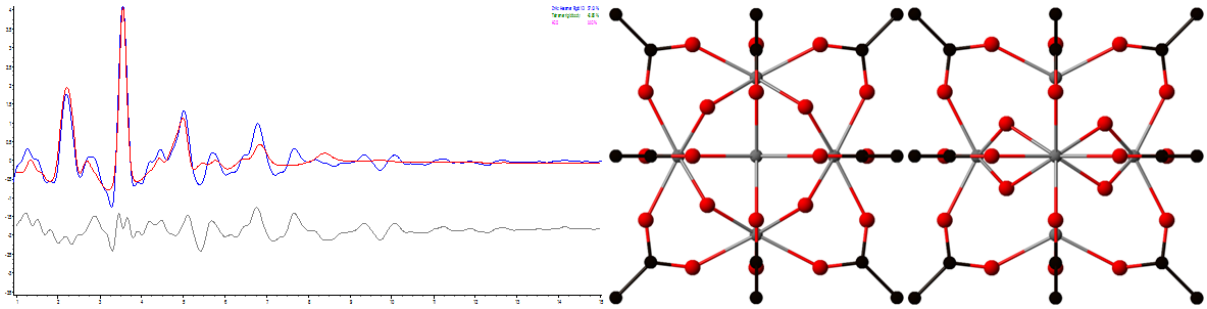

Figure 364: Observed and Calculated PDF from the chandelier core refinement of ZAA16A from the 18-month data collection and the resultant model viewed from the axial (left) and equatorial (right) positions.

Table 307: The atomic coordinates of the model resulting from the chandelier core refinement of ZAA16A from the 18-month data collection.

Atom Label	Atom Type	Multiplicity	Fractional X Coordinate	Fractional Y Coordinate	Fractional Z Coordinate	Fractional Occupancy
C1	C	1	0.5901275	0.5000000	0.5833742	1
C2	C	1	0.5000000	0.4098725	0.5833742	1
C3	C	1	0.4098725	0.5000000	0.5833742	1
C4	C	1	0.5000000	0.5901275	0.5833742	1
C5	C	1	0.5901275	0.5000000	0.4166258	1
C6	C	1	0.5000000	0.4098725	0.4166258	1
C7	C	1	0.4098725	0.5000000	0.4166258	1
C8	C	1	0.5000000	0.5901275	0.4166258	1
C9	C	1	0.5901275	0.4098725	0.5000000	1
C10	C	1	0.4098725	0.4098725	0.5000000	1
C11	C	1	0.4098725	0.5901275	0.5000000	1
C12	C	1	0.5901275	0.5901275	0.5000000	1
C13	C	1	0.6200311	0.5000000	0.6110371	1
C14	C	1	0.5000000	0.3799689	0.6110371	1
C15	C	1	0.3799689	0.5000000	0.6110371	1
C16	C	1	0.5000000	0.6200311	0.6110371	1
C17	C	1	0.6200311	0.5000000	0.3889629	1
C18	C	1	0.5000000	0.3799689	0.3889629	1
C19	C	1	0.3799689	0.5000000	0.3889629	1
C20	C	1	0.5000000	0.6200311	0.3889629	1
C21	C	1	0.6200311	0.3799689	0.5000000	1
C22	C	1	0.3799689	0.3799689	0.5000000	1
C23	C	1	0.3799689	0.6200311	0.5000000	1
C24	C	1	0.6200311	0.6200311	0.5000000	1
O1	O	1	0.5417338	0.4582662	0.4747455	1
O2	O	1	0.5417338	0.4582662	0.5252545	1
O3	O	1	0.4582662	0.4582662	0.4747455	1
O4	O	1	0.4582662	0.4582662	0.5252545	1
O5	O	1	0.4582662	0.5417338	0.4747455	1
O6	O	1	0.4582662	0.5417338	0.5252545	1
O7	O	1	0.5417338	0.5417338	0.4747455	1
O8	O	1	0.5417338	0.5417338	0.5252545	1

O9	O	1	0.59445	0.5000000	0.5503045	1
O10	O	1	0.59445	0.4456208	0.5000000	1
O11	O	1	0.59445	0.5000000	0.4496955	1
O12	O	1	0.59445	0.5543792	0.5000000	1
O13	O	1	0.5000000	0.59445	0.5503045	1
O14	O	1	0.5543792	0.59445	0.5000000	1
O15	O	1	0.5000000	0.59445	0.4496955	1
O16	O	1	0.4456208	0.59445	0.5000000	1
O17	O	1	0.40555	0.5000000	0.5503045	1
O18	O	1	0.40555	0.5543792	0.5000000	1
O19	O	1	0.40555	0.5000000	0.4496955	1
O20	O	1	0.40555	0.4456208	0.5000000	1
O21	O	1	0.5000000	0.40555	0.5503045	1
O22	O	1	0.4456208	0.40555	0.5000000	1
O23	O	1	0.5000000	0.40555	0.4496955	1
O24	O	1	0.5543792	0.40555	0.5000000	1
O25	O	1	0.5543792	0.5000000	0.5873728	1
O26	O	1	0.5000000	0.5543792	0.5873728	1
O27	O	1	0.4456208	0.5000000	0.5873728	1
O28	O	1	0.5000000	0.4456208	0.5873728	1
O29	O	1	0.5543792	0.5000000	0.4126272	1
O30	O	1	0.5000000	0.4456208	0.4126272	1
O31	O	1	0.4456208	0.5000000	0.4126272	1
O32	O	1	0.5000000	0.5543792	0.4126272	1
Zr1	Zr	1	0.5665231	0.5000000	0.5000000	1
Zr2	Zr	1	0.5000000	0.5665231	0.5000000	1
Zr3	Zr	1	0.4334769	0.5000000	0.5000000	1
Zr4	Zr	1	0.5000000	0.4334769	0.5000000	1
Zr5	Zr	1	0.5000000	0.5000000	0.5615385	1
Zr6	Zr	1	0.5000000	0.5000000	0.4384615	1

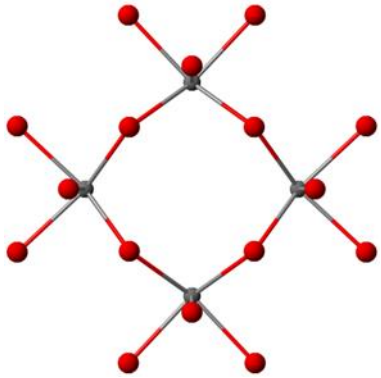

Figure 365: The tetrameric structure resulting from the chandelier core refinement of ZAA16A from the 18-month data collection.

Table 308: The atomic coordinates of the tetrameric phase of the chandelier core refinement of ZAA16A from the 18-month data collection.

Atom Label	Atom Type	Multiplicity	Fractional X Coordinate	Fractional Y Coordinate	Fractional Z Coordinate	Fractional Occupancy
O1	O	1	0.5143158	0.4856842	0.4731546	1
O2	O	1	0.4856842	0.4856842	0.5268454	1
O3	O	1	0.5143158	0.5143158	0.5268454	1
O4	O	1	0.4856842	0.5143158	0.4731546	1
O5	O	1	0.5000000	0.528352	0.5465312	1
O6	O	1	0.5000000	0.471648	0.5465312	1
O7	O	1	0.471648	0.5000000	0.4534688	1
O8	O	1	0.528352	0.5000000	0.4534688	1
O9	O	1	0.5145226	0.4599577	0.5000000	1
O10	O	1	0.4599577	0.4854774	0.5000000	1
O11	O	1	0.5400423	0.5145226	0.5000000	1
O12	O	1	0.4854774	0.5400423	0.5000000	1
O13	O	1	0.4599577	0.5145226	0.5000000	1
O14	O	1	0.5400423	0.4854774	0.5000000	1
O15	O	1	0.4854774	0.4599577	0.5000000	1
O16	O	1	0.5145226	0.5400423	0.5000000	1
O17	O	1	0.5143158	0.4856842	0.5268454	1
O18	O	1	0.4856842	0.4856842	0.4731546	1
O19	O	1	0.5143158	0.5143158	0.4731546	1
O20	O	1	0.4856842	0.5143158	0.5268454	1
O21	O	1	0.5000000	0.528352	0.4534688	1
O22	O	1	0.5000000	0.471648	0.4534688	1
O23	O	1	0.471648	0.5000000	0.5465312	1
O24	O	1	0.528352	0.5000000	0.5465312	1
Zr1	Zr	1	0.5000000	0.4754476	0.5000000	1
Zr2	Zr	1	0.4754476	0.5000000	0.5000000	1
Zr3	Zr	1	0.5245524	0.5000000	0.5000000	1
Zr4	Zr	1	0.5000000	0.5245524	0.5000000	1

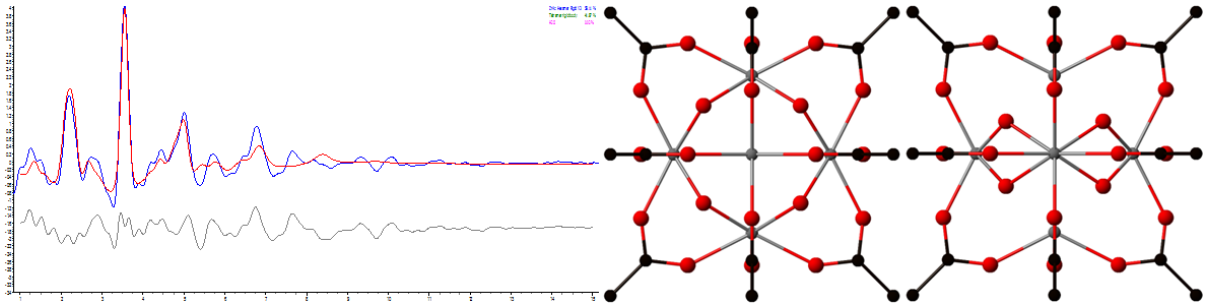

Figure 366: Observed and Calculated PDF from the chandelier core refinement of ZAA16C from the 18-month data collection and the resultant model viewed from the axial (left) and equatorial (right) positions.

Table 309: The atomic coordinates of the model resulting from the chandelier core refinement of ZAA16C from the 18-month data collection.

Atom Label	Atom Type	Multiplicity	Fractional X Coordinate	Fractional Y Coordinate	Fractional Z Coordinate	Fractional Occupancy
C1	C	1	0.5899993	0.5000000	0.5832556	1
C2	C	1	0.5000000	0.4100007	0.5832556	1
C3	C	1	0.4100007	0.5000000	0.5832556	1
C4	C	1	0.5000000	0.5899993	0.5832556	1
C5	C	1	0.5899993	0.5000000	0.4167444	1
C6	C	1	0.5000000	0.4100007	0.4167444	1
C7	C	1	0.4100007	0.5000000	0.4167444	1
C8	C	1	0.5000000	0.5899993	0.4167444	1
C9	C	1	0.5899993	0.4100007	0.5000000	1
C10	C	1	0.4100007	0.4100007	0.5000000	1
C11	C	1	0.4100007	0.5899993	0.5000000	1
C12	C	1	0.5899993	0.5899993	0.5000000	1
C13	C	1	0.6200513	0.5000000	0.6110558	1
C14	C	1	0.5000000	0.3799487	0.6110558	1
C15	C	1	0.3799487	0.5000000	0.6110558	1
C16	C	1	0.5000000	0.6200513	0.6110558	1
C17	C	1	0.6200513	0.5000000	0.3889442	1
C18	C	1	0.5000000	0.3799487	0.3889442	1
C19	C	1	0.3799487	0.5000000	0.3889442	1
C20	C	1	0.5000000	0.6200513	0.3889442	1
C21	C	1	0.6200513	0.3799487	0.5000000	1
C22	C	1	0.3799487	0.3799487	0.5000000	1
C23	C	1	0.3799487	0.6200513	0.5000000	1
C24	C	1	0.6200513	0.6200513	0.5000000	1
O1	O	1	0.5412124	0.4587876	0.4745766	1
O2	O	1	0.5412124	0.4587876	0.5254234	1
O3	O	1	0.4587876	0.4587876	0.4745766	1
O4	O	1	0.4587876	0.4587876	0.5254234	1
O5	O	1	0.4587876	0.5412124	0.4745766	1
O6	O	1	0.4587876	0.5412124	0.5254234	1
O7	O	1	0.5412124	0.5412124	0.4745766	1
O8	O	1	0.5412124	0.5412124	0.5254234	1

O9	O	1	0.5941909	0.5000000	0.55024	1
O10	O	1	0.5941909	0.4456905	0.5000000	1
O11	O	1	0.5941909	0.5000000	0.44976	1
O12	O	1	0.5941909	0.5543095	0.5000000	1
O13	O	1	0.5000000	0.5941909	0.55024	1
O14	O	1	0.5543095	0.5941909	0.5000000	1
O15	O	1	0.5000000	0.5941909	0.44976	1
O16	O	1	0.4456905	0.5941909	0.5000000	1
O17	O	1	0.4058091	0.5000000	0.55024	1
O18	O	1	0.4058091	0.5543095	0.5000000	1
O19	O	1	0.4058091	0.5000000	0.44976	1
O20	O	1	0.4058091	0.4456905	0.5000000	1
O21	O	1	0.5000000	0.4058091	0.55024	1
O22	O	1	0.4456905	0.4058091	0.5000000	1
O23	O	1	0.5000000	0.4058091	0.44976	1
O24	O	1	0.5543095	0.4058091	0.5000000	1
O25	O	1	0.5543095	0.5000000	0.5871331	1
O26	O	1	0.5000000	0.5543095	0.5871331	1
O27	O	1	0.4456905	0.5000000	0.5871331	1
O28	O	1	0.5000000	0.4456905	0.5871331	1
O29	O	1	0.5543095	0.5000000	0.4128669	1
O30	O	1	0.5000000	0.4456905	0.4128669	1
O31	O	1	0.4456905	0.5000000	0.4128669	1
O32	O	1	0.5000000	0.5543095	0.4128669	1
Zr1	Zr	1	0.5665532	0.5000000	0.5000000	1
Zr2	Zr	1	0.5000000	0.5665532	0.5000000	1
Zr3	Zr	1	0.4334468	0.5000000	0.5000000	1
Zr4	Zr	1	0.5000000	0.4334468	0.5000000	1
Zr5	Zr	1	0.5000000	0.5000000	0.5615664	1
Zr6	Zr	1	0.5000000	0.5000000	0.4384336	1

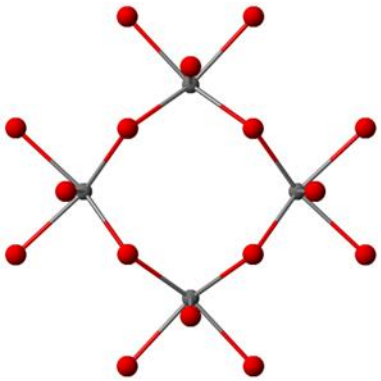

Figure 367: The tetrameric structure resulting from the chandelier core refinement of ZAA16C from the 18-month data collection.

Table 310: The atomic coordinates of the tetrameric phase of the chandelier core refinement of ZAA16C from the 18-month data collection.

Atom Label	Atom Type	Multiplicity	Fractional X Coordinate	Fractional Y Coordinate	Fractional Z Coordinate	Fractional Occupancy
O1	O	1	0.5143692	0.4856308	0.4734097	1
O2	O	1	0.4856308	0.4856308	0.5265903	1
O3	O	1	0.5143692	0.5143692	0.5265903	1
O4	O	1	0.4856308	0.5143692	0.4734097	1
O5	O	1	0.5000000	0.5285633	0.5464331	1
O6	O	1	0.5000000	0.4714367	0.5464331	1
O7	O	1	0.4714367	0.5000000	0.4535669	1
O8	O	1	0.5285633	0.5000000	0.4535669	1
O9	O	1	0.5145022	0.4599431	0.5000000	1
O10	O	1	0.4599431	0.4854978	0.5000000	1
O11	O	1	0.5400569	0.5145022	0.5000000	1
O12	O	1	0.4854978	0.5400569	0.5000000	1
O13	O	1	0.4599431	0.5145022	0.5000000	1
O14	O	1	0.5400569	0.4854978	0.5000000	1
O15	O	1	0.4854978	0.4599431	0.5000000	1
O16	O	1	0.5145022	0.5400569	0.5000000	1
O17	O	1	0.5143692	0.4856308	0.5265903	1
O18	O	1	0.4856308	0.4856308	0.4734097	1
O19	O	1	0.5143692	0.5143692	0.4734097	1
O20	O	1	0.4856308	0.5143692	0.5265903	1
O21	O	1	0.5000000	0.5285633	0.4535669	1
O22	O	1	0.5000000	0.4714367	0.4535669	1
O23	O	1	0.4714367	0.5000000	0.5464331	1
O24	O	1	0.5285633	0.5000000	0.5464331	1
Zr1	Zr	1	0.5000000	0.4755316	0.5000000	1
Zr2	Zr	1	0.4755316	0.5000000	0.5000000	1
Zr3	Zr	1	0.5244684	0.5000000	0.5000000	1
Zr4	Zr	1	0.5000000	0.5244684	0.5000000	1

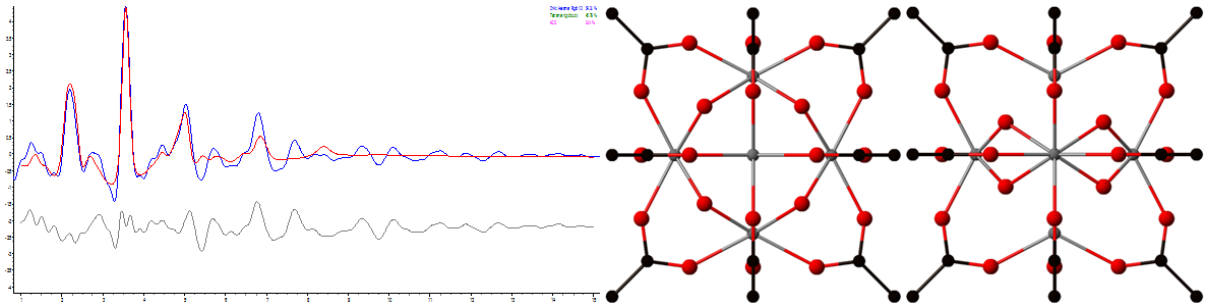

Figure 368: Observed and Calculated PDF from the chandelier core refinement of ZAA16I from the 18-month data collection and the resultant model viewed from the axial (left) and equatorial (right) positions.

Table 311: The atomic coordinates of the model resulting from the chandelier core refinement of ZAA16I from the 18-month data collection.

Atom Label	Atom Type	Multiplicity	Fractional X Coordinate	Fractional Y Coordinate	Fractional Z Coordinate	Fractional Occupancy
C1	C	1	0.5901367	0.5000000	0.5833827	1
C2	C	1	0.5000000	0.4098633	0.5833827	1
C3	C	1	0.4098633	0.5000000	0.5833827	1
C4	C	1	0.5000000	0.5901367	0.5833827	1
C5	C	1	0.5901367	0.5000000	0.4166173	1
C6	C	1	0.5000000	0.4098633	0.4166173	1
C7	C	1	0.4098633	0.5000000	0.4166173	1
C8	C	1	0.5000000	0.5901367	0.4166173	1
C9	C	1	0.5901367	0.4098633	0.5000000	1
C10	C	1	0.4098633	0.4098633	0.5000000	1
C11	C	1	0.4098633	0.5901367	0.5000000	1
C12	C	1	0.5901367	0.5901367	0.5000000	1
C13	C	1	0.6202225	0.5000000	0.6112142	1
C14	C	1	0.5000000	0.3797775	0.6112142	1
C15	C	1	0.3797775	0.5000000	0.6112142	1
C16	C	1	0.5000000	0.6202225	0.6112142	1
C17	C	1	0.6202225	0.5000000	0.3887858	1
C18	C	1	0.5000000	0.3797775	0.3887858	1
C19	C	1	0.3797775	0.5000000	0.3887858	1
C20	C	1	0.5000000	0.6202225	0.3887858	1
C21	C	1	0.6202225	0.3797775	0.5000000	1
C22	C	1	0.3797775	0.3797775	0.5000000	1
C23	C	1	0.3797775	0.6202225	0.5000000	1
C24	C	1	0.6202225	0.6202225	0.5000000	1
O1	O	1	0.5414553	0.4585447	0.4746644	1
O2	O	1	0.5414553	0.4585447	0.5253356	1
O3	O	1	0.4585447	0.4585447	0.4746644	1
O4	O	1	0.4585447	0.4585447	0.5253356	1
O5	O	1	0.4585447	0.5414553	0.4746644	1
O6	O	1	0.4585447	0.5414553	0.5253356	1
O7	O	1	0.5414553	0.5414553	0.4746644	1
O8	O	1	0.5414553	0.5414553	0.5253356	1

O9	O	1	0.5949845	0.5000000	0.5501229	1
O10	O	1	0.5949845	0.4458171	0.5000000	1
O11	O	1	0.5949845	0.5000000	0.4498771	1
O12	O	1	0.5949845	0.5541829	0.5000000	1
O13	O	1	0.5000000	0.5949845	0.5501229	1
O14	O	1	0.5541829	0.5949845	0.5000000	1
O15	O	1	0.5000000	0.5949845	0.4498771	1
O16	O	1	0.4458171	0.5949845	0.5000000	1
O17	O	1	0.4050155	0.5000000	0.5501229	1
O18	O	1	0.4050155	0.5541829	0.5000000	1
O19	O	1	0.4050155	0.5000000	0.4498771	1
O20	O	1	0.4050155	0.4458171	0.5000000	1
O21	O	1	0.5000000	0.4050155	0.5501229	1
O22	O	1	0.4458171	0.4050155	0.5000000	1
O23	O	1	0.5000000	0.4050155	0.4498771	1
O24	O	1	0.5541829	0.4050155	0.5000000	1
O25	O	1	0.5541829	0.5000000	0.5878673	1
O26	O	1	0.5000000	0.5541829	0.5878673	1
O27	O	1	0.4458171	0.5000000	0.5878673	1
O28	O	1	0.5000000	0.4458171	0.5878673	1
O29	O	1	0.5541829	0.5000000	0.4121327	1
O30	O	1	0.5000000	0.4458171	0.4121327	1
O31	O	1	0.4458171	0.5000000	0.4121327	1
O32	O	1	0.5000000	0.5541829	0.4121327	1
Zr1	Zr	1	0.566743	0.5000000	0.5000000	1
Zr2	Zr	1	0.5000000	0.566743	0.5000000	1
Zr3	Zr	1	0.433257	0.5000000	0.5000000	1
Zr4	Zr	1	0.5000000	0.433257	0.5000000	1
Zr5	Zr	1	0.5000000	0.5000000	0.5617419	1
Zr6	Zr	1	0.5000000	0.5000000	0.4382581	1

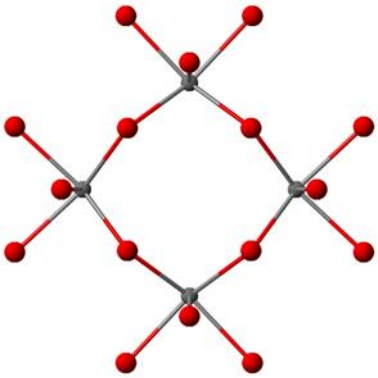

Figure 369: The tetrameric structure resulting from the chandelier core refinement of ZAA16I from the 18-month data collection.

Table 312: The atomic coordinates of the tetrameric phase of the chandelier core refinement of ZAA16I from the 18-month data collection.

Atom Label	Atom Type	Multiplicity	Fractional X Coordinate	Fractional Y Coordinate	Fractional Z Coordinate	Fractional Occupancy
O1	O	1	0.5142366	0.4857634	0.4747282	1
O2	O	1	0.4857634	0.4857634	0.5252718	1
O3	O	1	0.5142366	0.5142366	0.5252718	1
O4	O	1	0.4857634	0.5142366	0.4747282	1
O5	O	1	0.5000000	0.5294052	0.5463994	1
O6	O	1	0.5000000	0.4705948	0.5463994	1
O7	O	1	0.4705948	0.5000000	0.4536006	1
O8	O	1	0.5294052	0.5000000	0.4536006	1
O9	O	1	0.5145705	0.4598124	0.5000000	1
O10	O	1	0.4598124	0.4854295	0.5000000	1
O11	O	1	0.5401876	0.5145705	0.5000000	1
O12	O	1	0.4854295	0.5401876	0.5000000	1
O13	O	1	0.4598124	0.5145705	0.5000000	1
O14	O	1	0.5401876	0.4854295	0.5000000	1
O15	O	1	0.4854295	0.4598124	0.5000000	1
O16	O	1	0.5145705	0.5401876	0.5000000	1
O17	O	1	0.5142366	0.4857634	0.5252718	1
O18	O	1	0.4857634	0.4857634	0.4747282	1
O19	O	1	0.5142366	0.5142366	0.4747282	1
O20	O	1	0.4857634	0.5142366	0.5252718	1
O21	O	1	0.5000000	0.5294052	0.4536006	1
O22	O	1	0.5000000	0.4705948	0.4536006	1
O23	O	1	0.4705948	0.5000000	0.5463994	1
O24	O	1	0.5294052	0.5000000	0.5463994	1
Zr1	Zr	1	0.5000000	0.4753398	0.5000000	1
Zr2	Zr	1	0.4753398	0.5000000	0.5000000	1
Zr3	Zr	1	0.5246602	0.5000000	0.5000000	1
Zr4	Zr	1	0.5000000	0.5246602	0.5000000	1

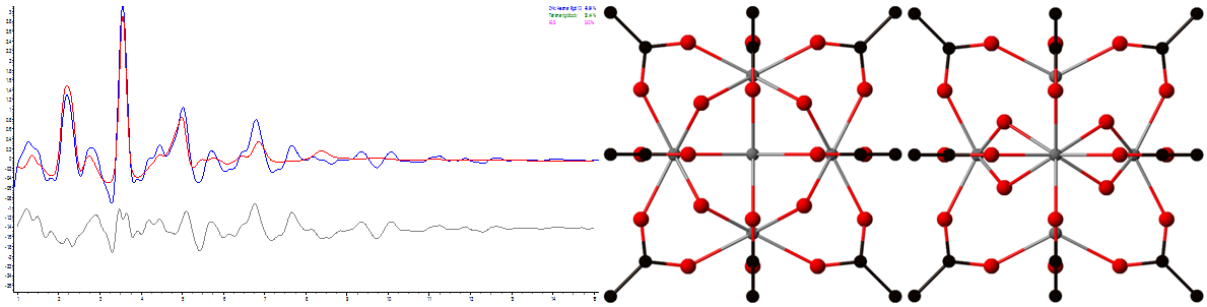

Figure 370: Observed and Calculated PDF from the chandelier core refinement of ZAA20A from the 18-month data collection and the resultant model viewed from the axial (left) and equatorial (right) positions.

Table 313: The atomic coordinates of the model resulting from the chandelier core refinement of ZAA20A from the 18-month data collection.

Atom Label	Atom Type	Multiplicity	Fractional X Coordinate	Fractional Y Coordinate	Fractional Z Coordinate	Fractional Occupancy
C1	C	1	0.5905718	0.5000000	0.5837852	1
C2	C	1	0.5000000	0.4094282	0.5837852	1
C3	C	1	0.4094282	0.5000000	0.5837852	1
C4	C	1	0.5000000	0.5905718	0.5837852	1
C5	C	1	0.5905718	0.5000000	0.4162148	1
C6	C	1	0.5000000	0.4094282	0.4162148	1
C7	C	1	0.4094282	0.5000000	0.4162148	1
C8	C	1	0.5000000	0.5905718	0.4162148	1
C9	C	1	0.5905718	0.4094282	0.5000000	1
C10	C	1	0.4094282	0.4094282	0.5000000	1
C11	C	1	0.4094282	0.5905718	0.5000000	1
C12	C	1	0.5905718	0.5905718	0.5000000	1
C13	C	1	0.6199662	0.5000000	0.6109771	1
C14	C	1	0.5000000	0.3800338	0.6109771	1
C15	C	1	0.3800338	0.5000000	0.6109771	1
C16	C	1	0.5000000	0.6199662	0.6109771	1
C17	C	1	0.6199662	0.5000000	0.3890229	1
C18	C	1	0.5000000	0.3800338	0.3890229	1
C19	C	1	0.3800338	0.5000000	0.3890229	1
C20	C	1	0.5000000	0.6199662	0.3890229	1
C21	C	1	0.6199662	0.3800338	0.5000000	1
C22	C	1	0.3800338	0.3800338	0.5000000	1
C23	C	1	0.3800338	0.6199662	0.5000000	1
C24	C	1	0.6199662	0.6199662	0.5000000	1
O1	O	1	0.5433838	0.4566162	0.4740783	1
O2	O	1	0.5433838	0.4566162	0.5259217	1
O3	O	1	0.4566162	0.4566162	0.4740783	1
O4	O	1	0.4566162	0.4566162	0.5259217	1
O5	O	1	0.4566162	0.5433838	0.4740783	1
O6	O	1	0.4566162	0.5433838	0.5259217	1
O7	O	1	0.5433838	0.5433838	0.4740783	1
O8	O	1	0.5433838	0.5433838	0.5259217	1

O9	O	1	0.5944039	0.5000000	0.550526	1
O10	O	1	0.5944039	0.4453814	0.5000000	1
O11	O	1	0.5944039	0.5000000	0.449474	1
O12	O	1	0.5944039	0.5546186	0.5000000	1
O13	O	1	0.5000000	0.5944039	0.550526	1
O14	O	1	0.5546186	0.5944039	0.5000000	1
O15	O	1	0.5000000	0.5944039	0.449474	1
O16	O	1	0.4453814	0.5944039	0.5000000	1
O17	O	1	0.4055961	0.5000000	0.550526	1
O18	O	1	0.4055961	0.5546186	0.5000000	1
O19	O	1	0.4055961	0.5000000	0.449474	1
O20	O	1	0.4055961	0.4453814	0.5000000	1
O21	O	1	0.5000000	0.4055961	0.550526	1
O22	O	1	0.4453814	0.4055961	0.5000000	1
O23	O	1	0.5000000	0.4055961	0.449474	1
O24	O	1	0.5546186	0.4055961	0.5000000	1
O25	O	1	0.5546186	0.5000000	0.5873302	1
O26	O	1	0.5000000	0.5546186	0.5873302	1
O27	O	1	0.4453814	0.5000000	0.5873302	1
O28	O	1	0.5000000	0.4453814	0.5873302	1
O29	O	1	0.5546186	0.5000000	0.4126698	1
O30	O	1	0.5000000	0.4453814	0.4126698	1
O31	O	1	0.4453814	0.5000000	0.4126698	1
O32	O	1	0.5000000	0.5546186	0.4126698	1
Zr1	Zr	1	0.5664731	0.5000000	0.5000000	1
Zr2	Zr	1	0.5000000	0.5664731	0.5000000	1
Zr3	Zr	1	0.4335269	0.5000000	0.5000000	1
Zr4	Zr	1	0.5000000	0.4335269	0.5000000	1
Zr5	Zr	1	0.5000000	0.5000000	0.5614923	1
Zr6	Zr	1	0.5000000	0.5000000	0.4385077	1

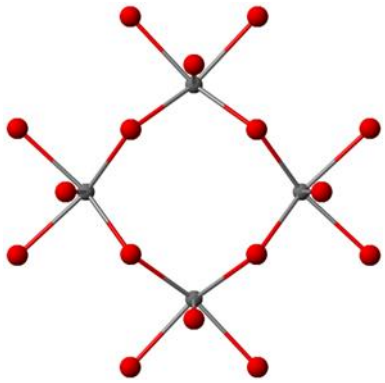

Figure 371: The tetrameric structure resulting from the chandelier core refinement of ZAA20A from the 18-month data collection.

Table 314: The atomic coordinates of the tetrameric phase of the chandelier core refinement of ZAA20A from the 18-month data collection.

Atom Label	Atom Type	Multiplicity	Fractional X Coordinate	Fractional Y Coordinate	Fractional Z Coordinate	Fractional Occupancy
O1	O	1	0.5143338	0.4856662	0.4766179	1
O2	O	1	0.4856662	0.4856662	0.5233821	1
O3	O	1	0.5143338	0.5143338	0.5233821	1
O4	O	1	0.4856662	0.5143338	0.4766179	1
O5	O	1	0.5000000	0.5291823	0.5473548	1
O6	O	1	0.5000000	0.4708177	0.5473548	1
O7	O	1	0.4708177	0.5000000	0.4526452	1
O8	O	1	0.5291823	0.5000000	0.4526452	1
O9	O	1	0.514537	0.4598083	0.5000000	1
O10	O	1	0.4598083	0.485463	0.5000000	1
O11	O	1	0.5401917	0.514537	0.5000000	1
O12	O	1	0.485463	0.5401917	0.5000000	1
O13	O	1	0.4598083	0.514537	0.5000000	1
O14	O	1	0.5401917	0.485463	0.5000000	1
O15	O	1	0.485463	0.4598083	0.5000000	1
O16	O	1	0.514537	0.5401917	0.5000000	1
O17	O	1	0.5143338	0.4856662	0.5233821	1
O18	O	1	0.4856662	0.4856662	0.4766179	1
O19	O	1	0.5143338	0.5143338	0.4766179	1
O20	O	1	0.4856662	0.5143338	0.5233821	1
O21	O	1	0.5000000	0.5291823	0.4526452	1
O22	O	1	0.5000000	0.4708177	0.4526452	1
O23	O	1	0.4708177	0.5000000	0.5473548	1
O24	O	1	0.5291823	0.5000000	0.5473548	1
Zr1	Zr	1	0.5000000	0.475427	0.5000000	1
Zr2	Zr	1	0.475427	0.5000000	0.5000000	1
Zr3	Zr	1	0.524573	0.5000000	0.5000000	1
Zr4	Zr	1	0.5000000	0.524573	0.5000000	1

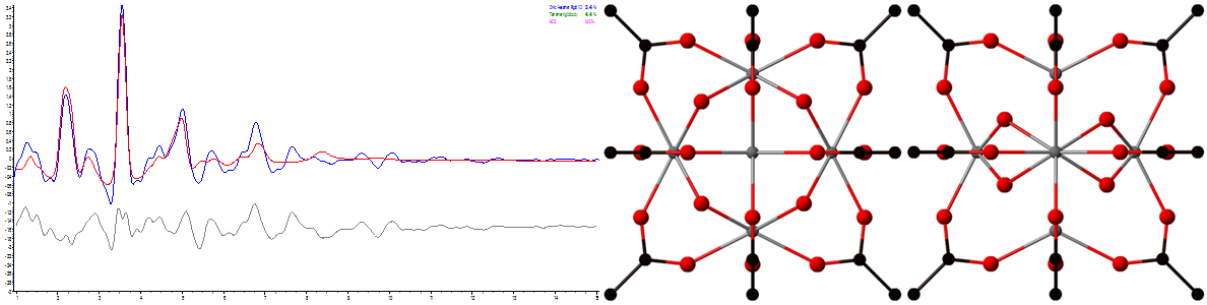

Figure 372: Observed and Calculated PDF from the chandelier core refinement of ZAA20C from the 18-month data collection and the resultant model viewed from the axial (left) and equatorial (right) positions.

Table 315: The atomic coordinates of the model resulting from the chandelier core refinement of ZAA20C from the 18-month data collection.

Atom Label	Atom Type	Multiplicity	Fractional X Coordinate	Fractional Y Coordinate	Fractional Z Coordinate	Fractional Occupancy
C1	C	1	0.5904031	0.5000000	0.5836291	1
C2	C	1	0.5000000	0.4095969	0.5836291	1
C3	C	1	0.4095969	0.5000000	0.5836291	1
C4	C	1	0.5000000	0.5904031	0.5836291	1
C5	C	1	0.5904031	0.5000000	0.4163709	1
C6	C	1	0.5000000	0.4095969	0.4163709	1
C7	C	1	0.4095969	0.5000000	0.4163709	1
C8	C	1	0.5000000	0.5904031	0.4163709	1
C9	C	1	0.5904031	0.4095969	0.5000000	1
C10	C	1	0.4095969	0.4095969	0.5000000	1
C11	C	1	0.4095969	0.5904031	0.5000000	1
C12	C	1	0.5904031	0.5904031	0.5000000	1
C13	C	1	0.6198631	0.5000000	0.6108818	1
C14	C	1	0.5000000	0.3801369	0.6108818	1
C15	C	1	0.3801369	0.5000000	0.6108818	1
C16	C	1	0.5000000	0.6198631	0.6108818	1
C17	C	1	0.6198631	0.5000000	0.3891182	1
C18	C	1	0.5000000	0.3801369	0.3891182	1
C19	C	1	0.3801369	0.5000000	0.3891182	1
C20	C	1	0.5000000	0.6198631	0.3891182	1
C21	C	1	0.6198631	0.3801369	0.5000000	1
C22	C	1	0.3801369	0.3801369	0.5000000	1
C23	C	1	0.3801369	0.6198631	0.5000000	1
C24	C	1	0.6198631	0.6198631	0.5000000	1
O1	O	1	0.5431439	0.4568561	0.4744346	1
O2	O	1	0.5431439	0.4568561	0.5255654	1
O3	O	1	0.4568561	0.4568561	0.4744346	1
O4	O	1	0.4568561	0.4568561	0.5255654	1
O5	O	1	0.4568561	0.5431439	0.4744346	1
O6	O	1	0.4568561	0.5431439	0.5255654	1
O7	O	1	0.5431439	0.5431439	0.4744346	1
O8	O	1	0.5431439	0.5431439	0.5255654	1

O9	O	1	0.5942568	0.5000000	0.5506091	1
O10	O	1	0.5942568	0.4452916	0.5000000	1
O11	O	1	0.5942568	0.5000000	0.4493909	1
O12	O	1	0.5942568	0.5547084	0.5000000	1
O13	O	1	0.5000000	0.5942568	0.5506091	1
O14	O	1	0.5547084	0.5942568	0.5000000	1
O15	O	1	0.5000000	0.5942568	0.4493909	1
O16	O	1	0.4452916	0.5942568	0.5000000	1
O17	O	1	0.4057432	0.5000000	0.5506091	1
O18	O	1	0.4057432	0.5547084	0.5000000	1
O19	O	1	0.4057432	0.5000000	0.4493909	1
O20	O	1	0.4057432	0.4452916	0.5000000	1
O21	O	1	0.5000000	0.4057432	0.5506091	1
O22	O	1	0.4452916	0.4057432	0.5000000	1
O23	O	1	0.5000000	0.4057432	0.4493909	1
O24	O	1	0.5547084	0.4057432	0.5000000	1
O25	O	1	0.5547084	0.5000000	0.5871941	1
O26	O	1	0.5000000	0.5547084	0.5871941	1
O27	O	1	0.4452916	0.5000000	0.5871941	1
O28	O	1	0.5000000	0.4452916	0.5871941	1
O29	O	1	0.5547084	0.5000000	0.4128059	1
O30	O	1	0.5000000	0.4452916	0.4128059	1
O31	O	1	0.4452916	0.5000000	0.4128059	1
O32	O	1	0.5000000	0.5547084	0.4128059	1
Zr1	Zr	1	0.5664535	0.5000000	0.5000000	1
Zr2	Zr	1	0.5000000	0.5664535	0.5000000	1
Zr3	Zr	1	0.4335465	0.5000000	0.5000000	1
Zr4	Zr	1	0.5000000	0.4335465	0.5000000	1
Zr5	Zr	1	0.5000000	0.5000000	0.5614741	1
Zr6	Zr	1	0.5000000	0.5000000	0.4385259	1

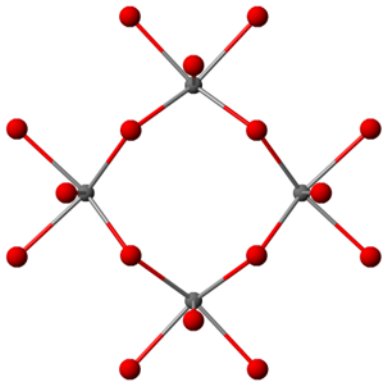

Figure 373: The tetrameric structure resulting from the chandelier core refinement of ZAA20C from the 18-month data collection.

Table 316: The atomic coordinates of the tetrameric phase of the chandelier core refinement of ZAA20C from the 18-month data collection.

Atom Label	Atom Type	Multiplicity	Fractional X Coordinate	Fractional Y Coordinate	Fractional Z Coordinate	Fractional Occupancy
O1	O	1	0.5142731	0.4857269	0.4752604	1
O2	O	1	0.4857269	0.4857269	0.5247396	1
O3	O	1	0.5142731	0.5142731	0.5247396	1
O4	O	1	0.4857269	0.5142731	0.4752604	1
O5	O	1	0.5000000	0.5289838	0.5467497	1
O6	O	1	0.5000000	0.4710162	0.5467497	1
O7	O	1	0.4710162	0.5000000	0.4532503	1
O8	O	1	0.5289838	0.5000000	0.4532503	1
O9	O	1	0.5145609	0.4598184	0.5000000	1
O10	O	1	0.4598184	0.4854391	0.5000000	1
O11	O	1	0.5401816	0.5145609	0.5000000	1
O12	O	1	0.4854391	0.5401816	0.5000000	1
O13	O	1	0.4598184	0.5145609	0.5000000	1
O14	O	1	0.5401816	0.4854391	0.5000000	1
O15	O	1	0.4854391	0.4598184	0.5000000	1
O16	O	1	0.5145609	0.5401816	0.5000000	1
O17	O	1	0.5142731	0.4857269	0.5247396	1
O18	O	1	0.4857269	0.4857269	0.4752604	1
O19	O	1	0.5142731	0.5142731	0.4752604	1
O20	O	1	0.4857269	0.5142731	0.5247396	1
O21	O	1	0.5000000	0.5289838	0.4532503	1
O22	O	1	0.5000000	0.4710162	0.4532503	1
O23	O	1	0.4710162	0.5000000	0.5467497	1
O24	O	1	0.5289838	0.5000000	0.5467497	1
Zr1	Zr	1	0.5000000	0.4754572	0.5000000	1
Zr2	Zr	1	0.4754572	0.5000000	0.5000000	1
Zr3	Zr	1	0.5245428	0.5000000	0.5000000	1
Zr4	Zr	1	0.5000000	0.5245428	0.5000000	1

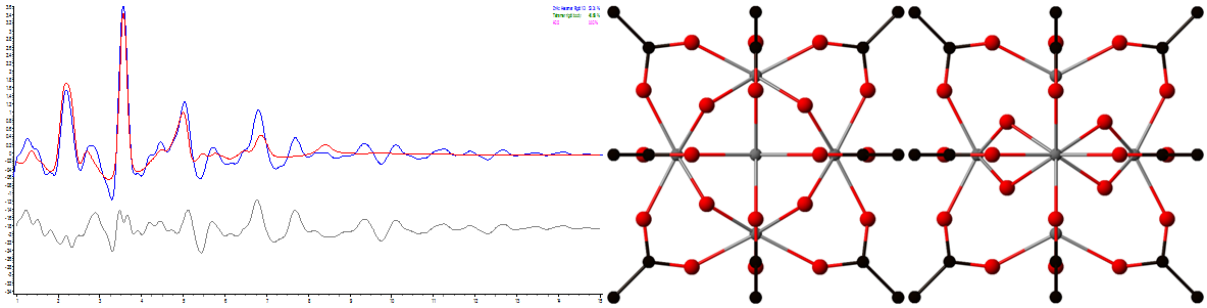

Figure 374: Observed and Calculated PDF from the chandelier core refinement of ZAA20I from the 18-month data collection and the resultant model viewed from the axial (left) and equatorial (right) positions.

Table 317: The atomic coordinates of the model resulting from the chandelier core refinement of ZAA20I from the 18-month data collection.

Atom Label	Atom Type	Multiplicity	Fractional X Coordinate	Fractional Y Coordinate	Fractional Z Coordinate	Fractional Occupancy
C1	C	1	0.5904586	0.5000000	0.5836805	1
C2	C	1	0.5000000	0.4095414	0.5836805	1
C3	C	1	0.4095414	0.5000000	0.5836805	1
C4	C	1	0.5000000	0.5904586	0.5836805	1
C5	C	1	0.5904586	0.5000000	0.4163195	1
C6	C	1	0.5000000	0.4095414	0.4163195	1
C7	C	1	0.4095414	0.5000000	0.4163195	1
C8	C	1	0.5000000	0.5904586	0.4163195	1
C9	C	1	0.5904586	0.4095414	0.5000000	1
C10	C	1	0.4095414	0.4095414	0.5000000	1
C11	C	1	0.4095414	0.5904586	0.5000000	1
C12	C	1	0.5904586	0.5904586	0.5000000	1
C13	C	1	0.620308	0.5000000	0.6112933	1
C14	C	1	0.5000000	0.379692	0.6112933	1
C15	C	1	0.379692	0.5000000	0.6112933	1
C16	C	1	0.5000000	0.620308	0.6112933	1
C17	C	1	0.620308	0.5000000	0.3887067	1
C18	C	1	0.5000000	0.379692	0.3887067	1
C19	C	1	0.379692	0.5000000	0.3887067	1
C20	C	1	0.5000000	0.620308	0.3887067	1
C21	C	1	0.620308	0.379692	0.5000000	1
C22	C	1	0.379692	0.379692	0.5000000	1
C23	C	1	0.379692	0.620308	0.5000000	1
C24	C	1	0.620308	0.620308	0.5000000	1
O1	O	1	0.5415943	0.4584057	0.4742214	1
O2	O	1	0.5415943	0.4584057	0.5257786	1
O3	O	1	0.4584057	0.4584057	0.4742214	1
O4	O	1	0.4584057	0.4584057	0.5257786	1
O5	O	1	0.4584057	0.5415943	0.4742214	1
O6	O	1	0.4584057	0.5415943	0.5257786	1
O7	O	1	0.5415943	0.5415943	0.4742214	1
O8	O	1	0.5415943	0.5415943	0.5257786	1

O9	O	1	0.5947861	0.5000000	0.5501672	1
O10	O	1	0.5947861	0.4457693	0.5000000	1
O11	O	1	0.5947861	0.5000000	0.4498328	1
O12	O	1	0.5947861	0.5542307	0.5000000	1
O13	O	1	0.5000000	0.5947861	0.5501672	1
O14	O	1	0.5542307	0.5947861	0.5000000	1
O15	O	1	0.5000000	0.5947861	0.4498328	1
O16	O	1	0.4457693	0.5947861	0.5000000	1
O17	O	1	0.4052139	0.5000000	0.5501672	1
O18	O	1	0.4052139	0.5542307	0.5000000	1
O19	O	1	0.4052139	0.5000000	0.4498328	1
O20	O	1	0.4052139	0.4457693	0.5000000	1
O21	O	1	0.5000000	0.4052139	0.5501672	1
O22	O	1	0.4457693	0.4052139	0.5000000	1
O23	O	1	0.5000000	0.4052139	0.4498328	1
O24	O	1	0.5542307	0.4052139	0.5000000	1
O25	O	1	0.5542307	0.5000000	0.5876838	1
O26	O	1	0.5000000	0.5542307	0.5876838	1
O27	O	1	0.4457693	0.5000000	0.5876838	1
O28	O	1	0.5000000	0.4457693	0.5876838	1
O29	O	1	0.5542307	0.5000000	0.4123162	1
O30	O	1	0.5000000	0.4457693	0.4123162	1
O31	O	1	0.4457693	0.5000000	0.4123162	1
O32	O	1	0.5000000	0.5542307	0.4123162	1
Zr1	Zr	1	0.5667164	0.5000000	0.5000000	1
Zr2	Zr	1	0.5000000	0.5667164	0.5000000	1
Zr3	Zr	1	0.4332836	0.5000000	0.5000000	1
Zr4	Zr	1	0.5000000	0.4332836	0.5000000	1
Zr5	Zr	1	0.5000000	0.5000000	0.5617173	1
Zr6	Zr	1	0.5000000	0.5000000	0.4382827	1

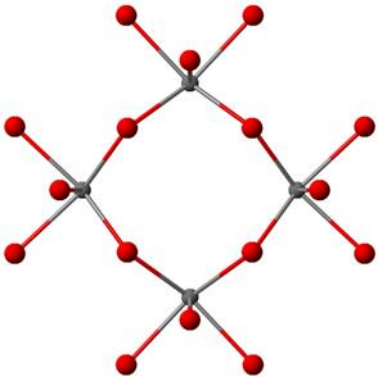

Figure 375: The tetrameric structure resulting from the chandelier core refinement of ZAA20I from the 18-month data collection.

Table 318: The atomic coordinates of the tetrameric phase of the chandelier core refinement of ZAA20I from the 18-month data collection.

Atom Label	Atom Type	Multiplicity	Fractional X Coordinate	Fractional Y Coordinate	Fractional Z Coordinate	Fractional Occupancy
O1	O	1	0.5143373	0.4856627	0.4758019	1
O2	O	1	0.4856627	0.4856627	0.5241981	1
O3	O	1	0.5143373	0.5143373	0.5241981	1
O4	O	1	0.4856627	0.5143373	0.4758019	1
O5	O	1	0.5000000	0.5299079	0.5463403	1
O6	O	1	0.5000000	0.4700921	0.5463403	1
O7	O	1	0.4700921	0.5000000	0.4536597	1
O8	O	1	0.5299079	0.5000000	0.4536597	1
O9	O	1	0.5145905	0.4597527	0.5000000	1
O10	O	1	0.4597527	0.4854095	0.5000000	1
O11	O	1	0.5402473	0.5145905	0.5000000	1
O12	O	1	0.4854095	0.5402473	0.5000000	1
O13	O	1	0.4597527	0.5145905	0.5000000	1
O14	O	1	0.5402473	0.4854095	0.5000000	1
O15	O	1	0.4854095	0.4597527	0.5000000	1
O16	O	1	0.5145905	0.5402473	0.5000000	1
O17	O	1	0.5143373	0.4856627	0.5241981	1
O18	O	1	0.4856627	0.4856627	0.4758019	1
O19	O	1	0.5143373	0.5143373	0.4758019	1
O20	O	1	0.4856627	0.5143373	0.5241981	1
O21	O	1	0.5000000	0.5299079	0.4536597	1
O22	O	1	0.5000000	0.4700921	0.4536597	1
O23	O	1	0.4700921	0.5000000	0.5463403	1
O24	O	1	0.5299079	0.5000000	0.5463403	1
Zr1	Zr	1	0.5000000	0.4753271	0.5000000	1
Zr2	Zr	1	0.4753271	0.5000000	0.5000000	1
Zr3	Zr	1	0.5246729	0.5000000	0.5000000	1
Zr4	Zr	1	0.5000000	0.5246729	0.5000000	1

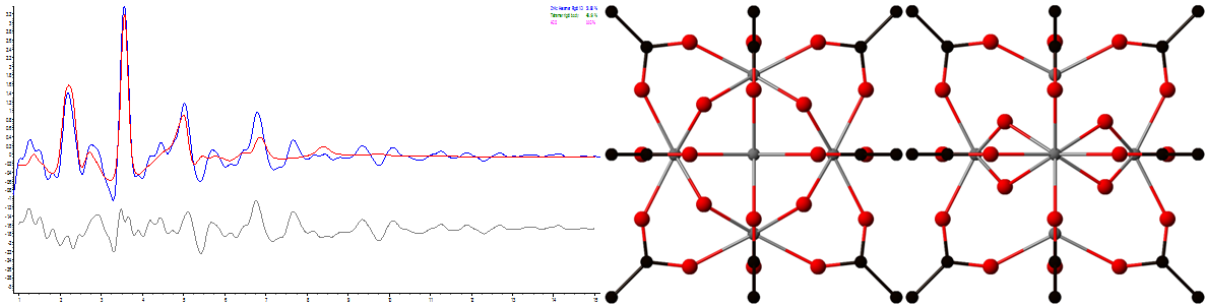

Figure 376: Observed and Calculated PDF from the chandelier core refinement of ZAA24A from the 18-month data collection and the resultant model viewed from the axial (left) and equatorial (right) positions.

Table 319: The atomic coordinates of the model resulting from the chandelier core refinement of ZAA24A from the 18-month data collection.

Atom Label	Atom Type	Multiplicity	Fractional X Coordinate	Fractional Y Coordinate	Fractional Z Coordinate	Fractional Occupancy
C1	C	1	0.5903724	0.5000000	0.5836008	1
C2	C	1	0.5000000	0.4096276	0.5836008	1
C3	C	1	0.4096276	0.5000000	0.5836008	1
C4	C	1	0.5000000	0.5903724	0.5836008	1
C5	C	1	0.5903724	0.5000000	0.4163992	1
C6	C	1	0.5000000	0.4096276	0.4163992	1
C7	C	1	0.4096276	0.5000000	0.4163992	1
C8	C	1	0.5000000	0.5903724	0.4163992	1
C9	C	1	0.5903724	0.4096276	0.5000000	1
C10	C	1	0.4096276	0.4096276	0.5000000	1
C11	C	1	0.4096276	0.5903724	0.5000000	1
C12	C	1	0.5903724	0.5903724	0.5000000	1
C13	C	1	0.6201584	0.5000000	0.6111549	1
C14	C	1	0.5000000	0.3798416	0.6111549	1
C15	C	1	0.3798416	0.5000000	0.6111549	1
C16	C	1	0.5000000	0.6201584	0.6111549	1
C17	C	1	0.6201584	0.5000000	0.3888451	1
C18	C	1	0.5000000	0.3798416	0.3888451	1
C19	C	1	0.3798416	0.5000000	0.3888451	1
C20	C	1	0.5000000	0.6201584	0.3888451	1
C21	C	1	0.6201584	0.3798416	0.5000000	1
C22	C	1	0.3798416	0.3798416	0.5000000	1
C23	C	1	0.3798416	0.6201584	0.5000000	1
C24	C	1	0.6201584	0.6201584	0.5000000	1
O1	O	1	0.5421741	0.4578259	0.4747166	1
O2	O	1	0.5421741	0.4578259	0.5252834	1
O3	O	1	0.4578259	0.4578259	0.4747166	1
O4	O	1	0.4578259	0.4578259	0.5252834	1
O5	O	1	0.4578259	0.5421741	0.4747166	1
O6	O	1	0.4578259	0.5421741	0.5252834	1
O7	O	1	0.5421741	0.5421741	0.4747166	1
O8	O	1	0.5421741	0.5421741	0.5252834	1

O9	O	1	0.5944771	0.5000000	0.5501789	1
O10	O	1	0.5944771	0.4457567	0.5000000	1
O11	O	1	0.5944771	0.5000000	0.4498211	1
O12	O	1	0.5944771	0.5542433	0.5000000	1
O13	O	1	0.5000000	0.5944771	0.5501789	1
O14	O	1	0.5542433	0.5944771	0.5000000	1
O15	O	1	0.5000000	0.5944771	0.4498211	1
O16	O	1	0.4457567	0.5944771	0.5000000	1
O17	O	1	0.4055229	0.5000000	0.5501789	1
O18	O	1	0.4055229	0.5542433	0.5000000	1
O19	O	1	0.4055229	0.5000000	0.4498211	1
O20	O	1	0.4055229	0.4457567	0.5000000	1
O21	O	1	0.5000000	0.4055229	0.5501789	1
O22	O	1	0.4457567	0.4055229	0.5000000	1
O23	O	1	0.5000000	0.4055229	0.4498211	1
O24	O	1	0.5542433	0.4055229	0.5000000	1
O25	O	1	0.5542433	0.5000000	0.5873979	1
O26	O	1	0.5000000	0.5542433	0.5873979	1
O27	O	1	0.4457567	0.5000000	0.5873979	1
O28	O	1	0.5000000	0.4457567	0.5873979	1
O29	O	1	0.5542433	0.5000000	0.4126021	1
O30	O	1	0.5000000	0.4457567	0.4126021	1
O31	O	1	0.4457567	0.5000000	0.4126021	1
O32	O	1	0.5000000	0.5542433	0.4126021	1
Zr1	Zr	1	0.5667897	0.5000000	0.5000000	1
Zr2	Zr	1	0.5000000	0.5667897	0.5000000	1
Zr3	Zr	1	0.4332103	0.5000000	0.5000000	1
Zr4	Zr	1	0.5000000	0.4332103	0.5000000	1
Zr5	Zr	1	0.5000000	0.5000000	0.5617851	1
Zr6	Zr	1	0.5000000	0.5000000	0.4382149	1

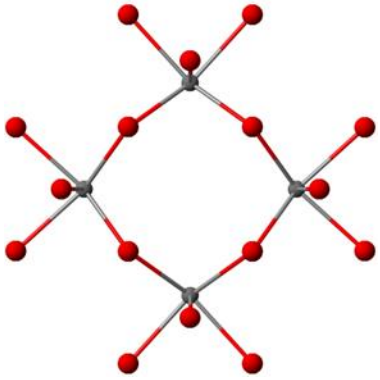

Figure 377: The tetrameric structure resulting from the chandelier core refinement of ZAA24A from the 18-month data collection.

Table 320: The atomic coordinates of the tetrameric phase of the chandelier core refinement of ZAA24A from the 18-month data collection.

Atom Label	Atom Type	Multiplicity	Fractional X Coordinate	Fractional Y Coordinate	Fractional Z Coordinate	Fractional Occupancy
O1	O	1	0.5143141	0.4856859	0.4746019	1
O2	O	1	0.4856859	0.4856859	0.5253981	1
O3	O	1	0.5143141	0.5143141	0.5253981	1
O4	O	1	0.4856859	0.5143141	0.4746019	1
O5	O	1	0.5000000	0.5296854	0.5490219	1
O6	O	1	0.5000000	0.4703146	0.5490219	1
O7	O	1	0.4703146	0.5000000	0.4509781	1
O8	O	1	0.5296854	0.5000000	0.4509781	1
O9	O	1	0.5142725	0.4597744	0.5000000	1
O10	O	1	0.4597744	0.4857275	0.5000000	1
O11	O	1	0.5402256	0.5142725	0.5000000	1
O12	O	1	0.4857275	0.5402256	0.5000000	1
O13	O	1	0.4597744	0.5142725	0.5000000	1
O14	O	1	0.5402256	0.4857275	0.5000000	1
O15	O	1	0.4857275	0.4597744	0.5000000	1
O16	O	1	0.5142725	0.5402256	0.5000000	1
O17	O	1	0.5143141	0.4856859	0.5253981	1
O18	O	1	0.4856859	0.4856859	0.4746019	1
O19	O	1	0.5143141	0.5143141	0.4746019	1
O20	O	1	0.4856859	0.5143141	0.5253981	1
O21	O	1	0.5000000	0.5296854	0.4509781	1
O22	O	1	0.5000000	0.4703146	0.4509781	1
O23	O	1	0.4703146	0.5000000	0.5490219	1
O24	O	1	0.5296854	0.5000000	0.5490219	1
Zr1	Zr	1	0.5000000	0.4754875	0.5000000	1
Zr2	Zr	1	0.4754875	0.5000000	0.5000000	1
Zr3	Zr	1	0.5245125	0.5000000	0.5000000	1
Zr4	Zr	1	0.5000000	0.5245125	0.5000000	1

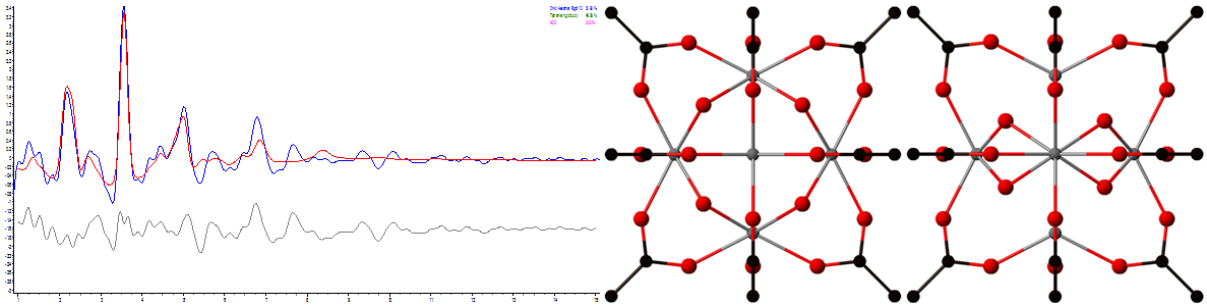

Figure 378: Observed and Calculated PDF from the chandelier core refinement of ZAA24C from the 18-month data collection and the resultant model viewed from the axial (left) and equatorial (right) positions.

Table 321: The atomic coordinates of the model resulting from the chandelier core refinement of ZAA24C from the 18-month data collection.

Atom Label	Atom Type	Multiplicity	Fractional X Coordinate	Fractional Y Coordinate	Fractional Z Coordinate	Fractional Occupancy
C1	C	1	0.5904418	0.5000000	0.583665	1
C2	C	1	0.5000000	0.4095582	0.583665	1
C3	C	1	0.4095582	0.5000000	0.583665	1
C4	C	1	0.5000000	0.5904418	0.583665	1
C5	C	1	0.5904418	0.5000000	0.416335	1
C6	C	1	0.5000000	0.4095582	0.416335	1
C7	C	1	0.4095582	0.5000000	0.416335	1
C8	C	1	0.5000000	0.5904418	0.416335	1
C9	C	1	0.5904418	0.4095582	0.5000000	1
C10	C	1	0.4095582	0.4095582	0.5000000	1
C11	C	1	0.4095582	0.5904418	0.5000000	1
C12	C	1	0.5904418	0.5904418	0.5000000	1
C13	C	1	0.6199874	0.5000000	0.6109967	1
C14	C	1	0.5000000	0.3800126	0.6109967	1
C15	C	1	0.3800126	0.5000000	0.6109967	1
C16	C	1	0.5000000	0.6199874	0.6109967	1
C17	C	1	0.6199874	0.5000000	0.3890033	1
C18	C	1	0.5000000	0.3800126	0.3890033	1
C19	C	1	0.3800126	0.5000000	0.3890033	1
C20	C	1	0.5000000	0.6199874	0.3890033	1
C21	C	1	0.6199874	0.3800126	0.5000000	1
C22	C	1	0.3800126	0.3800126	0.5000000	1
C23	C	1	0.3800126	0.6199874	0.5000000	1
C24	C	1	0.6199874	0.6199874	0.5000000	1
O1	O	1	0.5419409	0.4580591	0.4741445	1
O2	O	1	0.5419409	0.4580591	0.5258555	1
O3	O	1	0.4580591	0.4580591	0.4741445	1
O4	O	1	0.4580591	0.4580591	0.5258555	1
O5	O	1	0.4580591	0.5419409	0.4741445	1
O6	O	1	0.4580591	0.5419409	0.5258555	1
O7	O	1	0.5419409	0.5419409	0.4741445	1
O8	O	1	0.5419409	0.5419409	0.5258555	1

O9	O	1	0.5946277	0.5000000	0.5503982	1
O10	O	1	0.5946277	0.4455196	0.5000000	1
O11	O	1	0.5946277	0.5000000	0.4496018	1
O12	O	1	0.5946277	0.5544804	0.5000000	1
O13	O	1	0.5000000	0.5946277	0.5503982	1
O14	O	1	0.5544804	0.5946277	0.5000000	1
O15	O	1	0.5000000	0.5946277	0.4496018	1
O16	O	1	0.4455196	0.5946277	0.5000000	1
O17	O	1	0.4053723	0.5000000	0.5503982	1
O18	O	1	0.4053723	0.5544804	0.5000000	1
O19	O	1	0.4053723	0.5000000	0.4496018	1
O20	O	1	0.4053723	0.4455196	0.5000000	1
O21	O	1	0.5000000	0.4053723	0.5503982	1
O22	O	1	0.4455196	0.4053723	0.5000000	1
O23	O	1	0.5000000	0.4053723	0.4496018	1
O24	O	1	0.5544804	0.4053723	0.5000000	1
O25	O	1	0.5544804	0.5000000	0.5875372	1
O26	O	1	0.5000000	0.5544804	0.5875372	1
O27	O	1	0.4455196	0.5000000	0.5875372	1
O28	O	1	0.5000000	0.4455196	0.5875372	1
O29	O	1	0.5544804	0.5000000	0.4124628	1
O30	O	1	0.5000000	0.4455196	0.4124628	1
O31	O	1	0.4455196	0.5000000	0.4124628	1
O32	O	1	0.5000000	0.5544804	0.4124628	1
Zr1	Zr	1	0.5666135	0.5000000	0.5000000	1
Zr2	Zr	1	0.5000000	0.5666135	0.5000000	1
Zr3	Zr	1	0.4333865	0.5000000	0.5000000	1
Zr4	Zr	1	0.5000000	0.4333865	0.5000000	1
Zr5	Zr	1	0.5000000	0.5000000	0.5616222	1
Zr6	Zr	1	0.5000000	0.5000000	0.4383778	1

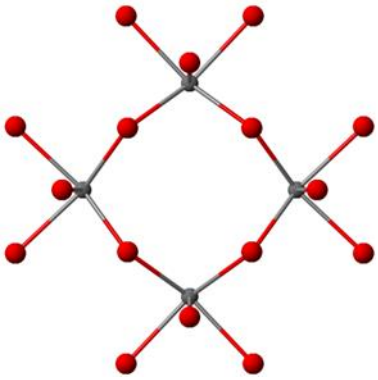

Figure 379: The tetrameric structure resulting from the chandelier core refinement of ZAA24C from the 18-month data collection.

Table 322: The atomic coordinates of the tetrameric phase of the chandelier core refinement of ZAA24C from the 18-month data collection.

Atom Label	Atom Type	Multiplicity	Fractional X Coordinate	Fractional Y Coordinate	Fractional Z Coordinate	Fractional Occupancy
O1	O	1	0.5143158	0.4856842	0.4754246	1
O2	O	1	0.4856842	0.4856842	0.5245754	1
O3	O	1	0.5143158	0.5143158	0.5245754	1
O4	O	1	0.4856842	0.5143158	0.4754246	1
O5	O	1	0.5000000	0.5293722	0.5461803	1
O6	O	1	0.5000000	0.4706278	0.5461803	1
O7	O	1	0.4706278	0.5000000	0.4538197	1
O8	O	1	0.5293722	0.5000000	0.4538197	1
O9	O	1	0.5146215	0.459896	0.5000000	1
O10	O	1	0.459896	0.4853785	0.5000000	1
O11	O	1	0.540104	0.5146215	0.5000000	1
O12	O	1	0.4853785	0.540104	0.5000000	1
O13	O	1	0.459896	0.5146215	0.5000000	1
O14	O	1	0.540104	0.4853785	0.5000000	1
O15	O	1	0.4853785	0.459896	0.5000000	1
O16	O	1	0.5146215	0.540104	0.5000000	1
O17	O	1	0.5143158	0.4856842	0.5245754	1
O18	O	1	0.4856842	0.4856842	0.4754246	1
O19	O	1	0.5143158	0.5143158	0.4754246	1
O20	O	1	0.4856842	0.5143158	0.5245754	1
O21	O	1	0.5000000	0.5293722	0.4538197	1
O22	O	1	0.5000000	0.4706278	0.4538197	1
O23	O	1	0.4706278	0.5000000	0.5461803	1
O24	O	1	0.5293722	0.5000000	0.5461803	1
Zr1	Zr	1	0.5000000	0.4754018	0.5000000	1
Zr2	Zr	1	0.4754018	0.5000000	0.5000000	1
Zr3	Zr	1	0.5245982	0.5000000	0.5000000	1
Zr4	Zr	1	0.5000000	0.5245982	0.5000000	1

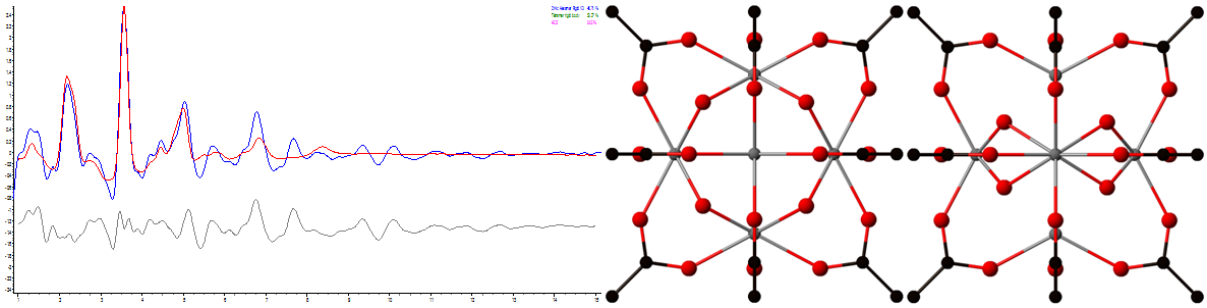

Figure 380: Observed and Calculated PDF from the chandelier core refinement of ZAA24I from the 18-month data collection and the resultant model viewed from the axial (left) and equatorial (right) positions.

Table 323: The atomic coordinates of the model resulting from the chandelier core refinement of ZAA24I from the 18-month data collection.

Atom Label	Atom Type	Multiplicity	Fractional X Coordinate	Fractional Y Coordinate	Fractional Z Coordinate	Fractional Occupancy
C1	C	1	0.5907704	0.5000000	0.5839689	1
C2	C	1	0.5000000	0.4092296	0.5839689	1
C3	C	1	0.4092296	0.5000000	0.5839689	1
C4	C	1	0.5000000	0.5907704	0.5839689	1
C5	C	1	0.5907704	0.5000000	0.4160311	1
C6	C	1	0.5000000	0.4092296	0.4160311	1
C7	C	1	0.4092296	0.5000000	0.4160311	1
C8	C	1	0.5000000	0.5907704	0.4160311	1
C9	C	1	0.5907704	0.4092296	0.5000000	1
C10	C	1	0.4092296	0.4092296	0.5000000	1
C11	C	1	0.4092296	0.5907704	0.5000000	1
C12	C	1	0.5907704	0.5907704	0.5000000	1
C13	C	1	0.6194463	0.5000000	0.6104961	1
C14	C	1	0.5000000	0.3805537	0.6104961	1
C15	C	1	0.3805537	0.5000000	0.6104961	1
C16	C	1	0.5000000	0.6194463	0.6104961	1
C17	C	1	0.6194463	0.5000000	0.3895039	1
C18	C	1	0.5000000	0.3805537	0.3895039	1
C19	C	1	0.3805537	0.5000000	0.3895039	1
C20	C	1	0.5000000	0.6194463	0.3895039	1
C21	C	1	0.6194463	0.3805537	0.5000000	1
C22	C	1	0.3805537	0.3805537	0.5000000	1
C23	C	1	0.3805537	0.6194463	0.5000000	1
C24	C	1	0.6194463	0.6194463	0.5000000	1
O1	O	1	0.5433771	0.4566229	0.4745819	1
O2	O	1	0.5433771	0.4566229	0.5254181	1
O3	O	1	0.4566229	0.4566229	0.4745819	1
O4	O	1	0.4566229	0.4566229	0.5254181	1
O5	O	1	0.4566229	0.5433771	0.4745819	1
O6	O	1	0.4566229	0.5433771	0.5254181	1
O7	O	1	0.5433771	0.5433771	0.4745819	1
O8	O	1	0.5433771	0.5433771	0.5254181	1

O9	O	1	0.5958761	0.5000000	0.5509513	1
O10	O	1	0.5958761	0.4449216	0.5000000	1
O11	O	1	0.5958761	0.5000000	0.4490487	1
O12	O	1	0.5958761	0.5550784	0.5000000	1
O13	O	1	0.5000000	0.5958761	0.5509513	1
O14	O	1	0.5550784	0.5958761	0.5000000	1
O15	O	1	0.5000000	0.5958761	0.4490487	1
O16	O	1	0.4449216	0.5958761	0.5000000	1
O17	O	1	0.4041239	0.5000000	0.5509513	1
O18	O	1	0.4041239	0.5550784	0.5000000	1
O19	O	1	0.4041239	0.5000000	0.4490487	1
O20	O	1	0.4041239	0.4449216	0.5000000	1
O21	O	1	0.5000000	0.4041239	0.5509513	1
O22	O	1	0.4449216	0.4041239	0.5000000	1
O23	O	1	0.5000000	0.4041239	0.4490487	1
O24	O	1	0.5550784	0.4041239	0.5000000	1
O25	O	1	0.5550784	0.5000000	0.5886921	1
O26	O	1	0.5000000	0.5550784	0.5886921	1
O27	O	1	0.4449216	0.5000000	0.5886921	1
O28	O	1	0.5000000	0.4449216	0.5886921	1
O29	O	1	0.5550784	0.5000000	0.4113079	1
O30	O	1	0.5000000	0.4449216	0.4113079	1
O31	O	1	0.4449216	0.5000000	0.4113079	1
O32	O	1	0.5000000	0.5550784	0.4113079	1
Zr1	Zr	1	0.5666516	0.5000000	0.5000000	1
Zr2	Zr	1	0.5000000	0.5666516	0.5000000	1
Zr3	Zr	1	0.4333484	0.5000000	0.5000000	1
Zr4	Zr	1	0.5000000	0.4333484	0.5000000	1
Zr5	Zr	1	0.5000000	0.5000000	0.5616574	1
Zr6	Zr	1	0.5000000	0.5000000	0.4383426	1

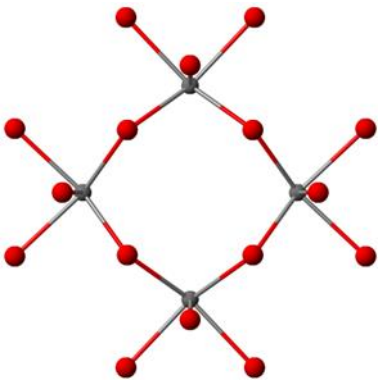

Figure 381: The tetrameric structure resulting from the chandelier core refinement of ZAA24I from the 18-month data collection.

Table 324: The atomic coordinates of the tetrameric phase of the chandelier core refinement of ZAA24I from the 18-month data collection.

Atom Label	Atom Type	Multiplicity	Fractional X Coordinate	Fractional Y Coordinate	Fractional Z Coordinate	Fractional Occupancy
O1	O	1	0.5143799	0.4856201	0.4746433	1
O2	O	1	0.4856201	0.4856201	0.5253567	1
O3	O	1	0.5143799	0.5143799	0.5253567	1
O4	O	1	0.4856201	0.5143799	0.4746433	1
O5	O	1	0.5000000	0.5292587	0.5467372	1
O6	O	1	0.5000000	0.4707413	0.5467372	1
O7	O	1	0.4707413	0.5000000	0.4532628	1
O8	O	1	0.5292587	0.5000000	0.4532628	1
O9	O	1	0.5146889	0.4598201	0.5000000	1
O10	O	1	0.4598201	0.4853111	0.5000000	1
O11	O	1	0.5401799	0.5146889	0.5000000	1
O12	O	1	0.4853111	0.5401799	0.5000000	1
O13	O	1	0.4598201	0.5146889	0.5000000	1
O14	O	1	0.5401799	0.4853111	0.5000000	1
O15	O	1	0.4853111	0.4598201	0.5000000	1
O16	O	1	0.5146889	0.5401799	0.5000000	1
O17	O	1	0.5143799	0.4856201	0.5253567	1
O18	O	1	0.4856201	0.4856201	0.4746433	1
O19	O	1	0.5143799	0.5143799	0.4746433	1
O20	O	1	0.4856201	0.5143799	0.5253567	1
O21	O	1	0.5000000	0.5292587	0.4532628	1
O22	O	1	0.5000000	0.4707413	0.4532628	1
O23	O	1	0.4707413	0.5000000	0.5467372	1
O24	O	1	0.5292587	0.5000000	0.5467372	1
Zr1	Zr	1	0.5000000	0.4754063	0.5000000	1
Zr2	Zr	1	0.4754063	0.5000000	0.5000000	1
Zr3	Zr	1	0.5245937	0.5000000	0.5000000	1
Zr4	Zr	1	0.5000000	0.5245937	0.5000000	1

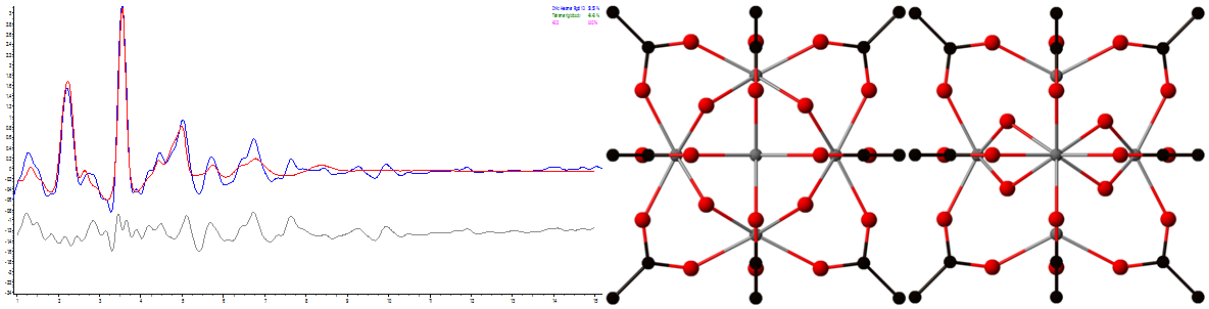

Figure 382: Observed and Calculated PDF from the chandelier core refinement of ZAA25A from the 18-month data collection and the resultant model viewed from the axial (left) and equatorial (right) positions.

Table 325: The atomic coordinates of the model resulting from the chandelier core refinement of ZAA25A from the 18-month data collection.

Atom Label	Atom Type	Multiplicity	Fractional X Coordinate	Fractional Y Coordinate	Fractional Z Coordinate	Fractional Occupancy
C1	C	1	0.5897555	0.5000000	0.5830301	1
C2	C	1	0.5000000	0.4102445	0.5830301	1
C3	C	1	0.4102445	0.5000000	0.5830301	1
C4	C	1	0.5000000	0.5897555	0.5830301	1
C5	C	1	0.5897555	0.5000000	0.4169699	1
C6	C	1	0.5000000	0.4102445	0.4169699	1
C7	C	1	0.4102445	0.5000000	0.4169699	1
C8	C	1	0.5000000	0.5897555	0.4169699	1
C9	C	1	0.5897555	0.4102445	0.5000000	1
C10	C	1	0.4102445	0.4102445	0.5000000	1
C11	C	1	0.4102445	0.5897555	0.5000000	1
C12	C	1	0.5897555	0.5897555	0.5000000	1
C13	C	1	0.6192565	0.5000000	0.6103205	1
C14	C	1	0.5000000	0.3807435	0.6103205	1
C15	C	1	0.3807435	0.5000000	0.6103205	1
C16	C	1	0.5000000	0.6192565	0.6103205	1
C17	C	1	0.6192565	0.5000000	0.3896795	1
C18	C	1	0.5000000	0.3807435	0.3896795	1
C19	C	1	0.3807435	0.5000000	0.3896795	1
C20	C	1	0.5000000	0.6192565	0.3896795	1
C21	C	1	0.6192565	0.3807435	0.5000000	1
C22	C	1	0.3807435	0.3807435	0.5000000	1
C23	C	1	0.3807435	0.6192565	0.5000000	1
C24	C	1	0.6192565	0.6192565	0.5000000	1
O1	O	1	0.5412556	0.4587444	0.4738121	1
O2	O	1	0.5412556	0.4587444	0.5261879	1
O3	O	1	0.4587444	0.4587444	0.4738121	1
O4	O	1	0.4587444	0.4587444	0.5261879	1
O5	O	1	0.4587444	0.5412556	0.4738121	1
O6	O	1	0.4587444	0.5412556	0.5261879	1
O7	O	1	0.5412556	0.5412556	0.4738121	1
O8	O	1	0.5412556	0.5412556	0.5261879	1

O9	O	1	0.5943172	0.5000000	0.5499470	1
O10	O	1	0.5943172	0.4460073	0.5000000	1
O11	O	1	0.5943172	0.5000000	0.4500530	1
O12	O	1	0.5943172	0.5539927	0.5000000	1
O13	O	1	0.5000000	0.5943172	0.5499470	1
O14	O	1	0.5539927	0.5943172	0.5000000	1
O15	O	1	0.5000000	0.5943172	0.4500530	1
O16	O	1	0.4460073	0.5943172	0.5000000	1
O17	O	1	0.4056828	0.5000000	0.5499470	1
O18	O	1	0.4056828	0.5539927	0.5000000	1
O19	O	1	0.4056828	0.5000000	0.4500530	1
O20	O	1	0.4056828	0.4460073	0.5000000	1
O21	O	1	0.5000000	0.4056828	0.5499470	1
O22	O	1	0.4460073	0.4056828	0.5000000	1
O23	O	1	0.5000000	0.4056828	0.4500530	1
O24	O	1	0.5539927	0.4056828	0.5000000	1
O25	O	1	0.5539927	0.5000000	0.5872500	1
O26	O	1	0.5000000	0.5539927	0.5872500	1
O27	O	1	0.4460073	0.5000000	0.5872500	1
O28	O	1	0.5000000	0.4460073	0.5872500	1
O29	O	1	0.5539927	0.5000000	0.4127500	1
O30	O	1	0.5000000	0.4460073	0.4127500	1
O31	O	1	0.4460073	0.5000000	0.4127500	1
O32	O	1	0.5000000	0.5539927	0.4127500	1
Zr1	Zr	1	0.5663757	0.5000000	0.5000000	1
Zr2	Zr	1	0.5000000	0.5663757	0.5000000	1
Zr3	Zr	1	0.4336243	0.5000000	0.5000000	1
Zr4	Zr	1	0.5000000	0.4336243	0.5000000	1
Zr5	Zr	1	0.5000000	0.5000000	0.5614022	1
Zr6	Zr	1	0.5000000	0.5000000	0.4385978	1

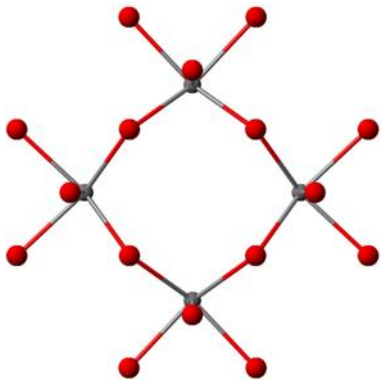

Figure 383: The tetrameric structure resulting from the chandelier core refinement of ZAA25A from the 18-month data collection.

Table 326: The atomic coordinates of the tetrameric phase of the chandelier core refinement of ZAA25A from the 18-month data collection.

Atom Label	Atom Type	Multiplicity	Fractional X Coordinate	Fractional Y Coordinate	Fractional Z Coordinate	Fractional Occupancy
O1	O	1	0.5143269	0.4856731	0.4714646	1
O2	O	1	0.4856731	0.4856731	0.5285354	1
O3	O	1	0.5143269	0.5143269	0.5285354	1
O4	O	1	0.4856731	0.5143269	0.4714646	1
O5	O	1	0.5000000	0.5278100	0.5479157	1
O6	O	1	0.5000000	0.4721900	0.5479157	1
O7	O	1	0.4721900	0.5000000	0.4520843	1
O8	O	1	0.5278100	0.5000000	0.4520843	1
O9	O	1	0.5143889	0.4601152	0.5000000	1
O10	O	1	0.4601152	0.4856111	0.5000000	1
O11	O	1	0.5398848	0.5143889	0.5000000	1
O12	O	1	0.4856111	0.5398848	0.5000000	1
O13	O	1	0.4601152	0.5143889	0.5000000	1
O14	O	1	0.5398848	0.4856111	0.5000000	1
O15	O	1	0.4856111	0.4601152	0.5000000	1
O16	O	1	0.5143889	0.5398848	0.5000000	1
O17	O	1	0.5143269	0.4856731	0.5285354	1
O18	O	1	0.4856731	0.4856731	0.4714646	1
O19	O	1	0.5143269	0.5143269	0.4714646	1
O20	O	1	0.4856731	0.5143269	0.5285354	1
O21	O	1	0.5000000	0.5278100	0.4520843	1
O22	O	1	0.5000000	0.4721900	0.4520843	1
O23	O	1	0.4721900	0.5000000	0.5479157	1
O24	O	1	0.5278100	0.5000000	0.5479157	1
Zr1	Zr	1	0.5000000	0.4754856	0.5000000	1
Zr2	Zr	1	0.4754856	0.5000000	0.5000000	1
Zr3	Zr	1	0.5245144	0.5000000	0.5000000	1
Zr4	Zr	1	0.5000000	0.5245144	0.5000000	1

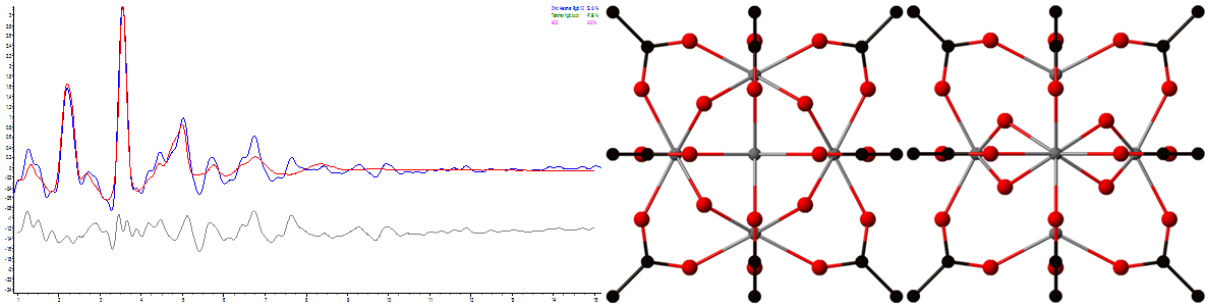

Figure 384: Observed and Calculated PDF from the chandelier core refinement of ZAA25C from the 18-month data collection and the resultant model viewed from the axial (left) and equatorial (right) positions.

Table 327: The atomic coordinates of the model resulting from the chandelier core refinement of ZAA25C from the 18-month data collection.

Atom Label	Atom Type	Multiplicity	Fractional X Coordinate	Fractional Y Coordinate	Fractional Z Coordinate	Fractional Occupancy
C1	C	1	0.5898947	0.5000000	0.5831589	1
C2	C	1	0.5000000	0.4101053	0.5831589	1
C3	C	1	0.4101053	0.5000000	0.5831589	1
C4	C	1	0.5000000	0.5898947	0.5831589	1
C5	C	1	0.5898947	0.5000000	0.4168411	1
C6	C	1	0.5000000	0.4101053	0.4168411	1
C7	C	1	0.4101053	0.5000000	0.4168411	1
C8	C	1	0.5000000	0.5898947	0.4168411	1
C9	C	1	0.5898947	0.4101053	0.5000000	1
C10	C	1	0.4101053	0.4101053	0.5000000	1
C11	C	1	0.4101053	0.5898947	0.5000000	1
C12	C	1	0.5898947	0.5898947	0.5000000	1
C13	C	1	0.6188292	0.5000000	0.6099253	1
C14	C	1	0.5000000	0.3811708	0.6099253	1
C15	C	1	0.3811708	0.5000000	0.6099253	1
C16	C	1	0.5000000	0.6188292	0.6099253	1
C17	C	1	0.6188292	0.5000000	0.3900747	1
C18	C	1	0.5000000	0.3811708	0.3900747	1
C19	C	1	0.3811708	0.5000000	0.3900747	1
C20	C	1	0.5000000	0.6188292	0.3900747	1
C21	C	1	0.6188292	0.3811708	0.5000000	1
C22	C	1	0.3811708	0.3811708	0.5000000	1
C23	C	1	0.3811708	0.6188292	0.5000000	1
C24	C	1	0.6188292	0.6188292	0.5000000	1
O1	O	1	0.5424078	0.4575922	0.4743067	1
O2	O	1	0.5424078	0.4575922	0.5256933	1
O3	O	1	0.4575922	0.4575922	0.4743067	1
O4	O	1	0.4575922	0.4575922	0.5256933	1
O5	O	1	0.4575922	0.5424078	0.4743067	1
O6	O	1	0.4575922	0.5424078	0.5256933	1
O7	O	1	0.5424078	0.5424078	0.4743067	1
O8	O	1	0.5424078	0.5424078	0.5256933	1

O9	O	1	0.5948328	0.5000000	0.5504678	1
O10	O	1	0.5948328	0.4454444	0.5000000	1
O11	O	1	0.5948328	0.5000000	0.4495322	1
O12	O	1	0.5948328	0.5545556	0.5000000	1
O13	O	1	0.5000000	0.5948328	0.5504678	1
O14	O	1	0.5545556	0.5948328	0.5000000	1
O15	O	1	0.5000000	0.5948328	0.4495322	1
O16	O	1	0.4454444	0.5948328	0.5000000	1
O17	O	1	0.4051672	0.5000000	0.5504678	1
O18	O	1	0.4051672	0.5545556	0.5000000	1
O19	O	1	0.4051672	0.5000000	0.4495322	1
O20	O	1	0.4051672	0.4454444	0.5000000	1
O21	O	1	0.5000000	0.4051672	0.5504678	1
O22	O	1	0.4454444	0.4051672	0.5000000	1
O23	O	1	0.5000000	0.4051672	0.4495322	1
O24	O	1	0.5545556	0.4051672	0.5000000	1
O25	O	1	0.5545556	0.5000000	0.587727	1
O26	O	1	0.5000000	0.5545556	0.587727	1
O27	O	1	0.4454444	0.5000000	0.587727	1
O28	O	1	0.5000000	0.4454444	0.587727	1
O29	O	1	0.5545556	0.5000000	0.412273	1
O30	O	1	0.5000000	0.4454444	0.412273	1
O31	O	1	0.4454444	0.5000000	0.412273	1
O32	O	1	0.5000000	0.5545556	0.412273	1
Zr1	Zr	1	0.5663835	0.5000000	0.5000000	1
Zr2	Zr	1	0.5000000	0.5663835	0.5000000	1
Zr3	Zr	1	0.4336165	0.5000000	0.5000000	1
Zr4	Zr	1	0.5000000	0.4336165	0.5000000	1
Zr5	Zr	1	0.5000000	0.5000000	0.5614094	1
Zr6	Zr	1	0.5000000	0.5000000	0.4385906	1

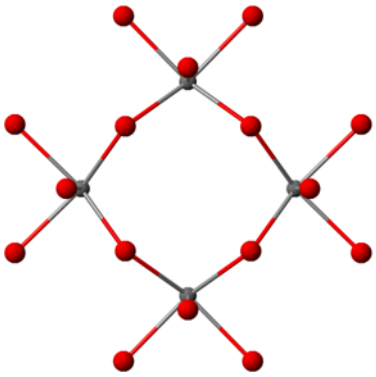

Figure 385: The tetrameric structure resulting from the chandelier core refinement of ZAA25C from the 18-month data collection.

Table 328: The atomic coordinates of the tetrameric phase of the chandelier core refinement of ZAA25C from the 18-month data collection.

Atom Label	Atom Type	Multiplicity	Fractional X Coordinate	Fractional Y Coordinate	Fractional Z Coordinate	Fractional Occupancy
O1	O	1	0.5143939	0.4856061	0.4723369	1
O2	O	1	0.4856061	0.4856061	0.5276631	1
O3	O	1	0.5143939	0.5143939	0.5276631	1
O4	O	1	0.4856061	0.5143939	0.4723369	1
O5	O	1	0.5000000	0.5279233	0.546399	1
O6	O	1	0.5000000	0.4720767	0.546399	1
O7	O	1	0.4720767	0.5000000	0.453601	1
O8	O	1	0.5279233	0.5000000	0.453601	1
O9	O	1	0.5147814	0.4602384	0.5000000	1
O10	O	1	0.4602384	0.4852186	0.5000000	1
O11	O	1	0.5397616	0.5147814	0.5000000	1
O12	O	1	0.4852186	0.5397616	0.5000000	1
O13	O	1	0.4602384	0.5147814	0.5000000	1
O14	O	1	0.5397616	0.4852186	0.5000000	1
O15	O	1	0.4852186	0.4602384	0.5000000	1
O16	O	1	0.5147814	0.5397616	0.5000000	1
O17	O	1	0.5143939	0.4856061	0.5276631	1
O18	O	1	0.4856061	0.4856061	0.4723369	1
O19	O	1	0.5143939	0.5143939	0.4723369	1
O20	O	1	0.4856061	0.5143939	0.5276631	1
O21	O	1	0.5000000	0.5279233	0.453601	1
O22	O	1	0.5000000	0.4720767	0.453601	1
O23	O	1	0.4720767	0.5000000	0.546399	1
O24	O	1	0.5279233	0.5000000	0.546399	1
Zr1	Zr	1	0.5000000	0.4753845	0.5000000	1
Zr2	Zr	1	0.4753845	0.5000000	0.5000000	1
Zr3	Zr	1	0.5246155	0.5000000	0.5000000	1
Zr4	Zr	1	0.5000000	0.5246155	0.5000000	1

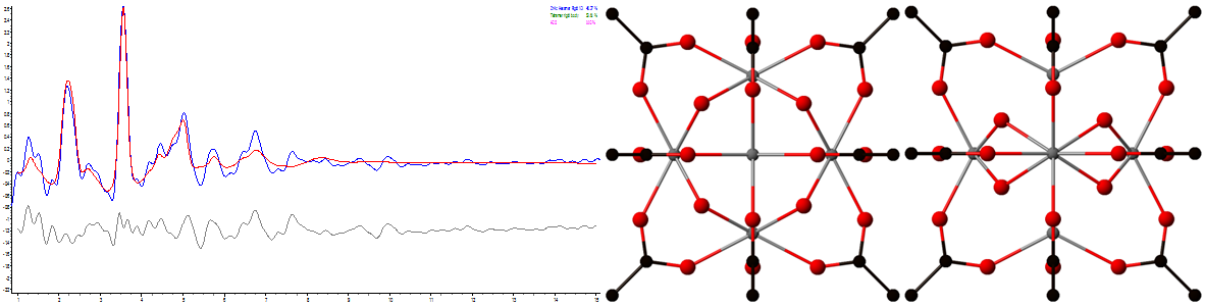

Figure 386: Observed and Calculated PDF from the chandelier core refinement of ZAA25I from the 18-month data collection and the resultant model viewed from the axial (left) and equatorial (right) positions.

Table 329: The atomic coordinates of the model resulting from the chandelier core refinement of ZAA25I from the 18-month data collection.

Atom Label	Atom Type	Multiplicity	Fractional X Coordinate	Fractional Y Coordinate	Fractional Z Coordinate	Fractional Occupancy
C1	C	1	0.590099	0.5000000	0.5833479	1
C2	C	1	0.5000000	0.409901	0.5833479	1
C3	C	1	0.409901	0.5000000	0.5833479	1
C4	C	1	0.5000000	0.590099	0.5833479	1
C5	C	1	0.590099	0.5000000	0.4166521	1
C6	C	1	0.5000000	0.409901	0.4166521	1
C7	C	1	0.409901	0.5000000	0.4166521	1
C8	C	1	0.5000000	0.590099	0.4166521	1
C9	C	1	0.590099	0.409901	0.5000000	1
C10	C	1	0.409901	0.409901	0.5000000	1
C11	C	1	0.409901	0.590099	0.5000000	1
C12	C	1	0.590099	0.590099	0.5000000	1
C13	C	1	0.6187114	0.5000000	0.6098163	1
C14	C	1	0.5000000	0.3812886	0.6098163	1
C15	C	1	0.3812886	0.5000000	0.6098163	1
C16	C	1	0.5000000	0.6187114	0.6098163	1
C17	C	1	0.6187114	0.5000000	0.3901837	1
C18	C	1	0.5000000	0.3812886	0.3901837	1
C19	C	1	0.3812886	0.5000000	0.3901837	1
C20	C	1	0.5000000	0.6187114	0.3901837	1
C21	C	1	0.6187114	0.3812886	0.5000000	1
C22	C	1	0.3812886	0.3812886	0.5000000	1
C23	C	1	0.3812886	0.6187114	0.5000000	1
C24	C	1	0.6187114	0.6187114	0.5000000	1
O1	O	1	0.5431123	0.4568877	0.474002	1
O2	O	1	0.5431123	0.4568877	0.525998	1
O3	O	1	0.4568877	0.4568877	0.474002	1
O4	O	1	0.4568877	0.4568877	0.525998	1
O5	O	1	0.4568877	0.5431123	0.474002	1
O6	O	1	0.4568877	0.5431123	0.525998	1
O7	O	1	0.5431123	0.5431123	0.474002	1
O8	O	1	0.5431123	0.5431123	0.525998	1

O9	O	1	0.5949803	0.5000000	0.5508227	1
O10	O	1	0.5949803	0.4450607	0.5000000	1
O11	O	1	0.5949803	0.5000000	0.4491773	1
O12	O	1	0.5949803	0.5549393	0.5000000	1
O13	O	1	0.5000000	0.5949803	0.5508227	1
O14	O	1	0.5549393	0.5949803	0.5000000	1
O15	O	1	0.5000000	0.5949803	0.4491773	1
O16	O	1	0.4450607	0.5949803	0.5000000	1
O17	O	1	0.4050197	0.5000000	0.5508227	1
O18	O	1	0.4050197	0.5549393	0.5000000	1
O19	O	1	0.4050197	0.5000000	0.4491773	1
O20	O	1	0.4050197	0.4450607	0.5000000	1
O21	O	1	0.5000000	0.4050197	0.5508227	1
O22	O	1	0.4450607	0.4050197	0.5000000	1
O23	O	1	0.5000000	0.4050197	0.4491773	1
O24	O	1	0.5549393	0.4050197	0.5000000	1
O25	O	1	0.5549393	0.5000000	0.5878634	1
O26	O	1	0.5000000	0.5549393	0.5878634	1
O27	O	1	0.4450607	0.5000000	0.5878634	1
O28	O	1	0.5000000	0.4450607	0.5878634	1
O29	O	1	0.5549393	0.5000000	0.4121366	1
O30	O	1	0.5000000	0.4450607	0.4121366	1
O31	O	1	0.4450607	0.5000000	0.4121366	1
O32	O	1	0.5000000	0.5549393	0.4121366	1
Zr1	Zr	1	0.5665342	0.5000000	0.5000000	1
Zr2	Zr	1	0.5000000	0.5665342	0.5000000	1
Zr3	Zr	1	0.4334658	0.5000000	0.5000000	1
Zr4	Zr	1	0.5000000	0.4334658	0.5000000	1
Zr5	Zr	1	0.5000000	0.5000000	0.5615488	1
Zr6	Zr	1	0.5000000	0.5000000	0.4384512	1

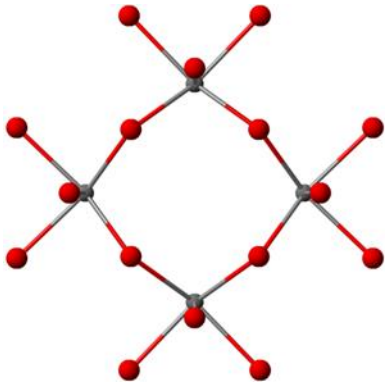

Figure 387: The tetrameric structure resulting from the chandelier core refinement of ZAA25I from the 18-month data collection.

Table 330: The atomic coordinates of the tetrameric phase of the chandelier core refinement of ZAA25I from the 18-month data collection.

Atom Label	Atom Type	Multiplicity	Fractional X Coordinate	Fractional Y Coordinate	Fractional Z Coordinate	Fractional Occupancy
O1	O	1	0.5143128	0.4856872	0.471698	1
O2	O	1	0.4856872	0.4856872	0.528302	1
O3	O	1	0.5143128	0.5143128	0.528302	1
O4	O	1	0.4856872	0.5143128	0.471698	1
O5	O	1	0.5000000	0.5280907	0.5465775	1
O6	O	1	0.5000000	0.4719093	0.5465775	1
O7	O	1	0.4719093	0.5000000	0.4534225	1
O8	O	1	0.5280907	0.5000000	0.4534225	1
O9	O	1	0.5146698	0.4601562	0.5000000	1
O10	O	1	0.4601562	0.4853302	0.5000000	1
O11	O	1	0.5398438	0.5146698	0.5000000	1
O12	O	1	0.4853302	0.5398438	0.5000000	1
O13	O	1	0.4601562	0.5146698	0.5000000	1
O14	O	1	0.5398438	0.4853302	0.5000000	1
O15	O	1	0.4853302	0.4601562	0.5000000	1
O16	O	1	0.5146698	0.5398438	0.5000000	1
O17	O	1	0.5143128	0.4856872	0.528302	1
O18	O	1	0.4856872	0.4856872	0.471698	1
O19	O	1	0.5143128	0.5143128	0.471698	1
O20	O	1	0.4856872	0.5143128	0.528302	1
O21	O	1	0.5000000	0.5280907	0.4534225	1
O22	O	1	0.5000000	0.4719093	0.4534225	1
O23	O	1	0.4719093	0.5000000	0.5465775	1
O24	O	1	0.5280907	0.5000000	0.5465775	1
Zr1	Zr	1	0.5000000	0.4754405	0.5000000	1
Zr2	Zr	1	0.4754405	0.5000000	0.5000000	1
Zr3	Zr	1	0.5245595	0.5000000	0.5000000	1
Zr4	Zr	1	0.5000000	0.5245595	0.5000000	1

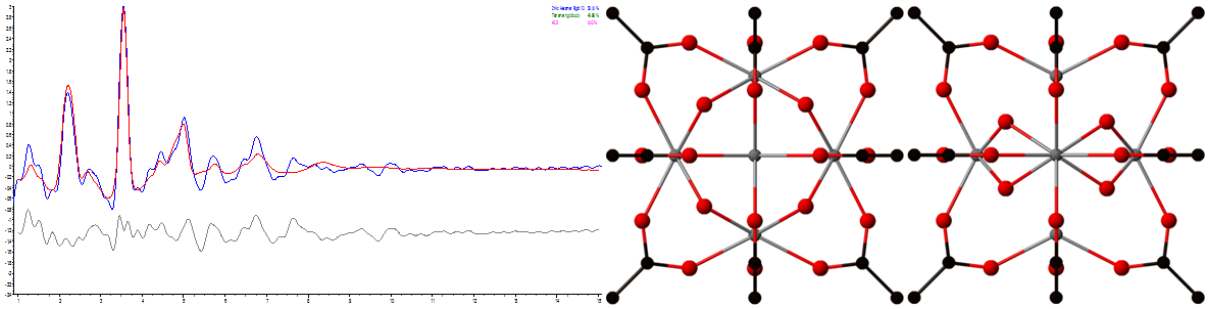

Figure 388: Observed and Calculated PDF from the chandelier core refinement of ZAA27A from the 18-month data collection and the resultant model viewed from the axial (left) and equatorial (right) positions.

Table 331: The atomic coordinates of the model resulting from the chandelier core refinement of ZAA27A from the 18-month data collection.

Atom Label	Atom Type	Multiplicity	Fractional X Coordinate	Fractional Y Coordinate	Fractional Z Coordinate	Fractional Occupancy
C1	C	1	0.5901257	0.5000000	0.5833725	1
C2	C	1	0.5000000	0.4098743	0.5833725	1
C3	C	1	0.4098743	0.5000000	0.5833725	1
C4	C	1	0.5000000	0.5901257	0.5833725	1
C5	C	1	0.5901257	0.5000000	0.4166275	1
C6	C	1	0.5000000	0.4098743	0.4166275	1
C7	C	1	0.4098743	0.5000000	0.4166275	1
C8	C	1	0.5000000	0.5901257	0.4166275	1
C9	C	1	0.5901257	0.4098743	0.5000000	1
C10	C	1	0.4098743	0.4098743	0.5000000	1
C11	C	1	0.4098743	0.5901257	0.5000000	1
C12	C	1	0.5901257	0.5901257	0.5000000	1
C13	C	1	0.6192476	0.5000000	0.6103123	1
C14	C	1	0.5000000	0.3807524	0.6103123	1
C15	C	1	0.3807524	0.5000000	0.6103123	1
C16	C	1	0.5000000	0.6192476	0.6103123	1
C17	C	1	0.6192476	0.5000000	0.3896877	1
C18	C	1	0.5000000	0.3807524	0.3896877	1
C19	C	1	0.3807524	0.5000000	0.3896877	1
C20	C	1	0.5000000	0.6192476	0.3896877	1
C21	C	1	0.6192476	0.3807524	0.5000000	1
C22	C	1	0.3807524	0.3807524	0.5000000	1
C23	C	1	0.3807524	0.6192476	0.5000000	1
C24	C	1	0.6192476	0.6192476	0.5000000	1
O1	O	1	0.5425433	0.4574567	0.474094	1
O2	O	1	0.5425433	0.4574567	0.525906	1
O3	O	1	0.4574567	0.4574567	0.474094	1
O4	O	1	0.4574567	0.4574567	0.525906	1
O5	O	1	0.4574567	0.5425433	0.474094	1
O6	O	1	0.4574567	0.5425433	0.525906	1
O7	O	1	0.5425433	0.5425433	0.474094	1
O8	O	1	0.5425433	0.5425433	0.525906	1

O9	O	1	0.5944926	0.5000000	0.5507601	1
O10	O	1	0.5944926	0.4451283	0.5000000	1
O11	O	1	0.5944926	0.5000000	0.4492399	1
O12	O	1	0.5944926	0.5548717	0.5000000	1
O13	O	1	0.5000000	0.5944926	0.5507601	1
O14	O	1	0.5548717	0.5944926	0.5000000	1
O15	O	1	0.5000000	0.5944926	0.4492399	1
O16	O	1	0.4451283	0.5944926	0.5000000	1
O17	O	1	0.4055074	0.5000000	0.5507601	1
O18	O	1	0.4055074	0.5548717	0.5000000	1
O19	O	1	0.4055074	0.5000000	0.4492399	1
O20	O	1	0.4055074	0.4451283	0.5000000	1
O21	O	1	0.5000000	0.4055074	0.5507601	1
O22	O	1	0.4451283	0.4055074	0.5000000	1
O23	O	1	0.5000000	0.4055074	0.4492399	1
O24	O	1	0.5548717	0.4055074	0.5000000	1
O25	O	1	0.5548717	0.5000000	0.5874122	1
O26	O	1	0.5000000	0.5548717	0.5874122	1
O27	O	1	0.4451283	0.5000000	0.5874122	1
O28	O	1	0.5000000	0.4451283	0.5874122	1
O29	O	1	0.5548717	0.5000000	0.4125878	1
O30	O	1	0.5000000	0.4451283	0.4125878	1
O31	O	1	0.4451283	0.5000000	0.4125878	1
O32	O	1	0.5000000	0.5548717	0.4125878	1
Zr1	Zr	1	0.5664756	0.5000000	0.5000000	1
Zr2	Zr	1	0.5000000	0.5664756	0.5000000	1
Zr3	Zr	1	0.4335244	0.5000000	0.5000000	1
Zr4	Zr	1	0.5000000	0.4335244	0.5000000	1
Zr5	Zr	1	0.5000000	0.5000000	0.5614946	1
Zr6	Zr	1	0.5000000	0.5000000	0.4385054	1

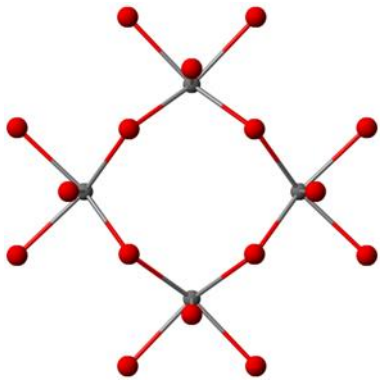

Figure 389: The tetrameric structure resulting from the chandelier core refinement of ZAA27A from the 18-month data collection.

Table 332: The atomic coordinates of the tetrameric phase of the chandelier core refinement of ZAA27A from the 18-month data collection.

Atom Label	Atom Type	Multiplicity	Fractional X Coordinate	Fractional Y Coordinate	Fractional Z Coordinate	Fractional Occupancy
O1	O	1	0.5143078	0.4856922	0.4716012	1
O2	O	1	0.4856922	0.4856922	0.5283988	1
O3	O	1	0.5143078	0.5143078	0.5283988	1
O4	O	1	0.4856922	0.5143078	0.4716012	1
O5	O	1	0.5000000	0.528152	0.5465663	1
O6	O	1	0.5000000	0.471848	0.5465663	1
O7	O	1	0.471848	0.5000000	0.4534337	1
O8	O	1	0.528152	0.5000000	0.4534337	1
O9	O	1	0.5146007	0.4601116	0.5000000	1
O10	O	1	0.4601116	0.4853993	0.5000000	1
O11	O	1	0.5398884	0.5146007	0.5000000	1
O12	O	1	0.4853993	0.5398884	0.5000000	1
O13	O	1	0.4601116	0.5146007	0.5000000	1
O14	O	1	0.5398884	0.4853993	0.5000000	1
O15	O	1	0.4853993	0.4601116	0.5000000	1
O16	O	1	0.5146007	0.5398884	0.5000000	1
O17	O	1	0.5143078	0.4856922	0.5283988	1
O18	O	1	0.4856922	0.4856922	0.4716012	1
O19	O	1	0.5143078	0.5143078	0.4716012	1
O20	O	1	0.4856922	0.5143078	0.5283988	1
O21	O	1	0.5000000	0.528152	0.4534337	1
O22	O	1	0.5000000	0.471848	0.4534337	1
O23	O	1	0.471848	0.5000000	0.5465663	1
O24	O	1	0.528152	0.5000000	0.5465663	1
Zr1	Zr	1	0.5000000	0.4754858	0.5000000	1
Zr2	Zr	1	0.4754858	0.5000000	0.5000000	1
Zr3	Zr	1	0.5245142	0.5000000	0.5000000	1
Zr4	Zr	1	0.5000000	0.5245142	0.5000000	1

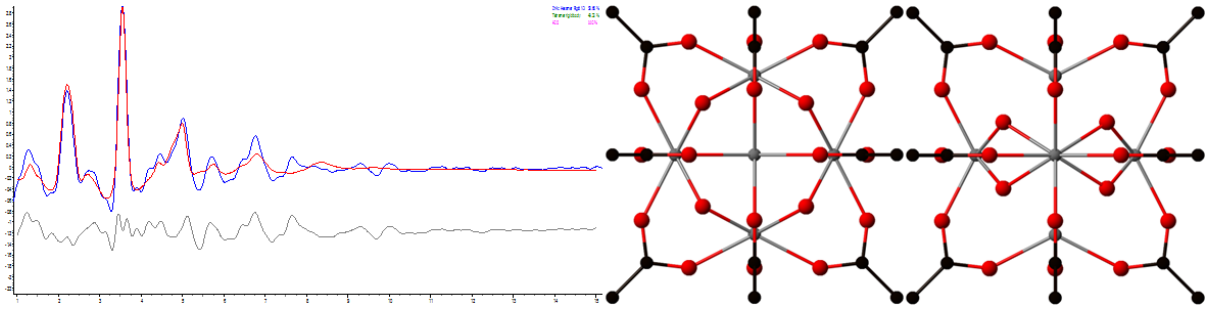

Figure 390: Observed and Calculated PDF from the chandelier core refinement of ZAA27C from the 18-month data collection and the resultant model viewed from the axial (left) and equatorial (right) positions.

Table 333: The atomic coordinates of the model resulting from the chandelier core refinement of ZAA27C from the 18-month data collection.

Atom Label	Atom Type	Multiplicity	Fractional X Coordinate	Fractional Y Coordinate	Fractional Z Coordinate	Fractional Occupancy
C1	C	1	0.5901489	0.5000000	0.5833941	1
C2	C	1	0.5000000	0.4098511	0.5833941	1
C3	C	1	0.4098511	0.5000000	0.5833941	1
C4	C	1	0.5000000	0.5901489	0.5833941	1
C5	C	1	0.5901489	0.5000000	0.4166059	1
C6	C	1	0.5000000	0.4098511	0.4166059	1
C7	C	1	0.4098511	0.5000000	0.4166059	1
C8	C	1	0.5000000	0.5901489	0.4166059	1
C9	C	1	0.5901489	0.4098511	0.5000000	1
C10	C	1	0.4098511	0.4098511	0.5000000	1
C11	C	1	0.4098511	0.5901489	0.5000000	1
C12	C	1	0.5901489	0.5901489	0.5000000	1
C13	C	1	0.6190695	0.5000000	0.6101476	1
C14	C	1	0.5000000	0.3809305	0.6101476	1
C15	C	1	0.3809305	0.5000000	0.6101476	1
C16	C	1	0.5000000	0.6190695	0.6101476	1
C17	C	1	0.6190695	0.5000000	0.3898524	1
C18	C	1	0.5000000	0.3809305	0.3898524	1
C19	C	1	0.3809305	0.5000000	0.3898524	1
C20	C	1	0.5000000	0.6190695	0.3898524	1
C21	C	1	0.6190695	0.3809305	0.5000000	1
C22	C	1	0.3809305	0.3809305	0.5000000	1
C23	C	1	0.3809305	0.6190695	0.5000000	1
C24	C	1	0.6190695	0.6190695	0.5000000	1
O1	O	1	0.5433221	0.4566779	0.474451	1
O2	O	1	0.5433221	0.4566779	0.525549	1
O3	O	1	0.4566779	0.4566779	0.474451	1
O4	O	1	0.4566779	0.4566779	0.525549	1
O5	O	1	0.4566779	0.5433221	0.474451	1
O6	O	1	0.4566779	0.5433221	0.525549	1
O7	O	1	0.5433221	0.5433221	0.474451	1
O8	O	1	0.5433221	0.5433221	0.525549	1

O9	O	1	0.594472	0.5000000	0.5507524	1
O10	O	1	0.594472	0.4451366	0.5000000	1
O11	O	1	0.594472	0.5000000	0.4492476	1
O12	O	1	0.594472	0.5548634	0.5000000	1
O13	O	1	0.5000000	0.594472	0.5507524	1
O14	O	1	0.5548634	0.594472	0.5000000	1
O15	O	1	0.5000000	0.594472	0.4492476	1
O16	O	1	0.4451366	0.594472	0.5000000	1
O17	O	1	0.405528	0.5000000	0.5507524	1
O18	O	1	0.405528	0.5548634	0.5000000	1
O19	O	1	0.405528	0.5000000	0.4492476	1
O20	O	1	0.405528	0.4451366	0.5000000	1
O21	O	1	0.5000000	0.405528	0.5507524	1
O22	O	1	0.4451366	0.405528	0.5000000	1
O23	O	1	0.5000000	0.405528	0.4492476	1
O24	O	1	0.5548634	0.405528	0.5000000	1
O25	O	1	0.5548634	0.5000000	0.5873932	1
O26	O	1	0.5000000	0.5548634	0.5873932	1
O27	O	1	0.4451366	0.5000000	0.5873932	1
O28	O	1	0.5000000	0.4451366	0.5873932	1
O29	O	1	0.5548634	0.5000000	0.4126068	1
O30	O	1	0.5000000	0.4451366	0.4126068	1
O31	O	1	0.4451366	0.5000000	0.4126068	1
O32	O	1	0.5000000	0.5548634	0.4126068	1
Zr1	Zr	1	0.5663781	0.5000000	0.5000000	1
Zr2	Zr	1	0.5000000	0.5663781	0.5000000	1
Zr3	Zr	1	0.4336219	0.5000000	0.5000000	1
Zr4	Zr	1	0.5000000	0.4336219	0.5000000	1
Zr5	Zr	1	0.5000000	0.5000000	0.5614044	1
Zr6	Zr	1	0.5000000	0.5000000	0.4385956	1

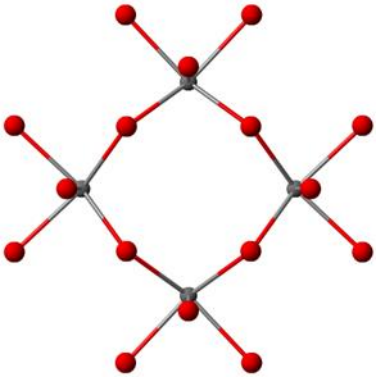

Figure 391: The tetrameric structure resulting from the chandelier core refinement of ZAA27C from the 18-month data collection.

Table 334: The atomic coordinates of the tetrameric phase of the chandelier core refinement of ZAA27C from the 18-month data collection.

Atom Label	Atom Type	Multiplicity	Fractional X Coordinate	Fractional Y Coordinate	Fractional Z Coordinate	Fractional Occupancy
O1	O	1	0.5142664	0.4857336	0.4715168	1
O2	O	1	0.4857336	0.4857336	0.5284832	1
O3	O	1	0.5142664	0.5142664	0.5284832	1
O4	O	1	0.4857336	0.5142664	0.4715168	1
O5	O	1	0.5000000	0.5279891	0.5466214	1
O6	O	1	0.5000000	0.4720109	0.5466214	1
O7	O	1	0.4720109	0.5000000	0.4533786	1
O8	O	1	0.5279891	0.5000000	0.4533786	1
O9	O	1	0.5144785	0.4600669	0.5000000	1
O10	O	1	0.4600669	0.4855215	0.5000000	1
O11	O	1	0.5399331	0.5144785	0.5000000	1
O12	O	1	0.4855215	0.5399331	0.5000000	1
O13	O	1	0.4600669	0.5144785	0.5000000	1
O14	O	1	0.5399331	0.4855215	0.5000000	1
O15	O	1	0.4855215	0.4600669	0.5000000	1
O16	O	1	0.5144785	0.5399331	0.5000000	1
O17	O	1	0.5142664	0.4857336	0.5284832	1
O18	O	1	0.4857336	0.4857336	0.4715168	1
O19	O	1	0.5142664	0.5142664	0.4715168	1
O20	O	1	0.4857336	0.5142664	0.5284832	1
O21	O	1	0.5000000	0.5279891	0.4533786	1
O22	O	1	0.5000000	0.4720109	0.4533786	1
O23	O	1	0.4720109	0.5000000	0.5466214	1
O24	O	1	0.5279891	0.5000000	0.5466214	1
Zr1	Zr	1	0.5000000	0.4754809	0.5000000	1
Zr2	Zr	1	0.4754809	0.5000000	0.5000000	1
Zr3	Zr	1	0.5245191	0.5000000	0.5000000	1
Zr4	Zr	1	0.5000000	0.5245191	0.5000000	1

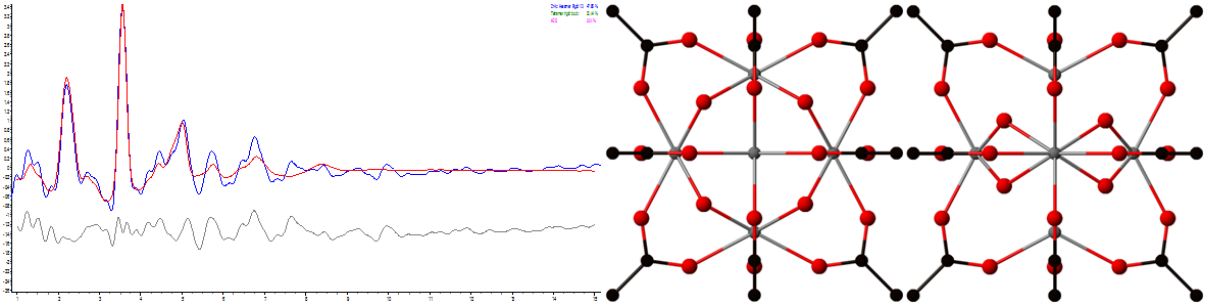

Figure 392: Observed and Calculated PDF from the chandelier core refinement of ZAA27I from the 18-month data collection and the resultant model viewed from the axial (left) and equatorial (right) positions.

Table 335: The atomic coordinates of the model resulting from the chandelier core refinement of ZAA27I from the 18-month data collection.

Atom Label	Atom Type	Multiplicity	Fractional X Coordinate	Fractional Y Coordinate	Fractional Z Coordinate	Fractional Occupancy
C1	C	1	0.5904682	0.5000000	0.5836894	1
C2	C	1	0.5000000	0.4095318	0.5836894	1
C3	C	1	0.4095318	0.5000000	0.5836894	1
C4	C	1	0.5000000	0.5904682	0.5836894	1
C5	C	1	0.5904682	0.5000000	0.4163106	1
C6	C	1	0.5000000	0.4095318	0.4163106	1
C7	C	1	0.4095318	0.5000000	0.4163106	1
C8	C	1	0.5000000	0.5904682	0.4163106	1
C9	C	1	0.5904682	0.4095318	0.5000000	1
C10	C	1	0.4095318	0.4095318	0.5000000	1
C11	C	1	0.4095318	0.5904682	0.5000000	1
C12	C	1	0.5904682	0.5904682	0.5000000	1
C13	C	1	0.6196272	0.5000000	0.6106635	1
C14	C	1	0.5000000	0.3803728	0.6106635	1
C15	C	1	0.3803728	0.5000000	0.6106635	1
C16	C	1	0.5000000	0.6196272	0.6106635	1
C17	C	1	0.6196272	0.5000000	0.3893365	1
C18	C	1	0.5000000	0.3803728	0.3893365	1
C19	C	1	0.3803728	0.5000000	0.3893365	1
C20	C	1	0.5000000	0.6196272	0.3893365	1
C21	C	1	0.6196272	0.3803728	0.5000000	1
C22	C	1	0.3803728	0.3803728	0.5000000	1
C23	C	1	0.3803728	0.6196272	0.5000000	1
C24	C	1	0.6196272	0.6196272	0.5000000	1
O1	O	1	0.5428478	0.4571522	0.4745182	1
O2	O	1	0.5428478	0.4571522	0.5254818	1
O3	O	1	0.4571522	0.4571522	0.4745182	1
O4	O	1	0.4571522	0.4571522	0.5254818	1
O5	O	1	0.4571522	0.5428478	0.4745182	1
O6	O	1	0.4571522	0.5428478	0.5254818	1
O7	O	1	0.5428478	0.5428478	0.4745182	1
O8	O	1	0.5428478	0.5428478	0.5254818	1

O9	O	1	0.5954009	0.5000000	0.5505762	1
O10	O	1	0.5954009	0.4453271	0.5000000	1
O11	O	1	0.5954009	0.5000000	0.4494238	1
O12	O	1	0.5954009	0.5546729	0.5000000	1
O13	O	1	0.5000000	0.5954009	0.5505762	1
O14	O	1	0.5546729	0.5954009	0.5000000	1
O15	O	1	0.5000000	0.5954009	0.4494238	1
O16	O	1	0.4453271	0.5954009	0.5000000	1
O17	O	1	0.4045991	0.5000000	0.5505762	1
O18	O	1	0.4045991	0.5546729	0.5000000	1
O19	O	1	0.4045991	0.5000000	0.4494238	1
O20	O	1	0.4045991	0.4453271	0.5000000	1
O21	O	1	0.5000000	0.4045991	0.5505762	1
O22	O	1	0.4453271	0.4045991	0.5000000	1
O23	O	1	0.5000000	0.4045991	0.4494238	1
O24	O	1	0.5546729	0.4045991	0.5000000	1
O25	O	1	0.5546729	0.5000000	0.5882525	1
O26	O	1	0.5000000	0.5546729	0.5882525	1
O27	O	1	0.4453271	0.5000000	0.5882525	1
O28	O	1	0.5000000	0.4453271	0.5882525	1
O29	O	1	0.5546729	0.5000000	0.4117475	1
O30	O	1	0.5000000	0.4453271	0.4117475	1
O31	O	1	0.4453271	0.5000000	0.4117475	1
O32	O	1	0.5000000	0.5546729	0.4117475	1
Zr1	Zr	1	0.5664572	0.5000000	0.5000000	1
Zr2	Zr	1	0.5000000	0.5664572	0.5000000	1
Zr3	Zr	1	0.4335428	0.5000000	0.5000000	1
Zr4	Zr	1	0.5000000	0.4335428	0.5000000	1
Zr5	Zr	1	0.5000000	0.5000000	0.5614776	1
Zr6	Zr	1	0.5000000	0.5000000	0.4385224	1

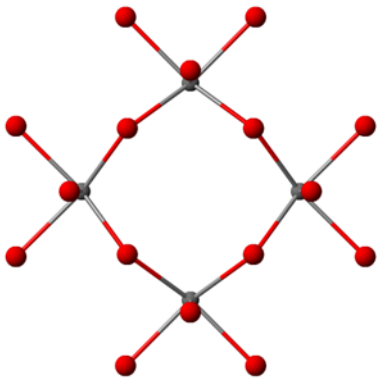

Figure 393: The tetrameric structure resulting from the chandelier core refinement of ZAA27I from the 18-month data collection.

Table 336: The atomic coordinates of the tetrameric phase of the chandelier core refinement of ZAA27I from the 18-month data collection.

Atom Label	Atom Type	Multiplicity	Fractional X Coordinate	Fractional Y Coordinate	Fractional Z Coordinate	Fractional Occupancy
O1	O	1	0.5143648	0.4856352	0.4725116	1
O2	O	1	0.4856352	0.4856352	0.5274884	1
O3	O	1	0.5143648	0.5143648	0.5274884	1
O4	O	1	0.4856352	0.5143648	0.4725116	1
O5	O	1	0.5000000	0.5275339	0.546851	1
O6	O	1	0.5000000	0.4724661	0.546851	1
O7	O	1	0.4724661	0.5000000	0.453149	1
O8	O	1	0.5275339	0.5000000	0.453149	1
O9	O	1	0.514831	0.460241	0.5000000	1
O10	O	1	0.460241	0.485169	0.5000000	1
O11	O	1	0.539759	0.514831	0.5000000	1
O12	O	1	0.485169	0.539759	0.5000000	1
O13	O	1	0.460241	0.514831	0.5000000	1
O14	O	1	0.539759	0.485169	0.5000000	1
O15	O	1	0.485169	0.460241	0.5000000	1
O16	O	1	0.514831	0.539759	0.5000000	1
O17	O	1	0.5143648	0.4856352	0.5274884	1
O18	O	1	0.4856352	0.4856352	0.4725116	1
O19	O	1	0.5143648	0.5143648	0.4725116	1
O20	O	1	0.4856352	0.5143648	0.5274884	1
O21	O	1	0.5000000	0.5275339	0.453149	1
O22	O	1	0.5000000	0.4724661	0.453149	1
O23	O	1	0.4724661	0.5000000	0.546851	1
O24	O	1	0.5275339	0.5000000	0.546851	1
Zr1	Zr	1	0.5000000	0.47521	0.5000000	1
Zr2	Zr	1	0.47521	0.5000000	0.5000000	1
Zr3	Zr	1	0.52479	0.5000000	0.5000000	1
Zr4	Zr	1	0.5000000	0.52479	0.5000000	1

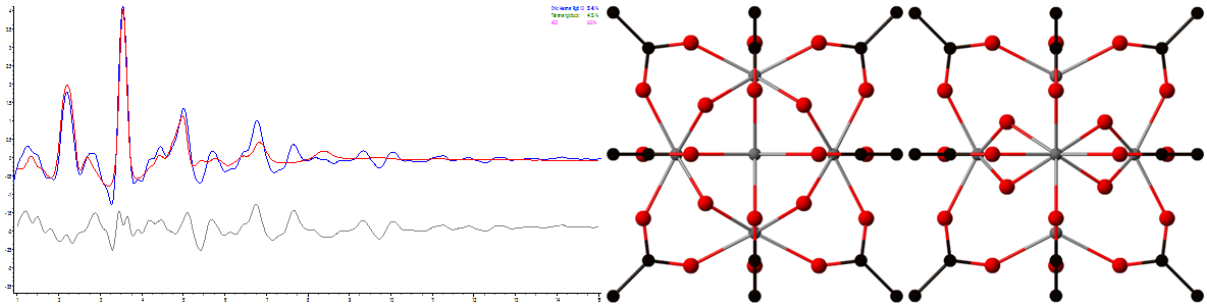

Figure 394: Observed and Calculated PDF from the chandelier core refinement of ZAA28A from the 18-month data collection and the resultant model viewed from the axial (left) and equatorial (right) positions.

Table 337: The atomic coordinates of the model resulting from the chandelier core refinement of ZAA28A from the 18-month data collection.

Atom Label	Atom Type	Multiplicity	Fractional X Coordinate	Fractional Y Coordinate	Fractional Z Coordinate	Fractional Occupancy
C1	C	1	0.5899761	0.5000000	0.5832341	1
C2	C	1	0.5000000	0.4100239	0.5832341	1
C3	C	1	0.4100239	0.5000000	0.5832341	1
C4	C	1	0.5000000	0.5899761	0.5832341	1
C5	C	1	0.5899761	0.5000000	0.4167659	1
C6	C	1	0.5000000	0.4100239	0.4167659	1
C7	C	1	0.4100239	0.5000000	0.4167659	1
C8	C	1	0.5000000	0.5899761	0.4167659	1
C9	C	1	0.5899761	0.4100239	0.5000000	1
C10	C	1	0.4100239	0.4100239	0.5000000	1
C11	C	1	0.4100239	0.5899761	0.5000000	1
C12	C	1	0.5899761	0.5899761	0.5000000	1
C13	C	1	0.61997	0.5000000	0.6109806	1
C14	C	1	0.5000000	0.38003	0.6109806	1
C15	C	1	0.38003	0.5000000	0.6109806	1
C16	C	1	0.5000000	0.61997	0.6109806	1
C17	C	1	0.61997	0.5000000	0.3890194	1
C18	C	1	0.5000000	0.38003	0.3890194	1
C19	C	1	0.38003	0.5000000	0.3890194	1
C20	C	1	0.5000000	0.61997	0.3890194	1
C21	C	1	0.61997	0.38003	0.5000000	1
C22	C	1	0.38003	0.38003	0.5000000	1
C23	C	1	0.38003	0.61997	0.5000000	1
C24	C	1	0.61997	0.61997	0.5000000	1
O1	O	1	0.5416467	0.4583533	0.4746614	1
O2	O	1	0.5416467	0.4583533	0.5253386	1
O3	O	1	0.4583533	0.4583533	0.4746614	1
O4	O	1	0.4583533	0.4583533	0.5253386	1
O5	O	1	0.4583533	0.5416467	0.4746614	1
O6	O	1	0.4583533	0.5416467	0.5253386	1
O7	O	1	0.5416467	0.5416467	0.4746614	1
O8	O	1	0.5416467	0.5416467	0.5253386	1

O9	O	1	0.5943671	0.5000000	0.5501597	1
O10	O	1	0.5943671	0.4457774	0.5000000	1
O11	O	1	0.5943671	0.5000000	0.4498403	1
O12	O	1	0.5943671	0.5542226	0.5000000	1
O13	O	1	0.5000000	0.5943671	0.5501597	1
O14	O	1	0.5542226	0.5943671	0.5000000	1
O15	O	1	0.5000000	0.5943671	0.4498403	1
O16	O	1	0.4457774	0.5943671	0.5000000	1
O17	O	1	0.4056329	0.5000000	0.5501597	1
O18	O	1	0.4056329	0.5542226	0.5000000	1
O19	O	1	0.4056329	0.5000000	0.4498403	1
O20	O	1	0.4056329	0.4457774	0.5000000	1
O21	O	1	0.5000000	0.4056329	0.5501597	1
O22	O	1	0.4457774	0.4056329	0.5000000	1
O23	O	1	0.5000000	0.4056329	0.4498403	1
O24	O	1	0.5542226	0.4056329	0.5000000	1
O25	O	1	0.5542226	0.5000000	0.5872961	1
O26	O	1	0.5000000	0.5542226	0.5872961	1
O27	O	1	0.4457774	0.5000000	0.5872961	1
O28	O	1	0.5000000	0.4457774	0.5872961	1
O29	O	1	0.5542226	0.5000000	0.4127039	1
O30	O	1	0.5000000	0.4457774	0.4127039	1
O31	O	1	0.4457774	0.5000000	0.4127039	1
O32	O	1	0.5000000	0.5542226	0.4127039	1
Zr1	Zr	1	0.5664916	0.5000000	0.5000000	1
Zr2	Zr	1	0.5000000	0.5664916	0.5000000	1
Zr3	Zr	1	0.4335084	0.5000000	0.5000000	1
Zr4	Zr	1	0.5000000	0.4335084	0.5000000	1
Zr5	Zr	1	0.5000000	0.5000000	0.5615094	1
Zr6	Zr	1	0.5000000	0.5000000	0.4384906	1

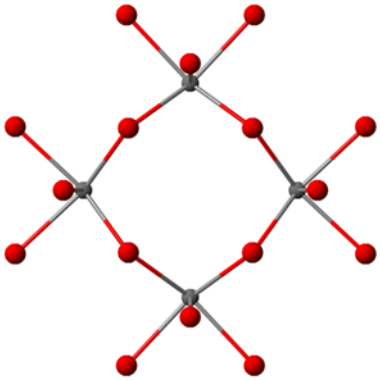

Figure 395: The tetrameric structure resulting from the chandelier core refinement of ZAA28A from the 18-month data collection.

Table 338: The atomic coordinates of the tetrameric phase of the chandelier core refinement of ZAA28A from the 18-month data collection.

Atom Label	Atom Type	Multiplicity	Fractional X Coordinate	Fractional Y Coordinate	Fractional Z Coordinate	Fractional Occupancy
O1	O	1	0.5142359	0.4857641	0.4742409	1
O2	O	1	0.4857641	0.4857641	0.5257591	1
O3	O	1	0.5142359	0.5142359	0.5257591	1
O4	O	1	0.4857641	0.5142359	0.4742409	1
O5	O	1	0.5000000	0.5290722	0.546617	1
O6	O	1	0.5000000	0.4709278	0.546617	1
O7	O	1	0.4709278	0.5000000	0.453383	1
O8	O	1	0.5290722	0.5000000	0.453383	1
O9	O	1	0.5145732	0.4599158	0.5000000	1
O10	O	1	0.4599158	0.4854268	0.5000000	1
O11	O	1	0.5400842	0.5145732	0.5000000	1
O12	O	1	0.4854268	0.5400842	0.5000000	1
O13	O	1	0.4599158	0.5145732	0.5000000	1
O14	O	1	0.5400842	0.4854268	0.5000000	1
O15	O	1	0.4854268	0.4599158	0.5000000	1
O16	O	1	0.5145732	0.5400842	0.5000000	1
O17	O	1	0.5142359	0.4857641	0.5257591	1
O18	O	1	0.4857641	0.4857641	0.4742409	1
O19	O	1	0.5142359	0.5142359	0.4742409	1
O20	O	1	0.4857641	0.5142359	0.5257591	1
O21	O	1	0.5000000	0.5290722	0.453383	1
O22	O	1	0.5000000	0.4709278	0.453383	1
O23	O	1	0.4709278	0.5000000	0.546617	1
O24	O	1	0.5290722	0.5000000	0.546617	1
Zr1	Zr	1	0.5000000	0.4755093	0.5000000	1
Zr2	Zr	1	0.4755093	0.5000000	0.5000000	1
Zr3	Zr	1	0.5244907	0.5000000	0.5000000	1
Zr4	Zr	1	0.5000000	0.5244907	0.5000000	1

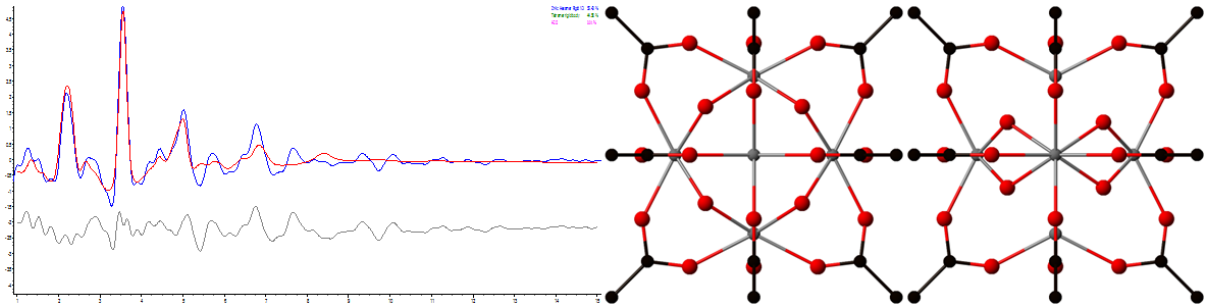

Figure 396: Observed and Calculated PDF from the chandelier core refinement of ZAA28C from the 18-month data collection and the resultant model viewed from the axial (left) and equatorial (right) positions.

Table 339: The atomic coordinates of the model resulting from the chandelier core refinement of ZAA28C from the 18-month data collection.

Atom Label	Atom Type	Multiplicity	Fractional X Coordinate	Fractional Y Coordinate	Fractional Z Coordinate	Fractional Occupancy
C1	C	1	0.5899239	0.5000000	0.5831859	1
C2	C	1	0.5000000	0.4100761	0.5831859	1
C3	C	1	0.4100761	0.5000000	0.5831859	1
C4	C	1	0.5000000	0.5899239	0.5831859	1
C5	C	1	0.5899239	0.5000000	0.4168141	1
C6	C	1	0.5000000	0.4100761	0.4168141	1
C7	C	1	0.4100761	0.5000000	0.4168141	1
C8	C	1	0.5000000	0.5899239	0.4168141	1
C9	C	1	0.5899239	0.4100761	0.5000000	1
C10	C	1	0.4100761	0.4100761	0.5000000	1
C11	C	1	0.4100761	0.5899239	0.5000000	1
C12	C	1	0.5899239	0.5899239	0.5000000	1
C13	C	1	0.6202374	0.5000000	0.6112279	1
C14	C	1	0.5000000	0.3797626	0.6112279	1
C15	C	1	0.3797626	0.5000000	0.6112279	1
C16	C	1	0.5000000	0.6202374	0.6112279	1
C17	C	1	0.6202374	0.5000000	0.3887721	1
C18	C	1	0.5000000	0.3797626	0.3887721	1
C19	C	1	0.3797626	0.5000000	0.3887721	1
C20	C	1	0.5000000	0.6202374	0.3887721	1
C21	C	1	0.6202374	0.3797626	0.5000000	1
C22	C	1	0.3797626	0.3797626	0.5000000	1
C23	C	1	0.3797626	0.6202374	0.5000000	1
C24	C	1	0.6202374	0.6202374	0.5000000	1
O1	O	1	0.5407696	0.4592304	0.4744576	1
O2	O	1	0.5407696	0.4592304	0.5255424	1
O3	O	1	0.4592304	0.4592304	0.4744576	1
O4	O	1	0.4592304	0.4592304	0.5255424	1
O5	O	1	0.4592304	0.5407696	0.4744576	1
O6	O	1	0.4592304	0.5407696	0.5255424	1
O7	O	1	0.5407696	0.5407696	0.4744576	1
O8	O	1	0.5407696	0.5407696	0.5255424	1

O9	O	1	0.5943557	0.5000000	0.5500657	1
O10	O	1	0.5943557	0.4458789	0.5000000	1
O11	O	1	0.5943557	0.5000000	0.4499343	1
O12	O	1	0.5943557	0.5541211	0.5000000	1
O13	O	1	0.5000000	0.5943557	0.5500657	1
O14	O	1	0.5541211	0.5943557	0.5000000	1
O15	O	1	0.5000000	0.5943557	0.4499343	1
O16	O	1	0.4458789	0.5943557	0.5000000	1
O17	O	1	0.4056443	0.5000000	0.5500657	1
O18	O	1	0.4056443	0.5541211	0.5000000	1
O19	O	1	0.4056443	0.5000000	0.4499343	1
O20	O	1	0.4056443	0.4458789	0.5000000	1
O21	O	1	0.5000000	0.4056443	0.5500657	1
O22	O	1	0.4458789	0.4056443	0.5000000	1
O23	O	1	0.5000000	0.4056443	0.4499343	1
O24	O	1	0.5541211	0.4056443	0.5000000	1
O25	O	1	0.5541211	0.5000000	0.5872856	1
O26	O	1	0.5000000	0.5541211	0.5872856	1
O27	O	1	0.4458789	0.5000000	0.5872856	1
O28	O	1	0.5000000	0.4458789	0.5872856	1
O29	O	1	0.5541211	0.5000000	0.4127144	1
O30	O	1	0.5000000	0.4458789	0.4127144	1
O31	O	1	0.4458789	0.5000000	0.4127144	1
O32	O	1	0.5000000	0.5541211	0.4127144	1
Zr1	Zr	1	0.566651	0.5000000	0.5000000	1
Zr2	Zr	1	0.5000000	0.566651	0.5000000	1
Zr3	Zr	1	0.433349	0.5000000	0.5000000	1
Zr4	Zr	1	0.5000000	0.433349	0.5000000	1
Zr5	Zr	1	0.5000000	0.5000000	0.5616568	1
Zr6	Zr	1	0.5000000	0.5000000	0.4383432	1

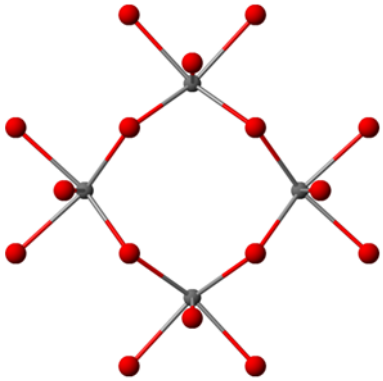

Figure 397: The tetrameric structure resulting from the chandelier core refinement of ZAA28C from the 18-month data collection.

Table 340: The atomic coordinates of the tetrameric phase of the chandelier core refinement of ZAA28C from the 18-month data collection.

Atom Label	Atom Type	Multiplicity	Fractional X Coordinate	Fractional Y Coordinate	Fractional Z Coordinate	Fractional Occupancy
O1	O	1	0.5143275	0.4856725	0.4739924	1
O2	O	1	0.4856725	0.4856725	0.5260076	1
O3	O	1	0.5143275	0.5143275	0.5260076	1
O4	O	1	0.4856725	0.5143275	0.4739924	1
O5	O	1	0.5000000	0.5291386	0.5471056	1
O6	O	1	0.5000000	0.4708614	0.5471056	1
O7	O	1	0.4708614	0.5000000	0.4528944	1
O8	O	1	0.5291386	0.5000000	0.4528944	1
O9	O	1	0.514383	0.4598657	0.5000000	1
O10	O	1	0.4598657	0.485617	0.5000000	1
O11	O	1	0.5401343	0.514383	0.5000000	1
O12	O	1	0.485617	0.5401343	0.5000000	1
O13	O	1	0.4598657	0.514383	0.5000000	1
O14	O	1	0.5401343	0.485617	0.5000000	1
O15	O	1	0.485617	0.4598657	0.5000000	1
O16	O	1	0.514383	0.5401343	0.5000000	1
O17	O	1	0.5143275	0.4856725	0.5260076	1
O18	O	1	0.4856725	0.4856725	0.4739924	1
O19	O	1	0.5143275	0.5143275	0.4739924	1
O20	O	1	0.4856725	0.5143275	0.5260076	1
O21	O	1	0.5000000	0.5291386	0.4528944	1
O22	O	1	0.5000000	0.4708614	0.4528944	1
O23	O	1	0.4708614	0.5000000	0.5471056	1
O24	O	1	0.5291386	0.5000000	0.5471056	1
Zr1	Zr	1	0.5000000	0.4755467	0.5000000	1
Zr2	Zr	1	0.4755467	0.5000000	0.5000000	1
Zr3	Zr	1	0.5244533	0.5000000	0.5000000	1
Zr4	Zr	1	0.5000000	0.5244533	0.5000000	1

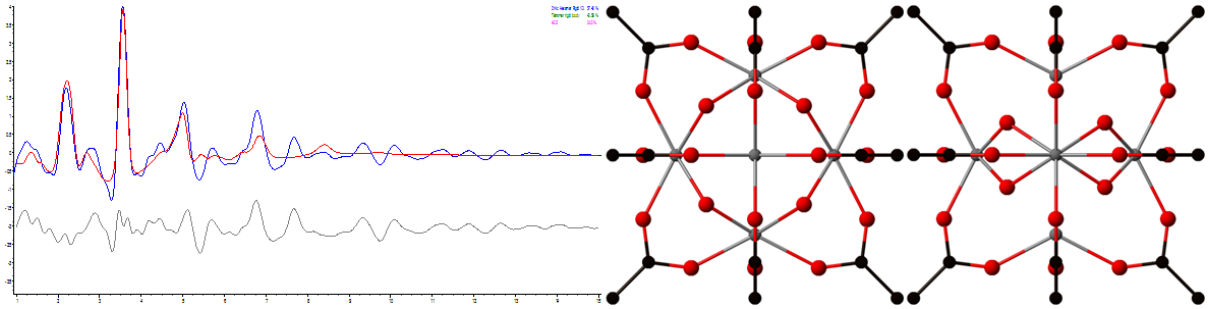

Figure 398: Observed and Calculated PDF from the chandelier core refinement of ZAA28I from the 18-month data collection and the resultant model viewed from the axial (left) and equatorial (right) positions.

Table 341: The atomic coordinates of the model resulting from the chandelier core refinement of ZAA28I from the 18-month data collection.

Atom Label	Atom Type	Multiplicity	Fractional X Coordinate	Fractional Y Coordinate	Fractional Z Coordinate	Fractional Occupancy
C1	C	1	0.5899277	0.5000000	0.5831894	1
C2	C	1	0.5000000	0.4100723	0.5831894	1
C3	C	1	0.4100723	0.5000000	0.5831894	1
C4	C	1	0.5000000	0.5899277	0.5831894	1
C5	C	1	0.5899277	0.5000000	0.4168106	1
C6	C	1	0.5000000	0.4100723	0.4168106	1
C7	C	1	0.4100723	0.5000000	0.4168106	1
C8	C	1	0.5000000	0.5899277	0.4168106	1
C9	C	1	0.5899277	0.4100723	0.5000000	1
C10	C	1	0.4100723	0.4100723	0.5000000	1
C11	C	1	0.4100723	0.5899277	0.5000000	1
C12	C	1	0.5899277	0.5899277	0.5000000	1
C13	C	1	0.6201604	0.5000000	0.6111567	1
C14	C	1	0.5000000	0.3798396	0.6111567	1
C15	C	1	0.3798396	0.5000000	0.6111567	1
C16	C	1	0.5000000	0.6201604	0.6111567	1
C17	C	1	0.6201604	0.5000000	0.3888433	1
C18	C	1	0.5000000	0.3798396	0.3888433	1
C19	C	1	0.3798396	0.5000000	0.3888433	1
C20	C	1	0.5000000	0.6201604	0.3888433	1
C21	C	1	0.6201604	0.3798396	0.5000000	1
C22	C	1	0.3798396	0.3798396	0.5000000	1
C23	C	1	0.3798396	0.6201604	0.5000000	1
C24	C	1	0.6201604	0.6201604	0.5000000	1
O1	O	1	0.5413242	0.4586758	0.4749006	1
O2	O	1	0.5413242	0.4586758	0.5250994	1
O3	O	1	0.4586758	0.4586758	0.4749006	1
O4	O	1	0.4586758	0.4586758	0.5250994	1
O5	O	1	0.4586758	0.5413242	0.4749006	1
O6	O	1	0.4586758	0.5413242	0.5250994	1
O7	O	1	0.5413242	0.5413242	0.4749006	1
O8	O	1	0.5413242	0.5413242	0.5250994	1

O9	O	1	0.5945797	0.5000000	0.549814	1
O10	O	1	0.5945797	0.4461511	0.5000000	1
O11	O	1	0.5945797	0.5000000	0.450186	1
O12	O	1	0.5945797	0.5538489	0.5000000	1
O13	O	1	0.5000000	0.5945797	0.549814	1
O14	O	1	0.5538489	0.5945797	0.5000000	1
O15	O	1	0.5000000	0.5945797	0.450186	1
O16	O	1	0.4461511	0.5945797	0.5000000	1
O17	O	1	0.4054203	0.5000000	0.549814	1
O18	O	1	0.4054203	0.5538489	0.5000000	1
O19	O	1	0.4054203	0.5000000	0.450186	1
O20	O	1	0.4054203	0.4461511	0.5000000	1
O21	O	1	0.5000000	0.4054203	0.549814	1
O22	O	1	0.4461511	0.4054203	0.5000000	1
O23	O	1	0.5000000	0.4054203	0.450186	1
O24	O	1	0.5538489	0.4054203	0.5000000	1
O25	O	1	0.5538489	0.5000000	0.5874928	1
O26	O	1	0.5000000	0.5538489	0.5874928	1
O27	O	1	0.4461511	0.5000000	0.5874928	1
O28	O	1	0.5000000	0.4461511	0.5874928	1
O29	O	1	0.5538489	0.5000000	0.4125072	1
O30	O	1	0.5000000	0.4461511	0.4125072	1
O31	O	1	0.4461511	0.5000000	0.4125072	1
O32	O	1	0.5000000	0.5538489	0.4125072	1
Zr1	Zr	1	0.5667892	0.5000000	0.5000000	1
Zr2	Zr	1	0.5000000	0.5667892	0.5000000	1
Zr3	Zr	1	0.4332108	0.5000000	0.5000000	1
Zr4	Zr	1	0.5000000	0.4332108	0.5000000	1
Zr5	Zr	1	0.5000000	0.5000000	0.5617847	1
Zr6	Zr	1	0.5000000	0.5000000	0.4382153	1

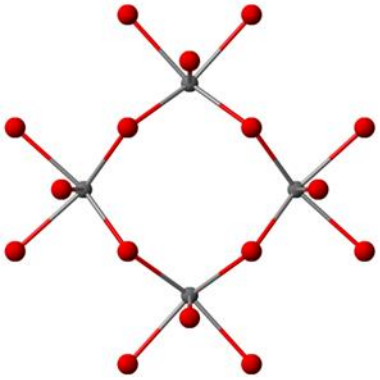

Figure 399: The tetrameric structure resulting from the chandelier core refinement of ZAA28I from the 18-month data collection.

Table 342: The atomic coordinates of the tetrameric phase of the chandelier core refinement of ZAA28I from the 18-month data collection.

Atom Label	Atom Type	Multiplicity	Fractional X Coordinate	Fractional Y Coordinate	Fractional Z Coordinate	Fractional Occupancy
O1	O	1	0.514272	0.485728	0.4744217	1
O2	O	1	0.485728	0.485728	0.5255783	1
O3	O	1	0.514272	0.514272	0.5255783	1
O4	O	1	0.485728	0.514272	0.4744217	1
O5	O	1	0.5000000	0.5295939	0.5480745	1
O6	O	1	0.5000000	0.4704061	0.5480745	1
O7	O	1	0.4704061	0.5000000	0.4519255	1
O8	O	1	0.5295939	0.5000000	0.4519255	1
O9	O	1	0.5142583	0.4597234	0.5000000	1
O10	O	1	0.4597234	0.4857417	0.5000000	1
O11	O	1	0.5402766	0.5142583	0.5000000	1
O12	O	1	0.4857417	0.5402766	0.5000000	1
O13	O	1	0.4597234	0.5142583	0.5000000	1
O14	O	1	0.5402766	0.4857417	0.5000000	1
O15	O	1	0.4857417	0.4597234	0.5000000	1
O16	O	1	0.5142583	0.5402766	0.5000000	1
O17	O	1	0.514272	0.485728	0.5255783	1
O18	O	1	0.485728	0.485728	0.4744217	1
O19	O	1	0.514272	0.514272	0.4744217	1
O20	O	1	0.485728	0.514272	0.5255783	1
O21	O	1	0.5000000	0.5295939	0.4519255	1
O22	O	1	0.5000000	0.4704061	0.4519255	1
O23	O	1	0.4704061	0.5000000	0.5480745	1
O24	O	1	0.5295939	0.5000000	0.5480745	1
Zr1	Zr	1	0.5000000	0.4755033	0.5000000	1
Zr2	Zr	1	0.4755033	0.5000000	0.5000000	1
Zr3	Zr	1	0.5244967	0.5000000	0.5000000	1
Zr4	Zr	1	0.5000000	0.5244967	0.5000000	1

10.6 Model Compound Analysis

Table 343:Percentage yields from the synthesis of a model compound umbite.

	Sep-19 Ambient Yield (%)	Jan-20 Ambient Yield (%)	Jan-20 Chilled Yield (%)	Sep-20 Ambient Yield (%)	Sep-20 Chilled Yield (%)	Sep-20 Incubated Yield (%)	April-21 Ambient Yield (%)	April-21 Chilled Yield (%)	April-21 Incubated Yield (%)
ZAA1	77.53	78.33	80.95	77.83	73.77	78.30	83.05	78.21	76.07
ZAA3	76.15	76.65	82.78	81.68	80.87	74.91	82.37	83.79	82.91
ZAA4	73.34	75.83	72.21	71.67	78.48	73.05	80.20	67.08	71.22
ZAA6	67.45	65.27	75.54	72.10	72.92	66.47	72.09	74.01	69.55
ZAA7	63.57	63.55	73.55	65.92	65.65	73.61	66.30	69.36	60.49
ZAA9	64.71	65.05	67.17	69.96	67.91	69.00	70.09	61.10	72.32
ZAA10	72.88	75.20	77.58	76.28	79.31	78.55	78.89	76.78	76.77
ZAA12	76.34	73.42	67.58	78.09	81.01	74.93	78.59	80.77	79.02
ZAA13	71.37	71.31	68.15	67.87	66.32	66.33	79.60	70.91	66.81
ZAA15	67.11	73.10	69.64	72.95	70.84	69.92	72.31	70.34	67.48
ZAA16	65.88	61.27	63.92	66.50	68.56	60.40	59.88	63.70	58.41
ZAA18	67.51	63.97	64.71	64.95	61.47	59.75	64.93	65.30	63.52
ZAA19	62.40	76.01	78.42	77.89	75.71	78.12	78.66	80.77	78.92
ZAA20	68.57	68.67		72.01	72.61	72.95	70.50	71.47	59.66
ZAA21	65.18	66.48		66.77	63.36	63.62	57.13	62.79	53.85
ZAA22	75.42	70.40		74.23	70.06	72.94	69.29	79.32	70.85
ZAA23	65.29	64.83		67.65	67.27	63.68	67.35	66.62	64.70
ZAA24	69.87	73.21		67.96	72.50	75.58	74.05	74.97	74.51
ZAA25	76.78	78.74		81.92	81.90	80.47	80.66	79.48	80.81
ZAA26	64.97	69.02		64.50	65.53	67.80	67.52	71.08	66.82
ZAA27	82.40	75.17		77.35	76.91	79.20	82.10	77.48	82.25

Table 344:Lattice parameter a values from the rietveld refinement of the umbite samples

Sample Name	Lattice Parameter *a*			
	Sep-19	Jan-20	Sep-20	Apr-21
ZAA1A	10.3034	10.3316	10.3026	10.3031
ZAA1C		10.3072	10.3092	10.3057
ZAA1I			10.3094	10.3000
ZAA3A	10.3069	10.3160	10.3025	10.3100
ZAA3C		10.3060	10.3056	10.2971
ZAA3I			10.3087	10.3007
ZAA4A	10.3085	10.3038	10.3095	10.3001
ZAA4C		10.3035	10.3105	10.3065
ZAA4I			10.3006	10.3070
ZAA6A	10.3117	10.2986	10.3099	10.3084
ZAA6C		10.3060	10.2955	10.3069
ZAA6I			10.3074	10.3015
ZAA7A	10.3084	10.3051	10.3079	10.3048
ZAA7C		10.3003	10.3084	10.3114
ZAA7I			10.2973	
ZAA9A	10.3108	10.2998	10.3144	10.3089
ZAA9C		10.3055	10.3023	10.3089
ZAA9I			10.3137	10.3073
ZAA10A	10.3044	10.3023	10.2999	10.3010
ZAA10C		10.2999	10.2954	10.2957
ZAA10I			10.3044	
ZAA12A	10.3052	10.2975	10.2946	10.3021
ZAA12C		10.3028	10.3186	10.3072
ZAA12I			10.3040	10.3100
ZAA13A	10.3005	10.2903	10.2999	10.3154
ZAA13C		10.3053	10.3006	10.3100
ZAA13I			10.2988	10.3045
ZAA15A	10.3072	10.2993	10.3021	10.3431
ZAA15C		10.3062	10.2965	10.3088
ZAA15I			10.2964	10.3121
ZAA16A	10.3175	10.3005	10.3079	10.3169
ZAA16C		10.3017	10.3103	10.3122
ZAA16I			10.3078	10.3171
ZAA18A	10.3031	10.2999	10.3054	10.3168
ZAA18C		10.3095	10.3028	10.3127
ZAA18I			10.3081	10.3126
ZAA19A	10.3091	10.2964	10.3056	10.3054
ZAA19C		10.3009	10.3008	10.3117
ZAA19I			10.3033	
ZAA20A	10.3033	10.3038	10.2983	10.3099

ZAA20C		10.3043	10.2995	
ZAA20I			10.3089	10.3101
ZAA21A	10.3126	10.3005	10.3123	10.3157
ZAA21C		10.3094	10.3073	10.3153
ZAA21I			10.3149	10.3134
ZAA22A	10.2984	10.3045	10.3063	
ZAA22C			10.3046	10.3202
ZAA22I			10.3143	10.3141
ZAA23A	10.3078	10.2986	10.3056	10.3073
ZAA23C			10.3023	10.3136
ZAA23I			10.3073	10.3080
ZAA24A	10.3056	10.3066	10.3113	10.3060
ZAA24C			10.3113	10.3088
ZAA24I			10.3109	10.3086
ZAA25A	10.3089	10.3160	10.3231	10.3142
ZAA25C			10.3236	10.3173
ZAA25I			10.3107	10.3076
ZAA26A	10.3060	10.3157	10.3093	10.3129
ZAA26C			10.3134	10.3046
ZAA26I			10.3041	10.3093
ZAA27A	10.3053	10.2968	10.3244	10.2986
ZAA27C			10.3250	10.3003
ZAA27I			10.3133	10.2986

Table 345: Lattice parameter b values from the rietveld refinement of the umbite samples

Sample Name	Lattice Parameter *b*			
	Sep-19	Jan-20	Sep-20	Apr-21
ZAA1A	13.3308	13.3612	13.3290	13.3273
ZAA1C		13.3388	13.3321	13.3286
ZAA1I			13.3280	13.3262
ZAA3A	13.3274	13.3504	13.3263	13.3342
ZAA3C		13.3279	13.3314	13.3302
ZAA3I			13.3310	13.3308
ZAA4A	13.3311	13.3281	13.3218	13.3315
ZAA4C		13.3344	13.3278	13.3211
ZAA4I			13.3266	13.3298
ZAA6A	13.3355	13.3275	13.3285	13.3237
ZAA6C		13.3332	13.3255	13.3260
ZAA6I			13.3306	13.3285
ZAA7A	13.3277	13.3282	13.3288	13.3284
ZAA7C		13.3277	13.3255	13.3279
ZAA7I			13.3252	
ZAA9A	13.3277	13.3286	13.3300	13.3261
ZAA9C		13.3270	13.3225	13.3234
ZAA9I			13.3284	13.3319
ZAA10A	13.3300	13.3320	13.3243	13.3180
ZAA10C		13.3293	13.3232	13.3210
ZAA10I			13.3267	
ZAA12A	13.3286	13.3302	13.3211	13.3196
ZAA12C		13.3272	13.3303	13.3232
ZAA12I			13.3240	13.3291
ZAA13A	13.3234	13.3192	13.3215	13.3299
ZAA13C		13.3278	13.3204	13.3294
ZAA13I			13.3206	13.3309
ZAA15A	13.3289	13.3259	13.3196	13.3243
ZAA15C		13.3289	13.3213	13.3223
ZAA15I			13.3226	13.3286
ZAA16A	13.3317	13.3283	13.3282	13.3270
ZAA16C		13.3307	13.3280	13.3190
ZAA16I			13.3262	13.3379
ZAA18A	13.3280	13.3314	13.3274	13.3292
ZAA18C		13.3321	13.3239	13.3335
ZAA18I			13.3283	13.3303
ZAA19A	13.3306	13.3249	13.3250	13.3206
ZAA19C		13.3326	13.3217	13.3277
ZAA19I			13.3330	
ZAA20A	13.3292	13.3312	13.3257	13.3264

ZAA20C		13.3299	13.3273	
ZAA20I			13.3264	13.3314
ZAA21A	13.3256	13.3284	13.3347	13.3330
ZAA21C		13.3291	13.3287	13.3318
ZAA21I			13.3143	13.3327
ZAA22A	13.3285	13.3337	13.3255	
ZAA22C			13.3298	13.3307
ZAA22I			13.3143	13.3327
ZAA23A	13.3286	13.3297	13.3222	13.3231
ZAA23C			13.3312	13.3262
ZAA23I			13.3294	13.3273
ZAA24A	13.3313	13.3311	13.3277	13.3299
ZAA24C			13.3340	13.3315
ZAA24I			13.3317	13.3361
ZAA25A	13.3301	13.3247	13.3232	13.3280
ZAA25C			13.3238	13.3273
ZAA25I			13.3245	13.3261
ZAA26A	13.3336	13.3374	13.3307	13.3323
ZAA26C			13.3318	13.3256
ZAA26I			13.3316	13.3306
ZAA27A	13.3217	13.3285	13.3180	13.3193
ZAA27C			13.3104	13.3176
ZAA27I			13.3071	13.3210

Table 346: Lattice parameter c values from the rietveld refinement of the umbite samples

Sample Name	Lattice Parameter *c*			
	Sep-19	Jan-20	Sep-20	Apr-21
ZAA1A	7.1938	7.2101	7.1922	7.1922
ZAA1C		7.1978	7.1955	7.1912
ZAA1I			7.1946	7.1889
ZAA3A	7.1949	7.2039	7.1882	7.1965
ZAA3C		7.1942	7.1912	7.1886
ZAA3I			7.1947	7.1902
ZAA4A	7.1957	7.1907	7.1944	7.1898
ZAA4C		7.1938	7.1948	7.1889
ZAA4I			7.1896	7.1926
ZAA6A	7.1982	7.1907	7.1950	7.1938
ZAA6C		7.1947	7.1880	7.1922
ZAA6I			7.1946	7.1892
ZAA7A	7.1939	7.1914	7.1949	7.1931
ZAA7C		7.1928	7.1950	7.1968
ZAA7I			7.1898	
ZAA9A	7.1956	7.1895	7.1981	7.1937
ZAA9C		7.1929	7.1906	7.1934
ZAA9I			7.1979	7.1925
ZAA10A	7.1917	7.1924	7.1899	7.1895
ZAA10C		7.1923	7.1884	7.1874
ZAA10I			7.1939	
ZAA12A	7.1924	7.1906	7.1883	7.1896
ZAA12C		7.1922	7.2002	7.1947
ZAA12I			7.1913	7.1959
ZAA13A	7.1929	7.1866	7.1890	7.1993
ZAA13C		7.1935	7.1876	7.1960
ZAA13I			7.1862	7.1918
ZAA15A	7.1949	7.1907	7.1901	7.1966
ZAA15C		7.1936	7.1874	7.1934
ZAA15I			7.1870	7.1978
ZAA16A	7.1991	7.1901	7.1940	7.1985
ZAA16C		7.1922	7.1945	7.1966
ZAA16I			7.1929	7.2016
ZAA18A	7.1935	7.1912	7.1913	7.1992
ZAA18C		7.1955	7.1917	7.1971
ZAA18I			7.1937	7.1964
ZAA19A	7.1947	7.1914	7.1922	7.1931
ZAA19C		7.1927	7.1902	7.1966
ZAA19I			7.1922	
ZAA20A	7.1923	7.1929	7.1903	7.1949

ZAA20C		7.1946	7.1911	
ZAA20I			7.1947	7.1958
ZAA21A	7.1958	7.1915	7.1977	7.1996
ZAA21C		7.1952	7.1935	7.1996
ZAA21I			7.1981	7.1991
ZAA22A	7.1900	7.1957	7.1929	
ZAA22C			7.1934	7.2024
ZAA22I			7.1986	7.1996
ZAA23A	7.1940	7.1916	7.1916	7.1933
ZAA23C			7.1926	7.1974
ZAA23I			7.1924	7.1944
ZAA24A	7.1928	7.1927	7.1961	7.1937
ZAA24C			7.1966	7.1962
ZAA24I			7.1962	7.1961
ZAA25A	7.1948	7.1989	7.2038	7.2003
ZAA25C			7.2046	7.2017
ZAA25I			7.1979	7.1953
ZAA26A	7.1930	7.2005	7.1938	7.1989
ZAA26C			7.1971	7.1925
ZAA26I			7.1948	7.1959
ZAA27A	7.1989	7.1957	7.2036	7.1927
ZAA27C			7.2010	7.1935
ZAA27I			7.1966	7.1940

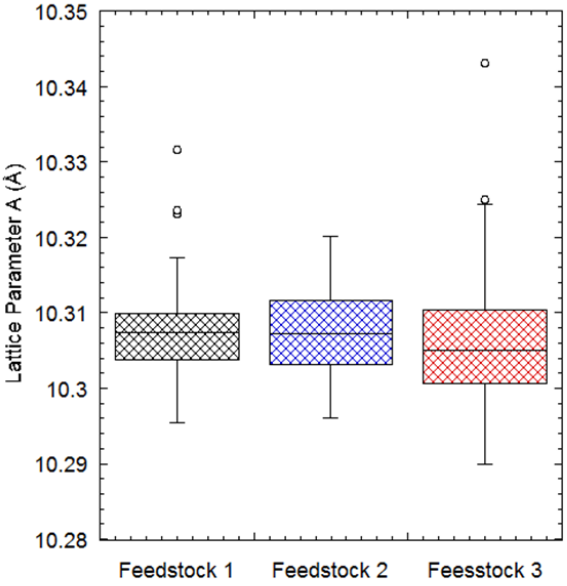

Figure 400: Distribution of lattice parameter a resulting from the rietveld refinement of umbite samples synthesised with the zirconium acetate precursor as a function of the feedstock of the zirconium acetate solution

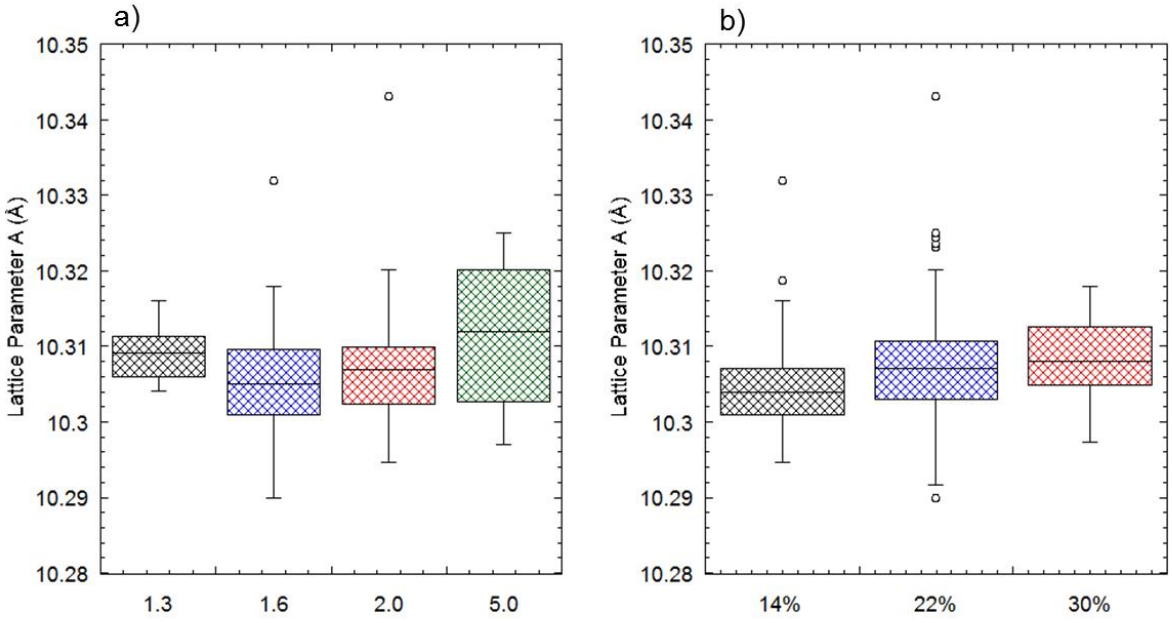

Figure 401: Distribution of lattice parameter a resulting from the rietveld refinement of umbite samples synthesised with the zirconium acetate precursor as a function of a) the acetic acid : zirconium ratio and b) the zirconium concentration of the zirconium acetate solution

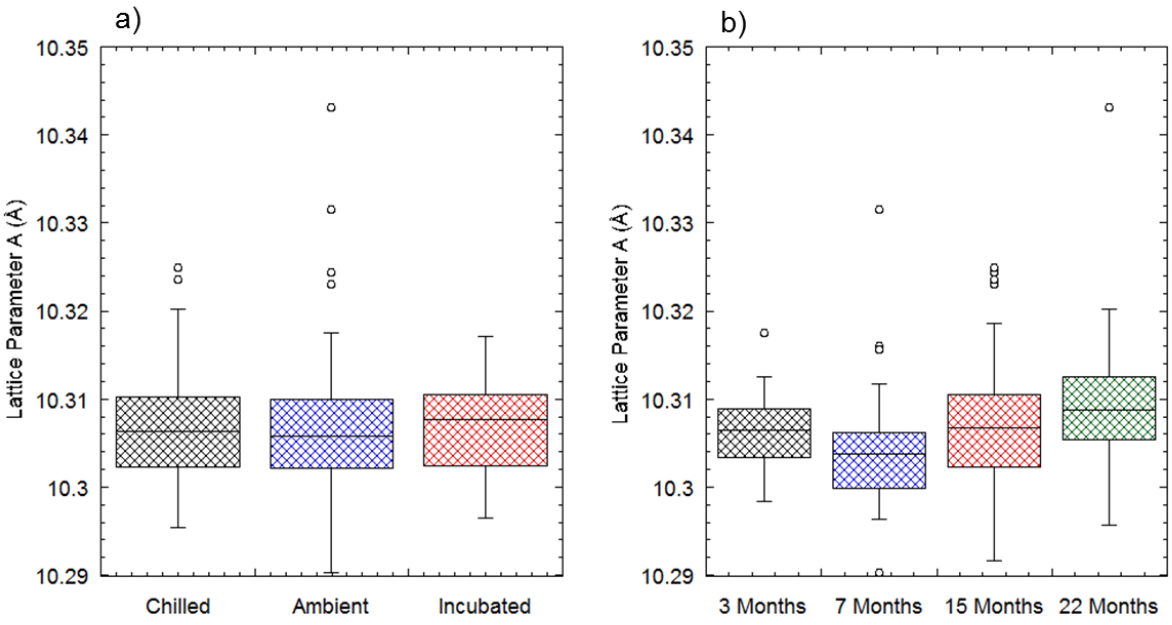

Figure 402: Distribution of lattice parameter a resulting from the rietveld refinement of umbite samples synthesised with the zirconium acetate precursor as a function of a) storage temperature and b) the age of the zirconium acetate solution

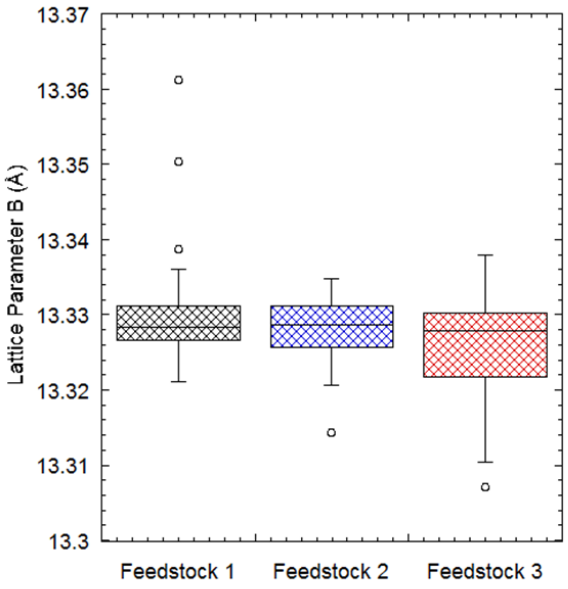

Figure 403: Distribution of lattice parameter b resulting from the rietveld refinement of umbite samples synthesised with the zirconium acetate precursor as a function of the feedstock of the zirconium acetate solution

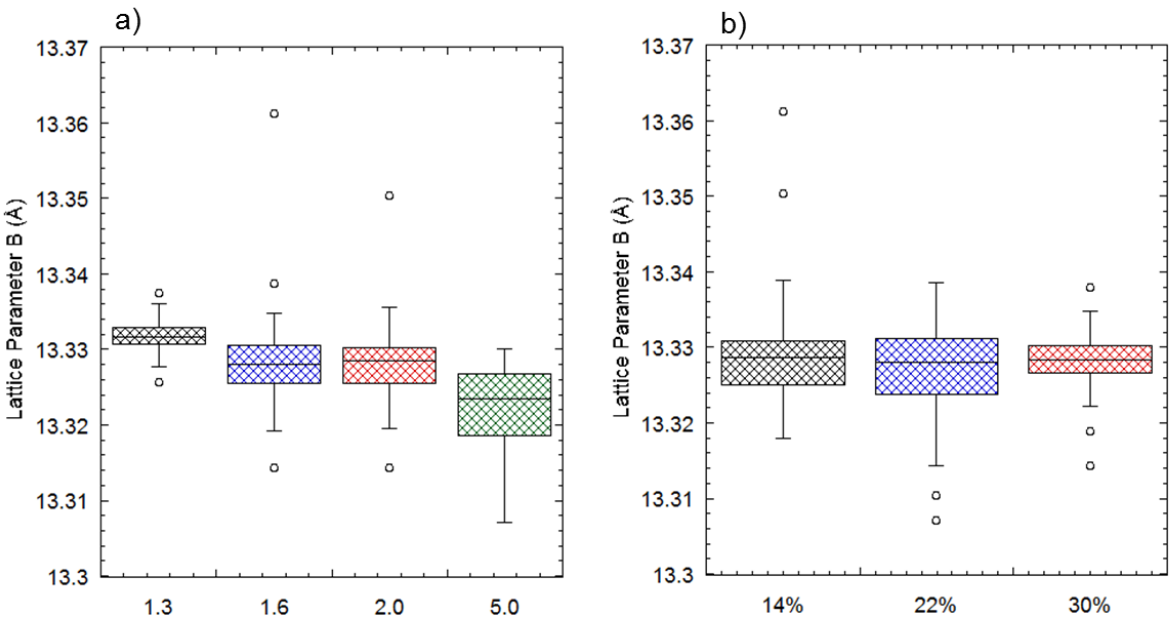

Figure 404: Distribution of lattice parameter b resulting from the rietveld refinement of umbite samples synthesised with the zirconium acetate precursor as a function of a) the acetic acid : zirconium ratio and b) the zirconium concentration of the zirconium acetate solution

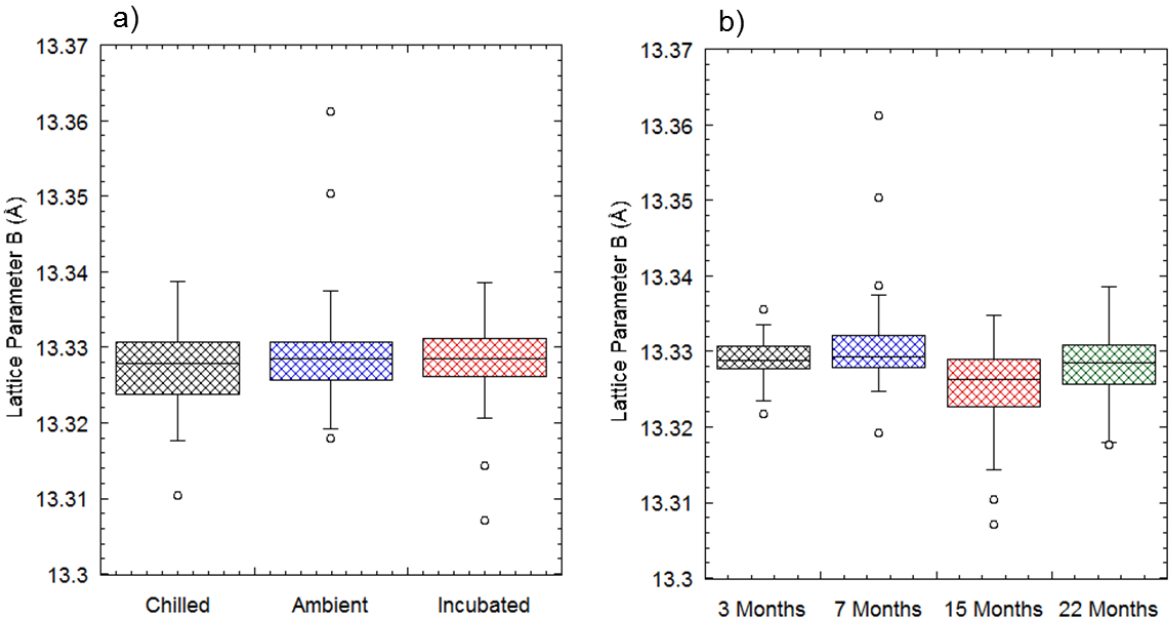

Figure 405: Distribution of lattice parameter b resulting from the rietveld refinement of umbite samples synthesised with the zirconium acetate precursor as a function of a) storage temperature and b) the age of the zirconium acetate solution

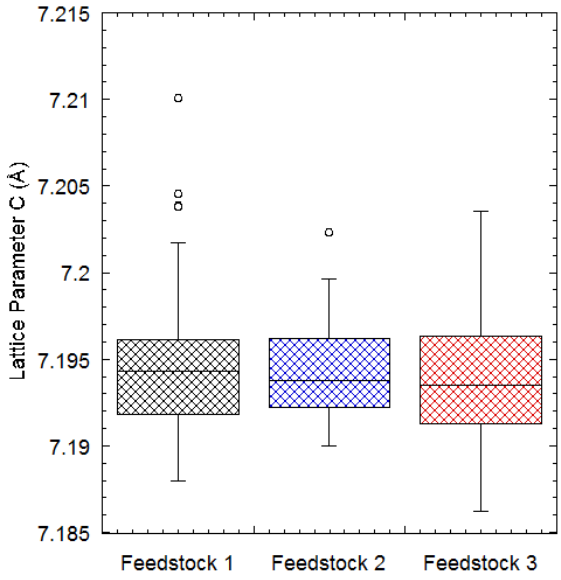

Figure 406: Distribution of lattice parameter c resulting from the rietveld refinement of umbite samples synthesised with the zirconium acetate precursor as a function of the feedstock of the zirconium acetate solution

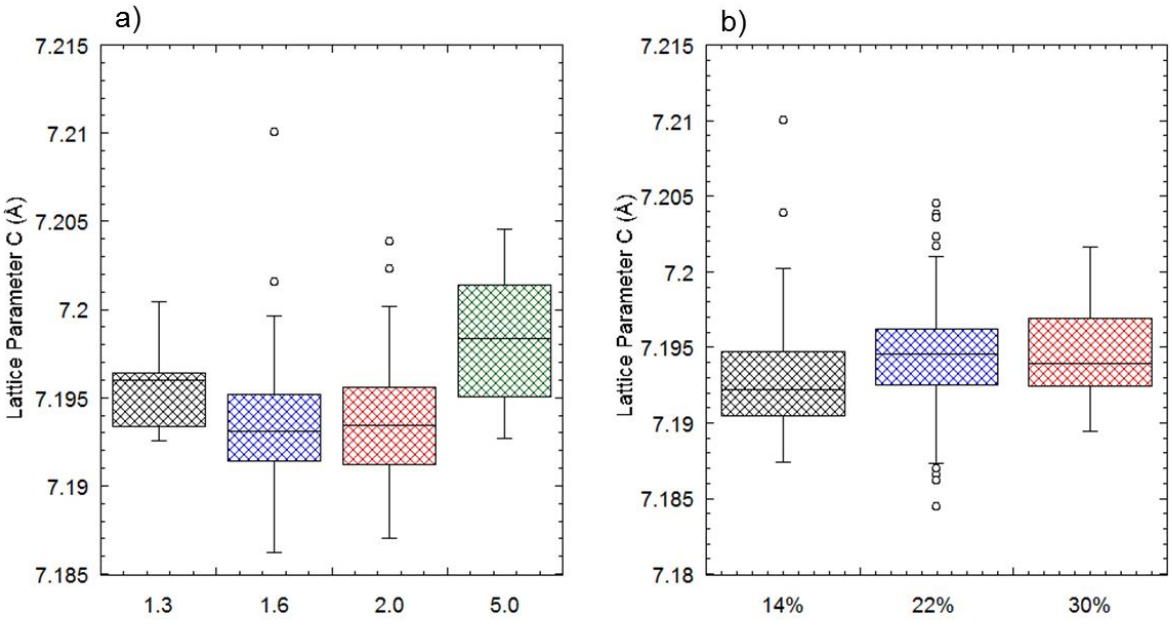

Figure 407: Distribution of lattice parameter c resulting from the rietveld refinement of umbite samples synthesised with the zirconium acetate precursor as a function of a) the acetic acid : zirconium ratio and b) the zirconium concentration of the zirconium acetate solution

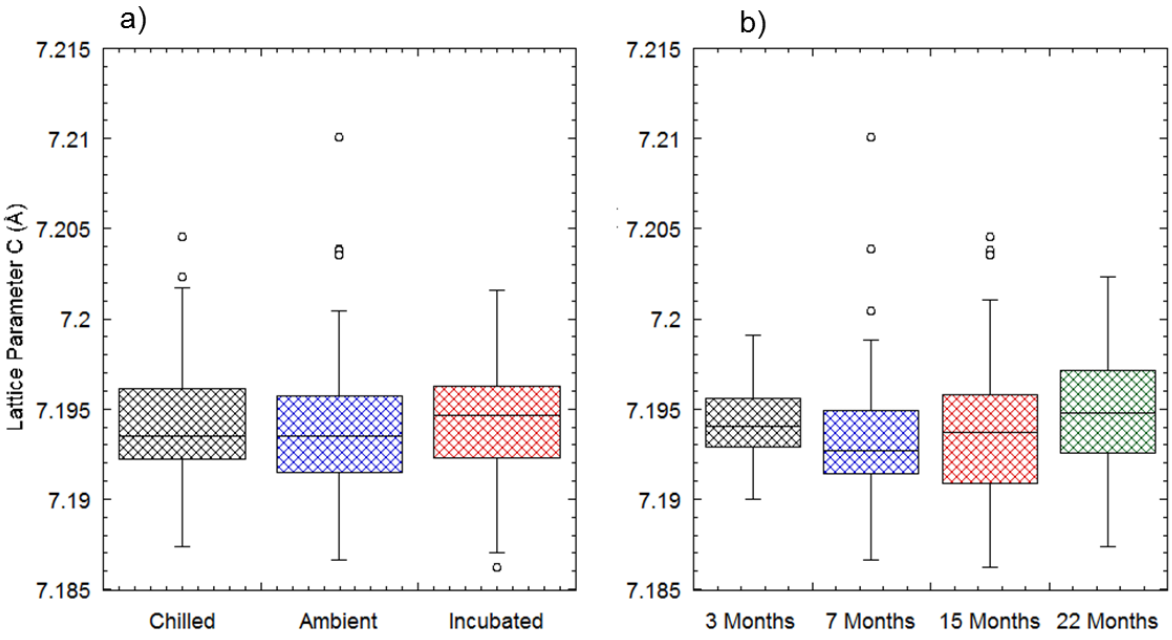

Figure 408: Distribution of lattice parameter c resulting from the rietveld refinement of umbite samples synthesised with the zirconium acetate precursor as a function of a) storage temperature and b) the age of the zirconium acetate solution

Table 347: Results of the structural refinements of samples of umbite synthesised from zirconium acetate, common to all samples.

Chemical formula	$K_2ZrSi_3O_9 \cdot H_2$	Radiation type	Cu Kα (1.5418 Å)
Crystal system	Orthorhombic	Collection Range (°)	10 – 120
Space Group	P 2_1 2_1 2_1 (#19)	Step Size (°)	0.02
Z	4	Collection Time (s)	21600
Background	35 point linear interpolation	Parameters refined	112

Table 348: Structural refinement parameters of samples of umbite synthesised from zirconium acetate solutions aged for 3-months

	Chi^2	R_{wp}	RF^2
ZAA1	8.142	0.0625	0.0671
ZAA3	6.252	0.0555	0.0623
ZAA4	7.062	0.0604	0.0743
ZAA6	6.242	0.0575	0.0719
ZAA7	6.686	0.0588	0.0705
ZAA9	5.721	0.0547	0.0727
ZAA10	6.659	0.0586	0.0752
ZAA12	6.74	0.0582	0.068
ZAA13	7.096	0.0604	0.0732
ZAA15	6.773	0.0589	0.0603
ZAA16	3.545	0.0435	0.0673
ZAA18	4.732	0.0495	0.0711
ZAA19	5.209	0.0535	0.0796
ZAA20	4.331	0.0494	0.0787
ZAA21	5.414	0.054	0.0804
ZAA22	5.738	0.0556	0.0684
ZAA23	5.321	0.0536	0.0687
ZAA24	4.304	0.0508	0.0689
ZAA25	3.907	0.0448	0.0704
ZAA26	6.18	0.0558	0.0563
ZAA27	2.64	0.0364	0.0977

Table 349: Structural refinement parameters of samples of umbite synthesised from zirconium acetate solutions aged for 7 months

	Ambient Samples			Chilled Samples			Incubated Samples		
	Chi^2	R_{wp}	RF^2	Chi^2	R_{wp}	RF^2	Chi^2	R_{wp}	RF^2
ZAA1	7.645	0.058	0.0593	6.415	0.0594	0.0691			
ZAA3	7.869	0.0591	0.0579	5.425	0.0846	0.0969			
ZAA4	7.865	0.0612	0.082	8.861	0.0677	0.0801			
ZAA6	6.819	0.057	0.0655	8.869	0.0687	0.092			
ZAA7	7.287	0.0587	0.0604	7.219	0.0601	0.0698			
ZAA9	7.175	0.0592	0.0708	4.385	0.0757	0.0669			
ZAA10	7.675	0.0618	0.0653	9.926	0.069	0.0814			
ZAA12	7.321	0.0607	0.0742	8.79	0.0647	0.0743			
ZAA13	6.38	0.055	0.056	7.206	0.0587	0.0649			
ZAA15	6.88	0.0576	0.0629	7.192	0.0589	0.0594			
ZAA16	7.913	0.0626	0.0625	7.047	0.0588	0.0605			
ZAA18	13.05	0.0794	0.0847	6.205	0.0552	0.0598			
ZAA19	7.755	0.0611	0.0791	6.194	0.0568	0.0686			
ZAA20	7.402	0.061	0.0735	7.226	0.0609	0.062			
ZAA21	7.323	0.0617	0.077	7.101	0.0593	0.0618			
ZAA22	5.704	0.0645	0.0798						
ZAA23	6.651	0.0569	0.0633						
ZAA24	6.723	0.0592	0.0689						
ZAA25	12.4	0.0792	0.0958						
ZAA26	7.282	0.0625	0.049						
ZAA27	7.41	0.0604	0.0718						
ZAA28	7.993	0.071	0.07						

Table 350: Structural refinement parameters of samples of umbite synthesised from zirconium acetate solutions aged for 15 months

	Ambient Samples			Chilled Samples			Incubated Samples		
	Chi^2	R_{wp}	RF^2	Chi^2	R_{wp}	RF^2	Chi^2	R_{wp}	RF^2
ZAA1	4.999	0.0825	0.0958	5.493	0.0873	0.1332	4.223	0.0747	0.0969
ZAA3	2.25	0.0549	0.1014	1.387	0.0588	0.1163	3.843	0.0718	0.1063
ZAA4	1.635	0.0607	0.064	2.199	0.0751	0.0964	2.165	0.0736	0.0746
ZAA6	4.729	0.0801	0.1119	4.438	0.0785	0.0895	4.416	0.0786	0.1022
ZAA7	4.335	0.076	0.0749	4.603	0.0791	0.0803	4.13	0.0748	0.078
ZAA9	3.998	0.0747	0.0829	4.474	0.0785	0.0834	4.601	0.0793	0.0834
ZAA10	6.291	0.0905	0.1101	5.722	0.0861	0.0908	4.406	0.0791	0.0928
ZAA12	4.256	0.0738	0.0646	3.89	0.0754	0.0935	3.935	0.0714	0.069
ZAA13	4.245	0.0738	0.0737	4.175	0.0733	0.0669	3.475	0.0669	0.0645
ZAA15	4.112	0.0707	0.0663	3.563	0.0656	0.0628	3.989	0.0713	0.06
ZAA16	3.874	0.069	0.0575	3.309	0.0658	0.077	2.743	0.0599	0.064
ZAA18	3.942	0.0722	0.0933	4.84	0.0807	0.0979	3.652	0.0691	0.0894
ZAA19	5.246	0.0829	0.0829	5.566	0.0856	0.1065	4.568	0.0789	0.0819
ZAA20	4.326	0.0725	0.0486	4.883	0.0815	0.0801	4.51	0.078	0.0741
ZAA21	5.954	0.0905	0.0997	4.416	0.0759	0.0801	3.046	0.0641	0.0926
ZAA22	4.504	0.0766	0.0997	4.677	0.0798	0.1122	5.032	0.083	0.0975
ZAA23	4.337	0.0758	0.0726	4.711	0.0822	0.1122	4.586	0.0779	0.1039
ZAA24	4.527	0.0779	0.0989	4.278	0.0768	0.0953	3.955	0.0762	0.1061
ZAA25	1.512	0.0452	0.1459	1.326	0.0425	0.1151	3.416	0.0699	0.1447
ZAA26	5.075	0.085	0.1102	3.114	0.0732	0.09	2.904	0.0628	0.0846
ZAA27	1.394	0.0433	0.1627	2.946	0.0614	0.1442	1.427	0.0432	0.1553
ZAA28	5.686	0.0866	0.1031	5.675	0.0864	0.1039	4.573	0.078	0.0812

Table 351: Structural refinement parameters of samples of umbite synthesised from zirconium acetate solutions aged for 22 months

	Ambient Samples			Chilled Samples			Incubated Samples		
	Chi^2	R_{wp}	RF^2	Chi^2	R_{wp}	RF^2	Chi^2	R_{wp}	RF^2
ZAA1	5.974	0.0883	0.0992	2.521	0.0597	0.1022	4.832	0.0804	0.0804
ZAA3	2.81	0.0702	0.0767	5.156	0.0851	0.092	4.686	0.0809	0.089
ZAA4	5.026	0.0839	0.0928	2.504	0.0528	0.0412	4.725	0.0812	0.0846
ZAA6	4.929	0.0812	0.0987	5.084	0.0839	0.0986	4.62	0.0803	0.0851
ZAA7	4.368	0.0768	0.0682	3.816	0.0716	0.0655	6.424	0.0944	0.0761
ZAA9	3.982	0.0735	0.0794	4.33	0.0762	0.0818	4.734	0.0813	0.1018
ZAA10	6.177	0.0896	0.097	5.363	0.086	0.0974	6.342	0.0914	0.1327
ZAA12	7.213	0.0982	0.1017	5.541	0.0884	0.0951	4.363	0.0742	0.0687
ZAA13	3.338	0.0655	0.0602	5.121	0.0849	0.083	3.534	0.067	0.053
ZAA15	4.448	0.0769	0.0713	3.941	0.07347	0.0635	4.716	0.0803	0.0886
ZAA16	3.465	0.0692	0.0684	5.605	0.0843	0.1095	2.892	0.0692	0.0503
ZAA18	4.634	0.0798	0.087	2.975	0.066	0.058	5.161	0.0869	0.1045
ZAA19	5.618	0.0839	0.0935	3.671	0.0671	0.0658	7.447	0.1023	0.1449
ZAA20	4.228	0.0749	0.0729	53.71	0.2756	0.2169	3.945	0.0708	0.0635
ZAA21	4.782	0.0819	0.0684	4.575	0.0781	0.0679	4.235	0.0766	0.0698
ZAA22				4.506	0.0789	0.0837	4.604	0.0798	0.0712
ZAA23	2.934	0.0607	0.0533	4.858	0.0816	0.0785	2.891	0.0602	0.0417
ZAA24	4.304	0.0774	0.0654	4.151	0.0735	0.0651	3.389	0.0742	0.0763
ZAA25	2.883	0.0648	0.0781	7.586	0.1004	0.1519	5.251	0.0851	0.0918
ZAA26	4.703	0.0814	0.0718	5.421	0.0808	0.0907	4.173	0.0738	0.0655
ZAA27	4.858	0.0801	0.1014	5.159	0.0829	0.108	2.959	0.0609	0.06
ZAA28	4.691	0.0795	0.0757	3.601	0.0666	0.052	3.234	0.068	0.0587